UTAH LOW-LEVEL RADIOACTIVE WASTE

DISPOSAL LICENSE - CONDITION 35 (RML UT2300249)

COMPLIANCE REPORT

June 1, 2011

For
Utah Division of Radiation Control
195 North 1950 West
Salt Lake City, UT 84114-4850

Energy*Solutions*, LLC
423 West 300 South, Suite 200
Salt Lake City, UT 84101

EXECUTIVE SUMMARY

In early 2009, the U.S. Nuclear Regulatory Commission voted to initiate rulemaking to require a site-specific analysis for disposal of large quantities of depleted uranium. Since that time, Energy*Solutions* has received (and intends to dispose) 3,577 metric tons of depleted uranium waste that has been declared surplus from the Savannah River Site. However, Utah Radiation Control Rule (URCR) Section R313-25-8(5) prohibits disposal of significant quantities of concentrated depleted uranium (more than one metric ton in total accumulation) after June 1, 2010, until the Utah Division of Radiation Control Executive Secretary's approves a performance assessment that demonstrates that Energy*Solutions* will meet the performance standards specified in 10 CFR Part 61 and corresponding provisions of Utah rules.

As required by URCR313-25-8(5) and in accordance with URCR313-25-8(2), Energy*Solutions* has competed and hereby submits to the Division's Executive Secretary for approval an in-depth site-specific performance assessment before disposal of depleted uranium. Once approved, it is Energy*Solutions*' objective to file documentation requesting its Radioactive Material License be amended to include disposal of depleted uranium.

Because of the processes, depleted uranium from the Savannah River Site also contains small quantities of waste fission products and transuranic elements. The estimated mass of depleted uranium from the Savannah River Site proposed for disposal at Energy*Solutions*' Clive Facility is 3,577 metric tons, (5,408 drums). Furthermore, this report also evaluates acceptance and disposal of up to 700,000 metric tons of similar depleted uranium waste from the gaseous diffusion plants at Portsmouth, Ohio and Paducah, Kentucky.

License Condition 35.B of Energy*Solutions*' Radioactive Material License (UT 2300249) states,

> "*Performance assessment: A performance assessment, in general conformance with the approach used by the Nuclear Regulatory Commission (NRC) in SECY-08-0147, shall be submitted for Executive Secretary review and approval no later than June 1, 2011. The performance assessment shall be revised as needed to reflect ongoing guidance and rulemaking from NRC. For purposes of this performance assessment, the compliance period will be a minimum of 10,000 years. Additional simulations will be performed for a minimum 1,000,000-year time frame for qualitative analysis.*"

Energy*Solutions* supports their claims of compliance with the license condition through the development and execution of a detailed, site-specific, probabilistic performance assessment using the GoldSim model. This model and the resulting findings demonstrate to the Division that Energy*Solutions*' proposed methods for disposal of depleted uranium will ensure that future operations, institutional control, and site closure can be conducted safely, and that the site will comply with the Division's radiological criteria contained in the Radioactive Material License.

While also included in this Compliance Report as part of improving qualitative understanding of facility performance, Energy*Solutions* recognizes that events that are projected to broadly disrupt the disposal site region should generally be expected to drive human populations away from the affected areas. Accordingly, "an appropriate assumption under these conditions would be that no individual is living close enough to the facility to receive a meaningful dose" (NRC, 2000).

TABLE OF CONTENTS

TABLE OF CONTENTS (continued)

LIST OF TABLES

LIST OF FIGURES

ACRONYMS AND ABBEVIATIONS

Term	Definition
11e.(2)	Section 11e.(2) of the Atomic Energy Act of 1954, as amended
2008 LRA renewal	License Renewal Application dated 20 June 2005
ABC ALA	Application for License Amendment (Classes A, B & C waste), dated December 13,2000
Ac	actinium
Act	Utah Radiation Control Act
ALARA	As Low As Reasonably Achievable
Am	americium
AMEC	AMEC Earth and Environmental, formerly AGRA Earth and
ASCE	American Society of Civil Engineers
ASTM	ASTM International, formerly American Society for Testing and
BLM	Bureau of Land Management
Bq	becquerel
BWF	Bulk Waste Facility
CCE	certified cost engineer
CEDE	committed effective dose equivalent
CFR	U.S. Code of Federal Regulations
Ci	curie
cm/sec	centimeters per second
cm/yr	centimeters per year
CQA/QC	Construction Quality Assurance/Quality Control
CSF	cancer slope factor
CSLM	Controlled Low Strength Material
CSM	conceptual site model
CTC	Cover Test Cell
CWF	Containerized Waste Facility
DCF	dose conversion factor
DDE	deep dose equivalent
Division	Utah Division of Radiation Control
DOE	U.S. Department of Energy
DOT	U.S. Department of Transportation
DRC	Utah Division of Radiation Control
DU	depleted uranium
EDIS	electronic document imaging system
EIS	environmental impact statement

ACRONYMS AND ABBEVIATIONS (continued)

Term	Definition
EPA	U.S. Environmental Protection Agency
ETTP	East Tennessee Technology Park
EWIS	Electronic Waste Information System
FEIS	Final Environmental Impact Statement
FEP	features, events, and processes
FR	Federal Register
ft	foot/feet
Ft	feet; foot
ft/ft	feet per foot
ft-lbf/ft^3	foot-pound force per cubic foot (unit of energy density)
g	gram
GDP	gaseous diffusion plant
GTCC	greater than Class C waste
GWPL	groundwater protection limit(s)
GWQDP	groundwater quality discharge permit
ha	hectare
hr	hour; hours
IAEA	International Atomic Energy Agency
ICRP	International Commission on Radiation Protection
in	inch; inches
in/yr	inches per year
ka	thousand years ago
K_d	soil/water partition coefficient
kg	kilogram
km	kilometer
ky	thousand years
L	liter
LARW	low-activity radioactive waste
LLRW	low-level radioactive waste
LRA	License Renewal Application
m	meter
Ma	million years ago
MCL	maximum contaminant level(s)
Mg	megagram (one metric ton)
mg	milligram

ACRONYMS AND ABBEVIATIONS (continued)

Term	Definition
MLLW	mixed [hazardous and] low-level radioactive waste
mm	millimeters
MPa	megapascal
mrem	millirem
mrem/yr	millirem/yr
My	million years
NORM	Naturally-Occurring Radioactive Materials
NQA	Nuclear Quality Assurance
NRC	U.S. Nuclear Regulatory Commission
NTS	Nevada Test Site
NUREG	an NRC publication
PA	performance assessment
Pa	protactinium
PAWG	Performance Assessment Working Group (DOE)
pCi	picocurie
pCi/g	picocuries per gram
pCi/m^2-s	picocuries per square meter-second
Po	polonium
ppm	part per million
Pu	plutonium
QA	quality assurance
QAM	Quality Assurance Manual
QAP	Quality Assurance Program
R	Roentgen
Ra	radium
RfD	reference dose
RML	Radioactive Material License (UT2300249), as amended May 10, 2011.
Rn	radon
S&H	safety and health
SLB&M	Salt Lake Baseline and Meridian
SNM	Special Nuclear Material
SRS	Savannah River Site
Tc	technetium
TDS	total dissolved solids

ACRONYMS AND ABBEVIATIONS (continued)

Term	Definition
TEDE	total effective dose equivalent
TF	Treatment Facility
Th	thorium
TSD	Treatment, Storage and Disposal
U	uranium
UAC	Utah Administrative Code
UDOGM	Utah Division of Oil, Gas and Mining
UDSHW	Utah Division of Solid and Hazardous Waste
UDWQ	Utah Division of Water Quality
UMTRA	Uranium Mill Tailing Remedial Action
UNF	used nuclear fuel
URCA	Utah Radiation Control Act
URCB	Utah Radiation Control Board
URCR	Utah Radiation Control Rules
USACE	US Army Corps of Engineers
USGS	United States Geologic Survey
UWQB	Utah Water Quality Board
yr	year

1. INTRODUCTION

Energy*Solutions*, headquartered in Salt Lake City, is a worldwide leader in the safe recycling, processing and disposal of nuclear material, providing innovations and technologies to the U.S. Department of Energy (DOE), commercial utilities, and medical and research facilities. At the Clive Facility, located 85 miles west of Salt Lake City, Energy*Solutions* operates a commercial treatment, storage and disposal facility for Class A low-level radioactive waste and Class A low-level mixed waste.

In early 2009, the U.S. Nuclear Regulatory Commission (NRC) voted to initiate rulemaking to require a site-specific analysis for the disposal of large quantities of depleted uranium (DU). Since that time, Energy*Solutions* has received 3,577 metric tons (5,408 drums) of uranium trioxide (DUO_3) waste that has been declared surplus from the Savannah River Site (SRS). In the future, Energy*Solutions* is also considering depleted uranium from the gaseous diffusion plants at Portsmouth, Ohio and Paducah, Kentucky. As is illustrated in Figure 1-1, Energy*Solutions* has evaluated a potential Federal Cell as ultimate destination for depleted uranium. In accordance with Utah Radiation Control Rule (URCR) Section R313-25-8(2), Energy*Solutions* is required to complete and submit to the Division's Executive Secretary for approval an in-depth site-specific performance assessment for the disposal of depleted uranium. Once approved, it is Energy*Solutions'* objective to file documentation requesting its Radioactive Material License be amended to include disposal of depleted uranium.

1.1 Licensing Overview

DOE remedial activities began for the Salt Lake City Vitro mill site in February 1985 and activities were completed in May 1989. Contaminated materials that remained at the site were excavated and relocated by the State of Utah to a newly acquired site, located 85 miles west of Salt Lake City at a location known as Clive, Utah. Adjacent to this operation, Energy*Solutions* (then known as Envirocare of Utah) began disposal operations at its Clive facility in 1988 under a State license (RML UT 2300249) to dispose of Naturally-Occurring Radioactive Materials (NORM). In 1990, Energy*Solutions* submitted a license application to modify its license to allow disposal of low-activity radioactive waste (LARW). In 1991, the Division granted this amendment request by issuing a license for LARW disposal. From time to time, the LARW disposal license has been amended to address Energy*Solutions'* changing needs and those of the public interest. Eventually, the license permitted disposal of Class A low-level radioactive waste (LLRW). In 2008, the Division renewed Energy*Solutions'* license (2008 RML renewal).

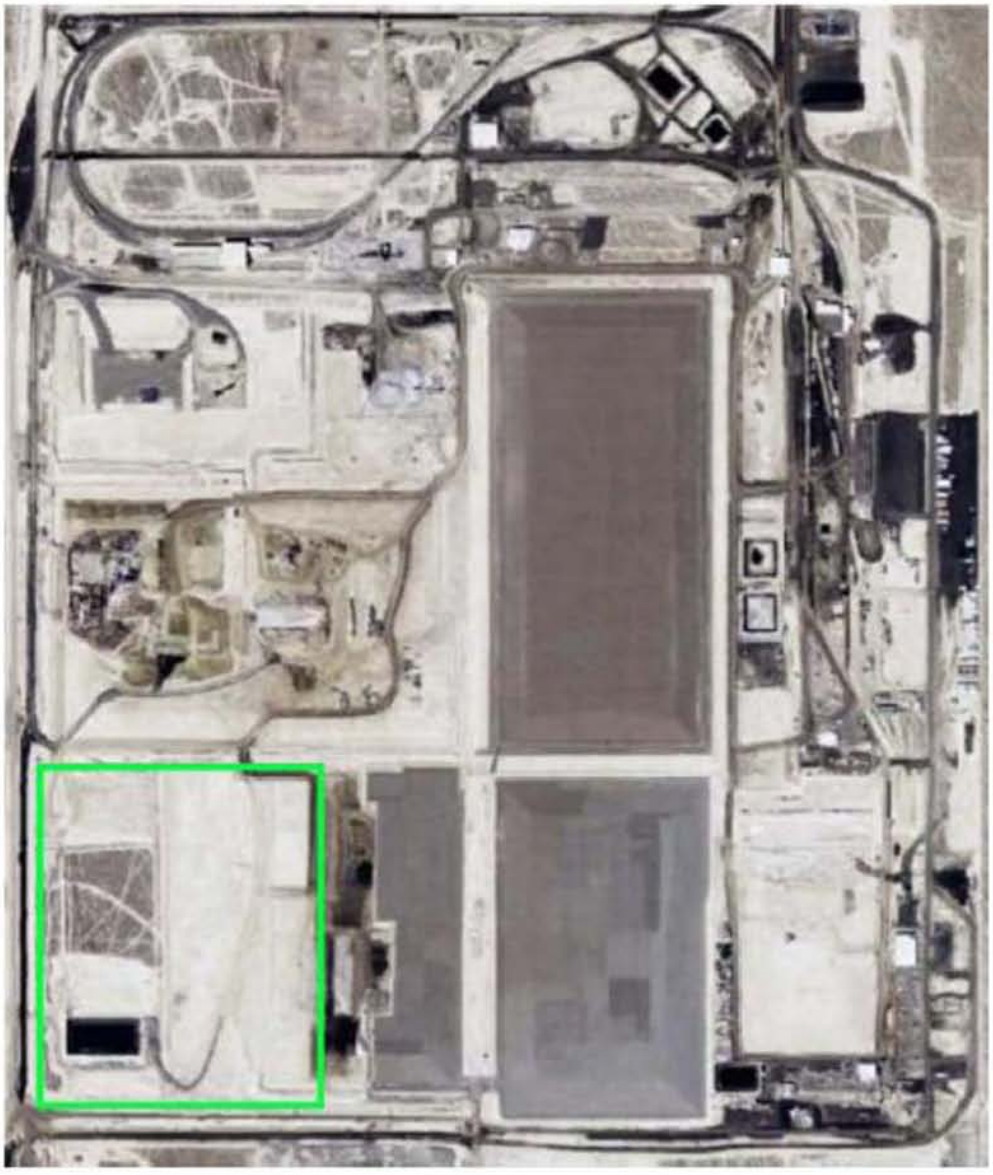

Figure 1-1, Energy*Solutions*' Proposed Depleted Uranium Disposal Location

Energy*Solutions* conducts other treatment and disposal operations in areas adjacent to its Class A embankments. These activities include mixed hazardous waste under a Treatment, Storage and Disposal (TSD) State-issued Part B RCRA Solid Waste Permit (re-issued by the Executive Secretary of the Utah Solid and Hazardous Waste Control Board on April 4, 2003). The nature of mixed waste managed at the facility includes contaminated soils, process waste, debris and sludges. The mixed waste portion of the Clive facility consists of a disposal cell, a treatment building, a storage building and an operations building. The treatment building is used for stabilization and solidification of certain waste streams and the operations building is used for alternative treatment technologies, such as macro-encapsulation and microencapsulation, as well as stabilization and storage of mixed waste.

Energy*Solutions* also disposes of uranium and thorium by-product material {11e.(2)} under a license issued by NRC as Byproduct Material License SMC-1559. Energy*Solutions*'11e.(2) license is now administered by the Division (RML UT2300478).

In conjunction with licensed activities, Energy*Solutions'* operations are also subject to the provisions of Ground Water Quality Discharge Permit (GWQDP) UGW450005, issued by the Utah Division of Water Quality (UDWQ). In 2008, Energy*Solutions* was awarded a renewal for this permit. This permit specifies that groundwater quality protection levels for radioactive constituents must be met for no fewer than 500 years following facility closure. Similarly, Energy*Solutions* also operates under Air Quality Approval Orders, issued by the Utah Division of Air Quality (UDAW).

1.2 Regulatory Summary

The Division regulates activities in the State of Utah that involve radioactive materials, some types of radioactive waste, and radiation. To assess whether Energy*Solutions*' Clive facility location and containment technologies are suitable for the disposal of depleted uranium and the continued protection of human health, specific performance objectives for land disposal of radioactive waste have been set forth in the URCR. Additionally, Energy*Solutions*' Clive facility is governed by the Department of Environmental Quality's groundwater and air regulatory requirements. Those rules potentially impacted by Energy*Solutions*' intent to dispose of depleted uranium include:

- "General Provisions" – URCR R313-12
- "Violations and Escalated Enforcement" – URCR R313-14
- "Standards for Protection Against Radiation" - URCR R313-15
- "Administrative Procedures" – URCR R313-17
- "Notices, Instructions and Reports to Workers by Licensees or Registrants—Inspections" – URCR R313-18
- "Requirements of General Applicability to Licensing of Radioactive Material" – URCR R313-19
- "Specific Licenses"- URCR R313-22
- "License Requirements of Land Disposal of Radioactive Waste" – URCR R313-25
- "Generator Site Access Permit Requirements for Accessing Utah Radioactive Waste Disposal Facilities" – URCR R313-26

- "Payments, Categories and Types of Fees" – URCR R313-70
- "Ground Water Quality Protection Rules" – Utah Administrative Code (UAC) Rule 317-6
- "Air Quality Protection Rules" – Utah Administrative Code Rule 307

1.3 Historical Management of Depleted Uranium

Large-scale uranium enrichment in the United States began as part of atomic bomb development by the Manhattan Project during World War II. Uranium enrichment activities were subsequently continued under the U.S. Atomic Energy Commission and its successor agencies, including DOE. The K-25 plant in Oak Ridge, Tennessee[1] was the first of three gaseous diffusion plants constructed to produce enriched uranium. The K-25 plant ceased operations in 1985, but uranium enrichment continues at facilities located in Paducah, Kentucky and Portsmouth, Ohio. These two plants are now operated by the United States Enrichment Corporation, created by law in 1993 to privatize uranium enrichment.

In the gaseous diffusion process, a stream of heated uranium hexafluoride (UF_6) gas is separated into a stream of UF_6 gas containing enriched U_{235} (EUF_6) and a stream of UF_6 gas depleted in U_{235} (DUF_6). The enriched uranium materials are used for manufacturing commercial reactor fuel, (typically contains 2 to 5% U_{235}), and military applications (requiring up to 95% U_{235}). The DUF_6 waste materials of interest to this Compliance Report typically contain U_{235} concentrations as low as 0.2 to 0.4%. Since the 1950s, DUF_6 waste materials have been stored at all three storage sites in large steel cylinders, similar to that illustrated in Figure 1-2.

Depleted uranium was also produced at DOE's Savannah River Site. The Savannah River Site produced depleted uranium as a byproduct of the nuclear material production programs, where irradiated nuclear fuels were reprocessed to separate out the fissionable Pu_{239}. Uranium billets were produced at the DOE Fernald, Ohio site, fabricated into targets at Savannah River Site, and then irradiated in the Savannah River Site production reactors to produce Pu_{239}. The irradiated targets were processed and fission products separated from the plutonium and uranium, which were then separated from each other. After additional purification, the depleted uranium-bearing waste stream was then processed into uranium trioxide (DUO_3). While still classified as depleted uranium, this DUO_3 also contains small quantities of waste fission products and transuranic elements. The Savannah River Site produced approximately 36,000 (55-gal) steel drums of DUO_3 during the production campaigns. This DUO_3, a solid powder at room temperature and pressure, is considered to be relatively homogeneous, based on known process controls and operations.

[1] The site of the K-25 plant is now called the East Tennessee Technology Park (ETTP), but is referred to by its original name, the K-25 site, in this Compliance Report.

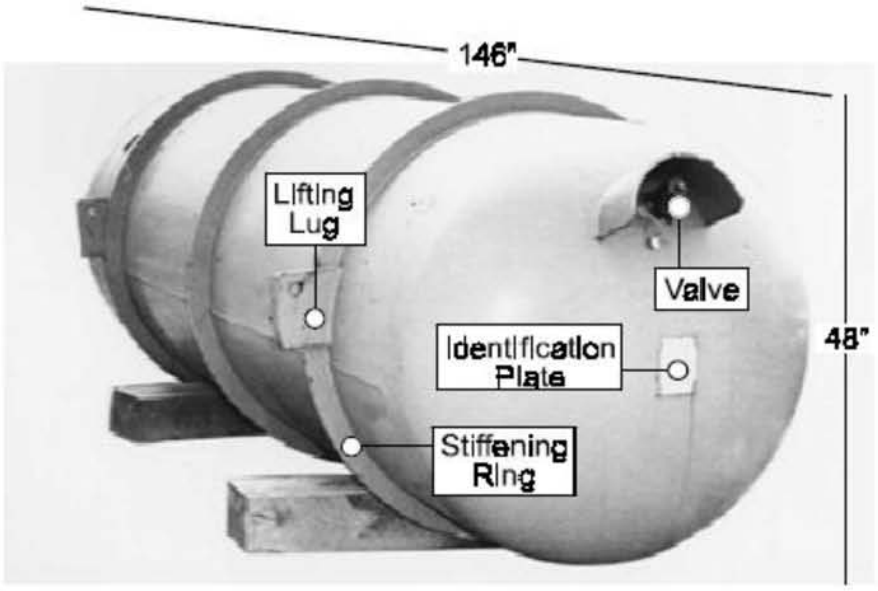

Figure 1-2, Typical Depleted Uranium Storage Cylinder (DOE, 1999)

Because storage began in the early 1950s, many of the drums and cylinders now show evidence of external corrosion and increased breach risk. When a DUF_6 container is breached, the contents react with moisture in air to form caustic hydrofluoric acid (HF) and solid uranyl fluoride (UO_2F_2). By 1998, breaches were identified in eight cylinders (two at Paducah, two at Portsmouth, and four at K-25), generally around spots previously damaged by handling activities. Similarly, a significant number of drums at the Savannah River Site have been placed into overpacks as a mitigating action for corrosion control and to prevent spills.

In an effort to reduce risks associated with container breach, Public Law 107-206, the 2002 Supplemental Appropriations Act for Further Recovery from and Response to Terrorist Attacks on the United States (commonly referred to as the "Terrorist Attack Response Act") requires DOE to design, construct, and operate facilities at Paducah and Portsmouth, for conversion of DUF_6 to the safer form, depleted triuranium octaoxide (U_3O_8). As part of this revised management strategy, all K-25 DUF_6 cylinders were shipped in 2004 to Portsmouth to be eventually converted to U_3O_8. The Terrorist Attack Response Act further required that the U_3O_8 be stored at Paducah and Portsmouth until there is a determination that all or a portion of the depleted uranium is no longer needed. At that point, the U_3O_8 is to be disposed of as low-level radioactive waste. DOE estimates the inventory of U_3O_8 that will eventually require disposal to be approximately 700,000 metric tons over a 20 to 25 year period (DOE, 2007).

Conversion to U_3O_8 is a preferential management strategy, because DUF_6 is a volatile, white, crystalline solid. Conversely, U_3O_8 is kinetically and thermodynamically stable and is the most common form of uranium found in nature. U_3O_8 can be produced in rotary kiln or fluidized-bed reactors by application of superheated steam and hydrogen (from dissociated ammonia) to DUF_6 (producing solid UO_2F_2 powder and gaseous HF). The powder UO_2F_2 is then defluorinated through heat and steam addition to create U_3O_8.

1.4 Basis for Performance Assessment

URCR R313-25-8 requires that a performance assessment be performed and approved by the Department of Environmental Quality prior to the disposal of significant quantities of depleted uranium. The required performance assessment must meet the provisions of section 2(a) of R313-25-8 that requires that the performance assessment:

> *"demonstrates that the performance standards specified in 10 CFR Part 61 and corresponding provisions of Utah rules will be met for the total quantities of concentrated depleted uranium and other wastes, including wastes already disposed of and the quantities of concentrated depleted uranium the facility now proposes to dispose. Any such performance assessment shall be revised as needed to reflect ongoing guidance and rulemaking from NRC. For purposes of this performance assessment, the compliance period shall be a minimum of 10,000 years. Additional simulations shall be performed for the period where peak dose occurs and the results shall be analyzed qualitatively."*

In performance of the required performance assessment, it is useful to consider the guidance the NRC has issued to assist applicants and licensees in applying these standards as they reflect years of experience with a variety of waste streams and disposal situations. NUREG-1573 is a key NRC guidance document for conducting performance assessments(NRC, 2000). More recent guidance is contained in NUREG-1854, (NRC, 2007).

In particular, there are four areas to consider in applying the performance standards. First is the compliance period. Second is the dose methodology. Third is the dose standard for the intruder. Fourth is site stability.

Section 2 (a) addresses the time period for compliance. It states:

> *"For purposes of this performance assessment, the compliance period shall be a minimum of 10,000 years. Additional simulations shall be performed for the period where peak dose occurs and the results shall be analyzed qualitatively."*

From a compliance period perspective, 10,000 years is the time period for a quantitative analysis and is consistent with Federal rules and guidance. Given the nature of depleted uranium, a qualitative analysis out to the peak dose period is also warranted to inform the performance assessment. Use of the 10,000 year time period for compliance is consistent with federal regulations (e.g., 40 CFR 191) and NRC guidance. Extending the analysis qualitatively until peak dose is also consistent with NUREG-1573 recommendations. The NRC has taken a similar approach with the NRC Decommissioning Criteria for the West Valley Demonstration Project at the West Valley Site (NRC, 2002). It is noteworthy that the only Federal standard that goes beyond 10,000 years for compliance is the standard for Yucca Mountain (NRC, 2002). That provision provides a two-level dose standard with a higher dose limit of 100 mrem after 10,000 years.

Consequently, for purposes of applying the performance standards for protection of the general public (URCR313-25-19) and for protection of individuals from inadvertent intrusion (URCR313-25-20), the Division should chosen to use the 10,000 year compliance period with a qualitative analysis to cover the period beyond to the peak dose.

The performance standard for protection of the general public (URCR313-25-19) is based on the 1959 standards of International Commission on Radiological Protection (ICRP) Publication 2 methodology. URCR313-15 rules are based on newer ICRP guidance in Publications 26 and 30. Part 20 uses the total effective dose equivalent (TEDE) rather than the whole body dose. NRC has recognized the inconsistency between the dose methodologies and has issued guidance to allow the use of newer guidance. This approach was taken for Yucca Mountain in 10 CFR Part 63, NUREGs -1854 and 1573, and in the NRC Decommissioning Criteria for West Valley. As noted in NUREG-1573:

> *"As a matter of policy, the Commission considers 0.25 mSv/year (25 mrem/year) TEDE as the appropriate dose limit to compare with the range of potential doses represented by the older limits that had whole-body dose limits of 0.25 mSv/year (25 mrem/year) (NRC, 1999, 64 FR 8644; see Footnote 1). Applicants do not need to consider organ doses individually because the*

low value of the TEDE should ensure that no organ dose will exceed 0.50 mSv/year (50 mrem/year)."

Consequently, the Division should use for purposes of applying the performance standards for protection of the general public (URCR313-25-19) the total effective dose equivalent rather than the whole body dose.

The performance standard for protection of individuals from inadvertent intrusion (URCR313-25-20) requires "*...protection of any individual inadvertently intruding into the disposal site and occupying the site or contacting the waste.*" However, these regulations are silent on the specific dose standard to apply. Since Part 61 has been issued, the standard used by NRC and others for low-level radioactive waste disposal licensing has been an intruder standard of 500 mrem/yr. The 500 mrem standard is also used in DOE's waste determinations implementing the Part 61 performance objectives (NUREG-1854). It is noted that 500 mrem/yr was also the standard proposed in Part 61 in 1981 (46 FR 38081, July 24, 1981). Additionally, the Statement of Considerations for the final rule did not object to the number. It was removed apparently at the request of EPA, because of its concern of how one would monitor it or demonstrate compliance with it, but not because EPA disagreed with it (47 FR57446, 57449, December 27, 1982). A dose standard of 500 mrem/yr is also used as part of the license termination rule dose standard for intruders (10 CFR 20.1403).

Consequently, DRC should use for purposes of applying the performance standard for protection of individuals from inadvertent intrusion (URCR313-25-20) a 500 mrem/yr threshold for the intruder dose.

The performance standard for stability requires the facility must be sited, designed, and closed to achieve long-term stability to eliminate to the extent practicable the need for ongoing active maintenance of the site following closure. The intent of this requirement is to provide reasonable assurance that long-term stability of the disposed waste and the disposal site will be achieved.

Prior to implementing Part 61, it had been a common practice at waste disposal facilities to randomly dump some waste. This practice jeopardized package integrity and did not permit access to voids between packages so that they could be properly backfilled. Consolidation of wastes would provide a less stable support which could contribute to failure of the disposal unit cover leading to increased precipitation infiltration and surface water intrusion.

To help achieve stability, NRC noted that to the extent practicable the waste should maintain gross physical properties and identity over 300 years, under the conditions of disposal. NRC believed that the use of design features to achieve stability was consistent with the concept of ALARA and the use of the best available technology. It was NRC's view that to the extent practicable, waste forms or containers should be designed to be stable (i.e., maintain gross physical properties and identity, over 300 years). NRC also noted that a site should be evaluated for at least a 500-year time frame to address the potential impacts of natural events or phenomena should also be applied.

About the same time as Part 61 was promulgated, NRC also put in place requirements for design of uranium mill tailings piles such as the Vitro site which is right next to the Clive site. In addressing

stability requirements for mill tailings, NRC recognized the need to set practicable standards. NRC specified that the design shall provide reasonable assurance of control of radiological hazards to be effective for 1,000 years, to the extent reasonably achievable, and, in any case, for at least 200 years.

In both cases (low-level radioactive waste and mill tailings disposal) NRC recognized the need to set practical standards that can be implemented. The design standards range from 200 up to 1,000 years. NRC recognized the design limitations and noted that reasonably achievable designs should be employed to the extent practicable. It is not practical to set design standards beyond 1,000 years.

Consequently, the Division should use for purposes of applying the performance standard for stability of the disposal site after closure (URCR313-25-22) an approach consistent with past standard setting practice.

Energy*Solutions* has demonstrated that its disposal site design and closure will provide reasonable assurance that long-term stability will be achieved and that the use of the best available technology in setting design standards in the range from 200 up to 1,000 years is appropriate to provide site stability to the extent practicable.

URCR Rule 313-25-8(2), as amended, requires Energy*Solutions* to demonstrate to the Division that proposed methods for disposal of depleted uranium will ensure that future operations, institutional control, and site closure can be conducted safely, and that the site will comply with the facility's performance objectives and the Division's regulatory requirements. Toward that end, Energy*Solutions* has conducted a detailed, site-specific, probabilistic performance assessment using GoldSim modeling software (GoldSim, 2011).

The GoldSim model, developed and managed by the GoldSim Technology Group, is a Monte Carlo simulation software solution for dynamically modeling complex systems in business, engineering and science. GoldSim supports decision and risk analysis by simulating future performance while quantitatively representing the uncertainty and risks inherent in all complex systems. GoldSim is a general purpose simulator that utilizes a hybrid of several simulation approaches, combining an extension of system dynamics with some aspects of discrete event simulation, and embedding the dynamic simulation engine within a Monte Carlo simulation framework. As part of a joint effort by NRC and DOE, the GoldSim model and the supporting sub-models have undergone extensive reviews concerning its use to demonstrate compliance with the individual protection standards (Pensado, et. al, 2002).

This Report demonstrates Energy*Solutions*' compliance with the URCR 313-25-8(2) and those other regulatory requirements affected by the proposed depleted uranium disposal.

2. REGULATORY COMPLIANCE AND PERFORMANCE OBJECTIVE SATISFACTION

As part of the renewal of its Radioactive Material License in 2008 (RML UT2300249), the Division certified that Energy*Solutions'* is in compliance with all applicable regulatory requirements (2008 RML renewal). As such, activities conducted at Energy*Solutions'* Clive site are designed to protect the health and safety of facility workers, the general public, and the environment. Energy*Solutions'* operations are conducted under the ongoing regulatory scrutiny of the Division, Utah Division of Solid and Hazardous Waste, Utah Division of Air Quality, and Utah Division of Water Quality. These inspectors provide continuing assurance that the interests of radiological and environmental safety are properly addressed.

Additionally, Energy*Solutions* continues to demonstrate that it is financially capable to carry out all licensed activities. Energy*Solutions* provides financial assurances sufficient to fund the safe closure of the facility, as well as the long-term monitoring and maintenance of the facility. Energy*Solutions* also provides information about the required qualifications of those persons who will operate the facility and about its existing training program.

For the majority of applicable regulatory requirements, disposal of depleted uranium does not impact the Division's prior certification of Energy*Solutions* compliance. However, as a result of a desire to dispose of depleted uranium and in compliance with URCR Rule 313-25-8(2), Energy*Solutions* has conducted a detailed, site-specific, probabilistic performance assessment to demonstrate to the Division that:

1) its proposed methods for disposal of depleted uranium will ensure that future operations, institutional control, and site closure will continue to be conducted safely,
2) the site will continue to comply with its performance objectives, and
3) it will continue to be in compliance with applicable Division requirements.

In addition to URCR R313-25-8(2), other regulatory requirements affected by the proposed depleted uranium disposal with which Energy*Solutions* must also demonstrate compliance are listed in Table 2-1 and addressed in further detail in this Section.

- Standards for Protection Against Radiation" - URCR R313-15
- Notices, Instructions and Reports to Workers by Licensees or Registrants" – URCR R313-18
- License Requirements of Land Disposal of Radioactive Waste" – URCR R313-25
- Ground Water Quality Protection Rules – R317-6
- Air Quality Protection Rules – R307

Table 2-1

Applicable Requirements Potentially Impacted by the Disposal of Depleted Uranium

URCR	REASON
R313-15-101	Radiation Protection Programs
R313-15-201	Occupational Dose Limits for Adults
R313-15-301	Dose Limits for Individual Members of the Public
R313-15-402	Radiological Criteria for Unrestricted Use
R313-15-601	Control of Access to High Radiation Areas
R313-15-801	Security and Control of Licensed or Registered Sources of Radiation
R313-15-902	Posting Requirements
R313-15-906	Procedures for Receiving and Opening Packages
R313-15-1002	Method for Obtaining Approval of Proposed Disposal Procedures
R313-15-1009	Waste Classification
R313-18-12	Instruction to Workers
R313-25-6(3)	General Information – Disposal Location and Expected Schedules
R313-25-7	Principal Design Features Potentially Impacted by the Disposal of Depleted Uranium (e.g., Waste Emplacement and Backfill, Land Disposal Facility Construction and Operation, and Classification and Specifications)
R313-25-8	Technical Analysis for the Protection of the General Population, Protection of Inadvertent Intruders, Protection during Normal and Abnormal Operations, and Demonstration of the Long-Term Disposal Site Stability.
R313-25-11	Requirements for Issuance of a License demonstrating no unreasonable risk to the General Public, Training and Qualification of Licensee Staff, Adequacy of Site to Protect the Public during operations and after closure, and the adequacy of financial resources to operate, close, and provide for appropriate institutional control of the facility.
R313-25-18	Licensee's facility shall be sited, designed, operated, closed, and controlled so that individual exposures are limited.
R313-25-19	Licensee's facility shall be sited, designed, operated, closed, and controlled so that general population exposures are limited.
R313-25-20	Licensee's facility shall be sited, designed, operated, closed, and controlled to limit exposures to individuals inadvertently intruding.
R313-25-21	Licensee's facility shall be sited, designed, and operated to limit exposures to individuals during operations.
R313-25-22	Licensee's facility shall be sited, designed, operated, closed, and controlled to achieve long-term stability of the site without ongoing active maintenance.
R313-25-23	Disposal Site Suitability Requirements for near-surface land disposal.
R313-25-24	Disposal site design requirements for near-surface land disposal.
R313-25-31	Licensee's assurance of financial capability to conduct necessary site closure and stabilization activities.
R313-25-32	Licensee's assurance of financial capability to conduct necessary institutional controls, following facility closure.

Table 2-1

Applicable Requirements Potentially Impacted by the Disposal of Depleted Uranium

URCR	REASON
R313-25-33	Specifies record keeping and reporting requirements of a person licensed for low-level radioactive waste disposal under URCR R313-25. As such, this is an issue for compliance monitoring rather than a criterion for granting a license amendment. However, the information and procedures provided in the 2008 LRA renewal and other submittals demonstrate that Energy*Solutions* intends to maintain information and records that are required by this regulation and that will be necessary to develop the required reports.
R313-25-34	Requires that Energy*Solutions* perform or allow the Executive Secretary to perform tests that the latter considers necessary. Tests may address any of (1) wastes, (2) facilities used for receipt, storage, treatment, handling or disposal of wastes, (3) radiation detection and monitoring instruments, and (4) other equipment and devices used in connection with the receipt, possession, handling, treatment, storage, or disposal of waste. As such, this is an issue for compliance monitoring rather than a criterion for initial licensing.
R313-25-35	Requires that Energy*Solutions* allow the Executive Secretary access to the disposal facility for facility and records inspections. As such, this is an issue for compliance monitoring rather than a criterion for granting a license amendment.
R313-R317-6	Groundwater protection limits

2.1 R313-15-101; Radiation Protection Programs

Requirement: Licensee shall develop, document, and implement a radiation protection program sufficient to ensure compliance, including operational procedures and engineering controls to achieve occupational doses and doses to members of the public that are as low as is reasonably achievable. Licensee's Radiation Protection Program shall constrain air emissions of radioactive material from operations to the environment, excluding radon-222 and its decay products, such that a member of the public likely to receive the highest dose will not be expected to receive a total dose equivalent in excess of 10 mrem per year from these emissions.

Compliance Basis: Energy*Solutions*' 2008 RML renewal references several plans and program descriptions that control operational activities that are carried on at the facility and which constitute the facility's Radiation Protection Program, including the Waste Characterization Plan, CQA/QC Manual, Radiation Safety Manual, ALARA Plan, Health and Safety Plan, Emergency Response and Contingency Plan, Site Radiological Security Plan, Environmental Monitoring Plan, and Quality Assurance Manual. Management and disposal practices documented therein do not require alteration to accommodate depleted uranium in a manner compliance with the R313-15-101 ALARA standards. Similarly, the 2008 RML renewal includes models demonstrating that atmospheric-pathway doses to the general public during operations will remain below regulatory required levels. Furthermore, Energy*Solutions*' Environmental Monitoring Program includes provisions to actively measure atmospheric radioactive contaminant concentrations at their Clive facility property boundary and to notify the Division in the event these concentrations approach levels of non-compliance.

2.2 R313-15-201; Occupational Dose Limits for Adults

Requirement: Licensee shall control the occupational dose to individual adults, except for planned special exposures, to the more limiting of a total effective dose equivalent of 5 rem or the sum of the deep dose equivalent and committed dose equivalent to any individual organ or tissue other than the eye of 50 rem. Furthermore, the Licensee shall control the occupational doses to the lens of the eye to 15 rem and skin to 50 rem of individual adults. Notwithstanding the annual dose limits, the Licensee shall limit the soluble uranium intake by an individual to 10 mg in a week in consideration of chemical toxicity.

Compliance Basis: Energy*Solutions*' 2008 RML renewal references several plans and program descriptions that control exposures from operational activities that are carried on at the facility, including the Radiation Safety Manual, ALARA Plan, Health and Safety Plan, Emergency Response and Contingency Plan, and Environmental Monitoring Plan. Management and disposal practices documented therein do not require alteration to accommodate depleted uranium in a manner compliance with the R313-15-201 occupational standards. As is documented therein, Energy*Solutions* regularly monitors and reports to the Division occupational exposures. Energy*Solutions*' Radiation Protection Program also includes provisions to notify the Division in the event these occupational exposures approach levels of non-compliance.

2.3 R313-15-301; Dose Limits for Individual Members of the Public

Requirement: Licensee shall conduct operations so that the annual total effective dose equivalent to individual members of the public during operations does not exceed 0.1 rem. Additionally, the dose in any unrestricted area from external sources does not exceed 2 mrem in any one hour.

Compliance Basis: Energy*Solutions*' 2008 RML renewal references several plans and program descriptions that control exposures to members of the public from operational activities that are carried on at the facility, including the Radiation Safety Manual, ALARA Plan, Health and Safety Plan, Emergency Response and Contingency Plan, Site Radiological Security Plan, and Environmental Monitoring Plan. Management and disposal practices documented therein do not require alteration to accommodate depleted uranium in a manner compliance with the R313-15-301 operational standards. As is documented therein, Energy*Solutions* regularly monitors and reports to the Division offsite contaminant concentrations and exposure levels. Energy*Solutions*' Radiation Protection Program also includes provisions to notify the Division in the event these occupational exposures approach levels of non-compliance.

2.4 R313-15-402; Radiological Criteria for Unrestricted Use

Requirement: By statute (R313-15-401), radiological criteria for unrestricted use apply to ancillary surface facilities that support radioactive waste disposal activities. As such, a site will be considered acceptable for unrestricted use if the residual radioactivity that is distinguishable from background radiation results in a total effective dose equivalent to an average member of the critical group that does not exceed 25 mrem per year, including no greater than 4 mrem committed effective dose equivalent or total effective dose equivalent to an average member of the critical group from groundwater sources, and the residual radioactivity has been reduced to levels that are as low as reasonably achievable (ALARA).

Compliance Basis: Chapter 6.4 of Appendix A and Energy*Solutions*' 2008 RML renewal references policies and procedures for decommissioning and releasing of ancillary surface facilities used in support of disposal operations, including the CQA/QC Manual, Radiation Safety Manual, ALARA Plan, Health and Safety Plan, and Quality Assurance Manual. Energy*Solutions* is currently storing drums containing depleted uranium from Savannah River Site's operations in a Depleted Uranium Storage Building built after the 2008 RML renewal. Prior to its construction, the Division reviewed and approved the Storage Building construction plans, use management, and eventual decommissioning and unrestricted release plans. No additional information is required to demonstrate compliance.

2.5 R313-15-601; Control of Access to High Radiation Areas

Requirement: The Licensee shall ensure that each entrance or access point to a high radiation area has 1) a control device that, upon entry into the area, causes the level of radiation to be reduced below that level at which an individual might receive a deep dose equivalent of 0.1 rem in one hour at 30 centimeters from the source of radiation or from any surface that the radiation penetrates; 2) a control device that energizes a conspicuous visible or audible alarm signal so that the individual entering the high radiation area and

the supervisor of the activity are made aware of the entry; or 3) entryways that are locked, except during periods when access to the areas is required, with positive control over each individual entry.

Compliance Basis: Energy*Solutions*' 2008 RML renewal references unrestricted and restricted area access protocols and protections contained in the Radiation Safety Manual, ALARA Plan, Health and Safety Plan, Emergency Response and Contingency Plan, and Site Radiological Security Plan. As was submitted to the Division prior to their approval of its construction, Energy*Solutions* continues to apply building access restriction controls to their Depleted Uranium Storage Building. No further information is necessary to demonstrate compliance.

2.6 R313-15-801; Security And Control Of Licensed Or Registered Sources Of Radiation

Requirement: The licensee shall secure licensed radioactive material from unauthorized removal or access.

Compliance Basis: Energy*Solutions*' 2008 RML renewal references security protocols and protections for radioactive materials in unrestricted and restricted area contained in their Radiation Safety Manual, Health and Safety Plan, Emergency Response and Contingency Plan, and Site Radiological Security Plan. As was submitted to the Division prior to their approval of its construction, Energy*Solutions* continues to apply material security and access controls to their Depleted Uranium Storage Building. No further information is necessary to demonstrate compliance.

2.7 R313-15-902; Posting Requirements

Requirement: The licensee shall post each radiation area with a conspicuous sign or signs bearing the radiation symbol and the words "CAUTION, RADIATION AREA."

Compliance Basis: Energy*Solutions*' 2008 RML renewal references radiation sign posting protocols and procedures for radioactive materials in unrestricted and restricted area contained in their Radiation Safety Manual. In compliance with these posting protocols and procedures, Energy*Solutions* has posted the required caution signs on its Depleted Uranium Storage Building. No further information is necessary to demonstrate compliance.

2.8 R313-15-906; Procedures for Receiving and Opening Packages

Requirement: The Licensee shall monitor the external surfaces of a labeled package for radioactive contamination, monitor the external surfaces of a labeled package for radiation levels, and monitor all packages known to contain radioactive material for radioactive contamination and radiation levels if there is evidence of degradation of package integrity, such as packages that are crushed, wet, or damaged.

Compliance Basis: Energy*Solutions*' 2008 RML renewal references waste receipt policies and procedures for radioactive materials received via rail and truck as contained in their Waste Characterization Plan, Radiation Safety Manual, ALARA Plan, and Health and Safety Plan. The Savannah River Site depleted

uranium drums currently in storage in Energy*Solutions'* Depleted Uranium Storage Building and any future depleted uranium packages will continue to be received and inspected according to these approved procedures.

2.9 R313-15-1002; Method for Obtaining Approval of Proposed Disposal Procedures

Requirement: The Licensee shall apply to the Executive Secretary for approval of proposed procedures to dispose of licensed or registered material.

Compliance Basis: Energy*Solutions*' 2008 RML renewal references waste disposal policies and procedures for radioactive materials contained in their CQA/QC Manual. Disposal of depleted uranium will be conducted according to these approved procedures. No further information is required to demonstrate compliance.

2.10 R313-15-1009; Waste Classification

Requirement: The Licensee shall only disposal of waste classified as "Class A", as defined by the procedures contained in this requirement. The definitions in this section are essentially identical to those in 10 CFR 61.55, with one exception: Utah adds Ra_{226} to the list of long-lived radionuclides in the regulations' Table I with a concentration limit of 100 nanoCuries per gam (nCi/g). Additionally, on April 13, 2010, the Utah Radiation Control Board approved a Depleted Uranium Performance Assessment Rule, R313-25-8, "Technical Analysis." The rule allows, subject to approval of the information contained in this Compliance Report, the Licensee to accept and disposal of depleted uranium as Class A waste.

Compliance Basis: URCR R313-15-1009 defines specific classifications (e.g., Class A, Class B, and Class C), based on a waste's source term. The Division has included Ra_{226} to the list of long-lived radionuclides in this regulations, with a concentration limit of 100 nCi/g (Utah, 2010). Since Ra_{226} is a decay product of uranium-238 (U_{238}), the principal component of depleted uranium, it is of direct relevance to the disposal of depleted uranium waste. Energy*Solutions*' Clive facility is licensed by the Division to dispose of Class A waste and has disposed of small quantities of depleted uranium waste under that license. However, as is presented in Table 2-2, the Savannah River Site wastes under consideration for disposal in this Compliance Report contain more than isotopes of uranium. In particular, the depleted uranium contains technetium-99 (Tc_{99}) and strontium-90 (Sr_{90}). Because of this, R313-15-1009 dictates that the determination of waste classification is driven not by the presence of uranium, but by the presence of radionuclides identified in the regulatory requirement. Based on the relative concentrations of isotopes other than uranium, the Savannah River Site wastes are Class A. Future shipments of other depleted uranium wastes that also contain isotopes other than uranium will be evaluated for waste classification purposes in accordance with the Radioactive Material License and Waste Characterization Plan, with wastes that are greater than Class A to be rejected for receipt.

Table 2-2

Savannah River Site Depleted Uranium Drum Waste Concentrations

Radionuclide	Mean Concentration (pCi/g)*	Standard Deviation (pCi/g)
Sr_{90}	47	75
Tc_{99}	23,800	11,000
$_{129}I$	19	9
$_{137}Cs$	12	4
$_{226}Ra$	317	110
$_{233}U$	5,290	480
$_{234}U$	33,100	2,170
$_{235}U$	2,970	750
$_{236}U$	4,910	1,170
$_{238}U$	272,000	6,640
$_{237}Np$	6	7
$_{238}Pu$	0.2	0.3
$_{239}Pu$	1	1
$_{240}Pu$	0.3	0.3
$_{241}Pu$	4	4
$_{241}Am$	14	5

* Radionuclide Concentrations in Savannah River Site drums in storage at Energy*Solutions* are generally normally distributed – See Appendix A, Chapter 9 for development methodology.

2.11 R313-18-12; Instruction to Workers

Requirement: All individuals who in the course of employment with the Licensee are likely to receive in a year an occupational dose in excess of 100 mrem a) shall be kept informed of the storage, transfer, or use of sources of radiation in the licensee's or registrant's workplace; b) shall be instructed in the health protection considerations associated with exposure to radiation or radioactive material to the individual and potential offspring, in precautions or procedures to minimize exposure, and in the purposes and functions of protective devices employed; c) shall be instructed in, and instructed to observe, to the extent within the worker's control, the applicable provisions of these rules and licenses for the protection of personnel from exposure to radiation or radioactive material; d) shall be instructed as to their responsibility to report promptly to the licensee or registrant a condition which may constitute, lead to, or cause a violation of the Act, these rules, or a condition of the licensee's license or unnecessary exposure to radiation or radioactive material; e) shall be instructed in the appropriate response to warnings made in the event of an unusual occurrence or malfunction that may involve exposure to radiation or radioactive material; and f) shall be advised as to the radiation exposure reports which workers shall be furnished.

Compliance Basis: Energy*Solutions*' 2008 RML renewal references employee training requirements for their plans and program descriptions that control operational activities that are carried on at the facility and which constitute the facility's Radiation Protection Program, including the Waste Characterization Plan, CQA/QC Manual, Radiation Safety Manual, ALARA Plan, Health and Safety Plan, Emergency Response and Contingency Plan, Site Radiological Security Plan, Environmental Monitoring Plan, and Quality Assurance Manual. Energy*Solutions*' Employee Training Program for management and disposal practices documented therein does not require alteration to accommodate depleted uranium.

2.12 R313-25-6(3); General Information - Expected Schedules

Requirement: The general information shall include the expected schedules for construction, receipt of waste, and first emplacement of waste at the existing land disposal facility.

Compliance Basis: As has been documented herein, Energy*Solutions* is currently in possession of depleted uranium from DOE's Savannah River Site, waiting a final disposal solution. It is Energy*Solutions*' target within 120 days of acceptance by the Division's Executive Secretary of the Performance Assessment (as documented herein), to apply for its Radioactive Material License be amended to include disposal of the depleted uranium wastes currently in storage at their Clive Facility. Within 120 days following successfully amending their Radioactive Material License, Energy*Solutions* intends to begin disposing of the Savannah River Site depleted uranium. Furthermore, subject to ongoing contract negotiations with DOE, Energy*Solutions* expects to receive and dispose of depleted uranium from the deconversion plants within one year of regulatory approval.

2.13 R313-25-7; Specific Technical Information - Principal Design Features: Descriptions, Design Criteria, Justification, and Codes

Requirement: The regulatory requirements of URCR R313-25-7(2) , -7(3) , -7(4) , and -7(5) form a system of requirements that apply to numerous principal design features at the existing low-level radioactive waste disposal facility and ensure that they will continue to perform adequately with the disposal of depleted uranium to achieve the performance objectives stated in URCR R313-25-18 through 26. The Licensee shall include the following information to determine whether or not they can continue to meet the performance objectives and the applicable technical requirements of URCR R313-25 in disposing of depleted uranium.

Descriptions of the design features of the land disposal facility and of the disposal units for near-surface disposal shall include those design features related to infiltration of water; integrity of covers for disposal units; structural stability of backfill, wastes, and covers; contact of wastes with standing water; disposal site drainage; disposal site closure and stabilization; elimination to the extent practicable of long-term disposal site maintenance; inadvertent intrusion; occupational exposures; disposal site monitoring; and adequacy of the size of the buffer zone for monitoring and potential mitigative measures. [URCR R313-25-7(2)] Descriptions of the principal design criteria and their relationship to the performance objectives. [URCR R313-25-7(3)] Descriptions of the natural events or phenomena on which the design is based and their relationship to the principal design criteria. [URCR R313-25-7(4)] Descriptions of codes and standards which Energy*Solutions* has applied to the design, and will apply to construction of the land disposal facilities. [URCR R313-25-7(5)]

Compliance Basis: Energy*Solutions* recognizes that the safe storage and disposal of depleted uranium waste is essential for mitigating releases of radioactive materials and reducing exposures to humans and the environment. Energy*Solutions*' Clive Facility design features are described in detail in the 2008 RML renewal. In its acceptance of Energy*Solutions'* 2008 RML renewal, the Division has determined that the principal design features identified perform the required functions (meaning that at least one required function is performed by each principal design feature). The principal design features potentially impacted by the intended disposal of depleted uranium, and for which satisfactory functional performance must herein be addressed are Waste Placement and Backfill, Land Disposal Facility Construction and Operation, and Classification and Specifications.

As they are potentially impacted by the intended disposal of depleted uranium, Waste Placement and Backfill, Land Disposal Facility Construction and Operation, and Classification and Specifications are described below, their design criteria identified, justification that they will perform as required is presented, and the codes and standards applicable are summarized. In review of the principal design features, the required functions that the principal design features must perform, as identified in URCR R313-25-7(2), include:

- Minimize infiltration of water.
- Ensure integrity of covers for disposal units.
- Ensure structural stability of backfill, wastes, and covers.
- Minimize contact of wastes with standing water.

- Provide disposal site drainage.
- Ensure disposal site closure and stabilization.
- Eliminate to the extent practicable long-term disposal site maintenance.
- Protect against inadvertent intrusion
- Limit occupational exposures.
- Provide for disposal site monitoring.
- Provide a buffer zone for monitoring and potential mitigative measures.

Waste Emplacement and Backfill - Description of Design Feature

Requirement: Descriptions of the design features of the land disposal facility and of the disposal units for near-surface disposal of depleted uranium shall include those design features related to infiltration of water; integrity of covers for disposal units; structural stability of backfill, wastes, and covers; contact of wastes with standing water; disposal site drainage; disposal site closure and stabilization; elimination to the extent practicable of long-term disposal site maintenance; inadvertent intrusion; occupational exposures; disposal site monitoring; and adequacy of the size of the buffer zone for monitoring and potential mitigative measures. [URCR R313-25-7(2)]

Compliance Basis: Energy*Solutions* proposes to dispose of depleted uranium in the western fraction of the Federal Cell. The eastern section is occupied by the 11e.(2) cell, which is dedicated to the disposal of uranium processing by-product waste, and which is not considered in the analysis. The general design aspect is that of a hipped cover, with relatively steep sloping sides nearer the edges. The upper part of the embankment has a more moderate slope than the sides. Only the top slope region is modeled in Appendix A, since no depleted uranium will be placed beneath the embankment's side slopes.

The 2008 LRA renewal addresses the pertinent characteristics of the principal design features for general waste placement and backfill including the waste types to be disposed in the existing embankments. Waste included in this analysis may take a variety of physical forms, including soil or soil-like material, compressible debris, incompressible debris, oversized debris, containerized Class A LLRW, and depleted uranium. Liquid waste may not be disposed in the embankments. Revisions to the waste placement management program for placement of depleted uranium are addressed in Chapters 4 and 6 of Appendix A and will be conducted in accordance with the CQA/QC Manual. As with other wastes, depleted uranium will be are disposed at Energy*Solutions*' Disposal Embankments in accordance with the provisions of the CQA/QC Manual. However, depleted uranium placement is expected to be subject to controls and license conditions.

With downward contaminant transport pathways influencing groundwater concentrations, and upward contaminant transport pathways influencing dose and uranium hazard, a balance is achieved in the placement of different kinds of waste. The Performance Assessment examined three different options for configuration of the depleted uranium waste within the embankment. The volume within the embankment that is available for waste disposal is 44.3 ft deep below the engineered cover. No depleted uranium waste is modeled beneath the embankment's side slopes in the Performance Assessment.

1. 3m Model
   Clean Fill from cover to 9.9 ft
   GDP contaminated waste from 9.9 ft to 11.6 ft
   SRS waste from 11.6 ft to 13.23 ft
   GDP uncontaminated waste from 13.23 ft to 44.65 ft

2. 5m Model
   Clean Fill from cover to 16.54 ft
   GDP contaminated waste from 16.54 ft to 18.19 ft
   SRS waste from 18.19 ft to 19.84 ft
   GDP uncontaminated waste from 19.84 ft to 44.65 ft

3. 10m Model
   Clean Fill from cover to 33.07 ft
   GDP contaminated waste from 33.07 ft to 34.72 ft
   SRS waste from 34.72 ft to 36.38 ft
   GDP uncontaminated waste from 36.38 ft to 44.65 ft

These options cover a fairly wide range of possible disposal options, from disposal below grade only to disposal throughout most of the system, exploring the range of possible options for disposal of depleted uranium waste.

The design of the facility enables isolation of each embankment after it has been filled and covered. Thus, once the embankment is closed, it will not be disturbed by continuing operations at the site. The final embankment cover integrates long-term water and erosion control methods into the overall design, thus eliminating the need for active maintenance of a closed embankment. Compliance with this requirement has therefore been sufficiently demonstrated.

Waste Emplacement and Backfill - Principal Design Criteria

Requirement: Descriptions of the principal design criteria and their relationship to the performance objectives. [URCR R313-25-7(3)]

Compliance Basis: The principal design criteria pertinent to the design of the depleted uranium waste placement and backfill are justified in Chapter 4 of Appendix A. A key design criterion is the limitation of allowable distortion in the cover to less than 0.02 ft/ft. That is, the depleted uranium waste placement and backfill must not result in a magnitude of differential settlement within the Disposal Embankment that would contribute to a distortion that exceeds 0.02 ft/ft in the cover. Practically, this means that cover system settlement is acceptable so long as it is less than 1 foot of vertical displacement in less than any 50-foot horizontal distance. Based on the foregoing summary of information contained in the 2008 RML renewal and the fact that waste placement procedures will not change, this report documents Compliance

by Energy*Solutions* with the requirements of URCR R313-25-7(3)) as they pertain to the disposal of depleted uranium in the disposal embankments.

Waste Emplacement and Backfill - Design Basis Conditions and Design Criteria Justification

Requirement: Descriptions of the natural events or phenomena on which the design is based and their relationship to the principal design criteria. [URCR R313-25-7(4)]

Compliance Basis: In development of the projected performance of the depleted uranium waste placement and backfill as presented and justified in Appendix A, Energy*Solutions* utilized applicable guidance issued by the NRC, including those described in SECY-08-0147, NRC NUREG-1199 and NUREG-1200, pertaining to normal, abnormal, and accident (where applicable) conditions that should be considered during design of NRC-licensed low-level radioactive waste disposal facilities. Chapter 4 of Appendix A summarizes the conditions considered in the design of the depleted uranium waste placement and backfill principal design feature and the relationship between the normal, and abnormal, and accident (as applicable) conditions evaluated to the principal design criteria.

Factors of safety associated with all of the normal and abnormal conditions evaluated represent the design criteria distortion of 0.02 ft/ft divided by the calculated distortions. Overall, the average safety factor associated with the three normal conditions and the average safety factor associated with the five abnormal conditions were ascertained. The safety factor is greater than or equal to 1.00 under abnormal conditions.

Based on the foregoing summary of information, this Report demonstrates Energy*Solutions*' compliance with requirements of URCR R313-25-7(4), as they pertain to the depleted uranium waste emplacement and backfill of the disposal embankment.

Waste Emplacement and Backfill - Applicable Codes and Standards

Requirement: Descriptions of codes and standards which Energy*Solutions* has applied to the design, and will apply to construction of the land disposal facilities. [URCR R313-25-7(5)]

Compliance Basis: The 2008 RML renewal provides a summary of the codes, standards, and guidelines that Energy*Solutions* considered and applied to the design. The primary standards considered by Energy*Solutions* in the design of the depleted uranium waste placement and backfill are those codified in URCR R313-25-24 and R313-25-25. Energy*Solutions* has also incorporated by reference minimum design criteria safety factors of 1.5 for static conditions and 1.2 for dynamic conditions from Utah Statutes and Administrative Rules for Dam Safety, Rule R625-11-6.

The CQA/QC Manual provides specifications for constructing the Class A Disposal Embankments (including sections associated with the disposal of depleted uranium). The CQA/QC Manual also includes QC and QA procedures to be used during its construction.

Based on the foregoing summary of information, this Report demonstrates Energy*Solutions*' compliance with requirements of URCR R313-25-7(5), as they pertain to the waste emplacement and backfill of the disposal embankment.

Land Disposal Facility Construction and Operation

Requirement: The Licensee shall provide certain technical information. The following information is needed to determine whether or not Energy*Solutions* can meet the performance objectives and the applicable technical requirements of URCR R313-25: Descriptions of the construction and operation of the land disposal facility. The description shall include as a minimum the methods of construction of disposal units; waste emplacement; the procedures for and areas of waste segregation; types of intruder barriers; onsite traffic and drainage systems; survey control program; methods and areas of waste storage; and methods to control surface water and ground water access to the wastes. The description shall also include a description of the methods to be employed in the handling and disposal of wastes containing chelating agents or other non-radiological substances which might affect meeting the performance objectives of URCR R313-25. [URCR R313-25-7(6)]

Compliance Basis: This Report demonstrates Compliance with the requirements of URCR R313-25-7(6) have been met. Energy*Solutions*' methods for constructing and operating the depleted uranium disposal embankment are those already approved as part of the 2008 RML renewal. Construction of the disposal unit will involve a continuous cut, backfill, and cover construction. To ensure that the depleted uranium disposal embankment is built to design requirements, construction activities will be performed under a QA/QC program and conform to the requirements of the CQA/QC Manual. The primary activities involved in construction of the disposal embankment (as target location for depleted uranium) include:

- Excavation.
- Preparation of the disposal area Foundation
- Construction of liner.
- Construction of run-on and runoff protection.
- Waste emplacement and backfill
- Construction of Temporary Cover over completed portions of disposal embankments
- Settlement monitoring to determine compliance with waste compaction / stability requirements. May include surcharging efforts to ensure embankment is stable for final cover,
- Construction of Final Cover, as per CQA/QC Manual requirements, and
- Construction of permanent drainage ditches surrounding the disposal unit(s).

Of particular interest is the placement of depleted uranium waste. Depleted uranium procedures for waste emplacement are the same as those already described in the 2008 RML renewal. After the Liner has been constructed over a specific area of the disposal embankment, at least 12 inches of debris-free soil will be placed on top of the liner; followed by another 12-inches of waste as a protection to the integrity of the liner. Both of these layers of protective soil will be compacted with rubber tired equipment.

The protection of inadvertent intruders from radiation exposures during facility operations focuses on prevention of inadvertent intrusion. Depleted uranium operational areas will be surrounded by fencing as described in Energy*Solutions*' CQA/QC Manual. Additional security features are presented in the Energy*Solutions'* Site Radiological Security Plan. Several features of the facility design have the effect of protecting an inadvertent intruder from exposure to the disposed depleted uranium materials and the effects of radiation. These features include:

- Lack of nearby residential population
- Embankment cover system

Onsite earth-roadways are continuously changing to meet the demands of current disposal needs. As the height of an active disposal cell increases, as the activity in a portion of the embankment decreases, or as the activity for a new portion of the embankment increases, access roads are constructed or removed to facilitate safe hauling and disposal of materials. Roadways are constructed to ensure that water properly drains off from them, thus minimizing ponding or ponded road conditions. Haul roads to disposal units generally are sloped at no greater than 3:1 in accordance with safety guidelines.

Energy*Solutions* describes the onsite drainage systems in the 2008 RML renewal. Energy*Solutions* has developed a berm system to direct water flow from precipitation, winter runoff, away from the site and stored materials. It also has developed an embankment drainage system surrounding each embankment to help minimize any water accumulation. The drainage systems are constructed of an erosion barrier rock of the same type used to cover the embankments. The design of the berms is sufficient to withstand the Probable Maximum Flood (PMF) without overtopping. The ditches will have triangular cross sections with side slopes of 1:5, and will have gentle longitudinal slopes, with depths great enough to carry the runoff from the 100-year, 1-hour storm event without exceeding their bounds.

Surveys at the disposal site will be tied to both the United States Geological Survey (USGS) survey of Section 32 T1S, R11E and to the state plane coordinate system. Energy*Solutions* performs an annual as-built survey of each embankment which is accomplished by a Utah licensed land surveyor. Survey control is the responsibility of the licensed land surveyor, in accordance with Utah licensing standards.

Energy*Solutions'* plans for controlling the access of surface water to the depleted uranium wastes are those already authorized as part of the 2008 RML renewal. The vertical minimum separation between the bottom of the disposed depleted uranium and the historic high water table is determined as being 13 feet. This value is based on: 1) the groundwater contour map, and 2) the minimum depth from the base of the liner to the groundwater below the liner for the disposal embankment over the past five years is approximately 13 feet.

Based on the information summarized above, this Report documents Energy*Solutions*' regulatory compliance in its methods for emplacing the depleted uranium waste in the disposal embankment.

Classification and Specifications

Requirement: The application shall include certain technical information. The following information is needed to determine whether or not Energy*Solutions* can meet the performance objectives and the applicable technical requirements of URCR R313-25: Descriptions of the kind, amount, classification and specifications of the radioactive material expected to be received, possessed, and disposed of at the land disposal facility. [URCR R313- 25-7(9)]

Compliance Basis: The information contained in Chapter 9 of Appendix A demonstrate that the requirements of URCR R313-25-7(9) have been met. Appendix A also describes the types and volumes of depleted uranium waste to be received for disposal, including the physical, chemical, and radiological properties of the waste. All depleted uranium waste accepted for disposal will be at or below the Class A concentration limits. Radionuclide release characteristics of the depleted uranium waste may vary, but the radionuclide release rates in the performance assessment are modeled in a conservative manner that does not take credit for package or improved waste forms.

In summary, the waste information presented are sufficiently complete and detailed to support the necessary calculations and analyses to show that the facility will meet the depleted uranium performance objectives and the applicable technical requirements of URCR R313-25.

2.14 R313-25-8; Technical Analysis

General Population Protection

Requirement: The Licensee's specific technical information shall include the following analyses needed to demonstrate that the performance objectives of URCR R313-25 will be met: Analyses demonstrating that the general population will be protected from releases of radioactivity shall consider the pathways of air, soil, ground water, surface water, plant uptake, and exhumation by burrowing animals. The analyses shall clearly identify and differentiate between the roles performed by the natural disposal site characteristics and design features in isolating and segregating the wastes. The analyses shall clearly demonstrate a reasonable assurance that the exposures to humans from the release of radioactivity will not exceed the limits set forth in URCR R313-25-19 [URCR R313-25-8(1)].

Compliance Basis: The information contained in Appendix A and other relevant documents Energy*Solutions* has submitted indicate that the requirements of R313-25-8(1) have been met. Each of the major media pathways of this requirement is addressed in the following paragraphs. The principal sources of information for the exposure assessment are Sections 4, 6, and 9 of Appendix A. Original evaluations contained in Energy*Solutions*' 2008 RML renewal demonstrate continued compliance for exposures from normal operating conditions and accident scenarios.

Air Pathway

Analysis conducted in support of the 2008 RML renewal demonstrated that the transport of dust to the site boundary during operations (affected mainly by the natural site characteristics, including wind speed, wind direction, and atmospheric stability conditions) is well below regulatory limits. Similarly, the Performance Assessment documented in Chapters 4, 6, and 9 of Appendix A projects potential releases of depleted uranium through the air pathway have been assessed for the facility far below regulatory limits. As stated in the 2008 RML renewal, Energy*Solutions*' engineering and operational controls prevent the resuspension and dispersion of particulate depleted uranium during operations. DOE is required to ship their depleted uranium in containers. Depleted uranium will not be dumped in bulk, but rather disposed in its shipping container, in CLSM. Water spray is used in the cells as need to prevent resuspension of radioactivity.

Haul roads are also wetted and maintained to prevent the resuspension and dispersion of particulate depleted uranium. Polymers are spread on inactive, open areas to bind the surface and prevent resuspension. Energy*Solutions* also performs routine air monitoring to identify if an airborne situation is developing that may require corrective actions.

After final placement of the depleted uranium waste and closure of the disposal embankment, the facility design prevents any further migration of radioactivity through the air pathway because all waste will be beneath a thick earthen cover. Analysis presented in Chapter 6 of Appendix A demonstrates that the maximum dose to a member of the public following site closure and institutional control is far below applicable regulatory limits.

During operations, radon releases are projected to be negligible because of low Ra_{226} parent waste concentrations and the cover design includes a clay radon barrier designed to limit the surface radon flux to less than 20 pCi/m^2-s, resulting in potential radon exposures well within limits. The design is based on the disposal of uranium mill tailings, which are initially higher in Ra_{226} than the depleted uranium (which require time periods exceeding the 10,000-year regulatory limit to in-grow due to uranium chain decay).

For accident conditions, depleted uranium dust or particulate matter could be released to the atmosphere and inhaled by individuals. The 2008 RML renewal and the analysis documented in Chapter 6 of Appendix A evaluate tornado and severe winds, train derailment, truck turnover or collision, and truck fire. All analyses show that the maximum dose to a member of the public is less than 25 mrem/yr, even if the individual is continually present at the disposal site boundary.

Soil Pathway

As summarized in Chapter 6 of Appendix A, the soil pathway involves the exposure of the public to contaminated depleted uranium from the facility. If an exposure occurred, doses could result from external radiation or ingestion of soil on dirty hands. The primary site characteristic that prevents the likelihood of such exposures during operations and institutional control is the site's remote location (the

low population density in the site vicinity, and the lack of natural resources to provide for population expansion). Therefore, this pathway was not considered.

The design of the disposal embankment also contributes to minimizing exposures to contaminated soil by members of the public. After closure of the embankment, all depleted uranium waste will be covered in the disposal cells. The cover system contains a surface layer of riprap to protect against erosion and human intrusion. Beneath the riprap, the cover system contains a drainage layer and a clay radon barrier.

During operation, the facility will be monitored as described in the 2008 RML renewal and Environmental Monitoring Program, to ensure that no releases or doses have occurred via the soil pathway.

Groundwater Pathway

As is described in Chapters 4 and 6 of Appendix A, the groundwater pathway is assessed using EPA's Hydrologic Evaluation of Landfill Performance (HELP) model and GoldSim. The primary site characteristics that prevent public exposures via the groundwater pathway are the very poor groundwater quality at the site, the low population density, and the relatively slow groundwater flow velocities. The groundwater is not potable because of its very high concentration of dissolved salts. This characteristic alone prevents any appreciable consumption of the water by humans or livestock. The horizontal groundwater flow velocity is approximately 0.5 meters per year, resulting in groundwater travel times of approximately 60 years from the toe of the side slope region of the embankment to the compliance well.

Several embankment design features provide additional protection of the public from exposure to depleted uranium via the groundwater pathway. The cover system to be placed over the disposal waste allows very little water to flow into the disposed waste. This limits the contamination of the groundwater by minimizing the contact of water with the depleted uranium waste. Another design feature of the disposal embankment is the bottom clay liner below the disposed depleted uranium waste. The clay absorbs many of the radionuclides and slows their potential release from the cell and subsequent transport to the water table aquifer.

The infiltration model for the embankment cover uses calculations with EPA's Hydrologic Evaluation of Landfill Performance (HELP) model (Schroeder et al., 1994) as a guide to defining the vertical and lateral flow rates in the individual layers of the cover, as a function of time. Additionally, annual water balances for the disposal embankment have been computed with the HELP model. By using HELP as input to GoldSim, Energy*Solutions* demonstrates that the infiltration and radionuclide transport models show that any depleted uranium waste disposed will satisfy all of the groundwater protection criteria, provided that the concentrations of Tc_{99} are limited to the concentrations used in the transport modeling. All other radionuclide concentrations are limited only by what is necessary for the waste to qualify as Class A. This groundwater modeling provides a conservative estimate for the groundwater exposure scenario.

Radionuclide transport was modeled with the GoldSim model assuming a 4 mrem/year groundwater protection level. The model calculated the release and transport of depleted uranium radionuclides from the waste cell, through the unsaturated zone, and horizontally through the shallow unconfined aquifer to a compliance-monitoring well located 90 feet from the edge of the disposal facility. The groundwater modeling included many conservative assumptions that helped to ensure that the radionuclide concentrations at the compliance monitoring well were not underestimated. For example, the distance from the bottom of the waste to the aquifer was decreased from its actual value by 1.3 feet to conservatively account for the effects of the capillary fringe at the water table and to account for variations in the water table level. No delay factors for waste container life were used to delay the onset of radionuclide releases from depleted uranium waste under side slopes. The transport modeling shows that, for most depleted uranium radionuclides at the Class A limits, groundwater protection levels are met for 500 years after disposal of the waste. Groundwater protection levels are met for all radionuclides present in the depleted uranium wastes.

Surface Water Pathway

Due mainly to the natural site characteristics, there are no radioactive releases expected through the surface water pathway from non-intruder scenarios. The annual precipitation is low and the evaporation is high. No permanent surface water bodies exist in the site vicinity. In addition, the site is far from populated areas. The disposal embankment design features also minimize the potential for releases by the surface water pathway. Embankment design includes drainage ditches around the waste disposal areas. After precipitation events, these ditches divert runoff from the disposal cell cover to areas away from the disposal cells.

Vegetation

Vegetation models developed for the depleted uranium disposal evaluate the redistribution of soils, and contaminants within the soil, by native flora and fauna. The biotic models are consistent with observed flora and fauna on and near the Clive facility, with flora and fauna characteristic of Great Basin alkali flat and Great Basin desert shrub communities.

The Compliance Report evaluates the effects of vegetation on the cover system. Vegetation had two primary effects on the cover system: increasing the hydraulic conductivity of the cover material and root clogging of the lateral drainage layers. During operation of the embankment, releases and doses through the plant pathway are limited by the design, operation, and maintenance of the facility. Plants on the site will be removed and prevented from contacting waste materials. After final placement of the cover, releases and doses from the plant pathway are limited by the site's natural characteristics, which include low rainfall, thin plant cover, and the presence of plants that are highly efficient at removing water from the soil and transpiring the moisture back to the atmosphere.

The plant uptake pathway is not a viable exposure pathway at the embankment because of natural site characteristics and design features of the embankment. Exposure by the plant uptake pathway could occur by (1) the production of food crops in contaminated soil at the site, and (2) root intrusion into the waste by native plants that are subsequently consumed by humans or animals. The natural site's characteristics help prevent exposures via the plant uptake pathway because there is insufficient water at the site for the production of food crops. In addition, saline soils present at the site limit the number and type of plant species that can tolerate such conditions. Additionally, there are few deep-rooted native plants in the site vicinity.

Design features of the facility also help limit exposures via the plant uptake pathway. A thick earthen cover will be placed over the disposal cells to make the waste less accessible to plant roots after closure of the facility. After closure, some limited plant species may set roots in the overlying Sacrificial Soil which possesses a higher moisture storage capacity. The overall scarcity of deep-rooted plant species in the site vicinity and the configuration of the earthen cover will offer an inhospitable environment for extension of these types of roots into the waste.

Burrowing Animals Pathway

In the arid environment of the Clive Facility, ants fill a broad ecological niche as predators, scavengers, trophobionts and granivores. However, it is their role as burrowers that is modeled. Ants burrow for a variety of reasons but mostly for the procurement of shelter, the rearing of young and the storage of foodstuffs. How and where ant nests are constructed plays a role in quantifying the amount and rate of subsurface soil transport to the ground surface at the Clive site. Factors relating to the physical construction of the nests, including the size, shape, and depth of the nest, are key to quantifying excavation volumes. Factors limiting the abundance and distribution of ant nests such as the abundance and distribution of plant species, and intra-specific or inter-specific competitors, also can affect excavated soil volumes. Parameters related to ant burrowing activities include nest area, nest depth, rate of new nest additions, excavation volume, excavation rates, colony density, and colony lifespan. The GoldSim model evaluates the impact of ant burrowing on the transport of contaminant using the following three steps:

1. Identification of which ant species overwhelmingly contribute to the rearrangement of soils near the surface at Clive.
2. Calculation of soil and contaminant excavated volume using maximum depth, nest area, nest volume, colony density, colony life span, and turnover rate for predominant ant species.
3. Calculation of burrow density as a function of depth to determine the distribution of contaminants within the vertical soil profile for each predominant ant species.

Other than ants, burrowing animals are not considered a viable exposure pathway, given the combination of site characteristics and design features. Burrowing animals at the site include jackrabbits, mice, foxes, and ants. The first deterrent to burrowing animals is the rip-rap erosion barrier. While this may be only partially effective in deterring animals, the primary protective barrier is the clay radon barrier. The burrowing species at the site are not known to dig to such a depth that their burrows could penetrate through the entire cover and into the waste. During operation of the facility, releases and doses from the burrowing animal pathway will be prevented by the design, operation, and maintenance of the facility.

Burrowing animals will be prevented from contacting the waste materials. After final placement of the cover, the design features of the facility, primarily the thick soil cover that isolates the waste from burrowing animals, will control releases and doses. Because of this, the likelihood of any animals burrowing through the entire cover and exhuming waste materials is sufficiently low that it was not included in the safety assessment calculations. As such, the burrowing animal pathway is not expected to result in any exposures to humans.

Doses to the Public

Chapter 6 of Appendix A shows that doses to members of the public will be within established regulatory limits. The groundwater pathway is not viable because of the high salinity and general poor quality of the groundwater; however, it was evaluated via the groundwater modeling and found to be less than 4 mrem/yr.

Protection of Inadvertent Intruders

Requirement: The specific technical information shall also include the following analyses needed to demonstrate that the performance objectives of URCR R313-25 will be met: Analyses of the protection of inadvertent intruders shall demonstrate a reasonable assurance that the depleted uranium waste classification and segregation requirements will be met and that adequate barriers to inadvertent intrusion will be provided. [URCR R313-25-8(2)]

Compliance Basis: Analyses of radiation exposure doses to inadvertent intruders were assessed by Energy*Solutions'* GoldSim model. Based upon current and reasonably anticipated future land uses, two future use exposure scenarios were identified: ranching and recreation. After institutional controls are no longer maintained, it is expected that exposures to contamination in the ranching and recreation scenarios could occur on the Clive facility site. The primary exposure routes for the ranching and recreation scenarios include ingestion, inhalation, and external irradiation. Chapter 6 of Appendix A discusses the design performance objectives of the facility to protect inadvertent intruders from exposure. As is demonstrated, the radiation dose to an inadvertent intruder is not expected to exceed radiation limits. Several design features provide the required protection. Overall features include:

- Lack of nearby residential population
- Embankment cover system
- Waste Form

Operations specific features include:

- Fences
- Buffer zone
- Security plan
- Post-Closure specific features include:
- Granite markers

Exposure Assessment

Requirement: The specific technical information shall also include the following analyses needed to demonstrate that the performance objectives of URCR R313-25 will be met: Assessments of expected exposures due to routine operations and likely accidents during handling, storage and disposal of depleted uranium waste. The analysis shall provide reasonable assurance that exposures will be controlled to meet the requirements of URCR R313-15. [URCR R313-25-8(3)]

Compliance Basis: The information contained Chapters 4 and 6 of Appendix A indicate that the requirements of URCR R313-25-8(3) have been met. The Radiation Protection Program that is required by URCR R313-15-101(1) outlines the facility's radiation protection program. Energy*Solutions*' Safety and Health Manual," describes site safety, incident reporting, emergency response, equipment operation, personal protective equipment, respiratory protection, medical surveillance, exposure monitoring, hazard communication, confined space entry, and other safety related programs. Included therein are descriptions of Energy*Solutions'* ALARA program, including dose goals that are significantly below the regulatory dose criteria for workers.

Long-Term Stability of Disposal Site

Requirement: The specific technical information shall also include the following analyses needed to demonstrate that the performance objectives of URCR R313-25 will be met: Analyses of the long-term stability of the disposal site shall be based upon analyses of active natural processes including erosion, mass wasting, slope failure, settlement of wastes and backfill, infiltration through covers over disposal areas and adjacent soils, and surface drainage of the disposal site. The analyses shall provide reasonable assurance that there will not be a need for ongoing active maintenance of the disposal site following closure. [URCR R313-25- 8(4)]

Compliance Basis: The description and justification of the principal design features of the facility are provided in Section 3.0 of the 2008 RML renewal. These principal design features have been designed to perform their required functions over the period of hundreds of years such that the facility will not require ongoing active maintenance following facility closure. Further discussion of these features is presented under URCR R313-25-7(2) through URCR R313-25-7(5) in sections dealing with the waste placement and backfill. Design features other than those discussed in this Compliance Report do not require alteration to accommodate the disposal of depleted uranium.

Geologic-Time Stability of Disposal Site

Requirement: The specific technical information shall also include the following analyses needed to demonstrate that the performance objectives of URCR R313-25 will be met: Analyses of the geologic-time stability of the disposal site shall be based upon qualitative analyses of active natural processes including submersion, erosion, mass wasting, infiltration through covers over disposal areas and adjacent soils, and surface drainage of the disposal site. The analyses shall provide reasonable assurance that there

will not be a need for critical design features to address geologic-time depleted uranium waste dispersal. [URCR R313-25- 8(5)]

Compliance Basis: While included in this Compliance Report as part of improving qualitative understanding of facility performance, Energy*Solutions* agrees with NRC cautions and recognizes that regulatory compliance should include limited, "consideration given to the issue of evaluating site conditions that may arise from changes in climate or the influences of human behavior should be limited so as to avoid unnecessary speculation"(NRC, 2000). Furthermore, "[t]hese events are envisaged as broadly disrupting the disposal site region to the extent that the human population would leave affected areas as the ice sheet or shoreline advances. Accordingly, an appropriate assumption under these conditions would be that no individual is living close enough to the facility to receive a meaningful dose." (NRC, 2000).

As such, geologic-time trends are examined in this Compliance Report, by exploring simulations until the time of peak radioactivity. For this Compliance Report, peak radioactivity associated with radon production from depleted uranium, occurs at about 2.1 million years (My). The time frame of this component requires consideration of climatic changes that have occurred historically on approximately 100 thousand years (ky) cycles for more than 1 My. These cycles include periods of extensive glaciation and inter-glacial periods.

The planet is currently in an inter-glacial period. In effect, the 10 ky model is projected under inter-glacial conditions, and the deep time model includes an evaluation of the effect on depleted uranium disposal of future 100-ky glacial cycles for the next 2.1 My. Analysis conducted in support of this Compliance Report qualitatively assesses the potential impact of glacial epoch pluvial lake events on the overall depleted uranium waste embankment from 10 ky through 2.1 My post-closure. A pluvial lake is a consequence of periods of extensive glaciation, and results from low evaporation, increased cloud cover, increased albedo, and increased precipitation in landlocked areas.

The Clive Facility's principal design features have been designed to perform their required functions over the period of hundreds of years, qualitative trends in depleted uranium transport away from the facility during geologic-time frames have also been evaluated (see Chapters 6 and 9 of Appendix A). In conjunction with this design feature, it is important to note that scenarios included in this Compliance Report demonstrate that waste placed below ground surface escape the effects of pluvial lake erosion. As such, it is concluded that the facility will not require further design changes or ongoing active maintenance following facility closure.

2.15 R313-25-10; Financial Qualifications to Carry Out Activities

Requirement: This information shall demonstrate that the applicant is financially qualified to carry out the activities for which the license is sought. The information shall meet other financial assurance requirements of URCR R313-25. [URCR R313-25-10(1)] A license for the receipt, possession, and disposal of waste containing radioactive material will be issued by the Executive Secretary upon finding that the financial or surety arrangements meet the requirements of URCR R313-25. [URCR R313-25-

11(9)] The applicant shall show that it either possesses the necessary funds, or has reasonable assurance of obtaining the necessary funds, or by a combination of the two, to cover the estimated costs of conducting all licensed activities over the planned operating life of the project, including costs of construction and disposal. [URCR R313-25-30(1)]

Compliance Basis: As required by License condition 73, Energy*Solutions* submits annual revised cost estimates from facility closure. In conjunction with the Surety Review, Energy*Solutions* submits annual revisions to a Letter of Credit complying with the requirements of URCR R313-25-10(1), 25-11(9), and 25-30(1). No revisions to Energy*Solutions*' current Letter of Credit are required as a result of the targeted disposal of depleted uranium.

2.16 R313-25-11; Requirements For Issuance Of A License

Risk to Health and Safety

Requirement: A license for the receipt, possession, and disposal of depleted uranium waste containing radioactive material will be issued by the Executive Secretary upon finding that the issuance of the license will not contribute an unreasonable risk to health and safety of the public [URCR R313-25-11(1)]

Compliance Basis: The information contained in Appendix A demonstrates that the requirements of URCR R313-25-11(1) have been or will be met. The analysis contained therein shows that the groundwater protection requirements will be met for at least 500 years, as required. Doses to offsite members of the public will be below the 25 mrem/yr limit.

Training and Experience

Requirement: A license for the receipt, possession, and disposal of waste containing radioactive material will be issued by the Executive Secretary upon finding that the applicant is qualified by reason of training and experience to carry out the described disposal operations in a manner that protects health and minimizes danger to life or property (URCR R313-25-11(2)].

Compliance Basis: No additional training and experience will be required as a result of the acceptance and disposal of depleted uranium. Once the Radioactive Material License has been amended to allow the disposal of depleted uranium, employee training and experience requirements of URCR R313-25-11(2) will continue to be met. Energy*Solutions'* training program contains detail about required worker experience, qualifications and training.

Protection to Public Health and Safety

Requirement: A license for the receipt, possession, and disposal of waste containing depleted uranium material will be issued by the Executive Secretary upon finding that the applicant's disposal site, disposal design, land disposal facility operations, including equipment, facilities, and procedures, disposal site

closure, and post-closure institutional control, are adequate to protect the public health and safety as specified in the performance objectives of URCR R313- 25-19 [URCR R313-25-11(3)]

Compliance Basis: The information contained in Appendix A of this Compliance Report indicate Energy*Solutions* will continue to comply with the requirements of URCR R313-25-11(3) as a result of accepting and disposing of depleted uranium. Energy*Solutions*' Clive Disposal site, disposal design, land disposal facility operations, including equipment, facilities, and procedures, disposal site closure, and post-closure institutional control features are addressed under several other requirements. Appendix A shows that the groundwater protection requirements will be met for at least 500 years, as required. Doses to offsite members of the public will be below the 25 mrem/yr limit, as described in Appendix A.

Health and Safety Performance Objectives

Requirement: A license for the receipt, possession, and disposal of depleted uranium waste will be issued by the Executive Secretary upon finding that the applicant's disposal site, disposal site design, land disposal facility operations, including equipment, facilities, and procedures, disposal site closure, and post-closure institutional control are adequate to protect the public health and safety in accordance with the performance objectives of URCR R313-25-20 [URCR R313-25-11(4)]

Compliance Basis: The information contained in Appendix A indicates that Energy*Solutions*' Clive disposal site, disposal site design, land disposal facility operations, including equipment, facilities, and procedures, disposal site closure, and post-closure institutional control are adequate to protect the public health and safety in accordance with requirements of URCR R313-25-11(4). The basis for this affirmative finding is presented in the description and justification of the design of the intruder barrier. The basis is presented under findings contained in this Compliance Report for Requirements URCR R313-25-7(2) through URCR R313-25-7(5) and are addressed in Appendix A.

Land Disposal Facility Operations, Including Equipment, Facilities, and Procedures

Requirement: A license for the receipt, possession, and disposal of depleted uranium waste containing radioactive material will be issued by the Executive Secretary upon finding that the applicant's proposed land disposal facility operations, including equipment, facilities, and procedures, are adequate to protect the public health and safety in accordance with R313-15 (URCR R313-25-11(5)]

Compliance Basis: In Appendix A, Energy*Solutions* projects that radiation exposures to members of the general public in unrestricted areas and to facility workers will not exceed the limits during facility operations. Furthermore, Energy*Solutions* will reduce radiation exposures to the extent reasonably achievable under the company's ALARA program. Energy*Solutions* has submitted operational procedures and descriptions of facilities which incorporate features to protect worker and public health and safety. These requirements are discussed further under requirements URCR R313-25-8(1) through URCR R313-25-8(3).

Long-Term Stability

Requirement: A license for the receipt, possession, and disposal of waste containing depleted uranium radioactive material will be issued by the Executive Secretary upon finding that the applicant's disposal site, disposal site design, land disposal facility operations, disposal site closure, and post-closure institutional control plans are adequate to protect the public health and safety in that they will provide reasonable assurance of the long-term stability of the disposed waste and the disposal site and will eliminate to the extent practicable the need for continued maintenance of the disposal site following closure. [URCR R313-25-11(6)]

Compliance Basis: As is repeated in Appendix A, Energy*Solutions* demonstrates that the disposal site, disposal site design, land disposal facility operations, disposal site closure, and post-closure institutional control plans are adequate to protect the public health and safety in that they will provide reasonable assurance of the long-term stability of the disposed waste and the disposal site and will eliminate to the extent practicable the need for continued maintenance of the disposal site through the 10,000 year compliance period following closure in accordance with the requirements of URCR R313-25-11(6). The basis for this affirmative finding is presented in the description and justification of the design of the principal design features planned for the disposal facility. These principal design features have been designed to perform their required functions over an appropriate period of time such that the facility will meet applicable performance objectives without the need for ongoing active maintenance following facility closure. The basis for this Compliance demonstration is presented under URCR R313-25-7(2) through URCR R313-25-7(5), URCR R313-25-8(4), and URCR R313-25-22(1).

Reasonable Assurance

Requirement: A license for the receipt, possession, and disposal of waste containing depleted uranium radioactive material will be issued by the Executive Secretary upon finding that the applicant's demonstration provides reasonable assurance that the requirements of URCR R313-25 will be met. [URCR R313-25-9(7)]

Compliance Basis: Energy*Solutions* demonstrates that the requirements of URCR R313-25 have been or will be met, as described and justified in this document. This finding is a global rollup of all the requirements contained in URCR R313-25. The basis for this demonstration of compliance is contained in the individual sections addressed in this Report.

Institutional Control Assurance

Requirement: A license for the receipt, possession, and disposal of waste containing radioactive material will be issued by the Executive Secretary upon finding that the applicant's proposal for institutional control provides reasonable assurance that control will be provided for the length of time found necessary to ensure the findings in URCR R313-25-11(3) through (6) and that the institutional control meets the requirements of URCR R313-25-28. [URCR R313-25-11(8)]

Compliance Basis: This Report demonstrates that reasonable assurance exists that control will be provided as necessary to ensure the findings in URCR R313-25-11(3) through (6) will be met. The information provided also indicates that reasonable assurance exists that the provisions for institutional control meet or will meet the requirements of URCR R313-25-28.

Financial or Surety Arrangements

Requirement: A license for the receipt, possession, and disposal of waste containing radioactive material will be issued by the Executive Secretary upon finding that the financial or surety arrangements meet the requirements of URCR R313-25. [URCR R313-25-9(9)]

Compliance Basis: As required by License condition 73, Energy*Solutions* submits annual revised cost estimates from facility closure. In conjunction with the Surety Review, Energy*Solutions* submits annual revisions to a Letter of Credit complying with the requirements of URCR R313-25-10(1), URCR R313-25-30(1), URCR R313-25-32(1), and URCR R313-32(2). No revisions to Energy*Solutions*' current Letter of Credit are required as a result of the targeted disposal of depleted uranium.

2.17 R313-25-18; Individual Exposure Assurance

Requirement: Land disposal facilities shall be sited, designed, operated, closed, and controlled after closure so that reasonable assurance exists that exposures to individuals do not exceed the limits stated in URCR R313-25-19 through 25-22. [URCR R313-25-19(1)]

Compliance Basis: The information contained in this Report demonstrate that the requirements of URCR R313-25-18 will be met (as embodied in the Technical Analyses required in support of each and are presented individually for each of the cited regulatory requirements as follows:

- R313-25-19 in Requirement 2508-1,
- R313-25-20 in Requirement 2508-2,
- R313-25-21 in Requirement 2508-3, and
- R313-25-22 in Requirement 2508-4.

2.18 R313-25-19; Protection Of The General Population From Releases Of Radioactivity

Requirement: Concentrations of radioactive material which may be released to the general environment in groundwater, surface water, air, soil, plants or animals shall not result in an annual dose exceeding an equivalent of 25 mrem to the whole body, 75 mrem to the thyroid, and 25 mrem to any other organ of any member of the public. Reasonable efforts should be made to maintain releases of radioactivity in effluents to the general environment as low as is reasonably achievable. [URCR R313-25-19(1)]

From a compliance period perspective, 10,000 years is the time period for a quantitative analysis and is consistent with Federal rules and guidance. Given the nature of depleted uranium, a qualitative analysis out to the peak dose period is also warranted to inform the performance assessment. Use of the 10,000 year time period for compliance is consistent with federal regulations (e.g., 40 CFR 191) and NRC

guidance. Extending the analysis qualitatively until peak dose is also consistent with NUREG-1573 recommendations. The NRC has taken a similar approach with the NRC Decommissioning Criteria for the West Valley Demonstration Project at the West Valley Site (NRC, 2002). It is noteworthy that the only Federal standard that goes beyond 10,000 years for compliance is the standard for Yucca Mountain (NRC, 2002). That provision provides a two-level dose standard with a higher dose limit of 100 mrem after 10,000 years.

Consequently, for purposes of applying the performance standards for protection of the general public (URCR313-25-19) and for protection of individuals from inadvertent intrusion (URCR313-25-20), the Division should chosen to use the 10,000 year compliance period with a qualitative analysis to cover the period beyond to the peak dose.

The performance standard for protection of the general public (URCR313-25-19) is based on the 1959 standards of International Commission on Radiological Protection (ICRP) Publication 2 methodology. URCR313-15 rules are based on newer ICRP guidance in Publications 26 and 30. Part 20 uses the total effective dose equivalent (TEDE) rather than the whole body dose. NRC has recognized the inconsistency between the dose methodologies and has issued guidance to allow the use of newer guidance. This approach was taken for Yucca Mountain in 10 CFR Part 63, NUREGs -1854 and 1573, and in the NRC Decommissioning Criteria for West Valley. As noted in NUREG-1573:

> *"As a matter of policy, the Commission considers 0.25 mSv/year (25 mrem/year) TEDE as the appropriate dose limit to compare with the range of potential doses represented by the older limits that had whole-body dose limits of 0.25 mSv/year (25 mrem/year) (NRC, 1999, 64 FR 8644; see Footnote 1). Applicants do not need to consider organ doses individually because the low value of the TEDE should ensure that no organ dose will exceed 0.50 mSv/year (50 mrem/year)."*

Consequently, the Division should use for purposes of applying the performance standards for protection of the general public (URCR313-25-19) the total effective dose equivalent rather than the whole body dose.

Compliance Basis: The information contained in this Report demonstrates that the requirements of URCR R313-25-19(1) have been met. Appendix A of this Compliance Report present the results of extensive analyses addressing the potential radionuclide releases to media including groundwater, surface water, air, soil, plants and animals, and discuss potential exposure pathways resulting from these releases. Transport of releases from disposed wastes was evaluated. The annual doses resulting from the postulated releases for reasonably likely conditions were found to be within the regulatory limit of 25 mrem to the whole body, 75 mrem to the thyroid, and 25 mrem to any other organ. The annual doses are found to be in compliance with the regulations. The following text provides a discussion of releases to all environmental media and their corresponding doses. The information on releases and dose assessment is included in Appendix A and is qualitatively summarized below to demonstrate that the construction, operation, and closure Clive operations will satisfy all applicable regulatory dose limits.

As is noted in the Technical Analysis and has been accepted by the Division as a result of prior licensing activities, future intruder constructor, intruder agriculture, and off-site receptor scenarios are considered unreasonable. An intruder explorer would not receive a significant dose. Conclusions are based upon the poor water quality, arid conditions and institutional controls.

Energy*Solutions*' radiological control program has successfully maintained worker exposures as a fraction of the regulatory limit, as demonstrated by worker dosimetry records and calculation of committed effective dose equivalents (CEDE). Energy*Solutions* actively reviews work practices, performs operational radiological surveys and has a functional ALARA review committee. The Division has recognized Energy*Solutions*' proactive approach that has resulted in successfully maintaining worker doses ALARA.

Maximum Dose

Table 2-3 presents the maximum dose to the general public at the Clive facility due to the disposal of depleted uranium. The reported 95% upper confidence interval of the mean peak doses is commonly used to represent reasonable maximum exposure in CERLCA risk assessments. Compliance with the performance objectives for the member of the general public of 25 mrem in a year is clearly established for all three disposal configurations. The doses increase as waste is placed nearer the top of the embankment, but the more stringent protection of the general public performance objectives are not exceeded for all cases. Compliance is demonstrated.

Groundwater Pathway

The groundwater protection criteria are based on an annual dose of 4 mrem to an individual drinking groundwater. The expected dose from the groundwater pathway is zero because of the poor groundwater quality. The high salinity of the groundwater, without rigorous treatment, prevents its use for drinking, livestock watering, or crop irrigation. Groundwater protection requirements place limits on the individual radionuclide concentrations in the groundwater at the compliance-monitoring well. The radionuclide concentration limits must not be exceeded for at least 500 years following closure of the facility.

Table 2-4 summarizes the distribution of the peak groundwater concentrations at the compliance point within the 500-year regulatory limit. As is illustrated, the 3m and 5m Models comply with the GWPLs. However, for the 10m Model, the situation is not as clear. Because the mean (of the peak of the means) and the 95th percentile for Tc_{99} and I_{129} exceed the GWPL in the 10m Model, it is reasonable to conclude that the 10m Model is not in compliance with the performance objective.

Table 2-3

Peak Total Effective Dose Equivalents to the General Public
(mrem/yr within 10,000 years)

Waste Model	Receptor	Mean	Median	95% Percentile
3m Model	Rancher	4.4	3.4	11.0
	Hunter	0.19	0.15	0.46
	OHV enthusiast	0.29	0.23	0.72
	I-80 receptor	0.00012	9.85e-5	0.00032
	Knolls receptor	0.0013	0.00099	0.0034
	Rail road receptor	0.00019	0.00016	0.0005
	Rest area receptor	0.0025	0.002	0.0063
	UTTR access road	0.062	0.049	0.166
5m Model	Rancher	0.60	0.47	1.5
	Hunter	0.026	0.021	0.063
	OHV enthusiast	0.039	0.032	0.095
	I-80 receptor	1.4e-5	1.20e-5	3.5e-5
	Knolls receptor	0.00015	0.00012	0.00038
	Rail road receptor	2.3e-5	1.9e-5	5.6e-5
	Rest area receptor	0.00029	0.00025	0.00073
	UTTR access road	0.0071	0.0059	0.018
10m Model	Rancher	0.0060	0.0047	0.015
	hunter	0.00025	0.00021	0.00062
	OHV enthusiast	0.00039	0.00031	0.00094
	I-80 receptor	1.5e-7	1.2e-7	3.9e-7
	Knolls receptor	1.6e-6	1.2e-6	4.3e-6
	Rail road receptor	2.4e-7	1.9e-7	6.1e-7
	Rest area receptor	3.1e-5	2.5e-6	7.8e-6
	UTTR access road	7.8e-5	6.2e-5	0.0002

Table 2-4

Peak Groundwater Concentrations
(pCi/L within 500 years)

Waste Model	GWPL	Mean	Median	95% Percentile
3m Model:				
Sr_{90}	42	0	0	0
Tc_{99}	3,790	86	1.4e-5	210
I_{129}	21	0.053	7.7e-21	0.13
Th_{230}	83	4.9e-17	4.2e-37	1.7e-26
Th_{232}	92	5.1e-23	0	1.3e-32
Np_{237}	7	1.9e-28	0	0
U_{233}	26	4.8e-13	5.2e-33	5.1e-22
U_{234}	26	2.3e-12	3.3e-32	3.3e-21
U_{235}	27	1.4e-13	2.7e-33	3.1e-22
U_{236}	27	4.4e-13	4.7e-33	4.1e-22
U_{238}	26	1.9e-11	2.7e-31	2.8e-20
5m Model:				
Sr_{90}	42	0	0	0
Tc_{99}	3,790	440	0.0026	1,700
I_{129}	21	0.37	3.4e-16	1.8
Th_{230}	83	2.2e-21	5e-37	1.5e-26
Th_{232}	92	1.6e-27	0	1.3e-32
Np_{237}	7	3.9e-25	0	4.2e-38
U_{233}	26	4.4e-17	6.3e-33	3.9e-22
U_{234}	26	2.7e-16	3.7e-32	2.4e-21
U_{235}	27	2.9e-17	3.0e-33	2.1e-22
U_{236}	27	3.6e-17	5.2e-33	3.4e-22
U_{238}	26	2.2e-15	3.0e-31	2.0e-20

Table 2-4
(continued)

Peak Groundwater Concentrations
(pCi/L within 500 years)

Waste Model	GWPL	Mean	Median	95% Percentile
10m Model:				
Sr_{90}	42	0	0	0
Tc_{99}	3,790	14,000	110	81,000
I_{129}	21	13	5.8e-07	81
Th_{230}	83	1.5e-21	3.8e-37	1.2e-26
Th_{232}	92	1.3e-27	0	9.3e-33
Np_{237}	7	7.6e-18	0	4.7e-26
U_{233}	26	2.9e-17	2.3e-32	4.7e-22
U_{234}	26	1.6e-16	3.0e-32	2.1e-21
U_{235}	27	1.6e-17	2.6e-33	1.8e-22
U_{236}	27	2.4e-17	4.3e-33	3.2e-22
U_{238}	26	1.4e-15	2.4e-31	1.7e-20

Surface Water Pathway

Long-term surface water pathway doses are expected to be zero because of the absence of permanent surface water bodies at the site. The nearest stream channel is greater than five miles east of the facility. Surface water from precipitation is directed away from the waste disposal embankment by drainage ditches and berms. During facility operations, possibly contaminated contact storm-water is recovered and conveyed to evaporation ponds where it is monitored and controlled. No contact storm-water is released offsite, thereby maintaining releases from surface water ALARA.

Air Pathway

As are described in Chapters 4 and 9 of Appendix A, gaseous and particle-bound contaminants that have migrated to the surface soil layer are potentially subject to dispersion in the atmosphere. The effect of mechanical disturbance on human exposure to soil particulates is evaluated in the Performance Assessment based on the effect of off-highway vehicle use. However, although this mechanism may be consequential for human exposure, it is not a significant contributor to the overall rate of fine particulates emissions from the embankment over time. Aeolian (wind-related) disturbance is the primary cause of particulates emissions from the embankment. Because the model projects massive dilution for windblown sediments, this pathway results in insignificant offsite accumulation of transported radionuclides and associated exposures to the general public. Compliance is demonstrated for the regulatory requirements for protecting members of the general public from the atmospheric pathway.

Soil Pathway

Soil pathway doses involve exposure of the public to contaminated soil from the facility. If an exposure occurred, doses could result from external radiation or ingestion of soil on dirty hands. External radiation levels at the top of the final cover will be at or below background radiation for the site, so no doses are anticipated. During operation, the facility will be monitored to ensure that no releases or doses occur via the soil pathway.

Plant Pathway

The plant pathway is not expected to cause any doses to humans. Edible crops or animal forage are not expected to grow on the waste embankment. During operations all plants will be prevented from contacting the waste. After closure, the site's low precipitation and cell cover design will prevent crop production or growth of domestic animal forage on the embankment.

Animal Pathway

Ants fill a broad ecological niche in arid ecosystem of the Clive facility as predators, scavengers, trophobionts and granivores. However, it is their role as burrowers that is of main concern for the purposes of this Compliance Report. Ants burrow for a variety of reasons but mostly for the procurement of shelter, the rearing of young and the storage of foodstuffs. How and where ant nests are constructed

plays a role in quantifying the amount and rate of subsurface soil transport to the ground surface at the Clive site. Factors relating to the physical construction of the nests, including the size, shape, and depth of the nest, are key to quantifying excavation volumes. Factors limiting the abundance and distribution of ant nests such as the abundance and distribution of plant species, and intra-specific or inter-specific competitors, also can affect excavated soil volumes. Parameters related to ant burrowing activities include nest area, nest depth, rate of new nest additions, excavation volume, excavation rates, colony density, and colony lifespan. These attributes are described in this section, along with other considerations involving the impact of ant species and their inclusion in the Clive PA model.

Other than ants, the burrowing animal pathway is not expected to cause any doses to humans. Burrowing animals at the site include jackrabbits, mice, and foxes. None of these species typically burrow deep enough to penetrate through the cover system and disturb the waste materials.

2.19 R313-25-20; Protection of Individuals From Inadvertent Intrusion

Requirement: Design, operation, and closure of the land disposal facility shall ensure protection of any individuals inadvertently intruding into the disposal site and occupying the site or contacting the waste after active institutional controls over the disposal site are removed. [URCR R313-25-20]

From a compliance period perspective, 10,000 years is the time period for a quantitative analysis and is consistent with Federal rules and guidance. Given the nature of depleted uranium, a qualitative analysis out to the peak dose period is also warranted to inform the performance assessment. Use of the 10,000 year time period for compliance is consistent with federal regulations (e.g., 40 CFR 191) and NRC guidance. Extending the analysis qualitatively until peak dose is also consistent with NUREG-1573 recommendations. The NRC has taken a similar approach with the NRC Decommissioning Criteria for the West Valley Demonstration Project at the West Valley Site (NRC, 2002). It is noteworthy that the only Federal standard that goes beyond 10,000 years for compliance is the standard for Yucca Mountain (NRC, 2002). That provision provides a two-level dose standard with a higher dose limit of 100 mrem after 10,000 years.

Consequently, for purposes of applying the performance standards for protection of the general public (URCR313-25-19) and for protection of individuals from inadvertent intrusion (URCR313-25-20), the Division should chosen to use the 10,000 year compliance period with a qualitative analysis to cover the period beyond to the peak dose.

The performance standard for protection of individuals from inadvertent intrusion (URCR313-25-20) requires "*...protection of any individual inadvertently intruding into the disposal site and occupying the site or contacting the waste.*" However, these regulations are silent on the specific dose standard to apply. Since Part 61 has been issued, the standard used by NRC and others for low-level radioactive waste disposal licensing has been an intruder standard of 500 mrem/yr. The 500 mrem standard is also used in DOE's waste determinations implementing the Part 61 performance objectives (NUREG-1854). It is noted that 500 mrem/yr was also the standard proposed in Part 61 in 1981 (46 FR 38081, July 24, 1981). Additionally, the Statement of Considerations for the final rule did not object to the number. It was removed apparently at the request of EPA, because of its concern of how one would monitor it or

demonstrate compliance with it, but not because EPA disagreed with it (47 FR57446, 57449, December 27, 1982). A dose standard of 500 mrem/yr is also used as part of the license termination rule dose standard for intruders (10 CFR 20.1403).

Consequently, DRC should use for purposes of applying the performance standard for protection of individuals from inadvertent intrusion (URCR313-25-20) a 500 mrem/yr threshold for the intruder dose.

Compliance Basis: For purposes of demonstrating compliance, it is important to note that occupation of the site by inadvertent intruders after site closure is not likely due to a lack of natural resources in the area, particularly a lack of potable water. As such, contacting the waste after site closure by an onsite resident is not likely due to the lack of natural resources (no reason to drill or dig) and the design of the embankment cover system. The design features and operations will minimize radiation dose to inadvertent intruders, as well. Several design features provide the required protection. Overall features include:

- Lack of nearby residential population
- Embankment cover system

Operations specific features include:

- Fences
- Buffer zone
- Security plan

Post-Closure specific features include:

- Granite markers

While onsite occupation is unlikely, the impact on facility performance by inadvertent intruders is modeled in the Performance Assessment via the possible formation of gullies that are caused by human intervention (e.g., OHV activity, cattle trails), which may result in direct human contact with the waste for future receptors. For those cases when gullies are formed, which is assumed to be affected by human intervention, comparison of doses is made to Inadvertent Intruder performance objectives.

Table 2-5 summarizes the maximum dose to the inadvertent intruder at the Clive facility due to the disposal of depleted uranium. The reported 95% upper confidence interval of the mean peak doses is commonly used to represent reasonable maximum exposure in CERLCA risk assessments. Compliance with the performance objectives for the inadvertent intruder of 500 mrem in a year is clearly established for all three disposal configurations.

Table 2-5

Peak Total Effective Dose Equivalents to the Inadvertent Intruder (mrem/yr within 10,000 years)

Waste Model	Receptor	Mean	Median	95% Percentile
3m Model	Rancher	21	11	72
	Hunter	0.8	0.47	2.6
	OHV enthusiast	1.2	0.73	4.0
5m Model	Rancher	0.60	0.44	1.4
	Hunter	0.024	0.02	0.063
	OHV enthusiast	0.037	0.03	0.090
10m Model	Rancher	0.0059	0.0046	0.015
	Hunter	0.00026	0.00020	0.00062
	OHV enthusiast	0.00039	0.00031	0.00096

2.20 R313-25-21; Protection of Individuals During Operation

Requirement: Operations at the land disposal facility shall be conducted in accordance with the standards for radiation protection set out in URCR R313-15, except for release of radioactivity in effluents from the land disposal facility, which are governed by URCR R313-25-19. Every reasonable effort shall be made to maintain radiation exposures as low as reasonably achievable, ALARA. [URCR R313-25-21]

Compliance Basis: The information contained in Appendix A of this report demonstrates that the requirements of URCR R313-25-21 will be met. NUREG-1199 describes the items that together encompass Conduct of Operations.

2.21 R313-25-22; Stability of the Disposal Site After Closure

Requirement: The disposal facility shall be sited, designed, used, operated, and closed to achieve long-term stability of the disposal site and to eliminate, to the extent practicable, the need for ongoing active maintenance of the disposal site following closure so that only surveillance, monitoring, or minor custodial care are required. [URCR R313-25-21]

The performance standard for stability requires the facility must be sited, designed, and closed to achieve long-term stability to eliminate to the extent practicable the need for ongoing active maintenance of the site following closure. The intent of this requirement is to provide reasonable assurance that long-term stability of the disposed waste and the disposal site will be achieved.

Prior to implementing Part 61, it had been a common practice at waste disposal facilities to randomly dump some waste. This practice jeopardized package integrity and did not permit access to voids between packages so that they could be properly backfilled. Consolidation of wastes would provide a less stable support which could contribute to failure of the disposal unit cover leading to increased precipitation infiltration and surface water intrusion.

To help achieve stability, NRC noted that to the extent practicable the waste should maintain gross physical properties and identity over 300 years, under the conditions of disposal. NRC believed that the use of design features to achieve stability was consistent with the concept of ALARA and the use of the best available technology. It was NRC's view that to the extent practicable, waste forms or containers should be designed to be stable (i.e., maintain gross physical properties and identity, over 300 years). NRC also noted that a site should be evaluated for at least a 500-year time frame to address the potential impacts of natural events or phenomena should also be applied.

About the same time as Part 61 was promulgated, NRC also put in place requirements for design of uranium mill tailings piles such as the Vitro site which is right next to the Clive site. In addressing stability requirements for mill tailings, NRC recognized the need to set practicable standards. NRC specified that the design shall provide reasonable assurance of control of radiological hazards to be effective for 1,000 years, to the extent reasonably achievable, and, in any case, for at least 200 years.

In both cases (low-level radioactive waste and mill tailings disposal) NRC recognized the need to set practical standards that can be implemented. The design standards range from 200 up to 1,000 years. NRC recognized the design limitations and noted that reasonably achievable designs should be employed to the extent practicable. It is not practical to set design standards beyond 1,000 years.

Consequently, the Division should use for purposes of applying the performance standard for stability of the disposal site after closure (URCR313-25-22) an approach consistent with past standard setting practice.

Compliance Basis: Compliance with the regulatory requirements related to URCR R313-25-22 is addressed in this Report's sections for URCR R313-25-23(1) through URCR R313-25-23(11), URCR R313-25-7(2) through URCR R313-25-7(5), URCR R313-25-11(1) through URCR R313-25-11(5), URCR R313-25-8, and URCR R313-11(6) through URCR R313-25-11(9).

2.22 R313-25-24; Disposal Site Design For Near-Surface Land Disposal

Requirement: Site design features shall be directed toward long-term isolation and avoidance of the need for continuing active maintenance after site closure. [URCR R313-25-24(1)]

Compliance Basis: URCR R313-25-8 discuss the primary emphasis in determining disposal site suitability was given to isolation of depleted uranium wastes and to disposal site features that ensure that the long-term performance objectives will be met. URCR R313-25-7(1) through URCR R313-25-7(5) also demonstrate that the Principal Design Features have been designed to perform as intended for more than 500 years following the Institutional Control period without reliance on active ongoing maintenance.

2.23 R313-25-31; Funding for Disposal Site Closure and Stabilization

Requirement: The applicant shall provide assurances prior to the commencement of operations that sufficient funds will be available to carry out disposal site closure and stabilization, including: (a) decontamination or dismantlement of land disposal facility structures, and (b) closure and stabilization of the disposal site so that following transfer of the disposal site to the site owner, the need for ongoing active maintenance is eliminated to the extent practicable and only minor custodial care, surveillance, and monitoring are required.

Compliance Basis: The supporting documentation for the 2008 RML renewal indicates that the requirements of URCR R313-25-31, 25-32(1) , and 25-32(2) have been or will be met. Energy*Solutions* annually submits supplemental information to justify the financial assurances it proposes. These annual reports supplement sureties already provided for licensed activities, in an amount adequate to cover any additional costs attributable to closing, stabilizing, decontaminating, decommissioning, monitoring, and maintaining the depleted uranium disposal embankment.

Energy*Solutions* has provided a binding arrangement between Energy*Solutions*, the Division, and the Energy*Solutions*' fiduciary agent that ensures that sufficient funds will be available to cover the costs of

closing and stabilizing the depleted uranium disposal facility, and monitoring and maintaining it during the institutional control period.

The binding arrangement has been and continues to be periodically reviewed by the Executive Secretary to ensure that changes in inflation, technology, and disposal facility operations are reflected in the arrangements. Energy*Solutions* is required by regulation to support similar reviews on an annual basis. Any changes to the binding arrangement will be submitted to the Executive Secretary for review and approval before becoming effective.

2.25 R313-25-32; Financial Assurances For Institutional Control

Requirement: The applicant shall provide assurances prior to the commencement of operations that sufficient funds will be available to carry out disposal site closure and stabilization, including: (a) decontamination or dismantlement of land disposal facility structures, and (b) closure and stabilization of the disposal site so that following transfer of the disposal site to the site owner, the need for ongoing active maintenance is eliminated to the extent practicable and only minor custodial care, surveillance, and monitoring are required.

These assurances shall be based on Executive Secretary approved cost estimates reflecting the Executive Secretary approved plan for disposal site closure and stabilization. The Applicant's cost estimates shall take into account total costs that would be incurred if an independent contractor were hired to perform the closure and stabilization work. [URCR R313-25-31(1)]

Requirement: Prior to the issuance of the license, the applicant shall provide for Executive Secretary approval, a binding arrangement, between the applicant and the disposal site owner that ensures that sufficient funds will be available to cover the costs of monitoring and required maintenance during the institutional control period. The binding arrangement shall be reviewed annually by the Executive Secretary to ensure that changes in inflation, technology, and disposal facility operations are reflected in the arrangements. [URCR R313-25-32(1)]

Requirement: Subsequent changes to the binding arrangement specified in URCR R313-25-32(1) relevant to institutional control shall be submitted to the Executive Secretary for prior approval. [URCR R313-25-32(2)]

Compliance Basis: The supporting documentation in the 2008 RML renewal indicates that the requirements of URCR R313-25-31, 25-32(1) , and 25-32(2) have been or will be met. Energy*Solutions* annually submits supplemental information to justify the financial assurances it proposes. These annual reports supplement sureties already provided for licensed activities, in an amount adequate to cover any additional costs attributable to closing, stabilizing, decontaminating, decommissioning, monitoring, and maintaining the depleted uranium disposal embankment.

Energy*Solutions* has provided a binding arrangement between Energy*Solutions*, the Division, and the Energy*Solutions* fiduciary agent that ensures that sufficient funds will be available to cover the costs of closing and stabilizing the depleted uranium disposal facility, and monitoring and maintaining it during the institutional control period.

The binding arrangement has been and continues to be periodically reviewed by the Executive Secretary to ensure that changes in inflation, technology, and disposal facility operations are reflected in the arrangements. Energy*Solutions* is required by regulation to support similar reviews on an annual basis. Any changes to the binding arrangement will be submitted to the Executive Secretary for review and approval before becoming effective.

2.26 R317-6; Groundwater Protection Limits

Requirement: In addition to these radiological criteria, the Division imposes limits on groundwater contamination, as stated in the Ground Water Quality Discharge Permit (the Permit) (UWQB, 2011). Part I.C.1 of the Permit specifies that Ground Water Protection Limits (GWPLs) in Table 1A of the Permit shall be used for depleted uranium. Table 1A in the Permit specifies general mass and radioactivity concentrations for several constituents of interest to depleted uranium waste disposal. These GWPLs are derived from Ground Water Quality Standards listed in UAC R317-6-2 Ground Water Quality Standards.

Compliance Basis: It is noted that according to the Permit, groundwater at Clive is classified as Class IV, saline ground water, according to UAC R317-6-3 Ground Water Classes. As presented in Appendix A, the Performance Assessment estimates groundwater concentrations at a virtual well near the depleted uranium disposal embankment for comparison with these GWPLs.

3. CONCLUSIONS

This report demonstrates Energy*Solutions*' continued regulatory compliance resulting from their proposed disposal of depleted uranium as Class A waste. As such, it is concluded that acceptance and disposal of depleted uranium produced at DOE's Savannah River Site can be completed compliant with URDR regulatory requirements. Furthermore, this report also demonstrates that Energy*Solutions* may accept and dispose of similar depleted uranium waste from the gaseous diffusion plants at Portsmouth, Ohio and Paducah, Kentucky, and depleted uranium waste from the National Enrichment Facility currently under construction in New Mexico (up to the limits and configurations modeled in the Performance Assessment).

Energy*Solutions* further supports their claims of compliance with URCR Rules through the development and execution of a detailed, site-specific, probabilistic performance assessment using the GoldSim model. This model and the resulting findings demonstrate to the Division that Energy*Solutions*' proposed methods for disposal of depleted uranium will ensure that future operations, institutional control, and site closure can be conducted safely, and that the site will comply with the Division's radiological criteria contained in the URCR.

While included in this Compliance Report as part of improving qualitative understanding of facility performance, Energy*Solutions* agrees with NRC cautions and recognizes that regulatory compliance should include limited, "consideration given to the issue of evaluating site conditions that may arise from changes in climate or the influences of human behavior should be limited so as to avoid unnecessary speculation"(NRC, 2000). Furthermore, "[t]hese events are envisaged as broadly disrupting the disposal site region to the extent that the human population would leave affected areas as the ice sheet or shoreline advances. Accordingly, an appropriate assumption under these conditions would be that no individual is living close enough to the facility to receive a meaningful dose." (NRC, 2000).

4. REFERENCES

Energy*Solutions*, 2008. "Radioactive Material License renewal application", Energy*Solutions*, 2008.

DOE, 1999. "Final Programmatic Environmental Impact Statement for Alternative Strategies for the Long-Term Management and Use of Depleted Uranium Hexaflouride." (DOE/EIS-0269), U.S. Department of Energy, Office of Nuclear Energy, Science and Technology, Washington D.C., April 1999.

DOE, 2007. "Draft Supplement Analysis for Location(s) to Dispose of Depleted Uranium Oxide Conversion Product Generated from DOE's Inventory of Depleted Uranium Hexaflouride." (DOE/EIS-0359-SA1), U.S. Department of Energy, Office of Environmental Management, Washington D.C., 2007.

GoldSim (www.GoldSim.com) accessed 12 May 2011.

Pensado, Osvaldo, P. LaPlante, et. al. "Evaluation of Goldsim Implementation of Total System Performance Assessment – Site Recommenation – CNWRA Input." Center for Nuclear Waste Regulatory Analyses, San Antonio, Texas, November 2002.

NRC, 2000. "A Performance Assessment Methodology for Low-Level Radioactive Waste Disposal Facilities." NUREG-1573. Division of Waste Management, Office of Material Safety and Safeguards, U.S. Nuclear Regulatory Commission, Washington D.C., October 2000.

NRC, 2002. "NRC Decommissioning Criteria for the West Valley Demonstration Project at the West Valley Site (67 FR 5003, 5006, February 1, 2002)." Washington D.C., October 2000.

NRC, 2007. "NRC Staff Guidance for Activities Related to U.S. Department of Energy Waste Determinations." NUREG-1854. U.S. Nuclear Regulatory Commission, Washington D.C., October 2000.

Schroeder, P.R., Aziz, N.M., Lloyd, C.M., and P.A. Zappi, 1994. The Hydrologic Evaluation of Landfill Performance (HELP) Model: User's Guide for Version 3, EPA/600/R-94/168A; US EPA Office of Research and Development, Washington, D.C., 1994.

SRS, 2002. SRS Interoffice Memorandum 071802 Sampling Plan for DU. Westinghouse Savannah River Company, SRS, NMM-ETS-2002-00108, Revision 0. Dated July 18, 2002. To Robertson, Breidenback, Howell, from Loftin, McWhorter.

Utah, 2010. Utah Administrative Code Rule 313-15. "Standards for Protection Against Radiation.", Utah Division of Radiation Control, March 1, 2010.

APPENDIX A

Final Report for the Clive DU PA Model – version 1.0

[provided via attached digital DVD]

Final Report for the Clive DU PA Model version 1.0

1 June 2011

Prepared by

Neptune and Company, Inc.

This page intentionally left blank, aside from this statement.

CONTENTS

FIGURES

TABLES

Executive Summary

Neptune and Company, Inc., under contract to Energy*Solutions*, LLC (Energy*Solutions*), has developed a computer model (the Clive DU PA Model—the Model) to support decision making related to the proposed disposal of depleted uranium (DU) wastes at the low-level radioactive waste (LLW) disposal facility at Clive, Utah, operated by Energy*Solutions*. The model provides a platform on which to conduct analyses relevant to performance assessment (PA), as required by the State of Utah in Utah Administrative Code (UAC) R313-25, License Requirements for Land Disposal of Radioactive Waste (Utah 2010). Specifically, a PA is required in UAC R313-25-8, Technical Analyses. The model may also serve to inform decisions made by the Site operator in order to gain maximum utility of the resource that is the Clive Facility.

Depleted uranium is the remains of the uranium enrichment process, of which the fissionable uranium isotope ^{235}U is the product. The leftover uranium, depleted in ^{235}U, is predominantly ^{238}U, but may include small amounts of other U isotopes. In general, DU will contain very small amounts of decay products in the uranium, thorium, actinium, and neptunium series of decay chains. Some specific DU waste, resulting from introduction of uranium retrieved from used nuclear reactor fuel (reactor returns) into the separations process, contains varying amounts of contaminants, in the form of fission and activation products. Since the DU is not all pure uranium and its decay products, it is here termed "DU waste". The national inventory of DU is on the order of 700 Gg (700,000 Mg, or metric tons) in mass, and the bulk of it exists in its original storage cylinders as uranium hexafluoride (DUF_6), awaiting conversion to an oxide form (U_3O_8) for disposal. This conversion is to be performed at the Portsmouth, Ohio, and Paducah, Kentucky gaseous diffusion plant (GDP) sites, using new purpose-build "deconversion" plants. A much smaller mass of DU waste was generated by the Savannah River Site (SRS) in the form of UO_3, a powder stored in several thousand 200-L (55-gal) drums. While the composition of the SRS DU is reasonable well known, the content of the GDP DU is not well documented. For the purposes of this assessment, it was necessary to assume that some uncertain fraction of the GDP DU waste was contaminated to the same extent as the SRS DU. DU waste from both sources is considered in the Clive DU PA Model.

The Model is written using the GoldSim probabilistic systems analysis software, which is well-suited for the purpose. In order to provide decision makers with a broad perspective of the behavior and capabilities of the Facility, the model considers uncertainty in input parameters and to some extent in modeling approaches. This probabilistic assessment methodology is encouraged by the Nuclear Regulatory Commission (NRC) and the Department of Energy (DOE) in constructing PAs and the models that support them. The Model can be run in deterministic mode, where a single set of model inputs is used, but running in probabilistic *Monte Carlo* mode provides greater insight into the model behavior, and especially into model sensitivity. In *Monte Carlo* mode, a large number of equally-probably realizations are executed, and the results reflect the uncertainty in the model. To the extent that the model reflects the uncertain state of knowledge at a site, the model provides insight about how the site works, and what should be expected if different actions are taken or different wastes are disposed. In this way, the model aids in decision making, even in the face of uncertainty.

The Clive Facility is located at the eastern edge of the Great Salt Desert, west of the Cedar Mountains, and approximately 100 km (60 mi) west of Salt Lake City, Utah. Clive is a remote and environmentally inhospitable area. Human activity at Clive has, historically, been very limited, due largely to the lack of potable water, or even water suitable for irrigation. The site is located on flat ground, with the bottom of the waste disposal cells shallowly excavated into local lacustrine silts, sands, and clays. A single waste disposal cell, or embankment, is considered in this model: the Class A South embankment. This is modeled with an engineered cover, as per design documents. The top of the cell is above grade, and the cover has layers of engineered materials of earthen origin. In time, this cover is expected to become infilled with loess (windblown silt from local lacustrine deposits), vegetated with native plants, and occupied to a limited extent by insects and mammals. As plant communities become established, they are likely to keep the cover system fairly dry through transpiration.

Some water is modeled as penetrating the cover system, however, and this infiltration leaches radionuclides and transports them down through the cell liner and unsaturated zone to the aquifer. In the saturated zone (aquifer), contaminants are transported laterally to a hypothetical monitoring well located about 27 m (90 ft) from the edge of the interior of the cell. Since the side slopes of the cell are modeled to not contain DU waste, the effective distance to the well from the DU waste itself is about 73 m (240 ft). This pathway is significant for long-lived and readily-leached radionuclides such as ^{99}Tc. Contributions to groundwater radionuclide concentration from the proposed DU waste are calculated for comparison to groundwater protection limits (GWPLs) during the next 500 years (UWQB 2009).

In addition to water advective transport, radionuclides are transported via diffusion in both water and air phases, which can provide upward pathways. Gaseous radionuclides, such as ^{222}Rn, partition between air and water. Soluble constituents partition between water and solid porous media. Coupled with all these process are the activities of biota, with plants transporting contaminants to the ground surface in their tissues, and burrowing animals (ants and small mammals) moving bulk materials upward and downward through burrow excavation and collapse. Biota do not play a major role in contaminant transport, according to model results, but the potential effect of black greasewood, with its long tap root, is occasionally apparent. The cover, with its upper layers infilled with loess, will be largely self-healing from the effects of roots, burrows, and desiccation, but the degree to which the compacted clay radon barriers at the bottom of the cover would be affected is not well understood. The model does not consider the effects of enhanced infiltration or radon diffusion from a compromised radon barrier.

Once radionuclides reach the ground surface at the top of the engineered cover, they are subject to suspension into the atmosphere and dispersion to the surrounding landscape. Atmospheric transport of gases (^{222}Rn) and contaminants sorbed to suspended particles is modeled using a standard modeling platform approved by the Environmental Protection Agency (EPA), called AERMOD. The results of this model are abstracted into the Clive DU PA Model, and contributions of airborne radionuclides to dose and uranium toxicity hazard are evaluated.

The potentially significant cover degradation process of gully formation is evaluated using a simple modeling construct, in order to determine whether it warrants more sophisticated modeling approaches. The Model employs the geometry of gully formation. It is assumed that a gully could form, as the result of natural or anthropogenic processes, as a wedge-shaped incision

into the cover, with the top end at the cover ridge, and the mouth at the change in slope. Outwash from the gully forms a fan-shaped deposit on the side of the embankment. A small number of gullies (1 to 20) is posited, to determine if the number of gullies is significant. Materials exposed in the gully bottom are presumed to be spread across the top of the fan. If these materials include DU waste components, then this leads to some contribution to doses and uranium hazards. No associated effects, such as biotic processes, effects on radon dispersion, or local changes in infiltration are considered. When gullies encounter DU waste, doses and uranium hazards are increased, but when wastes are buried sufficiently deep the gullies have essentially no effect on human exposures.

Given the remote and inhospitable environment of Clive, it is not reasonable to assume that the traditional residential receptors considered in PA will be present. Traditionally, and based on DOE (DOE M 435.1) and NRC guidance (10 CFR 61), members of the public are evaluated outside the fence line or boundary of the disposal facility, and inadvertent intruders are assumed to access the disposal facility and the disposed waste directly, in activities such as well drilling or house construction. For disposal facilities in the arid west, these types of strictly defined default scenarios do not adequately describe likely human activities. Their inclusion in a PA for a site in the arid west, such as Clive, will usually result in underestimation of the performance of a disposal system, which does not lend itself to effective decision making for the Nation's needs to dispose of radioactive waste.

At Clive, there is no potable water resource to drill for, and historical evidence suggests there is little likelihood that anyone would construct a residence on or near the site. There are present day activities in the vicinity, however, that might result in receptor exposures if these activities are projected into the future when the facility is closed and after institutional control is lost. Large ranches operate in the area, so ranch hands will work in the vicinity. Pronghorn antelope are found in the region, and hunters will follow them. Both of these activities are facilitated by the use of off-highway vehicles (OHVs). OHV enthusiasts also ride recreationally for sport in areas adjacent to the facility.

In addition to these receptors, there are specific points of exposure within the vicinity of the Clive Facility where individuals might be exposed. About 12 km (8 miles) to the west, OHV enthusiasts use the Knolls Recreation Area. Interstate-80 and a railroad are located to the north, with an associated rest area on the highway. Closer to the Clive Facility, the Utah Test and Training Range access road is used on occasion. The Model hence evaluates dose, or risk, to site-specific receptors.

The State of Utah follows federal guidance by categorizing receptors in a PA in UAC Rule R313-25-8 and 10 CFR 61.41 according to the labels "member of the public" (MOP) and "inadvertent human intruder" (IHI). NRC offers two definitions of inadvertent intruders in 10 CFR 61:

> **§ 61.2 Definitions**. *Inadvertent intruder* means a person who might occupy the disposal site after closure and engage in normal activities, such as agriculture, dwelling construction, or other pursuits in which the person might be unknowingly exposed to radiation from the waste.

> **§ 61.42 Protection of individuals from inadvertent intrusion.** Design, operation, and closure of the land disposal facility must ensure protection of any individual inadvertently intruding into the disposal site and occupying the site or contacting the waste at any time after active institutional controls over the disposal site are removed.

NRC offers one reference to an MOP:

> **§ 61.41 Protection of the general population from releases of radioactivity.** Concentrations of radioactive material which may be released to the general environment in ground water, surface water, air, soil, plants, or animals must not result in an annual dose exceeding an equivalent of 25 millirems [0.25 mSv] to the whole body, 75 millirems [0.75 mSv] to the thyroid, and 25 millirems [0.25 mSv] to any other organ of any member of the public. Reasonable effort should be made to maintain releases of radioactivity in effluents to the general environment as low as is reasonably achievable.

DOE definitions in DOE M 435.1 (the Manual accompanying DOE Order 435.1) are much more specific. However, the applicable federal agency that regulates disposal of low-level radioactive waste at the Clive Facility is NRC. For the Clive Facility and the Model, based on the NRC definitions, the ranch hand, hunter and OHV enthusiast are expected to engage in activities both on and off the site. As such, these receptors fit the NRC definition of inadvertent intrusion. This is the case whether or not gullies are included in the model, although inclusion of gullies presents a mechanism for more direct intrusion into the DU waste. The receptors that are located at specific offsite locations, instead, fit the NRC definition of member of the public. The Model presents predicted doses to the receptors identified above, under the conditions and assumptions that provide the basis for the Model. These doses are presented as the results of the Model. The effect of comparison with MOP and IHI performance objectives is also presented.

The Model addresses radiation dose to human receptors who might come in contact with radionuclides released from the disposal facility into the environment subsequent to facility closure. In accordance with UAC Rule R313-25-8, doses are calculated within a 10,000-year compliance period and may be compared to a performance criterion of 25 mrem in a year for a MOP, and 500 mrem in a year for an inadvertent intruder. The dose assessment component of the PA model, like the transport modeling components described above, supports probabilistic *Monte Carlo* analysis. Spatio-temporal scaling is a critical component of the Model development. For example, the Model differentiates the impact of short-term variability in exposure parameters (values applicable over a few years or decades, such as individual physiological and behavioral parameters) from the longer-term variability of transport parameters (values applied over the full 10,000-year performance period, such as hydraulic and geochemical parameters). This distinction facilitates assessment of uncertainties that relate to physical processes from uncertainties relating to inter-individual differences in potential future receptors.

In addition to radiation dose, uranium is also associated with non-radiological toxicity, e.g. kidney damage. The potential chemical toxicity of uranium disposed at the Clive Facility is evaluated in the Model. Potential receptor exposure to uranium is compared to toxicological criteria that pertain to a threshold of adverse effect associated with kidney toxicity.

These doses and the supporting contaminant transport modeling that provides the dose model with radionuclide concentrations in exposure media, are evaluated for 10,000 yr, in accordance with UAC R313-25-8(2). After that time, active contaminant transport and exposure modeling is no longer useful, and the focus turns to long-term, or "deep time" scenarios. Peak activity of the waste occurs when the principal parent ^{238}U (with a half-life that is approximately the age of the earth— over 4 billion years), reaches secular equilibrium with its decay products. This occurs at roughly 2.1 My from the time of isotopic separation, and the model evaluates the potential future of the site in this context. This time frame borders on geologic, and needs to take into account the likely possibility of future large lakes in the Bonneville Basin. The return of such lakes is understood to be inevitable, and the Clive Facility, as constructed, will not survive in its current configuration. Many lakes, of intermediate and large size, are expected to occur in the 2.1-My time frame, following the climate cycle periodicity of about 100,000 yr, based on current scientific understanding of paleoclimatology.

As each lake returns, estimates are made of the radionuclide concentrations in a local part of the lake, and in the sediments surrounding and subsuming the site. Because the exact behavior of lake intrusion and site destruction is speculative, the model makes several conservative assumptions. The entirety of the DU waste is assumed to comingle with sediments, dispersed over an uncertain area. In the presence of a lake, the radionuclides migrate into the water column, in accordance with their aqueous solubility. For U_3O_8, which is considered to be the only form of uranium oxide remaining by the time the first lake arrives (since UO_3 has a relative high solubility and will be washed out of the embankment in roughly 50,000 yr), the solubility of U is very low, so its sediment concentration is relatively high. As each lake recedes, radionuclides are co-deposited with the sediment, only to be dissolved into the water column again with the next lake. This is a very conservative approach, since in reality each blanket of sediment could entrap constituents, and the concentrations in water and sediment over time should decrease consequently. The analysis, therefore, focuses on the arrival of the first lake, which will be the most destructive in terms of sudden release of radionuclides, and would provide the least amount of sediment to encapsulate them. Subsequent lakes would see progressively less radionuclide activity as the site is slowly buried under ever-deeper lacustrine deposits through the eons.

The utility of such a calculation, aside from responding to the UAC, is to inform decisions regarding the placement of wastes in the embankment. With downward pathways influencing groundwater concentrations, and upward pathways influencing dose and uranium hazard, a balance must be achieved in the placement of different kinds of waste. The Model reported herein includes three different options for configuration of the DU waste within the CAS embankment. The volume within the embankment that is available for waste disposal is about 13.5m deep below the engineered cap. The 13.5m is divided into 27 layers that are all 0.5m thick. The layers are labeled 1 through 27 from top to bottom of the available volume. No DU waste is included under the side slopes for this PA.

1. GDP contaminated waste in Layer 7 – SRS waste in Layer 8 – GDP uncontaminated waste in Layers 9-27. This model is termed the 3-m model, because the top of Layer 7 is 3 m below the embankment cover. Note that clean fill material is assumed for the 3 m between the cap and Layer 7.

2. GDP contaminated waste in Layer 11 – SRS waste in Layer 12 – GDP uncontaminated waste in Layers 13-27. This model is termed the 5-m model, because the top of Layer 11 is 5 m below the cap. Note that fill material is assumed for the 5 m between the cap and Layer 11.

3. GDP contaminated waste in Layer 21 – SRS waste in Layer 22 – GDP uncontaminated waste in Layers 23-27. This model is termed the 10-m model, because the top of Layer 21 is 10 m below the cap. Note that fill material is assumed for the 10 m between the cap and Layer 21. This model places all waste below grade.

These options cover a fairly wide range of possible disposal options, from disposal below grade only to disposal throughout most of the system, which helps explore the range of possible options for disposal of DU waste. In addition to these options, two scenarios are considered that are related to erosion. The first essentially assumes a stable embankment for 10 ky, with infilling of the cap and continual airborne deposition replacing fine sediments that are resuspended themselves and subsequently dispersed offsite. This model assumes a balance so that substantial erosion from air and water borne forces is unlikely. The second scenario is one in which gullies are formed that, depending on the DU waste disposal configuration, might intersect and expose the DU waste to the environment. Consequently, six different models are considered for the dose and groundwater concentration endpoints. Dose results for ranch workers are presented in Tables ES-1 (without gullies) and ES-2 (with gullies). Doses to ranch workers are more than an order of magnitude greater than doses to hunters and OHV enthusiasts. Groundwater results for ^{99}Tc in Table ES-3.

There is a question of which statistic is most appropriate for comparison. The statistics in Tables ES-1 and ES-2 represent summaries of the peak of the mean doses. If the model is constructed properly, and considering that doses increase with time given the model construction and assumptions so that the peak mean dose occurs at or near 10 ky, then the 95th percentile is analogous to the 95% upper confidence interval of the mean that is commonly used to represent reasonable maximum exposure in CERLCA risk assessments. The mean, instead represents a central tendency estimate of risk under CERCLA.

When gullies are not included in the model, compliance with the performance objectives for the inadvertent intruder of 500 mrem in a year, and for the MOP of 25 mrem in a year is clearly established for all three disposal configurations. The doses increase as waste is placed nearer the top of the embankment, but the more stringent MOP performance objectives are not exceeded in all cases. This implies that disposal configurations exist, under the conditions of this model, for which it is reasonable to dispose of DU waste.

When gullies are included (Table ES-2), all doses are still less than the 500-mrem in a year inadvertent intruder performance objective. However, the 95th percentile peak mean dose to ranch workers exceeds the MOP performance objective of 25 mrem in a year.

Results are also available for the offsite (MOP) receptors. None of the 95th percentile dose estimates for these receptors exceeds 1 mrem in a year, and most of the peak mean dose estimates are much less than 1 mrem in a year.

Table ES-1. Peak mean TEDE, without consideration of gullies: statistical summary

	Peak TEDE (mrem in a yr) within 10,000 yr*		
receptor	**mean**	**median (50th %ile)**	**95th %ile**
waste emplaced > 3 m below embankment cover			
ranch worker	4.37	3.44	11.3
waste emplaced > 5 m below embankment cover			
ranch worker	0.598	0.473	1.52
waste emplaced > 10 m below embankment cover			
ranch worker	0.00596	0.00471	0.0152

* - Results based on 5,000 simulations of the Model

Table ES-2. Peak mean TEDE, with gully screening calculation: statistical summary

	Peak TEDE (mrem in a yr) within 10,000 yr*		
receptor	**mean**	**median (50th %ile)**	**95th %ile**
waste emplaced > 3 m below embankment cover			
ranch worker	20.9	11.6	72.3
waste emplaced > 5 m below embankment cover			
ranch worker	0.564	0.443	1.44
waste emplaced > 10 m below embankment cover			
ranch worker	0.00594	0.00457	0.0155

* - Results based on 5,000 simulations of the Model

Summary statistics for the distribution of the peak of the mean ^{99}Tc concentrations are presented in Table ES-3. For the 3-m and 5-m models, compliance with the GWPLs is clearly demonstrated. For the 10-m model the situation is not as clear. However, both the mean (of the peak of the means) and the 95th percentile exceed the GWPL, in which case, it is probably not unreasonable to conclude that the 10-m model is not in compliance with the performance objective.

The results depend critically on the model structure, specification and underlying assumptions. Infiltration rates and ^{99}Tc inventory concentrations might be overestimated. However, based on the model assumptions the 10-m model does not comply with the GWPL performance objective for ^{99}Tc. These results suggest, however, that there are configurations that comply with the GWPLs.

Table ES-3. Peak groundwater activity concentrations for 99Tc within 500 yr, compared to GWPLs

radionuclide	GWPL (pCi/L)	peak activity concentration within 500 yr (pCi/L)*		
		mean	median (50^{th} %ile)	95^{th} %ile
waste emplaced > 3 m below embankment cover				
^{99}Tc	3790	85.9	1.43e-5	209
waste emplaced > 5 m below embankment cover				
^{99}Tc	3790	437	0.00264	1710
waste emplaced > 10 m below embankment cover				
^{99}Tc	3790	14400	113	81400

* - Results based on 5,000 simulations of the Model

Groundwater concentrations for all other radionuclides are much less than their respective GWPLs, with the exception of ^{129}I, which has never been detected in the DU waste proposed for disposal at Clive.

The dose and groundwater concentration results indicate that the downward pathway is dominated by groundwater concentrations of ^{99}Tc, whereas, the upward pathway is dominated by dose from radon. A trade-off is indicated in terms of DU waste placement. The lower the DU waste is placed, particularly the ^{99}Tc contaminated DU waste, the greater the groundwater concentrations of ^{99}Tc, but the lower the doses. Conversely the higher the DU waste is placed in the embankment, the lower the ^{99}Tc groundwater concentrations, and the greater the dose to ranch workers. However, there is a wide range of DU waste configurations in the CAS embankment that satisfy both dose and groundwater performance objectives.

In addition to the individual dose assessments, the structure of the model allows population dose to be tracked. In keeping doses as low as reasonably achievable (ALARA) estimated dose to the entire population of individuals over time is needed. One such calculation is the cumulative dose to all ranch workers, hunters, and OHV enthusiasts, summed across all individuals and all years of the 10,000-yr simulation. These cumulative population doses, as TEDE, are shown in Table ES-4, considering the various cases of waste placement and whether the gully screening calculation is included in the analysis.

The population doses presented in Table ES-4 are very small. This is because the populations of receptors are small, and the individual doses that they might receive are small. Both NRC and DOE have suggested ALARA-based costs of $1,000 (without discounting) and $2,000 (with discounting) per person rem. With costs like these, the total ALARA costs are negligible compared to the cost of waste operations and disposal.

Table ES-4. Peak cumulative population TEDE: statistical summary

	Peak population TEDE (rem) within 10,000 yr*		
simulation scenario	**mean**	**median (50th %ile)**	**95th %ile**
no gullies; waste > 3 m below cover	35.2	29.2	87.3
no gullies; waste > 5 m below cover	4.07	3.46	9.78
no gullies; waste > 10 m below cover	0.0434	0.0356	0.103
with gullies; waste > 3 m below cover	378	172	1430
with gullies; waste > 5 m below cover	4.46	3.7	10.7
with gullies; waste > 10 m below cover	0.0448	0.0364	0.108

* - Results based on 5,000 simulations of the Model

This simple ALARA analysis is consistent with the inhospitable environment and the remoteness of the Clive facility, and confirms the findings of the individual dose assessment. ALARA is intended to support evaluation of options to reduce doses in a cost-effective manner, however, given the results of this ALARA analysis, it is not clear that further reduction in risk (dose) is necessary. It is important to realize that the ALARA analysis depends on the Model structure, specification and assumptions, and that it focuses on a specific aspect of a more complete benefit-cost or decision analysis. However, the results are otherwise compelling.

The final set of analyses that are important are the deep-time analyses. As described above, the deep-time model is very conservative in many ways with respect to dispersal of the DU waste material. Large lakes that obliterate the CAS embankment are assumed to return periodically, but the models of dispersion of the waste are very constraining.

Given the model, peak mean concentrations of 238U in lake water and sediment for the next 100 ky are presented in Tables ES-5 and ES-6. These results simply show the concentrations that might occur in response to obliteration of the site, and subsequent dispersal of the waste in a relatively confined system. The concentrations presented would decrease with each lake and climate cycle as more sediment is deposited with each lake event, and each lake event allows the remnants of the DU waste to be dispersed ever further afield.

Table ES-5. Statistical summary of peak mean uranium-238 concentrations in lake water within the first 100-ky climate cycle

	Peak mean lake water concentration of uranium-238 within 100 ky (pCi/L)		
simulation scenario	**mean**	**median (50th %ile)**	**95th %ile**
no gullies; waste > 3 m below cover	0.18	0.0010	1.1
no gullies; waste > 5 m below cover	0.17	0.0009	1.0
no gullies; waste > 10 m below cover	0.18	0.0009	1.3

* - Results based on 5,000 simulations of the Model

Table ES-6. Statistical summary of peak mean uranium-238 concentrations in sediment within the first 100-ky climate cycle

	Peak mean sediment concentration of uranium-238 within 100 ky (pCi/g)*		
simulation scenario	**mean**	**median (50^{th} %ile)**	**95^{th} %ile**
no gullies; waste > 3 m below cover	1,600	1,300	3,600
no gullies; waste > 5 m below cover	1,500	1,300	3,400
no gullies; waste > 10 m below cover	1,500	1,300	3,400

* - Results based on 5,000 simulations of the Model

The quantitative results are summarized in Table ES-7. Doses are always less than 500 mrem in a year, and doses to the offsite receptors are always much less than 25 mrem in a year. Groundwater concentrations of ^{99}Tc are always less than its GWPL except when the ^{99}Tc contaminated waste is disposed below grade. Even in this case, the median groundwater concentration is only 113 pCi/L.

Table ES-7. Summary of the results of the Clive DU PA Model

	without gullies: top of waste at			with gullies: top of waste at		
performance objective	**3 m**	**5 m**	**10 m**	**3 m**	**5 m**	**10 m**
Dose to MOP below regulatory threshold of 25 mrem/year	Yes	Yes	Yes	Maybe[1]	Yes	Yes
Dose to IHI below regulatory threshold of 500 mrem/year	Yes	Yes	Yes	Yes	Yes	Yes
Groundwater maximum concentration of ^{99}Tc in 500 years < 3790 pCi/L[3]	Yes	Yes	No[2]	Yes	Yes	No[2]
ALARA average total population cost equivalent over 10,000 years	$35,000	$4,000	$43	$378,000	$4,500	$45

The results overall suggest clearly that there are disposal configurations that can be used to dispose of the quantities of DU included in the Model that are adequately protective of human health and the environment.

1.0 Background

One of the responsibilities of the Nuclear Regulatory Commission (NRC) is to ensure the safe disposal of commercially generated low-level radioactive waste. Non-defense-related depleted uranium (DU) waste falls under the jurisdiction of NRC, and requires a disposal option that is protective of human health and the environment. NRC currently regulates the disposal of DU waste as a low-level radioactive waste, in cooperation with "Agreement States". The Energy*Solutions* low-level radioactive waste disposal facility at Clive, Utah is a candidate for disposal of DU waste, and Utah is an Agreement State that has regulatory authority to determine if such disposal can occur in compliance with Utah and NRC regulatory requirements.

Adequate protection of human health and the environment is evaluated by conducting a Performance Assessment (PA). A PA is used to model potential transport of radionuclides from the disposed inventory to the accessible environment, and to estimate radiation dose to potential human receptors. The estimated doses are compared to performance objectives, which are specified as dose limits. If the estimated doses are less than the performance objectives, then adequate protection of human health has been demonstrated.

The purpose of this report is to present the results of a the Clive DU PA Model v1.0 (the Model), a computer model developed to inform performance assessment (PA) for disposal of some specific DU waste materials at the Clive Facility. This report provides a summary of the approach taken and the results that can be obtained from the Model, and is accompanied by supporting documentation that includes details of the Model development and quality assurance program.

1.1 Depleted Uranium

In order to produce suitable fuel for nuclear reactors and/or weapons, uranium has to be enriched in the fissionable ^{235}U isotope. Uranium enrichment in the US began during the Manhattan Project in World War II. Enrichment for civilian and military uses continued after the war under the U.S. Atomic Energy Commission, and its successor agencies, including the DOE.

The uranium fuel cycle begins by extracting and milling natural uranium ore to produce "yellow cake," which is a varying mixture of uranium oxides. Low-grade natural ores contain about 0.05 to 0.3% by weight of uranium oxide while high-grade natural ores can contain up to 70% by weight of uranium oxide. Uranium found in natural ores contains two principal isotopes – uranium-238 (99.3% ^{238}U) and uranium-235 (0.7% ^{235}U). The uranium is enriched in ^{235}U before being made into nuclear fuel, which generates a product consisting of 3% to 5% ^{235}U for use as nuclear fuel and a by-product of DU (between 0.1% and 0.5 ^{235}U). The DU has some commercial applications including counterweights and military applications as artillery. However, the commercial demand for depleted uranium is currently much less than the amounts generated for nuclear fuel. Use of ^{238}U as fuel for breeder reactors has not been seriously considered in this country. The U.S. Department of Energy (DOE) has about 700 Gg (700,000 Mg or metric tons) of DU in storage. Hence, the need to find disposal options for DU waste.

1.2 The Clive Waste Disposal Facility

Energy*Solutions* operates a low-level radioactive waste disposal facility west of the Cedar Mountains in Clive, Utah, as shown in Figure 1. Clive is located along Interstate-80, approximately 5 km (3 mi) south of the highway, in Tooele County. The facility is approximately 80 km (50 mi) east of Wendover, Utah and approximately 100 km (60 mi) west of Salt Lake City, Utah. The facility sits at an elevation of approximately 1302 m (4275 ft) above mean sea level (amsl) and is accessed by both road and rail transportation.

Currently, the Clive Facility receives low-level radioactive waste shipped via truck and rail. The Clive disposal facility is licensed to accept Class A low-level radioactive waste. Under current NRC regulations, DU waste is considered Class A waste, in which case the Clive site is an option for disposal. However, NRC and the State of Utah are currently considering options for updating their regulations and rules (10 CFR 61 for NRC, and UAC R313-25-8(2) for the State of Utah), which is likely to force the requirement of a PA for disposal of DU. Pending the findings of the Clive DU PA, DU waste will be disposed in an above-ground engineered disposal embankment that is clay-lined with a composite clay and rock cap. The disposal embankment is designed to perform for a minimum of 500 years based on requirements of 10 CFR 61.7, and hence provides a possible solution for the long-term disposal of DU.

Clive is a remote and environmentally inhospitable area. Human activity at Clive has, historically, been very limited. The regulations (10 CFR 61 and Utah regulations R313-25-8) indicate the need to evaluate performance with respect to members of the public and inadvertent human intruders. However, the difference between these two categories of human receptors is somewhat blurred because of the types of human activities that are reasonable to consider in the general area of the disposal facility. These two categories of receptors are described further below in the context of the regulatory context of the Clive DU PA.

1.3 Regulatory Context

Energy*Solutions* is permitted by the State of Utah to receive Class A Low Level under Utah Administrative Code (UAC) R313 25, *License Requirements for Land Disposal of Radioactive Waste.* The wastes that are received must be classified in accordance with the UAC R313 15 1008, *Classification and Characteristics of Low-Level Radioactive Waste.* The classification requirements in UAC R313-15-1008 reflect those outlined in NRC's 10 CFR 61 Section 55, but include additional references to radium 226 (^{226}Ra). Further, groundwater protection levels (GWPLs) must be adhered to, as outlined in the site's *Ground Water Quality Discharge Permit* (UWQB, 2010).

Title 10 CFR 61 (Code of Federal Regulations, 2007) is the Federal regulation for the disposal of certain radioactive wastes, including land disposal at privately-operated facilities such as that managed and operated by Energy*Solutions* at Clive, Utah. It contains procedural requirements, performance objectives, and technical requirements for near-surface disposal, including disposal in engineered facilities with protective earthen covers, which may be built fully or partially above-grade. Near-surface disposal is defined as disposal in or within the upper 30 m (100 ft) of the earth's surface (10 CFR 61.2).

Figure 1. Location of the Clive site operated by Energy*Solutions* (base image from Google Earth).

Performance objectives are evaluated by preparing a PA model. DU presents an interesting case because the uranium is nearly all ^{238}U, meaning that secular equilibrium is not attained for more than 2 My, and during that time, activity associated with the DU continues to increase. At the time of the development of the regulation, DU waste as such did not, and was not expected to, exist in significant quantities. The nature of the radiological hazards associated with DU presents challenges to the estimation of long-term effects from its disposal. Recognition of this special behavior of DU has prompted the NRC to revisit the regulation. Until that process is complete, however, 10 CFR 61 stands as the controlling regulation.

The key endpoints of a PA are estimated future potential doses to members of the public (MOP). The performance objectives specified in Subpart C of 10 CFR 61 are in the following section:

> **§ 61.41 Protection of the general population from releases of radioactivity.** Concentrations of radioactive material which may be released to the general environment in ground water, surface water, air, soil, plants, or animals must not result in an annual dose exceeding an equivalent of 25 millirems [0.25 mSv] to the whole body, 75 millirems [0.75 mSv] to the thyroid, and 25 millirems

> [0.25 mSv] to any other organ of any member of the public. Reasonable effort should be made to maintain releases of radioactivity in effluents to the general environment as low as is reasonably achievable.

The location of a member of the public (MOP) is not defined clearly in the NRC statute. Under DOE Order 435.1 the MOP is defined as someone who does not access the disposal facility, but is located outside of the fence line or boundary of the facility. However, NRC does not similarly define an MOP, unless the disposal facility is not considered part of the natural environment. Otherwise, an MOP is not restricted other than through the activities in which the MOP might engage.

In addition to addressing MOP, 10 CFR 61 requires additional assurance of protecting individuals from the consequences of inadvertent intrusion. An inadvertent intruder is someone who is exposed to waste without intent, and without realizing that exposure might occur (after loss of institutional control). This is distinct from the intentional intruder, who might be interested in deliberately disturbing the site, or extracting materials from it, or who might be driven by curiosity or scientific interest. Intentional intruders are not evaluated in a PA.

> **§ 61.42 Protection of individuals from inadvertent intrusion.** Design, operation, and closure of the land disposal facility must ensure protection of any individual inadvertently intruding into the disposal site and occupying the site or contacting the waste at any time after active institutional controls over the disposal site are removed.

The distinction between MOP and an inadvertent intruder is clear in DOE Order 435.1, but is not as clear in NRC 10 CFR 61. Under DOE Orders, a MOP does not engage in activities within the boundaries of the disposal facility, and an inadvertent intruder inadvertently accesses the waste material directly. Consequently, the locations of MOP and intruder are different under DOE Orders. However, the NRC indicates that an inadvertent intruder is defined as follows:

> **§ 61.2 Definitions**. *Inadvertent intruder* means a person who might occupy the disposal site after closure and engage in normal activities, such as agriculture, dwelling construction, or other pursuits in which the person might be unknowingly exposed to radiation from the waste.

Because of the remoteness of the Clive Facility and, hence, the types of activities in which humans might engage, the distinction is made for this PA that ranchers, hunters and OHV enthusiasts are inadvertent intruders because they "engage in normal activities, such as agriculture, dwelling construction, or other pursuits in which the person might be unknowingly exposed to radiation from the waste". This facility is regulated under NRC, in which case the definitions in 10 CFR 61 are most relevant. However, it is noted that the ranchers, hunters and OHV enthusiasts do not intrude into the waste to create a direct exposure. Other receptors evaluated in the PA Model who are located offsite are regarded as MOPs. The results of this Model are calculated without regard for MOP and IHI categorization. The Model simply evaluates dose to each receptor, providing the information necessary for comparison with performance objectives.

No dose limit is specified in 10 CFR 61 for the inadvertent intruder. However, since Part 61 has been issued, the standard used by NRC and others for LLW disposal licensing has been an annual dose of 500 mrem. The 500 mrem-in-a-year standard is also used in the DOE waste determinations implementing the Part 61 performance objectives (NUREG-1854), and as part of the license termination rule dose standard for intruders (10 CFR 20.1403).

The scope of a PA may be limited to the evaluation of MOP and inadvertent intrusion, and also to the issue of site stability. The performance standard for stability requires the facility to be sited, designed, and closed to achieve long-term stability to eliminate to the extent practicable the need for ongoing active maintenance of the site following closure. The intent was to provide reasonable assurance that long-term stability of the disposed waste and the disposal site will be achieved. To help achieve stability, the NRC suggested to the extent practicable that disposed waste should maintain gross physical properties and identity over 300 years, under the conditions of disposal, with a further suggestion that the disposal facility should be evaluated for at least a 500-year time frame. About the same time as Part 61 was promulgated, the NRC also put in place requirements for design of uranium mill tailings piles such as the Vitro site which is collocated with the Clive Facility. The NRC specified that the design shall provide reasonable assurance of control of radiological hazards to be effective for 1,000 years to the extent reasonably achievable, and, in any case, for at least 200 years.

This raises the issue of appropriate compliance periods for a waste form that does not reach peak radioactivity for more than 2 My. Section 2(a) of R313-25-8 states:

> For purposes of this performance assessment, the compliance period shall be a minimum of 10,000 years. Additional simulations shall be performed for the period where peak dose occurs and the results shall be analyzed qualitatively.

The intent of this Model, therefore, is to evaluate impacts to receptors for a period of 10,000 years, and long-term performance of the disposal system beyond that time. The regulation does not address time frame for site stability. Given the long period of time before DU reaches secular equilibrium, it is difficult to determine when peak dose might occur. Consequently, the Clive DU PA Model has been implemented quantitatively for 10 ky, and has run additional simulations for 2.1 My, the time at which DU reaches peak activity. The results of the PA Model will be used to inform decisions about the suitability of the Clive facility for disposal of DU waste, the amount of DU waste that can be disposed safely, and different options for the engineered design and the placement of the waste within the disposal system. These decisions will be made in light of the doses to the receptors identified for the Model, groundwater concentrations of ^{99}Tc and other radionuclides, and the long-term effects on site stability and dispersal of DU waste in returning lakes and lake sediment.

Site stability might also be considered to be a qualitative criterion for evaluating the concept of maintaining receptor impacts to be "as low as reasonably achievable" (ALARA). However, the CFR (Section 61.42) also defines ALARA in the context of dose to populations. The regulation states that "reasonable effort should be made to maintain releases of radioactivity in effluents to the general environment as low as is reasonably achievable". The ALARA process is described in more detail in the white paper *Decision Analysis Methodology for Assessing ALARA Collective*

Radiation Doses and Risks (Appendix 12). ALARA is evaluated in terms of population doses for the design options that are considered. This allows design options to be compared, and, ultimately, to be optimized. NRC also offers options for discounting costs of human exposures over time. NRC suggests a value of $2000 for the cost per person rem, with a possible range of $1000 to $6000. This range will be considered in the ALARA analysis. The ALARA analysis complements the compliance analysis for MOP and inadvertent intruders, since only those options that are in compliance are considered.

In addition to the radiological criteria, the State of Utah imposes limits on groundwater contamination, as stated in the Ground Water Quality Discharge Permit (UWQB, 2010). Part I.C.1 of the Permit specifies that GWPLs in Table 1A of the Permit shall be used for the Class A LLW Cell. Table 1A in the Permit specifies general mass and radioactivity concentrations for several constituents of interest to DU waste disposal. These GWPLs are derived from Ground Water Quality Standards listed in UAC R317-6-2 *Ground Water Quality Standards*. Exceptions to values in that table are provided for specific constituents in specific wells, tabulated in Table 1B of the Permit. This includes values for mass concentration of total uranium, radium, and gross alpha and beta radioactivity concentrations for specific wells where background values were found to be in exceedence of the Table 1A limits.

According to the Permit, groundwater at Clive is classified as Class IV, saline ground water, according to UAC R317-6-3 *Ground Water Classes,* and is highly unlikely to serve as a future water source. The underlying groundwater in the vicinity of the Clive site is of naturally poor quality because of its high salinity and, as a consequence, is not suitable for most human uses, and is not potable for humans. However, the Clive DU PA Model calculates estimates of groundwater concentrations at a virtual well near the Class A South Cell for comparison with these GWPLs. Part I.D.1 of the Permit specifies that the performance standard for radionuclides is 500 years.

1.4 Performance Assessment

Within the regulatory framework described above, a PA addresses doses to potential human receptors within a time frame of compliance. The Clive DU PA Model also addresses performance of the system for approximately 2.1 My—until secular equilibrium of ^{238}U and its decay products is reached. The PA process starts with the regulatory context, but is itself a decision support process. Decisions may be made based on the results of the PA modeling that is performed. In the context of decision analysis, this requires steps that include:

1. State a problem,
2. Identify objectives (and measures of those objectives – i.e., attributes or criteria),
3. Identify decision alternatives or options,
4. Gather relevant information, decompose and model the problem (structure, uncertainty, preferences),
5. Choose the "best" alternative (the option that maximizes the overall benefit),

6. Conduct uncertainty analysis, sensitivity analysis and value of information analysis to determine if the decision should be made, or if more data/information should be collected to reduce uncertainty and, hence, increase confidence in the decision, and
7. Go back (iterate) if more data/information are collected.

The problem addressed here is one of potential disposal of DU waste at the Clive Facility. The objectives are to minimize risk to human health and the environment. Risk is measured in terms of dose and uranium toxicity hazard to the human receptors that are identified for analysis. The decision options that are evaluated relate to different waste configuration options for DU waste disposal. Given that context, the next step of the PA process is to gather information, and build a PA model. There are several steps involved, each one building on the previous step. The modeling process starts with evaluating features, events and processes (FEPs) that might be important for evaluating performance, and using the FEPs analysis to build a conceptual site model (CSM). These steps are described in full in the *FEP Analysis for Disposal of Depleted Uranium at the Clive Facility* (Appendix 1), and the *Conceptual Site Model for Disposal of Depleted Uranium at the Clive Facility* (Appendix 2).

Development of the CSM sets the stage for subsequent model structuring, which is the first step needed to build the numerical model of the system. All relevant FEPs are captured in the model structure, from waste inventory, mechanisms for transport through the engineered system, migration through the natural environment to the accessible environment, to identification of human receptors, exposure pathways and dose assessment. The model structure leads to specification of the model. Probability distributions are specified for each input parameter. The type of information available for each input parameter is highly variable, hence requiring varied approaches for specification. Different methods that are used are described in the white paper *Development of Probability Distributions* (Appendix 14).

Model structuring and specification completes the numerical model. The model is computed using the GoldSim systems analysis software (GTG, 2010). GoldSim is probabilistic simulation software that includes a graphical user-interface that is convenient for developing PA models. GoldSim is inherently a systems-level software framework. The focus of a GoldSim model is on the decision making process, which includes managing uncertainty and coupling all processes. This PA model is intended to reflect the current state of knowledge with respect to the proposed DU disposal, and to support environmental decision making in light of inherent uncertainties.

The development of the model is iterative, where the iterations depend on model evaluation, which is performed at various levels. During model construction the model is evaluated iteratively as new components are added. Once a complete model is assembled then the model is subjected to uncertainty and sensitivity analysis. The goals of the uncertainty analysis are to evaluate results against the performance objectives and to understand the values of the results with respect to the model formation. The sensitivity analysis is used to identify components of the model that are most influential on the output. This leads to model iteration as suggested in Step 7 above.

Building a model to inform PA is a large undertaking. There are many intricacies that must be accommodated starting with development of FEPs, moving through the CSM, mathematical

abstraction of environmental processes, numerical model structuring, development of probability distributions for the input parameters, and model evaluation. This complex process is described briefly in this document, and is described in more detail in the supporting documents (see Appendices). In addition to complete documentation, the GoldSim model itself is fully contained, with internal documentation of every aspect of the model structure. The extensive documentation is provided for two reasons: The first is simply that it provides access to all information used in the Model. This is done in the spirit of openness, transparency and, hence, defensibility. The second is in the context of the quality assurance program that requires tracking of all information from its source through to the final model. The QA program implemented for this Model is described in full in the *Quality Assurance Project Plan* (Appendix 17).

1.5 Technical Evolution of PA and PA Modeling

Since PA modeling began in the late 1970s through early 1990s at many of the radioactive waste disposal facilities around the U.S., many different approaches to modeling have been used. These approaches span the range from deterministic process-level modeling to probabilistic systems-level modeling. Early PA models tended towards deterministic modeling for several reasons: 1) PA modeling was initially performed with a focus on groundwater modeling, which was, and still is, often performed using deterministic process-level models, 2) there were computational or technological difficulties with taking a probabilistic approach, and 3) PA regulations and guidance were established mostly with deterministic performance objectives, which was interpreted as a reason for performing deterministic modeling. In particular, PA for low-level radioactive waste (LLW) disposal facilities followed deterministic performance objectives. However, the regulations for the Waste Isolation Pilot Plant and the Yucca Mountain Project (YMP) (Title 40, *Code of Federal Regulations* (CFR), Part 191, "Environmental Radiation Protection Standards for Management and Disposal of Spent Nuclear Fuel, High-Level and Transuranic Radioactive Wastes," and Title 40, CFR Part 197, "Public Health and Environmental Radiation Protection Standards for Yucca Mountain, Nevada") provide an exception to the deterministic objectives, and consequently, PA models for these radioactive waste disposal facilities have been developed probabilistically.

Technological advances in the last decade have also allowed more PA modeling to move towards a probabilistic approach. Finally, PA modeling is multi-disciplinary, and as more technical disciplines have been brought into PA modeling, there has been increased recognition of the potential benefits of probabilistic systems-level modeling.

Systems-level models are usually computationally simpler than process-level models. However, the systems-level PA model might still have large numbers of parameters, which reveals the complexity of dealing with PA modeling even at a systems-level scale. The large number of parameters is a consequence of the many constituents of concern that are usually included in PA models, and the need to characterize transport properties for each of these constituents (e.g., partitioning coefficients, solubility, plant uptake factors). However, it is unlikely that more than a few of these parameters are important predictors for a given PA endpoint (e.g., dose to a member of the public, groundwater protection levels). Along these lines, another advantage of systems-level modeling performed in a probabilistic environment is the ability to identify parameters that are most important or sensitive for a given endpoint. Because system-level

models may be probabilistic, global sensitivity analysis methods can be used to identify the most sensitive parameters (see the white paper entitled *Sensitivity Analysis* in Appendix 15).

The advantages of system-level models are that they are capable of 1) coupling of different processes without the need for the application of ad hoc boundary conditions, 2) using an appropriate spatial and temporal scaling relative to the decisions that need to be made, 3) having the ability to characterize and manage uncertainty through probabilistic modeling, and 4) being used to perform global sensitivity analysis. Use of the global sensitivity analysis can potentially lead to refinement and enhancements of the underlying models or the identification and collection of new data (e.g., research studies or monitoring) as necessary to reduce uncertainty of certain parameters or variables. Use of a system-level model can also provide the ability to rapidly and efficiently explore alternative conceptualizations of the system, which allows a greater ability to address scenario and conceptual model uncertainties.

System-level models are often supported by process-level models. Each component of a system-level model requires model building, which can include abstraction from a process-level model. The purpose of the abstraction is to be able to capture the essence of the process-level model in the probabilistic system-level model, so that its relative importance or sensitivity can be evaluated. As a consequence of the development of system-level modeling frameworks such as GoldSim, PA models are often developed following this approach, with global sensitivity analysis driving iteration until the model results indicate a clear response and decision path.

1.6 Report Structure

The remainder of this report provides a more complete introduction to the PA modeling process applied to the Clive DU waste disposal option, briefly describes the FEPs process, and follows with a brief description of the CSM. The CSM description is aimed more at identifying components of the model that might be significant in the model results. Model building always leads to insights into the important components of a model, and that is conveyed in terms of important aspects of the CSM.

The model structure is described prior to presentation of results, which are the main focus of this report. Results are presented for the 10-ky quantitative model and for the deep-time model. For the 10-ky model, the important results from a regulatory perspective include doses to the receptors that have been identified as critical. Groundwater concentrations are evaluated for the next 500 yrs. For the deep-time model, which models the performance of disposal of DU at Clive for the next 2.1 My, results are presented in terms of lake water concentrations assuming the return of a large pluvial lake in the Bonneville Basin, and sediment concentrations that remain after the pluvial lake recedes.

A summary is provided that includes further interpretation of results and comparison with performance objectives. More complete documentation of the details of the model development is contained in the Appendices, and also in the GoldSim model itself. This compendium of documents provides a thorough treatise of the Clive DU PA Model v1.0.

2.0 Introduction

The safe storage and disposal of DU waste is essential for mitigating releases of radioactive materials and reducing exposures to humans and the environment. Currently, a radioactive waste facility located in Clive, Utah and operated by Energy*Solutions* is proposed to receive and store DU waste that has been declared surplus from radiological facilities across the nation. The Clive Facility has been tasked with evaluating disposal of the DU waste in an economically feasible manner that protects humans from future radiological releases.

To assess whether the Clive Facility location and containment technologies are suitable for protection of human health, specific performance objectives for land disposal of radioactive waste set forth in Title 10 Code of Federal Regulations Part 61 (10 CFR 61) Subpart C, and promulgated by the Nuclear Regulatory Commission (NRC), must be met. In order to support the required radiological PA, a model is needed to evaluate doses to human receptors that would result from the disposal of DU and its associated radioactive contaminants.

This section provides an introduction to the general approach taken to developing version 1.0 of the Clive DU PA Model. The focus is on methods that have been undertaken at each step along the path, from description of the problem and the disposal facility under consideration, FEPs identification, CSM development, approaches to numerical modeling and evaluation of results.

2.1 General Approach

Performance Assessment models are complex probabilistic systems-level models that evaluate the long-term effects to human health and the environment of disposal of radioactive waste. The approach includes the following steps:

1. Identification of disposal options – in this case use of the Class A South embankment at the Clive Facility in Utah for disposal of DU waste, and specifics of the disposal configuration. This includes consideration of the regulatory environment in which the PA model is to be evaluated.

2. Identification of important FEPs that should be considered in the evaluation of the Clive disposal facility. This includes identification of human receptors who might be engaged in activities near or on the disposal facility.

3. Development of a CSM that captures the relevant FEPs. This includes cursory evaluation of the FEPs for the likelihood of occurrence and their consequence. If, for a given FEP the likelihood of occurrence or consequence is considered too small, then the FEP is not included in the CSM.

4. Development of a numerical or computational model for the PA. This translates the CSM into numerical code for processing. This includes model structure and model specification. The Clive DU PA Model is developed fully probabilistically, with coupling of all processes included in the model.

5. Model evaluation, including:

   a. uncertainty analysis, which compares the probabilistic output to the performance objectives,

   b. sensitivity analysis, which is used to identify the important parameters or components of the model in terms of prediction of the model output. This leads to model refinement or data collection if the uncertainties in the decisions that need to be made are considered to be too large.

6. Reporting of the PA model and its results, including:

   a. Doses to potential human receptors

   b. Population doses evaluated in the context of ALARA

   c. Groundwater concentrations

   d. Deep time concentrations in lake water and lake sediment

7. Quality Assurance.

A PA is a type of systematic (risk) analysis that addresses (a) what can happen, (b) how likely it is to happen, (c) what the resulting impacts are, and (d) how these impacts compare to regulatory standards. The essential elements of a performance assessment are (a) a description of the site and engineered system, (b) an understanding of events and processes likely to affect long-term facility performance, (c) a description of processes controlling the movement of contaminants from waste sources to the general environment, (d) a computation of metrics reflecting system performance including concentrations, doses, and other human health risk metrics to members of the general population, and (e) an evaluation of uncertainties in the modeling results that support the assessment.

Because of the long-term nature of the analysis, the intent of a PA is not necessarily to estimate actual long-term human health impacts or risks from a closed facility. Rather, the purpose of the Model is to provide a robust analysis that can examine and identify the key elements and components of the site, the engineered system, and the environmental setting that could contribute to potential long-term impacts. Because of the time-scales of the analysis and the associated uncertainty in knowledge of characteristics of the site, the waste inventory, the engineered system and its potential to degrade over time, and changing environmental conditions, a critical part of the PA process is also the consideration of uncertainty and evaluation of model and parameter sensitivity in interpretation of PA modeling results.

A probabilistic model includes a mathematical analysis of stochastic events or processes and their consequences. Probabilistic analysis acknowledges that events and processes are inherently uncertain, and hence involves characterization of uncertainty around expectation. Model output hence is expressed with the same characteristics of expectation and uncertainty, which lends itself to a global or probabilistic sensitivity analysis. Sensitivity analysis for probabilistic models is used to identify the parameters (variables) that are the most important predictors of the output for a given endpoint (e.g., dose to a resident, concentrations in groundwater). The important

predictors are those that explain most of the variability in the output variable of interest. Usually, for a given endpoint of interest, this is no more than a handful of input or explanatory variables. Because PA models are usually complex, dynamic, non-linear systems, these global sensitivity analysis methods involve complex non-linear regression models that capture the input of each input variable across its specified range (range of its probability distribution).

PA concerns modeling radioactive waste disposal facilities into the long-term future. As such, PA models must address both the spatial and temporal magnitude of PA. It is critical in a PA model to addresses the scale of the decisions that need to be made. Modeling is performed at the spatial and temporal scale that is needed to support PA decisions related to closure. In effect, system-level models might be fairly coarse, but this has advantages for evaluating how the system evolves over time. For example, all processes involved are fully coupled in the same model, probabilistic modeling can be performed to both characterize and manage uncertainty, and statistics and decision analysis can be incorporated into the modeling framework.

Results from a systems-level model are aimed at the decision objectives at the spatial and temporal scales of interest. These results are presented as probability distributions for the endpoints of interest (doses, concentrations, etc.), and comparisons are made with performance objectives where appropriate (dose, groundwater concentrations).

Given the PA model construction with respect to the spatio-temporal scales of the model, there are two levels of response. The first is for each hypothetical individual included in the model. Dose results are available for each receptor in every year of the model, up to 10 ky. Each dose result at this level represents individual dose to the concentrations in various media predicted by the model at that time. The dose parameters, however, are specific to the individual. This approach to modeling dose was taken for a few reasons: 1) There are not many receptors at Clive, in which case, from a computational perspective it was feasible to consider each individual receptor, and 2) This approach allows population dose to be estimated directly from the individual doses.

Although individual doses are available in the model, the output of interest is the mean dose. Traditionally this has been estimated as the mean dose to a hypothetical average individual. With this model, the mean dose is estimated directly from the individual doses. Mean doses are evaluated in each year of the model, however, traditionally for PA, interest lies primarily in the worst case year, in which case the peak mean dose across time is the metric of interest.

The effect is that average (mean) doses are available at multiple scales. Traditional comparison with performance objectives is performed with the peak mean dose, meaning the highest mean dose in a year across the 10-ky performance period. This simplification might have been taken previously because of technical practicability. However, with modern computer technology, such short-cuts are not necessary, and the mean dose within each model year can be evaluated directly. However, in the interest of precedent, the "peak of the means" is used in this document for comparison purposes. The problem with the peak of the means is that the peak might vary in time form simulation to simulation. Considering the peak of the means in this way overestimates dose, and, consequently, underestimates disposal system performance. In this model, for which radioactivity is increasing with time for the DU waste, the peak almost always occurs close to 10 ky, in which case this is not a major issue. The distribution of the peak of the means is presented

in this report. Note that there are 5,000 estimates of the peak of the mean for each receptor from the 5,000 simulations that are run. This is usually enough simulations to stabilize an estimate of the mean. The dose assessment model is described in detail in the white paper entitled *Dose Assessment* (Appendix 11).

If the distribution of the peak of the means is treated as if each simulation result is independent, then, because the model is constructed at the spatial and temporal scales as described above, the 95th percentile of the distribution is somewhat analogous to the notion of a 95% upper confidence limit that is commonly used under CERCLA. Comparisons may be made with the PA performance objectives using the median, mean and 95th percentile of the output distribution for each endpoint of interest.

For the ALARA analysis, the model is set up so that the population dose can be estimated for each receptor class in each year of the model. The 5,000 realizations provide 5,000 estimates of population dose in each year of the model. The population dose distribution can also be processed to include the cost to human health and society by assigning a dollar value to person rem. This process is described in detail in the *Decision Analysis* white paper (Appendix 12).

Once the results are obtained and compared to the performance objectives, a global sensitivity analysis is performed to identify the parameters that are the most influential in predicting each endpoint of interest. Often this is only a handful of parameters for each endpoint. The results of the sensitivity analysis can be used to determine if it might be useful to collect more data or otherwise refine the model before making final decisions. This is ostensibly a decision analysis task, which can be performed using the sensitivity analysis results as a basis for determining the benefit of collecting new data. The potential benefits would be seen in reduction in uncertainty in the model results. The sensitivity analysis methods used for this model are described in the white paper entitled *Sensitivity Analysis Methods* (Appendix 15).

This holistic approach to PA modeling is aimed at providing insights into disposal system performance. Although the model predicts or estimates doses to human receptors, among other endpoints, the more important aspect of this type of modeling is to gain an understanding of how the system might evolve over the time frames of interest, and to use this understanding to support decision making including ability to safely dispose of waste and optimization of waste placement within the disposal system.. No matter what doses are predicted, it is important to understand why those modeled doses are observed, and hence, what are the important features of the disposal system with regards to protection of human health and the environment.

2.2 General Facility Description

The Energy*Solutions* low-level radioactive waste disposal facility is west of the Cedar Mountains in Clive, Utah, as shown in Figure 2. Clive is located along Interstate-80, approximately 5 km (3 mi) south of the highway, in Tooele County. The facility is approximately 80 km (50 mi) east of Wendover, Utah and approximately 100 km (60 mi) west of Salt Lake City, Utah. The facility sits at an elevation of approximately 1302 m (4275 ft) above mean sea level (amsl). The Clive Facility is adjacent to the above-ground disposal cell used for uranium mill tailings that were

removed from the former Vitro Chemical company site in South Salt Lake City between 1984 and 1988 (Baird et al., 1990).

Currently, the Clive Facility receives waste shipped via truck and rail. Pending the findings of the PA, DU waste will be stored in a permanent above-ground engineered disposal embankment that is clay-lined with a composite clay and rock cap. The disposal embankment is designed to perform for a minimum of 500 years based on requirements of 10 CFR 61.7. The Energy*Solutions* Clive Facility is divided into three main areas (Figure 2):

- the Bulk Waste Facility, including the Mixed Waste, Low Activity Radioactive Waste (LARW), 11e.(2), and Class A LLW areas,
- the Containerized Waste Facility (CWF), located within the Class A LLW area, and
- the Treatment Facility (TF), located in the southeast corner of the Mixed Waste area.

Figure 2. Disposal and Treatment Facilities operated by Energy*Solutions*.

The DU waste under consideration is proposed for disposal in the Class A South (CAS) cell. The terms "cell" and "embankment" are here used interchangeably. That is, this Clive DU PA Model considers only to the long-term performance of DU disposed in this waste cell. The CAS embankment, or cell, is the western fraction of the Federal Cell (Figure 2). The eastern section is occupied by the 11e.(2) cell, which is dedicated to the disposal of uranium processing by-product waste, but not considered in this analysis.

The general aspect of the CAS embankment is that of a hipped cap, with relatively steeper sloping sides nearer the edges. The upper part of the embankment, known as the top slope, has a moderate slope, while the side slope is markedly steeper (20% as opposed to 2.4%). For this PA Model, no waste is placed under the side slopes, in which case modeling focuses on waste placed under the top slope. The embankment is also constructed such that a portion of it lies below-grade. Details of the design of the embankment are contained in the white paper entitled *Embankment Modeling* (Appendix 3).

DU waste from the Savannah River Site (SRS) and the gaseous diffusion plants (GDP) at Portsmouth, Ohio and Paducah, Kentucky has been proposed for disposal at the Clive facility. There are three categories of DU waste that are considered:

1. Depleted uranium oxide (UO_3) waste from the Savannah River Site (SRS) proposed for disposal at the Clive facility,
2. DU from the GDPs, which exists in two principal populations:
    a) DU contaminated with fission and activation products from reactor returns introduced to the diffusion cascades, and
    b) DU consisting of only "clean" uranium, with no such contamination.

The DU oxides that are to be produced at these sites "deconversion" plants will be primarily U_3O_8. The contamination problem arises from the past practice of introducing irradiated nuclear materials (reactor returns) into the isotopic separations process. Irradiated nuclear fuel underwent a chemical separation process to remove the plutonium for use in nuclear weapons. Uranium, then thought to be a rare substance, was also separated out, but contained some residual contamination from activation and fission products. This uranium was again converted to UF_6 for re enrichment, and was introduced to the gaseous diffusion cascades, contaminating them and the storage cylinders as well. Decay products (^{226}Ra), activation products (^{241}Am, ^{237}Np, ^{238}Pu, ^{239}Pu, ^{240}Pu, ^{241}Pu, ^{242}Pu), and fission products (^{90}Sr, ^{99}Tc, ^{129}I, ^{137}Cs) potentially contaminate the DU waste. The proposed inventory that is evaluated in the Model is described fully in the white paper entitled *Waste Inventory* (Appendix 4).

3.0 Features, Events and Processes

The conceptual site model (CSM) describes the physical, chemical, and biological characteristics of the Clive facility. The CSM, therefore, encompasses everything from the inventory of disposed wastes, the migration of radionuclides contained in the waste through the engineered and natural systems, and the exposure and radiation doses to hypothetical future humans. These site characteristics are used to define variables for the quantitative PA model that is used to provide insights and understanding of the future potential human radiation doses from the disposal of DU waste.

The content of the CSM informs the Model with respect to regional and site-specific features, events and processes, such as climate, groundwater, and human receptor scenarios. The CSM accounts for and defines relevant features, events, and processes (FEPs) at the site, materials and their properties, interrelationships, and boundaries. These constitute the basis of the Model, on which, or through which, radionuclides are transported to locations where receptors might be exposed.

A key activity in developing a PA for a radiological waste repository is the comprehensive identification of relevant external factors that should be included in quantitative analyses. These factors, termed "features, events, and processes" (FEPs), form the basis for scenarios that are evaluated to assess site performance.

The universe of FEPs that were screened and identified as relevant for the Clive Facility PA are documented in the white paper entitled *FEP Analysis for Disposal of Depleted Uranium at the Clive Facility* (Appendix 1) and further elaborated in the CSM document (*Conceptual Site Model for Disposal of Depleted Uranium at the Clive Facility* – Appendix 2).

4.0 Conceptual Site Model

The important components of the conceptual site model are described in the following sections. Details are contained in the white paper entitled *Conceptual Site Model for Disposal of Depleted Uranium at the Clive Facility* (Appendix 2).

4.1.1 Disposal Site Location

Energy*Solutions* operates a low-level radioactive waste disposal facility west of the Cedar Mountains in Clive, Utah, as shown in Figure 1. Clive is located along Interstate-80, approximately 5 km (3 mi) south of the highway, in Tooele County. The facility is approximately 80 km (50 mi) east of Wendover, Utah and approximately 100 km (60 mi) west of Salt Lake City, Utah. The facility sits at an elevation of approximately 1,302 m (4,275 ft) above mean sea level (amsl) and is accessed by both highway and rail transportation. The Clive Facility is adjacent to the above-ground disposal cell used for uranium mill tailings that were removed from the former Vitro Chemical company site in South Salt Lake City between 1984 and 1988 (Baird et al., 1990).

4.1.2 Disposal Site Description

Currently, the Clive Facility receives waste shipped via truck and rail. DU waste is proposed for disposal in a permanent above-ground engineered disposal embankment that is clay-lined with a composite clay and rock cap. The disposal embankment is designed to perform for a minimum of 500 years based on requirements of 10 CFR 61.7, which provides a long-term disposal solution with minimal need for active maintenance after site closure. More detail relating to the properties of the disposal embankment is provided in Section 4.1.2.1.

The Energy*Solutions* Clive Facility is divided into three main areas (Figure 2): the Bulk Waste Facility, including the Mixed Waste, Low Activity Radioactive Waste (LARW), 11e.(2), and Class A LLW areas, the Containerized Waste Facility (CWF), located within the Class A LLW area, and the Treatment Facility (TF), located in the southeast corner of the Mixed Waste area. This analysis considers only the Class A South (CAS) embankment.

4.1.2.1 Embankment

Depleted uranium waste is proposed for disposal in the Class A South disposal cell. The Class A South (CAS) Cell, which is part of the Federal Cell, is about 541 × 436 m (1,775 × 1,430 ft), with an area of approximately 24 ha (58 acres), and an estimated total waste volume of about 2.7 million m^3 (96 million ft^3). A drainage ditch surrounds the disposal cell on three sides, with 11e.(2) waste on the fourth side. The cell is constructed on top of a compacted clay liner covered by a protective cover. Waste will be placed above the liner and will be covered with a layered engineered cover constructed of natural materials. The top slopes will be finished at a 4% grade while the side slopes will be no steeper than 5:1 (20% grade).

The design of the Class A South Cell cover has been engineered to discourage erosion, reduce the effects of infiltration, and to protect workers and the public from radionuclide exposure. The cell cover is a layered composite of a clay radon barrier, filter material, sacrificial soil, and rip rap. The clay radon barrier is designed to minimize infiltration of precipitation and runoff and reduce the migration of radon from the waste cell. The filter material is intended to confine dew and condensates in order to reduce the likelihood of the radon barrier clay from drying out. The purpose of the rip rap cover is to ensure the integrity of the underlying layers and overall waste cell by providing protection from physical weathering sources such as erosion by water and wind. The detailed properties of each cell layer may be found in the white paper on *Embankment Modeling* (Appendix 3).

4.1.2.2 Waste Inventory

The waste inventory is limited to the disposal of DU wastes of two general waste types: 1) depleted uranium trioxide (DUO_3) waste from the Savannah River Site (SRS) and 2) anticipated DU waste as U_3O_8 from gaseous diffusion plants (GDPs) at Portsmouth, Ohio and Paducah, Kentucky. The quantity and characteristics of DU waste from other sources that has that already been disposed of at the Clive Facility was not included. A full list of radionuclides has been established for the PA modeling effort. The radionuclide species list was based upon process knowledge, radionuclides analyzed for (though not necessarily detected) in the DU waste

material, and decay products with half-lives over five years. The species list consists of the following radionuclides:

fission products:
Sr-90, Tc-99, I-129, Cs-137

progeny of uranium isotopes:
Pb-210, Rn-222, Ra-226, -228, Ac-227, Th-228, -229, -230, -232, Pa-231

uranium isotopes:
U-232, -233, -234, -235, -236, -238

transuranic radionuclides:
Np-237, Pu-239, -239, -240, -241, -242, Am-241

The waste inventory is discussed in more detail in the *Waste Inventory* white paper (Appendix 4) and in the *Conceptual Site Model* white paper (Appendix 1).

4.1.2.3 Climate

The following sections briefly describe the aspects of the regional climate that influence the performance of the site and engineered features. Further details are provided in the *Conceptual Site Model* white paper (Appendix 1), and in the *Unsaturated Zone Modeling* white paper (Appendix 5). In general the climate is dry, with evapotranspiration potential that exceeds precipitation on an annual basis. This leads to low infiltration rates, and subsequent relatively slow movement of radionuclides to groundwater. Also, the embankment is largely above grade, and the dry, sometimes windy, environment could lead to drying out of the embankment beyond what is considered in typical unsaturated zone models.

4.1.2.3.1 Temperature

Regional climate is regulated by the surrounding mountain ranges, which restrict movement of weather systems in the vicinity of the Clive facility. The most influential feature affecting regional climate is the presence of the Great Salt Lake, which can moderate downwind temperatures since it never freezes (NRC, 1993). The climatic conditions at the Clive Facility are characterized by hot and dry summers, cool springs and falls, and moderately cold winters (NRC, 1993). Frequent invasions of cold air are restricted by the mountain ranges in the area. Data from the Clive Facility from 1992 through 2009 indicate that monthly temperatures range from about -2°C (29°F) in December to 26°C (78°F) in July (Whetstone, 2006).

4.1.2.3.2 Precipitation

The Clive Facility is characterized as being an arid to semi-arid environment where evaporation greatly exceeds annual precipitation (Adrian Brown, 1997). Data collected at the Clive Facility from 1992 through 2004 indicate that average annual rainfall is on the order of 22 cm (8.6 in) per year (Whetstone, 2006). Precipitation generally reaches a maximum in the spring (1992-2004 monthly average of 3.2 cm [1.25 in] in April), when storms from the Pacific Ocean are strong

enough to move over the mountains (NRC, 1993; Whetstone, 2006). Precipitation is generally lighter during the summer and fall months (1992-2004 monthly average of 0.8 cm [0.32 in] in August) with snowfall occurring during the winter months (Whetstone, 2006; NRC, 1993; Baird et al., 1990).

4.1.2.3.3 Evaporation

Because of warm temperatures and low relative humidity, the Clive Facility is located in an area of high evaporation rates. NRC (1993) indicates that average annual pond evaporation rate at the Clive Facility is 150 cm/yr (59 in/yr), with the highest evaporation rates between the months of May and October. Previous modeling studies indicate that the Dugway climatological station nearby is comparable to the Clive site with respect to evaporation and have reported pan-evaporation estimates of 183 cm/yr (72 in/yr), which is considerably greater than average annual rainfall (Adrian Brown, 1997). Because of the high evaporation rate, the amount of groundwater recharge due to precipitation is likely very small except during high intensity precipitation events (Adrian Brown, 1997).

4.1.2.4 Unsaturated Zone

The engineered features of the landfill, including cap, waste, and liner, are all in the unsaturated zone (UZ), at least within the 10,000-yr duration of the quantitative model. The part of the UZ that extends from the bottom of the cell liner to the water table consists of naturally-occurring lake sediments from the ancestral Lake Bonneville. Since the cap is intentionally designed to restrict permeability, interstitial water in the UZ below the facility is not expected to migrate upwards through the cap to surface soils, as it might otherwise do naturally given the strong evaporation potential at the surface. Rather, it is expected to migrate slowly down to the water table, at a rate equal to the rate at which the engineered liner leaks.

Diffusion in the water phase may also play a role in the transport of waterborne contaminants in the UZ, since the advective flux is expected to be small. The concentration gradients in the UZ are also expected to be predominantly vertical, so diffusion will also occur in the vertical direction, oriented with the column of cells.

Diffusion in the air phase within the UZ below the facility will not be modeled, since the only diffusive species would be radon, which is of greater concern at the ground surface. Upward radon diffusion to the ground surface will be dominated by radon parents in the waste zone, and is modeled within the engineered cap. Unsaturated zone processes, material properties, and parameters represented in the PA model are described in detail in the *Unsaturated Zone Modeling* White Paper. The primary concerns for the PA are movement through the unsaturated zone of mobile radionuclides, such as ^{90}Sr, ^{99}Tc, and ^{129}I to groundwater and the upward diffusive movement of radon.

4.1.2.4.1 Infiltration

The infiltration model for the cap and cell uses calculations from the HELP program to develop vertical and lateral flow rates in the individual layers of the cap. The results of the HELP modeling determine the vertical flow of water through the engineered cell layers, the waste, and

the unsaturated zone. A numerical solution of Darcy's equation is used to determine the moisture contents in the radon barriers, waste layer, clay liner, and unsaturated zone from the vertical flow rates.

Comparisons of HELP modeling results with results from mechanistic unsaturated zone modeling programs such as UNSAT-H and HYDRUS at arid and semi-arid sites suggest that the HELP model will generally overestimate the vertical flow rates through waste cell covers (Meyer et al. 1996, Khire et al. 1997, Albright et al. 2002). These model comparisons indicate that the vertical flow rates through the CAS cell calculated using the HELP model are likely to be overestimated in the PA Model.

The cell and unsaturated zone infiltration modeling approaches and results are described in more detail in the *Unsaturated Zone Modeling* white paper (Appendix 5).

4.1.2.5 Geochemical

The conceptual model for the transport of radionuclides at the Clive Facility allows sufficient meteoric water infiltration into the waste zone to allow dissolution of uranium and daughters, fission products and potential transuranic contaminants (along with native soluble minerals). At first, leaching is likely to be solubility-limited with respect to uranium, and the leachate will migrate away from the source with the uranium concentration at the solubility limit. The other radionuclides are unlikely to be at a solubility limit. Depending upon the amount of water available, these radionuclides will either re-precipitate, once the thermodynamic conditions for saturation are reached, or remain in solution and be transported to the saturated zone. This water is expected to be oxidizing, with circum-neutral to slightly alkaline pH (similar to the upper unconfined aquifer), and an atmospheric partial pressure of carbon dioxide. However, the amount of total dissolved solids (TDS) is expected to be initially lower than the upper aquifer.

The composition of this aqueous phase will change as it reaches the saturated zone, with some increase in dissolved solids and potentially lower dissolved oxygen and carbon dioxide. The saturated zone for this PA model includes only the shallow, unconfined aquifer. Transport of radionuclides is expected to be restricted to this aquifer and not migrate to the lower aquifer due to a natural upward gradient at the facility. The chemical composition of the saturated zone is characterized as somewhat alkaline pH likely due to the presence of carbonates, mainly oxidizing though transient reduced conditions may exist, with high levels of dissolved ions of mainly sodium and chlorine.

The transport of dissolved radionuclides can also be limited by sorption onto the solid phase of associated minerals and soils within each of the zones considered in this PA model. The transport of uranium is limited by both solubility and the sorption of radionuclides in groundwater. Sorption consists of several physicochemical processes including ion exchange, adsorption, and chemisorption. Sorption is represented in the PA model as a partitioning coefficient (K_d) value.

Distributions of radionuclide-specific partitioning coefficients and solubilities were developed for the PA model considering the geochemical conditions in the cell, the unsaturated zone, and the shallow aquifer at the Clive facility. The development of these distributions is described in detail in the *Geochemical Modeling* white paper (Appendix 6). The primary concerns for the model

include the geochemical properties of ^{99}Tc as they affect movement to groundwater, and of uranium in its different chemical forms for the 10-ky and deep-time models.

4.1.2.6 Saturated Zone

Contaminants moving vertically in the UZ below the cell enter the saturated zone (SZ) beneath the disposal facility. The rate of recharge is the same as the Darcy flux (the rate of volume flow of water per unit area) through the overlying UZ, and is expected to be small enough that vertical transport within the SZ would be small. Most SZ waterborne contaminant transport will be in the horizontal direction, following the local pressure gradients, which are reflected in water table elevations in the shallow aquifer. A point of compliance in the groundwater has been established at 27 m (90 ft) from the edge of the embankment interior, so saturated transport is modeled to that point. Note that in the case of the proposed DU waste disposal, only the top slope section of the embankment would contain DU waste, so the effective distance from the DU waste to the well is lengthened by the width of the side slope section, to about 73 m (240 ft).

Saturated zone groundwater transport generally involves the processes of advection-dispersion and diffusion. Mean pore water velocity in the saturated zone is assumed to be determined by the Darcy flux and the porosity of the sediment. A range of values will allow the sensitivity analysis (SA) to determine if this is a sensitive parameter in the determination of concentrations at the compliance well and resultant potential doses. Modeling of fate and transport for the saturated zone pathway will include advection, linear sorption, mechanical dispersion, and molecular diffusion. Saturated zone processes and parameters represented in the PA model are described in detail in the *Saturated Zone Modeling* white paper (Appendix 7). The primary concern for the model is the breakthrough of ^{99}Tc at the monitoring well.

4.1.2.7 Air Modeling

Gaseous and particle-bound contaminants that have migrated to the surface soil layer are potentially subject to dispersion in the atmosphere. The effect of mechanical disturbance on human exposure to soil particulates is evaluated in the PA based on the effect of off-highway vehicle (OHV) use. However, although this mechanism may be consequential for human exposure, it is not likely to be a significant contributor to the overall rate of fine particulates emissions from the embankment over time. Aeolian (wind-related) disturbance is the primary cause of particulates emissions from the embankment and is the process modeled in the PA to estimate particulate emissions.

In addition to particulate emissions of contaminated surface soil due to aeolian erosion, emissions of gas-phase radionuclides diffusing across the surface of the embankment into the atmosphere are considered in the PA model. Note that this effect is counter-balanced by replacement with aeolian material that moves onto the cap. Diffusion modeling of radionuclide gases in the embankment, and estimation of flux into the atmosphere, is described in the *Unsaturated Zone* white paper (Appendix 5). For both particulate-bound and gaseous radionuclides, atmospheric dispersion modeling employing local meteorological data is conducted to calculate breathing-zone air concentrations above the embankment and at specific locations in the area where off-site receptors may be exposed (see *Dose Assessment* white paper – Appendix 11).

Atmospheric dispersion may result in significant bulk transport of fine particles modeling off of the embankment. Atmospheric dispersion modeling is also used to calculate the deposition flux of resuspended embankment particles in the areas adjacent to the embankment where ranchers and recreational receptors may be exposed. As particulates from the embankment are deposited on surrounding land, this surrounding area may become a secondary source of radionuclide exposure.

Atmospheric dispersion modeling was conducted outside of the GoldSim modeling environment, into which the model was abstracted. An atmospheric dispersion model is a mathematical model that employs meteorological and terrain elevation data, in conjunction with information on the release of contamination from a source, to calculate breathing-zone air concentrations at locations above or downwind of the release. Some models may also be used to calculate surface deposition rates of contamination at locations downwind of the release.

Both particle resuspension and atmospheric dispersion are first modeled outside of the GoldSim PA model, and the results are then incorporated into GoldSim. The particulate emission model used is a relatively simple model that has been adopted by EPA to estimate an annual-average emission rate of respirable particulates (approximately 10 μm and less, i.e., PM_{10}) from the ground surface. The air dispersion model used is AERMOD, which is EPA's recommended regulatory air modeling system for steady-state releases and suitable for calculating annual-average contaminant breathing zone air concentrations at various distances and in various directions from a source release. These models are described in detail in the *Atmospheric Transport Modeling* white paper (Appendix 8). Given the massive dilution that occurs for windblown sediments, it seems unlikely that this pathway will result in offsite accumulation of large amounts of transported radionuclides. Accumulation onsite seems more likely.

4.1.2.8 Biological

Biological organisms play an important role in soil mixing processes, and therefore are potentially important mediators of transport of buried wastes from deeper layers to shallower layers or the soil surface. Three broad categories are evaluated for their potential effect on the redistribution of radionuclides at the Clive facility: plants, ants, and burrowing mammals. The impact of these flora and fauna will be limited largely to the top several meters, in which case, the severity of their effect on radionuclides transport might be small. Details for all three categories can be found in the *Biological Modeling* white paper (Appendix 9).

4.1.2.8.1 Plants

Biotic fate and transport models have been developed to evaluate the redistribution of soils, and contaminants within the soil, by native flora and fauna. The Clive Facility is located in the eastern side of the Great Salt Lake Desert, with flora and fauna characteristic of Great Basin alkali flat and Great Basin desert shrub communities.

Plant-induced transport of contaminants is assumed to proceed by absorption of contaminants into the plants roots, followed by redistribution throughout all the tissues of the plant, both above ground and below ground. Upon senescence, the above-ground plant parts are incorporated into surface soils, and the roots are incorporated into soils at their respective depths.

Functional factors that contribute to the plant section of the biotic transport model include identifying dominant plant species, grouping plant species into categories that are significantly similar in form and function with respect to the transport processes, estimating net annual primary productivity (NAPP, a measure of combined above-ground and below-ground biomass generation), determining relative abundance of plants or plant groups, evaluating root/shoot mass ratios, and representing the density of plant roots as a function of depth below the ground surface.

Field surveys of the Clive site and surrounding areas were conducted by SWCA Environmental Consultants in September and December 2010 to identify plant species present in different vegetative associations around the Clive Site (SWCA, 2011). Five different vegetative associations were surveyed, with three associations representing the alkali flat/desert flat type soils found in the vicinity of Clive, and two associations representative of desert scrub/shrub-steppe habitat characteristic of slopes and slightly higher elevations with less-saline soil chemistry. A one hectare (100 m × 100 m) plot was established in each vegetative association, and each plot was surveyed for dominant plant species present, and the percent cover and density of each species. In addition, a small number of black greasewood, shadscale, halogeton, and Mojave seablite plants were excavated to obtain root profile measurements and above-ground plant dimensions. Plots 3 through 5 represent current vegetation at the Clive site, while Plots 1 and 2 are representative of less-saline soils that may develop on top of the waste cell cover.

A total of 41 plant species were identified on the five survey plots. Eighteen species each comprised at least 1% of the total cover on at least one plot. These 18 species were considered the most important for the purpose of modeling plant mediated transport of radiochemical contaminants at Clive. Species were grouped into five functional plant groups: grasses, forbs, greasewood, other shrubs, and trees. Greasewood is separated from other shrubs because of its status as a phreatophyte that can extend taproots in excess of five meters to reach groundwater. Annual and perennial grasses were grouped due to similar maximum rooting depths. Despite the ability of Greasewood to extend taproots, it will only do so if there is a water source to mine. There is no evidence in the Clive data that greasewood in the area of Clive extends to the water table. Also, the radon barrier acts as an impediment to deep rooting. Consequently, plant pathways for radionuclide transport are likely to have a limited effect in the current model.

4.1.2.8.2 Ants

Ants fill a broad ecological niche in arid ecosystems as predators, scavengers, trophobionts and granivores. However, it is their role as burrowers that is of main concern for the purposes of this model. Ants burrow for a variety of reasons but mostly for the procurement of shelter, the rearing of young and the storage of foodstuffs. How and where ant nests are constructed plays a role in quantifying the amount and rate of subsurface soil transport to the ground surface at the Clive site. Factors relating to the physical construction of the nests, including the size, shape, and depth of the nest, are key to quantifying excavation volumes. Factors limiting the abundance and distribution of ant nests such as the abundance and distribution of plant species, and intra-specific or inter-specific competitors, also can affect excavated soil volumes. Important parameters related to ant burrowing activities include nest area, nest depth, rate of new nest additions, excavation volume, excavation rates, colony density, and colony lifespan.

Modeling soil and contaminant transport by ant species assumes that ants move materials from lower cells to those cells above while excavating chambers and tunnels within a nest. These chambers and tunnels are assumed to collapse over time and return soil from upper cells back to lower cells.

Surveys for ants at Clive were limited to surface surveys of ant colonies, including identification of ant species, measurements (length, width, and height) of ant mounds, and determination of ant nest densities in each vegetative association (SWCA, 2011). No excavations of ant nests were performed at Clive to support this initial PA model, although excavations could be conducted to support future model iterations if ant nest depth and volume are found to be sensitive parameters. Total nest depth and nest volume were extrapolated from mound surface dimensions based on correlations reported in the literature for the dominant ant species at Clive. Only two species of ants were identified during the surveys, with the western harvester ant, *Pogonomyrmex occidentalis*, accounting for 62 of the 64 nests identified. The second ant species, a member of the genus *Lasius,* was only encountered twice, both times in the mixed grassland plot. Harvester ants also tend to create the largest and deepest burrows. Consequently, the characteristics of the harvester ants were included in the model.

Although the effect of burrowing ants is modeled, it is not expected to have a large influence on model results because ant nests are not assumed to get into the waste, which is about 5m or more below ground surface for the disposal configurations considered. In addition, the design of the cap is likely to limit the potential presence of ants on the embankment. That is, the rip rap and gravel layers included in the design are not conducive to the development of ant nests.

4.1.2.8.3 Burrowing Mammals

Burrowing mammals can have a profound impact on the distribution of soil and its contents near the soil surface. The degree to which mammals influence soil structure is dependent on the behavioral habits of individual species. While some species account for a large volume of soil displacement, others are less influential. Functional factors such as burrowing depth, burrow depth distributions, percent burrow by depth, tunnel cross-section dimension, tunnel lengths, soil displacement by weight, soil displacement by volume and animal density per hectare play a critical role in determining the final soil constituent mass by depth within the soil.

Modeling soil and contaminant transport by mammal species within the Clive PA model assumes animals move materials from lower cells to those cells above while excavating burrows. Burrows are assumed to collapse over time and return soil from upper cells back to lower cells. Thus, the balance of materials is preserved through time.

Each Clive plot was surveyed for small mammal burrows during September and October 2010 (SWCA 2011). Burrows were identified by animal category. Within the survey area four categories of mammal burrows were identified: ground squirrels, kangaroo rats, mouse/rats/voles, and one badger. Due to the small number of badger and ground squirrel burrows, the decision was made to treat all burrowing mammals as a single unit for modeling purposes. Small mammal trapping was conducted on the five Clive plots during the new moon in October 2010 to identify the principal small mammal fauna present in each vegetative association. Each 1-ha plot was

subdivided into 25 20-m × 20-m subplots. At the center of the each subplot, two Sherman® live traps were placed, for a total of 50 traps per plot.

Deer mice (*Peromyscus maniculatus*) were the most abundant small mammal captured during trapping, and were the only mammal captured in the plots located on the Clive Facility (Plots 3, 4, and 5). Plots 3, 4, and 5 were characterized by very low mammal densities, as evidenced by both the trapping results and the burrow surveys. With such a small population in plots 3, 4, and 5, the decision was made to average these plots. It is not clear if the cap layering of the Clive embankment will be conducive to the development of mammal burrows, however, the burrows are sufficiently shallow that it is unlikely that they will have a significant impact on radionuclide transport, and hence on doses to human receptors.

4.1.2.9 Erosion

The Class A South embankment is subject to erosion by the forces of wind and water. The conceptual model assumes that wind-blown material will infill the pore space between the larger materials of the cap, including the rip rap, in a short period of time. This wind-blown material has a finer particle size and moves more readily with wind or water forces acting on the cap than the rip rap or gravel. Wind blows material off-site (see Section 4.1.2.7), even while it replaces material that is removed from the cap. Water removes cap material through the formation of gullies. The large particle-sized material of the rip rap is generally considered to be resistant to movement by erosion. However, if there is sufficient disturbance by animals or OHVers, gullies are expected to form.

Once an initiating event has occurred, wherein a "nick" is formed in the rip rap of the cover (by natural or anthropogenic events), gully formation follows from water flowing in narrow channels, particularly during heavy rainfall events. Gully erosion typically results in a gully that has an approximate "V" cross section which widens (lateral growth) and deepens (vertical growth) through time until the gully stabilizes. The formation of gullies is a concern on uranium mill tailings sites and other long-term above-ground radioactive waste sites (NRC 2010). Gully erosion has the potential to move substantial quantities of both cover materials and waste, should the waste material be buried close to the surface. Gully outwash forms depositional fans on the slopes of the embankment. Gullies might form initially on the embankment through disturbance attributed to animal burrowing, or by human induced mechanisms such as cattle paths or OHV tracks.

In the Clive DU PA Model, a gully is assumed to have a triangular cross-section, with the bottom of the gully being a curved line, steeper where it initiates and flatter where the gully emerges from the embankment. The slope of the thalweg (bottom) of the gully depends on:

- the height of the gully thalweg above the mouth of the gully,
- the horizontal distance from the ridge of the embankment downslope,
- the steepness of the slope, and
- the curve of the gully thalweg, characterized by a shape parameter b.

Several parameters are given probability distributions to incorporate uncertainty, including *b*, the angle of repose of the gully, the angle of repose of the fan formed by the gully outwash, and the distance from the ridge at which the gully initiates. Some of these parameters may be more likely to affect whether or not a gully gets into the waste than other parameters. After parameter values are chosen for the input parameters, a system of equations is solved so that the volume of the fan (made up of the gully outwash) is the same as the volume of the gully, and so that the height of the fan is the same as the height of the gully bottom where the gully emerges from the embankment. More detail on gully calculations can be found in the *Erosion Modeling* white paper (Appendix 10).

The gully model is a simplistic model of gully erosion and landscape evolution. For example, the model assumes that 1) a gully forms instantly and doesn't change with time, 2) that between 1 and 20 gullies only are allowed to form, and 3) that gullies do not interact with other model processes such as biotic transport (e.g., no plants grow in a gully). This stylized model was used to provide a basis for discussion of whether or not gully formation is an important consideration in this waste disposal system, and to evaluate the consequences of human activities that inadvertently cause doses to future humans. To apply the effects of gully formation to doses, the average waste concentrations exposed by the gully and the average waste concentration of material removed by the gully are used. The exposure area for this waste concentration is the surface area of the fan plus the surface area of the gully for which waste layers are exposed. More detail on the dose calculations for the gully model can be found in the *Dose Assessment* white paper (Appendix 11).

4.1.2.10 Dose Assessment

The dose assessment in the Model addresses potential radiation dose to any receptor who may come in contact with radioactivity released from the disposal facility into the general environment (10 CFR 61.41).The objective of a dose assessment in a radiological PA is to provide estimates of potential doses to humans over time from radioactive releases from a disposal facility after closure, as described in Section 3.3.7 of NRC (2000 – NUREG 1573). As described below, the critical groups in the Model are defined as ranchers and recreationalists.

The radiation dose limit for protection of the general population is 25 mrem/yr, as a total effective dose equivalent (TEDE). Dose limits for radiological PAs are defined in UAC Rule R313-25-19 and10 CFR 61.41as an equivalent of 0.25 mSv (25 mrem) to the whole body, 0.75 mSv (75 mrem) to the thyroid, and 0.25 mSv (25 mrem) to any other organ of any member of the public. However, the radiation dosimetry underlying these dose metrics is based on a methodology published by the International Commission on Radiation Protection (ICRP) in 1959. More recent dose assessment methodology has been published as ICRP Publication 30 (ICRP, 1979) and ICRP Publication 56 (ICRP, 1989), employing the TEDE approach. As stated in Section 3.3.7.1.2 of NRC (2000), "As a matter of policy, the Commission considers 0.25 mSv/year (25 mrem/year) TEDE as the appropriate dose limit to compare with the range of potential doses represented by the older limits…"

The period of performance for a radiological PA defined in UAC Rule R313-25-8 requires evaluation for a minimum compliance period of 10 ky, with additional simulations for a qualitative analysis for the period where peak hypothetical dose occurs. The scope of this Model

includes modeling of the disposal system performance to the time of peak hypothetical radiological dose (or peak radioactivity, as a proxy), and to quantify dose within the time frame of 10 ky.

4.1.2.10.1 Receptors and Exposure Scenarios

Receptors in a PA are categorized in UAC Rule R313-25-8 and10 CFR 61.41 according to the labels "member of the public" (MOP) and "inadvertent human intruder" (IHI). The regulatory basis for, and interpretation of these categories of receptors is provided in Section 1.3. The MOP is essentially a receptor who is exposed outside the boundaries of the facility, and the IHI is someone who intrudes onto the facility and may directly contact the waste (e.g., by well drilling, or basement construction). The "critical group" receptors evaluated are modeled to receive exposure both upon the disposal embankment and in adjacent areas according to the activities foreseen (ranching and recreational uses). Both scenarios are evaluated under post-institutional control conditions. The Model may be run with or without the formation of gullies.

Ranching Scenario. The land surrounding the Clive Facility is currently utilized for cattle and sheep grazing. Ranchers typically use off-highway vehicles (OHVs, including four-wheel drive trucks) for transport. Activities are expected to include herding, maintenance of fencing and other infrastructure, and assistance in calving and weaning. Ranchers may be exposed to contamination via the pathways outlined in Table 1.

Recreational Scenario. Recreational uses on the land surrounding the Clive Facility may involve OHV use, hunting, target shooting of inanimate objects, rock-hounding, wild-horse viewing, and limited camping. As soil develops on the rip-rap surface of the cap and plant succession proceeds, the disposal unit may become more attractive for different types of recreational activities. It is assumed in the Clive DU PA Model that recreational OHV riders ("Sport" OHVers; i.e., OHV users who use their vehicles for recreation alone) and hunters using OHVs ("Hunters"), both of whom may also camp at the site, represent the most highly-exposed recreational receptors. Recreationalists may be exposed to contamination via the pathways outlined in Table 1.

Table 1. Exposure Pathways Summary

Exposure Pathway	Ranching	Recreation
Inhalation (wind derived dust)	×	×
Inhalation (mechanically-generated dust)	×	×
Inhalation (gas phase radionuclides)	×	×
Ingestion of surface soils (inadvertent)	×	×
Ingestion of game meat		× (Hunter)
Ingestion of beef	×	
External irradiation – soil	×	×
External irradiation – immersion in air	×	×

The ranching and recreation scenarios are characterized by potential exposure related to activities both on the disposal site and in the adjoining area. Specific off-site points of potential exposure also exist for other receptors based upon present-day conditions and infrastructure. Unlike ranching and recreational receptors who might be exposed by a variety of pathways on or adjacent to the site, these off-site receptors would likely only be exposed to wind-dispersed contamination, for which inhalation exposures are likely to predominate. Five specific off-site locations and receptors are evaluated in the Clive PA, including:

- Travelers on Interstate-80, which passes 4 km to the north of the site;
- Travelers on the main east-west rail line, which passes 2 km to the north of the site;
- Workers at the Utah Test and Training Range (UTTR, a military facility) to the south of the Clive facility, who may occasionally drive on an access road immediately to the west of the Clive Facility fence line;
- The resident caretaker at the east-bound Interstate-80 rest facility (the Grassy Mountain Rest Area at Aragonite) approximately 12 km to the northeast of the site, and,
- OHV riders at the Knolls OHV area (BLM land that is specifically managed for OHV recreation) 12 km to the west of the site.

4.1.2.11 ALARA

CFR (Section 61.42) defines a second decision rule that pertains to populations as well as individuals. The regulation states "reasonable effort should be made to maintain releases of radioactivity in effluents to the general environment as low as is reasonably achievable" (or ALARA). The ALARA concept can be applied to either individuals or populations. In the context of the Clive DU PA Model, ALARA is applied to collective doses germane to the receptor populations described in the Section 4.1.2.10.

The ALARA process is also described in DOE regulations and associated guidance documents such as 10 CFR Part 834 and DOE 5400.5 ALARA (10 CFR 834; DOE 1993, 1997), and in other NRC documents (NRC, 1995, 2000). The definitions in each case are very similar; indicating that exposures should be controlled so that releases of radioactive material to the environment are as low as is reasonable taking into account social, technical, economic, practical, and public policy considerations.

The probabilistic Clive DU PA Model is designed to estimate individual annual doses to hypothetical individuals in future populations that may be exposed to radionuclide releases from the Clive Facility. The model is also able to aggregate individual doses into estimates of collective and cumulative population dose on an annual basis as well as over the 10-ky period of performance. Given this model structure, an opportunity exists with the Clive DU PA Model to evaluate ALARA in the context of population dose.

The overall implication of the various Agency regulations and guidance documents regarding ALARA is that many factors should be taken into account when considering the potential benefits of different options for disposal of radioactive waste. In order to implement ALARA in a

logical system, and so that economic factors are taken into consideration, a decision analysis is implied. Decision analysis is the appropriate mechanism for evaluating and optimizing disposal, closure and long term monitoring and maintenance of a radioactive waste disposal system. Decision options for disposal at Clive include engineering options and waste placement. More generally, if decision analysis is applied, then a much wider range of options can be factored into the decision model, such as transportation of waste, risk to workers, and effect on the environment. However, for the current Model, the focus is on different options for waste disposal within the current proposed configuration of the Class A South embankment.

The decision analysis in this context is essentially a benefit-cost analysis, within which different options for the placement of waste are evaluated. For each option, the Model predicts doses to the array of receptors, and the consequences of those doses are assessed as part of an overall cost model, which also includes the costs of disposal of waste for each option. The goal is to find the best option, which is the option that provides the greatest overall benefit. The consequences of risk can be measured through a simplification that is available in ALARA guidance, including NRC 1995, which provides the basis for, and history of, assigning a dollar value to person-rem as a measure of radiation dose. Prior to the NRC (1995) guidance, a single value of $1,000 per person-rem was recommended, with the accompanying assumption that a discount rate would not be applied. The history of the selection of this value is described in NRC, 1995, and further references to prior documents. In 1995, NRC instead promoted the idea of using $2,000 per person-rem as the relevant value, subject to present worth considerations. This appears to be an overt attempt by the NRC to allow an economic decision analysis to be performed, allowing for a discount factor to be used in the assessment of ALARA. This is made clearer in NRC, 2000, which provides examples and formulas for how to implement ALARA, which include discount factors of 7% for the first 100 years, and 3% thereafter. These are steep discounting rates that result in small costs comparatively at 100 years into the future. DOE guidance also suggests that a range of $1,000 to $6,000 could be considered (DOE, 1997), but that the $2,000 value is sufficient for most purposes. The allowable range presented by DOE, however, could be used to describe uncertainty over the appropriate value.

In assigning a value to the person-rem cost to society of radiation dose, the agencies have short-circuited a full decision analysis. This is reasonable for a first pass at a decision analysis associated with the proposed disposal at Clive. Hence, the value of $2,000 is applied to the population dose. Application of the ALARA process to the Clive DU PA Model is described more completely in the *Decision Analysis* white paper (Appendix 12).

4.1.2.12 Groundwater Concentrations

Apart from individual and population dose evaluations, evaluation of the PA also requires comparison of groundwater concentrations with groundwater protection levels, or GWPLs. That is, the State of Utah imposes limits on groundwater contamination, as stated in the Ground Water Quality Discharge Permit (UWQB, 2010). Part I.C.1 of the Permit specifies that GWPLs in Table 1A of the Permit shall be used for the Class A LLW Cell. Table 1A in the Permit specifies general mass and radioactivity concentrations for several constituents of interest to DU waste disposal. This includes values for mass concentration of total uranium, radium, and gross alpha and beta radioactivity concentrations for specific wells where background values were found to

be in exceedence of the Table 1A limits. Part I.D.1 of the Permit specifies that the performance standard for radionuclides is 500 years. Relevant GWPLs for Clive are:

- Strontium-90 42 pCi/L,
- Technetium-99 3,790 pCi/L,
- Iodine-129 21 pCi/L,
- Thorium-230 83 pCi/L,
- Thorium-232 92 pCi/L,
- Neptunium-237 7 pCi/L,
- Uranium-233 26 pCi/L,
- Uranium-234 26 pCi/L,
- Uranium-235 27 pCi/L,
- Uranium-236 27 pCi/L, and
- Uranium-238 26 pCi/L.

The main concern for the PA model is the potential for transport of ^{99}Tc, a contaminant in the DU waste, to the point of compliance.

Note that according to the Permit, groundwater at Clive is classified as Class IV, saline ground water, according to UAC R317-6-3 *Ground Water Classes,* and is highly unlikely to serve as a future water source. The underlying groundwater in the vicinity of the Clive site is of naturally poor quality because of its high salinity and, as a consequence, is not suitable for most human uses, and is not potable for humans. However, the Clive DU waste PA will calculate estimates of groundwater concentrations at a the location of a virtual well near the CAS embankment for comparison with the GWPLs.

4.1.2.13 Deep Time Assessment

The approach to deep time modeling is briefly described in the *Conceptual Site Model for Disposal of Depleted Uranium at the Clive Facility* white paper (Appendix 2). A more in-depth discussion of the deep time modeling methodology is described in *Deep Time Assessment for the Clive PA* white paper (Appendix 13). The focus of the deep time evaluation is to assess the potential impact of glacial epoch pluvial lake events on the CAS waste embankment from 10 ky through 2.1 My post-closure. (note that this model is termed the "deep-time" model.) A pluvial lake is a consequence of periods of extensive glaciation, and results from low evaporation, increased cloud cover, increased albedo, and increased precipitation in landlocked areas. Given that long-term climatic cycles of 100 ky are considered very likely in the next 2.1 My, it is assumed that large lakes will return to the Bonneville Basin in the future. In addition to large lakes, intermediate sized lakes are also assumed to occur, periodically during a 100-ky glacial cycle. Events that might occur in deep time other than the occurrence of intermediate lakes and the cyclic return of large lakes (e.g., meteor strikes and a large eruption at Yellowstone) are not considered further in this model because their likelihood is relatively small, and their consequences are likely to be much greater and far reaching for human civilization.

For the deep time scenarios, the PA model provides a qualitative assessment of the future consequences of present-day disposal of DU waste to the environment. While no exposure or dose assessment is attempted, tracking of radioactive species concentrations provides insight into waste disposal and embankment construction design and performance. Long-term historical information on the area surrounding the Clive site is sparse, providing only a broad depiction of historical behavior of lake cycles in the Bonneville Basin. Thus, the model utilized for projecting into the long-term future is largely conceptual or stylized, providing a similarly broad depiction of future behavior

There are two components of the model used to represent the deep time scenarios. The first is modeling lake formation and dynamics in the Bonneville Basin. The second is modeling the fate of the CAS embankment and disposed DU waste.

For the first component, the deep time evaluation focuses on potential releases of radioactivity following a series of pluvial lake events caused by glacial cycles assumed to occur (approximately) every 100 ky. The 100-ky glacial periodicity is based on historical ice core and the benthic marine isotope data for the past 800 ky. These cycles are also consistent with information regarding orbital forcing, and the periodicity suggested by the Milankovitch cycles.

These 100 ky glacial cycles form the basis for modeling the return and recurrence of lake events in the Bonneville Basin. The lake formation model is applied to each 100 ky cycle similarly. One large lake is assumed to occur every in each 100 ky cycle, and several intermediate lakes are allowed to form during the transgressive and regressive phases of the large lake. Note that the current 100-ky cycle is not modeled differently than future glacial cycles, despite evidence that the current inter-glacial period might last for another 50 ky (Berger and Loutre, 2002). In the model, therefore, an intermediate lake can return sooner than might be expected in the current 100-ky cycle. The precise timing of the return of a lake at or greater than the elevation of Clive is not as important as the event itself.

For the second component, it is assumed that destruction of the CAS embankment and fate of the DU waste will result from the effects of wave action from an intermediate or large lake. In effect, it is assumed that a lake is large enough that obliteration of the embankment will occur. In this obliteration scenario, all of the embankment material above grade is dispersed across a large localized area through wave action, although this includes all the DU waste, even if some DU waste was disposed below grade. Inclusion of the below grade waste is conservative, since it allows more DU waste to migrate into returning lakes and future sediment. The waste material is mixed with sediment and then enters the lake system via dissolution. A simplifying, conservative assumption is to limit dissolution to a column above the waste dispersal area. This assumption is conservative because lake water will probably mix more extensively, creating greater dilution. As a result, these assumptions lead to greater concentrations of waste than is probably reasonable. The conservatism is included in this model because of the lack of data that exists to quantify the processes.

The deep-time model assumes that the form of DU available for deep-time transport is U_3O_8, which is far less soluble than UO_3. Fate and transport modeling performed using the PA Model indicates that the relative soluble UO_3 will have migrated transported to groundwater within 50 ky. Consequently, the deep time model focuses on U_3O_8 as the form of DU available for deep-

time transport. While the lake is present, some waste in the water column will bind with carbonate ions and precipitate out into oolitic sediments, while the remaining waste will fall out with the sediment as the lake eventually recedes. The model assumes the waste is fully mixed with the accumulated sediments, a conservative assumption, since some waste is likely to be buried rather than mixed with future lake sediments. The extent of mixing of previous sediment with new sediment is not well understood; hence an assumption that the sediments completely mix is expedient, and probably leads to conservative results. All of the waste that has dissolved into the lake re-enters the lake sediment once the lake recedes. Overall sediment concentrations decrease over time because the amount of waste does not change other than through decay and ingrowth, whereas more sediment is added over time.

Thus the deep-time model should be regarded as conceptual and heuristic. The intent is to present a picture of what the long-term future might hold for the DU waste disposal embankment, rather than to provide a quantitative, temporally-specific, prediction of future conditions, or an assessment of exposure or dose to human receptors. The type of glacial climate change envisioned in the deep-time model will probably have wide-reaching consequences for the planet and human society, that are far beyond the scope of a PA for disposal of radioactive waste.

5.0 Model Structure

5.1 Summary of Important Assumptions

The results of the Clive DU PA Model depend critically on the model structure, the model specification (input probability distributions, for example) and the assumptions that underlie the model. That is, the results are fully dependent, or conditional, on the Model. The most important assumptions are identified in this section.

5.1.1 Points of Compliance

Points of compliance in a PA are usually defined in terms of the location in the accessible environment at which human health is evaluated in the dose assessment, and the location at which groundwater concentrations are used for comparison to GWPLs. For this model, the primary receptors (ranchers, recreators) are assumed to spend time on the site, and off the site in the general vicinity. Other receptors are defined at points in space (See Section 4.1.2.10.1). Note that the ALARA analysis addresses the same points of compliance.

Groundwater concentrations are evaluated at a virtual well located 27 m (90 ft) from the interior of the waste embankment. In the case of the proposed DU waste disposal, only the top slope section of the embankment would contain DU waste, so the effective distance from the DU waste to the well is lengthened by the width of the side slope section, to about 73 m (240 ft).

For the deep-time model, there are no receptors that are considered, and doses are not calculated. Instead, concentration of radionuclides are estimated in lake water and in lake sediment in the general vicinity of the CAS embankment.

5.1.2 Time Periods of Concern

There are four time periods that have import in this PA. The PA model is run fully quantitatively for dose endpoints for 10 ky. Peak mean dose is estimated and used for comparison with performance objectives for this time frame. The ALARA analysis is also performed for this period of time.

An institutional control period of 100 y is assumed, during which time doses are not calculated, because access to the site is assumed to be not possible.

Groundwater concentrations are compared to GWPLs for the first 500 years of the model, since this is the compliance period that is applied to the GWPLs under Utah Code.

The deep-time model is run for 2.1 My because the DU does not achieve secular equilibrium until about that time. That is, the model is run to peak activity of the DU, rather than to peak dose, which is undefined that far into the future.

5.1.3 Closure Cover Design Options

The engineered system in the PA model allows for evaluation of many different disposal configurations. DU waste is assumed to not be disposed under the side slopes. Otherwise there are 27 waste layers in the model, each about 0.5 m thick, starting with Layer 1 directly under the cap. The layers are numbered one through 27, with the 27th layer at the bottom of the waste cell. Layers 21 through 27 are below grade. Only one type of waste can be placed in a specific layer. Three disposal configurations are considered in this PA:

1. GDP contaminated waste in Layer 7 – SRS waste in Layer 8 – GDP uncontaminated waste in Layers 9-27. This model is termed the 3-m model, because Layer 7 is 3 m below the cap. Note that fill material is assumed for the 3 m between the cap and Layer 7.

2. GDP contaminated waste in Layer 11 – SRS waste in Layer 12 – GDP uncontaminated waste in Layers 13-27. This model is termed the 5-m model, because Layer 11 is 5 m below the cap. Note that fill material is assumed for the 5 m between the cap and Layer 11.

3. GDP contaminated waste in Layer 21 – SRS waste in Layer 22 – GDP uncontaminated waste in Layers 23-27. This model is termed the 10-m model, because Layer 21 is 10 m below the cap. Note that fill material is assumed for the 10 m between the cap and Layer 21. This model places all waste below grade.

These three configurations span a fairly wide range of options, from disposal near the cap, to disposal below grade.

5.1.4 Waste Concentration Averaging

Within each waste layer the contents of the waste are assumed to include the waste material and the fill material needed to occupy the layer volume. Since each layer represents a mixing cell, the concentration of the radionuclides is averaged throughout the layer. That is, each drum or cylinder is not modeled separately. This is typical of PA models, and is reasonable provided transport from the actual configuration does not differ greatly from transport from the modeled configuration.

5.1.5 Environmental Media Concentration Averaging

Similarly to the waste layers, concentrations in the environmental media are averaged throughout the cell that represents the medium. For example, the concentration of uranium in deep-time lake sediment is the average concentration throughout the sediment layer that is defined by its model cell.

5.1.6 Members of the Public

MOP is defined in terms of the receptors who perform activities in the vicinity of the Clive facility. This includes receptors at specific locations offsite as described in Section 4.1.2.10.

5.1.7 Inadvertent Human Intrusion

Following NRC 10 CFR 61, inadvertent intrusion is defined in terms of receptors who might perform some activities onsite. This includes ranchers, hunters and OHV enthusiasts. Inadvertent intrusion is often used in terms of direct but inadvertent access to the waste (e.g. through well drilling or basement construction), for which the initiator is exposed. However, such direct activities are unlikely at this site. The types of activities here do not result in direct exposure to the waste by the initiator, but potentially to future receptors. However, the receptors identified here are engaged in onsite activities, and are hence indirectly exposed to the DU waste.

5.1.8 Deep Time evaluation

The deep-time evaluation depends on the return of a lake in the Bonneville Basin that is large enough to obliterate the CAS embankment. Such a lake is assumed to occur more than once in each 100-ky glacial cycle. Once the CAS embankment is obliterated, the material is assumed to disperse within the vicinity of Clive. The dispersed waste then migrates into lake water through diffusion. All wastes that leave the sediment return to the sediment as the lake recedes, either physically or chemically. The wastes are assumed to mix with lake sediment in each lake cycle.

The outputs of interest are concentrations of radionuclides in lake water and in lake sediment.

5.2 Distribution Averaging

Most parameters in the Clive DU PA Model correspond to physical quantities that represent an average of some type. Some parameters represent averages over time, as they represent typical behavior that will be used throughout the 10-ky performance period, such as annual precipitation. Other parameters represent averages over space. For example, properties of vegetation represent an average vegetation effect across a model area, while soil properties represent an average across a volume of material represented by a model cell. When data are available that represent small amounts of time relative to the 10,000 years, or small areas/volumes relative to the model cells, then it is the *mean* of the data distribution that needs to be modeled.

To capture the temporal domain of the model, time steps in this type of systems-level dynamic probabilistic model are usually on the order of several to many years. Consequently, the average effects over long time frames, assuming no catastrophic changes in the system, are far more important than the effects on the scale of days, hours, minutes or seconds. Spatial and temporal scaling of available data, which are usually collected at points in time and space, is critical for the success of systems-level models. Scaling in this context is essentially an averaging process both spatially and temporally. Simple averaging works well if the effect on the response of a variable or parameter is linear. Otherwise, some care needs to be taken in the spatio-temporal averaging process. In addition, these types of models are characterized by differential equations and multiplicative terms. Averaging is a linear construct that does not translate directly in non-linear systems. Again, care needs to be taken to capture the appropriate systems-level effect when dealing with differential equations and multiplicative terms.

Another important statistical issues that is often overlooked in PA is correlation between inputs. Many parameters in the Clive DU PA Model are related to one another. One parameter may be physically constrained by the value of another parameter, or they may simply tend to vary together. When joint data are available, a simple approach is to simply calculate the sample correlation of the parameters in the data and apply the same correlation to the parameters in the model to induce a joint distribution. A simple correlation structure may not fully capture the relationship between two parameters but often provides a reasonable first approximation. Where a correlation structure is used in the Clive DU PA Model, the correlation algorithms implemented in GoldSim for Gaussian copula are used (Iman and Conover 1982, Embrechts et al. 2001).

Where data and expertise are available, it is generally preferable to construct joint distributions for the parameters by constructing a marginal distribution for one parameter and *conditional* distributions for the remaining parameters. By fitting a distinct conditional distribution of the second parameter for each possible value of the first parameter, a more realistic relationship might be constructed than can be achieved through simple correlation

The statistical methods used for appropriate spatio-temporal scaling and correlation effects are described in the *Development of Probability Distributions* white paper (Appendix 14).

5.3 Model Evaluation through Uncertainty and Sensitivity Analysis

The Clive DU PA is built as a probabilistic systems-level model. Systems-level modeling is geared towards decision objectives, and is a style of bottom-up modeling for which model refinement and iteration is performed in response to model evaluation. Model evaluation is performed throughout model development, but in the final stages it involves uncertainty analysis and sensitivity analysis. Quantitative assessment of the importance of inputs is necessary when the level of uncertainty in the system response exceeds the acceptable threshold specified in the decision making framework. One of the goals of sensitivity analysis is to identify which variables have distributions that exert the greatest influence on the response.

Uncertainty is captured directly for probabilistic system-level models. The input probability distributions are used to capture the range of possible parameter values. For probabilistic models, sensitivity analysis is performed simultaneously for all input parameters. This approach is termed global sensitivity analysis. It is a very powerful tool at the disposal of probabilistic modeling for identifying parameters that are important predictors of the model output, and it is not constrained by the user's preconceptions of what may be important. In addition to global sensitivity analysis, probabilistic models can be evaluated numerically in an uncertainty analysis and for value of information. Uncertainty analysis in this context involves comparison of the output distribution to performance metrics. A determination can then be made based on the comparison of the compliance of the disposal system. Value of information analysis can be performed to identify parameters for which uncertainty reduction in the output of interest might best be achieved, if it is necessary to reduce uncertainty. This approach can also be used in the context of ALARA contamination goals, to determine if further uncertainty reduction can reasonably be performed.

Sensitivity analysis is a very important tool for understanding the model. For those parameters that are deemed as important, and if the uncertainty analysis indicates, then there are options for

further model refinement. These options include further data collection, and refinement of the model. Uncertainty and sensitivity analysis are applied to each endpoint (model output) separately. Consequently, it is reasonable to expect that some of the endpoints are sensitive to different inputs. For example, output doses might be sensitive to parameters that are related to radon production and transport, whereas the groundwater concentrations might be sensitive to ^{99}Tc inventory or Kd. Consequently, each endpoint might have different needs regarding further data collection or model refinement.

Sensitivity analysis can be used to help identify those inputs for which uncertainty reduction through further information collection will have the most impact on reducing uncertainty in the model response. However, sensitivity analysis of high dimensional probabilistic models can be computationally challenging. These challenges can be met through machine learning methods applied to probabilistic simulation results. Further details are provided in the *Sensitivity Analysis Methods* white paper (Appendix 15).

Another aspect of uncertainty when running probabilistic simulations is simulation stability. The final statistics of interest might relate to the mean output, or a percentile of the output, and therefore may require a large number of simulations for stability of the estimate of the statistic. The question is, how large? The number of simulations needed can be determined by running a different number of simulations for each endpoint and statistic of interest. Otherwise, simulation uncertainty could interfere with the uncertainty and sensitivity analysis.

5.4 Clive DU PA Model Structure

The Clive DU PA Model is written using the GoldSim systems modeling software. Like other such models, its structure is hierarchical, with nested "Containers" providing the means to organize the model into different conceptual parts (see Figure 3). This model uses Containers to basic modeling constructs such as Materials, and contaminant transport Processes that are global (model-wide) in scope. Other containers are devoted to distinct topics, such as Inventory definitions, Disposal calculations, Exposure and Dose calculations, comparisons to GWPLs, and the development of Deep Time Scenarios. Supplemental containers define dashboards used for running the model and displaying results, collected Results from calculations around the model, Simulation Settings for model controls, and Documentation. The role of each of these is discussed below. For instructions on how to use the model, consult the *Clive DU PA Model User Guide*.

The purpose of this model is to simulate, to a degree sufficient for decision making, the fate and transport of radionuclides proposed for disposal in the Clive Facility, and to assess their potential effects on future individuals and populations. This is done in the realm of environmental transport modeling coupled with the modeling of health physics and toxicity to humans.

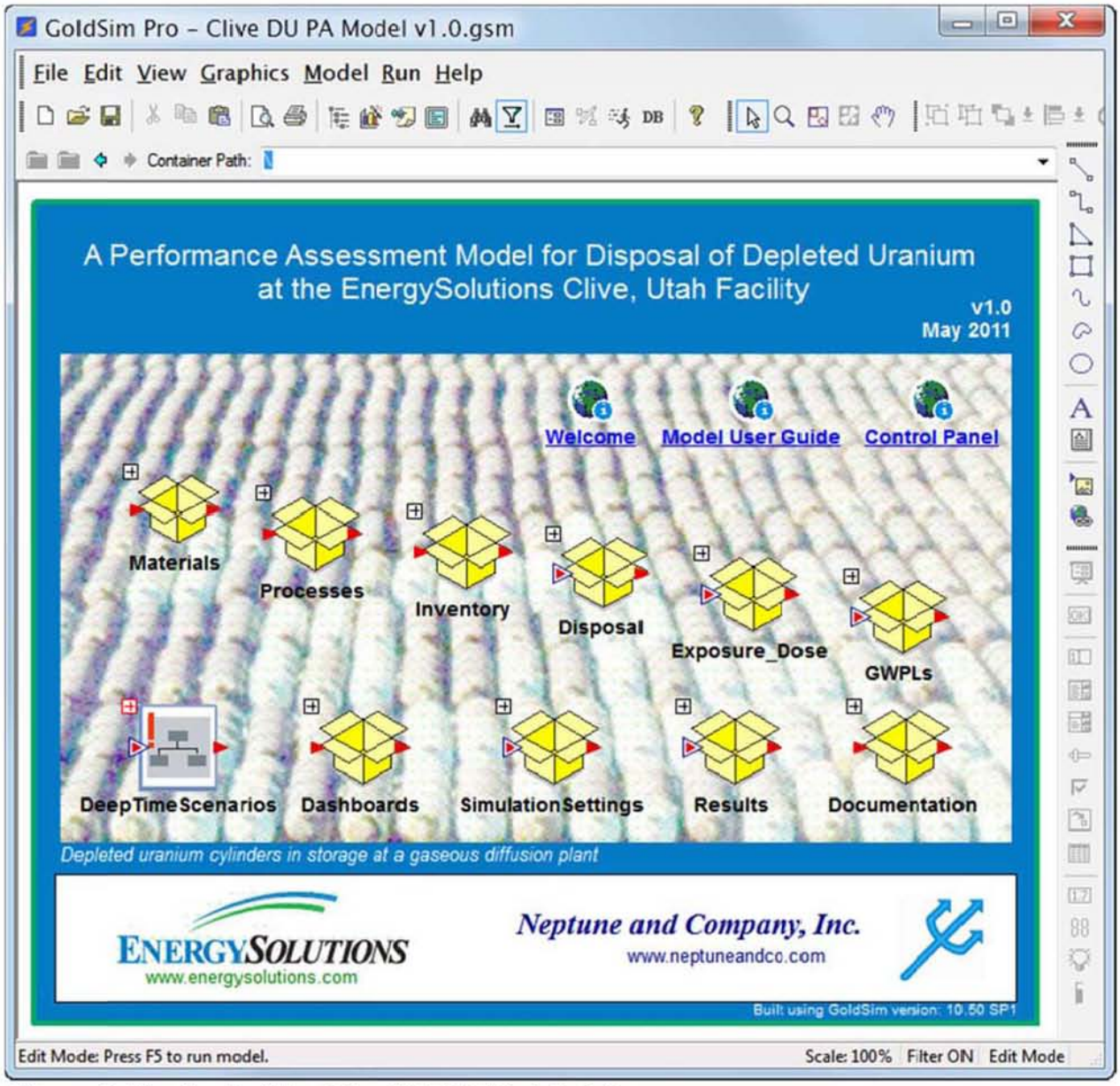

Figure 3. Top level of the Clive DU PA Model v1.0.

5.4.1 Materials

Any physical model of an environmental system must contains some sort of materials as a basis for representing the physical environment. Water, air, waste, soils, and other porous media are

defined in this container, and are referenced throughout the model. The arrangement of these materials in space, and their interconnectivity, is intended to represent a large block of the environment, including the Clive Facility, or in this case the Class A South Embankment within that facility, and its surroundings. The spatial definition of the environment is in the Disposal container.

5.4.2 Processes

Contaminant transport in the environment is driven by several processes in this model, including advection in water, diffusion in water, diffusion in air, uptake and redistribution by plants, and disturbance by burrowing animals. These parameters defining these processes are global in model scope, and so are defined at this high level. The actual implementation of these processes in moving radionuclides in the environment, is done mostly in the Disposal container.

Radioactive decay and ingrowth, chemical solubility in water, soil/water partitioning, air/water partitioning are also fundamental processes that determine fate and transport of radionuclides, though these are defined in the Materials container, since they are directly related to materials.

5.4.3 Inventory

The mass of radionuclides introduced as waste into the model is called the inventory. Inside this container, the total mass of various types of DU waste is defined, as are the concentrations of the radionuclides in each type of waste. These inventories can be selected individually or in combination by the user by using the Control Panel dashboard (see Figure 4), and is then introduced to the modeling cells that represent the waste layers, in the Disposal container.

5.4.4 Disposal

For the first 10,000 yr following disposal, calculations are performed for the fate and transport of radionuclides from the inventory, into and throughout the modeled environment, in the Disposal container. Here the physical location of modeling cells is defined, each with materials representing what would be found at that location. For example, modeling cells representing the cover container rip rap, loess (windblown sediment), clays, and other porous media, as well as water and air. Cells representing the aquifer contain Unit 2 sediments and water, but no air, since this regions is saturated with water by definition. Waste cells contain waste and backfill as porous media, air and water, and are provided a mass of radionuclides from the inventory. As the model progresses through time, these radionuclides migrate into other part of the physical system, and eventually are found in environmental media (air, water, soils) that receptors will encounter. The Disposal container performs essentially all the contaminant transport calculations to necessary to estimate future concentrations of radionuclides in these exposure media.

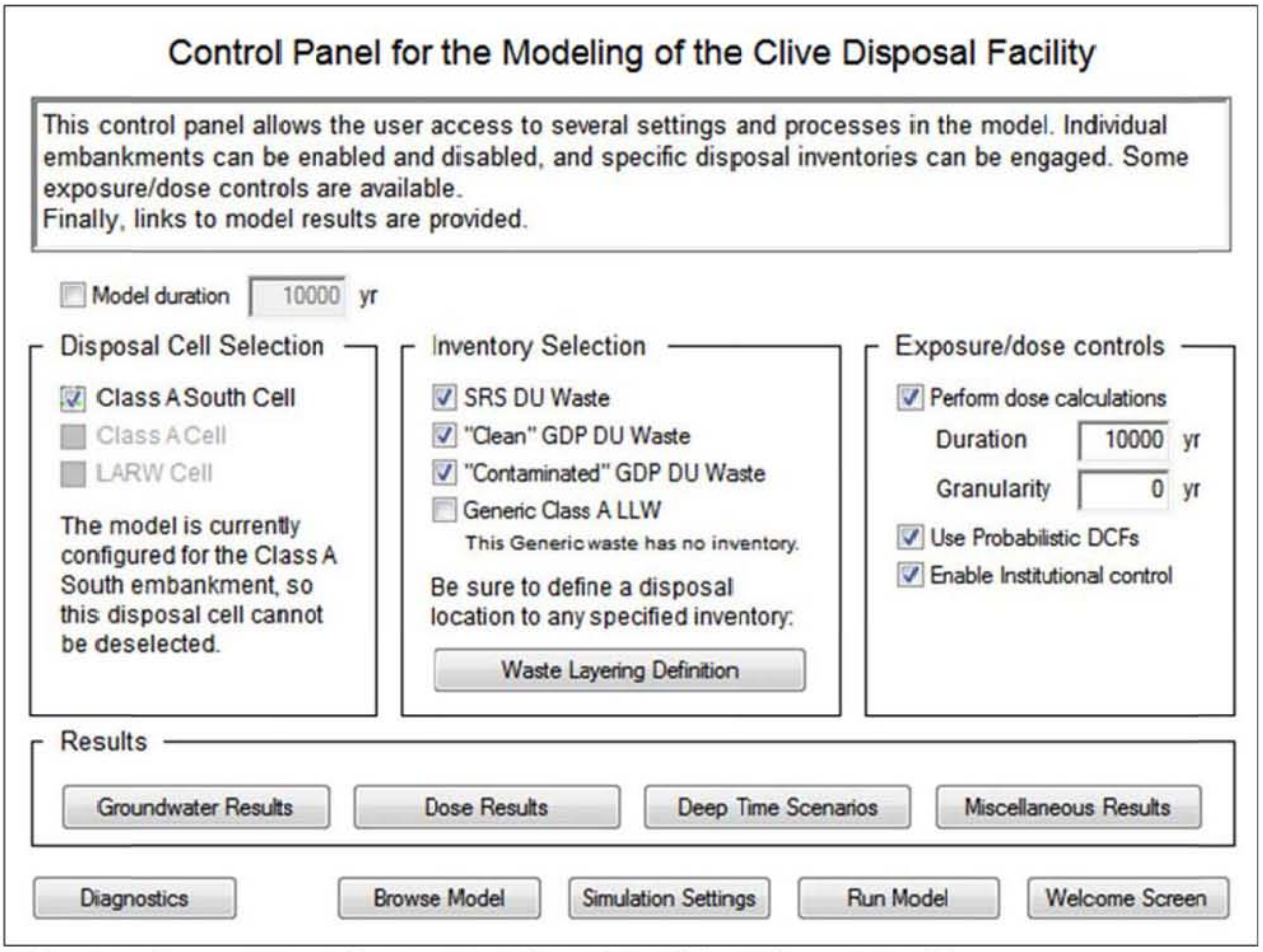

Figure 4. Control Panel for the Modeling of the Clive Disposal Facility.

5.4.5 Exposure and Dose

The exposure and dose calculations, which also include estimates of uranium toxicity hazard, are performed in this Exposure_Dose container. Receptors are hypothetical future humans who have behaviors similar to those of people around the site today: There are ranch workers, hunters, and OHV enthusiasts, all of whom are expected to have direct access to the site after institutional control is lost. There are also receptors who travel in the area, using highways, railroads, and access roads. These receptors are represented with a range of attributes and behaviors, from age to time spent on an OHV, and each encounters exposure media. As they breathe dust-laden air and walk on contaminated soils, for example, their exposures result in doses from radionuclides and toxic effects from uranium as a heavy metal. All of these calculations are performed in this container, and provide results that can be compared to performance objectives such as peak dose limits.

5.4.6 Groundwater Protection Level Calculations

In addition to the performance objectives provided by the State of Utah and the NRC for dose limits, there are GWPLs to be considered. In the Disposal container, the model provides

radionuclide concentrations at a hypothetical monitoring well located about 27 m (90 ft) from the interior of the waste embankment. In the case of the proposed DU waste disposal, only the top slope section of the embankment would contain DU waste, so the effective distance from the DU waste to the well is lengthened by the width of the side slope section, to about 73 m (240 ft). For those radionuclides that have GWPLs defined, the maximum well concentrations within 500 yr are compared to the GWPL values. These comparison calculations are performed in the GWPLs container.

5.4.7 Deep Time

All the calculations described above are aimed at producing results for comparisons to performance objectives that pertain to the first 10,000 yr after disposal. Following that, and out to the time of peak activity, is considered deep time. Peak activity of the DU waste, which is predominantly ^{238}U, is the time at which the decay products of the parent reach secular equilibrium with the parent. In this case, the peak activity is at about 2.1 million years. For the purposes of the model, then deep time is that duration from 10,000 y to 2.1 My.

Given the distinct time frame, the deep time calculations are independent of much of the rest of the model, except that the radionuclide mass in the embankment, as calculated in the Disposal container, is used as a source of radionuclides for dispersal in future lakes. The DeepTimeScenarios container produces estimates of radionuclide concentrations in the water column of future lakes, and in the sediments that they deposit.

5.4.8 Supplemental Containers

The Dashboards container is simply a location in the model for storing Dashboard elements, which are dialog-box-like controls for operating the model and for conveniently viewing results. The model can be executed and browsed without using any dashboards, though their convenience makes them quite useful.

The Simulation Settings container hosts a small number of elements that are used simply to control the simulation. Logical switches and values controlled by the dashboards are kept here, and the container will probably be of little interest to the average user.

The dashboards provide access to several results of general interest, most of which are collected in the Results container. In addition to those referenced by the dashboards, there are many other results that provide a more detailed look into the model. Also inside this container are the results needed for performing sensitivity analyses, such as those discussed later in this report.

Documentation contains records pertinent to model development, such as the Change Log, illustrations about particular model processes, and a large collection of references supporting the model. The subcontainer Documentation\References holds nearly 1 GB of reference materials in PDF format, and links to many more copyrighted materials that cannot be provided directly.

6.0 Results of Analysis

The Clive DU PA Model was run for several scenarios, in order to ascertain the effects of various assumptions. The different scenarios involved placing the DU wastes in different positions inside the waste volume in the embankment, and using the gully screening calculations. Endpoints of interest include

- groundwater concentrations of radionuclides for which GWPLs are specified,
- dose and uranium toxicity hazard to various receptors, and
- lake water and sediment concentrations of ^{238}U in the deep time analysis.

Statistical results (e.g. mean, median, 95th percentile) are based on simulations of 5,000 realizations.

The waste layering scenarios include filling the embankment waste volume with the three types of DU waste, to within 3 m, 5 m, and 10 m of the bottom of the embankment cover. The top 3 to 10 m is assumed to have been backfilled with clean material. In all these cases, the waste is arranged as follows: The bottom layers, variable in number depending on the amount of clean fill used, contain Clean GDP DU, the top waste layer contains SRS DU, and the layer directly below that contains Contaminated GDP DU. Details regarding these wastes can be found in the *Waste Inventory* white paper.

Each waste layer is roughly 0.5 m (20 in) in thickness. In general, the effect of the layer is that the higher the waste is emplaced in the volume, the greater influence it has on doses, which are derived from surface soils. The lower the waste, the greater its influence on groundwater concentrations. For this reason, the contaminated DU wastes are placed above the clean DU wastes, in order to position the ^{99}Tc that is present in contaminated wastes as far from the groundwater as possible. Details on this modeling can be found in the *Embankment Modeling* white paper. This arrangement allows exploration of a few different alternatives that help explore the PA model, and hence the performance of the system.

Groundwater protection levels are defined in the Clive Facility's groundwater discharge permit (UWQB 2009). Radionuclides with GWPLs and for which concentrations are evaluated include ^{90}Sr, ^{99}Tc, ^{129}I, ^{230}Th, ^{232}Th, ^{237}Np, ^{233}U, ^{234}U, ^{235}U, ^{236}U, and ^{238}U (see Section 4.1.2.12). The Clive DU PA Model estimates contributions to groundwater concentrations from the DU wastes for 500 yr, assuming transport to a hypothetical monitoring well. Details on the groundwater transport calculations are provided in the *Unsaturated Zone Modeling* and *Saturated Zone Modeling* white papers (Appendices 5 and 7).

Possible human receptors are of the following basic types, and details are available in the *Dose Assessment* white paper (Appendix 11):

- Ranch workers (mostly ranch hands), hunters, and OHV enthusiasts are expected to be present on and near the embankment.

- Other receptors have doses evaluated at specific locations, including the nearby highway (I-80), the Knolls OHV Recreations Area (Knolls), the nearby rail road (Railroad), the Grassy Mountain Rest Area on I-80 (Rest Area), and the Utah Test and Training Range access road (UTTR).
- All receptors are considered in population dose calculations.

The formation of gullies in the embankment cap is not modeled in detail in this version of the Clive DU PA Model, but is considered rather as a screening exercise in order to assess the influence of gullies on dose and hazard calculations. The model may be run with or without consideration of this screening calculation, so that their effect may be considered, as least qualitatively. In the following presentation of results, gully screening calculations are considered in addition to the case of no gully formation. Details on the gully calculations are provided in the *Erosion Modeling* white paper (Appendix 10).

Deep time is considered to be that time after 10,000 yr, the period of performance for assessing dose as specified in the Utah regulation. Endpoints related to the deep time assessment include lake sediment concentrations of ^{238}U, and concentrations of ^{238}U in lakewater, when lakes are present. Details on these calculations are provided in the *Deep Time Assessment* white paper (Appendix 13).

Results for all these endpoints are presented below, summarized in tables. Graphs of time histories and of sensitivity analysis results are also shown, although in cases where results are qualitatively similar, only a single representative graph is presented.

6.1 Groundwater Concentrations

Peak groundwater activity concentrations within 500 yr resulting from proposed waste disposals are calculated for all radionuclides at a hypothetical monitoring well placed about 27 m (90 ft) from the interior of the waste embankment. In the case of the proposed DU waste disposal, only the top slope section of the embankment would contain DU waste, so the effective distance from the DU waste to the well is lengthened by the width of the side slope section, to about 73 m (240 ft).

6.1.1 Summary of Results for Groundwater

For those radionuclides for which GWPLs exist, as specified in the facility's permit (UWQB 2009), results are shown in Table 2. It should be noted that these statistics summarize the peak mean concentrations for the 500-yr period. In general, concentrations increase with time, in which case the statistics presented are the mean concentrations on or near 500 yrs. Since all modeled estimates are of mean concentrations, the statistics represent the mean, median and 95th percentile of the (peak of the) mean concentration. As such, the 95th percentile is analogous to a 95% upper confidence limit on the mean. Note that most of the distributions are markedly positively skewed, as demonstrated by the large difference between the mean and median concentrations.

Table 2. Peak groundwater activity concentrations within 500 yr, compared to GWPLs

radionuclide	GWPL[1] (pCi/L)	peak activity concentration within 500 yr (pCi/L)		
		mean	median (50th %ile)	95th %ile
waste emplaced > 3 m below embankment cover				
^{90}Sr	42	0	0	0
^{99}Tc	3790	85.9	1.43e-5	209
^{129}I	21	0.0528	7.74e-21	0.131
^{230}Th	83	4.85e-17	4.19e-37	1.69e-26
^{232}Th	92	5.06e-23	0	1.33e-32
^{237}Np	7	1.91e-28	0	0
^{233}U	26	4.84e-13	5.2e-33	5.05e-22
^{234}U	26	2.27e-12	3.3e-32	3.3e-21
^{235}U	27	1.36e-13	2.7e-33	3.07e-22
^{236}U	27	4.41e-13	4.69e-33	4.07e-22
^{238}U	26	1.91e-11	2.68e-31	2.75e-20
waste emplaced > 5 m below embankment cover				
^{90}Sr	42	0	0	0
^{99}Tc	3790	437	0.00264	1710
^{129}I	21	0.368	3.35e-16	1.77
^{230}Th	83	2.16e-21	5e-37	1.5e-26
^{232}Th	92	1.61e-27	0	1.28e-32
^{237}Np	7	3.93e-25	0	4.22e-38
^{233}U	26	4.43e-17	6.32e-33	3.85e-22
^{234}U	26	2.66e-16	3.65e-32	2.44e-21
^{235}U	27	2.93e-17	2.99e-33	2.08e-22
^{236}U	27	3.61e-17	5.16e-33	3.35e-22
^{238}U	26	2.23e-15	2.98e-31	1.97e-20
waste emplaced > 10 m below embankment cover				
^{90}Sr	42	0	0	0
^{99}Tc	3790	14400	113	81400
^{129}I	21	12.7	5.8e-07	81.2
^{230}Th	83	1.53e-21	3.81e-37	1.23e-26
^{232}Th	92	1.34e-27	0	9.28e-33
^{237}Np	7	7.6e-18	0	4.69e-26
^{233}U	26	2.92e-17	2.25e-32	4.67e-22
^{234}U	26	1.57e-16	2.99e-32	2.14e-21

^{235}U	27	1.61e-17	2.64e-33	1.82e-22
^{236}U	27	2.4e-17	4.28e-33	3.23e-22
^{238}U	26	1.4e-15	2.41e-31	1.68e-20

[1]GWPLs are from UWQB (2009) Table 1A.

Based on these results, it can be seen that as the waste is emplaced lower in the embankment, monitoring well concentrations increase. This makes sense for two reasons: 1) The waste is closer to the groundwater, and so has a shorter travel distance, bringing the peak closer in time, and 2) the waste is more concentrated since it is arranged into a smaller volume, thereby decreasing the duration of breakthrough at the well, and increasing its amplitude.

For most radionuclides in Table 2 the groundwater concentrations are negligible compared to the GWPLs. The exceptions are ^{99}Tc and ^{129}I. For the 10-m model, the 95th percentiles for these two radionuclides exceed their GWPLs (this is also the case for the mean for ^{99}Tc). However, the median is still much less than the respective GWPLs. The distributions of these concentrations are very skewed, largely because of the skew in some if the input distributions. For example, the distributions for K_d are expressed as log-uniform.

In the case of ^{129}I, this radionuclide was not detected in any samples collected from the SRS drums (see the *Waste Inventory* white paper – Appendix 4). Not only was ^{129}I not detected, but it was not identified in any sample. However, the detection limits were used directly for creating the input distribution for inventory of ^{129}I. Consequently, the results presented are based on data that suggest that ^{129}I does not exist in the SRS inventory.

In the case of ^{99}Tc there are concerns over both the inventory concentration distribution, the concentration of ^{99}Tc in the GDP waste, and the infiltration modeling. The ^{99}Tc inventory concentration distribution is derived from three datasets that suggest very different concentrations. Consequently, the input distribution covers more than one order of magnitude of possible ^{99}Tc concentrations. With more data or better information, it is reasonable to expect that this uncertainty could be reduced. In addition, the use of HELP for infiltration modeling in an arid setting is known to over-estimate infiltration rates (see Section 4.1.2.4). The model results suggest that groundwater concentrations of ^{99}Tc are less than the GWPL for the 3-m and 5-m configurations, but that some of the simulations exceed this threshold in the 10-m model. With some model refinements that address the inventory distributions and the infiltration rates, the results are more likely to be reduced.

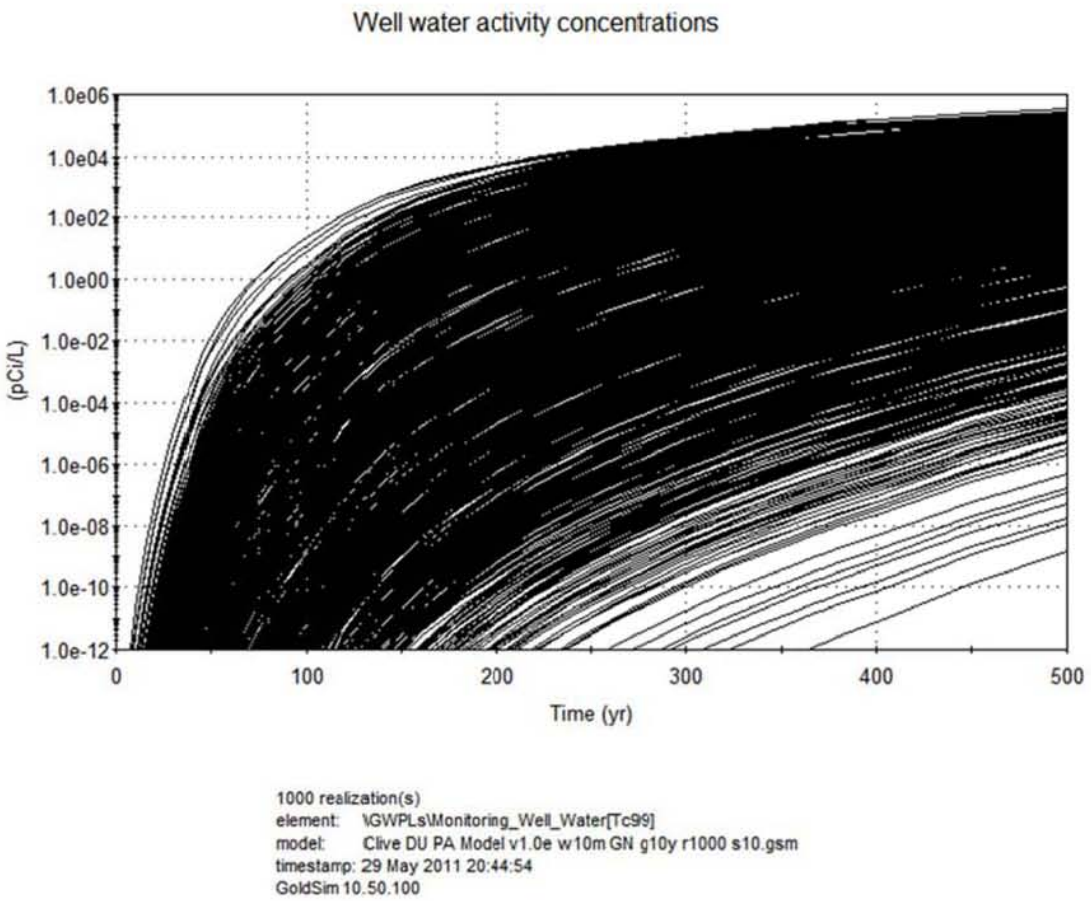

Figure 5. Time history of mean peak ^{99}Tc well concentrations: all realizations.

Technetium-99 is selected to represent a time history of monitoring well concentrations, as shown in Figure 5. This time history is for the case where waste is emplaced greater than 10 m below the embankment cover, and therefore represents the highest concentrations of the three waste layering cases. Figure 5 shows each of the 1,000 realizations, and Figure 6 shows a statistical summary of those realizations. For clarity of presentation, these graphs show a suite of 1,000 realizations rather than the full 5,000 realizations on which the summary statistics in Table 2 are based. Subsequent time histories will show only the statistical summaries. Of particular interest is the increase in concentrations of ^{99}Tc over time up to the 500-yr compliance period.

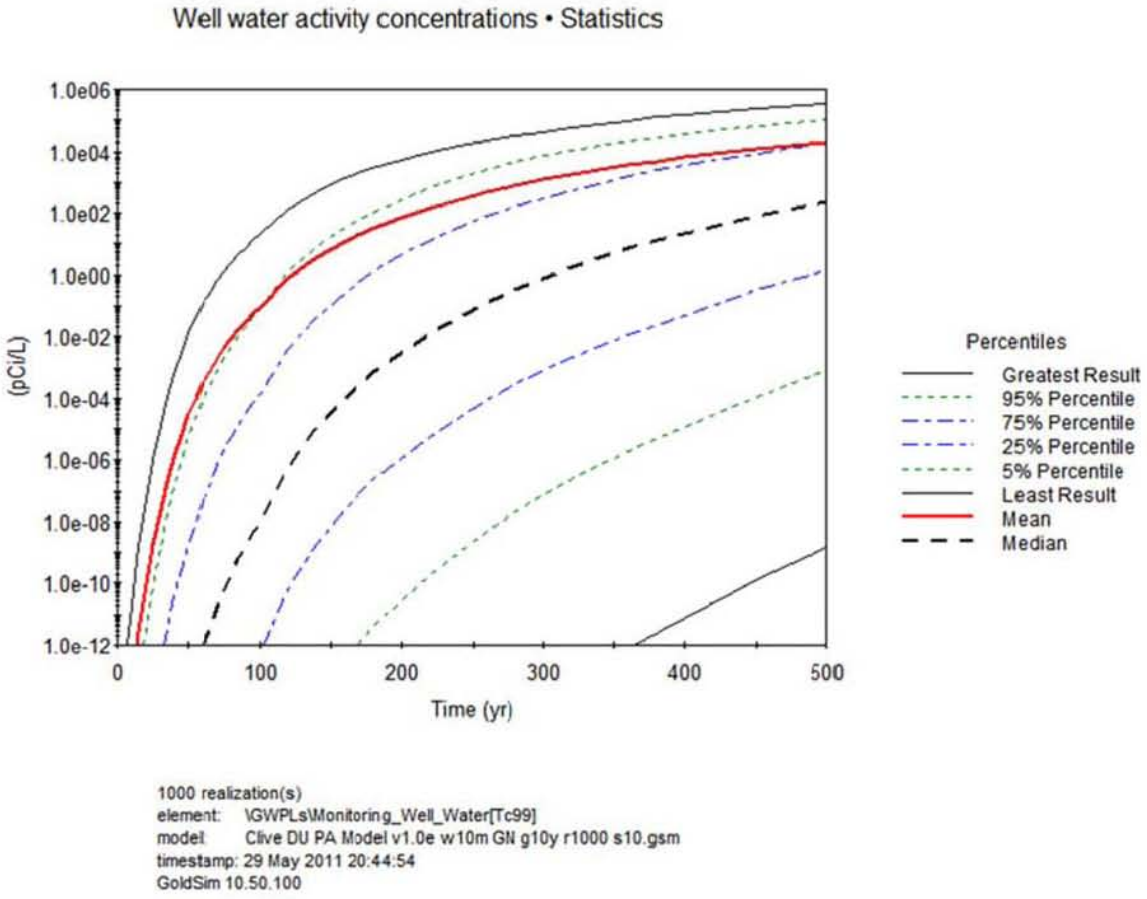

Figure 6. Time history of mean peak ^{99}Tc well concentrations: statistical summary.

6.1.2 Sensitivity Analysis for Groundwater

A sensitivity analysis of the ^{99}Tc groundwater concentrations was performed in order to determine which modeling parameters are most significant in predicting its value. As seen in Figure 7, the concentration is sensitive to the value of the soil/water partition coefficient, K_d, for Tc in the Unit 3 sand, which is used to represent the waste as well as the unsaturated zone below the embankment. In this case, which is for waste emplaced 3 m below the cover, the sand K_d for Tc accounts for 83.4% of the variation. No other model input parameters account for more than 5%, and so are not shown. In all other cases of ^{99}Tc groundwater concentrations, a similarly strong and almost exclusive dependence on sand K_d is seen.

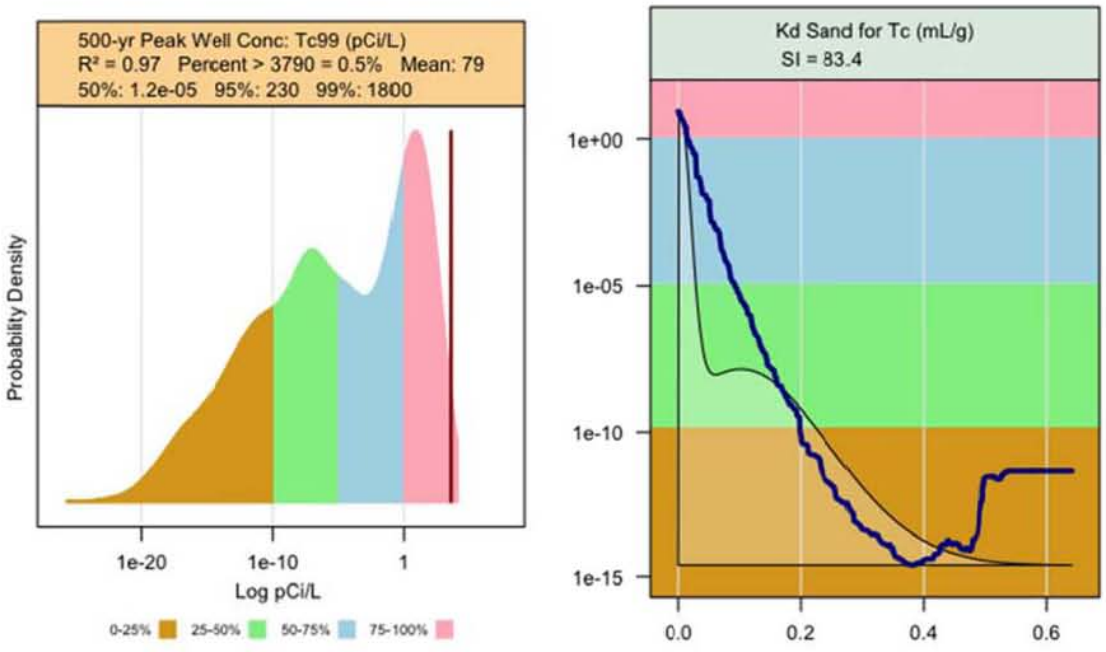

Figure 7. Partial dependence plot for peak ^{99}Tc groundwater concentration, assuming waste at 3 m.

Note that the input distribution is bimodal. This is because the distribution assumes a non-negligible probability that the K_d is zero, and a complementary probability that the K_d is greater than zero. The partial dependence plot looks reasonable for the range of values of K_d up to about 0.4. After that, there are too few data simulated from the input distributions to provide a good fit, however, the response is very small concentrations.

6.2 Receptor Doses

Doses to receptors are calculated as total effective dose equivalent (TEDE), and are to be compared to the performance objective of a peak dose of 0.25 mSv (25 mrem) in a year, achieved within 10,000 yr (Utah 2010). Comparison with the inadvertent intrusion standard of 5 mSv (500 mrem) in a year can also be considered for the models that include human induced gully erosion.

6.2.1 Summary of Results for Doses

These are summarized in two tables: Table 3 shows the statistics for mean TEDE for all receptors, without the gully screening calculations, for the cases of waste emplaced at 3 m, 5 m, and 10 m below the embankment cover.

Table 3. Peak mean TEDE, without consideration of gullies: statistical summary

	Peak TEDE (mrem in a yr) within 10,000 yr		
receptor	**mean**	**median (50th %ile)**	**95th %ile**
waste emplaced > 3 m below embankment cover			
ranch worker	4.37	3.44	11.3
hunter	0.187	0.152	0.462
OHV enthusiast	0.286	0.234	0.721
I-80 receptor	0.000124	9.85e-5	0.000318
Knolls receptor	0.00129	0.000989	0.00336
rail road receptor	0.000194	0.000155	0.0005
rest area receptor	0.00249	0.002	0.00633
UTTR access road receptor	0.0617	0.0493	0.156
waste emplaced > 5 m below embankment cover			
ranch worker	0.598	0.473	1.52
hunter	0.0258	0.021	0.0628
OHV enthusiast	0.039	0.0321	0.0947
I-80 receptor	1.44e-5	1.20e-5	3.54e-5
Knolls receptor	0.000147	0.000117	0.000383
rail road receptor	2.26e-5	1.89e-5	5.56e-5
rest area receptor	0.000289	0.000245	0.00073
UTTR access road receptor	0.0071	0.00589	0.0177
waste emplaced > 10 m below embankment cover			
ranch worker	0.00596	0.00471	0.0152
hunter	0.000253	0.000205	0.000624

OHV enthusiast	0.000388	0.000313	0.00094
I-80 receptor	1.54e-7	1.21e-7	3.89e-7
Knolls receptor	1.62e-6	1.22e-6	4.33e-6
rail road receptor	2.42e-7	1.9e-7	6.11e-7
rest area receptor	3.13e-5	2.51e-6	7.84e-6
UTTR access road receptor	7.81e-5	6.16e-5	0.0002

Table 4 shows the same information, but with the gully screening calculations included. That is, these doses evaluate the effects of the formation of a small number of gullies on the TEDE for all receptors.

Note that the doses to the offsite receptors are very small. Consequently, these receptors are not considered further. Of greater interest are the doses to the ranchers, hunters and OHVers. These three classes of receptors were modeled with the intent of capturing dose to each hypothetical individual in the relevant populations (see the *Dose Assesssment* white paper – Appendix 11). The data presented hence represent summary statistics for the peak average dose to each group of receptors. The peak of the average doses is a reasonable surrogate for average doses at 10,000 years in this PA model, because dose increases with time for DU. Consequently, the 95th percentile is analogous to a 95% upper confidence limit of the mean dose that is typically used under CERCLA, for example.

The output dose distributions are very positively skewed, with long tails. The long tails are probably due to a combination of factors that include: skewed input distributions that reasonably reflect uncertainty in upper values of a parameter; multiplicative effects in the model; and, missing correlations between some input parameters, which can lead to implausible combinations of input values. Consequently, dose results that are far into the tail of the output dose distributions might be unreliable. The mean and 95th percentile are used for comparison with performance objectives.

The greatest doses are shown for the 3-m configuration, as would be expected. The doses to ranch workers are greater than to the other receptors. However, in all cases the summary statistics present values that are less than the MOP performance objective of 0.25 mSv.

When gullies are included in the model, in the stylized fashion in which they are modeled, the doses are increased. This is because of both thinning of the cover layers (cap and fill material), and possible direct exposure to the DU waste. Given the flexibility available in the configuration options in the model, other options could also be considered than the three configurations presented here.

Table 4. Peak mean TEDE, with gully screening calculation: statistical summary

	Peak TEDE (mrem in a yr) within 10,000 yr		
receptor	**mean**	**median (50th %ile)**	**95th %ile**
waste emplaced > 3 m below embankment cover			
ranch worker	20.9	11.6	72.3
hunter	0.8	0.467	2.62
OHV enthusiast	1.22	0.729	3.99
I-80 receptor	0.000123	0.0001	0.000315
Knolls receptor	0.0013	0.001	0.00341
rail road receptor	0.000193	0.000157	0.000495
rest area receptor	0.00247	0.00202	0.00621
UTTR access road receptor	0.061	0.0499	0.156
waste emplaced > 5 m below embankment cover			
ranch worker	0.564	0.443	1.44
hunter	0.0244	0.0198	0.0603
OHV enthusiast	0.0367	0.0298	0.0898
I-80 receptor	1.47e-5	1.18e-5	3.76e-5
Knolls receptor	0.000154	0.00012	0.000405
rail road receptor	2.32e-5	1.86e-5	5.90e-5
rest area receptor	0.000298	0.000241	0.000746
UTTR access road receptor	0.00732	0.00587	0.0185
waste emplaced > 10 m below embankment cover			
ranch worker	0.00594	0.00457	0.0155
hunter	0.000257	0.000203	0.000636
OHV enthusiast	0.000386	0.000306	0.00096
I-80 receptor	1.58e-7	1.25e-7	3.95e-7
Knolls receptor	1.64e-6	1.24e-6	4.35e-6
rail road receptor	2.48e-7	1.97e-7	6.2e-7
rest area receptor	3.17e-6	2.49e-6	7.86e-6
UTTR access road receptor	7.83e-5	6.18e-5	0.000199

6.2.2 Sensitivity Analysis for Doses

Sensitivity analysis was performed on the results for the mean TEDE to ranch workers, hunters, and to OHV enthusiasts. The partial dependence plots for the ranch worker, assuming waste emplacement at 3 m and no gullies, is shown in Figure 8. In this case, the radon E/P ratio (escape-to-production ratio) is the most significant predictor of dose, followed by the moisture content in the sacrificial soil layer, and the K_d for radium in sandy soils. All other cases of the sensitivity analysis for dose are qualitatively similar. It is not surprising that all these receptors have such similar influences from the same parameters, since they engage in similar behaviors.

The sensitive parameters are all associated with the impact of radon on the doses. Radium is the pre-cursor to radon in the decay chain; increased moisture content mitigates radon transport; and, the radon E/P ratio affects the amount of radon that can leave the system. Radon is the greatest dose driver in the model. Of interest is the approach to estimating radon dose, which is documented in the *Dose Assessment* white paper (Appendix 11). Radon dose is not often calculated in a PA. Instead, radon flux at the surface of a disposal system is calculated. This example perhaps indicates the important of radon in a dose calculation, although it also indicates that the predicted doses are very low without the contribution from radon.

Similar sensitivity results are found for the no gully models, and for the gully models in the 5-m and 10-m cases. In these cases the gullies have limited effect because the depth of the gullies does not penetrate the waste.

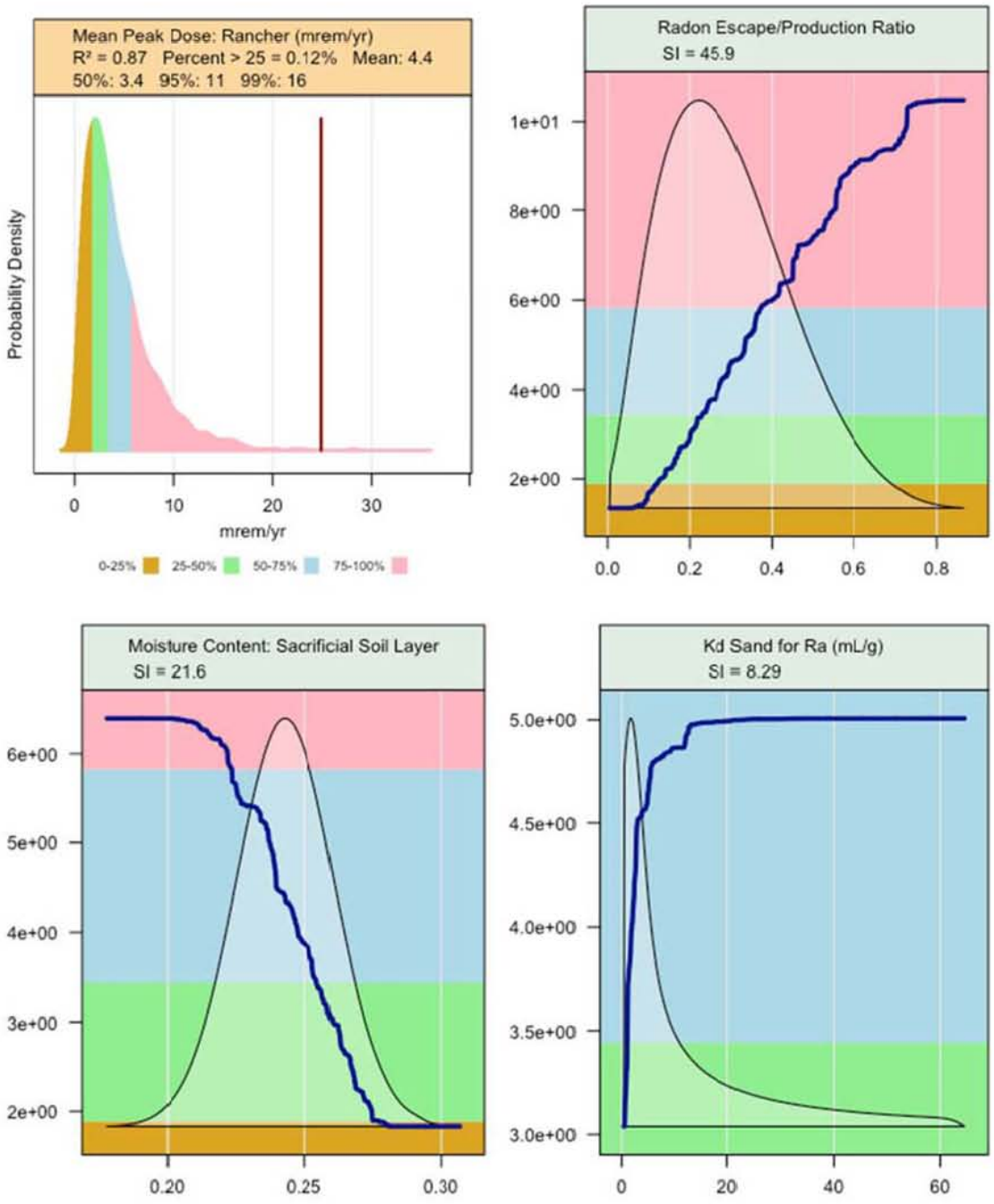

Figure 8. Partial dependence plots for the mean ranch worker dose, assuming waste at 3 m and no gullies

However, very different sensitivities are found for the gully screening calculations with waste emplaced up to 3 m below the embankment cover. As seen in Figure 9, the sensitive parameters are all gully-related: Angle of repose of the debris fan is the most significant, describing about half of the variation.

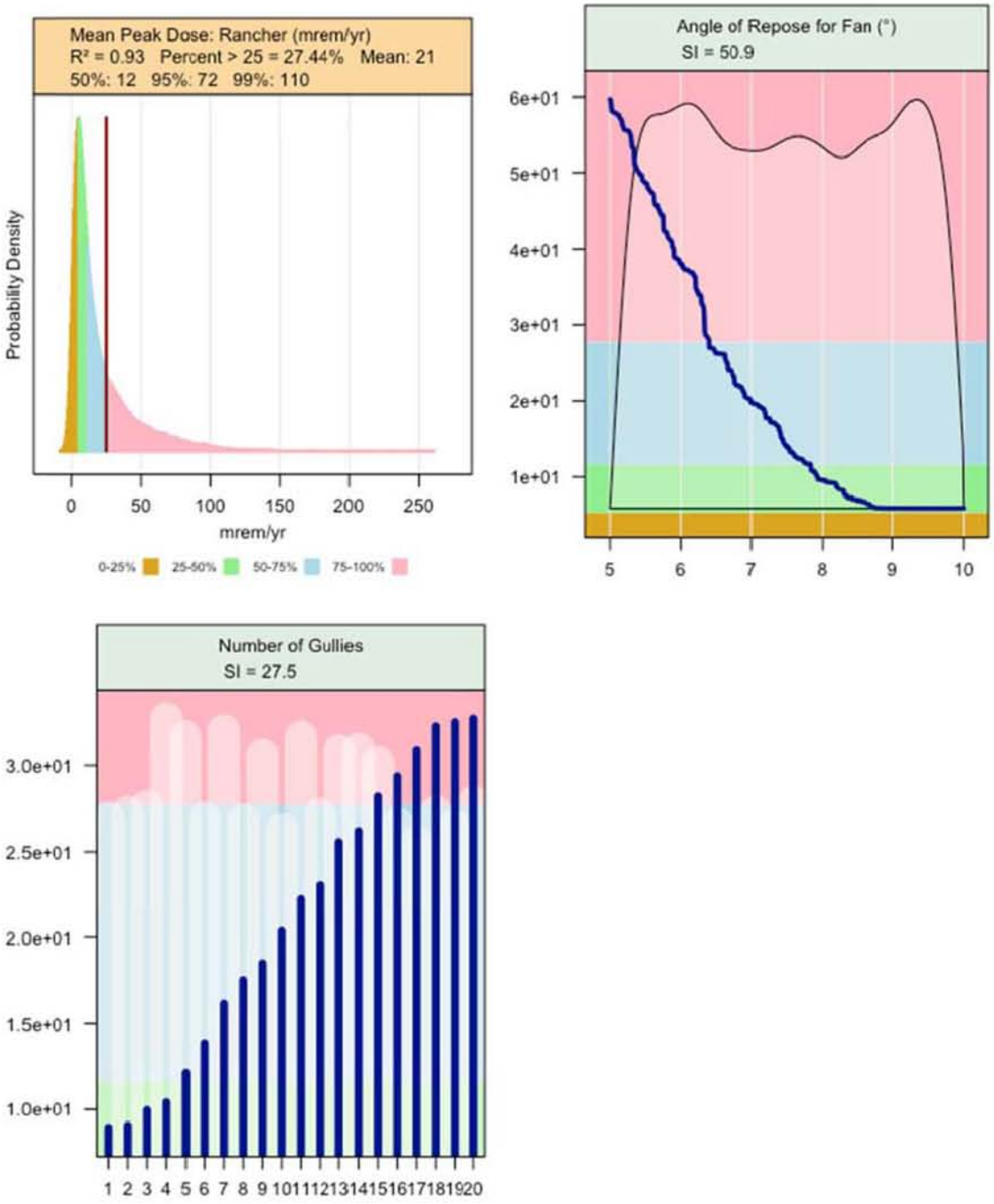

Figure 9. Partial dependence plots for the mean ranch worker dose, assuming waste at 3 m, with gullies

This is followed by the number of gullies, which was defined as a small number (1 to 20) just to see if they were significant. It is clear from these results that, if the waste is buried within 3 m of the cover, gullies are quite significant in contributing to doses. If the waste is emplaced at 5 or 10 m below the embankment cover, this sensitivity to gully formation goes away. A summary of sensitive parameters for each endpoint is provided in the following tables, showing for each of the principal receptors (ranch worker, hunter, and OHV enthusiast) the sensitivity to input parameters for the various waste emplacement depth cases, and with (Table 5) or without (Table 6) gullies. Only those input parameters with a sensitivity index (SI) over 5% are shown.

Table 5. Sensitivities of peak mean TEDE within 10,000 yr, with gully screening calculation

receptor	SI rank	input parameter	sensitivity index (SI)
waste emplaced > 3 m below embankment cover			
ranch worker	1	Angle of repose of the outwash fan	51
	2	Number of gullies	28
hunter	1	Angle of repose of the outwash fan	52
	2	Number of gullies	29
OHV enthusiast	1	Angle of repose of the outwash fan	54
	2	Number of gullies	29
waste emplaced > 5 m below embankment cover			
ranch worker	1	Radon escape/production ratio	46
	2	Sacrificial soil water content	16
hunter	1	Radon escape/production ratio	49
	2	Sacrificial soil water content	18
	3	Radium K_d in sand	7.7
OHV enthusiast	1	Radon escape/production ratio	50
	2	Sacrificial soil water content	18
	3	Radium K_d in sand	7.7
waste emplaced > 10 m below embankment cover			
ranch worker	1	Radon escape/production ratio	35
	2	Sacrificial soil water content	14
hunter	1	Radon escape/production ratio	26
	2	Sacrificial soil water content	9.6
OHV enthusiast	1	Radon escape/production ratio	30
	2	Sacrificial soil water content	11

Table 6. Sensitivities of peak mean TEDE within 10,000 yr, with no gullies

receptor	SI rank	input parameter	sensitivity index (SI)
waste emplaced > 3 m below embankment cover			
ranch worker	1	Radon escape/production ratio	46
	2	Sacrificial soil water content	22
	3	Radium K_d in sand	8.3
hunter	1	Radon escape/production ratio	50
	2	Sacrificial soil water content	24
	3	Radium K_d in sand	9.0
OHV enthusiast	1	Radon escape/production ratio	51
	2	Sacrificial soil water content	24
	3	Radium K_d in sand	9.1
waste emplaced > 5 m below embankment cover			
ranch worker	1	Radon escape/production ratio	42
	2	Sacrificial soil water content	19
	3	Radium K_d in sand	8.4
hunter	1	Radon escape/production ratio	47
	2	Sacrificial soil water content	23
	3	Radium K_d in sand	9.5
OHV enthusiast	1	Radon escape/production ratio	49
	2	Sacrificial soil water content	23
	3	Radium K_d in sand	9.9
waste emplaced > 10 m below embankment cover			
ranch worker	1	Radon escape/production ratio	37
	2	Sacrificial soil water content	18
hunter	1	Radon escape/production ratio	38
	2	Sacrificial soil water content	18
	3	Radium K_d in sand	8.7
OHV enthusiast	1	Radon escape/production ratio	37
	2	Sacrificial soil water content	17
	3	Radium K_d in sand	8.6

In the cases where gullies do not form, or they do not encounter waste, receptor doses are sensitive to three parameters related to radon, implying that the dose from radon is important. The

most sensitive is the radon E/P ratio, which defines the fraction of ^{222}Rn that escapes into the mobile environment, when formed by radioactive decay from its parent, ^{226}Ra. Radon that does not escape, such as that trapped in a crystalline matrix, stays in place and decays to polonium and then to ^{210}Pb. Note that the higher the E/P ratio, the higher the dose.

The significance of the water content in the sacrificial soil layer is that as radon diffuses upward through the engineered cover system, whatever small amount gets through the radon barrier then migrates up through the sacrificial soil. Since radon has a propensity to partition from air into water (a high Henry's Law constant), the wetter a porous medium is, the slower radon will migrate through it. In this case, the higher the moisture content, the lower the dose.

The third most significant parameter in these cases is the soil/water partition coefficient (K_d) in sand for radium. The link to dose is most likely through radon, given the other two parameters. In the Clive DU PA Model, the DU wastes are assigned K_d values assuming the geochemistry of their constituents is dominated by the fill materials surrounding the waste. This fill material is derived from the Unit 3 stratum, which is a sandy soil assigned K_d for sand. The sensitivity plot (Figure 8) shows that as the Ra K_d increases, especially at low values, the dose increases. A high K_d value would tend to make the radium partition onto soils, rather than migrate with local infiltrating water. If ^{226}Ra is not leaving the waste layers due to a high K_d, then it remains behind as a source for ^{222}Rn. A plausible transport and exposure scenario is that ^{222}Rn is formed by the decay of ^{226}Ra, the radon diffuses upward to the ground surface, partitioning into pore water along the way, and there enters the atmosphere where it is dispersed and inhaled by receptors. A combination of high radium K_d in sand, low water content in sacrificial soil, and high radon E/P ratio makes for high doses, and *vice versa*.

Also of significance is the formation of gullies in the 3-m model. It is no surprise that in the presence of gullies, the parameters defining gully formation are the most important. The angle of repose of the outwash fan is part of what defines the area of that fan (which is much larger than the area of the narrow but deep gully), and the number of fans multiplies that area directly. Since these receptors spend time on the fans as a proportion of the total fan area compared to the entire embankment area, the amount of time spent on the fan (and in the gullies themselves), where wastes may be exposed, is important in determining the doses. If wastes are not exposed, as in the cases of waste emplacement greater than 5 or 10 m below the embankment cover, the gullies do not generally encounter wastes, and therefore the outwash is not contaminated, and there is no associated contribution to dose. This analysis strongly indicates that the intrusion of gullies into waste-bearing layers nearer the top of the embankment is what is important.

6.3 Receptor Uranium Hazard Quotients

Uranium hazard quotients (HQs) to receptors within 10,000 yr are calculated, and are compared to EPA's standard point of departure for hazard index of 1. Uranium hazard is not regulated for disposal of radioactive waste. However, it provides another point of reference for evaluating site performance for the disposal of DU.

6.3.1 Summary of Results for Uranium Hazard

The uranium hazard results are summarized in two tables: Table 7 shows the statistics for mean uranium hazard quotient for all receptors, without the gully screening calculations, for the cases of waste emplaced at 3 m, 5 m, and 10 m below the embankment cover.

Table 8 shows the same information, but with the gully screening calculations included. That is, these results evaluate the effects of the formation of a small number of gullies on the uranium hazard quotient for all receptors. In the case of no gullies the hazard quotients for uranium are extremely small, indicating essentially no risk from uranium toxicity. The results in Table 8 are similar for both the 5-m and 10-m waste configurations. However, the 3-m configuration shows some simulations with comparatively large uranium hazard quotients. For example, the 95th percentile is 47.8 for ranchers. Several other values are greater than 1. Similar to the dose results presented above, this indicates that disposal of DU waste near to the top of the embankment is not as protective of human health and the environment. However, disposal of DU waste below 5 m appears to demonstrate clear compliance with the performance objectives.

Table 7. Peak mean uranium hazard quotient, without consideration of gullies: statistical summary

	Peak uranium hazard quotient within 10,000 yr		
receptor	**mean**	**median (50th %ile)**	**95th %ile**
waste emplaced > 3 m below embankment cover			
ranch worker	4.81e-7	1.15e-10	5.24e-7
hunter	1.15e-8	3.38e-12	1.32e-8
OHV enthusiast	1.07e-8	1.31e-12	7.53e-9
waste emplaced > 5 m below embankment cover			
ranch worker	5.35e-8	9.64e-14	8.51e-9
hunter	1.34e-9	2.65e-15	2.57e-10
OHV enthusiast	1.27e-9	9.6e-16	1.66e-10
waste emplaced > 10 m below embankment cover			
ranch worker	1.23e-10	3.23e-21	7.83e-12
hunter	3.44e-12	9.62e-23	2.42e-13
OHV enthusiast	2.37e-12	3.86e-23	1.1e-13

Table 8. Peak mean uranium hazard quotient, with gully screening calculation: statistical summary

	Peak uranium hazard quotient within 10,000 yr		
receptor	**mean**	**median (50th %ile)**	**95th %ile**
waste emplaced > 3 m below embankment cover			
ranch worker	8.62	1.47	47.8
hunter	0.199	0.0331	1.11
OHV enthusiast	0.238	0.0394	1.34
waste emplaced > 5 m below embankment cover			
ranch worker	0.00566	7.02e-6	0.024
hunter	0.000129	1.62e-7	0.000514
OHV enthusiast	0.000155	1.97e-7	0.000642
waste emplaced > 10 m below embankment cover			
ranch worker	5.15e-6	1.05e-12	8.29e-7
hunter	1.55e-7	2.75e-14	1.92e-8
OHV enthusiast	2.22e-7	3.43e-14	2.46e-8

6.3.2 Sensitivity Analysis for Uranium Hazard Quotient

Sensitivity analysis was performed on the results for the mean uranium hazard quotient to ranch workers, hunters, and to OHV enthusiasts. The partial dependence plots for the ranch worker, assuming waste emplacement at 3 m and no gullies, is shown in Figure 10. In this case, the water content exponent for the water tortuosity model is the most significant predictor of the hazard quotient, followed by the molecular diffusivity in water, the porosity exponent for the water tortuosity model, the solubility of UO_3, and the vegetation association selector. The graphs in Figure 10 are specific to the ranch worker receptor, but as can be seen from consulting the values in Table 9, this is representative to all three major receptor types, in the case of waste emplacement at 3 m below the embankment cover, and no consideration of gullies.

Two of these are related to the water tortuosity model, where tortuosity in the water phase equals the water content (to a power "water content exponent") divided by porosity (to the power "porosity exponent"). Therefore, higher values of "water content exponent" cause higher values of water tortuosity, and, higher values of "porosity exponent" cause lower values of water tortuosity, because it is in the denominator. A higher value of water tortuosity means that constituents diffusing in water have to travel farther, along a more tortuous path, so the overall rate of diffusion is lower. Figure 10 shows that as the "water content exponent" increases, uranium hazard decreases. Concurrently, as the "porosity exponent" increases, uranium hazard increases. Both of these indicate that as water tortuosity increases, the uranium HQ decreases.

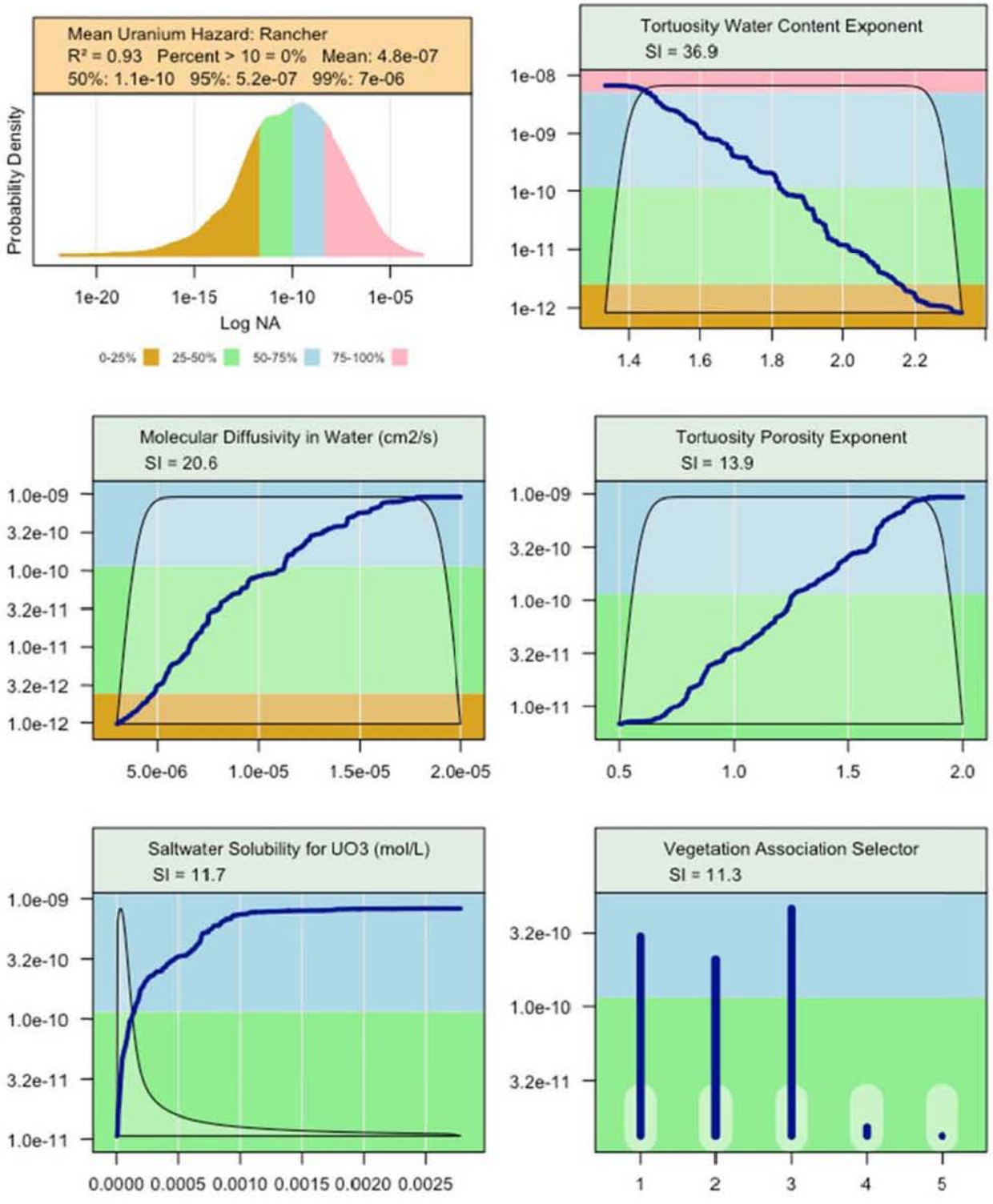

Figure 10. Partial dependence plots for the mean ranch worker uranium hazard quotient, assuming waste at 3 m and no gullies

In addition to the effects of tortuosity on diffusion, and ultimately on uranium HQ, the molecular diffusivity D_m in water is also identified as a sensitive parameter. As the diffusivity increases, so does the uranium HQ. Together, these three variables identify water phase diffusion as being positively correlated to the uranium HQ.

Uranium hazard quotient is obviously tied directly to uranium, and no other radionuclides except uranium parents (of which there are very few) could influence this endpoint. The significance of water diffusion indicates that uranium is migrating by diffusion in the water phase. While the bulk of the uranium in the DU waste is U_3O_8, and therefore essentially insoluble, the SRS DU is UO_3, which is much more soluble. The fourth sensitive variable is the solubility of UO_3 in water (all water in the embankment is assumed to be salty water), bolstering the argument that uranium is diffusing in the water phase.

The final piece of this transport and exposure pathway puzzle is hinted at by the fifth-ranked variable: the vegetation associate selector. This stochastic chooses at random from one of five future vegetation associations, each of which is currently found in the vicinity of Clive. These five plots and their vegetation associations are:

- Plot 1: Mixed Grassland,
- Plot 2: Juniper – Sagebrush,
- Plot 3: Black Greasewood,
- Plot 4: Halogeton – Disturbed, and
- Plot 5: Shadscale - Gray Molly.

It is interesting to note that Plot 3 is correlated to the highest values of uranium HQ, implicating black greasewood as a plant of interest. While the black greasewood vegetation association is not entirely made up of that plant type, it is the association with the most black greasewood. Of all the plant types considered in the model, black greasewood has the greatest rooting depth, with a maximum of 5.7 m. With an embankment cover of about 1.65 m, this leaves black greasewood delving about 4 m into the waste below the cover. With the waste emplaced at 3 m below the cover, black greasewood can tap directly into the waste. But even without such deep roots, plants can access uranium that is diffusing upward into the cover. Thus, the following contaminant transport pathway for uranium is suggested: Uranium is leached into infiltrating water, and can diffuse upward to the point that it is within reach of plant roots. With black greasewood in the mix, it does not even have to move upward.

Adding gullies into the mix changes the uranium hazard quotient results significantly for wastes emplaced up to 3 m below the embankment cover. Uranium HQs are much higher, and the variables influencing the value are quite different. As seen in Figure 11, the sensitive parameters are mostly gully-related: Angle of repose of the debris fan is the most significant, describing about two thirds of the variation. This is followed by the gully shape parameter b, defining the degree of curvature of the gully thalweg, and thereby related to the depth and volume of the gully. Greater values of b mean larger gullies, leading to increases uranium HQ. The fourth-ranked variable is the angle of repose of the gully walls, also influencing gully outwash volume.

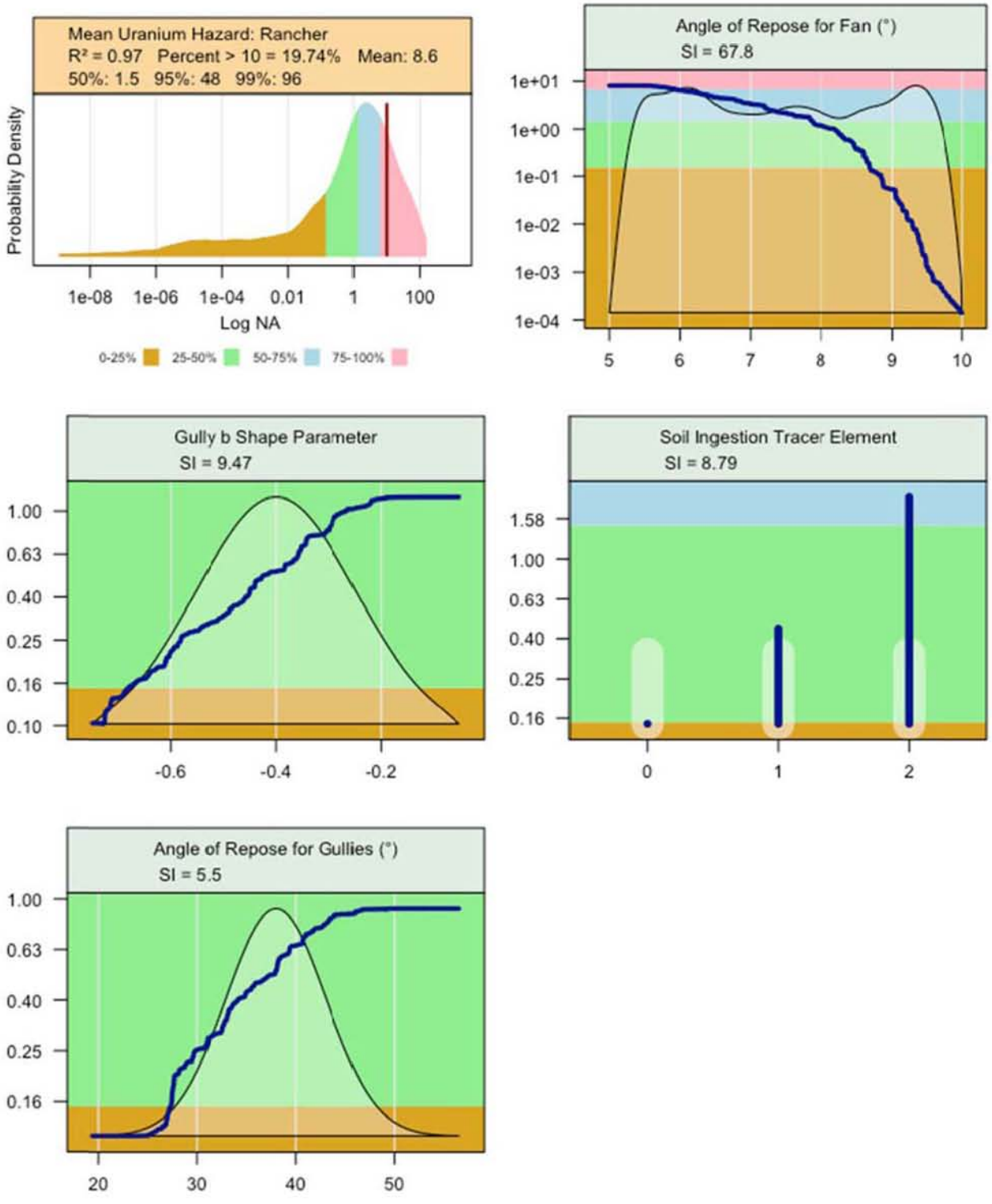

Figure 11. Partial dependence plots for the mean ranch worker uranium hazard quotient, assuming waste at 3 m, with gullies

A new variable here is the third one: the selection of the soil ingestion tracer element. In the estimation of soil ingestion rates by humans, as described in the *Dose Assessment* white paper (Appendix 11), various tracers are used, including silicon, aluminum, and titanium. The choice of which of these to use has an effect on this endpoint, but the real message is that soil ingestion is the exposure pathway leading to the uranium exposure.

For the cases where waste is emplaced below 5 m or 10 m, the influences on uranium hazard quotient are much more like those found in the cases where no gullies are considered at all.

A summary of sensitive parameters for each endpoint is provided in the following tables, showing for each of the principal receptors (ranch worker, hunter, and OHV enthusiast) the sensitivity to input parameters for the various waste emplacement depth cases, and with (Table 9) or without (Table 10) gullies. Only those input parameters with a sensitivity index (SI) over 5% are shown.

Table 9. Sensitivities of peak mean uranium hazard quotient within 10,000 yr, with gully screening calculation

receptor	SI rank	input parameter	sensitivity index (SI)
waste emplaced > 3 m below embankment cover			
ranch worker	1	angle of repose for outwash fan	68
	2	gully thalweg shape parameter b	9.5
	3	soil ingestion tracer element	8.8
	4	angle of repose in gullies	5.5
hunter	1	angle of repose for outwash fan	68
	2	gully thalweg shape parameter b	9.5
	3	soil ingestion tracer element	9.0
	4	angle of repose in gullies	5.5
OHV enthusiast	1	angle of repose for outwash fan	67
	2	gully thalweg shape parameter b	9.4
	3	soil ingestion tracer element	9.3
	4	angle of repose in gullies	5.4
waste emplaced > 5 m below embankment cover			
ranch worker	1	angle of repose for outwash fan	50
	2	water content exponent for tortuosity model	14
	3	aqueous solubility of UO_3	10
	4	molecular diffusivity in water	9.1
	5	porosity exponent for tortuosity model	6.0
hunter	1	angle of repose for outwash fan	50
	2	water content exponent for tortuosity model	14

	3	aqueous solubility of UO_3	10
	4	molecular diffusivity in water	9.2
	5	porosity exponent for tortuosity model	6.0
OHV enthusiast	1	angle of repose for outwash fan	49
	2	water content exponent for tortuosity model	14
	3	aqueous solubility of UO_3	10
	4	molecular diffusivity in water	9.2
	5	porosity exponent for tortuosity model	6.0
waste emplaced > 10 m below embankment cover			
ranch worker	1	water content exponent for tortuosity model	38
	2	molecular diffusivity in water	24
	3	porosity exponent for tortuosity model	16
	4	angle of repose for outwash fan	9.4
	5	uranium K_d in sand	7.5
hunter	1	water content exponent for tortuosity model	38
	2	molecular diffusivity in water	25
	3	porosity exponent for tortuosity model	16
	4	angle of repose for outwash fan	9.3
	5	uranium K_d in sand	7.3
OHV enthusiast	1	water content exponent for tortuosity model	38
	2	molecular diffusivity in water	25
	3	porosity exponent for tortuosity model	16
	4	angle of repose for outwash fan	9.3
	5	uranium K_d in sand	7.2

Table 10. Sensitivities of peak mean uranium hazard quotient within 10,000 yr, with no gullies

receptor	SI rank	input parameter	sensitivity index (SI)
waste emplaced > 3 m below embankment cover			
ranch worker	1	water content exponent for tortuosity model	37
	2	molecular diffusivity in water	21
	3	porosity exponent for tortuosity model	14
	4	aqueous solubility of UO_3	12
	5	vegetation association selector	11
hunter	1	water content exponent for tortuosity model	37
	2	molecular diffusivity in water	21

	3	porosity exponent for tortuosity model	14
	4	vegetation association selector	12
	5	aqueous solubility of UO_3	12
OHV enthusiast	1	water content exponent for tortuosity model	37
	2	molecular diffusivity in water	21
	3	porosity exponent for tortuosity model	14
	4	aqueous solubility of UO_3	11
	5	vegetation association selector	8.3
waste emplaced > 5 m below embankment cover			
ranch worker	1	water content exponent for tortuosity model	41
	2	molecular diffusivity in water	27
	3	porosity exponent for tortuosity model	16
	4	aqueous solubility of UO_3	5.3
hunter	1	water content exponent for tortuosity model	41
	2	molecular diffusivity in water	27
	3	porosity exponent for tortuosity model	16
	4	aqueous solubility of UO_3	5.3
OHV enthusiast	1	water content exponent for tortuosity model	41
	2	molecular diffusivity in water	26.8
	3	porosity exponent for tortuosity model	17
	4	aqueous solubility of UO_3	5.2
waste emplaced > 10 m below embankment cover			
ranch worker	1	water content exponent for tortuosity model	34
	2	molecular diffusivity in water	23
	3	porosity exponent for tortuosity model	14
	4	uranium K_d in sand	13
hunter	1	water content exponent for tortuosity model	31
	2	molecular diffusivity in water	22
	3	porosity exponent for tortuosity model	13
	4	uranium K_d in sand	12
OHV enthusiast	1	water content exponent for tortuosity model	31
	2	molecular diffusivity in water	22
	3	porosity exponent for tortuosity model	13
	4	uranium K_d in sand	11

Like the sensitivity analysis for the dose endpoints, this analysis shows that in the presence of gullies in the 3-m configuration, the parameters defining gully formation are the most important. If wastes are not exposed, as in the cases of deeper waste emplacement, the gullies do not generally encounter wastes, and therefore the outwash is not contaminated, and there is no associated contribution to uranium HQ. Overall, the conclusion of the sensitivity analyses for both the dose and uranium hazard clearly show that the intrusion of gullies into waste-bearing layers has a detrimental effect.

6.4 ALARA

In keeping doses as low as reasonably achievable (ALARA) it is necessary to estimate doses not to individuals, but to the entire population of individuals. One such calculation is the cumulative dose to all ranch workers, hunters, and OHV enthusiasts, summed across all individuals and all years of the 10,000-yr simulation. These cumulative population doses, as TEDE, are shown in Table 11, considering the various cases of waste placement and whether the gully screening calculation is included in the analysis.

Table 11. Peak cumulative population TEDE: statistical summary

	Peak population TEDE (rem) within 10,000 yr		
simulation scenario	**mean**	**median (50th %ile)**	**95th %ile**
no gullies; waste > 3 m below cover	35.2	29.2	87.3
no gullies; waste > 5 m below cover	4.07	3.46	9.78
no gullies; waste > 10 m below cover	0.0434	0.0356	0.103
with gullies; waste > 3 m below cover	378	172	1430
with gullies; waste > 5 m below cover	4.46	3.7	10.7
with gullies; waste > 10 m below cover	0.0448	0.0364	0.108

These population doses represent sum of the average population dose in each year summed over the three classes of receptors. These population doses are very small for five of these six scenarios. A measure for these population doses can be obtained by considering the person-rem costs suggested in NRC and DOE guidance (see the *Decision Analysis* white paper – Appendix 12). Prior to 1995, NRC suggested a flat $1,000 per person-rem cost. Subsequent to 1995, NRC suggested a value of $2,000 with a discounting factor of 7% for the first 100 years, and 3% thereafter. NRC also suggested that a range of $1,000 to $6,000 might be reasonable, with a best estimate of $2,000. NRC noted that the intent of raising the person-rem costs from $1,000 to $2,000 was to accommodate discounting in an economic analysis. Note that the intent of the NRC approach is to capture the societal effects of added dose to the public.

If a flat rate of $1,000 is applied to the population dose estimates provided above, then the costs associated with these scenarios are provided in Table 12. These are the total costs over 10 ky. The costs per year are very small, even in the worst case scenario of gullies and a 3-m configuration.

Table 12. Statistical summary of the flat rate ALARA costs

	Peak population ALARA costs within 10,000 yr		
simulation scenario	**mean**	**median (50th %ile)**	**95th %ile**
no gullies; waste > 3 m below cover	$35,000	$29,000	$87,000
no gullies; waste > 5 m below cover	$4,000	$3,000	$10,000
no gullies; waste > 10 m below cover	$43	$36	$100
with gullies; waste > 3 m below cover	$378,000	$172,000	$1,430,000
with gullies; waste > 5 m below cover	$4,500	$3,700	$10,000
with gullies; waste > 10 m below cover	$45	$36	$110

An approach to discounting could also be applied as suggested by NRC, but this would simply result in lower costs again. For simplicity, assume that the population doses are the same every year, apply the cost of $2,000 per person rem, and the NRC discount factor. If a discount factor of 7% is applied for the first 100 years, then the ALARA costs are negligible. If a 3% factor is applied across all time, then the total ALARA costs is less than 1% of the undiscounted ALARA costs presented in Table 12 even with the change in starting point from $1,000 to $2,000 per person-rem.

In using this approach to ALARA for informed decisions, the ALARA costs involved are very small. The reason the ALARA costs are small is because there are not many receptors in the model that are involved in ranching, hunting or OHV activities at the site. The disposal site is located in a hostile environment, far from most human population centers, and groundwater is not potable. This analysis shows that the number of people engaged in the general vicinity of Clive over the next 10 ky is small, and the doses they are likely to receive are small.

6.5 Deep Time Results

The deep time model addresses in a heuristic fashion the fate of the CAS embankment from 10 ky to 2.1 My, the time at which DU reaches secular equilibrium. The model addresses the needs identified in the Section 2(a) of R313-25-8 of the UAC to perform additional simulations for the period where peak dose occurs, for which the results are to be analyzed qualitatively. The deep-time model runs simulations to 2.1 My, but does not calculate dose because of the huge uncertainty in predicting human society and evolution that far into the future, and because the requirement is to analyze simulation results qualitatively. Instead the output of the deep time model is presented in terms of concentrations of radionuclides in relevant environmental media.

The deep-time model considers the return of lakes in the Bonneville Basin that reach or exceed the elevation of Clive. Two classes of lakes are considered. The first is a large lake similar to Lake Bonneville that not only inundates the Clive facility, but also is deep enough and has sufficient duration that lake sedimentation will add to the materials that are currently on Bonneville Basin floor. This type of lake is assumed to occur once every 100 ky in line with the 100-ky climate cycles that have occurred for the past 1 My or so. The second type of lake is

shallower, and is termed an intermediate lake. It is also assumed to inundate the Clive facility, but is not a deep lake like Lake Bonneville. It is more similar to the Gilbert Lake that occurred at the end of the last ice age. This type of lake is assumed to occur several times in each climate cycle in response to colder, wetter conditions.

Return of a lake at or above the elevation of Clive is assumed to result in the destruction of the CAS embankment. The above grade embankment material and all of the DU waste is assumed to be dispersed through wave action. The dispersal area forms the basis for the volume of water in which DU waste is dissolved, and ultimately settles back to the basin floor through precipitation or through evaporation as the lake recedes. The lake cycle involves movement of the DU waste, subject to continuing decay and ingrowth, from the sediment into lake water, and back to sediment as the lake forms and recedes. The DU waste is assumed to be fully mixed with the accumulated sediment. Sediment accumulates on average at the rate of about 17 m per 100 ky climate cycle. The current Unit 3 layer of sediment at Clive, which is derived from Lake Bonneville, is assumed to be a confining layer.

The lake cycle effects on transport processes are complex. Sediment core records show significant mixing of sediment, but also can be used to identify significant lake events in the past several hundred thousand years. The extent of sediment mixing is not well understood. The mechanisms for dispersal of a relatively soft pile of material in the middle of a desert flat is not well understood. The extent of mixing of dissolved materials in a large lake is also not well understood. The Model, consequently, is simplified to the point of acknowledging lake return, destruction of the CAS embankment, and cycling of DU waste material between periodic lakes and basin sediments.

In particular, the model overly simplifies the lake cycle processes, and the effect of those processes on the transport of DU waste, and limits the dispersal of DU waste through time. Destruction of the CAS embankment is assumed to occur with a lake that at least reaches the elevation of Clive. This means that even a very shallow lake is assumed to destroy the embankment. It is possible that such lakes, that barely exceed the elevation of Clive would not possess sufficient power to destroy the embankment, and that a different threshold for intermediate lake elevation would be more appropriate. Once the embankment is destroyed, the amount of sedimentation is tied to lake elevation, and the volume of lake water into which DU waste can mix is similarly limited. At the extremes of the input distributions for these factors, some (perhaps unreasonably) high lake water and sediment concentrations are predicted by the Model.

The area of dispersal of the CAS embankment is captured with a simple model that allows the embankment material to spread out according to a specified depth of material that limits the dispersal area. This fixes a dispersal area, but wave action is unlikely to limit the effects of dispersal to such a uniform layer.

Dissolution into the lake is assumed to occur only in the lake volume immediately above the dispersed area. This limits the volume of water within which dissolved materials might mix, and limits the area in which precipitates and evaporates can return. In addition, radon does not escape from the modeled system.

Although the embankment material is dispersed within a dispersal area, isolation of any part of the sediment profile is assumed not to occur. That is, the sediment is assumed to completely mix with previous sediment for every lake event. Lake sedimentation does not allow burial or isolation of previously formed sediment layers. Since different lakes can be identified in sediment cores, this again limits the dispersal of the DU waste.

Initial dispersal of the embankment includes all of the DU waste, even if some of the DU waste is disposed below grade. Return of a lake results in some mixing of sediments with new lake material, but the depth of sediment mixing is not well known. Consequently, all waste is assumed to be mixed with the sediment from the first returning lake. A consequence is that all DU waste in the sediment is available for dissolution into a new lake, no matter how thick the completely mixed sediment.

The model, therefore, represents a closed system that cycles DU waste from lake water to sediment and back again. Decreased concentrations in sediment are obtained because of the increased sediment load, but the mass of DU waste in each lake is not different except from decay and ingrowth.

In light of the simplifications that are included in the model, the results for the deep time scenario are presented for the first 100-ky cycle only, in which the first intermediate or large lake will return and the CAS embankment will be obliterated. The effect of dispersal on concentrations in lake water and sediment are presented for that time frame with a focus on ^{238}U. Conceptually, deep time will result in a combination of repeated isolation of sediment layers and much greater dispersal than modeled. This will cause mixing over ever increasing areas and volumes, rather than mixing within a closed system. Consequently, concentrations of radionuclides in the DU waste will decrease with each lake cycle and with each climate cycle. However, the constraints of the model do not allow lake water concentrations to decrease with each cycle, and sediment concentrations decrease only because of the additional mass of sediment in which the DU waste is mixed.

The focus of the deep-time results is, consequently, concentrations of ^{238}U in lake water and sediments within the first 100-ky climate cycle.

6.5.1 Lake Water Concentrations of Uranium-238

A summary of lake water concentrations of ^{238}U is presented in Table 13. Results are presented only for the "no gullies" model scenarios. Based on the model structure, the results should be the same for each of these three models (and also for the cases with gullies if they were included). This is because the entire existing inventory of DU waste is dispersed upon destruction of the embankment, including the waste disposed below grade. The inventory might differ to some relatively small extent because of transport of radionuclides to groundwater or to the accessible environment prior to the return of the lake. However, the lack of systematic differences in the results presented in Table 13 is more suggestive of simulation uncertainty. A time history plot is presented in Figure 12. The jagged nature of the plot is because lake water concentrations are zero when there is no lake present, and intermediate lakes only occur a handful of times prior to formation of the large lake at the end of the 100-ky climate cycle. The peak lake water

concentrations occur near the end of the period of the large lake, which provides time for the ^{238}U to dissolve into the lake.

Table 13. Statistical summary of peak mean uranium-238 concentrations in lake water within the first 100-ky climate cycle

	Peak mean lake water concentration of ^{238}U within 100 ky (pCi/L)		
simulation scenario	**mean**	**median (50th %ile)**	**95th %ile**
no gullies; waste > 3 m below cover	0.18	0.0010	1.1
no gullies; waste > 5 m below cover	0.17	0.0009	1.0
no gullies; waste > 10 m below cover	0.18	0.0009	1.3

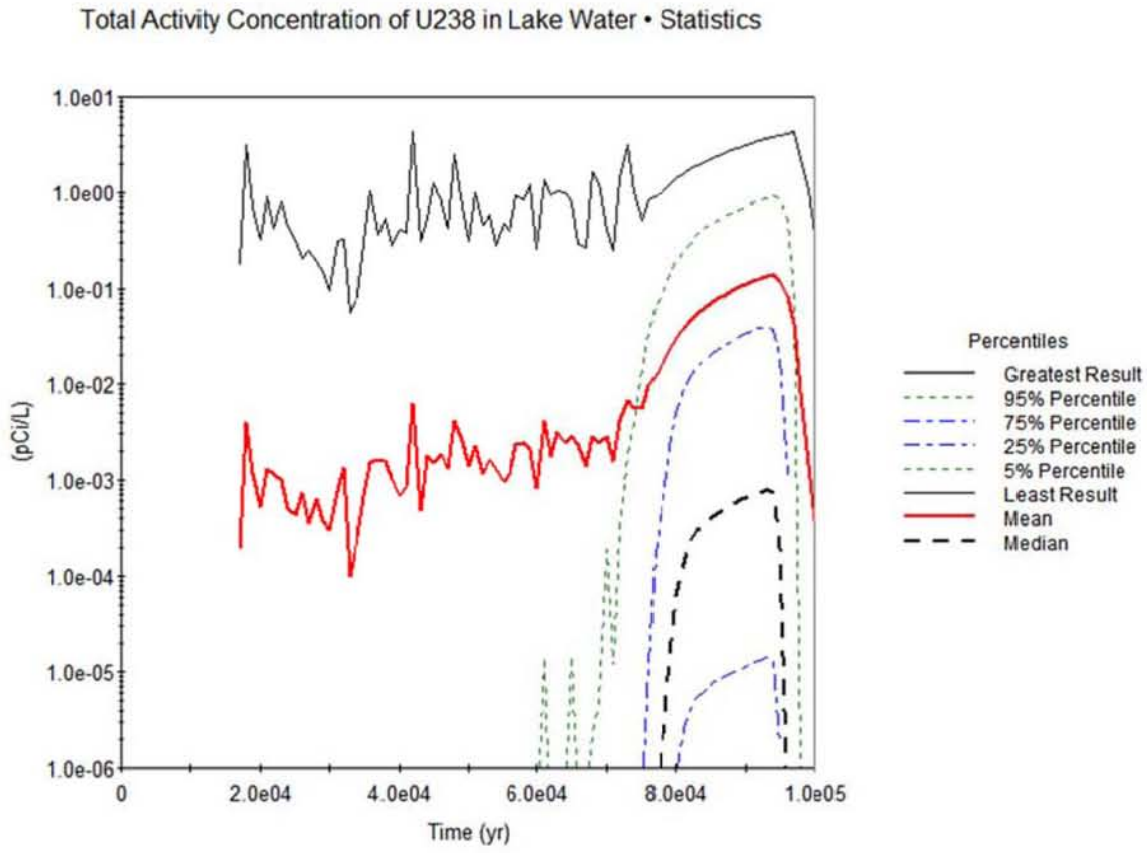

Figure 12. Time history of mean concentrations of uranium-238 in lake water

6.5.2 Lake Sediment Concentrations of Uranium-238

Results are presented similarly in Table 14 for concentrations of ^{238}U in sediment derived from successive lakes. The slight differences are, again due to simulation uncertainty.

Table 14. Statistical summary of peak mean uranium-238 concentrations in sediment within the first 100-ky climate cycle

	Peak mean sediment concentration of ^{238}U within 100 ky (pCi/g)		
simulation scenario	**mean**	**median (50th %ile)**	**95th %ile**
no gullies; waste > 3 m below cover	1,600	1,300	3,600
no gullies; waste > 5 m below cover	1,500	1,300	3,400
no gullies; waste > 10 m below cover	1,500	1,300	3,400

A time history of ^{238}U concentrations in future lake sediments is presented in Figure 13. This shows a large increase in concentrations as a consequence of the first lake event, with subsequent decreases as the sediment load increases.

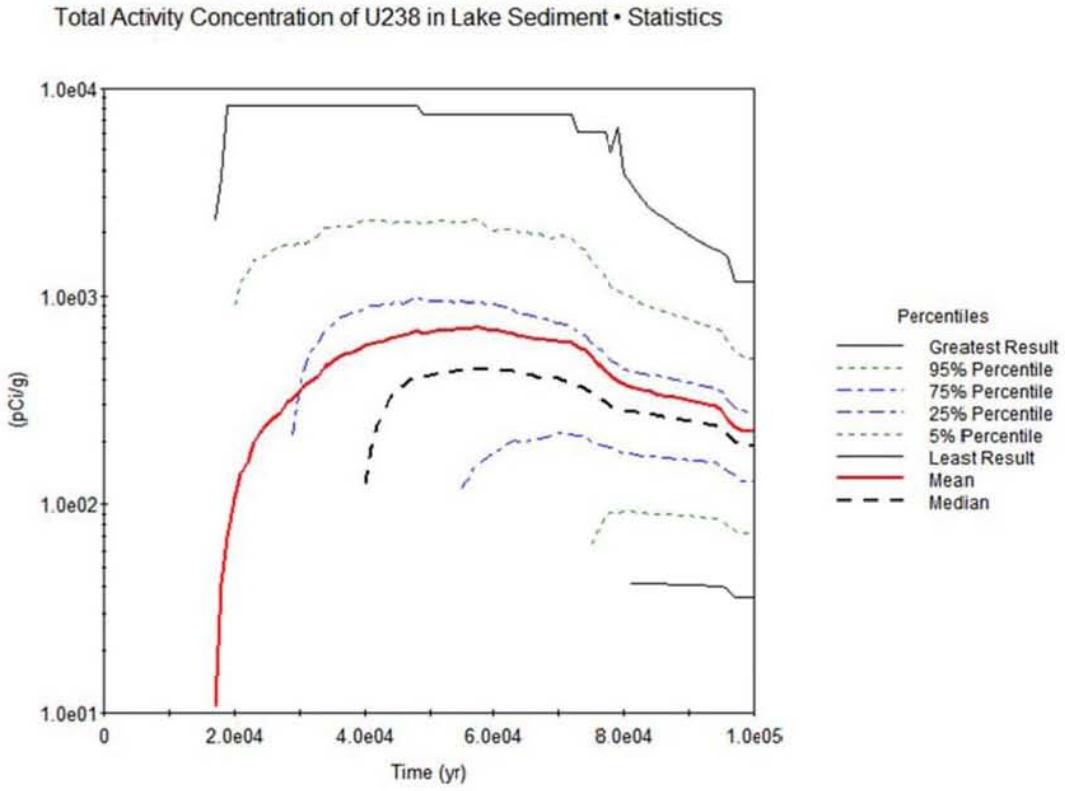

Figure 13. Time history of mean concentrations of uranium-238 in sediments

One of the objectives of a PA, as defined in the UAC R313-25-8 is site stability. The performance standard for stability requires the facility must be sited, designed, and closed to achieve long-term stability to eliminate to the extent practicable the need for ongoing active maintenance of the site following closure. If the intent is the need to minimize the need for ongoing active maintenance, as stated, then obliteration of the CAS embankment in deep time achieves this goal. The DU waste material is broadly dispersed with the embankment material, resulting in substantial dilution so that concentrations are low and the need to maintain the site disappears completely.

7.0 Summary

This report has laid out the approach taken to developing the PA model for DU waste disposal options at the Clive facility, and has presented results of the initial model (Clive DU PA Model v1.0) with accompanying sensitivity analyses. The purpose of this section is to provide an interpretation of the results in the context of the model, and to compare the results more directly to performance objectives in a compliance evaluation.

7.1 Interpretation of Results

Important results of the quantitative PA Model can be summarized, given the compliance time frames of interest, in terms of doses to ranch workers, groundwater concentrations of ^{99}Tc, and the effect of including gullies in the model. Three waste configurations have been considered, with waste placed at different depths to explore possible disposal configurations. Results of the simplistic ALARA analysis and concentrations in lake water and lake sediments in deep time are also of interest.

Doses to ranch workers increase as the waste is emplaced nearer to the embankment surface in the disposal facility. These doses are driven primarily by exposure to radon. However, groundwater concentrations of ^{99}Tc increase as the waste is emplaced lower in the disposal facility. These concentrations are driven primarily by the K_d for ^{99}Tc in sand, but the magnitude of the concentrations is also affected by the concentration distributions used for ^{99}Tc in the model, and the infiltration rates estimated from the HELP model. That is, the ^{99}Tc groundwater concentrations could be overestimated. These results highlight the trade-off between disposal configurations that place DU waste higher or lower in the disposal facility. Transport mechanisms move waste either up into the accessible environment or down towards groundwater. A balance is indicated so that performance objectives can be satisfied for these competing endpoints.

The dose results are sensitive to radon. Radon dose assessment is controversial, and takes a different path than dose assessment for other radionuclides, as described in the *Dose Assessment* white paper (Appendix 11).

Once gullies are involved, the doses increase (groundwater concentrations do not change noticeably). However, the effect is most noticeable for the 3-m configuration because sometimes gullies cut into the waste when the waste is placed that high in the embankment. The gully model is a stylized model, developed to examine the potential effects of inclusion of gullies in the Model. The calculation of the depth of gullies is sound, but the number of possible gullies of between 1 and 20 is included in the model only to evaluate sensitivity. The depth of gullies appears as more sensitive than the number of gullies, but both factors are important. Gullies are assumed to be caused by an initiating event such as OHV activity, cattle trails, or biotic impacts (animal burrowing). However, the impact of gullies has not been fully developed in terms of their effect on biotic activity, radon transport, or infiltration.

The ALARA analysis results are interesting mostly because the population doses are very small, which leads to very small ALARA costs, especially if the costs are discounted over time. The

population doses are small because the population itself is small, and the doses are also small. Taking this ALARA approach to site performance would suggest that this is a good site for disposal of DU waste. There is room for improvement in this crude ALARA decision analysis. For example, other factors could be included in the analysis such as transportation and worker safety factors, and the cost per person rem could be reevaluated. However, the small population because of the remoteness of the facility, and the low doses suggest that the disposal system would meet ALARA-based performance objectives.

The deep-time model should be regarded as heuristic or highly stylized. Nevertheless, it models the basic concepts of the return of lakes in the Bonneville Basin at or above the elevation of the Clive facility. A sufficiently large lake destroys the DU disposal facility, redistributes DU waste with the lake sediment, and repeats the cycles of DU waste moving into lake water, and settling back into sediment. Sedimentation rates are about 17 m per 100 ky, and the DU waste is assumed to mix with the sediment across time. There are several components of this heuristic model that could be regarded as conservative in the sense of over predicting concentration in both lake water and lake sediment. For example, all of the DU waste that is still in the disposal system is assumed to be dispersed when the embankment is obliterated, even though it might be reasonable to assume that the waste disposed below grade would be covered by lake sediment. Also, in the model a lake can destroy the site when it reaches the Clive elevation, which can cause mixing of waste in a very shallow lake, a lake that perhaps does not have sufficient power to destroy the facility. Research into the power needed for a lake to destroy the facility might indicate the minimum elevation needed for such an event. The embankment is dispersed over a comparatively small area in some simulations. Research into physical dispersal as a consequence of lake-induced destruction might be revealing. A water column is assumed above the dispersal area, which limits the amount of water available for mixing with DU waste. And, sediment mixing is assumed to occur with every lake cycle, even though some lake cycles might bury some sediment. Despite these possible conservatisms in the deep-time model, the lake water and lake sediment concentrations are small. They reflect concentrations associated with the first lake event, consistent with the timing of the maximum lake water and lake sediment concentrations.

Lake water concentrations of ^{238}U in the first 100-ky climate cycle average less than 1 pCi/L, even given the conservatism in the model. The peak of the mean concentrations of ^{238}U in sediment average about 1,500 pCi/g, with a 95th percentile of about 3,500 pCi/g. Given the simplified model structure, these lake water and sediment concentrations are probably considerable overestimates, and the concentrations should decrease with time as a consequence of further dispersal of the DU waste with other material over time.

7.2 Comparison to Performance Objectives

Comparisons to performance objectives are presented for doses to ranch workers, since dose to other receptors are considerably less, and groundwater concentration for ^{99}Tc. The evaluations address the three disposal configuration scenarios (3-m, 5-m, and 10-m) and exclusion/inclusion of gullies. Quantitative performance objectives do not exist for the ALARA analysis or for the deep-time concentrations endpoints.

The concentrations reported by the PA model represent estimates of the mean concentration in each year. The peak of those mean concentrations is collected across the 500-yr compliance period. Because the groundwater concentration of ^{99}Tc increases with time, the peak of the mean concentration occurs at 500 yrs. The 5,000 simulations provide 5,000 estimates of the peak of the mean concentrations. Summary statistics for the distribution of the peak of the mean ^{99}Tc concentrations are presented in Table 15. For the 3-m and 5-m models, compliance with the GWPLs is clearly demonstrated. For the 10-m model the situation is not as clear. However, both the mean (of the peak of the means) and the 95th percentile exceed the GWPL, in which case, it is probably reasonable to conclude that the 10-m scenario is not in compliance with the performance objective.

The results depend critically on the model structure, specification and underlying assumptions. Infiltration rates might be overestimated, and ^{99}Tc inventory concentrations might be overestimated. However, based on the model assumptions the 10-m model does not comply with the GWPL performance objective for ^{99}Tc. These results suggest that there are configurations that comply with the GWPLs.

Table 15. Peak groundwater activity concentrations for ^{99}Tc within 500 yr, compared to GWPLs

radionuclide	GWPL (pCi/L)	peak activity concentration within 500 yr (pCi/L)		
		mean	median (50th %ile)	95th %ile
waste emplaced > 3 m below embankment cover				
^{99}Tc	3790	85.9	1.43e-5	209
waste emplaced > 5 m below embankment cover				
^{99}Tc	3790	437	0.00264	1710
waste emplaced > 10 m below embankment cover				
^{99}Tc	3790	14400	113	81400

The dose results for ranch workers are presented in Table 16 for the no gully scenario, Table 17 for the scenario with gullies, and for all three disposal configurations. The statistics represent summaries of the peak of the mean doses. Considering that doses increase with time given the model construction and assumptions, then the 95th percentile is analogous to the 95% upper confidence interval of the mean that is common in CERLCA risk assessments. The mean and the 95th percentile are compared to the performance objectives.

The doses increase as waste is placed nearer the top of the embankment, but the MOP performance objectives are not exceeded in all cases. This implies that disposal configurations exist, under the conditions of this model, for which it is reasonable to dispose of DU waste.

Table 16. Peak mean TEDE, without consideration of gullies: statistical summary

	Peak TEDE (mrem in a yr) within 10,000 yr		
receptor	**mean**	**median (50th %ile)**	**95th %ile**
waste emplaced > 3 m below embankment cover			
ranch worker	4.37	3.44	11.3
waste emplaced > 5 m below embankment cover			
ranch worker	0.598	0.473	1.52
waste emplaced > 10 m below embankment cover			
ranch worker	0.00596	0.00471	0.0152

Table 17. Peak mean TEDE, with gully screening calculation: statistical summary

	Peak TEDE (mrem in a yr) within 10,000 yr		
receptor	**mean**	**median (50th %ile)**	**95th %ile**
waste emplaced > 3 m below embankment cover			
ranch worker	20.9	11.6	72.3
waste emplaced > 5 m below embankment cover			
ranch worker	0.564	0.443	1.44
waste emplaced > 10 m below embankment cover			
ranch worker	0.00594	0.00457	0.0155

8.0 Conclusions

Model results are dependent on the model structure, specification and assumptions upon which it is based. With the expertise and assumptions upon which the Clive DU PA Model v1.0 is based, the Model demonstrates that there are disposal configuration options for the subject DU waste that are adequately protective of human health and the environment as projected for the next 10,000 years. Protectiveness is assessed under Utah Administrative Code R313-25-8 Section 2(a) by consideration in this PA Model of:

- dose to site-specific receptors,
- concentrations in groundwater,
- ALARA, and
- considerations of deep-time scenarios.

The model was run using three different configurations: 3 m, 5 m, and 10 m of extra fill material. It was also run with and without expectation of gullies forming. Simplified results for these scenarios are presented in Table 18.

Table 18. Summary of results of the Clive DU PA Model

	without gullies: top of waste at			with gullies: top of waste at		
performance objective	**3-m**	**5-m**	**10-m**	**3-m**	**5-m**	**10-m**
Dose to MOP below regulatory threshold of 25 mrem/year	Yes	Yes	Yes	Maybe[1]	Yes	Yes
Dose to IHI below regulatory threshold of 500 mrem/year	Yes	Yes	Yes	Yes	Yes	Yes
Groundwater maximum concentration of ^{99}Tc in 500 years < 3790 pCi/L[3]	Yes	Yes	No[2]	Yes	Yes	No[2]
ALARA average total population cost equivalent over 10,000 years	$35,000	$4,000	$43	$378,000	$4,500	$45

[1]The expected dose to MOP is acceptable under this scenario, but the 95th percentile of the expected dose exceeds the regulatory threshold.

[2]These results might overestimate groundwater concentrations because of potential overestimation of infiltration rates and of the ^{99}Tc inventory.

[3]Groundwater concentrations of all other radionuclides are significantly less than their respective GWPLs, with the exception of ^{129}I inventory which is evaluated separately.

The three configurations that are evaluated for the Clive DU PA Model v1.0, with and without consideration of gullies, demonstrate that the disposal facility can adequately protect human health and the environment when disposing of the subject DU waste:

- all disposal options evaluated exhibit doses that are less than the inadvertent intrusion performance objective,
- there are clearly disposal configurations for which the predicted doses are less than the MOP performance objective, and
- there are clearly disposal options for which groundwater concentrations do not exceed GWPLs.

In addition, the ALARA analysis indicates that ALARA costs from population doses that might be realized for the duration of the 10 ky model are very small. On a per year basis, the ALARA costs are always less than $1 per day.

The deep-time model indicates that concentrations in media such as lake water and sediment will continue to decrease with each lake and climate cycle, and that destruction of the site will lead to dispersal of the DU waste in the Bonneville Basin. The CAS embankment will be destroyed and buried by the return of a large lake, but long-term maintenance will be unnecessary.

All conclusions depend on the model structure, specification and assumptions. Changes in any aspect of the model could cause different results.

9.0 References

Adrian Brown (Adrian Brown Consultants), 1997. *Volume I, LARW Infiltration Modeling Input Parameters and Results*, Report 3101B.970515.

Albright, W.H., G.W. Gee, G.V. Wilson, and M.J. Fayer. 2002. *Alternative Cover Assessment Project Phase I Report*. Desert Research Institute Publication No. 41183. Reno, NV.

Baird R.D., Bollenbacher, M.K., Murphy, E.S., et al. 1990. *Evaluation of the Potential Public Health Impacts Associated with Radioactive Waste Disposal at a Site Near Clive, Utah*. Rogers and Associates Engineering Corporation, Salt Lake City UT.

Berger, A. and M. F. Loutre, 2002. "An exceptionally long interglacial ahead?" *Science*, 297: 1287- 1288.

DOE (US Department of Energy). 1997. Applying the ALARA Process for Radiation Protection of the Public and Environmental Compliance with 10 CFR Part 834 and DOE 5400.5 ALARA Program Requirements, Volume 1 Discussion, DOE-STD-ALARA1draft. United States Department of Energy, Washington DC. April 1997.

Embrechts, P., Lindskog, F., and McNeil, A. (2001). *Modelling Dependence with Copulas and Applications to Risk Management*, Department of Mathematics, Swiss Federal Institute of Technology, Zurich.

Iman, R.L., and Conover, W.J. (1982). "A Distribution-Free Approach to Inducing Rank Correlation Among Input Variables," Communications in Statistics: Simulation and Computation,11 (3): 311-334.

Khire, M.V, C.H. Benson, and P.J. Bosscher, Water Balance Modeling of Earthen Final Covers, *Journal of Geotechnical and Geoenvironmental Engineering*, Vol. 23, No. 8, August 1997.

Meyer, P.D., M.L. Rockhold, W.E. Nichols, and G.W. Gee. 1996. *Hydrologic evaluation methodology for estimating water movement through the unsaturated zone at commercial low-level radioactive waste disposal sites.* NUREG/CR-6346. U.S. Nuclear Regulatory Commission. Washington, D.C.

NRC (U.S. Nuclear Regulatory Commission). 1993. *Final Environmental Impact Statement to Construct and Operate a Facility to Receive, Store, and Dispose of 11e.(2) Byproduct Material Near Clive, Utah*, NUREG-1476, US Nuclear Regulatory Commission, Washington, DC.

NRC. 1995. *Reassessment of NRC's Dollar Per Person-Rem Conversion Factor Policy*, NUREG-1530, US Nuclear Regulatory Commission, Washington, DC. December 1995.

NRC, 2000. *A Performance Assessment Methodology for Low-Level Radioactive Waste Disposal Facilities*. NUREG-1573. Division of Waste Management, Office of Material Safety and Safeguards, U.S. Nuclear Regulatory Commission, Washington D.C., October 2000

NRC, 2010. Workshop on Engineered Barrier Performance Related to Low-Level Radioactive Waste, Decommissioning, and Uranium Mill Tailings Facilities. Nuclear Regulatory Commission. August 3 – 5, 2010.

SWCA 2011. *Field Sampling of Biotic Turbation of Soils at the Clive Site, Tooele County, Utah*. SWCA Environmental Consultants Inc. Prepared for Energy*Solutions*, Salt Lake City, UT.

Utah 2010. License Requirements for Land Disposal of Radioactive Waste. Utah Administrative Code Rule R313-25.

UWQB (State of Utah, Division of Water Quality, Utah Water Quality Board), 2009. Ground Water Quality Discharge Permit No. 450005, 23 Dec 2009.

Whetstone, 2006. EnergySolutions Class A Combined (CAC) Disposal Cell Infiltration and Transport Modeling Report, Salt Lake City Utah, May 2006.

List of Appendices

Neptune and Company Inc.

June 1, 2011 Report for EnergySolutions

Clive DU PA Model, version 1

Appendix 1

FEP Analysis for Disposal of

Depleted Uranium at the Clive Facility

FEP Analysis for Disposal of Depleted Uranium at the Clive Facility

28 May 2011

Prepared by

Neptune and Company, Inc.

This page intentionally left blank, aside from this statement.

CONTENTS

TABLES

1.0 Introduction

The safe storage and disposal of depleted uranium (DU) waste is essential for mitigating releases of radioactive materials and reducing exposures to humans and the environment. Currently, a radioactive waste facility located in Clive, Utah (the "Clive facility") operated by Energy*Solutions* is proposed to receive and store DU waste that has been declared surplus from radiological facilities across the nation. The Clive facility has been tasked with disposing of the DU waste in an economically feasible manner that protects humans from radiological releases.

To assess whether that the proposed Clive facility DU disposal location and containment technologies are suitable for protection of human health, specific performance objectives for land disposal of radioactive waste set forth in Title 10 Code of Federal Regulations Part 61 (10 CFR 61) Subpart C, promulgated by the U.S. Nuclear Regulatory Commission (NRC), must be met. In order to support the required radiological performance assessment (PA), a detailed computer model is being developed to evaluate the potential detrimental effects on human health that would result from the disposal of DU and its associated radioactive contaminants.

A key activity in developing a PA for a radiological waste repository is the comprehensive identification of relevant external factors that should be included in quantitative analyses. These factors, termed "features, events, and processes" (FEPs), form the basis for scenarios that are evaluated to assess site performance.

Although it is not a governing regulation for the disposal of LLW and DU at Clive, Title 40 CFR Part 191, promulgated by the U.S. Environmental Protection Agency (EPA), provides a useful and general definition for the scope of a PA analysis of a radiological disposal facility. The PA 1) identifies the processes and events that might affect the disposal system, 2) examines the effects of these processes and events on the performance of the disposal system, and 3) estimates the cumulative releases of radionuclides considering the associated uncertainties caused by all significant processes and events (40 CFR 191). The identification of FEPs is essential to the development of the conceptual site model (CSM) and model scenario development process (see *Conceptual Site Model for Disposal of Depleted Uranium at the Clive Facility*).

This report serves to document and examine the universe of FEPs that may apply to the disposal of depleted uranium (DU) waste at the Clive Facility. FEPs that are screened and identified as relevant for the Clive facility PA are identified in this white paper and are further elaborated in the CSM document.

This document is considered to be a living document that is synchronized with current conceptual models, analysis, and modeling of the PA. As concepts and modeling evolve, so too will this document.

2.0 Identification of Features, Events, and Processes

The identification of FEPs for use in the Clive facility PA was an iterative process that began with compiling an exhaustive list of candidate FEPs that could affect the long-term performance of the radiological waste repository. As an initial step, all potentially relevant FEPs from a

variety of reference sources were collected. The initial list from external sources was modified as additional FEPs were identified that are specific to the Clive facility.

This exhaustive initial compilation of FEPs led to significant redundancy across the original sources. Redundancy was addressed by the modification of the candidate list of FEPs through normalization (removal of redundant FEPs) and assignment of FEPs categories (grouping of common FEPs). This section describes the FEP identification process, including implementation of the normalization, categorization and screening processes.

2.1 Compilation of FEPs

The initial list of FEPs pertaining to the efficacy of disposal of radioactive wastes in general was compiled from several scenario development documents published for other nuclear waste disposal facilities, including those for Yucca Mountain Project, the Waste Isolation Pilot Plant, and several foreign radioactive waste projects. The primary literature source for FEP analysis is Guzowski and Newman (1993). They compiled over 700 potentially disruptive FEPs from a review of scenario documentation from other waste repositories around the world.

The facilities considered in Guzowski and Newman have substantially different geological, environmental and regulatory settings from those of the Clive facility. Consequently, the collection of FEPs in Guzowski and Newman provides a substantial list that should be considered for any PA, but they are also missing FEPs that pertain more particularly to the waste disposal facility at Clive. Site-specific understanding of the environmental and engineered attributes of the Clive facility, and the potentially affected region and population, was used to augment the initial compilation of FEPs.

Additional FEPs were also identified from the Nuclear Energy Agency database (NEA, 2000). In this initial compilation step, nearly 1,000 FEPs were identified from the literature and site-specific considerations. Initial FEPs compiled from all sources are listed in Table A in the Appendix.

2.2 Normalization and Consolidation of FEPs

Subsequent to the initial compilation of FEPs, steps were taken to reduce redundancy. Initially, FEPs were sorted alphabetically and duplicates were deleted. Recorded FEP values that were different only in vernacular/diction (e.g., “climate change” versus “change in climate”) were normalized to capture a single primary FEP value for a series of identical or closely-related concepts.

To address duplication of FEPs where similar terminology was stated dissimilarly, initial FEPs were grouped by keyword content (e.g., “climate,” “waste,” “groundwater,” etc.) and evaluated for possible normalization or consolidation. Where possible, FEPs were normalized to a standard terminology.

Similar but not identical FEPs were maintained, to be evaluated as part of the consolidation step. At this point, each FEP was considered for its similarity to other FEPs, so that they could be grouped into fewer classes, making the list more manageable. For example, all geochemical processes were grouped together. These would be easier to address as a group for inclusion in the CSM. Likewise, all coastal processes could be considered for exclusion as a group. For each

FEP, the rationale behind its grouping was noted. No FEPs were excluded at this step, but nearly all were consolidated with others. This consolidation process reduced the total number to 135 unique FEP groupings.

3.0 Classifying Features, Events, and Processes

Following the normalization and consolidation steps, the 135 unique FEP groups were carried forward to the classification step and were considered for inclusion in the conceptual model scenarios. The classification is principally an organizational tool for the FEP analysis, although the categories identified also relate to components of the CSM. The 135 unique FEP groups were classified into the following 18 categories:

- Celestial
- Climate change
- Containerization
- Contaminant Migration
- Engineered Features
- Exposure
- Hydrology
- Geochemical
- Geological
- Human Processes
- Hydrogeological
- Marine
- Meteorology
- Model Settings
- Other Natural Processes
- Source Release
- Tectonic/Seismic/Volcanic
- Waste

These categories are relevant to the development of scenarios and are integral to the CSM for the Clive Facility. Occasionally, a FEP could have been classified into more than one category. However, the overall goal of the FEP analysis is to identify those processes that should be carried forward into the CSM, and subsequently into the modeling. Provided each FEP is identified in one of the categories, it was carried forward to the CSM. Ultimately, each FEP was given due consideration, and the implementation of relevant FEPs in the final modeling was rather independent of the classification.

4.0 Screening of FEPs

The long list of FEPs was screened in consideration of regulatory concern and professional judgment based on physical reasonableness, probability of occurrence, severity of consequence, and assessment scope.

The most basic screening criterion is regulatory concern. Regulatory requirements for performance of EnergySolutions' Clive facility are published in 10 CFR 61 and Utah Administrative Code R313. While the mention of something that can be construed as a feature, event, or process in the text of a regulation triggers its consideration in this FEP analysis, it does not mean that the FEP must become part of the PA analysis or modeling.

A subjective element of the FEP screening process is consideration of assessment scope and physical reasonableness. Physical reasonableness is a professional judgment based on logical arguments using available data and information to support a conclusion of whether or not conditions can exist within the period of regulatory concern that will result in the occurrence of a particular event or process that affects disposal system performance. In addition to meeting screening criteria, some FEPs were retained as model parameters specifically because they pertain to scenario development itself (e.g., exposure terms).

The inclusion or dismissal of FEPs and associated rationale is documented in support of constructing the conceptual model and scenarios. The product of this screening procedure is the identification of those FEPs that, either alone or in conjunction with others, could affect the performance of the disposal system.

4.1 Regulatory Considerations, Guidance, and Supporting Information

This section discusses the regulatory language, guidance, and other supporting information to be considered in developing scenarios and conceptual models for the Clive Facility PA. Specific considerations of NRC's land disposal performance requirements (10 CFR 61 Subpart C) are required for the PA scenario development and are important to document as part of the FEP compilation and screening activity. In addition, observations and recommendations previously published by radioactive waste disposal facility working groups and technical advisers are also considered, although most of these are focused on geologic disposal of radioactive wastes.

Specific provisions of regulations for the operation and closure of a land-disposal LLW facility were specifically considered if they were mentioned in a regulatory document.

Based on these provisions, 55 of 135 FEPs were identified as relevant for evaluation in the conceptual model or exposure scenarios. The remaining FEPs were dismissed from further consideration for various reasons. Some, like a direct impact from a large meteorite, are simply beyond the scope of the PA analysis. Tsunami and other marine phenomena obviously do not apply at the Clive facility. Several FEPs from the original sources were dismissed because they apply only to geologic repositories, or to specific types of containment, like copper canisters for used nuclear fuel.

4.1.1 Nuclear Regulatory Commission: 10 CFR 61

This regulation contains Federal procedural requirements and performance objectives applicable to land disposal of radioactive waste. Specific considerations of 10 CFR 61 include attributes of facility siting, facility engineering (including post-closure stability and control), site monitoring, record-keeping, protection of health and safety, and a minimum time frame for which an assessment must be conducted to ensure long-term stability of the disposal site. The types of FEPs mentioned in 10 CFR 61 include:

- long-term effectiveness based on physical siting of the disposal unit (including site geology and hydrology),
- protection of the general population (in terms of radiological dose),
- protection of inadvertent intruders (dose),
- protection of individuals during operations (dose),
- isolation and segregation of wastes,
- releases of radionuclides via pathways in air, water, surface water, plant uptake, or exhumation by burrowing animals,
- long-term stability of the disposal site,
- evaluation of engineering failures, including erosion, mass wasting, slope failure, settlement of wastes and backfill, infiltration through covers, and surface drainage,
- site monitoring requirements,
- identification of natural resources whose exploitation could result in inadvertent exposure, and
- efficacy of institutional controls.

4.1.2 Utah Administrative Code R313: Radiation Control

The Utah Administrative Code (UAC) Rules 313-15 (*Standards for Protection Against Radiation*) and 313-25 (*License Requirements for Land Disposal of Radioactive Waste*) mirror the provisions for land disposal of radioactive waste provided in 10 CFR 61. Notable technical performance objectives of near-surface disposal sites established of UAC Rule R313-25 include:

- protection of the general population,
- protection of inadvertent intruders,
- consideration of releases of radionuclides through pathways via air, water, surface water, plant update, and exhumation of burrowing animals,
- protection of individuals during operations,
- long-term stability of the disposal site,
- prevention of erosion, mass wasting, slope failure, settlement of wastes and backfill, infiltration through covers, and surface drainage,
- site monitoring requirements, and
- identification of natural resources whose exploitation could result in inadvertent exposure.

The majority of the FEPs identified as relevant under 10 CFR 61 are also applicable under UAC Rule R313-25 and are retained for analysis.

4.1.3 Additional Guidance

The NRC's PA working group has identified additional considerations in NRC's *Performance Assessment Methodology* (NRC 2000). The working group identifies two specific areas of interest in conducting a PA: pathway analysis and dose assessment.

Pathway analysis involves the mechanisms of radionuclide transfer through the biosphere to humans. These mechanisms, or transport and exposure pathways, must be identified and modeled. Pathway analysis should result in the determination of the total intake of radionuclides by the average member of the critical group. The critical group is defined as the "...group of individuals reasonably expected to receive the greatest dose from radioactive releases from the disposal facility over time, given the circumstances under which the analysis would be carried out" (NRC 2000).

Various considerations should be taken into account when analyzing the transport of radionuclides through the biosphere (to humans). These considerations should include

- modeling the movement of radionuclides through the environment and the food chain, adequately reflecting complex symbiotic systems and relationships,
- considering mechanisms of (biotic and) human uptake of radionuclides, and
- identifying usage, production, and consumption parameters, for various food products and related systems, that may vary widely, depending on regional climate conditions, local or ethnic diet, and habits.

The dose assessment requires that the dosimetry of the exposed individual be modeled. The objective of dose modeling in a LLW PA is to provide estimates of potential doses to humans, in terms of the average member of the critical group, from radioactive releases from a LLW disposal facility, after closure.

A "current conditions" philosophy is initially applied to determine which pathways are to be evaluated. That is to say that current regional land use and other local conditions in place at the time of the analysis will strongly influence pathways that are considered to be significant. The conceptual model and scenarios must consider each of the general pathways discussed in 10 CFR 61.13. Additional pathways for consideration are published in NUREG/CR-5453 (Shipers, 1989) and NUREG-1200 (NRC, 1994). NUREG-1200 discusses example potential "scenarios by which radioactivity may be released from the disposal facility and cause the potential for radiological impacts on individuals." Shipers (1989) identifies exposure pathways, and scenarios regarding transport mechanisms that could contribute to the release of radioactive materials from the disposal facility leading to human exposure, in the context of near-surface LLW disposal.

4.2 Scope of Assessment and Physical Reasonableness

The final phase of FEP screening is the application of professional judgment in terms of the scope of the PA and the physical reasonableness of evaluating those FEPs in the CSM and scenarios. Performance objectives include protection of the general population from releases of radioactivity (10 CFR 61.41), protection of individuals from inadvertent intrusion (§61.42), and stability of the site after closure (§61.44). Assumptions of the scope of the PA include:

- Performance assessment reflects post-closure conditions. Because PA considers the site only after closure, consideration of the protection of individuals during operations (§61.43) is not within the scope of the evaluation and FEPs related to operations are not considered relevant to the CSM or scenarios.
- Land-use assumptions relative to human exposures post-closure are based on current conditions and likely future conditions. Therefore urban settlement, residential use, farming, and aquaculture and FEPs pertaining to these incongruous uses are not included in the CSM or scenarios because of the high concentrations of salt in the soil and groundwater of this site. However, hunting, ranching, and recreational use are considered viable scenarios.
- Intentional human intruders are not protected.

5.0 Screening Results

Using the identification and screening processes described in Sections 1 through 3, FEPs were consolidated from an exhaustive list of over 900 to 135 FEPs or FEP categories. Of this consolidation, 90 FEPs are retained for further consideration and 45 FEPs were dismissed from inclusion in the PA model. All FEPs considered and retained for inclusion in the CSM and scenarios are reported in Table B in the Appendix. FEPs that were considered and dismissed from evaluation in the CSM and scenarios are listed in Table C, along with a brief rationale for their exclusion.

In summary, FEPs retained for consideration in the PA, CSM, and scenarios pertain to regulatory aspects of post-closure protection of human health and long-term stability of the disposal facility for the duration and spatial scope of the assessment period. FEPs that were dismissed from consideration in the PA include those that do not fall within the scope of the PA, were characterized as extremely unlikely to occur or having a low magnitude of consequence of affecting the performance of the repository, or were dismissed based on site-specific considerations.

6.0 Use of FEPs for Conceptual Model and Scenario Development

The CSM provides detailed descriptions of the physical environment, the engineered disposal facility, the sources and chemical forms of disposed wastes, potentially affected media, potential release pathways and exposure routes, and potential receptors. The CSM considers broad categories of FEPs that are relevant to these attributes, but individual FEPs may or may not be

addressed in the CSM based on the scope of the assessment and the scenarios developed. This section identifies the FEPs that are considered for inclusion in the CSM and are addressed in the development of scenarios for the PA model. These are grouped into several categories, and listed in tabulated form in Appendix B. Those FEPs that were dismissed from consideration in the modeling are listed in Appendix C. Some FEPs may overlap or repeat between categories.

Meteorology

Frost weathering and other meteorological events (e.g., precipitation, atmospheric dispersion, resuspension) are considered in the conceptual model. Weathering may occur from frost cycles. Resuspension of particulates from surface soils allows them to be redistributed by atmospheric dispersion, which is a meteorological phenomenon. Dust devils are also possible at the site and a tornado occurred in Salt Lake City in 1999, which was the first tornado in Utah in over 100 years.

Climate change

Features, events, and processes of climate change considered in the conceptual model include effects on hydrology (including lake effects), hydrogeology, biota, and human behaviors. Lake effects include appearance/disappearance of large lakes and associated phenomena (sedimentation, wave action, erosion/inundation). Wave action, including seiches, is included in the CSM.

Hydrology

Hydrology is addressed in the conceptual model since it influences many processes in contaminant transport. Examples of FEPs considered for the conceptual model include groundwater transport, inundation, and water table changes.

Hydrogeological

Several hydrogeological FEPs were identified for consideration in the conceptual model. Groundwater transport, in both the unsaturated and saturated zones, is potentially a significant transport pathway. For some model endpoints, such as groundwater concentrations that are compared to groundwater protection levels (GWPLs), it is the only pathway of concern.

Groundwater flow and transport processes include advection-dispersion, diffusion, fluid migration, waterborne contaminant transport, changes in the flow system, recharge, water table movements, and brine interactions. Inundation of the site may occur due to changes in lakes or reservoirs, which is included in lake effects of climate change.

Geochemical

Geochemical effects include chemical sorption and partitioning between phases, aqueous solubility, precipitation, chemical stability, complexation, changes in water chemistry (redox potential, pH, Eh), fluid interactions, speciation, interactions with clays and other host materials, and leaching of radionuclides from the waste form. These processes are addressed in the model.

Other Natural Processes

The broad category of other natural processes considered for the conceptual model include ecological changes and pedogenesis (soil formation). Ecological changes are associated with catastrophic events (e.g., inundation), evolution, or climate change. Pedogenesis is expected on the cap, giving rise to vegetation growth or habitation by wildlife.

Denudation (cap erosion) may be sufficient to expose waste. Erosion of the repository resulting from pluvial, fluvial or aeolian processes can result from extreme precipitation, changes in surface water channels, and weathering. Sediment transport is an inherent aspect of erosion. Sedimentation/deposition onto the repository would also affect disposal at the site.

Note that seismic activity is unlikely to impact the Clive facility. Faults are not present within the vicinity of Clive, although effects of isostatic rebound are still possible in the Lake Bonneville area.

Engineered Features

Engineered features are intended to promote containment and inhibit migration of contaminants. Conditions potentially affecting site performance include failure of general engineered features, repository design, repository seals, material properties, and subsidence of the repository.

Containerization

Two key components of containerization were identified as FEPs: containment degradation and corrosion. Canister degradation, including fractures, fissures, and corrosion (pitting, rusting) could result in containment failure. These processes are evaluated in the conceptual model.

Waste

Attributes of waste that could influence the performance of the Clive facility include the inventory of radionuclides, physical and chemical waste forms, container performance, matrix performance, leaching, radon emanation, and other waste release mechanisms.

Source Release

Source release can result from many mechanisms, including containment failure, leaching, radon emanation, plant uptake, and translocation by burrowing animals. FEPs that fit in the category of source release include gas generation, radioactive decay and in-growth, and radon emanation.

Contaminant Migration

Contaminant migration for the CSM includes the mechanisms and processes by which radionuclides may come to be located outside of the containment unit. The following contaminant migration processes were identified for consideration in the conceptual model: resuspension, atmospheric dispersion, biotically-induced transport, contaminant transport, diffusion, dilution, advection-dispersion, dissolution, dust devils, tornados, infiltration, and preferential pathways.

Animal ingestion is part of the human exposure model, both as ingestion of fodder and feed by livestock, and ingestion of livestock by humans. Transport by atmospheric dispersion is modeled and is associated with limited resuspension, dust devils, and tornados. Modeling of biotic (plant- and animal-mediated) processes leading to contaminant transport, and the evolution of these processes in response to climate change and other influences, including bioturbation, burrowing, root development, and contaminant uptake and translocation are considered. Contaminant transport includes transport media (water, air, soil), transport processes (advection-dispersion, diffusion, plant uptake, soil translocation), and partitioning between phases. Diffusion occurs in gas and water phases. Dilution occurs when mixing with less concentrated water. Hydrodynamic dispersion is associated with water advection. Dissolution in water is limited by aqueous solubility. Transport in the gas phase includes gas generation in the waste, partitioning between air and water phases, diffusion in air and water, and radioactive decay and ingrowth. Infiltration of water through the cap, into wastes, and potentially to the groundwater is another contaminant migration concern. Preferential pathways for contaminant transport are also addressed.

Human Processes

The FEPs identified as human processes encompass human behaviors and activities, resource use, and unintentional intrusion into the repository. Human process FEPs identified for assessment are related to the human exposure model and include anthropogenic climate change, human behavior, human-induced processes related to engineered features at the site, human-induced transport, inadvertent human intrusion, institutional control, land use, post-closure subsurface activities, waste recovery, water resource management, and weapons training such as that occurring at nearby bombing ranges.

Exposure

Exposure is an integral part of the conceptual model, and may result from reduced site performance. Exposure-relevant FEPs identified for evaluation include those related to dosimetry, exposure media, human exposure, ingestion pathways, and inhalation pathways. Dosimetry as a science is not a FEP *per se* but physiological dose response is accounted for in the PA model.

Transport pathways (e.g. food chains) that lead to foodstuff contamination, and human exposures due to inhalation of gaseous radionuclides and particulates are included. Exposure media include are foodstuffs, drinking water, and environmental media. Exposure pathways (ingestion, inhalation, etc.) and physiological effects from radionuclides and toxic contaminants (e.g. uranium) are also assessed.

Model Settings

Model settings that were identified during the FEP compilation process include model parameterization, period of performance, regulatory requirements, and spatial domain. While these are not FEPs in and of themselves, they are important considerations in the performance assessment model and are included with the FEPs for completeness.

7.0 References

Andersson, J., T. Carlsson, T., F. Kautsky, E. Soderman, and S. Wingefors, 1989. *The Joint SKI/SKB Scenario Development Project*. SKB-TR89-35, SvenskKarnbranslehantering Ab, Stockholm, Sweden.

Burkholder, H.C., 1980. "Waste Isolation Performance Assessment—A Status Report", in *Scientific Basis for Nuclear Waste Management*, Ed. C.J.M. Northrup, Jr., Plenum Press, New York, NY, Vol. 2, p. 689-702.

Code of Federal Regulations, Title 10, Part 61 (10 CFR 61), *Licensing Requirements for Land Disposal of Radioactive Waste*, Government Printing Office, 2007.

Code of Federal Regulations, Title 40, Part 191 (40 CFR 191), *Environmental Radiation Protection Standards for Management and Disposal of Spent Nuclear Fuel, High-Level and Transuranic Radioactive Waste*, Government Printing Office, 1993.

Guzowski, R.V., 1990. *Preliminary Identification of Scenarios That May Affect the Escape and Transport of Radionuclides From the Waste Isolation Pilot Plant, Southeastern New Mexico*, SAND89-7149, Sandia National Laboratories, Albuquerque, NM.

Guzowski, R.V., and G. Newman, 1993, *Preliminary Identification of Potentially Disruptive Scenarios at the Greater Confinement Disposal Facility, Area 5 of the Nevada Test Site*, SAND93-7100, Sandia National Laboratories, Albuquerque, NM.

Hertzler, C.L., and C.L. Atwood, 1989. *Preliminary Development and Screening of Release Scenarios for Greater Confinement Disposal of Transuranic Waste at the Nevada Test Site*, EGG-SARE-8767, EG&G Idaho, Inc., Idaho Falls, ID.

Hunter, R.L., 1983. *Preliminary Scenarios for the Release of Radioactive Waste From a Hypothetical Repository in Basalt of the Columbia Plateau*, SAND83-1342 (NUREG/CR-3353), Sandia National Laboratories, Albuquerque, NM.

Hunter, R.L., 1989. *Events and Processes for Constructing Scenarios for the Release of Transuranic Waste From the Waste Isolation Pilot Plant*, Southeastern New Mexico, SAND89-2546, Sandia National Laboratories, Albuquerque, NM.

Koplik, C.M., M.F. Kaplan, and B. Ross, 1982. "The Safety of Repositories for Highly Radioactive Wastes," *Reviews of Modern Physics*, Vol. 54, no. 1, p. 269-310.

Merrett, GJ., and P.A. Gillespie, 1983. *Nuclear Fuel Waste Disposal: Long-Term Stability Analysis*, AECL-6820, Atomic Energy of Canada Limited, Pinawa, Manitoba.

NEA (Nuclear Energy Agency), 1992, *Systematic Approach to Scenario Development. A report of the NEA Working Group on the Identification and Selection of Scenarios for Performance Assessment of Radioactive Waste Disposal*, Nuclear Energy Agency, Paris, France.

NEA, 2000. *Features, Events, and Processes (FEPs) for Geologic Disposal of Radioactive Waste. An International Database*. Nuclear Energy Agency, Organization for Economic Cooperation and Development.

NRC (U.S. Nuclear Regulatory Commission), 1994. *Standard Review Plan for the Review of a License Application for a Low-Level Radioactive Waste Disposal Facility*, NUREG-1200, U.S. Nuclear Regulatory Commission, Washington, D.C.

NRC, 2000. *A Performance Assessment Methodology for Low-Level Radioactive Waste Disposal Facilities*, NUREG-1573, U.S. Nuclear Regulatory Commission, Washington, D.C.

Shipers, L.R., 1989, *Background Information for the Development of a Low-Level Waste Performance Assessment Methodology, Identification of Potential Exposure Pathways*, NUREG/CR-5453, Vol. 1 , U.S. Nuclear Regulatory Commission, December 1989.

Appendix: FEP Listings

This appendix lists the features, events, and processes (FEPs) identified for evaluation in the Conceptual Site Model and Performance Assessment Scenario development. Table A contains all initial FEP values, listed and numbered by reference document. Table B lists those FEPs retained for analysis, and Table C includes all those FEPs that were dismissed from further consideration.

Table A. List of Initial FEPs by Reference

Table A (continued)

FEP ID	Initial FEP	Reference[1]
1	meteorite	Andersson et al., 1989
2	change in sea level	Andersson et al., 1989
3	desert and unsaturation	Andersson et al., 1989
4	no ice age	Andersson et al., 1989
5	glaciation	Andersson et al., 1989
6	permafrost	Andersson et al., 1989
7	creeping of copper	Andersson et al., 1989
8	common cause canister defects - Quality control	Andersson et al., 1989
9	cracking along welds	Andersson et al., 1989
10	degradation of hole- and shaft seals	Andersson et al., 1989
11	electro-chemical cracking	Andersson et al., 1989
12	internal pressure	Andersson et al., 1989
13	radiation effects on canister	Andersson et al., 1989
14	random canister defects - Quality control	Andersson et al., 1989
15	reactions with cement pore water	Andersson et al., 1989
16	role of chlorides in copper corrosion	Andersson et al., 1989
17	thermal cracking	Andersson et al., 1989
18	corrosive agents, sulphides, oxygen etc	Andersson et al., 1989
19	pitting	Andersson et al., 1989
20	stress corrosion cracking	Andersson et al., 1989
21	accumulation in peat	Andersson et al., 1989
22	colloid generation and transport	Andersson et al., 1989
23	colloid generation - source	Andersson et al., 1989
24	colloids, complexing agents	Andersson et al., 1989
25	accumulation in sediments	Andersson et al., 1989
26	loss of ductility	Andersson et al., 1989
27	matrix diffusion	Andersson et al., 1989
28	saturation of sorption sites	Andersson et al., 1989
29	solubility and precipitation	Andersson et al., 1989
30	sorption	Andersson et al., 1989
31	extreme channel flow of oxidants and nuclides	Andersson et al., 1989
32	radiation effects on bentonite	Andersson et al., 1989
33	solubility within fuel matrix	Andersson et al., 1989
34	thermal buoyancy	Andersson et al., 1989
35	thermochemical changes	Andersson et al., 1989
36	diffusion - surface diffusion	Andersson et al., 1989

Table A (continued)

FEP ID	Initial FEP	Reference[1]
37	dilution	Andersson et al., 1989
38	dispersion	Andersson et al., 1989
39	dissolution chemistry	Andersson et al., 1989
40	dissolution of fracture fillings/precipitations	Andersson et al., 1989
41	methane intrusion	Andersson et al., 1989
42	accumulation of gases under permafrost	Andersson et al., 1989
43	gas transport	Andersson et al., 1989
44	gas transport in bentonite	Andersson et al., 1989
45	flow through buffer/backfill	Andersson et al., 1989
46	preferential pathways in the buffer/backfill	Andersson et al., 1989
47	poorly designed repository	Andersson et al., 1989
48	backfill effects on copper corrosion	Andersson et al., 1989
49	backfill material deficiencies	Andersson et al., 1989
50	changed hydrostatic pressure on canister	Andersson et al., 1989
51	degradation of the bentonite by chemical reactions	Andersson et al., 1989
52	erosion of buffer/backfill	Andersson et al., 1989
53	excavation/backfilling effects on nearby rock	Andersson et al., 1989
54	external stress	Andersson et al., 1989
55	hydraulic conductivity change - excavation/backfilling effect	Andersson et al., 1989
56	hydrostatic pressure on canister	Andersson et al., 1989
57	movement of canister in buffer/backfill	Andersson et al., 1989
58	thermal effects on the buffer material	Andersson et al., 1989
59	voids in the lead filling	Andersson et al., 1989
60	swelling of bentonite into tunnels and cracks	Andersson et al., 1989
61	swelling of corrosion products	Andersson et al., 1989
62	uneven swelling of bentonite	Andersson et al., 1989
63	mechanical effects - excavation/backfilling effects	Andersson et al., 1989
64	mechanical failure of buffer/backfill	Andersson et al., 1989
65	mechanical failure of repository	Andersson et al., 1989
66	sudden energy release	Andersson et al., 1989
67	coagulation of bentonite	Andersson et al., 1989
68	chemical toxicity of wastes	Andersson et al., 1989
69	complexing agents	Andersson et al., 1989
70	far field hydrochemistry - acids, oxidants. nitrate	Andersson et al., 1989
71	change of ground-water chemistry in nearby rock	Andersson et al., 1989
72	chemical effects of rock reinforcement	Andersson et al., 1989
73	coupled effects (electrophoresis)	Andersson et al., 1989
74	effects of bentonite on ground-water chemistry	Andersson et al., 1989
75	isotopic dilution	Andersson et al., 1989
76	near field buffer chemistry	Andersson et al., 1989
77	oxidizing conditions	Andersson et al., 1989
78	Pb-I reactions	Andersson et al., 1989
79	pH-deviations	Andersson et al., 1989
80	recrystallization	Andersson et al., 1989
81	redox front	Andersson et al., 1989
82	redox potential	Andersson et al., 1989
83	diagenesis	Andersson et al., 1989
84	accidents during operation	Andersson et al., 1989
85	human-induced climate change	Andersson et al., 1989
86	non-sealed repository	Andersson et al., 1989
87	unsealed boreholes and/or shafts	Andersson et al., 1989

Table A (continued)

FEP ID	Initial FEP	Reference[1]
88	explosions	Andersson et al., 1989
89	geothermal energy production	Andersson et al., 1989
90	enhanced rock fracturing	Andersson et al., 1989
91	thermo-hydro-mechanical effects	Andersson et al., 1989
92	altered surface water chemistry by humans	Andersson et al., 1989
93	city on the site	Andersson et al., 1989
94	underground dwellings	Andersson et al., 1989
95	loss of records	Andersson et al., 1989
96	archeological intrusion	Andersson et al., 1989
97	postclosure monitoring	Andersson et al., 1989
98	underground test of nuclear devices	Andersson et al., 1989
99	unsuccessful attempt of site improvement	Andersson et al., 1989
100	poorly constructed repository	Andersson et al., 1989
101	future boreholes and undetected past boreholes	Andersson et al., 1989
102	other future uses of crystalline rock	Andersson et al., 1989
103	reuse of boreholes	Andersson et al., 1989
104	chemical sabotage	Andersson et al., 1989
105	nuclear war	Andersson et al., 1989
106	waste retrieval, mining	Andersson et al., 1989
107	human-induced actions on ground-water recharge	Andersson et al., 1989
108	human-induced changes in surface hydrology	Andersson et al., 1989
109	water producing well	Andersson et al., 1989
110	weathering of flow paths	Andersson et al., 1989
111	erosion on surface/sediments	Andersson et al., 1989
112	geothermally induced flow	Andersson et al., 1989
113	sedimentation of bentonite	Andersson et al., 1989
114	changes of ground-water flow	Andersson et al., 1989
115	enhanced ground-water flow	Andersson et al., 1989
116	groundwater recharge/discharge	Andersson et al., 1989
117	resaturation	Andersson et al., 1989
118	saline or fresh ground-water intrusion	Andersson et al., 1989
119	river meandering	Andersson et al., 1989
120	microbes	Andersson et al., 1989
121	repository induced Pb/Cu electrochemical reactions	Andersson et al., 1989
122	Gas generation	Andersson et al., 1989
123	gas generation: He production	Andersson et al., 1989
124	radiolysis	Andersson et al., 1989
125	radiolysis	Andersson et al., 1989
126	recoil of alpha-decay	Andersson et al., 1989
127	reconcentration	Andersson et al., 1989
128	chemical reactions (copper corrosion)	Andersson et al., 1989
129	I, Cs-migration to fuel surface	Andersson et al., 1989
130	interactions with corrosion products and waste	Andersson et al., 1989
131	internal corrosion due to waste	Andersson et al., 1989
132	natural telluric electrochemical reactions	Andersson et al., 1989
133	perturbed buffer material chemistry	Andersson et al., 1989
134	radioactive decay; heat	Andersson et al., 1989
135	release of radionuclides from failed canister	Andersson et al., 1989
136	role of the eventual channeling within the canister	Andersson et al., 1989
137	soret effect	Andersson et al., 1989
138	earthquakes	Andersson et al., 1989

Table A (continued)

FEP ID	Initial FEP	Reference[1]
139	faulting	Andersson et al., 1989
140	intruding dikes	Andersson et al., 1989
141	changes of the magnetic field	Andersson et al., 1989
142	stress changes of conductivity	Andersson et al., 1989
143	creeping of rock mass	Andersson et al., 1989
144	intrusion into accumulation zone in the biosphere	Andersson et al., 1989
145	uplift and subsidence	Andersson et al., 1989
146	effect of plate movements	Andersson et al., 1989
147	tectonic activity - large scale	Andersson et al., 1989
148	undetected discontinuities	Andersson et al., 1989
149	undetected fracture zones	Andersson et al., 1989
150	volcanism	Andersson et al., 1989
151	criticality	Andersson et al., 1989
152	H2/02 explosions	Andersson et al., 1989
153	co-storage of other waste	Andersson et al., 1989
154	damaged or deviating fuel	Andersson et al., 1989
155	decontamination materials left	Andersson et al., 1989
156	near storage of other waste	Andersson et al., 1989
157	stray materials left	Andersson et al., 1989
158	Meteorites	Burkholder, 1980
159	climate modification	Burkholder, 1980
160	Glaciation	Burkholder, 1980
161	corrosion	Burkholder, 1980
162	Transport Agent Introduction	Burkholder, 1980
163	fluid migration	Burkholder, 1980
164	dissolutioning	Burkholder, 1980
165	biochemical gas generation	Burkholder, 1980
166	decay product gas generation	Burkholder, 1980
167	differential elastic response	Burkholder, 1980
168	dewatering	Burkholder, 1980
169	canister movement	Burkholder, 1980
170	fluid pressure changes	Burkholder, 1980
171	material property changes	Burkholder, 1980
172	non-elastic response	Burkholder, 1980
173	shaft seal failure	Burkholder, 1980
174	geochemical alterations	Burkholder, 1980
175	diagenesis	Burkholder, 1980
176	gas or brine pockets	Burkholder, 1980
177	reservoirs	Burkholder, 1980
178	undiscovered boreholes	Burkholder, 1980
179	Undetected Past Intrusion	Burkholder, 1980
180	Intentional Intrusion	Burkholder, 1980
181	archeological exhumation	Burkholder, 1980
182	irrigation	Burkholder, 1980
183	establishment of new population center	Burkholder, 1980
184	improper waste emplacement	Burkholder, 1980
185	resource mining (mineral hydrocarbon, geothermal, salt)	Burkholder, 1980
186	mine shafts	Burkholder, 1980
187	sabotage	Burkholder, 1980
188	war	Burkholder, 1980
189	waste recovery	Burkholder, 1980

Table A (continued)

FEP ID	Initial FEP	Reference[1]
190	intentional artificial ground-water recharge or withdrawal	Burkholder, 1980
191	weapons testing	Burkholder, 1980
192	Denudation and Stream Erosion	Burkholder, 1980
193	sedimentation	Burkholder, 1980
194	flooding	Burkholder, 1980
195	radiolysis	Burkholder, 1980
196	waste package - geology interactions	Burkholder, 1980
197	breccia pipes	Burkholder, 1980
198	diapirism	Burkholder, 1980
199	far-field faulting	Burkholder, 1980
200	near-field faulting	Burkholder, 1980
201	faults, shear zones	Burkholder, 1980
202	static fracturing	Burkholder, 1980
203	impact fracturing	Burkholder, 1980
204	surficial fissuring	Burkholder, 1980
205	local fracturing	Burkholder, 1980
206	Igneous emplacement	Burkholder, 1980
207	intrusive magmatic activity	Burkholder, 1980
208	hydraulic fracturing	Burkholder, 1980
209	isostasy	Burkholder, 1980
210	lava tubes	Burkholder, 1980
211	Orogenic Diastrophism	Burkholder, 1980
212	Epeirogenic Displacement	Burkholder, 1980
213	undetected features	Burkholder, 1980
214	extrusive magmatic activity	Burkholder, 1980
215	criticality	Burkholder, 1980
216	chemical liquid waste disposal	Burkholder, 1980
217	storage of hydrocarbons or compressed air	Burkholder, 1980
218	non-nuclear waste disposal	Burkholder, 1980
219	Celestial bodies	Guzowski, 1990
220	meteorite impact	Guzowski, 1990
221	sea-level variations	Guzowski, 1990
222	pluvial periods	Guzowski, 1990
223	glaciation	Guzowski, 1990
224	seiches	Guzowski, 1990
225	formation of dissolution cavities	Guzowski, 1990
226	excavation induced stress/fracturing in host rock	Guzowski, 1990
227	subsidence and caving	Guzowski, 1990
228	thermally induced stress/fracturing in host rock	Guzowski, 1990
229	shaft and borehole seal degradation	Guzowski, 1990
230	explosions	Guzowski, 1990
231	Inadvertent Future Intrusions	Guzowski, 1990
232	injection wells	Guzowski, 1990
233	irrigation	Guzowski, 1990
234	drilling	Guzowski, 1990
235	mining	Guzowski, 1990
236	damming of streams or rivers	Guzowski, 1990
237	withdrawal wells	Guzowski, 1990
238	mass wasting	Guzowski, 1990
239	erosion/ sedimentation	Guzowski, 1990
240	flooding	Guzowski, 1990

Table A (continued)

FEP ID	Initial FEP	Reference[1]
241	hydrologic stresses	Guzowski, 1990
242	hurricanes	Guzowski, 1990
243	tsunamis	Guzowski, 1990
244	diapirism	Guzowski, 1990
245	faulting	Guzowski, 1990
246	formation of interconnected fracture systems	Guzowski, 1990
247	regional subsidence or uplift (also applies to subsurface)	Guzowski, 1990
248	seismic activity	Guzowski, 1990
249	magmatic activity	Guzowski, 1990
250	volcanic activity	Guzowski, 1990
251	meteorite impact	Hertzler and Atwood, 1989
252	climatic change	Hertzler and Atwood, 1989
253	sea level change	Hertzler and Atwood, 1989
254	dam and reservoir formation from natural causes	Hertzler and Atwood, 1989
255	glacial activity	Hertzler and Atwood, 1989
256	radial dispersion	Hertzler and Atwood, 1989
257	fluid interactions	Hertzler and Atwood, 1989
258	dissolution	Hertzler and Atwood, 1989
259	decay product gas generation	Hertzler and Atwood, 1989
260	infiltration and evapotranspiration	Hertzler and Atwood, 1989
261	thermal changes in burial zone caused by heat generation	Hertzler and Atwood, 1989
262	mechanical effects	Hertzler and Atwood, 1989
263	shaft/borehole seal failure	Hertzler and Atwood, 1989
264	geochemical changes from natural causes	Hertzler and Atwood, 1989
265	diagenesis	Hertzler and Atwood, 1989
266	landslide	Hertzler and Atwood, 1989
267	local subsidence/caving	Hertzler and Atwood, 1989
268	climate control	Hertzler and Atwood, 1989
269	fire and explosion	Hertzler and Atwood, 1989
270	fire and explosion of waste after burial	Hertzler and Atwood, 1989

Table A (continued)

FEP ID	Initial FEP	Reference[1]
271	geochemical changes from manmade causes	Hertzler and Atwood, 1989
272	earthquake from man-made causes	Hertzler and Atwood, 1989
273	human surface activities	Hertzler and Atwood, 1989
274	hydrology change from man-made causes	Hertzler and Atwood, 1989
275	unanticipated intrusion	Hertzler and Atwood, 1989
276	undetected past intrusion	Hertzler and Atwood, 1989
277	undetected features or processes	Hertzler and Atwood, 1989
278	intentional intrusion	Hertzler and Atwood, 1989
279	improper waste emplacement	Hertzler and Atwood, 1989
280	mining inadvertent intruder	Hertzler and Atwood, 1989
281	dam and reservoir, man-made	Hertzler and Atwood, 1989
282	well-drilling inadvertent intruder	Hertzler and Atwood, 1989
283	weapons testing	Hertzler and Atwood, 1989
284	land erosion	Hertzler and Atwood, 1989
285	sedimentation/ aggradation	Hertzler and Atwood, 1989
286	lateral ground-water flow in the unsaturated zone	Hertzler and Atwood, 1989
287	hydrology change from natural causes	Hertzler and Atwood, 1989
288	hurricane	Hertzler and Atwood, 1989
289	tornado	Hertzler and Atwood, 1989
290	brush fire	Hertzler and Atwood, 1989
291	chemical effects	Hertzler and Atwood, 1989
292	diapirism	Hertzler and Atwood, 1989
293	earthquake from natural causes	Hertzler and Atwood, 1989
294	faulting	Hertzler and Atwood, 1989
295	igneous activity	Hertzler and Atwood, 1989

Table A (continued)

FEP ID	Initial FEP	Reference[1]
296	regional subsidence or uplift	Hertzler and Atwood, 1989
297	criticality	Hertzler and Atwood, 1989
298	chemical liquid waste disposal	Hertzler and Atwood, 1989
299	unanticipated waste composition	Hertzler and Atwood, 1989
300	permafrost affects repository	Hunter, 1983
301	fluids do not recirculate in response to thermal gradients	Hunter, 1983
302	fluids leave along new fault	Hunter, 1983
303	fluids recirculate in response to thermal gradients	Hunter, 1983
304	fluids recirculate in response to thermal gradients	Hunter, 1983
305	normal flow increases	Hunter, 1983
306	diffusive mixing occurs	Hunter, 1983
307	flux through repository is altered	Hunter, 1983
308	head is above outfall	Hunter, 1983
309	head is below outfall	Hunter, 1983
310	subsidence fractures end above repository	Hunter, 1983
311	subsidence fractures reach repository	Hunter, 1983
312	fluids carry waste to rivers or tributaries	Hunter, 1983
313	fluids carry waste to wells or springs	Hunter, 1983
314	ground-water flow paths are shortened	Hunter, 1983
315	water from a confined aquifer enters repository	Hunter, 1983
316	water from the unconfined aquifer enters repository	Hunter, 1983
317	location of river channel changes	Hunter, 1983
318	location of river channel changes and flow through repository is altered	Hunter, 1983
319	flow channels close and reopen later	Hunter, 1983
320	meteorite impact	Hunter, 1989
321	climatic change	Hunter, 1989
322	glaciation	Hunter, 1989
323	leaching	Hunter, 1989
324	diffusion out of the repository	Hunter, 1989
325	dissolution	Hunter, 1989
326	dissolution other than leaching	Hunter, 1989
327	thermal effects	Hunter, 1989
328	seal performance	Hunter, 1989
329	subsidence	Hunter, 1989
330	exhumation	Hunter, 1989
331	drilling into repository	Hunter, 1989
332	effects of mining for resources	Hunter, 1989
333	sabotage	Hunter, 1989
334	warfare	Hunter, 1989
335	sedimentation	Hunter, 1989
336	ground-water flow	Hunter, 1989
337	migration of brine aquifer	Hunter, 1989
338	migration of intracrystalline brine inclusions	Hunter, 1989
339	effects of brine pocket	Hunter, 1989
340	gas generation waste effect	Hunter, 1989
341	radiolysis waste effect	Hunter, 1989

Table A (continued)

FEP ID	Initial FEP	Reference[1]
342	waste/rock interaction	Hunter, 1989
343	breccia-pipe formation	Hunter, 1989
344	induced diapirism	Hunter, 1989
345	faulting	Hunter, 1989
346	Igneous intrusion	Hunter, 1989
347	nuclear criticality	Hunter, 1989
348	meteorite impact	IAEA 1983
349	climatic change	IAEA 1983
350	sea level change	IAEA 1983
351	glacial erosion	IAEA 1983
352	geochemical change	IAEA 1983
353	corrosion	IAEA 1983
354	transport agent introduction	IAEA 1983
355	fluid interactions	IAEA 1983
356	fluid migration	IAEA 1983
357	decay-product gas generation	IAEA 1983
358	faulty design	IAEA 1983
359	exploration bore-hole seal failure	IAEA 1983
360	thermal effects	IAEA 1983
361	canister movement	IAEA 1983
362	fluid pressure, density, viscosity changes	IAEA 1983
363	differential elastic response	IAEA 1983
364	material property changes	IAEA 1983
365	mechanical effects	IAEA 1983
366	non-elastic response	IAEA 1983
367	shaft seal failure	IAEA 1983
368	geochemical change	IAEA 1983
369	diagenesis	IAEA 1983
370	gas or brine pockets	IAEA 1983
371	climate control	IAEA 1983
372	reservoirs	IAEA 1983
373	inadvertent future intrusion	IAEA 1983
374	undetected past intrusion	IAEA 1983
375	undiscovered boreholes	IAEA 1983
376	Intentional intrusion	IAEA 1983
377	archeological exhumation	IAEA 1983
378	irrigation	IAEA 1983
379	faulty operation	IAEA 1983
380	faulty waste emplacement	IAEA 1983
381	resource mining (mineral, water, hydrocarbon, geothermal, salt, etc)	IAEA 1983
382	exploratory drilling	IAEA 1983
383	mine shafts	IAEA 1983
384	sabotage	IAEA 1983
385	war	IAEA 1983
386	waste recovery	IAEA 1983
387	intentional artificial ground-water recharge or withdrawal	IAEA 1983
388	denudation	IAEA 1983
389	stream erosion	IAEA 1983
390	sedimentation	IAEA 1983
391	flooding	IAEA 1983

Table A (continued)

FEP ID	Initial FEP	Reference[1]
392	ground-water flow	IAEA 1983
393	brine pockets	IAEA 1983
394	large-scale alterations of hydrology	IAEA 1983
395	hydrology change	IAEA 1983
396	gas generation	IAEA 1983
397	radiolysis	IAEA 1983
398	waste package-rock interactions	IAEA 1983
399	breccia pipes	IAEA 1983
400	diapirism	IAEA 1983
401	faulting/seismicity	IAEA 1983
402	faults, shear zones	IAEA 1983
403	local fracturing	IAEA 1983
404	intrusive	IAEA 1983
405	intrusive dikes	IAEA 1983
406	Isostatic	IAEA 1983
407	lava tubes	IAEA 1983
408	orogenic	IAEA 1983
409	uplift/subsidence	IAEA 1983
410	epeirogenic	IAEA 1983
411	magmatic activity	IAEA 1983
412	extrusive	IAEA 1983
413	nuclear criticality	IAEA 1983
414	chemical liquid waste disposal	IAEA 1983
415	meteorites	Koplik et al., 1982
416	climate modification	Koplik et al., 1982
417	climatic fluctuations	Koplik et al., 1982
418	glaciation	Koplik et al., 1982
419	corrosion	Koplik et al., 1982
420	biosphere alteration	Koplik et al., 1982
421	local fluid migration	Koplik et al., 1982
422	dissolutioning	Koplik et al., 1982
423	decay product gas generation	Koplik et al., 1982
424	Improper design of operation	Koplik et al., 1982
425	Thermal effects	Koplik et al., 1982
426	canister movement	Koplik et al., 1982
427	change in local state of stress	Koplik et al., 1982
428	readjustment of rock along joints	Koplik et al., 1982
429	fluid pressure changes	Koplik et al., 1982
430	canister migration	Koplik et al., 1982
431	convection	Koplik et al., 1982
432	differential elastic response	Koplik et al., 1982
433	material property changes	Koplik et al., 1982
434	Mechanical effects	Koplik et al., 1982
435	nonelastic response	Koplik et al., 1982
436	stored energy	Koplik et al., 1982
437	shaft seal failure	Koplik et al., 1982
438	seal - rock interactions	Koplik et al., 1982
439	subsidence of canister	Koplik et al., 1982
440	geochemical alterations	Koplik et al., 1982
441	diagenesis	Koplik et al., 1982
442	gas or brine pockets	Koplik et al., 1982

Table A (continued)

FEP ID	Initial FEP	Reference[1]
443	reservoirs	Koplik et al., 1982
444	Inadvertent future intrusion	Koplik et al., 1982
445	Undetected past intrusion	Koplik et al., 1982
446	undiscovered boreholes	Koplik et al., 1982
447	Intentional intrusion	Koplik et al., 1982
448	archeological exhumation	Koplik et al., 1982
449	irrigation	Koplik et al., 1982
450	establishment of population center	Koplik et al., 1982
451	improper waste emplacement	Koplik et al., 1982
452	resource mining (salt, mineral, hydrocarbon, geothermal)	Koplik et al., 1982
453	mine shafts	Koplik et al., 1982
454	sabotage	Koplik et al., 1982
455	war	Koplik et al., 1982
456	waste recovery	Koplik et al., 1982
457	Perturbation of ground-water system	Koplik et al., 1982
458	intentional artificial ground-water recharge or withdrawal	Koplik et al., 1982
459	weapons testing	Koplik et al., 1982
460	Denudation and stream erosion	Koplik et al., 1982
461	Sedimentation	Koplik et al., 1982
462	Flooding	Koplik et al., 1982
463	Modification of hydrologic regime	Koplik et al., 1982
464	gas generation	Koplik et al., 1982
465	Radiation effects	Koplik et al., 1982
466	radiolysis	Koplik et al., 1982
467	Chemical effects	Koplik et al., 1982
468	waste package - geology interactions	Koplik et al., 1982
469	breccia pipes	Koplik et al., 1982
470	diapirism	Koplik et al., 1982
471	far-field faulting	Koplik et al., 1982
472	near-field faulting	Koplik et al., 1982
473	faults, shear zones	Koplik et al., 1982
474	Static fracturing	Koplik et al., 1982
475	impact fracturing	Koplik et al., 1982
476	surficial fissuring	Koplik et al., 1982
477	local fracturing	Koplik et al., 1982
478	Igneous emplacement	Koplik et al., 1982
479	intrusive magmatic activity	Koplik et al., 1982
480	hydraulic fracturing	Koplik et al., 1982
481	isostasy	Koplik et al., 1982
482	lava tubes	Koplik et al., 1982
483	Orogenic diastrophism	Koplik et al., 1982
484	Epeirogenic displacement	Koplik et al., 1982
485	Magmatic activity	Koplik et al., 1982
486	extrusive magmatic activity	Koplik et al., 1982
487	criticality	Koplik et al., 1982
488	storage of hydrocarbons, compressed air, or hot water	Koplik et al., 1982
489	non-nuclear waste disposal	Koplik et al., 1982
490	chemical liquid waste disposal	Koplik et al., 1982
491	Meteorite impact	Merrett and Gillespie, 1983

Table A (continued)

FEP ID	Initial FEP	Reference[1]
492	determination of meteorite impact frequencies	Merrett and Gillespie, 1983
493	probability of meteorite damage	Merrett and Gillespie, 1983
494	Glaciation	Merrett and Gillespie, 1983
495	glacial erosion	Merrett and Gillespie, 1983
496	fracture mechanics analysis	Merrett and Gillespie, 1983
497	vault-related events	Merrett and Gillespie, 1983
498	presence of a heat source	Merrett and Gillespie, 1983
499	excavation	Merrett and Gillespie, 1983
500	use of explosive devices	Merrett and Gillespie, 1983
501	drilling and mining	Merrett and Gillespie, 1983
502	Denudation and fluvial erosion	Merrett and Gillespie, 1983
503	denudation	Merrett and Gillespie, 1983
504	fluvial erosion	Merrett and Gillespie, 1983
505	alteration of hydrological conditions	Merrett and Gillespie, 1983
506	new fault formation	Merrett and Gillespie, 1983
507	rapid fault growth	Merrett and Gillespie, 1983
508	slow fault growth	Merrett and Gillespie, 1983
509	stress analysis	Merrett and Gillespie, 1983
510	glacially induced faulting	Merrett and Gillespie, 1983
511	subsidence and rebound	Merrett and Gillespie, 1983
512	Seismic activity	Merrett and Gillespie, 1983
513	jointed rock motion	Merrett and Gillespie, 1983
514	Volcanic activity	Merrett and Gillespie, 1983
515	hot-spot volcanic activity	Merrett and Gillespie, 1983
516	rift system volcanic activity	Merrett and Gillespie, 1983

Table A (continued)

FEP ID	Initial FEP	Reference[1]
517	Presence of a radioactive source	Merrett and Gillespie, 1983
518	Meteorite impact	NEA OECD, 2000
519	Climate change, Global	NEA OECD, 2000
520	Climate change, regional and local	NEA OECD, 2000
521	Ecological response to climate changes	NEA OECD, 2000
522	Hydrological/hydrogeological response to climate changes	NEA OECD, 2000
523	Sea Level change	NEA OECD, 2000
524	Warm climate effects (tropical and desert)	NEA OECD, 2000
525	Glacial and ice sheet effects, local	NEA OECD, 2000
526	Periglacial effects	NEA OECD, 2000
527	Container materials and characteristics	NEA OECD, 2000
528	Atmospheric transport of contaminants	NEA OECD, 2000
529	Vegetation	NEA OECD, 2000
530	Animal populations	NEA OECD, 2000
531	Biological/biochemical processes and conditions (in geosphere)	NEA OECD, 2000
532	Biological/biochemical processes and conditions (in waste and EBS)	NEA OECD, 2000
533	Species evolution	NEA OECD, 2000
534	Animal, plant and microbe mediated transport of contaminants	NEA OECD, 2000
535	Colloids. contaminant interactions and transport with	NEA OECD, 2000
536	Contaminant transport path characteristics (in geosphere)	NEA OECD, 2000
537	Chemical/complexing agents, effects on contaminant speciation/transport	NEA OECD, 2000
538	Solid-mediated transport of contaminants	NEA OECD, 2000
539	Sorption/desorption processes, contaminant	NEA OECD, 2000
540	Speciation and solubility, contaminant	NEA OECD, 2000
541	Dissolution, precipitation, and crystallization, contaminant	NEA OECD, 2000
542	Noble gases	NEA OECD, 2000
543	Volatiles and potential for volatility	NEA OECD, 2000
544	Gas-mediated transport of contaminants	NEA OECD, 2000
545	Geological resources	NEA OECD, 2000
546	Geological units, other	NEA OECD, 2000
547	Host rock	NEA OECD, 2000
548	Repository assumptions	NEA OECD, 2000
549	Thermal processes and conditions (in geosphere)	NEA OECD, 2000
550	Excavation disturbed zone, host rock	NEA OECD, 2000
551	Buffer/backfill materials and characteristics	NEA OECD, 2000
552	Other engineered features materials and characteristics	NEA OECD, 2000
553	Thermal processes and conditions (in wastes and EBS)	NEA OECD, 2000
554	Emplacement of wastes and backfilling	NEA OECD, 2000
555	Repository design	NEA OECD, 2000
556	Mechanical processes and conditions (in geosphere)	NEA OECD, 2000
557	Mechanical processes and conditions (in wastes and EBS)	NEA OECD, 2000
558	Seals. cavern/tunnel/shaft	NEA OECD, 2000
559	Closure and repository sealing	NEA OECD, 2000
560	Dose response assumptions	NEA OECD, 2000
561	Dosimetry	NEA OECD, 2000
562	Drinking water, foodstuffs and drugs, contaminant concentrations in	NEA OECD, 2000

Table A (continued)

FEP ID	Initial FEP	Reference[1]
563	Environmental media, contaminant concentrations in	NEA OECD, 2000
564	Impacts or concern	NEA OECD, 2000
565	Human characteristics (physiology, metabolism)	NEA OECD, 2000
566	Chemical/organic toxin stability	NEA OECD, 2000
567	Exposure modes	NEA OECD, 2000
568	Non-food products, contaminant concentrations in	NEA OECD, 2000
569	Nonradiological toxicity/effects	NEA OECD, 2000
570	Radiological toxicity/effects	NEA OECD, 2000
571	Radon and radon daughter exposure	NEA OECD, 2000
572	Diet and fluid Intake	NEA OECD, 2000
573	Food and water processing and preparation	NEA OECD, 2000
574	Food chains, uptake of contaminants in	NEA OECD, 2000
575	Chemical/geochemical processes and conditions (in geosphere)	NEA OECD, 2000
576	Chemical/geochemical processes and conditions (In wastes and	NEA OECD, 2000
577	Organics and potential for organic forms	NEA OECD, 2000
578	Diagenesis	NEA OECD, 2000
579	Gas sources and effects (in geosphere)	NEA OECD, 2000
580	Human influences on climate	NEA OECD, 2000
581	Social and Institutional developments	NEA OECD, 2000
582	Excavation/construction	NEA OECD, 2000
583	Explosions and crashes	NEA OECD, 2000
584	Future human action assumptions	NEA OECD, 2000
585	Future human behavior (target group) assumptions	NEA OECD, 2000
586	Habits (non-diet related behavior)	NEA OECD, 2000
587	Leisure and other uses of environment	NEA OECD, 2000
588	Human response to climate changes	NEA OECD, 2000
589	Surface environment, human activities	NEA OECD, 2000
590	Technological developments	NEA OECD, 2000
591	Adults, children, Infants and other variations	NEA OECD, 2000
592	Human-action-mediated transport of contaminants	NEA OECD, 2000
593	Community characteristics	NEA OECD, 2000
594	Dwellings	NEA OECD, 2000
595	Motivation and knowledge issues (inadvertent/deliberate human actions)	NEA OECD, 2000
596	Administrative control , repository site	NEA OECD, 2000
597	Records and markers, repository	NEA OECD, 2000
598	Unintrusive site investigation	NEA OECD, 2000
599	Site Investigation	NEA OECD, 2000
600	Rural and agricultural land and water use (incl. fisheries)	NEA OECD, 2000
601	Urban and Industrial land and water use	NEA OECD, 2000
602	Wild and natural land and water use	NEA OECD, 2000
603	Monitoring of repository	NEA OECD, 2000
604	Remedial actions	NEA OECD, 2000
605	Schedule and planning	NEA OECD, 2000
606	Quality control	NEA OECD, 2000
607	Retrievability	NEA OECD, 2000
608	Drilling activities (human intrusion)	NEA OECD, 2000
609	Mining and other underground activities (human intrusion)	NEA OECD, 2000
610	Accidents and unplanned events	NEA OECD, 2000

Table A (continued)

FEP ID	Initial FEP	Reference[1]
611	Water management (wells, reservoirs. dams)	NEA OECD, 2000
612	Coastal features	NEA OECD, 2000
613	Topography and morphology	NEA OECD, 2000
614	Erosion and deposition	NEA OECD, 2000
615	Erosion and sedimentation	NEA OECD, 2000
616	Hydraulic/hydrogeological processes and conditions (in geosphere)	NEA OECD, 2000
617	Hydraulic/hydrogeological processes and conditions (in wastes and EBS)	NEA OECD, 2000
618	Hydrological/hydrogeological response to geological changes	NEA OECD, 2000
619	Hydrothermal activity	NEA OECD, 2000
620	Marine features	NEA OECD, 2000
621	Soil and sediment	NEA OECD, 2000
622	Aquifers and water-bearing features, near surface	NEA OECD, 2000
623	Water-mediated transport of contaminants	NEA OECD, 2000
624	Hydrological regime and water balance (near-surface)	NEA OECD, 2000
625	Lakes, rivers, streams and springs	NEA OECD, 2000
626	Atmosphere	NEA OECD, 2000
627	Meteorology	NEA OECD, 2000
628	Model and data Issues	NEA OECD, 2000
629	Timescale of concern	NEA OECD, 2000
630	Regulatory requirements and exclusions	NEA OECD, 2000
631	Spatial domain or concern	NEA OECD, 2000
632	Ecological/biological microbial systems	NEA OECD, 2000
633	Microbial/biological/plant-mediated processes,	NEA OECD, 2000
634	Gas sources and effects (in wastes and EBS)	NEA OECD, 2000
635	Radioactive decay and in-growth	NEA OECD, 2000
636	Radiation effects (In wastes and EBS)	NEA OECD, 2000
637	Inorganic solids/solutes	NEA OECD, 2000
638	Salt diapirism and dissolution	NEA OECD, 2000
639	Discontinuities, large scale (in geosphere)	NEA OECD, 2000
640	Metamorphism	NEA OECD, 2000
641	Deformation, elastic, plastic or brittle	NEA OECD, 2000
642	Seismicity	NEA OECD, 2000
643	Undetected features (In geosphere)	NEA OECD, 2000
644	Tectonic movements and orogeny	NEA OECD, 2000
645	Volcanic and magmatic activity	NEA OECD, 2000
646	Nuclear criticality	NEA OECD, 2000
647	Inventory, radionuclide and other material	NEA OECD, 2000
648	Waste form materials and characteristics	NEA OECD, 2000
649	Waste allocation	NEA OECD, 2000
650	meteorite impact	NEA, 1992
651	no ice age	NEA, 1992
652	sea-level rise/fall	NEA, 1992
653	ecological response to climatic change	NEA, 1992
654	glaciation (erosion/deposition, glacial loading, hydrogeological change)	NEA, 1992
655	periglacial effects (permafrost, high seasonality)	NEA, 1992
656	river flow and lake level changes	NEA, 1992
657	fracturing	NEA, 1992
658	embrittlement and cracking	NEA, 1992

Table A (continued)

FEP ID	Initial FEP	Reference[1]
659	metallic corrosion (pitting/uniform, internal and external agents, gas generation e.g. H2)	NEA, 1992
660	animal uptake	NEA, 1992
661	plant uptake	NEA, 1992
662	uptake by animal, plant, root	NEA, 1992
663	uptake by deep rooting species	NEA, 1992
664	soil and sediment bioturbation	NEA, 1992
665	plant and animal evolution	NEA, 1992
666	colloid formation, dissolution and transport	NEA, 1992
667	accumulation in soils and organic debris	NEA, 1992
668	advection and dispersion	NEA, 1992
669	matrix diffusion	NEA, 1992
670	multiphase flow and gas driven flow	NEA, 1992
671	solubility limit	NEA, 1992
672	sorption (linear/non-linear, reversible/irreversible)	NEA, 1992
673	non-radioactive solute plume in geosphere (effect on redox, ph and sorption)	NEA, 1992
674	diffusion	NEA, 1992
675	mass, isotopic and species dilution	NEA, 1992
676	dissolution, precipitation, and crystallization	NEA, 1992
677	natural gas intrusion	NEA, 1992
678	gas flow	NEA, 1992
679	gas mediated transport	NEA, 1992
680	inadequate backfill or compaction voidage	NEA, 1992
681	dewatering of host rock	NEA, 1992
682	common cause failures	NEA, 1992
683	investigation borehole seal failure and degradation	NEA, 1992
684	stress field changes, settling, subsidence or caving	NEA, 1992
685	thermal effects (concrete hydration)	NEA, 1992
686	Thermal (nuclear and chemical)	NEA, 1992
687	canister or container movement	NEA, 1992
688	changes in in-situ stress field	NEA, 1992
689	subsidence / collapse	NEA, 1992
690	differential elastic response	NEA, 1992
691	material defects (e.g. early canister failure)	NEA, 1992
692	material property changes	NEA, 1992
693	Mechanical	NEA, 1992
694	non-elastic response	NEA, 1992
695	Design and construction	NEA, 1992
696	design modification	NEA, 1992
697	shaft or access tunnel seal failure and degradation	NEA, 1992
698	altered soil or surface water chemistry	NEA, 1992
699	chemical transformations	NEA, 1992
700	chemical gradients (electrochemical effects and osmosis)	NEA, 1992
701	complexing agents	NEA, 1992
702	diagenesis	NEA, 1992
703	land slide	NEA, 1992
704	accidents during operation	NEA, 1992
705	agricultural and fisheries practice changes	NEA, 1992
706	anthropogenic climate changes (greenhouse effect)	NEA, 1992
707	abandonment of unsealed repository	NEA, 1992

Table A (continued)

FEP ID	Initial FEP	Reference[1]
708	poor closure	NEA, 1992
709	tunneling	NEA, 1992
710	underground construction	NEA, 1992
711	geothermal energy production	NEA, 1992
712	repository flooding during operation	NEA, 1992
713	co-disposal of reactive wastes (deliberate)	NEA, 1992
714	undetected past intrusions (boreholes, mining)	NEA, 1992
715	injection of liquid wastes	NEA, 1992
716	loss of records	NEA, 1992
717	archeological investigation	NEA, 1992
718	irrigation	NEA, 1992
719	demographic change, urban development	NEA, 1992
720	land use changes	NEA, 1992
721	post-closure monitoring	NEA, 1992
722	underground nuclear testing	NEA, 1992
723	effects of phased operation	NEA, 1992
724	Operation and closure	NEA, 1992
725	poor quality construction	NEA, 1992
726	radioactive waste disposal error	NEA, 1992
727	Post-closure surface activities	NEA, 1992
728	exploitation drilling	NEA, 1992
729	exploratory drilling	NEA, 1992
730	resource mining	NEA, 1992
731	quarrying, near surface extraction	NEA, 1992
732	sabotage	NEA, 1992
733	malicious intrusion (sabotage, act of war)	NEA, 1992
734	recovery of repository materials	NEA, 1992
735	recovery of repository materials	NEA, 1992
736	ground-water abstraction	NEA, 1992
737	dams and reservoirs, built/drained	NEA, 1992
738	coastal erosion and estuarine development	NEA, 1992
739	denudation (eolian and fluvial)	NEA, 1992
740	chemical denudation and weathering	NEA, 1992
741	freshwater sediment transport and deposition	NEA, 1992
742	fracture mineralization and weathering	NEA, 1992
743	rock heterogeneity (permeability, mineralogy), affecting water and	NEA, 1992
744	river, stream, channel erosion (downcutting)	NEA, 1992
745	marine sediment transport and deposition	NEA, 1992
746	extremes of precipitation, snow melt and associated flooding	NEA, 1992
747	effects at saline-freshwater interface	NEA, 1992
748	ground-water conditions (saturated/unsaturated)	NEA, 1992
749	ground-water discharge (to surface water, springs, soils, wells, and marine)	NEA, 1992
750	ground-water flow (Darcy, non-Darcy, intergranular fracture,	NEA, 1992
751	recharge to ground water	NEA, 1992
752	saline or freshwater intrusion	NEA, 1992
753	natural thermal effects	NEA, 1992
754	induced hydrological changes (fluid pressure, density convection, viscosity)	NEA, 1992
755	site flooding	NEA, 1992

Table A (continued)

FEP ID	Initial FEP	Reference[1]
756	rivers rechanneled	NEA, 1992
757	river meander	NEA, 1992
758	frost weathering	NEA, 1992
759	solar insolation	NEA, 1992
760	coastal surge, storms, and hurricanes	NEA, 1992
761	precipitation, temperature, soil, water balance	NEA, 1992
762	ecological change (ex. forest fire cycles)	NEA, 1992
763	microbial interactions	NEA, 1992
764	microbiological (effects on corrosion/degradation, solubility/complexation, gas generation, ex. CH.C02)	NEA, 1992
765	pedogenesis	NEA, 1992
766	gas effects (pressurization, disruption, explosion, fire)	NEA, 1992
767	radioactive decay and ingrowth (chain decay)	NEA, 1992
768	radiolysis	NEA, 1992
769	Radiological	NEA, 1992
770	heterogeneity of waste forms (chemical, physical)	NEA, 1992
771	cellulosic degradation	NEA, 1992
772	interactions of host materials and ground water with repository material (ex. concrete carbonation, sulphate attack)	NEA, 1992
773	interactions of waste and repository materials with host materials (electrochemical corrosive agents)	NEA, 1992
774	introduced complexing agents and cellulosics	NEA, 1992
775	induced chemical changes (solubility sorption, species equilibrium, mineralization)	NEA, 1992
776	diapirism	NEA, 1992
777	fault activation	NEA, 1992
778	fault generation	NEA, 1992
779	host rock fracture aperture changes	NEA, 1992
780	metamorphic activity	NEA, 1992
781	changes in the earth's magnetic field	NEA, 1992
782	uplift and subsidence (orogenic, isostatic)	NEA, 1992
783	seismicity	NEA, 1992
784	plate movement/tectonic change	NEA, 1992
785	undetected features (faults, fracture networks, shear zones, brecciation, gas pockets)	NEA, 1992
786	magmatic activity (intrusive, extrusive)	NEA, 1992
787	nuclear criticality	NEA, 1992
788	inadvertent inclusion of undesirable materials	NEA, 1992
789	Recurrance of Lake Bonneville	Neptune
790	Wave action	Neptune
791	Animal burrowing	Neptune
792	Dust devils	Neptune
793	Barrier stability during inundation	Neptune
794	inhalation pathways	Neptune
795	human induced hydraulic fracturing	Neptune
796	natural hydraulic fracturing (hydrogeological)	Neptune
797	Sedimentation	Neptune
798	Inundation	Neptune
799	radon emanation	Neptune
800	natural hydraulic fracturing (tectonic/seismic/volcanic)	Neptune

Table A (continued)

FEP ID	Initial FEP	Reference[1]
801	Off-Site Residents: impacts on the site by people who might use the area but don't live on the site itself.	Neptune
802	On-Site Residents: water well with desalinization; construction-related activities like basements, footings, and utilities; enhanced infiltration from septic; altered plant/animal communities; effect of grading on infiltration; effect of buildings and pavement on evapotranspiration.	Neptune
803	Agricultural activities	Neptune
804	Explosions and Crashes related to plane crashes, bombs	Neptune
805	Accidental Intrusion, facility properties intact: mineral, oil and gas, geothermal or other resource exploration; water well with desalinization; construction-related activities	Neptune
806	Accidental Intrusion, facility properties altered due to prior volcanic or seismic event	Neptune
807	FEPs related to post-closure inhabitation of the area	Neptune
808	Deliberate Intrusion (purposeful waste retrieval; archeology; terrorism, etc)	Neptune
809	FEPs related to post-closure intrusion by nonresidents who come looking for something, or to some kind of major accident like a plane crash either before or after closure	Neptune
810	meteorite	Prij et al. 1991
811	climatic variability	Prij et al. 1991
812	minor climatic changes	Prij et al. 1991
813	sea-level changes	Prij et al. 1991
814	ecological response to climate	Prij et al. 1991
815	glaciation	Prij et al. 1991
816	periglacial effects	Prij et al. 1991
817	canister defects	Prij et al. 1991
818	common cause (canister) failures	Prij et al. 1991
819	fracturing	Prij et al. 1991
820	embrittlement, cracking	Prij et al. 1991
821	metallic corrosion	Prij et al. 1991
822	bioturbation of soil sediment	Prij et al. 1991
823	radiocolloid formation	Prij et al. 1991
824	accumulation in soils, organic debris	Prij et al. 1991
825	transport of radionuclides	Prij et al. 1991
826	advection and dispersion	Prij et al. 1991
827	matrix diffusion	Prij et al. 1991
828	multiphase flow	Prij et al. 1991
829	leaching of nuclides	Prij et al. 1991
830	non-radioactive solute in geosphere	Prij et al. 1991
831	diffusion	Prij et al. 1991
832	dilution of mass	Prij et al. 1991
833	dissolution/precipitation reactions	Prij et al. 1991
834	natural gas intrusion	Prij et al. 1991
835	gas mediated transport	Prij et al. 1991
836	inadequate backfill compaction, voidage	Prij et al. 1991
837	convergence of openings	Prij et al. 1991
838	dewatering of host rock	Prij et al. 1991
839	stress field changes	Prij et al. 1991
840	thermal effects	Prij et al. 1991

Table A (continued)

FEP ID	Initial FEP	Reference[1]
841	Thermal	Prij et al. 1991
842	degradation of buffer/backfill	Prij et al. 1991
843	canister or container movement	Prij et al. 1991
844	changes in in-situ stress field	Prij et al. 1991
845	readjustment of host rock along joints	Prij et al. 1991
846	heat production	Prij et al. 1991
847	fracture aperture changes	Prij et al. 1991
848	canister migration	Prij et al. 1991
849	dehydration of salt minerals	Prij et al. 1991
850	differential elastic response	Prij et al. 1991
851	material defects	Prij et al. 1991
852	swelling of backfill (clay)	Prij et al. 1991
853	swelling of corrosion products	Prij et al. 1991
854	material property changes	Prij et al. 1991
855	Mechanical	Prij et al. 1991
856	non-elastic response	Prij et al. 1991
857	release of stored energy	Prij et al. 1991
858	Design and construction	Prij et al. 1991
859	design modification	Prij et al. 1991
860	seal failure	Prij et al. 1991
861	subsidence, collapse	Prij et al. 1991
862	alteration of soil, surface water chemistry	Prij et al. 1991
863	Geochemical	Prij et al. 1991
864	chemical transformations	Prij et al. 1991
865	ionic strength	Prij et al. 1991
866	speciation equilibrium reactions	Prij et al. 1991
867	texture	Prij et al. 1991
868	acidity	Prij et al. 1991
869	adsorption and desorption reactions	Prij et al. 1991
870	chemical equilibrium reactions	Prij et al. 1991
871	counter, competitive, and potential determining ions	Prij et al. 1991
872	physico-chemical characteristics influencing chemical equilibria	Prij et al. 1991
873	redox conditions	Prij et al. 1991
874	geochemical alterations	Prij et al. 1991
875	diagenesis	Prij et al. 1991
876	land slide	Prij et al. 1991
877	accidents during operation	Prij et al. 1991
878	agricultural developments and changes	Prij et al. 1991
879	anthropogenic climate changes (greenhouse effect)	Prij et al. 1991
880	abandonment of unsealed repository	Prij et al. 1991
881	poor closure	Prij et al. 1991
882	tunneling	Prij et al. 1991
883	underground construction	Prij et al. 1991
884	fisheries developments and changes	Prij et al. 1991
885	geothermal energy production	Prij et al. 1991
886	co-disposal of reactive wastes (deliberate)	Prij et al. 1991
887	Human Induced Phenomena	Prij et al. 1991
888	undetected past intrusions	Prij et al. 1991
889	injection of fluids	Prij et al. 1991
890	loss of records	Prij et al. 1991

Table A (continued)

FEP ID	Initial FEP	Reference[1]
891	archaeological investigation	Prij et al. 1991
892	irrigation	Prij et al. 1991
893	changes in land use	Prij et al. 1991
894	demographic developments and changes	Prij et al. 1991
895	urban developments and changes	Prij et al. 1991
896	post-closure monitoring	Prij et al. 1991
897	underground nuclear testing	Prij et al. 1991
898	Operation and closure	Prij et al. 1991
899	phased operation effects	Prij et al. 1991
900	attempt of site Improvement	Prij et al. 1991
901	poor quality construction	Prij et al. 1991
902	improper waste emplacement	Prij et al. 1991
903	radioactive waste disposal error	Prij et al. 1991
904	Post-closure sub-surface activities	Prij et al. 1991
905	Post-closure subsurface activities (intrusion)	Prij et al. 1991
906	Post-closure surface activities	Prij et al. 1991
907	exploitation drilling	Prij et al. 1991
908	exploratory drilling	Prij et al. 1991
909	resource mining	Prij et al. 1991
910	quarrying, surface mining	Prij et al. 1991
911	sabotage	Prij et al. 1991
912	malicious intrusion, sabotage/war	Prij et al. 1991
913	ground-water abstraction/recharge	Prij et al. 1991
914	construction of dams/reservoirs	Prij et al. 1991
915	drainage of dams reservoirs	Prij et al. 1991
916	coastal erosion development of estuaries	Prij et al. 1991
917	denudation, erosion	Prij et al. 1991
918	channel erosion	Prij et al. 1991
919	chemical denudation	Prij et al. 1991
920	channeling and preferential pathways	Prij et al. 1991
921	effects on suberosion	Prij et al. 1991
922	sediment transport	Prij et al. 1991
923	solifluction	Prij et al. 1991
924	rock heterogeneity	Prij et al. 1991
925	subrosion	Prij et al. 1991
926	flooding of repository during operation	Prij et al. 1991
927	extreme precipitation	Prij et al. 1991
928	flooding of site	Prij et al. 1991
929	changes in ground-water system	Prij et al. 1991
930	ground-water conditions	Prij et al. 1991
931	ground-water discharge	Prij et al. 1991
932	ground-water flow	Prij et al. 1991
933	ground-water recharge	Prij et al. 1991
934	saline-freshwater interface	Prij et al. 1991
935	brine migration	Prij et al. 1991
936	natural thermal effects	Prij et al. 1991
937	induced hydrological changes	Prij et al. 1991
938	changes in river regime, lake levels	Prij et al. 1991
939	intrusion of saline/fresh water	Prij et al. 1991
940	rechanneling of rivers	Prij et al. 1991
941	meandering of river	Prij et al. 1991

Table A (continued)

FEP ID	Initial FEP	Reference[1]
942	water table changes	Prij et al. 1991
943	frost weathering	Prij et al. 1991
944	solar insolation	Prij et al. 1991
945	coastal surge, storms	Prij et al. 1991
946	precipitation, temperature, soil, water balance	Prij et al. 1991
947	temperature	Prij et al. 1991
948	ecological response to sudden change (forest fires)	Prij et al. 1991
949	evolution	Prij et al. 1991
950	microbial interactions	Prij et al. 1991
951	microbiological effects	Prij et al. 1991
952	pedogenesis	Prij et al. 1991
953	gas generation, explosions	Prij et al. 1991
954	gas generation effects	Prij et al. 1991
955	radioactive decay/ingrowth	Prij et al. 1991
956	Radiological	Prij et al. 1991
957	radiolysis	Prij et al. 1991
958	heterogeneity of waste forms; chemical or physical	Prij et al. 1991
959	cellulosic degradation	Prij et al. 1991
960	electrochemical reactions	Prij et al. 1991
961	introduced complexing agents, cellulosics	Prij et al. 1991
962	material interactions	Prij et al. 1991
963	redox potential, pH	Prij et al. 1991
964	induced chemical changes	Prij et al. 1991
965	diapirism, halokinesis	Prij et al. 1991
966	fault activation	Prij et al. 1991
967	fault generation	Prij et al. 1991
968	fracturing	Prij et al. 1991
969	metamorphic activity	Prij et al. 1991
970	changes in magnetic field	Prij et al. 1991
971	creep of rock	Prij et al. 1991
972	uplift and subsidence	Prij et al. 1991
973	seismicity	Prij et al. 1991
974	undetected geological features	Prij et al. 1991
975	plate tectonics	Prij et al. 1991
976	undetected features	Prij et al. 1991
977	magmatic activity	Prij et al. 1991
978	nuclear criticality	Prij et al. 1991
979	inadvertent inclusion of undesirable materials	Prij et al. 1991
980	radon emanation	Neptune
981	resuspension	Neptune

1 References for Andersson et al. (1989), Burkholder (1980), Guzowski (1990), Hertzler and Atwood (1989), Hunter (1983), Hunter, (1989), IAEA (1983), Koplik et al. (1982), Merrett and Gillespie, NEA (1992) and Prij et al. (1991) were found in Guzowski and Newman (1993).

Table B. List of consolidated FEPs evaluated for inclusion in the conceptual site model and scenarios

Table B (continued)

Neptune Subgroup	Normalized FEP (accepted)	Discussion	Representative FEP IDs[1]
Climate change	climate change	Climate change can have a large influence on site performance. Climate change includes natural and anthropogenic changes and its effects on hydrology (including lake effects), hydrogeology, glaciation, biota, and human behaviors.	2, 3, 4, 159, 221, 222, 252, 253, 254, 321, 349, 350, 416, 417, 519, 520, 521, 522, 523, 524, 651, 652, 653, 811, 812, 813, 814
	lake effects	A large lake could have detrimental effects on the repository. Lake effects include appearance/ disappearance of large lakes and associated phenomena (sedimentation, wave action, erosion/inundation, isostasy). This is covered within climate change scenarios. Regulations suggest consideration.	656, 789
	wave action	Wave action, including seiches, could influence site performance and is included in long-term scenarios. See lake effects and erosion/inundation.	224, 790
Containerization	containment degradation	A number of processes can contribute to degradation of waste containment. These are accounted for in release of the source term. It is expected that no credit will be given to containment. Regulations suggest consideration.	7, 8, 9, 10, 11, 12, 13, 14, 15, 16, 17, 352, 496, 527, 657, 658, 817, 818, 819, 820
	corrosion	Corrosion is one of the processes that would contribute to degradation of waste containment. Regulations suggest consideration.	18, 19, 20, 161, 353, 419, 659, 821
Contaminant Migration	biotically-induced transport	Plant uptake and burrow excavation are potential contaminant transport (CT) pathways. Modeling includes biotic (plant- and animal-mediated) processes leading to contaminant transport, and the evolution of these processes in response to climate change and other influences, including bioturbation, burrowing, root development, and contaminant uptake and translocation. Regulations suggest consideration.	21, 420, 529, 530, 531, 532, 533, 534, 661, 662, 663, 664, 665, 791, 822
	colloid transport	Colloid formation could be a CT pathway. This process will be considered in the geochemistry conceptual model.	22, 23, 24, 535, 666, 823

Table B (continued)

Neptune Subgroup	Normalized FEP (accepted)	Discussion	Representative FEP IDs[1]
	contaminant transport	CT is a large class of processes that govern the migration of contaminants in the environment, including transport media (water, air, soil) processes (advection-dispersion, diffusion, plant uptake, soil translocation) and partitioning between phases; much overlap with atmospheric, groundwater, surface water, and biotically-induced transport. Regulations suggest consideration.	25, 26, 27, 28, 29, 30, 31, 32, 33, 34, 35, 162, 163, 257, 301, 302, 303, 304, 305, 323, 354, 355, 356, 421, 536, 537, 538, 539, 540, 667, 668, 669, 670, 671, 672, 673, 824, 825, 826, 827, 828, 829, 830
	diffusion	Diffusion is a basic CT process that could affect performance. Diffusion occurs in gas and water phases.	36, 306, 324, 674, 831
	dilution	Dilution is a basic CT process that could affect performance. Dilution occurs when mixing with less concentrated water.	37, 675, 832
	dispersion	Dispersion is a basic CT process that could affect performance. Hydrodynamic dispersion is associated with water advection.	38
	dissolution	Dissolution will govern leaching of the waste form into water, limited by aqueous solubility.	39, 40, 164, 225, 258, 325, 326, 422, 541, 676, 833
	dust devils	Dust devils are common on the flats, and could disperse contaminants. These are included in atmospheric dispersion.	792
	gas transport	Radon produced in the waste is likely to be transported via gaseous diffusion. Transport in the gas phase includes gas generation in the waste, partitioning between air and water phases, diffusion in air and water, and radioactive decay and ingrowth.	42, 43, 44, 165, 166, 259, 357, 423, 542, 543, 544, 678, 679, 835
	infiltration	Infiltration through the cap materials, the waste, and unsaturated zone could be an important CT mechanism. This includes infiltration of meteoric water (precipitation minus abstractions) through the cap, into wastes, and potentially to the groundwater.	45, 260, 307
	local geology	This feature will control some aspects of CT and is included implicitly in other processes. Regulations suggest consideration.	545, 546, 547

Table B (continued)

Neptune Subgroup	Normalized FEP (accepted)	Discussion	Representative FEP IDs[1]
	preferential pathways	Preferential pathways could contribute to CT. Their presence is accounted for in the definition of advective and diffusive processes. Regulations suggest consideration.	46
Engineered Features	compaction error	Inadequate compaction could result in subsidence. This overlaps with subsidence and closure failure.	680, 836
	engineered features	Many engineered features are intended to improve performance. This large collection of features is intended to promote containment and inhibit migration of contaminants. Regulations suggest consideration.	48, 49, 50, 51, 52, 53, 54, 55, 56, 57, 58, 59, 167, 168, 169, 170, 226, 227, 228, 261, 308, 309, 327, 359, 360, 361, 362, 363, 425, 426, 427, 428, 429, 430, 431, 432, 497, 498, 548, 549, 550, 551, 552, 553, 554, 555, 681, 682, 683, 684, 685, 686, 687, 688, 689,690
	material properties	Material properties are an essential feature of any model, and include density, porosity, hydraulic conductivity, permeability, texture, tortuosity, etc. of waste, backfill, cap materials, and naturally occurring materials.	60, 61, 62, 171, 364, 433, 692, 852, 853, 854
	repository design	Respository design clearly influences its performance. This is accounted for implicitly in the modeling of the repository. Regulations suggest consideration.	695, 696, 858, 859
	source release	Source release is an essential part of the model, and can result from many mechanisms, including containment failure, leaching, radon emanation, plant uptake, and translocation by burrowing animals.	128, 129, 130, 131, 132, 133, 134, 135, 136, 137, 196, 291, 342, 398, 467, 468, 637, 770, 771, 772, 773, 774, 775, 958, 959, 960, 961, 962, 963, 964

Table B (continued)

Neptune Subgroup	Normalized FEP (accepted)	Discussion	Representative FEP IDs[1]
	subsidence of repository	Subsidence can compromise performance, leading to failure of the cap, and enhanced infiltration. Regulations suggest consideration.	310, 311, 329, 439, 861
	waste	Waste form and inventory are essential parts of the model. Inventory and source release includes initial inventory of radionuclides and its physical and chemical form, container performance, matrix performance, leaching, and other release mechanisms.	517, 647, 648, 649
Exposure	animal ingestion	Human ingestion of livestock and game exposed to contaminants is an exposure pathway, and is implemented as part of the human exposure model, as ingestion of fodder and feed by livestock, and ingestion of livestock by humans, and similar pathways for game. Regulations suggest consideration.	660
	dosimetry	Dosimetry hints at human dose response, which is an integral part of PA. Physiological dose response will be estimated in the PA model. Dosimetry as a science is not a FEP, *per se.* Regulations suggest consideration.	560, 561
	exposure media	Exposure media are a fundamental part of exposure pathways, and include foodstuffs, drinking water, other environmental media. These are included in the human exposure model. Regulations suggest consideration.	562, 563
	human behavior	Behavior is part of human exposure pathway. Future human behaviors include activities and their frequency and duration, distinct from food and water ingestion. Regulations suggest consideration.	584, 585, 586, 587, 588
	human exposure	Human exposure, in terms of dose and toxicity, is considered in the model, and includes exposure pathways (ingestion, inhalation, etc.) and physiological effects from radionuclides and toxic contaminants. Regulations suggest consideration.	68, 564, 565, 566, 567, 568, 569, 570, 571, 801, 802
	ingestion pathways	Ingestion of food, water, and soils are modeled human exposure pathways. These include human exposures due to ingestion of water and foodstuffs, and transport pathways (e.g. food chains) that lead to foodstuffs. Regulations suggest consideration.	572, 573, 574

Table B (continued)

Neptune Subgroup	Normalized FEP (accepted)	Discussion	Representative FEP IDs[1]
	inhalation pathways	Inhalation of gases and fine particles are modeled human exposure pathways. Regulations suggest consideration.	794
Geochemical	geochemical effects	Geochemical processes control CT in waste sources, water, and geologic media. These include chemical sorption and partitioning between phases, aqueous solubility, precipitation, chemical stability, complexing, changes in water chemistry (redox potential, pH, Eh), fluid interactions, halokinesis, diagenesis, speciation, cellulosic degradation effects, interactions with clays and other host materials, effects of corrosion products, effects of cementitious materials, and leaching.	69, 70, 71, 72, 73, 74, 75, 76, 77, 78, 79, 80, 81, 82, 174, 264, 368, 440, 575, 576, 577, 698, 699, 700, 701, 862, 863, 864, 865, 866, 867, 868, 869, 870, 871, 872, 873, 874
Human Processes	anthropogenic climate change	This is addressed as part of climate change in general.	85, 580, 706, 879
	community development	Development of communities and other human habitation overlaps with land use and habitation, and is considered in the human exposure assessment, albeit unlikely. See inhabitation, land use. Regulations suggest consideration.	581
	excavation	Excavation includes construction of basements and other construction, and is included as part of the human intrusion scenarios.	330, 499, 582, 709, 710, 882, 883
	explosions	Human-caused explosions include bombs, plane crashes, and conventional weapons training.	230, 500, 583, 804
	human-induced processes	Human-induced processes are limited to repository design, inadvertent human intrusion, or human-induced climate change. Engineered features include repository design and new technological developments. Intentional intrusion is not considered. Anthropogenic climate change is considered under climate change.	90, 91, 92, 177, 271, 272, 372, 443, 589, 590, 712, 713, 886
	human-induced transport	Human activities that could contribute to release are considered. Humans can induce contaminant transport through a variety of activities. See inadvertent human intrusion.	273, 274, 591, 592, 795, 887
	inadvertent human intrusion	Inadvertent human intrusion into the waste is considered in the development of exposure pathways. Regulations suggest consideration.	178, 179, 231, 275, 276, 277, 373, 374, 375, 444, 445, 446, 714, 805, 806, 888

Table B (continued)

Neptune Subgroup	Normalized FEP (accepted)	Discussion	Representative FEP IDs[1]
	inhabitation	Inhabitation on or near the site, including the establishment of surface or underground dwellings, communities, or cities, is extremely unlikely. See community development, land use. Regulations suggest consideration.	93, 94, 593, 594, 807
	institutional control	Institutional control affects human exposures, and includes records of site knowledge, markers, barriers, and security, and the loss thereof. Regulations suggest consideration.	95, 595, 596, 597, 716, 890
	land use	Land use in general could affect exposure scenarios. Land use changes are related to demographics, including development of agricultural, industrial, urban, or wild land uses. Regulations suggest consideration.	183, 450, 600, 601, 602, 719, 720, 893, 894, 895
	post-closure subsurface activities	Subsurface human activities are covered to the extent that they are inadvertent. This could include intrusion, construction, investigation, drilling, or mining. Regulations suggest consideration.	727, 904, 905, 906
Hydrogeological	denudation	Denudation could expose wastes, and is combined with erosion and inundation. Regulations suggest consideration.	192, 388, 460, 502, 503, 739, 917
	erosion	Erosion of the repository resulting from pluvial, fluvial, or aeolian processes can result from extreme precipitation, changes in surface water channels, and weathering. Regulations suggest consideration.	110, 238, 284, 389, 504, 613, 740, 918, 919, 920, 921
	erosional transport	Erosional (sediment) transport could be a CT mechanism. Sediments may move during erosion; includes solifluction. Regulations suggest consideration.	111, 239, 614, 615, 741, 742, 922, 923
	hydrogeological effects	Hydrogeological and groundwater hydraulics changes may occur in response to geological changes, including hydrothermal activity. This is generally covered under groundwater transport. Regulations suggest consideration.	112, 616, 617, 618, 619, 743, 744, 796, 924
	sedimentation	Sedimentation would occur on a lake bottom, and could affect performance. This includes sedimentation/aggradation onto the repository.	113, 193, 285, 335, 390, 461, 621, 797

Table B (continued)

Neptune Subgroup	Normalized FEP (accepted)	Discussion	Representative FEP IDs[1]
Hydrology	groundwater transport	Groundwater transport includes waterborne contaminant transport (CT) in the unsaturated and saturated zones, and is a principal CT mechanism. Groundwater flow and transport mechanisms include advection-dispersion, diffusion, fluid migration, waterborne contaminant transport, changes in the flow system, recharge and discharge, water table movements, and brine interactions.	114, 115, 116, 117, 118, 286, 312, 313, 314, 315, 316, 336, 337, 338, 339, 392, 393, 622, 623, 747, 748, 749, 750, 751, 752, 929, 930, 931, 932, 933, 934, 935, 942
	hydrological effects	Hydrological processes are considered under the topics of surface water and groundwater. Regulations suggest consideration.	463, 505, 624, 753, 754, 936, 937
	inundation	Inundation by a large lake or reservoir is likely to affect the site in the long term. (See also: wave action, and lake effects). Regulations suggest consideration.	755, 798, 938, 939
Meteorology	frost weathering	Weathering from frost cycles is included in cap degradation modeling.	758, 943
	meteorology	Meteorology is considered indirectly; meteorology as a science is not a FEP, *per se*, but contributes to other processes, such as precipitation and atmospheric dispersion, which are covered elsewhere. Regulations suggest consideration.	626, 627, 761, 946, 947
	resuspension	Resuspension will affect site performance, allowing particulates from surface soils to be redistributed by atmospheric dispersion.	981
	atmospheric dispersion	Atmospheric dispersion is a potential CT pathway and is modeled. See also: dust devils. Regulations suggest consideration.	256, 528
	tornado	Tornados are possible in the area.	289
Model Settings	model parameteri-zation	Parameterization is a fundamental part of modeling, though is not a FEP, *per se*.	628
	period of performance	Definition of a period of performance is a fundamental part of PA modeling, though is not a FEP, *per se*.	629
	regulatory requirements	Regulatory requirements drive much of the modeling in PA, though is not a FEP, *per se*.	630
	spatial domain	Definition of a spatial domain is a fundamental part of modeling, though is not a FEP, *per se*.	631

Table B (continued)

Neptune Subgroup	Normalized FEP (accepted)	Discussion	Representative FEP IDs[1]
Other Natural Processes	ecological changes	Changes in the types and abundance of plants and animals could affect performance. Changes in the ecology can be associated with catastrophic events (e.g. fire, inundation), evolution, or climate change.	762, 948, 949
	gas generation	Uranium wastes are expected to produce radon which will affect site performance in terms of doses. See also gas transport.	122, 123, 340, 396, 464, 634, 766, 953, 954
	pedogenesis	Soils are likely to develop on the cap and may affect performance.	765, 952
	radioactive decay and in-growth	Radioactive decay and ingrowth processes are essential to the model.	635, 767, 799, 955
	radon emanation	Radon emanation directly affects the mass of radon released into the environment, and hence site performance.	980
	reconcentration	Possible reconcentration of radiological materials during transport is accounted for in the CT modeling.	127
Tectonic/ Seismic/ Volcanic	geophysical effects	Geophysical changes to the engineered features of the site are accounted for in degradation. Geophysical effects include pressure, stress, density, viscosity, deformation, magnetics, creep, and elasticity.	141, 142, 143, 509, 641, 781, 970, 971

[1]The Representative FEP IDs correspond to the FEP IDs given in Table A.

Table C. List of FEPs dismissed from further consideration.

Table C (continued)

Neptune Subgroup	Normalized FEP (dismissed)	Discussion	Representative FEP IDs[1]
Celestial	meteorite impact	The occurrence and consequences of a direct hit by a meteorite are out of the scope of this model.	1, 158, 219, 220, 251, 320, 348, 415, 491, 492, 493, 518, 650, 810
Climate change	glacial effects	Glacial effects include presence of continental glaciers and resulting isostatic effects, glacial erosion, and periglacial effects. Glaciers in the basin are not modeled. Return of a large lake is expected should a glacial epoch return and is covered within climate change scenarios.	5, 160, 223, 255, 322, 351, 418, 494, 495, 525, 526, 654, 655, 815, 816
	permafrost	The effects of permafrost are bounded by those of cap degradation, which considers more damaging freeze/thaw cycles. See frost weathering.	6, 300
Contaminant Migration	gas intrusion	No mechanism for intrusion of naturally-produced gases into the repository has been identified.	41, 677, 834
Engineered Features	convergence of openings	This FEP applies to mined repositories only.	837
	design error	Errors in design could compromise performance but are not included in the modeling. Design error is distinct from construction or operational error.	47, 358, 424
	material defects	Material defects are covered by degradation, and include material defects in source containment, closure cap, and other engineered materials.	691, 851
	mechanical effects	Mechanical effects are covered implicitly by degradation, and include changes in mechanical properties and conditions, including failure.	63, 64, 65, 172, 262, 365, 366, 434, 435, 556, 557, 693, 694, 855, 856
	release of stored energy	No significant energy is stored within the wastes.	66, 436, 857
	repository seals	Regulations suggest consideration, but, the sealing of the repository shafts, boreholes, and construction and failure of such is applicable only to mined repositories.	67, 173, 229, 263, 328, 367, 437, 438, 558, 559, 697, 860

Table C (continued)

Neptune Subgroup	Normalized FEP (dismissed)	Discussion	Representative FEP IDs[1]
Exposure	agriculture	Agriculture includes establishment, evolution, and abandonment of agriculture and aquaculture at and near the site. Regulations suggest consideration, however, none of these are expected to occur because of the high salinity of soils and groundwater at the site.	705, 803, 878
Geological	diagenesis	Diagenesis in local lacustrine sediments could include the formation of interstitial evaporites, but is not expected to change site performance.	83, 175, 265, 369, 441, 578, 702, 875
	gas or brine pockets	No gas or brine pockets have been identified below the site.	176, 370, 442, 579
	landslide	Regulations suggest consideration, but landslides are not expected to occur in the flat lacustrine basin. Mass wasting of the site itself is covered under erosion.	266, 703, 876
	local subsidence	Geological subsidence in the area is unlikely to seriously affect performance, and is not expected in the basin of lacustrine sediments.	267
Human Processes	accidents during operations	Regulations suggest consideration, but operational performance is not within the scope of the PA model.	84, 704, 877
	climate control	No climate control at the facility is assumed. Climate control is a feature of certain mined repositories.	268, 371
	closure failure	Regulations suggest consideration; however, poor closure includes abandonment or other failure to close the facility as planned, and is not modeled.	86, 87, 707, 708, 880, 881
	fire	The waste is not combustible or explosive. Fires in the waste itself or following explosions are distinct from wildfire.	269, 270
	fisheries	Regulations suggest consideration, but development of fisheries is not credible at the site.	884
	geothermal energy production	No geothermal resources are identified at the site.	89, 711, 885
	injection wells	Given the regional history, the construction of injection wells nearby for disposal of liquid wastes is possible. The effect of drilling such wells in the vicinity would be negligible, however.	232, 715, 889

Table C (continued)

Neptune Subgroup	Normalized FEP (dismissed)	Discussion	Representative FEP IDs[1]
	intentional intrusion	Intentional intruders are not protected and are not modeled as receptors. Intentional intrusion includes exhumation of waste, sabotage, terrorism, or archeological research.	96, 180, 181, 278, 376, 377, 447, 448, 717, 808, 891
	investigation	Site investigation is considered intentional, and receptors are not covered.	598, 599, 809
	irrigation	Regulations suggest consideration, and irrigation could affect site performance, but will not occur since there is no suitable water source.	182, 233, 378, 449, 718, 892
	monitoring	Monitoring of the site is required, but persons performing the activity are not protected since it is intentional and informed. Monitoring activities will not affect the performance of the site.	97, 603, 721, 896
	nuclear testing	Regulations suggest consideration; however, testing of nuclear devices underground, at the ground surface, or in the atmosphere is considered intentional disruption of the site and is not covered.	98, 722, 897
	operational effects	Operations could affect performance, and include normal site operation, closure, and later attempts at site improvement. Regulations suggest consideration; however, operations are not part of the PA.	99, 604, 605, 723, 724, 898, 899, 900
	operational error	Covered under operational effects. Operational errors include poor quality site construction, waste emplacement, and site closure. Regulations suggest consideration, however, operations are not part of the PA.	100, 184, 279, 379, 380, 451, 725, 726, 901, 902, 903
	quality control	Quality control is important to site operations, but is not a FEP that lends itself to modeling.	606
	resource extraction	Regulations suggest consideration. Resource extraction is a type of intentional intrusion, including drilling, mining, or quarrying into the repository, or in such a way as to affect performance, in search of resources such as petroleum, natural gas, salt, rock, or geothermal resources. See intentional intrusion.	101, 102, 103, 185, 186, 234, 235, 280, 331, 332, 381, 382, 383, 452, 453, 501, 608, 609, 728, 729, 730, 731, 907, 908, 909, 910
	sabotage	Sabotage is by its nature intentional. See intentional intrusion.	104, 187, 333, 384, 454, 732, 733, 911, 912

Table C (continued)

Neptune Subgroup	Normalized FEP (dismissed)	Discussion	Representative FEP IDs[1]
	unplanned events	This category is too vague to be considered explicitly; unplanned events are generally subsumed by other FEPs.	610
	war	Intrusion or disruption as part of an act of war would be intentional. See intentional intrusion.	105, 188, 334, 385, 455
	waste recovery	Regulations suggest consideration, but waste recovery, retrieval, or mining are considered intentional acts. See intentional intrusion.	106, 189, 386, 456, 607.734, 735
	water resource management	Water resource activities include construction of dams, reservoirs, and wells, and could affect the site as water is extracted or retained. Regulations suggest consideration; however, this is not specifically modeled, as it is bounded by the large lake scenario.	107, 108, 109, 190, 236, 237, 281, 282, 387, 457, 458, 611, 736, 737, 913, 914, 915
	weapons testing	Any nuclear and conventional weapons testing would be done with cognizance of the site, and is intentional. See also explosions and intentional intrusion.	191, 283, 459
Hydrogeological	subrosion	No subsurface erosion has been reported in the vicinity.	925
Hydrology	flooding	Regulations suggest consideration; however, temporary flooding of the site due to extreme precipitation is not plausible due to site topography in the midst of the flats. This is distinct from inundation by the return of a large lake, which is included.	194, 240, 391, 462, 746, 926, 927, 928
	surface water transport	Surface water transport includes formation and changes in rivers, lakes, and streams, and transport of dissolved and suspended solids, and sediments. Such effects are not anticipated at the facility. This is distinct from inundation by the return of a large lake, which is included.	119, 241, 287, 317, 318, 319, 394, 395, 625, 756, 757, 940, 941
Marine	coastal processes	Coastal processes will not apply at the site, since no sea or ocean is expected in relevant time frames. However, see wave action.	612, 738, 760, 916, 945
	hurricanes	No hurricanes occur in the area.	242, 288
	insolation	Insolation (the amount of sunshine on the site) has no direct effect on site performance. See ecological changes.	759, 944

Table C (continued)

Neptune Subgroup	Normalized FEP (dismissed)	Discussion	Representative FEP IDs[1]
	marine effects	Marine processes will not apply at the site, since no sea or ocean is expected in relevant time frames. Marine processes include sea-level change. See also coastal processes and tsunami.	620, 745
	tsunami	No tsunami will occur at the site. See coastal processes and marine effects.	243
Natural Processes	microbial effects	Microbial action is not expected to affect performance. Microbial processes include corrosion, changes in chemistry, and dissolution of glasses, but biotically-induced transport is limited to macrobiological processes.	120, 632, 633, 763, 764, 950, 951
	radiological effects	Regulations suggest consideration. Radiological processes such as radiolysis are a concern for waste containment in some geological repositories, but are not modeled here, since waste containment is not given credit.	124, 125, 126, 195, 341, 397, 465, 466, 636, 768, 769, 956, 957
	wildfire	Occasional wildfire (brush fire, forest fire, either local or widespread) is not likely to affect site performance in the long run, since this is a natural part of plant community dynamics.	290
Source Release	electrochemical effects	Electrochemical effects are not a relevant process at the site. Electrochemical reactions are a concern for the SKB repository.	121
	explosions	Explosive gases are not present in the repository.	88
Tectonic/ Seismic/ Volcanic	breccia pipes	Regulations suggest consideration, and the formation of breccia pipes or mud volcanoes could affect performance, but is considered highly unlikely.	197, 343, 399, 469
	diapirism	Salt deposits in the strata below the site will not result in the formation of diapirs.	198, 244, 292, 344, 400, 470, 638, 776, 965
	discontinuities	No major geological discontinuities are envisioned at the site.	639
	earthquake	Earthquakes, either from natural or man-made causes, would not change the performance of this shallow unconsolidated site.	138, 293

Table C (continued)

Neptune Subgroup	Normalized FEP (dismissed)	Discussion	Representative FEP IDs[1]
	faulting	Faulting is unlikely to significantly affect performance of this shallow unconsolidated site and is not explicitly modeled. Geologic faulting includes all type of faults, shear zones, diastrophism, existing and future. See also see fracturing.	139, 199, 200, 201, 245, 294, 345, 401, 402, 471, 472, 473, 506, 507, 508, 777, 778, 966, 967
	fracturing	Tectonic fracturing will not affect unconsolidated site performance.	202, 203, 204, 205, 246, 403, 474, 475, 476, 477, 779, 968
	geological intrusion	Magmatic and intrusive igneous activity has not been identified in the vicinity of the site. Geological intrusion includes dikes, intrusive and magmatic activity, and metamorphism due to such activity. This is distinct from breccia pipes (mud volcanoes) and human intrusion.	140, 206, 207, 295, 346, 404, 405, 478, 479, 640, 780, 969
	hydraulic fracturing	Hydraulic fracturing is performed in solid rock, and has no applicaton at the site. Hydraulic fracturing ("hydrofracking") is induced by humans to enhance resource recovery or liquid waste disposal by injection.	208, 480
	intrusion into accumulation zone in the biosphere	No accumulation zone in the biosphere has been identified at the site.	144
	isostatic effects	Isostatic changes could influence lake levels, which are accounted for elsewhere. Isostasy includes that caused by tectonics, large bodies of water, and by continental glaciers.	209, 406, 481, 510, 511
	lava tubes	No lava tubes exist at the site or are expected in the future.	210, 407, 482
	orogeny	No significant orogeny is expected in relevant time frames. Orogeny (mountain-building) caused by tectonic movements or regional uplift.	211, 247, 296, 408, 483
	regional subsidence	Regional subsidence could influence lake levels, which are accounted for elsewhere.	145, 409, 782, 972
	seismic effects	Regulations suggest consideration, but effects of seismic activity (see also earthquakes) would be insignificant for shallow land burial.	248, 512, 513, 642, 783, 973

Table C (continued)

Neptune Subgroup	Normalized FEP (dismissed)	Discussion	Representative FEP IDs[1]
	tectonic effects	Tectonic effects could influence lake levels, which are accounted for elsewhere.	146, 147, 148, 149, 212, 213, 410, 484, 643, 644, 784, 785, 974, 975, 976
	volcanism	No significant volcanism is expected in relevant time frames.	150, 214, 249, 250, 411, 412, 485, 486, 514, 515, 516, 645, 786, 800, 977
Waste	nuclear criticality	Nuclear criticality, while a concern for repositories of used nuclear fuel, is not a concern at this LLW site.	151, 152, 215, 297, 347, 413, 487, 646, 787, 978
	other waste	The current analysis is constrained to examine depleted uranium wastes only, including associated "contaminant" waste. This rather vague reference to "other waste" will be addressed as the scope of wastes under consideration expands.	153, 154, 155, 156, 157, 216, 217, 218, 298, 299, 414, 488, 489, 490, 788, 979

[1]The Representative FEP IDs correspond to the FEP IDs given in Table A.

Neptune and Company Inc.

June 1, 2011 Report for EnergySolutions

Clive DU PA Model, version 1

Appendix 2

Conceptual Site Model for Disposal of Depleted Uranium at the Clive Facility

Conceptual Site Model for Disposal of Depleted Uranium at the Clive Facility

28 May 2011

Prepared by

Neptune and Company, Inc.

This page is intentionally blank, aside from this statement.

CONTENTS

FIGURES

TABLES

Acronyms and Abbrev.

Ac	actinium
Am	americium
amsl	above mean sea level
bgs	below ground surface
BLM	Bureau of Land Management
Bq	becquerel (1 disintegration per second)
CAS	Class A South (embankment)
CEDE	committed effective dose equivalent
CFR	U.S. Code of Federal Regulations
Ci	curie (37 GBq)
CSF	cancer slope factor
CSM	conceptual site model
CWF	Containerized Waste Facility
DCF	dose conversion factor
DOE	U.S. Department of Energy
DU	depleted uranium
DUF_6	depleted uranium hexafluoride
EIS	Environmental Impact Statement
EPA	U.S. Environmental Protection Agency
ETTP	East Tennessee Technology Park
FEIS	Final Environmental Impact Statement
FEP	features, events, and processes
FR	Federal Register
ft	foot/feet
g	gram
GDP	gaseous diffusion plant
GWPL	groundwater protection limit(s)
GTCC	greater than Class C waste
ha	hectare
IAEA	International Atomic Energy Agency
ICRP	International Commission on Radiation Protection
IHI	inadvertent human intruder
ka	thousand years ago
K_d	soil/water partition coefficient
kg	kilogram
K_H	Henry's Law constant (air/water partition coefficient)
km	kilometer
ky	thousand years
L	liter

LARW	low-activity radioactive waste
LLW	low-level radioactive waste
MCL	maximum contaminant level(s)
m	meter
Ma	million years ago
mg	milligram
Mg	megagram (one metric ton)
MLLW	mixed [hazardous and] low-level radioactive waste
MOP	member of the public
MPa	megapascal
mrem	millirem
mSv	millisievert
My	million years
NRC	U.S. Nuclear Regulatory Commission
NTS	Nevada Test Site
NUREG	an NRC publication
OHV	off-highway vehicle
Pa	protactinium
PA	performance assessment
PAWG	Performance Assessment Working Group (DOE)
pCi	picocurie
Po	polonium
ppm	part per million
Pu	plutonium
QA	quality assurance
Ra	radium
RfD	reference dose
Rn	radon
SRS	Savannah River Site
Sv	Sievert
Tc	technetium
TDS	total dissolved solids
TEDE	total effective dose equivalent
TF	Treatment Facility
Th	thorium
U	uranium
UAC	Utah Administrative Code
UNF	used nuclear fuel
UWQB	Utah Water Quality Board
yr	year

1 Introduction

The safe storage and disposal of depleted uranium (DU) waste is essential for mitigating releases of radioactive materials and reducing exposures to humans and the environment. Currently, a radioactive waste facility located in Clive, Utah (the "Clive facility") operated by Energy*Solutions* is proposed to receive and store DU waste that has been declared surplus from radiological facilities across the nation. The Clive facility has been tasked with disposing of the DU waste in an economically feasible manner that protects humans from future radiological releases.

To assess whether the proposed Clive facility location and containment technologies are suitable for protection of human health, specific performance objectives for land disposal of radioactive waste set forth in Title 10 Code of Federal Regulations Part 61 (10 CFR 61) Subpart C, and promulgated by the Nuclear Regulatory Commission (NRC), must be met. In order to support the required radiological performance assessment (PA), a detailed computer model will be developed to evaluate the doses to human receptors that would result from the disposal of DU and its associated radioactive contaminants (collectively termed "DU waste"), and conversely to determine how much DU waste can be safely disposed at the Clive facility.

This conceptual site model (CSM) document describes the site conditions, chemical and radiological characteristics of the wastes, contaminant transport pathways, and potential exposure routes at the Clive facility that are used to structure the quantitative PA model. The PA model will be developed as a probabilistic model taking into account uncertainties inherent to model variables and site-specific conditions. The GoldSim systems analysis software (GTG, 2010) will be used to construct the probabilistic PA model. This PA model is intended to reflect the current state of knowledge with respect to the proposed DU disposal, and to support environmental decision making in light of inherent uncertainties.

The CSM report, and the associated features, events and processes report, are regarded as "living documents." That is, as further information is gathered during the course of model development, the CSM might evolve and, consequently, be updated. Changes to the CSM will be tracked so that the evolution is well documented. Nevertheless, this version of the CSM (revision 1) is expected to include most of the features, events and processes that need to be included in the evaluation of the Clive facility for disposal of DU waste.

2 Scope of the Conceptual Site Model

The overall scope of this PA is to evaluate the long term siting and performance integrity of the Class A Embankment at the Clive facility for the proposed disposal of DU waste. The need for the PA is driven by Federal and State of Utah regulations, which require an evaluation of the potential human radiation doses and consequences of disposal of radioactive waste. The regulations contain procedural requirements, performance objectives, and technical requirements for near-surface disposal, including disposal in engineered facilities with protective earthen/rock covers, which may be built fully or partially above-grade, such as the radioactive waste disposal cells at the Clive facility. The overall PA process is illustrated in Figure 1.

This CSM describes the physical, chemical, and biological characteristics of the Clive facility. The CSM, therefore, encompasses everything from the inventory of disposed wastes, the migration of radionuclides contained in the waste through the engineered and natural systems, and the exposure and radiation doses to hypothetical future humans. These site characteristics are used to define variables for the quantitative PA model that is used to provide insights and understanding of the future potential human radiation doses from the disposal of DU waste.

The content of the CSM informs the PA model with respect to regional and site-specific features, events and processes, such as climate, groundwater, and human receptor scenarios. The CSM accounts for and defines relevant features, events, and processes (FEPs) at the site, materials and their properties, interrelationships, and boundaries. These constitute the basis of the PA model, on which, or through which, radionuclides are transported to locations where receptors might be exposed.

The quantitative probabilistic PA model will be used to evaluate the migration of radionuclides contained in the DU wastes, and the subsequent human doses resulting from potential exposure to radionuclides, based on projecting current societal conditions up to 10,000 years into the future. However, because the radioactivity from the DU wastes (including progeny) will increase for more than 2 million years, and will persist for at least a billion years, further modeling of potential long-term future scenarios will be performed beyond the 10,000 year compliance period. The longer term model will address mechanisms by which radionuclides might be dispersed in the environment, suggesting concentrations of radionuclides in various media.

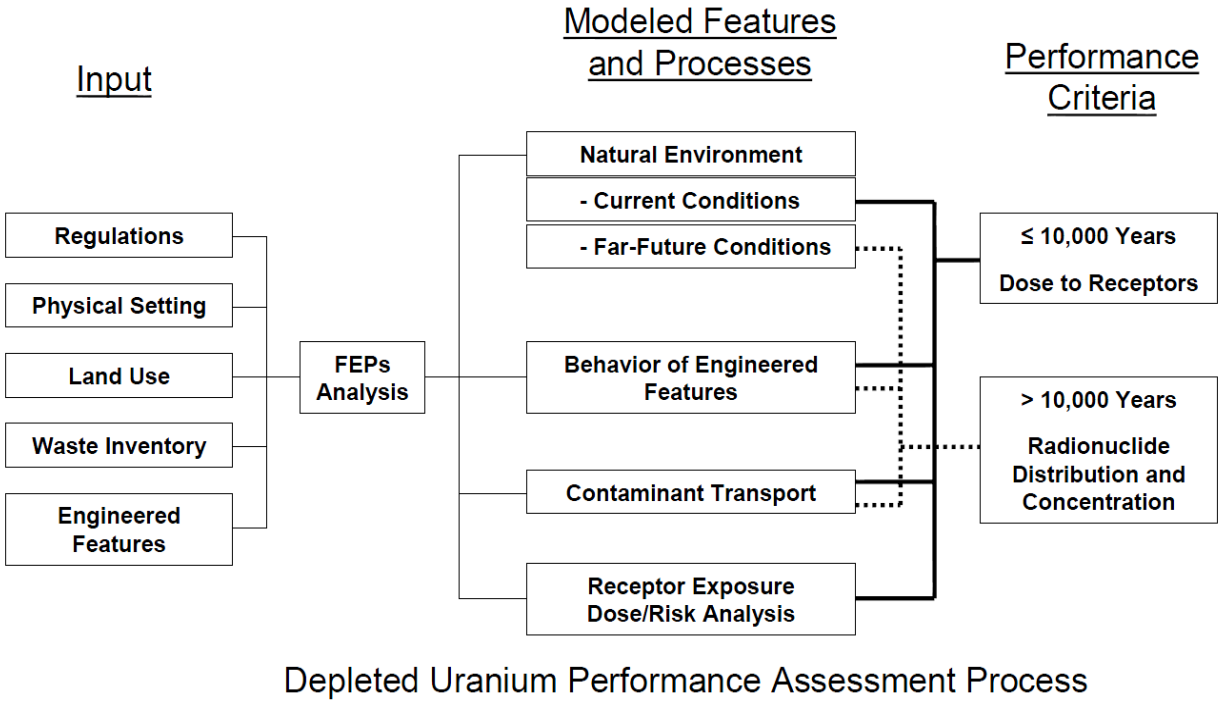

Figure 1. Conceptual diagram of the performance assessment process

However, the long term future model will not directly address human doses, because it is not clear what human exposure scenarios might be reasonable given events in the long term future that might dramatically alter human society and civilization. Therefore, the focus of the longer-term modeling will be scenarios developed to represent potential features, events and processes that affect contaminant fate and transport over these much longer periods.

The quantitative model will be used to evaluate potential human radiation doses from exposure to radionuclides contained in the DU wastes that may result from migration through the engineered and natural systems to the potentially exposed population. Note that regulations specify estimation of *dose*, rather than risk; however, there are risks implied in the regulatory dose limits (see Section 4). Risk-based decision-making is best supported with probabilistic modeling, and has been used to assess compliance and inform decision making at many challenging radioactive waste sites under various regulatory requirements. The U.S. Environmental Protection Agency (EPA) has published probabilistic risk assessment guidance for human exposure to chemicals (EPA, 2001) and promotes the use of probabilistic methods for performance assessments of radioactive disposal facilities in its *Environmental Radiation Protection Standards* (40 CFR 191). The U.S. Department of Energy (DOE) has implemented a probabilistic PA at the Waste Isolation Pilot Plant, at the Yucca Mountain Project, and for low-level radioactive waste (LLW) disposal facilities at the Nevada Test Site (NTS), and the Los Alamos National Laboratory, and has more recently initiated similar efforts at the Savannah River Site. The NRC has adopted this approach as well, as documented in its *Performance Assessment Methodology for LLW Disposal Facilities* (NRC, 2000). Further, the National Research Council has argued in favor of the risk-based approach in its recent book, *Risk and Decisions* (National Research Council, 2005). More generally, various agencies and professional organizations (e.g., EPA's Council for Regulatory Environmental Modeling, Society for Risk Analysis) have consistently moved in the direction of supporting risk-based decisions with probabilistic analysis so that the potential risks are modeled more realistically (as opposed to conservatively) and uncertainty is numerically characterized.

Thus, the quantitative PA model will be probabilistic; with uncertainties associated with the complex evolution from waste disposal to human exposure and dose captured through input parameter probability distributions. Attention will be paid to developing model input parameter distributions that reflect both the uncertain state of knowledge and the appropriate spatio-temporal scaling. The focus of the uncertainty analysis in the PA model will be parameter uncertainty. The PA model will also be developed with the capability of running the model under various FEP scenarios to allow for an assessment of scenario uncertainty. This will be important for the longer-term scenarios in particular.

As noted above, the probabilistic approach models future conditions by projecting current conditions as reasonably as possible while including uncertainty in the parameters or assumptions of the model. This is differentiated from "conservative" (i.e., biased toward safety) modeling that is sometimes performed, typically using point values for parameters (implying a great deal of confidence; i.e., no uncertainty). This type of conservative modeling is often termed "deterministic" modeling, and has often been been used to support compliance decisions. However, supposed conservatism in parameter estimates (or distributions) is often difficult to judge in fully coupled models in which all transport processes are contained in the same overall

PA model. More importantly perhaps, conservative dose results from PA models do not support the full capability of a disposal facility. Conservative, deterministic models may have utility at a "screening" level, but, they do not provide the full range of information that is necessary for important decisions such as compliance or rule-making (Bogen 1994, Cullen 1994).

Of further concern is the type of modeling environment that is needed to support the types of decisions that are made on the basis of PA models. The GoldSim modeling environment is focused on development of "systems-level" models. These models are intended to characterize the effects and consequences of system level dynamics. In this case, the system consists of the waste disposal facility and the interaction of the facility with the environment (e.g., weather, water, biota, etc.) in the 10,000-yr duration for which quantitative modeling will be performed with human dose as the endpoint of interest, as well as the longer duration for which media concentrations resulting from potential future scenarios involving, for example, climate change, re-occurrence of large lakes, will be evaluated. That is, the domain of the model is large both spatially and temporally. However, decisions need to be made in the face of uncertainty regarding the applicability of the Clive facility for disposal of DU, and, more generally, for the design of the disposal facility.

Systems-level models are aimed precisely at supporting decision making in this type of context. More detailed "process-level" models, which might model at a much more refined spatial scale (and perhaps temporal scale), can provide useful input to the systems-level model, but they do not as readily support decision-making at the more holistic scale of the systems-level response. For example, a systems-level model will evaluate the movement of radionuclides from the waste zone, through the unsaturated zone, to the saturated zone, by considering the average effects across those system components, as opposed to the effects at a more refined scale such as every cubic meter, which is more common for process-level modeling. Process-level models are often geared towards capturing variability at small spatial scales, whereas systems-level models are aimed at capturing uncertainty in the system as a whole. PA modeling is concerned with the latter, including demonstration of compliance followed by a decision analysis in the spirit of achieving ALARA (as low as reasonably achievable; see Section 4) releases and doses to optimize disposal and closure (e.g., engineered barriers, institutional controls).

To capture the temporal domain of the model, time steps in this type of systems-level dynamic probabilistic model are usually on the order of several to many years. Consequently, the average effects over long time frames, assuming no catastrophic changes in the system, are far more important than the effects on the scale of days, hours, minutes or seconds. Spatial and temporal scaling of available data, which are usually collected at points in time and space, is critical for the success of systems-level models. Scaling in this context is essentially an averaging process both spatially and temporally. Simple averaging works well if the effect on the response of a variable or parameter is linear. Otherwise, some care needs to be taken in the spatio-temporal averaging process. In addition, these types of models are characterized by differential equations and multiplicative terms. Averaging is a linear construct that does not translate directly in non-linear systems. Again, care needs to be taken to capture the appropriate systems-level effect when dealing with differential equations and multiplicative terms.

A further statistical issue of concern is the challenge of capturing dependencies or correlation structures with this type of dynamic probabilistic system. Inputs for parameters (variables) are usually provided independently of each other. However, it is very important to capture correlations between variables in a multiplicative model. Otherwise, system uncertainty is not adequately constrained. GoldSim provides some limited capability to introduce correlation into a PA model, but steps will be taken to evaluate the correlation effects of some variables.

Processes that contribute to the fate and transport of these contaminants are also abstracted into mathematical models. That is, process-level models are sometimes important for providing input to PA models. Model abstraction is best performed by running process-level models for some cases or scenarios that correspond to a design over the inputs. The response can be modeled using a statistical response surface, which can then be carried or abstracted into the PA model. The systems-level PA model is then fully coupled across processes, meaning that inputs and outputs from each process affect the prior and posterior processes.

With a probabilistic dynamic PA model, a global sensitivity analysis can be performed to identify those parameters that are most important for predicting the model results. This type of sensitivity analysis is performed using statistical methods from data mining allowing all input parameters to be varied simultaneously. This allows the combined effect of changes in parameters to be evaluated. The sensitivity analysis tools can then be used to determine whether more information should be collected to reduce uncertainty. This is fully consistent with the concepts underlying the PA maintenance program that DOE uses under DOE M 435.1 to reduce uncertainty in LLW PAs (DOE, 1999).

3 Site Description

Energy*Solutions* operates a low-level radioactive waste disposal facility west of the Cedar Mountains in Clive, Utah, as shown in Figure 2. Clive is located along Interstate-80, approximately 5 km (3 mi) south of the highway, in Tooele County. The facility is approximately 80 km (50 mi) east of Wendover, Utah and approximately 100 km (60 mi) west of Salt Lake City, Utah. The facility sits at an elevation of approximately 1302 m (4275 ft) above mean sea level (amsl) and is accessed by both highway and rail transportation. The Clive facility is adjacent to the above-ground disposal cell used for uranium mill tailings that were removed from the former Vitro Chemical company site in South Salt Lake City between 1984 and 1988 (Baird et al., 1990).

Currently, the Clive facility receives waste shipped via truck and rail. Pending the findings of the PA, DU waste will be stored in a permanent above-ground engineered disposal embankment that is clay-lined with a composite clay and rock cap. The disposal embankment is designed to perform for a minimum of 500 years based on requirements of 10 CFR 61.7, which provides a long-term disposal solution with minimal need for active maintenance after site closure. More detail relating to the properties of the disposal embankment is provided in Section 3.6.1 .

Figure 2. Location of the Clive site operated by Energy*Solutions* (from Google Earth)

The Energy*Solutions* Clive facility is divided into three main areas (Figure 3; Energy*Solutions*, 2008):

- the Bulk Waste Facility, including the Mixed Waste, Low Activity Radioactive Waste (LARW), 11e.(2), and Class A LLW areas,
- the Containerized Waste Facility (CWF), located within the Class A LLW area, and
- the Treatment Facility (TF), located in the southeast corner of the Mixed Waste area.

The subject of this CSM and associated modeling is DU waste disposed or to be disposed in the Class A South cell. The terms "cell" and "embankment" are here used interchangeably.

3.1 Land Management

The Bureau of Land Management (BLM) administers much of the land around the Clive facility; this land is public domain (NRC, 1993). The disposal site is located within a 260-ha (640-acre) section of land that was originally selected for the disposal of the Vitro Chemical Company uranium tailings (see "Vitro" in Figure 3). This section of land occupies approximately 40 ha (100 acres), while the remaining 220 ha (540 acres) is owned and operated by Energy*Solutions*. The Tooele County Commission zoned the Clive site as a "Hazardous Industrial District," which

falls within the West Desert Hazardous Industry Area, an area that prohibits future residential housing in the near vicinity of the Clive site (NRC, 1993).

NRC (1993) and the BLM (BLM staff, personal communication, 2010) indicates that the area surrounding the Clive facility is used for cattle and sheep grazing purposes and recreation. While the site is zoned for hazardous waste disposal by Tooele County, the lack of potable water at this site makes the surrounding area an unlikely location for any residential, commercial, or industrial developments (Baird et al., 1990).

Figure 3. Disposal and Treatment Facilities operated by Energy*Solutions*

3.2 Climate

3.2.1 Temperature

Regional climate is regulated by the surrounding mountain ranges, which restrict movement of weather systems in the vicinity of the Clive facility. The most influential feature affecting regional climate is the presence of the Great Salt Lake, which can moderate downwind temperatures since it never freezes (NRC, 1993). The climatic conditions at the Clive facility are characterized by hot and dry summers, cool springs and falls, and moderately cold winters (NRC, 1993). Frequent invasions of cold air are restricted by the mountain ranges in the area. Data from the Clive facility from 1992 through 2009 indicate that monthly temperatures range from about -2°C (29°F) in December to 26°C (78°F) in July (Whetstone, 2006).

3.2.2 Precipitation

The Clive facility is characterized as being an arid to semi-arid environment where evaporation greatly exceeds annual precipitation (Adrian Brown, 1997a). Data collected at the Clive facility from 1992 through 2004 indicate that average annual rainfall is on the order of 22 cm (8.6 in) per year (Whetstone, 2006). Precipitation generally reaches a maximum in the spring (1992-2004 monthly average of 3.2 cm [1.25 in] in April), when storms from the Pacific Ocean are strong enough to move over the mountains (NRC, 1993; Whetstone, 2006). Precipitation is generally lighter during the summer and fall months (1992-2004 monthly average of 0.8 cm [0.32 in] in August) with snowfall occurring during the winter months (Whetstone, 2006; NRC, 1993; Baird et al., 1990).

3.2.3 Evaporation

Because of warm temperatures and low relative humidity, the Clive facility is located in an area of high evaporation rates. NRC (1993) indicates that average annual pond evaporation rate at the Clive facility is 150 cm/yr (59 in/yr), with the highest evaporation rates between the months of May and October. Previous modeling studies indicate that the Dugway climatological station nearby is comparable to the Clive site with respect to evaporation and have reported pan-evaporation estimates of 183 cm/yr (72 in/yr), which is considerably greater than average annual rainfall (Adrian Brown, 1997a). Because of the high evaporation rate, the amount of groundwater recharge due to precipitation is likely very small, except during high intensity precipitation events (Adrian Brown, 1997a).

3.3 Geology

3.3.1 Site Geology

The Clive facility rests on lacustrine deposits from the ancestral Lake Bonneville, which was a pluvial lake that existed during the late Pleistocene. The geology is characterized by north-south trending mountain ranges surrounded by sediment filled basins. The site is bounded by the Cedar Mountains to the east and the Great Salt Lake Desert to the west. Surficial drainage is generally in a westward direction away from the nearest mountain range.

NRC (1993) indicates that based on subsurface borehole logs, lacustrine deposits extend to at least 75 m (250 ft) underneath the site, however these estimates are limited to the depths of boreholes drilled from previous hydrogeologic investigations (e.g., Envirocare [2004]). Oviatt et

al. (1999) examined the upper 110 m (361 ft) of the Burmester core, a sediment core that was collected to a depth of 307 m (1007 ft) in the 1970s to characterize major pluvial lake cycles in the Bonneville Basin. Brodeur (2006) also indicates that sediments can be up to a thousand meters thick in some regions of the basin and greater than 200 m (700 ft) thick in the basin at the Clive site.

The sediments underlying the Clive site are described as four separate stratigraphic units based on grain size and sediment characteristics. These units are described in NRC (1993), Adrian Brown (1997a), and Envirocare (2004) and are introduced from the ground surface down:

- Unit 4 (surface) is composed primarily of silt and clay between 1.8 and 5 m (6 and 16.5 ft) thick, with an average thickness of 3 m (10 ft). Minor amounts of sand within the silt and clay can be found along with some evaporite mineral content. This layer is rather impermeable due to the silt and clay composition and therefore makes it difficult for water to readily pass through it.
- Unit 3 lies beneath Unit 4 and is composed of a silty sand between 2.1 and 7.6 m (7 and 25 ft thick, with an average thickness of 3 m (10 ft). The water table of a shallow, unconfined aquifer occurs near the bottom of this Unit on the western side of the site. This shallow aquifer is saline.
- Unit 2 lies beneath Unit 3 and is composed of clay with occasional lenses or interbeds of silty sand. This unit is between 0.76 and 7.6 m (2.5 and 25 ft) thick and is saturated with saline groundwater.
- Unit 1 underlies Unit 2 and is composed of silty sand with interbedded layers of clay and silt. The Envirocare investigation indicates that the total thickness of Unit 1 is at least 75 m (250 ft) (Envirocare, 2004). The deepest borehole at the time of this investigation was drilled to 250 ft below ground surface (bgs) without encountering bedrock. Unit 1 is saturated beneath the facility and contains a locally confined aquifer. Envirocare (2004) also indicated that a borehole drilled at an area north of the facility did not encounter bedrock at a depth of 200 m (700 ft) bgs.

3.3.2 Site Seismotectonics

The Clive site does not have any known active faults in its vicinity. NRC (1993) indicates that the nearest faulting is located 29 km (18 miles) to the north, having occurred between 1 million to 25 million years ago (1 to 25 Ma). Although the site is not located near any active faults, isostatic rebound is suspected to be the cause of any recent seismic activity in the Lake Bonneville area.

NRC (1993) cites two seismic investigations that were conducted for the Vitro tailings disposal facility and a proposed site for a supercollider that was to encompass a 24-km (15-mile) elliptical ring around the Clive site. Based on these studies, NRC (1993) indicated that nearby structures and seismogenic areas that could pose a hazard include the fault zones within a 72-km (45-mile) radius of the site. These include the eastern flank of the Cedar Mountains, western flank of the Lakeside Mountains, Northwest Puddle Valley, eastern flank of the Newfoundland mountains, and the western flank of the Stansbury Mountains. However, NRC (1993) concluded that no

active fault zones lie beneath the Clive site, and there is no macroseismic evidence of a capable fault in the vicinity of the site.

3.4 Hydrology

3.4.1 Surface Water

The Clive site is located within a hydrologically closed basin west of the Cedar Mountains. As there is no outlet from the basin, any water that would flow by the site would pond several miles to the west in a playa (NRC, 1993).

No surface water bodies are present on the Clive site and any stream flows from higher elevations usually evaporate and/or infiltrate before reaching flatter land (NRC, 1993). Indicators of channelized flow are not present on the Clive site (Baird et al., 1990). The nearest stream channel ends about 3.2 km (2mi) east of the site, and the nearest water body that is utilized is approximately 45 km (28 mi) to the east. The only significant water body in the region is Great Salt Lake. NRC (1993) indicates that no historical (chronic) flooding has occurred in the vicinity of the site. Given the 1300-m elevation of the Clive facility, it is not subject to flooding from the Great Salt Lake, which is not expected to exceed 1285 m (4217 ft) amsl (NRC, 1993).

3.4.2 Groundwater

The NRC recognizes "groundwater" to include all subsurface water, in both unsaturated and saturated zones. This convention is used in the following descriptions.

3.4.2.1 Groundwater Flow Regime

Local groundwater recharge from meteoric sources is generally limited, since pan-evaporation greatly exceeds precipitation (NRC, 1993). Recharge is more likely to occur in areas adjoining the surrounding mountain ranges, moving as subsurface flow to the center of the basin.

Given the strong evaporation potential at the site, it may be expected that some unsaturated zone (vadose zone) groundwater may actually move upward. An upward gradient is not only due to evaporation of water at the ground surface, it is also driven by the transpiration of plants, which pull water from the ground and release it to the dry atmosphere. The coupled effect of these two processes, or evapotranspiration, serves to keep near-surface soils dry enough that precipitation often does not penetrate to lower soils.

Groundwater at the Clive site is found within a low-permeability saline aquifer starting near the bottom of the Unit 3 stratigraphic unit, and saturating the Unit 2 stratigraphic unit. The depth to groundwater is between approximately 6 and 9 m (20 and 30 ft) bgs at an approximate elevation of 1295 m (4250 ft) amsl (Brodeur, 2006).

The regional (saturated) groundwater system flows primarily to the east-northeast toward the Great Salt Lake (Envirocare 2004) and the local shallow groundwater follows a slight horizontal gradient to the north-northeast (Brodeur, 2006).

3.4.2.2 Groundwater Quality

The underlying groundwater in the vicinity of the Clive site is of naturally poor quality because of its high salinity and, as a consequence, is not suitable for most human uses (NRC, 1993).

Brodeur (2006) reports that groundwater beneath the Clive site had a total dissolved solid (TDS) content of 40,500 mg/L (40.5 ‰). The majority of the cations and anions are sodium and chloride, respectively. This is not potable for humans. For comparison purposes, sea water typically has a TDS content of 35,000 mg/L (35 ‰), thus the salinity content at the site is much higher than average sea water.

3.5 Ecology

NRC (1993) and Envirocare (2000) characterized the Clive facility as a homogeneous, semi-desert low shrubland, primarily composed of shadscale (*Atriplex confertifolia*). The shrubland is part of the Northern Great Basin Desert Shrub Biome and has been described as a saltbrush-greasewood shrub complex. The development of modeling of biotic processes is detailed in the Biological Modeling white paper.

3.5.1 Local Vegetation

Several plant communities identified include shadscale-gray molly (*Kochia americana* var. *vestita*), shadscale-gray molly-black greasewood (*Sarcobatus vermiculatus*), and black greasewood-gardner saltbrush (*Atriplex nuttallii*). Envirocare (2000) and SWCA (2011) confirmed that the predominant vegetation over most of the site is shadscale. Shrubs are widely spaced, totaling between 1.5% and 20% ground cover, depending upon vegetation association. The shadscale-gray molly community covers most of the South Clive site, with black greasewood becoming prominent only on the eastern quarter of the site. SWCA (2011) found very little transition between the shadscale-gray molly and black greasewood vegetation associations, and that shadscale and gray molly totaled less than 0.5% cover in the geasewood association, suggesting that the shadscale-gray molly-black greasewood community identified by Envirocare (2000) is perhaps better classified as a pure greasewood community. Envirocare reported that the black greasewood-gardner saltbush community only occurs in the far northeast corner of the Clive site. Seepweed (*Suaeda torreyana*), perfoliate pepperweed (*Lepidium perfoliatum*), and halogeton (*Halogeton glomeratus*) are the most common understory plants. Sage (A*rtemisia* spp.) and rabbitbrush (*Chrysothamnus* spp.) which are characteristic of much of the Great Basin shrubland, do not occur on the valley floors around Clive due to their low salt tolerance, but may occur on bajadas and well-drained slopes. No threatened or endangered plant species are known to occur in the near vicinity of the Clive site (NRC, 1993).

3.5.2 Local Wildlife

The Clive site consists of two main habitat types, shadscale flats and greasewood. Comprehensive faunal surveys have not been conducted around the Clive site, but NRC (1993) indicates that species diversity is low. Species typical of these shrubland habitats include black-tailed jackrabbit (*Lepus californicus*), Townsend's ground-squirrel (*Spermophilus townsendii*), Ord's kangaroo rat (*Dipodomys ordii*), deer mouse (*Peromyscus maniculatus*), horned lark (*Eremophila alpestris*), and the desert horned lizard (*Phrynosoma platyrhinos*). Jackrabbits, deer mice, and grasshopper mice (*Onychomys leucogaster*) were the only mammals trapped during surveys conducted for the 1993 Environmental Impact Statement (EIS) (NRC 1993). Additional trapping conducted in October 2010 collected only deer mice at the Clive site, and deer mice, grasshopper mice, Ord's kangaroo rat, and chisel-toothed kangaroo rat in neighboring areas with steeper slopes and greater density of grasses (SWCA 2011). Pronghorn antelope can also be

found near the facility, but the area is considered to be poor habitat (NRC, 1993). The bald eagle and the peregrine falcon are two federally-listed species that could occur in the project area. However, NRC (1993) indicates that the U.S. Fish and Wildlife Service concurs with the conclusion that the project site would not affect either species due to the distance to the nearest nesting site.

A variety of invertebrates is expected to occur at the Clive site. Invertebrates, particularly ants, play a key role in maintenance of desert shrub communities. Harvester ants of the genus *Pogonomyrmex* create large, easily recognizable nests, and play an important role in the development of desert soils and the dispersal of plant seeds. Surveys conducted in 2010 found that the Western harvester ant (*Pogonomyrmex occidentalis*) was by far the dominant ant species at the site, independent of vegetative association (SWCA 2011).

3.6 Engineered Features

3.6.1 Class A South Disposal Cell Design

Depleted uranium waste is proposed for disposal in the Class A South disposal cell. The Class A South Cell, which is part of the Federal Cell, is about 541 × 436 m (1,775 × 1,430 ft), with an area of approximately 24 ha (58 acres), and an estimated total waste volume of about 2.7 million m^3 (96 million ft^3). A drainage ditch surrounds the disposal cell on three sides, with 11e.(2) waste on the fourth side. The cell is constructed on top of a compacted clay liner covered by a protective cover. Waste will be placed above the liner and will be covered with a layered engineered cover constructed of natural materials. The top slopes will be finished at a 4% grade while the side slopes will be no steeper than 5:1 (20% grade).

The design of the Class A South Cell cover has been engineered to prevent the effects of erosion, reduce the effects of infiltration, and to protect workers and the public from radionuclide exposure. The cell cover is a layered composite of a clay radon barrier, filter material, sacrificial soil, and rip rap. The clay radon barrier is designed to minimize infiltration of precipitation and runoff and reduce the migration of radon from the waste cell. The filter material is intended to confine dew and condensates in order to reduce the likelihood of the radon barrier clay from drying out. The purpose of the rip rap cover is to ensure the integrity of the underlying layers and overall waste cell by providing protection from physical weathering sources such as erosion by water and wind. The detailed properties of each cell layer may be found in engineering drawings (Energy*Solutions*, 2009a) and in the white paper on Embankment Modeling.

3.6.2 Degradation of Engineered Features

While the engineered liner and cap are expected to be constructed as designed, and to perform well over the coming decades, they will likely degrade with time. Sheet erosion by wind and water is expected to be minor while the rip rap is intact, and is likely to be counteracted by aeolian deposition of loess (wind-blown sediment) filling the interstices of the gravel, cobbles and boulders. It is possible, however, that the rip rap may be displaced or degraded by processes such as unusual weather events (e.g., tornadoes), animal activity, or human activities after the loss of institutional control. These events may result in damage to the rip rap and cap, though the damage is likely to be localized. This could result in gully erosion, and possibly the exposure of

deeper parts of the cap or the waste itself. Details are provided in the Erosion Modeling white paper.

4 Regulatory Context

Energy*Solutions* is permitted by the State of Utah to receive Class A Low Level and Mixed Low-Level Radioactive Waste (LLW and MLLW) under Utah Administrative Code (UAC) R313-25, *License Requirements for Land Disposal of Radioactive Waste.* The wastes that are received must be classified in accordance with the UAC R313-15-1008, *Classification and Characteristics of Low-Level Radioactive Waste.* The classification requirements in UAC R313-15-1008 reflect those outlined in NRC's 10 CFR 61 Section 55, but include additional references to radium-226 (Ra-226). Further, groundwater protection levels (GWPLs) must be adhered to, as outlined in the site's *Ground Water Quality Discharge Permit* (UWQB, 2010). The regulatory context within the Federal and State regulations is discussed in the following sections.

4.1 Nuclear Regulatory Commission Regulations

Title 10 CFR 61 (Code of Federal Regulations, 2007) is the Federal regulation for the disposal of certain radioactive wastes, including land disposal at privately-operated facilities such as that managed and operated by Energy*Solutions* at Clive, Utah. It contains procedural requirements, performance objectives, and technical requirements for near-surface disposal, including disposal in engineered facilities with protective earthen covers, which may be built fully or partially above-grade. Near-surface disposal is defined as disposal in or within the upper 30 meters of the earth's surface (10 CFR 61.2).

The promulgation of 10 CFR 61 required a Final Environmental Impact Statement (FEIS) which was issued in 1982 (NRC, 1982). The FEIS focused on the waste streams typically disposed by NRC licensees at the time, and did not take into account facilities that generated high concentrations and large quantities of DU, which was not then considered to be waste. As a result, the NRC did not establish a concentration limit for uranium isotopes in the waste classification tables presented in 10 CFR 61.55.

4.1.1 Section 61.55: Waste Classification

Section 61.55 defines three classes of radioactive waste for near surface disposal—Class A, Class B, Class C—and discusses the fourth, commonly called "greater than Class C" (GTCC) waste, which, "in the absence of specific requirements in this part […] must be disposed of in a geologic repository […] unless proposals for disposal of such waste in a disposal site licensed pursuant to this part are approved by the Commission" (§61.55[2][iv]). The Class A, B, and C wastes are defined based on concentrations of specific long-lived radionuclides (defined in Table 1 of §61.55), or, in the absence of long-lived ones, on specific short-lived radionuclides (defined in Table 2 of §61.55). These tables are reproduced in Figure 4 for convenience.

Wastes containing radionuclides listed on both tables are classified using a combination approach as specified in §61.55(5):

> §61.55(5) Classification determined by both long- and short-lived radionuclides. If radioactive waste contains a mixture of radionuclides, some of which are listed in Table 1, and some of which are listed in Table 2, classification shall be determined as follows:

> (i) If the concentration of a nuclide listed in Table 1 does not exceed 0.1 times the value listed in Table 1, the class shall be that determined by the concentration of nuclides listed in Table 2.
> (ii) If the concentration of a nuclide listed in Table 1 exceeds 0.1 times the value listed in Table 1 but does not exceed the value in Table 1, the waste shall be Class C, provided the concentration of nuclides listed in Table 2 does not exceed the value shown in Column 3 of Table 2.

The scope of this PA includes the disposal of DU, which by default falls into the category of Class A waste:

> §61.55(6) Classification of wastes with radionuclides other than those listed in Tables 1 and 2. If radioactive waste does not contain any nuclides listed in either Table 1 or 2, it is Class A.

Nevertheless, DU presents an interesting case, as the uranium it contains is fundamentally different from the Class A wastes that NRC had in mind when it devised the classifications. Uranium does not appear in Table 1 of 10 CFR 61.55 (Figure 4) because, at the time of the development of the regulation, uranium waste did not, and was not expected to, exist in significant quantities. The nature of the radiological hazards associated with DU presents challenges to the estimation of long-term effects from its disposal. As DU evolves toward secular equilibrium with its progeny, a process that will take over 2 million years, it becomes a greater radiological hazard due to the in-growth of its decay products. Recognition of this special behavior of DU has prompted the NRC to revisit the regulation in a rule-making. This is discussed in Section 4.1.5 , below. Until that rule-making is complete, however, 10 CFR 61 stands as the controlling regulation.

TABLE 1

Radionuclide	Concentration curies per cubic meter
C–14	8
C–14 in activated metal	80
Ni–59 in activated metal	220
Nb–94 in activated metal	0.2
Tc–99	3
I–129	0.08
Alpha emitting transuranic nuclides with half-life greater than 5 years	[1] 100
Pu–241	[1] 3,500
Cm–242	[1] 20,000

[1] Units are nanocuries per gram.

TABLE 2

Radionuclide	Concentration, curies per cubic meter		
	Col. 1	Col. 2	Col. 3
Total of all nuclides with less than 5 year half-life	700	([1])	([1])
H–3	40	([1])	([1])
Co–60	700	([1])	([1])
Ni–63	3.5	70	700
Ni–63 in activated metal	35	700	7000
Sr–90	0.04	150	7000
Cs–137	1	44	4600

[1] There are no limits established for these radionuclides in Class B or C wastes. Practical considerations such as the effects of external radiation and internal heat generation on transportation, handling, and disposal will limit the concentrations for these wastes. These wastes shall be Class B unless the concentrations of other nuclides in Table 2 determine the waste to be Class C independent of these nuclides.

Figure 4: Waste classification Tables 1 and 2 from 10 CFR 61.55

4.1.2 Section 61.41: Protection of the Public

The key endpoints of a PA are estimated future potential doses to members of the public (MOP). The performance objectives specified in Subpart C of 10 CFR 61 are in the following section:

> **§ 61.41 Protection of the general population from releases of radioactivity.**
> Concentrations of radioactive material which may be released to the general environment in ground water, surface water, air, soil, plants, or animals must not result in an annual dose exceeding an equivalent of 25 millirems [0.25 mSv] to the whole body, 75 millirems [0.75 mSv] to the thyroid, and 25 millirems [0.25 mSv] to any other organ of any member of the public. Reasonable effort should be made to maintain releases of radioactivity in effluents to the general environment as low as is reasonably achievable.

However, the approach to dose assessment suggested by §61.41 is now dated, and NRC recommends the current International Commission on Radiological Protection 30 (ICRP 1984) methodology in their Performance Assessment Methodology, NUREG-1573 (NRC 2000):

> **3.3.7.1.2 Internal Dosimetry**
> The NRC performance objective set forth in Section 61.41, is based on the ICRP 2 dose 3-79 methodology (ICRP, 1979), but current health physics practices follow the dose methodology used in Part 20, which is currently based on ICRP 30 methodology (ICRP, 1979). The license application will contain many other assessments of potential exposures (e.g., worker exposure, accident exposures, and operational releases) that will need to use ICRP 30 dose methodology. For internal consistency in the application, it is recommended that the performance assessment be consistent with the methodology approved by the NRC in Part 20 for comparison with the performance objective. Therefore, PAWG [the performance assessment working group] believes that calculation of a TEDE [total effective dose equivalent] for the LLW performance assessment—a summation of the annual external dose and the CEDE [committed effective dose equivalent]—is acceptable for comparison with the performance objective.
> As a matter of policy, the Commission considers 0.25 mSv/year (25 mrem/year) TEDE as the appropriate dose limit to compare with the range of potential doses represented by the older limits that had whole-body dose limits of 0.25 mSv/year (25 mrem/year) (NRC, 1999, 64 FR 8644; see Footnote 1). Applicants do not need to consider organ doses individually because the low value of the TEDE should ensure that no organ dose will exceed 0.50 mSv/year (50 mrem/year).

The estimation of dose to a MOP in the PA model therefore uses the ICRP 30 TEDE approach.

There are a number of implicit assumptions in using dose as a performance metric, in that it is being used as a proxy for risk. Risk involves a biological effect. The biological effect of greatest interest at the doses evaluated here is cancer. The risk of cancer to an exposed individual depends upon a large number of assumptions, the most influential being 1) that the major source of data for radiological risk assessment; i.e., the Hiroshima/Nagasaki atomic bomb survivors, is relevant for the doses evaluated, and 2) that risks can be extrapolated from large doses to small doses in a linear fashion, with no threshold of effect (i.e., no dose is without some risk of cancer). Both of these assumptions are controversial, yet provide the basis for most radiation regulation. The implications of these assumptions are discussed in the Dose Assessment white paper.

4.1.3 Section 61.42: ALARA and Collective Dose

A second potential decision rule pertains to populations. There is no clear decision rule as far as collective (cumulative population) doses are concerned. However, the regulations state that "reasonable effort should be made to maintain releases of radioactivity in effluents to the general environment as low as is reasonably achievable" (ALARA). There are, however, other competing objectives, and the resource implications are large to achieving ALARA on a collective level. Additionally, the words "reasonably" and "achievable" are not precise. The two words perhaps imply some degree of consideration of trade-offs, but no clear definition is published. Assuming that there are trade-offs, then this implies that an analysis that explicitly evaluates the trade-offs, and how different disposal options, designs, or sites may differentially satisfy the objectives and resource constraints (e.g., a decision or economic analysis) should be performed. Yet, at present, this has yet to be conducted in the context of the PA process, and there are no current specific regulations. However, the ICRP (1984) provides guidance regarding potential approaches.

4.1.4 Section 61.42: Protection of the Inadvertent Intruder

In addition to protecting any member of the public, 10 CFR 61 requires additional assurance of protecting individuals from the consequences of inadvertent intrusion. An inadvertent intruder is someone who is exposed to waste without meaning to, and without realizing it is there (after loss of institutional control). This is distinct from the intentional intruder, who might be interested in deliberately disturbing the site, or extracting materials from it, or who might be driven by curiosity or scientific interest.

> **§ 61.42 Protection of individuals from inadvertent intrusion.**
> Design, operation, and closure of the land disposal facility must ensure protection of any individual inadvertently intruding into the disposal site and occupying the site or contacting the waste at any time after active institutional controls over the disposal site are removed.

Because the definition of inadvertent intruders encompasses exposure of individuals who engage in normal activities without knowing that they are receiving radiation exposure, there is no practical distinction made here between a member of the public (MOP) and inadvertent intruders with regard to exposure/dose assessment.

4.1.5 Proposed Rule-Making Regarding 10 CFR 61

In 2005, the NRC proposed to consider whether or not the quantities of DU from uranium enrichment facilities warrant an amendment of the waste classification tables currently defined in 10 CFR 61 (NRC, 2005). In 2008, NRC staff responded to the October 2005 order which evaluated a generic case to determine if Part 61 standards could be met for near-surface disposal of DU (NRC, 2008). The results of this evaluation indicated that it may be possible, given certain conditions, to meet the standards for near-surface disposal of DU. Furthermore the NRC staff prepared several regulatory options. NRC staff also recommended that no classification change be made for DU, retaining its status as Class A waste, but that additional language be included requiring a site-specific PA prior to the acceptance of DU for disposal. In March 2009, the NRC agreed with the course of action recommended by the NRC staff in SECY-08-0147 and decided to keep DU classified as a Class A waste (NRC, 2009a). They also decided to initiate rule-making that would propose enhanced PA requirements for those facilities that plan to dispose of large quantities of DU (NRC, 2009b).

Most of the proposed changes to 10 CFR 61 involve the concept that no matter what classification DU is given, any disposal of the material should involve an analysis that will inform decision makers about the doses associated with such a disposal to individuals who might be exposed at some time after site closure. This position is substantially in concordance with that put forth by the National Research Council (2005), and with the approach that will be used in this PA.

4.2 State of Utah Regulations

Utah is an NRC agreement state, meaning that it is granted authority to enforce NRC regulation, or regulations of its own drafting that are substantially compatible with the NRC regulation, 10 CFR 61. The State of Utah has done so, in two Rules of the Utah Administrative Code (UAC): UAC Rule R313-25 *License Requirements for Land Disposal of Radioactive Waste*, and Rule R313-15 *Standards for Protection Against Radiation* (Utah, 2010). Each of these is discussed below.

4.2.1 Section R313-25: Licensing Requirements

Section R313-25-8 *Technical Analyses*. Parts (1)(a) and (b) of this Section are patterned closely after 10 CFR 61.41 and 42:

> (1) The specific technical information shall also include the following analyses needed to demonstrate that the performance objectives of R313-25 will be met:
> (a) Analyses demonstrating that the general population will be protected from releases of radioactivity shall consider the pathways of air, soil, ground water, surface water, plant uptake, and exhumation by burrowing animals. The analyses shall clearly identify and differentiate between the roles performed by the natural disposal site characteristics and design features in isolating and segregating the wastes. The analyses shall clearly demonstrate a reasonable assurance that the exposures to humans from the release of radioactivity will not exceed the limits set forth in R313-25-19.
> (b) Analyses of the protection of inadvertent intruders shall demonstrate a reasonable assurance that the waste classification and segregation requirements will be met and that adequate barriers to inadvertent intrusion will be provided.

In addition, a new section for R313-25-8 has recently been adopted, and is reproduced here:

> (2)(a) Any facility that proposes to land dispose of significant quantities of depleted uranium, more than one metric ton in total accumulation, after June 1, 2010, shall submit for the Executive Secretary's review and approval a performance assessment that demonstrates that the performance standards specified in 10 CFR Part 61 and corresponding provisions of Utah rules will be met for the total quantities of depleted uranium and other wastes, including wastes already disposed of and the quantities of concentrated depleted uranium the facility now proposes to dispose. Any such performance assessment shall be revised as needed to reflect ongoing guidance and rulemaking from NRC. For purposes of this performance assessment, the compliance period will be a minimum of 10,000 years. Additional simulations will be performed for an analysis for the period where peak dose occurs and the results shall be analyzed qualitatively.

4.2.2 Section R313-15-1008: Waste Classification

Rule R313-15 contains section R313-15-1008 *Classification and Characteristics of Low-Level Radioactive Waste*. The definitions in this section are essentially identical to those in 10 CFR 61.55, with one exception: Utah adds Ra-226 to the list of long-lived radionuclides in the regulations' Table I (see Figure 5), with a concentration limit of 100 nCi/g (Utah, 2010). Since Ra-226 is a decay product of uranium-238 (U-238), the principal component of DU, it is of direct interest to the disposal of DU waste.

The Energy*Solutions* Clive facility is licensed by the State of Utah for disposal of Class A waste, and has disposed of DU waste under that license. The wastes under consideration for disposal in the present PA, however, contain more than simply isotopes of uranium, potentially including some radionuclides listed in the tables shown in Figure 7 in addition to the Ra-226 added by Utah (Figure 5). In particular, the DU from certain sources contains some amount of technetium-99 (Tc-99). Therefore, for now at least, the determination of classification is driven not by the presence of uranium, but by the presence of radionuclides in the tables, as discussed in the quotation from §61.55(5) above.

TABLE I

Radionuclide	Concentration curie/cubic meter(1)	Concentration nanocurie/gram(2)
C-14	8	
C-14 in activated metal	80	
Ni-59 in activated metal	220	
Nb-94 in activated metal	0.2	
Tc-99	3	
I-129	0.08	
Alpha emitting transuranic radionuclides with half-life greater than five years		100
Pu-241		3,500
Cm-242		20,000
Ra-226		100

NOTE: (1) To convert the Ci/m^3 values to gigabecquerel (GBq)/cubic meter, multiply the Ci/m^3 value by 37.
(2) To convert the nCi/g values to becquerel (Bq)/gram, multiply the nCi/g value by 37.

Figure 5. Waste classification Table I from R313-15-1008

4.2.3 Groundwater Protection Limits

In addition to these radiological criteria, the State of Utah imposes limits on groundwater contamination, as stated in the Ground Water Quality Discharge Permit (UWQB, 2010). Part I.C.1 of the Permit specifies that GWPLs in Table 1A of the Permit shall be used for the Class A

LLW Cell. Table 1A in the Permit specifies general mass and radioactivity concentrations for several constituents of interest to DU waste disposal. These GWPLs are derived from Ground Water Quality Standards listed in UAC R317-6-2 *Ground Water Quality Standards*. Exceptions to values in that table are provided for specific constituents in specific wells, tabulated in Table 1B of the Permit. This includes values for mass concentration of total uranium, radium, and gross alpha and beta radioactivity concentrations for specific wells where background values were found to be in exceedence of the Table 1A limits. Note that according to the Permit, groundwater at Clive is classified as Class IV, saline ground water, according to UAC R317-6-3 *Ground Water Classes,* and is highly unlikely to serve as a future water source. As noted in Section 3.4.2.2 , the underlying groundwater in the vicinity of the Clive site is of naturally poor quality because of its high salinity and, as a consequence, is not suitable for most human uses, and is not potable for humans.

The DU waste PA will calculate estimates of groundwater concentrations at a virtual well near the Class A South Cell for comparison with these GWPLs.

5 Summary of Features, Events, and Processes (FEPs)

A requirement for the PA scenario development process is the preliminary identification of possible future states of the disposal system as it is subjected to external changes and factors (e.g., climate, weathering, demographic changes) over time. The identification of features, events, and processes (FEPs) is a key activity in developing scenarios for the Clive facility PA model. The identification, compilation, and screening of FEPs form the basis for scenarios and quantitative analyses used to evaluate site performance.

The list of FEPs pertaining to the efficacy of disposal and storage of DU waste at the Clive Facility was compiled from several PA-related FEPs documents published for other radiological waste disposal facilities (e.g., NEA, 1992; NEA, 2000; Guzowski, 1990; Guzowski and Newman, 1993). In addition to existing PA literature sources for FEPs, site-specific understanding of the environmental and engineered attributes of the Clive facility, geographical region, and population were also addressed in the compilation of FEPs for this assessment.

All FEPs identified in the literature and developed internally were compiled into an exhaustive initial list. This list was iteratively reviewed to reduce duplication among sources and to more broadly (or more precisely) group related FEPs for incorporation in the CSM. For each group of related FEPs, the rationale for its inclusion in or dismissal from the model was documented.

This section of the CSM identifies the FEPs and conditions pertaining to the conceptual model that are retained for use in developing the PA model. Details related to the identification and screening processes are discussed in the accompanying document *FEP Analysis for Disposal of Depleted Uranium at the Clive Facility*. Features, events, and processes were grouped into several categories based on groupings listed in the original source documents, and include some overlap and redundancy. Nevertheless, the groupings are not significant with respect to the CSM. What is important is that the FEPs are considered in the appropriate parts of the model. Only those FEPs retained for further consideration are discussed here. Once identified, these FEPs are qualitatively evaluated for inclusion in the CSM based on considerations of their likelihood and consequence.

Meteorology

Frost weathering and other meteorological events (e.g., precipitation, atmospheric dispersion, resuspension) are included in the CSM. Weathering may occur from frost cycles. Resuspension of particulates from surface soils allows them to be redistributed by atmospheric dispersion, which is a meteorological phenomenon. Dust devils are also possible at the site and a tornado occurred in Salt Lake City in 1999, which was the first tornado in Utah in over 100 years.

Climate change

Features, events, and processes of climate change considered in the conceptual model include effects on hydrology (including lake effects), hydrogeology, biota, and human behaviors. Lake effects include appearance/disappearance of large lakes and associated phenomena (sedimentation, wave action, erosion/inundation). Wave action, including seiches, is included in the CSM.

Hydrology

Several hydrogeological FEPs were identified for consideration in the conceptual model. Groundwater transport, in both the unsaturated and saturated zones, is potentially a significant transport pathway. For some model endpoints, such as groundwater concentrations that are compared to groundwater protection levels (GWPLs), it is the only pathway of concern.

Groundwater flow and transport processes include advection-dispersion, diffusion, changes in the flow system, recharge, and brine interactions. Inundation of the site may occur due to changes in lakes or reservoirs, which is included in lake effects of climate change.

Geochemical

Geochemical effects include chemical sorption and partitioning between phases, aqueous solubility, precipitation, chemical stability, complexation, changes in water chemistry (redox potential, pH, Eh), speciation, and leaching of radionuclides from the waste form. These processes are addressed in the model.

Other Natural Processes

The broad category of other natural processes considered for the conceptual model include ecological changes and pedogenesis (soil formation). Ecological changes are associated with catastrophic events (e.g., inundation), evolution, or climate change. Pedogenesis is expected on the cap, giving rise to vegetation growth or habitation by wildlife.

Denudation (cap erosion) may be sufficient to expose waste. Erosion of the repository resulting from pluvial, fluvial or aeolian processes can result from extreme precipitation, changes in surface water channels, and weathering. Sediment transport is an inherent aspect of erosion. Sedimentation/deposition onto the cell may also affect cell performance.

Note that seismic activity is unlikely to impact the Clive facility. Faults are not present within the vicinity of Clive, although effects of isostatic rebound are still possible in the Lake Bonneville area.

Engineered Features

Engineered features are intended to promote containment and inhibit migration of contaminants. Conditions potentially affecting site performance include failure of engineered features, cell design, material properties, and subsidence of the cell.

Containerization

Two key components of containerization were identified as FEPs: containment degradation and corrosion. Canister degradation, including fractures, fissures, and corrosion (pitting, rusting) could result in containment failure. These processes are evaluated in the conceptual model.

Waste

Attributes of waste that could influence the performance of the Clive facility include the inventory of radionuclides, physical and chemical waste forms, container performance, matrix performance, leaching, radon emanation, and other waste release mechanisms.

Source Release

Source release can result from many mechanisms, including containment failure, leaching, radon emanation, plant uptake, and translocation by burrowing animals. FEPs that fit in the category of source release include gas generation, radioactive decay and in-growth, and radon emanation.

Contaminant Migration

Contaminant migration for the CSM includes the mechanisms and processes by which radionuclides may come to be located outside of the containment unit. The following contaminant migration processes were identified for consideration in the CSM: resuspension, atmospheric dispersion, biotically-induced transport, contaminant transport, diffusion, dilution, advection-dispersion, dissolution, dust devils, tornadoes, infiltration, and preferential pathways.

Human exposure pathways could include animal ingestion, both as ingestion of fodder and feed by livestock, and ingestion of livestock by humans. Transport by atmospheric dispersion could be associated with limited resuspension, dust devils, and tornadoes. Modeling of biotic (plant- and animal-mediated) processes leading to contaminant transport, and the evolution of these processes in response to climate change and other influences, including bioturbation, burrowing, root development, and contaminant uptake and translocation are considered.

Contaminant transport includes transport media (water, air, soil), transport processes (advection-dispersion, diffusion, plant uptake, soil translocation), and partitioning between phases. Diffusion occurs in gas and water phases. Dilution occurs when mixing with less concentrated water. Hydrodynamic dispersion is associated with water advection. Dissolution in water is limited by aqueous solubility. Transport in the gas phase includes gas generation in the waste, partitioning between air and water phases, diffusion in air and water, and radioactive decay and ingrowth. Infiltration of water through the cap, into wastes, and potentially to the groundwater is another contaminant migration concern. Preferential pathways for contaminant transport are also addressed.

Human Processes

The FEPs identified as human processes encompass human behaviors and activities, resource use, and unintentional intrusion into the repository. Human process FEPs identified for assessment are related to the human exposure model and include anthropogenic climate change, human behavior, human-induced processes related to engineered features at the site, human-induced transport, inadvertent human intrusion, institutional control, land use, post-closure subsurface activities, waste recovery, water resource management, and military activities.

Exposure

Exposure is an integral part of the conceptual model, and may result from reduced site performance. Exposure-relevant FEPs identified for evaluation include those related to dosimetry, exposure media, human exposure, ingestion pathways, and inhalation pathways. Dosimetry as a science is not a FEP *per se* but physiological dose response is accounted for in the PA model.

Transport pathways (e.g. food chains) that lead to foodstuff contamination, and human exposures due to inhalation of gaseous radionuclides and particulates are included. Exposure media include soil/dust and food. Exposure pathways (ingestion, inhalation, etc.) and physiological effects from radionuclides and toxic contaminants (e.g. uranium) are also assessed.

6 Waste Forms

The scope of this CSM is limited to the disposal of DU wastes of two general waste types: 1) depleted uranium trioxide (DUO_3) waste from the Savannah River Site (SRS) 2)anticipated DU waste as U_3O_8 from gaseous diffusion plants (GDPs) at Portsmouth, Ohio and Paducah, Kentucky. The quantity and characteristics of DU waste from other sources that has that already been disposed of at the Clive Facility was not included.

The quantity and characteristics of DU waste will constitute source terms in the PA model. This section provides background on the uranium cycle and origins and nature of DU waste in particular.

Depleted uranium consists of three isotopes of uranium (U-238, U-235, and U-234) and progeny from radioactive decay. The wastes proposed for disposal contain these isotopes of uranium, but some also include other "contaminants" in varying amounts (ORNL 2000, Energy*Solutions*, 2009b). These associated radionuclides are the result of introduction of used nuclear fuel (UNF) into the uranium enrichment process. In order to clarify that these wastes contain more than just DU (uranium isotopes), they are termed "DU waste." When this term is used, it refers to wastes, such as those from SRS, that contain DU and a small amount of contamination from actinides and fission products. If uranium hexafluoride derived from irradiated reactor returns is introduced to the cascade, the associated fission products and actinides migrate to the depleted end of the cascade, with the U-238.

6.1 Depleted Uranium Background

The uranium fuel cycle begins by extracting and milling natural uranium ore to produce "yellow cake," a mixture of various uranium oxides. Low-grade natural ores contain about 0.05 to 0.3%

by weight of uranium oxide while high-grade natural ores can contain up to 70% by weight of uranium oxide (NRC, 2010). Naturally occurring uranium contains the isotopes U-238, U-235, and U-234, and radioactive decay products in secular equilibrium with these primordial parents. Each uranium isotope has the same chemical properties, but differs in terms of radiological properties. Naturally occurring uranium has a typical isotopic composition of about 99.283% U-238, 0.711% U-235, and 0.006% U-234 by mass, although there are varying assays and estimates.

In order to produce fuel for nuclear reactors and weapons, uranium has to be enriched in the fissionable U-235 isotope. Uranium enrichment began in support of the Manhattan Project during World War II. Enrichment for civilian and military uses continued after the war under the U.S. Atomic Energy Commission, and its successor agencies, including the DOE.

Three large GDPs were constructed in order to produce enriched uranium. The first of these diffusion cascades was built in Oak Ridge, Tennessee, at what was originally called K-Site (later called the K-25 Site, after its largest GDP cascade), and is now known as the East Tennessee Technology Park (ETTP). Two others of similar design were constructed in Paducah, Kentucky, and Portsmouth, Ohio (DOE 2004a and 2004b). The ETTP halted operations in 1985, the Portsmouth plant ceased in 2001, and the Paducah GDP continues to operate. The two more recent GDPs are host to a large inventory of depleted uranium hexafluoride (DUF_6), since the ETTP material was moved to Portsmouth.

The official definition of DU given by the NRC is uranium in which the percentage fraction by weight of uranium-235 is less than 0.711%. (its natural abundance) According to the International Atomic Energy Agency (IAEA), typical DU percentage concentration by weight of the uranium isotopes used for military purposes is 99.8% U-238, 0.2% U-235, and 0.001% U-234. Depleted uranium isotopic ratio values from gaseous diffusion plants, which processed material for both military and commercial purposes, are reported to be 99.75% U-238, 0.25% U-235, and 0.0005% U-234 (Rich et al. 1988). Because processing of uranium has only been practiced for roughly 60 years, there has not been sufficient time for noticeable in-growth of the daughter radionuclides in this by-product. Depleted refined uranium is therefore considerably less radioactive than natural uranium because it has less U-234, U-235, and progeny, per unit mass.

6.2 Savannah River Site Uranium Trioxide

The SRS produced DU as a byproduct of the nuclear material production programs, where irradiated nuclear fuels were reprocessed to separate out the fissionable plutonium-239 (Pu-239) (Fussell and McWhorter, 2002). Uranium billets were produced at the DOE Fernald, Ohio site, fabricated into targets at SRS, then irradiated in one of the SRS production reactors to produce Pu-239. The irradiated targets were processed in F-Canyon, where in acid solution, the fission products were separated from the plutonium and uranium, which were then separated from each other. After additional purification, the DU-bearing waste stream was transferred to the FA-Line Facility where it was processed into uranium trioxide which is now a focus of this PA. This DUO_3 contains small quantities of waste fission products and transuranic elements (Energy*Solutions*, 2009b), which will also be included in the PA model.

The DU waste was produced at the SRS from the 1950s to the late 1980s as a by-product in the manufacture of nuclear materials, as described above. The DUO_3 was produced from DUF_6 using a classic chemical separation process to separate and recover plutonium and uranium product. The DU was purified through multiple processing steps, and then transferred to a final production plant for conversion to uranium trioxide. Some of this material was sent off-site for commercial or military use, and the rest was stored on site, and is now slated for disposal.

The chemical separation process was performed in two separate processing cycles. The more highly radioactive processing, such as dissolution of irradiated target material from the SRS reactors, and removal of the vast majority of the highly radioactive fission products and actinides, was performed in the first processing cycle. The final purification of the uranium product stream to remove the remaining fission product and actinide "contaminants" was performed in a second processing cycle. A small fraction of these contaminants was carried forward with the uranium product. This process ceased operations in the late 1980s.

The SRS produced approximately 36,000 200-L (55-gal) steel drums of DUO_3 during the production campaigns (Fussell and McWhorter, 2002). This DUO_3, a solid powder at room temperature and pressure, is considered to be relatively homogeneous, based on known process controls and operations. The drums have an average mass of 680 kg (weight of 1,500 lb) apiece (Fussell and McWhorter, 2002). The condition of the drums varies from good to poor with a high percentage of the drums having some degree of outer surface corrosion. A significant number of drums in two facilities (221-21F and 221-22F) have been placed into overpacks as a mitigating action for corrosion control and to prevent spills. The estimated mass of DU from SRS proposed for disposal at Clive is 24,500 Mg (megagrams, or metric tons), assuming disposal of all 36,000 drums.

This material was characterized by SRS for uranium isotopes, fission products, and transuranics, as well as some metals and organic compounds (pesticides, herbicides, semi-volatile and volatile organic compounds) as recorded in the Waste Profile Record (Energy*Solutions*, 2009b). No organic compounds were detected, though low levels (0 to 2 mg/kg) of lead, arsenic, cadmium, chromium, selenium, silver, zinc and copper were found. These low levels of metal make up less than 5 parts per million (ppm) mass of the DU waste. Based on the physical properties description in the Waste Profile Record, the DU is stoichiometrically 83.22% uranium (100% UO_3) with over 99% U-238. Beals et al., (2002) provide additional information on trace radionuclides in the SRS DU waste.

6.3 Depleted Uranium Oxide from the Gaseous Diffusion Plants

Three large GDPs were constructed to produce enriched uranium. The first diffusion cascades were built in Oak Ridge, Tennessee, at what was the K-25 Site, but is now known as the East Tennessee Technology Park (ETTP). Two others of similar design were constructed in Paducah, Kentucky (PGDP), and Portsmouth, Ohio (PORTS) (DOE 2004a and 2004b). The cascades at the K-25 Site ceased operations in 1985, the Portsmouth plant ceased in 2001, the Paducah GDP continues to operate. The two more recent GDPs are host to a large inventory of stored DUF_6, including the ETTP material that was moved to Portsmouth.

The DOE is currently managing approximately 60,000 cylinders at both PGDP and PORTS (DOE 2004a, 2004b). For many years, interest has been expressed in converting the DUF_6 in these cylinders to an oxide form to support their long-term disposal. In May, 1995 an independent DOE oversight board recommended a study to determine a suitable chemical form for long-term storage of DU. Two Environmental Impact Statements (EIS) were prepared as part of the plan, one for Paducah, DOE/EIS-0359, (DOE 2004a) and one for Portsmouth, EIS-0360, DOE 2004b). These EISs describe the background and alternatives for DUF_6 conversion. With the completions of the EISs, "deconversion" plants were built at both the PORTS and PGDP locations. In 2002, DOE awarded a contract to Uranium Disposition Service, LLC (UDS) to design, construct, and operate two DUF_6 deconversion facilities at these locations. As of this writing, both plants have been built by UDS and have begun test processing DUF_6 into oxide form.

Of the DUF_6 cylinders that will be reused for disposal of the DU oxide, a fraction are contaminated with fission and activation products from introduction of reactor returns into the diffusion cascades. The contamination is similar in nature to that found in the SRS DU, and is modeled as such until more information is gained from the generation of DU oxide at Portsmouth and Paducah. Since the contaminated cylinders are a low priority for conversion, this information is unlikely to be available for several years.

6.4 Depleted Uranium Already Disposed at the Clive Facility

The DU PA Model does not account for DU that is already disposed at the Clive site, some of which is from the same SRS DU population (Fussell and McWhorter, 2002).

6.5 Modeled Radionuclides

A full list of radionuclides has been established for the CSM and the contaminant transport modeling effort:

fission products:
Sr-90, Tc-99, I-129, Cs-137

progeny of uranium and transuranics:
Pb-210, Rn-222, Ra-226, -228, Ac-227, Th-228, -229, -230, -232, Pa-231

uranium isotopes:
U-232, -233, -234, -235, -236, -238

transuranic radionuclides:
Np-237, Pu-239, -239, -240, -241, -242, Am-241

This radionuclide species list is based upon process knowledge, radionuclides analyzed for (though not necessarily detected) in the DU waste material, and decay products with half-lives over five years. A diagram showing each decay species is shown in the Radionuclide Transport section (Section 9). The decay chains are informative as they provide an understanding of how each species derived from a parent radionuclide. Many more short-lived progeny are accounted for in dose assessment calculations. Note that in several instances where the inventory has been

set to zero, these species may be daughters of a known parent with inventory of a potential future inventory species.

6.6 Chemical Characteristics of DU Wastes

Both forms of uranium oxide have some limited solubility in water, thus hydrologic transport is expected to occur to some extent. The solubilities of the two waste forms are dependent upon the geochemistry and their own inherent solubility. Other specific waste forms will be modeled as information becomes available if needed. This transport will start with release from the containment (e.g., drums, cylinders), followed by leaching of the radionuclides from the DU waste which is primarily a function of solubility. The solubility of the radionuclide species, including uranium, will depend upon two main geochemical processes: dissolution/precipitation and adsorption/desorption. These processes are largely controlled by the redox condition, pH, carbonate chemistry, and ionic strength of the local environments. The parameters used to model the transport of the uranium oxides and associated radionuclides are described in Section 9 . Retarded transport will be modeled using a solid/water partition (or distribution) coefficient (K_d) for each radionuclide species. The values (represented as statistical distributions) used for each radionuclide will depend upon the expected geochemical conditions within the various wastes and natural media.

The release of radon-222 (Rn-222) from its Ra-226 parent in the U-238/U-234 decay chain is also described in Section 9 . The transport of radon in both the saturated and unsaturated zones will be included in the PA model. Radon transport is controlled by the emanation factor, diffusion, advection, and partitioning parameters that will be incorporated into the transport modeling.

7 Modeling of the Natural Environment

The natural environment consists of those materials that surround the engineered facility, and make up its environs. This includes the lacustrine sediments of the Great Salt Lake Desert underlying the site, the groundwater within those sediments, the air above, and the biota living on and near the ground surface. Each of these environments is introduced below, along with their conceptual models for the PA.

7.1 Current Conditions

The basic conceptual model of the present day site is that the facility is located on a desert flat, with a biotic community established on the ground surface, and with unsaturated and saturated zones of groundwater below. This scenario is assumed to apply for the 10,000-yr duration of the quantitative model for this base case.

In general, natural processes in the environs will tend to make the site and its engineered features more like the natural environment. Wind and water will modify the cap, and biota will populate it. Throughout this evolving and mixing system, radionuclides that have been disposed within the facility will tend to migrate out to the natural system. A fundamental function of the PA is to estimate the rate and extent of that migration.

7.1.1 Groundwater Flow and Transport

Groundwater is considered in two parts: unsaturated zone (UZ) and the saturated zone (SZ). The UZ, often called the vadose zone, extends from the ground surface down to the water table, and is characterized by having both water and air in the porous spaces in the sediment. The SZ lies below the water table, and extends deep into the earth's crust. For the purposes of modeling, however, contaminants are assumed to penetrate only so far into the saturated sediments, which include natural horizontal barriers confining the vertical flow, as discussed in Section 3.3.1 .

7.1.1.1 The Unsaturated Zone

The engineered features of the landfill, including cap, waste, and liner, are all in the UZ, at least within the 10,000-yr duration of the quantitative model. The part of the UZ that extends from the bottom of the landfill liner to the water table consists of naturally-occurring lake sediments from the ancestral Lake Bonneville. Since the cap is intentionally designed to restrict permeability, interstitial water in the UZ below the facility is not expected to migrate upwards through the cap to surface soils, as it might do naturally given the strong evaporation potential at the surface. Rather, it is expected to migrate slowly down to the water table, at a rate equal to the rate at which the engineered liner leaks.

The natural UZ below the facility will be modeled as a column of discrete elements, called Cell Pathway elements in the GoldSim modeling framework. Each of these is connected in series to model the one-dimensional advective flow path to the water table. Diffusion in the water phase may also play a role in the transport of waterborne contaminants in the UZ, since the advective flux is expected to be small. The concentration gradients in the UZ are also expected to be predominantly vertical, so diffusion will also occur in the vertical direction, oriented with the column of cells.

Diffusion in the air phase within the UZ below the facility will not be modeled, since the only diffusive species would be radon, which is of greater concern at the ground surface. Upward radon diffusion to the ground surface will be dominated by radon parents in the waste zone, and is modeled within the engineered cap.

7.1.1.2 The Saturated Zone

Contaminant transport in the water phase in the SZ is fed by contaminants entering the water table beneath the disposal facility as recharge. The rate of recharge is the same as the Darcy flux (the rate of volume flow of water per unit area) through the overlying UZ, and is expected to be small enough that vertical transport within the SZ would be small. Most SZ waterborne contaminant transport will be in the horizontal direction, following the local pressure gradients which are reflected in water table elevations in an unconfined aquifer such as this. A point of compliance in the groundwater has been established to be 27 m (90 ft) from the toe of the waste embankment, so transport will be modeled to that point.

Saturated zone groundwater transport generally involves the processes of advection-dispersion and diffusion. Mean pore water velocity in the saturated zone is assumed to be determined by the Darcy flux and the porosity of the sediment. A range of values will allow the sensitivity analysis (SA) to determine if this is a sensitive parameter in the determination of concentrations at the

compliance well and resultant potential doses. Modeling of fate and transport for the saturated zone pathway will include advection, linear sorption, mechanical dispersion, and molecular diffusion.

The modeling of the SZ is similar to the modeling of the UZ, except that the "column" of GoldSim Cell Pathway elements is arranged horizontally. This will be modeled as a row of cells between the region below the disposal unit and the compliance well. These cells are saturated with water that flows along the row, in order to represent the aquifer.

7.1.2 Surface Water

The Clive facility is sited in an area of extremely low topographic relief, and surface water features such as stream channels are rare. The ancestral lake bed is quite flat, so there is little in the way of land surface gradients which might drive surface water flow. Most if not all meteoric water that lands on the ground is assumed to be returned to the atmosphere by evapotranspiration, and essentially none is abstracted by runoff.

The embankment cells on the waste disposal site have significant relief, and surface water runoff should be expected from these structures. The runoff and associated sediment transport will be local, and is likely to remain in the vicinity of the site. The principal effect of surface water flow is expected to be contribution to the formation of gullies, as discussed in Section 8.3 .

7.1.3 Air and Atmosphere

Contaminant transport in the air phase takes on two distinct forms: diffusion in the interstitial air in porous media below ground, and dispersion by the atmosphere above. Diffusion in interstitial air of porous media is a means by which contaminants reach the atmosphere at the ground surface. Dispersion of contaminants in the atmosphere can occur through direct diffusion of gaseous contaminants into ambient air, and through resuspension and movement of wind borne contaminated soil particles.

Airborne transport is a secondary contaminant transport mechanism at the Clive Facility. As containment features such as the cap become contaminated from the result of natural processes (e.g. radon diffusion, burrow excavation, plant senescence), radionuclides will migrate to surface soils, serving as a source for atmospheric transport. As these contaminants accumulate on the ground surface, either in a gaseous form (e.g. radon) or attached to solid particles, they undergo resuspension or volatilization into the atmosphere, leading to airborne transport. Airborne contaminants will be carried into ambient air by the wind and either inhaled directly by receptor populations or deposited onto exposure media such as vegetation or soils in the vicinity.

7.1.3.1 Diffusion Through Air in Porous Media

Contaminants released from the waste (or generated by decay of parents in any location) may be transported via the air pathway by migration of gaseous species through soil pore space. Over time, cracks, fissures, animal burrows, and plant roots can also provide preferential diffusion pathways that reduce the effectiveness of the engineered barrier.

Factors that influence the diffusion of contaminants through porous media include the volatility of the chemical species, its molecular weight, physical properties of the soil matrix (e.g.,

porosity, grain size distribution, and moisture content, which determine phasic tortuosity – that is, tortuosity in either the air or water phase), and temperature gradients. Diffusion in porous media and along preferential pathways is also driven by concentration gradients and mediated by effective diffusion coefficients through the tortuous diffusion path.

Diffusion rates are determined from the defined values for effective diffusivities, diffusive areas, diffusive lengths, and the calculated concentration gradients between adjacent cells, which varies as time progresses. Diffusion can take place in both air and water. In coordination with diffusion is radioactive decay and ingrowth, advection of water, partitioning of contaminants between water and air and between water and soils, and biotic processes. All these differential equations and transfer functions are solved at each time step by the PA model.

An important consideration related to the disposal of DU is the production of radon. Since Rn-222 is a descendent of U-238 and U-234, through Th-230 and Ra-226, it will be generated wherever Ra-226 occurs. As the radium, or any parent in the chain, migrates into the cap, either by diffusion in the water phase or translocation by biotic processes (see Section 7.1.4), it provides a source for Rn-222 in more locations beyond the disposed waste. Furthermore, not all of the radon that is produced enters the environment for transport. Some of it is retained within the solid material that held its parent, and decays to polonium-218 (Po-218) without moving. This phenomenon is called radon emanation, and is discussed in the radionuclide transport section (Section 9).

Radon that does enter the environment readily partitions between air and water, with a strong preference for the latter. Soil moisture therefore retards the migration of radon as it partitions into the soil, making it less available to diffusion in air under wetter soil conditions.

7.1.3.2 Atmospheric Dispersion

Atmospheric dispersion of airborne gaseous and particulate contaminants found in surface soils is expected. To the extent that contaminated subsurface soils are exposed or exhumed and plant litter is deposited on the surface, they become surface soils and as such will also be subject to atmospheric dispersion.

Atmospheric dispersion of contaminants is regulated by several factors. Contaminant chemistry, contaminant mobility, soil texture, effects of vegetation on the atmospheric boundary layer, topography, and meteorological conditions (predominant wind direction and speed, precipitation, temperature, and humidity) may influence dispersion of airborne contaminants as well as soil erosion and contaminant resuspension rates.

The Clive facility is sited in an exposed area, with little around it to protect from the winds. Wind dispersion is a likely mechanism of airborne transport. Contaminants deposited over or adsorbed onto soil may migrate from this area source as airborne particulates. Depending on the particle-size distribution and associated settling rates, these particulates may be deposited downwind or remain suspended, resulting in contamination of surface soils and/or exposure of regional receptors through inhalation, immersion, or external irradiation pathways.

Ancestral lake sediments prevalent at the Clive facility are fine-grained, and are susceptible to resuspension and entrainment in the wind, and to subsequent atmospheric dispersion. This

resuspension of naturally-occurring sediments, however, is moderated by local plant growth, which tends to create a boundary layer of lower-velocity air at the ground surface, and by the formation of desert crust, making the cemented particles of sediment in effect much larger.

The embankment cells on the site have significant relief in relation to the surrounding environment. A cover of gravel- and boulder-sized rip rap on the embankment cells would curtail atmospheric re-suspension relative to flat and more uniform areas. Eventually, however the rip rap may trap enough wind-driven (aeolian) sediment that the disposal site will approach the surrounding natural lake bed in appearance and behavior. Although these aeolian deposits will consist of uncontaminated material at first, they may become contaminated by the process of radon diffusion upward from the waste (with radon progeny left behind in the soils) and through the biotic processes discussed in the following section. Once radon gas and resuspended particles have entered the atmosphere directly above the cells, they can be dispersed over a wide area by the wind. Given these possible transport pathways, atmospheric dispersion of gases (e.g. radon and other volatile constituents) and of fine particles of sediment must be taken into consideration in the model.

Entrainment of contaminants into the atmosphere will contribute to the air inhalation exposure pathways for receptors that are present on the site itself. As particulates eroding from the embankment are deposited on surrounding land, this surrounding area may become a secondary source of radionuclide exposure. Atmospheric dispersion calculations in the PA model will support estimation of of gas and particulate air concentrations above the embankment, and off-site particulate deposition rates that can be used to estimate radionuclide soil concentrations in the area surrounding the embankment.

7.1.4 Biota

Biota of primary importance for movement of buried waste and subsurface soils are burrowing animals (both vertebrates and invertebrates, which provide constant mixing of the soil column) and plants, which can move buried wastes through root-uptake and translocation of contaminants to various parts of the plant.

7.1.4.1 Native Plants

Plants represent an important potential pathway for waste transport by way of rooting and conditioning of soil aggregates and particulates, nutrient exchange with soil surfaces, transport of nutrients from soil through plant tissues, deposition of organic materials and non-nutritive waste products at or near the soil surface, and physical mixing of soils through the addition of organic materials to soil due to root collapse and surface deposition. In particular, nutrient exchanges between the subsurface and surface also create the potential for the exchange of non-nutritive chemicals, such as with anthropogenic wastes.

Plant-induced transport of contaminants is assumed to occur primarily through absorption of contaminants into the roots, after which the contaminants are redistributed throughout all the tissues of the plant, both above-ground and below-ground. Upon senescence, the above-ground plant parts are incorporated into surface soils, and the roots are incorporated into soils at their respective depths. This process is illustrated in Figure 6, which shows the conceptual model for plant uptake, redistribution, and senescence. Note that relatively clean surface soils become more

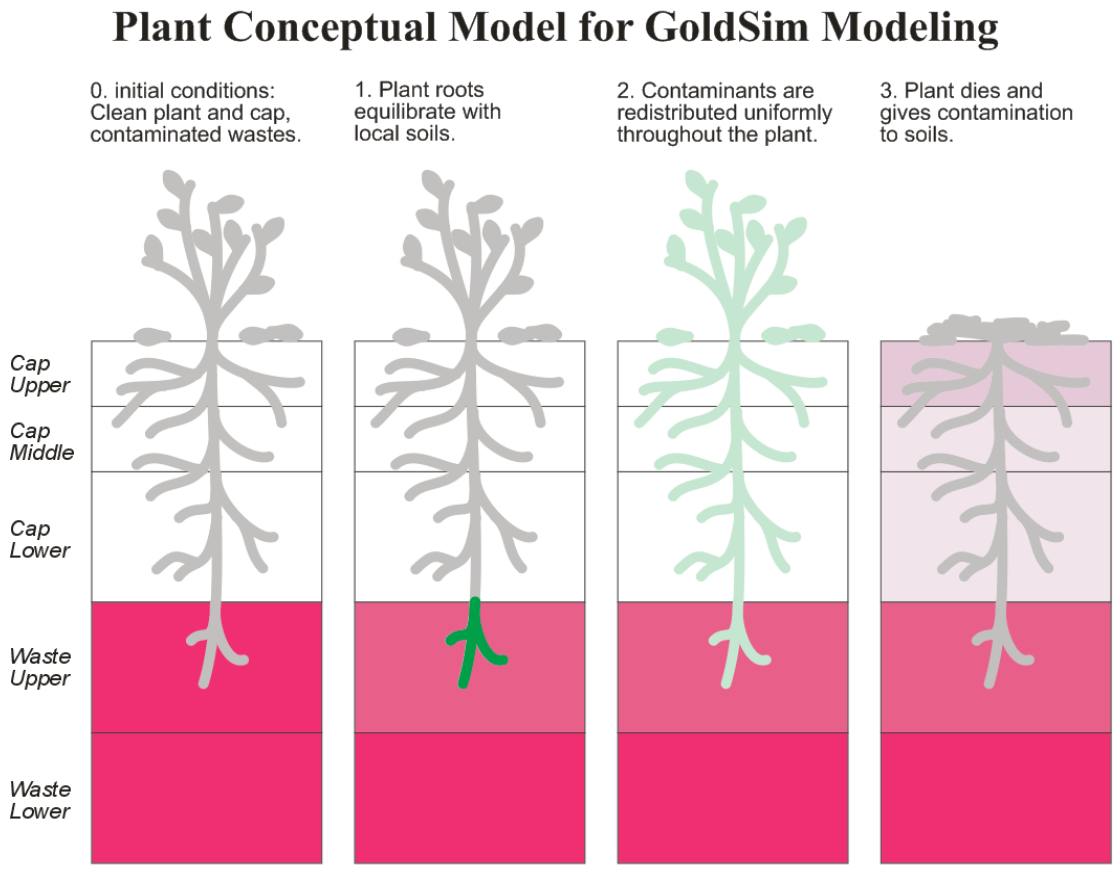

Figure 6. Conceptual model for plant transport

contaminated over time as subsurface contaminants are translocated to above ground portions of the plant, and ultimately to the surface soil as the plant senesces.

The degree to which plants can move contaminants from the subsurface, and the rate at which that transport can occur are dependent upon a number of factors such as plant rooting depth, total above ground plant biomass, total below ground plant biomass, relative abundance of plants, and density of plants roots by depth.

Plant rooting depths are influenced by a number of physical and physiological factors, but the ultimate limiting factor is the availability of water. Roots of desert plants generally do not exceed the depth to which water from precipitation infiltrates on a consistent basis. The maximum rooting depth of any desert plant is physically limited to the maximum depth from which the plant can obtain water. Of the plants that dominate the Clive site, black greasewood (*Sarcobatus vermiculatus*) is likely the most deeply rooted. Black greasewood is phreatophytic, meaning that it can utilize shallow groundwater, or derive supplementary water from the overlying capillary fringe and deplete soil water potential to values less than 4.0 megapascals (MPa). However, in areas where precipitation does not infiltrate to groundwater, black greasewood will not form taproots and will maintain a more shallowly rooted growth form. Excavations of several greasewood plants at the Clive site by SWCA (2011) found roots that did not exceed one meter

in depth. Several investigators have documented the types and metrics of plant species in bajadas, desert valleys, and saline mounds (Robinson 1958, Meinzer 1927, Groenveld 1990, Blank et al. 1998, Hansen and Ostler 2003, Rundel and Nobel 1991, and Holmgren and Brewster 1972).

The plant species currently inhabiting the Clive site are generally halophytic, meaning that they are adapted to saline environments. Dominant plant species in the saline environments around Clive include the halophytic shrubs black greasewood, shadscale, and the non-native forb halogeton. Soil chemistry of the alkali flat environment is a limiting factor that regulates the local plant community assemblages. It could be anticipated that the soil chemistry of constructed mounds such as the disposal cells may change over time as precipitation leaches salts from the mound soils, which are elevated above the surrounding terrain and decoupled from the saline groundwater. This change in soil chemistry could allow for the establishment of less salt-tolerant species, such as sage (*Artemesia spp)* and rabbit brush (*Chrysothamnus spp.),* which are common in less saline cool desert habitats. It is expected that plants will be the first colonizers of the Clive cap, though that is not expected to occur until the uppermost riprap layer has silted in sufficiently to allow for germination and root establishment.

7.1.5 Native Animals

Only limited biotic surveys of the Clive site have conducted, so site-specific information about the utilization of the site by specific animal species is likewise limited. However, based on the limited Clive studies and more comprehensive studies at other sites, burrowing animals, including invertebrates and mammals, are of importance when evaluating the mixing of soils and the potential for transporting buried wastes from the subsurface to the surface.

Ants

Ants fill a broad ecological niche as predators, scavengers, trophobionts and granivores, but it is their role as burrowers that is of main concern for evaluating transport of buried materials from the subsurface to the surface. Ants burrow for a variety of reasons but mostly for the procurement of shelter, the rearing of young and the storage of foodstuffs.

In arid areas of the Great Basin and southwestern U.S., harvester ants of the genera *Pogonomyrmex* and *Messor* are widespread, form large colonies, and often construct elaborate nests. A preliminary survey of the Clive site and surrounding areas in October 2010 found that the Western harvester ant (*Pogonomrymex occidentalis*) is by far the most common ant at the site, with nest densities ranging from two nests per hectare in mixed sage/juniper community, to 33 nests per hectare in areas with abundant grasses (SWCA 2011). Only a single other ant species (*Lasius* sp.) was identified at the Clive site during the preliminary surveys, and it occurred only in the mixed grass vegetative association.

Several investigations have focused on ants as a taxonomic group of importance for the potential to move buried waste at locations such as the Idaho National Laboratory (INL), and the Hanford Site in southeastern Washington (Blom 1990, Fitzner et al. 1979, Gano et al., 1985). These studies indicate that large colonies of *Pogonomyrmex* spp. may nest to depths of 3 to 4 meters (10 to 13 ft) and may colonize areas with great densities of nests (over 100 per hectare), thus potentially excavating large volumes of contaminated soil to the ground surface.

How and where ant nests are constructed plays a role in quantifying the amount and rate of soil movement and the mixing of the soil column. Factors relating to the physical construction of the nests including the size, shape, and depth of the nest are necessary in order to quantify excavation volumes. Factors limiting the abundance and distribution of ant nests such as the abundance and distribution of plant species, and intra- and inter-species competition also can affect excavated soil volumes. Therefore, the amount and rate of soil movement is based on a variety of factors, including nest area, nest depth, rate of new nest additions, colony density and colony lifespan.

Due to its dominance at the Clive site, the initial model will be parameterized using available data for *Pogonomyrmex occidentalis*. The geometry and structure of ant nests appears to be more of a species-specific trait that does not exhibit significant flexibility in variable environments (MacKay 1981). The mound's height, width, distribution of particles, color, and exposure significantly impact the colony for predatory defense and environmental regulation, but for any given species, these mound traits are the same from place to place (MacKay 1981). Therefore, there is defensibility for using data collected elsewhere for the same species in order to parameterize the potential for ant-mediated transport in the Clive model. Site specific data collected by SWCA (2011) on mound surface dimensions will be used to predict overall nest volume and depth, and habitat-specific information of ant nest density will be used to help predict the overall rate of soil movement on a per hectare basis for each habitat type. Additional site specific data may be needed dependent on the outcome of the initial model.

A number of authors contend that it is reasonable to expect that over the 15 to 30-year life of some *Pogonomyrmex* colonies, the entire soil column of the nest is turned over at least once (Mandel and Sorenson 1981). For important and long-lived *Pogonomyrmex* ants in the desert southwestern U.S., Lavigne (1969) and MacKay (1981) have investigated nest structure rather extensively, and conclude that the net effect of soil movement within an ant colony's lifetime is a general homogenization of soils throughout the nest profile. In general, it is likely that this homogenization occurs more rapidly in the top third of the nest, as this is where most of the colony's burrowing takes place, but over the life of the nest, burrowing at the greatest depths of the nest can be extensive (Lavigne 1969, MacKay 1981). However, at the Clive site the top layers of the cap are comprised of riprap and gravel layers. It is expected that after these layers silt in, ants will colonize the cap. However, ants will not directly transport the larger particles comprising the riprap and gravel layers of the cap, and these will affect the size and distribution of chambers within the upper layers of the nest since gallery and chamber construction will be limited to the void spaces between cobbles. Therefore, mixing of the riprap and gravel particles downward will be minimal, though transport of soil and clay particles from lower layers of the cap upward through the gravel and riprap is expected.

Mammals

Burrowing mammals such as gophers, pocket gophers, moles, voles, squirrels, mice, rats, kangaroo rats, and their predators have a profound influence on soil mixing. Burrowing mammals rework the entire near-surface of soil over most of the North American continent on a persistent basis, but at varying rates (Nevo 1999). Each of these mammalian species contributes to soil turnover to a varying degree, depending upon their burrowing habits, geographic location,

and prevailing climate and soil conditions (Laundré and Reynolds 1993). Mammalian biotic transport of soils also includes the deposition of fecal material in soils, the intermixing of vegetation, and the significant aeration of upper layers. All of these actions dramatically affect soil fertility, permeability by air and water, and increase soils' susceptibility to invasion by microorganisms (e.g., bacteria, fungi, nematodes, microarthropods).

Some mammals such as pocket gophers (*Thomomys* spp.), ground squirrels (*Spermophilus* spp., *Sciuridae* spp., and others), and kangaroo rats are considered obligately fossorial, i.e., they spend most of their time underground, including foraging underground. Other organisms, however, will utilize burrows only for shelter (temporary or permanent) and reproduction. These include hares (*Lepus* spp.), rabbits (*Sylvilagus* spp.), sagebrush voles (*Lagurus curtatus*), pocket mice (*Perognathus* spp.), kangaroo mice (*Microdipodops* spp.), foxes (*Vulpes* spp., *Urocyon cinereoargenteus*), and coyotes (*Canis latrans*).

Biotic transport of soils by mammals at waste burial sites includes the potential direct movement of waste from the subsurface to the surface, as well as secondary transport, such as food chain transfer, transport by way of fecal deposition, and carcass degradation (Arthur and Markham 1982, Smallwood et al. 1998). Intrusion into buried wastes and active physical transport occur when animals penetrate protective barriers and cause vertical or horizontal redistribution of waste material (Hakonson et al. 1982, Arthur and Markham 1982). As animals excavate burrows they either relocate buried material to the surface, or relocate soils from depth into below-ground chambers lateral to the point of entry, as is common with pocket gophers or other obligately fossorial mammals (Smallwood et al. 1998).

Because mammal burrows facilitate natural ventilation and aeration of the soils, burrowing activity may also enhance the potential for contaminant release in gaseous form by allowing increased communication between the atmosphere and buried waste. Mammal burrows also provide preferential pathways for water infiltration, as studies have shown that recharge quantities and depth of recharge were positively correlated with burrow density, and also found that ground squirrels can increase precipitation infiltration into the soils by as much as 34% as a consequence of burrowing activity (Laundré, 1993).

Preliminary investigations of mammals at Clive have focused on surveying the different habitat associations for mammal burrows, quantification of the amount of soil excavated by burrowing mammals, and trapping to determine dominant small mammal species in each vegetative association. Results suggest that burrowing mammals are relatively scarce on the alkali flat habitats (greasewood, shadscale), becoming more abundant in the less saline soils associated with mixed grass and juniper-sage habitats. Deer mice were the most abundant mammals trapped in all habitat types, with lesser numbers of kangaroo rats (two species), and grasshoppper mice also found in the traps.

At Clive it is expected that small mammals such as mice may use the void spaces in the riprap as refugia. As gravel and riprap layers silt in, the cap may be utilized by small mammals such as mice, but the riprap and gravel are expected to create less than optimal conditions for burrow construction, and the gravel layers may well serve as a barrier to mammalian borrowing altogether.

7.2 Far-Future Conditions

The deep time frame over which the analysis is concerned is defined by the period of time beyond 10,000 years until radioactivity from the DU parents and its progeny is at its peak. This occurs when the progeny, identified in Section 9.1.2 , are in secular equilibrium with the parent. For decay of a refined U-238 parent (the longest-lived uranium isotope), progeny reach secular equilibrium at about 2.1 million years (My). With its exceedingly long half-life of over 4 billion years, the parent U-238 decays only by about one half-life before the end of the solar system, and the peak achieved at 2.1 My wanes only slightly in that time. The analysis devoted to deep time scenarios is sufficiently representative of this entire duration when considered out to only 2.1 My in the future, as changes in radioactivity are minor after that time.

The model developed to evaluate the ultra-long term performance of the Clive disposal facility will focus on concentrations in various media, and will not attempt to translate these concentrations into human dose metrics. This approach will be used because of the overwhelming uncertainty associated with evaluating human receptor scenarios that far into the future. This uncertainty is associated both with projecting human behavior and environmental conditions.

A scenario is considered that involves the return of large lakes in the Bonneville Basin over the next few million years, since secular equilibrium is reached at about 2.1 My. Following that, the radioactivity of the DU will persist effectively forever. When the duration of interest is expanded to billions of years, however, on such a time scale, such major geologic processes are at work to make any predictions absurd—even for a geologic repository.

Understanding the phases associated with the change from current climatic conditions to future climatic conditions can help construct a qualitative picture of how the Clive facility will respond to those changes. The following section provides a brief overview of how major environmental changes in the past are directly coupled to major shifts in climatic regimes. This section also provides context with respect to how these past changes may occur in the future and their implications on the stability of the Clive storage facility.

7.2.1 Background on Long-term Controls on Site Conditions

7.2.1.1 Climate processes

Large-scale climatic fluctuations over the last 2.58 My (the beginning of the Quaternary Period) have been studied extensively in order to understand the mechanism underlying those changes (Hays et al., 1976, Berger, 1988, Paillard, 2001, Berger and Loutre, 2002). These large-scale fluctuations in climate have resulted in glacial and interglacial cycles which have waxed and waned throughout the Quaternary Period. The causes of the onset of the Northern Hemisphere glaciation about 3 million years ago (3 Ma) remain uncertain, but several studies suggest that the closing of the Isthmus of Panama caused a marked reorganization of ocean circulation patterns that resulted in continental glaciation (Haug and Tiedemann, 1998, Driscoll and Haug, 1998).

Changes in the periodicity of glacial cycles have been linked to variations in Earth's orbit around the Sun. These variations were described by Milankovitch and are based on changes that occur due to:

- the eccentricity of Earth's orbit – around every 100,000 years (100 ky),
- the obliquity of Earth's axis every – around 41 ky, and,
- the precession of the equinoxes (or solstices) – around 21 ky.

For the first two million years of the Pleistocene (the first major Epoch of the Quaternary Period), Northern Hemispheric glacial cycles occurred about every 41 ky, while the last million years have indicated larger glacial cycles occurring about once every 100 ky, with strong cyclicity in solar radiation every ~23 ky (Berger and Loutre, 2002; Paillard, 2006). The results of Hays et al. (1976), who analyzed changes in the isotopic $\delta^{18}O$ composition of deep-sea sediment cores, suggest that major climatic changes have followed both the variations in obliquity and precession through their impact on planetary insolation. Variations in $\delta^{18}O$ reflect changes in oceanic isotopic composition caused by the waxing and waning of Northern Hemispheric ice sheets, and are thus used as a proxy for the climatic record. However, the shift from shorter to longer cycles is one of the greatest uncertainties associated with utilizing the Milankovitch orbital theory to explain the onset of glacial cycles alone (Paillard, 2006).

Various studies have highlighted the importance of atmospheric carbon dioxide (CO_2) variations in the dynamics of glaciations across the Northern Hemisphere in addition to the insolation due to orbital forcing (Clark et al., 2009; Paillard, 2006). Direct measurement of past CO_2 trapped in the Vostok and EPICA Dome C ice cores from Antarctica show that atmospheric CO_2 concentrations decreased during glacial periods due to greater storage in the deep ocean, thereby causing cooler temperatures from a reduction of the atmosphere's greenhouse effect (EPICA, 2004). Warmer temperatures resulting from elevated concentrations of CO_2 that are released from the ocean on the other hand contribute to further warming and could support hypotheses of rapid wasting at the end of glacial events (Hays et al., 1976). Berger and Loutre (2002) conducted simulations forced with insolation and CO_2 variations over the next 100 ky and report that the current interglacial period could last another 50 ky with the next glacial maximum occurring about 100 ky from now. They also report, however, that future increases in atmospheric CO_2 from anthropogenic activity along with small insolation variations could result in a transition between the Quaternary and the next geologic period due to the potential wasting of the Greenland and west Antarctic Ice Sheets.

There is a strong likelihood that there will be major climatic shifts within the next million years, and strong evidence that the 100 ky cycle has impacted the Bonneville basin in the form of large lake recurrence (Oviatt, 1997; Asmerom et al., 2010). Thus, due to the destructive potential of a lake to the waste embankment, the deep time scenarios of most interest are the return of large lakes in the Bonneville Basin.

7.2.1.2 Large Lake Cycle Events

The Clive facility is located in the Bonneville Basin where Lake Bonneville, the largest of the late Pleistocene pluvial lakes, last existed between 30-10 ka. Pluvial lakes are lakes that show evidence of expansion due to pluvial episodes (wetter climatic phases) as well as contraction due to what is assumed to reflect interpluvial episodes (warmer, dryer climatic phases). Various FEPs fall within the lake cycle scenario which include wave action, sedimentation, and site inundation.

At its maximum (between ~15-16 ka BP), Lake Bonneville is estimated to have covered an area of 51,300 km^2 (~19,800 sq mi) and was over 370 m (1200 ft) deep (Lowe and Walker, 1997). Following the Bonneville flood around ~14.5 ka, during which the lake level dropped by ~114 m (~375 ft) as it spilled over and eroded a spill point, the lake level continued to decline leaving behind modern-day Great Salt Lake. Geomorphological evidence is present that shows the variability in the levels of the last major lake cycle as indicated by the exposed shoreline features in areas of the Bonneville basin.

Oviatt et al. (1999) examined sediments from the Burmester core and suggested that a total of four deep-lake cycles occurred during the past 780 ky. They found that the four lake cycles correlated with marine oxygen isotope stages 2 (Bonneville lake cycle: ~24-12 ka), 6 (Little Valley lake cycle: ~186-128 ka), 12 (Pokes Point lake cycle: ~478-423 ka), and 16 (Lava Creek lake cycle: ~659-620 ka), which suggests that large lake formation in the Bonneville basin occurred only during the most extensive Northern Hemisphere glaciations. In addition to these large lake cycles, a smaller cycle known as the Cutler Dam cycle occurred between ~80-40 ka (Link et al., 1999). Each major lake cycle and its corresponding estimated maximum shoreline elevations are listed in Table 1. As a point of reference, the Clive facility is located at an elevation of 1302 m (4275 ft) amsl, and the airport at Salt Lake City, SLC, is at 1288 m (4227 ft).

During the large pluvial lake events, large amounts of calcium carbonate were precipitated as tufas, marls, shells (of mollusks), and ostracodes (Hart et al., 2004). Brimhall and Merritt (1981) reviewed previous studies that analyzed sediment cores of Utah Lake, a freshwater remnant of Lake Bonneville that formed ~10 ka. It is suggested that up to 8.5 m (28 ft) of sediment has accumulated since the beginning of Utah Lake, implying an average sedimentation rate of ~0.00085 m/y (nearly 1 mm/y) over 10 ky. Within the Bonneville basin as a whole it is suggested that the major lake cycles resulted in substantial accumulations of sediment based on the depth of the cores analyzed (e.g., 110-meter core that corresponds to the past 780 ky, or four major lake cycles for an average sedimentation rate of 0.00014 m/yr including non-lake phases; Oviatt et al., 1999).

Table 1: Known lake cycles in the Bonneville Basin

Lake Cycle	Approximate Age*	Maximum Elevation	Lake level control
Great Salt Lake (current level)	present	1284 m (4212 ft) in 1873	climate; human intervention
Gilbert	11–10 ka	1295 m (4250 ft)	climate
Provo	14.5–13.5 ka	1445 m (4740 ft)	threshold at Zenda near Red Rock Pass, Idaho
Bonneville	~28–12 ka (^{14}C)	1552 m (5090 ft)	threshold at Zenda near Red Rock Pass, Idaho
Stansbury	23–20 ka	1372 m (4500 ft)	climate
Cutler Dam	~80–40 ka	< 1380 m (< 4525 ft)	
Little Valley	~128–186 ka	1490 m (4887 ft)	
Pokes Point	417–478 ka	1428 m (4684 ft)	
Lava Creek	~620–659 ka	1420 m (4658 ft)	

*Approximate ages derived from Currey, et al. (1984) Link et al. (1999) and Oviatt et al. (1999).
Elevations are not corrected for isostatic variations

There is a lack of peer-reviewed literature that considers the direct effects of future climate change on major lake formation in the Bonneville basin. However, if the current geologic era continues, the probability of another major lake cycle occurring in the Bonneville basin within the next 100 ky in conjunction with variation in Earth's orbital characteristics is high, considering the correspondence between past global temperature fluctuations and past known lake events. Assuming that past conditions will apply in the future, variations in orbital characteristics are very likely lead to another major ice age and thus alter long-term climatic patterns in the Bonneville region making it suitable for lake formation. Each 100 ky glacial cycle is different, depending on orbital forcing, but it is clear from the historical record that the current period is inter-glacial, and colder conditions are likely in the future. Unless the current geologic period ends in response to anthropogenic forcing effects on atmospheric CO_2 concentrations (Berger and Loutre, 2002), it is expected that the Clive facility will be subjected to lake formation in the future. Return of a large lake is considered unlikely without climatic change.

7.2.1.3 Isostatic Rebound

Isostasy refers to the gravitational equilibrium between Earth's lithosphere (the rocky outer crust) and asthenosphere (the semiliquid layer below the crust) such that the lithosphere "floats" at an elevation that depends on its local thickness and density. When large amounts of sediment, water, (in the case of Lake Bonneville) or ice occur over a particular region over time, the weight of the new mass may cause the crust below to sink. Hetzel and Hampel (2005) examined the effects of the removal of Lake Bonneville on isostatic rebound of the lithosphere. They found that the

removal of Lake Bonneville triggered an increase in fault slip rates in the Wasatch region resulting in clustering of earthquakes during the early Holocene. Former islands present during the Lake Bonneville cycle also indicate that isostatic rebound occurred after the regression of the lake. This is evidenced by the palæo-shorelines on the islands which are located tens of meters above the palæo-shorelines along the lake periphery (Hetzel and Hampel, 2005).

Although it is difficult to predict potential impacts from future seismic events, it is expected that if isostatic rebound effects were to occur, the effects of future seismic events would be mitigated by the site's burial by lacustrine sediment.

7.2.1.4 Volcanism

The principal effects of volcanism on the Clive site are indirect. Hart et al. (1997) suggest that lava flows near Grace, Idaho during the Pleistocene diverted the upper Bear River between the Snake River drainage to the Bonneville Basin through the formation of lava dams. Link et al. (1999) report that the permanent addition of the Bear River discharge to Lake Bonneville likely occurred around 50 ka (±10 ka), and in conjunction with cooler and wetter conditions during this time, it is thought to be responsible for the lake reaching its highest level (i.e., the Bonneville shoreline). Although the lava dams resulted in the alteration of the path of the Bear River, at certain times during the Pleistocene the upper Bear River was diverted into the Snake River which deprived the Bonneville basin of significant discharge. Future changes in the regional hydrology in response to any future lava flows or regional volcanic activity could result in similar implications for future pluvial lake events (i.e., increase or decrease in discharge to the basin).

7.2.1.5 Ecological Changes

Changes in biotic assemblages have been shown to occur in the past (Davis and Moutoux, 1998) and will likely occur in the future in response to shifts in climatic regimes. Temperature and precipitation have a profound effect on plant community assemblages, as does soil chemistry. Areas where salt pans remain in place will remain largely unvegetated regardless of changes in temperature and precipitation. Valley areas around the margins of salt pans will remain restricted to halophytic plants until salinity levels drop. Because Clive is somewhat centrally located within the Great Basin cold desert biome, vegetation assemblage changes associated with climate change will occur more slowly than in areas closer to biome transition zones. As the climate changes, vegetation changes will occur on steppes and slopes, but soil chemistry will remain the constraining factor on the valley floors.

Pollen studies from sediment cores in the Great Salt Lake show that the vegetation of the Bonneville Basin and surrounding area has been desert for approximately the last 5 My (Davis and Moutoux, 1998). The pollen studies indicate that *Sarcobatus*, *Artemisia,* and various Chenopodaceae (the family that includes the various saltbush species) have dominated during interglacial periods, with montane conifers (*Picea*, *Abies*, and *Pseudotsuga*) increasing during glacial periods. For the purposes of this CSM, it is assumed that climatic shifts could occur resulting in any one of four different conditions: cooler-wetter, cooler-drier, warmer-wetter, warmer-drier. The direction of the climatic shift will affect both the vegetative and faunal assemblages occupying the site. Figure 7 illustrates a general biome diagram based on

temperature and precipitation, as well as the approximate location of the Clive site within this temperature-precipitation gradient.

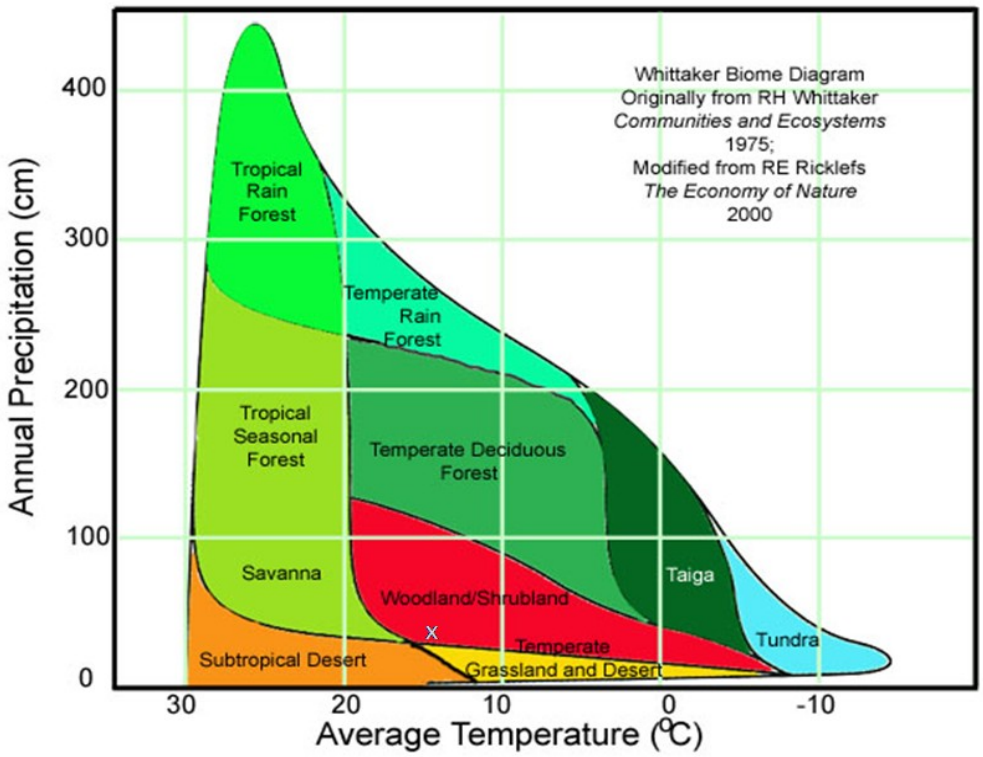

Figure 7: Whittaker Biome Diagram

Cooler, wetter conditions will likely result in transition first to *Artemisia* sage communities, then to Pinyon-Juniper woodland characterized by the presence of *Juniperus osteosperma* and *Pinus monophylla*, and finally to montane spruce/fir woodlands as seen during past glacial periods. These woodlands are not likely to ever occupy the valley floor unless profound changes in soil chemistry occur. All of these changes occur over geologic time, and prediction of the occurrence of specific species represents a great uncertainty. Cooler, drier conditions will likely maintain similar plant communities as are currently present, unless temperatures get cold enough to support taiga/tundra conditions.

Warmer, drier conditions will result in plant assemblages similar to those that occur in the Mojave desert, where valley floors are dominated by creosote bush (*Larrea tridentata*), white bursage (*Ambrosia dumosa),* and pale desert-thorn (*Lycium pallidum*). Warmer, wetter conditions could lead to establishment of grasslands, and eventually temperate forest, as existed more than 10 Ma when the pollen record shows that elm (*Ulmus*), hickory (*Carya*), yew (*Taxus*), and hemlock (Tsuga) were common in the area (Davis and Moutoux, 1998). Again, establishment of

these vegetative complexes on the valley floor would require a major shift in soil structure and chemistry.

7.2.1.6 Human Intervention

Various scenarios can be constructed that look at each of these impacts on the Clive facility in the ultra long-term future. One major difference between the past 3 My and the present is the existence of well-developed human civilization, technology, and greater ability to adapt to changing conditions. If the future is more in line with reentering another ice age similar to those that have occurred during the Pleistocene, human intervention could help to mitigate the effects of future events that could jeopardize the stability of the engineered facility at Clive. For example, the disposal cell could be protected by adding more rip-rap material, a seawall, or berm (or other engineered barriers) to prevent the deleterious effects of wave action in the event of future lake formation.

In the event of another major lake cycle, human intervention is likely to be employed in surrounding areas (e.g., Salt Lake City) and could result in modifying engineered features like those that were installed to alleviate the effects of flooding in the early 1980s, when a pumping system was built to divert flood waters into the west desert (see `www.water.utah.gov/Construction/GSL/GSLpage.htm`). In fact, the Utah Division of Water Resources proposed various options to handle flooding events of Great Salt Lake due to natural variations in precipitation (see `www.water.utah.gov/Construction/GSL/GSLflood.htm`). Some of the options that were proposed included the exportation of flood flows from the Great Salt Lake drainage basin to the Bear River and Sevier River drainages, consumption of water via evapotranspiration through the development of new agricultural lands, and creating a dike around the lake to protect major facilities and resources.

While it is difficult to predict the level of human intervention in response to these events, it should be taken into consideration for all future scenarios considered for the performance assessment of Clive facility.

7.2.2 Long-Term Scenarios

The primary scenario of concern in the deep time scenario is the return of a lake to the Bonneville Basin that reaches the elevation of the Clive facility. There is historical evidence of large lakes covering the Clive site with more than 100 meters of water, so large lakes will be modeled as recurring in the future. There is weaker historical record of intermediate-sized lakes, lakes that are relatively shallow at the Clive elevation. The lack of historical record for intermediate lakes is not necessarily surprising, since sedimentation from subsequent lakes is likely to bury evidence of intermediate lakes. However, there is evidence of two relatively recent intermediate lakes – Cutler Dam and Gilbert, as well as stratigraphy in sediment cores that suggest many lakes rising and falling at the Clive elevation (Oviatt, 1997), which might be associated with either intermediate lakes or fluctuations in large lake transgression and regression. The expected consequence of the formation of a lake in the Bonneville Basin is the destruction of the waste embankment due to wave energy, resulting in physical dispersal of the site material. Waste entrained in the sediment can partially dissolve into the lake, and contaminant complexes will precipitate from the lake water back into the sediment. This process is depicted in the conceptual model shown in Figure 8.

The deep time model is thus constructed to represent the following components:

- *Continuation of natural processes in the waste embankment.* After 10,000 years, natural processes such as air dispersal, groundwater transport, and biotic uptake will continue to be modeled as long as the embankment is intact.

- *Returns of large and intermediate lakes to the Clive site*. Large lakes will be treated as occurring regularly with the 100,000-year orbital cycle, while intermediate lakes will occur according to a random process between large lake cycles, with greater probability of occurrence further in time from the end of the inter-glacial period (i.e., as the temperature decreases and precipitation increases).

- *Site destruction*. When the first lake returns at or above the elevation of Clive, the waste embankment will be treated as destroyed. The result is dispersal of above-grade waste into the sediments near the site, along with dissolution into the lake water. Once the waste embankment is destroyed, the evolution of the waste embankment is no longer modeled.

- *Sedimentation and mixing*. The presence of a lake implies sedimentation at the site. As the waste is dispersed, it will be mixed with the embankment materials and sediment. Waste material that dissolves into the water column will be assumed to precipitate out of the water column back into the sediment at the site as the lake recedes. Subsequent lakes are likely to at least partially bury the waste beneath subsequent sediment. However, since the deep time model is intended to be qualitative, a conservative choice is made to model all sediments containing waste as mixing with sediments of subsequent lakes.

- *Activity levels*. The results tracked in the deep time model are the radioactive concentrations in lake water and in sediment.

8 Modeling of Engineered Features

The engineered features of the disposal facility are the waste form itself (including containment), and the liner and cap, which surround the wastes. Other than these, the natural environment is relied upon to moderate the migration of contaminants. These engineered features are expected to degrade with time, gradually assuming a form more like the natural surroundings. The model will attempt to capture the performance of the engineered features, including the essential processes contributing to their degradation, as described in this section.

8.1 Waste Form and Containment

The waste forms are discussed in detail in Section 6 , but a brief discussion is included here for completeness as an engineered feature. The waste form, for the purposes of this discussion, includes the matrix that contains radionuclides, and any drums, boxes, or other materials that contain that matrix. Generally, wastes are not designed with their long-term resistance to

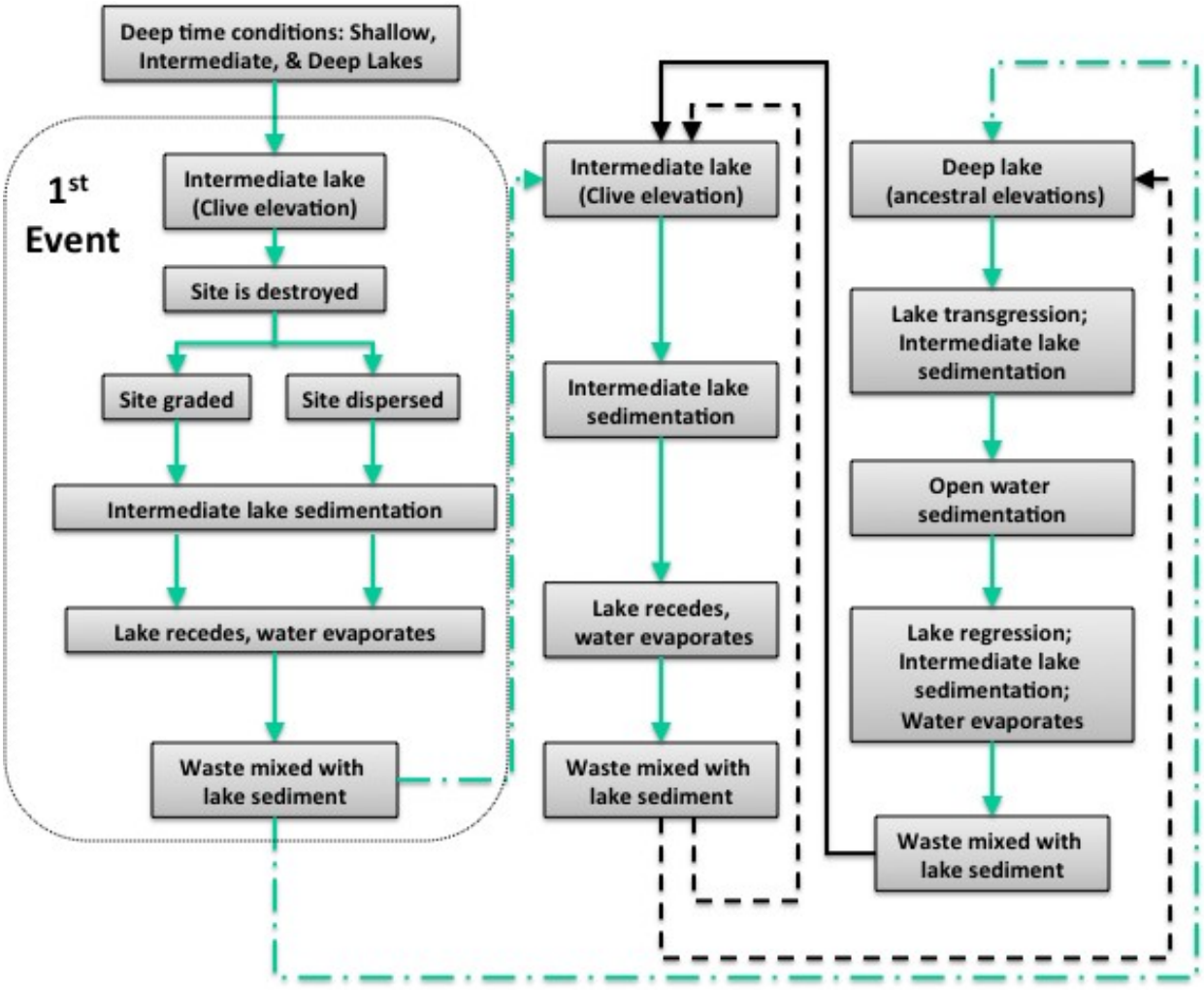

Figure 8: Scenarios for the long-term fate of the Clive facility

degradation in mind, but rather for the convenience of the generator and shipper. Also, waste form and containment on waste profiles or shipping manifests are sufficient for disposal purposes, but not necessarily for PA purposes.

Low-level radioactive waste matrices are in general quite heterogeneous, including bulk soils, debris from decontamination and decommissioning activities, protective equipment, tools, laboratory wastes, chemical residues, resins and filters, and such, but in the case of DU waste, the form is unusually uniform. Leachability and solubility can be modeled for well-documented DU oxide waste forms. Details on the chemical characteristics of DU waste are given in Section 6.6 .

Steel barrels and boxes, "burrito-wrap" fabrics, cardboard, or even bulk uncontainerized materials are common in LLW. Most of these offer little in the way of long-term containment, especially after compaction to reduce void spaces, which often crushes or otherwise compromises containment. Container integrity is not typically given credit in LLW PA models. In the case of DU, the containers, which consist of steel 200-L (55-gal) drums or the various specialized designs of steel UF_6 cylinders, are not expected to provide much in the way of long-term containment. Pitting, rusting, and other forms of corrosion have already been documented for the cylinders, and a number of steel drums have had to be repackaged. This degradation has taken place in the last few decades, so it would be unreasonable to assume that containers would remain intact for any appreciable length of time in the environment of the embankment cell. The model, therefore, will not take credit for containment. All wastes are assumed to have the characteristics of local Unit 3 sandy soil.

8.2 Liners

The Clive facility's embankment cells are constructed similarly to those designed for landfills under the Resource Conservation and Recovery Act (RCRA), using a variety of natural and engineered materials. Liners are constructed on the floor of the facility, and the waste is placed on top of them. Caps are constructed over the waste, and are designed to shed water. Despite careful construction to exacting standards and conscientious maintenance, both the caps and liners are subject to failure in the long-term (Smith et al., 1997), as entropy returns them to what approaches a natural state.

Previous PA modeling at the Clive site, which addressed a performance period of hundreds of years, included modeling of the installed performance of the cap and liner, degradation of the cap, and bio-intrusion scenarios (Whetstone, 2000). Liner degradation allows for increased contaminant transport from the waste layers to the UZ below the facility, and subsequently to the SZ through recharge. The performance of the liner is not expected to degrade significantly. The principal role of the liner in the contaminant transport model is to regulate flow from the waste to the underlying UZ, so all that matters, in the end, is the rate at which water may penetrate it, plus any chemical retardation involved as it flows through.

8.3 Cap

The engineered cap is likely to return to nature faster than the liner, due to biointrusion and erosion. These processes are discussed in the following paragraphs.

Changes in evapotranspiration fluxes due to time dependent evolution of the cap after closure will have the most significant influence on net infiltration. The potential changes in evapotranspiration and lateral drainage as the cap evolves are driven by the following processes:

- Aeolian dust begins to fill the void spaces between the armor (Layer 1) and the smaller cobbles in the upper filter (Layer 2), providing a soil base for plant cover on the top layer of the cap. The dust deposition process is augmented by fracturing of some large cobbles into smaller particles due to weathering. The presence of plant cover and soil on the cap is expected to increase evapotranspiration, thereby reducing the infiltration into the waste.

  The results of dust deposition, weathering, and plant growth were observed on the Vitro cell during a visit to the Clive site on September 16, 2010. The Vitro cell was closed in December 1988, and provides a site-specific measure of dust deposition, weathering, and plant growth since closure. A partial plant cover of grasses and small shrubs has been established within the past 22 years, based on the growth on the side slope and top slope of the Vitro cell.

  Evaporation will likely occur from greater depth once aeolian dust fills the void spaces between cobbles in the rip rap and plant cover is reestablished on the top surface of the cap. The measured moisture content in the Cover Test Cell at the site provides evidence for an evaporative zone depth greater than 18 in (Envirocare 2005). The measured data from the Cover Test Cell show that the middle of the sacrificial soil, at a depth of 30 in below the top of the cap, experiences seasonal drying during the six months with very low precipitation at the site (Envirocare 2005, Figures 3 and 4). Some of this drying is due to evapotranspiration, although drainage to the underlying clay layers (i.e., the radon barrier) may also play a role.

- Smaller mammals and ants are not expected to populate the cap in sufficient numbers to cause bioturbation and homogenization of the armor and upper filter (Layers 1 and 2). It is likely that smaller mammals may burrow to some extent in the silted rip rap, but not find the underlying cobbles hospitable compared to the virgin soil surrounding the cell. It is also unlikely that ants will find sufficient room amongst the cobbles and gravel to build chambers in Layers 1 and 2.

- The lower layers of the cap, Layers 3 and 4, will be a good habitat for deeper plant roots, based on a biological survey of the site. Observations made during a biological survey at the Clive facility (SWCA, 2011) indicate that plant roots often form on top of clay layers that are a meter or more below the top surface, such as the upper radon barrier (Layer 5). Some of these roots may penetrate the radon barriers, based on observations of plant roots in clay layers in boring logs, although the recent biological survey did not dig through clay layers to confirm this. It is possible that ants may also penetrate the clay layers by following root holes or possible cracks in the clay layers. On balance, the evidence suggests that bioturbation and homogenization of the radon barriers will probably occur very slowly relative to the 10,000-year time frame for the PA.

Sheet erosion is a uniform process over the area of the cap, and depends largely on its slope. In the central area of the embankment, where slopes are gradual, sheet erosion would be slower than on the steeper side slopes of the cell. As soil and loess move downslope, however, it is expected that their volumes would be replenished by deposition of clean loess from the surrounding environs. In the end, the soil volumes do not change, though there would be a slow movement of soils downslope, along with the contaminants they could potentially contain. Sheet erosion is not included in this model since the top slope of the cap is gradual (about 2%), and since the overall effect of sheet erosion is likely to be considerably less than the effect of gully erosion.

Gully erosion has the potential to move substantial quantities of both cap materials and waste. Once a "nick" is started somewhere on the surface of the cap, by an animal burrow or OHV track, for example, the feedback processes inherent in gully formation will cause erosion upward to the top of the slope, and downward to the surrounding grade. This process continues until the sides of the gully have met the angle of repose of the various materials within the facility, removing a wedge-shaped volume of material, and depositing it on the neighboring flat as a sort of small alluvial fan. As a first approximation of this volume, a simple wedge is calculated using the angle of repose.

Freeze/thaw cycles will also tend to degrade performance of the cap. This process is anticipated in the design, however, which includes a sacrificial layer to accommodate it (Whetstone, 2000). It is assumed in this model that although sacrificial soil will include plant roots and animal burrows, the overall effectiveness of the sacrificial soil layer is sufficient for this site.

Subsidence of the wastes could also contribute to decreased performance of the cap (Smith et al., 1997). Differential subsidence would be expected to cause vertical shearing of the cap layers, creating enhanced transport pathways, and the formation of depressions which could capture water, increasing local infiltration. However, it is expected that any depression would fill in rather quickly by windblown sediments. Subsidence is not expected to be an important process at the Clive facility, since the waste is aggressively compacted in order to prevent this occurrence (Energy*Solutions*, 2009c).

9 Radionuclide Transport

This section describes the aspects of modeling that involve radionuclides. The modeling of the natural environment, including groundwater flow, atmospheric dispersion, and other processes that are not specific to radionuclides, is discussed in Section 7 . Following the determination of the list of radionuclide species under consideration, this section discusses the mechanisms governing their fate and transport in the environment.

9.1 Modeled Radionuclides

Unlike general LLW, DU waste contains only a select number of radionuclides. These are mostly uranium isotopes (by mass), the most common of which is U-238. The non-uranium radionuclides are either fission products or actinides.

9.1.1 Reported Inventory

Based on laboratory analysis of the contents of DU waste (including all radionuclides in the containers), the species in the disposed inventory include (Beals, et al. 2002, Energy*Solutions* 2009b, Johnson 2010):

uranium isotopes	^{233}U, ^{234}U, ^{235}U, ^{236}U, ^{238}U
other actinides (and radium)	^{226}Ra, ^{241}Am, ^{237}Np, ^{238}Pu, ^{239}Pu, ^{240}Pu, ^{241}Pu
fission products	^{90}Sr, ^{99}Tc, ^{129}I, ^{137}Cs

9.1.2 Radioactive Decay and In-growth

Radioactive decay and in-growth are fundamental physical processes. There are several types of radiological transformations, including alpha, beta, gamma, electron capture, spontaneous fission, etc. While these processes are not specifically detailed in this subsection, they are accounted for in terms of their dose effects on humans, and their change in elemental (chemical) nature. As they experience decay and in-growth, the radionuclides in the reported inventory will change and these progeny must also be included in the modeling.

Simplified decay chains for the actinides are shown in Figure 9. Decay and in-growth continue until a stable nuclide is reached. In the case of the actinides, the stable nuclide is always bismuth or lead.

9.1.3 Short-lived Radionuclides

Not all of the members of a decay chain are modeled in the fate and transport calculations. Given the long duration of the analysis, and the short half-life of many of the radionuclides, it is impractical to model their transport, as they could not travel any appreciable distance before decaying to the next nuclide of the decay chain. Attempting to include short-lived radionuclides in the fate and transport model adds unnecessary complexity to the model. Therefore, radionuclides with half-lives less than five years are excluded from the fate and transport analysis, with one exception: Rn-222. Radon is a special case, since as a noble gas it has unique transport characteristics, even though it has a half-life of under four days. It diffuses in both air and water, partitioning between the two, and can migrate significant distances.

It must be noted that while the short-lived radionuclides are not included in the fate and transport calculations, they are included in the dose assessment. It is often short-lived nuclides that contribute most to dose.

9.1.4 Radionuclides with Small Branching Fractions

Similar to the short-lived radionuclides, there are radionuclides that have exceedingly small branching fractions, in addition to being short-lived. These are included in neither the fate and transport calculations, nor the dose calculations, as their omission is invariably inconsequential and promotes computational efficiency. In addition, most of these small branching fraction radionuclides have no dose conversion factors available.

The detailed sections of the actinide decay chains that contain these radionuclides, showing all the short-lived and small-branching-fraction radionuclides, are provided in Figure 10.

List of Radionuclides Species for Fate and Transport

The complete list of radionuclides accounted for in the fate and transport model follows, organized into decay chains:

$^{241}Pu \rightarrow {}^{241}Am \rightarrow {}^{237}Np \rightarrow {}^{233}U \rightarrow {}^{229}Th$

$^{242}Pu \rightarrow {}^{238}U \rightarrow {}^{234}U \rightarrow {}^{230}Th \rightarrow {}^{226}Ra \rightarrow {}^{222}Rn \rightarrow {}^{210}Pb$

$^{238}Pu \rightarrow {}^{234}U \rightarrow$ (joins above chain)

$^{239}Pu \rightarrow {}^{235}U \rightarrow {}^{231}Pa \rightarrow {}^{227}Ac$

$^{236}U \rightarrow {}^{232}Th \rightarrow {}^{228}Ra \rightarrow {}^{228}Th$

$^{232}U \rightarrow {}^{228}Th \rightarrow$ (joins above chain)

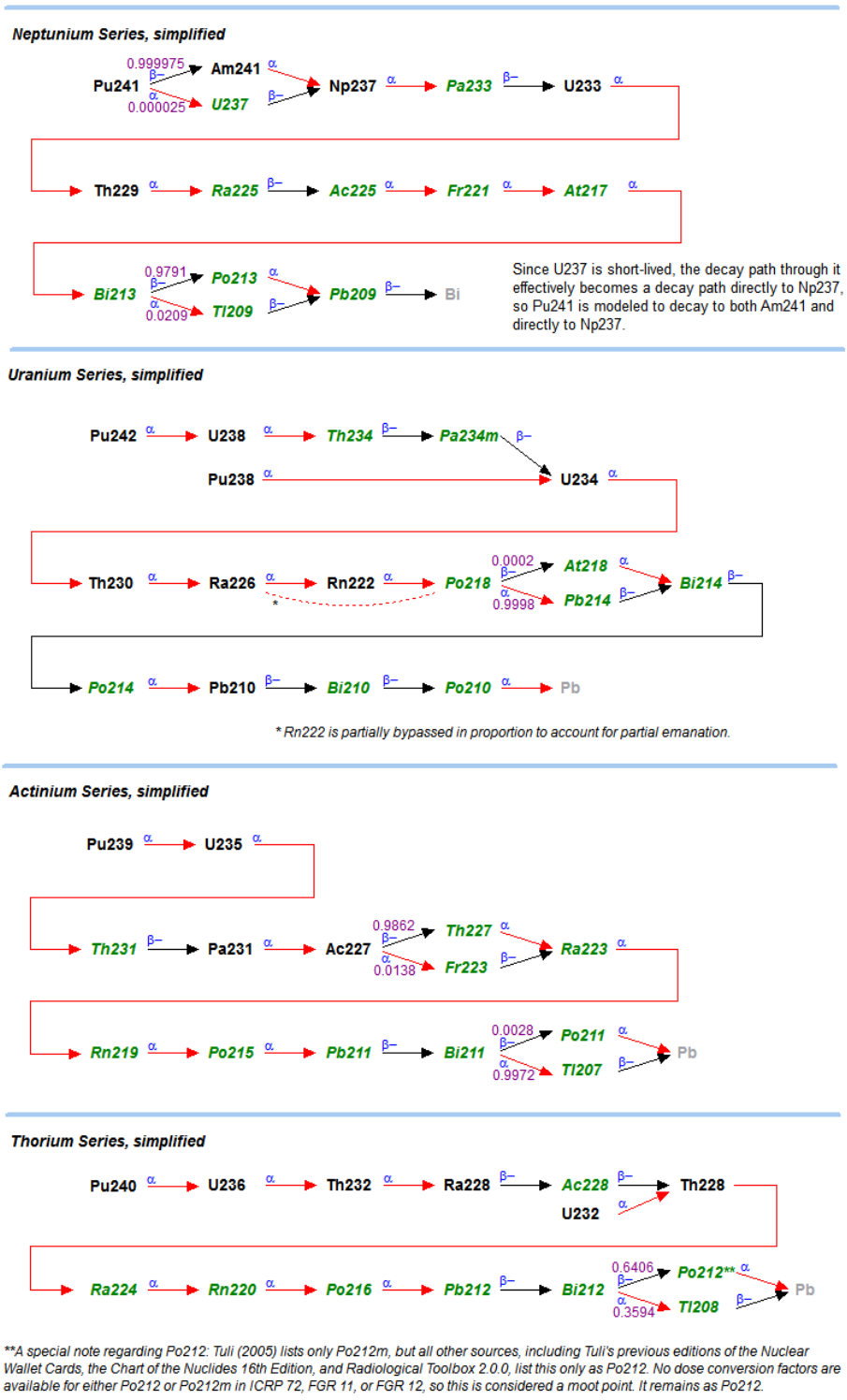

Figure 9: Principal decay chains for the four actinide series. Radionuclides in black are included in the fate and transport model, and those in green are considered only in the dose model.

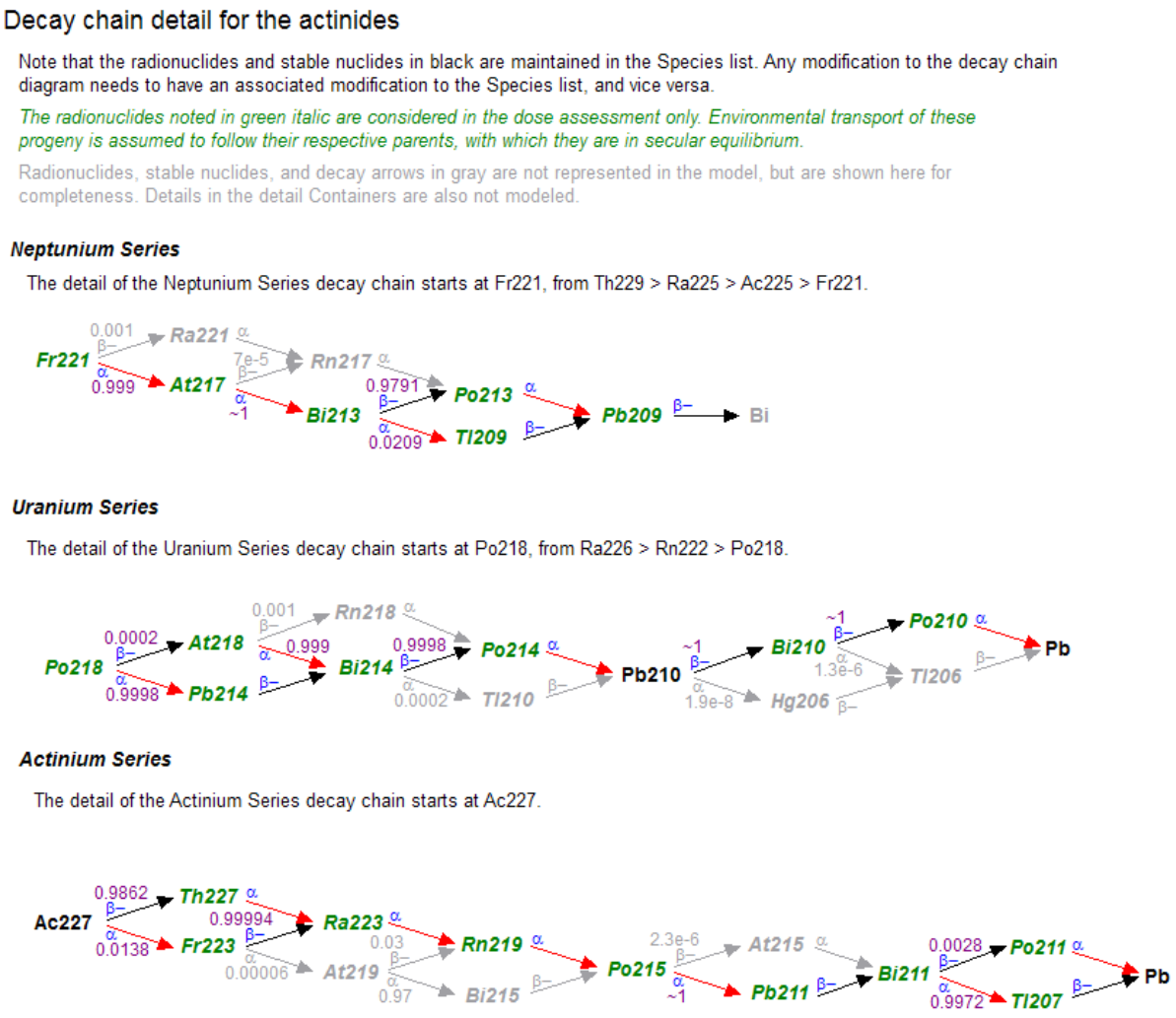

Figure 10: Detailed decay chains for actinides. Radionuclides in black are included in the fate and transport model, those in green are considered only in the dose model. and those in gray are not modeled.

Several radionuclides are not part of the actinide series:

$^{137}Cs \rightarrow {}^{137m}Ba$

^{129}I

$^{90}Sr \rightarrow {}^{90}Y$

^{99}Tc

The decay of the last species listed in the chain is also included in the fate and transport modeling.

9.2 Source Release

The disposed DU waste is assumed to be uncontainerized, since standard operations at the site include significant compaction of disposed waste.

9.2.1 Containment Degradation

As discussed in Section 8.1 , no credit will be given to the ability of steel containers to inhibit release of wastes.

9.2.2 Matrix Release

In the absence of detailed information regarding the chemical and physical form of the uranium oxides, release of radionuclides from the waste matrix will be assumed to be instantaneous. That is, release into infiltrating water that migrates through the waste will be controlled only by the geochemical constraints of the waste/water partition coefficient (K_d) and solubility (see Section 9.3). If information can be provided for a basis of a measured release from the waste matrix, that can also be incorporated into the model.

9.2.3 Radon Emanation

A special consideration for DU is the production and release of radon, especially Rn-222. As Rn-222 is produced by alpha decay from Ra-226, the recoil from the ejection of the alpha particle may be of sufficient energy to expel the Rn-222 atom from the waste matrix. If it is not so energetic, the radon atom will stay in the matrix, and will in a matter of days decay to Po-218 and then to other progeny, and will not be available for environmental transport as radon.

The fraction of decaying radium atoms that result in a radon atom being expelled into a transport medium (water or air) is called the radon emanation factor or the escape/production ratio (E/P) ratio, and has a value between 0 and 1. If the E/P ratio for a given waste form is 0, no radon ever escapes the matrix; if it is 1, all radon escapes. A dense solid matrix such as metal, crystal, or glass could have a low E/P ratio, and a fine powder or surface contamination would have a relatively high value.

9.3 Waterborne Radionuclide Transport

Water enters the modeled system as infiltration from meteoric waters (precipitation) at the embankment cell surface, and as groundwater below the ground surface. The approach to modeling different groundwater zones is discussed in Section 7.1.1 . This section focuses on the transport of radionuclides within that water system. For many contaminants waterborne transport is influenced by geochemical processes.

While the radiogeochemistry of contaminant transport is in reality exceedingly complex, it is typically simplified for the purposes of PA. A full geochemical model considers the mineralogy of neighboring geological materials and the full geochemical makeup of water, on a highly refined scale. It considers the speciation and complexation of ions, which is especially involved for those cations with multiple valence states, such as uranium and plutonium. It considers the formation and transport of colloids, and the fine-scale adsorption of chemical species onto sediment particles and fracture coatings. For the PA modeling, the geochemistry of contaminant transport in groundwater is approached at the macro scale, and a few key concepts are assumed

to account for all the small-scale variation. A simple equilibrium sorption model using soil/water partition coefficients or K_ds is used to model the partitioning process. While simplified, the K_d approach is conservatively representative of the solid-water partitioning process and is in common usage in PA models. The K_d model assumes that a given constituent dissolved in the water (e.g. uranium) has some propensity to sorb to the solid phase of a porous medium, while maintaining some presence dissolved in the aqueous phase as well. The definition of the solid/water distribution coefficient, with units of mL/g (or sometimes m^3/kg) is:

$$K_d = \frac{mass\ of\ constituent\ sorbed\ on\ a\ unit\ mass\ of\ solid\ (g/g)}{mass\ of\ constituent\ within\ a\ unit\ volume\ of\ water\ (g/mL)}. \quad (1)$$

The sorption is assumed to be instantaneously reversible and independent of concentration. That is, no dynamics are accounted for, and the ratio is always simply linear—a constituent's concentration in water is always the same ratio with respect to its sorbed concentration onto the solid, and it takes no time for the change between solid or liquid phases to occur. This is the linear isotherm assumption, and is commonly employed.

Aqueous solubility, however, places limits on the amount of a constituent that can be dissolved in the water phase. Each chemical species (in this case, each chemical element, including all isotopes) has a limit as to how much of that chemical can exist in the water phase. Solubility is expressed in moles per unit volume of water (typically mol/L), where one mole is Avogadro's number of atoms (or molecules). If, then, the solubility of uranium were 1 mol/L, one liter of water could hold one mole of uranium, which could be a mix of U-235, U-236, U-238, or other isotopes. Any attempt to add uranium to the water will result in the precipitation of uranium.

The K_d model expressed in Equation 1 is applied only when the solubility limit for a given constituent is not in effect. This is a particularly important point to keep in mind when modeling the leaching of a concentrated waste form, such as uranium oxides. At first, the leaching is likely to be solubility-limited with respect to uranium, and the leachate will migrate away with uranium at the solubility limit. Eventually, as enough uranium is removed from the source, the leachate concentration will be limited only by K_d, and will be less and less concentrated until the source is depleted. This occurs for all other elements as well, though the synergistic effect of various similar chemicals (e.g. other heavy metals like plutonium and lead) is not modeled.

Note that partitioning and solubility are independent of isotopic variation, as the radiological aspect of contaminants does not enter into their chemistry. That is, isotopes all behave identically, chemically speaking. U-234, U-235 and U-238 are isotopes, and therefore compete together for sorption sites, or for aqueous solubility. A model that considers U-235 and U-238 in separate simulations cannot couple these effects, and may produce inaccurate results, especially in the presence of solubility limitations. GoldSim recognizes the concept of isotopes, and accounts for their interrelated chemical behavior.

9.4 Airborne transport

As discussed in the section on modeling the natural environment (Section 7.1.3), the two distinct types of airborne transport include diffusion in the air-filled pore spaces of porous media, and

dispersion above the ground surface by wind. Radiological aspects of these processes are discussed below.

9.4.1 Diffusion Through Porous Media

Diffusion within porous media, in either air or water, is driven by concentration gradients. Diffusion is mediated by diffusion coefficients, and it follows tortuous paths through the specific medium. Partitioning between air and water phases also occurs, which adds to the number of simultaneous equations to be solved.

The principal radionuclides of interest in the modeling of DU waste are the isotopes of radon, since radon, a noble gas, is the only radionuclide to be found in a gaseous form. The parents and progeny of radon isotopes are of interest as well. Radon has several isotopes that occur in the various actinide decay series, including: Rn-217, -218, -219, -220, and -222 (see Figures 8 and 10). Radon isotopes with half-lives ranging from milliseconds to just under 1 minute quickly undergo decay to polonium and therefore can travel no appreciable distance. Radon-222, however, has a half-life of just under 4 days, and is able to migrate for some distance by diffusion in interstitial air before it, too, decays to polonium. When regulations such as DOE's Radioactive Waste Management Order 435.1 address radon ground surface flux as a performance objective, Rn-222 is the isotope of concern.

Since Rn-222 is a direct descendent of U-238 and U-234, and hence Th-230 and Ra-226, it will be generated anywhere in the environment that Ra-226 occurs. As the radium migrates into the embankment cell cap, either by diffusion in the water phase or translocation by biotic processes (see Section 9.5), it provides a source for Rn-222 in more locations than just the disposed waste. This form of translocation and transport is accounted for in the modeling.

A phenomenon unique to the production and release of radon is the E/P ratio, introduced in Section 9.2.3 with respect to release from the waste form. If, however, the Ra-226 parent is present in other locations, such as cap materials or surface soils, radon will be in water or adsorbed onto solids, rather than bound in some crystalline matrix. The E/P ratio in the environment is assumed to be 1, and thereby all of the decay of Ra-226 outside the waste form results in Rn-222 that is available for transport.

Radon readily partitions into both air and water, per its Henry's Law constant (K_H) and exhibits preference for the water phase. For this reason, wet soils are much better at attenuating radon migration than dry soils. To mitigate the diffusion of radon through the engineered cap, the layering within the cap design includes a substantial layer of clay. Clay has a low permeability to air and to water, and also can maintain a high moisture content, which retards the migration of radon as it partitions into soil (Ota et al., 2007). The effectiveness of this clay radon barrier, however, depends on its resistance to degradation by erosion and biotic processes. Cracks, fissures, animal burrows, and plant roots can all provide fast diffusion pathways that reduce the effectiveness of the radon barrier.

Diffusion in the porous medium air phase, as well as the water phase, is implemented in the Clive DU PA Model through diffusive flux links between all GoldSim Cells in a column, from the atmosphere to the water table.

9.4.2 Atmospheric Dispersion

The basic modeling of atmospheric dispersion is covered in Section 7.1.3.2 . The only effect of radon and radionuclides attached to particles that is related to radioactive processes is that during transport, as in other transport pathways, radionuclides undergo radioactive decay and in-growth. For the purposes of this model, however, the assumption is made that atmospheric transport is sufficiently fast relative to rates of decay that no decay need be accounted for during the transport.

9.5 Biotically-Induced Transport

Plants and fossorial (burrowing) animals have the potential to move radioactive material in addition to the more commonly implemented waterborne and airborne transport pathways. The full conceptual model of biota at the site is discussed in Section 7.1.4 , and the relevance to radionuclide transport is discussed here.

9.5.1 Transport via Plants

Plants obtain many nutrients and minerals from the soil, through root uptake. Some chemical species are preferred over others, and this preference differs between plant species, as does the effectiveness of uptake. This selective uptake is coupled with radioactive decay and in-growth. Plants are conceived to selectively absorb chemical species from the soils, with roots exposed to different soil layers and thus different suites of chemicals at various depths. The absorbed radionuclides, then, are distributed evenly within the plant tissues, both above-ground and below-ground.

When the plant dies, the below-ground parts return radionuclides to whatever soil layer they are in, and the above-ground plant parts all return their constituents to the top layer of soil.

9.5.2 Burrowing Animals

Burrowing animals include various mammals, reptiles, and insect species. They move bulk soil from the depths where they construct burrows directly to the ground surface. Bulk soil includes soil and any interstitial water and air, and all radionuclides contained in the volume that the animals remove.

After a burrow is abandoned, it eventually collapses, moving bulk soils back down from the surface, in accordance with the volume excavated. This preserves the mass balance of soil in the soil column. The overall effect of this burrowing activity is a consistent churning of the soil layers (bioturbation). This effect may be surprisingly deep, with ant nests having been observed to penetrate over 4 meters (~13 ft) below the ground surface at another western radioactive waste disposal site (see Section 7.1.5).

10 Modeling Dose and Risk to Humans

Evaluation of radiation dose (with implied risk) to potential human receptors is a requirement of the PA. The individual dose assessment addresses potential radiation dose to any member of the public who may come in contact with radioactivity released from the disposal facility into the general environment (10 CFR 61.41). Radiation dose limits for protection of the general population are defined in 10 CFR 61.41. Design, operation, and closure of the land disposal

facility must also ensure protection of any individual inadvertently intruding into the disposal site and occupying the site or contacting the waste at any time after loss of active institutional control of the site (10 CFR 61.42). Because the definition of inadvertent intruders encompasses exposure of individuals who engage in normal activities without knowing that they are receiving radiation exposure (10 CFR 61.2), there is no practical distinction made in the dose assessment between any MOP and inadvertent intruders with regard to modeling radiation dose for protection of the general population.

Protection of inadvertent intruders from the consequences of disturbing disposed waste can involve two principal controls: 1) institutional control over the site after operations by the site owner to ensure that no such occupation or improper use of the site occurs, or 2) designating which waste could present an unacceptable risk to an intruder, and disposing of this waste in a manner that provides some form of intruder barrier that is intended to prevent contact with the waste (10 CFR 61.7(3)).

The objective of modeling annual radiation dose to an individual in a radiological PA is to provide estimates of potential doses to humans, in terms of an "average" member of the critical group, from radioactive releases from a disposal facility after closure, as described in Section 3.3.7 of NUREG-1573, *A Performance Assessment Methodology for Low-Level Radioactive Waste Disposal Facilities* (NRC, 2000). As described below, the critical groups in this PA are defined as Ranchers, Sport OHVers, and Hunters. An "average" member of such a group may be considered as either a statistical construct, or more subjectively as simply a hypothetical individual whose behavioral and physiological attributes do not place them on either the lower of higher extreme of the range of possible individual doses.

NUREG-1573 describes two aspects of dose modeling: First, the mechanisms of radionuclide transfer through the biosphere, to humans, needs to be identified and modeled. This is termed the pathway analysis. Second, the dosimetry of the exposed individual must be modeled. This is termed the individual dose assessment.

Pathway analysis, as defined in NUREG-1573, results in the determination of the total intake of radionuclides by the average member of the critical group. The critical group is defined as the group of individuals reasonably expected to receive the greatest dose from radioactive releases from the disposal facility over time, given the circumstances under which the analysis would be carried out. Modeling of radionuclide transport by plants and animals, and of human activities, is captured within the scope of this pathway analysis. The dosimetry component of the dose modeling refers to estimation of the effective dose equivalent from internal radiation dose following radionuclide intake, and from external radiation dose.

In order to estimate collective doses for the purpose of determining whether disposal options satisfy ALARA, a population needs to be assessed. A population is comprised of multiple individuals, so individual doses need to be added over some period of time to estimate the collective dose. The 'answer', at the end of the performance period (10,000 years post-closure, in this case) might then be the individual annual doses added up over a period of 10,000 years. Although there is no collective dose performance metric that currently exists, this analysis may be useful in the context of comparing how one site or disposal option might perform compared to another.

10.1 Period of Performance

No specific time frame is defined in 10 CFR 61 for the dose assessment. In the context of inadvertent human intrusion, Section 61.42 states,

> "Design, operation, and closure of the land disposal facility must ensure protection of any individual inadvertently intruding into the disposal site and occupying the site or contacting the waste *at any time* after active institutional controls over the disposal site are removed." (emphasis added.)

Proposed modifications to UAC Rule R313-25-8 are more specific, requiring a PA for DU to have a minimum compliance period of 10,000 years, with additional simulations for a qualitative analysis for the period where peak hypothetical dose occurs. The estimation of doses at such long time frames is tenuous at best, but if total radioactivity is used for a proxy, accounting for decay and ingrowth from the disposed DU, then a peak value would occur once the progeny of U-238 have reached secular equilibrium in about 2.1 million years.

The scope of this PA is to model the disposal system performance to the time of peak hypothetical radiological dose (or peak radioactivity, as a proxy), but to quantify dose only within the regulatory time frame of 10,000 yr. This approach is consistent with the proposed amendments to UAC R313-25-8(2).

10.2 Site Characteristics and Assumptions

Key land use characteristics and assumptions for the Clive facility that pertain to the development of receptor scenarios and dose modeling are summarized in the Site Description (Section 3).

As addressed in *FEP Analysis for Disposal of Depleted Uranium at the Clive Facility*, the distinction between deliberate and inadvertent intrusion for this PA is based on the motive underlying the activity. Intrusive activities not related to a deliberate attempt to excavate materials underlying the protective cover will be considered inadvertent. The performance objectives of 10 CFR 61.43 specifically address protection of individuals from the consequences of inadvertent intrusion after active institutional controls are removed. Because deliberate intrusion at the site is omitted from the performance objectives, whereas inadvertent intrusion is specifically mentioned, modeling of dose resulting from deliberate intrusion into the disposal site is not included in this PA. Therefore, radiation doses due to intrusion based on motives such as archeology, sabotage, or waste retrieval for constructive or malicious reasons, are not evaluated.

10.3 Receptor Scenarios

Potential activities of interest for this model are based on the predominant present day uses of the general area as identified in the FEP analysis: ranching and recreation. Other scenarios that are often considered for PAs, including agriculture and homesteading, are not applicable for the Clive site for reasons described below. There are other populations that might be exposed at locations remote from the disposal embankment, such as drivers along Interstate 80, a resident caretaker at the Aragonite rest area off I-80, rail workers and riders, and workers at the Utah Test and Training Range. Although these receptors are likely exposed for short amounts of time

and/or at lower concentrations compared to ranchers and recreationists, these off-site receptors will also be evaluated in the PA model.

From a regulatory perspective, two categories of receptors require consideration. These are often labeled "member of the public" (MOP) and "inadvertent human intruder" (IHI). Both categories are described in related guidance: the MOP essentially as a receptor who resides at the boundary of the facility, and the IHI as someone who directly contacts the waste (e.g., by well drilling, or basement construction). There is no historical evidence of non-transient human activities in the near vicinity of Clive, however, other than current activities and a temporary maintenance camp at the nearby railroad over 50 years ago. Furthermore, while the area in which the site is located is zoned for hazardous waste disposal by Tooele County, the lack of potable water makes the surrounding area an unlikely location for other residential, commercial, or industrial developments (Baird et al., 1990). Consequently, an IHI or MOP receptor as described in regulatory guidance is extremely unlikely. Therefore, consideration will be given to ranching and recreational scenarios to describe plausible human activities under current conditions. The potential for these human activities to result in inadvertent human intrusion will also be considered.

10.3.1 Ranching Scenario

The land surrounding the disposal facility is used for cattle and sheep grazing (NRC, 1993; BLM, 2010). Leases are administered by the BLM, and are generally up to 6 months in length, from autumn to spring. The ranching exposure scenario includes exposure to radionuclides that have entered the available environment due to natural processes described in the transport model. Receptors may be directly exposed while working upon or in the vicinity of the disposal unit. Evaluation of potential radiation dose in this scenario is partially dependent upon assumptions regarding the nature of plant community succession on the disposal unit over time. Because ecological succession on the disposal unit over time could potentially result in grazing habitat upon the disposal unit, a variety of potential future plant community assemblages are evaluated in the PA model.

Inputs for developing exposure parameter values under the ranching scenario include information on the characteristic activities of ranch hands and restrictions related to BLM leases for ranching. Activities are expected to include herding, maintenance of fencing and other infrastructure, and assistance in calving and weaning. The primary exposure pathways for the ranching scenario include incidental ingestion of soil, inhalation, external irradiation, and ingestion of beef from cattle grazing in contaminated areas. Exposure to respirable particulates may occur from natural wind disturbance of surface soil as well as mechanical disturbance due to rancher use of off-highway vehicles (OHVs) for transportation within the impacted area.

10.3.2 Recreational Scenario

The recreational exposure scenario encompasses receptors such as hunters and recreational OHV riders on, or in the vicinity of, the disposal unit. Based upon discussions with the BLM and reasonable judgment regarding anticipated land use, all recreational activities are likely to involve some OHV use and may encompass sport OHV riding, hunting, target shooting of

inanimate objects, rock-hounding, wild-horse viewing, looking for ghost towns, and limited camping. The recreational scenario evaluated in the PA model includes two distinct receptor groups:

1. "Sport OHVers" who use their vehicles primarily for recreation and who may visit the area as either a day trip or by camping overnight; and,
2. "Hunters" who, in addition to purely recreational visits, also visit the area for the purpose of hunting game and who may also visit the area as either a day trip or by camping overnight.

The desirability of recreational activities on or around the Clive facility is, like suitability for ranching, dependent on assumptions regarding ecological succession at the Clive facility over time. With the possible exception of OHV use and use of the cap as a vantage point for hunting, recreational uses of Clive facility in an as-closed state of bare rip rap surfaces is likely to be minimal. As soil develops on the cap and plant succession proceeds, the Clive facility may become more attractive for activities such as camping and therefore support higher exposure intensity.

The primary exposure pathways for the Sport OHV scenario modeled in the PA (described in more detail below) include incidental ingestion of soil, inhalation, and external irradiation. The Hunter scenario includes these same pathways and adds ingestion of game meat from animals grazing in contaminated areas. Exposure to respirable particulates is evaluated for both natural wind disturbance of surface soil as well as mechanical disturbance due to Sport OHV and Hunter use of OHVs for transportation within the impacted area.

10.3.3 Remote Off-Site Receptors

The ranching and recreation scenarios are characterized by potential exposure related to activities both on the disposal site and in the adjoining area. Specific off-site points of potential exposure also exist for other receptors based upon present-day conditions and infrastructure. Unlike ranching and recreational receptors who may be exposed by a variety of pathways, these off-site receptors are likely to be exposed solely to wind-dispersed contamination, for which inhalation exposures are likely to predominate. The remote locations and receptors for which inhalation exposures are evaluated in the PA model include:

- Travelers on Interstate-80, which passes 4 km to the north of the site;
- Travelers on the main east-west rail line, which passes 2 km to the north of the site;
- Workers at the Utah Test and Training Range (a military facility) to the south of the Clive facility, who may occasionally drive on an access road immediately to the west of the Clive facility fenceline;
- The resident caretaker at the east-bound Interstate-80 rest facility (Aragonite [Grassy Mountain]) approximately 12 km to the northeast of the site, and,
- Recreational OHVers at the Knolls OHV area (BLM land that is specifically managed for OHV recreation) 12 km to the west of the site.

10.4 Transport Pathways

Various considerations should be taken into account when analyzing the transport of radionuclides through the biosphere to humans. Pathway identification is discussed in various literature sources, such as Volume 1 of NUREG/CR-5453 (NRC, 1989) and NUREG-1200 (NRC, 1994), and NUREG-1573 (NRC, 2000). Components of the disposal system that can affect transport include aspects of the source term and engineered barriers. Principal transport media at many low-level waste disposal sites include groundwater, surface water, and air (NRC, 2000).

Pathways that will be evaluated for the protection of exposed individuals from releases of radioactivity include those related to air (gas diffusion, air dispersion, and aeolian erosion of soil), soil (contaminant migration via upward flux from subsurface soil, deposition of wind-borne material), groundwater (groundwater flow, geochemical effects, radon emanation), surface water (water erosion leading to gullies, infiltration), plants (uptake of contaminants in the waste, engineered cap, or soil), and animals (exhumation by burrowing). . Exposure media subsequently affected by transport processes include air, surface soil, plants, game, and livestock. Figure 11 depicts the conceptual model for contaminant transport at the Clive facility.

The transport processes figure depicts those processes relating contaminant release mechanisms to environmental media that are the subject of the dose assessment. Many of these transport pathways may not be complete or may not contribute sufficiently to exposures to warrant explicit modeling.

10.5 Exposure Pathways

Exposure pathways describe the activities and exposure routes between the environmental media described in Section 7 and human receptors in the ranching and recreation exposure scenarios. The primary exposure routes related to radionuclides in environmental media include ingestion, inhalation, and external irradiation.

The ingestion exposure route may pertain to inadvertent ingestion of contaminated soil at either on-site or off-site locations for the ranching and recreation scenarios. In addition to incidental ingestion of soil, ingestion of meat containing radionuclides taken up from contaminated soil by grazing animals is possible. Ingestion of meat from livestock grazing on or around the Clive facility is characterized in the Ranching scenario. Ingestion of hunted meat from pronghorn grazing in the region of the Clive facility is characterized for the Hunter receptor in the recreational scenario.

The inhalation exposure route consists of the inhalation of either gas-phase radiological contaminants or of respirable particulates originating from contaminated soil. The inhalation exposure route is evaluated for both the ranching and recreational scenarios. Concentrations of respirable particulates in air is assessed as a function of both wind erosion and mechanical disturbance from the use of OHVs for all potential receptors.

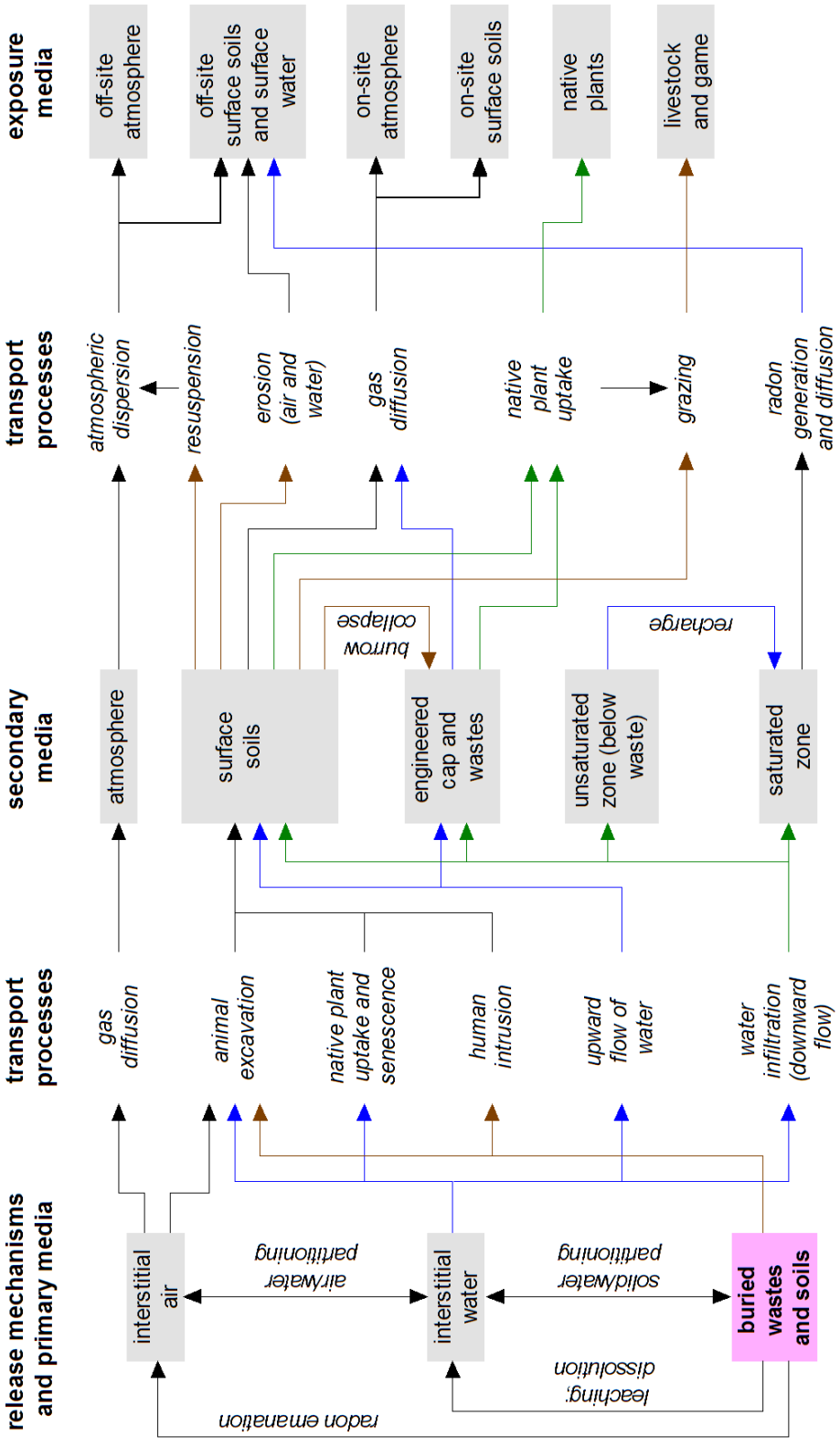

Figure 11. Conceptual model for contaminant transport at the Clive facility

External irradiation refers to the external exposure to a radiological source such as contaminated surface soil (a two-dimensional source) or air (a three-dimensional source). External irradiation from contaminated soil may occur when a receptor travels across the ground surface during either ranching or recreational activities. Atmospheric immersion occurs when a receptor is exposed to external irradiation via bodily immersion in contaminated air. Atmospheric immersion is tied to the gaseous diffusion and air dispersion transport pathways, and is a viable exposure route for both the ranching and recreational scenarios.

10.6 Risk Assessment Endpoints

Title 10 CFR 61.41 specifies assessment endpoints related to radiation dose. The specific metrics described in §61.41 are organ-specific doses, and restrict the annual dose to an equivalent of 0.25 mSv (25 mrem) to the whole body, 0.75 mSv (75 mrem) to the thyroid, and 0.25 mSv (25 mrem) to any other organ of any member of the public. However, as described below, the dose assessment for the PA will employ a total effective dose equivalent (TEDE) for comparison with the 0.25-mSv/yr threshold.

As discussed in Section 3.3.7.1.2 of NUREG-1573 (NRC, 2000), the radiation dosimetry underlying these dose metrics was based on a methodology published by the International Commission on Radiation Protection (ICRP) in 1959. More recent dose assessment methodology has been published as ICRP Publication 30 (ICRP, 1979) and ICRP Publication 56 (ICRP, 1989), employing the TEDE approach. The TEDE uses weighting factors related to the radiosensitivity of each target organ to arrive at an effective dose equivalent across all organs. The text of Section 3.3.7.1.2 of NUREG-1573 (NRC, 2000) states

> "As a matter of policy, the Commission considers 0.25 mSv/year (25 mrem/year) TEDE as the appropriate dose limit to compare with the range of potential doses represented by the older limits... Applicants do not need to consider organ doses individually because the low value of TEDE should ensure that no organ dose will exceed 0.50 mSv/year (50 mrem/year)."

Radiation dose conversion factors (DCFs) applicable for calculating the TEDE are published by DOE, EPA, and the ICRP. Section 3.3.7.3 of NUREG-1573 specifies DCFs published by EPA in Federal Guidance Reports 11 (EPA, 1988) and 12 (EPA, 1993). EPA subsequently made use of age-specific DCFs published in ICRP Publication 72 (ICRP, 1996) to compute radionuclide cancer slope factors in Federal Guidance Report 13 (EPA, 1999). DCFs published in Federal Guidance Report 13 are employed in this PA where possible.

DU waste can also be associated with toxicological risks that are independent of radioactive properties. Unlike carcinogenic agents, EPA typically views toxicants with non-cancer effects as having thresholds; i.e., levels below which effects would be unlikely. Reference doses (RfDs) essentially amount to such thresholds, usually with several layers of 'safety' factors added. The basic modeling process for evaluating uranium toxicity is very similar to that conducted for radionuclides, except that kidney toxicity (as opposed to radiation dose) of DU is evaluated, and the toxicity of DU does not change over time (as radioactive decay is not important in this context).

11 Summary

This CSM describes the dynamic systems model that will be implemented for the Clive DU PA. The CSM describes the regulatory environment that constrains the PA, and the technical components that transport radionuclides associated with the DU waste to the accessible environment. Transport starts with characterization of the waste, and continues with release of radionuclides from the waste, migration through the engineered barriers system that initially confines the waste, fate and transport through the local environment to the accessible environment where human receptors might be exposed, including radioactive decay and ingrowth through time and space. The dynamic systems model will be implemented using the GoldSim systems modeling platform, which facilitates fully-coupled dynamic systems modeling and is ideally suited to performing radiological performance assessments. The modeling will be performed in a probabilistic manner so that uncertainties are fully captured and global sensitivity analysis can be performed in order to identify the critical parameters. Consideration will be given to spatio-temporal scaling and correlation in the modeling, so that input probability distributions are properly specified. For some inputs to the model (e.g., radon diffusion, water content in the unsaturated zone, erosion of the cover) process-level models may be developed and then abstracted into the GoldSim systems-level model so that these model components are fully integrated into the overall model.

The modeling effort will be split into two overlapping but distinct time frames of primary interest. The regulatory compliance period for the first time frame is 10,000 years, requiring a quantitative model that predicts radioactive dose to potential receptors. For this model, current conditions of society and the environment will be projected into the future. Potential receptors of interest for this model are based on present day use of the general area, as discussed in Section 10.3 , including ranching, hunting, and recreation.

The second modeling time frame will consider much longer term consequences of disposal of DU waste at Clive, since peak radioactivity of the DU waste occurs beyond 2 million years into the future. This model will overlap the short term assessment in that it will share many of the same modeling components, such as waste inventory, source release, and fate and transport through the local environment. However, this model will consider changes in the general environment that might effect major changes in the environmental conditions of Clive. For example, climate change is inevitable within this time frame, so its consequences will be considered. Earth is in a glacial epoch, consisting of long glacial periods interspersed with shorter interglacial periods. For example, the current interglacial period is one in which the population of the human race has expanded to unprecedented levels. This interglacial period is likely to continue for tens of thousand of years. However, based on the historical record, return of a glacial period is inevitable. Based on geological evidence, the return of a glacial period will probably result in the re-formation of a large lake covering most of northwestern Utah, so lake recurrence is included in this model. Human exposure scenarios, however, will not be evaluated that far into the future, because receptor scenarios cannot be defensibly developed and the consequences of radioactive dose cannot be reasonably understood that far into the future. Many changes in climate will have occurred within the next 2.1 My, the period over which it takes DU to reach secular equilibrium. During such a long time frame there is likely to be massive disruption in human society and changes in human evolution. Consequently, instead of

attempting to model dose to hypothetical human receptors that far into the future, the spatial distribution and concentrations of radionuclides that might migrate from the disposal cells to the environment will be modeled. The processes by which the radionuclides might move around , include the formation of large lakes and the return to lower lake levels once the lake subsides again. Consideration will also be given to the potential effects of wave action at the Clive facility as the lake forms.

This two-tiered approach is consistent with the requirements of the Utah regulations to perform fully quantitative modeling for 10,000 years, and qualitative modeling until peak activity. Consequently, these two models will be used together to support the required regulatory analysis of DU waste disposal at the Clive facility.

12 References

Code of Federal Regulations, Title 10, Part 61 (10 CFR 61), *Licensing Requirements for Land Disposal of Radioactive Waste*, Government Printing Office, 2007.

Code of Federal Regulations, Title 40, Part 191 (40 CFR 191), *Environmental Radiation Protection Standards for Management and Disposal of Spent Nuclear Fuel, High-Level and Transuranic Radioactive Waste*, Government Printing Office, 1993.

Adrian Brown (Adrian Brown Consultants), 1997a. *Volume I, LARW Infiltration Modeling Input Parameters and Results*, Report 3101B.970515, 15 May 1997.

Arthur, W.J. and O.D. Markham, 1983. "Small Mammal Soil Burrowing as a Radionuclide Transport Vector at a Radioactive Waste Disposal Area in Southeastern Idaho," *J. Environ. Qual.* 12: 117–122.

Asmerom, Y., Polyak, V. J., and S. J. Burns, 2010. "Variable winter moisture in the southwestern United States linked to rapid glacial climate shifts," *Nature Geoscience* 3: 114-117.

Baird, R. D., Bollenbacher, M. K., Murphy, E. S., Shuman, R., and R. B. Klein, 1990. *Evaluation of the Potential Public Health Impacts Associated with Radioactive Waste Disposal at a Site Near Clive, Utah*. Rogers and Associates Engineering Corporation, Salt Lake City Utah.

Beals, D., S.P. LaMont, J.R. Cadieux, C.R. Shick, Jr., and G. Hall, 2002. *Determination of Trace Radionuclides in SRS Depleted Uranium*, WSRC-TR-2002-00536, Westinghouse Savannah River Company, Aiken, SC, 19 November 2002.

Berger, A., 1988. "Milankovitch Theory and Climate," *Reviews of Geophysics*, 26(4): 624-657.

Berger, A. and M. F. Loutre, 2002. "An exceptionally long interglacial ahead?" *Science*, 297: 1287-1288.

Blank, R.R., Young, J.A., Trent, J.D., and D.E. Palmquist, 1998. "Natural History of a Saline Mound," *Great Basin Naturalist*, 58(3): 217-230.

BLM (U.S. Bureau of Land Management). 2010. Rangeland Administration System. U.S.

Blom, P.E., 1990. *Potential Impacts of Radioactive Waste Disposal Situations by the Harvester Ant, Pogonomyrmex salinus Olsen (Hymenoptera: Formicidae)*. A thesis for degree of Masters of Science. Regents of the University of Idaho, Moscow, ID. 198 pp.

Bogen, K.T., "A Note on Compounded Conservatism", *Risk Analysis*, 14 (4) , pp. 379 – 381, August 1994

Brimhall W. H. and L. B. Merritt, 1981. "The Geology of Utah Lake – Implications for Resource management," *Great Basin Naturalist Memoirs*, 5: 24-42.

Brodeur, J. R., 2006. *Mixed Low-Level Radioactive and Hazardous Waste Disposal Facilities, Energy Sciences and Engineering*, Kennewick, Washington.

Clark, P. U., Dyke, A. S., Shakun, J. D., Carlson, A. E., Clark, J., Wohlfarth, B., Mitrovica, J. X., Hostetler, S. W., and A. M. McCabe, 2009. "The Last Glacial Maximum," *Science*, 325: 710-714.

Cullen, A. C., "Measures of Compounding Conservatism in Probabilistic Risk Assessment", *Risk Analysis*, 14 (4) , pp. 389 – 393, August 1994

Currey, D.R., G. Atwood, and D.R. Mabey, *Map 73 Major Levels of Great Salt Lake and Lake Bonneville*, Utah Geological and Mineral Survey, Salt Lake City, UT, May 1984

Davis, O.K., and T.E. Moutoux, 1998. "Tertiary and Quaternary Vegetation History of the Great Salt lake, Utah, USA." *J. Paleolimnology*, 19: 417-427.

DOE (U.S. Department of Energy), 1999. M*aintenance Guide for U.S. Department of Energy Low-Level Waste Disposal Facility Performance Assessments and Composite Analyses*, U.S. DOE, 10 November 1999

DOE, 2004a. *Final Environmental Impact Statement for Construction and Operation of a Depleted Uranium Hexafluoride Conversion Facility at the Paducah, Kentucky, Site*, DOE/EIS-0359, U.S. DOE Environmental Management, June 2004.

DOE, 2004b. *Final Environmental Impact Statement for Construction and Operation of a Depleted Uranium Hexafluoride Conversion Facility at the Portsmouth, Ohio, Site*, DOE/EIS-0360, U.S. DOE Environmental Management, June 2004.

Driscoll, N. W. and G. H. Haug, 1998. "A Short Circuit in Thermohaline Circulation: A Cause for Northern Hemisphere Glaciation," *Science*, 282: 436-438.

Energy*Solutions*, 2008. *Bulk Waste Disposal and Treatment Facilities Waste Acceptance Criteria*, Rev. 7, Clive, Utah.

Energy*Solutions*, 2009a. Energy Solutions Clive Facility, *EnergySolutions License Amendment Request: Class A South/11e.(2) Embankment, Revision 1*, 9 Jun 2009, Clive, Utah.

Energy*Solutions*, 2009b. *Radioactive Waste Profile Record*, EC-0230, Rev. 7, plus attachments (Form 9021-33), Clive, Utah.

Energy*Solutions*, 2009c, *LLRW and 11e.(2) Construction Quality Assurance/Quality Control Manual, rev 24e*, Energy*Solutions*, Salt Lake City, Utah, 16 September 2009

Envirocare, 2000. *Assessment of Vegetative Impacts on LLRW*, Salt Lake City, Utah, November 2000.

Envirocare 2004. *Revised Hydrogeologic Report for the Envirocare Waste Disposal Facility Clive, Utah*, Version 2.0, Salt Lake City Utah, August 2004.

Envirocare, 2005. *Cover Test Cell Data Report Addendum: Justification to Change EZD from 18-inches to 24-inches*. Attachment to letter dated October 13, 2005 from Daniel B. Shrum, Director of Safety and Compliance, Envirocare of Utah, LLC, to Dane L. Finefrock, Executive Secretary, Division of Radiation Control.

EPA (U.S. Environmental Protection Agency), 1988. *Limiting Values of Radionuclide Intake and Air Concentration and Dose Conversion Factors for Inhalation, Submersion, and Ingestion*, EPA 520/1-88-020, Federal Guidance Report (FGR) 11.

EPA, 1993. *External Exposure to Radionuclides in Air, Water, and Soil*, EPA 402-R-93-81, FGR 12.

EPA, 1999. *Cancer Risk Coefficients for Environmental Exposure to Radionuclides: Updates and Supplements*, EPA 402-R-99-001, FGR 13.

EPA, 2001. *Risk Assessment Guidance for SuperFund: Volume III, Part A, Process for Conducting Probabilistic Performance Assessment*. EPA 540-R-02-002, December 2001.

EPICA (European Project for Ice Coring in Antarctica). 2004. Eight glacial cycles from and Antarctic ice core. *Nature*. 429, 623-628.

Fitzner, R.E., K.A. Gano, W.H. Rickard, and L.E. Rogers, 1979. *Characterization of the Hanford 300 Area Burial Grounds: Task IV - Biological Transport,* PNL-2774, Pacific Northwest Laboratory, Richland, Washington. Pp. 24–27.

Fussell, G.M, and D. L. McWhorter, 2002. *Project Plan for the Disposition of the SRS Depleted, Natural, and Low-Enriched Uranium Materials*. WSRC-RP-2002-00459, Washington Savannah River Site, November 21, 2002.

Gano, K.A., D.W. Carlile and L.E. Rogers, 1985. *A Harvester Ant Bioassay for Assessing Hazardous Chemical Waste Sites,* Pacific Northwest Laboratory, Battelle Memorial Institute, Richland, Washington. 19 pp., appendices.

Groenveld, D.P., 1990. *Shrub Rooting and Water Acquisition in Threatened Shallow Groundwater Habitats in the Owens Valley, California*. Symposium on Cheatgrass Invasion, Shrub Die-off, and Other Aspects of Shrub Biology and Management. pp. 221-236, in: U.S. Dept. Agr. General Technical Report INT-267. Intermountain Research Station, Ogden, Utah.

GTG (GoldSim Technology Group), 2010. *GoldSim: Monte Carlo Simulation Software for Decision and Risk Analysis*, `http://www.goldsim.com`

Guzowski, R.V., 1990. *Preliminary Identification of Scenarios That May Affect the Escape and Transport of Radionuclides From the Waste Isolation Pilot Plant, Southeastern New Mexico*, SAND89-7149, Sandia National Laboratories, Albuquerque, NM.

Guzowski, R.V., and G. Newman, 1993, *Preliminary Identification of Potentially Disruptive Scenarios at the Greater Confinement Disposal Facility, Area 5 of the Nevada Test Site*, SAND93-7100, Sandia National Laboratories, Albuquerque, NM.

Hakonson, T.E., J.L. Martinez, and G.C. White, 1982. "Disturbance of a Low-level Waste Burial Site Cover by Pocket Gophers," *Health Physics* 42: 868–871.

Hansen, D.J., and W.K. Ostler, 2003. *Rooting Characteristics of Vegetation Near Areas 3 and 5 Radioactive Waste Management Sites at the Nevada Test Site,* DOE/NV/11718-595, U.S. Department of Energy National Nuclear Security Administration Nevada Site Office, 125 pp.

Hart, W. S., Quade, J., Madsen, D. B., Kaufmann, D. S., and C. G. Oviatt, 2004. "The $^{87}Sr/^{86}Sr$ Ratios of Lacustrine Carbonates and Lake-level History of the Bonneville Paleolake System," *GSA Bulletin*, 116: 1107-1119.

Haug, G. H. and R. Tiedemann, 1998. "Effect of the Formation of the Isthmus of Panama on Atlantic Ocean Thermohaline Circulation," *Nature*, 393: 673-676.

Hays, J. D., Imbire, J., and N. J. Shackleton, 1976. "Varitations in the Earth's Orbit: Pacemaker of the Ice Ages," *Science*, 194: 1121-1132.

Hetzel, R. and A. Hampel, 2005. "Slip rate variations on normal faults during glacial-interglacial changes in surface loads," *Nature*, 435: 81-84.

Holmgren. R.C. and S.F. Brewster, 1972. *Distribution of Organic Matter Reserve in a Desert Shrub Community,* Paper INT-130, U.S. Dept. Agr. Forest Serv. Research, Intermountain Forest and Range Experiment Station, Ogden, Utah.

ICRP (International Commission on Radiation Protection), 1979. ICRP Publication 30 *Limits for Intakes of Radionuclides by Workers*, Ann. ICRP 2(3-4), 1979.

ICRP, 1984. ICRP Publication 30. *Cost-Benefit Analysis in the Optimization of Radiation Protection*. Ann ICRP. 1983;10(2-3):1-75.

ICRP, 1989. ICRP Publication 56 *Age-Dependent Doses from Intakes of Radionuclides: Part 1*, Ann. ICRP 20(2), 1989.

ICRP, 1996. ICRP Publication 72 *Age-Dependent Doses to Members of the Public from Intake of Radionuclides, Part 5: Compilation of Ingestion and Inhalation Dose Coefficients*, Ann. ICRP 26(1), 1996. P 072 errata in SG 03 JAICRP 32 (1-2).

Johnson R. 2010. State of Utah, DEQ. Memo – April 6, 2010 Subj. Savannah River Depleted Uranium Sampling

Laundré, J.W., 1993. "Effects of Small Mammal Burrows on Water Infiltration in a Cool Desert Environment," *Oecologia,* 94: 43–48.

Laundré, J.W. and T.D. Reynolds, 1993. "Effects of Soil Structure on Burrowing Characteristics of Five Small Mammal Species," *Great Basin Naturalist* 53(4): 358–366.

Lavigne, R.J. ,1969. "Bionomics and Nest Structure of *Pogonomyrmex occidentalis* (Hymenoptera: Formicidae)," *Ann. Ent. Soc. Am*. 62: 1166–1175.

Link, P. K., Kaufman, D. S., and G. D. Thackray, 1999. *Field guide to Pleistocene lakes Thatcher and Bonneville and the Bonneville Flood, southeastern Idaho*, in Hughes, S. S. and G. D. Thackray (eds.), *Guidebook to the Geology of Eastern Idaho*, Idaho Museum of Natural History, pp. 251-266.

Lowe, J. J. and M. J. C. Walker, 1997.*Reconstructing Quaternary Environments*, 2nd Edition. Prentice Hall, London, 446 pp.

MacKay, W.P., 1981. "A Comparison of the Nest Phenologies of Three Species of *Pogonomyrmex* Harvester Ants (Hymenoptera: Fomicidae)," *Psyche* 88: 25–74.

Mandel, R.D. and C.J. Sorenson, 1981. "The Role of the Western Harvester Ant (*Pogonomyrmex occidentalis*) in Soil Formation," *Soil Sci. Soc. Am. J.* 46: 785–788.

Meinzer, O.E., 1927. *Plants As Indicators of Groundwater*, United States Department of Interior Geological Survey Water Supply Paper 577. Washington, D.C.

National Research Council, 2005. *Risk and Decisions*, National Academies Press, Washington, DC, 2005.

NEA (Nuclear Energy Agency), 1992, *Systematic Approach to Scenario Development. A Report of the NEA Working Group on the Identification and Selection of Scenarios for Performance Assessment of Radioactive Waste Disposal*, Nuclear Energy Agency, Paris, France.

NEA, 2000. *Features, Events, and Processes (FEPs) for Geologic Disposal of Radioactive Waste. An International Database*. Nuclear Energy Agency, Organization for Economic Cooperation and Development.

Nevo, E., 1999. *Mosaic Evolution of Subterranean Mammals: Regression, Progression and Global Convergence*. Oxford University Press, Oxford England. 413 pp.

NRC (U.S. Nuclear Regulatory Commission), 1982. *Final Environmental Impact Statement on 10 CFR Part 61 Licensing Requirements for Land Disposal of Radioactive Waste*, NUREG-0945, Nuclear Regulatory Commission, Washington, DC, November 1982.

NRC, 1989a. *Methodology, Identification of Potential Exposure Pathways*, NUREG/CR-5453, Nuclear Regulatory Commission, Washington, DC.

NRC, 1993. *Final Environmental Impact Statement to Construct and Operate a Facility to Receive, Store, and Dispose of 11e.(2) Byproduct Material Near Clive, Utah*, NUREG-1476, Nuclear Regulatory Commission, Washington, DC.

NRC, 1994. *Standard Review Plan for the review of a license application for a Low-Level Radioactive Waste Disposal Facility*, NUREG-1200, Rev. 3, Nuclear Regulatory Commission, April 1994.

NRC, 2000. *A Performance Assessment Methodology for Low-Level Radioactive Waste Disposal Facilities*, NUREG-1573, Nuclear Regulatory Commission, Washington, DC, October 2000.

NRC, 2005. In the Matter of Louisiana Energy Services (National Enrichment Facility), CLI-05-10, Docket 70-3103-ML, Nuclear Regulatory Commission, Washington, DC, October 19, 2005.

NRC, 2008. Response to Commission Order CLI-05-20 Regarding Depleted Uranium, SECY-08-0147, Nuclear Regulatory Commission, Washington, DC.

NRC, 2009a. Memorandum, Staff requirements – SECY-08-0147 – Response to commission order CLI-05-20 regarding depleted uranium, Nuclear Regulatory Commission, Washington, DC, March 18, 2009.

NRC, 2009b. *NRC News*, No. 09-052, Nuclear Regulatory Commission, Washington, DC, March 18, 2009.

NRC, 2010. "Stages of the Nuclear Fuel Cycle," U.S. Nuclear Regulatory Commission website, `http://www.nrc.gov/materials/fuel-cycle-fac/stages-fuel-cycle.html`

ORNL. 2000. *Strategy for Characterizing Transuranics and Technetium Contamination in Depleted UF6 Cylinders*, ORNL/TM-2000/242, Oak Ridge National Laboratory, October 2000.

Ota, M., Iida, T., Yamazawa, H., Nagara, S., Ishimori, Y., Sato, K., and T. Tokizawa, 2007. "Suppression of Radon Exhalation from Soil by Covering with Clay-mixed Soil," *Journal of Nuclear Science and Technology*, 44(5): 791-800.

Oviatt, C. G., 1997. Lake Bonneville fluctuations and global climate change. Geology, 25(2): 155-158.

Oviatt, C. G., Thompson, R. S., Kaufman, D. S., Bright, J., and R. M. Forester, (1999). "Reinterpretation of the Burmester Core," Bonneville Basin, Utah, *Quaternary Research*, 52, 180-184.

Paillard, D., 2001. Glacial cycles: toward a new paradigm, *Reviews of Geophysics*, 39(3): 325-346.

Paillard, D., 2006. "What drives the Ice Age cycle?" *Science*, 313: 455-456.

Rich, B.L., S.L. Hinnefeld, C.R. Lagerquist, W.G. Mansfield, L.H. Munson, E.R. Wagner, and E.J. Vallario, 1988. *Health Physics Manual of Good Practices for Uranium Facilities*, EGG-2530, Idaho National Engineering Laboratory, Idaho Falls, ID, June 1988.

Robinson, T.W., 1958. *Phreatophytes*. United States Department of Interior Geological Survey Water Supply Paper 577, Washington, D.C.

Rundel, P.W., and P.S. Nobel, 1991. "Structure and Function in Desert Root Systems," In: D. Atkinson (Ed.), *Plant Root Growth: An Ecological Perspective,* Special Publication #10 of the British Ecological Society. Blackwell Scientific Pub. London, England. Pp. 349-378.

Smallwood, K.S., M.L. Morrison, and J. Beyea, 1998. Animal Burrowing Attributes Affecting Hazardous Waste Management. *Environmental Management,* 22(6): 831–847.

Smith, E.D., R.J. Luxmoore, and G.W. Suter, II, 1997. *Natural Physical and Biological Processes Compromise the Long-Term Performance of Compacted Soil Caps*, Barrier Technologies for Environmental Management: Summary of a Workshop. National Academy of Sciences, 1997.

SWCA, 2011, *Field Sampling of Biotic Turbation of Soils at the Clive Site, Tooele County, Utah*, SWCA Environmental Consultants, Salt Lake City, Utah, January 2011.

Utah, State of, 2010, Utah Administrative Code Rule R313-15. *Standards for Protection Against Radiation*. As in effect on March 1, 2010. (`http://www.rules.utah.gov/publicat/code/r313/r313-015.htm`, accessed 17 Mar 2010)

UWQB (State of Utah, Division of Water Quality, Utah Water Quality Board), 2010. *Ground Water Quality Discharge Permit No. 450005*, 23 Dec 2010.

Whetstone (Whetstone Associates, Inc.), 2000. *Revised Envirocare of Utah Western LARW Cell Infiltration and Transport Modeling*, Lakewood, Colorado, 19 July 2000.

Whetstone, 2006. *EnergySolutions Class A Combined (CAC) Disposal Cell Infiltration and Transport Modeling Report*, Salt Lake City Utah, May 2006.

Neptune and Company Inc.

June 1, 2011 Report for EnergySolutions

Clive DU PA Model, version 1

Appendix 3

Embankment Modeling

Embankment Modeling for the Clive DU PA Model

28 May 2011

Prepared by

Neptune and Company, Inc.

This page is intentionally blank, aside from this statement.

CONTENTS

FIGURES

TABLES

1.0 Summary of Parameter Values

The parameters that define the characteristics of the Class A South embankment at the Clive facility are summarized in Table 1. Following this summary are sections describing the basis for these values. Of principal interest to the model are the interior dimensions of the volume occupied by waste, and the thicknesses of the various layers in the engineered cover.

Table 1. Summary of embankment engineering parameters

parameter	value	units	reference / comment
average original grade elevation	4272	ft amsl*	USGS (1973) see §4.1 below
elevation of top of the waste at the ridgeline	4317.25	ft amsl	EnergySolutions (2009) see eq. (1) in §3.1.1
elevation of top of the waste at the break in slope	4299.20	ft amsl	EnergySolutions (2009) see eq. (2) in §3.1.1
average elevation of the bottom of the waste	4264.17	ft amsl	EnergySolutions (2009) see eq. (3) in §3.1.1
average elevation of the bottom of the clay liner	4262.17	ft amsl	see eq. (6)(3) in §3.1.2
length overall	1429.6	ft	EnergySolutions (2009) see eq. (4) in §3.1.1
width overall	1775.0	ft	EnergySolutions (2009) see eq. (5) in §3.1.1
length from edge to the break in slope	153.2	ft	EnergySolutions (2009) see §3.1.1
width from edge to the break in slope	152.1	ft	*ibid*.
length along the ridge	542.1	ft	*ibid*.
type A rip rap thickness	18	in	EnergySolutions (2009) see Table 2
type B rip rap thickness	18	in	*ibid*.
type A filter zone thickness	6	in	*ibid*.
sacrificial soil thickness	12	in	*ibid*.
type B filter zone thickness (top slope only)	6	in	*ibid*.
type B filter zone thickness (side slope only)	18	in	*ibid*.
5×10^{-8} cm/s radon barrier clay thickness	12	in	*ibid*.
1×10^{-6} cm/s radon barrier clay thickness	12	in	*ibid*.
clay liner thickness	24	in	Whetstone (2000) see end of §3.1.2

* above mean sea level

2.0 Introduction

The safe storage and disposal of depleted uranium (DU) waste is essential for mitigating releases of radioactive materials and reducing exposures to humans and the environment. Currently, a radioactive waste facility located in Clive, Utah (the "Clive facility") operated by the company Energy*Solutions* Inc. is being considered to receive and store DU waste that has been declared surplus from radiological facilities across the nation. The Clive facility has been tasked with disposing of the DU waste in a manner that protects humans and the environment from future radiological releases.

To assess whether the proposed Clive facility location and containment technologies are suitable for protection of human health, specific performance objectives for land disposal of radioactive waste set forth in Utah Administrative Code (UAC) Rule R313-25 *License Requirements for Land Disposal of Radioactive Waste - General Provisions* must be met—specifically R313-25-8 *Technical Analyses*. In order to support the required radiological performance assessment (PA), a probabilistic computer model has been developed to evaluate the doses to human receptors and concentrations in groundwater that would result from the disposal of radioactive waste, and conversely to determine how much waste can be safely disposed at the Clive facility. The GoldSim systems analysis software (GTG, 2010) was used to construct the probabilistic PA model.

The site conditions, chemical and radiological characteristics of the wastes, contaminant transport pathways, and potential human receptors and exposure routes at the Clive facility that are used to structure the quantitative PA model are described in the conceptual site model documented in the white paper entitled *Conceptual Site Model for Disposal of Depleted Uranium at the Clive Facility* (Clive DU PA CSM.pdf).

The purpose of this white paper is to address specific details relating to the dimensional components of the Class A South (CAS) section of the Federal Cell, located at the Clive facility. This paper is organized to give a brief overview of where the CAS section is located at the Clive facility followed by a description of the parameters and calculations used to estimate the various dimensional components of the CAS embankment.

This probabilistic PA takes into account uncertainty in many input parameters, but the dimensions of the CAS embankment are not considered to be uncertain. Given that the disposal cell is carefully designed and constructed, any uncertainty in its dimensions is considered insignificant. Stochastic representation of parameters is reserved for those values about which there is uncertainty.

3.0 Physical Dimensions

The Clive DU PA model considers only a single embankment. For the purposes of this PA, only the CAS section of the Federal Cell is considered for disposal (Figure 1).

3.1 Class A South Embankment Dimensions

The CAS embankment, or cell, is the western fraction of the Federal Cell (Figure 1). The eastern section is occupied by the 11e.(2) cell, which is dedicated to the disposal of uranium processing by-product waste, but not considered in this analysis. A stylized drawing of the CAS and its relationship to the 11e.(2) cell is shown in Figure 2.

The general aspect of the CAS embankment is that of a hipped cap, with relatively steeper sloping sides nearer the edges. The upper part of the embankment, known as the top slope, has a moderate slope, while the side slope is markedly steeper (20% as opposed to 2.4%). These two distinct areas, shown in different colors in Figure 2, are modeled separately in the Clive DU PA model. Each is modeled as a separate one-dimensional column, with an area equivalent to the embankment footprint. The embankment is also constructed such that a portion of it lies below-grade (Figure 2).

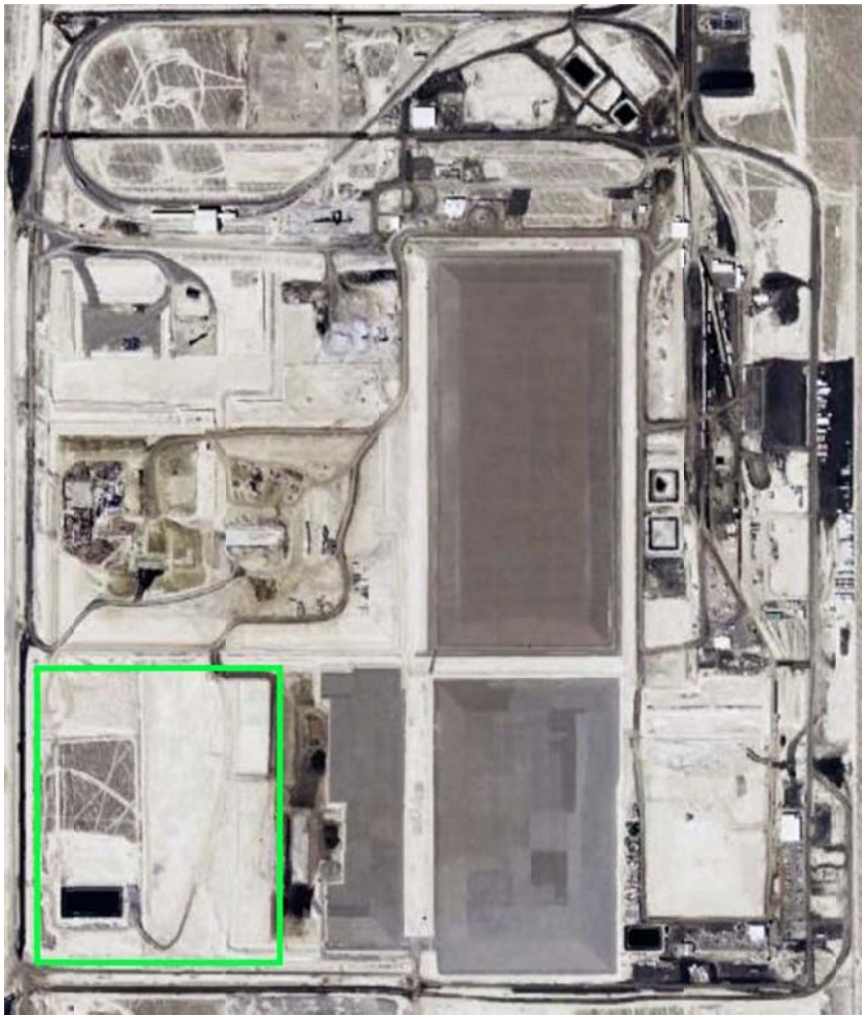

Figure 1. The Clive Facility, with the location of the Class A South embankment outlined in green. This orthophotograph is roughly 1 mile across, and north is up.

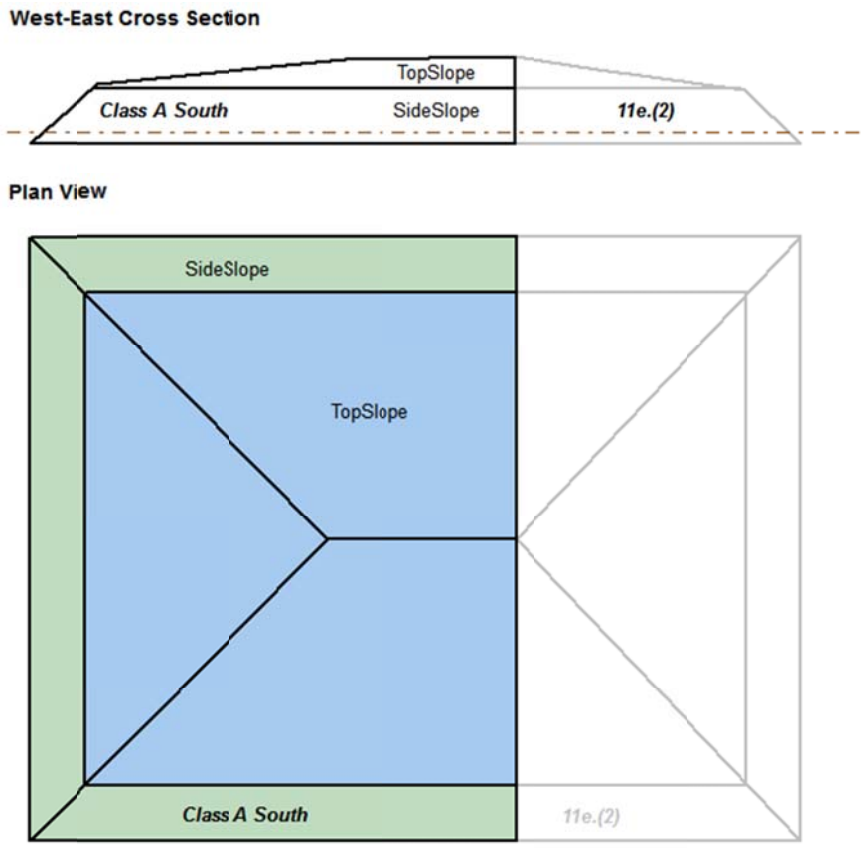

Figure 2. Section and Plan views of the Class A South embankment, with top slope shown in blue and side slope in green. The brown dotted line in the West-East Cross section represents below-grade (below the line) and above-grade (above the line) regions of the embankment.

3.1.1 Class A South Embankment Interior Waste

The Clive DU PA model requires information about embankment dimensions to be able to determine the footprint areas and the volumes of waste within each area. From this, an average thickness of the waste is determined, since the 1-D column has but one thickness over its entire area. All dimensions provided in this white paper are with respect to the waste itself, and do not include the liner or cover materials. The dimensions of interest that are used in the Clive DU PA model are shown in Figure 3. The values of the dimensions shown in Figure 3 are derived from various engineering drawings in Energy*Solutions* (2009) which are herein referred to in this white paper as drawings 07021 V1, 07021 V3, and 07021 V7. These drawings are all reproduced from Energy*Solutions* (2009) in Figures 4 through Figure 6.

As shown in the engineering drawings, the exact dimensions of the CAS are somewhat irregular, with a gently sloping bottom and ridge line. The shape of the cell has been somewhat idealized to facilitate calculations, and it is assumed to have a horizontal floor and ridge line. Elevations for

the top of the waste are derived from drawing 07021 V1 (Figure 4), which has the note "*1. All elevations shown are for top of waste...*". Elevation of the bottom of waste is derived from drawing 07021 V3 (Figure 5). Details on each of these values are provided below.

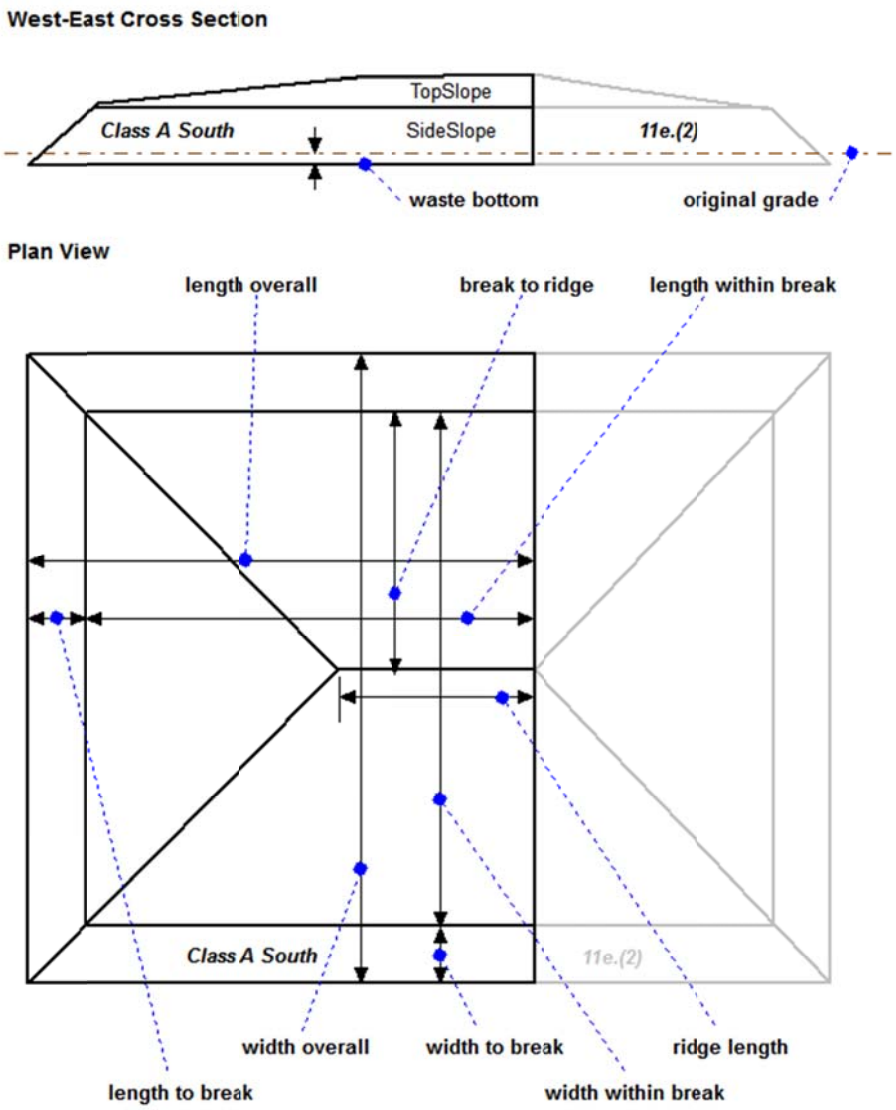

Figure 3. Dimensions of the Class A South embankment that are used in the Clive DU PA model.

Elevation of the top of the waste at the ridge line: This is calculated as an average of the values from drawing 07021 V3 (Figure 5), West-East Cross Section A, accounting for the 2-ft thick radon barrier. The thickness of the radon barrier, 24 in. (2 ft) is shown in the CAS top slope and CAS side slope sections of drawing 07021 V7 (Figure 6). The top of the radon barrier at the west peak is at 4318.80 ft, so the top of the waste is 2 ft lower at an elevation of 4316.80 ft.

Likewise, the top of the radon barrier at the east peak is 4319.70 ft, so the top of the waste is 2 ft lower at an elevation of 4317.70 ft, after adjusting for the thickness of the radon barrier. The average of the west and east peak elevations is:

$$(4316.80 \text{ ft} + 4317.70 \text{ ft}) / 2 = 4317.25 \text{ ft} \quad (1)$$

Elevation of the top of the waste at the slope break: The elevation of the top of the radon barrier derived from the upper drawing 07021 V3 (Figure 5), West-East Cross Section A, is 4301.20 ft. Subtracting the 2-ft thick radon barrier as described above shows the elevation of the top of the waste to be:

$$4301.20 \text{ ft} – 2 \text{ ft} = 4299.20 \text{ ft} \quad (2)$$

Elevation of the bottom of the waste: This is calculated as the average of the values derived from the lower drawing 07021 V3 (Figure 5), West-East Cross Section A. The top of the clay liner is at an elevation of 4262.14 ft at the west end, and 4266.19 ft at the east end, which includes the area under the 11e.(2) section of the Federal Cell. The average of these elevations is:

$$(4262.14 \text{ ft} + 4266.19 \text{ ft}) / 2 = 4264.17 \text{ ft} \quad (3)$$

Length (east-west) overall: The overall length of the CAS is the sum of the values derived from drawing 07021 V1 (Figure 4). Following along the dimensions shown just below the centerline running west-east, the length is:

$$153.2 \text{ ft} + 734.3 \text{ ft} + 542.1 \text{ ft} = 1429.6 \text{ ft} \quad (4)$$

Width (north-south) overall: The overall width of the CAS is the sum of values from drawing 07021 V1 (Figure 4). Following along the dimensions shown down the centerline running north-south, the width is:

$$152.1 \text{ ft} + 735.4 \text{ ft} + 735.4 \text{ ft} + 152.1 \text{ ft} = 1775.0 \text{ ft} \quad (5)$$

Length from edge to break in slope: This is derived from drawing 07021 V1 (Figure 4) at the western slope which is 153.2 ft.

Width from edge to break in slope: This is derived from drawing 07021 V1 (Figure 4) at the north or south slope which is 152.1 ft.

Length along the ridge: The length along the ridge is derived from drawing 07021 V1 (Figure 4) which is 542.1 ft.

3.1.2 Class A South Cover and Liner Dimensions

The engineered cover designs for the top slope and side slope sections of the CAS are shown in drawing 07021 V7 (Figure 6). The values chosen from the sections labeled "*Class A South Top Slopes*" and "*Class A South Side Slopes*" are summarized in Table 2. The properties of the various layers within the engineered cover and liner are discussed in detail in *Unsaturated Zone Modeling* white paper.

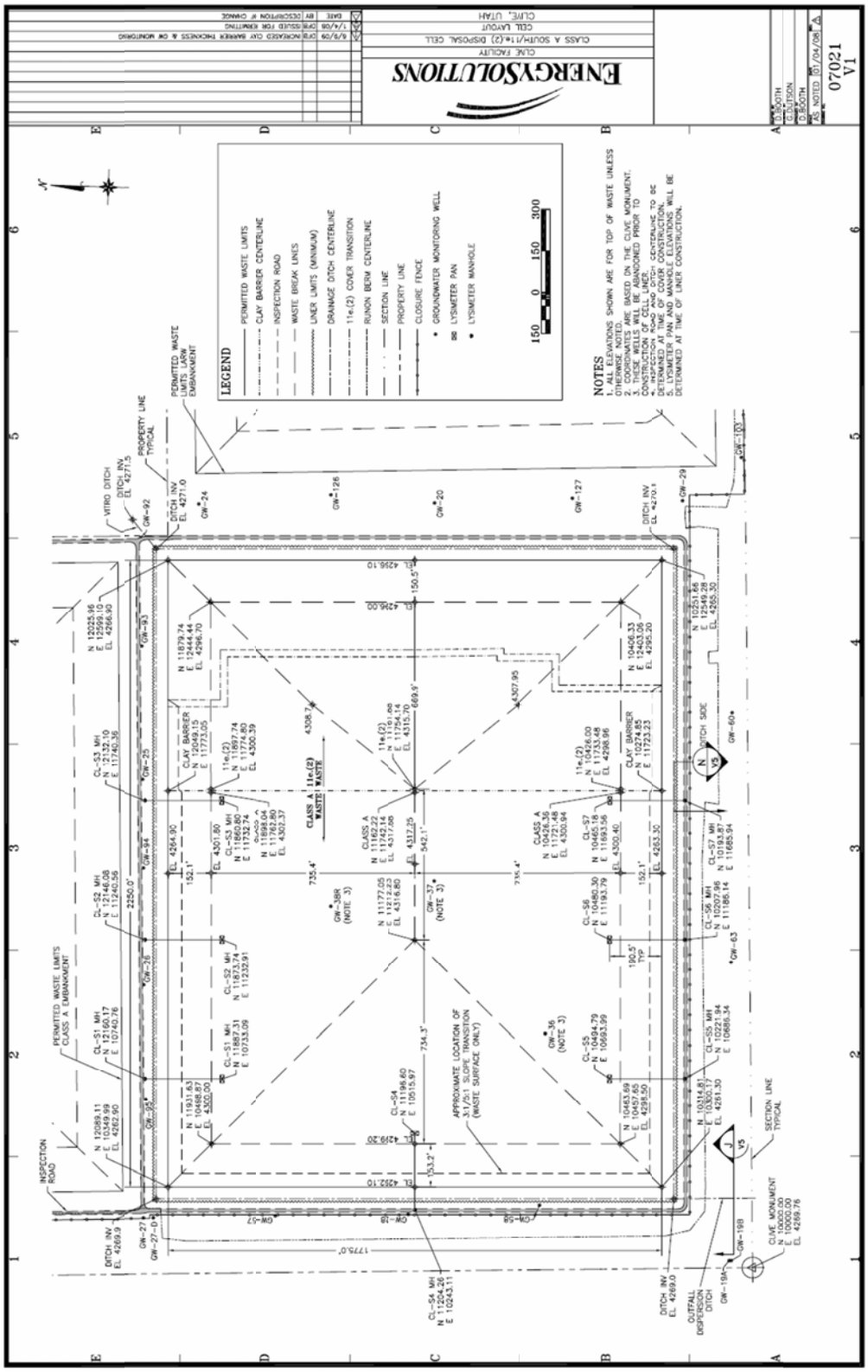

Figure 4. Class A South and 11e.(2) cell engineering drawing 07021 V1

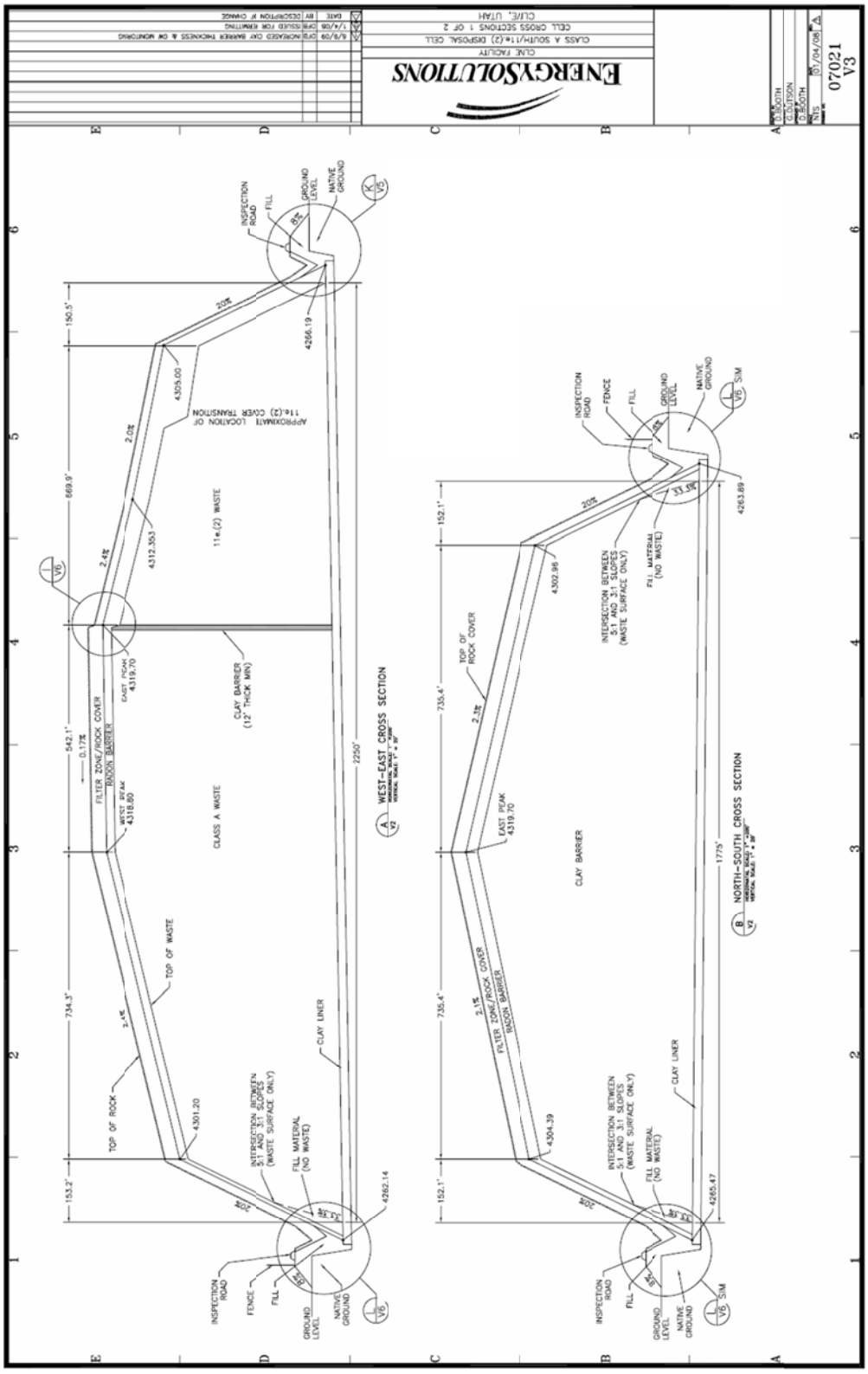

Figure 5. Class A South and 11e.(2) cell engineering drawing 07021 V3

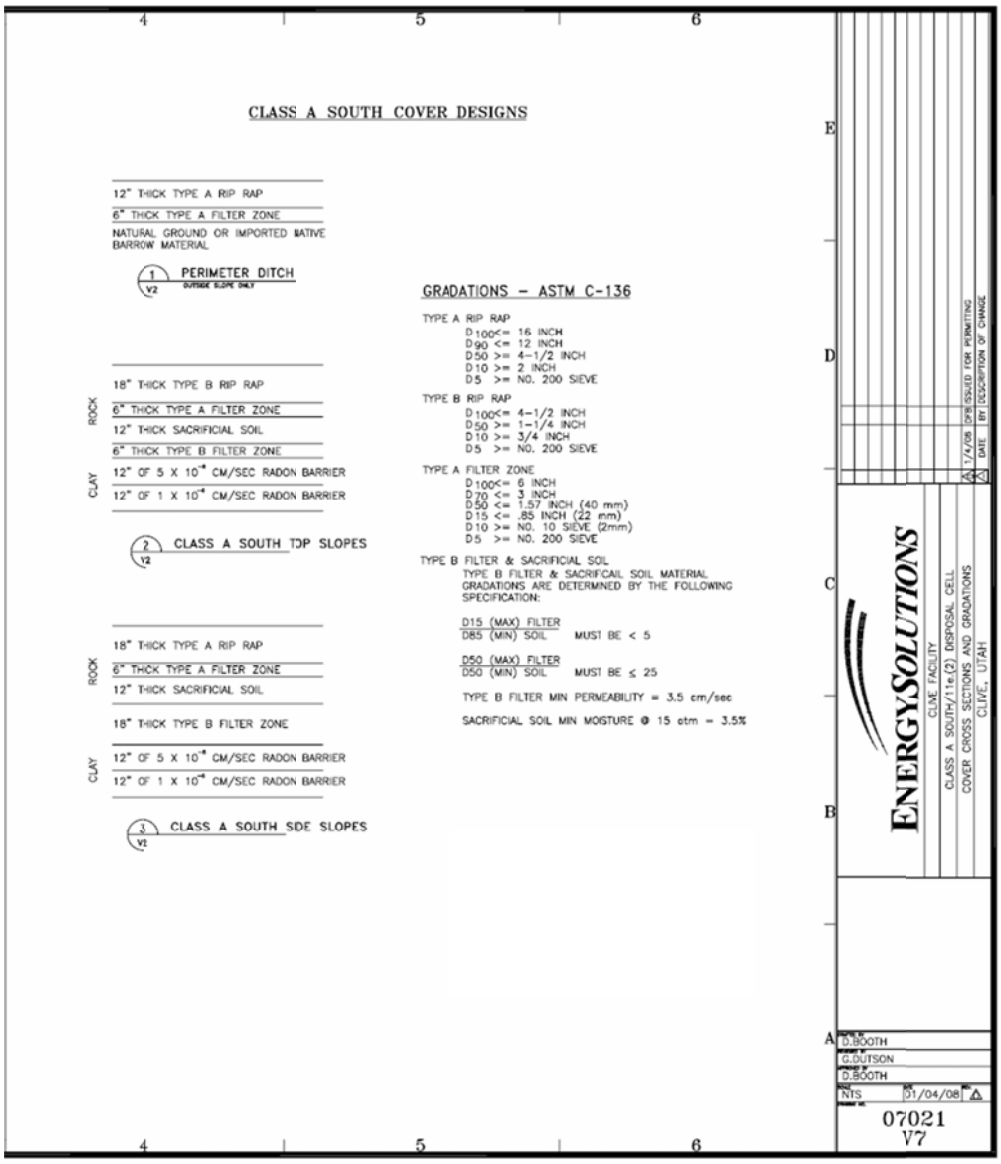

Figure 6. Class A South cell engineering drawing 07021 V7: cap dimensions

Table 2. Cover layer thicknesses for the CAS cell

layer	thickness (in)	
	top slope	side slope
type A rip rap	—	18
type B rip rap	18	—
type A filter zone	6	6
sacrificial soil	12	12
type B filter zone	6	18
5×10^{-8} cm/s radon barrier clay	12	12
1×10^{-6} cm/s radon barrier clay	12	12

The waste layers of the embankment are underlain by a clay liner, as shown in Figure 5, but no thickness is provided in this engineering drawing set. The thickness of the clay liner is defined in a previous modeling report as 24 in (2 ft) (Table 7 in Whetstone, 2000).

Elevation of the bottom of the clay liner: This is calculated simply the average elevation of the bottom of the waste in eq. (3) minus the thickness of the liner. The elevation of the bottom of the clay liner is then is:

$$4264.17 \text{ ft} - 2 \text{ ft} = 4262.17 \text{ ft} \quad (6)$$

Note that this is also the elevation of the top of the unsaturated zone.

4.0 Original Grade Elevation

The original grade is of interest in determining the vertical location of wastes inside the embankment. One might consider any above-ground waste or other material to be erodible, and conversely below-ground portions to be inherently not erodible. It is therefore of interest to determine the disposal volume that lies below grade since placing waste below grade greatly reduces the potential for erosion during lake cycles. Again, only the CAS is considered at this time.

4.1 Class A South Embankment Original Grade

The elevation of the original grade is interpreted from the elevations indicated on a 1:24,000 scale quadrangle map for Aragonite, UT (USGS, 1973). The relevant section of this map as it applies to the CAS embankment is shown in Figure 7. This 1-square mile section, Section 32, is the site of the Clive Facility (Figure 7). The southwest corner of Section 32 is at elevation 4270 ft amsl (above mean sea level) while the ground surface (original grade) slopes gently and fairly uniformly up to the northeastern corner, crossing the 4280-ft amsl contour.

The CAS occupies the southwestern corner of Section 32 (refer to Figure 1), and its center is approximately at an elevation of 4272 ft amsl. This is the value used for original grade of the CAS.

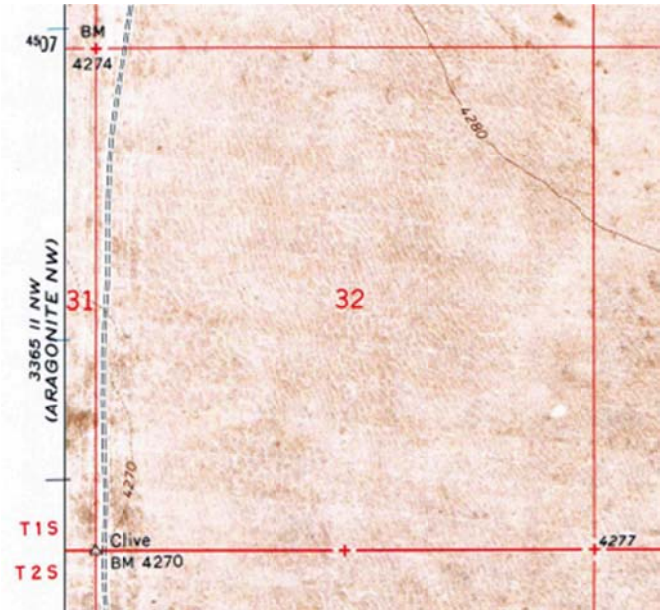

Figure 7. Section 32 within the Aragonite quadrangle, as it appeared in 1973, before construction of the Clive Facility. Note elevation contours at 4270 and 4280 ft amsl. *ARAGONITE NW* is the next quadrangle to the west.

5.0 Implementation in the GoldSim Model

5.1 Representation of the CAS Embankment

The representation of the CAS embankment in the Clive DU PA Model is essentially one-dimensional (1-D), and is therefore necessarily simplified. The top slope and side slope sections of the embankment are modeled as independent 1-D columns, as discussed below. The volumes of waste and each layer of engineered cap and liner are preserved. Since the cap and liner are laterally continuous and do not vary in dimension within a column, the thicknesses in the model correspond directly to thicknesses in the real world. The waste layers, however, are of a shape that changes in the horizontal, and must be rearranged to produce a shape that is a rectangular prism of equal volume to the actual waste volume.

5.1.1 CAS Embankment Dimensions

The dimensions developed in Section 3.1.1 are documented in the model in the container \Disposal\ClassASouthCell\ClassASouth_Cell_Dimensions. The calculation of the waste volumes within the side slope and within the top slope, as identified in Figure 2, is done within the GoldSim model by assembling pieces that have volumes that are easily calculated using basic geometry, as shown in Figure 8. Once the waste volumes for top and side slope are known, the average waste thicknesses are calculated. These are used as the waste thicknesses in the columns within the GoldSim model, as described in the following section.

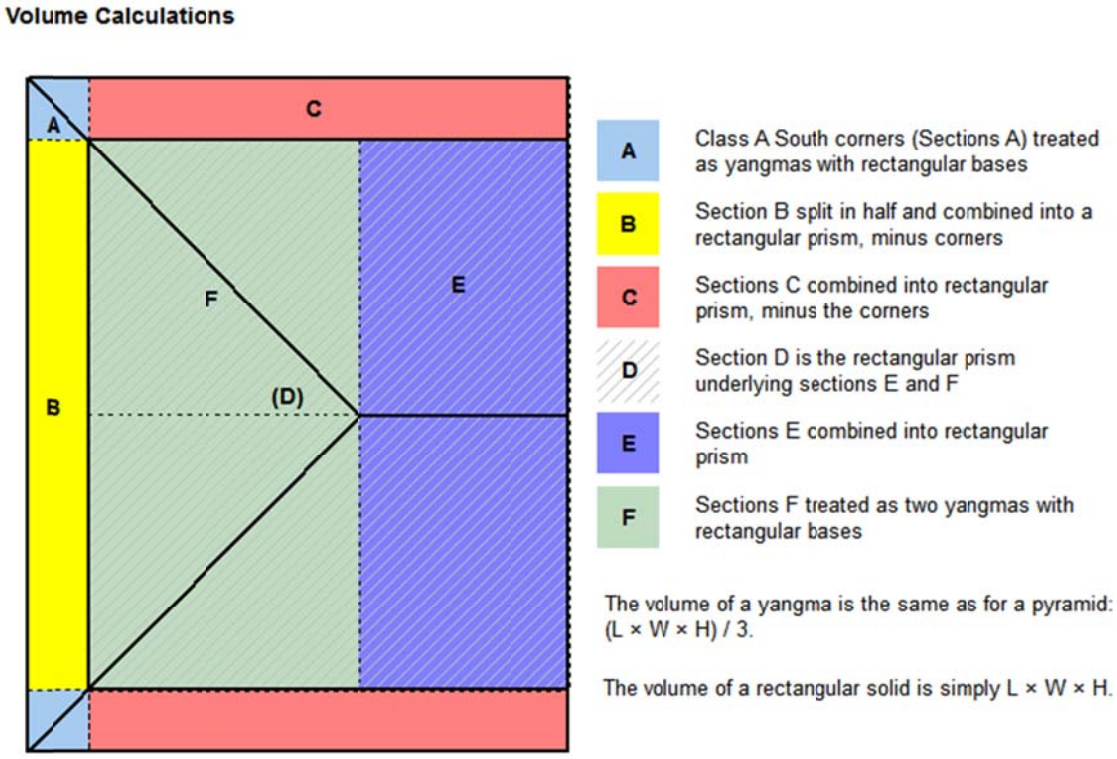

Figure 8. Geometrical deconstruction of the CAS cell waste volumes

5.1.2 CAS Columns

The top slope and side slope columns are modeled in parallel, since they have different waste and cap layer thicknesses. That is, each column has primarily vertical flow of water, with some lateral flows in the cover. Both feed into the unsaturated zone and thence to groundwater at the bottom. The top slope column has a much thicker waste layer than the side slope, and this is reflected in the overall thickness of the two columns. In order to capture the flexibility available in locating waste during disposal operations, the user can select which waste types go where in the top slope column, using the Waste Layering Definition dashboard. No DU wastes are to be disposed in the side slope column in this model. An example of this selection is shown in Figure 9.

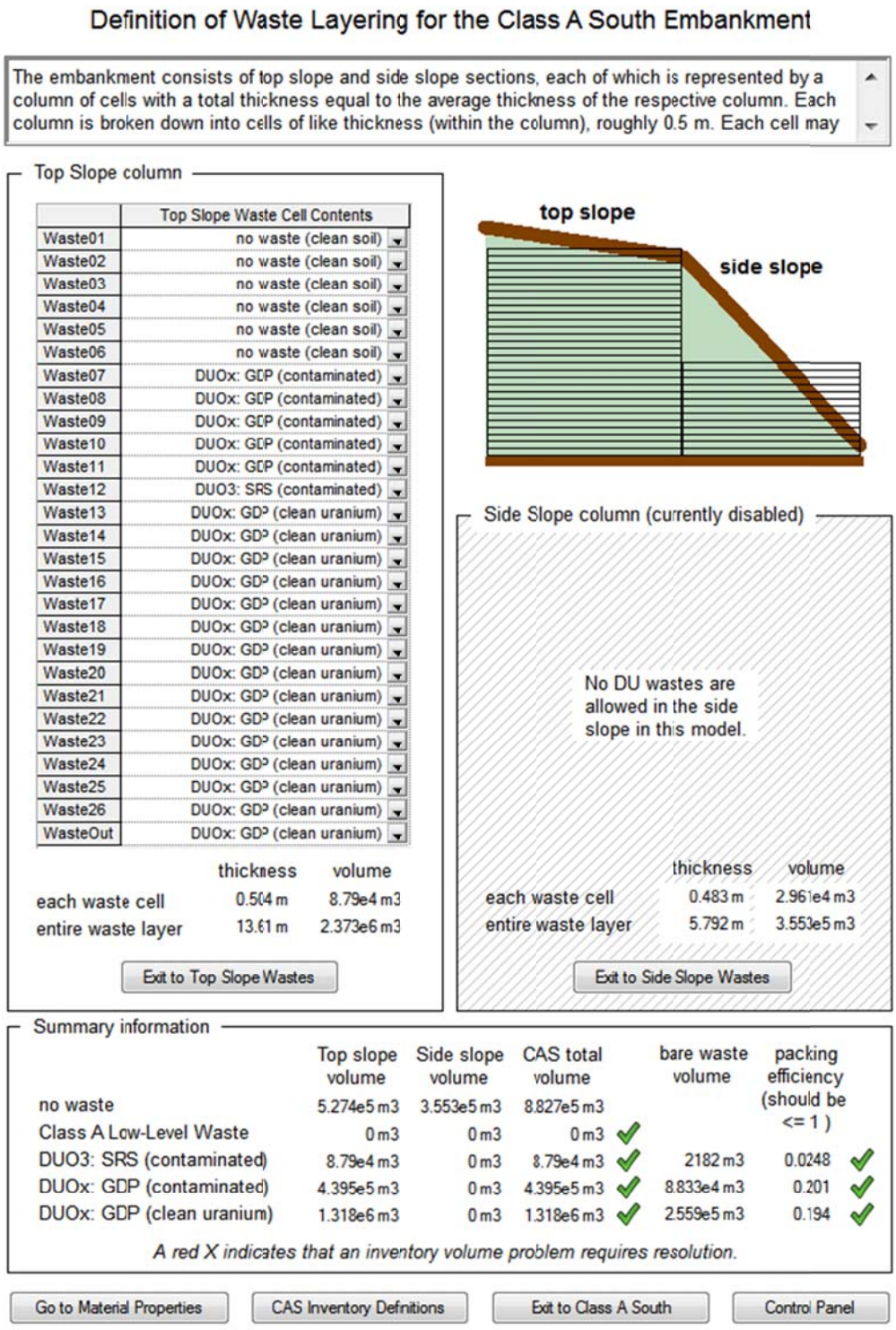

Figure 9. Waste layering definitions within the two columns of the CAS cell

6.0 References

Energy*Solutions*, 2009. *EnergySolutions License Amendment Request: Class A South/11e.(2) Embankment, Revision 1*, 9 June 2009 (file: Class A South-11e.(2) Eng Drawings.pdf)

GTG (GoldSim Technology Group), 2010. *GoldSim: Monte Carlo Simulation Software for Decision and Risk Analysis*, http://www.goldsim.com

USGS (United States Geological Survey), 1973. 1:24,000 topographic quadrangle map for Aragonite, UT, revised 1973 (file: UT_Aragonite_1973_geo.pdf)

Whetstone (Whetstone Associates, Inc.), 2000. Revised Envirocare of Utah Western LARW Cell Infiltration and Transport Modeling (file: 2000, July 19 - Whetstone, Western LARW Cell Infiltration Modeling.pdf)

Implementation of Diffusion in GoldSim

Kate Catlett
John Tauxe
Neptune and Co.
April 2011

Introduction

This paper outlines how diffusion in air and water is to be implemented in GoldSim models that include diffusion in the unsaturated zone. The need for this discussion arises from the assumption in GoldSim that diffusion occurs only in saturated porous media. In the modeling of radioactive waste facilities, we have the definite need to include diffusion in both the air phase (e.g. diffusion of radon from buried wastes to the ground surface) and often in the water phase. These processes can be independently enabled or disabled by setting logical "switches" in the model.

We have tested diffusion-specific models built in GoldSim for consistency with analytical results, and have verified our interpretation of GoldSim's internal calculations, and the appropriateness of our modifications to definitions of diffusive flux.

Diffusion Math

To introduce basic diffusive transport mathematics, we turn to Jury (1991), who provides the following 1-dimensional gas phase conservation (transport) equation:

$$\frac{\partial \theta_a C_g}{\partial t} = -\frac{\partial J}{\partial z} \qquad [1]$$

where

θ_a = volumetric air content (constant in space and time),
C_g = gas concentration in air,
t = time, and
z = the single spatial dimension,

and the diffusive mass flux J is given by

$$J = -D_g^s \frac{\partial C_g}{\partial z} \qquad [2]$$

where the effective diffusion coefficient D_g^s is

$$D_g^s = \tau_a \cdot D \qquad [3]$$

where

τ_a = tortuosity of the air phase and

D = free air molecular diffusion coefficient (also called the free air diffusivity).

Combining equations [1], [2], and [3], we find that

$$\frac{\partial \theta_a C_g}{\partial t} = \frac{\partial}{\partial z}\left(\tau_a \cdot D \frac{\partial C_g}{\partial z} \right) \quad [4]$$

Diffusion in GoldSim

In the GoldSim modeling environment, the flux equation looks like (GoldSim CT manual p. B-4, Eq. B-3):

$$J = D_{cs}\left(C_i - C_j \right) \quad [5]$$

where

J = diffusive mass flux,
D_{cs} = GoldSim's "diffusive conductance",
C_i = concentration in cell i in air (essentially C_g), and
C_j = concentration in cell j in air (essentially C_g).

Note that GoldSim uses the concentration difference, not the gradient, in the fluid medium in question. The gradient is the difference divided by the diffusive length (in GoldSim, this is the sum of the diffusive lengths defined in each adjacent cell). Diffusive conductance is defined as (GoldSim CT manual p. B-5, Eq. B-5):

$$D_{cs} = \frac{A_c}{\dfrac{L_{ci}}{f_{ms} \cdot d_{ms} \cdot t_{Pci} \cdot n_{Pci}} + \dfrac{L_{cj}}{f_{ns} \cdot d_{ns} \cdot t_{Pcj} \cdot n_{Pcj} \cdot K_{nms}}} \quad [6]$$

where

A_c = the bulk cross-sectional area of diffusive mass flux link,
L_{ci} = diffusive length in cell i,
L_{cj} = diffusive length in cell j,
f_{ms} = available porosity for species s in medium m (i.e., the fraction of the pore volume of solid m that is accessible to species s),
f_{ns} = available porosity for species s in medium n (i.e., the fraction of the pore volume of solid n that is accessible to species s),
d_{ms} = diffusivity for species s for fluid m (in cell i),
d_{ns} = diffusivity for species s for fluid n (in cell j),
t_{Pci} = tortuosity for the porous medium in cell i ($t \leq 1$),
t_{Pcj} = tortuosity for the porous medium in cell j ($t \leq 1$),
n_{Pci} = porosity for the porous medium in cell i,
n_{Pcj} = porosity for the porous medium in cell j, and
K_{nms} = partition coefficient between fluid medium n (in cell j) and fluid medium m (in cell i) for species s.

This equation can be greatly simplified if we ignore the "available porosity" factors (let the equal 1) and assume no suspended solids, one porous medium (partition coefficients, porosities and tortuosities are the same) and one fluid medium (diffusivities are the same):

$$D_{cs} = \frac{A\,n\,D\,\tau}{L} \qquad [7]$$

where

A = diffusive area, or bulk cross-sectional area of the porous medium,
n = total porosity of the porous medium,
D = free air diffusivity (same as D above),
τ = tortuosity of the entire pore space in the porous medium, and
L = the sum of the diffusive lengths in adjacent cells i and j.

It is useful to determine at this point exactly where each of these values comes from in GoldSim. The diffusive area and diffusive lengths are provided explicitly to GoldSim in the definition of each diffusive flux link, using Diffusive Fluxes tab in the Cell Pathway Properties dialog box shown in Figure 1.

Diffusion in Partially-Saturated Porous Media

This dialog box also provides for the definition of the porous medium, in this example "Alluvium", which has the properties of porosity and tortuosity as part of its definition as a solid material. It is important to note that the values of porosity and tortuosity used in GoldSim's calculation of diffusive flux are taken from the definition of the solid material, and *GoldSim assumes that the porous medium is saturated with respect to the fluid through which diffusion is occurring*. This assumption is violated for unsaturated conditions. In the current example, we wish to allow diffusion in both Water and Air fluids, so some corrections have to be applied to the values for porosity n and tortuosity τ. Instead of using the Alluvium's defined n and τ, we need to use values appropriate for the fluid of interest. For example, for air, we want to use volumetric air content θ_a instead of n, and air-phase tortuosity τ_a instead of a generalized τ. Since GoldSim is hard-coded to apply the n and τ for the solid material (Alluvium), we need to account for the differences carefully.

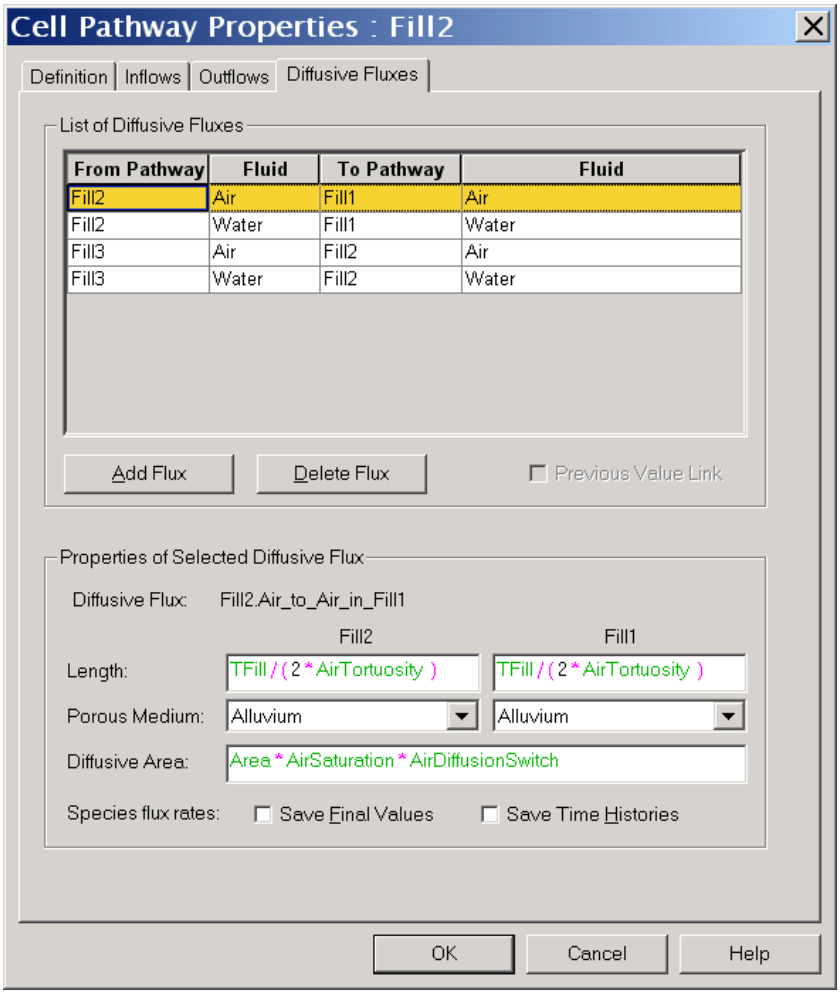

Figure 1. The definition of diffusive flux in GoldSim

In order to use volumetric air content instead of porosity, we insert a multiplicative factor into the definition of the Diffusive Area, so that we get the cross-sectional area of the fluid of interest, rather than the entire porous medium (see Figure 1). GoldSim internally multiplies the Diffusive Area times the Alluvium porosity n, so we must multiply that by the Air phase saturation, S_a, to get

$$D_{cs} = \frac{A S_a n D \tau}{L} \qquad [8]$$

so that GoldSim ends up working with the cross-sectional area of just the Air phase, which is $A\theta_a$:

$$D_{cs} = \frac{A \theta_a D \tau}{L} \qquad [9]$$

An alternative approach would be to define the porosity of the Alluvium to be unity, and correct the Diffusive Area by θ_a rather than by S_a. This approach, however, has

unintended consequences since other processes (such as retardation) use the porosity value defined for Alluvium.

In addition to the area correction to account for partially-saturated media, we need to use an appropriate value for tortuosity. What we want is the tortuosity of the phase in which diffusion occurs, but again, GoldSim assumes saturation and is hard-coded to use the bulk tortuosity defined for the porous medium, Alluvium. In this case, it is simplest to effectively remove the porous medium tortuosity by setting it equal to 1 in the definition of the Alluvium, and to apply fluid-specific tortuosities in the definition of the Diffusive Flux. The logical parameter to modify is the Diffusive Length, since the concept of porosity is one of increased distance of travel that a diffusive species must travel due to its tortuous path through the partially-saturated porous medium. Fortunately, no other processes in GoldSim use the tortuosity value specified for Alluvium, so defining it as unity does not affect other parts of the model.

We have adopted the definition of tortuosity as the straight-line path between points A and B in the porous medium divided by the actual path through the fluid, tortuosity values are always between 0 and 1, with lower values implying more tortuous paths. The corrected Diffusive Length, therefore, is L / τ_a (for Air in this case). This correction can be seen in Figure 1. In effect, GoldSim is then solving the equation (for Air)

$$D_{cs} = \frac{A \theta_a D \tau_a}{L} \qquad [9]$$

For the water phase, the analogous equation is found by substituting θ_w and τ_w for θ_a and τ_a. While values for θ_w and θ_a are simple in concept and derivation, the fluid-specific tortuosities are not. Their derivation is the subject of a discussion below.

Grappling with Tortuosity

Jury (1991) discusses models for estimating air-phase tortuosity from other material properties, such as water content and porosity. In Jury's Table 6.1, the following three models are presented:

Table 1. Air phase tortuosity equations.

equation for air phase tortuosity	reference
$\tau_a = \frac{\theta_a^{10/3}}{n^2}$	Millington and Quirk (1961)
$\tau_a = 0.66^{\theta_a}$	Penman (1940)
$\tau_a = \theta_a^{3/2}$	Marshall (1959)

At air contents and porosities typical of arid sites, however, these models give markèdly different results. If we assume a porosity of 0.39 and a water content of 0.06, then we have an air content of 0.30. The three models return values for air phase tortuosity of 0.12, 0.88, and 0.16, respectively, showing wide variation in their estimates. Which model is most appropriate for a given material is a matter of site-specific investigation.

Also undetermined is an appropriate model for water phase tortuosity.

Modeling with GoldSim vs FEHM

The solution to GoldSim's unsaturated diffusive flux problem was originally developed while modeling the Radioactive Waste Management Sites (RWMSs) at the Nevada National Security Site (NNSS, formerly the Nevada Test Site). Since the issues surrounding the migration of water in the unsaturated zone at the NNSS were addressed by practitioners at Los Alamos National Laboratory (LANL) using the FEHM modeling program, we examined the implementations of diffusive flux in GoldSim and in a FEHM-based unsaturated zone model developed by Walvoord, Wolfsberg and Stauffer. This is important for consistency between the GoldSim and FEHM models of the unsaturated zone at the RWMSs.

Returning to the simplified version of GoldSim's equation for Diffusive Flux modified for a single fluid phase (equation [9]), we can substitute that equation into the mass balance equation (GoldSim CT manual p. B-2, Eq. B-1), giving

$$\frac{\partial m}{\partial t} = \frac{A}{L}\theta_a \tau_a \cdot D\left(C_i - C_j\right) \qquad [10]$$

We can convert mass to concentration (in air, rather than bulk concentration) since $m = C_g \theta_a V$, and rearrange to look more like the equation from Jury (Eq. 4)

$$\frac{\partial \theta_a C_g}{\partial t} = \frac{A}{V L}\left[\theta_a \tau_a \cdot D\left(C_i - C_j\right)\right] \qquad [11]$$

where V is the volume of the cell. Dividing through by θ_a gives

$$\frac{\partial C_g}{\partial t} = \frac{A}{V L}\left[\tau_a \cdot D\left(C_i - C_j\right)\right] \qquad [12]$$

The key is seeing that the definition of D_g^s in the Jury text does not explicitly include volumetric air content. From Eq. 11, we can see that GoldSim *does* explicitly include volumetric air content (or rather, porosity) in the definition of D_g^s (or D_{cs}), so that D_g^s is defined as

$$D_g^s = \theta_a D \tau_a$$

Note that FEHM, like GoldSim, includes volumetric air content explicitly.

Thus we must be careful when we define the air phase tortuosity τ_a in our model in order to understand how D_g^s is defined in the literature that the various tortuosity equations come from. For example, Jury (1991) writes the Millington-Quirk (1961) equation for air phase tortuosity as $\frac{\theta_a^{10/3}}{n^2}$ (where *n* is porosity) and in GoldSim we need to use $\frac{\theta_a^{7/3}}{n^2}$ for tortuosity.

References

Jury, W.A., W.R. Gardner, and W.H. Gardner, 1001. *Soil Physics* Fifth Edition, Wiley, New York, NY

Marshall, T.J., 1959. "The diffusion of gas through porous media." *Journal of Soil Science* (10) pp. 79-82

Millington, R.J., and J.P. Quirk, 1961. "Permeability of porous solids." *Trans. Faraday Society* (57) pp. 1200-1207

Penman ----1940 -----(referenced in Jury 1991)

Ionic Diffusion Coefficients for Transport Modeling in GoldSim

Dave Gratson
Neptune and Company
February 2010

Recent discussions about the diffusion coefficients currently used in contaminant transport models in GoldSim have centered on exploring ion-specific D_m values, as opposed to the single value of 4.3×10^{-5} cm^2/s for transuranics (TRU) as used in the Performance Assessment (PA) for the Greater Confinement Disposal (GCD) boreholes at the NTS (Cochran, et al. 2001). The GCD PA justifies the use of this value thus: "The molecular diffusion coefficient is not radionuclide -specific ... because the radionuclides themselves are of similar size." While that may hold true for the TRU waste in the GCD boreholes, it most definitely is not true for the wide variety of radionuclides found in low-level radioactive wastes disposed in other facilities.

I investigated approaches for incorporating individual D_m values for the chemical elements in the model, a long list spanning most of the periodic table with extreme ranges of ion sizes. Thus it would seem prudent to derive D_m values for each element used in the model. However, after investigating this issue I will provide two arguments for using a range of D_m values, rather than attempting to provide individual values.

D_m derivation: Ionic and molecular diffusion coefficients are derived in theory from the Stokes-Einstein equation:

$$D_{AB} = RT/6\pi\,\eta_B\,r_A,$$

where

- R = universal gas constant,
- T = temperature,
- η_B = absolute viscosity of the solvent (water), and
- r_A = radius of the "spherical" solute.

A variety of empirical equations have been derived based on the Stokes-Einstein equation for different scenarios. For a dilute solution of a single salt the diffusion coefficient can be derived from the Nernst-Haskell equation (Reid et al., 1987). This equation includes the valence of the cation and anions as well as ionic conductances. Specific ionic conductances are required for each cation and anion species. When two or more chemical species are present at different concentrations, interdiffusion (counterdiffusion) must be included to satisfy electroneutrality (Lerman 1979). For a geochemical system as large as that found in LW disposal facilities this quickly becomes too complex to model, even if ionic conductivities are available for each species.

The second difficulty in deriving diffusion coefficients lies in the large number of potential ions. The number of LLW elements typically modeled may be 30 to 40, and for each element in this list one can expect multiple forms. For example, U has 4 redox states, and many soluble species for each of these. Assuming oxic conditions U will be primarily found as $UO_2(CO_3)_3^{-4}$, $UO_2(CO_3)_2^{-2}$, and $UO_2CO_3^{0}$, however there are at least 8

additional forms of U(+6) that may be found. Thus the potential number of ions that would need to be included in the model would easily be in the hundreds. Obtaining the parameters for each species that would be required to model the ionic diffusion would be difficult.

Solution: I propose a D_m range be incorporated. This range can be derived from Table 3.1 in Lerman (1979). For conditions near 25°C, the range of D_m for the elements of interest is 4×10^{-6} to 2×10^{-5} cm^2/s. For cooler temperatures, which would be expected in the deeper subsurface, the values are somewhat lower. The values for 25°C are reproduced in the following table:

Cation	D_m (10^{-6} cm^2/s)	Anion	D_m (10^{-6} cm^2/s)
K^+	19.6	Cl^-	20.3
Cs^+	20.7	I^-	20.0
Sr^{2+}	7.94	IO_3^-	10.6
Ba^{2+}	8.48		
Ra^{2+}	8.89		
Co^{2+}	6.99		
Ni^{2+}	6.79		
Cd^{2+}	7.17		
Pb^{2+}	9.45		
UO_2^{2+}	4.26		
Al^{3+}	5.59		

from Table 3.1 in Lerman (1979)

Based on this discussion, the value chosen for the GoldSim element \Materials\Water_Properties\Dm is a uniform stochastic, varying from 3×10^{-6} to 2×10^{-5} cm^2/s.

References

Cochran, J.R., W.E. Beyeler, D.A. Brosseau, L.H. Brush, T.J. Brown, B.M. Crowe, S.H. Conrad, P.A. Davis, T. Ehrhorn, T. Feeney, W. Fogleman, D.P. Gallegos, R. Haaker, E. Kalinina, L.L. Price, D.P. Thomas, and S. Wirth, 2001. *Compliance Assessment Document for the Transuranic Wastes in the Greater Confinement Disposal Boreholes at the Nevada Test Site, Volume 2: Performance Assessment*, SAND2001-2977, September 2001

Lerman, A. 1979. *Geochemical Processes in Water and Sediment Environments*. Wiley-Interscience. QES71.L45

Reid, Prausnitz, and Poling, 1987. *The Properties of Gases and Liquids*, 4th Edition. McGraw-Hill, Inc. TP242.R4

Neptune and Company Inc.

June 1, 2011 Report for EnergySolutions

Clive DU PA Model, version 1

Appendix 4

Waste Inventory

Radioactive Waste Inventory for the Clive DU PA

28 May 2011

Prepared by

Neptune and Company, Inc.

This page is intentionally blank, aside from this statement.

CONTENTS

FIGURES

TABLES

1.0 Waste Inventory Parameters Summary

This section is a brief summary of parameters and distributions employed in the waste inventory component of the Clive Depleted Uranium Performance Assessment Model that is the subject of this white paper.

For distributions, the following notation is used:

- N(μ, σ, [*min*, *max*]) represents a normal distribution with mean μ and standard deviation σ, and optional truncation at the specified *min*imum and *max*imum, and
- Beta(μ, σ, *min*, *max*) represents a generalized beta distribution with mean μ, standard deviation σ, minimum *min*, and maximum *max*.

A summary of values and distributions for waste inventory modeling inputs is provided in Table 1.

Table 1. Summary input parameter values and distributions

parameter	value or distribution	units	comments
Number of SRS DU drums	5,408	-	see Section 2.2.1
Mass of a 208-L (55-gal) drum	20	kg	see Section 2.2.1
Total mass of SRS DUO_3 proposed for disposal	3,577	Mg	see Section 3.1.1
Number of DUF_6 cylinders from Paducah GDP	36,191	-	see Section 3.5.1
Number of DUF_6 cylinders from Portsmouth GDP	16,109	-	see Section 3.5.1
Number of DUF_6 cylinders from K-25 GDP	4,822	-	see Section 3.5.1
Mass of DUF_6 from Paducah GDP	436,400	Mg	see Section 3.5.1
Mass of DUF_6 from Portsmouth GDP	195,800	Mg	see Section 3.5.1
Mass of DUF_6 from K-25 GDP	54,300	Mg	see Section 3.5.1
Diameter of cylinders	4	ft	see Section 2.3.1
Length of cylinders	12	ft	see Section 2.3.1
Fraction of GDP DU that is contaminated	Beta(0.0392, 0.0025, 0, 1)	-	see Section 3.5.2.3

Mean and standard deviation values for uranium isotopes and other fission products in the uranium trioxide (UO_3) from the Savannah River Site (SRS) are developed in Section 3.0. These concentrations are summarized in Table 2. Note that the standard deviations are those used in the GoldSim PA model. They are intended to be estimates of the standard deviation of the mean concentration, hence addressing the spatio-temporal scale of the input distribution.

Table 2. Summary of mean and standard deviations for SRS DUO_3 concentrations, assuming a normal distribution

radionuclide	SRS DUO_3 concentration	
	mean (pCi/g)	standard deviation (pCi/g)
^{90}Sr	4.70E+1	1.28E+1
^{99}Tc	2.38E+4	1.10E+4
^{129}I	1.86E+1	1.59E+0
^{137}Cs	1.21E+1	7.10E-1
^{210}Pb	0	0
^{222}Rn	0	0
^{226}Ra	3.17E+2	1.91E+1
^{228}Ra	0	0
^{227}Ac	0	0
^{228}Th	0	0
^{229}Th	0	0
^{230}Th	0	0
^{232}Th	0	0
^{231}Pa	0	0
^{232}U	0	0
^{233}U	5.29E+3	4.78E+2
^{234}U	3.31E+4	2.17E+3
^{235}U	2.97E+3	7.50E+2
^{236}U	4.91E+3	1.17E+3
^{238}U	2.72E+5	6.64E+3
^{237}Np	5.68E+0	1.17E+0
^{238}Pu	2.10E-1	4.00E-2
^{239}Pu	1.28E+0	2.00E-1
^{240}Pu	3.40E-1	5.00E-2
^{241}Pu	4.04E+0	7.40E-1
^{242}Pu	0	0
^{241}Am	1.42E+1	9.10E-1

The DU inventories from the gaseous diffusion plants (GDPs) are based upon estimates from the DOE (DOE 2004a and 2004b) for mass of DUF_6 and U_3O_8 produced. The inventories for the other actinides and fission products is highly uncertain, but is informed by studies performed by Oak Ridge National Laboratory (ORNL 2000a, 2000b, 2000c, 2000d). Until adequate information concerning DU inventory is received from the GDPs, which may not happen until the DU oxide product has been produced and sampled, the actinides and fission products are assumed to be in equal concentrations in the DUF_6 waste as has been found in the SRS DUO_3

waste, as shown in Table 2. This is only a rough approximation and will need to be revised as data from the GDP waste are provided.

2.0 Uranium Oxide Inventory

This document describes three categories of depleted uranium waste form at the Clive, Utah disposal facility:

1. Depleted uranium oxide (UO_3) waste from the Savannah River Site (SRS) proposed for disposal at the Clive facility,
2. DU from the GDPs at Portsmouth, Ohio and Paducah, Kentucky, which exists in two principal populations:

    a) DU contaminated with fission and activation products from reactor returns introduced to the diffusion cascades, and

    b) DU consisting of only "clean" uranium, with no such contamination.

The DU oxides that are to be produced at these sites' "deconversion" plants will be primarily U_3O_8. The remainder of this section provides background on the uranium cycle and origins and nature of DU waste in particular.

2.1 Depleted Uranium

In order to produce suitable fuel for nuclear reactors and/or weapons, uranium has to be enriched in the fissionable ^{235}U isotope. Uranium enrichment in the US began during the Manhattan Project in World War II. Enrichment for civilian and military uses continued after the war under the U.S. Atomic Energy Commission, and its successor agencies, including the DOE.

The uranium fuel cycle begins by extracting and milling natural uranium ore to produce "yellow cake," a varying mixture of uranium oxides. Low-grade natural ores contain about 0.05 to 0.3% by weight of uranium oxide while high-grade natural ores can contain up to 70% by weight uranium oxide (NRC, 2010). Naturally occurring uranium contains three isotopes, ^{238}U, ^{235}U, and ^{234}U. Each isotope has the same chemical properties, but they differ in radiological properties. Naturally occurring U has an isotopic composition of about 99.2739±.0007% ^{238}U, 0.7204±.0007% ^{235}U, and 0.0057±.0002% ^{234}U (Rich et al., 1988).

The milled ore is refined to remove the decay products (^{226}Ra, ^{230}Th, etc.) that have built up in the material naturally to the degree of secular equilibrium, leaving more or less pure uranium oxide. This uranium, still at natural isotopic abundances, is enriched to obtain the ^{235}U, with vast quantities of ^{238}U as a by-product. Although a variety of technologies exist for enrichment, the most prevalent enrichment process at the time was by gaseous diffusion, which requires that the uranium be converted to a gaseous form: uranium hexafluoride (UF_6). This gas is introduced to a diffusion cascade, which separates the isotopes, generating enriched uranium as a product, and depleted uranium hexafluoride (DUF_6) as a waste stream. Depleted uranium isotopic ratio values from gaseous diffusion plants are roughly 99.75% ^{238}U, 0.25% ^{235}U, and 0.0005% ^{234}U (Rich, et al., 1988), but the ^{235}U assay found in the cylinders today varies with fluctuating enrichment goals, operational conditions, and where in the cascade process the DU was removed. Because

processing of uranium has been practiced for only about 60 years, there has not been sufficient time for appreciable in-growth of decay products in this by-product. Depleted uranium is therefore considerably less radioactive than natural uranium because it has less ^{234}U and other decay products per unit mass. The bulk of this material is still stored in the original cylinders in which it was first collected at the GDPs.

Uncontaminated (clean) depleted uranium consists principally of three isotopes of uranium (^{238}U, ^{235}U, and ^{234}U) and a small amount of progeny from radioactive decay of these isotopes. Trace amounts of other uranium isotopes (^{232}U, ^{233}U, and ^{236}U) may also exist. The bulk of the DU at the GDPs is clean uranium, but a significant amount of contaminated DU also exists, both at the GDPs and in all the DU waste from the SRS.

The contamination problem arises from the past practice of introducing irradiated nuclear materials (reactor returns) into the isotopic separations process. Irradiated nuclear fuel underwent a chemical separation process to remove the plutonium for use in nuclear weapons. Uranium, then thought to be a rare substance, was also separated out, but contained some residual contamination from activation and fission products. This uranium was again converted to UF_6 for re-enrichment, and was introduced to the gaseous diffusion cascades, contaminating them and the storage cylinders as well. Based on laboratory analysis of the contents of contaminated DU waste (including all radionuclides in the containers), the species in the disposed inventory include those in Table 3 (Beals, et al. 2002, Energy*Solutions* 2009b, and ORNL 2000c).

Table 3. Radionuclide constituents of contaminated depleted uranium

category	radionuclides
uranium isotopes	^{232}U, ^{233}U, ^{234}U, ^{235}U, ^{236}U, ^{238}U
decay products	^{226}Ra
activation products	^{241}Am, ^{237}Np, ^{238}Pu, ^{239}Pu, ^{240}Pu, ^{241}Pu, ^{242}Pu
fission products	^{90}Sr, ^{99}Tc, ^{129}I, ^{137}Cs

In order to clarify that the contaminated DU wastes contain more than just uranium or DU, they are termed "DU waste". When this term is used, it refers to wastes that contain DU and a perhaps small but potentially significant amount of contamination from actinides and fission products.

2.2 Savannah River Site Depleted Uranium

Depleted uranium was generated at the SRS as a byproduct of the nuclear material production programs (Fussell and McWhorter, 2002). Depleted uranium billets were produced at the DOE Fernald, Ohio, site, fabricated into targets at SRS, then irradiated in one of the SRS production reactors. The irradiated targets were transported to F-Canyon where the targets were dissolved. After dissolution, the fission products were separated from the plutonium and uranium which were then separated from each other. After additional purification, the uranium stream was transferred to the FA-Line Facility where it was processed into uranium trioxide (UO_3) for storage in about 36,000 drums. Since the chemical separations process is imperfect, the DUO_3

contains trace quantities of fission products and transuranic elements (Beals et al, 2002, Energy*Solutions*, 2009b) as discussed above.

2.2.1 Mass of SRS Depleted Uranium Proposed for Disposal

The SRS DUO_3 is a solid powder at room temperature and pressures. This DU oxide is stored in 208-L (55-gal) steel drums, with plastic liners. Steel drums have a tare mass of about 20 kg each. The drums are approximately 2/3 full with an average mass of about 1500 lbm (750 kg) apiece (Fussell and McWhorter, 2002). This DUO_3 is considered to be relatively homogeneous, based on known process controls and operations. The condition of the drums varies from good to poor with a high percentage of the drums having some degree of outer surface corrosion.

In December 2009, SRS made a shipment of drums to the Clive, Utah facility. This shipment contained 52 rail-cars (referred to as gondolas in the manifests), each holding 104 drums, for a total of 5,408 drums. This shipment of DU waste is considered in this PA.

2.2.2 Composition of SRS Depleted Uranium

There are three main sources of data for establishing the concentration of uranium isotopes, fission products, and transuranics in the SRS DU. In 2002 SRS sampled and analyzed their DU oxide in preparation for shipment to Utah (Beals, et al., 2002). A total of 33 drums were sampled; this is approximately 1% of 3300 drums that were available for sampling. The samples were analyzed at the Savannah River Technology Center (SRTC) and by a Utah certified laboratory (BWXT Services, Inc) for uranium, fission, and transuranic radionuclides. The analytical results from SRTC are presented in Beals et al, 2002, and in an Energy*Solutions* Radioactive Waste Profile Record, referred to here as the 2002 Waste Profile Record (Energy*Solutions*, 2009b).

The 2002 Waste Profile Record (Energy*Solutions*, 2009b) provides activity concentration data for isotopes of uranium and for potential contaminants such as ^{99}Tc. The latter are used to characterize the contaminant radionuclides for the PA (see Section 3). The data for uranium isotopes are in the form of both activity concentration by alpha spectrometry, and atomic percent by mass spectrometry. ^{233}U was not detected by mass spectrometry. The alpha spectrometry, also used to characterize the samples, cannot differentiate between ^{233}U and ^{234}U (or ^{235}U and ^{236}U) thereby requiring the mass spectrometry analysis. Note, the ^{235}U and ^{236}U results are also based on mass spectrometry analysis.

The 33 samples were characterized for uranium isotopes, fission products, transuranics, and some metals and organic compounds (pesticides, herbicides, semi-volatile and volatile organic compounds) as recorded in the Waste Profile Record (Energy*Solutions*, 2009b). No organic compounds were detected but low levels (mg/kg) of lead, arsenic, cadmium, chromium, selenium, silver, zinc and copper were found. These low levels of metal make up less than 5 ppm of the DU, and are not considered in this PA because they are not radioactive, and they are not in excess of minimum regulated concentrations for hazardous waste (i.e., the DU waste is not classified as “mixed waste”).

Data for other characteristics of the DU waste are also available from the 52 Waste Manifests (Energy*Solutions*, 2009d). The shipment consisted of 52 gondola railroad cars, each car

containing 104 drums. The 2009 Waste Manifests from that shipment provide the volume (total 1,133.2 m^3) and weight (total of 7,886,738 pounds, corresponding to a mass of 3,577 Mg).

Based on the physical properties description in the Waste Profile Record (Energy*Solutions*, 2009b), the DU is stoichiometrically 83.22% uranium, indicating that the DU is essentially 100% UO_3. The isotopic mass percent of ^{238}U is over 99%.

Since the arrival in Clive of the 52 gondolas of SRS DU waste, Energy*Solutions* has performed two separate sampling and analysis events. In January of 2010 Energy*Solutions* collected 15 samples that were analyzed for uranium isotopes (Table 14, in the Appendix). In April 2010 Energy*Solutions* collected 11 samples that were analyzed for uranium isotopes and ^{99}Tc (Table 15, in the Appendix). In August of 2010 the State of Utah analyzed 173 samples that Energy*Solutions* collected from the drums (Johnson, 2010). These samples were analyzed for ^{99}Tc only. The data are described in greater detail in Section 3, in which input distributions for the GoldSim PA model are developed.

2.3 Depleted Uranium Oxide from the Gaseous Diffusion Plants

Three large GDPs were constructed to produce enriched uranium. The first diffusion cascades were built in Oak Ridge, Tennessee, at what was the K-25 Site, but is now known as the East Tennessee Technology Park (ETTP). Two others of similar design were constructed in Paducah, Kentucky (PGDP), and Portsmouth, Ohio (PORTS) (DOE 2004a and 2004b). The cascades at the K-25 Site ceased operations in 1985, the Portsmouth plant ceased in 2001, the Paducah GDP continues to operate. The two more recent GDPs are host to a large inventory of stored DUF_6, including the ETTP material that was moved to Portsmouth.

The DOE is currently managing approximately 60,000 cylinders at both PGDP and PORTS (DOE 2004a, 2004b). For many years, interest has been expressed in converting the DUF_6 in these cylinders to an oxide form to support their long-term disposal. In May, 1995 an independent DOE oversight board recommended a study to determine a suitable chemical form for long-term storage of DU. Also, in 1994 the DOE began work on a *Programmatic Environmental Impact Statement for Alternative Strategies for the Long-Term Management and Use of Depleted Uranium Hexafluoride* (DOE 1999a). Later, DOE issued the *Final Plan for the Conversion of Depleted Uranium Hexafluoride as Required by Public Law 105-204* (DOE 1999b). As a result of these efforts the DOE developed a Conversion Plan that describes the steps that would allow DOE to convert the DUF_6 inventory to a more stable chemical form. Two Environmental Impact Statements (EIS) were prepared as part of the plan, one for Paducah, DOE/EIS-0359, (DOE 2004a) and one for Portsmouth, EIS-0360 (DOE 2004b). These EISs describe the background and alternatives for DUF_6 conversion. With the completions of the EISs, "deconversion" plants were built at both the PORTS and PGDP locations. In 2002, DOE awarded a contract to Uranium Disposition Service, LLC (UDS) to design, construct, and operate two DUF_6 deconversion facilities at these locations. As of this writing, both plants have been built by UDS and have begun test processing DUF_6 into oxide form.

The UDS dry conversion is a continuous process in which DUF_6 is vaporized and converted to a mixture of uranium oxides (primarily DU_3O_8 but with some UO_2) by reaction with steam and hydrogen in a fluidized-bed conversion unit. The hydrogen is generated using anhydrous ammonia (NH_3). Nitrogen is also used as an inert purging gas and is released to the atmosphere

through the building stack as part of the clean off-gas stream. The DU_3O_8 powder is collected and packaged in the former DUF_6 cylinders for disposition. The process equipment is arranged in parallel lines. Each line consists of two autoclaves, two conversion units, a HF recovery system, and process off-gas scrubbers (DOE 2004a).

2.3.1 Mass of GDP Depleted Uranium

According to the EISs the PGDP facility has been designed to convert approximately 18,000 Mg (one Mg is one metric tonne, or about 2,200 lbm) of DUF_6 per year, which will require approximately 25 years for full conversion of the PGDP inventory. At Portsmouth, 13,500 Mg of DUF_6 per year (approximately 1,000 cylinders per year) is expected to be converted.

Several different cylinder types are in use. Most cylinders are expected to range from 11 to 12 Mg full. The cylinders with a 12-Mg capacity are 12 ft (3.7 m) long by 4 ft (1.2 m) in diameter; most have a steel wall that is 5/16 in (0.79 cm) thick. Similar but slightly smaller cylinders with a capacity of 9 Mg are also in use. Most of the cylinders were manufactured in accordance with an American National Standards Institute standard (ANSI N14.1, Uranium Hexafluoride Packaging for Transport) as specified in 49 CFR 173.420, the Federal regulations governing transport of DUF_6.

To develop an estimate for the mass of DU oxide from the two GDPs, the mass of DUF_6 was converted to mass of uranium and thence to mass of U_3O_8. This simple stoichiometric conversion, based on moles of uranium, fluorine, and oxygen, is performed within the Clive DU PA Model. Details are provided in Section 3.5.1.

2.3.2 Composition of GDP Depleted Uranium

The depleted uranium oxides from Portsmouth and Paducah that are proposed for disposal have yet to be manufactured. Until their production is complete, with associated testing of composition, estimates of composition must be relied upon to construct distributions and make decisions. At the most coarse level, there are two distinct populations of GDP DU composition: 1) DU derived from "clean" (a.k.a. "green") uranium, which contains no contamination, and 2) contaminated DU, which contains varying amounts of fission and activation products, as well as transuranics, resulting from the introduction of reactor returns into the gaseous diffusion cascade.

The clean DU is characterized by its abundance of uranium isotopes, and includes those radionuclides as well as their decay products. Isotopic abundance analyses were focused on determining the amount of U-235 in the DU, since this isotope was the "product" of the entire enrichment enterprise, and little attention was given to the exact abundance of other uranium isotopes, all of which were considered waste products.

Little information is available at this time regarding the exact nature and extent of the contamination within the contaminated DU population. The uranium isotopic abundance estimates are the same as for the clean DU. Estimates of the contamination by reactor return radionuclides, however, must rely on the SRS DU as a proxy until better GDP-specific information becomes available. For the purposes of this PA, then, the contaminated fraction of the GDP DU is assumed to have the same contaminant composition as the SRS DU.

3.0 Input Parameter Distribution Development

The probabilistic Clive DU PA Model relies on stochastic parameters in order to evaluate uncertainty and sensitivity. The statistical development of input parameter distributions is provided here.

3.1 Parameters for Depleted Uranium from the Savannah River Site

Parameters of interest for the PA include the mass of DU waste, and the concentrations of each radio-isotope contained in the DU waste. The contents of the SRS drums were described in Section 2.1. The purpose of this section is to describe the characterization of the mass of DU, and the concentrations of the radioisotopes. The mass of DU is considered fixed for the purpose of this PA, and is presented without uncertainty. The concentrations are presented in terms of the best estimate of the mean concentration, and the uncertainty of the mean concentration for each radio-isotope.

3.1.1 Mass of SRS Depleted Uranium

The single source of information regarding the mass of total depleted uranium shipped from SRS to Clive are shipping manifests (Energy*Solutions*, 2009d). Key pieces of information on these forms include the following

- Total mass in kg and corresponding weight in US tons
- Total volume in cubic meters and in cubic feet
- Net waste volume in cubic meters and in cubic feet
- Net mass in kg and corresponding net weight in US tons

Reviewing these manifests suggest that each gondola rail car was weighed empty (tared) and fully loaded, and the tare weight was subtracted to arrive at the "Net Waste Weight" reported on the manifests. Since this is a measured amount, it will be considered a fixed value and a distribution will not be assigned. There is no reason to believe that the mass of the drums was deducted from this net weight. Such drums do not have a standardized tare weight, but for the purposes of calculation it is assumed that each drum has a mass of 20 kg. This is considered a representative weight for a 55-gallon drum.

The net weights from the manifests were summarized by W. Johns in a spreadsheet ("100105 9021-33 Iso With Calcs.xls") sent to Neptune. These values have been summed to create a total mass data value for total mass of the depleted uranium shipped from SRS to Clive, Utah. Weights of DU plus drums for the individual 52 rail cars range from 50.37 Mg to 75.56 Mg. The total amount shipped is 3,577 Mg.

3.1.2 Composition of SRS Depleted Uranium

Three data sources are available for the development of probability distributions for the concentrations of radio-isotopes in the SRS DU waste: The SRS-2002 dataset consists of activity concentration data and uranium isotopic abundance as atomic percent from Beals, et al. (2002). The ES-2010 dataset has uranium activity concentration and total uranium mass concentrations from two Energy*Solutions* sampling and analysis events: GEL (2010a and 2010b), and GEL (2010c). Finally, the Utah-2010 analysis obtained activity concentrations of ^{99}Tc from

Energy*Solutions* sampling and State of Utah requested analysis (Johnson 2010). These datasets are briefly described in Table 4 and the individual values are presented in Appendix A.

Table 4: Summary of available uranium and technetium data for the SRS DU

Source	Date	Number	Constituents	Units
SRS-2002: Table 16 of Beals et al, (2002)	2002	6 (2 replicates per sample)	^{233}U, ^{234}U, ^{235}U, ^{236}U, ^{238}U	Isotopic abundances (atomic % U)
SRS-2002: Table 17 and Table 4 of Beals et al, (2002)	2002	33	$^{233+234}$U, $^{235+236}$U, ^{238}U, ^{99}Tc	Activity % U
ES-2010 (GEL, 2010 a,b)	January 2010	15	Total U, $^{233+234}$U, $^{235+236}$U, ^{238}U	µg/g for Total U; pCi/g for others
ES-2010 (GEL 2010 c)	April 2010	11	Total U, ^{99}Tc, $^{233+234}$U, $^{235+236}$U, ^{238}U	µg/g for Total U; pCi/g for others
Utah-2010 (Johnson, 2010)*	August 2010	173 (plus 30 duplicates)	^{99}Tc	pCi/g

* Note that splits of these samples were also submitted for analysis by Energy*Solutions.*

Note that the 33 samples included in the SRS-2002 data also include concentrations of the other contaminants presented in Table 3 (decay, activation and fission products), which are used to developed input probability distributions for the concentrations of these radionuclides.

The spatio-temporal scale of interest for the Clive DU PA Model includes a large volume of DU waste and fill material in the Class A South embankment, a 10 ky quantitative analysis followed by a 2.1 My qualitative analysis. This, and the dynamic nature of the PA modeling environment in which time steps of many years are used, affects the approach to characterizing probability distributions of the inventory. Conceptually, the PA model incorporates compartments or cells that are fully mixed at each time step. The physical samples used in this statistical analysis represent very small volumes of waste, but the mean concentrations are representative of the entire inventory. This approach is reasonable so long as there is not a strong non-linear effect due to spatial variation within the waste cell. For this model the waste is fully mixed within a waste layer. The appropriate spatio-temporal scaling suggests that characterization of the mean activity concentration of each radionuclide is needed. This is the basic approach that is taken in each case, however, because the data sources are different for some of the radionuclides, different approaches are needed for estimation of the probability distributions (Table 5 and Table 6):

- The probability distribution of mean activity concentration for uranium isotopes is estimated from the ES-2010 data. Because activity from combinations of isotopes $^{233+234}$U and $^{235+236}$U is reported in ES-2010, the atomic percent data from SRS-2002 is used to partition these isotopes.
- There are three sources of ^{99}Tc data: SRS-2002, ES-2010, and Utah-2010. These datasets are used to estimate mean ^{99}Tc activity concentrations. Note that the duplicate measurements in Utah-2010 were not used because there are many samples (173) without

the duplicates, and the duplicates were found to be dependent on their original samples (separating out those dependencies statistically is complicated and unnecessary given the large number of samples available).

- The SRS-2002 data provide the only data available for the other radionucludes (americium, cesium, radon, iodine and plutonium). Consequently, these data are used to estimate distributions of mean activity concentrations for these radionuclides. The parameter estimates for the probability distributions of the mean activity concentrations for these radionuclides are presented in Table 5.

Therefore, the approach for distribution development is to establish the uncertainty distribution of the mean activity concentration for each radionuclide. Each individual data set available is reasonably well-behaved statistically, not exhibiting large skew or multi-modality. There are also enough data that the Central Limit Theorem can be applied, implying a normal distribution for the distribution of the mean. The normal distributions are characterized with the mean concentration and the standard error (i.e., the standard deviation of the mean). However, different sampling events for ^{99}Tc and U indicate potentially different measurement types between sampling events. Consequently, for ^{99}Tc and uranium isotopes, bootstrap re-sampling of the samples and the sampling events is used to address possible differences between sampling events. For the remaining radionuclides, the SRS data are used directly to estimate the parameters. The final distributions are presented in Table 5 and Table 6. Details of the development of these distributions are in the following sections.

Table 5: Summary of probability distributions of mean activity concentrations (pCi/g) for uranium and technetium

Radioisotope	Mean	Standard Error	Source
^{99}Tc	23,800	11,000	SRS-2002, ES-2010 (Jan), Utah-2010
^{233}U*	5,290	478	ES 2010 (Jan/Apr)
^{234}U*	33,100	2,170	ES 2010 (Jan.Apr)
^{235}U*	2,970	750	ES 2010 (Jan.Apr)
^{236}U*	4,910	1,170	ES 2010 (Jan.Apr)
^{238}U	272,000	6,640	ES 2010 (Jan.Apr)

* Isotopes are partitioned using SRS 2002 atomic percentage data.

Table 6: Summary of probability distributions for mean activity concentrations (pCi/g) for other radioisotopes. (Source: SRS-2002.)

Radioisotope	N	Mean	Std. Error
^{241}Am	33	14.2	0.91
^{137}Cs	33	12.1	0.71
^{129}I	33	18.6	1.59
^{237}Np	33	5.68	1.17
^{238}Pu	31*	0.21	0.04

Radioisotope	N	Mean	Std. Error
^{239}Pu	31*	1.28	0.20
^{240}Pu	31*	0.34	0.05
^{241}Pu	31*	4.04	0.74
^{226}Ra	33	316.8	19.1
^{90}Sr	33	47.0	12.8

* - note that results for plutonium isotopes were not reported for 2 samples in the SRS-2002 data

3.2 Analysis of Uranium Composition in SRS Depleted Uranium

Direct comparison between uranium concentrations represented in the SRS-2002 data and in the ES-2010 data is complicated by several factors. The ES-2010 data represent activity concentrations for uranium, where the SRS-2002 data represent isotopic abundance as activity percent (%) of uranium, rather than activity concentration. These different expressions of uranium activity cannot be reconciled without recourse to the total proportion of uranium in each sample—information that is not available. Further, the pedigree of the SRS-2002 data is not clear. Information is available in Beals et al. (2002) about the analytical methods performed in the laboratory, but the actual laboratory reports for the SRS-2002 data are not available. In contrast, the pedigree of the ES-2010 data is well known, and the laboratory reports are available to support the reported uranium activity concentrations. Consequently, only the ES-2010 data are used to generate distributions of the mean uranium activity concentration for each uranium isotope. However, an exploratory comparison is made between the SRS-2002 and the ES-2010 activity data to understand the differences between the SRS and ES uranium data. Development of input probability distributions is presented after the exploratory comparison.

For the PA model, separation is also needed for the uranium isotopes in the pairs $^{233+234}$U and $^{235+236}$U. The ES-2010 laboratory analysis and subsequent uranium data do not distinguish between these pairs of isotopes, but report $^{233+234}$U and $^{235+236}$U activity concentrations combined. However, the SRS-2002 study also includes some uranium isotopic abundance data presented as atomic percent (%) for all uranium isotopes. These SRS-2002 atomic% data are used to partition the $^{233+234}$U and $^{235+236}$U activity concentration data obtained from ES-2010.

3.2.1 Exploratory Comparison of Uranium Data

In SRS-2002, activity% for all uranium isotopes was measured at SRS using alpha spectrometry. In ES-2010, activity concentrations (pCi/g) were measured for $^{233+234}$U, $^{235+236}$U, and ^{238}U. As noted above, only the ES-2010 data will be used to develop input distributions for uranium concentrations for the PA model. However, a comparison of the ES-2010 and SRS-2002 data is presented to better understand the limitations of the SRS-2002 data, and to support the contention that the ES-2010 data are more appropriate for use in developing input distributions for uranium activity concentrations for the PA model.

A major consideration in the decision to focus on the ES-2010 for development of input distributions for the PA model is the lack of supporting documentation for the SRS-2002 data and the difficulty of converting from data presented in activity% to activity concentration. The ES-2010 and SRS-2002 data are compared by first translating one of the datasets to the units of the other dataset. The approach taken is to convert the ES-2010 data to activity%. This is a relatively simple step that facilitates comparison of the SRS-2002 and ES-2010 datasets.

Activity% can be calculated directly from activity concentrations (Equation 1).

$$A_i = \frac{c_i}{\sum_j c_j} \times 100 \quad (1)$$

where

A_i = activity% of uranium component *i*, and

c_i = activity concentration for uranium component *i,* which indexes $^{233+234}U$, $^{235+236}U$, ^{238}U

The results of this conversion are presented graphically in Figure 1. This figure shows pairs of scatter plots for the different uranium components. These plots show clear difference between the datasets. For example, there is a cluster of points from the SRS-2002 dataset (circles). As originally ordered and labeled in Beals et al. (2002), the first 21 samples form the close cluster of points while the last 12 points form the more dispersed cluster of points. Without any further information, this is suggestive of either sampling or laboratory differences or biases within the SRS-2002 data. Sample IDs could be surrogates for sample location, perhaps representing samples from barrels of similar wastes, which would be an example of a potential sampling bias if the entire waste stream is not relatively homogeneous. Alternatively, the samples could have been analyzed in separate batches on different days – with different ambient background concentrations being subtracted from each batch, which would be an example of laboratory bias. No information has been found to explain these differences, but this provides further evidence for why these data are not included in the development of the probability distributions for uranium isotopic inventory for the Clive DU PA.

Data from the two 2010 ES sampling events form clusters that are different but with some overlap. The data from the ES-2010-January sampling event have greater standard deviation than those from the April sampling event. The $^{235+236}U$ data tend to be slightly greater for the January sampling event, whereas the ^{238}U data tend to be slightly greater for the April sampling event.

The greatest overall difference is between the first cluster (21 samples) from SRS-2002 and the rest of the data. This cluster has markedly lower $^{233+234}U$ activity% values than the remainder of the data, and, consequently, markedly greater ^{238}U activity% values.

The summary statistics for each dataset in Figure 1 are presented in Table 7. They further demonstrate the differences between the datasets. The questionable pedigree and difference between the two clusters in the SRS-2002 data are sufficient to justify not using these data for distribution development for the PA. The differences, particular in standard deviation, between the two ES datasets suggest that these two datasets should not be combined when estimating input probability distributions for the uranium activity concentrations for the PA model.

The next stage in this exploratory analysis of the SRS-2002 and ES-2010 Uranium data is to convert the SRS-2002 data from activity% to activity concentrations. This is done to see if the same basic results are obtained, considering different inputs are needed for this conversion.

Table 7: Summary statistics for the Uranium activity% data

Radioisotope	SRS-2002 (33 samples)		ES-2010-January (11)		ES-2010-April (15)	
	Mean	Std. Dev.	Mean	Std. Dev.	Mean	Std. Dev.
$^{233+234}U$	8.0%	1.8%	11.6%	1.1%	12.4%	2.0%
$^{235+236}U$	2.0%	0.3%	1.7%	0.4%	3.2%	1.2%
^{238}U	90.0%	2.0%	86.7%	1.1%	84.4%	2.3%

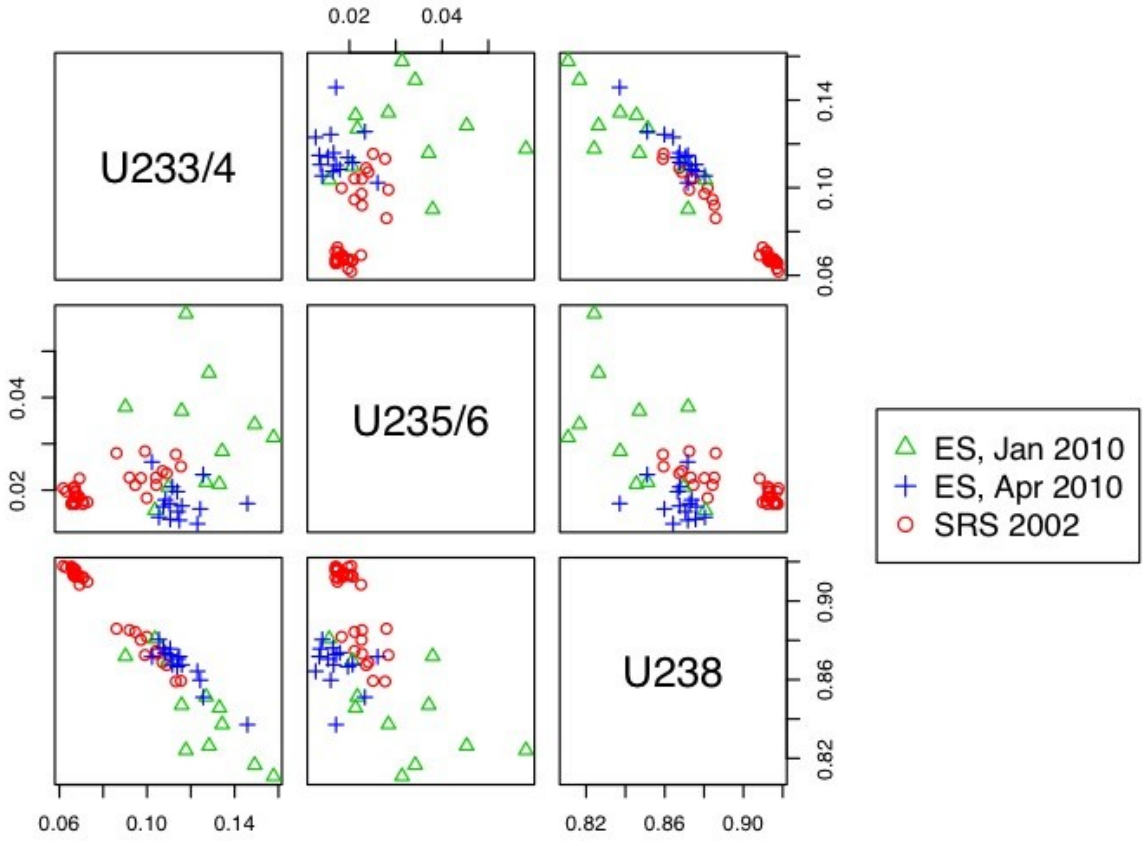

Figure 1. Comparison of activity percent for the SRS DU uranium isotopes

3.2.2 Partitioning $^{233+234}U$ and $^{235+236}U$

The Clive DU PA model requires probability distributions of activity concentration for each uranium isotope. Because of the methods used to measure radioactivity, most samples collected in 2002 and in 2010 do not distinguish between ^{233}U and ^{234}U or between ^{235}U and ^{236}U, but rather report combined quantities. To separate the isotopes some data on the relative contributions of each isotope in each pair is needed.

From the SRS-2002 data, 6 samples were analyzed using mass spectrometry. These 6 samples are from the original 33 samples that were analyzed for activity% of uranium. The mass spectrometry method identified all uranium isotopic abundances and the results are expressed as atomic% (see Table 12). The dataset provides two values for each sample. These values are treated as duplicates and the values are averaged for use in subsequent analyses.

All abundance values for ^{233}U are reported as 0.0000%, because it was not identified in any sample. However, to allow for the possibility of a trace quantity of ^{233}U in the SRS DU, for both SRS-2002 and ES-2010 datasets, ^{233}U atomic percentage values are assumed to be 0.00005%, a value that was chosen because any value smaller than that would be recorded as 0.0000% to four decimal places.

To partition activity% and activity concentrations for $^{235+236}U$ and $^{233+234}U$, uranium abundances expressed as atomic% are multiplied by their respective specific activities, and renormalized to calculate activity%. Ratios are presented in Table 8. The atomic% data do not sum to exactly 100%, hence the renormalization causes small differences in the ^{233}U activity% values.

Table 8: Partitioning Ratios for Uranium Isotopes

	Radionuclide				Ratios	
Sample	**^{233}U**	**^{234}U**	**^{235}U**	**^{236}U**	**$^{234}U/^{233}U$**	**$^{236}U/^{235}U$**
3	1.29%	7.03%	0.73%	1.12%	5.45	1.54
9	1.29%	6.73%	0.73%	1.11%	5.20	1.53
17	1.29%	7.13%	0.73%	1.14%	5.54	1.56
20	1.28%	7.33%	0.74%	1.16%	5.70	1.58
25	1.22%	11.50%	0.83%	1.56%	9.43	1.89
30	1.25%	9.80%	0.78%	1.46%	7.87	1.86

Both sets of ratios show similar patterns, clearly demonstrating that the last two samples are different than the first four samples. This also matches the differences observed in the activity% data reported in the 33 samples, for which the first 21 samples are clearly different than the last 12 samples (see Figure 1). However, all six samples are used to separate these isotopes for the PA model, the effect of which is to increase the variance of the ratios, which introduces more uncertainty in the PA model. In general, the differences this causes in uranium activity concentrations are fairly small relative to the likely effect on the PA model results, however, this will be tested in the model evaluation and sensitivity analysis. If the uranium isotopic distributions prove to be sensitive in the PA model, then it might be necessary to collect data that are aimed more specifically at the needs of the PA.

3.2.3 SRS Depleted Uranium Activity Concentration

As illustrated in Figure 1, there are differences between concentrations measured by ES in the January and April, 2010, data. (Note, as described in Section 3.2.1, the SRS-2002 uranium data are not included in the development of input distributions for uranium activity concentrations for the PA model.) The focus is on the ES-201 datasets. The data from these two ES-2010 dataset are not considered independent or exchangeable, in which case they cannot be directly combined.

Consequently, in order to estimate the population mean and the standard deviation of the mean, a bootstrap method is used giving equal weight to both ES-2010 sampling events.

To simulate the two sampling events, all combinations of the ES-2010 January and April sampling events were used. The samples are bootstrapped within each sampling event, the mean value is calculated for each study, and the study means are averaged to obtain an overall mean value. The bootstrap method is applied as follows:

1. The two sampling events are selected with replacement. Since there are only 4 possible combinations of sampling events (select the January event twice, select the April event twice, select the January event followed by the April event, and select the April event followed by the January event – this is analagous to the results that could be obtained by tossing a coin twice), all combinations are used and weighted equally.
2. For each sampling event selected, the data are sampled with replacement and a mean mean calculated. An overall mean is calculated as an average of the two means.
3. This simulation is repeated 10,000 times for each of the 4 sampling event combinations, to construct a distribution of means. The simulations were selected at random. This large number of simulations provided adequate convergence of the distribution of the mean.

The effect of this approach is that the effective sample size is related more to the two sampling events than to the 26 samples. This leads to a comparatively wide distribution. If instead, all 26 samples had been treated as independent, then the standard deviation would be considerably smaller. The conceptual difference between the two possible approaches is that treating the data as independent assigns the information content, or uncertainty, to each sample, whereas, the approach used assigns the information content to the sampling events. That is, the sampling events themselves are considered more important for characterizing the distribution of the uranium isotopes than the individual sample results.

10,000 bootstrap samples are used, to create the distributions of mean values for each uranium component shown in Figure 2. The distributions for the uranium components are presented to show how the distributions relate to the two ES-2010 datasets. The red lines on the plots show how the April data exhibit greater activity concentrations for all three uranium components. The plots also show how the distributions bound the means of the two datasets for all three uranium components. If an approach had been taken that treated all 26 data points as independent, then the distributions of the means would probably have fallen between the two means.

The distributions of the uranium components $^{233+234}$U and $^{235+236}$U are partitioned using a randomly assigned ratio from one of the 6 ratios presented in Table 8. That is, each of the 10,000 simulated means is partitioned, so that there are 10,000 realizations of the distributions of the individual uranium isotopes. The resulting distributions of the mean uranium isotope activity concentrations were fit using a normal distribution. The resulting distributions are presented in Table 5.

The activity concentrations of uranium are dominated by ^{238}U at an average of 272,000 pCi/g. This is to be expected, although the mean activity concentration of ^{234}U is also large compared to the other isotopes. These distributions could be narrowed (i.e., reduced uncertainty) by collecting new data under an experimental design that is aimed at the needs of the PA. This includes activity concentrations over a wide range of drums, locations in drums, and laboratory

analysis that provides activity concentrations for every uranium isotope. The ES-2010 datasets provide reasonable data, but the two datasets present different mean uranium activity concentrations, in which case there would be benefit from a more complete study of uranium in the SRS DU waste. If, given these relatively broad distributions, the uranium isotopes are not sensitive to any PA model endpoint, then the need to refine these distributions will be less.

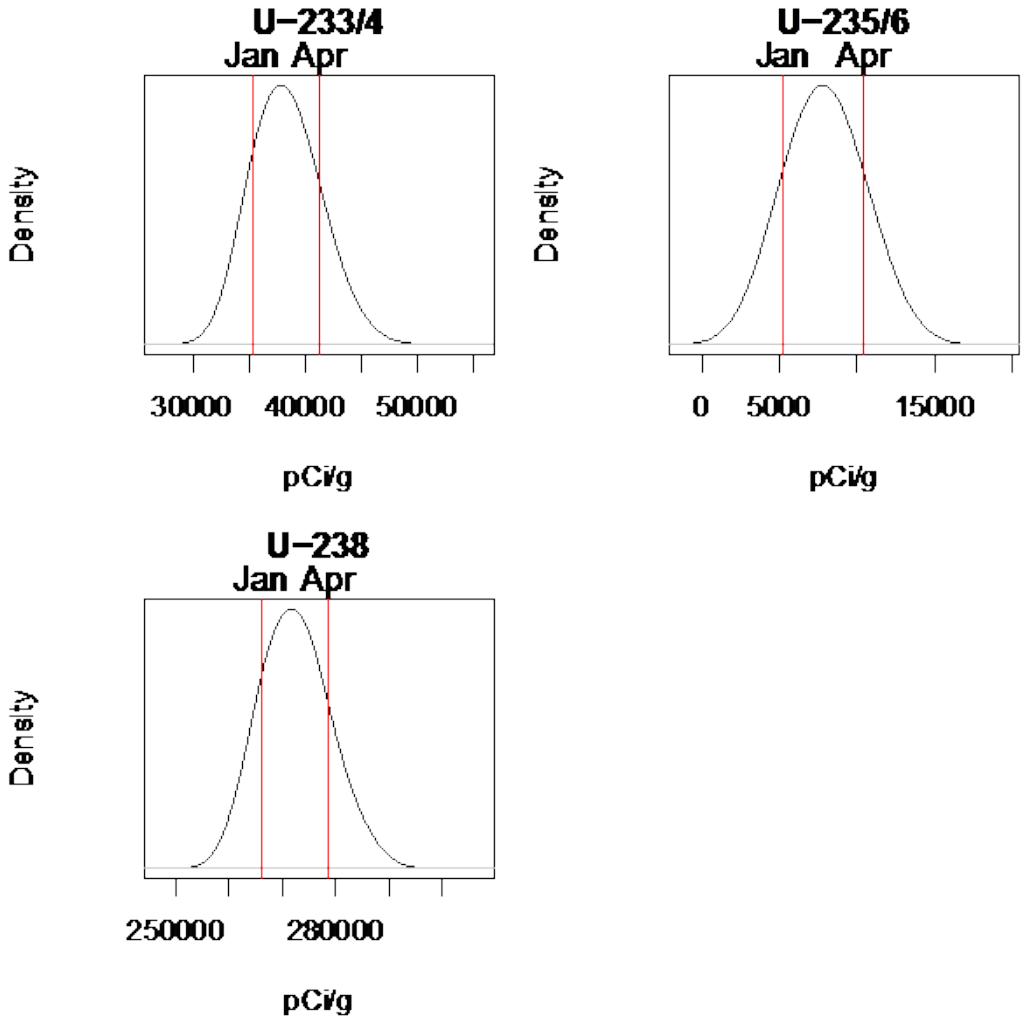

Figure 2. Distribution of mean activity concentration values from bootstrap resampling.

Mean concentration from each input data set are denoted by vertical red lines. To compare with original ES data, mean concentrations of $^{233+234}U$, $^{235+236}U$ and ^{238}U components are shown (red lines) for both the ES-2010 January and April datasets.

3.3 Analysis of Technetium Concentrations in SRS DU

Technetium-99 is the most important of the contaminants contained in the SRS DU waste, because of its potential for relatively fast transport to groundwater. Other mobile radionuclides were reported as not detected in the SRS-2002 samples.

Three sources of data exist for ^{99}Tc from the following sampling events: SRS-2002 (33 samples), ES-2010 (11 samples), and Utah-2010 (173 samples – without duplicates). Figure 3 shows that the samples from these three sampling events have different mean concentrations and different standard deviations. The original SRS-2002 data show the greatest concentrations. Energy*Solutions* attempted to verify these concentrations in January 2011. However, the ES-2010 ^{99}Tc showed lower concentrations. Given the uncertainty and importance of understanding the ^{99}Tc concentrations, the State of Utah commissioned a study involving sampling and analysis of ^{99}Tc for 173 samples (Johnson, 2010). However, these exhibited lower concentrations again.

Table 9: Summary statistics for Technetium data (concentration in pCi/g)

	Data Source		
Statistic	**SRS-2002**	**ES-2010 (January)**	**Utah-2010**
Number of Samples	33	11	173
Mean	49,370	17,800	4,340
Standard Deviation	29,260	5,910	3,550

The pattern of ^{99}Tc concentrations in the SRS-2002 data is similar to the pattern seen in the uranium data. That is, the concentrations are considerably greater in the last 12 samples (particularly in the last 9 samples) than in the first 21 samples, by sample ID (see Table 13). This could be reason to exclude the SRS-2002 ^{99}Tc data from the distribution development. The data do not seem to come from one population, possibly because of sampling or laboratory differences or biases, and the pedigree of the data is lacking because there are no laboratory reports available for the data. However, these data have been included because they show greater concentrations than the two datasets from 2010, which causes the developed distribution of ^{99}Tc concentrations to extend out to cover the SRS-2002 data. The effect of the inclusion of these data has been tested during model evaluation and is reported as part of the sensitivity analysis. If, as might be expected, the ^{99}Tc concentrations are a sensitive part of the model, then it might warrant reconsideration of the available data.

Of further concern is the difference between the ES-2010 data and the Utah-2010 data. These data were collected less than a year apart, and several of the samples from the Utah-2010 data were from the same drums used for the ES-2010 samples. The only clear difference between the two datasets is that different analytical laboratories were used in each case. The ES-2010 samples were analyzed by GEL Laboratories. The Utah-2010 samples were analyzed at a different laboratory. It is possible that the differences are analytical.

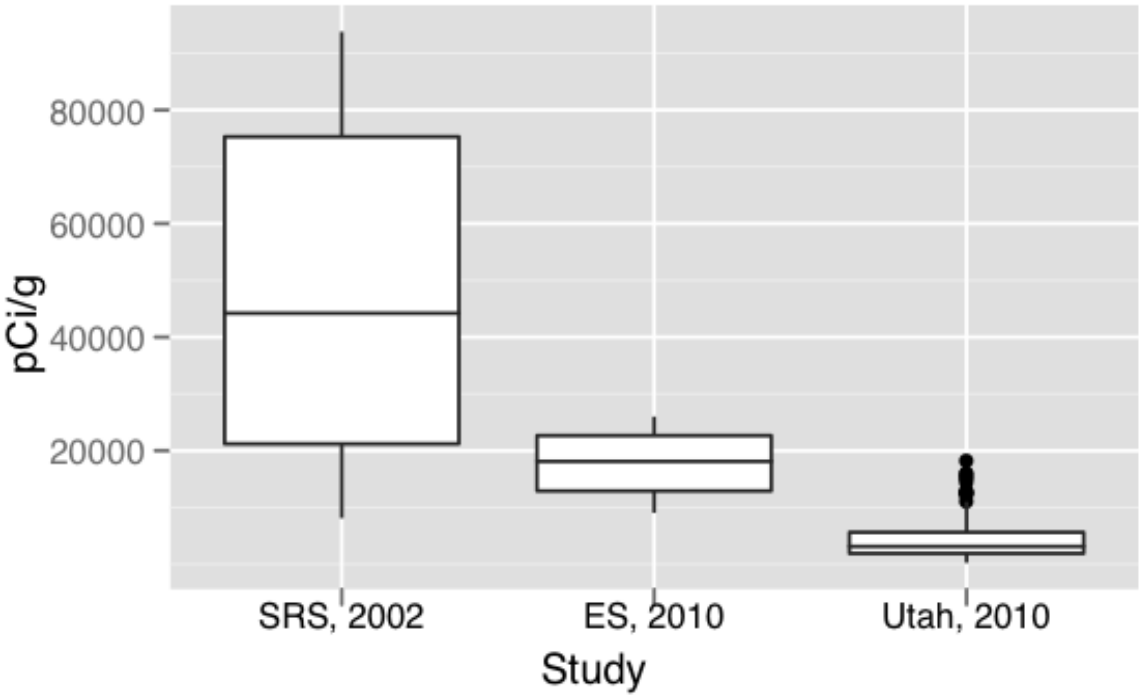

Figure 3. Tc-99 Activity Concentration. Sample sizes: SRS-2002 = 33; ES-2010 = 11; Utah-2010 = 173.

As a consequence of the differences in ^{99}Tc concentrations between the different sampling events, the approach taken to development of an input distribution of mean ^{99}Tc concentrations is similar to the one used for uranium. That is, it is considered more important to model the information content in the sampling events rather than each individual sample. This approach reduces the effect of the Utah-2010 data, which would otherwise dominate estimation of the input distribution.

A simple approach to distribution development is to treat each measurement across all three sampling events as independent and identically distributed and calculate the mean and standard error using all the data. However, this approach weights the data based on the number of samples, giving the Utah-2010 data the most influence. Further, to the extent that the data within each study are not independent, the standard error would be artificially small. The individual data points might not be independent because analyses were often performed on samples from the same drum. To address these issues, a bootstrap method was developed and used to estimate the distribution of the mean ^{99}Tc value that treats the three datasets as independent, rather than each data point across sampling events.

Note that the Utah-2010 dataset contains 18 laboratory and 12 field duplicate measurements. These data were examined and found to be correlated with the associated primary samples.

Since these measurements cannot be considered independent and a relatively large number of samples (173) were analyzed, the duplicates are not included in this distribution analysis.

The three datasets are treated independently in the bootstrap approach, which leads to a wide distribution that covers the range of all three datasets combined. The more simple approach of treating each data point as independent across the three sampling events would result in a very narrow distribution, because of the large number of data points, and the center of the distribution would be lower because the Utah-2010 dataset would dominate given the large sample size.

The bootstrap method is applied as follows:

1. The three studies are selected with replacement from the three available sources of ^{99}Tc data (SRS-2002, ES-201o and Utah-2010). Since there are only 27 possible combinations of sampling events, all combinations were used and weighted equally.
2. For each study, the data are sampled with replacement and a study mean calculated. An overall mean is calculated as an average of the three study means.
3. This simulation is repeated 10,000 times for each of the 27 study combinations, to construct a distribution of the estimated mean concentrations for ^{99}Tc.

The density plot describes the distribution of the overall mean (Figure 4). Because of smoothing in the plotting algorithm, the distribution appears to include negative values, however, the smallest value from the simulations is 3,800 pCi/g. This distribution is reasonably described by a normal distribution, which is used in the PA model (see Table 5). The mean of the distribution is 23,800 pCi/g, and the standard deviation is 11,000 pCi/g. In the PA model, the distribution is truncated at zero, so that negative mean concentrations are not possible. Since this is a distribution of the mean concentration, this distribution indicates that the mean concentration of ^{99}Tc could be as low as zero, or greater than 60,000 pCi/g (see Figure 4). This is a large range, and reflects the uncertainty in the three data sources because of their differences. Different decisions regarding combination of the available data would almost certainly lead to a narrower distribution of the mean concentration, given the large number of data points available. For example, if the Utah-2010 data were used alone, then the 173 data points would lead to a mean of about 4,340 pCi/g and a standard error of about 270 pCi/g, which is the distribution that would then be used in the PA. That is, most of the distribution of the mean concentration would fall between 3,800 pCi/g and 4,880 pCi/g. This is very different than the distribution that is currently proposed for use in the PA.

Note in Figure 4 that the mean concentrations for the three data sources are also presented. These show clearly that the distribution of the mean ^{99}Tc concentration spans the means of the available datasets. As noted above, if the mean ^{99}Tc concentrations proves to be sensitive for any given endpoint of the PA model (dose, groundwater concentrations, or deep time concentrations), then the development of this input distribution should be revisited, including a re-examination of how the three data sources have been combined. Given the mobility of ^{99}Tc and the width of the input distribution defined above, it is reasonable to expect that concentration of ^{99}Tc will be a sensitive parameter.

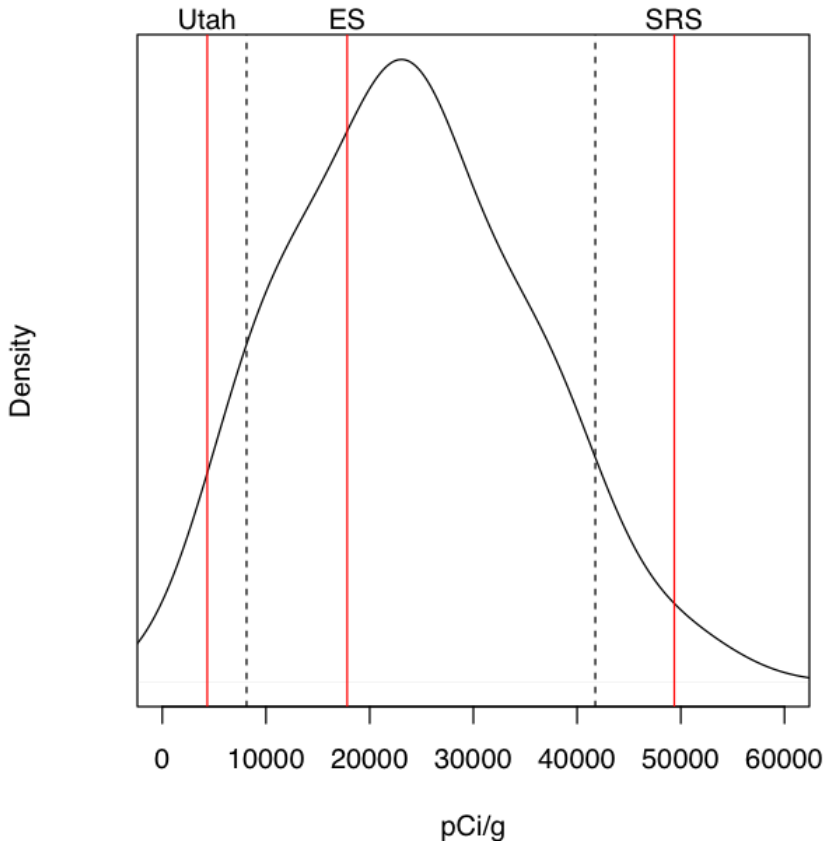

Figure 4. Distribution of Tc-99 mean values. Red lines indicate mean values of Utah-2010, ES-2010, and SRS-2002.

3.4 Concentrations of Other Radionuclides in the SRS Depleted Uranium

As noted in Section 2.1, there are other potential contaminants in the SRS DU, including decay, activation and fission products (see Table 3). Given the only source of data for these radionuclides in SRS-2002, the concentrations are very low, and are unlikely to significantly contribute to the PA, however, input distributions for the mean concentrations of each of these radionuclides are developed and included in the PA to confirm that this is the case.

The measurement of other radionuclides is reported only in the SRS-2002 dataset. These include ^{241}Am, ^{226}Ra, ^{137}Cs, ^{90}Sr, ^{237}Np, ^{238}Pu, ^{239}Pu, ^{240}Pu, ^{241}Pu and ^{129}I. Distributions of these values are shown in Figure 5. With the exception of the plutonium isotopes, all measurements were below the detection limit. Non-detects were set to their detection limits for this analysis. This is a conservative approach, which over-estimates the activity concentrations of these radionuclides. However, the impact of these radionuclides on the PA is likely to be very small, in which case use of the detection limits probably has insignificant effect on the concentrations and doses output by the PA model.

The final distributions are presented in Table 6. The distributions are assumed to be normal, and they are truncated at zero in the PA model.

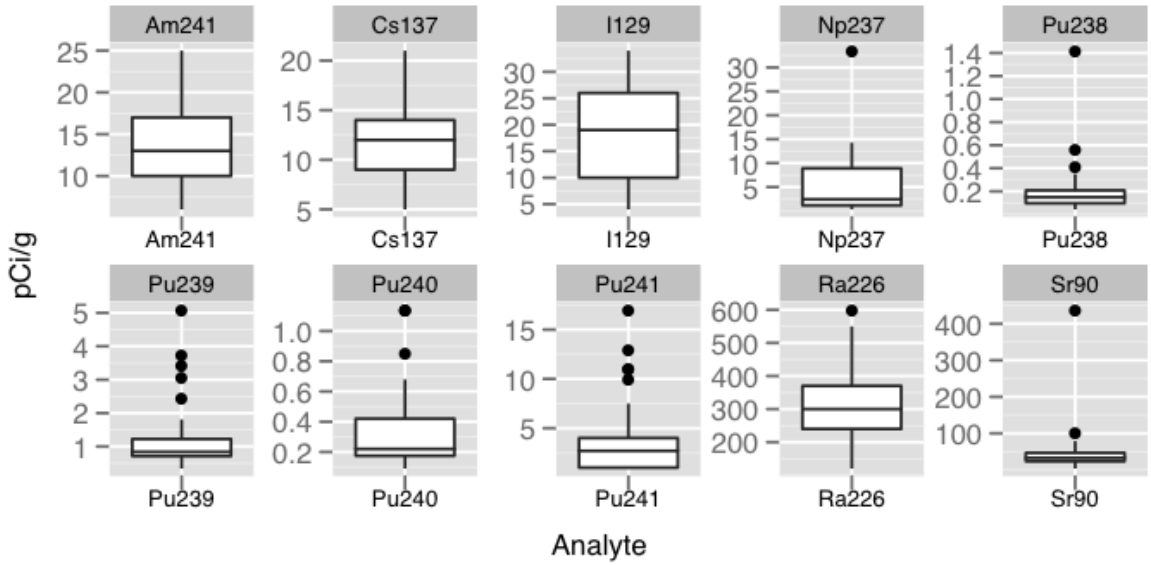

Figure 5. Additional radionuclide data (SRS-2002). Sample size = 33.

3.5 Parameters for Depleted Uranium Oxide from the GDPs

The exact nature of the DU oxides that will be generated by the deconversion plants at Portsmouth and Paducah will not be known until their production, so this PA relies on the best information available to develop estimates. What is known is that the oxides will be primarily U_3O_8, and that they will be shipped and disposed in used DUF_6 cylinders, some of which will contain residual contamination from reactor returns.

3.5.1 Mass of GDP DU

The total mass of anticipated GDP DU oxide is estimated from the reported mass of DUF_6 currently residing in the cylinder yards and a mass conversion from DUF_6 to DU_3O_8.

Although the exact number of cylinders at each facility varies from day to day, the Depleted Uranium Management Information Network reports the numbers as 36,191 at Paducah, 16,109 from the Portsmouth GDP, and 4,822 from the K-25 GDP, now moved to Portsmouth (DOE, 2010). However, there are discrepancies in the available information regarding the numbers of cylinders. Consequently, these numbers are used only for rough estimates of the volume needed for disposal.

Estimates of the total mass of DUF_6 from each of the GDPs is also provided at the Depleted UF_6 Management Information Network web site (DOE, 2010). These estimates are 436,400 Mg for Paducah, 195,800 Mg for Portsmouth, and 54,300 Mg for the K-25 GDP, now stored at Portsmouth. These estimates are used in the PA model. No uncertainty is assigned to them. They are a condition of the PA model until more information is made available. Uncertainty is,

instead, included in the concentration estimates, which serves as a reasonable measure in this PA model for inventory uncertainty

3.5.2 Composition of GDP DU

As of this writing, only a single cylinder of oxide has been produced from the deconversion plants, and only one sample from that cylinder has been analyzed. The DUF_6 processed for this sample was of low ^{235}U assay, and contained no TRU or fission product contaminants, and is therefore not representative of the entire populations of GDP DU oxides.

The GDP DU is considered to have two distinct compositions: Clean DU is pure uranium, derived from natural sources, and Contaminated DU includes at least some TRU and fission products from reactor returns. Each of these is discussed below, and the fraction of the total that is contaminated is estimated for use in the PA model.

3.5.2.1 Clean GDP DU

The constituents comprising the clean DU are naturally-occurring isotopes of uranium, significantly depleted in everything but ^{238}U, and whatever decay products may have developed in the short time since their purification and separation. No quantitative information is available about the relative abundance of the uranium isotopes that characterizes the entire waste stream. Given the lack of definitive information about the relative abundances of the uranium isotopes, it is assumed that Clean DU from the GDPs shares the same uranium composition as the DU from SRS. The same isotopic abundances and contaminant concentrations developed for the SRS DU in Section 3.2.3 are therefore applied to the uranium fraction of GDP DU cylinders.

3.5.2.2 Contaminated GDP DU

No quantitative information is available about the contamination of the GDP DU Cylinders, other than limited research determining that some are contaminated and some are not. Given the lack of definitive information about the degree of contamination, it is assumed that contaminated DU from the GDPs shares the same composition as the DU from SRS. The same isotopic abundances and contaminant concentrations developed for the SRS DU in Section 3.2.3 are therefore applied to the contaminated fraction of GDP DU cylinders. There are no other data that are available at this time. The processes under which the DU waste is generated is similar in both case, with material being processed in a diffusion cascade. In both cases the cascades were contaminated, and this is the source of the contaminants in the DU. Without further information on the contamination concentration levels, use of the SRS DU contaminant concentrations is the only information available, even though it is surrogate information.

3.5.2.3 Fraction of Contaminated GDP DU

Assuming that each GDP cylinder is either “clean” or “contaminated”, an estimate is needed for the number of each type, so that the total amount of contaminant radionuclides in the GDP inventory can be estimated. At the time of this writing, the best available information about this comes from a study by Henson (2006): DUF6-G-G-STU-003 (Draft for UDS review). This document reviews information about the Paducah population of cylinders as recorded on cylinder history cards, which were used until 1988, and all contaminated cylinders are represented in this

population. Table 1 (reproduced here as Table 10) in Henson (2006) categorizes the cylinders as follows:

- "Category 1 – 13,240 cylinders: Cleared" cylinders, which are not contaminated,
- "Category 2 – 1,335 cylinders: TRU and/or Tc" cylinders, which are confirmed to have some degree of contamination,
- "Category 3 – 971 cylinders: >1% U235" cylinders, which do not contain DU and so are not considered in this PA, and
- "Category 4 – 22,382 cylinders: To Be Determined" cylinders which have unknown status regarding contamination. 9,407 of these cylinders have history cards and 12,975 do not.

Note that these values are in numbers of cylinders, rather than mass of DU, so an assumption is made for the purposes of estimating the fraction of waste that is contaminated that each cylinder contains the same mass of DU. Note also that the total number of cylinders here is not the same as the number of cylinders suggested in Section 3.5.1. This reflects both uncertainty in the total number of cylinders, and the change in number through time as cylinders are reprocessed or transferred.

The Paducah data can be summarized as follows for the purposes of building a distribution for the fraction of cylinders that are contaminated:

- 13,240 are known to not be contaminated
- 1,335 are known to be contaminated
- Of the unknowns 9,407 have history cards, and, hence, can be considered part of the same population of reconciled cylinders. These are assumed to be pre-1988 cylinders.
- Of the unknowns, 12,975 do not have history cards. These are post-1988 cylinders.

The cylinder history card system at Paducah was discontinued May 31, 1988 (Henson, 2006). Paducah cylinders post-1988 are considered much more likely to be clean of contaminants. Consequently, unknown cylinders are modeled differently for pre-1988 and post-1988.

The cylinders at Portsmouth also need to be considered. The Depleted Uranium Management Information Network reports the numbers as 16,109 from the Portsmouth GDP, and 4,822 from the K-25 GDP, now moved to Portsmouth (DOE, 2010). These cylinders are also considered unlikely to be contaminated (personal communication, Tammy Stapleton, April 2011).

This completes the summary of the population of cylinders that are considered for disposal at the Clive facility. The available information is used to construct an estimate of the total fraction of the cylinders that are contaminated. In effect the proportion contaminated at Paducah for the cylinders that have known status is used as an estimate of the fraction of all cylinders with history cards that are contaminated. These are presumed to be all of the pre-1988 cylinders. For the post-1988 cylinders at Paducah, which have no history cards, and the Portsmouth cylinders, a much smaller fraction of the cylinders is assumed to be contaminated.

Consequently, the fraction of Pre-1988 cylinders at Paducah that is assumed to be contaminated is about 9% [1,335 / (1,335 + 13,240)]. The Portsmouth cylinders might also have a small fraction that are contaminated. Using expert opinion, this is estimated at less than 1%, with a best guess at no more than 10 cylinders contaminated (personal communication, Tammy Stapleton, April 2011). These values were interpreted as expert judgment of the 95th and 50th percentiles of the distribution, respectively. A beta distribution was fit to these values, following the procedures outlined in the Fitting Probability Distributions white paper.

The total number of contaminated cylinders was then simulated by adding the number of confirmed contaminated cylinders with simulated numbers for the unknown cylinders. Table 11 shows the inputs that were used for the simulations. A distribution was constructed based on the simulation output for the overall proportion of cylinders that are contaminated. This Beta(0.0392, 0.0025) probability density function is shown in Figure 6.

In terms of the number of contaminated cylinders, this distribution has 1st, 50th, and 99th percentiles of 1,946, 2,266, and 2,619, respectively. This is a fairly narrow distribution given the lack of information available. It is narrow because nearly 15,000 of the Paducah cylinders have been characterized, an assumption is made that all other pre-1988 cylinders will be show a similar ratio, and the remaining cylinders are expected to be clean of contamination. As more information is gathered when the depleted uranium is prepared for disposal, then input distributions used to characterize the GDP waste should be revisited. Information that will be needed will include total amount of DU, chemical speciation of DU, and activity concentrations of the DU and contaminants.

Table 10: Categorization of Paducah Cylinders Using Cylinder History Cards (reproduced from Table 1 in Henson, 2006)

Category 1: Cleared	Category 2: TRU and/or Tc	Category 3: >1% ^{235}U	Category 4: To Be Determined
Filled once with natural normal or depleted material. (9,728)	Never filled with 1% or greater assay, but have a history of containing recycled feed material. These cylinders may have "hidden heels" containing both transuranics (TRU) and Tc. (1,334)	Filled at some time with material >1% assay, and also used to contain recycled material. These cylinders may have "hidden heels" containing both transuranics (TRU) and Tc. (584)	No Paducah history card. (12,975)
Filled more than once, but only with natural normal or depleted material. (2,681)	No history of recycled feed service, but used to hold Paducah product (at <1% enrichment). These cylinders may also have "hidden heels" which could contain Tc. (1)	No history of recycled feed service, but used to hold Paducah product (at >1% enrichment). These cylinders may also have "hidden heels" which could contain Tc. (387)	History card does not provide enough information. (9,407)
Washed and subsequently filled with only natural normal or depleted material. (832)		Filled at some time with >1% assay, but have never contained recycled uranium or Paducah product. (n/a for Phase II)	
TOTAL = 13,240	TOTAL = 1,335	TOTAL = 971	TOTAL = 22,382

Table 11: Inputs for the Simulation of the Fraction of Contaminated GDP Cylinders

Cylinder Type	Paducah Category 2	Paducah Category 1	Paducah Category 4 Pre-1988	Paducah Category 4 Post-1988	Portsmouth (not from Oak Ridge)	Portsmouth (from Oak Ridge)
Number	1,335	13,240	9,407	12,975	16,109	4,822
Simulated Binomial Proportion	NA (confirmed value)	NA (confirmed value)	Beta(0.092, 0.0024)	Beta(0.0020, 0.0042)		

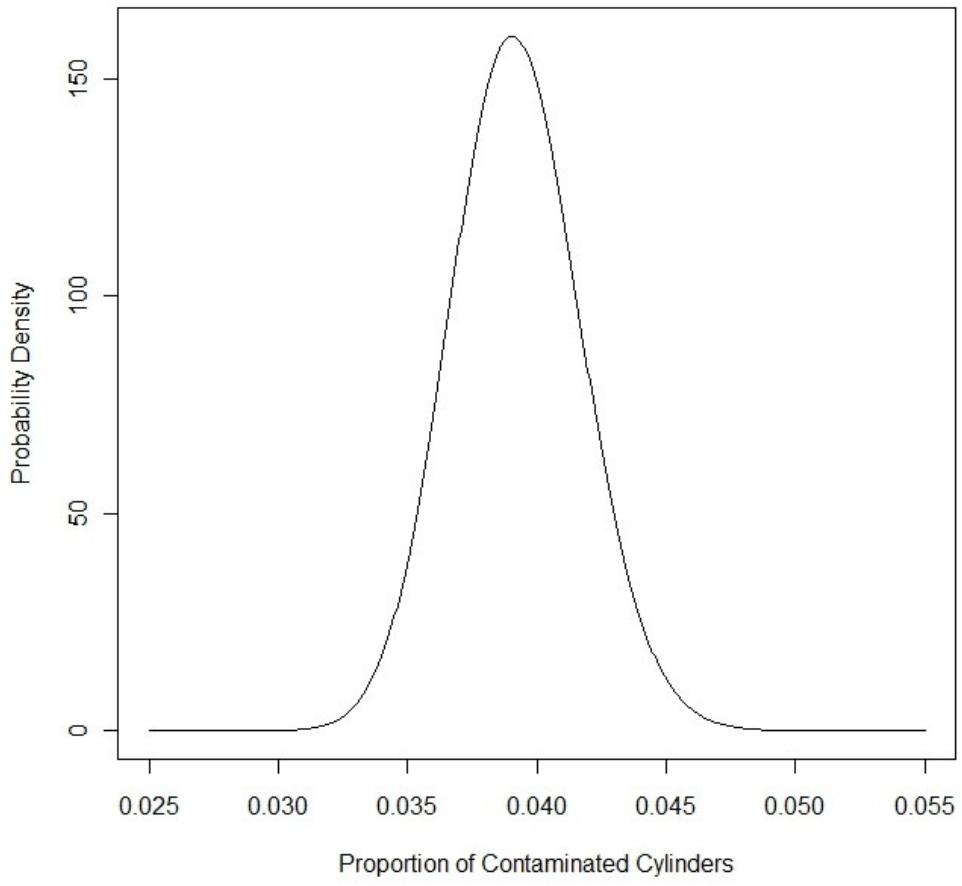

Figure 6. Probability density function for the proportion of contaminated cylinders.

4.0 References

Beals D.M., LaMont S.P., Cadieux J.R., et al. 2002. Determination of Trace Radionuclides in SRS Depleted Uranium (DU). WSRC-TR-2002-00536, Westinghouse Savannah River Company, Savannah River Site, Aiken, SC.

DOE (U.S. Department of Energy) 1999a. Programmatic Environmental Impact Statement for *Alternative Strategies for the Long-Term Management and Use of Depleted Uranium Hexafluoride* (DUF6 PEIS) (DOE/EIS-0269) .

DOE 1999b. Final Plan for the Conversion of Depleted Uranium Hexafluoride as Required by Public Law 105-204.

DOE, 2004a. *Final Environmental Impact Statement for Construction and Operation of a Depleted Uranium Hexafluoride Conversion Facility at the Paducah, Kentucky, Site*, DOE/EIS-0359, U.S. DOE Environmental Management, June 2004.

DOE, 2004b. *Final Environmental Impact Statement for Construction and Operation of a Depleted Uranium Hexafluoride Conversion Facility at the Portsmouth, Ohio, Site*, DOE/EIS-0360, U.S. DOE Environmental Management, June 2004.

DOE. 2010. *Depleted UF_6 Management Information Network*. URL: http://web.ead.anl.gov/uranium/mgmtuses/storage/index.cfm

Energy*Solutions*. 2009b. *Radioactive Waste Profile Record, EC 0230, Rev. 7, plus attachments* (Form 9021 33), EnergySolutions Inc. Clive UT.

Energy*Solutions*. 2009d. *Uniform Low-level Radioactive Waste Manifest Shipping Papers,* (Form 540), Energy*Solutions* Inc. Clive UT.

Fussell, G.M, and D. L. McWhorter, 2002. *Project Plan for the Disposition of the SRS Depleted, Natural, and Low-Enriched Uranium Materials*. WSRC-RP-2002-00459, Washington Savannah River Site, November 21, 2002.

GEL 2010a. GEL Work Order 243721. Laboratory report dated January 12, 2010.

GEL 2010b. GEL Work Order 244495. Laboratory report dated January 19, 2010.

GEL 2010c. GEL Work Order 249710. Laboratory report dated April 8, 2010.

Henson (Henson Technical Projects, LLC), 2006, *Contents Categorization of Paducah DUF6 Cylinders Using Cylinder History Cards – Phase II*, DUF6-G-G-STU-003, Draft for UDS Review, Uranium Disposition Services, LLC, Lexington, KY, 30 September 2006 (file: DUF6-G-G-STU-003 Henson 2006.pdf)

Johnson R. 2010. State of Utah, DEQ. Memo – April 6, 2010 Subj. Savannah River Depleted Uranium Sampling

NRC (U.S. Nuclear Regulatory Commission). 2010. *Stages of the Nuclear Fuel Cycle*, URL: http://www.nrc.gov/materials/fuel-cycle-fac/stages-fuel-cycle.html

ORNL (Oak Ridge National Laboratory). 2000a. *Depleted Uranium Storage and Disposal Trade Study: Summary Report*, ORNL/TM 2000/10, Oak Ridge National Laboratory, Oak Ridge TN, February, 2000

ORNL. 2000b. *Assessment of Preferred Depleted Uranium Disposal Forms*, ORNL/TM 2000/161, Oak Ridge National Laboratory, Oak Ridge TN, June 2000

ORNL. 2000c. *Strategy for Characterizing Transuranics and Technetium Contamination in Depleted UF6 Cylinders*, ORNL/TM-2000/242, Oak Ridge National Laboratory, October 2000.

ORNL. 2000d. *Evaluation of the Acceptability of Potential Depleted Uranium Hexafluoride Conversion Products at the Envirocare Disposal Site*, ORNL/TM-2000/355, Oak Ridge National Laboratory, October 2000.

Rich, B.L., S.L. Hinnefeld, C.R. Lagerquist, W.G. Mansfield, L.H. Munson, E.R. Wagner, and E.J. Vallario, 1988. *Health Physics Manual of Good Practices for Uranium Facilities*, EGG-2530, Idaho National Engineering Laboratory, Idaho Falls, ID, June 1988.

SRS (Savannah River Site). 2002. SRS Interoffice Memorandum 071802 Sampling Plan for DU. Westinghouse Savannah River Company, SRS, NMM-ETS-2002-00108, Revision 0. Dated July 18, 2002. To Robertson, Breidenback, Howell, from Loftin, McWhorter.

Appendix

Table 12. Uranium isotopic abundances by mass spectrometry, atomic percent, including replicates (data summarized in Table 16, Beals, et al. 2002)

Sample	Replicate	^{234}U	^{235}U	^{236}U	^{238}U
3	a	0.0004%	0.1270%	0.0065%	99.87%
3	b	0.0004%	0.1260%	0.0065%	99.87%
9	a	0.0004%	0.1260%	0.0064%	99.87%
9	b	0.0004%	0.1250%	0.0064%	99.87%
17	a	0.0004%	0.1260%	0.0066%	99.87%
17	b	0.0004%	0.1260%	0.0066%	99.87%
20	a	0.0005%	0.1270%	0.0068%	99.87%
20	b	0.0004%	0.1290%	0.0067%	99.86%
25	a	0.0008%	0.1510%	0.0096%	99.84%
25	b	0.0007%	0.1510%	0.0095%	99.84%
30	a	0.0006%	0.1410%	0.0088%	99.85%
30	b	0.0006%	0.1400%	0.0086%	99.85%

Table 13. Uranium isotopic abundances by alpha spectrometry (as percent of total uranium activity) (Table 17, Beals, et al. 2002) and Technetium concentrations in the SRS-2002 data (Beals, et al. 2002)

Sample	^{238}U	$^{235+\ 236}U$	^{234}U	^{99}Tc (nCi/g)
1	91.7	1.72	6.57	44.2
2	91.0	1.74	7.28	57.5
3	91.3	2.04	6.63	21.2
4	91.3	1.86	6.82	33.3
5	91.6	1.73	6.67	15.7
6	91.2	1.76	7.07	19.1
7	91.2	1.85	6.91	18.5
8	91.6	1.71	6.67	24.5
9	91.3	1.98	6.72	90.2
10	91.8	1.7	6.55	79.7
11	91.6	1.7	6.75	89.8
12	91.8	2.04	6.18	79.7
13	91.3	1.95	6.74	37.5
14	91.2	1.7	7.09	75.3
15	91.6	1.74	6.63	34.2
16	91.4	1.86	6.7	74.2
17	91.2	2.07	6.7	41.4
18	91.4	1.86	6.71	64.7
19	91.7	1.97	6.32	16.1
20	90.8	2.25	6.92	14.9
21	91.6	1.73	6.69	27.2
22	87.5	2.11	10.42	8.1
23	88.4	2.11	9.46	15.7
24	85.9	2.51	11.55	9
25	86.9	2.41	10.71	93.8
26	86.7	2.36	10.9	92.7
27	87.3	2.27	10.41	32.5
28	88.0	2.26	9.72	55.3
29	87.3	2.84	9.91	53.8
30	88.5	2.27	9.2	88.5
31	85.9	2.77	11.32	93.7
32	88.6	2.8	8.61	54.3
33	88.2	1.83	9.99	73
Mean	90	2.05	7.99	49.37
Std.Dev	2.03	0.34	1.77	29.26

Table 14. January 2010 Energy*Solutions* Data Analyzed by GEL (GEL 2010a and 2010b)

Sample ID	bulk density (g/cm^3)	^{99}Tc (pCi/g)	total uranium (µg/g)	$^{233+234}U$ (pCi/g)	$^{235+236}U$ (pCi/g)	^{238}U (pCi/g)
243721001	3.31	2.28E+4	7.93E+5	4.84E+4	1.11E+4	2.65E+5
243721002	3.45	9.78E+3	8.54E+5	4.50E+4	7.21E+3	2.86E+5
243721003	2.84	1.78E+4	8.06E+5	3.83E+4	1.89E+4	2.68E+5
243721004	3.15	9.04E+3	8.27E+5	3.26E+4	4.92E+3*	2.77E+5
243721005	2.50	1.44E+4	8.48E+5	4.25E+4	7.27E+3*	2.85E+5
243721006	3.21	2.08E+4	8.80E+5	3.04E+4	1.28E+4	2.94E+5
243721007	4.00	2.25E+4	9.90E+5	6.44E+4	1.28E+4	3.31E+5
243721008	2.36	1.14E+4	6.50E+5	3.37E+4	1.19E+4	2.17E+5
244495001	3.46	2.60E+4	8.44E+5	3.57E+4	6.72E+3	2.83E+5
244495002	3.66	2.35E+4	8.00E+5	3.65E+4	1.17E+4	2.67E+5
244495003	4.00	1.81E+4	8.76E+5	4.70E+4	9.94E+3	2.93E+5
Mean	3.27	1.78E+4	8.33E+5	4.13E+4	1.15E+4	2.79E+5
Std.Dev	0.54	5.91E+3	8.15E+3	9.73E+3	3.57E+3	2.74E+3

* - reported as non-detects – detection limits used for statistical analysis.

Table 15. April 2010 Energy*Solutions* Data Analyzed by GEL (GEL 2010c)

Sample ID	bulk density (g/cm^3)	^{99}Tc (pCi/g)	total uranium (µg/g)	$^{233+234}U$ (pCi/g)	$^{235+236}U$ (pCi/g)	^{238}U (pCi/g)
249710001	-	-	7.95E+5	3.42E+4	6.34E+3	2.66E+5
249710002	-	-	8.31E+5	3.65E+4	6.31E+3	2.78E+5
249710003	-	-	8.15E+5	3.35E+4	5.12E+3	2.73E+5
249710004	-	-	8.74E+5	3.84E+4	5.17E+3	2.93E+5
249710005	-	-	8.28E+5	3.66E+4	4.30E+3	2.78E+5
249710006	-	-	8.74E+5	4.17E+4	4.31E+3	2.93E+5
249710007	-	-	7.07E+5	2.94E+4	4.86E+3	2.37E+5
249710008	-	-	6.46E+5	3.78E+4	4.43E+3	2.17E+5
249710009	-	-	7.42E+5	3.66E+4	6.80E+3	2.48E+5
249710010	-	-	7.97E+5	3.86E+4	4.95E+3	2.67E+5
249710011	-	-	8.29E+5	3.51E+4	4.36E+3	2.78E+5
249710012	-	-	7.58E+5	2.98E+4	7.60E+3	2.54E+5
249710013	-	-	7.45E+5	3.16E+4	4.89E+3	2.50E+5
249710014	-	-	7.71E+5	3.09E+4	4.14E+3	2.58E+5
249710015	-	-	8.97E+5	4.02E+4	5.75E+3	3.01E+5
Mean			7.88E+5	3.54E+4	5.34E+3	2.64E+5
Std.Dev.			6.61E+4	3.60E+3	1.07E+3	2.21E+4

Table 16. Technetium-99 concentrations collected by State of Utah, (Johnson, 2010)

Sample ID	pCi/g	Sample ID	pCi/g	Sample ID	pCi/g
1337	6.30E+3	3800	1.24E+4	0249	3.28E+3
1348	1.27E+4	3824	5.59E+3	0370	4.77E+3
1423	2.13E+3	3849	4.13E+3	0434	2.80E+3
1428	3.45E+3	3857	2.56E+3	0461	4.09E+3
1429	7.05E+3	3870	1.55E+4	0488	3.09E+3
1467	2.66E+3	3951	1.79E+3	0499	8.22E+2
1584	3.50E+3	4052	2.07E+3	0555	1.12E+3
1622	7.99E+3	4104	2.44E+3	0562	2.08E+3
1697	3.09E+3	4138	4.23E+3	0565	7.19E+3
1712	5.21E+3	4162	3.51E+3	0571	4.11E+3
1739	5.62E+3	4172	6.85E+3	0626	1.78E+3
1794	2.74E+3	4185	2.64E+3	0629	4.41E+3
1808	2.54E+3	4207	2.01E+3	0662	2.74E+2
1834	1.53E+4	4244	1.56E+3	0670	1.95E+3
1835	7.12E+3	4275	1.22E+3	0697	1.63E+3
1853	2.49E+3	4303	8.86E+2	0739	2.37E+3
1876	1.47E+3	4322	1.01E+3	0756	3.56E+3
1918	2.90E+3	4362	3.06E+3	0800	1.57E+3
1946	2.08E+3	4376	6.66E+3	0809	5.73E+2
2061	1.84E+4	4384	2.32E+3	0813	2.22E+3
2077	1.83E+3	4385	9.72E+3	0852	4.45E+3
2098	1.10E+4	4393	3.58E+3	0853	2.31E+3
2102	7.65E+2	4414	3.78E+3	0854	2.83E+3
2140	7.86E+3	4415	8.86E+3	0879	4.52E+3
2250	6.71E+3	4425	5.87E+3	0884	4.76E+3
2256	7.19E+3	4431	1.29E+4	0893	2.02E+3
2343	1.30E+3	4486	5.83E+3	0910	2.24E+2
2424	6.27E+2	4487	2.63E+3	0911	8.23E+2
2449	4.86E+3	4504	8.48E+3	0927	6.38E+2
2481	1.32E+3	4535	5.25E+3	0928	7.42E+2
2497	1.62E+4	4606	1.72E+3	1000	5.85E+3
2517	8.06E+2	4611	3.47E+3	1021	1.24E+3
2528	1.66E+3	4687	1.51E+3	1030	1.63E+3
2550	3.02E+3	4760	3.04E+3	1117	6.56E+3
2614	1.49E+3	4790	2.28E+3	1140	1.76E+3
2674	1.89E+3	4817	2.25E+3	1147	1.29E+3
2675	2.92E+3	4822	2.62E+3	1216	1.44E+3
2823	4.89E+3	4851	1.32E+4	1505	2.26E+3

Sample ID	pCi/g	Sample ID	pCi/g	Sample ID	pCi/g
2827	1.61E+4	4866	1.45E+4	1511	3.96E+3
2878	2.86E+3	4940	4.41E+3	1646	6.19E+3
3035	7.59E+3	4955	3.68E+3	1678	1.00E+4
3059	5.01E+3	4962	5.89E+3	2393	4.08E+3
3067	1.77E+3	5023	1.89E+3	2657	5.52E+3
3080	4.36E+3	5054	2.36E+3	2693	1.97E+3
3085	1.53E+3	5061	1.68E+3	3127	3.31E+3
3089	2.37E+3	5084	6.22E+3	3160	6.34E+3
3197	2.28E+3	5191	1.13E+4	3288	7.08E+3
3234	4.62E+3	5224	5.75E+3	3336	5.12E+3
3303	5.61E+3	5277	1.58E+3	3337	5.37E+3
3347	5.53E+3	5322	7.33E+2	3446	3.25E+3
3543	1.67E+3	0023	3.89E+3	3471	2.86E+3
3668	3.12E+3	0057	1.15E+3	3546	4.73E+3
3685	3.03E+3	0157	1.28E+3	4016	1.09E+4
3695	7.46E+3	0162	6.53E+3	4098	8.93E+3
3717	4.56E+3	0168	3.42E+3	4200	1.68E+3
3726	4.94E+3	0180	2.80E+3	4514	3.28E+3
3728	1.28E+4	0210	3.72E+3	4581	1.81E+3
3760	2.38E+3	0214	2.24E+3		

Number of samples = 173

Average ^{99}Tc concentration = 4,340 pCi/g

Standard Deviation = 3,550 pCi/g

Table 17. Concentration data for other radioisotopes, SRS 2002. (Beals, et al. 2002)

Sample	^{241}Am *(<) pCi/g	^{226}Ra *(<) pCi/g	^{137}Cs *(<) pCi/g	^{90}Sr *(<) pCi/g	^{237}Np pCi/g	^{238}Pu pCi/g	^{239}Pu pCi/g	^{240}Pu pCi/g	^{241}Pu pCi/g	^{129}I *(<) pCi/g
1	6	120	6	8.6	0.44	0.114	0.53	0.14	2.80	13
2	24	500	19	5.9	2.34	0.099	0.69	0.15	nd	7
3	21	450	17	3.4	0.33	0.065	0.48	0.12	1.00	7
4	17	330	14	6.7	4.61	0.129	0.84	0.17	nd	4
5	25	600	20	7.2	12.8	0.086	0.95	0.23	2.50	12
6	20	390	15	14	8.89	0.163	0.40	0.10	nd	10
7	16	314	13	8	14.3	0.090	0.34	0.10	1.60	9
8	16	310	12	7.7	3.85	1.420	0.91	0.48	10.00	4
9	10	240	9	50.7	6.52	0.350	3.43	1.14	11.00	8
10	21	470	19	32.7	2.43	0.244	0.48	0.18	3.80	6
11	16	370	14	23.4	13.6	0.240	3.10	0.68	13.00	20
12	11	250	10	29.3	11.9	0.090	1.15	0.29	2.70	14
13	11	260	10	46.6	8.55	0.230	5.09	1.14	17.00	18
14	13	340	12	31.2	1.3	0.123	2.46	0.55	7.50	20
15	17	360	13	40	6.38	0.127	0.36	0.09	0.90	16
16	12	300	11	68.2	33.5	0.099	0.66	nd	nd	16
17	11	230	10	28.4	6.08	0.125	1.63	0.50	4.00	17
18	11	230	8	38.3	2.86	0.081	0.75	0.20	nd	19
19	10	210	7	51	10.2	0.043	3.74	0.86	11.00	26
20	6	170	5	45.6	11.3	0.088	1.07	0.27	nd	32
21	14	300	13	27.1	1.92	0.094	0.50	0.12	1.10	33
22	9	250	8	28.6	0.77	0.149	0.81	0.22	3.40	27
23	18	380	15	45.7	1.67	0.186	1.81	0.52	5.30	24
24	16	340	13	26.9	0.69	0.242	1.30	0.36	nd	27
25	13	280	11	45.7	1.18	0.178	0.88	0.24	2.60	26
26	9	250	9	100.5	0.65	0.560	0.79	0.22	2.70	7
27	10	280	10	59.1	0.94	0.181	0.79	0.22	2.80	30
28	25	550	21	28	1.61	0.154	0.74	0.21	3.40	34
29	16	410	14	57.9	11.1	0.420	0.79	0.18	nd	24
30	10	190	10	32.9	0.87	0.123	0.85	0.22	4.00	27
31	16	350	15	78.9	1.04	0.250	1.02	nd	nd	26
32	9	190	7	438.2	1.32	0.155	1.09	0.32	2.50	22
33	9	240	9	35.8	1.58	0.153	0.82	0.24	1.70	28

Appendix References

Beals D.M., LaMont S.P., Cadieux J.R., et al. 2002. *Determination of Trace Radionuclides in SRS Depleted Uranium (DU)*. WSRC-TR-2002-00536, Westinghouse Savannah River Company, Savannah River Site, Aiken, SC.

GEL 2010a. GEL Work Order 243721. Laboratory report dated January 12, 2010.

GEL 2010b. GEL Work Order 244495. Laboratory report dated January 19, 2010.

GEL 2010c. GEL Work Order 249710. Laboratory report dated April 8, 2010.

Johnson R. 2010. State of Utah, DEQ. Memo – April 6, 2010 Subj. Savannah River Depleted Uranium Sampling

Neptune and Company Inc.

June 1, 2011 Report for EnergySolutions

Clive DU PA Model, version 1

Appendix 5

Unsaturated Zone Modeling

Unsaturated Zone Modeling for the Clive PA

28 May 2011

Prepared by

Neptune and Company, Inc.

and

Michael B. Gross

This page is intentionally blank, aside from this statement.

CONTENTS

FIGURES

TABLES

1.0 Summary of Parameter Values

A summary of parameter values used in the Clive DU PA Model is provided in Table 1. For distributions, the following notation is used:

- N(μ, σ, [*min*, *max*]) represents a normal distribution with mean μ and standard deviation σ, and optional truncation at the specified *min*imum and *max*imum,
- LN(*GM*, *GSD*, [*min*, *max*]) represents a log-normal distribution with geometric mean GM and geometric standard deviation GSD, and optional *min* and *max*,
- U(*min*, *max*) represents a uniform distribution with lower bound *min* and upper bound *max*,
- Beta(μ, σ, *min*, *max*) represents a generalized beta distribution with mean μ, standard deviation σ, minimum *min*, and maximum *max*,
- Gamma(μ, σ) represents a gamma distribution with mean μ and standard deviation σ, and
- TRI(*min*, *m*, *max*) represents a triangular distribution with lower bound *min*, mode *m*, and upper bound *max*.

Note that a number of these distributions are truncated at a minimum value of 0 and a maximum of Large, an arbitrarily large value defined in the GoldSim model. The truncation at the low end is a matter of physical limits (e.g. precipitation cannot be negative), and in GoldSim's distribution definitions, if truncations are made, they must be made at both ends, so the very large value is chosen for the upper end.

Table 1: Summary of Parameter Values and Distributions

Parameter	Distribution [*Comments*]	Units	Internal Reference
Average precipitation	N(8.61, 0.822, min=0 , max=Large)	in/yr	Section 3.1
Average surface runoff	LN(0.0252, 3.33, min=0 , max=0.1)	in/yr	Section 3.1
Average evapotranspiration	N(5.14, 0.762, min=0 , max=Large)	in/yr	Section 3.1
Armor layer moisture content	N(0.125, 0.0175, min=small , max=porosity of Unit 4)	—	Section 3.3, Table 9
Upper filter layer moisture content	same as Armor layer	—	Section 3.3, Table 9
Sacrificial soil moisture content	N(0.243, 0.0175, min=small , max=porosity of silt sand gravel)	—	Section 3.3, Table 9
Lower filter layer moisture content	same as sacrificial soil	—	Section 3.3, Table 9
Water tortuosity water content exponent	U(4/3, 7/3)	—	Section 9.1.3

Parameter	Distribution [*Comments*]	Units	Internal Reference
Water tortuosity porosity exponent	U(0.5, 2)	—	Section 9.1.3
Henry's Law constant ($K_{H,cp}$) for radon	9.3×10^{-3}	mol/L·atm	Section 9.3
Soil temperature	N(12, 1)	°C	Section 9.3
Escape-to-production ratio for uranium in DU oxide wastes	beta(0.290, 0.156, min=0, max=1)	—	Section 9.4.1
Free air diffusivity for radon	0.11	cm^2/s	Section 9.2.2
Thickness of the atmosphere layer	N(μ=2.0, σ=0.5, min=Small, max=Large)	m	Section 9.2.2, Table 15
Wind speed	N(μ=3.14, σ=0.5, min=Small, max=Large)	m/s	Section 9.2.2, Table 15
Atmospheric diffusion length	N(μ=0.1, σ=0.02, min=Small, max=Large)	m	Section 9.2.2, Table 15
Thickness of the Unsat zone (below the embankment clay liner)	N(12.9, 0.25, min=small, max=Large)	ft	Section 7.0
As-Designed Cover			
Mean lateral diversions by upper filter	N(0.0427, 0.0111, min=0, max=Large)	in/yr	Section 3.1
Mean lateral diversions by lower filter	N(3.39, 0.214, min=0 , max=Large)	in/yr	Section 3.1
Mean vertical flow through clay barrier	N(0.104, 0.00417, min=0 , max=Large)	in/yr	Section 3.1
Naturalized Cover			
Time to cover naturalization	N(40, 10, min=10, max=Large)	yr	Section 3.2
Mean lateral diversions by upper filter	0.0	in/yr	Section 3.2
Mean lateral diversions by lower filter	N(0.345, 0.0815, min=small , max=Large)	in/yr	Section 3.2
Mean vertical flow through clay barrier	N(0.0482, 0.00351, min=small , max=Large)	in/yr	Section 3.2
Unit 3			
Porosity_Unit3	equal to MCsat_Unit3	—	Section 4.3
BulkDensity_Unit3	N(ParticleDensity_Unit3 × (1 – Porosity_Unit3), 0.1, min=Small, max=Large)	g/cm^3	Section 4.3
ParticleDensity_Unit3	2.65	g/cm^3	Section 4.3
D_Unit3	N(2.73, 5.21e-3, min=0, max=3)	—	Section 4.4.1

Parameter	Distribution [*Comments*]	Units	Internal Reference
Hb_Unit3	N(8.85, 0.929, min=Small, max=Large); [*correlated to D_Unit3 as -0.85*]	cm	Section 4.4.1
MCres_Unit3	N(6.78e-3, 2.05e-3, min=Small, max=Large); [*truncated just above 0*]	—	Section 4.4.1
MCsat_Unit3	N(0.393, 6.11e-3, min=Small, max=1-Small), [*truncated just above 0 and just below 1*]	—	Section 4.4.1
Ksat_Unit3	N(5.14e-5, 5.95e-6, min=Small, max=Large); [*correlated to D_Unit3 as -0.98*]	cm/s	Section 4.4.1
Unit 4			
Porosity_Unit4	equal to MCsat_Unit4	—	Section 4.3
BulkDensity_Unit4	N(ParticleDensity_Unit4 × (1 – Porosity_Unit4), 0.1, min=Small, max=Large); [*truncated just above 0*]	g/cm^3	Section 4.3
ParticleDensity_Unit4	2.65	g/cm^3	Section 4.3
D_Unit4	N(2.81, 9.93e-5, min=0, max=3)	—	Section 4.4.2
Hb_Unit4	N(104., 1.72, min=Small, max=Large); [*correlated to D_Unit4 as -0.66*]	cm	Section 4.4.2
MCres_Unit4	N(0.108, 8.95e-4, min=Small, max=Large); [*truncated just above 0*]	—	Section 4.4.2
MCsat_Unit4	N(0.428, 6.08e-3, min=Small, max=1-Small); [*truncated just above 0 and just below 1*]	—	Section 4.4.2
Ksat_Unit4	N(5.16e-5, 5.97e-7, min=Small, max=Large); [*truncated just above 0; correlated to D_Unit4 as -0.37*]	cm/s	Section 4.4.2
Fine Cobble Mix			

Parameter	Distribution [*Comments*]	Units	Internal Reference
Porosity_FineCobbleMix	N (0.19, 0.01, min=Small, max=1-Small)	—	Section 5.1.2
BulkDensity_FineCobbleMix	N (ParticleDensity_ FineCobbleMix × (1 – Porosity_FineCobbleMix), 0.1, min=Small, max=Large)	g/cm^3	Section 5.1.2, Section 4.3
ParticleDensity_FineCobbleMix	2.65	g/cm^3	Section 5.1.2, Section 4.3
Fine Gravel Mix			
Porosity_FineGravelMix	N (0.28, 0.01, min=Small, max=1-Small)	—	Section 5.1.4
BulkDensity_FineGravelMix	N (ParticleDensity_FineGravelMix × (1 – Porosity_FineGravelMix), 0.1, min=Small, max=Large)	g/cm^3	Section 5.1.4, Section 4.3
ParticleDensity_FineGravelMix	2.65	g/cm^3	Section 5.1.4, Section 4.3
Rip Rap			
Porosity_RipRap	N (0.18, 0.01, min=Small, max=1-Small)	—	Section 5.1.1
BulkDensity_RipRap	N (ParticleDensity_RipRap × (1 – Porosity_RipRap), 0.1, min=Small, max=Large)	g/cm^3	Section 5.1.1, Section 4.3
ParticleDensity_RipRap	2.65	g/cm^3	Section 5.1.1, Section 4.3
Silt Sand Gravel			
Porosity_SiltSandGravel	N (0.31, 0.01, min=Small, max=1-Small)	—	Section 5.1.3
BulkDensity_SiltSandGravel	N (ParticleDensity_SiltSandGravel × (1 – Porosity_SiltSandGravel), 0.1, min=Small, max=Large)	g/cm^3	Section 5.1.3, Section 4.3
ParticleDensity_SiltSandGravel	2.65	g/cm^3	Section 5.1.3, Section 4.3

Parameter	Distribution [*Comments*]	Units	Internal Reference
Upper Radon Barrier Clay			
Porosity_UpperRnBarrierClay	assigned value for Unit 4	—	Section 4.4.2
BulkDensity_UpperRnBarrierClay	assigned value for Unit 4	g/cm^3	Section 4.3
D_UpperRnBarrierClay	assigned value for Unit 4	—	Section 4.4.2
Hb_UpperRnBarrierClay	assigned value for Unit 4	cm	Section 4.4.2
MCres_UpperRnBarrierClay	assigned value for Unit 4	—	Section 4.4.2
MCsat_UpperRnBarrierClay	assigned value for Unit 4	—	Section 4.4.2
Ksat_UpperRnBarrierClay	LN(5e-8, 1.2)	cm/s	Section 5.1.5
Lower Radon Barrier Clay			
Porosity_LowerRnBarrierClay	assigned value for Unit 4	—	Section 4.4.2
BulkDensity_LowerRnBarrierClay	assigned value for Unit 4	g/cm^3	Section 4.3
D_LowerRnBarrierClay	assigned value for Unit 4	—	Section 4.4.2
Hb_LowerRnBarrierClay	assigned value for Unit 4	cm	Section 4.4.2
MCres_LowerRnBarrierClay	assigned value for Unit 4	—	Section 4.4.2
MCsat_LowerRnBarrierClay	assigned value for Unit 4	—	Section 4.4.2
Ksat_LowerRnBarrierClay	LN(1e-6, 1.2)	cm/s	Section 5.1.6
Generic Waste			
Porosity_Generic_Waste	assigned value for Unit 3	—	Section 4.4.1, Section 6.0
BulkDensity__Generic_Waste	assigned value for Unit 3	g/cm^3	Section 4.3, Section 6.0
D_Generic_Waste	assigned value for Unit 3	—	Section 4.4.1, Section 6.0
Hb_Generic_Waste	assigned value for Unit 3	cm	Section 4.4.1, Section 6.0
MCres_Generic_Waste	assigned value for Unit 3	—	Section 4.4.1, Section 6.0
MCsat_Generic_Waste	assigned value for Unit 3	—	Section 4.4.1, Section 6.0
Ksat_Generic_Waste	assigned value for Unit 3	cm/s	Section 4.4.1, Section 6.0
UO3 Waste			
Porosity_Generic_Waste	assigned value for Unit 3	—	Section 4.4.1, Section 6.0
BulkDensity__Generic_Waste	assigned value for Unit 3	g/cm^3	Section 4.3, Section 6.0
D_Generic_Waste	assigned value for Unit 3	—	Section 4.4.1, Section 6.0

Parameter	Distribution [*Comments*]	Units	Internal Reference
Hb_Generic_Waste	assigned value for Unit 3	cm	Section 4.4.1, Section 6.0
MCres_Generic_Waste	assigned value for Unit 3	—	Section 4.4.1, Section 6.0
MCsat_Generic_Waste	assigned value for Unit 3	—	Section 4.4.1, Section 6.0
Ksat_Generic_Waste	assigned value for Unit 3	cm/s	Section 4.4.1, Section 6.0
U3O8 Waste			
Porosity_Generic_Waste	assigned value for Unit 3	—	Section 4.4.1, Section 6.0
BulkDensity__Generic_Waste	assigned value for Unit 3	g/cm^3	Section 4.3, Section 6.0
D_Generic_Waste	assigned value for Unit 3	—	Section 4.4.1, Section 6.0
Hb_Generic_Waste	assigned value for Unit 3	cm	Section 4.4.1, Section 6.0
MCres_Generic_Waste	assigned value for Unit 3	—	Section 4.4.1, Section 6.0
MCsat_Generic_Waste	assigned value for Unit 3	—	Section 4.4.1, Section 6.0
Ksat_Generic_Waste	assigned value for Unit 3	cm/s	Section 4.4.1, Section 6.0
Liner Clay			
Porosity_LinerClay	assigned value for Unit 4	—	Section 4.4.2
BulkDensity__LinerClay	assigned value for Unit 4	g/cm^3	Section 4.3
D_LinerClay	assigned value for Unit 4	—	Section 4.4.2
Hb_LinerClay	assigned value for Unit 4	cm	Section 4.4.2
MCres_LinerClay	assigned value for Unit 4	—	Section 4.4.2
MCsat_LinerClay	assigned value for Unit 4	—	Section 4.4.2
Ksat_LinerClay	LN(1e-6, 1.2)	cm/s	Section 5.1.7

Porous medium solid/water partition coefficients for various radionuclides in these materials are assigned one of three representative and rather generic collections of K_d values for the materials sand, silt and clay. These assignments are listed in Table 2, with discussion in the relevant sections below. Distributions for the values themselves are documented in the *Geochemical Modeling* white paper.

Table 2. Assignment of solid/water partition coefficients K_d values.

material	K_d material
Unit 2 (includes saturated zone medium)	clay
Unit 3 (includes unsaturated zone medium and all wastes)	sand
Unit 4 (includes loess, clay liner, and upper and lower radon barrier clays)	silt
rip rap	none
fine cobble mix	sand
silt sand gravel	sand
fine gravel mix	sand

2.0 Introduction

Energy*Solutions* operates a low-level radioactive waste (LLW) and mixed waste disposal facility at Clive, Utah. The waste disposal cells (or embankments—the terms are used interchangeably) at the facility are permanent, clay-lined cells with composite caps composed of clay, soil, and cobble layers above the waste. The focus of this white paper is on the hydrologic response of the facility's Class A South (CAS) cell, which has been proposed as a burial site for depleted uranium waste (DU waste). Neptune and Company has been tasked with developing a performance assessment (PA) to evaluate the proposed disposal of DU waste streams in the CAS cell from the Savannah River Site and from the gaseous diffusion plants in Portsmouth, Ohio, and Paducah, Kentucky.

This white paper defines an infiltration model for unsaturated flow through the CAS cell and down to the water table where it enters the saturated zone as recharge. This infiltration model is incorporated into the overall Clive DU PA Model, which is developed using the GoldSim systems analysis modeling software. The infiltration model for the engineered cover is based on calculations for the top and side slopes of the CAS cell that were performed using the EPA's Hydrologic Evaluation of Landfill Performance (HELP) program (Schroeder, et al., 1994). The hydraulic properties for the unsaturated media are based on laboratory measurements by Colorado State University (CSU) for the moisture retention and hydraulic conductivity of core samples from Unit 3 (a silty sand) and Unit 4 (a silty clay) at the site (Bingham Environmental, 1991). The flow analysis determines the suction head, moisture content, and hydraulic conductivity from a solution of the Darcy equation (Buckingham, 1907) for steady state unsaturated flow in the downward direction as a function of vertical infiltration rate.

A detailed description of the hydrogeology of the Clive facility, including the local stratigraphy and construction of the waste cells, has been given in previous reports (Bingham Environmental 1991, 1994) and is not repeated here. Similarly, detailed numerical solutions using the HELP and UNSAT-H modeling programs for infiltration through the engineered cover, waste, clay liners, and soil at the various cells of the facility have been presented in previous reports, most recently for the CAS cell (Whetstone, 2007), and is not repeated here. These reports provide data for analyzing infiltration through the engineered cover and representative soil characteristics for

Units 3 and 4. The latter report also provides numerical results for validating the computational method for solving Darcy's equation that is presented in this white paper.

The infiltration model, soil characteristics, and solution technique for unsaturated flow have been incorporated into the GoldSim-based Clive DU PA Model, for the CAS cell. A major difference between this white paper and the previous work is the effort to incorporate uncertainty in hydrogeologic response into the analysis of unsaturated flow through the CAS cell.

This white paper further describes the contaminant transport mechanisms in unsaturated porous media. This includes gaseous diffusion, water advection and diffusion, and fate and transport of radon.

Section 3.0 defines the infiltration model for the engineered cover on the top and side slopes of the CAS cell's engineered cover. Section 4.0 defines the moisture retention and hydraulic conductivity for Units 3 and 4, based on measurements of core properties by CSU, as well as porosity and bulk density distributions for these materials. Section 5.0 defines the material properties for the engineered materials. Section 6.0 describes material properties for waste materials. Section 7.0 discusses properties of the natural unsaturated zone below the embankment liner and above the water table. Section 8.0 defines the numerical technique for solving Darcy's equation, provides verification of the numerical technique by comparison with results from UNSAT-H, and presents typical results for a range of infiltration rates through the CAS cell. Section 9.0 is devoted to porous medium contaminant transport topics such as advection and diffusion, including the fate and transport of radon in the waste and cover.

3.0 HELP Calculation and Infiltration Model for the Top and Side Slopes

The infiltration model for the engineered cover uses calculations with the HELP program as a guide to defining the vertical and lateral flow rates in the individual layers of the engineered cover as a function of time. The HELP model is a quasi-two-dimensional representation that analyzes the water balance in the cover layers using weather data, soil properties, and landfill design data. The major layers of the as-designed cover and their hydraulic properties are listed in Tables 3 and 4. The names in parentheses under the "Layer No." headings in the Tables are the names of Layers in the PA model. These layers are subdivided into thinner GoldSim Cell Pathway elements, analogous to 1-D finite-difference modeling cells, in the Clive DU PA Model. Differences in construction between the two sections of the cover for the parameters shown are: The porosity of the rip-rap on the top slope is slightly higher than that on the side slope, the hydraulic conductivity of the rip-rap on the side slope is nearly twice that of the rip-rap on the top slope, and the Type-B filter (lower filter) is three times thicker on the side slope than on the top slope.

Table 3. Major layers of the engineered cover on the top slope of the CAS cell.

Layer No.	Material	Thickness	Porosity (-)	K_s (cm/s)	Function	Description
1 (Armor)	Type-B Rip Rap	18 in (~45 cm)	0.19	42	Vertical Percolation	Coarse gravel to fine cobble, 0.75 to 4.5 in
2 (Upper Filter)	Type-A Filter	6 in (~15 cm)	0.19	42	Lateral Drainage	Coarse sand to cobble, 0.08 to 6 in
3	Sacrificial Soil	12 in (~30 cm)	0.31	0.004	Barrier Soil	Silty sand and gravel (coarser than Unit 3)
4 (Lower Filter)	Type-B Filter	6 in (~15 cm)	0.28	3.5	Lateral Drainage	Coarse sand to fine gravel, 0.2 to 1.5 in
5	Upper Radon Barrier	12 in (~30 cm)	0.43	5×10^{-8}	Barrier Soil	Silty clay (Unit 4)
6	Lower Radon Barrier	12 in (~30 cm)	0.43	1×10^{-6}	Vertical Percolation	Silty clay (Unit 4)
7	Waste	100 in (~250 cm)	0.437	5×10^{-4}	Vertical Percolation	Sand
8	Clay Liner	24 in (~60 cm)	0.430	1×10^{-6}	Barrier Soil	Silty clay (Unit 4)

Based on (Whetstone 2007, Table 8)

Table 4. Major layers of the engineered cover on the side slope of the CAS cell.

Layer No.	Material	Thickness (inches)	Porosity (-)	K_s (cm/s)	Function	Description
1 (Armor)	Type-A Rip Rap	18 in (~45 cm)	0.17	80	Vertical Percolation	Coarse gravel to boulders, 2 to 16 in
2 (Upper Filter)	Type-A Filter	6 in (~15 cm)	0.19	42	Lateral Drainage	Coarse sand to cobble, 0.08 to 6 in
3	Sacrificial Soil	12 in (~30 cm)	0.31	0.004	Barrier Soil	Silty sand and gravel (coarser than Unit 3)
4 (Lower Filter)	Type-B Filter	18 in (~45 cm)	0.28	3.5	Lateral Drainage	Coarse sand to fine gravel, 0.2 to 1.5 in
5	Upper Radon Barrier	12 in (~30 cm)	0.43	5×10^{-8}	Barrier Soil	Silty clay (Unit 4)
6	Lower Radon Barrier	12 in (~30 cm)	0.43	1×10^{-6}	Vertical Percolation	Silty clay (Unit 4)
7	Waste	100 in (~250 cm)	0.437	5×10^{-4}	Vertical Percolation	Sand
8	Clay Liner	24 in (~60 cm)	0.430	1×10^{-6}	Barrier Soil	Silty clay (Unit 4)

Based on (Whetstone 2007, Table 9)

Annual water balances for the top and side slopes of the CAS cell computed with the HELP model by Whetstone (2007, Table 12) are shown in Tables 5 and 6.

Table 5. Water balance for the top slope of the CAS cell.

Flow Process	Flow Rate or Head	
Annual Precipitation	22.15 cm/yr	8.72 in/yr
Surface Runoff	0.132 cm/yr	0.052 in/yr
Evapotranspiration	13.1 cm/yr	5.14 in/yr
Lateral Drainage from Type-A (Upper) Filter	0.11 cm/yr	0.043 in/yr
Net Percolation into Sacrificial Soil	8.85 cm/yr	3.483 in/yr (= 8.72 – 0.052 – 5.142 – 0.043)
Head on Top of Sacrificial Soil	0.0025 cm	0.001 in
Lateral Drainage from Type-B (Lower) Filter	8.57 cm/yr	3.374 in/yr
Net Percolation into Upper Radon Barrier	0.277 cm/yr	0.109 in/yr (= 3.483 – 3.374)
Head on Top of Upper Radon Barrier	0.041 cm	0.016 in
Net Percolation through bottom clay layer	0.277 cm/yr	0.109 in/yr

Based on (Whetstone 2007, Table 12, first subtable)

Table 6. Water balance for the side slope of the CAS cell.

Flow Process	Flow Rate or Head	
Annual Precipitation	22.15 cm/yr	8.72 in/yr
Surface Runoff	0.147 cm/yr	0.058 in/yr
Evapotranspiration	12.85 cm/yr	5.058 in/yr
Lateral Drainage from Type-A (Upper) Filter	0.572 cm/yr	0.225 in/yr
Net Percolation into Sacrificial Soil	8.58 cm/yr	3.379 in/yr (= 8.72 – 0.058 – 5.058 – 0.225)
Head on Top of Sacrificial Soil	0.0025 cm	0.001 in
Lateral Drainage from Type-B (Lower) Filter	8.29 cm/yr	3.265 in/yr
Net Percolation into Upper Radon Barrier	0.287 cm/yr	0.113 in/yr (= 3.379 – 3.265)
Head on Top of Upper Radon Barrier	0.005 cm	0.002 in

Based on (Whetstone 2007, Table 12, second subtable)

While there are small differences in the amount of lateral drainage from the upper and lower filter layers for the top and side slope of the cell, the net infiltration entering the upper radon barrier is 0.28 cm/yr (0.11 in/yr) in both cases. Given that net infiltration is essentially the same for both slopes and that the current Clive DU PA Model assumes no placement of waste below the side slope, the infiltration through the engineered cover will be represented with the same

values for both slopes in the GoldSim model. If at a later time modeling will include disposal below the side slope, estimates of infiltration rates for the side slope will be refined.

It is important to note that these deterministic (fixed, constant) values from the HELP modeling were calculated external to GoldSim, not directly in the probabilistic Clive DU PA Model itself. They are used in the development of the uncertain stochastic distributions that are used in the GoldSim model, as developed in subsequent sections, and summarized in Section 1.0, Table 1.

3.1 Cell Infiltration Modeling Approach – As-Designed Condition

Given that the development of the engineered cover over time will likely result in differences in the water balance of the cover, the approach adopted for the PA is to model the cover in its as-designed condition for several decades and then in a condition reflecting development of the materials and colonization by plants for the remaining time period—its "naturalized" condition. Infiltration is assumed to be steady-state.

The calculations for the infiltration model for the as-designed cover are described in Table 7. The input parameter distributions are described in Table 1. The modeled net infiltration and lateral flows are described beginning at the bottom of the cell and moving upwards. For steady-state infiltration, the net infiltration through the upper radon barrier in Layer 5 and through the clay liner in Layer 8 are the same since there are no sources or sinks of water within or between those layers. For example see HELP results for the CAS cell in Table 12 of Whetstone (2007).

The distributions for the net infiltration through the clay liner and lateral flow through the upper and lower filter layers are based on the output of the Whetstone (2007) HELP model. The HELP model simulated 100 years of data. Year 1 results were not included in the analysis in order to avoid the influence of model initial moisture conditions on the calculated annual mean values. The remainder of the data were interpreted as a sample from the underlying distribution for the annual infiltration, except that, since the 100 year simulation time was rather arbitrary, the 99 remaining samples do not necessarily reflect 99 years worth of information. Due to the complexity of the interactions of the inputs, it is not a simple matter to determine how much information is contained in the inputs. Many of the inputs are based on over 100 years of data from the Salt Lake City area. However, due to year-to-year correlation in weather data, these data do not represent 100 independent pieces of information. Therefore, the input information is treated as effectively equivalent to 18 years worth of data (e.g.,the amount of data available for the Clive site).

Since it is the long-term average infiltration rate that is of interest, the distribution represents uncertainty about the mean rate for each of these parameters. While there was some slight right-skewness in the simulated values for each of the three parameters, the uncertainty about the mean is well-represented by a normal distribution. The mean of the normal distribution is set equal to the average simulated value, while the standard deviation of the normal distribution is set equal to the standard error of the mean when treating the simulation as equivalent to 18 years worth of data: the sample standard deviation divided by the square root of 18.

A distribution was developed for the mean annual net infiltration through the clay liner based on 99 mean annual values calculated using the Whetstone HELP model (Whetstone 2007, Appendix

1). Year 1 results were not included in the analysis to avoid the influence of model initial moisture conditions on the calculated annual mean values. The distribution for net infiltration through the clay liner is normal with a mean of 0.264 cm/yr (0.104 in/yr) and a standard deviation of 0.011 cm/yr (0.00417 in/yr). This parameter describes the net infiltration through the upper and lower radon barriers, the waste, the clay liner, and into the unsaturated zone below the cell.

The layer above the upper radon barrier is the lower filter layer (Layer 4). The distribution for lateral flow through the lower filter layer is normal with a mean of 8.61 cm/yr (3.39 in/yr) and a standard deviation of 0.544 cm/yr (0.214 in/yr). The sum of the lateral flow from the lower filter layer and the net infiltration through the clay liner gives the vertical flow through the sacrificial soil in Layer 3 above the lower filter layer.

The layer above the sacrificial soil layer is the upper filter layer (Layer 2). The distribution for lateral flow through the upper filter layer is normal with a mean of 0.108 cm/yr (0.0427 in/yr) and a standard deviation of 0.028 cm/yr (0.0111 in/yr).

Infiltration into Layer 1 (armor) is calculated in the model by subtracting the runoff and evapotranspiration losses from the precipitation.

A probability distribution for precipitation was developed using 12 years of site-specific meteorological data described in Whetstone (2007). Since the parameter of interest is the *mean* annual precipitation, the uncertainty in characterized by a normal distribution with mean equal to the sample mean of 21.9 cm/yr (8.61 in/yr) and standard deviation equal to the sample standard error of 2.09 cm/yr (0.822 in/yr).

The monthly means and standard deviations from HELP model runs listed in Attachment 1 of Whetstone (2007) were utilized as data to develop distributions for runoff and evapotranspiration, following the approach outlined in the *Fitting Probability Distributions* white paper using the mean annual rates from the model runs, with uncertainty propagated across the months to produce standard deviations for the rates. For runoff, the resulting distribution was lognormal with a geometric mean of 0.064 cm/yr (0.0252 in/yr) and a geometric standard deviation of 8.46 cm/yr (3.33 in/yr), with the upper tail truncated at 0.25 cm/yr (0.1 in/yr). The distribution for evapotranspiration was normal with a mean of 13.1 cm/yr (5.14 in/yr) and a standard deviation of 1.94 cm/yr (0.762 in/yr).

Table 7. Infiltration model for top and side slopes of the CAS embankment for the cover as designed.

Layer No.	Material	Flows for as-designed material properties:
1 (Armor)	Type-B Rip Rap	Annual precipitation: distribution from HELP results. Surface runoff: distribution from HELP results. Evapotranspiration (ET): distribution from HELP results. Vertical Flow Armor Layer = Annual Precipitation – Surface Runoff – ET.
2 (Upper Filter)	Type-A Filter	Lateral Flow Upper Filter Layer: distribution from HELP results. Vertical Flow Upper Filter Layer = Vertical Flow Clay Liner + Lateral Flow Lower Filter Layer.

Layer No.	Material	Flows for as-designed material properties:
3	Sacrificial Soil	Vertical Flow Sacrificial Soil = Vertical Flow Clay Liner + Lateral Flow Lower Filter Layer.
4 (Lower Filter)	Type-B Filter	Lateral Flow Lower Filter Layer = distribution from HELP results Vertical Flow Lower Filter Layer = Vertical Flow Clay Liner.
5	Upper Radon Barrier Clay	Vertical Flow Radon Barrier Clay = Vertical Flow Clay Liner.
6	Lower Radon Barrier Clay	Vertical Flow Lower Radon Barrier Clay = Vertical Flow Clay Liner.
7	Waste	Vertical Flow Waste = Vertical Flow Clay Liner.
8	Clay Liner	Vertical Flow Clay Liner: distribution from HELP results.

3.2 Cell Infiltration Modeling Approach – Naturalized Condition

The water balance values for cell layers for the as-designed cover calculated by Whetstone (2007) using HELP are described in Tables 5 and 6. These results demonstrate that evapotranspiration and lateral drainage from the lower filter (Layer 4) provide the main "sinks" that reduce the net infiltration rate into the radon barriers. Assuming that the lower filter layer will remain operational, it follows that changes in evapotranspiration fluxes due to time dependent naturalization of the cover after closure will have the most significant influence on net infiltration. The potential changes in evapotranspiration and lateral drainage as the cover evolves are driven by the following processes:

- Aeolian dust (loess) begins to fill the void spaces between the armor (Layer 1) and the smaller cobbles in the upper filter (Layer 2), providing a soil base for plant (and animal) communities on the top layer of the cover. The dust deposition process is augmented by fracturing of some large cobbles into smaller particles due to weathering. The presence of plants and soil on the cover is expected to increase evapotranspiration, thereby reducing the infiltration into the waste.

  The results of dust deposition, weathering, and plant growth were observed by Neptune and Company staff on the similarly-constructed Vitro cell during an inspection on September 16, 2010. The Vitro cell was closed in December 1988, and provides a site-specific measure of dust deposition, weathering, and plant growth since closure. A partial plant cover of grasses and small shrubs had been established within the past 22 years, based on the growth on the side slope and top slope of the Vitro cell. Based on this information, the time to naturalization of the cover is assigned a normal distribution, with a mean of 40 yr and a standard deviation of 10 yr, truncated with a minimum value of 10 yr.

  Evaporation will likely occur from greater depth once loess fills the void spaces between cobbles in the rip rap and plant cover is reestablished on the top surface of the engineered cover. The measured moisture content in the Cover Test Cell at the site provides evidence for an evaporative zone depth greater than about 45 cm (18 in) (Envirocare

2005). The measured data from the Cover Test Cell show that the middle of the sacrificial soil, at a depth of 76 cm (30 in) below the top of the cover, experiences seasonal drying during the six months with very low precipitation at the site (Envirocare 2005, Figures 3 and 4). Some of this drying is due to evapotranspiration, although drainage to the underlying clay layers (i.e., the radon barrier) may also play a role.

- Although burrowing mammals and ants will cause some bioturbation, they are not expected to populate the engineered cover in sufficient numbers to cause homogenization of the armor and upper filter (Layers 1 and 2). It is likely that smaller mammals may burrow a bit in the silted rip rap, but would not find the underlying cobbles hospitable compared to the virgin soil surrounding the embankment. It is also unlikely that ants will find sufficient room amongst the cobbles and gravel to build satisfactory chambers in Layers 1 and 2.
- The lower layers of the engineered cover, Layers 3 and 4, will be a good habitat for deeper plant roots, based on a biological survey of the site. Observations made during a biological survey at the Clive facility (SWCA, 2011) indicate that plant roots often form on top of clay layers that are a meter or more below the top surface, such as the upper radon barrier (Layer 5). Some of these roots may penetrate the radon barriers, based on observations of plant roots in clay layers in boring logs. However, Energy*Solutions* excavated into the first clay unit in the shallow subsurface and observed that the roots did not appear to penetrate the clay, but rather, spread and stayed in the more silty sandy unit above the clay. It is possible that ants may also penetrate the clay layers by following root holes or possible cracks in the clay layers. On balance, the evidence suggests that bioturbation and homogenization of the radon barriers will probably occur very slowly relative to the 10,000-yr time frame for the quantitative part of the PA.

To simulate the performance of the cover system as the designed system is affected by natural forces and becomes colonized by vegetation, several changes were made to the properties of the upper two layers to represent their long-term characteristics. The rip-rap layer and upper filter layer porosity are assumed to be filled with loess within a few decades after closure. Layer 1 as designed is 45 cm (18 in) thick, with a design porosity of 0.19. Layer 2 as constructed is 15 cm (6 in) thick composed of coarse sand, coarse gravel and cobbles, also with a design porosity of 0.19. There is then an equivalent 60 cm (24 in) × 0.19 = 11.7 cm (4.6 in) of available pore space that will be filled with loess. For the HELP model of the naturalized cover, these two layers will be replaced with a single equivalent layer of soil 11.7 cm (4.6 in) thick, having the characteristics of the surface soils in the vicinity of the cell.

The sacrificial soil layer in the HELP model of the as-designed cover is located directly below the upper filter layer, a lateral drainage layer. Since HELP cannot model capillary flow across the filter layer, the soil layer had to be classified as a barrier soil liner. In HELP, a barrier layer is assumed to be saturated at all times and allows flow only when there is a positive head on the top surface. HELP allows only downward saturated flow in barriers and no evapotranspiration. By combining the upper two layers into an equivalent soil layer, the sacrificial soil layer can be re-classified in the HELP model as a vertical percolation layer, and the evaporative zone can be extended to the top of the lower filter layer. Values of field capacity and wilting point moisture content data for both soils were obtained from the National Resources Conservation Service Web

Soil Survey (USDA, 2011). The average wilting point and field capacity weighted by area are 0.286 and 0.148 respectively (see Section 3.3). An average value of saturated hydraulic conductivity from the NRCS Web Soil Survey (USDA, 2011) was reported as 2.2×10^{-4} cm/s for both soils. A value of 0.5 was used for the total porosity considering the mean porosity of unit 4 soil cores of 0.43 and some porosity increase due to the presence of vegetation. An initial value for moisture content of 0.13 was used for the sediment filled layer and for the sacrificial soil layer. This value is the mean of the distribution for moisture content estimated for the upper soil layers described in Section 3.3 below. The lower filter layer was assumed to remain functional.

Vegetation was included in the system, described in HELP as "a poor stand of grass" with an evaporative zone depth of 42.2 cm (16.6 in). A leaf area index of 1.26 was assigned to the vegetation corresponding to the value used for cheatgrass by Ward et al. (2005) for an area on the Hanford site in eastern Washington.

For estimating runoff, the upper surface was characterized as bare gravel for the as-designed cover. These inputs were changed to a HELP default soil texture of 9 representing a silt loam soil (Schroeder et al. 1994) and a vegetation index of 2, representing a "poor stand of grass" as described in the HELP User's Guide (Schroeder et al. 1994).

The HELP model was run for 100 years with these changes in structure and inputs and the mean annual flows from the lower filter layer and net infiltration from the clay liner were used to develop distributions for the GoldSim model as described previously for the as-designed condition. The distribution for lateral flow in the lower filter layer is normal with a mean of 0.876 cm/yr (0.345 in/yr) and a standard deviation of 0.207 cm/yr (0.0815 in/yr). The distribution for the mean annual net infiltration through the clay liner is normal with a mean of 0.122 cm/yr (0.0482 in/yr) and a standard deviation of 0.0089 cm/yr (0.00351 in/yr). Since the upper filter layer is assumed to have been silted up and is therefore ineffective at diverting infiltrating water, it is assigned a lateral flow of 0 cm/yr (0 in/yr).

Comparisons of HELP modeling results with results from mechanistic unsaturated zone modeling programs such as UNSAT-H at arid and semi-arid sites suggest that the HELP model will generally overestimate the net infiltration through the waste in the CAS cell (Meyer et al. 1996, Khire et al. 1997, Albright et al. 2002). The results from the calculation with the HELP model for the CAS cell provide a reasonable estimate of the steady-state infiltration for the PA model.

3.3 Embankment Layer Moisture Contents

GoldSim uses Cell Pathway Elements to model compartments in the 1-D contaminant transport columns. Part of the definition of each Cell is the specification of the amount of various materials in the Cell, including the volume of water. It is therefore necessary to determine the volume of water that should be specified for each Cell in the column, and this is done by knowing the entire volume of the Cell, and multiplying by the water (moisture) content of the porous material in it. This section discusses the determination of moisture contents in the various model layers and materials.

The radionuclide transport and diffusion calculations in the Clive DU PA Model require the moisture content of layers 1 through 4 that are described in Tables 3 and 4, as well as the net

infiltration rates, described previously in Sections 3.1 and 3.2. Calculation of moisture contents for the upper radon barrier and underlying layers is discussed in Section 8.3. In assigning probability distributions for moisture content, layers 1 and 2 (armor layer and upper filter) were combined, since loess is expected to infill both layers. Likewise, layers 3 and 4 (sacrificial soil and lower filter) were combined. Natural Resource Conservation Service mapping of the site indicated that approximately 85 percent of the soils on and near the site were classified as the Skumpah series and the remaining 15 percent as the Timpie series (USDA, 2011). Field capacity and wilting point moisture content data for both soils obtained from (USDA, 2011) are shown in Table 8. The average wilting point and field capacity weighted by area are 0.148 and 0.286 respectively. Daily precipitation data were used to estimate the fraction of time the soil would be at a moisture content corresponding to the wilting point and the fraction of time the soil would be at a moisture content corresponding to field capacity. These fractions, combined with the average wilting point and field capacity moisture contents, provide an estimate of the mean moisture content over time. The precipitation data set was then divided into six equal periods and each period was analyzed in the same manner as the entire data set to obtain an estimate of the standard deviation. The resulting distributions for moisture content for layers 1 through 4 are summarized in Table 9.

Table 8: Wilting point and field capacity water contents for Skumpah and Timpie Soil Series.

Soil Series	Wilting Point Water Content	Field Capacity Water Content
Skumpah	0.154	0.288
Timpie	0.115	0.272

Table 9. Moisture contents in layers 1 through 4 of the top slope and side slope cover.

Layer No.	Material	Moisture Content Distribution
1 (Armor)	Rip Rap	Normal distribution with a mean of 0.125 and a standard deviation of 0.0175.
2 (Upper Filter)	Type-A Filter	
3 (Sacrificial Soil)	Sacrificial Soil	Normal distribution with a mean of 0.243 and a standard deviation of 0.0175.
4 (Lower Filter)	Type-B Filter	

4.0 Soil Characteristics of Unit 3 and Unit 4

4.1 Laboratory Measurements

The hydraulic properties for Units 3 and 4 are based on laboratory measurements by CSU for the moisture retention and hydraulic conductivity of core samples from Units 3 and 4 at the Clive site (Bingham Environmental 1991). Measurements of water retention as a function of matric pressure (called suction head in this report) are available for the drying and wetting cycles. These measurements were performed on four cores: GW19A-B1 and GW17A-B2 from Unit 4 (a silty clay), and GW18-B4 and GW17A-B5 from Unit 3 (a silty sand). Measurements of hydraulic

conductivity as a function of moisture content are available for three cores: GW19A-B1, GW18-B4, and GW17A-B5. The focus in this work (and in previous work) is on the wetting cycle data because infiltration after a heavy rain, which is a major driver for downward flow and transport, is driven by a rewetting front that passes through the engineered cover, waste, and clay layers. The Appendix documents the hydraulic data for Units 3 and 4, based on data reported in (Bingham Environmental 1991, pp. B-19 through B-31).

4.2 Grain Size Distributions for the Cores

Tables 10 and 11 summarize the grain size distributions according to the Unified Soil Classification System (Bingham Environmental, 1991) for cores from Units 4 and 3, respectively. Table 10 is sorted by increasing percent of clay plus silt content. Table 11 is sorted by increasing percent of sand content. The four cores that were tested by CSU have the following properties:

- GW17A-B2 has 55.6% clay, the highest measured clay content with a trace of sand in Table 10 for Unit 4,
- GW19A-B1 has 56.2% silt, the highest measured silt content with a trace of sand in Table 10 for Unit 4,
- GW18-B4 has 45.5% sand, the lowest measured sand content in Table 11 for Unit 3, and
- GW17A-B5 has 83.3% sand, the highest measured sand content in Table 11 for Unit 3.

The core samples that were selected for testing span the extremes of the clay, silt, and sand contents for Units 3 and 4. The core samples that were tested are in a bold font in Tables 10 and 11.

The water retention data are consistent with these material distributions, as shown in Figure 1. In particular, the core that has the greatest clay content retains a greater moisture content than the cores that are high in silt or sand at a given suction head, and the core that has the greatest sand content demonstrates the abrupt changes in moisture content that are typical of a sandy material.

Table 10. Grain size distributions for cores* from Unit 4, a silty clay.

Well/Sample No.	Depth (ft)	Description	% Gravel	% Sand	% Silt	% Clay	% Clay + Silt	Reference
I-3-50 (SE)	1.5	Silty Clay	0	39.3			60.7	Bingham 1994, page 23
I-4-50 (SE)	10.5	Silty Clay	0	19.6			80.4	Bingham 1994, page 32
I-3-50 (SE)	10.5	Silty Clay	0	16.6			83.4	Bingham 1994, page 24
I-1-50 (NW)	7.5	Silty Clay	0	11.7			88.3	Bingham 1994, page 13
GW-16/S-1	3 - 5	Brown Silty Clay w/Trace Fine Sand	0.1	11.2	50.3	38.4	88.7	Bingham 1991, page B-13
GW-19A/S-1	**5-7**	**Brown Silty Clay w/Trace Fine Sand**	**0**	**2.8**	**56.2**	**41.0**	**97.2**	**Bingham 1991, page B-17**

Well/Sample No.	Depth (ft)	Description	% Gravel	% Sand	% Silt	% Clay	% Clay + Silt	Reference
GW-17A/L-2	**7-9.5**	**Brown Silty Clay w/Trace Fine Sand**	**0**	**2.1**	**42.3**	**55.6**	**97.9**	**Bingham 1991, page B-15**
GW-18/B-1	5-6.5	Brown Silty Clay w/Trace Fine Sand	0	2.0	49.9	48.1	98.0	Bingham 1991, page B-16
I-4-50 (SE)	7.5	Silty Clay	0	1.2			98.8	Bingham 1994, page 31

*Cores in bold font were tested by CSU

Table 11. Grain size distributions for cores* from Unit 3, a silty sand.

Well/Sample No.	Depth (ft)	Description	% Gravel	% Sand	% Silt	% Clay	% Clay + Silt	Reference
GW-18/S-4	**20-22**	**Brown Silty Fine Sand w/Some Clay**	**0**	**45.5**	**38.7**	**15.8**	**54.5**	**Bingham 1991, page B-16**
I-1-50 (NW)	18.0	Silty Sand	0	48.2			51.8	Bingham 1994, page 15
DH-48/B-2	17-19	Tan Silty Sand	0	55.5			44.5	Bingham 1994, page B-11
GW-16/B-4	19.5-21	Tan Silty Fine Sand	0	59.4			40.6	Bingham 1991, page B-14
I-3-50 (SE)	19.5	Silty Sand	0	62.3			37.7	Bingham 1994, page 26
GW-41/B-6	10-12	Tan Silty Sand	0	65.3			34.7	Bingham 1994, page B-10
GW-41/B-9	16-18	Tan Silty Sand	0	66.3			33.7	Bingham 1994, page B-10
I-1-50 (NW)	10.5	Silty Sand	0	66.6			33.4	Bingham 1994, page 14
GW-19B/B-4	17-19	Tan Silty Fine Sand	0	66.7			33.3	Bingham 1991, page B-18
GW-55/B-8	14-16	Tan Silty Sand	1.1	69.5			29.4	Bingham 1994, page B-11
DH-33/L-7	16.5	Tan Silty Sand	0.1	72.9			27	Bingham 1994, page B-9
GW-16/B-3	14.5-16	Tan Silty Fine Sand	0.2	74.7			25.1	Bingham 1991, page B-13
I-3-50 (SE)	15	Silty Sand	0	75.8			24.2	Bingham 1994, page 25
I-4-50 (SE)	21	Silty Sand	0	76.4			23.6	Bingham 1994, page 33

Well/Sample No.	Depth (ft)	Description	% Gravel	% Sand	% Silt	% Clay	% Clay + Silt	Reference
GW-16/B-2	9.5-11	Tan Silty Fine Sand	1.6	79.8			18.6	Bingham 1991, page B-13
GW-19A/S-3	15-16	Brown Silty Fine Sand	0	82.0			18	Bingham 1991, page B-17
GW-17A/L-5	**19.5-22**	**Brown Silty Fine Sand w/Trace Clay**	**0**	**83.8**	**8.4**	**7.8**	**16.2**	**Bingham 1991, page B-15**
GW-19B/L-5	22-24.5	Tan Silty Fine Sand	0	83.8			16.2	Bingham 1991, page B-18

*Cores in bold font were tested by CSU

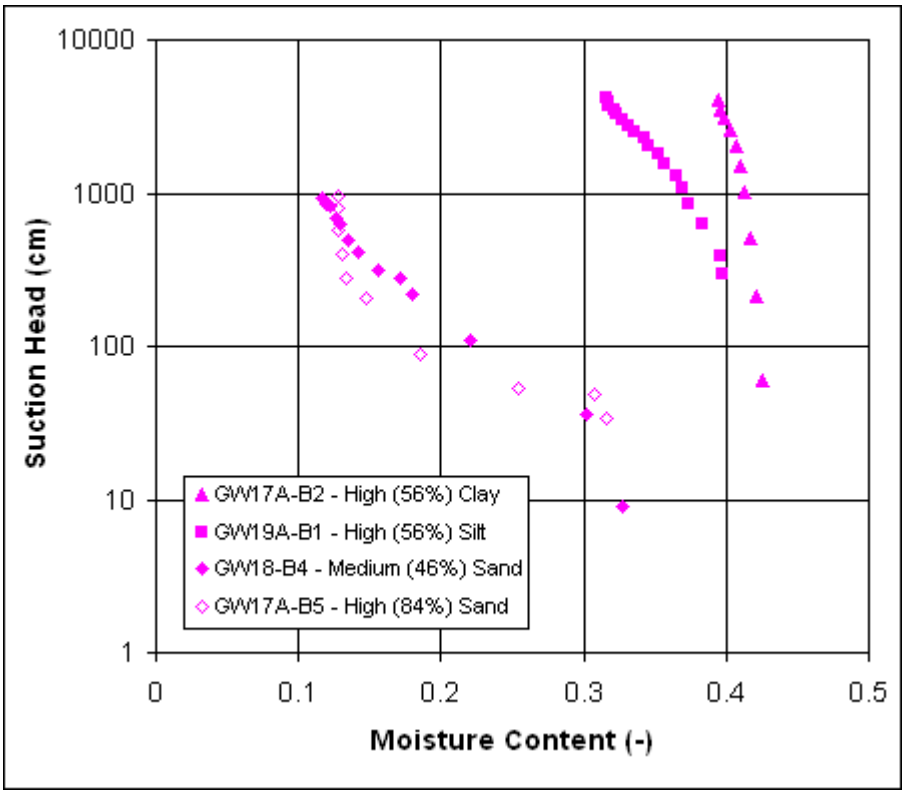

Figure 1. Comparison of water retention data (wetting cycle) for four core samples

4.3 Soil Material Properties

Particle density ρ_s is defined as the ratio of the mass of the solid to the volume of the solid:

$$\rho_s = M_{solid} / V_{solid}.$$

Particle density depends on the chemical composition and crystalline structure of the mineral particles. Particle density is not influenced by particle size, packing arrangement, or pore space.

Dry bulk density ρ_b is defined as the ratio of the mass of dried alluvium to its total volume,

$$\rho_b = M_{solid} / V_{total}.$$

For a dried sample, $V_{total} = V_{solid} + V_{gas}$.

Porosity, ϕ, (often also denoted as n) is the relative pore volume of the medium,

$$V_{liquid} + V_{gas} / V_{solid} + V_{liquid} + V_{gas}.$$

For a dry sample, porosity is $V_{gas} / (V_{solid} + V_{gas})$. Total porosity can be determined from dry bulk density and particle density by $\phi = 1 - \rho_b / \rho_s$. Therefore, relating these equations,

$$\phi = 1 - \rho_b / \rho_s = (\rho_s - \rho_b)/\rho_s = [\, M_{solid} / V_{solid} - M_{solid} / (\, V_{solid} + V_{gas}\,)\,] / (\, M_{solid} / V_{solid}\,) = V_{gas} / (\, V_{solid} + V_{gas}\,)$$

The structure of coarse dry alluvium is generally single grained. The actual packing arrangement depends on grain size distribution, grain shape, and the processes under which the alluvium was deposited. The grain size distribution can consist of a single grain size (monodisperse) or multiple grain sizes (polydisperse). The packing arrangements of spherical grains of uniform size can be represented by models for regular packing that allow the calculation of the spacing of layers, the volume of a unit cell and thus the bulk density. Although monodisperse systems are idealizations of natural porous materials such as alluvium, calculated relationships between particle density and bulk density gives some insight into potential particle density – bulk density correlation. The unit cell volume, bulk density, and porosity are given in the table below for for five models of regular packing of uniform spheres.

Table 12. Theoretical porosities based on particle packing geometry.

Model	Unit Cell Volume (*R* is grain radius)	Bulk Density	Porosity
simple cubic	$8R^3$	$\Pi\rho_s/6$	47.64
cubic tetrahedral	$4\sqrt{3}\ R^3$	$\Pi\rho_s/3\sqrt{3}$	39.54
tetragonal sphenoidal	$6R^3$	$2\Pi\rho_s/9$	30.19
pyramidal	$4\sqrt{2}R^3$	$\Pi\rho_s/3\sqrt{2}$	25.95
tetrahedral	$4\sqrt{2}R^3$	$\Pi\rho_s/3\sqrt{2}$	25.95

Source: Deresiewicz (1958, Table 1) reported in Hillel (1980, Table 6.1)

These calculations show that the bulk density of a volume of monodisperse spheres of constant particle density depends on the packing arrangement. Thus, correlation between particle density and bulk density would only be expected for a sample characterized by a single packing arrangement.

Polydisperse systems are more complex with grains of smaller radii filling in the pore spaces between larger grains. The increase in bulk density due to infilling by smaller particles depends on the grain size distribution. Natural materials are more likely to be characterized by a range of

particle sizes leading to many diverse packing arrangements. The large range of possible packing arrangements in coarse alluvium makes a physically based correlation between particle density and bulk density unlikely.

Given the conclusion that particle density and bulk density are not physically dependent and given the need to restrict the sampling of material properties and moisture content parameters to physically meaningful and consistent values the following approach was taken:

1) Separate up-scaled distributions for Unit 3 and 4 for saturated water content and residual water content are estimated from borehole water retention curve and hydraulic conductivity data. This estimation approach is detailed in subsequent sections.

2) Porosity is assumed to be equal to the saturated water content.

3) Based on particle density data presented in Table 13 and best professional judgement a constant value of 2.65 g/cm^3 was chosen for particle density for both Unit 3 and 4, fine cobble mix, fine gravel mix, rip rap, silt sand gravel.

4) Based on bulk density data presented in Table 13 and best professional judgement an up-scaled distribution for bulk density was specified as a normal distribution with a mean of (1- porosity) times particle density and a standard deviation of 0.1. This was applied to both Unit 3 and 4, fine cobble mix, fine gravel mix, rip rap, silt sand gravel..

This approach allows the uncertainty in water content and bulk density to be modeled while maintaining a physically coherent probabilistic unsaturated zone model.

Table 13: Bulk density, porosity, and calculated particle density data from water retention experiments.

Borehole	Unit	Bulk Density (g/cm)	Porosity	Calculated Particle Density (g/cm^3)
GW18-B4	3	1.567	0.409	2.65
GW17A-B5	3	1.673	0.32	2.46
GW19A-B1	4	1.397	0.473	2.65
GW17A-B2	4	1.326	0.505	2.68

from Colorado State University Porous Media Laboratory

4.4 Soil Moisture Content

The flow of water in porous media occurs in response to a gradient in the total potential energy of water. The total potential can be composed of a number of components but this analysis will be restricted to gravitational and matric potentials. Water potential components are often expressed in units of energy per unit weight rather than units of energy per unit mass. When the quantity of water is expressed as a weight, the units of potential are defined in terms of head. The gravitational potential refers to the energy of water with respect to reference elevation and is written here as Z. Although not a formal definition, the matric potential relates to the energy of

the tension imposed on the pore water by the soil matrix. Matric potential is a negative value and is written here as ψ. The total potential is then $H = \psi + Z$.

Steady-state fluid flow in an unsaturated medium is defined by the Buckingham-Darcy equation (Jury and Horton, 2004, p.95). In the following discussion this equation will be referred to simply as the Darcy equation. The one dimensional form of Darcy's equation for unsaturated flow is given by Fayer (2000, Eqns. 4.2 and 4.5):

$$q = -K_L(\psi)\frac{\partial H}{\partial z}, \tag{1}$$

where

- q is the flux of liquid per unit area,
- K_L is the unsaturated conductivity as a function of the matric head ψ,
- H is the matric plus gravitational potentials [cm], and
- z is the depth below ground surface [cm].

It is convenient to define two sign conventions for the total potential (Fayer 2000, page 4.2): (1) the z-coordinate is zero at the soil surface and positive downward. With this convention, the gravitational head in the soil, which is defined as the elevation of a point with respect to the soil surface, and negative and defined as $-z$; and (2) the suction head, h, is the negative of the matric potential or matric head, ψ. With this convention, the suction head, h, is always greater than zero for an unsaturated soil. It follows that

$$H = \psi + Z = -(h + z) \tag{2}$$

and the flux is then given by

$$q = K_L(h)\left(\frac{\partial h}{\partial z} + 1\right). \tag{3}$$

The unsaturated conductivity, K_L, is formulated based on the Brooks-Corey representation for moisture content as a function of suction head

$$\begin{aligned} \Theta &= \left(\frac{h}{h_b}\right)^{-\lambda} \quad for\ h > h_b, \\ &= 1 \qquad for\ 0 \le h \le h_b \end{aligned} \tag{4}$$

where

- Θ is the effective saturation,
- h is the suction head (cm),
- h_b is the bubbling pressure head (cm) at which moisture first drains from the material, and
- l is a constant that is fit to data.

Alternatively, expressed in terms of the fractal dimension, D

$$\Theta = \left(\frac{h}{h_b}\right)^{D-3} \quad for\ h > h_b, \qquad = 1 \quad for\ 0 \le h \le h_b \tag{5}$$

The suction head is positive for an unsaturated material and 0 at saturation. Θ, the effective saturation, is defined as

$$\Theta = \frac{\theta - \theta_r}{\theta_s - \theta_r}, \tag{6}$$

where

- Θ is the moisture content,
- Θ_r is the residual moisture content, and
- Θ_s is the saturated moisture content.

Combining Equations

$$\theta = \theta_r + \left(\theta_s - \theta_r\right)\left(\frac{h}{h_b}\right)^{-\lambda} \tag{7}$$

This equation can then be fit to core data.

Alternatively, expressing in terms of D and assuming

$$\theta = \theta_r + (\theta_s - \theta_r)\left(\frac{h}{h_b}\right)^{(D-3)} \tag{8}$$

Using the Mualem theory for predicting hydraulic conductivity (Mualem 1976), the unsaturated hydraulic conductivity is defined as

$$K_L = K_S \Theta^{2+\frac{2}{\lambda}}. \tag{9}$$

Substituting Equation 6 into Equation 9 gives:

$$K_L = K_S \left(\frac{\theta - \theta_r}{\theta_s - \theta_r}\right)^{2+\frac{2}{\lambda}}. \tag{10}$$

Setup (e.g. unit 3)

1) from 4 measurements estimate mean and standard error for porosity (ϕ) and θ_r, use these as priors for θ_s and θ_r (assumes $\theta_s = \phi$).
2) for each borehole core there are 2 separate measurements
    1. moisture content, θ; and suction head, h

2. moisture content, θ; and hydraulic conductivity K_L
3. estimate h_b, D, θ_s, θ_r, and K_s as described below

Here's the Brooks-Corey $\theta \sim f(h)$ equation:

$$\theta = \theta_r + (\theta_s - \theta_r)\left(\frac{h}{h_b}\right)^{(D-3)} \tag{11}$$

Here's $K_L \sim f(\theta)$

$$K_L = K_S\left(\frac{\theta - \theta_r}{\theta_s - \theta_r}\right)^{-(\tau + 2/(D-3))} \tag{12}$$

where the data are

θ	the water content,
h	is the suction head (cm),
K_L	is hydraulic conductivity (cm/sec),

and the parameters to be fit are

h_b	is the air entry pressure head (cm),
D	is the soil fractal dimension,
θ_s	is the saturated water content,
θ_r	is the residual water content,
τ	is the Mualem empirical parameter = 2,
K_S	is saturated hydraulic conductivity (cm/sec),

Typically these relationships are fit using non-linear least squares. However, it seems for these boreholes the optimization has trouble converging and the uncertainty in parameter estimates is difficult to estimate. To allow combining of information available across the available borehole moisture content and hydraulic conductivity datasets and to provide an estimate of the uncertainty in these parameter estimates a Bayesian Markov Chain Monte Carlo (MCMC) simulation approach was taken that allows the parameters to be constrained via prior distributions and generates parameter posterior distributions. This also allows the two sets of information from a borehole to be combined as well as allowing for combing information across boreholes for a unit (borehole data are presented in the Appendix).

In a Bayesian approach sources of information on model parameters can be combined through a prior distribution or through a data likelihood. The priors integrate expert judgment and scientific knowledge while the likelihood integrates information available in observed data. In effect, the prior can be used to constrain the results parameter distribution to physical meaningful values.

The priors listed below (Equations 13-19) are all non-informative distributions which allow the data to determine the distribution and also constrain the parameter values to a physically meaningful range.

$$p(\theta_s) = U[0.3, 0.55] \tag{13}$$

$$p(\theta_r) = U[0.001, 0.2] \tag{14}$$

$$p(h_b) = U[1, 500] \tag{15}$$

$$p(D) = U[1, 2.999] \tag{16}$$

$$p(\sigma) = U[0.001, 1000] \tag{17}$$

$$p(K_{sat}) = U[\text{10e-10}, \text{10e-3}] \tag{18}$$

$$p(\sigma_{K_s}) = U[\text{1e-9}, \text{1e-4}] \tag{19}$$

and the likelihood based on the moisture content matrix pressure data:

$$\begin{aligned} p(\theta_s, h_b, D, \sigma \mid \theta_{borehole1}, \theta_{borehole2}, h_{borehole1}, h_{borehole2}) = \\ N_{borehole1}\left[\theta_r + (\theta_s - \theta_r)\left(\frac{h_{borehole1}}{h_b}\right)^{(D-3)}, \sigma\right] \\ N_{borehole2}\left[\theta_r + (\theta_s - \theta_r)\left(\frac{h_{borehole2}}{h_b}\right)^{(D-3)}, \sigma\right] \end{aligned} \tag{20}$$

and the likelihood based on the moisture content hydraulic conductivity data:

$$\begin{aligned} p(\theta_s, \theta_r, D, K_S, \sigma_{K_s} \mid \theta_{borehole1}, \theta_{borehole2}, K_{L_{borehole1}}, K_{L_{borehole2}}) = \\ N_{borehole1}\left[K_S\left(\frac{(\theta - \theta_r)}{(\theta_s - \theta_r)}\right)^{-(2+2/(D-3))}, \sigma_{K_s}\right] \\ N_{borehole2}\left[K_S\left(\frac{(\theta - \theta_r)}{(\theta_s - \theta_r)}\right)^{-(2+2/(D-3))}, \sigma_{K_s}\right] \end{aligned} \tag{21}$$

Markov Chain Monte Carlo (MCMC) simulation of the joint distribution define by equations 13-21 was used to generate samples from the marginal parameter distributions for the moisture content and hydraulic conductivity models. Results for Unit 3 and 4 are presented in the following sections.

4.4.1 Unit 3 Brooks-Corey Parameters

The MCMC sampling using likelihoods incorporating the two Unit 3 borehole cores resulted in the the following marginal parameter distributions:

$$p(h_b) = N[mean = 8.85, sd = 0.929] \tag{22}$$

$$p(D) = N[mean = 2.73, sd = 5.21\text{e-}3] \quad (23)$$

$$p(K_S) = N[mean = 5.14\text{e-}05, sd = 5.95\text{e-}6] \quad (24)$$

$$p(\theta_s) = N[mean = 0.393, sd = 6.11\text{e-}03] \quad (25)$$

$$p(\theta_r) = N[shape = 6.78\text{e-}3, scale = 2.05\text{e-}3] \quad (26)$$

Significant correlations from these simulations was found between D and H_b (-0.85) and between K_{sat} and D (-0.98).

4.4.2 Unit 4 Brooks-Corey Parameters

The MCMC sampling using likelihoods incorporating the two Unit 4 borehole cores resulted in the the following marginal parameter distributions:

$$p(h_b) = N[mean = 104., sd = 1.72] \quad (27)$$

$$p(D) = N[mean = 2.81, sd = 9.93\text{e-}5] \quad (28)$$

$$p(K_S) = N[mean = 5.16\text{e-}05, sd = 5.97\text{e-}7] \quad (29)$$

$$p(\theta_s) = N[mean = 0.428, sd = 6.08\text{e-}3] \quad (30)$$

$$p(\theta_r) = N[shape = 0.108, scale = 8.95\text{e-}4] \quad (31)$$

Significant correlations from these simulations was found between D and H_b (-0.66) and between K_{sat} and D (-0.37).

5.0 Engineered Materials

The cap over the facility is constructed of engineered materials that are derived from natural materials. These generally consist of various grades of sorted aggregates, or of clay compacted to specific tolerances. Properties for these materials are described in Whetstone (2000, Tables 7 and 8).

5.1.1 Rip Rap

Rip Rap is used to construct the uppermost layer: Armor. The Rip Rap itself is assumed to be an inert material. The Class A South cover design (EnergySolutions, 2009, drawing 07021 V7) assigns Type A rip rap to the side slopes, and Type B rip rap to the top slope, we have adopted common properties for the two types for the purposes of this assessment. This is justified, since the only role of the rip rap in the dimensional and hydraulic properties of the cap is to take up space as an inert material. In that sense, it is sufficient to average the two porosities of 0.17 and 0.19, for Types A and B respectively (Whetstone, 2000, Tables 7 and 8), to be 0.18, with a standard deviation of 0.01, so that the range is suitably covered.

As the pore space of the rip rap becomes becomes infilled with loess within decades after closure, the original porosity of the rip rap takes on the properties similar to the Unit 4 soil (Section 3.2).

5.1.2 Fine Cobble Mix

Fine Cobble Mix is used to construct the upper filter layer. Distributions for the as-designed upper filter layer (fine cobble mix) parameters are described in Table 1. The Fine Cobble Mix

itself is assumed to be an inert material. As the pore space of the upper filter layer becomes infilled with loess within decades after closure, the original porosity of the upper filter layer takes on the properties similar to the Unit 4 soil (Section 3.2).

5.1.3 Silt Sand Gravel

Silt Sand Gravel is used to construct the sacrificial soil layer. Distributions for the sacrificial soil layer (silt sand gravel) parameters are described in Table 1. Properties of the sacrificial soil layer are not expected to change with time.

5.1.4 Fine Gravel Mix

Fine Gravel Mix is used to construct the lower filter layer. Distributions for the lower filter layer (fine gravel mix) parameters are described in Table 1. The lower filter layer is assumed to remain operational during the modeled time period. The Fine Gravel Mix itself is assumed to be an inert material.

5.1.5 Upper Radon Barrier Clay

The Radon Barrier layers are divided into upper and lower layers. Both are constructed of local clay, compacted to different hydraulic conductivities. UpperRnClay represents the upper of the two layers. Distributions for upper radon barrier clay parameters are described in Table 1. The distribution for saturated hydraulic conductivity was developed using the design value (Table 3) for the clay layer of 5×10^{-8} cm/s as the geometric mean of a lognormal distribution. A geometric standard deviation of 1.2 was chosen to provide an approximate order of magnitude variation above and below the geometric mean.

5.1.6 Lower Radon Barrier Clay

The Lower Radon Barrier is constructed of compacted local clay. LowerRnClay represents the lower of the two layers. Distributions for the lower radon barrier clay parameters are described in Table 1. The distribution for saturated hydraulic conductivity was developed using the design value (Table 3) for the clay layer of 1×10^{-6} cm/s as the geometric mean of a lognormal distribution. A geometric standard deviation of 1.2 was chosen to provide an approximate order of magnitude variation above and below the geometric mean.

5.1.7 Liner Clay

The Liner is constructed of compacted local clay, here defined as LinerClay. Distributions for the liner clay parameters are described in Table 1. The distribution for saturated hydraulic conductivity was developed using the design value (Table 3) for the clay layer of 1×10^{-6} cm/s as the geometric mean of a lognormal distribution. A geometric standard deviation of 1.2 was chosen to provide an approximate order of magnitude variation above and below the geometric mean.

6.0 Porous Media Properties of Waste Materials

Test data are not available for the unsaturated porous media properties of the wastes. However, the DU waste is expected to be in a powdered form or possibly compressed into small "briquettes" for safety during transportation to the Clive facility. In this condition, the DU waste will behave like a mixture of fine sand to fine gravel. Since there is so little information on which to base material properties for the waste, it is assigned the properties of Unit 3.

Three types of waste materials are considered in the DU PA: Generic LLW, the UO_3 waste from the SRS, and the U_3O_8 wastes from the gaseous diffusion plants (GDPs) at Portsmouth, OH, and Paducah KY. The generic LLW is used only as an inert filler in the model, with no inventory, and is assumed to simply have the properties of local silty sandy soil: Unit 3.

The uranium oxide wastes, both UO_3 and U_3O_8, will be disposed in an indeterminate mix of materials, including containers (55-gallon drums and DU cylinders of various types) and possibly concrete, grout, bulk LLW, and local soils as backfill. This complex mix of heterogeneous materials is not modeled at this point, and the assumption is made instead that the overall material properties are again simply that of local silty sandy soil: Unit 3.

So, in summary, all waste materials in the Clive DU PA Model are assumed to have the same physical properties as Unit 3 soils.

7.0 Properties of the Natural Unsaturated Zone

The CAS embankment is constructed by excavating through the uppermost stratum, Unit 4, and into the top of Unit 3. The entire unsaturated zone below the embankment, from the bottom of the clay liner to the top of the saturated zone, is modeled as Unit 3 material, sharing all the properties and characteristics of Unit 3 as outlined in this white paper. The saturated zone is modeled as Unit 2 (see the *Saturated Zone Modeling* white paper). In the GoldSim PA Model, this zone below the embankment is called the Unsat zone, and does not include overlying waste and cover materials. It is part of both the top slope and side slope columns.

The thickness of the Unsat zone below the CAS is determined by the difference in average elevations of the bottom of the clay liner and the water table. The clay liner is uniformly about 60 cm (2 ft)-thick by design, though the bottom of the waste cell has a gentle slope to it, as documented in the *Embankment Modeling* white paper.

A distribution for the thickness of the unsaturated zone was established based on measurements for groundwater wells, engineering drawings for the CAS embankment (see the *Embankment Modeling* white paper), and consideration of the accuracy of the elevation measurements. The four wells are selected from a map of wells (Figure 7 in Bingham Environmental, 1991): GW-19A, GW-25, GW-27, and GW-60 as shown in Figure 2, since the location of these four wells bound the Class A waste cell. Each groundwater well is in the vicinity of one of the four corners of the CAS cell, so their measurements are treated as approximations to the water table elevation at the four corners. These water table elevations are also used to establish the distributions for the thickness of the saturated zone, and are documented in the *Saturated Zone Modeling* white paper.

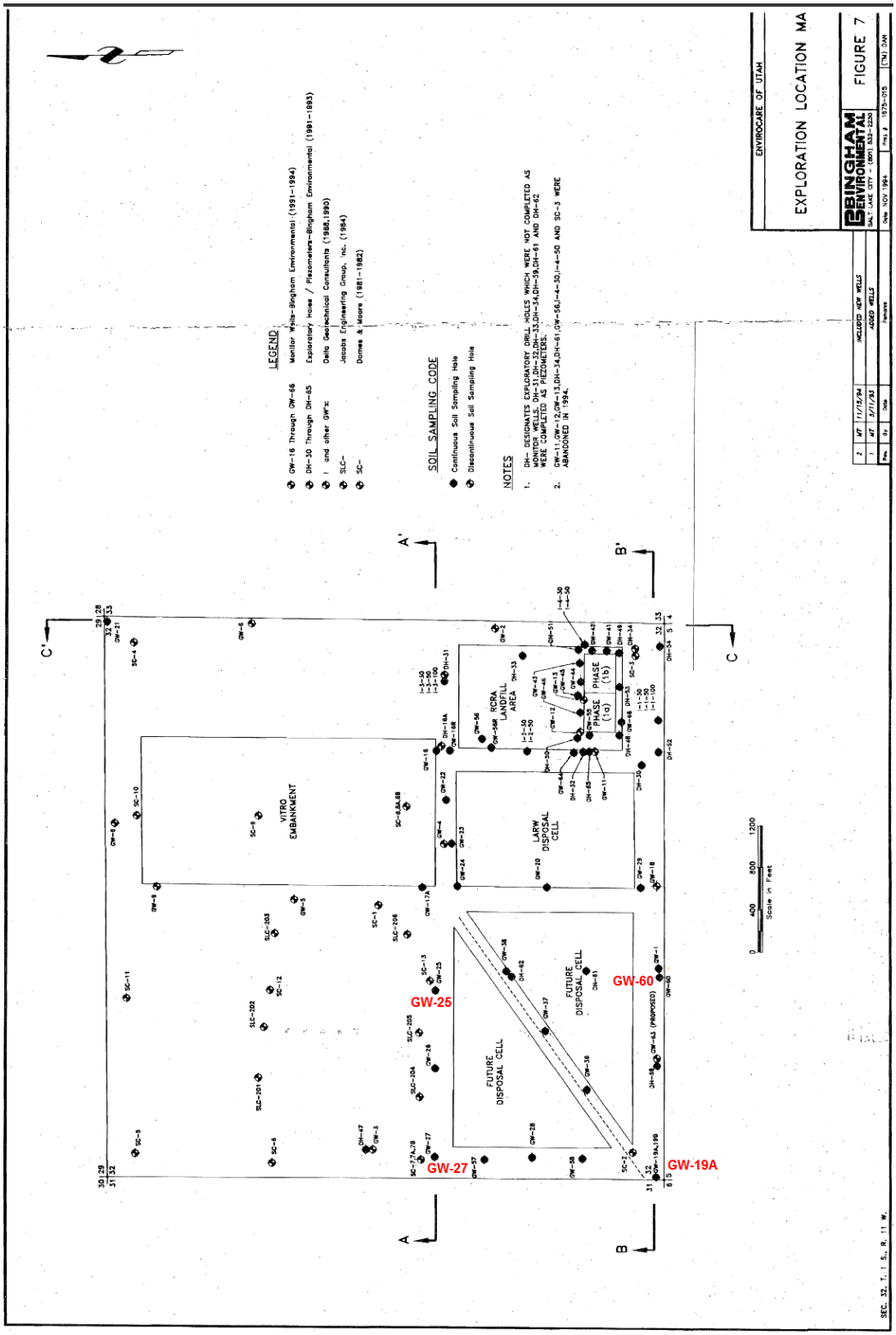

Figure 2. Locations of wells GW-1, GW-25, GW-27, and GW-19 (Figure 7 from Bingham Environmental, 1991)

In order to establish unsaturated zone thickness, the elevations for the water table are subtracted from the elevations for the bottom of the clay liner (see the *Embankment Modeling* white paper). The elevations of the bottom of the clay liner are interpolated for each of the four corners of the CAS cell to compute an unsaturated zone thickness for each corner. Based on the accuracy of the water table elevation measurements and the approximations involved in computing thicknesses, the calculated thickness for each corner was deemed to have measurement and reporting error with a standard deviation of 15 cm (0.5 ft). Since the average elevation across the cell is computed as the average elevation of the four corners, the standard error of the mean is 15 cm (0.5 ft) divided by the square root of 4. The resulting distribution for the mean thickness of the unsaturated zone was thus chosen as a normal distribution with mean equal to 3.93 m (12.9 ft) and a standard deviation of 7.6 cm (0.25 ft).

8.0 Numerical Solution for Unsaturated Flow

The computational method implemented in the Clive DU PA Model solves Equation 3 for steady state flow at constant infiltration flux, q. (At steady state, the vertical infiltration flux must be constant in all layers of the cell below the radon barriers, which includes the waste, the clay liner, and the Unsat zone.) No iterations are required with the selected solution technique. The approach in the Clive DU PA Model differs from the solution technique in the UNSAT-H code, which solves the transient (unsteady) equation for one-dimensional unsaturated flow and iterates to a steady state solution with constant infiltration rate.

8.1 Solution of the Darcy Equation by the Runge-Kutta Method

Equation 3 is a nonlinear, first order differential equation for the suction head that can be solved by numerical approximation. The Runge-Kutta method is attractive for this application because it allows variable spacing (i.e., variable Δz) between nodes, because it is highly stable, and because it does not require iteration to converge to a solution. Equation 3 can be rewritten as a first order differential equation in the form $h' = f(h)$:

$$\frac{\partial h}{\partial z} = \frac{q}{K_L(h)} - 1 \tag{32}$$

A second order Runge-Kutta solution for this first order differential equation is given by Abramowitz and Stegun (1970, Section 25.5.6):

$$h_{n+1} = h_n + \frac{k_1 + k_2}{2} + O(h^3), \tag{33}$$

with

$$k_1 = \Delta z \left(\frac{q}{K_L(h_n)} - 1 \right) \tag{34}$$

$$k_2 = \Delta z \left(\frac{q}{K_L(h_n + k_1)} - 1 \right) \tag{35}$$

and

$$\Delta z = z_{n+1} - z_{n.} \tag{36}$$

Equations 33 through 36 define a procedure for calculating h_{n+1} from the known values of h_n, Δz, and the (constant) infiltration flux, q. These equations constitute a predictor-corrector calculation, where k_1 is the predictor and k_2 is the corrector. No iteration is involved in this solution because Equations 34, 35, and 33 can be solved sequentially for each node of the grid, beginning with the lowest node at the top of the water table with $h = 0$ (because the suction head is zero for a saturated soil) and $K_L = K_s$, and integrating upward through the various unsaturated soil layers. Stable solutions do require a finer discretization than the layers that are defined for the 1-D columns used in the Clive PA model.

The value of Δz does not have to be constant over the domain of integration, and has been adjusted to provide reasonable accuracy where the head gradient is greatest. In practice, these regions occur at the capillary fringe just above the water table and at the interface between the clay liner and waste. The value of Δz has to be small enough that the predictor step (Equation 34) does not generate a value of k_1 that is so large and negative that $(h_n + k_1)$ becomes negative. Suction head is always positive, and $K_L(h_n + k_1)$ in Equation 35 cannot be evaluated for negative values of $(h_n + k_1)$. In practice, an initial node spacing of 2 cm provides a stable solution in Unit 3, directly above the water table, for the infiltration fluxes of interest. However, an initial node spacing of 0.1 mm was required to provide a stable solution in the waste, directly above the clay liner, at high infiltration rates. This fine spacing is required because the head gradient at the interface between the waste and clay liner is quite large. A node spacing of 25 cm provides a stable solution in the main body of the waste and in Unit 3 where the head gradients are smaller. A constant node spacing of 15 cm provides adequate resolution in the clay liner and in the upper and lower radon barrier. Solutions at these variable grid spacings are mapped to the Clive DU PA Model's regular grid that is used to represent wastes and other layers, in the top slope and side slope columns.

8.2 Verification of the Runge-Kutta Method

The UNSAT-H modeling program (Fayer 2000) has been used to analyze infiltration through the CAS cell at the Energy*Solutions* facility (Whetstone 2007). A model built with UNSAT-H predicted moisture content and suction head from the radon barriers in the cover downward through the waste, clay liner, and Unit 3 silty sand to the top of the aquifer (Whetstone 2007, Section 4 and Table 17). The results from the UNSAT-H calculation for the top and side slope models have been used to verify the steady state unsaturated flow solutions with the Runge-Kutta method outlined in Section 8.1.

The UNSAT-H calculations are based on a van Genuchten representation for soil moisture content and for soil hydraulic conductivity. For verification purposes, the Runge-Kutta solution was programmed into a spreadsheet using the identical van Genuchten models as UNSAT-H. The Runge-Kutta verification used the same total thicknesses for the radon barriers, waste, clay liner, and Unit 3 sand as the UNSAT-H model, but the spacing of individual nodes (i.e., the values of Δz) is different. Table 14 summarizes the thicknesses of the major components.

Table 14. Layer thicknesses and coordinates for top slope validation calculations.

Layer	Thickness	z-Coordinate
Upper Radon Barrier	1 ft (30.48 cm)	0 to 30.48 cm
Lower Radon Barrier	1 ft (30.45 cm)	30.48 cm to 60.96 cm
Waste	45 ft (1371.6 cm)	60.96 cm to 1432.56 cm
Clay Liner	2 ft (60.96 cm)	1432.56 cm to 1493.52 cm
Unit 3 Silty Sand	10.8 ft (329.2 cm)	1493.52 cm to 1822.7 cm

Figure 3(a) compares the calculated values for moisture content from the UNSAT-H model (Whetstone 2007, Table 17) and from the Runge-Kutta solution for the top slope model with an infiltration rate of 0.276 cm/yr. Both solutions encompass the radon barriers, the waste, the clay liner beneath the waste, and Unit 3 from the bottom of the clay liner to the top of the water table. The results are essentially identical, providing validation for the Runge-Kutta method. Figure 3(b) provides a more detailed comparison of moisture content near the bottom and top of the clay liner, again demonstrating the close agreement between the UNSAT-H model and the Runge-Kutta method.

A similar comparison was also performed for the side slope model with an infiltration rate of 0.595 cm/yr. The side slope model is similar to the top slope model, except the average waste thickness is 5.64 m (18.5 ft) rather than 13.7 m (45 ft). Figures 4(a) and 4(b) again demonstrate the close agreement between the UNSAT-H model and the Runge-Kutta method.

The calculated values for suction head from the UNSAT-H model and from the Runge-Kutta method were also compared for the top and side slope models. The suction head profiles in the radon barriers, waste, clay liner and Unit 3 are shown in Figure 5 for the top and side slope models. A qualitative comparison between the Runge-Kutta solution and the UNSAT-H results was performed because the UNSAT-H data for suction head were not tabulated, only presented graphically (Whetstone 2007, Figures 8 and 9). The comparison of suction heads from both methods again demonstrates that the Runge-Kutta solution is in excellent agreement with the results from the UNSAT-H model.

The results in Figures 3 and 4 highlight three important features of the response of the CAS cell to infiltration. First, the clay liner has a moisture content of about 0.42 (see Figures 3(b) and 4(b)) in the top and side slope models. This value is just below θ_s, which is 0.432 for the van Genuchten model. The radon barriers have slightly higher moisture contents, approximately 0.425 to 0.43 (see left-hand side of Figures 3(a) and 4(a)), again just below the saturated moisture content of 0.432. These results confirm that the clay liner and radon barriers remain very close to saturation for either model (top or side slope) and for two different infiltration rates (0.276 cm/yr or 0.595 cm/yr) in the CAS cell. Second, the waste drains to a relatively low moisture content, on the order of 0.06 for either slope model and infiltration rate. This behavior is consistent with the low moisture retention of a sandy material. Finally, suction head shows greater differences than moisture content for the top and side slope models. The suction head is more directly dependent

on flow rate (see Equation 32) than moisture content, and the factor of two difference in the flow rates for the top and side slope models is the probable cause of the differences in Figure 5(a) and 5(b).

8.3 Clive PA Model of the CAS Cell

The Runge-Kutta method has been incorporated into the Clive PA model for infiltration through the radon barriers, waste, clay liner and Unit 3 of the CAS cell at the Energy*Solutions* facility. The PA model of the CAS cell has a number of differences with the verification calculations discussed in the previous section. The major differences are as follows:

1. The moisture retention and hydraulic conductivity of the radon barriers and clay liner are defined by a Brooks-Corey/Mualem model that is based on the test data from CSU for Unit 4 cores GW17A-B2 and GW19A-B1.

2. The moisture retention and hydraulic conductivity of the Unit 3 silty sand between the clay liner and water table are defined by a Brooks-Corey/Mualem model that is based on the test data from CSU for Unit 3 cores GW18-B4 and GW17A-B5.

Integration of the Darcy equation from node n, with a known value of the suction head, h_n, and a known value of $\Delta z_n = z_{i+1} - z_n$, to node n+1 is based on the following sequential steps:

1. Calculate the moisture content, θ_n, corresponding to the suction head, h_n. The calculation of θ_n is based on Equations 4 and 6 in Section 4.4.

2. Calculate the conductivity, $K(h_n)$, based on the effective saturation, Θ_n, at θ_n. Equations 6 and 9 in Section 4.4 define the formulas.

3. Calculate $k_1 = \Delta z_n(q/K(h_n) - 1)$ (see Equations 34 and 36 in Section 8.1).

4. Calculate the trial value of the suction head, $h_n + k_1$.

5. Calculate the trial value of the moisture content, $\theta(h_n + k_1)$ using Equations 4 and 6 found in Section 4.4.

6. Calculate the trial value of the conductivity, $K(h_n + k_1)$, based on the effective saturation at $\theta(h_n + k_1)$. Equations 6 and 9 in Section 4.4 define the formulas.

7. Calculate $k_2 = \Delta z_n(q/K(h_n + k_1) - 1)$ (see Equations 35 and 36 in Section 8.1).

8. Calculate $h_{n+1} = h_n + (k_1 + k_2)/2$ (see Equation 33 in Section 8.1)

Numerical testing demonstrated that the trial value of the suction head, $h_n + k_1$, can become negative, leading to an undefined value for $K(h_n + k_1)$. Negative values of $K(h_n + k_1)$ occurred at the interface between the waste and clay liner when the infiltration rate increased from 0.3 to 0.5 cm/yr for the as-designed cover to approximately 5 cm/yr. The numerical problem appears in the waste, adjacent to its interface with the clay liner, because the gradient of suction head is greatest at this location (for example, see Figure 5(a) at a depth of about 1,400 cm).

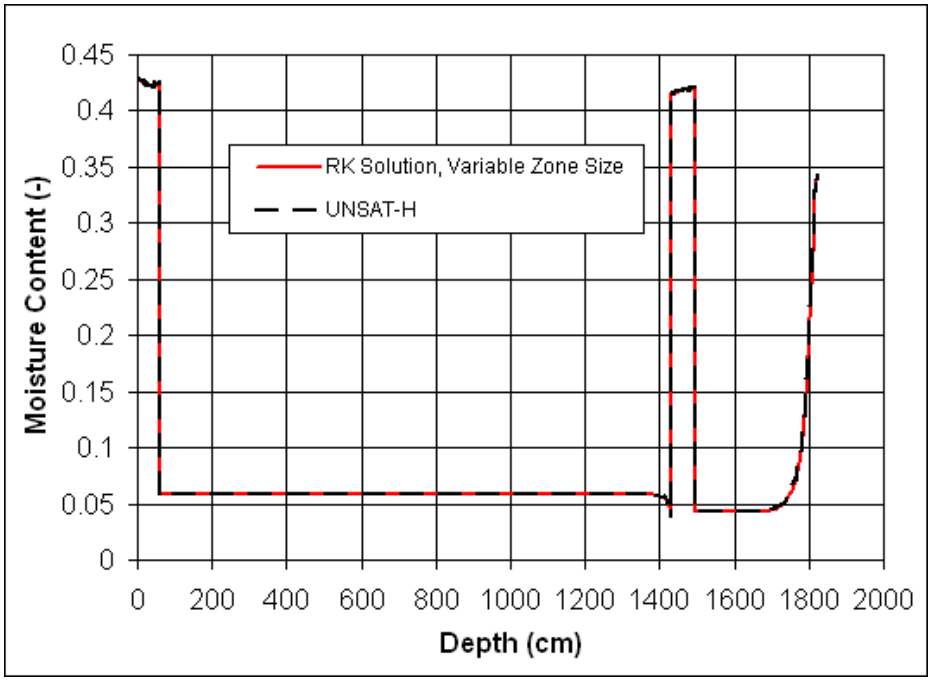

(a) Comparison of moisture content in Unit 3, clay liner, waste, and radon barriers

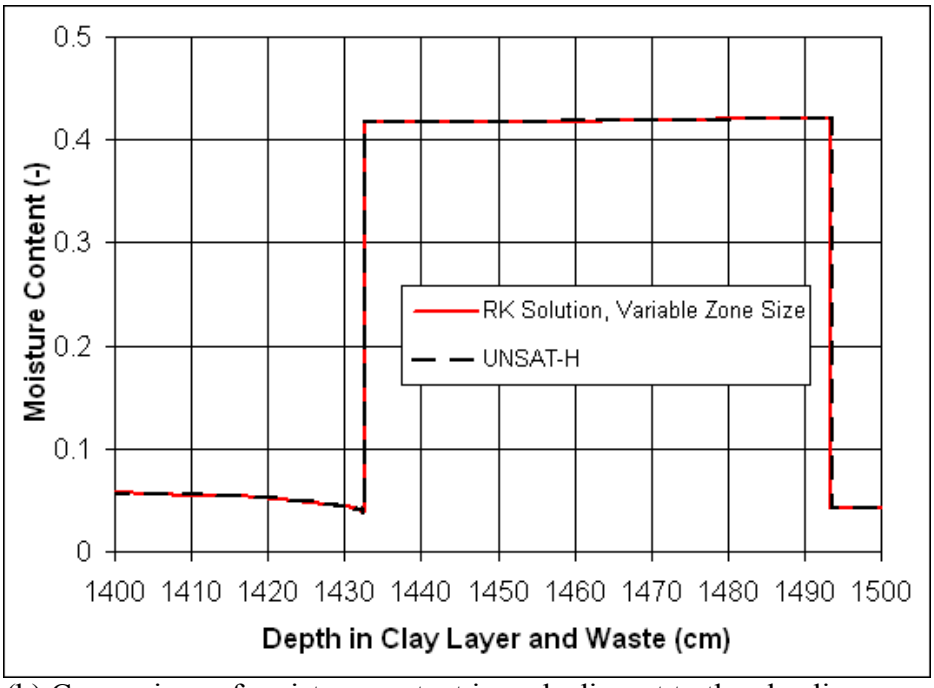

(b) Comparison of moisture content in and adjacent to the clay liner

Figure 3. Comparison of the Runge-Kutta and UNSAT-H solutions for top slope model.

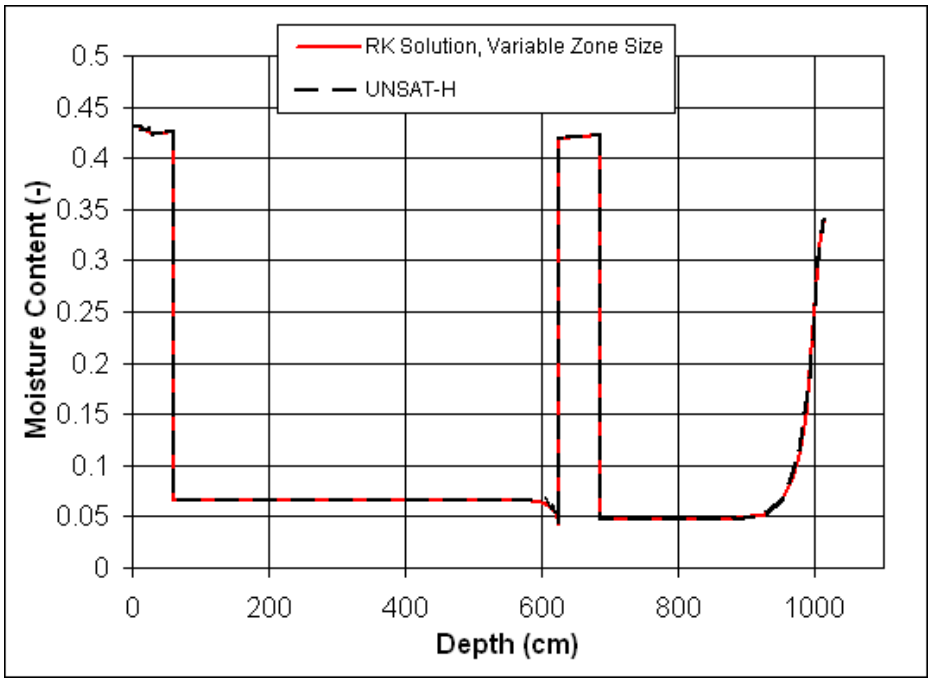

(a) Comparison of moisture content in Unit 3, clay liner, waste, and radon barriers

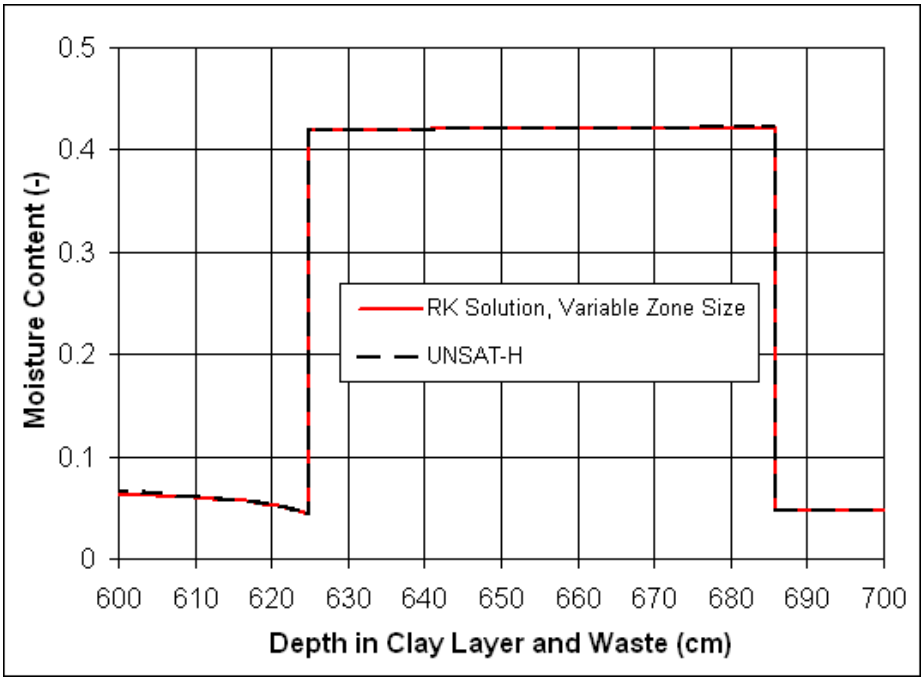

(b) Comparison of moisture content in and adjacent to the clay liner

Figure 4. Comparison of the Runge-Kutta and UNSAT-H solutions for side slope model.

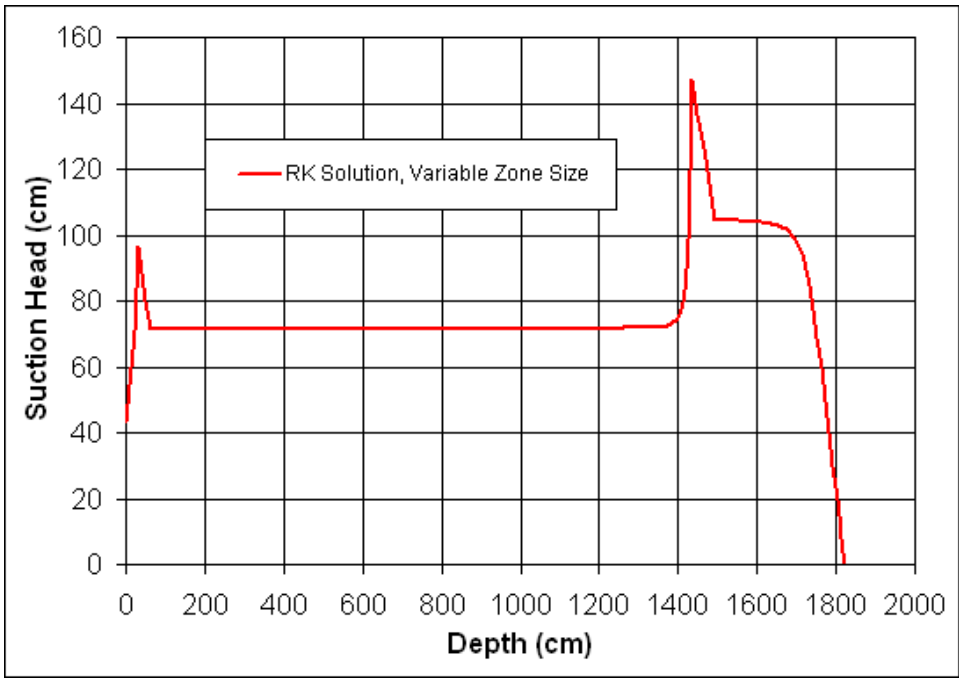

(a) Top Slope Model

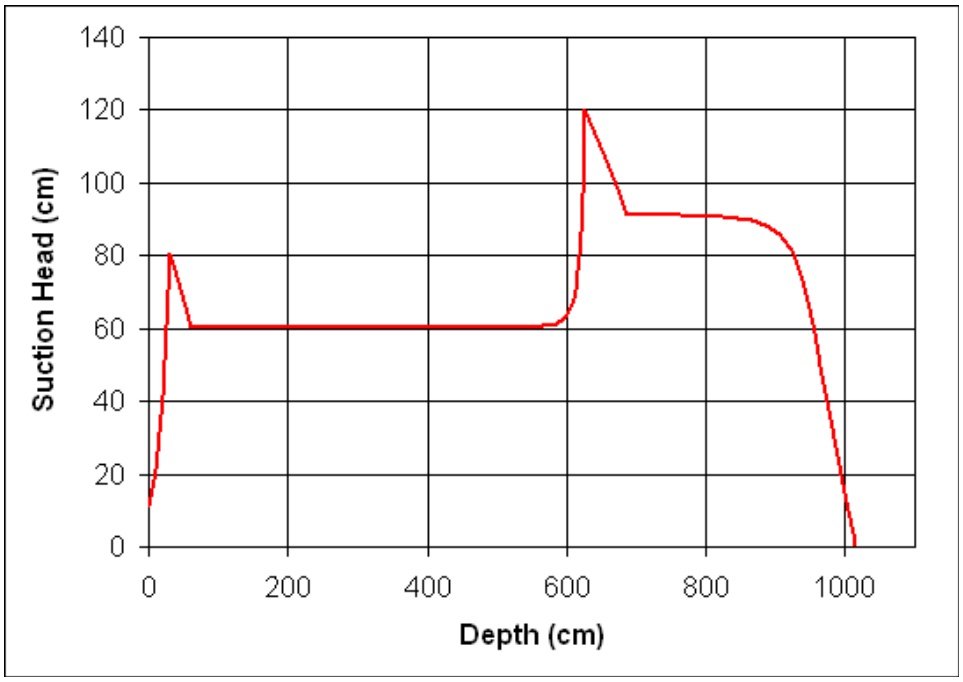

(b) Side Slope Model

Figure 5. Suction head profiles in Unit 3, clay liner, waste, and radon barriers for the top slope and side slope models.

The verification testing in Section 8.2 used the following spacing for nodes in the waste, adjacent to the clay liner: (1) 2-cm node spacing for the first five nodes in the waste, (2) 5-cm node spacing for the next 4 nodes in the waste, and (3) 25-cm node spacing for all other nodes in the waste. The GoldSim implementation of this solution uses a geometric spacing between the first 12 nodes in the waste, beginning with an initial spacing of 0.1 mm, which increases by a ratio of approximately 1.93 for each subsequent node. The spacing between the 11^{th} and 12^{th} nodes is 0.135 m and the total width of the 12 nodes with geometric zoning is 0.281 m. All subsequent nodes in the waste have a constant spacing of 0.281 m in the GoldSim implementation. Numerical testing demonstrated that the geometric zoning produces stable solutions for the top slope and side slope models with the Runge-Kutta method up to flow rates of 5 cm/year.

8.4 Numerical Testing of the Top Slope Model in GoldSim

Validation of a top slope infiltration model for the CAS cell was performed in GoldSim, using the same Runge-Kutta method and the same descriptions of soil properties, providing a direct comparison of results and a means of identifying errors in programming. Deterministic calculations were performed with Brooks-Corey/Mualem models for the individual cores (Unit 4 core GW17A-B2 or GW19A-B1, and Unit 3 core GW17A-B5 or GW18-B4) to compare unsaturated flow conditions calculated using GoldSim. Stochastic calculations were performed with GoldSim for 20 realizations using randomly sampled values for the Brooks-Corey/Mualem input parameters for Units 3 and 4. The GoldSim results for Realization 18 were identical to a calculation for Realization 18 to 5 or 6 significant digits. This testing also provided useful insights into the range of conditions in the CAS cell during unsaturated flow.

Figures 6 and 7 compare the profiles for moisture content and suction head, respectively, in the radon barriers, waste, clay liner, and Unit 3 for the four deterministic calculations that use Unit 3 (silty sand) properties for GW18-B4 or GW17A-B5 and use Unit 4 (silty clay) properties for GW17A-B2 or GW19A-B1. All calculations have an infiltration rate of 0.276 cm/yr (0.109 in/yr). These results confirm previous observations: (1) The moisture contents of the clay liner and radon barriers remain close to saturation, and (2) the waste retains a low moisture content of 0.06. In addition, the suction heads in the radon barriers are identical because the hydraulic conductivity is identical for either core (because conductivity was only measured for one of the two cores).

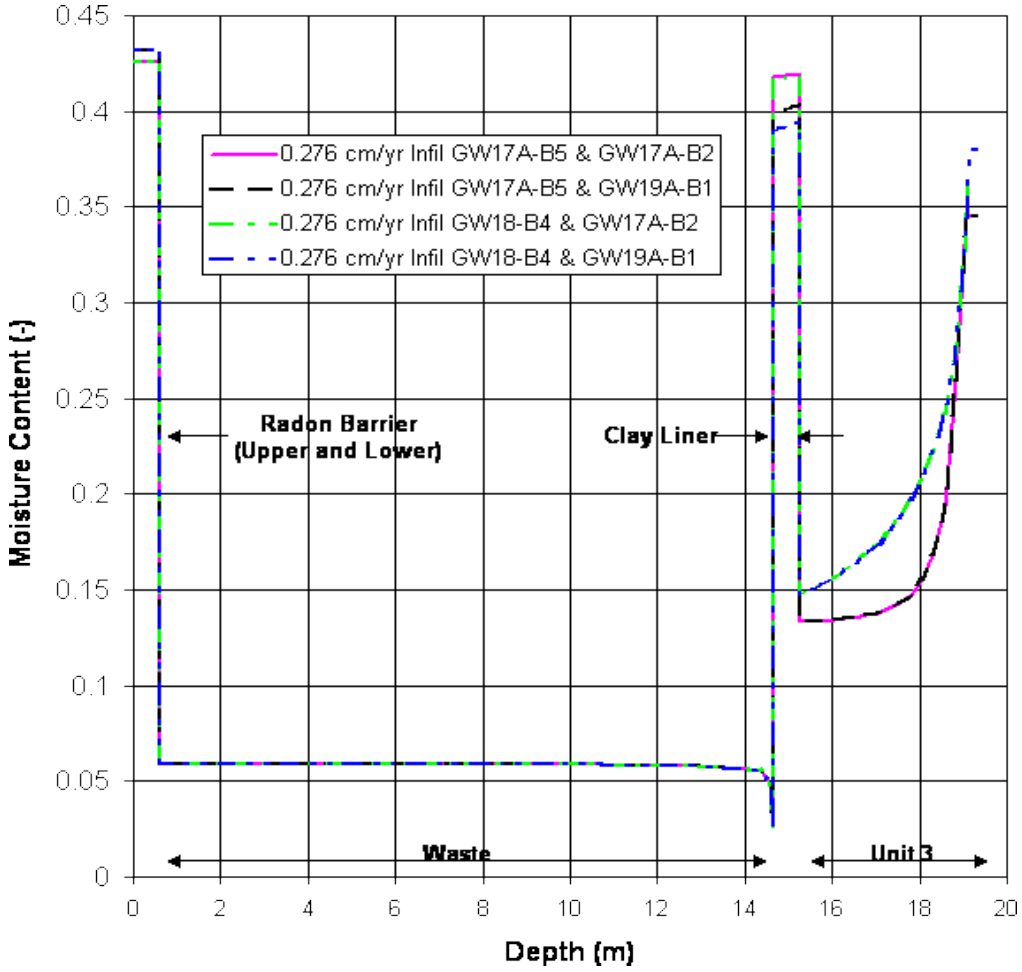

Figure 6. Profiles of moisture content in Unit 3, clay liner, waste, and radon barriers for the top slope model with 0.276 cm/yr infiltration.

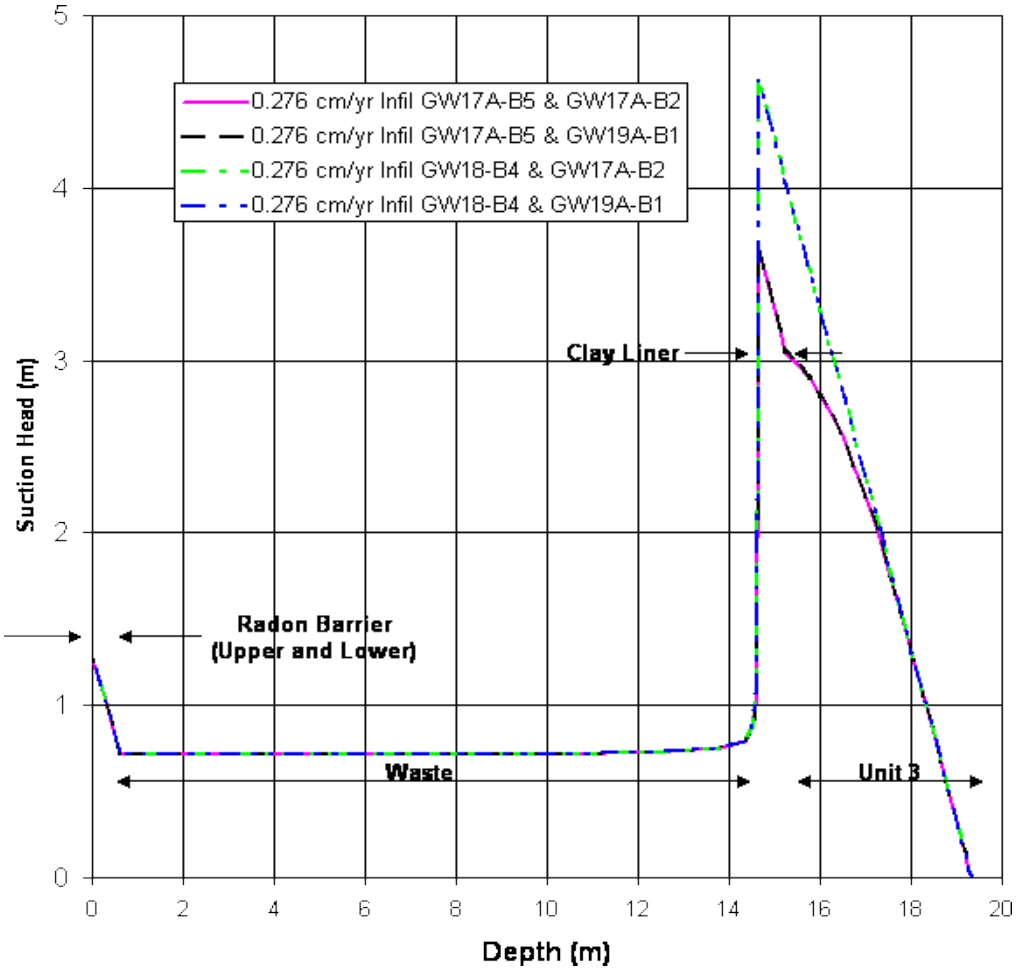

Figure 7. Profiles of suction head in Unit 3, clay liner, waste, and radon barriers for the top slope model with 0.276 cm/yr infiltration.

Figures 8 and 9 compare the profiles for moisture content and suction head, respectively, in the radon barriers, waste, clay liner, and Unit 3 for deterministic calculations that use soil properties for GW17A-B5 (Unit 3) and GW17A-B2 (Unit 4) at three different infiltration rates: 0.168 cm/year, 0.276 cm/yr, and 5.0 cm/yr. In general, Figures 8 and 9 demonstrate that moisture content is more sensitive to infiltration rate than to the differences between soil properties for the various cores. The major difference in Figure 8 is the degree of drainage in the waste, with the high infiltration rate increasing the retained moisture from 0.055 at 0.168 cm/yr to 0.084 at 5.0 cm/yr infiltration. The moisture content in the waste also shows a small oscillation between 0.082 to 0.086 at the 5.0-cm/yr infiltration rate. This could have be eliminated by having finer spacing between the nodes in the waste, but the accuracy of the current solution is considered more than adequate.

Similar calculations were also performed for soil properties with GW17A-B5 for Unit 3 and GW19A-B1 for Unit 4. The results are very similar to those shown in Figures 8 and 9 and are not repeated here.

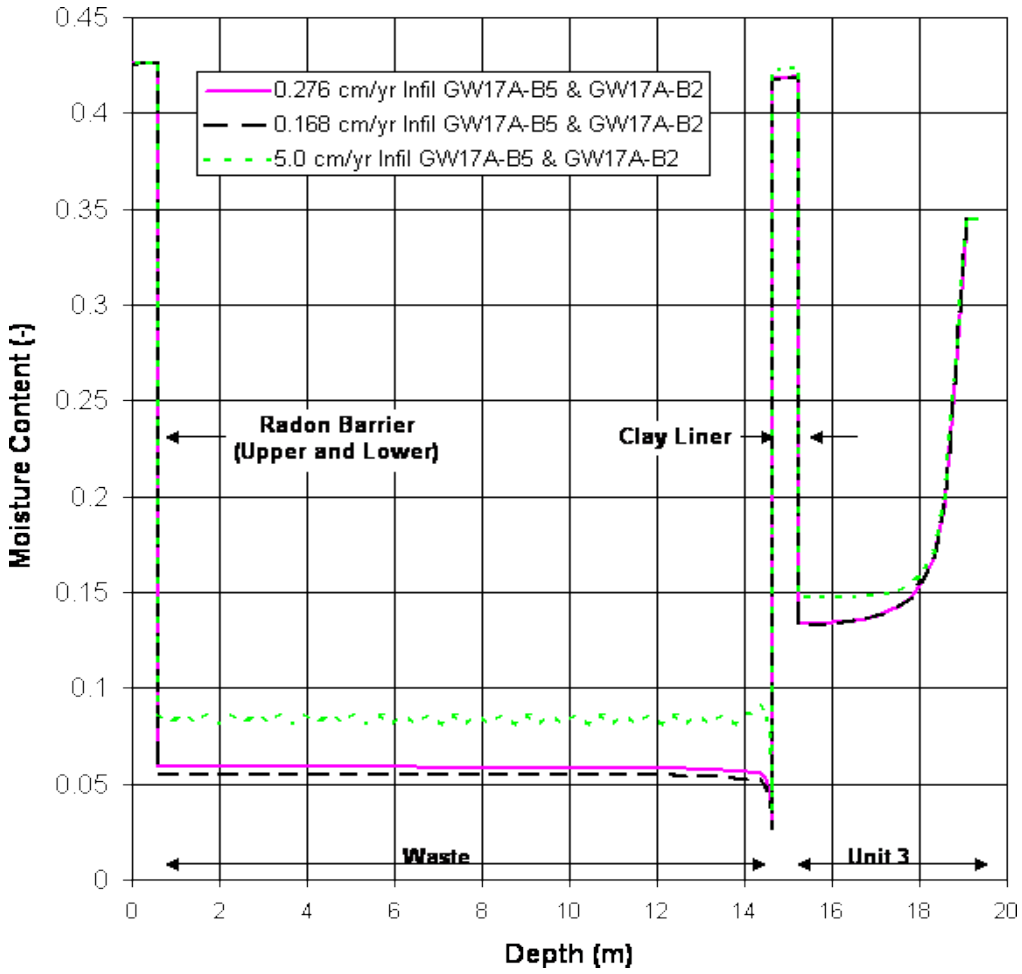

Figure 8. Profiles of moisture content in Unit 3, clay liner, waste, and radon barriers for the top slope model with different infiltration rates.

Figures 10 through 14 compare the time dependent moisture content at the mid-points of Unit 3, of the clay liner, of the waste, of the lower radon barrier, and of the upper radon barrier, respectively, for a GoldSim calculation with 20 realizations and randomly sampled soil properties for Units 3 and 4. The duration of each realization is 3,000 years and the lower filter layer is assumed to become degraded at 2,640 years after closure for test purposes.

The results in Figures 10 through 14 confirm the observations from the previous calculations: (1) the moisture contents in the clay liner, lower radon barrier, and upper radon barrier remain close to saturation (note the expanded vertical scale for Figures 13 and 14), and (2) the waste drains to low moisture content, 0.03 to 0.08, for these 20 realizations, and (3) the moisture content in Unit 3 also has a limited range of 0.13 to 0.20 for the infiltration rates generated by the cover infiltration model.

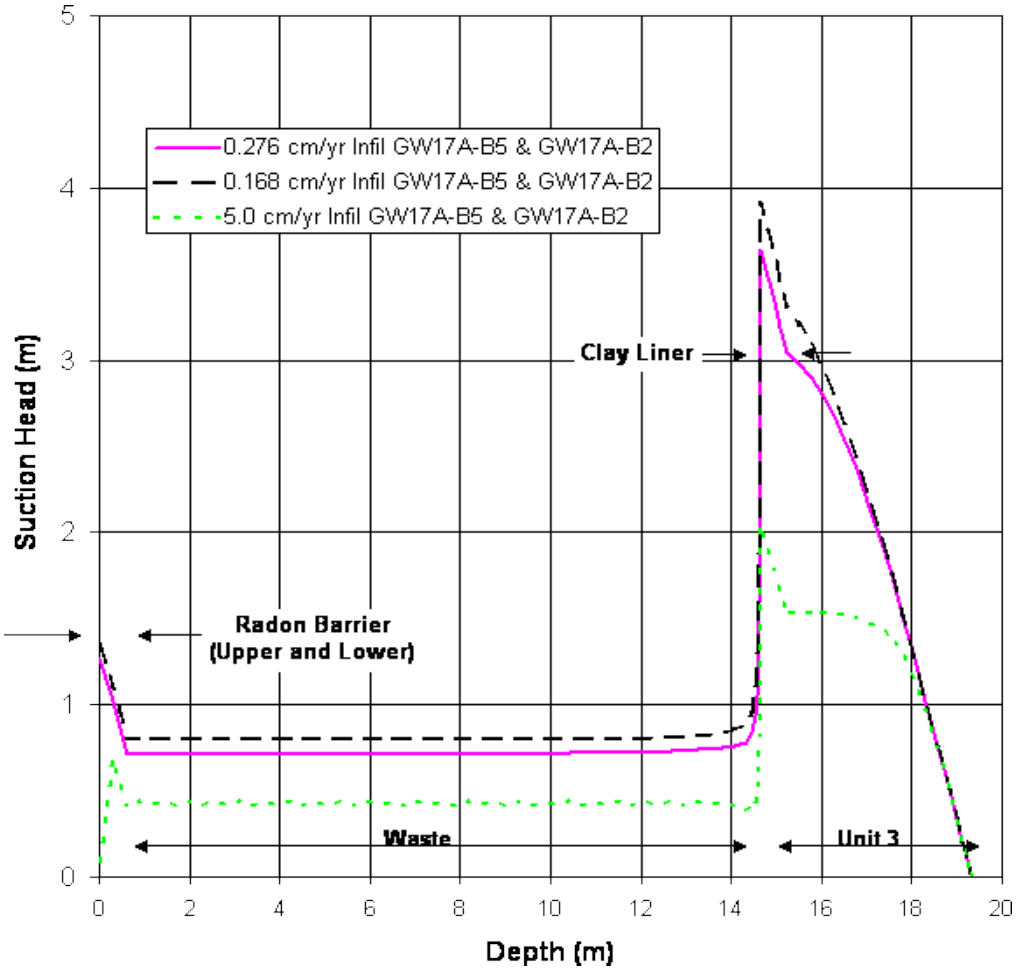

Figure 9. Profiles of suction head in Unit 3, clay liner, waste, and radon barriers for the top slope model with different infiltration rates.

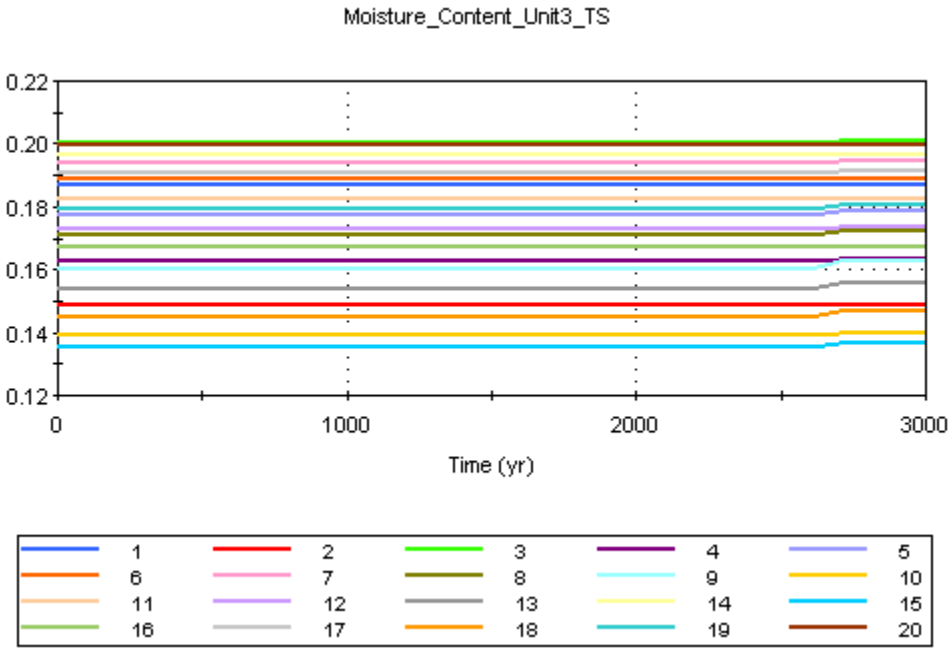

Figure 10. Time dependent moisture content from 20 realizations at the mid-height of Unit 3 with sampled soil properties for Units 3 and Unit 4.

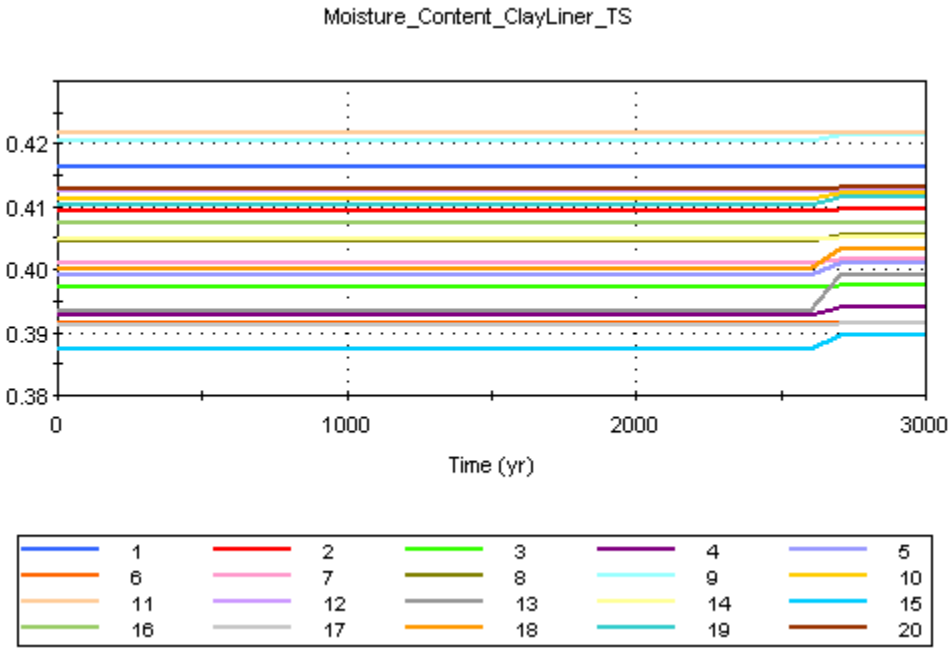

Figure 11. Time dependent moisture content from 20 realizations at the mid-height of the clay liner with sampled soil properties for Units 3 and Unit 4.

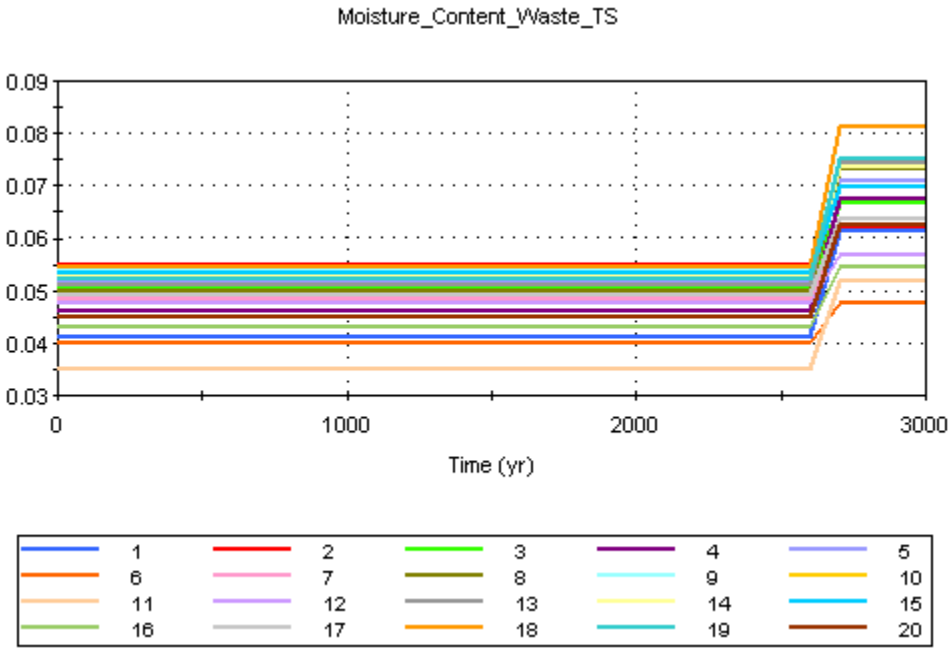

Figure 12. Time dependent moisture content from 20 realizations at the mid-height of the waste with sampled soil properties for Units 3 and Unit 4.

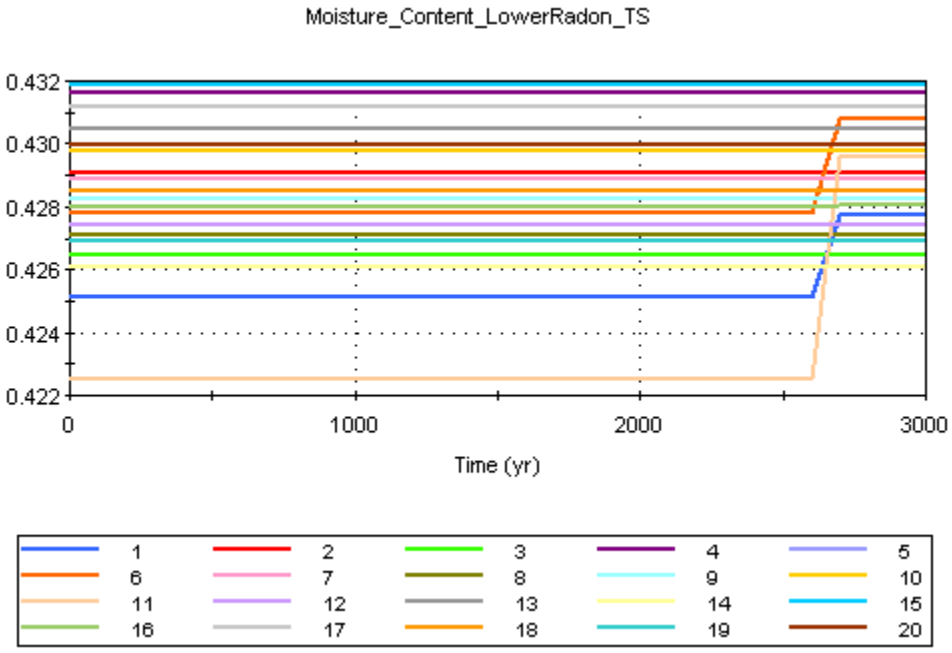

Figure 13. Time dependent moisture content from 20 realizations at the mid-height of the lower radon barrier with sampled soil properties for Units 3 and Unit 4.

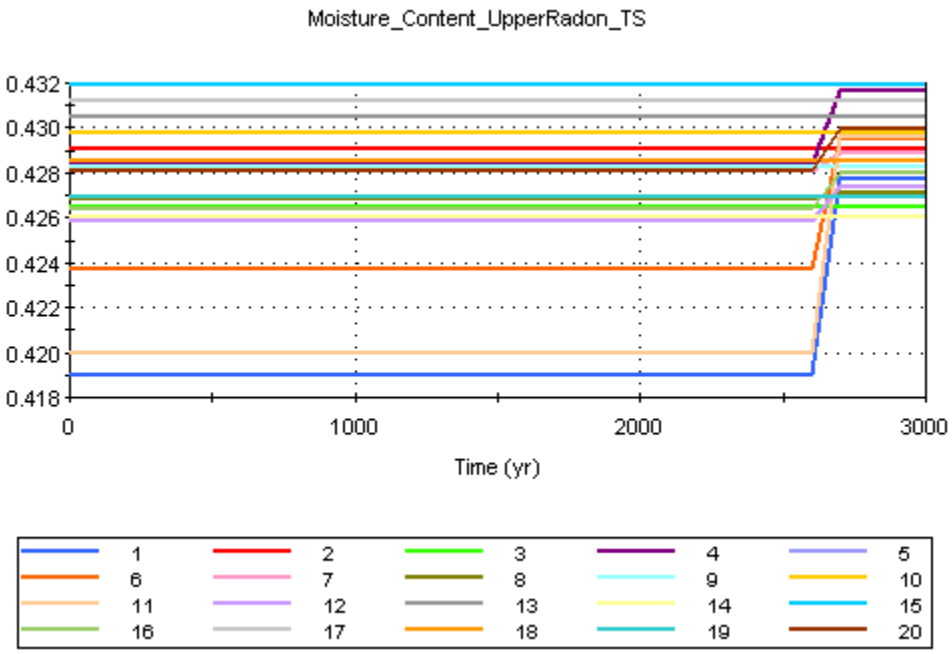

Figure 14. Time dependent moisture content from 20 realizations at the mid-height of the upper radon barrier with sampled soil properties for Units 3 and Unit 4.

9.0 Contaminant Fate and Transport in Porous Media

Once all the hydraulic properties and states have been developed, as in the previous sections, we can turn to transport mechanisms within the various porous media. Contaminant transport takes place in fluid phases—in the present case, this is limited to air and water. Fluids move through the pores by advection in response to fluid pressure gradients, carrying dissolved contaminants with them. Fluids are also a medium for diffusive transport, in which contaminants move simply in response to concentration gradients, and do not require movement of the fluid. Both these processes occur simultaneously, along with all the other mechanisms identified in the model for contaminant transport (radioactive decay and ingrowth, geochemical partitioning, biotically-induced transport, erosion, etc.) This section discusses advective and diffusive contaminant transport mechanisms in fluids.

9.1 Porous Medium Water Transport

Water is a significant transport mechanism at Clive, and the conceptual model is that water slowly percolates down from the ground surface to the water table, and that diffusion can occur in the water phase as well.

9.1.1 Advection of Water

The flow of water is discussed at length in the previous sections of this document. Contaminant transport in this flowing water is essentially passive, with solutes moving along with the fluid, though of course concentrations are affected by other simultaneous processes.

9.1.2 Diffusion in Water

The Clive DU PA Model employs a modified version of GoldSim's native diffusive flux links to calculate diffusive fluxes in porous media. The modifications are necessary to account for unsaturated media, since GoldSim assumes that porous media are saturated in its basic implementation of diffusive flux calculations. The standard GoldSim diffusive flux mathematics are covered in Appendix B of the GoldSim User's Guide (GTG, 2011), and the modifications that have been developed by Neptune are discussed in detail in the Neptune document entitled *Modeling Diffusion in GoldSim*, but are also covered briefly here. The modifications required to model diffusion in unsaturated media take two phenomena into consideration: 1) The diffusive area is reduced by the saturation (with respect to air or water, whichever medium is of interest) and 2) the diffusive length is increased to account for tortuosity in the respective medium.

If a porous medium contains only a single fluid phase, the diffusive area between two cells containing that medium is simply the total area times the porosity, since the pores are occupied by the fluid, and the diffusion takes place only in the fluid. In the case of two fluids, such as air and water in unsaturated media, the diffusive area is further reduced, since the area of the fluid of interest across the plane of diffusion is less. If we are interested in diffusion in the water phase, for example, the area of water that intersects the plane is equal to the total area times the water content, which equals the total area times the porosity times the saturation with respect to water. If we are interested in diffusion in the air phase, we use the same construct, substituting air for water. Because the diffusive area is always less, the diffusion in a unsaturated medium will always be less than that in a fully saturated medium.

Diffusion in unsaturated media is also attenuated because of increased tortuosity. In any porous medium, a diffusing solute must travel through pores, following a tortuous path that is always longer than if it were traveling in a straight line. The ratio of the straight line distance to this tortuous path is called the tortuosity. If the porous medium is unsaturated, this path becomes even longer, since the three dimensional shape of the fluid of interest gets even more tortuous. This increases the diffusive length, which is used in calculating the concentration gradient. The gradient in concentration of a solute is what drives diffusion.

9.1.3 Water phase Tortuosity

Tortuosity is a term used to describe the resistive and retarding influence of pore structure for a variety of transport processes (Clennell, 1997). Definitions of tortuosity are not consistent in the literature and depend on the discipline and the particular transport process of interest. The tortuosity τ for molecular diffusion in porous media can be written as the ratio of effective diffusivity D_{eff} to bulk diffusivity D_{bulk}, often seen in two forms:

$$\tau_1 = \frac{D_{eff}}{D_{bulk}} \tag{37}$$

or alternatively, if exclusion of the measured porosity n is desired (Clennell, 1997), as

$$\tau_1 = \frac{D_{eff}}{n D_{bulk}}. \tag{38}$$

In this definition, consistent with the assumptions of GoldSim, the value of tortuosity varies between 0 and 1, with lower values indicating a longer path for porous medium solute transport via advection or diffusion. For unsaturated systems n is replaced in equation (38) by water content θ_w for water phase diffusion, or by the volumetric air content θ_a, for gaseous phase diffusion. The form shown in equation (37) is found in Freeze and Cherry (1979) and Marsily (1986) while that in equation (38) is used by Hillel (1980) and Koorevaar et al. (1983).

For consistency with GoldSim the second form is used. The equations for diffusive conductance in GoldSim explicitly specify the effective porosity (or in the case of unsaturated flow, water content or air filled porosity) as in equation (38). For more information on the diffusion equations in GoldSim, see Appendix B of the GoldSim User's Guide (GTG 2011). In the following sections, the equations from the literature have been converted where necessary to be consistent with equation (38) so that they can be directly applied to PA models.

Two options were considered for modeling liquid phase tortuosity in the Models. The Millington-Quirk model is commonly used to estimate tortuosity in non-fractured porous media (Millington and Quirk, 1961) (see Jury and Horton, 2004, eq. 7.14, modified by division by water content for consistency with GoldSim.) The water phase tortuosity τ_w is calculated as

$$\tau_w = \frac{D_{eff}}{\theta_w D_{bulk}} = \frac{\theta_w^{7/3}}{n^2}. \tag{39}$$

An alternative estimate of tortuosity has been developed from an empirical relationship between D_{eff} and θ_w from measurements provided by Conca and Wright (1992). Effective diffusivities for over 300 samples were determined for NaCl and KCl solutions using their Unsaturated Flow Apparatus (UFA) to establish the water content and other physical conditions in the sample. The relationship between D_{eff} and θ_w for a range of soils and gravels is shown in Figure 15. The relationship is remarkably consistent over a wide range of materials, indicating that it is insensitive to the grain size of the porous medium.

The model is expressed as

$$\log_{10} D_{eff} = -4.1 + 2.7 \log_{10}(\theta_w) + 0.32 \log_{10}(\theta_w)^2. \tag{40}$$

Volumetric water content is expressed as a fraction and D_{eff} has implied units of cm^2/s. Using D_{bulk} of 2.03×10^{-5} cm^2/s for chloride (Domenico and Schwartz 1990, p. 369), water tortuosity can be estimated from equations (39) and (40) for all solutes:

$$\tau_w = \frac{D_{eff}}{\theta_w D_{bulk}} = \frac{10^{-4.1 + 2.7 \log_{10}\theta_w + 0.32 \log_{10}\theta_w^2}}{\theta_w \, 2.03 \times 10^{-5} \, cm^2/s}. \tag{41}$$

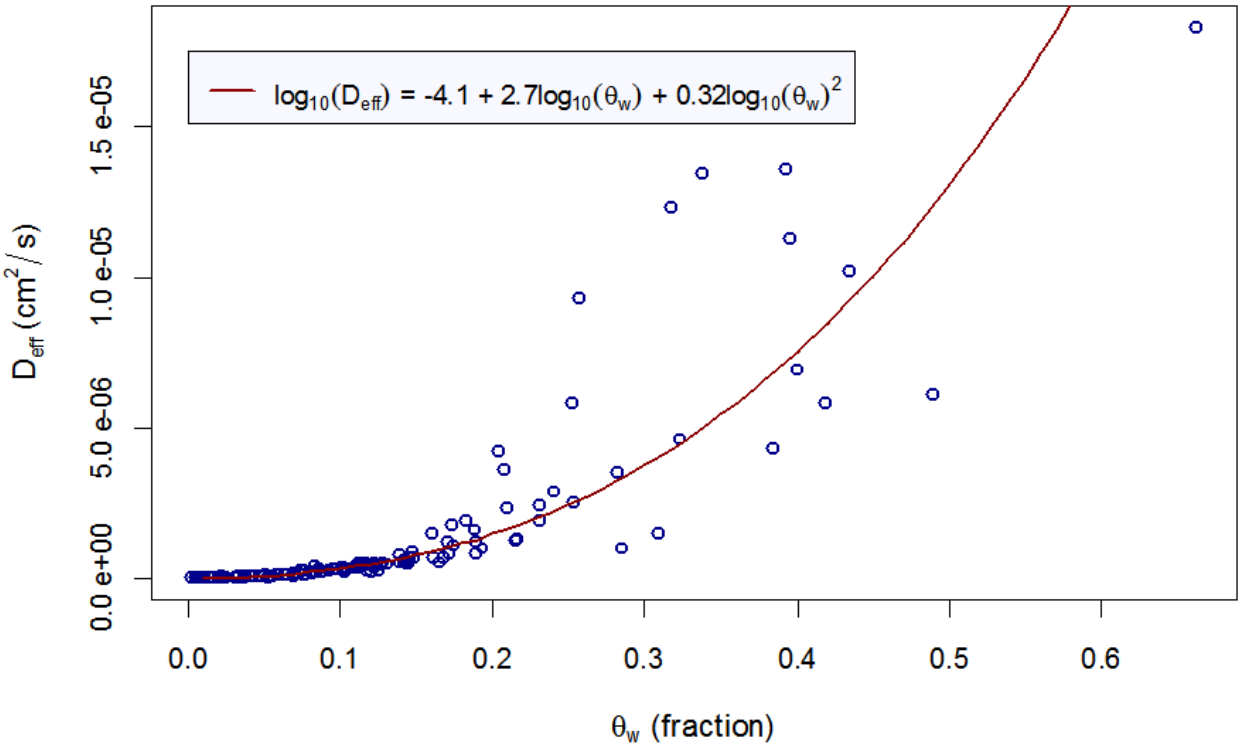

Figure 15. Estimated values of effective diffusivity D_{eff} for a range of volumetric water content for the Conca and Wright (1992) model. (After Conca and Wright, 1992).

The two tortuosity models are compared in Figure 16 using an effective porosity value of 0.37 for the Millington-Quirk model. Over the range of volumetric water contents from 0.10 to 0.20 the models differ by factors ranging from approximately 5 to 2.

Millington and Quirk (1961) concluded that, when considering porosity as the effective area of flow, the range on the porosity exponent in Equation (39) could be between 0.5 and 2 depending on the characteristics of the medium. This provided the foundation for developing input distributions for the exponents in porosity and water content in the Millington-Quirk model that model a range of behaviors that spanned the Millington-Quirk model and the Conca and Wright data. Generalizing the Millington-Quirk model gives:

$$\tau_w = \frac{D_{eff}}{\theta_w D_{bulk}} = \frac{\theta_w^{\beta_\theta}}{n^{\beta_n}} \tag{42}$$

where

β_θ is the water content exponent, and
β_n is the porosity exponent.

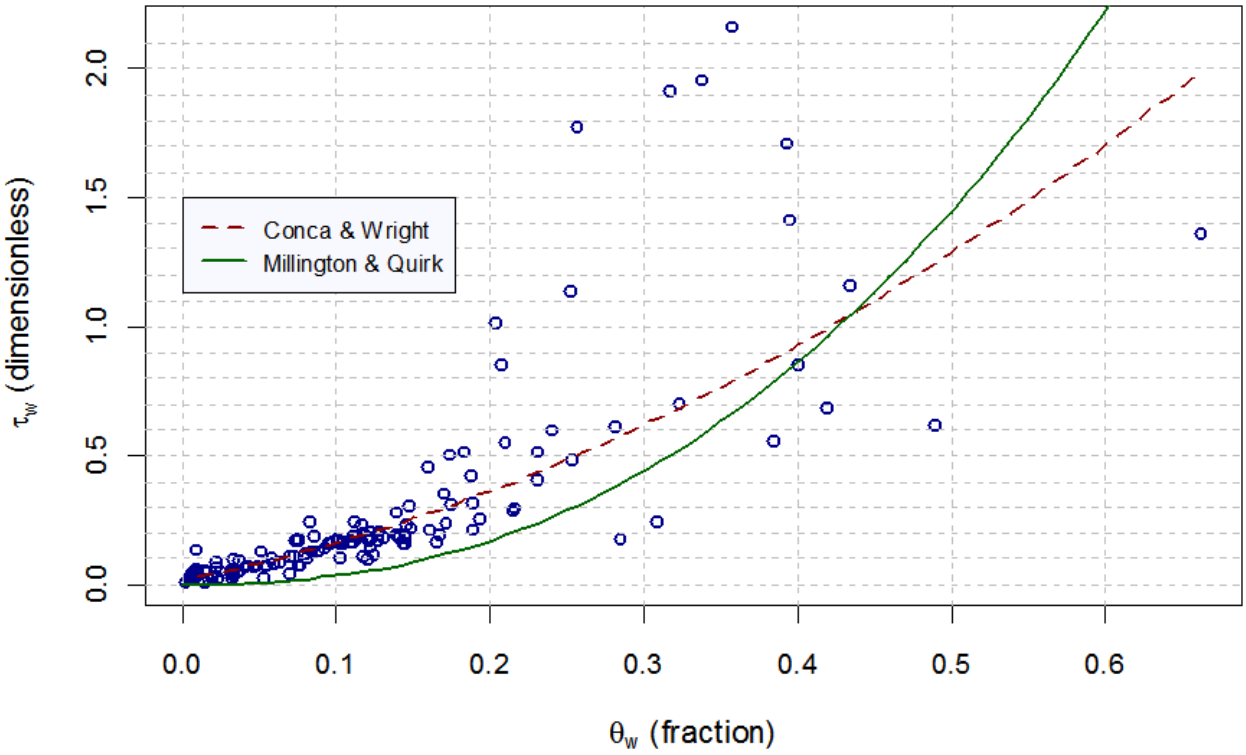

Figure 16. Water phase tortuosity function comparison between Millington-Quirk (Jin and Jury 1996) and Conca and Wright (1992).

Choosing a uniform distribution with a minimum of 0.5 and a maximum of 2.0 for β_n and a uniform distribution with a minimum of 4/3 and a maximum of 7/3 for β_θ results in the range of behaviors presented in Figure 17. These values are utilized in the Clive PA Model parameters to provide a conservatively high estimate of uncertainty, to allow the sensitivity analysis to determine the model is sensitive to the value of β_n. The upper bound on simulated tortuosity is given by $\beta_n = 2$ and $\beta_\theta = 4/3$ and the lower bound is given by $\beta_n = 1/2$ and $\beta_\theta = 7/3$. This appears to adequately describe a range of behaviors that includes the original Millington-Quirk model, the Conca and Wright data and a modeling analysis of unsaturated zone behavior in arid environments (Wolfsberg and Stauffer, 2003).

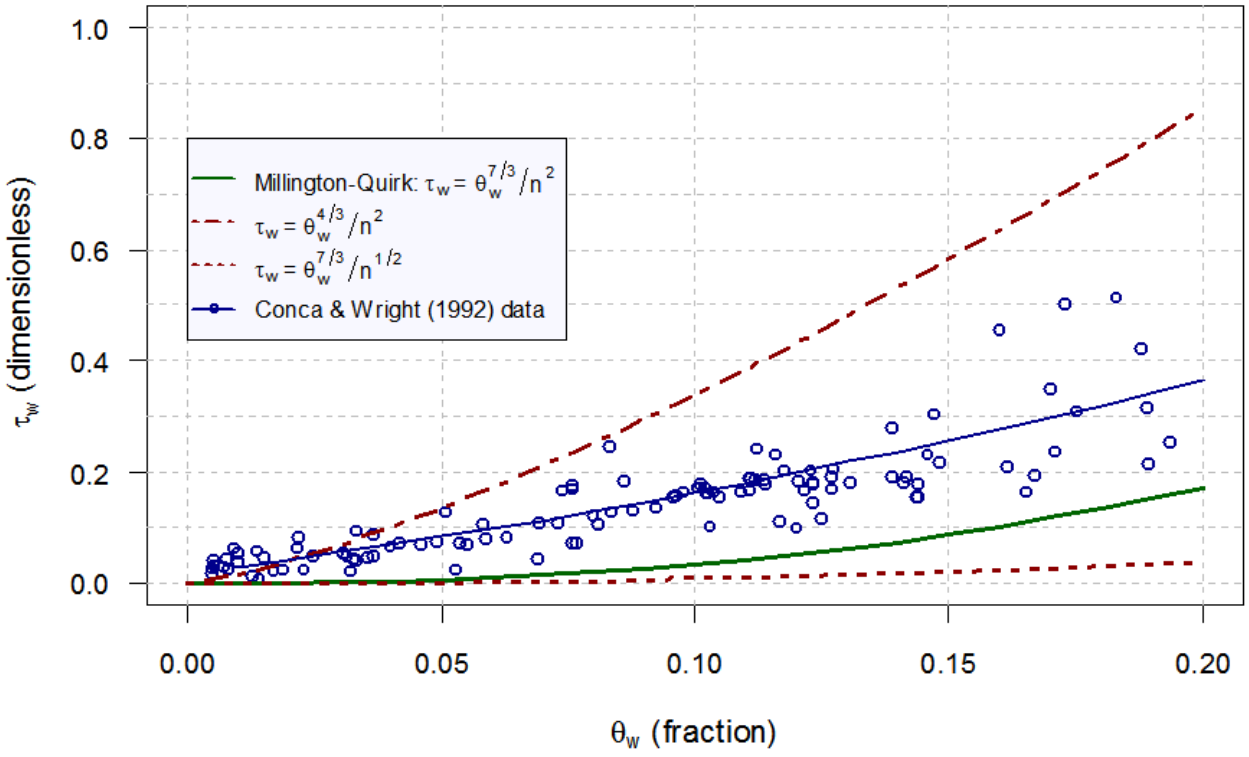

Figure 17. Comparison of the Millington-Quirk (1961) based water phase tortuosity formulation and the Conca and Wright model and data (1992).

9.2 Porous Medium Air Transport

9.2.1 Advection of Air

Air-phase advection is not included in the Clive DU PA Model. It is assumed that the advective flux of gases is negligible compared to the diffusive gas flux.

9.2.2 Diffusion in Air

Air-phase diffusion is included in the model, and this is the principal process by which gases are moved. The "built-in" diffusion calculations in GoldSim are used to estimate diffusion in the air phase. These gaseous diffusive fluxes are modified to handle the unsaturated porous media (described above in Section 9.1.2), but also include a calibration to counteract numerical dispersion for radon (discussed below in Section 9.4.2), which at this time is the only radionuclide that is considered to be present in the gaseous phase. The free-air diffusion coefficient for radon is fixed at 0.11 cm^2/s (Rogers and Nielson, 1991, p.226), since this is a well-established value with little uncertainty. Partitioning between the air and water phases is also handled internally by GoldSim, with the aid of the definition of Henry's Law constants for the various gas-phases constituents, discussed in Section 9.3.

Diffusion in the air phase is modeled throughout the top slope and side slope columns, bounded at the bottom by the saturated zone, and at the top by the atmosphere. The bottom boundary condition is one of no diffusion, since there is no air in the saturated zone to diffuse into, by definition. The boundary condition at the top is effectively a zero-concentration sink, since the volume of air in the atmosphere flowing over the embankment is sufficiently large that concentrations are kept much lower than in the pore air of the cover and wastes below. In order to model this, the air directly above the embankment is represented by an Atmosphere Cell Pathway element in GoldSim. The volume of air is defined by a thickness times the area of each respective modeled column, and this air volume is flushed out by the wind. The diffusive flux from the uppermost cover cell in the column to the Atmosphere cell is defined by the diffusive area, as discussed above, and the diffusive length, discussed in the following section. Since the atmosphere is not a porous medium, a diffusive length unrelated to its thickness is adopted. Since the wind will maintain low concentrations in the atmosphere, amounting to a zero-concentration boundary condition, the choice of the parameters defining the Atmosphere is not expected to have much influence on the diffusive flux from the embankment cover. Small uncertainties have been selected for these values, as shown in Table 15, in order to evaluate the model's sensitivity.

Table 15. Atmosphere volume parameters for creating a surface boundary condition in the porous medium air diffusion model.

Parameter	Distribution	Units
Thickness of the atmosphere layer	N(μ=2.0, σ=0.5, min=Small, max=Large)	m
Wind speed	N(μ=3.14, σ=0.5, min=Small, max=Large)	m/s
Atmospheric diffusion length	N(μ=0.1, σ=0.02, min=Small, max=Large)	m

9.2.3 Air-Phase Tortuosity

A number of tortuosity models have been proposed for air phase diffusion in porous media. Using the form for tortuosity shown in (38) above, models reviewed by Jin and Jury (1996) include the Penman model (Penman, 1940) and two models attributed to Millington and Quirk. In the Penman model, air phase tortuosity τ_a is a constant:

$$\tau_a = 0.66 . \tag{43}$$

In the more commonly used Millington-Quirk model (MQ1), which is analogous to equation (39), tortuosity is expressed as

$$\tau_a = \frac{\theta_a^{7/3}}{n^2} . \tag{44}$$

And, in an alternative Millington-Quirk model (MQ2) evaluated by Jin and Jury (1996), tortuosity is expressed as

$$\tau_a = \frac{\theta_a}{n^{2/3}} . \tag{45}$$

Note that as θ_a approaches n (e.g. as the porous medium becomes drier), τ_a approaches $n^{1/3}$ for both formulations (44) and (45).

An air-phase tortuosity model was developed by Lahvis et al. (1999) by calibrating a transport model to steady-state gas concentration data obtained from seven column experiments using silt and fine sand sediments. In this model, air phase tortuosity is dependent only on the volumetric water content:

$$\tau_a = 0.765 - 2.02\ \theta_w. \tag{46}$$

Comparison of these models for alluvium with an effective porosity of 0.37 and tortuosity as defined in equation (38) is shown in Figure 18. Due to the similarity of the Lahvis et al. (1999) model to the MQ2 model over a wide range of volumetric water content, it will not be considered further.

The Penman and the two Millington-Quirk models were compared by Jin and Jury (1996) with measured D_{eff}/D_{bulk} ratios from six studies that included a total of approximately 50 measurements on predominantly agricultural soils. While this ratio corresponds to the definition of tortuosity given in equation (38), it is useful in comparing the predictions of the various models. Over the range of air phase porosity investigated (0.05 to 0.5), the Penman model tended to overestimate tortuosity, while the MQ1 model in equation (44) underestimated tortuosity. Of the three models, the MQ2 model given by (45) provided the best fit to the measured tortuosities.

A comparison of the Penman and Millington-Quirk models for a material with an effective porosity of 0.37 is shown in Figures 18 and 19. Note that in both these figures, the points are merely points of calculation, and do not represent data. The values produced by the Penman and Millington-Quirk models converge for dry and wet conditions but diverge at intermediate values of air porosity. Given its median behavior as seen in Figures 18 and 19, the alternative Millington-Quirk model (MQ2, equation (45)) is used in the Clive DU PA model.

Tortuosity is implemented in the GoldSim model as a multiplier to the diffusive length, which is defined for each Cell Pathway element using the common method of setting it equal to 1/2 the cell length that is parallel to flow. In this case, that is the vertical dimension.

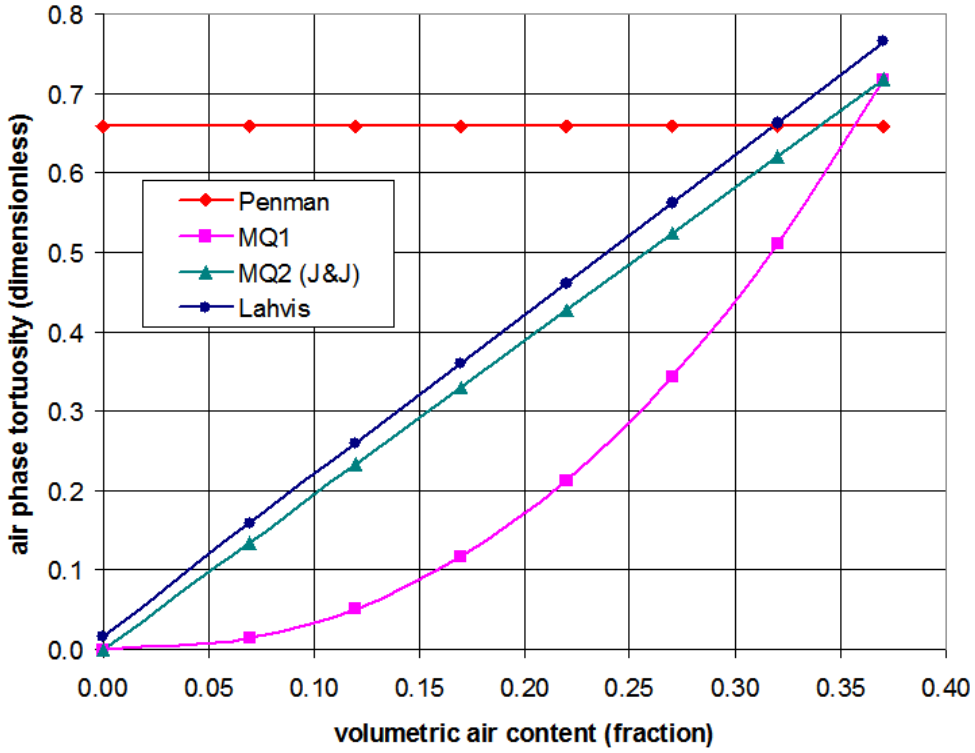

Figure 18. Comparison of air-phase tortuosity models by Penman (equation (43)), Millington and Quirk (MQ1, equation (44)), Millington and Quirk as modified by Jin and Jury (1996) (MQ2, equation (45)), and Lahvis et al. (1999) (equation (46)).

9.3 Air/water partitioning: Henry's Law

Most volatile solutes exist to varying degrees in both air and water. In the absence of other processes, a solute will partition between air and water phases in a given proportion (for a given temperature), following Henry's Law. The ratio of the concentration of a chemical in water to its concentration in air in known as its Henry's Law constant, which can have many functional forms. In the Clive DU PA Model, only one radionuclide has a gaseous phase: radon. Sander (1999, Table 7, p.13) provides a Henry's Law constant for radon of 9.3×10^{-3} mol/L·atm, defined using a form of Henry's Law that relates the partial pressure of the solute in the gas above the water to the concentration of the water:

$$K_{H,cp} = \frac{c}{p} \tag{47}$$

where

$K_{H,cp}$ is the Henry's Law constant relating c to p, in units of mol/L·atm
c is the concentration of the solute, in mol/L, and
p is the partial pressure of the solute in the gas phase, in atm.

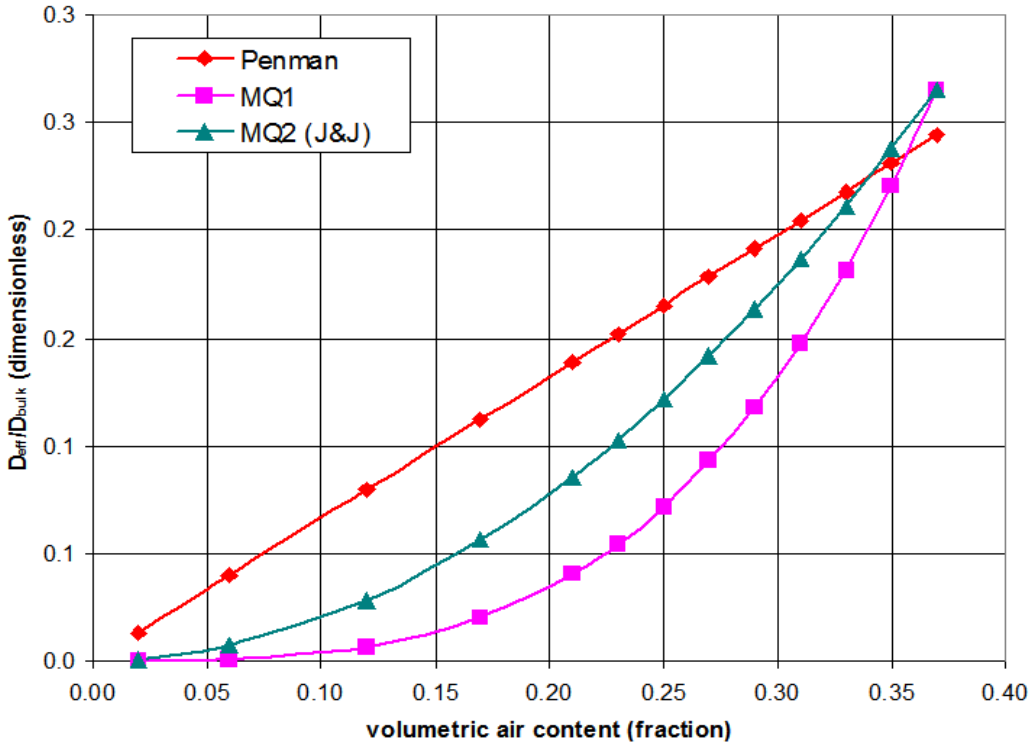

Figure 19. Comparison of effective to bulk diffusivity ratios with air phase porosity for air phase tortuosity models.

This Henry's Law constant must be converted to the dimensionless form—a ratio of the concentration in water to that in gas (air):

$$K_H = \frac{C_{(water)}}{C_{(air)}} \tag{48}$$

This conversion is done using the following equation:

$$K_H = \frac{1}{K_{H,cp} R T_{soil}} \tag{49}$$

where

R is the ideal gas constant, and
T_{soil} is the soil temperature.

The gas constant R is conveniently provided as a defined constant in GoldSim. The soil temperature at the Clive facility is estimated from the Clive Test Cell data provided by Energy*Solutions* in the spreadsheet "Temp and Dose Data 9-19-01 to 1-15-09.xls", with a normal distribution with a mean of 12°C and a standard deviation of 1 °C.

This dimensionless Henry's Law constant K_H for radon is an attribute of the fluid material Air defined in the Clive DU PA Model. The value of K_H for radon is therefore 4.5, meaning that the noble gas strongly favors dissolution in water.

9.4 Transport of Radon

The Clive DU PA Model is dominated by a single waste form: depleted uranium. This material predominantly consists of ^{238}U. This uranium isotope is a parent of ^{222}Rn, its rate of production controlled by the decay rate of the ^{238}U. Using a basic representation of fate and transport, radon emanation is accounted for, as is Henry's Law partitioning into water, and the gas is allowed to diffuse in pore air using GoldSim's internal diffusion processes, as corrected for unsaturated media and for numerical dispersion. Radon emanation and diffusion are discussed below.

9.4.1 Radon Emanation (Escape/Production Ratio)

The fraction of ^{222}Rn produced by decay of radium-226 (^{226}Ra) that is released from the solid matrix is known as the escape-to-production (E/P) ratio, as well as the emanation coefficient, the emanation factor, or emanating power (Nielson and Sandquist, 2011). When ^{226}Ra decays, a small fraction of the decay energy, 0.1 MeV, is carried by the recoiling ^{222}Rn atom. This is sufficient energy for the recoiling atom to travel about 45 nm in a mineral matrix, 0.1 μm in water, and about 63 μm in air. Recoiling atoms with just sufficient energy to stop in the air or water filled pore space will be released from the matrix and become available for transport. If there is too little energy available, the atom will remain trapped in the solid matrix. If there is too much energy, the atom will cross the pore space and be embedded in the solid matrix of a nearby grain. The E/P ratio describes that fraction of ^{222}Rn that stops in the air or water-filled pore space and is free to diffuse. The E/P ratio can physically vary from a minimum of 0 to a maximum of 1.

Predicting the E/P ratio for a material is difficult as numerous factors have been identified that affect it: The E/P ratio is inversely related to grain size. The closer decaying atoms are to the surface of a grain, the more likely they will be released to the pore space. The adsorption or coprecipitation of ^{226}Ra on surficial coatings increases emanation, as will cracks, fissures, or pitting of grains. In contrast, the E/P ratio is directly related to pore size. As the pore size increases, it is more likely that recoiling atoms will stop in the pore space and emanation increases. The presence of water in the pore space increases emanation, because the reduced particle range in water increases the likelihood that the recoiling atom will stop in the pore space. Predicting the E/P ratio of a material is particularly difficult because it requires detailed knowledge of the microscopic physical structure of the material, microscopic distribution of ^{226}Ra in the material, and water content.

The E/P ratios for different types of common geologic materials have been reported. From geometrical considerations, the maximum emanation expected from a thick slab source is 0.5 and from a thin film, 1.0. The maximum E/P ratio of natural materials will lie somewhere between these two extremes. The maximum value reported for common materials is approximately 0.7 to 0.8. Reported E/P ratios for soils and rocks range from 0.02 to 0.7 (UNSCEAR 2000; NCRP 1988). The emanation factor of a single material may vary over a substantial portion of this range depending on the water content. Rock and uncrushed ores usually have lower emanation factors ranging from 0.02 to 0.26 (Nazaroff 1992). Concrete emanation factors may range from 0 to 0.3 (Rogers et al. 1994; Cozmuta et al. 2003).

Nielson and Sandquist (2011, Table 1, p. 11) discuss radon modeling at length, and have assembled information about E/P ratios in uranium ores (in Table 1 of that document), which are reasonable analogs for uranium oxides that are the subject of this PA. Following the principles outlined in the *Fitting Probability Distributions* white paper, a beta distribution is chosen to represent the E/P ratio, with a mean of 0.290, with a standard deviation of 0.156.

9.4.2 Radon diffusion

The transport of the radioactive noble gas radon presents special modeling challenges. The diffusion of gas phase constituents follows concentration gradients, and these vary along the diffusive path. These concentrations are subject to other transport processes, notably partitioning into water (according to the Henry's Law constant) and encountering sinks like the atmosphere. In the modeling of radioactive constituents, most radionuclides have relatively long half-lives, and the concentration gradients are not much affected by decay and ingrowth. Radon isotopes, however, have short half-lives relative to the rate of diffusive transport processes, can move quickly in pore air, and decay to a chain of radionuclides that can be significant in terms of dose and risk. In the Clive DU PA Model, the radon isotope of interest is ^{222}Rn, with a half-life of about 3.8 days. With this short half-life, ^{222}Rn decays away quickly enough that the decay alone can produce strong concentration gradients, causing additional challenges in numerical simulation.

Chemical engineers are faced with similar issues in process plants, where chemicals in a process that moves through the plant are simultaneously undergoing chemical transformation to other substances. The quantification of this effect is called the Damköhler number. The value can be expressed in a number of different ways for different applications, and in the case of this model, it is the ratio of the decay rate to the diffusive mass transport rate. For ^{222}Rn, with its high rate of decay, the Damköhler number is also high, indicating that diffusive transport will be overpredicted in a coarsely-discretized model such as the Clive DU PA Model.

Approaches to correcting for this overprediction include calibration to analytical solutions for radon diffusive transport and refining the discretization of the modeling grid. If the contaminant transport modeled column is of one or two layers of uniform materials, analytical solutions are possible, such as those presented in the Nuclear Regulatory Commission's Regulatory Guide on the estimation of radon attenuation in earthen covers for uranium mill tailings piles (NRC 1989b).

9.4.3 Calibration of Air Diffusion to Counteract Numerical Dispersion

In the Clive DU PA Model, where wastes and other materials with a variety of porous medium properties can be intermixed, calibration to analytical solutions is prohibitively difficult. The only way to refine the solution is by refining the grid, which is the approach that is taken in the model. This refinement reduces numerical dispersion, providing a realistic simulation of the diffusion process. To refine the top slope and side slop columns, which integrate all the contaminant transport processes, would introduce an unreasonable computational burden, since most of the processes would not appreciably benefit from the finer discretization. By taking advantage of a clever side calculation, the model can benefit from the increased accuracy of the finer discretization, without significant computational effort.

Within the GoldSim container for the Class A South Top Slope contaminant transport calculations, an additional container is added, with a switch for enabling and disabling its calculations. This container is devoted to determining the appropriate measure by which the radon diffusivity of 0.11 cm^2/s should be reduced in order to exactly counter the effects of numerical dispersion. The calculation consists of two columns: one coarsely- and one finely-discretized. The coarse discretization matches that of the main Top Slop column, with GoldSim Cell pathway elements representing layers in the cover of about 15 cm (6 in) thickness, and layers in the waste about 50 cm (20 in) thick. Each of the Cells is populated with air, water, porous media, and initial inventory just as is the main column, but the only processes represented include retardation, solubility, and air diffusion. This protects the coarse column from all the confounding factors of water advection and diffusion, biotic processes, etc.

The fine column is built the same way, but with 15 times as many Cells. That is, the cover cells in the fine column are about 1 cm thick, and those in the waste are about 3 cm. This fine column has significantly less numerical dispersion for the air diffusion calculations, and is used for calibration of the coarse column. The calibrated diffusion coefficients for radon in the coarse column, then, are also applied to the main Top Slope and Side Slope columns, thereby counteracting the effects of numerical dispersion there as well.

Both the coarse and fine columns are populated with porous materials that exactly match those in the Top Slope column. These reside in three distinct zones. From the bottom up, these zones are: 1) the waste zone, where radioactive wastes are disposed, and are of similar material properties as far as air diffusion is concerned, 2) the radon barrier clay layers, which consist of tightly compacted clays overlying the wastes, and 3) the upper cover materials, which are uncompacted fill materials. The radon fluxes (mass flow per area, with dimensions of M/L^2-T and units of g/m^2-s or pCi/m^2-s) are recorded at the top of each of these three zones in both the coarse and fine columns. With less numerical dispersion, the finer column always has a lower rate of diffusion out the top of the zone.

If the coarse column's diffusion coefficient for radon is adjusted downward, it can be forced to match the finer column, producing a more accurate flux. This correction is performed sequentially, from the bottom up, and a different correction factor is applied for each material within the three zones. This results in one radon diffusion correction factor for the waste zone, one for the clays, and one for the upper cover layers. The correction factor for wastes is applied to the waste layers in the Top Slope and Side Slope contaminant transport columns. Likewise, the correction factors for the clay layers is applied to the radon barrier clay and liner clay layers in the Top Slope and Side Slope columns, and the correction factors for the upper cover layers is applied to both columns as well.

This radon calibration need be done only once, unless the layer geometries and/or material properties change significantly. Fortunately, performing the calibration in deterministic mode is sufficient, as it is robust and holds quite well even using stochastic inputs in probabilistic mode. Once the calibration has been completed, the radon calibration container may be disabled, so that it does not impose further computational burden on the model.

10.0 References

Abramowitz, Milton, and Irene A. Stegun, 1970. *Handbook of Mathematical Functions with Formulas, Graphs, and Mathematical Tables*. National Bureau of Standards, Applied Mathematics Series 55, ninth printing. November, 1970.

Albright, W.H., G.W. Gee, G.V. Wilson, and M.J. Fayer. 2002. *Alternative Cover Assessment Project Phase I Report.* Desert Research Institute Publication No. 41183. Reno, NV.

Bingham Environmental, 1991. *Hydrogeologic Report Envirocare Waste Disposal Facility South Clive, Utah*. Final version October 9, 1991.

Bingham Environmental, 1994. *Hydrogeologic Report Mixed Waste Disposal Area Envirocare Waste Disposal Facility South, Clive, Utah*. Final version November 18, 1994.

Buckingham, E. 1907. *Studies on the Movement of Soil Moisture*. Bulletin 38. U.S. Dept. of Agriculture Bureau of Soils. Washington, D.C.

Clennell, M.B. 1997. *Tortuosity: a guide through the maze*. in Developments in Petrophysics, Lovell, M.A. and P.K. Harvey (eds). Geological Society Special Publication No. 122, pp. 299-344.

Conca, J.L., and J.V. Wright. 1992. Flow and Diffusion of Unsaturated Gravel, Soils and Whole Rock, *Applied Hydrogeology*, International Association of Hydrogeologists, Vol. 1, 1992, pp. 5-24.

Cozmuta, I., E. R. van der Graaf, and R. J. de Meijer, 2003. Moisture Dependence of Radon Transport in Concrete: Measurements and Modeling. *Health Physics* 85(4): 438 – 456.

Domenico, P.A. and F.W. Schwartz. 1990. *Physical and Chemical Hydrogeology*. John Wiley & Sons, New York, NY.

EnergySolutions, 2009. *Class A South Cover Designs. Drawing 07021 V7*, Clive, Utah.

Envirocare, 2005. *Cover Test Cell Data Report Addendum: Justification to Change EZD from 18-inches to 24-inches*. Attachment to letter dated October 13, 2005 from Daniel B. Shrum, Director of Safety and Compliance, Envirocare of Utah, LLC, to Dane L. Finefrock, Executive Secretary, Division of Radiation Control.

Fayer, M.J., 2000. *UNSAT-H Version 3.0: Unsaturated Soil Water and Heat Flow Model, Theory, User Manual, and Examples*. PNNL-13249. Pacific Northwest National Laboratory, Richland, Washington. June, 2000.

Freeze, R.A and J.A. Cherry. 1979. *Groundwater*. Prentice-Hall, Inc., Englewood Cliffs, NJ.

GTG (GoldSim Technology Group), 2011. *User's Guide: GoldSim Contaminant Transport Module*, GoldSim Technology Group, Issaquah, WA, December 2010

Hillel, D. 1980. *Fundamentals of Soil Physics*. Academic Press Inc. San Francisco, CA.

Jin, Y., and W.A. Jury. 1996. *Characterizing the Dependence of Gas Diffusion Coefficient on Soil Properties*, Soil Science Society of America Journal, Vol. 60, pp. 66-71.

Jury, W.A. and R. Horton. 2004. *Soil Physics.* 6th ed. John Wiley and Sons Inc. New Jersey.

Khire, M.V., C.H. Benson, and P.J. Bosscher. 1997. Water balance modeling of earthen final covers. *J. Geotechnical and Geoenvironmental Engineering* . Vol. 23, No. 8.

Koorevaar, P., G. Menelik, and C. Dirksen. 1983. *Elements of Soil Physics*. Elsevier. New York, NY.

Lahvis, M.A., A.L. Baehr, and R.J. Baker. 1999. *Quantification of Aerobic Biodegradation and Volatilization Rates of Gasoline Hydrocarbons Near the Water Table Under Natural Attenuation Conditions*. Water Resour. Res. v. 27, 753-765.

Marsily, G. de. 1986. *Quantitative Hydrogeology*. Academic Press Inc. San Diego, CA.

Meyer, P.D., M.L. Rockhold, W.E. Nichols, and G.W. Gee. 1996. *Hydrologic evaluation methodology for estimating water movement through the unsaturated zone at commercial low-level radioactive waste disposal sites.* NUREG/CR-6346. U.S. Nuclear Regulatory Commission. Washington, D.C.

Millington, R.J., and J.P. Quirk. 1961. "Permeability of porous solids." Trans. Faraday Society (57) pp. 1200-1207

Mualem, Yechezkel, 1976. *A New Model for Predicting the Hydraulic Conductivity of Unsaturated Porous Media*. Water Resources Research, Vol. 12, No. 3, pp. 513-522. June, 1976.

Nazaroff, W. W., 1992. Radon Transport from Soil to Air. Rev. of Geophysics 30(2): 137 – 162.

NCRP (National Council on Radiation Protection and Measurements). 1988. Measurements of Radon and Radon Daughters in Air. NCRP Report No. 97, NCRP Bethesda, Maryland, November 1988.

NRC (U.S. Nuclear Regulatory Commission). 1989b. *Calculation of Radon Flux Attenuation by Earthen Uranium Mill Tailings Covers, Regulatory Guide 3.64*, Nuclear Regulatory Commission, June 1989.

Nielson, K.K., and G.M. Sandquist. 2011. *Radon Emanation from Disposal of Depleted Uranium at Clive, Utah*. Report for Energy*Solutions* by Applied Science Professionals, LLC. February 2011.

Penman, H.L. 1940. "Gas and vapor movements in the soil. I. The diffusion of vapors through porous solids." Journal of Agricultural Science (30) pp. 437-462

Rogers, V.C., and K.K. Nielson. 1991. Correlations for Predicting Air Permeabilities and Rn-222 Diffusion Coefficients of Soils, Health Physics (61) 2

Rogers, V.C., K. K. Nielson, M. A. Lehto, and R. B. Holt, 1994. Radon Generation and Transport Through Concrete Foundations. EPA/600/SR-94/175, U. S. Environmental Protection Agency, Research Triangle Park, North Carolina, November 1994.

Sander. 1999. Compilation of Henry's Law Constants for Inorganic and Organic Species of Potential Importance in Environmental Chemistry, version 3, 8 Apr 1999 http://www.mpch-mainz.mpg.de/~sander/res/henry.html

Schroeder, P.R., Aziz, N.M., Lloyd, C.M., and P.A. Zappi, 1994. *The Hydrologic Evaluation of Landfill Performance (HELP) Model: User's Guide for Version 3*, EPA/600/R-94/168A; US EPA Office of Research and Development, Washington, D.C.

SWCA, 2011, *Field Sampling of Biotic Turbation of Soils at the Clive Site, Tooele County, Utah*, SWCA Environmental Consultants, Salt Lake City, Utah, January 2011.

UNSCEAR (United Nations Scientific Committee on the Effects of Atomic Radiation). 2000. UNSCEAR Report to the General Assembly – Sources and Effects of Ionizing Radiation.

USDA (United States Department of Agriculture) 2011. Web Soil Survey. US Department of Agriculture, National Resources Conservation Service. 2011. Retrieved from URL http://websoilsurvey.nrcs.usda.gov/.

Ward, A.L., M.D. White, E.J. Freeman, and Z.F. Zhang. 2005. STOMP: *Subsurface transport over multiple phases. Version 1.0. Addendum: Sparse vegetation evapotranspiration model for the water-air-energy operational mode.* PNNL-15465. Pacific Northwest National Laboratory, Richland, WA.

Whetstone Associates, Inc., 2000, *Revised Envirocare of Utah Western LARW Cell Infiltration and Transport Modeling.* July 19, 2000.

Whetstone Associates, Inc., 2007. *EnergySolutions Class A South Cell Infiltration and Transport Modeling*. December 7, 2007.

Wolfsberg, A. and P. Stauffer. 2003. *Vadose Zone Fluid and Solute Flux: Advection and Diffusion at the Area 5 Radioactive Waste Management Site*. LA-UR-03-4819, Los Alamos National Laboratory, Los Alamos, New Mexico.

Appendix

Soil Moisture Data for Units 3 and 4

The data for soil moisture characteristics in Unit 3, a silty sand, and in Unit 4, a silty clay, are reproduced in the following tables, and are based on testing performed by Colorado State University (Bingham Environmental 1991, Appendix B, pages B-20 and B-26). Cores GW18-B4 and GW79A-B5 are from Unit 3, and cores GW19A-B1 and GW17A-B2 are from Unit 4. Bulk density is defined in the units of g/cm^3. Conductivity data have units of cm/s.

	GW18-B4		GW19A-B1		GW17A-B5		GW17A-B2	
	WATER CONTENT	MATRIC PRESSURE (cm)	WATER CONTENT	MATRIC PRESSURE (cm)	WATER CONTENT	MATRIC PRESSURE (cm)	WATER CONTENT	MATRIC PRESSURE (cm)
DRYING CYCLE	0.409	0	0.442	0	0.377	0	0.505	0
	0.409	6	0.438	383	0.376	19	0.505	49
	0.404	24	0.426	468	0.319	60	0.485	455
	0.362	94	0.405	683	0.207	274	0.466	954
	0.321	131	0.370	1074	0.188	569	0.453	1947
	0.262	171	0.344	2029			0.429	2563
	0.213	230	0.337	3025			0.397	4815
	0.180	349	0.316	4921				
	0.144	664						
	0.132	828						
WETTING CYCLE	0.117	932	0.316	4211	0.1279	946	0.395	4030
	0.119	852	0.317	3961	0.128	807	0.396	3537
	0.122	817	0.317	3736	0.128	578	0.399	3092
	0.126	683	0.322	3465	0.130	403	0.403	2545
	0.129	633	0.323	3265	0.134	282	0.407	2045
	0.135	491	0.327	3010	0.148	204	0.410	1524
	0.142	417	0.332	2774	0.186	88	0.413	1005
	0.156	314	0.335	2540	0.254	53	0.417	504
	0.171	262	0.343	2284	0.307	49	0.422	211
	0.180	221	0.345	2054	0.316	34	0.426	60
	0.220	110	0.352	1804				
	0.302	36	0.357	1534				
	0.327	9	0.365	1300				
			0.369	1079				
			0.373	845				
			0.383	625				
			0.398	391				
			0.397	300				
			0.432	0				
BULK DENSITY	1.567		1.397		1.673		1.326	
POROSITY	0.409		0.473		0.320		0.505	
WETTING CYCLE FIT PARAMETERS								
θ_s	0.380		0.432		0.345		0.429	
θ_s	0.0		0.0		0.130		0.172	
α	0.05222		0.00295		0.0177		0.0012	
n	1.3068		1.1202		3.6477		1.1000	
m	0.2347		0.1073		0.7259		0.0909	

	GW18-B4		GW19A-B1		GW17A-B5	
	WATER CONTENT	D(θ) (cm^2/s)	WATER CONTENT	D(θ) (cm^2/s)	WATER CONTENT	D(θ) (cm^2/s)
DIFFUSIVITY DATA	0.380	0.005559	0.430	0.004502	0.345	0.005559
	0.360	0.010385	0.420	0.004024	0.340	0.012307
	0.340	0.008981	0.400	0.003327	0.320	0.008794
	0.320	0.008246	0.380	0.002838	0.300	0.007767
	0.300	0.007759	0.360	0.002471	0.280	0.007184
	0.280	0.007401	0.340	0.002184	0.260	0.006785
	0.260	0.007119	0.320	0.001952	0.240	0.006485
	0.240	0.006889	0.315	0.001900	0.220	0.006247
	0.220	0.006696	0.312	0.001870	0.200	0.006051
	0.200	0.006529	0.262	0.001468	0.180	0.005885
	0.180	0.006383	0.212	0.001186	0.160	0.005742
	0.160	0.006254	0.162	0.000974	0.140	0.005616
	0.140	0.006138	0.112	0.000809	0.135	0.005586
	0.120	0.006034			0.132	0.005569
	0.100	0.005938			0.1308	0.005563
	0.080	0.005850			0.1305	0.005561
	0.060	0.005770				
	0.040	0.005695				
	0.020	0.005625				
	0.010	0.005591				
CONDUCTIVITY DATA	0.380	3.38E-5	0.430	1.89E-7	0.345	5.59E-5
	0.360	3.28E-5	0.420	1.33E-7	0.340	9.60E-6
	0.340	2.42E-5	0.400	6.74E-8	0.320	1.72E-5
	0.320	1.74E-5	0.380	3.41E-8	0.300	1.76E-5
	0.300	1.22E-5	0.360	1.71E-8	0.280	1.55E-5
	0.280	8.39E-6	0.340	8.38E-9	0.260	1.25E-5
	0.260	5.59E-6	0.320	4.01E-9	0.240	9.16E-6
	0.240	3.61E-6	0.315	3.32E-9	0.220	6.09E-6
	0.220	2.25E-6	0.312	2.96E-9	0.200	3.53E-6
	0.200	1.34E-6	0.262	3.84E-10	0.180	1.65E-6
	0.180	7.56E-7	0.212	3.49E-10	0.160	5.01E-7
	0.160	4.00E-7	0.162	1.79E-12	0.140	3.62E-8
	0.140	1.95E-7	0.112	3.28E-14	0.135	6.65E-9
	0.120	8.54E-8			0.132	6.45E-10
	0.100	3.22E-8			0.1308	4.73E-11
	0.080	9.83E-9			0.1305	9.10E-12
	0.060	2.14E-9				
	0.040	2.50E-10				
	0.020	6.44E-12				
	0.010	1.67E-13				
FIT PARAMETER Ks	4.4E-3		2.00E-4		2.00E-4	

Neptune and Company Inc.

June 1, 2011 Report for EnergySolutions

Clive DU PA Model, version 1

Appendix 6

Geochemical Modeling

Radionuclide Geochemical Modeling for the Clive DU PA

28 May 2011

Prepared by

Neptune and Company, Inc.

This page is intentionally blank, aside from this statement.

CONTENTS

FIGURES

TABLES

1.0 Summary of Solubility, Partitioning (Kd), and Diffusion Parameters

This section is a brief summary of parameters and distributions used for modeling geochemical processes for the Clive Depleted Uranium Performance Assessment Model. For distributions, the following notation is used:

- N(μ, σ, [*min*, *max*]) represents a normal distribution with mean μ and standard deviation σ, and optional truncation at the specified *min*imum and *max*imum, and
- LN(*GM*, *GSD*, [*min*, *max*]) represents a log-normal distribution with geometric mean.

Water partitioning coefficients for the sand, clay and silt fractions used in the GoldSim transport model are summarized in Table 1 (discussed in Section 4.0). The minimum and maximum values used in the log uniform distribution of the aqueous solubility ranges used in the GoldSim transport model are summarized in Table 2 (discussed in Section 5.0). Minimum and maximum values for a uniform distribution for ionic and molecular diffusion coefficients are summarized in Table 3 (see Section 6.0)

Table 1: Distribution Parameters for Partitioning Coefficients (K_d) for materials (mL/g). Unless noted otherwise, distributions are described by the log uniform distribution.

Chemical Element	Sand		Silt		Clay	
	Min	Max	Min	Max	Min	Max
Ac	1.68E+1	5.35E+2	1.57E+1	1.91E+3	8.36E+1	2.99E+3
Am	4.32E+1	8.11E+2	8.80E+1	1.14E+3	8.80E+1	1.14E+3
Cs	2.70E+0	2.22E+1	4.23E+0	1.18E+2	6.69E+0	2.39E+2
I	N(4.28e-1, 6.05e-1)		N(4.28e-1, 6.05e-1)		N(4.28e-1, 6.05e-1)	
Np	3.92E-1	5.10E+1	8.05E-1	6.21E+001	4.32E+0	8.11E+1
Pa	8.32E+0	3.31E+2	1.84E+2	9.78E+2	1.80E+2	1.56E+3
Pb	2.70E+0	2.22E+1	4.23E+0	1.18E+2	6.69E+0	2.39E+2
Pu	6.69E+1	2.39E+3	8.05E+1	6.21E+3	9.14E+2	5.47E+3
Ra	3.87E-1	6.46E+1	7.97E-1	7.53E+1	1.42E+0	1.41E+3
Rn	0.00E+0	0.00E+0	0.00E+0	0.00E+0	0.00E+0	0.00E+0
Sr	2.70E+0	2.22E+1	4.23E+0	1.18E+2	6.69E+0	2.39E+2
Tc	N(1.02e-1, 1.45e-1)		N(1.02e-1, 1.45e-1)		N(1.02e-1, 1.45e-1)	
Th	1.92E+1	4.16E+1	3.44E+1	6.97E+2	8.47E+1	2.36E+3
U	3.44E-1	6.77E+0	8.80E-1	1.14E+1	9.05E+0	6.63E+001

Table 2: Log Uniform Parameters for Solubilities

Chemical Element	Min (mol/L)	Max (mol/L)
Ac	6.81E-9	1.47E-5
Am	6.81E-10	1.47E-6
Cs	6.81E-3	1.47E+1
I	5.99E-5	1.67E+0
Np	6.81E-6	1.47E-2
Pa	6.81E-9	1.47E-5
Pb	6.81E-9	1.47E-5
Pu	5.27E-11	1.90E-5
Ra	5.99E-10	1.67E-5
Rn	7.74E-4	1.29E-1
Sr	6.81E-7	1.47E-3
Tc	7.74E-5	1.29E-2
Th	7.74E-9	1.29E-6
U*	3.58E-6	2.79E-3
U_3O_8	1.0E-16	6.5E-10
UO_3	3.58E-6	2.79E-3

* See GoldSim model note Section 5.1.14.3.

Table 3: Distribution Parameters for Ionic and Molecular Diffusion Coefficients

Parameter	Ion/Molecule	Units	Distribution
D_m	All	cm^2/s	$U(3 \times 10^{-6}, 2 \times 10^{-5})$

2.0 Geochemical Conditions

The Clive Disposal Facility is located on the eastern side of the Great Salt Lake Desert. The geochemistry of the Clive, Utah location is dominated by weathering and erosion of the local basin and mountains and by recharge via meteorological precipitation. The area consists of a large basin surrounded by mountains formed of Paleozoic limestones, dolomites, shales, quartzites, and sandstones. Isolated areas of the Great Salt Lake desert region are underlain with tertiary extrusive igneous basaltic flows and pyroclasts. The valley sediments consist of alluvial fans, evaporites, and unconsolidated and semi-consolidated valley fill (Bingham Environmental 1991, Schaefer et al., 2003). Within the valley, where the Clive facility is located, the valley fill is formed by quaternary-age lacustrine lake deposits associated with the former Lake Bonneville. The surface deposits are mainly low-permeability silty clays with sand and gravel outcrops and lenses in the subsurface. Bedrock appears to be at least 75 m (250 ft) below ground surface (bgs) and potentially much lower. The regional groundwater flow is to the east-northeast towards the Great Salt Lake.

There are four zones within the PA model domain that are included in the radionuclide transport model, moving downward beginning with the depleted uranium waste cell there is a clay liner beneath this waste—part of the engineered closure system. Beneath the clay liner is the unsaturated zone which extends to the upper aquifer in the saturated zone. Each zone has unique properties that will influence the dissolved transport of the radionuclides modeled. The depleted uranium in the waste cell, like the unsaturated zone below it, is expected to be largely devoid of a significant water phase during the period of this PA model. The depleted uranium waste will be initially contained in cylinders or drums within the embankment. For the Conceptual Site Model (CSM) and associated geochemical modeling, there is no assumption that the waste cell will have any type of grout or concrete added. However, it is likely that fill will be placed between the waste containers before the cell is closed. It is expected that within the 10,000-year time period the containers will fail to a significant extent such that the depleted uranium (DU) oxide will be mixed with the degraded steel containers and surrounding fill material. No credit is given for containment by the steel drums or cylinders. Water will occur as inclusions in the waste and fill pores. Transport through this zone, either downward or upward, via a dissolved phase, is modeled using the solubility conditions and partitioning (K_d) values described below.

The conceptual model for the transport of radionuclides at the Clive Facility allows sufficient meteoric water infiltration into the waste zone such that dissolution of uranium and daughters, fission products and potential transuranic contaminants (along with native soluble minerals) will occur. Depending upon the amount of water available, these radionuclides will either re-precipitate, once the thermodynamic conditions for saturation are reached or remain in solution and be transported to the saturated zone. This water is expected to be oxidizing, with circumneutral to slightly alkaline pH (similar to the upper unconfined aquifer), and an atmospheric partial pressure of carbon dioxide. However, the amount of total dissolved solids (TDS) is expected to be initially lower than the upper aquifer. The composition of this aqueous phase will change as it reaches the unsaturated zone, with some increase in dissolved solids and potentially lower dissolved oxygen and carbon dioxide. This is a fairly simplistic representation geochemically, yet the use of stochastics for the material properties, element solubilities, and sorption parameters provides for variability in this model.

The saturated zone for this PA model includes only the shallow, unconfined aquifer. Transport of radionuclides is expected to be restricted to this aquifer and not migrate to the deep aquifer due to a natural upward gradient at the facility. The *Unsaturated Zone Modeling* and *Saturated Zone Modeling* white papers discuss transport in more detail. The chemical composition of the saturated zone was established by using site-specific groundwater quality measurements. This groundwater is characterized as somewhat alkaline pH likely due to the presence of carbonates, oxidizing, with high levels of dissolved ions of mainly sodium and chlorine. The presence of carbonates can have a significant influence on uranium solubility.

The aqueous chemistry for the unsaturated zone is expected to be relatively oxidizing. However, reducing conditions can exist in some areas of the saturated zone as evidenced by low Eh values and zero dissolved oxygen in some wells at the Clive Facility.

The radionuclides of interest for this PA model include uranium and its daughter products with relatively long half lives, along with fission products and potential contaminant transuranic elements (ORNL 2000, Beals, et al. 2002). The inventory and speciation of the radionuclides in

the waste layer will determine the source term. The total inventory and uranium oxide waste forms are described in a separate white paper (Waste Inventory).

The three major types of chemical reactions that affect water composition include dissolution and precipitation, ion-exchange and sorption, occurring as gas-phase and aqueous reactions. Precipitation and dissolution are the major reactions between the solid and aqueous phases. When the dissolved concentration of a radionuclide exceeds the solubility limit for any possible mineral form, the solid phase will theoretically precipitate and control the maximum concentration. Precipitation and dissolution are governed by thermodynamic and kinetic considerations that include water temperature, redox conditions, concentration (activity) of dissolved constituents, pH, and partial pressure of gases including carbon dioxide. The rate of dissolution (kinetics) is not considered in the PA model. Due to the ratio of dissolution rate to the time frame of interest for contaminant transport (10,000 years), it is assumed that any dissolution is instantaneous within this time frame. Ionic strength is also a critical parameter, especially in waters with high dissolved solids, as activity is influenced by this parameter. The thermodynamic activity of a dissolved species is the product of its actual concentration and activity coefficient. For dilute systems, the activity is close to unity but will deviate substantially at high ionic concentrations. Under equilibrium conditions, the composition of the aqueous phase within each zone will react with the surrounding solid phases to establish the chemistry that will define the radionuclide solubilities discussed in Section 5.0. Sorption at the solid-solution interface is also important in transport modeling and is discussed in Section 4.0.

By definition, isotopes behave identically from a chemical standpoint. As such, both solubility and sorption parameters are treated as equal for each isotope of a single element. For example, uranium-234, -235 and -238, is isotopes, are given equal solubility and sorption constraints, competing for sorption sites and for aqueous solubility.

2.1 Hydrostratigraphic Units

Sediments at the Clive site are divided into four hydrostratigraphic units within the unsaturated and saturated zones (Table 4) . Unit 4 is the uppermost unit, with Unit 1 beginning approximately 12 to 14 m (40 to 45 feet) bgs (Envirocare 2004).

The Unit 4 soils have cation exchange capacity (CEC) values in the range of 10 to 20 meq/100 g (USDA, 2009). These values were used qualitatively in the derivation of sorption parameters described below.

The waste zone will contain two forms of depleted uranium oxide: UO_3 produced from the Savannah River Site (SRS) and other DOE facilities, and what is predominantly U_3O_8 from the gaseous diffusion plants (GDPs). In both cases the waste will be initially stored in steel cylinders and drums that are assumed to be backfilled with Unit 3 soils.

Table 4: Soil and Mineralogy within the Four Hydrostratigraphic Units

Unit Number	Soil and Mineral Type	Unit Description
4	Fine-grained silty clay, clay silt. Carbonates, quartz, feldspars, clay minerals (kaolinite, smectite, and illite/mica) trace gypsum.	From 6 to16.5 ft thick with an average thickness of 10 ft. Unsaturated.
3	Silty sand, occasional silty to sandy clay lenses.	10 to 25 ft thick with an average of thickness of 15 ft. Largely unsaturated, with lower portion saturated in western part of site. The unconfined water-bearing zone in Unit 3 and the upper part of Unit 2 has been designated as the shallow aquifer.
2	Silty clay.	2.5 to 25 ft thick with an average of thickness of 15 ft. Unit 2 is saturated below the Clive Facility.
1	Silty sand with occasional silty clay. Confined aquifer.	Begins at a depth of approximately 45 ft bgs. The thickness of Unit 1 is unknown.

Geochemical conditions and water movement have not been extensively studied in the unsaturated zone at the Clive Facility. As described above, the upper level pore water within the unsaturated zones is expected to contain lower TDS than is found within the saturated zone, though these levels could increase with depth in the unsaturated zone. The relative anion and cation constituents of this pore water are likely very similar to those in the saturated zone. This is expected as the ions in the saturated zone appear to be largely due to the presence of evaporites and alluvium from the valley and former Lake Bonneville. Dissolved oxygen and carbon dioxide are expected to be largely in equilibrium with atmospheric conditions, at least in the upper profile including the DU waste zone. For derivation of the solubility and sorption parameters a pH range of 6.5-8.5, pCO_2 range of slightly above atmospheric to slightly below atmospheric, and geochemical make up similar to the saturated zone but lower TDS was used.

2.2 Shallow Unconfined Aquifer

The geochemistry of the shallow, unconfined aquifer consists of very high levels of dissolved solutes as outlined above. The groundwater table occurs near the bottom of Unit 3, with the shallow aquifer mainly within Unit 2. For the purposes of the PA model, the water table is assumed to be coincident with this stratigraphic interface. This unconfined aquifer contains very high dissolved solids, with TDS values ranging from 20 to 70 parts per thousand and specific gravity from 1.02 to 1.06 g/mL (Envirocare 2004, and recent site specific groundwater data acquired by Energy*Solutions*). The shallow aquifer consists of a brine with sodium and chloride comprising approximately 90 percent of the ions (see Tables 5 and 6) This brine is likely a result of the dissolution from the Lake Bonneville evaporite sediments. Prior geochemical modeling (Bingham Environmental, 1991) indicates the aquifer is supersaturated with calcite and dolomite. Geochemical modeling for this PA also indicats these minerals to be at saturated conditions.

The deep confined aquifer, in Unit 1, also has high values of TDS of up to 20 parts per thousand, but the average is well below the average of the shallow aquifer. The higher salinity of the shallow aquifer is thought to be due to concentration of salts through evapotranspiration (ET) and/or localized dissolution of evaporite deposits in the unsaturated zone.

The Clive Facility has a large number of monitoring wells with completion zones in this aquifer and monitoring data are currently collected from these wells on at least an annual basis. Prior to geochemical modeling performed for this PA, geochemical data from seven of these monitoring wells were summarized and are provided in Tables 5 and 6 below. These wells are in close proximity to the DU waste cell. All wells are completed within the upper unconfined aquifer, and are located surrounding the cell in all four horizontal directions. Data ranges and averages were taken from from quarterly, and in some cases monthly, monitoring reports. At least two years of data were used, and in most cases data goes back to at least the year 2000.

Table 5: Geochemical parameter ranges from Groundwater Wells at Clive, Utah

Well ID	pH	TDS (mg/L)	Eh (mV)	DO (mg/L)	Bicarbonate (mg/L)	Temp (°C)
GW-16R	6.65 to 7.63	26,000 to 46,400	-21 to 489	0.2 to 3	300 to 350	11.40 to 13.60
GW-25	6.62 to 7.62	40,000 to 55,000	-34 to 500	0 to 6.7	160 to 330	10.90 to 15.50
GW-19A	7.16 to 7.25	69,000 to 75,000	61 to 212	1.6 to 2.51	120 to 140	13.40 to 14.29
GW-57	6.64 to 7.69	35,000 to 52,700	-43.70 to 480	0.19 to 5.37	102 to 140	10.80 to 15.10
GW-100	6.95 to 7.63	31,000 to 42,000	30.8 to 209	0.4 to 4.0	120 to 140	12.13 to 14.00
GW-110	7.24 to 7.57	29,000 to 38,000	-18 to 168	0.14 to 7.52	160 to 204	12.60 to 13.59
GW-125	7.09 to 7.52	28,000 to 40,000	48 to 233	0.76 to 4.58	160 to 180	12.60 to 13.84
Max Range	6.62 to 7.69	26,000 to 75,000	-43.70 to 500	0 to 7.52	102 to 350	10.8 to 15.5

Table 6: Ion Concentrations from GW Wells Surrounding the Waste Cell

GW Well	Br^- (mg/L)	F^- (mg/L)	Cl^- (mg/L)	NO_3^- (mg/L)	SO_4^{2-} (mg/L)	Ca^{2+} (mg/L)	Mg^{2+} (mg/L)	K^+ (mg/L)	Na^+ (mg/L)
GW-16R	22	3.8	22,914	1.4	1,769	354	486	476	14,263
GW-25	23	8.8	25,783	1.1	4,420	527	853	565	16,465
GW-19A	0	0.0	37,800	0.0	0	1,028	1,580	616	23,800
GW-57	18	8.5	23,110	1.9	4,652	707	844	530	14,398
GW-100	26	1.8	20,254	1.1	2,911	496	683	457	12,993
GW-110	17	1.5	17,989	2.1	2,226	322	469	432	11,400
GW-125	16	0.9	20,813		2,494	427	637	488	12,813
Average	20	4.2	24,094	1.5	3,079	552	793	509	15,162

The groundwater is considered a brine, with TDS values as high as 72,000 mg/L. The redox conditions are fairly oxidizing with an average Eh of 125 mV. Sodium and chloride are clearly the dominant ions with slightly alkaline pH. Excellent charge balance is obtained using these data, indicating all major ions are being accounted for. Groundwater temperatures range from 11.5 to 14.5 °C. Using the data from the average of all wells shown in Table 5, the stoichiometric ionic strength is calculated at 0.73 M (mol/L).

3.0 Method for Estimating Distributions for Solubility and Partitioning Parameters

The process for developing probability distributions for the geochemical parameters utilized the following basic scheme:

1. Perform a literature search for parameter values.
2. Based on site characteristics, screen the literature studies to those that could potentially apply to the Clive site.
3. Weight the remaining literature values based on expert judgment.
4. Develop a distribution based on the weighting.

In nearly every case, once the site specific data and the general literature were screened to retain studies relevant to the Clive site. Any value within the range of those studies was deemed to be "equally viable," given the uncertainty associated with various soil and water characteristics for the site. “Equally viable” indicates that the probability of one order of magnitude range is equally likely as any other order of magnitude range within the overall viable range. Therefore, the default probability distribution is a log-uniform distribution. To establish a range for the log-uniform distribution, the range of values from the relevant literature was considered. To ensure that the distribution represented the minimum and maximum literature values, these values were treated as the 5th ($Q_{0.05}$) and 95th ($Q_{0.95}$) percentiles of the distribution, respectively, effectively extending the support of the distribution a small amount beyond the range of literature values. That is, the geometric mean of the distribution is set to the geometric mean of the quantiles:

$$GM = \exp\left(\frac{\ln Q_{0.05} + \ln Q_{0.95}}{2}\right) \tag{1}$$

To calculate the range of the distribution in log-space, the range of the log-percentiles is extended from 90% to 100%:

$$R_l = \frac{\ln Q_{0.95} - \ln Q_{0.05}}{0.9} \tag{2}$$

To get the endpoints of the log-uniform distribution, the half-range is subtracted and added to the geometric mean:

$$Min = \exp\left(\ln GM - \frac{R_l}{2}\right) \qquad Max = \exp\left(\ln GM + \frac{R_l}{2}\right) \tag{3}$$

For example, the literature values for K_d values of Ac in silt ranged from 20 mL/g to 1500 mL/g. Treating these values as 5th and 95th percentiles gives a geometric mean of GM=173, and a log-range of R_l=4.80, leading to a log-uniform distribution from 15.7 mL/g to 1910 mL/g. This distribution is illustrated in Figure 1.

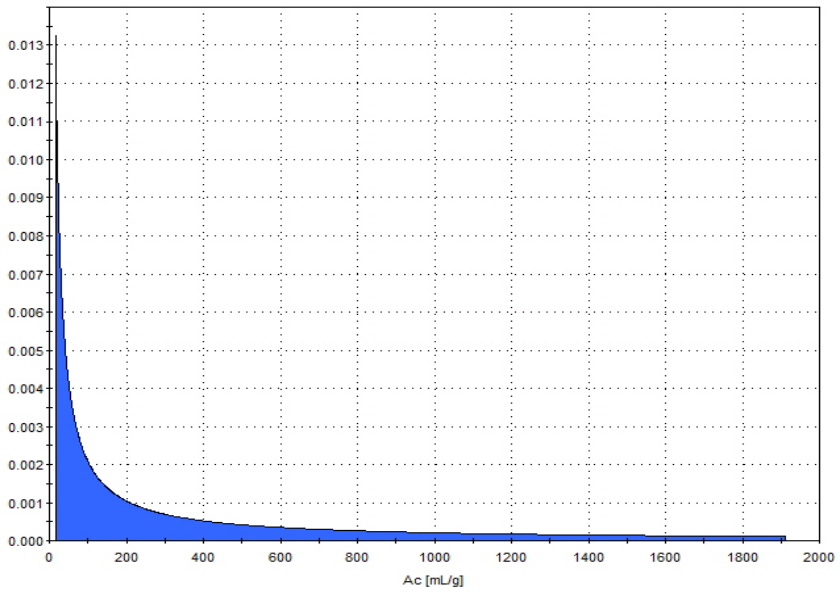

Figure 1: Example of probability distribution function for log-uniform distribution. Value for K_d of Ac in silt with a range of values from 15.7 to 1,910 mL/g.

The exceptions to the log-uniform fit were the K_d values for Tc and I. For these parameters, values of 0 are possible, yet a log-uniform distribution cannot represent that possibility naturally. For these parameters, it was decided to fit a distribution that would give an approximate 25% chance of a 0 value and a median near the Clive-specific data (Adrian Brown Consultants, Response to UDEQ K_d Interrogatories, 1997). The median values used were 0.11 mL/g for Tc and 0.46 mL/g for I. For Tc, a maximum literature value of 0.33 was considered as a 95th percentile. These distributions were fitted using the standard approach of fitting distributions based on quantiles that is described in the *Fitting Probability Distributions* white paper. A normal distribution fit these percentiles well, when values less than 0 were treated as 0. The I distribution was then scaled to match the shape of the Tc distribution. Figure 2 illustrates how the distribution for I is represented in GoldSim. Values less than zero are set equal to zero.

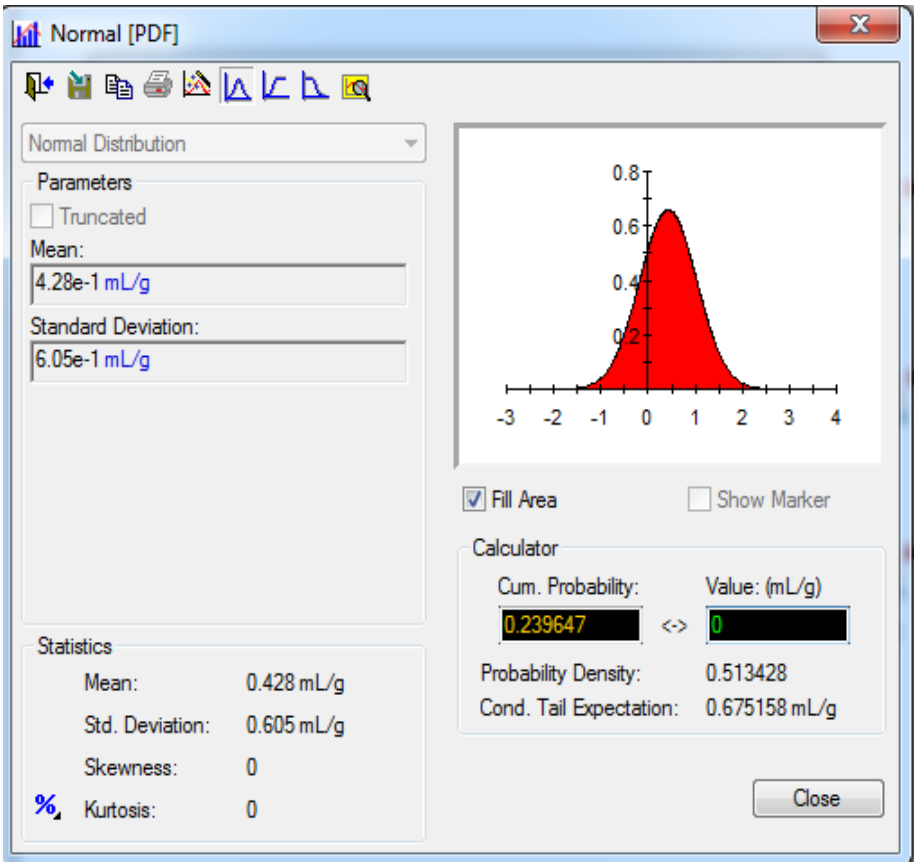

Figure 2: Distribution of K_d values for I in sand. Values less than 0 are set equal to zero.

4.0 Solid/Water Partition Coefficients (K_d)

The transport of dissolved radionuclides can be limited by sorption onto the solid phase of associated minerals and soils within each of the zones considered in this PA model. The transport of uranium is limited by both solubility and the sorption of radionuclides in groundwater. Sorption consists of several physicochemical processes including ion exchange, adsorption, and chemisorption.

Sorption is represented in the PA model as a K_d value. While the geochemistry of contaminant transport is complex, a representative and standard approach was taken for the purposes of the PA. Distribution parameters for radionuclide solubilities are derived in Section 5.0 below. The current section focuses on the description of sorption and the derivation of parameters for K_d distributions.

Solid/water partition coefficients, or K_ds, are based on a simple equilibrium sorption model, and are a simplification of the wide range of geochemical processes discussed above. Despite the simplicity of the K_d models, they are commonly used in performance assessments because of their ease of implementation in transport codes. Site-specific monitoring tests were used in the process to derive distributions when this information was available. The K_d model assumes that a given constituent dissolved in the water (e.g., uranium) has some propensity to sorb to the solid

phase of a porous medium, while maintaining an aqueous phase. The definition of the solid/water distribution coefficient, with units of mL/g is:

$$K_d = \frac{mass\ of\ constituent\ sorbed\ on\ a\ unit\ mass\ of\ solid\ (g/g)}{mass\ of\ constituent\ within\ a\ unit\ volume\ of\ water\ (g/mL)}. \quad (4)$$

The sorption is assumed to be instantaneously reversible and independent of concentration. That is, no dynamics are accounted for, and the ratio is always simply linear—a constituent's concentration in water is always the same ratio with respect to its sorbed concentration onto the solid, and sorption is instantaneous. This is the commonly used linear isotherm assumption.

Applying the K_d model outside of the range of concentrations used to obtain the values can lead to over- or under-estimation of sorption. To account for ranges of geochemical conditions and the potential deviation from the assumptions underlying the linear sorption model which may result in variation in K_d values, this PA model includes parameter distributions (stochastics) for the sorption values. Nominal K_d values were selected using both site-specific monitoring tests (when available) and the general scientific literature. Data were taken from literature that most closely matched the geochemical conditions at the site, including TDS range, pH and alkaline conditions, temperature, and soil properties (CEC, clay types) to the extent possible. K_d values have been chosen for five individual materials: silt, sand, clay, UO_3 waste and U_3O_8 waste. In all natrual zones the silt, sand, and clay are mixed to some extent. After including the uranium oxide material amounts into the GoldSim model, it became apparent that they form such a small fraction of the profile relative to the other materials that sorption processes within the waste could be neglected, so these materials are assigned values for Unit 3, represented using the K_ds for sand. It is also recognized that essentially no information on sorption to uranium oxides (as the waste inventory) is available in the published literature.

The process for selecting K_d values for the elements entailed an extensive literature search to identify sorption values used in other transport models, and in particular from locations that have similar solid phase properties and geochemical conditions. The sorption values used by Whetstone Associates (2009), Bingham Environmental (1995, 1996), Scism (2006), Sheppard and Thibault (1990), the Yucca Mountain Site Characterization Project (LANL 1997), DOE (2003), and Envirocare (2000) were evaluated. In addition, the EPA three volume series *Understanding Variation In Partition Coefficient, K_d, Values* (EPA, 1999b, 1999c, 2004) was referenced extensively in this process. The reader is advised to consult that EPA series as it was used for the derivation of many K_d values and much of that information is not repeated here.

Work by Serne (2007) was also reviewed during this investigation. Serne focused on surface agricultural soils and Columbia River bank near-surface sediment associated with the Hanford site. Serne specifically states that the values are not to be used in water-borne scenarios except when the modeling is used to estimate accumulation of contaminants by future surface soils from irrigation practices, and that they are not appropriate for unsaturated zone transport to the groundwater. Nevertheless, the results are important from a semi-quantitative perspective. Of note is that the Hanford soils are slightly acidic, with organic content of 0.5 to 1.5% organic carbon somewhat different from the Clive location. Serne (2007) also reviews a number of studies that are also somewhat applicable to the Clive facility and the range of K_d values provided are useful as a first comparison. As such, a number of values compiled by Serne are provided

below. Serne also refers to work by Last et al. (2004) and Krupka et al. (2004) for systems that include migration to groundwater, as envisioned in this PA model. Values described by these authors are discussed below for individual species.

4.1 Partitioning by Element

This section provides a description of the derivation of the partition coefficient for each element used in the transport model. Data were derived first from site-specific monitoring studies where this information was available. Second, the data was taken from literature searches, with values chosen from locations with similar geochemistry and soil/mineral conditions as the Clive facility as described in Section 3.0 above.

4.1.1 Actinium

Minimal K_d information was found for this element. Values from Sheppard and Thibault (1990) are as follows: 450 mL/g (sand), 1,500 mL/g (loam, here used to represent silt), 2,400 mL/g (clay), 5,400 mL/g (organic). In order to derive values for this PA for each of the three materials (sand, silt, and clay) a range similar to those from Sheppard and Thibault (1990) was incorporated with adjustments made for each of the three materials.

4.1.2 Americium

Americium will likely occur predominantly as carbonate complex cation Am (III) in the pH range at the Clive facility, though some speciation as an anion is also possible. This rare earth element will have a large sorption coefficient. The largest source of K_d values for this element was found in Serne (2007) with discussion on a number of studies by other researchers. In the Hanford system, americium adsorbs fairly strongly to soils and sediments. Serne chose a best value of 500 mL/g with a recommended range of 60 mL/g to 5,000 mL/g for the non-groundwater scenarios. This range is consistent with studies by others using a matrix within a groundwater system, with the exception of those done on <1 mm size particles by Tanaka and Muraoka found in Serne. Krupka et al. (2004) chose a best value of 300 mL/g. Sanchez (in EPA 2004) found no apparent effect of salinity on K_d values and no additional information was obtained during this research. For the transport model a range from 43 mL/g to 1,140 mL/g was chosen as shown in Table 1.

4.1.3 Cesium

Cesium sorption is strong in most soils (EPA 1999c). Sorption commonly occurs as the Cs^+ cation via cation exchange. In calcareous soils with mica minerals, cesium was essentially completely absorbed above pH 4.0. However, high salt solution does decrease sorption. At Idaho National Laboratory (INL) (Hull, 2008), a release of cesium in 1972 has been found to be essentially immobile. This effect is thought to largely be a function of cation exchange with clays in the exchange on both the planar and frayed edge sites of clays. The binding on the frayed edge is considered stronger, resulting in a high K_d.

Serne (2007) chose a recommended value of 2,000 mL/g for the low ionic strength, circum-neutral waters in the near surface sediments at Hanford. This was consistent with the value from Krupka et al. (2004). Serne (2007) recommended a range of 200 to 5,000 mL/g for the non water-borne (e.g., unsaturated, agriculture zone) scenarios at that location and a log normal probability distribution to describe the variation.

Because cesium sorbs by an ion exchange process, sorption can be depressed by high TDS of the groundwater. Vandergraaf et al. (1993) has performed sorption experiments with Cs examining the relationship between Cs concentrations and TDS and were able to fit a quadratic equation to the data. For this PA model, cesium K_d values were selected largely from the look up tables in EPA (1999c), but were adjusted lower due to the high TDS in the saturated zone. Also note that the CEC values of 10-20 meq/100 g at the Clive facility are indicative of some but not a significant presence of clay minerals within the saturated zone. These CEC values apply to the materials within the saturated zone. The liner especially, and some native materials within the unsaturated zone do contain clay minerals.

4.1.4 Iodine

Iodine is expected to largely exist as the anion, I^- or IO_3^-, though volatile organic forms are also possible. Because of the negative charge, sorption will likely not be strong, due to the typical negative charge of the soils at the Clive site under neutral to alkaline conditions. This is especially true in the saturated zone where high concentrations of chloride ions will compete for any available sites to sorb. Sorption appears to increase with increasing organic matter for iodine (EPA 2004), which may be largely due to microbial processes. Studies of iodine sorption under oxic conditions on Hanford Site sediments (Kaplan 1998b from EPA 2004) indicated very low K_d values. Serne (2007) recommended a value of 3 mL/g with a range of 0 to 15 mL/g. Last et al. (2004) recommended a range of 0 to 2 mL/g. The very low concentrations of organic compounds found in the sediments at the Clive facility would support the use of of a low range for the K_d. This range is largely derived from *Summary of Results, Radionuclide Kd Tests* (Bingham Environmental, Inc. August 3, 1995) where a value of 0.7 mL/g was derived for the Clive facility using samples from Unit 3 samples. The grain size distributions from these Unit 3 samples indicated the material was largely sand. Clive site groundwater was used for the sorption studies. This K_d value was then changed in Adrian Brown Consultants (1997), with a recommended value of 0.46 mL/g.

4.1.5 Lead

Lead speciation is largely anticipated to be in the form of dissolved $PbCO_3$ at least in the saturated zone. Lead may be largely in the hydroxide ion form in waters of lower carbonate concentration, though this is not anticipated to any significant extent. As $PbCO_3$ is expected to be the dominant form above pH 7, sorption will not be especially significant. Lead has such low solubility, especially in presence of phosphate and chloride, that solubility often can control movement. Table 1 in Appendix D of the Bingham Environmental (1991) shows an EPA Arid Site value of 220 mL/g for lead, with an applicable range of 1 to 10,000 mL/g. Serne (2007) recommended a value of 400 mL/g for the non-groundwater scenarios at Hanford, within the range of Sheppard and Thibault (1990). Based on the Pauling ionic radii of Sr^{2+} and Pb^{2+} (1.12 and 1.19 Å, respectively), the sorption of lead is expected to be similar to strontium and also to be somewhat suppressed by high ionic strength solutions. For this model, the lead K_d values were chosen in a range from 2 to 200 mL/g with lower values for the sand material. This range was based upon the expected similarity with strontium and cesium.

4.1.6 Neptunium

Neptunium will most probably exist in the Np(V) form with some as Np(IV), principally as an uncharged hydroxide, where reducing conditions exist. In the Np(V) form as NpO_2^+, this species can sorb to iron oxides and clays but not to a significant extent to common minerals. Np(V) has a pH dependence, with negligible sorption at values less than pH 5. This ion can also form carbonate complexes above pH 8.5 or under high carbonate concentration conditions (Serne, 2007).

The transient, mildly reducing conditions that can exist at Clive and the presence of carbonates may lead to the formation of Np(VI) carbonate complexes above pH 7. However, there are a limited number of K_d studies for this element. Heberling et al. (2008) studied Np(V) adsorption to calcite at four pH values at constant ionic strength. The K_d was found to vary with both pH and concentration with a value range of 0.0090 ± 0.004 mL/g to 0.0610 ± 0.002 mL/g. Wooyong et al. (2009) measured K_d values from sediment collected at the Hanford site and found a range of 0.6 to 4.8 mL/g. The EPA (2004) suggests a minimum K_d of 0.2 mL/g. Serne (2007) chose a range of 2 to 50 mL/g for the non-groundwater scenario at Hanford with a best value of 25 mL/g. This range is approximately two times higher than the range recommended by Last et al. (2004) and Krupka et al. (2004) for groundwater systems.

Vandergraaf et al. (1993) reported values ranging from 0.5 to 68 mL/g. In the presence of Fe(II), reduction of Np(V) has been observed (Cui and Eriksen 1996, Nakata et al. 2002). Kumata et al. (1993) observed retention of Np in columns of crushed granite from solutions with low Eh values finding a relationship between retention and flow rate that suggested that the kinetics of the redox process were relatively slow. Values from Sheppard and Thibault (1990) are as follows: sand: 5 mL/g, loam (silt): 25 mL/g, clay: 55 mL/g, and organic: 1200 mL/g. For the Clive facility, a similar range is recommended, though this range is reduced for the sand matrix.

4.1.7 Plutonium

Plutonium can be found in a number of valence states under the conditions at Clive. The most likely states are as Pu(V) and Pu(VI) both as cations and complexed with hydroxide and carbonate. Plutonium sorption is known to occur on many common minerals, clays, and oxides. Some studies indicate the sorption is non-reversible. It is noted that experiments by Linsalata and Cohen (1980) did not find a reduction in K_d with high ionic strength (salinity increased to 24%). Serne (2007) chose a range of 200 to 5,000 mL/g and a best value of 600 mL/g for the Hanford non-groundwater scenario. Last et al. (2004) and Krupka et al. (2004) recommended values of 600 mL/g and 150 mL/g, respectively, with a high range value of 2000 mL/g. Data by Glover et al. (1976) found in the EPA (EPA 1999c) series may be of particular relevance to the Clive location. These data, along with K_d values collected on basalt sediments were used to develop the EPA look up table. For the Clive location, K_d values corresponding to lower clay content especially within the saturated zone, and medium to highly soluble carbonate throughout are most applicable. These K_d values range from 80 mL/g to 520 mL/g. These values appear to be slightly low compared to other studies. For the Clive facility, a slightly higher range was chosen, with the upper limit increased because of the clay matrix.

4.1.8 Protactinium

Little information was identified that provided sorption values for this element. Serne (2007) discusses the use of neptunium as an analog for protactinium. In sea water environments, where particles of very high surface area are encountered, K_d values of greater than 10,000 mL/g have been measured. Serne recommended a most probable K_d value of 400 mL/g for protactinium, similar the values used for bismuth and polonium. Serne's recommended range is 150 to 10,000 mL/g. Again, this is for a non-groundwater scenario, different from that at the Clive facility. Sheppard and Thibault (1990) categorize K_d values by sand, clay, loam, and organic with values ranging from 550 to 2,700, sand-clay respectively. These values from Sheppard and Thibault (1990) formed the basis for the distribution used for this PA model. These values were reduced to account for the high TDS in the saturated zone.

4.1.9 Radium

Based on the compilation by Serne (2007), radium is a fairly strongly sorbing species in low ionic solutions at circumneutral pH. Radium will co-precipitate with calcium sulfate in high ionic strength waters and may also do so in barite. Sheppard and Thibault (1990) recommended the following values: sand: 500 mL/g, loam (silt): 36,000 mL/g clay: 9,100 mL/g and organic: 2,400 mL/g. Serne recommended a best value of 200 mL/g and a range of 5 mL/g to 500 mL/g. This range was lower than Sheppard and Thibault (1990) based on studies that indicated cation exchange is a dominant sequestration mechanism and the low CEC of the Hanford soils. Krupka et al. (2004) recommended a K_d of 14 mL/g with a range of 5 mL/g to 200 mL/g. A range based on all of the above data was chosen for each material class.

4.1.10 Strontium

Strontium has little tendency to form complexes with inorganic ligands (EPA 1999c). Reversible cation exchange is expected to be the most important mechanism impacting sorption in the pH conditions at the Clive facility. This behavior is similar to that of cesium though sorption is generally not as strong. A point worth noting in this context is that natural Sr in the groundwater will dilute any radioactive Sr isotopically. The high sulfate concentration in the groundwater at Clive (4,420 mg/L average for GW-25) may lead to precipitation of $SrSO_4$ or co-precipitation with $CaSO_4$.

A study at the INL (Hull, 2008) indicated strontium sorption was dependent upon other cations, primarily Ca^{2+}, Mg^{2+}, and Na^{+} with K_d decreasing with increasing concentrations of these ions. The K_d value decreased from 85 mL/g to 4.7 mL/g. This effect was considered a cation exchange phenomenon, where the divalent strontium cation competes with calcium. This effect is similar to that observed by Patterson and Spoel (1981, as referenced in Hull) at the Chalk River Nuclear Laboratories. The EPA look up table (EPA 1999) was developed using pH and CEC values. Using this table, along with the known applicable parameter ranges for Clive of relatively low abundance of clay minerals within the saturated zone but somewhat higher within the unsaturated zone, a CEC of 10 to 20 meq/100 g, and pH range of 6.6 to 8.5, the listed K_d values are within a range from 15 mL/g to approximately 200 mL/g. Note, a higher clay content will act to increase these values. However, under very high TDS conditions as in the saturated zone, lower sorption is expected and is reflected in the ranges chosen for this transport model.

4.1.11 Technetium

In oxic conditions technetium will exist as the TcO_4^- metal oxyanion, which is essentially non-adsorptive (EPA 2004). EPA did not develop a lookup table for technetium but cite data indicating K_d ranges from slightly negative to generally less than 1 mL/g. Under chemically reducing conditions, either in the bulk groundwater or locally on the surface of Fe(II) containing minerals (biotite, magnetite), or in the presence of microbes, reduction of Tc(VII) to Tc(IV) can occur and the reduced form of Tc will either sorb strongly or will precipitate (Vandergraaf et al. 1984, Cui and Eriksen 1996). This process will fix technetium to geological material. However, if redox conditions change, there is the possibility that Tc could be resolubilized and transported through the geosphere as an anion without retardation. Sheppard and Thibault (1990) indicate very low K_d values for this species ranging from 0.1 to 1. This low propensity for the TcO_4^- ion to sorb, has been noted by many researchers. Wooyong et al. (2009) measured K_d values from sediment collected at the Hanford site and found a range of 0.08 to 0.4 mL/g. For this model, the technetium sorption distributions were chosen based on the information above and the derivation that is provided in Adrian Brown Associates (1997). These data are derived from sorption on to Unit 3 sand and site-specific groundwater under oxidizing conditions.

4.1.12 Thorium

The solubility of thorium is low (circa 10^{-9} molar), which has made sorption measurements difficult. This element occurs only in the +4 oxidation state in natural waters. Thorium can form many different species including carbonate complexes. The Canadian high level waste program uses a K_d value of 800 mL/g. Values for thorium were chosen largely based upon the information in the EPA literature (1999b, 1999c, 2004) though the values were reduced to some extent to account for the high TDS based upon recommendations from Vandergraaf (personal communication 2010).

4.1.13 Uranium

The K_d for uranium is important in this PA due to the large mass of this element in the inventory relative to any other radionuclide. The transport of uranium is expected to be mainly a factor of the solubility within the waste zone (near source), and potentially within the saturated zone with time. However, retardation of the uranium via sorption will be important in the clay liner beneath the waste zone and within both the unsaturated and saturated zones.

Uranium (VI) sorption can be controlled by cation exchange and adsorption processes, especially in low ionic strength systems (EPA 1999c). As the ionic strength increases, other cations will displace the uranyl $(UO_2)^{2+}$ ion. Uranium sorption on iron oxide minerals and smectite clays is extensive except in the presence of carbonate where this is reduced (EPA 1999c). Aqueous pH values also influence uranium sorption, affecting the speciation as described above as well as influencing the number of exchange sites on variably charged surfaces. Dissolved carbonate concentrations and pH appear to be the most important factors influencing adsorption of U(VI). However, under the slightly alkaline and carbonate dominated conditions expected in the saturated zone, uranium will likely occur in several forms including a uranyl-carbonate or oxy-carbonate anion or a non-charged uranyl hydoxide. The speciation results from the solubility modeling are described in Section 5.0.

In the range of pH 7 to 9, there were 4 to 5 orders of magnitude variation in K_d values noted in the data collected by the EPA (1999b, 1999c, 2004). For the pH range of 7 to 8, which is most likely at the Clive site, the EPA listed a minimum K_d of 0.4 mL/g and a maximum of 630,000 mL/g. The minimum value was based on values calculated for quartz with the maximum value based on data calculated for ferrihydrite and kaolinite. These very high K_d values are considered potentially biased by one order of magnitude. Values from Sheppard and Thibault (1990) are as follows: sand: 35 mL/g, loam (slit): 15 mL/g clay: 1,600 mL/g and organic: 410 mL/g.

Last et al. (2004) and Krupka et al. (2004) recommend ranges for uranium of 0.2 mL/g to 4 mL/g and 0.1 mL/g to 80 mL/g respectively. Wooyong et al. (2009) measured K_d values from sediment collected at the Hanford site and found a range of 0.2 mL/g to 1.5 mL/g. In most cases these authors found that higher K_d values were associated with the less-than-2-mm particle size fraction as one would expect based purely on surface area. However in some of their sediments this relationship was reversed. They attributed this to highly reactive surfaces on gravel at their location.

Site-specific sorption data for uranium are also available from the Adrian Brown and Associates (1997) report, performed by Barringer Laboratories. Two data points at a single uranium concentration (at day 7 and 16) were obtained with tests performed at two higher concentrations resulting in the precipitation of the uranium. The average K_d value in this study was 6.0 mL/g.

The K_d values chosen for this PA were based on both the site-specific data and literature information. The U(VI) species in the aqueous environment will not have particularly strong sorption tendencies. The uranyl ion is mobile in the high ionic-strength solutions and this mobility is also found with waters containing high carbonates. This indicates uranium sorption is more likely to be found at the lower ranges of those cited by the EPA and Sheppard and Thibault (1990).

5.0 Element and Species Solubility

Modeling transport of radionuclides of interest at the Clive Disposal Facility area requires an understanding of the expected concentration of these species in the dissolved phase starting in the DU oxide waste zone. Once dissolved from the waste, the radionuclides have the potential for transport vertically down into the unsaturated zone below and then into the shallow aquifer. Diffusion both upward and downward in the aqueous phase is also possible. At first, leaching is likely to be solubility-limited with respect to uranium, and the leachate will migrate away from the source with uranium concentration at the solubility limit. The other radionuclides are unlikely to be at a solubility limit but establishing boundaries is necessary for the modeling. The concentrations of radionuclides limited by sorption will be less in the dissolved phase farther from the source.

The importance of solubilities of the individual species in this PA model varies. Uranium is expected to be solubility limited at the source, but most other elements in the inventory likely will not be so limited. Therefore, the majority of effort for solubility distribution development was focused on uranium. Solubilities for the other species were drawn from literature reviews of studies conducted at locations with similar water chemistry.

At the Clive site, four major physical zones or systems are encountered and can influence the aqueous movement of radionuclides. These zones include the waste cell, the clay liner beneath the waste zone, the unsaturated zone, and the saturated zone (shallow aquifer). As described in the *Unsaturated Zone Modeling* and *Saturated Zone Modeling* white papers, the waste zone and unsaturated zone are considered very similar in terms of the expected geochemistry of the aqueous phase. Due to the small ratio of DU waste to native materials they are also relatively similar in mineral composition and both are modeled using physical and chemical properties of Unit 3 (represented chemically as a sand). The clay liner will mainly influence retardation via sorption, in addition to decreasing water infiltration. The important saturated zone geochemical conditions, including aqueous and solid state chemistry, are those that influence the precipitation and dissolution of the species of interest in this PA. Differences between the saturated and unsaturated zones are mainly associated with ionic strength and redox conditions with pH expected to be fairly similar in both saturated and unsaturated zones. The interstitial water in the waste and unsaturated zones is considered to be highly oxidizing, more so than the aquifer, and with neutral to slightly alkaline pH. However, the differences in ionic strength and oxidizing conditions between the unsaturated zone and saturated zone did not have a significant effect on the calculated solubilities. Data from the saturated zone (Tables 5 and 6) indicate it is susceptible to localized, transient, anoxic conditions with zero to slightly negative Eh values. These areas will have a large influence on uranium solubilities since U(IV) is much less soluble (circa 10^{-8} M) than U(VI). Other species of interest to this PA model will also have reduced solubilities in anoxic regions.

Microbial influences on the transport of the radionuclides are not expected to be important. Little or no organic materials (cellulosics, plastic) are expected in the waste. Therefore, no microbial influence is included in this model, nor are organic materials such as humic and fulvic acids expected to be present in any significant amounts. However, radiolytic effects could cause transient changes in redox conditions or generate carboxylic acids as described below.

Anoxic corrosion of the steels and iron-based alloys used to construct the DU cylinders and drums can affect the release of actinides. Corrosion would be expected to reduce the oxidation state of some actinides. The most significant effect would be to decrease the mobility of uranium, technetium, and plutonium. Uranium transport is again strongly influenced by redox conditions. However, it is highly uncertain whether anoxic corrosion would take place since this would require consumption of oxygen. A more conservative approach was taken, where largely oxidizing conditions are assumed to remain to some extent within the unsaturated zone.

The potential for colloidal transport of actinides at the Clive facility is not incorporated into the PA model. Actinide intrinsic colloids are formed by condensation of hydrolyzed actinide ions and consist of actinide cations linked by anions. The Pu(IV) instrinsic colloid is a well studied example (Johnson and Toth 1978). However, plutonium, and Pu (IV) in particular, is apparently unique in its propensity to form an intrinsic colloid. Due to the expected very low mass of plutonium from the DU, this colloidal process has not been included in the source term. There are approaches for including colloidal transport into an effective retardation factor (Contardi et al. 2001). However this approach requires colloid concentration data which are not available. While colloid transport is unlikely for the uranium isotopes, there is greater potential for colloid transport for americium and plutonium species. Geckeit et al. (2008) have developed a scenario

for colloid transport of trivalent actinides. Their modeling supports the theory that colloidal actinide transport is driven by radionuclide-colloid interaction, agglomeration, filtration, and sorption of colloids to mineral surfaces in the bulk phase. Polyvalent actinides appear to be the most prone to colloid transport but the relevance of colloid transport in general is controversial. Retention of colloids is favored at high ionic strength, low pH and in impermeable rock. The high ionic strength conditions in the saturated zone at Clive are counter to conditions considered favorable for colloid transport.

In many cases the solubility of radionuclide species used in the transport model was based to some extent on the data provided in the proposed Yucca Mountain Project (LANL 1997) and the Nevada National Security Site (NNSS, formerly the Nevada Test Site) (Sandia 2001) modeling. These data provide a starting basis for the central tendency value used in the solubility distributions for several of the radionuclide species. The Yucca Mountain, NNSS, and the Clive, Utah locations have many common geochemical conditions such that the solubility for the minor constituents (those other than uranium) can be modeled similarly. There are noted differences between the three sites but these references provide a good basis for selecting solubility since much of the chemistry is similar with respect to redox, carbonate chemistry, low organic matter content, and pH.

The Yucca Mountain unsaturated zone water is characterized as oxidizing (Eh estimated at 400 to 600 mV) and the partial pressure of carbon dioxide will be variable with depth resulting in a pH of 7 to 8. The saturated zone water at Yucca Mountain is characterized as having a pH also in the range of 7 to 8 and oxidizing to reducing conditions depending upon whether the waters have access to atmospheric oxygen or to reducing agents (Kerrisk, 1987). With the exception of the very high ionic strength of the shallow aquifer, this is similar to the conditions at the Clive site. The waste zone at the Clive facility will likely have redox conditions very similar to those in the unsaturated zone at Yucca Mountain. The high ionic strength brine found in the shallow aquifer at Clive can increase the solubilities of some actinides (DOE 2009) and this influence was incorporated into the decision making for solubility selection and modeling. However, the three locations do also have very different mineralogy and soil properties that can influence the ion-exchange and sorption constraints in this model.

At the NNSS, data from Frenchman Flat (Sandia 2001) indicate that elemental composition of minerals and total oxide concentrations of the sediments remain fairly constant with depth. The alluvium has a composition of approximately 65% SiO_2 and 13% Al_2O_3. Very little clay is present. Some accumulation of calcium carbonate, in certain horizons are found as coatings on clasts and with pendants of pebbles and sand beneath, indicating repeated periods of surface stability in the Quaternary. Water does not move downward under current climate conditions in the unsaturated zone and this is expected to continue within the next 10,000 years. The unsaturated zone moisture content is low, roughly 5 to 10% to 40 meters with a pH range of 7 to 9 and a high Eh. The alluvium is dominated by quartz, feldspar, cristobalite, with calcite, gypsum, and minor amounts of clays and zeolites.

5.1 Solubility by element

5.1.1 Actinium

The only stable oxidation form of actinium is the +3 ion (Morss et al., 1977). Actinium forms hydrolysis complexes with the $Ac(OH)_3$ species and the solubility is reported at 0.74 mg/L (2.6 x 10^{-6} M).

At Yucca Mountain the actinium solubility used in the Total System Performance Assessment (TSPA) model ranges from 10^{-10} M to 10^{-6} M (LANL 1997). For this PA model, a similar range was used, though the lower end was raised by a factor of 100.

5.1.2 Americium

Americium exists in the +3 oxidation state in natural waters and forms carbonate complexes at pH values above 7 (EPA 2004, Serne 2007). The americium solids that would likely control the solubility include Am $(OH)_3$, $AmOHCO_3$, and $Am_2(CO_3)_3$. At Yucca Mountain the americium solubility used in the TSPA model ranged from 10^{-10} M to 10^{-6} M (LANL 1997). A similar range is used in this PA model.

5.1.3 Cesium

Cesium exists in the +1 oxidation state (EPA 1999c) with little tendency to form aqueous complexes. The dominant form at the site would be as the Cs^+ ion. Cesium has a high solubility, with little tendency to precipitate, therefore a conservatively high solubility was used for this PA model, with a fairly narrow range.

5.1.4 Iodine

Iodine can form a number of oxidation states, but within the Eh and pH conditions expected at the Clive facility, iodine is expected to exist in the -1 oxidation form. This is consistent with the modeling provided by EPA (1999c). In addition to dissolving and sorbing reactions, iodine can also volatilize to the gas phase either as I_2 (molecular iodine) or hydrogen iodide and organic (e.g. methyl) iodides. Iodine is not likely to form minerals due to the very low concentrations that would be encountered. Nevertheless, solubility could be controlled via iodine minerals. The distribution used for iodine in this PA model reflects the high solubility.

5.1.5 Lead

Under the environmental conditions at the site lead will exist in the +2 oxidation state (EPA 1999c). However, lead has very low solubility with values of 10^{-8} M in natural waters, with the dissolved species $PbCO_3$ the dominant form above pH 7. Lead species include hydrolysis and carbonate complexes, with the later more prevalent above pH 7. Lead carbonate (e.g cerussite, hydrocerussite), sulfate (anglesite) and phosphates (chlorophyromorphite) minerals control lead solubility under oxidizing conditions (EPA 1999c). At Yucca Mountain the lead solubility used in the TSPA model ranged from 10^{-8} M to 10^{-5} M, with an expected value of $10^{-6.5}$ M. (LANL 1997). This same general range is used in all three zones for this PA model.

5.1.6 Neptunium

Neptunium can exist in several oxidation states, but only +4 and +5 are reasonable for the Clive site. Np(V) is relatively mobile due to the high solubilities of associated minerals and low

sorption. Np (V) is expected to be present as NpO_2^+ (EPA 2004). Np (IV) however, forms solids of low solubility though these are restricted to reducing conditions. Neptunium can form carbonate complexes but this is generally limited to pH conditions above 8. In carbonate rich systems with high sodium and potassium, as found at the Clive facility, several sodium (e.g. $2NaNpO_2CO_3 \bullet 7H_2O$) and potassium based mineral forms of Np can control the solubility. Due to the high solubilities of these minerals Np can be found at levels in the 10^{-4} M or greater concentration. At Yucca Mountain the neptunium solubility used in the TSPA model ranged from 10^{-8} M to 10^{-2} M, with an expected value of 10^{-4} M (LANL 1997).

5.1.7 Plutonium

Plutonium can exist in four different oxidation states: +3, +4, +5, and +6 with Pu(IV), Pu(V), and Pu(VI) expected under oxidizing conditions, such as those found at the site (EPA 1999c). Plutonium forms strong hydroxy-carbonate complexes with the tetravalent complex $[Pu(OH)_2(CO_3)_2^{2-}]$ a likely dominant form at the Clive site. Pu(VI) can also form complexes with chloride ion under oxidizing conditions in high ionic strength solutions (Clark and Tait, 1996). Dissolved plutonium in the natural environmental is typically very low, in the 10^{-15} M range (EPA 1999c), though higher levels are possible where a solid phase is present. At Yucca Mountain the plutonium solubility used in the TSPA model ranged from 10^{-10} M to 10^{-6} M, with an expected value of 10^{-8} M. (LANL 1997). A similar range is used for this PA model.

5.1.8 Protactinium

Protactinium can exist in two oxidation states in natural waters, +4 and +5. Both forms have a propensity to form hydrolysis complexes (Morss, et al. 1977). Protactinium will also form complexes with halides (F^-, Cl^-, Br^-, I^-) and sulfate. Very little information is available on the protactinium species in circumneutral pH range. At Yucca Mountain the protactinium solubility used in the TSPA model ranged from 10^{-10} M to 10^{-5} M (LANL 1997). A similar range is used for this model.

5.1.9 Radium

Radium only exists in the +2 oxidation state in nature and is generally found uncomplexed as Ra^{2+} (EPA 2004). Radium has similar chemical behavior as barium and forms a co-precipitate as a sulfate [(Ba,Ra) SO_4]. This co-precipitate would likely control the solubility at the Clive site if radium reaches levels for saturation. At Yucca Mountain, the radium solubility used in the TSPA model ranged from 10^{-9} M to 10^{-5} M, with an expected value of 10^{-7} M. (LANL 1997). For this PA, a similar range was used with a central tendency value higher by a factor of 10.

5.1.10 Radon

Radon, in the form of ^{222}Rn, is the longest-lived of all radon isotopes with a half life of 3.8 days and is considered the most environmentally important isotope. Radon exists as an essentially inert gas and does not precipitate or sorb to any significant extent, but will partition between aqueous and gas phases, according to its Henry's Law constant, as discussed in the *Unsaturated Zone Modeling* white paper. In the unsaturated zone radon will mainly exist in the gas phase, but is soluble and within all zones the solubility is temperature sensitive. A fairly narrow solubility range based on values from Langmuir (1997) was used in this PA model since temperature is likely the largest factor impacting this species solubility.

5.1.11 Strontium

Strontium is expected to exist in the Sr^{2+} form in the aqueous environments at the Clive site. Strontium has minimal tendency to form inorganic complexes (EPA 1999c), has a similar ionic radius to that of calcium, and forms similar minerals including celestite ($SrSO_4$) and strontianite ($SrCO_3$). In alkaline conditions with sufficient concentration, strontianite, or co-precipitation with calcite and anhydrite, is expected to control the Sr^{2+} concentration. At Yucca Mountain the strontium solubility used in the TSPA model ranged from 10^{-6} M to 10^{-3} M. (LANL 1997). A similar range was used for this PA model.

5.1.12 Technetium

Technetium can exist in multiple oxidation states, but +7 is dominant under oxidizing conditions (EPA 2004, Langmuir 1997, Wildung et al. 2004). In oxidizing conditions the species is the oxyanion TcO_4^- which is highly soluble and is not known to form complexes. Under slightly reducing conditions technetium exists an an uncharged hydroxide. Under stronger reducing conditions technetium can form a very insoluble form. For this PA model, a solubility centered around 10^{-3} M was used.

5.1.13 Thorium

Thorium is expected to exist in the 4+ form at the Clive site. Thorium forms hydroxyl complexes as well as carbonate and inorganic anion complexes. Thorium has very low solubility (EPA 1999c). Hydrous thorium oxide can be used to develop a maximum solubility. At Yucca Mountain the thorium solubility used in the TSPA model ranged from 10^{-10} M to 10^{-7} M. (LANL 1997). This value is consistent with values in EPA (1999c), which described a range of $10^{-8.5}$ M to 10^{-9} M for a pH range of 5 to 9. The solubility of hydrous thorium oxide increases 2 to 3 orders of magnitude with increasing ionic strength (EPA 1999c). This behavior is significant for the shallow aquifer zone of this model resulting in a solubility range that was chosen near the upper end of that used in the Yucca Mountain repository study.

5.1.14 Uranium

5.1.14.1 Uranium Forms and Geochemical Model Parameters

The DU waste proposed for disposal at the Clive facility is in two main uranium oxide forms: UO_3 and U_3O_8. Uranium trioxide, UO_3, is the waste form received from SRS. The uranium oxides expected to be produced at the deconversion plants in Portsmouth, OH, and Paducah KY (the GDP DU) are anticipated to be predominantly U_3O_8, with small amounts of UO_2. The U.S. DOE has characterized U_3O_8 as insoluble (ANL 2010, DOE 2001). The exact solid phase that will control uranium solubility for the Clive Facility is not known and would require extensive laboratory testing to determine. Based upon the results outlined by the several research groups described above, schoepite likely is the major contributor, and this solid was selected to develop the solubility distribution in this PA for the UO_3 form. This is a conservative assumption in that schoepite is more soluble than uranyl carbonate and much more soluble than U_3O_8. The solubility of U_3O_8 is also incorporated into the GoldSim model.

Due to the importance of uranium solubility to this PA, the input distribution was derived from geochemical modeling. The model Visual MINTEQ (Gustafsson 2011) was utilized. This geochemical code is based on the EPA MINTEQA2 program, and was used with its default

database. MINTEQ allows for a large number of uranium mineral forms to be examined. The following were considered the most important for this PA: schoepite, U_3O_8 (crystalline), U_4O_9 (crystalline), UO_2 (amorphous), B_$UO_2(OH)_2$, rutherfordine, and uraninite.

Under oxidizing subsurface conditions U(VI) as the UO_2^{2+} uranyl complex, is the predominant oxidation state and is not easily reduced geochemically. Experiments by Reed et al. (1996) indicate the uranyl complex can persist for over two years, even under high ionic strength anoxic conditions. However, with strongly reducing conditions the U(IV) species can form. Based on the pH and redox conditions at Clive, aqueous uranium is expected to be predominantly in the +6 form [U(VI)] in all three zones (Langmuir 1997, EPA 1999c). However, some of the groundwater measurements do indicate areas of negative Eh (reducing conditions) where uranium could exist in either the U(V) or U(IV) form if bioreduction or reduced iron exists. Under low carbonate levels uranium exists as a polynuclear hydrolysis species. However, the carbonate chemistry associated with the groundwater and the atmospheric CO_2 partial pressure will promote the formation of carbonate complexes with uranium. These complexes can increase the overall uranium solubility. The carbonate complex $UO_2(CO_3)_3^{4-}$ is accepted as a major complex at high carbonate concentrations (Clark et al., 1995, Langmuir 1997). The solid, uranyl carbonate, UO_2CO_3, can also potentially limit the uranium solubility (DOE 2009). Studies where this was the dominant species indicates that solubilities decreases with increasing ionic strength. Divalent metal uranium carbonate complexation [e.g., $Ca_2UO_2(CO_3)_{3(aq)}$] is also possible (Bernhard, et al. 2001, Wan et al. 2008).

The scenario within the waste and unsaturated zones is expected to be somewhat analogous to the experimental system described by Wronkiewics et al. (1992) and also modeled by De Windt et al. (2003). In the work by Wronkiewics et al. the Unsaturated Test Method was used to study the dissolution and precipitation of UO_2 at 90 degrees Celsius. Note that UO_2 is uncommon in the Clive inventory, but may make up a small amount of the GDP DU. The UO_2 was freshly prepared containing natural uranium isotope abundances and leached with water from well J-13 near Yucca Mountain, Nevada that had been equilibrated with local tuff. During the course of the test, this leachate was periodically injected into the top of the system, water samples were collected, and the UO_2 was visually inspected. They found an initially low concentration of uranium in the outflow followed by a slug of uranium that leveled off over the circa 238-week (4.5-yr) period. Formic and oxalic acids were detected in the leachate but not found in the starting material. This was attributed this to a potential radiolytic effect. Of particular importance was the change in uranium oxide phases with time. A number of secondary uranium oxides were formed as the uranium first dissolved, then later precipitated as a different oxide. Schoepite ($UO_3 \bullet xH_2O$), dehydrated schoepite (UO_3), uranophane and a number of other uranium hydroxide minerals including uranium alkali silicates were formed. In all cases these indicated uranium was present only in the U(VI) redox state. The solubility limit, based upon the steady-state uranium release after two years of leaching, was attributed to precipitation of uranyl silicates on the surface, limiting additional dissolution. De Windt et al. (2003) modeled UO_2 oxidative dissolution in a saturated zone under oxidizing conditions. They found that uranium mobility was controlled by schoepite, the dominant mineral formed. The total uranium concentration decreased for the first 100 years from a maximum of approximately 400 μM to a constant 10^{-5} M after consumption of all of the UO_2. This mineral paragenesis is similar to that observed for oxidized zones in natural uraninite. Modeling by Langmuir (1997) indicates that

uranium solubility based on schoepite ranges from 10^{-6} M to 10^{-4} M, depending upon pCO_2 levels. This is consistent with the values in the Wronkiewics et al. (1992) study and modeled by De Windt (2003). Though analogous to what can happen at the Clive facility, it is critical to realize Wronkiewics et al. and De Windt started with a very soluble form of uranium, UO_2, as compared with the much more stable UO_3 and especially U_3O_8 DU waste at Clive. U_3O_8 is considered one of the most thermodynamically and kinetically stable forms of uranium. Also of note above was the potential for dissolution to be reduced by the formation of less soluble uranyl silicates on the surface of the starting material.

At the Clive Facility, should formic and oxalic acid be formed radiolytically, they also could increase the overall uranium solubility (Langmuir, 1997). However, the generation of these acids is not expected to be significant nor should it have a significant effect on pH. This is especially true for any water that leaches from the waste zone into the shallow aquifer due to the buffering capacity of this aquifer. As such, this effect would be transitory at best.

To derive uranium solubility distributions and speciation, the geochemical modeling program was run in individual batches, where for a given run the parameters pH, temperature (13°C), pe (Eh), and water density were fixed. Multiple runs were performed by adjusting a single parameter. The effect of temperature on solubility, with a range of approximately 10°C to 25°C, is insignificant relative to the uncertainty of measurements and modeling. A single temperature value of 13°C was used in the geochemical modeling. To account for the thermodynamic activity in this high TDS saturated zone system, the Bronsted-Guggenheim-Scatchard specific ion interaction theory (SIT) (Nordstrom and Munoz, 1994) model is utilized. The SIT model is applicable to high ionic strength solutions up to approximately 4 molal. When lower TDS parameters were utilized the Davies equation was employed. Most of the thermodynamic parameters used in Visual MINTEQ for the uranium species are derived from the Nuclear Energy Agency database (2003) available in the Visual MINTEQ program.

The level of ions other than uranium used in the geochemical modeling was set for two different conditions. The first condition was set based on the ions found as the average of the data from well GW-25 at the Clive facility. The groundwater chemistry of this well and several others is shown in Tables 5 and 6, representing the conditions in the very high TDS shallow aquifer. Modeling indicated that pH and bicarbonate/pCO_2 had the largest influence on total uranium concentrations within the Eh range of 800 to -200 mV. When the redox conditions were reduced to -500 mV, U_3O_8 precipitated at very low uranium concentrations. These low redox conditions are not anticipated at Clive except under transient conditions. A second set of geochemical modeling runs was performed under much lower TDS conditions. In this set lower sodium and chlorine levels were chosen to more closely represent the water phase in the unsaturated zones, at least in the upper waste prior to significant salt dissolution. The mineral form of uranium anticipated from the two main sites SRS (as schoepite, a form of UO_3,) and the GDPs (as U_3O_8) were included as infinite solids in separate geochemical models. Basing solubility limits solely on a solid phase is not without uncertainty (OECD 1997, Chapter IV). So, solubility distributions are incorporated into the PA to account for this uncertainty. The pH, Eh, and carbonate conditions were varied and the resulting total uranium concentration was calculated. Uranium solubility limits were based on the concentration at which each mineral reached saturation. Differences between the high ionic strength modeling runs and those with lower

sodium and chloride were not significant enough, relative to the uncertainty of the modeling, to justify separate solubility distributions. Complete reports from each of the model runs are available.

5.1.14.2 Uranium Solubilities based on Schoepite

The solubility of uranium for the UO_3 waste form was derived using the mineral schoepite in the geochemical code Visual MINTEQ as described above. The parameters were adjusted so that they would mimic the range of conditions at the site, with schoepite provided as an infinite solid source. TDS values were elevated, similar to the shallow aquifer. The total uranium solubility outputs from these geochemical models are shown in Table 7. As shown from these model results, uranium solubilities range from 10 mg/L to 100 mg/L. Using schoepite [U(VI)] as the controlling mineral indicates uranium levels could reach as high as 100 mg/L (4.2×10^{-4} M) under several scenarios. These values are similar to those found experimentally by Wronkiewics et al. (1992). Choppin (2000) performed batch solubility studies using a synthetic water and mixed uranium oxides under both anoxic and oxidizing conditions. In the absence of humic compounds, the solubility of uranium was 114±2 mg/L and 94±2 mg/L under oxic (Eh of 220 mV) and anoxic (Eh 138 mV) conditions respectively. The pH of the solution ranged from 8 to 8.2. A 1 ppm humic acids level had little effect on solubility. The data by Choppin (2000) are also similar to estimates from this geochemical modeling for schoepite. Tomasko (2001) modeled uranium transport using UF_4 as the disposed form. This is a very soluble form of uranium, much more so than the uranium oxides that are expected in the Clive facility inventory. The study by Tomasko considered uranium tetrafluoride disposed in 30- or 50-gallon drums. After exposure to water the uranium underwent hydrolysis to form schoepite or U_3O_8. No solubility experiments were performed by Tomasko though he cited work by others to develop the solubility limits. Under oxidizing conditions Tomasko envisioned the schoepite being formed from the U_3O_8. Tomasko used a range of uranium solubilities from 24 mg/L, the solubility he cited for schoepite, to a much higher value of to 23,000 mg/L. This higher value was based on the potential formation of ammonium carbonate uranium complexes . These complexes are not considered significant species at the Clive location due to the low nitrogen availability of the system.

Table 7: Model Results for High TDS System analogous to the Upper Aquifer. Uranium solubility limit based on Schoepite*.

pH	Bicarbonate (mg/L)	Eh (mV)	Total Uranium (mg/L)	Total Uranium (mol/L)
6.5	190	200	28.1	1.18E-4
7.2	10	200	2.3	9.72E-6
7	190	200	75.4	3.17E-4
7.3	190	811	58.5	2.46E-4
7.2	300	200	241	1.01E-3
7.5	500	200	421	1.77E-3
8	300	200	428	1.80E-3

*Data in this table include the following constant parameters: specific gravity of water 1.03, stoichiometric ionic strength 0.88, and anions and cations levels as shown in Table 5 and 6 above for GW-25.

The geochemical model runs listed in Table 6 were also repeated at a reduced TDS condition as shown in Table 8. The results were sufficiently similar that the model is considered to be applicable to both the saturated and unsaturated regions. When the model is adjusted so that levels of sodium and chloride are reduced significantly (Na = 6,465 mg/L, Cl = 10,783 mg/L) at pH 7.25, the uranium solubilities with schoepite are not significantly different, as shown in Table 8. As such, the GoldSim model did not utilize different solubilities for the different levels of TDS and instead the higher maximum values for the distributions were chosen as a conservative approach. Though this approach is a bit conservative, as indicated above the range of TDS that is expected throughout the unsaturated and saturated zones does not have a large impact on uranium solubility.

Table 8: Total uranium, low TDS (ionic strength 0.127 M). Uranium solubility limit based on schoepite.

pH	Bicarbonate (mg/L)	Eh (mV)	Total Uranium (mg/L)	Total Uranium (mol/L)
6.5	190	200	152.8	6.42E-4
7.2	10	200	2.28	9.58E-6
7	190	200	162.32	6.82E-4
7.3	190	811	172.55	7.25E-4
7.2	300	200	278.46	1.17E-3
7.5	500	200	485.52	2.04E-3
8	300	200	307.02	1.29E-3

The major dissolved uranium species considered in the geochemical model simulations included those shown in Table 9. A mixture of primarily anions, but also uncharged and cations are included. The uncharged and anionic species make up the major species under the conditions modeled for schoepite as shown in Table 9.

Table 9: Major dissolved uranium species included in geochemical models.

Uranium Species
$UO_2(CO_3)_3^{-4}$
$UO_2(CO_3)_2^{-2}$
$Ca_2\ UO_2(CO_3)_3$ (aq)
$CaUO_2(CO_3)_3^{-2}$
$(UO_2)_3(CO_3)_6^{-6}$
$UO_2(OH)_2$ (aq)
$UO_2(OH)^{3-}$
$(UO_2)_4(OH)^{7+}$
$(UO_2)_3(OH)^{5+}$

5.1.14.3 Uranium Solubilities based on U_3O_8

The solubility of uranium for the U_3O_8 waste form was derived by directly setting this solid form as an infinite source in the geochemical code Visual MINTEQ as described above. Results are provided in Table 10 .

Table 10: Total Uranium, low TDS (ionic strength 0.127 M). Uranium solubility limit based on the mineral U_3O_8*.

pH	Bicarbonate (mg/L)	Eh (mV)	Total Uranium (mg/L)	Total Uranium (mol/L)
6.5	190	200	1.87E-10	7.85E-16
7	190	200	7.14E-11	3.00E-16
8	300	200	2.38E-11	1.00E-16
7.3	190	-10	1.19E-6	4.98E-12
7.3	190	-40	6.00E-6	2.52E-11
7.3	190	-100	1.54E-4	6.45E-10
7.3	190	-300	7.57E+0	3.18E-5

*Data in this table include the following constant parameters: specific gravity of water 1.03, stoichimetric ionic strength 0.88, and anion and cation levels as shown in Table 5 and 6 above for GW-25.

The differences in solubility between schoepite and U_3O_8 are pronounced. U_3O_8 has significantly lower solubility within the geochemical conditions expected at the Clive Facility. Only at very anoxic conditions does U_3O_8 show a solubility approaching that of UO_3. The amount of current experimental data on the solubility of this mineral is limited. As stated above, the DOE considers U_3O_8 insoluble.

GoldSim Model Note: The GoldSim model cannot incorporate solubilities for both UO_3 and U_3O_8 simultaneously within a single 10,000 year simulation because solubility is based only on the element uranium. To account for the differences in solubility between the two uranium oxide wastes in the inventory, the Control Panel for the model provides the ability to use either the default solubility based on UO_3 or to select the solubility based on U_3O_8. One may also select either or both waste inventories. Based upon evaluation of the Clive DU PA Model, the UO_3 solubility is governing the uranium concentrations into the groundwater for about 50,000 yr. This indicates that the inability to have two separate solubilities in the model for the two waste forms of DU is not affecting the simulation results.

6.0 Ionic and Molecular Diffusion Coefficients

The diffusion coefficient (D_m) is required for calculating the movement of solutes due to differences in concentration gradient. Movement by diffusion can occur without advective flow of water. Ionic and molecular diffusion coefficients are derived in theory from the Stokes-Einstein equation:

$$D_m = RT / 6\pi\eta_B r_A \quad (5)$$

where

R = universal gas constant,

T = temperature,

η_B = absolute viscosity of the solvent (water), and

r_A = radius of the assumed spherical solute.

A variety of empirical equations have been derived based on the Stokes-Einstein equation for different scenarios. For a dilute solution of a single salt the diffusion coefficient can be derived from the Nernst-Haskell equation (Reid et al., 1987). This equation includes the valence of the cation and anions as well as ionic conductances. Specific ionic conductances are required for each cation and anion species. When two or more chemical species are present at different concentrations, interdiffusion (counterdiffusion) must be included to satisfy electroneutrality (Lerman 1979). For a geochemical system as large as that found in radioactive waste disposal facilities this quickly becomes too complex to model, even if ionic conductivities are available for each species.

An additional difficulty in deriving ion-specific diffusion coefficients lies in the large number of potential ions. The number of radioactive waste elements typically modeled may be 30 to 40, and for each element in this list one can expect multiple forms. For example, U has 4 redox states, and many soluble species for each of these. Assuming oxic conditions U will be primarily found as $UO_2(CO_3)_3^{4-}$, $UO_2(CO_3)_2^{2-}$, and UO_2CO_3, but there are at least 8 additional forms of U(+6) that may be found. Thus the potential number of ions that would need to be included in the model would easily be in the hundreds. Obtaining the parameters for each species that would be required to model the ionic diffusion would be difficult.

Given these issues with developing ion-specific values of D_m, the approach used in modeling diffusion in the PA model is to use a range of D_m values. This range can be derived from Table 3.1 in Lerman (1979). For conditions near 25°C, the range of D_m for the elements of interest is 4×10^{-6} to 2×10^{-5} cm^2/s. For cooler temperatures, which would be expected in the deeper subsurface, the values are somewhat lower. The values for 25°C are reproduced in Table 11.

Table 11. Diffusion coefficients for selected cations and anions.

Cation	D_m (10^{-6} cm^2/s)	Anion	D_m (10^{-6} cm^2/s)
K^+	19.6	Cl^-	20.3
Cs^+	20.7	I^-	20
Sr^{2+}	7.94	IO^{3-}	10.6
Ba^{2+}	8.48		
Ra^{2+}	8.89		
Co^{2+}	6.99		
Ni^{2+}	6.79		
Cd^{2+}	7.17		
Pb^{2+}	9.45		
UO_2^{2+}	4.26		
Al^{3+}	5.59		

SOURCE: Table 3.1 Lerman (1979)

Based on these values, the diffusion coefficient is represented in the Clive DU PA Model as a uniform distribution with a minimum of 3×10^{-6} cm^2/s and a maximum of 2×10^{-5} cm^2/s, and is the same for all elements.

7.0 References

Adrian Brown Consultants, Response to UDEQ Kd Interrogatories, Dated April 22, 1997 Report 3101B.970422.

ANL Characteristics of Uranium. Web site accessed 2010. http://web.ead.anl.gov/uranium/guide/ucompound/propertiesu/octaoxide.cfm

Beals, D. M., S. P. LaMont, J. R. Cadieux, C. R. Shick, and G. Hall. Determination of Trace Radionuclides in SRS Depleted Uranium (DU). November 19, 2002. WSRC-TR-2002-00536 Westinghouse Savannah River Company, SRS, Aiken, SC 29808.

Bernhard G, G Geipel, T Riech, V Brendler, S Amayri, and H Nitsche. 2001. Uranyl (VI) Carbonate Complex Formation: Validation of the Ca2UO2(CO3)3 (aq) Species. Radiochimica Acta 89:511-518.

Bingham Environmental, 1991. Hydrogeologic Report Envirocare Waste Disposal FacilitySouth Clive, Utah. Final version October 9, 1991.

Bingham Environmental, Project Memorandum. Summary of Results, Radionuclide Kd Tests, Envirocare Disposal Landfills, Clive, Utah. August 3, 1995.

Bingham Environmental, Project Memorandum. Summary of Results, Radionuclide Kd Tests, Envirocare Disposal Landfills, Clive, Utah. January 25, 1996.

Choppin, Gregory R. Idaho National Engineering and Environmental Laboratory Publication. INEEL/EXT-01-00762 Rev. 0. November 2000. Actinide Solubility Experiments in INEEL Perched Simulant Solution.

Clark, D. L. and Tait, C. D. 1996. Monthly Reports Under SNL Contract AP2274, Sandia WIPP Central File A:WBS 1.1.10.1.1. These data are qualified under LANL QAPjP CST-OSD-QAP1-001/0. WPO 31106.

Clark, D. L., D. E. Hobart, and M. P. Neu. Actinide Carbonate Complexes and Their Importance in Actinide Environmental Chemistry. Chemical Reviews, Vol 95: 25. 1995

Contardi, J. S., D. R. Turner, and T. M Ahn. Modeling Colloid Transport for Performance Assessment. Journal of Contaminant Hydrology 47, 323-333, 2001.

Cui, D. and Eriksen, T. 1996. Reduction of Tc(VII) and Np(V) in solution by ferrous iron. SKP TR 96-03.

De Windt L., Burnol A., Montaranl P., van der Lee J. 2003. Intercomparison of reactive transport models applied to UO2 oxidative dissolution and uranium migration. Journal of Contaminant Hydrology 61, 303-312, 2003.

DOE 2001. http://web.ead.anl.gov/uranium/pdf/UraniumCharacteristicsFS.pdf

DOE. 2003. Publication 45185. Evaluation of Surface Complexation Models for Radionuclide Transport at the Nevada Test Site: Data Availability and Parameter Evaluation. D. Decker and C. Papelis. May, 2003.

DOE. 2009. Waste Isolation Pilot Plant (WIPP), SOTERM-2009. Title 40 CFR Part 191 Subparts B and C Compliance Recertification Application for the Waste Isolation Pilot Plant. Appendix SOTERM-2009 Actinide Chemistry Source Term.

Envirocare of Utah. Revised Hydrogeological Report for the Envirocare Waste Disposal Facility, Clive, Utah. Version 2.0, 2004.

Envirocare of Utah. Metals Distribution Coefficient Values Relevant to the EnvirocareSite. Memorandum and Report to the US Nuclear Regulatory Commission. 2000.

EPA. 1999b. Understanding Variation in Partition Coefficient, Kd, Values. Volume I. 402-R-99-004A. US Environmental Protection Agency, Washington, DC.

EPA. 1999c. Understanding Variation in Partition Coefficient, Kd, Values. Volume II (1999). 402-R-99-004C. US Environmental Protection Agency, Washington, DC.

EPA. 2004. Understanding Variation in Partition Coefficient, Kd, Values. Volume III. 402-R-04-002C. US Environmental Protection Agency, Washington, DC.

Geckeit, H. and T. Rabung. Actinide Geochemistry: From the Molecular Level to the Real System. Journal of Contaminant Hydrology 102, 187-195, 2008.

Glover, P. A., F. J. Miner and W. O. Polzer. 1976. "Plutonium and Americium Behavior in the Soil/Water Environment. I. Sorption of Plutonium and Americium by Soils." In Proceedings of Actinide-Sediment Reactions Working Meeting, Seattle, Washington, pp. 225-254, BNWL-2117, Battelle Pacific Northwest Laboratories, Richland, Washington.

Gustafsson, J.P., 2011. Visual MINTEQ ver 3.0. Based on the USEPA MINTEQA2 software, (http://www2.lwr.kth.se/English/OurSoftware/vminteq/)

Heberling, F., B. Brendebach, and D. Bosbach. Neptunium(V) Adsorption to Calcite. Journal of Contaminant Hydrology 102, 246-252, 2008.

Hull, L. C, and A. L. Schaefer. 2008. Accelerated transport of 90Sr following a release of a high ionic strength solution in vadose zone sediments. Journal of Contaminant Hydrology 97, 135-157.

Johnson, G.L., and L.M. Toth. 1978. Plutonium(IV) and Thorium(IV) Hydrous Polymer Chemistry. ORNL/TM-6365. Oak Ridge, TN: Oak Ridge National Laboratory, Chemistry Division.

Kerrisk, Jerry F. Ground-Water Chemistry at Yucca Mountain, Nevada and Vicinity. LA-10929-MS February 1987

Krupka KM, RJ Serne, and DI Kaplan. 2004. Geochemical Data Package for the 2005 Hanford Integrated Disposal Facility Performance Assessment. PNNL-13037, Rev 2, Pacific Northwest National Laboratory, Richland, Washington.

Kumata, M., Vandergraaf, T.T. And Jujnke, D. G. 1993. The migration behavior of neptunium under deep geological conditions. Migration '93 Abstracts, p 73.

LANL (Los Alamos National Laboratory), LA-13262-MS. 1997. Summary and Synthesis Report on Radionuclide Retardation for the Yucca Mountain Site Characterization Project.

Last GV, EJ Freeman, KJ Cantrell, MJ Fayer, GW Gee, WE Nichols, BN Bjornstad, and DG Horton. 2004. Vadose Zone Hydrogeology Data Package for the 2004 Composite Analysis. PNNL-14702 Rev. 0, Pacific Northwest National Laboratory, Richland, Washington.

Lerman, A. 1979. Geochemical Processes in Water and Sediment Environments. Wiley-Interscience. QES71.L45

Langmuir, D. Aqueous Environmental Chemistry. Prentice Hall 1997.

Linsalata, P. and N. Cohen. Determination of the Distribution Coefficient of Plutonium in WATER-Secimetn Systems. Health Physics 39:1040-1041. 1980.

Morss, Lester, Norman M Edelstein, Jean Fuger, and Joseph Katz. The Chemistry of the Actinide and Transactinide Elements. Third Edition, Volume 1. 1977 Springer.

Nakata, K., Nagasaki, S., Tanaka, S., Sakamoto, Y., Tanaka, T. and Ogawa, H. 2002. Sorption and reduction of neptunium (V) on surface or iorn oxides. Radiochim. Acta 90 pp 665-669.

Nordstrom, D. K, and J. L. Munoz. 1994. Geochemical thermodynamics. 2nd edition. Cambridge, MA; Blackwell Scientific Publications, Inc.

OECD Publication 1997. Modelling in Aquatic Chemistry. Chapter IV, Raulf Grauer. Scientific Editors Ingmar Grenthe and Ignasi Puigdomenech

ORNL (Oak Ridge National Laboratory). 2000. J. R. Hightower, et al. Strategy for Characterizing Transuranics and Technetium Contamination in Depleted UF6 Cylinders. ORNL/TM-2000-242 Chemical Technology Division, ORNL. 2000.

Patterson, R.J., Spoel, T., 1981. Laboratory measurements of strontium distribution coefficeint Kd -Sr for sediments from a shallow sand aquifer. Water Resources Research 17 (3), 513-520.

Reed, D.T., D. R. Wygmans, and M. K. Richman. Actinide Stability/Solubility in Simulated WIPP Brines. Argonne National Laboratory, Actinide Speciation and Chemistry Group, Chemical Technology Group. Interim Report 1996.

Reid, R.C., Prausnitz, J.M., and Poling B.E., 1987. The Properties of Gases and Liquids, 4th Edition. McGraw-Hill, Inc. TP242.R4.

Sandia (Sandia National Laboratories) 2001. Compliance Assessment Document for the Transuranic Wastes in the Greater Confinement Disposal Boreholes at the Nevada Test Sites. Volume 2: Performance Assessment. Version 2.0.

Schaefer, Donald H., S. A. Thiros, and M. R. Rosen. Ground-Water Quality in the Carbonate-Rock Aquifer of the Great Basin, Nevada and Utah, 2003. U.S. Geological Survey, National Water-Quality Assessment Program. Scientific Investigations Report 2005-5232.

Scism, Cynthia D. 2006. The Sorption/Desorption Behavior of Uranium in Transport Studies using Yucca Mountain Alluvium. Los Alamos National Laboratory LA-14271-T. 2006.

Serne, R. Jeff. 2007. Kd Values for Agricultural and Surface Soils for Use in Hanford Site Farm, Residential, and River Shore Scenarios. Technical Report for Ground-Water Protection Project. PNNL-16531. August 2007.

Sheppard, Marsha., D. H. Thibault. 1990. Default Soil Solid/Liquid Partition Coefficients, KdS, for Four Major Soil Types: A Compendium. Health Physics Vol 59, No 4, pp 471-482. October 1990.

Tomasko, D., 2001, Groundwater Calculations for Depleted Uranium Disposed of as Uranium Tetrafluoride (UF4). ANL/EAD/TM-111, Argonne National Laboratory, Argonne, Ill.

USDA. Nat Resources Conservation Service, Tooele Area Soil Survey Utah, Version 5, Sept 2, 2009.

Vandergraaf, T. T., Ticknor, K.V., and George, I. M. 1984. Reactions between Technetium in Solution and Iron-Containing Minerals Under Oxic and Anoxic Conditions. ACS Symposium Series, 246, pp.25-43, Atomic Energy of Canada Limited Report, AECL-7957.

Vandergraaf, T. T., Ticknor, K.V., and Melnyk, T. W. 1993. The selection of a sorption data base for the geosphere model in the Canadian Nuclear Fuel Waste Management Program. Journal of Contaminant Hydrology, 13, 327-345.

Wan, J., T.K. Tokunaga, Y. Kim, Z. Wang, A. Lanzirotti, E. Saiz, and R.J. Serne, Effect of saline waste solution infiltration rates on uranium retention and spatial distribution in Hanford sediments, Environ. Sci. Technol., 42, 1973-1978, 2008.

Whetstone Associates. Technical Memorandum to Energy Solutions from Whetstone Associates, Oct 30, 2009.

Wildung, R. E., Li S. W., Murray, C. J., Krupka, K. M., Xie, Y., Hess, H. J., and Rogen, E.E. Technetium reduction in sediments of a shallow aquifer exhibiting dissimilatory iron reduction potential. FEMS Microbiology Ecology. 49, 151-162, 2004.

Wooyong Um, R. Jeffrey Serne, G. V. Last, R. E. Clayton, and E. T. Glossbrenner. The Effect of Gravel Size Fractions on the Distribution Coefficients of Selected Radionuclides. Journal of Contaminant Hydrology 107, 82-90, 2009.

Wronkiewicz, David J , Bates, J. K., Gerding, T. J., Veleckis, E., and Tani B. S. Journal of Nuclear Materials 190. 107-127. 1992.

Neptune and Company Inc.

June 1, 2011 Report for EnergySolutions

Clive DU PA Model, version 1

Appendix 7

Saturated Zone Modeling

Saturated Zone Modeling for the Clive DU PA

28 May 2011

Prepared by

Neptune and Company, Inc.

This page is intentionally blank, aside from this statement.

CONTENTS

FIGURES

TABLES

1.0 Summary of Parameters and Distributions

This section is a brief summary of parameters and distributions used for modeling saturated zone processes for the Clive Depleted Uranium Performance Assessment (PA) Model. For distributions, the following notation is used:

- N(μ, σ, [*min*, *max*]) represents a normal distribution with mean μ and standard deviation σ, and optional truncation at the specified *min*imum and *max*imum,
- LN(*GM*, *GSD*, [*min*, *max*]) represents a log-normal distribution with geometric mean GM and geometric standard deviation GSD, and optional *min* and *max*,
- U(*min*, *max*) represents a uniform distribution with lower bound *min* and upper bound *max*,
- Beta(μ, σ, *min*, *max*) represents a generalized beta distribution with mean μ, standard deviation σ, minimum *min*, and maximum *max*,
- Gamma(μ, σ) represents a gamma distribution with mean μ and standard deviation σ, and
- TRI(*min*, *m*, *max*) represents a triangular distribution with lower bound *min*, mode *m*, and upper bound *max*.

Note that a number of these distributions are truncated at a minimum value of 0 and a maximum of Large, an arbitrarily large value defined in the GoldSim model. The truncation at the low end is a matter of physical limits (e.g. precipitation cannot be negative), and in GoldSim's distribution definitions, if truncations are made, they must be made at both ends, so the very large value is chosen for the upper end.

Table 1: Summary of saturated zone parameter distributions

Parameter	Distribution	Units	Comment
Saturated Hydraulic Conductivity	N(9.6e-4, 9.67e-5, min=Small, max=Large)	cm/s	See Section 3.1
Bulk Density	N(1.57, 0.05, min=Small, max=Large) [standard deviation is a placeholder]	g/cm^3	See Section 3.2
Porosity	N(0.29, 0.05, min=Small, max=1-Small) [standard deviation is a placeholder]	—	See Section 3.2
Hydraulic Gradient	N (6.94×10^{-4}, 1.27×10^{-4}, min=0 , max=Large)	—	See Section 3.3
Aquifer Thickness	N (16.2, 0.25, min=0, max=Large)	ft	See Section 4.1

2.0 Clive Site Hydrogeology

The site hydrogeology for the Energy*Solutions*' Clive facility has been described by Bingham Environmental (1991, 1994) and Envirocare (2000, 2004). The most recent revised hydrogeologic report prepared by Envirocare (2004) noted that the interpretations of structure

and stratigraphy presented in their report were consistent with previous presentations described in Bingham Environmental (1991, 1994) and Envirocare (2000).

The following description of the Clive site hydrology is taken from the review prepared by Envirocare (2004). The site is described as being located on lacustrine (lake bed) deposits associated with the former Lake Bonneville. The sediments underlying the facility are principally interbedded silt, sand, and clay. While the depth of the sediments below the site is not known, the sediments extend to a depth of at least 250 feet (ft). This minimum depth is based on a borehole log for the deepest well on the site which did not encounter bedrock at its total depth of 250 ft.

Sediments at the site are described by Bingham Environmental (1991, 1994) and Envirocare (2000, 2004) as being classified into four hydrostratigraphic units (HSU). Predominant sediment textural class, layer thickness range, and average layer thickness for each unit are listed in Table 2.

Unit 4: This unit begins at the ground surface and extends to between 6 ft and 16.5 ft below the ground surface (bgs). The average thickness of this unit is 10 ft. This unit is composed of finer grained low permeability silty clay and clay silt.

Unit 3: Unit 3 underlies Unit 4 and ranges from 7 ft to 25 ft in thickness. The average thickness of this unit is 15 ft. Unit 3 is described as consisting of silty sand with occasional lenses of silty to sandy clay.

Unit 2: Unit 2 underlies Unit 3 and ranges from 2.5 ft to 25 ft in thickness. The average thickness of this unit is 15 ft. Unit 2 is described as being composed of clay with occasional silty sand interbeds. A structure map was prepared by Envirocare (2004, Figure 5) with contours representing the elevations of the top of the unit. This map shows that the top surface of Unit 2 slopes downward gradually from east to west in the vicinity of the Class A South cell.

Unit 1: Unit 1 is the bottom layer of this sequence. This unit is described as silty sand interbedded with clay and silt layers. The thickness of this layer has not been estimated.

Table 2: Texture class, thickness range, and average thickness for the hydrostratigraphic units underlying the Clive site.

Unit	Sediment Texture Class	Thickness Range (ft)	Average Thickness (ft)
4	silt and clay	6 – 16.5	10
3	silty sand with interbedded silt and clay layers	7 - 25	15
2	clay with occasional silty sand interbeds	2.5 - 25	15
1	silty sand with interbedded clay and silt layers	?-?	?

The aquifer system in the vicinity of the Clive Facility is described by Bingham Environmental (1991, 1994) and Envirocare (2000, 2004) as consisting of unconsolidated basin-fill and alluvial-fan aquifers. Characterization of the aquifer system is based on subsurface stratigraphy observations from borehole logs and from potentiometric measurements.

The aquifer system is described as being composed of two aquifers; a shallow, unconfined aquifer and a deep confined aquifer. The shallow unconfined aquifer extends from the water table to a depth of approximately 40 ft to 45 ft bgs. The deep confined aquifer is encountered at approximately 45 ft bgs and extends through the valley fill (Bingham 1994). The water table in the shallow aquifer is reported to be located in Unit 3 on the west side of the site and in Unit 2 on the east side.

Deeper saturated zones in Unit 1 below approximately 45 ft bgs are reported to show higher potentiometric levels than the shallow unconfined aquifer. Differences in potentiometric levels are attributed to the presence of the Unit 2 clays. These observations are interpreted as indicating that the shallow unconfined aquifer below the site does not extend into Unit 1 but is contained within Units 2 and 3. Unit 1 extends from approximately 45 ft bgs and contains the deep aquifer.

3.0 Groundwater Flow Parameter Distributions

The parameters used to calculate the groundwater flux are the saturated hydraulic conductivity and the hydraulic gradient. The porosity is needed to calculate the mean groundwater velocity from the flux.

3.1 Saturated Hydraulic Conductivity

To develop a distribution for saturated hydraulic conductivity (K_s), 253 measurements were obtained for 122 locations in the vicinity of the cells and ponds. These measurements were provided to N&C by Energy*Solutions* in an Excel spreadsheet named "Hydraulic Cond" prepared by R. Sobocinski.

There are multiple measurements per location. Thus, in order to not over-represent those locations, a random effects analysis of variance model was fitted, treating location as a random effect, to produce estimates of the mean K_s and its associated standard error.

The average K_s across locations ranges from 2.23×10^{-6} cm/s to 5.95×10^{-3} cm/s There is some right-skew to the average K_s values, which results in a slight overestimate of the standard error in the random-effects model. However, with 122 locations, the distribution of the mean will be well-approximated with a normal distribution. The random effects model produces a mean K_s of 9.6×10^{-4} cm/s and standard error of 9.67×10^{-5} cm/s.

3.2 Bulk Density and Porosity

Although no data have been provided, Whetstone (2000) provides some values for material properties of the shallow aquifer. In Section 7.1.2 of that report, a deterministic value for bulk density of 1.566 g/cm^3 is is listed as an input for the Whetstone (2000) model. That value was adopted as a mean of a normal distribution, and was assigned a placeholder standard deviation of 0.05 g/cm^3.

Similarly, section 7.1.3 of Whetstone (2000) offers a porosity for the shallow aquifer of 0.29. That value was used as the mean of a normal distribution, and a placeholder standard deviation of 0.05 was assigned.

3.3 Hydraulic Gradient

Monthly averages of the site-wide hydraulic gradient from 1999 through 2010 were calculated by Energy*Solutions* from water level measurements. These data were used to establish a distribution for the mean site-wide gradient. The uncertainty related to the mean is typically well-modeled by a normal distribution, due to the effect of averaging. A difficulty with the gradient data is in establishing an appropriate standard error for the mean, since there is considerable time correlation in the data. That is, the values change less from month to month than they do over longer time periods. To account for this behavior several auto-regressive, moving-average (ARMA) models (Brockwell and Davis 1996) were fit to determine a model that adequately captured the time with an adequate fit for the time correlation. Amongst these models, a best model was chosen based on the Akaike information criterion (AIC), and a standard error for the mean was established based on this model's fit. The uncertainty distribution for site-wide gradient was thus established as a normal distribution with a mean of 6.94×10^{-4} and a standard deviation of 1.27×10^{-4}.

4.0 Groundwater Transport Parameter Distributions

Parameters in the PA model that are needed for estimating transport in the shallow aquifer include the aquifer thickness, porosity, ionic and molecular diffusion coefficients, and the dispersion coefficient. The distribution for porosity has been described previously in Section 3.2. Aquifer thickness and dispersion coefficient parameters are described in following sections. The distribution for ionic and molecular diffusion coefficients is described in the *Geochemical Modeling* white paper.

4.1 Aquifer Thickness

The unsaturated zone and the shallow aquifer are represented in the Clive PA Model as cell pathways. A cell pathway consists of a series of linked mixing cells. The transport of contaminants in water through the vadose zone is modeled as advective mass flux links from cell to cell though the network to the first cell representing the shallow aquifer. The cell pathways for the unsaturated zone and the shallow aquifer are represented schematically in Figure 1.

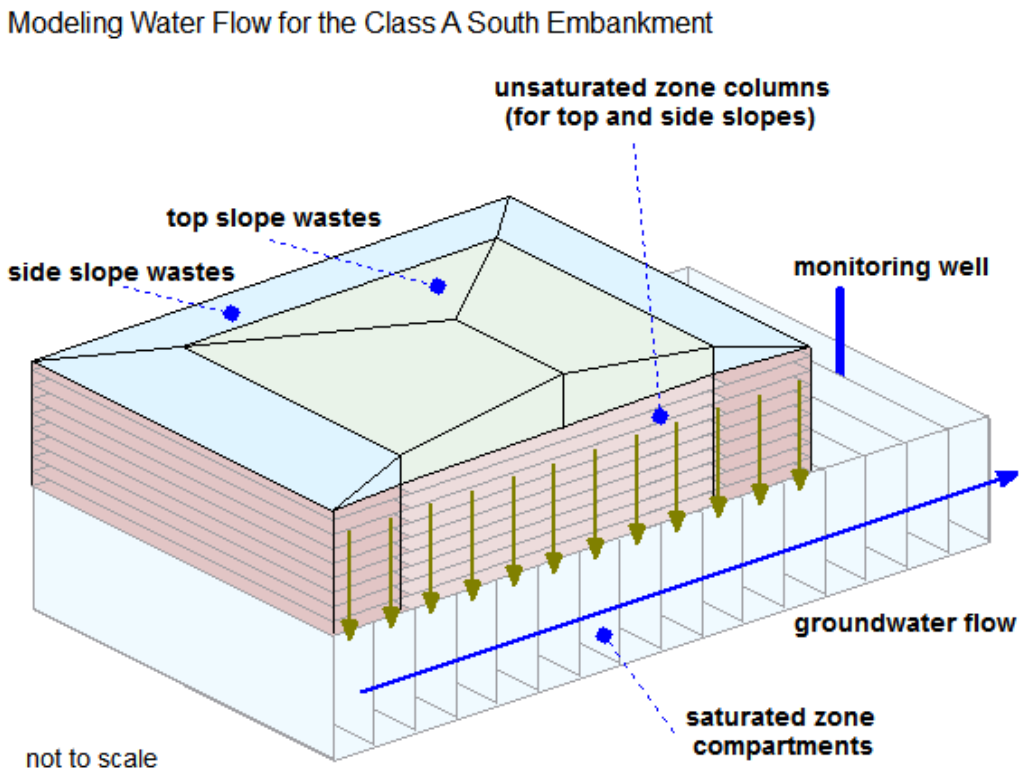

Figure 1: Schematic representation of unsaturated zone and shallow aquifer transport using cell pathways.

The advective mass flux in a cell pathway is calculated as the concentration of the contaminant in water multiplied by the rate at which the water is flowing:

$$\text{Advective Mass Flux} = \text{Concentration} \times \text{Flow Rate} \quad (1)$$

An assumption of the mixing cell approach is that all mass that enters the cell is completely mixed and equilibrated among all media in the cell. To provide contaminant mass balance, GoldSim requires information specifying the volume of the cells. For the Clive PA model, the extent of the saturated zone below the Class A South cell and the distance from the toe of the disposal cell to the compliance point are represented as a horizontal network of linked cells (Figure 1). GoldSim requires the specification of the length of the cell in the direction of flow and the cross-sectional area of the cell. The dimensions of the cell are determined in the following manner. The length of the cell is determined by the selection of the number of cells used to represent the transport distance. The length of each cell is then the transport distance divided by the number of cells. The choice of the number of cells used is arbitrary. The cross sectional area is the product of the cell width and height. For the Clive PA model, the cell width is set to the width of the Class A South cell perpendicular to the direction of flow. The height of the cell corresponds to the aquifer thickness.

Aquifer thickness in the subsurface at the Class A South cell was estimated considering water table elevations, mapped stratigraphy, and interpretations described in Envirocare (2000, 2004). Water table maps provided in Envirocare (2000, 2004) indicate that the flow in the shallow aquifer in the vicinity of the Class A South cell is generally to the north. This northerly flow direction is representative of the current conditions reflecting the effects of mounding due to surface water infiltration. The natural gradient is approximately to the northeast. Given the predominant flow direction, wells GW-19B, GW-27D, GW-25, and GW-1 were selected as locations providing the best available borehole logs for estimating the elevation of the bottom of the aquifer. Well construction details are provided in Table 3 and well locations are shown in Figure 2.

Table 3. Construction details for selected wells used for estimating the elevation of the bottom of the shallow aquifer.

Well Number	State Plane Coordinates (NAD 83)		Surface Elevation (ft)	Well Depth (ft bgs)	Date Drilled
	Easting (ft)	Northing (ft)			
GW-19B	1189865	7420999	4269	102	02/06/91
GW-27D	1190080	7423071	4270	100	12/28/98
GW-25	1191693	7423029	4274	34	12/19/91
GW-1	1191843	7420942	4273	42	03/03/88

Since the shallow aquifer is described as unconfined, the elevation of the top of the aquifer is determined by the water table elevation. At three of the locations, nearby wells with shallow screened intervals were used to obtain more representative values for the shallow water table elevation. Well construction details for the wells used for measurement of water level elevations are provided in Table 4 and well locations are shown in Figure 2. Well GW-19A is located 8 ft from well GW-19B, well GW-27 is located 45.6 ft from well GW-27D, and well GW-60 is located 37.6 ft from well GW-1. Given the average hydraulic gradient of 6.94×10^{-4}, the maximum error in water table elevation due to distance between the wells will be 0.03 ft. This error was considered small enough to be neglected in the estimate of aquifer thickness.

A map of the shallow aquifer showing fresh water equivalent head surface elevation contours was prepared by Envirocare (2004) using groundwater elevation measurements from February, 2004. These elevations are used for this analysis to provide continuity with past work describing the shallow aquifer. The fresh water elevations for the four wells were taken from Table 4 of Envirocare (2004) and are listed in Table 5.

The bottom elevations of the shallow aquifer at wells GW-19B and GW-27D were estimated from hydrologic cross-sections described in Envirocare (2000, 2004). A south to north cross-section on the west side of the Class A South cell is shown in Figure 3. At well GW-19B the elevation of the bottom of the aquifer is estimated to be where the silty sand interval grades into a clay interval. The borehole log for this well indicates that this transition occurs at an elevation of 4,229 ft.

Table 4. Construction details for selected wells used for water table elevations.

Well Number	State Plane Coordinates (NAD 83)		Screened Interval (ft bgs)	Well Depth (ft bgs)	Date Drilled
	Easting (ft)	Northing (ft)			
GW-19A	1189866	7421007	18 – 27.5	31.5	02/07/91
GW-27	1190121	7423091	20 – 29.5	32	12/11/91
GW-25	1191693	7423029	24 – 33.5	34	12/19/91
GW-60	1191832	7420906	22.5 - 27	28	02/02/93

The lower boundary is extended to the top of an extensive clay layer mapped in well GW-27D shown in Figure 3. The borehole log for this well indicates that the top of the clay layer occurs at an elevation of 4,238 ft.

Well GW-25 is 40 ft deep and screened in the bottom 10 ft of the well in a unit described as silty clay. The elevation of the bottom of the well is 4,240 ft. The saturated hydraulic conductivity measured in this well is reported by Envirocare (2004) as 1.05×10^{-3} cm/s. Comparing this result with a site-wide mean value of saturated hydraulic conductivity of 9.6×10^{-4} cm/s indicates that this well is completed within the shallow aquifer. The elevation of the bottom of the aquifer at this well may be deeper than the bottom of the well but is conservatively taken as 4,240 ft, the elevation of the bottom of the well.

Well GW-1 is 41.5 ft deep and is screened from 20 ft bgs to 40 ft bgs. The driller's log describes the sediments as a silty sand from 14 ft to 29 ft depth and sandy clay from 29 ft to the bottom of the borehole at 41.5 ft. Well GW-60 located 37.6 ft from well GW-1 is completed to a depth of 28 ft in sediments described as a silty clay. The interval from 22.5 ft bgs to 27 ft bgs within the silty clay is screened. Saturated hydraulic conductivity in well GW-60 was determined to be 3.4×10^{-3} cm/s or three times the site-wide average. This relatively high value of saturated hydraulic conductivity measured in a silty clay indicates the the shallow aquifer extends at least as deep as the bottom of well GW-1. Given this interpretation, the elevation of the bottom of the aquifer at this borehole is estimated to be 4,231 ft. The estimated elevations of the bottom of the shallow aquifer and the resulting saturated thicknesses are listed in Table 5.

A distribution for the thickness of the saturated zone was established based on four location measurements (GW-19B, GW-27D, GW-25, and GW-1), and professional judgment regarding the accuracy of the measurements. An aquifer thickness for each of the four locations was calculated as the difference between the recorded elevation of the water table and the elevation of the bottom of the shallow aquifer. Since the four locations do not quite form a square, triangulation was used to calculate an average thickness across the region. Only two possible triangulations exist for these four points, so both were computed, and the average of the two was used as the mean of the distribution for saturated zone thickness. Professional judgment was that the measurements are accurate to within 1 foot. Thus, 1 foot was interpreted as a two standard deviation range, giving a measurement standard deviation of 0.5 ft. Since four measurements are being averaged (with nearly equal weights), the resulting standard error for the mean is then

0.5 ft divided by the square root of 4. The resulting distribution for the mean thickness of the saturated zone was thus chosen as a normal distribution with mean equal to 16.2 ft with a standard deviation of 0.25 ft.

Table 5. Water table elevations, aquifer bottom elevations and estimated saturated thickness of the shallow aquifer.

Well Number	Water Table Elevation (ft)*	Bottom Elevation of Shallow Aquifer (ft)	Saturated Thickness (ft)
GW-19B	4251	4229	22
GW-27D	4250	4238	12
GW-25	4250	4240	10
GW-1	4251	4231	20

*GW-19B, GW-27D, and GW-1 water table elevations estimated from the elevation in nearby shallow aquifer wells.

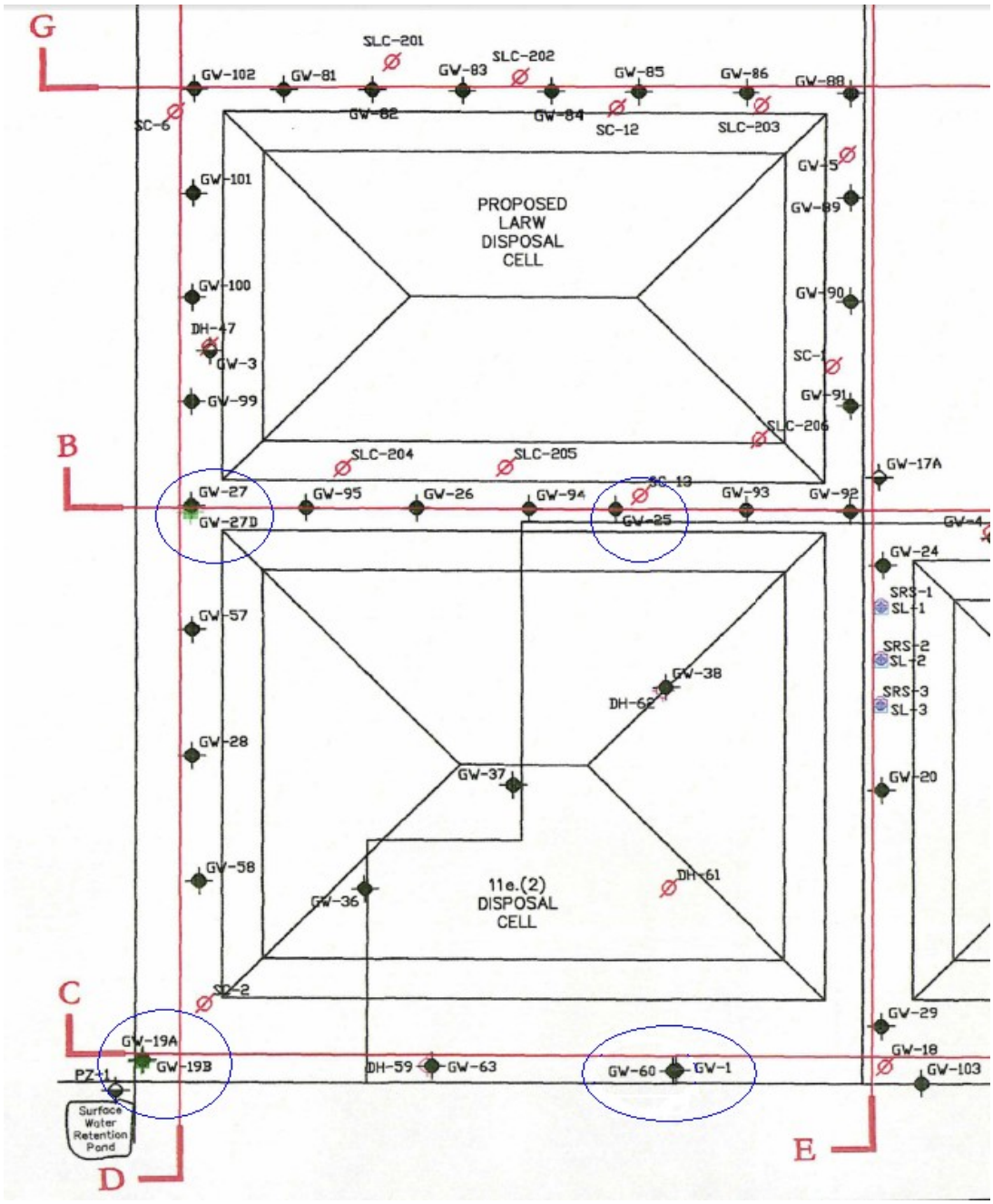

Figure 2: Well locations used for estimating shallow aquifer thickness.
Diagram is modified from Envirocare (2004).

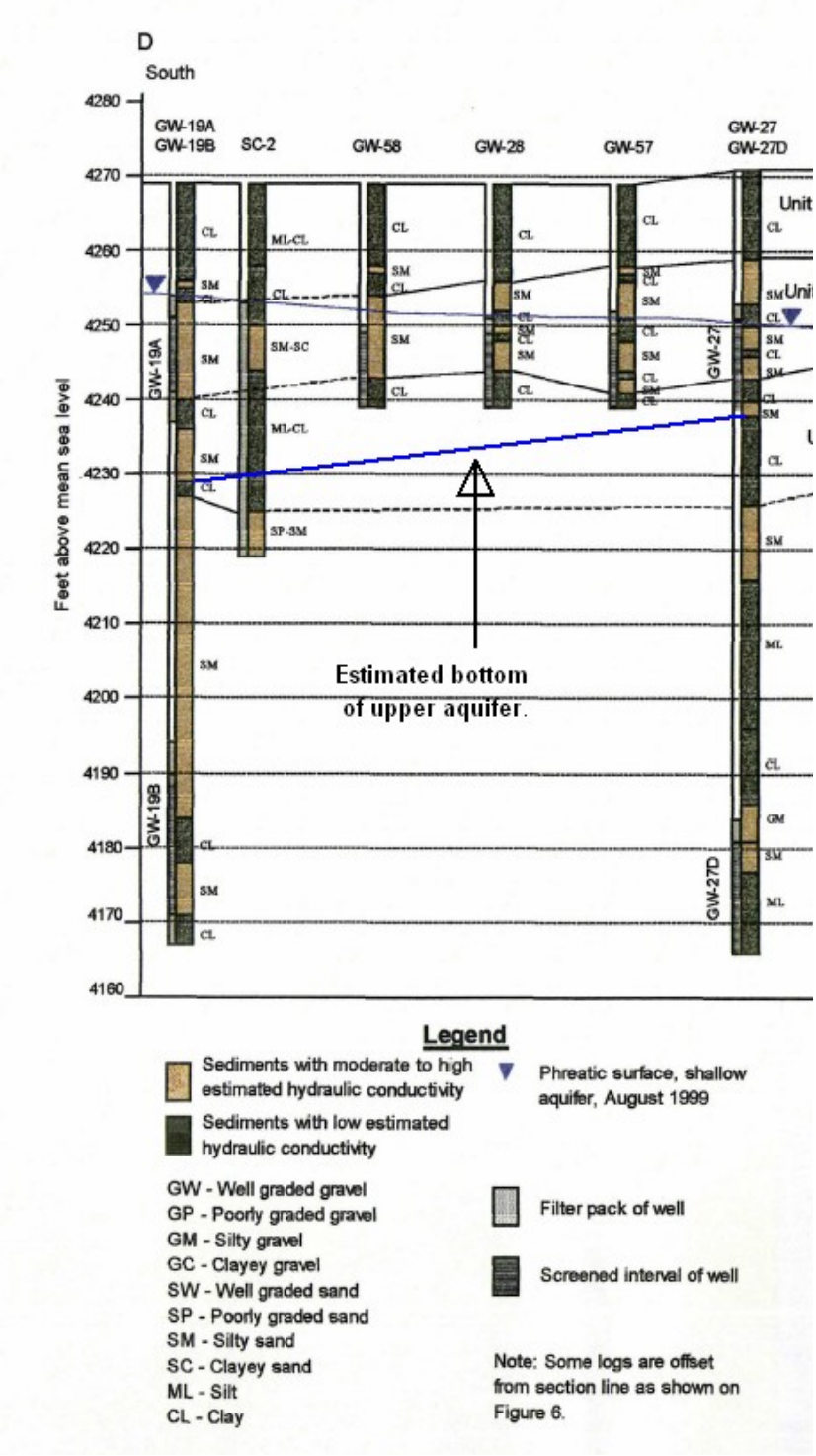

Figure 3: Cross-section D-D' modified from Envirocare (2004) showing estimated elevation of the bottom of the shallow aquifer.

4.2 Dispersion

The process of spreading of a contaminant in groundwater that occurs in addition to movement by advective flow is represented in mathematical models by the dispersion coefficient. The dispersion coefficient represents both the mechanical and chemical components of mixing and is written as:

$$D_l = \alpha_l \bar{v} + D_m \quad (2)$$

Where

D_l = longitudinal dispersion coefficient

α_l = longitudinal dispersivity

v = mean pore water velocity

D_m = molecular diffusion coefficient

Only longitudinal dispersion will be considered for this discussion because of the geometry of the transport pathway. The width of the disposed waste is the dimension perpendicular to the groundwater flow direction. This distance is 1,276.4 ft (Whetstone 2007, Figure 6). The distance from the edge of the waste to the compliance point is 250 ft (Whetstone 2007). With this geometry, the width of the source is more than 5 times the distance from the edge of the source to the point of compliance, making transverse dispersion insignificant.

In a numerical model such as the Clive DU PA Model, the discretization of the flow path into cells results in an apparent dispersion due to small numerical errors even with a value of zero for the dispersivity. Because of the inherent numerical dispersion, the dispersion coefficient is not explicitly included in the shallow aquifer transport calculations in the Clive DU PA Model.

5.0 References

Bingham Environmental. 1991. Hydrogeologic report Envirocare Waste Disposal Facility South Clive, Utah. October 9, 1991. Prepared for Envirocare of Utah. Salt Lake City, UT.

Bingham Environmental. 1994. Hydrogeologic report Mixed Waste Disposal Area Envirocare Waste Disposal Facility South Clive, Utah. November 18, 1994. Prepared for Envirocare of Utah. Salt Lake City, UT.

Brockwell, P. J. and Davis, R. A. 1996. *Introduction to Time Series and Forecasting*. Springer, New York.

Domenico, P.A. and F.W. Schwartz. 1990. *Physical and chemical hydrology*. New York: John Wiley and Sons.

Envirocare of Utah, Inc. 2000. Revised hydrogeologic report for the Envirocare Waste Disposal Facility Clive, Utah. Version 1.0. Envirocare of Utah, Inc. Salt Lake City, UT.

Envirocare of Utah, Inc. 2004. Revised hydrogeologic report for the Envirocare Waste Disposal Facility Clive, Utah. Version 2.0. Envirocare of Utah, Inc. Salt Lake City, UT.

Whetstone Associates. 2000, *Revised Envirocare of Utah Western LARW Cell Infiltration and Transport Modeling.* July 19, 2000.

Whetstone Associates. 2007. Energy*Solutions* Class A South Cell Infiltration and Transport Modeling. December 7, 2007.

Neptune and Company Inc.

June 1, 2011 Report for EnergySolutions

Clive DU PA Model, version 1

Appendix 8

Air Modeling

Atmospheric Transport Modeling for the Clive DU PA

28 May 2011

Prepared by

Neptune and Company, Inc.

This page is intentionally blank, aside from this statement.

CONTENTS

FIGURES

TABLES

1 Summary of PA Model Inputs

A summary of parameter values and distributions employed in the atmospheric modeling component of the Clive Performance Assessment (PA) model is provided here. Additional information on the derivation and basis for these inputs is provided in subsequent sections of this report. With the exception of particulate resuspension flux, the PA model inputs related to atmospheric modeling are derived from AERMOD air dispersion modeling results. The term Chi/Q refers to the ratio of breathing-zone air concentration (*Chi*) to the emission rate (*Q*) used in the AERMOD simulations. The term PM_{10} refers to particulates with a mean aerodynamic diameter of 10 μm and less, the size fraction employed in regulatory air modeling to represent respirable particles.

PA Model Parameter	Units	Value	Notes
Chi / Q ratios for PM_{10}	$\mu g/m^3$ per g/s	See Table 3	Based on AERMOD modeling; see Section 6.2.1 .
Chi / Q ratios for gases	$\mu g/m^3$ per g/s	See Table 4	Based on AERMOD modeling; see Section 6.2.1 .
Embankment PM_{10} redeposition	g/m2-yr per g/yr	See Table 5	Based on AERMOD modeling; see Section 6.2.2 .
Resuspension flux of PM_{10}	kg/m^2-yr	LogUniform (2.5e-7, 0.3)	Implementation of Cowherd et al (1985); see Section 6.4 .
Fraction PM_{10} deposition in off-site exposure area	—	See Table 5	Based on AERMOD modeling; see Section 6.2.2 .

2 Introduction

The safe storage and disposal of depleted uranium (DU) waste is essential for mitigating releases of radioactive materials and reducing exposures to humans and the environment. Currently, a radioactive waste facility located in Clive, Utah (the "Clive facility") operated by the company Energy*Solutions* Inc. is being considered to receive and store DU waste that has been declared surplus from radiological facilities across the nation. The Clive facility has been tasked with disposing of the DU waste in a manner that protects humans from future radiological releases.

To assess whether the proposed Clive facility location and containment technologies are suitable for protection of human health, specific performance objectives for land disposal of radioactive waste set forth in Utah Administrative Code (UAC) Rule R313-25 *License Requirements for Land Disposal of Radioactive Waste - General Provisions* must be met—specifically R313-25-8 *Technical* Analyses (Utah 2010). In order to support the required radiological performance assessment (PA), a probabilistic computer model has been developed to evaluate the doses to human receptors that would result from the disposal of radioactive waste, and conversely to determine how much waste can be safely disposed at the Clive facility. The GoldSim systems analysis software (GTG 2011) was used to construct the probabilistic PA model.

The site conditions, chemical and radiological characteristics of the wastes, contaminant transport pathways, and potential human receptors and exposure routes at the Clive facility that are used to structure the quantitative PA model are described in the conceptual site model documented in *Conceptual Site Model for Disposal of Depleted Uranium at the Clive Facility* (Clive DU PA CSM.pdf). Based on current and reasonably anticipated future land uses, the two future use exposure scenarios described in the CSM for evaluation in the PA are ranching and recreation.

The Neptune and Company, Inc. (Neptune) white paper *Dose Assessment for the Clive PA* (Dose Assessment.pdf) details the assumptions and computational methods for estimating radiation doses to future human receptors associated with DU and its decay products. This present white paper focuses on one aspect of the exposure and radiation dose calculations; atmospheric modeling to support the calculation of breathing zone air concentrations of radionuclides for future human receptors. Specifically, this paper addresses the modeling of:

1. Rates of particle resuspension by aeolian (wind derived) processes;
2. Air concentrations of radionuclides above the disposal embankment and at specific locations of potential off-site exposure; and,
3. Deposition flux of resuspended embankment particles at locations beyond the embankment.

Particle resuspension related to mechanical disturbances from off-highway vehicle (OHV) use is also addressed in the PA model and is discussed in the white paper *Dose Assessment for the Clive PA*.

3 Overview and Framework

Atmospheric dispersion modeling was conducted using computer software outside of the GoldSim modeling environment, as the GoldSim PA model is a system-level model. An atmospheric dispersion model is a mathematical model that employs meteorological and terrain elevation data, in conjunction with information on the release of contamination from a source, to calculate breathing-zone air concentrations at locations above or downwind of the release. Some models may also be used to calculate surface deposition rates of contamination at locations downwind of the release.

Air dispersion models, including the AERMOD (EPA, 2011a) and CAP-88 (EPA, 2011b) models used in this exercise, commonly assume a Gaussian distribution for estimating vertical and horizontal dispersion of contamination away from the source. Factors affecting the amount of dispersion include atmospheric turbulence, the height of the release (e.g., a virtual stack versus ground level), the buoyancy of the plume, and terrain features. Although they employ different mathematical models for assessing horizontal and vertical dispersion, both AERMOD and CAP-88 ultimately calculate annual-average contaminant breathing zone air concentrations at various distances and in various directions from a source release.

The Clive facility waste disposal embankment will be a large-area emissions source with a gently sloping surface that will be raised approximately 15 m above the surrounding terrain. There are two types of future radioactive emissions associated with the embankment:

1. Particulate emissions of contaminated surface soil due to aeolian erosion; and,
2. Emissions of gas-phase radionuclides diffusing across the surface of the embankment into the atmosphere.

With respect to potential human receptors exposed upon the embankment itself (ranchers and recreationalists, including hunters, and OHV sport riders—see the *Dose Assessment* white paper), the surface of the embankment represents a ground-level (0-m height) emissions source. For estimating the annual dose to these individuals, the air modeling endpoint of interest is the annual-average breathing-zone concentration of respirable particles or gaseous radionuclides above the embankment. For individuals exposed at locations other than the embankment, the embankment represents a 15-m elevation emissions source, as transport by wind will be necessary for exposure at these locations. A second air modeling endpoint of interest for these "off-site" receptors is the same as for the "on-site" receptors; i.e., the annual-average breathing-zone concentration of respirable particles or gaseous radionuclides released from the embankment at some specific off-site location.

A third endpoint of interest is the off-site deposition rate of embankment particulates. As particulates eroding from the embankment are deposited on surrounding land, this surrounding area may become a secondary source of radionuclide exposure for ranchers and recreationists. The relative importance of exposure on-site and off-site depends in part on the fraction of total exposure time a rancher or recreationist spends in each area. However, the importance of on-site vs. off-site exposure also depends on the rate of aeolian particle erosion from the embankment and the rate at which contamination from the disposed waste is transported to the the surface of the embankment by processes such as biotic transport (see *Biological Modeling* white paper) and radon diffusion. If transport rates of radioactivity are much higher than the rate at which aeolian particle erosion removes radioactivity, then embankment surface soil radionuclide concentrations will steadily increase over time relative to off-site levels. However, if aeolian particle erosion rates are greater than the transport/accumulation rate of radioactivity in surface soil, then embankment soil radioactivity will be minimal throughout the modeling period. Because only a portion of wind-eroded particles remain within the overall receptor exposure area, and because receptor exposure intensity varies between the embankment and the off-site exposure area, this can have significant consequences for dose assessment results.

In summary, there are three air modeling endpoints:

1. Annual-average breathing-zone concentration of respirable particles and gaseous radionuclides above the embankment;
2. Annual-average breathing-zone concentration of respirable particles and gaseous radionuclides at specific off-site locations; and,
3. Off-site aeolian deposition rate of embankment particulates.

For gas-phase radionuclides, the contaminant transport component of the GoldSim PA model (see *Unsaturated Zone Modeling* white paper) provides the diffusive flux (activity per area per time, as in $Bq/m^2 \cdot s$) at the surface of the disposal embankment. A particulate resuspension model, described below, is employed to calculate the particle flux from the surface of the disposal embankment. The gas-phase radionuclide and particle fluxes are the site-specific inputs to the air dispersion model. The third endpoint, the off-site deposition rate of embankment particulates, is used as an input for modeling radionuclide soil concentrations over time in the off-site exposure area for ranchers and recreationists.

AERMOD, a United States Environmental Protection Agency (EPA)-recommended regulatory air modeling system that incorporates state-of-the-art modeling approaches (EPA, 2011a), is used for the air dispersion modeling to address the three endpoints. As a quality assurance measure, a second EPA regulatory air dispersion model (CAP-88; EPA, 2011b) is employed to confirm the AERMOD results (see Section 6.3).

4 Model Descriptions

The following subsections provide a summary of the particle resuspension and air dispersion models used to support the modeling endpoints described above.

4.1 Cowherd Particle Resuspension Model

Air dispersion models for estimating radionuclide concentrations above, or at some distance from, a release source require a radionuclide emission rate as an input. In the case of aeolian soil particulates in ambient air (e.g., dust), an area-averaged particulate resuspension rate is needed. For screening of potential inhalation risks at contaminated soil sites, EPA recommends a particulate emission factor (PEF) model to estimate annual average concentrations of respirable particulates (approximately 10 μm and less; i.e., PM_{10}) in ambient air above contaminated soil (EPA, 1996; EPA, 2002).

The PEF incorporates PM_{10} emission models (Cowherd et al, 1985) related to wind erosion under one of two conditions. The particulate emission model for PM_{10} used in EPA (1996; 2002) pertains to a surface with unlimited erosion potential. Cowherd et al (1985) also provide a model for estimating PM_{10} particle emissions from surfaces with a limited reservoir of erodible particles. The decision criterion in choosing between these model types is provided in Figure 3-2 of Cowherd et al. (1985) as, "Is threshold friction velocity > 75 cm/s?" For surfaces not covered by continuous vegetation, including assumed future states of the disposal embankment (see *Biological Modeling* white paper), surfaces with a threshold friction velocity larger then 75 cm/s tend to be composed of elements too large to be eroded, or of erosion-resistant crusts. An erosion-resistant crust might be of cryptogamic nature (particles bound by a biological community consisting of one or more types of cyanobacteria, lichens, mosses, and fungi), or simply by aggregation of very fine silty-clay particles.

Methods for characterizing threshold friction velocity in Cowherd et al. (1985) rely on site inspection, which is problematic for this modeling because the future surface characteristics of the embankment are uncertain. The foreseeable future state of the cap surface likely includes a range of particle sizes due to contributions from windblown loess, from decaying plant material,

and from degrading rip rap. A practical constraint on the use of the limited-reservoir model of soil erosion is that this model is dependent upon the frequency of disturbance of the surface. When a surface has limited erosion potential, disturbances to expose fresh surface material are considered necessary to restore erodibility. For the Clive PA model, a range of input parameter values are used with the unlimited-reservoir model to estimate possible PM_{10} emission rates based on the presumption of dynamic steady-state conditions, where PM_{10} emissions are presumed to be balanced by deposition of particles from upwind locations.

The equation for particle emissions from a surface with *unlimited* erosion potential, originally published as Equation 4-4 in Cowherd et al. (1985), has the form:

$$E_{10} = 0.036 \times (1 - V) \times ([u] / u_{t\text{-}7})^3 \times F(x) \quad (1)$$

where:

E_{10} is the annual-average PM_{10} emission rate per unit area of contaminated soil ($g/m^2 \cdot hr$);
V is the fraction of vegetative cover (-);
$[u]$ is the mean annual wind speed (m/s);
$u_{t\text{-}7}$ is the threshold value of wind speed at 7 m (m/s); and,
$F(x)$ is a function dependent on the ratio u / u_t (-).

and, from Equation 4-3 in Cowherd et al. (1985):

$$u_{t\text{-}7} = (u_t \times F_{adj} / 0.4) \times \ln(700 \text{ cm} / z_0) \quad (2)$$

where:

u_t is the unadjusted threshold friction velocity (m/s);
F_{adj} is the threshold friction velocity adjustment factor; and,
z_0 is the surface roughness height (cm).

Values of $F(x)$ are estimated based on the function shown graphically in Figure 4-3 of Cowherd et al. (1985). The value of x is calculated as defined in Equation 4-4 of Cowherd et al. (1985):

$$x = 0.886 \times (u_{t\text{-}7} / [u]) \quad (3)$$

and the function $F(x)$ is approximated using the following equations:

when $x < 1$, $F(x) = (6 - x^3)/\pi$
when $x \geq 1$ and < 2, $F(x) = (-1.3 \times x) + 2.89$
when $x \geq 2$, $F(x) = [(8 \times x^3) + (12 \times x)] \times e^{-(x\text{^}2)}$.

With the exception of the case where $x \geq 2$, these equations were fit by Neptune and Company based on visual approximation to the graphic in Figure 4-3 of Cowherd et al. (1985). For the case $x \geq 2$, the equation is taken from Appendix B of Cowherd et al (1985).

4.2 AERMOD

AERMOD is EPA's recommended regulatory air modeling system for steady-state emissions. It is defined by EPA (2011a) as

> "A steady-state plume model that incorporates air dispersion based on planetary boundary layer turbulence structure and scaling concepts, including treatment of both surface and elevated sources, and both simple and complex terrain."

AERMOD supports source characterization as an area of user-defined dimensions and elevation and is thus suitable for modeling the disposal embankment. AERMOD employs two pre-processors related to handling of meteorological data and terrain data. The AERMET pre-processor is used to estimate boundary layer parameter values such as mixing height and friction velocity needed for the air dispersion modeling. AERMET inputs include albedo (a measure of the reflectivity of the ground surface), surface roughness, and Bowen ratio (a measure of heat flux to the atmosphere), plus meteorological measurements such as wind speed and direction, temperature, and cloud cover. The AERMAP pre-processor uses gridded terrain elevation data to generate receptor grids for the air dispersion modeling.

In the stable boundary layer nearest the earth's surface, AERMOD assumes a Gaussian concentration distribution on the vertical and horizontal axes. In the convective boundary layer above, the horizontal distribution is also assumed to be Gaussian, but the vertical distribution is described using a linear combination of two separate Gaussian functions. In this manner AERMOD addresses heterogeneity in the planetary boundary layer where wind and associated mixing is influenced by friction with the earth's surface.

4.3 CAP-88

The Clean Air Assessment Package – 1988 (CAP-88) modeling program (EPA, 2011b) is recommended for demonstrating regulatory compliance with the requirements of Subpart H of 40 CFR Part 61 (NESHAPS; National Emission Standards for Emissions of Radionuclides Other Than Radon from Department of Energy Facilities). As described in 10 CFR 40 Part 61.93, 12-15-1989:

> "To determine compliance with the standard, radionuclide emissions shall be determined and effective dose equivalent values to members of the public calculated using EPA approved sampling procedures, computer models CAP–88 or AIRDOS-PC, or other procedures for which EPA has granted prior approval."

CAP-88 employs a modified Gaussian plume dispersion model to compute ground-level radionuclide air concentrations for a circular grid around an emission source. Meteorological data must be processed into STability ARray (STAR) files for CAP-88, which include assignments of atmospheric turbulence into one of six stability classes labeled A through F.

5 Meteorological and Terrain Elevation Data

Raw meteorological data from the the Energy*Solutions* monitoring station at Clive, Utah were collected (MSI, 2010). The monitoring station is at 1,306 m above sea level, and is equipped to measure horizontal wind speed, wind direction, 2-and 10-meter temperature, delta-temperature

for the derivation of atmospheric stability class, solar radiation, precipitation, and evaporation (MSI, 2010).

Meteorological Solutions Inc. (MSI), processed the raw meteorological data to create AERMET files (for AERMOD air dispersion modeling) and STAR files (for CAP-88 air dispersion modeling). STAR files were created by MSI using two different methods. The sigma-theta method (STAR-ST) assigns an atmospheric stability class based on the standard deviation of the horizontal wind direction. A second method (STAR-SR) assigns an atmospheric stability class based on solar radiation and delta-temperature measurements. The processed meteorological data were then employed by Neptune for the air dispersion modeling. AERMET, STAR-ST, and STAR-SR input files for the years 2003, 2004, 2006, 2007, and 2009 were made available to Neptune by MSI. Composite STAR-SR and STAR-ST files integrating meteorological data for all five years were also created by MSI and provided to Neptune.

A Clive, Utah wind rose from MSI (2010), showing wind speed and direction for the period January 2009 through December 2009, is duplicated here as Figure 1. As shown in Figure 4.1 of MSI (2010), the wind rose integrating data for the period 1993 through 2009 is very similar to that for 2009 shown here. For example, average annual wind speed for both time periods is 7.2 mph and stability class variability for 1993-2009 and just 2009 is less than 5% (MSI, 2010).

Terrain elevation information for each grid cell was derived from the AERMAP interface within the AERMOD View™ (Version 6.7.1) software package (Lakes Environmental, 2010). AERMAP accesses digital elevation model (DEM) data from webGIS (http://www.webgis.com), which is then processed for input into AERMOD. For this project, DEM data from the United States Geological Survey (USGS) for Tooele County, Utah are employed. These data have a nominal resolution of 90 m and were interpolated to the uniform Cartesian grid (i.e., the modeling area) using the inverse distance weighting setting, which is the recommended setting in AERMAP. The nature of the AERMOD View™ interface, and the basis of the spatial receptor grid, are described in Section 6.1 .

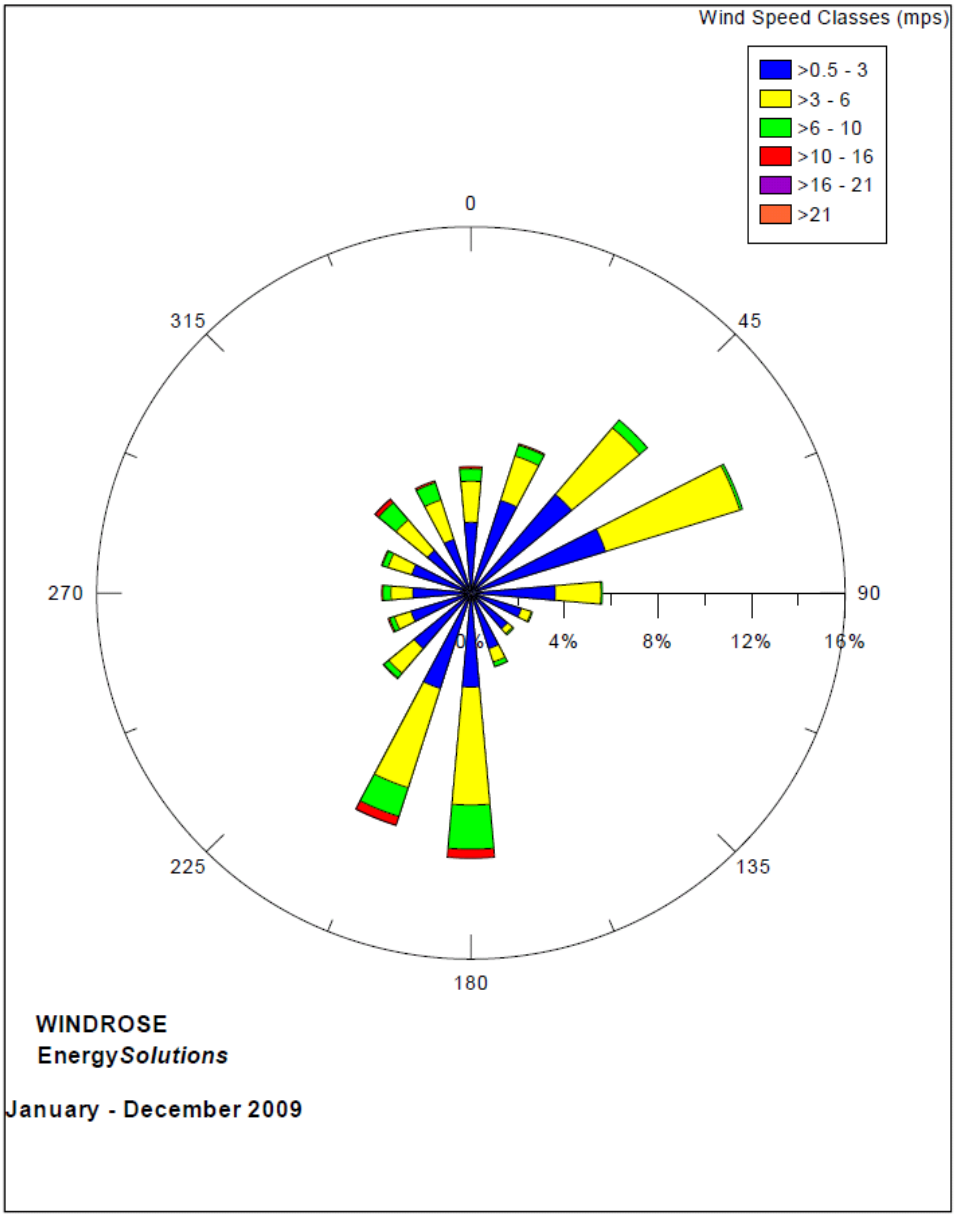

Figure 1. Wind Rose for Clive, Utah (courtesy of Meteorological Solutions, Inc.)

6 Implementation of Resuspension and Dispersion Models

Neptune implemented AERMOD within the graphical user interface AERMOD View™ (Lakes Environmental, 2010). This software package provides an interface for using base maps to define sources and receptors, importing digital elevation data from USGS, and producing graphical displays of results.

6.1 Spatial Attributes of Air Dispersion Modeling

As described in Section 1, the intent of the air dispersion modeling was to estimate air concentrations of radionuclides above the disposal embankment, and for receptors at specific locations of potential off-site exposure. These receptors and off-site locations, described in the Dose Assessment white paper, include:

- Travelers on Interstate-80 which passes 4 km to the north of the site;
- Travelers on the main east-west rail line which passes 2 km to the north of the site;
- The resident caretaker present at the east-bound Grassy Mountain (Aragonite) Interstate-80 rest area 12 km to the northeast of the site;
- Recreational users of the Knolls OHV area (BLM land that is specifically managed for OHV recreation) 12 km to the west of the site; and,
- Workers at the Utah Test and Training Range (UTTR, a military facility) to the south of the Clive facility, who may occasionally drive on an access road immediately to the west of the Energy*Solutions* fenceline.

These five locations are shown in Figure 2. A uniform Cartesian grid using 1-km^2 resolution grid cells was employed in the AERMOD air dispersion modeling to support calculation of air concentrations at the first four locations. This grid was constructed of 299 grid cells (23 grid cells longitudinally by 14 grid cells latitudinally).

To support the estimation of air concentrations above the disposal embankment and particle deposition onto the embankment, AERMOD was also run with a smaller 0.3-km^2 grid size, which corresponds to the area of the disposal embankment. In this AERMOD simulation, one grid cell was centered directly above the 0.3-km^2 area emissions source representing the embankment. The results for this grid cell were also applied to the UTTR access road, which is in close proximity to the disposal embankment.

Figure 2. Off-site air dispersion locations (Note: red line is the rail; green line is UTTR access road).

6.2 AERMOD Results for Air Concentrations and Off-Site Deposition

Two sets of simulations were conducted using AERMOD; one to estimate air concentrations and total deposition of particulates, and a second to estimate gas concentrations at the specified receptor locations in Section 6.1 . The air concentration outputs (particulate and gas) from AERMOD were then used to calculate χ/Q ratios, which are the ratio of breathing-zone air concentration (χ) to the emission rate (Q) used in the AERMOD simulations (Section 6.2.1). These χ/Q ratios are then employed in the GoldSim model for each receptor location by multiplying χ/Q by the gas or particle emission rate generated in the model. Particle deposition rates from AERMOD were used to calculate the fraction of particulates that are redeposited on the embankment (Section 6.2.2). This off-site deposition fraction was used in conjunction with the particle emission rate generated in the model to calculate the mass of embankment particles deposited onto the off-site air dispersion area over time.

6.2.1 AERMOD Simulated Air Concentrations and Chi/Q Values

As described in Section 6.1 , AERMOD was run using either a 0.3-km^2 or a 1.0-km^2 resolution grid, depending on whether the air concentrations above the embankment or at distant off-site locations were simulated. A consideration in the air dispersion modeling is the elevation of the area source. For modeling air concentrations in the breathing zone above an area source, it is necessary to define a zero meter-elevation release height in AERMOD. For modeling air

concentrations at the locations of distant off-site receptors, however, the disposal embankment is more accurately represented as an area source with a 15-m release height (where 15 m is the approximate height of the gently sloping top of the embankment).

An assumed PM_{10} emission rate of 0.25 g/sec was used for all AERMOD simulations. This value corresponds to an area flux of approximately 0.025 kg/m^2-yr, which is near the upper end of PM_{10} emission rates derived using Cowherd et al (1985) (see Section 6.4). The AERMOD results are used to develop χ/Q ratios, which in principle are independent of the specific emission rate used in the simulations. The emission rate input to AERMOD was varied over several orders-of-magnitude, and it was confirmed that the ratio χ/Q is independent of emission rate.

The relative mass associated with two particle size fractions within the PM_{10} category can be distinguished in AERMOD: 0 to 2.5 micron particle diameter, and 2.5 to 10 micron particle diameter. The actual particle size distribution of future PM_{10} emissions from the embankment is unknown. To explore the influence of particle size fraction on on-site and off-site PM_{10} air concentrations, the mass of particles in the two categories for a series of eight simulations was varied as presented in Table 1:

Table 1: Allocation of particle mass in particle size fraction bins for PM_{10} emissions.

Simulation	0 to 2.5 microns	2.5 to 10 microns
1	0%	100%
2	5%	95%
3	10%	90%
4	20%	80%
5	40%	60%
6	60%	40%
7	80%	20%
8	100%	0%

Note that these fractions represent fine particle fractions only, and assume that less than 10% of the particle emissions is composed of dust greater than or equal to 10 microns in diameter.

The AERMOD particulate simulations in Table 1 were conducted using meteorological input data for year 2009, as previously discussed. Additional simulations were conducted using meteorological data from 2003, 2004, 2006, and 2007. The differences in modeled air concentrations among the five data sets was minimal. Uncertainty related to meteorological conditions is overwhelmingly due to extrapolating current conditions (as represented by any of these five years) to the 10,000-year performance period, which is not possible to quantify at this time. Therefore, uncertainty related to the slight differences in AERMOD results based upon the five data sets has not been propagated in the GoldSim PA model.

As described above, two sets of simulations were conducted at different spatial resolutions (0.3-km^2 and 1.0-km^2) for the particle size fractions outlined in Table 1. The outputs from these simulations are summarized in Table 2.

Table 2: Air concentration estimates (ug/m^3 of PM_{10}) by location and particle diameter fraction; 0.25 g/s emission rate.

Simulation	Knolls OHV Area	Grassy Mt. (Aragonite) Rest Area	I-80	Railroad	Embankment	UTTR Access Road
1	0.011	0.0017	0.065	0.11	56	56
2	0.011	0.0017	0.066	0.11	56	56
3	0.011	0.0017	0.066	0.11	56	56
4	0.011	0.0017	0.067	0.11	56	56
5	0.012	0.0018	0.068	0.11	57	57
6	0.013	0.0018	0.069	0.11	58	58
7	0.014	0.0018	0.070	0.11	59	59
8	0.015	0.0019	0.071	0.11	59	59

Concentration estimates for the Embankment and UTTR Access Road receptors are based on simulations conducted at 0.3-km^2 resolution. All other concentrations correspond to simulations conducted at 1.0-km^2 resolution. Values for I-80 and Railroad are the largest values for any grid cell containing these features (i.e. at points close to the Clive facility). Note that the simulation numbers in this table correspond to the particle diameter fractions in Table 1.

The AERMOD input emission rate and the air concentration outputs from AERMOD were then used to construct χ/Q ratios for each receptor, as shown in Table 3. The Q term for this ratio is 0.25 g/sec, as described above. The χ term ($\mu g/m^3$) is from Table 2. These χ/Q ratios were then directly imported into the GoldSim PA model. For each model realization, one of the eight simulations is selected and the associated χ/Q ratios are used in the dose calculations. Differences among the eight sets of χ/Q ratios represent uncertainty in the particle size distribution of future PM_{10} emissions from the embankment.

Table 3: Receptor-specific χ/Q ratios for PM_{10} particulates.

Simulation	Knolls OHV Area	Grassy Mt. (Aragonite) Rest Area	I-80	Railroad	Embankment	UTTR Access Road
1	0.043	0.0069	0.26	0.43	222	222
2	0.044	0.0069	0.26	0.43	223	223
3	0.044	0.0069	0.26	0.43	224	224
4	0.046	0.0070	0.27	0.43	225	225
5	0.049	0.0071	0.27	0.43	228	228
6	0.052	0.0072	0.28	0.44	231	231
7	0.055	0.0073	0.28	0.44	234	234
8	0.058	0.0074	0.28	0.44	238	238

χ/Q ratios for the Embankment and UTTR Access Road receptors are based on simulations conducted at 0.3-km^2 resolution. All other off-site receptors correspond to simulations conducted at 1.0-km^2 resolution. Values for I-80 and Railroad are the largest values for any grid cell containing these features. Note that the simulation numbers in this table correspond to the particle diameter fractions in Table 1.

As described in Section 3 , air concentrations of gases in the off-site air dispersion area are based on air dispersion of gas emissions from the cap. The size and basis of the off-site air dispersion area (see Figure 3) is discussed in the *Dose Assessment* white paper, and is that area surrounding the embankment in which ranchers and recreationists may be exposed to contaminants originating from the embankment. Radon-222 is the only gas-phase radionuclide evaluated in the Clive PA model. Breathing zone concentrations of radon-222 in the off-site air dispersion area are based on releases from the cap, rather than evolution from any radium-226 deposited with particulates in dispersion area surface soil, because the former will be by far the more significant source. Radon transport in the embankment is discussed in the *Unsaturated Zone Modeling for the Clive PA* white paper.

Radon-222 air concentrations in the off-site air dispersion area have been calculated based on the smallest potential size of this area (16,000 acres, or approximately 65 km^2). The gas concentration in air for this area was calculated as the arithmetic average of the gas concentrations in the 65 AERMOD 1-km grid areas with the highest concentrations.

Radon-222 air concentrations were estimated using the gas deposition module in AERMOD for the embankment and the 5 other receptor locations described in Section 6.1 . Similar to estimating air concentrations for PM_{10} dust, these simulations were conducted with a 0-m elevation source for a 0.3-km^2 grid size (over the embankment and for the adjacent UTTR access road) and a 15-m elevation source with a 1.0-km^2 grid size (all other receptor locations). However, only one simulation each was conducted for radon gas dispersion because uncertainty related to particle size fraction is inapplicable to gases.

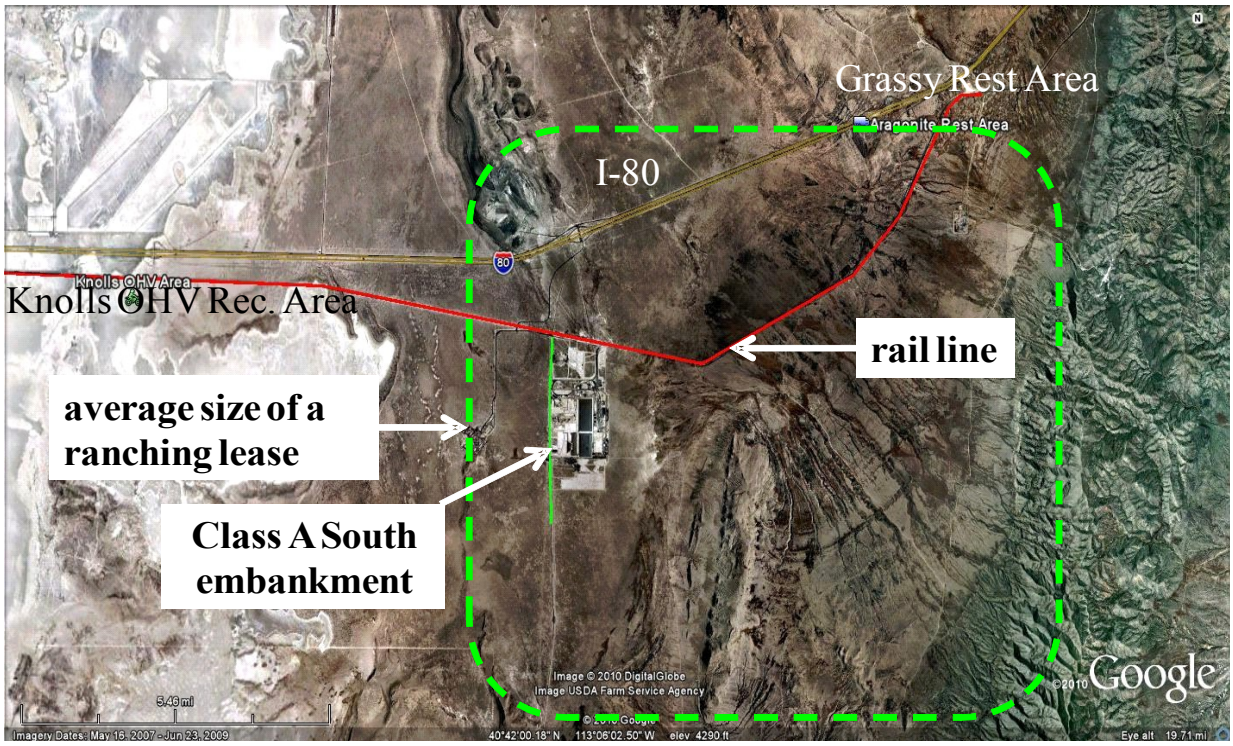

Figure 3. Off-site air dispersion area (approximate dimensions of largest receptor exposure area shown as dashed green line).

The input parameters required by AERMOD include diffusivity of the modeled gas in air and water, cuticular resistance, and Henry's Law constant. For radon diffusivity in air, a value of 0.11 cm^2/sec was assumed (Rogers and Nielson, 1991; Nielson and Sandquist, 2011). For radon diffusivity in water, a value of 100,000 cm^2/sec was assumed (Volkovitsky, 2004), while Henry's Law constant was assumed to be 0.0093 mol/kg-bar (NIST, 2011). The landcover properties were assigned the default values from AERMOD corresponding to category 8, or "barren land, mostly desert". Cuticular resistance, a measure of gas uptake by plants, was set to an arbitrarily low value of 0.1 sec/cm because this parameter was expected to have little influence for AERMOD simulations in a desert environment. The low influence of the value of cuticular resistance on modeled gas concentrations was confirmed by setting the value to 100 sec/cm and observing no change in radon air concentrations. As with particulates, radon air concentrations were simulated using meteorological data for year 2009.

Table 4 presents the output air concentrations for radon for each receptor location and their associated χ/Q ratios that are input into the GoldSim model.

Table 4: Radon air concentrations (0.25 g/s emissions) and χ/Q ratios for each receptor location.

Receptor Location	Air Concentration (μg/m^3)	χ/Q ratio (μg/m^3 per g/s)
Embankment (OnSite)	59	234
Knolls OHV Area	0.013	0.053
Grassy Mt. (Aragonite) Rest Area	0.0022	0.0088
I-80	0.070	0.28
Railroad	0.11	0.44
UTTR Access Road	59	234
Off-Site Exposure Area	0.096	0.38

χ/Q ratios for the Embankment and UTTR Access Road receptors are based on simulations conducted at 0.3-km^2 resolution. All other off-site receptors correspond to simulations conducted at 1.0-km^2 resolution. Values for I-80 and Railroad are the largest values for any grid cell containing these features.

6.2.2 AERMOD Off-Site Particulate Deposition

In addition to calculating air concentrations of gases and particulates, AERMOD was used to calculate the fraction of annual mass deposition (g/yr) of resuspended embankment particles outside the perimeter of the embankment. The total mass of deposited particulates within AERMOD is a function of the size of the grid area, and is therefore only approximated with a finite grid area. However, suspended particle re-deposition on the embankment is available as an output of AERMOD using the 0.3-km^2 grid size described in Section 6.1 . The fraction of total particulate mass deposited outside the embankment area can be calculated by mass balance as:

$$Dep_{off\text{-}site} = 1 - (Dep_{site} / E_{site}) \quad (4)$$

where:

$Dep_{off\text{-}site}$ is the fraction of annual PM_{10} emissions deposited beyond the embankment;

E_{site} is the annual-average PM_{10} emission rate per unit area of contaminated soil (g/m^2·yr); and,

Dep_{site} is the annual deposition rate of resuspended site PM_{10} within the site perimeter per unit area of contaminated soil (g/m^2·yr).

The majority of PM_{10} particulates deposited outside the embankment are carried by atmospheric transport to regions far beyond the vicinity of the embankment. The fraction of all PM_{10} emissions that is deposited within the combined area of the embankment and the largest potential size of the off-site dispersion area (64,000 acres, or 260 km^2; see the *Dose Assessment* white paper) varies depending on PM_{10} particle size fraction (see Table 1) between approximately 4% and 11%.

The remaining PM_{10} mass (89% to 96%) can be expected to be deposited over some very large region outside the receptor grid at rates no greater than the low values that were calculated with AERMOD near the receptor grid boundaries. The exact size of this region is influenced by regional atmospheric conditions and terrain features. At distances beyond approximately 20 to 50 km, AERMOD is unsuitable for air dispersion modeling and a long-range regional model would be required for quantifying concentrations and deposition rates. The fraction of total particulate mass deposited within the off-site exposure area is calculated as:

$$Dep_{off\text{-}site\ dispersion\ area} = f_{local} \times Dep_{off\text{-}site} \quad (5)$$

where:

f_{local} is the fraction of annual PM_{10} deposition occurring within the off-site dispersion area (see Table 5, Column 4); and ,

$Dep_{off\text{-}site}$ is the fraction of annual PM_{10} emissions deposited beyond the embankment from Equation 4.

To estimate the total amount of particulate matter deposited on the disposal embankment (Dep_{site}) for Equation 4, AERMOD simulations were performed using the 0.3-km^2 resolution grid for each of the eight particle size fraction combinations given in Table 1. Table 5 presents the AERMOD output for total deposition over the disposal embankment. To estimate the amount of redeposited material, the total mass emitted on an annual basis was calculated based on the AERMOD input emission rate of 0.25 g/sec. The total annual mass of particulates emitted each year from the source area is therefore 7,884,000 g. The total mass of particulate matter deposited per square meter over the embankment (Table 5, Column 2) was then divided by the annual mass emitted to give an estimate of on-site redeposition of particulate matter (Table 5, Column 3) for each of the eight simulations. These results were integrated into the GoldSim PA model in a manner analogous to that described for particle air concentrations in Section 6.2.1 .

Table 5: Total deposition of PM_{10} particulate matter on the disposal embankment.

Simulation	Total Deposition (g/m^2-yr)	On-site redeposition (g/m^2-yr per g/yr)	Fraction off-site deposition occurring in off-site exposure area
1	3.3	4.2E-07	0.11
2	3.2	4.1E-07	0.11
3	3.2	4.0E-07	0.11
4	3.0	3.8E-07	0.099
5	2.6	3.3E-07	0.086
6	2.2	2.8E-07	0.072
7	1.8	2.3E-07	0.057
8	1.4	1.8E-07	0.041

6.3 Confirmation of AERMOD Results with CAP-88

Version 3 of the CAP-88 air dispersion model was used to confirm the results of the AERMOD simulations. The purpose of this comparison was to perform a quality assurance check on AERMOD data preparation. As described in Section 5 , two types of STAR files for input of meteorological data to CAP-88 were prepared by MSI. The variability in CAP-88 results using STAR-ST vs STAR-SR files was about 10-20%, and a number of user input variables (such as the height of the tropospheric “lid” on mixing) were set at default values. On the AERMOD side, air concentrations and particle depositions varied by up to a factor of two depending on the particle size fractions assumed for emissions (see Table 2). Particle size fraction for the emission rate is not a variable input in the CAP-88 model. These sources of variance are in addition to the underlying differences in the model frameworks. AERMOD does not employ atmospheric stability class categories and troposhere "lid" inputs but instead implements planetary boundary layer methods of estimating atmospheric mixing. Therefore, comparison of AERMOD results with CAP-88 results is considered on an order-of-magnitude scale, where results within a factor of 10 or less of each other may be considered nominally equivalent.

Both AERMOD and CAP-88 output air concentrations and ground deposition rates, although with AERMOD these results are integrated over a receptor grid cell while in CAP-88 they are associated with specific x,y coordinates. Particle deposition rates were selected as the output for this comparison. CAP-88 results were obtained for distances of 1 km, 5 km, and 10 km from the embankment at each of 16 orientations (N, NNW, NW, WNW, etc). Particle deposition results from AERMOD grid cells overlapping these coordinates were identified. A comparison of these results for the four cardinal directions is shown in Table 6.

Table 6: Comparison of CAP-88 and AERMOD particle deposition results (g/m^2-yr).

Direction	Distance (km)	CAP-88 deposition	AERMOD deposition	Ratio CAP-88 / AERMOD
N	1	0.14	0.11	1.2
N	5	0.015	0.016	0.92
N	10	0.0054	0.0047	1.2
W	1	0.13	0.097	1.3
W	5	0.013	0.0037	3.5
W	10	0.0045	0.00084	5.3
S	1	0.082	0.099	0.83
S	5	0.0081	0.0096	0.85
S	10	0.0029	0.0033	0.89
E	1	0.042	0.21	0.20
E	5	0.0042	0.0045	0.93
E	10	0.0015	0.00056	2.7

Of the 12 comparisons shown in Table 6, CAP-88 and AERMOD particle deposition results were within a factor of two for all but four results. The largest discrepancies were approximately a factor of five, for the 10-km distance to the west and the 1-km distance to the east. This comparison indicates that that there is relatively low variability between the CAP-88 and AERMOD results considering the differences between these models, and suggests that the AERMOD results are reliable.

6.4 Implementation of Cowherd Unlimited-Reservoir Resuspension Model

A range of input parameter values for the unlimited-reservoir particle resuspension model were employed to evaluate the possible particle emission rates. Input parameters include fraction of vegetative cover (V), average annual wind speed (u), surface roughness height (z_0), the unadjusted threshold friction velocity (u_t), and the friction velocity adjustment factor. The range of potential adjustment factors is shown in Figure 3-5 of Cowherd et al (1985). High-end, middle, and low-end estimates (based on impact to the calculated emission rate (E_{10}) are shown in Table 7 and discussed in the following paragraphs.

Table 7: Range of input parameter values for particle resuspension modeling.

Parameter	units	High E_{10}	Middle E_{10}	Low E_{10}
vegetative cover (V)	–	0.058	0.172	0.318
average annual wind speed (u)	m/s	3.20	3.14	3.10
surface roughness height (z_0)	cm	5	3.5	2
unadjusted threshold friction velocity (u_t)	m/s	0.1	0.25	0.7
Friction velocity adjustment factor	–	3	4	5

Values for the range of V are based on means for each of the five plant communities evaluated in test plots near the disposal facility site. The range of u is based on review of five years of Clive meteorological data. High-end and low-end values are approximate. Values of z_0 are based on Figure 3-6 of Cowherd et al (1985). The value for High E_{10} is a slightly larger z_0 than that of a wheat field and comparable to "suburban dwellings". This is possibly analogous to widely spaced shrubs. The z_0 of 2 is the lower part of the range for "grassland".

Estimates for u_t are the most critical for calculating particle erosion. The range of other parameters can be estimated, whereas the outcome of soil development on the cap after many millenia (with respect to particle size distribution, formation of soil crust, amount of projecting rip rap, etc) is essentially unknown. However, based upon professional judgment, the values used here are based on examination of Figure 3-4 of Cowherd et al (1985). The value of High E_{10} is a factor of 10 below the lowest value for aggregate size distribution (100 µm) shown on the scale, or 10 µm. This corresponds, by extending the linear function in Figure 3-4, to a u_t value of 0.1 m/s. The value of Low E_{10} corresponds to an aggregate erodible particle size distribution mode of ~1 mm (1,000 µm). The middle value equates to a 100 µm size. The High E_{10} value equates to an aggregate particle diameter smaller than that of silt-size particles (0.05 mm), below

which one may presume a more crusted surface that is not associated with an unlimited-reservoir erosion model. For the Low E_{10} value, an aggregate diameter of 1 mm suggests a relatively large contribution from weathering of rip rap and particle aggregation.

The u_t adjustment factor estimates were developed based on correlation of expected cap conditions with photographs in Appendix A of Cowherd et al (1985). Figure A-3, was selected as the best representation of the likely future cap surface. The associated value of 5 for Figure A-3, however, is approximately equal to the upper end of the range of adjustment factors shown in Figure 3-5 of Cowherd et al (1985). Therefore, to capture some range of possible values, factors of 3, 4, and 5 were used for High E_{10}, Mid E_{10}, and Low E_{10} calculations, respectively. Adjustment factors shown in Figure 3-5 span a range between 1 and 7, with the function steepening rapidly between values of 2 and 7.

The average-annual PM_{10} emission rates (E_{10}) calculated using Equation 1 are as follows:

- High E_{10}: 0.30 kg/m^2-yr;
- Mid E_{10}: 2.5E-07 kg/m^2-yr; and,
- Low E_{10}: 1.4E-94 kg/m^2-yr.

Because the middle value is effectively zero, these results were represented in the GoldSim PA model using a log-uniform distribution with boundaries of 2.5E-07 and 0.30 kg/m^2-yr.

7 Electronic Reference

Atmospheric Modeling Appendix.pdf

This file contains graphical output of air concentrations and particulate deposition related to the AERMOD simulations described in this white paper.

8 References

Cowherd, C., G. E. Muleski, P. J. Englehart, and D. A. Gillette, 1985, Rapid Assessment of Exposure to Particulate Emissions from Surface Contamination Sites, prepared for U.S. Environmental Protection Agency, Office of Health and Environmental Assessment, by Midwest Research Institute, Kansas City, Missouri, EPA/600/8-85/002, February, 1985.

EPA, 1996, *Soil Screening Guidance: Technical Background Document*, EPA/540/R-95/128, OSWER Directive 9355.4-17A, Office of Solid Waste and Emergency Response, U.S. Environmental Protection Agency, Washington, D.C., May 1996.

EPA, 2002, *Supplemental Guidance for Developing Soil Screening Levels for Superfund Sites,* OSWER Directive 9355.4-24, U.S. Environmental Protection Agency, Office of Solid Waste and Emergency Response, Washington, D.C., December 2002.

EPA, 2011a. AERMOD modeling system, model and documentation available on-line at: http://www.epa.gov/ttn/scram/dispersion_prefrec.htm#aermod

EPA, 2011b. CAP-88 radiation risk assessment software, model and documentation available on-line at: http://www.epa.gov/rpdweb00/assessment/CAP88/index.html

GTG (GoldSim Technology Group), 2011. *GoldSim: Monte Carlo Simulation Software for Decision and Risk Analysis*, http://www.goldsim.com

Lakes Environmental, 2010. *AERMOD View™*, air dispersion modeling package, available on-line at: http://www.weblakes.com/products/aermod/.

MSI, 2010, *January 2009 Through December 2009 and January 1993 Through December 2009 Summary Report of Meteorological Data Collected at EnergySolutions' Clive, Utah Facility*, prepared for Energy*Solutions*, LLC by Meteorological Solutions Inc, February, 2010.

NESHAPS, National Emission Standards for Emissions of Radionuclides Other Than Radon from Department of Energy Facilities, 10 CFR 40 Part 61.93, available on-line at: http://ecfr.gpoaccess.gov/cgi/t/text/text-idx?c=ecfr&sid=3ae5812c554c6c41807e0fd4dc157bac&rgn=div5&view=text&node=40:8.0.1.1.1&idno=40

Nielson, K.K., and G.M. Sandquist. 2011. Radon Emanation from Disposal of Depleted Uranium at Clive, Utah. Report for EnergySolutions by Applied Science Professionals, LLC. February 2011.

NIST, 2011, NIST Chemistry WebBook, National Institute of Standards and Technology, available on-line at: http://webbook.nist.gov/cgi/cbook.cgi?ID=C10043922&Mask=10#Solubility

Rogers, V. C., and K. K. Nielson, 1991. Correlations for predicting air permeabilities and 222Rn diffusion coefficients of soils, *Health Physics* 61(2): 225-230.

Utah 2010. License Requirements for Land Disposal of Radioactive Waste. Utah Administrative Code Rule R313-25.

Volkovitsky, P., 2004. Radon diffusion and the emanation fraction for NIST polyethylene capsules containing radium solution. National Institute of Standards and Technology, Ionizing Radiation Division, available on-line at: http://www.aarst.org/proceedings/2004/2004_11_Radon_Diffusion_Emanation_Fraction_for_NIST_Poly.pdf

Electronic Appendix

AERMOD

Air Dispersion Modeling

Electronic Appendix

Air Concentration Maps for Year 2009
Particulates
0.3-km^2 Resolution
0-m Release Height

AERMOD Air concentration (ug/m^3)

0% of particulate fraction between 0-2.5 microns

0.3 km^2 resolution, 0-m release height, 0.25 g/sec emission rate

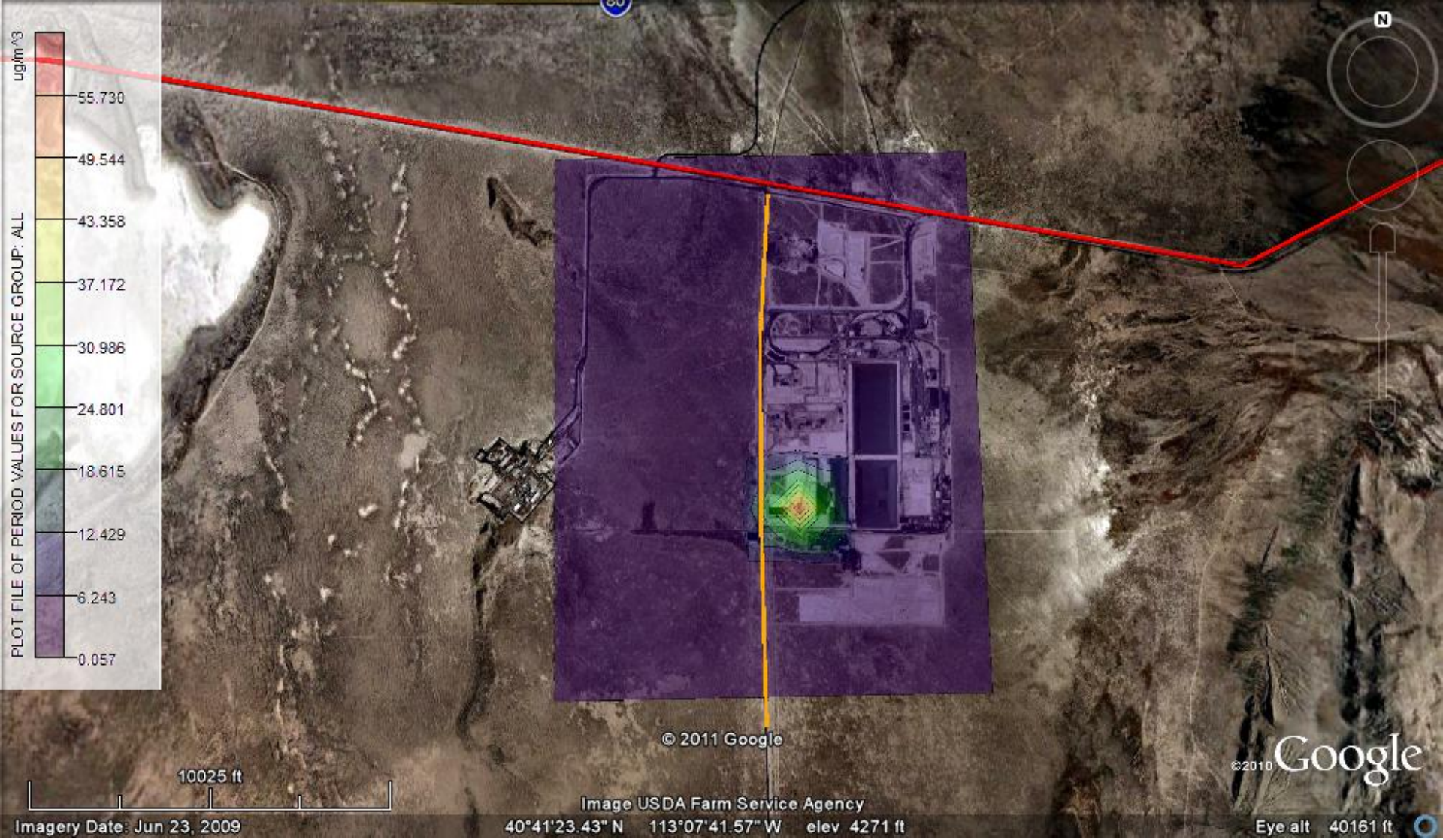

AERMOD Air concentration (ug/m^3)

5% of particulate fraction between 0-2.5 microns

0.3 km^2 resolution, 0-m release height, 0.25 g/sec emission rate

AERMOD Air concentration (ug/m^3)
10% of particulate fraction between 0-2.5 microns
0.3 km^2 resolution, 0-m release height, 0.25 g/sec emission rate

AERMOD Air concentration (ug/m^3)

20% of particulate fraction between 0-2.5 microns

0.3 km^2 resolution, 0-m release height, 0.25 g/sec emission rate

AERMOD Air concentration (ug/m^3)

40% of particulate fraction between 0-2.5 microns

0.3 km^2 resolution, 0-m release height, 0.25 g/sec emission rate

AERMOD Air concentration (ug/m^3)

60% of particulate fraction between 0-2.5 microns

0.3 km^2 resolution, 0-m release height, 0.25 g/sec emission rate

AERMOD Air concentration (ug/m^3)

80% of particulate fraction between 0-2.5 microns

0.3 km^2 resolution, 0-m release height, 0.25 g/sec emission rate

AERMOD Air concentration (ug/m^3)

100% of particulate fraction between 0-2.5 microns

0.3 km^2 resolution, 0-m release height, 0.25 g/sec emission rate

Electronic Appendix

Air Concentration Maps for Year 2009
Particulates
1-km^2 Resolution
15-m Release Height

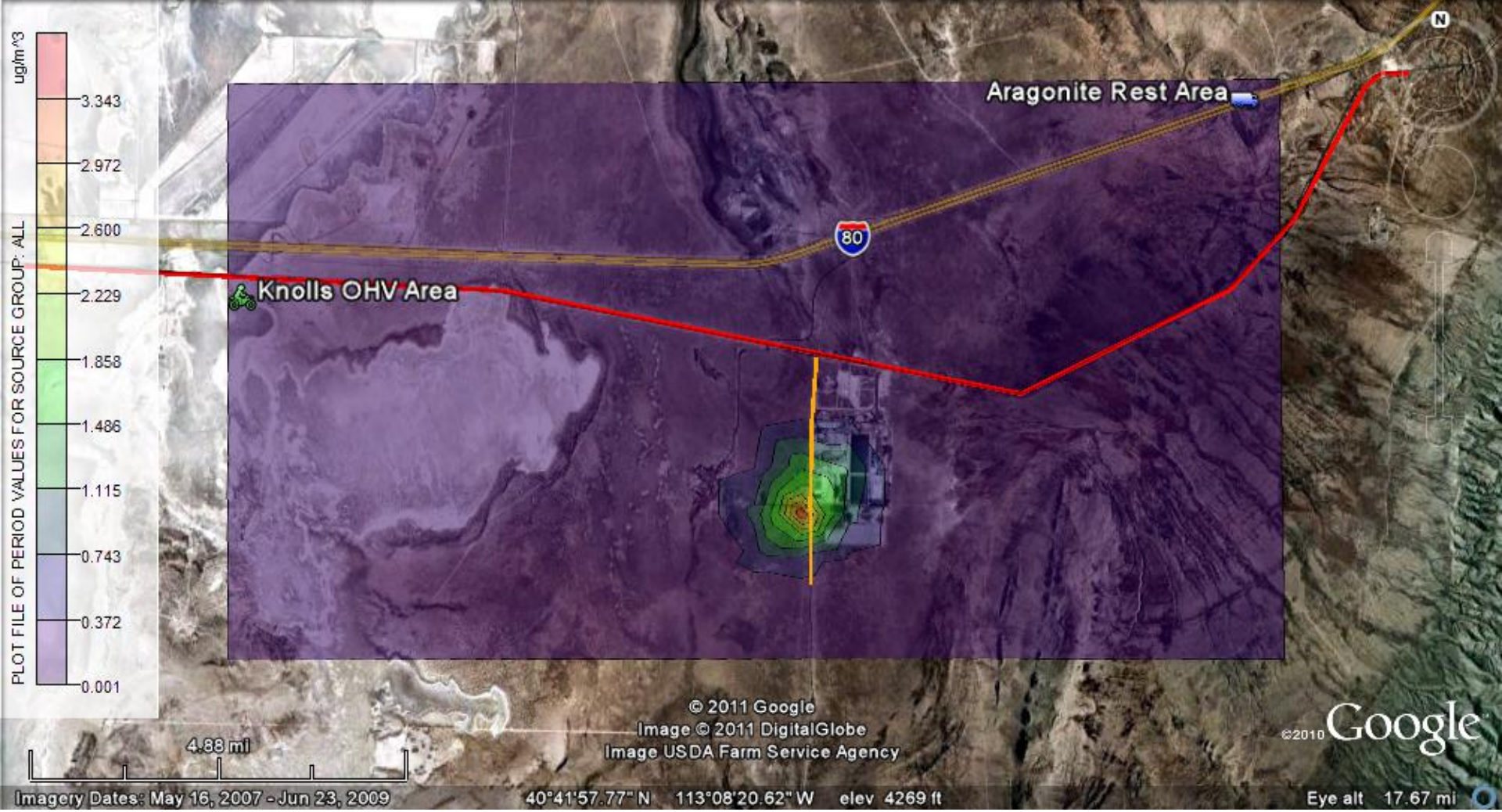

AERMOD Air concentration (ug/m^3)

0% of particulate fraction between 0-2.5 microns

1-km^2 resolution, 15-m release height, 0.25 g/sec emission rate

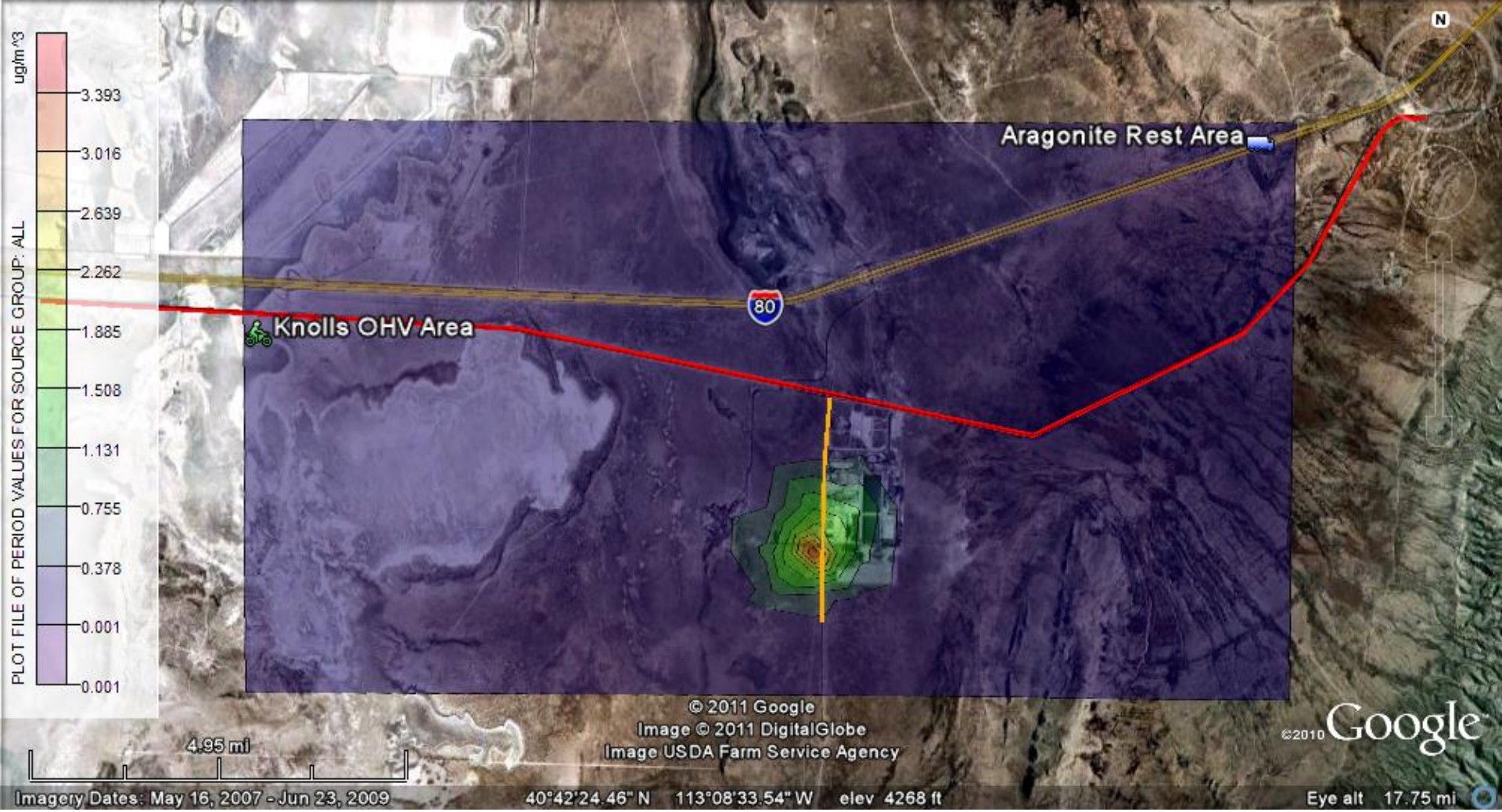

AERMOD Air concentration (ug/m^3)

5% of particulate fraction between 0-2.5 microns

1-km^2 resolution, 15-m release height, 0.25 g/sec emission rate

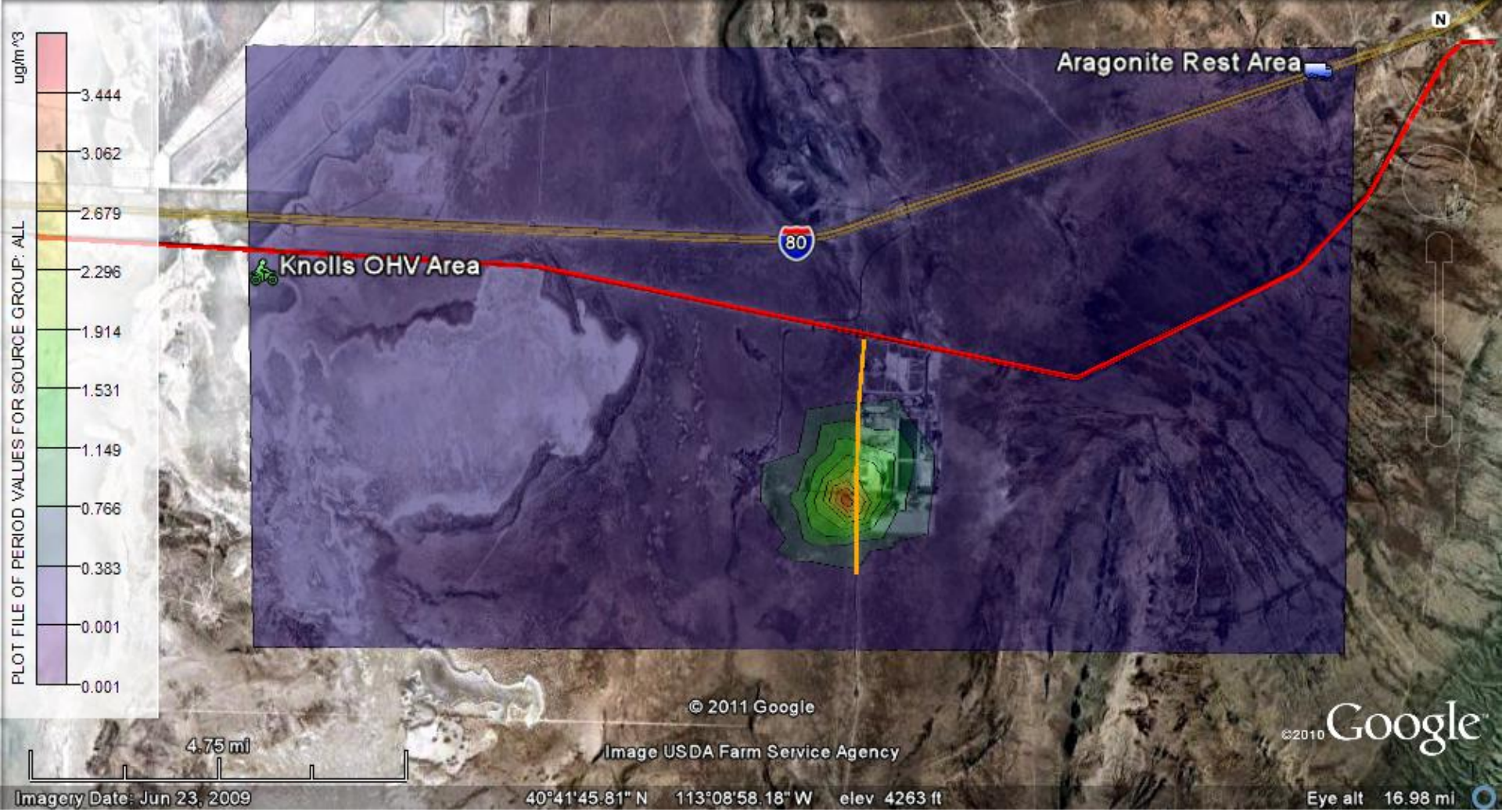

AERMOD Air concentration (ug/m^3)

10% of particulate fraction between 0-2.5 microns

1-km^2 resolution, 15-m release height, 0.25 g/sec emission rate

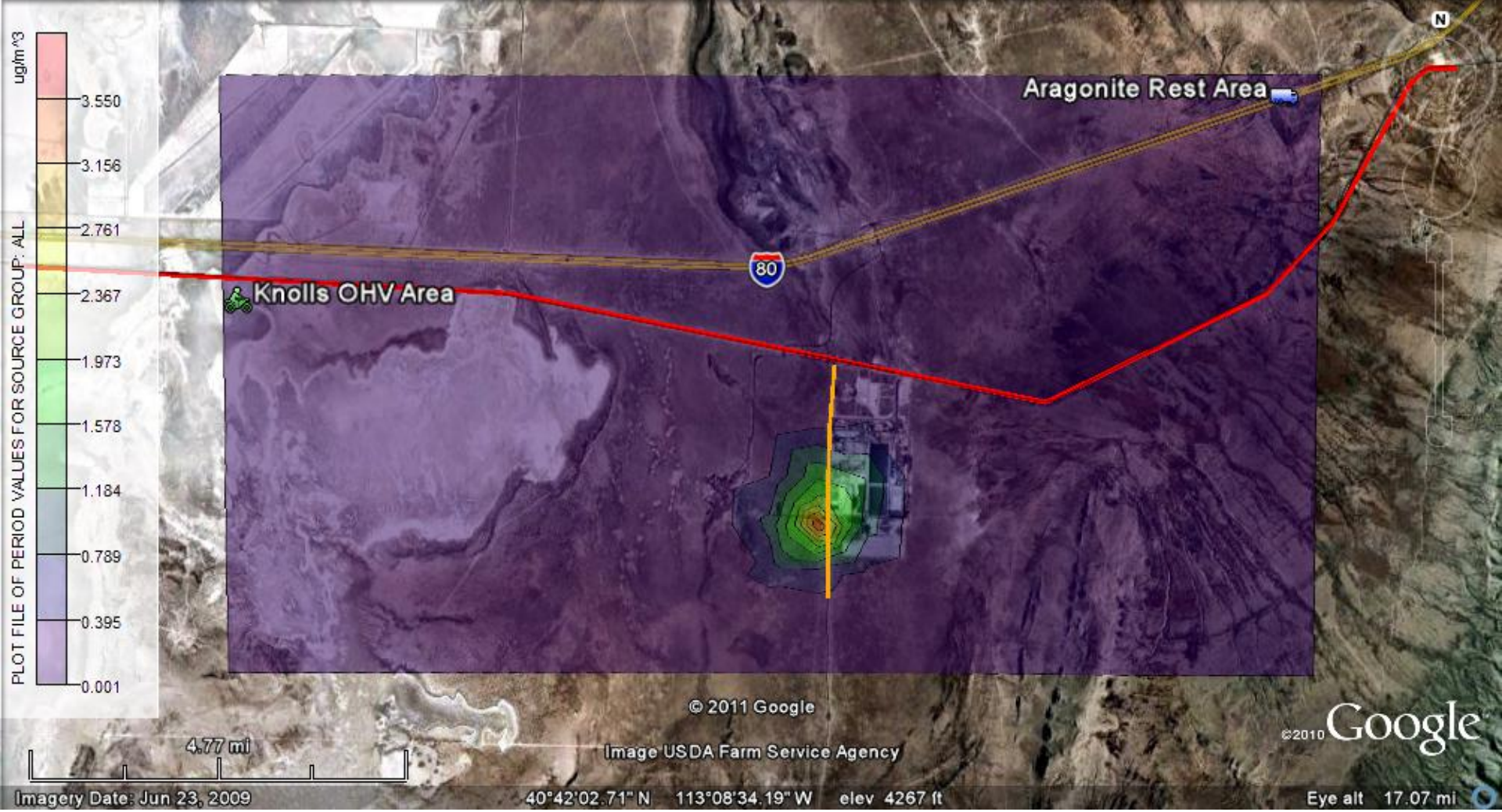

AERMOD Air concentration (ug/m^3)

20% of particulate fraction between 0-2.5 microns

1-km^2 resolution, 15-m release height, 0.25 g/sec emission rate

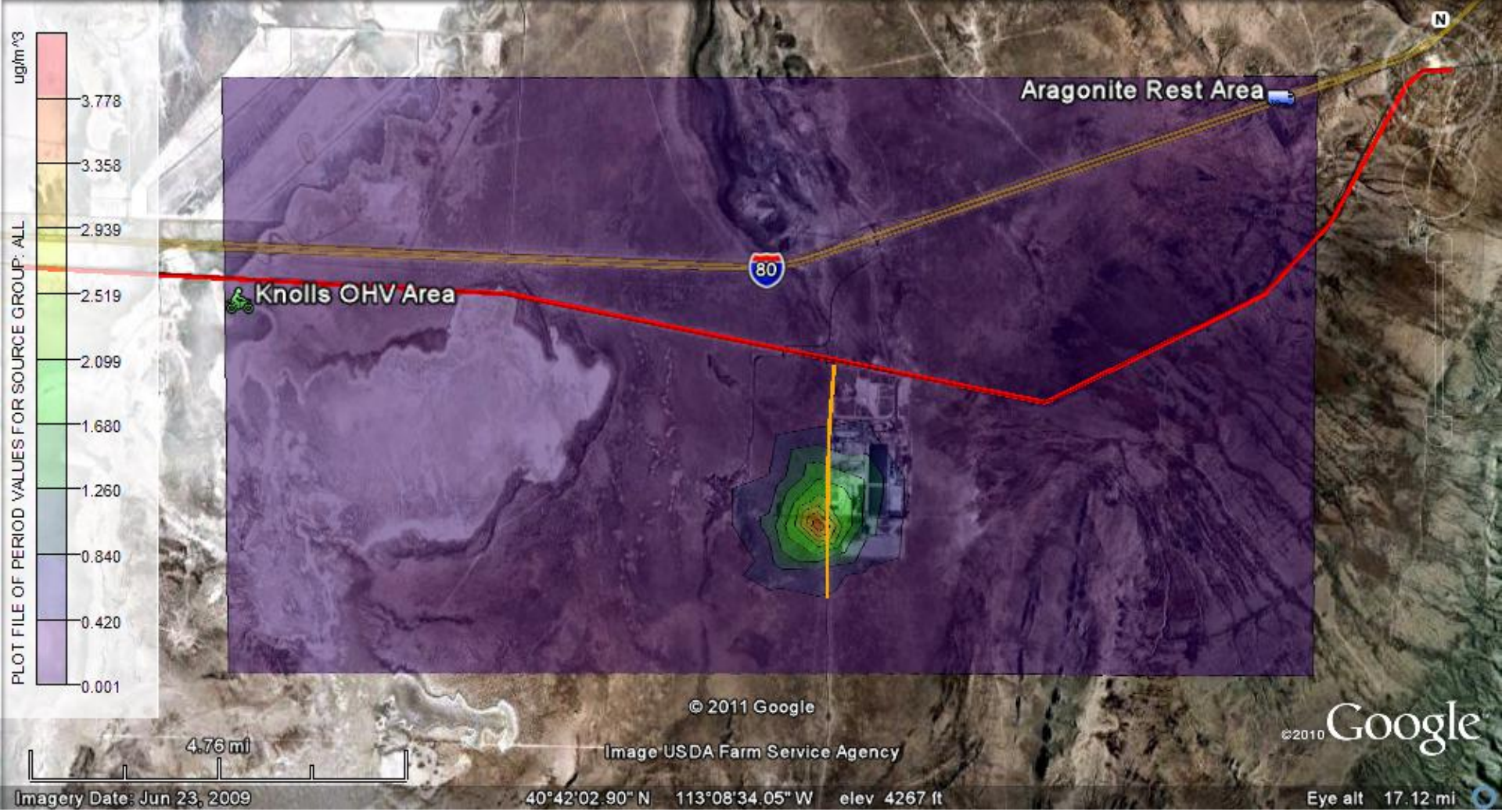

AERMOD Air concentration (ug/m^3)

40% of particulate fraction between 0-2.5 microns

1-km^2 resolution, 15-m release height, 0.25 g/sec emission rate

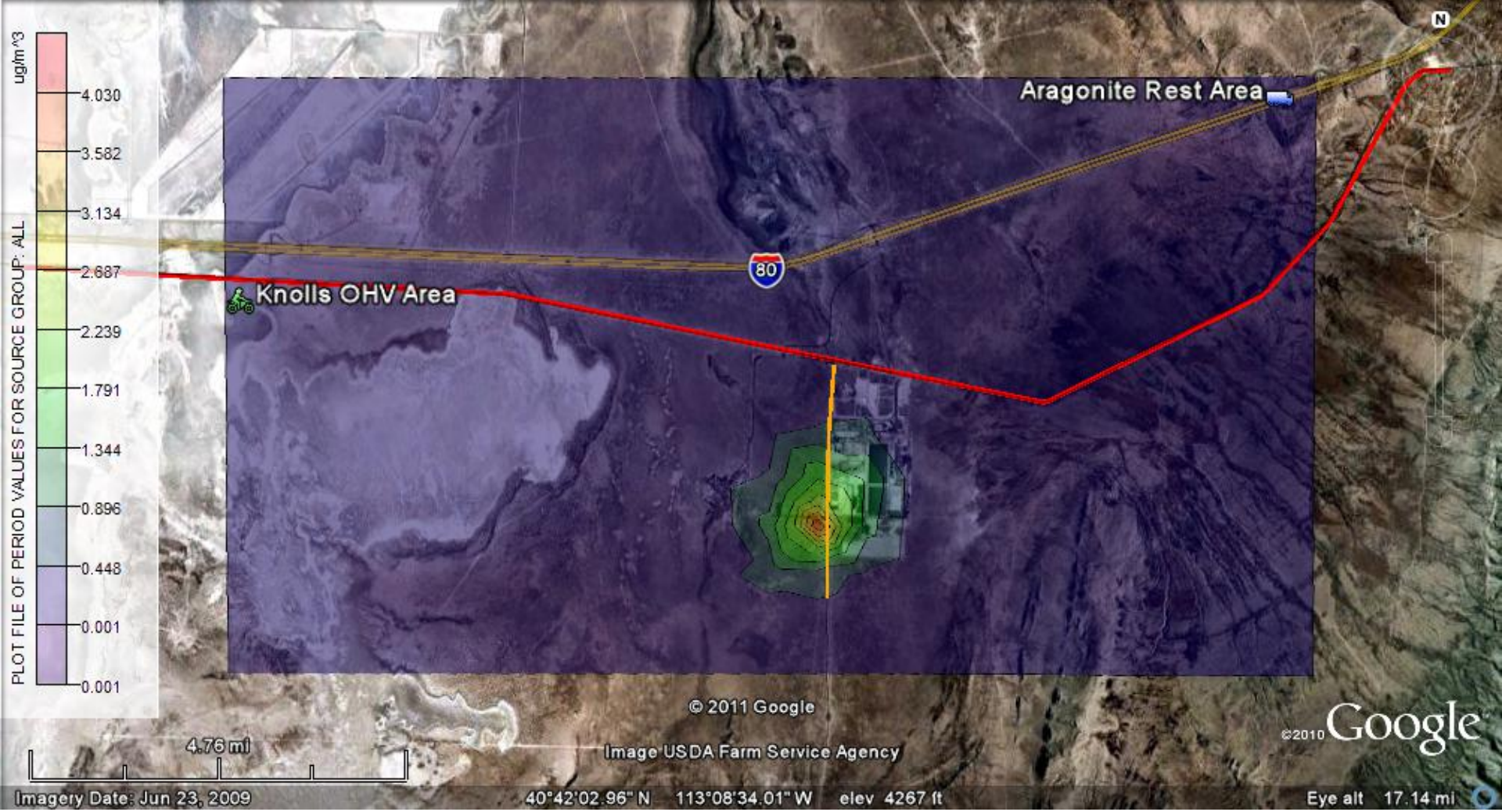

AERMOD Air concentration (ug/m^3)

60% of particulate fraction between 0-2.5 microns

1-km^2 resolution, 15-m release height, 0.25 g/sec emission rate

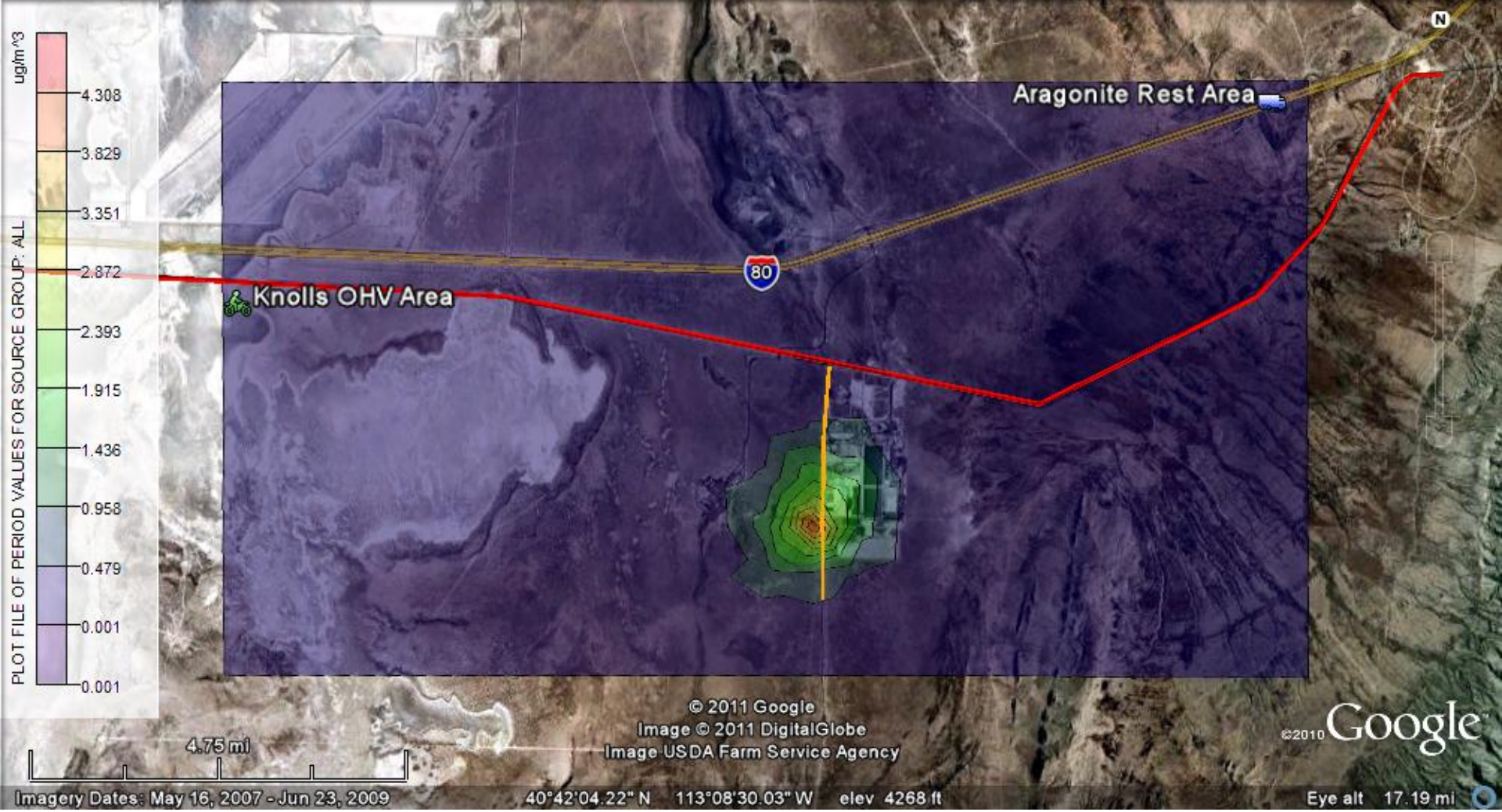

AERMOD Air concentration (ug/m^3)

80% of particulate fraction between 0-2.5 microns

1-km^2 resolution, 15-m release height, 0.25 g/sec emission rate

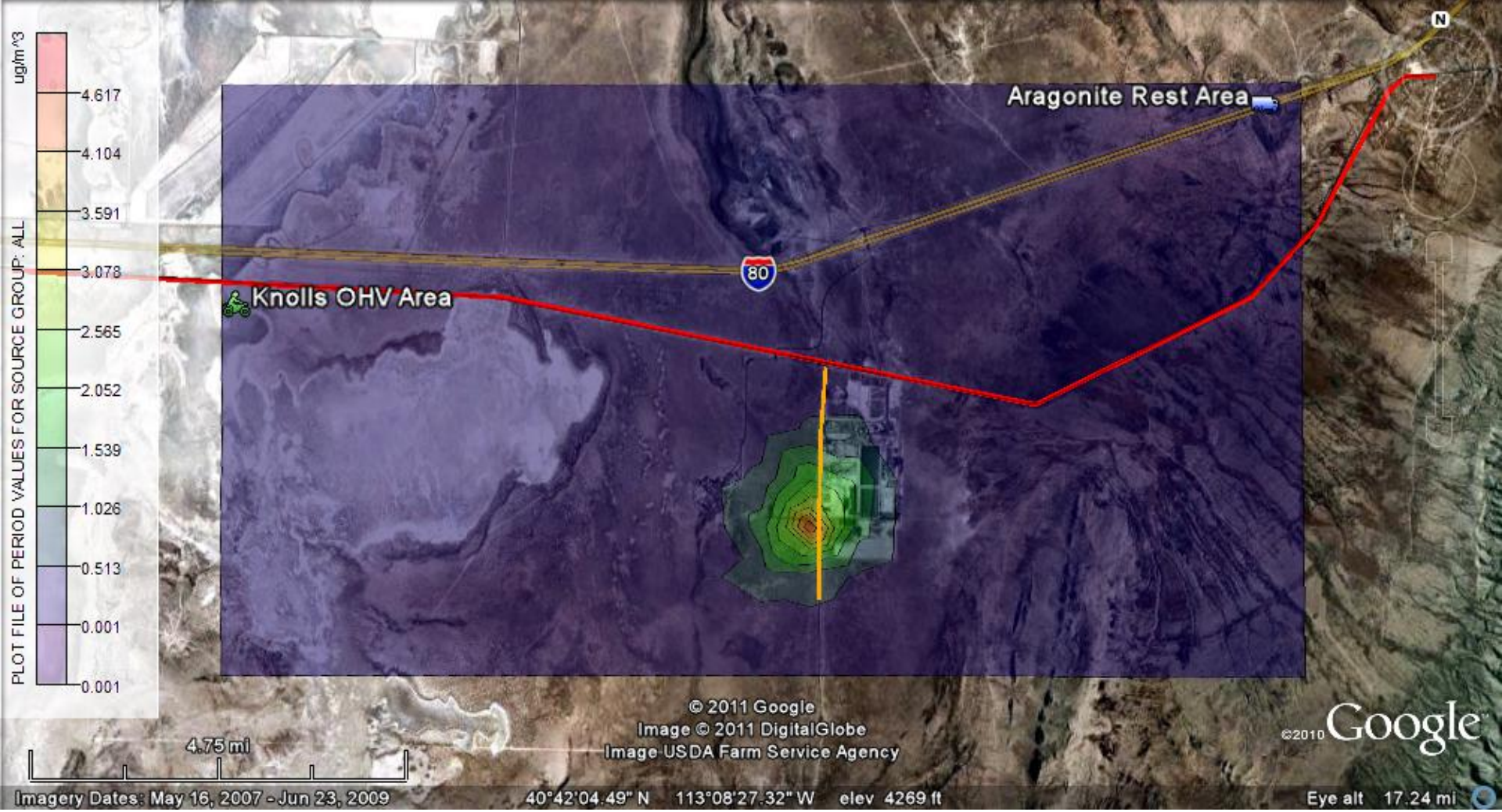

AERMOD Air concentration (ug/m^3)

100% of particulate fraction between 0-2.5 microns

1-km^2 resolution, 15-m release height, 0.25 g/sec emission rate

Electronic Appendix

Air Concentration Maps for Year 2009
Particulates
0.3-km^2 Resolution
0-m Release Height

AERMOD Air concentration (ug/m^3)
0.3-km^2 resolution, 0-m release height

Electronic Appendix

Air Concentration Maps for Year 2009
Radon Gas
1-km^2 Resolution
15-m release height

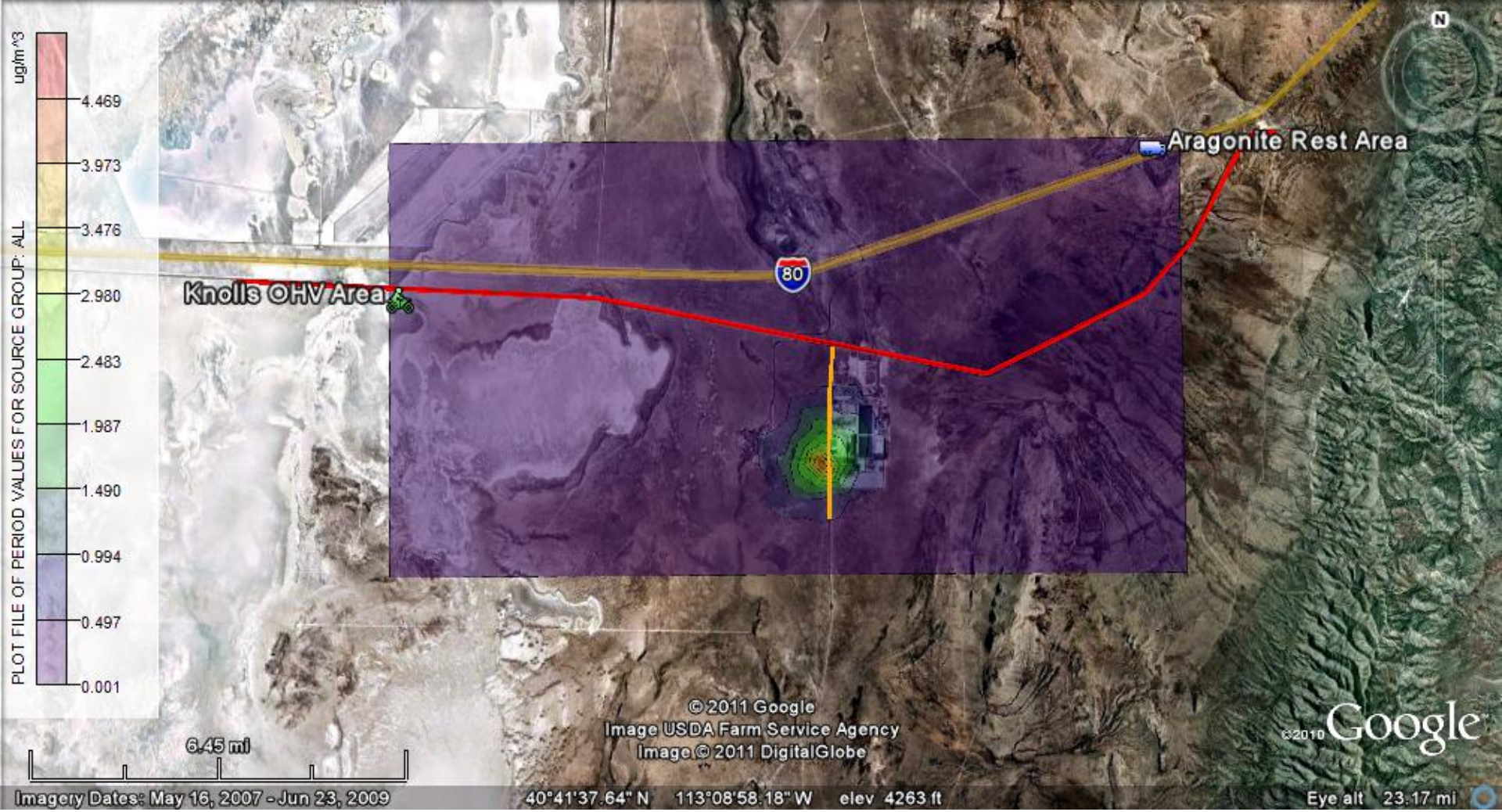

AERMOD Air concentration (ug/m^3)
1-km^2 resolution, 15-m release height

Neptune and Company Inc.

June 1, 2011 Report for EnergySolutions

Clive DU PA Model, version 1

Appendix 9

Biological Modeling

Biologically-Induced Transport Modeling for the Clive DU PA

28 May 2011

Prepared by

Neptune and Company, Inc.

This page is intentionally blank, aside from this statement.

CONTENTS

FIGURES

TABLES

1.0 Summary of Parameters

Following is a brief summary of input values used parameters employed in the biotic transport component of the Clive Performance Assessment (PA) model that is the subject of this white paper.

Table 1 lists the biological transport model parameter distributions for the Clive DU waste cell GoldSim Model that are summarized in this document. For a number of biotic parameters, site specific data were not available for the Clive site, so the GoldSim model makes use of biotic parameters for the same or similar species developed for the performance assessment of disposal cells at the Nevada National Security Site (NNSS, formerly the Nevada Test Site), with the assumption that these species-specific parameters do not vary greatly across North American desert types. The derivation of these NNSS parameters is detailed in the relevant NNSS documents (Neptune 2005a, 2005b, 2006).

For distributions, the following notation is used:

- N(μ, σ, [*min*, *max*]) represents a normal distribution with mean μ and standard deviation σ, and optional truncation at the specified *min*imum and *max*imum,
- LN(*GM*, *GSD*, [*min*, *max*]) represents a log-normal distribution with geometric mean *GM* and geometric standard deviation *GSD*, and optional *min* and *max*,
- U(*min*, *max*) represents a uniform distribution with lower bound *min* and upper bound *max*,
- Beta(μ, σ, *min*, *max*) represents a generalized beta distribution with mean μ, standard deviation σ, minimum *min*, and maximum *max*,
- Gamma(μ, σ) represents a gamma distribution with mean μ and standard deviation σ, and
- TRI(*min*, *m*, *max*) represents a triangular distribution with lower bound *min*, mode *m*, and upper bound *max*.

Table 1. Summary of Biotic Transport Parameters

Parameter	Value	Units	Reference / Comment
Ant Transport Parameters			
Volume of Each Nest	N(μ=0.161, σ=0.024, min=0, max=Large)	m^3	SWCA, 2011 (Sec 2.3, Appendix A1) and Neptune, 2006. See Section 4.3
Lifespan of Each Colony	N(μ=20.2, σ=3.6, min=0, max=Large)	yr	Neptune, 2006 (Section 6.8, p. 16)
ColonyDensity - area density of colonies on the ground	___	___	SWCA, 2011 (Table 20, p. 23). See Section 4.7
ColonyDensity_Plot1	Gamma(33,1, min=0, max=Large)	1/ha	*Ibid.*
ColonyDensity_Plot2	Gamma(2, 1, min=0, max=Large)	1/ha	*Ibid.*
ColonyDensity_Plot3	Gamma(7, 1, min=0, max=Large)	1/ha	*Ibid.*
ColonyDensity_Plot4	Gamma(17, 1, min=0, max=Large)	1/ha	SWCA, 2011 (Based on provided data. Information for this plot in Table 20, p. 23 in the SWCA report is incorrect.)
ColonyDensity_Plot5	Gamma(6, 1, min=0, max=Large)	1/ha	*Ibid*
MaxDepth - maximum depth for any colony	212	cm	SWCA, 2011 and Neptune, 2006. See Section 4.4.
b - fitting parameter for nest shape	N(μ=10, σ=0.71, min=1, max=Large)	—	Neptune, 2006 (Section 7.3, p. 21)

Mammal Transport Parameters			
MoundDensity - area density of mounds on the ground	see below for each plot	---	SWCA, 2011 (Section 2.2.2, p. 18 – 22)
_Plot1	Gamma(235, 1, min=0, max=Large)	1/ha	
_Plot2	Gamma(239, 1, min=0, max=Large)	1/ha	
_Plot3	Gamma(1.33, 1, min=0, max=Large)	1/ha	
_Plot4	Gamma(1.33, 1, min=0, max=Large)	1/ha	
_Plot5	Gamma (1.33, 1, min=0, max=Large)	1/ha	
ExcavationRate - volumetric rate of a single burrow excavation	N(μ=0.0006, σ=0.00015, min=Small, max=Large)	m^3/yr	Mean of excavated volumes at each sample location from SWCA, 2011 (Tables 13, 15, 17, 19), corrected for the number of burrows reported at each sample location (See Table 14 of this white paper)
MaxDepth - maximum depth for any burrow	200	cm	Neptune 2005b (Table 2)
b - fitting parameter for burrow shape	N(μ=4.5, σ=0.84, min=1, max=Large)	—	Fitting parameter for rodent burrows from Neptune 2005b (Fig. 10, p. 22)
Plant Transport Parameters			
BiomassProductionRate	U(300,1500)	kg/ha yr	Approximate Range for Great Basin from Smith, et al 1997(Fig 7, p. 37)
PctCover_Plot*_[plant]	Tabulated in Clive PA Model Parameters.xls workbook	—	Simulations based on SWCA (2011) percent cover data. See Section 3.3

Percent cover random selector	randomly select between values 1 to 1000, inclusive	—	Modeling construct
Vegetation Association Picker	Discrete (1, 2, 3, 4, 5)	—	Modeling construct
Greasewood Parameters			
RootShoot_Ratio	U(0.30, 1.24)	—	Assumed similar to creosote, Neptune, 2005a (Table 16, p. 38)
MaxDepth	570	cm	Robertson, 1983 (p. 311)
b - fitting parameter for root shape	N(μ=14.6, σ=0.0807, min=1, max=Large)	—	Assumed similar to creosote, Neptune, 2005a (Fig. 9, p. 51)
RootShoot_Ratio	T(1, 1.2, 2)	—	Mode based on Bethlenfalvay and Dakessian, 1984 (Table 2, p. 314); bounds based on Neptune, 2005a
MaxDepth	150	cm	Based on H. comata from Zlatnik, 1999a (p. 7)
b - fitting parameter for root shape	N(μ=2.19 σ=0.036, min=1, max=Large)	—	For perennial grasses, from Neptune 2005a (Fig. 12, p. 55)
Forb Parameters			
RootShoot_Ratio	U(0.40, 1.80)	—	Distribution of “Other Shrubs” used for conservatism, see Section 3.4
MaxDepth	51	cm	Based on Halogeton, from Pavek, 1992 (p. 5)
b – fitting parameter for root shape	N(μ=23.9 σ =0.313, min=1, max=Large)	—	Distribution same as “Other Shrubs”, see Section 3.5
Tree Parameters			
RootShoot_Ratio	U(0.55, 0.76)	—	For Juniperus occidentalis from Miller et al., 2005 (p. 16)

MaxDepth	450	cm	For J. occidentalis from Zlatnik, 1999b (p. 6)
b – fitting parameter for root shape	N(μ=14.6 σ=0.0807, min=1, max=Large)	—	Distribution for creosote used due to similar taproot depth, see Section 3.5
Other Shrub Parameters			
RootShoot_Ratio	U(0.4, 1.8)	—	Based on range for Artemisia sp. from Neptune, 2005a (Table 16, p. 38),
MaxDepth	110	cm	Branson et al. 1976 (Fig. 19, p. 1120)
b - fitting parameter for nest shape	N (μ= 23.9, σ=0.313, min=1, max=Large)	—	Based on fitting parameter for Atriplex canascens at NNSS, from Neptune 2005a (Fig 10, p. 52)
Plant/Soil Concentration Ratios			
PlantCRs by chemical element	tabulated in Clive PA Model Parameters.xls workbook	—	See Table 10
Plant CR GM for Rn	Small	—	See Table 10
Plant CR GSD for Rn	1	—	See Table 10

2.0 Introduction

Biotic fate and transport models have been developed for the depleted uranium (DU) waste cell at the Clive repository to evaluate the redistribution of soils, and contaminants within the soil, by native flora and fauna. The biotic models are part of a larger Performance Assessment (PA) model that has been built to evaluate the consequences of contaminant migration over time from the DU waste cell. The purpose of the PA model is to provide a decision management system that will support future disposal, closure and long term monitoring decisions, as well as supporting all regulatory requirements of PAs and other environmental assessments for these waste disposal systems. The Clive facility is located in the eastern side of the Great Salt Lake Desert, with flora and fauna characteristic of Great Basin alkali flat and Great Basin desert shrub communities.

3.0 Plant Specifications and Parameters

The purpose of this chapter is to explain the component of the Clive PA model that addresses calculation of plant-mediated contaminant mass distributions by depth, and the rate of contaminant transport from subsurface strata to the ground surface.

3.1 Plant Conceptual Model

Plant-induced transport of contaminants is assumed to proceed by absorption of contaminants into the plants roots, followed by redistribution throughout all the tissues of the plant, both above ground and below ground. Upon senescence, the above-ground plant parts are incorporated into surface soils, and the roots are incorporated into soils at their respective depths (Figure 1).

The calculations of contaminant transport due to plant uptake and redistribution take place in a series of steps:

1. Calculate the fraction of plant roots in each layer for each plant type.

2. Calculate uptake of contaminants into plant roots in each layer.

3. Sum the contaminant uptake to determine the total uptake by the roots for each contaminant.

4. Determine the average concentration in the roots, assuming complete redistribution within the root mass.

5. Assuming that the plant returns all fixed contaminants to adjacent soils upon senescence, determine how much of each contaminant is returned to each layer. The aboveground plant parts are mixed in the uppermost layer.

6. Calculate uptake of contaminants into aboveground parts of the plant ("shoots"), based on the fractions of roots fixing contaminants within each layer and sending it up to the shoots.

7. Calculate the net flux of contaminants into (or out of) each layer due to steps 1 through 6. This value is used to adjust contaminant inventories in each layer (each layer is a GoldSim cell).

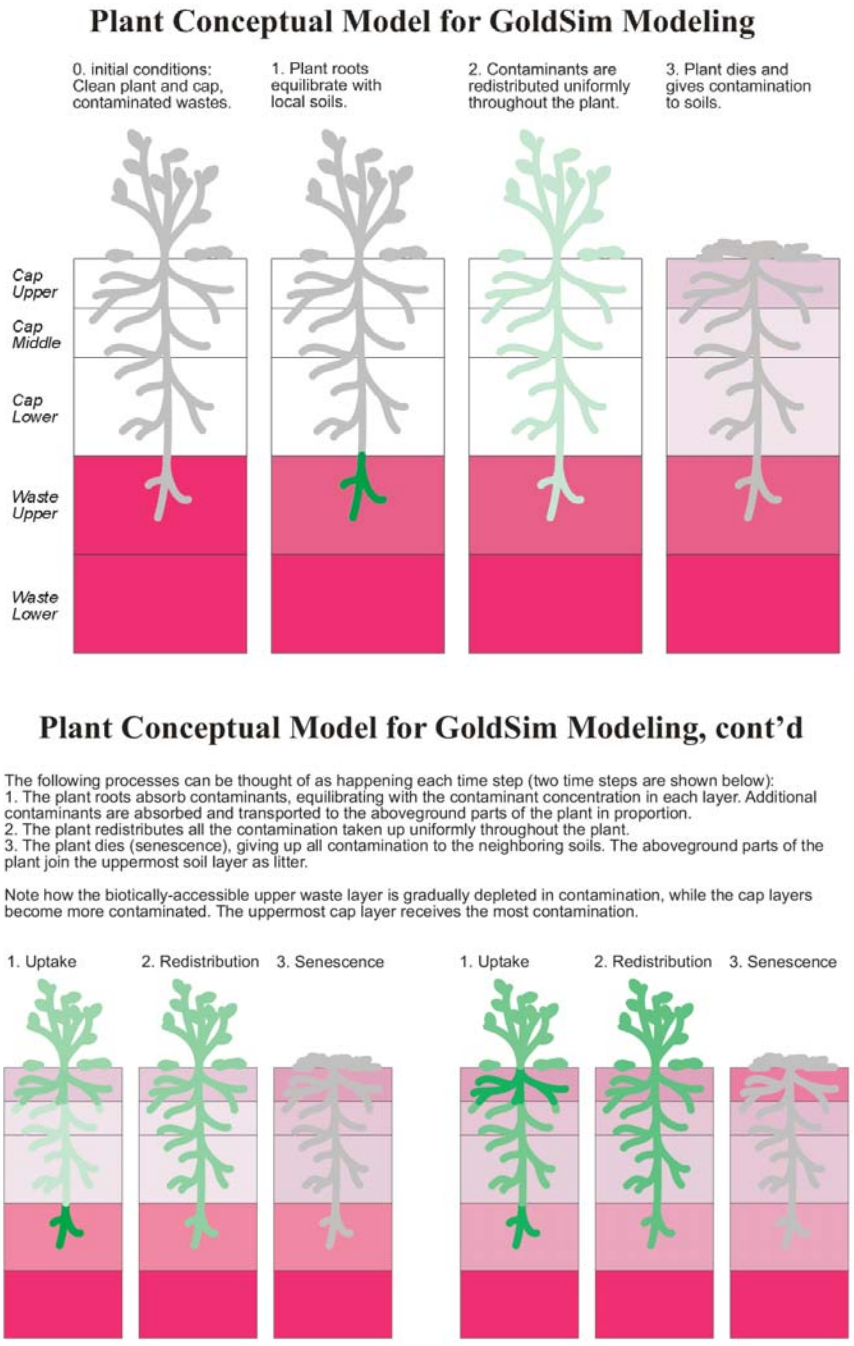

Figure 1. Conceptual model of contaminant uptake and redistribution by plants

This section describes the functional factors that contribute to the parameterization of the plant section of the biotic transport model. Such factors include identifying dominant plant species, grouping plant species into categories that are significantly similar in form and function with respect to the transport processes, estimating net annual primary productivity (NAPP, a measure of combined above-ground and below-ground biomass generation), determining relative abundance of plants or plant groups, evaluating root/shoot mass ratios, and representing the density of plant roots as a function of depth below the ground surface. The data used for each of the seven steps of the algorithm are presented, outstanding issues with the available data are identified, and the issues that deserve attention for the next model iteration are described.

In the Clive DU PA model, the vertical soil horizon is discretized into horizontal layers based on various functional attributes of the soil-based biotic communities (plants and animals), requirements related to gas and liquid transport, and the configuration of the disposal cell cover. The model is ultimately used to simulate radionuclide transport throughout the soil layers. Utilizing the information provided in 1 through 6 above, distributions of above-ground and below-ground NAPP for grasses, forbs, shrubs and trees are developed. Radionuclide activity associated with above-ground biomass is assigned to the uppermost soil/cover layer in the model. Radionuclide activity associated with below-ground NAPP is apportioned by depth interval according to root mass distribution. In order to reflect the redistribution of radionuclides, these calculations require the use of plant uptake factors (plant-soil concentration ratios) to model the relative uptake of contaminants from soil by plants.

3.2 Identification of Plant Functional Groups

Field surveys of the Clive site and surrounding areas were conducted by SWCA Environmental Consultants in September and December 2010 to identify plant species present in different vegetative associations around the Clive Site (SWCA Environmental Consultants, 2011). Five different vegetative associations were surveyed, with three associations representing the alkali flat/desert flat type soils found in the vicinity of Clive, and two associations representative of desert scrub/shrub-steppe habitat characteristic of slopes and slightly higher elevations with less-saline soil chemistry. A one hectare (100 m × 100 m) plot was established in each vegetative association, and each plot was surveyed for dominant plant species present, and the percent cover and density of each species. In addition, a small number of black greasewood, shadscale, halogeton, and Mojave seablite plants were excavated to obtain root profile measurements and above-ground plant dimensions. The vegetative associations for each plot are shown in Table 2. Plots 3 through 5 represent current vegetation at the Clive site, while Plots 1 and 2 are representative of less-saline soils that may develop on top of the waste cell cover.

A total of 41 plant species were identified on the five survey plots. Eighteen species each comprised at least 1% of the total cover on at least one plot. These 18 species were considered the most important for purposes of modeling plant mediated transport of chemical contaminants at Clive. Species were grouped into five functional plant groups, as shown in Table 3. The five functional groups are: grasses, forbs, greasewood, other shrubs, and trees. Greasewood is separated from other shrubs due to its status as a phreatophyte that can extend taproots in excess of five meters to reach groundwater. Annual and perennial grasses were grouped due to similar maximum rooting depths.

Table 2. Vegetative associations surveyed for embankment cover modeling

Plot Number	Plot Name
1	Mixed Grassland
2	Juniper-sagebrush
3	Black Greasewood
4	Halogeton-disturbed
5	Shadescale-Gray Molly

Table 3. Species identified at Clive included within each plant group

Plant Group	Common Name	Species Name
Forbs	Halogeton	*Halogeton glomeratus*
Forbs	Mojave seablite	*Suaeda torreyana*
Forbs	Curveseed butterwort	*Ranunculus testiculatus*
Grasses	Needle and thread	*Hesperostipa comata*
Grasses	Intermediate wheatgrass	*Thinopyrum intermedium*
Grasses	Sandberg bluegrass	*Poa secunda*
Grasses	Crested wheatgrass	*Agropyron cristatum*
Grasses	Muttongrass	*Poa fendleriana*
Grasses	Tall wheatgrass	*Thinopyrum ponticum*
Grasses	Slender wheatgrass	*Elymus trachycaulus*
Grasses	Western wheatgrass	*Pascopyrum smithii*
Grasses	Cheatgrass	*Bromus tectorum*
Greasewood	Black greasewood	*Sarcobatus vermiculatus*
Shrubs	Big sagebrush	*Artemisia tridentata*
Shrubs	Shadscale saltbush	*Atriplex confertifolia*
Shrubs	Gray molly	*Bassia americana*
Shrubs	Broom snakeweed	*Gutierrezia sarothrae*
Trees	Utah juniper	*Juniperus osteosperma*

3.3 Estimation of Net Annual Primary Production

Net annual primary productivity has not been measured at the Clive site or in the adjacent vegetative associations. NAPP can vary widely on an annual basis and is strongly correlated with mean annual water availability, and in desert ecosystems, correlates moderately well with annual precipitation (Smith et al., 1997). Smith et al. (1997, Figure 7, p. 37) show Great Basin NAPP ranging from approximately 300 to 1500 kg/ha/yr, and report mean NAPP for Great Basin terrestrial systems of 920 kg/ha/yr. Given the lack of site-specific NAPP data, the variability of

NAPP, and the dependence of NAPP on annual water availability, it is reasonable to assume for the initial modeling effort that NAPP in the area of Clive has a uniform distribution of 300 to 1500 kg/ha/yr. A total biomass production for the selected plot is drawn from this distribution. Since these data are not on a per-plant or per-species basis, percent cover of each plant group will be used to apportion NAPP by vegetation type. This biomass is then apportioned based on the percent of vegetation from each plant type. Percent cover of each plant species was measured in 100 separate 1-m^2 quadrats located along ten transects in each Plot. Mean percent cover for each species was reported by SWCA (2011, Tables 1 through 5) for plant species recorded in each vegetation association, and this information is summarized by plant group in Table 4.

A distribution for percent plant cover was developed using a bootstrap resampling approach to estimate the sampling distribution of the mean percent plant cover (Efron 1998). The percent plant cover is to be applied for the full 10 ka performance period, and thus it is the distribution of the *mean* percent plant cover that is being modeled, to account for the time averaging. The bootstrap resampling simulation needs to reflect the same sort of sampling structure as the field sampling, in order to capture the underlying structure of the data. To simulate this structure, five transects from two subplots were selected at random from each plot, then 10 quadrats within those five transects were selected at random. This means that quadrat data originally within a transect were resampled together, and transect data from within a subplot were resampled together. Subplot data within a plot were resampled together, and data between plots were not mixed. As in standard bootstrap resampling, each random selection was done with replacement. A mean value was then calculated for percent cover of each plant type from the two subplots. To calculate total percent coverage, percent coverage for each plant type in each simulation was aggregated. The percent coverage for each plot, for each plant type, and for each simulation was saved in a table, with the entire process being repeated 1,000 times. Since data was collected on only two of the four subplots within a plot, there are only four ways in which the two subplots can be selected. Therefore, in this phase of the bootstrap resampling, all four possibilities are calculated and assigned equal weight. No standard statistical distribution provided an adequate fit to the resulting mean percent cover values. Thus, the simulated values were recorded in a table, and each simulated value is drawn with equal likelihood in the Clive PA GoldSim model. All percent cover simulation results are shown in the Clive PA Model Parameters Workbook.

To calculate total biomass by plant type, these percent cover simulations are used with the Total Biomass distribution to apportion biomass by plant type. For example, if a plot with 20% shrubs 30% grasses, and 50% bare ground is assumed to produce 1000 kg of biomass, 400 kg is assumed to be produced by shrubs and 600 kg is assumed to be produced by grasses (Table 5), since bare ground, which for purposes of this model includes litter and biological crust, is assumed to produce no biomass.

3.4 Root/Shoot Ratios

Distributions of above-ground and below-ground biomass production for plant groups will be developed from the total NAPP based on root/shoot ratio for each plant group. The root/shoot ratio is the ratio of below-ground (root) mass to above-ground (shoot) mass. Estimates of below-ground NAPP are determined by multiplying total NAPP by the root-shoot ratio of the species of concern. Above-ground NAPP is equivalent to the remaining portion of total NAPP. Root/shoot ratios for each plant group are shown in Table 6. A triangular distribution was developed for the

grasses root/shoot ratio. Data from Bethlenfalvay and Dakessian (1984, Table 2, p. 314) for *Hesperostipa comata* suggesting a root/shoot ratio of 1.2 in ungrazed systems was used for the mode of the distribution. Furthermore, since root/shoot ratios for grasses generally range from 1:1 to 2:1 (Neptune, 2005a) the endpoints of the distribution were set at a minimum of one and a maximum of two. For greasewood, the root/shoot ratio is based on information in Neptune (2005a) for creosote (*Larrea tridentata*), a warm desert shrub with a similar growth form to greasewood. The root/shoot ratio for the "Other Shrubs" category is based on the range of root/shoot ratios reported for sage (*Artemesia* spp) by Neptune, 2005a (Table 16, p. 38) . Utah juniper (*Juniperus osteosperma*) is the only tree found in any of the five survey plots. The root/shoot ratio for trees is based on western juniper (*Juniperus occidentalis*), a closely related species, as reported by Miller et al. (2005, p. 16). No root shoot information was available for the primary forbs occupying the site (halogeton and curveseed butterwort). This lack of information represents a data gap, though biointrusion modeling at NNSS showed that forbs, due to their more shallow rooting system and smaller contribution to NAPP, contributed very minimally to the biotic transport of buried wastes. To parameterize this model input, the root/shoot ratio for other shrubs was used, because this ratio represents a uniform distribution with a wide range and relatively large upper bound. For modeling of contaminant uptake, this means that the distribution tends to be conservative, since a large proportion of the plant mass can be determined to be underground, which results in increased absorption and upward movement of any contaminants in a given layer where roots occur.

Table 4. Measured percent cover of plant groups within each vegetation type (From Tables 1 through 5 in SWCA, 2011)

	Plot 1: Mixed Grassland	**Plot 2: Juniper - Sagebrush**	**Plot 3: Greasewood**	**Plot 4: Halogeton - Disturbed**	**Plot 5: Shadscale - Gray Molly**
% Tree	0	6.2	0	0	0
% Greasewood	0	0	4.5	0.2	0.2
% Other Shrub	2.0	18.9	0.6	5.0	13.1
% Forb	2.2	1.4	0.8	3.9	1
% Grass	26.4	9.8	0	0	0.1
% Bare Ground	69.4	63.7	94.1	90.9	85.6

Table 5. Great Basin net annual primary productivity

Group	Value or Distribution	Units	References
Total Biomass (Primary productivity)	U(300, 1500)	kg/ha/yr	Range for Great Basin from Smith, et al 1997. Mean of 920 kg/ha/yr reported by Le Houerou 1984. Net primary productivity dependent upon total moisture availability
Biomass Greasewood Biomass Shrubs Biomass Grasses Biomass Forbs Biomass Trees	Apportioned from above by % cover of each vegetation type		

Table 6. Root/shoot ratios for plant groups at Clive Site.

ES Plant Type	Value or Distribution	Units	References
Forbs	U(0.40, 1.80)	—	Distribution of "Other Shrubs" used for conservatism, see text
Grasses	Tri(1, 1.2, 2)	—	Based on *H. comata* (ungrazed), Bethlenfalvay and Dakessian, 1984
Greasewood	U(0.30, 1.24)	—	Assumed similar to creosote, from NTS (Neptune, 2005a)
Other Shrubs	U(0.4, 1.8)	—	Based on range for *Artemisia* spp. from Barbour, 1973
Trees	U(0.55, 0.76)	—	For Western Juniper, Miller et al, 2005

3.5 Maximum Root Depths and Biomass

Maximum root depths for each of the plant groups are based on literature values as shown in Table 7. Forbs are the most shallowly rooted plant group at Clive, with halogeton roots extending half a meter or less based on excavations conducted by SWCA (2011, Table 6). Though roots of some perennial grasses have been shown to extend up to two and a half meters (Zlatnik, 1999c), maximum rooting depths for the two most abundant grasses identified in the 2011 SWCA surveys of the Clive plots [needle and thread grass (*Hesperostipa comata*) and cheatgrass (*Bromus tectorum*)], extend about 1.5 meters (Zlatnik, 1999a, and Zouhar, 2003). Greasewood has been reported to extend taproots up to 19 meters to reach groundwater (SWCA Environmental Consultants, 2000, p. 2), though this extreme situation will only occur when precipitation can infiltrate to groundwater, as greasewood roots cannot penetrate the very dry soil that occurs below the zone of infiltration. The vegetative survey of the Clive site found that the majority of greasewood plants are less than one meter tall, and studies have found that greasewood of that size tend not to produce taproots (Robertson, 1983). Still, larger plants do occupy parts of the Clive site, especially where precipitation runoff is concentrated, and these plants may extend taproots to exploit deeper water. A maximum root depth of 5.7 meters (Robertson, 1983, p. 311) is used in this model. Maximum root depth for the "Other Shrub" category is based on rooting depths for shadscale as reported in Branson et al., (1976, Fig. 19, P. 1120). The maximum rooting depth of three shadscale excavated at the Clive site (Table 6 in SWCA, 2011) was approximately 75 cm. The proportion of root biomass as a function of depth was determined for greasewood, shadscale (i.e. other shrubs), and halogeton and mojave seablite (i.e. forbs) based on root profile excavations conducted by SWCA Environmental Consultants (2011) and is presented in Table 8. Maximum rooting depth for the only tree species found on any of the five survey plots (Utah juniper, *Juniperus osteosperma*) was based on rooting depths of the similar Western juniper (*Juniperus occidentalis*), which has been found to extend taproots as deep as 4.5 meters (Zlatnik, 1999b, p. 6). Understanding root biomass by depth is necessary to apportion below-ground biomass production to depth layers or "cells" within the cover component of the Clive PA model. The first step entails modeling the depth distribution of plant mass for each shrub and grass species. Once this is accomplished, a model is applied to the aggregate within each layer. The PA model utilizes the work done by Neptune (2005a) at NNSS to fit mathematical functions describing the root mass by depth for each of the plant groups. Fitting parameters (β) describing the root biomass as a function of depth for each of the Clive plant groups are presented in Table 9. All plant types use the same generic mathematical function to represent the density of roots with depth, from which is derived the value for f_i^N, the fraction of root in each layer N. Each plant type, however, is assigned specific distributions of parameter values z_i^{max} and β_i to change the shape of the function in order to fit available root density data.

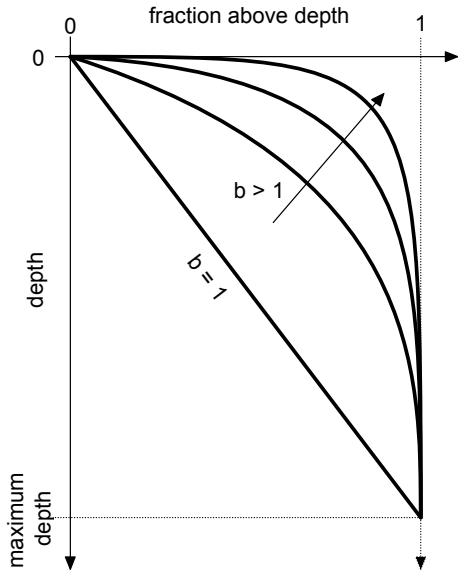

The function f_i used to represent root densities actually defines the fraction of all roots above any given depth. At depth $z = 0$, the value is obviously 0, and at the maximum

root depth $z = z_i^{max}$ the value is 1, meaning that all roots are above that depth (the definition of maximum root depth). The fraction of roots for plant *i* above any depth *z* is

$$f_i^z = 1 - \left(1 - \frac{z}{z_i^{max}}\right)^{\beta_i}. \quad \textbf{(1)}$$

Where:

f_i^z	Fraction of roots for plant *i* above any depth *z*
z_i^{max}	Maximum root depth for plant *i*
β_i	Fitting parameter for the root density equation, for plant *i*

A $\beta = 1$ indicates a uniform cylindrical "can-shape" distribution of roots from the surface to maximum rooting depth. Increasing β values result in a narrowing of overall rooting width with depth, with $\beta = 3$ resulting in a "cone-shaped" distribution of roots, and β values greater than 4 indicating increasingly "funnel-shaped" distributions with depth, as might be found in plants producing taproots. Neptune's work at the NNSS did not develop β parameters for forbs and trees. However, as shown in Table 8, excavations of halogeton, the dominant forb at the Clive site, show that all root mass is in the top 50 cm of soil. Tilley et al. (2008) report that halogeton does form a taproot that can extend to approximately 50 cm below the surface. Therefore, the selected β for forbs at Clive was based on the β for "other shrubs" at the NNSS, which though had deeper maximum rooting depths, had similar "shape" of root apportionment with depth. As discussed previously, the NNSS biointrusion modeling excluded evaluation of forbs due to their minimal contribution to the biotic transport of buried wastes. Additional excavations of halogeton to better define distribution of root mass with depth could be performed in the future if this uncertainty influences modeling results. Neptune's work at the NNSS also did not derive β parameters for trees. Therefore, the fitting parameter for juniper roots is based upon the β derived for creosote, which also forms a taproot and has a fairly deep maximum rooting depth [315 cm (Neptune, 2005a)] as that used here for juniper [450 cm (Zlatnik, 1999b)].

Table 7. Maximum root depths for plant groups at the Clive Site

ES Plant Type	Value or Distribution	Units	References
Forbs	51	cm	For Halogeton from Pavek, 1992
Grasses	150	cm	Based on *H. comata* (Zlatnik, 1999a) and *B. tectorum* (Zouhar, 2003), the two most abundant grasses at Clive
Greasewood	570	cm	Robertson, 1983
Other Shrubs	110	cm	Based on shadscale from Branson et al, 1976
Trees	450	cm	Value for Western Juniper from Zlatnik, 1999b

Table 8. Proportion root biomass by depth from Clive excavations conducted by SWCA Environmental Consultants (extrapolated by multiplying average number of roots per cm in each layer by the total rooting width in each layer, with all layers summing to 1)

Depth Interval (cm)	Proportion Rootmass in Layer					
	Black Greasewood		Other Shrubs		Forbs	
	Mean	St. Dev.	Mean	St. Dev.	Mean	St. Dev.
0-10	0.029	0.025	0.096	0.023	0.217	0.109
10-20	0.405	0.315	0.344	0.227	0.434	0.219
20-30	0.292	0.18	0.306	0.059	0.268	0.213
30-40	0.15	0.065	0.197	0.124	0.07	0.099
40-50	0.078	0.029	0.042	0.019	0.012	0.016
50-60	0.03	0.041	0.003	0.006	0	0
60-70	0.015	0.014	0.002	0.003	0	0
70-80	0.001	0.001	0.003	0.006	0	0
80-90	0	0	0.003	0.006	0	0
90-100	0	0	0.005	0.009	0	0

Table 9. Fitting parameter b describing root biomass above a given depth for each plant type

ES Plant Type	Value or Distribution	References
Forbs	N(μ=23.9 σ =0.313, min=1, max=Large)	Fitting parameter based on "other shrubs" at NNSS (Neptune, 2005a). See Section 3.5
Grasses	N(2.19, 0.036, min=1, max=Large)	Fitting parameter for perennial grasses (Neptune, 2005a)
Greasewood	N(μ=14.6, σ=0.0807, min=1, max=Large)	Based on fitting parameter for creosote at NNSS (Neptune, 2005a)
Other Shrubs	N(23.9, 0.313, min = 1, max=Large)	Based on fitting parameter for four-winged saltbush at NNSS (Neptune, 2005a)
Trees	N(μ=14.6 σ=0.0807, min=1, max=Large)	Based on fitting parameter for creosote at NNSS (Neptune 2005a). See Section 3.5

3.6 Estimation of Plant Uptake

Radionuclide concentrations in plant tissues are calculated based on root uptake using plant-soil concentration ratios ($K_{p\text{-}s}$), expressed as activity per dry weight plant tissue divided by activity per dry weight of bulk soil (Bq/g per Bq/g). Element-specific $K_{p\text{-}s}$ values were preferentially obtained from a recent publication of the International Atomic Energy Agency (IAEA, 2010). A report by Pacific Northwest National Laboratory (Staven et al., 2003) was used as a secondary reference when element-specific values were not available in IAEA (2010).

Element-specific values of $K_{p\text{-}s}$ were available in IAEA (2010) for all Clive PA radionuclides of concern with the exception of actinium, iodine, protactinium, and radon. For actinium and protactinium, americium values were employed as a surrogate as suggested in Staven et al., 2003). A $K_{p\text{-}s}$ value for iodine was obtained from Stave et al. (2003). A summary of $K_{p\text{-}s}$ values used in the Clive PA is provided in Table 10.

Distributional form for the values of geometric mean and geometric standard deviation reported in IAEA (2010) was not discussed in this reference. In order to provide a common set of inputs, values obtained from IAEA (2010) and Staven et al. (2003) were processed to conform to an assumed lognormal distribution. The value for iodine originally reported as an arithmetic mean was transformed to a geometric mean equivalent. $K_{p\text{-}s}$ data were reported in IAEA (2010) as a geometric mean, geometric standard deviation, minimum, and maximum. The geometric standard deviations are greater than 2 in nearly every case, suggested high right-skewness in the data, and the minimum and maximum were consistent with samples from a lognormal distribution. In order to establish a distribution for the mean, a parametric bootstrap approach was taken (Efron 1998), simulating bootstrap samples from the lognormal distribution using the maximum likelihood estimates of the lognormal parameters. A lognormal distribution was then fit to the resulting

bootstrap simulations of the mean, since some right-skewness was still present in the sampling distribution.

Plant-soil concentration ratios reflect an assumption that there is a linear and unchanging relationship between soil and plant tissue concentrations. In reality, $K_{p\text{-}s}$ values are liable to overestimate plant tissue concentrations as soil concentrations increase to levels higher than those employed in the studies from which the values are derived. This concern may apply in the Clive PA to conditions where plant roots are in contact with relatively high uranium concentrations, such as in disposed DU waste. The GoldSim model assumes that plant roots are in contact with soils in various layers belowground, each of which has its own concentration of contaminants ("Species" in GoldSim parlance). The roots present in each layer absorb each Species proportionally to the concentration of that Species in the soil in that layer. These absorbed Species are distributed uniformly throughout all the plant's tissues, aboveground and belowground. The plant is then assumed to die off, and all the Species contained within it are returned to soils in each layer according to the fraction of roots present in that layer. Aboveground plant parts are returned to the topmost soil layer. All of these processes take place in a single time step.

Table 10. Plant/soil concentration ratios

Element	Sample Size	Geometric Mean	Geometric St. Dev.	Notes
Actinium	27	0.0037	1.50	Americium used as a surrogate, based on Staven et al. (2003)
Americium	27	0.0037	1.50	
Cesium	401	0.67	1.13	
Iodine	1	0.066	3.87	Geo mean based on Staven et al. (2003). Geo SD from Sheppard and Evenden (1997).
Neptunium	16	0.095	1.35	
Protactinium	27	0.0037	1.50	Americium used as a surrogate, based on Staven et al. (2003).
Lead	34	0.29	1.54	
Plutonium	22	0.0010	1.35	
Radium	42	0.44	1.82	
Radon	NA	arbitrarily small number	1	Radon gas is inert and has effectively no potential to establish equilibrium in plant tissue.
Strontium	172	1.8	1.07	
Technetium	18	131	1.39	
Thorium	64	0.39	1.47	
Uranium	53	0.17	1.49	

The concentration of Species *j* in the plant *i* with roots in layer *N* is simply

$$C_{i,j}^{N} = CR_j \cdot C_s^N . \quad \textbf{(2)}$$

Where:

$C_{i,j}^{N}$ Concentration of Species *j* in plant *i* roots in layer *N*

CR_j Concentration ratio for all plants and Species *j* (Table 10)

C_s^N Concentration in soil on layer N

The total mass of Species *j* extracted by roots of plant *i* from soils (or wastes) in layer *N* is

$$M_{i,j}^{N} = C_{i,j}^{N} \cdot MP_i \cdot f_i^N \cdot f_{root} + C_{i,j}^{N} \cdot MP_i \cdot f_i^N \cdot f_{shoot} \quad \textbf{(3)}$$

Where:

f_i^{root} Mass fraction of plant *i* that is in the roots (belowground fraction)

f_i^N Mass fraction of root of plant *i* that is in layer *N* (so that the fraction of the entire plant in layer *N* is $f_i^{root} \times f_i^N$)

f_i^{shoot} Mass fraction of plant *i* that is in the shoots (aboveground fraction)

$M_{i,j}^{N}$ Mass of Species *j* extracted by the roots of plant *i* in layer *N*

MP_i Mass of all individuals of plant *i* over the site (M)

The model assumes that all absorbed Species are distributed uniformly throughout all the plant tissues, both aboveground parts and roots. The total mass of Species *j* in plant *i* is the total mass extracted by the roots of the plant summed across all *N* layers:

$$M_{i,j}^{T} = \sum_N M_{i,j}^{N} . \quad \textbf{(4)}$$

Where:

$M_{i,j}^{T}$ Total mass of Species *j* extracted by the roots of plant *i* and redistributed throughout the plant tissues

$M_{i,j}^{N}$ Mass of Species *j* extracted by the roots of plant *i* in layer *N*

This total amount of Species mass is divided up into the parts of the plant that occupy each layer, as well as the aboveground parts, so that we may calculate the mass of contamination ${}^{+}M_{i,j}^{N}$ that the plant returns to the various soil layers upon senescence. The total amount of contamination returned to the soils must equal the amount that was absorbed (not accounting for decay of the Species), in order to conserve mass of the Species. This total absorbed Species mass is returned to the soil in proportion to the amount of plant in each layer, with the topmost soil layer also receiving the aboveground plant parts:

$$\begin{aligned} {}^{+}M_{i,j}^{1} &= M_{i,j}^{T} \cdot f_{root} \cdot f_{i}^{1} + M_{i,j}^{T} \cdot f_{shoot} \\ {}^{+}M_{i,j}^{2} &= M_{i,j}^{T} \cdot f_{root} \cdot f_{i}^{2} \\ &\vdots \\ {}^{+}M_{i,j}^{N} &= M_{i,j}^{T} \cdot f_{root} \cdot f_{i}^{N} \end{aligned} \quad \textbf{(5)}$$

The net mass added to each layer is the redistributed mass from Equation 5 minus the absorbed mass from Equation 3. For plant *i*, this net mass added is simply

$${}^{+}M_{i,j}^{N} - M_{i,j}^{N}. \quad \textbf{(6)}$$

The GoldSim model contains various plant types. For the sake of simplicity in defining changes to each cell's inventory, the Species redistribution for all plants can be combined to result in a net addition (or subtraction) of mass effected by all plants. To do so, we sum Equation 6 over all the plant types:

$${}^{+}M_{j}^{N} = \sum_{i} {}^{+}M_{i,j}^{N} \quad \text{and} \quad M_{j}^{N} = \sum_{i} M_{i,j}^{N}. \quad \textbf{(7)}$$

4.0 Ant Specifications and Parameters

4.1 Ant Conceptual Model

Ants fill a broad ecological niche in arid ecosystems as predators, scavengers, trophobionts and granivores. However, it is their role as burrowers that is of main concern for the purposes of this model. Ants burrow for a variety of reasons but mostly for the procurement of shelter, the rearing of young and the storage of foodstuffs. How and where ant nests are constructed plays a role in quantifying the amount and rate of subsurface soil transport to the ground surface at the Clive site. Factors relating to the physical construction of the nests, including the size, shape, and depth of the nest, are key to quantifying excavation volumes. Factors limiting the abundance and distribution of ant nests such as the abundance and distribution of plant species, and intra-specific or inter-specific competitors, also can affect excavated soil volumes. Parameters related to ant burrowing activities include nest area, nest depth, rate of new nest additions, excavation volume, excavation rates, colony density, and colony lifespan. These attributes are described in this section, along with other considerations involving the impact of ant species and their inclusion in the Clive PA model.

The calculations of contaminant transport due to ant burrowing involves three steps:

1. Identify which of the ant species overwhelmingly contribute to the rearrangement of soils near the surface at Clive.

2. Calculate soil and contaminant excavated volume using maximum depth, nest area, nest volume, colony density, colony life span, and turnover rate for predominant ant species.

3. Calculate burrow density as a function of depth to determine the distribution of contaminants within the vertical soil profile for each predominant ant species.

4.2 Clive Field Surveys

Surveys for ants at Clive were limited to surface surveys of ant colonies, including identification of ant species, measurements (length, width, and height) of ant mounds, and determination of ant nest densities in each vegetative association (SWCA Environmental Consultants, 2011). No excavations of ant nests were performed at Clive to support the initial GoldSim model, though excavations could be conducted to support future model iterations if ant nest depth and volume are found to be sensitive parameters. Only two species of ants were identified during the surveys, with the western harvester ant, *Pogonomyrmex occidentalis*, accounting for 62 of the 64 nests identified. The second ant species, a member of the genus *Lasius,* was only encountered twice, both times in the mixed grassland plot. A summary of ant nests in each vegetative association is shown in Table 11.

Table 11. Summary of ant nests in each vegetative association

Vegetative Association	Number of Mounds/Hectare	Average Mound Surface Area (sq dm)
Plot 1: Mixed Grassland	33	95.03
Plot 2: Juniper-Sagebrush	2	39.77
Plot 3: Greasewood	7	120.18
Plot 4: Halogeton-disturbed	17	84.43
Plot 5: Shadscale-Gray Molly	6	137.73

4.3 Ant Nest Volume

Ant nests were not excavated at the Clive site, so only nest surface area – not nest volume or depth data was available. Generally, the surface areas of the Clive sites were smaller than the surface areas at the sites studied at the NNSS. To obtain estimates of nest volumes, a regression was made using *Pogonomyrmex* nest volume surface area data collected at the NNSS (Neptune, 2006) with nest surface area data described in Table 11. The NNSS data and associated regressions are shown in Figure 2. To be consistent with the data available from NNSS, the areas calculated are the two-dimensional areas of the mound – not the conical surface area.

To predict nest volume as a function of surface area, the following steps were taken:

1. Using data from NNSS, a linear model was fit to log transformed surface area and volume data to predict nest volume. Figure 2 shows the fitted model along with the predicted values based on measured surface area values from the Clive study.

2. To estimate the uncertainty in the predicted volume values, a model-based resampling method was used. With the statistical model created with the NNSS data, data from Clive were resampled with replacement. New values were estimated by drawing from a normal distribution whose mean was the predicted value and whose standard deviation is a function of both the fitting error and the residual error. This was repeated 10,000 times
3. The distribution of the mean volume is summarized by the mean and standard deviation of the resampled values.

Modeling all sample plots together resulted in a volume distribution of N(0.161m^3, 0.024 m^3). Predicted nest volumes were smaller than those observed at NNSS, where the volume distribution was N(0.64 m^3, 0.091 m^3).

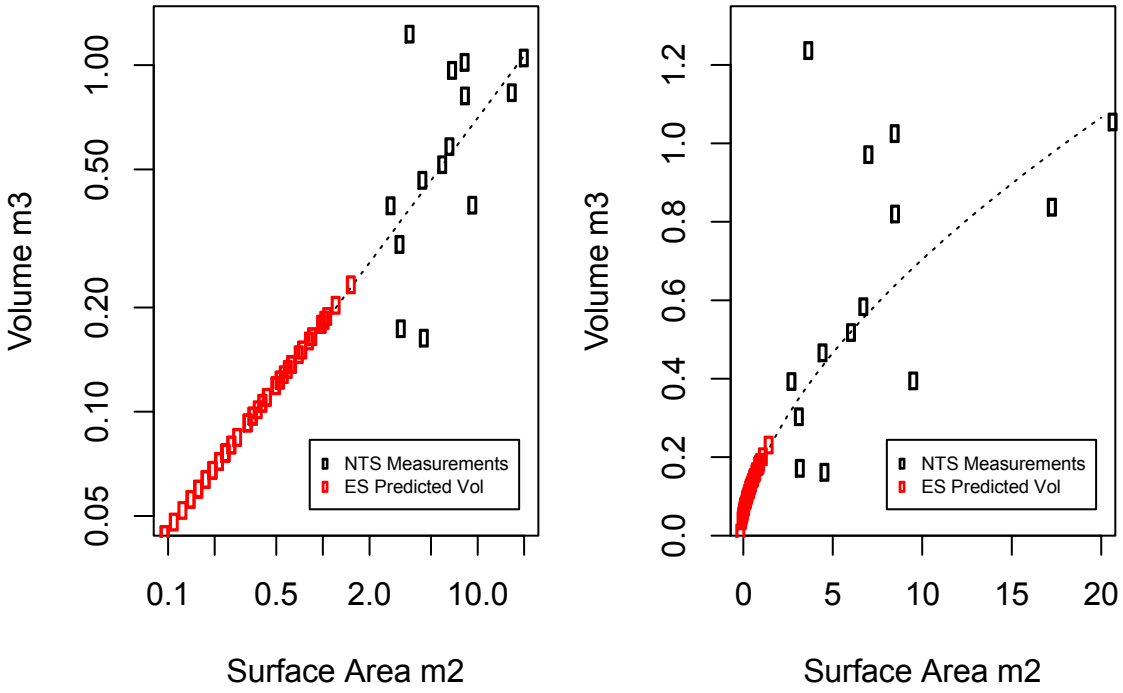

Figure 2. Linear regression model to predict ant nest volume based on nest surface area

4.4 Maximum Nest Depth

Again, since ant nests were not excavated, maximum nest depth had to be determined by other means. As shown in Figure 2, NNSS data support the assumption that larger mound surface area features correlate with larger nest volumes and deeper maximum depths, therefore the mound dimension data collected by SWCA (2011, Table 20, p. 23) was used to predict nest depths. The upper 95% prediction interval of SWCA-measured surface area was used with the NNSS linear model predicting depth as a function of surface area. The upper 95% prediction interval was used in lieu of a maximum value because taking the maximum of simulated values from an unbounded

normal distribution could result in an unrealistically large value. Using this approach, the predicted maximum nest depth at Clive is 212 cm.

4.5 Colony Lifespan

A critical component in modeling excavation volume is the turnover rate, or the fraction of the volume of the ant nest that is excavated in any given year. The turnover rate itself is inversely related to the life span of the colony. Table 12 shows four literature studies that report colony lifespan for *P. occidentalis* or *Pogonomyrmex* spp. These *Pogonomyrmex* spp. entries are included because the *P. occidentalis* study simply suggests colony lifespan is greater than 7 years, indicating that the study did not continue until colony failure. The non-specific studies include one entry that suggests a range of 15-20 yrs, one that suggests a range for the Queen of 17-30 but only 2-17 for the nest, and an entry of 20.2 ± 8.1 (standard deviation) based on 5 observations. The NNSS cover modeling (Neptune, 2006) used the latter entry, including the information that there were 5 data points. Since the standard deviation was based on 5 observations, the standard deviation of 8.1 was divided by the square of 5 to arrive at a normal distribution with a mean of 20.2 years and standard deviation of 3.6 years. This same distribution was used here. To ensure non-negative values as well as allow division by colony life, the distribution is truncated at 1e-20.

Table 12. Summary of *Pogonomyrmex* nest longevity reported in literature (Adapted from Neptune 2006, Table 6, p. 32)

Genera and species	Max nest (n) or queen (q) longevity (years)	Number of observations	Authors
Pogonomyrmex	17–30 (q)		Hölldobler and Wilson 1990
	2–17 (n)		Hölldobler and Wilson 1990
	20.2 ± 8.1	5	Porter and Jorgensen 1988
Pogonomyrmex occidentalis (Cresson)	>7 (n)		Hölldobler and Wilson 1990

4.6 Burrow Density as a Function of Depth

Excavation volume gives an overall picture of how much soil is being transported to the soil surface, however, it is also important to determine the density of burrowing activities as a function of depth within the vertical soil profile. The shape of the nest under the surface expression of the nest gives insight into the quantity of contaminated soils at various depths being excavated to the surface. The burrow density as a function of depth is described by the fitting

parameter β. Lacking site-specific nest excavations at Clive, the fitting parameter developed in the NNSS study (Neptune, 2006) for all *Pogonomyrmex* species is used in the model. Based on bootstrapping, a normal distribution with a mean of 10 and standard deviation of 0.71, truncated at 1, was estimated for β (Figure 4) for *Pogonomyrmex* nests at NNSS (Neptune, 2006).

4.7 Colony Density

Colony densities in the five Clive plots ranged from two colonies per hectare in the Juniper-Sage habitat to 33 colonies per hectare in the mixed grassland (SWCA 2011, Table 20, p. 23). For the initial model, the colony density will use the non-informative prior distribution and the Bayesian posterior, meaning that for an observed count of X, the posterior distribution for the rate would be Gamma(X, 1) (where the 1 is in the units of data collection, i.e. 1/ha). Expressed another way, Bayesian statistics combines knowledge about a process generating data (in this case colony counts) with assumptions about the process. It is reasonable to assume that the colony counts are non-negative - making the gamma distribution more appropriate than a normal distribution. A non-informative prior indicates that other than the fact that counts cannot be negative, there is no data which might suggest how the colony counts are distributed for each location. In other circumstances, other data might be used to reduce uncertainty. In this case, the distributions are conservative and reflect this lack of prior knowledge. Figure 3 illustrates the shape of the distributions used to describe colony counts for each plot area.

Modeling soil and contaminant transport by ant species within the Clive PA model assumes that ants move materials from lower cells to those cells above while excavating chambers and tunnels within a nest. These chambers and tunnels are assumed to collapse over time and return soil from upper cells back to lower cells. Through this process the balance of materials is preserved through time. Soil and contaminant movement from one cell to another is calculated as follows. Within each layer, the fraction of excavated ant nest volume and the fraction of contaminants contained within that layer are determined. The fraction of contaminants within the excavated volume is based on the ratio of the excavated volume to total volume of each layer and is assumed to be distributed homogeneously within the layer. Secondly, the sum of contaminants from each layer associated with ant nest is calculated with the assumption that all excavations from layers below are deposited in the uppermost layer. Finally, downward movement of contaminants associated with chamber and tunnel collapse from each layer to the layer below is calculated and the net movement of contaminants into each layer is determined. The amount of contaminants in each layer is then used to adjust contaminant inventory in each layer for the next time step.

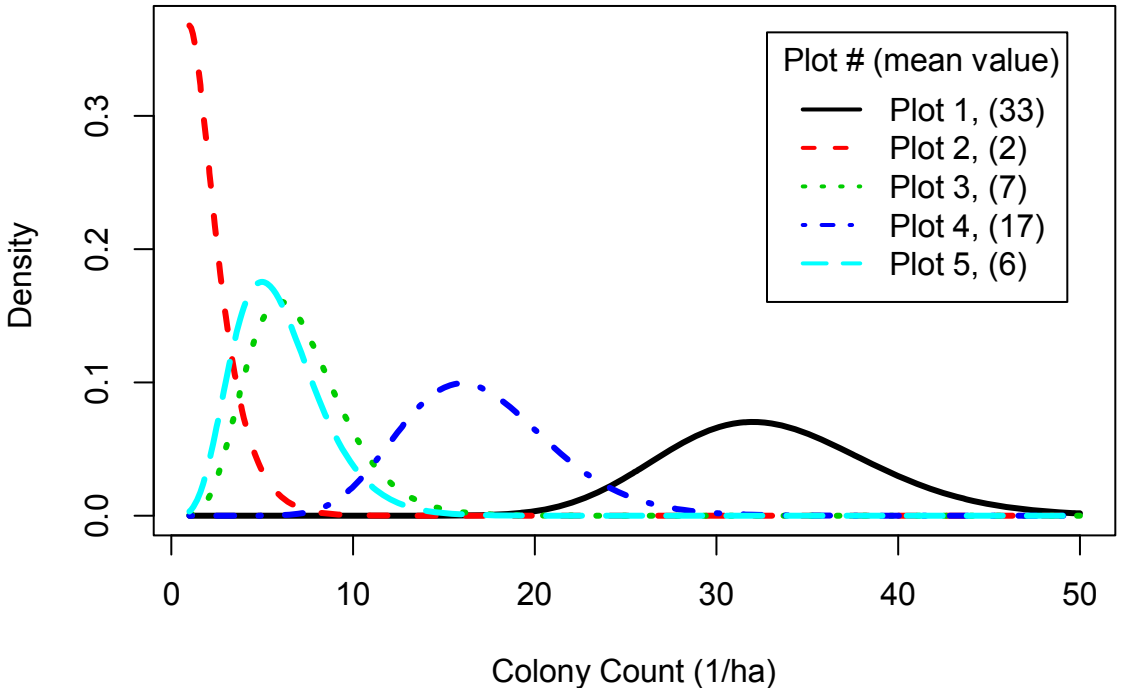

Figure 3 Distribution of ant colony counts for each plot area.

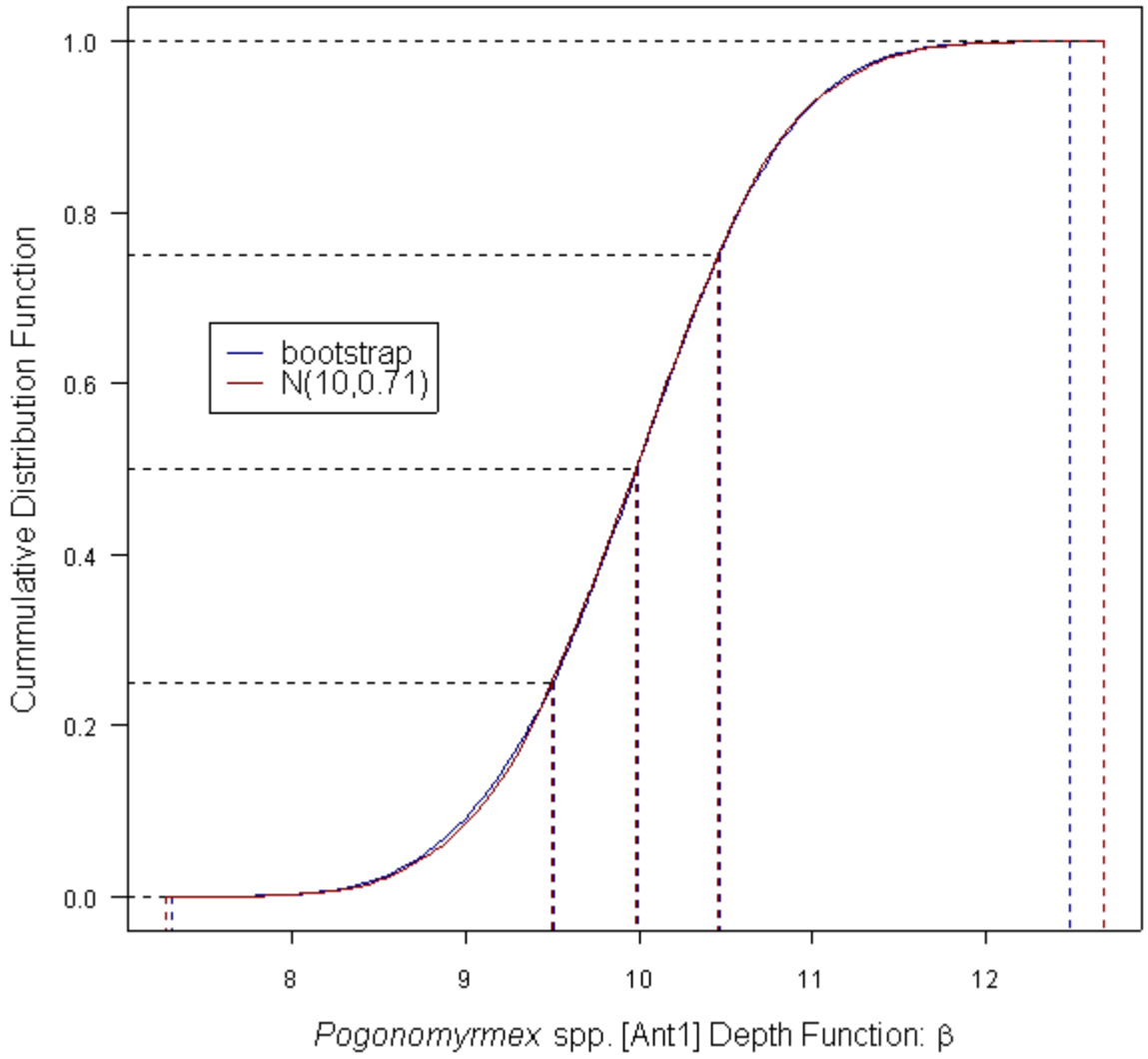

Figure 4. Comparison of bootstrapped and a normal distribution for *Pogonomyrmex spp.* nest density with depth β parameter

5.0 Mammal Specifications and Parameters

5.1 Mammal Conceptual Model

Burrowing mammals can have a profound impact on the distribution of soil and its contents near the soil surface. The degree to which mammals influence soil structure is dependent on the behavioral habits of individual species. While some species account for a large volume of soil displacement, others are less influential. This section presents the functional factors used to parameterize the Clive PA model. Factors such as burrowing depth, burrow depth distributions, percent burrow by depth, tunnel cross-section dimension, tunnel lengths, soil displacement by weight, soil displacement by volume and animal density per hectare play a critical role in determining the final soil constituent mass by depth within the soil.

Modeling soil and contaminant transport by mammal species within the Clive PA model assumes animals move materials from lower cells to those cells above while excavating burrows. Furthermore, burrows are assumed to collapse over time and return soil from upper cells back to lower cells (Figure 5). Thus, the balance of materials is preserved through time. Calculating soil and contaminant movement from one cell to another is straightforward. Within each layer, the fraction of burrow volume and the fraction of contaminants contained within the burrowed volume are determined. The fraction of contaminants within the burrowed volume is based on the ratio of burrow volume to total volume of each layer and is assumed to be distributed homogeneously within the layer. Secondly, the sum of contaminants from each layer associated with burrow excavation by all animal types is calculated with the assumption that all excavations from layers below are deposited in the uppermost layer. Finally, downward movement of contaminants associated with burrow collapse from each layer to the layer below is calculated and the net movement of contaminants into each layer is determined. The amount of contaminants in each layer is then used to adjust contaminant inventory in each layer for the next time step.

The calculations of contaminant transport due to mammal burrowing involves four steps:

1. Identify which of the mammal species overwhelmingly contribute to the rearrangement of soils near the surface.

2. Assign these mammal species to categories and determine the excavated volumes.

3. Calculate burrow density as a function of depth for mammal categories.

4. Determine the distribution of the burrow depth fitting parameter β for mammal categories.

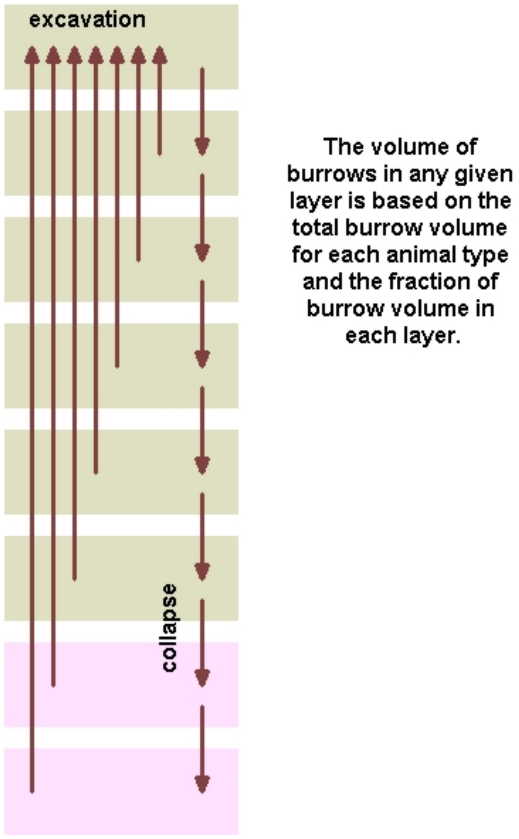

Figure 5. Conceptual diagram of soil movement by burrowing animals

5.2 Clive Site Surveys

Each Clive plot was surveyed for small mammal burrows during September and October 2010 (SWCA 2011). Burrows were identified by animal category, as shown in Table 13. Within the survey area four categories of mammal burrows were identified: ground squirrels, kangaroo rats, mouse/rats/voles, and one badger. Due to the small number of badger and ground squirrel burrows, the decision was made to treat all burrowing mammals as a single unit for modeling purposes. Small mammal trapping was conducted on the five Clive plots during the new moon in October 2010 to identify the principal small mammal fauna present in each vegetative association. Each 1.0-ha plot was subdivided into 25 20–m × 20–m subplots. At the center of the each subplot, two Sherman® live traps were placed, for a total of 50 traps per plot. Results of the small mammal trapping are presented in Table 14.

Table 13. Summary of Clive small mammal burrow surveys

	Badger	Ground Squirrel	Kangaroo Rat	Mouse/Vole/ Rat	Total
Plot 1: Mixed Grassland	0	2	102	131	235
Plot 2: Juniper-Sage	1	0	222	16	239
Plot 3: Greasewood	0	1	1	1	3
Plot 4: Halogeton-disturbed	0	0	0	0	0

Plot 5: Shadscale-Gray Molly	0	0	0	1	1

Deer mice (*Peromyscus maniculatus*) were the most abundant small mammal captured during trapping, and were the only mammal captured in the plots located on the Clive facility (Plots 3, 4, and 5). Plots 3, 4, and 5 were characterized by very low mammal densities, as evidenced by both the trapping results and the burrow surveys. With such a small population in plots 3, 4, and 5, the decision was made to average these plots. Similar to how the ant mound density data was used to develop distributions for the model, the resulting mammal burrow population counts were used to develop Gamma distributions for mound density. For the GoldSim model mound density is defined as Gamma(X, 1) where X is the number of mammal mound counts for each plot.

5.3 Mound Volume

After burrow surveys were completed, soil volumes were collected in a randomly selected ¼-plot (0.25 ha) within each plot. The obviously mounded or disturbed soil around a burrow entrance was collected and its volume measured. This provides an estimate of the volume of soil excavated to the surface from each burrow, with the assumption that the mounded soil represents excavations for a single year. Results of the mound volume measurements are shown in Table 15. Based on analysis of the data presented in Table 15, the per-mound volume is defined as a normal distribution with a mean of 0.0006 m^3/yr, and a standard deviation of 0.00015 m^3/yr. Total annual excavated volume is equal to the per mound volume multiplied by the mound density.

5.4 Maximum Burrow Depth

Maximum burrow depth was set at 200 cm based on best professional judgment. This depth is consistent with that used at NNSS by Neptune (2005b), and represents the likely average vertical extent of multiple badger excavations (Kennedy et. al, 1985).

5.5 Burrow Density as a Function of Depth

The β parameter describes the burrow density as a function of depth, and alters the form and volume of the excavated burrow. As the value of β increases, the fraction of burrow excavated at each depth moves from being evenly distributed to a highly skewed distribution with most of the excavation occurring near the soil surface. Since no below-ground measurements were obtained on mammal burrows at Clive, this version of the PA model uses the β parameter derived by Neptune (2005b) for rodents at NNSS. The β parameter, defined based on analysis of NNSS data, resulted in a parameter estimate of 4.5 and a standard error of 0.84. Badger data were not used in the derivation of the β parameter do to the overall scarcity of badgers in the survey area, where only one badger burrow was recorded in the five hectares surveyed across all vegetation types.

Table 14. Results of Clive small mammal trapping

Plot	Date	Species	Count - Species	Sum - # Recaptured	Sum - # Deceased
1			24	7	3
	10/5/2010		4	0	0
		Peromyscus maniculatus	4	0	0
	10/6/2010		4	0	1
		Peromyscus maniculatus	4	0	1
	10/7/2010		8	3	1
		Peromyscus maniculatus	6	3	1
		Dipodomys microps	1	0	0
		Onychomys leucogaster	1	0	0
	10/8/2010		8	4	1
		Peromyscus maniculatus	8	4	1
2			43	5	0
	10/5/2010		7	0	0
		Peromyscus maniculatus	7	0	0
	10/6/2010		8	2	0
		Peromyscus maniculatus	8	2	0
	10/7/2010		14	0	0
		Peromyscus maniculatus	10	0	0
		Dipodomys microps	3	0	0
		Dipodomys ordii	1	0	0
	10/8/2010		14	3	0
		Peromyscus maniculatus	11	3	0
		Dipodomys microps	3	0	0
3			2	1	0
	10/6/2010		1	0	0
		Peromyscus maniculatus	1	0	0
	10/7/2010		1	1	0
		Peromyscus maniculatus	1	1	0
4			1	0	0
	10/8/2010		1	0	0
		Peromyscus maniculatus	1	0	0
5			4	1	0
	10/6/2010		1	0	0
		Peromyscus maniculatus	1	0	0
	10/7/2010		1	0	0
		Peromyscus maniculatus	1	0	0
	10/8/2010		2	1	0
		Peromyscus maniculatus	2	1	0
Total			74	14	3

Table 15. Soil volume (m^3) of excavated mammal burrows

Plot	Burrow ID	Number of Burrows	Kangaroo Rat	Mouse/Vole/Rat	Badger	Grand Total
1			0.01203	0.00059		0.01262
	1SW104	2	0.0035			0.0035
	1SW105	1		0.00001		0.00001
	1SW106	2		0.0002		0.0002
	1SW107	1		0.00001		0.00001
	1SW108	1	0.00005			0.00005
	1SW110	1	0.00125			0.00125
	1SW111	2	0.0003			0.0003
	1SW112	4	0.00056			0.0006
	1SW113	1		0.00003		0.00003
	1SW114	1		0.00001		0.00001
	1SW115	1	0.00025			0.00025
	1SW116	1	0.00005			0.00005
	1SW117	3	0.0025			0.0025
	1SW118	4		0.00008		0.00008
	1SW119	1	0.00003			0.00003
	1SW120	1	0.00003			0.00003
	1SW121	3	0.00009			0.00009
	1SW122	2	0.00003			0.00003
	1SW123	1	0.00003			0.00003
	1SW124	1	0.0002			0.0002
	1SW125	1	0.00015			0.00015
	1SW126	1	0.0001			0.0001
	1SW127	1		0.00001		0.00001
	1SW128	4	0.00286			0.00286
	1SW129	1	0.00005			0.00005
	1SW130	1		0.00004		0.00004
	1SW131	2		0.00005		0.00005
	1SW132	2		0.00003		0.00003
	1SW133	1		0.0001		0.0001
	1SW134	1		0.00002		0.00002
2			0.037845	0.00019	0.006	0.044035
	2NE002	1	0.00005			0.00005
	2NE006	1		0.00001		0.00001
	2NE007	1	0.00001			0.00001
	2NE009	6	0.00015			0.00015
	2NE010	1		0.06000		0.00006
	2NE012	1	0.000225			0.000225
	2NE015	1			0.006	0.006
	2NE019	2	0.00135			0.00135

Plot	Burrow ID	Number of Burrows	Kangaroo Rat	Mouse/Vole/Rat	Badger	Grand Total
	2NE020	11	0.00683			0.00683
	2NE021	14	0.002975			0.002975
	2NE025	1	0.00006			0.00006
	2NE026	3	0.000185			0.000185
	2NE027	1		0.0001		0.0001
	2NE028	1	0.00005			0.00005
	2NE029	1	0.0002			0.0002
	2NE037	1		0.00001		0.00001
	2NE040	1	0.00001			0.00001
	2NE041	4	0.00004			0.00004
	2NE044	1		0.00001		0.00001
	2NE046	3	0.0003			0.0003
	2NE048	2	0.0001			0.0001
	2NE051	10	0.01501			0.01501
	2NE052	3	0.0095			0.0095
	2NE104	2	0.0008			0.0008
3				0.001		0.001
	3NE003	1		0.001		0.001
5				0.01375		0.01375
	5SW001	1		0.01375		0.01375
Grand Total		124	0.049875	0.01553	0.006	0.071405

6.0 References

Bethlenfalvay, G.J., and S. Dakessian. 1985. Grazing effects on mycorrhizal colonization and floristic composition of the vegetation on a semiarid range in Northern Nevada. *J. Range Management*. 37(4): 312-316.

Branson, F.A., Miller, R.F., and I.S. McQueen. 1976. Moisture relationships in twelve northern desert shrub communities near Grand Junction, Colorado. *Ecology*. 57: 1104-1124.

Efron B., and Tibshirani R.J. 1998. Introduction to the Bootstrap, CRC Press, Boca Raton, FL.

Hölldobler B. and E.O. Wilson. 1990. The Ants. The Belknap Press of Harvard University Press, Cambridge, Massachusetts. 732 pp.

IAEA, 2010. *Handbook of Values for the Prediction of Radionuclide Transfer in Terrestrial and Freshwater Environments*, Technical Report Series No. 472, International Atomic Energy Agency, Vienna, 2010.

Kennedy, W.F., L.L. Cadwell, and D.H. McKenzie. 1985. Biotic transport of radionuclide wastes from a low-level radioactive waste site. *Health Physics* 49(1): 11–24.

Neptune. 2005a. Plant Parameter Specifications for the Area 5 and Area 3 RWMS Models. Neptune and Company, Inc.

Neptune. 2005b. Mammal Parameter Specifications for the Area 5 and Area 3 RWMS Models. Neptune and Company, Inc.

Neptune. 2006. Ant Parameter Specifications for the Area 5 and Area 3 RWMS Models. Neptune and Company, Inc.

Pavek, Diane S. 1992. *Halogeton glomeratus*. In: Fire Effects Information System, [Online]. U.S. Department of Agriculture, Forest Service, Rocky Mountain Research Station, Fire Sciences Laboratory (Producer). Available: http://www.fs.fed.us/database/feis/ [2011, February 22]

Robertson, J.H., 1983. Greasewood (Sarcobatus vermiculatus (Hook.) Torr.). *Phytologia*. 54(5): 309-324.

Sheppard, S.C. and W.G. Evenden. 1997. Variation in Transfer Factors for Stochastic Models: Soil-to-Plant Transfer, *Health Physics*, 72: 727-33.

Smith, S.D., Monson, R.K., and J.E. Anderson. 1997. *Physiological Ecology of North American Desert Plants*. Springer-Verlag, Berlin. 286 pages.

Staven L.H., Napier B.A., Rhoads K., Strenge DL. 2003. *A Compendium of Transfer Factors for Agricultural and Animal Products,* Pacific Northwest National Laboratory, Richland WA.

SWCA Environmental Consultants. 2000. *Assessment of Vegetative Impacts on LLRW*. Prepared for Envirocare of Utah, Inc. Salt Lake City, UT. 12 pages.

SWCA Environmental Consultants. 2011. *Field Sampling of Biotic Turbation of Soils at the Clive Site, Tooele County, Utah*. Prepared for Energy Solutions, Salt Lake City, UT. 31 pp.

Tilley, D., Ogle, D., and L. St. John. 2008. Halogeton, *Halogeton glomeratus* (M. Bieb.) C. Meyer. USDA NRCS Plant Guide. United States Department of Agriculture. Available: http://plants.usda.gov/plantguide/pdf/pg_hagl.pdf [2011, May 11]

Zlatnik, Elena. 1999a. *Hesperostipa comata*. In: Fire Effects Information System, [Online]. U.S. Department of Agriculture, Forest Service, Rocky Mountain Research Station, Fire Sciences Laboratory (Producer). Available: http://www.fs.fed.us/database/feis/ [2011, February 22].

Zlatnik, Elena. 1999b. *Juniperus osteosperma*. In: Fire Effects Information System, [Online]. U.S. Department of Agriculture, Forest Service, Rocky Mountain Research Station, Fire Sciences Laboratory (Producer). Available: http://www.fs.fed.us/database/feis/ [2011, February 22].

Zlatnik, Elena. 1999c. *Agropyron cristatum*. In: Fire Effects Information System, [Online]. U.S. Department of Agriculture, Forest Service, Rocky Mountain Research Station, Fire Sciences Laboratory (Producer). Available: http://www.fs.fed.us/database/feis/ [2011, February 22].

Zouhar, Kris. 2003. *Bromus tectorum*. In: Fire Effects Information System, [Online]. U.S. Department of Agriculture, Forest Service, Rocky Mountain Research Station, Fire Sciences Laboratory (Producer). Available: http://www.fs.fed.us/database/feis/ [2011, February 22].

Neptune and Company Inc.

June 1, 2011 Report for EnergySolutions

Clive DU PA Model, version 1

Appendix 10

Erosion Modeling

Erosion Modeling for the Clive PA

28 May 2011

Prepared by
Neptune and Company, Inc.

This page is intentionally blank, aside from this statement.

CONTENTS

FIGURES

TABLES

1.0 Erosion Model Input Distribution Summary

A summary of parameter values and distributions employed in the erosion modeling component of the Clive Performance Assessment (PA) model is provided in Table 1. Additional information on the derivation and basis for these inputs is provided in subsequent sections of this report.

For distributions, the following notation is used:

- N(μ, σ, [*min*, *max*]) represents a normal distribution with mean μ and standard deviation σ, and optional truncation at the specified *min*imum and *max*imum,
- LN(*GM*, *GSD*, [*min*, *max*]) represents a log-normal distribution with geometric mean *GM* and geometric standard deviation *GSD*, and optional *min* and *max*,
- U(*min*, *max*) represents a uniform distribution with lower bound *min* and upper bound *max*,
- Beta(μ, σ, *min*, *max*) represents a generalized beta distribution with mean μ, standard deviation σ, minimum *min*, and maximum *max*,
- Gamma(μ, σ) represents a gamma distribution with mean μ and standard deviation σ, and
- TRI(*min*, *m*, *max*) represents a triangular distribution with lower bound *min*, mode *m*, and upper bound *max*.

Table 1. Summary of distributions for gully modeling

GoldSim Model Parameter	Symbol	Units	Distribution or Value	Notes
Gully_b_parameter	b	—	normal(μ = -0.4, σ = 0.15, min = -0.75, max = -0.05)	See Section 5.1
L_init	L_0	m	uniform(Small[1], 5)	See Section 4.1
AngleOfRepose_Gully	α_{gully}	deg	normal(μ = 38, σ = 5, min = Small, max = 90 – Small)	Clover, 1998 (for gravel); See Section 4.1
AngleOfRepose_Fan	α_{fan}	deg	uniform(5, 10)	See Section 4.1
Number_of_Gullies		—	Discrete uniform(min=1, max=20)	See Section 4.0 and Section 6.0
ConvergenceCriterion		m^3	0.01	modeling construct

2.0 Introduction

The safe storage and disposal of depleted uranium (DU) waste is essential for mitigating releases of radioactive materials and reducing exposures to humans and the environment. Currently, a radioactive waste facility located in Clive, Utah (the "Clive facility") operated by the company EnergySolutions Inc. is being considered to receive and store DU waste that has been declared surplus from radiological facilities across the nation. The Clive facility has been tasked with

disposing of the DU waste in a manner that protects humans and the environment from future radiological releases.

To assess whether the proposed Clive facility location and containment technologies are suitable for protection of human health, specific performance objectives for land disposal of radioactive waste set forth in Utah Administrative Code (UAC) Rule R313-25 *License Requirements for Land Disposal of Radioactive Waste - General Provisions* must be met—specifically R313-25-8 *Technical Analyses*. In order to support the required radiological performance assessment (PA), a probabilistic computer model has been developed to evaluate the doses to human receptors and concentrations in groundwater that would result from the disposal of radioactive waste, and conversely to determine how much waste can be safely disposed at the Clive facility. The GoldSim systems analysis software (GTG, 2010) was used to construct the probabilistic PA model.

The site conditions, chemical and radiological characteristics of the wastes, contaminant transport pathways, and potential human receptors and exposure routes at the Clive facility that are used to structure the quantitative PA model are described in the conceptual site model documented in the white paper entitled *Conceptual Site Model for Disposal of Depleted Uranium at the Clive Facility* (Clive DU PA CSM.pdf).

The purpose of this white paper is to address specific details of the erosional processes that may affect cap performance and thus potentially result in the exposure of waste. This paper is organized to give a brief overview of erosional processes, present the overall modeling approach and assumptions, followed by the presentation of the mathematical formulae that are used to represent these processes in the GoldSim PA model.

3.0 Erosion Overview

Above-ground caps of waste repositories are subject to erosion by the forces of wind and water. The proposed waste disposal cell for DU at the Clive facility, which has an engineered above-ground cap, is subject to these erosional processes. Both wind and water erosion are represented in the Clive PA model. Wind erosion is briefly discussed below but is addressed in detail in the white paper, *Atmospheric Transport Modeling for the Clive Performance Assessment* (Atmospheric Modeling.pdf). Water erosion via the return of Lake Bonneville or a small lake is not discussed in this document, but is addressed in the Neptune white paper, *Deep Time Assessment for the Clive PA* (Deep Time Assessment.pdf). Other water erosional processes are described below.

The composition of the above-ground cap is an important factor in determining its erodibility. At the Clive facility, the top slope of the cap is composed of 18 inches of armor material (rip rap) above a 6-inch gravel layer, a 12-inch sacrificial soil layer, and a 6-inch lower gravel layer (Energy*Solutions,* 2009). The side slope has the same composition as the top slope, except with an 18-inch lower gravel layer. The large particle-sized material of the rip rap is generally considered to be resistant to movement by erosion. However, if there is sufficient disturbance by animals or OHVers, this may trigger erosion. The conceptual model for the Clive PA model assumes that wind-blown material will infill the pore space between the larger materials of the

cap, including the rip rap. This wind-blown material has a finer particle size and moves more readily with wind or water forces acting on the cap compared to the rip rap or gravel, which has larger particle sizes.

The following sections give conceptual overviews that relate to the various erosional processes that are considered as part of the Clive PA conceptual model. These sections set the conceptual basis for the modeling assumptions described in Section 5.0.

3.1 Wind Erosion

At the Clive facility, wind is expected to cause infilling of the spaces in the rip rap and the gravel layers over a relatively short period of time. For modeling simplification and because the overall time period of the model is so long, it is assumed that infill happens immediately at the beginning of the modeling run. Wind will also be the primary mechanism for blowing materials off-site. Once the cap infills with wind-blown material, it is assumed that the amount of soil removed off-site by wind erosion is the same as what is transported on-site, which results in a net mass balance of zero change by wind erosion. Details of wind erosion modeling for the Clive PA and the effects on dose to potential receptors are presented in the white paper, *Atmospheric Transport Modeling for the Clive Performance Assessment*.

3.2 Water Erosion

There are two types of water erosion in the Clive PA conceptual model: 1) sheet erosion and 2) gully erosion. These erosional processes are discussed in the following sections.

3.2.1 Sheet Erosion

Sheet erosion is erosion of soil particles by water flowing overland as a "sheet" in a downslope direction. During extremely high rainfall events when rain falls faster than water can infiltrate, runoff can occur, which acts as a mechanism for removing/eroding cap materials. Sheet erosion is a uniform process over the area of the cap and depends largely on its slope, as well as rainfall intensity. This is different than erosion that flows in defined channels (i.e., Gully Erosion), which is discussed in Section 3.2.2.

In the central area, or top slope, of the embankment, where slopes are gradual (about 2% slope), sheet erosion would be slower than on the steeper side slopes of the cell (about 20% slope) (*Embankment Modeling for the Clive PA Model* white paper). As soil and loess move down slope by sheet erosion, it is likely that their volumes would be replenished by deposition of clean loess from the surrounding environs (i.e., a net balance of zero change). In the end, the total soil volume on the embankment would not change, though there would be a slow movement of soils down slope, along with the contaminants they could potentially contain if the cap were breached. However, sheet erosion is not included in the Clive PA model given that the top slope of the cap is nearly horizontal and that the side slope will not have DU waste buried under it in the current engineering design, so that not much contamination would likely be moved off site. Sheet erosion likely would have little effect, except possibly to move a small amount of potentially contaminated soil down slope. The potential contribution from sheet erosion could be evaluated

further by examining surface concentrations in the cap. Sheet erosion is not included in the Clive PA model since gully erosion is included and has a much more significant impact.

3.2.2 Gully Erosion

Gully erosion is a process that occurs when water flows in narrow channels, particularly during heavy rainfall events. Gully erosion typically results in a gully that has an approximate "V" cross section which widens (lateral growth) and deepens (vertical growth) through time until the gully stabilizes. The formation of gullies is a concern on uranium mill tailings sites and other long-term above-ground radioactive waste sites (NRC 2010). Gully erosion has the potential to move substantial quantities of both cap materials and waste, should the waste material be buried close to the surface. It occurs when surface water runoff becomes channeled and repeatedly removes soil along drainage lines, creating a fan of the removed materials.

There are two important features of the gully that need to be considered when modeling gully erosion: the thalweg and the angle of repose. The thalweg is a line that joins the lowest points of the gully along the entire length of the gully in its downward slope defining the gully's deepest channel. It can conceptually be thought of as the bottom of the gully that runs along a downward slope. The angle of repose is the angle the side of the gully makes with the horizontal; it is a property of the material that is eroding.

The engineered cap at the Clive facility may be subject to gully erosion via a disturbance attributed to either an animal burrow or off-highway vehicle (OHV) track. It is assumed that a notch or nick will be created from these activities at some location on the surface of the cap and the feedback processes inherent in gully formation will cause erosion downward to the surrounding grade and erosion upward toward the top slope of the embankment. As water flows across the inner walls of the notch, erodible solid materials will be transported with it, creating a larger notch (both vertically and laterally) and thus a greater capacity to remove solid material. As this process continues, more material will erode down-gradient from the notch, as well as up-gradient from the notch. Also, as water flows down the thalweg it can undercut the gully banks, causing materials to slump into the thalweg, where they get washed along the downward slope until the angle of repose is reached. A wedge-shaped volume of material is removed and deposited on the neighboring flat as a sort of small alluvial fan, forming its own angle of repose. This process continues until the mouth of the gully has met the top of the removed material (Figure 1). With a brief screening assessment, gully erosion was evaluated as having the potential to occur at the Clive facility and is included using a simplified approach for the Clive PA model.

4.0 Gully Model Assumptions

In the development of the erosion modeling approach, Dr. Garry Willgoose, a geomorphologist with expertise in gully formation at The University of Newcastle, Australia, was consulted for advice relating to the modeling of gully formation at the Clive Site. Dr Willgoose is author of the erosion model SIBERIA (Willgoose, 2005) and has experience with gully formation on uranium mill tailings (Willgoose, 2010; Willgoose and Shermeen, 2006). The purpose of the initial gully

model in the Clive PA model is to determine whether gullies and fans are significant contributors to dose and whether a more sophisticated erosion model is needed. A simple screening-type gully model was developed with the advice of Dr. Willgoose. To that end, several simplifying assumptions are made:

- Gullies are assumed to form instantaneously, from the time of loss of institutional control. They do not evolve over time. To provide some understanding of what could happen if gullies were allowed to form at different times, concentrations in the gully material that is moved to the fan changes over time, as if the gully were formed instantaneously at any moment in time. These concentrations are used in the dose assessment. By this means, the effects of time are considered in the gully model.
- Gully formation occurs independently of main model processes. For example, processes such as biotic intrusion do not occur in gullies, nor does particle resuspension via wind erosion occur from the gully. In addition, the embankment remains intact – top and side slopes of the waste cell do not change in area or geometry with the formation of gullies.
- A small number of gullies are allowed to form, to evaluate the effects of more than one gully on dose and on model sensitivity. The distribution for the number of gullies allowed is a discrete uniform distribution from 1 to 20. Each gully has the same geometry for any given model realization.
- Types of gully-initiating events are not modeled. Conceptually, these could be either natural (e.g., animal burrows) or anthropogenic (e.g., OHV track). It is simply assumed that some triggering event occurs.
- The parameters for angles of repose, which are some of the parameters that dictate the geometry of the gullies, are based on the assumption of a homogenous cap material.
- The cross section of a gully is an inverted isosceles triangle, with the bottom vertex of the triangle following along a curved, downward sloping line that is the bottom of the gully (the thalweg).

As shown in Figure 1, gullies that form in the embankment may be of different depths or slightly different shapes. Thus, a different amount of material may be removed for different realizations, resulting in a different amount of potentially expose waste in different realizations. The first picture in Figure 1 shows the intact embankment, with different color shades demonstrating different layers of the cap and waste. The second picture in Figure 1 illustrates a shallow gully formed so that the gully and fan have equal volumes. It is clear that the height of the fan aligns with the mouth of the gully. The third picture in Figure 1 shows another, deeper gully formed. These gully depictions show the mouth of the gully and the height of the fan aligning, as well as equal volumes of fan and gully.

Gully geometry parameters are simulated probabilistically and are constant over a realization, assuming homogeneous materials. These parameters are then used to calculate the depth and volume of the formed gully. Based on this geometry, the amount of exposed waste is then calculated and included in the dose assessment as a soil concentration across the surface area of the fan and the gully.

The remainder of this document describes gully geometry and the derivation of a simple model of a gully, based on recommendations from Dr. Willgoose, as well as the implementation of this model in the Clive PA GoldSim model.

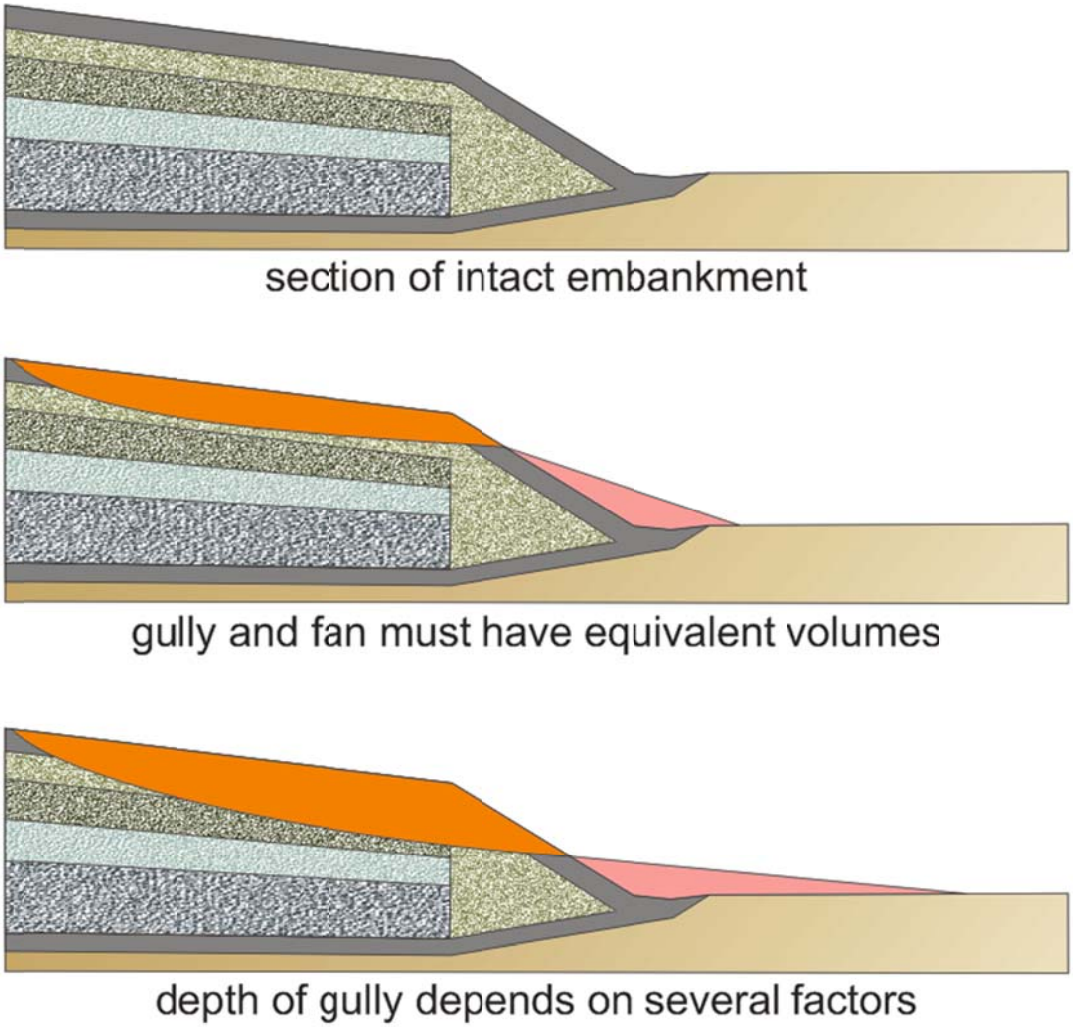

Figure 1. Illustration of the embankment with and without gullies

4.1 Gully Geometry Overview

The overall geometry of the simplified gully used in the Clive PA GoldSim model is illustrated in Figure 2. Both Figure 1 and Figure 2 show a representation of half of the embankment, with the ridge of the top slope on the vertical axis. The vertical axis in Figure 2 is the elevation above ground surface, and the horizontal axis is the distance from the ridge of the embankment. The thalweg of the gully is the blue curved line in Figure 2; it forms the bottom of the gully, sloping downward toward the fan.

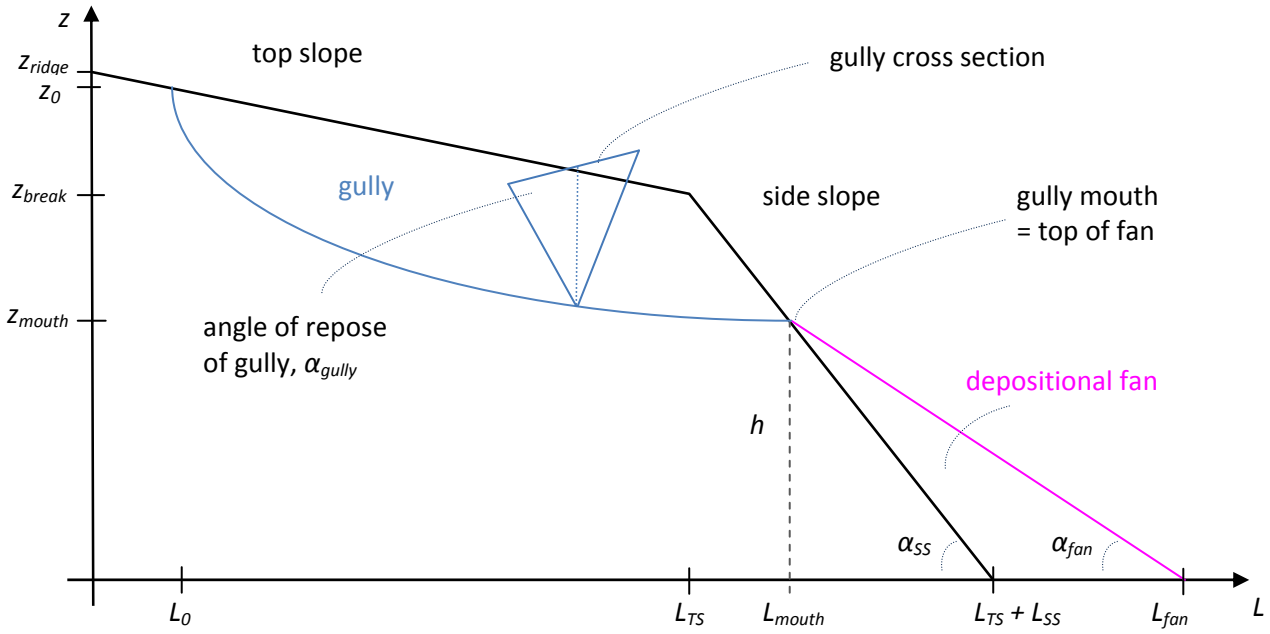

Figure 2. Longitudinal cross-section of a gully in the embankment.

Any cross section of the gully is assumed to be triangular, with the angle of repose of the gully being the angle that the gully makes with a horizontal line. The height of the thalweg when it comes out of the embankment through the side slope is also the height of the fan. This parameter, h, is also denoted as z_{mouth}, the elevation of the mouth of the gully. The break in slope is where the top slope and the side slope meet, denoted in Figure 2 by the point (L_{TS}, z_{break}).

The geometry of the gully is fully described by the engineering design of the cap, as described above, and by stochastic parameters for the angle of repose of the gully in the cap material (α_{gully}), the angle of repose of the eroded cap material (α_{fan}), the point of initiation of the gully on the cap (L_0), and the shape parameter of the longitudinal cross section of the gully (b). For these distributions, best professional judgment was used to create reasonably wide distributions that capture uncertainty in these parameters.

The angle of repose of the materials in the gully was represented by choosing values based on gravel, with a mean of 38 degrees, from an estimated range of 30 – 45 degrees (Clover, 1998). A standard deviation of 5 degrees was chosen to allow a slightly wider range of angles, since there is uncertainty in this parameter. Thus a normal distribution was assigned with a mean of 38 degrees, a standard deviation of 5 degrees, a minimum of near zero (1E-30) and a maximum of near 90 degrees (90 - 1E-30). The minimum and maximum were chosen by physical constraints.

The gully is assumed to begin less than 2 m from the ridge of the cap (Garry Willgoose, personal communication, 3 Jan 2011). As the point of initiation of the gully gets closer to the ridge, the slope of the gully approaches infinity, so the cap should not start at the ridge itself. A uniform distribution was assigned to L_0, ranging from near zero (1E-30) to 5 m. A gully is not allowed to begin at L_0 equal to zero, exactly at the ridge of the cap; rather, it is kept to one side of the ridge.

The angle of repose of the fan is limited on the high end by the angle created by the side slope and the ground surface, which is about 12 degrees. Since the fan partially lies on top of the side slope, the fan must form a smaller angle. As well, there is some limitation for the smallest angle this fan can form. Considering the large particle size of the gravel and rip rap, it is assumed that the minimum angle of the fan is 5 degrees. So the distribution for α_{fan} is chosen as a uniform distribution from 5 degrees to 10 degrees.

The distribution for *b* is described in Section 5.2.

The notation for parameters in Figure 2 is used in the equations below. The following section describes geometry of the gullies as represented by the model and how the dimensions of the gullies are calculated.

5.0 Gully Calculations

The following subsections present the various mathematical formulae for calculating the components of the overall gully model.

5.1 Equation for thalweg elevation (gully bottom)

The following form for the slope of the thalweg of the gully as suggested by Dr. Garry Willgoose (personal communication, 3 Jan 2011) is:

$$Slope = \frac{\mathrm{d}z_{gully}}{\mathrm{d}L} = aL^b \,. \qquad (1)$$

where

z_{gully} is the height of the gully thalweg above natural ground surface (m)
L is the horizontal distance from the ridge of the cap downslope (m),
a is an amplitude parameter of the steepness of the thalweg slope (unitless), and
b is a power parameter (unitless), representing the curve of the thalweg.

Conditional on the value of b, the value of *a* can be calculated so that the elevation of the mouth of the gully matches the elevation of the fan of material that is washed out of the gully. In order to include the uncertainty in the model, a probability distribution was chosen to represent *b*. A mean value for *b* of -0.4 was estimated from the geomorphology of erosion profiles (Garry Willgoose, personal communication, 3 Jan 2011), and uncertainty about that value was implemented by representing *b* with a truncated normal distribution with a mean of -0.4 and a standard deviation of 0.15, truncated to be between -0.75 and -0.05.

Integrating each side of this equation results in an equation for z_{gully}, the height above ground surface of the thalweg along any point of the thalweg:

$$z_{gully} = \int aL^b dL \tag{2}$$

So,
$$z_{gully} = \frac{a}{b+1} L^{b+1} + C \tag{3}$$

where

C is the constant of integration.

To find a value for C, the point of intersection of the gully and the top slope of the cap, i.e., where the gully begins, can be used. The top slope of the cap can be represented by the line

$$z_{TS} = \frac{(z_{break} - z_{ridge})}{L_{TS}} L + z_{ridge} \tag{4}$$

Setting z_{gully} equal to z_{TS} at the start of the gully, i.e., at L_0, yields

$$\frac{a}{b+1} L_0^{b+1} + C = \frac{(z_{break} - z_{ridge})}{L_{TS}} L_0 + z_{ridge} \tag{5}$$

Solving for C:

$$C = \frac{(z_{break} - z_{ridge})}{L_{TS}} L_0 + z_{ridge} - \frac{a}{b+1} L_0^{b+1} \tag{6}$$

Let

$$B_1 = -\frac{1}{b+1} L_0^{b+1} \tag{7}$$

and

$$B_0 = \frac{(z_{break} - z_{ridge})}{L_{TS}} L_0 + z_{ridge} = S_{TS} L_0 + z_{ridge} \tag{8}$$

where

S_{TS} is the slope of the top slope of the cap.

Note that this expression, B_0, is the same as the height of the gully where the gully initiates.

Now there is an expression for the elevation of the bottom of the gully (z_{gully}) in terms of the distance from the ridge of the cap:

$$z_{gully} = \frac{a}{b+1} L^{b+1} - B_1 a + B_0 \quad (9)$$

5.2 Solving for Gully Elevation

There are two sets of equations that are fundamental to solving this system. First, it is assumed that if a gully forms, it comes out of the side slope, so that the mouth of the bottom of the gully must intersect the line that forms the top of the side slope. In other words, the equation for the height of the bottom of the gully, evaluated where the gully emerges, must be equal to the elevation of the side slope, evaluated where the mouth of the gully emerges. Written mathematically, this becomes:

$$z_{gully}\Big|_{L_{mouth}} = z_{SS}\Big|_{L_{mouth}} \quad (10)$$

where

z_{SS} is the elevation of the side slope at any distance L from the break to the ground surface (m).

The second key equation is that, the volume of cap materials removed by the gully must equal the volume of the material in the fan, following conservation of mass:

$$V_{gully} = V_{fan} \quad (11)$$

where

V_{gully} is the volume of the gully in the cap (m^3), and
V_{fan} is the volume of the gully in the fan (m^3).

In terms of the top slope and side slope, this equation can be written

$$V_{gully}^{TS} + V_{gully}^{SS} = V_{fan} \quad (12)$$

where

V^{TS}_{gully} is the volume of the gully in the top slope of the cap (m^3), and
V^{SS}_{gully} is the volume of the gully in the side slope of the cap (m^3).

These equations can be used to express all other unknown variables in terms of two variables: *a* and *h*, which is the elevation of the mouth of the gully. Using these key equations, the system of equations can be solved for *a* and *h*.

5.2.1 Volume of the Gully in the Top Slope of the Cap

As shown in Figure 2 and Figure 3, the cross-sectional area of the gully is assumed to be an isosceles triangle (Willgoose, personal communication, 3 Jan 2011). The height of the triangle is the difference between the height of the top slope and the height of the bottom of the gully. The angle of repose of the gully walls is the angle the gully makes with the horizontal. The base of the triangle is twice the height divided by the tangent of that angle.

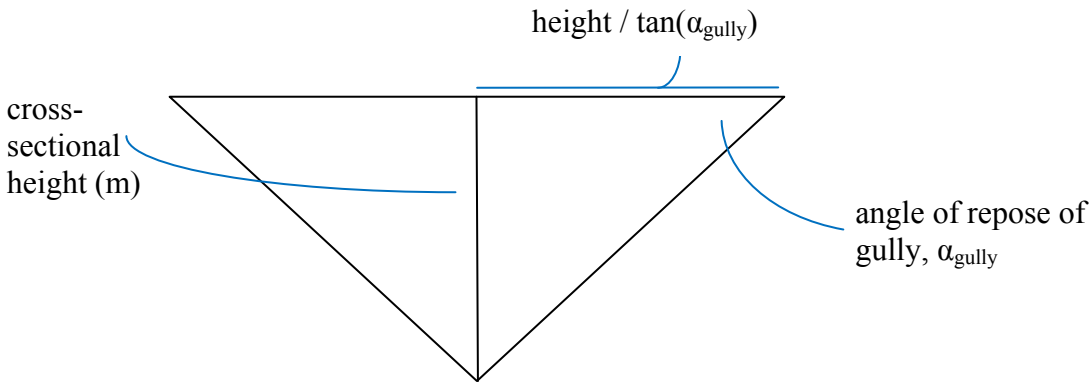

Figure 3. Cross-sectional view of gully

The cross-sectional area of the gully (m^2) can be represented by

$$A = \frac{1}{2} base \times height \tag{13}$$

$$A = \frac{height \times height}{\tan \alpha_{gully}} \tag{14}$$

and

$$A = \frac{(z_{TS} - z_{gully})^2}{\tan \alpha_{gully}} \tag{15}$$

$$A = \frac{(S_{TS} L + z_{ridge} - (\frac{a}{b+1} L^{b+1} - B_1 a + S_{TS} L_0 + z_{ridge}))^2}{\tan \alpha_{gully}} \tag{16}$$

This equation simplifies to

$$A = \frac{(S_{TS}L - \frac{a}{b+1}L^{b+1} + B_1 a - S_{TS}L_0)^2}{\tan\alpha_{gully}} \quad (17)$$

So, the volume of the gully in the top slope (m^3) is the integral of the cross-sectional area from the initial point of the gully, L_0 to the break between the top slope and the side slope, which corresponds to the length of the top slope, L_{TS}.

$$V_{gully}^{TS} = \int_{L_0}^{L_{TS}} \frac{(S_{TS}L - \frac{a}{b+1}L^{b+1} + (B_1 a - S_{TS}L_0))^2}{\tan\alpha_{gully}} dL \quad (18)$$

Simplifying, the volume becomes

$$V_{gully}^{TS} = \frac{1}{\tan\alpha_{gully}} \int_{L_0}^{L_{TS}} ({S_{TS}}^2 L^2 - \frac{2aS_{TS}}{b+1}L^{b+2} + \frac{a^2}{(b+1)^2}L^{2b+2} + 2(B_1 a - S_{TS}L_0)S_{TS}L - \frac{2a(B_1 a - S_{TS}L_0)}{b+1}L^{b+1} + (B_1 a - S_{TS}L_0)^2)dL \quad (19)$$

$$V_{gully}^{TS} = \frac{1}{\tan\alpha_{gully}} \left[\frac{{S_{TS}}^2 L^3}{3} - \frac{2aS_{TS}L^{b+3}}{(b+1)(b+3)} + \frac{a^2 L^{2b+3}}{(b+1)^2(2b+3)} + (B_1 a - S_{TS}L_0)S_{TS}L^2 - \frac{2a(B_1 a - S_{TS}L_0)}{(b+1)(b+2)}L^{b+2} + (B_1 a - S_{TS}L_0)^2 L \right] \Bigg|_{L_0}^{L_{TS}} \quad (20)$$

and finally,

$$V_{gully}^{TS} = \frac{1}{\tan\alpha_{gully}} \left[\frac{{S_{TS}}^2({L_{TS}}^3 - {L_0}^3)}{3} - \frac{2aS_{TS}({L_{TS}}^{b+3} - {L_0}^{b+3})}{(b+1)(b+3)} + \frac{a^2({L_{TS}}^{2b+3} - {L_0}^{2b+3})}{(b+1)^2(2b+3)} + (B_1 a - S_{TS}L_0)S_{TS}({L_{TS}}^2 - {L_0}^2) - \frac{2a(B_1 a - S_{TS}L_0)}{(b+1)(b+2)}({L_{TS}}^{b+2} - {L_0}^{b+2}) + (B_1 a - S_{TS}L_0)^2(L_{TS} - L_0) \right] \quad (21)$$

5.2.2 Volume of the Gully in the Side Slope of the Cap

The volume of the gully in the side slope is derived in a similar fashion to how the volume was derived for the gully in the top slope. The only differences are that the equation for the line made by the top of the side slope is used instead of the equation of the line made by top slope and that the limits of integration are from the edge of the top slope (the break) to the mouth of the gully, at an unknown value, L_{mouth}.

The side slope of the cap can be represented by the line

$$z_{SS} = -\frac{z_{break}}{L_{SS}}L + B_2 \quad (22)$$

where

$$B_2 = \frac{z_{break}}{L_{SS}}(L_{SS} + L_{TS}) \tag{23}$$

So, the volume of the gully in the side slope is the integral of the cross-sectional area of the gully in the side slope between the break (L_{TS}) and the distance at which the gully mouth comes out the side slope (L_{mouth}).

$$V_{gully}^{SS} = \int_{L_{TS}}^{L_{mouth}} \frac{(-\frac{z_{break}}{L_{SS}}L + B_2 - (\frac{a}{b+1}L^{b+1} + (B_0 - aB_1))^2}{\tan\alpha_{gully}} dL \tag{24}$$

$$V_{gully}^{SS} = \frac{1}{\tan\alpha_{gully}} \int_{L_{TS}}^{L_{mouth}} \left(-\frac{z_{break}}{L_{SS}}L - \frac{a}{b+1}L^{b+1} + (aB_1 - B_0 + B_2) \right)^2 dL \tag{25}$$

Simplifying, the volume becomes

$$V_{gully}^{SS} = \frac{1}{\tan\alpha_{gully}} \int_{L_{TS}}^{L_{gully}} (\frac{z_{break}^2}{L_{SS}^2}L^2 + \frac{2az_{break}}{L_{SS}(b+1)}L^{b+2} + \frac{a^2}{(b+1)^2}L^{2b+2} - 2\frac{z_{break}}{L_{SS}}(aB_1 - B_0 + B_2)L$$
$$- \frac{2a(aB_1 - B_0 + B_2)}{b+1}L^{b+1} + (aB_1 - B_0 + B_2)^2)dL \tag{26}$$

$$V_{gully}^{SS} = \frac{1}{\tan\alpha_{gully}} \left[\frac{z_{break}^2}{L_{SS}^2}\frac{L^3}{3} + \frac{2az_{break}L^{b+3}}{L_{SS}(b+1)(b+3)} + \frac{a^2L^{2b+3}}{(b+1)^2(2b+3)} - \frac{z_{break}}{L_{SS}}(aB_1 - B_0 + B_2)L^2 \right.$$
$$\left. - \frac{2a(aB_1 - B_0 + B_2)}{(b+1)(b+2)}L^{b+2} + (aB_1 - B_0 + B_2)^2 L \right] \Bigg|_{L_{TS}}^{L_{gully}} \tag{27}$$

and finally,

$$V_{gully}^{SS} = \frac{1}{\tan\alpha_{gully}} \left[\frac{z_{break}^2}{L_{SS}^2}\frac{({L_{gully}}^3 - {L_{TS}}^3)}{3} + \frac{2az_{break}({L_{gully}}^{b+3} - {L_{TS}}^{b+3})}{L_{SS}(b+1)(b+3)} + \frac{a^2({L_{gully}}^{2b+3} - {L_{TS}}^{2b+3})}{(b+1)^2(2b+3)} \right.$$
$$\left. - \frac{z_{break}}{L_{SS}}(aB_1 - B_0 + B_2)({L_{gully}}^2 - {L_{TS}}^2) - \frac{2a(aB_1 - B_0 + B_2)}{(b+1)(b+2)}({L_{gully}}^{b+2} - {L_{TS}}^{b+2}) + (aB_1 - B_0 + B_2)^2(L_{gully} - L_{TS}) \right] \tag{28}$$

5.2.3 Volume of the Fan

The fan comes from the mouth of the gully, lies along the side slope, and continues to the ground surface (Figure 2). Figure 4 shows a 3-dimensional view of the fan. Figure 5 depicts a birds-eye view of the fan, looking through the fan to the bottom footprint of the fan. The base of the fan is the circular segment. The triangular area is the shadow of the part of the fan that lies on the

surface of the side slope. The apex of the fan represents the point of the bottom of the gully mouth.

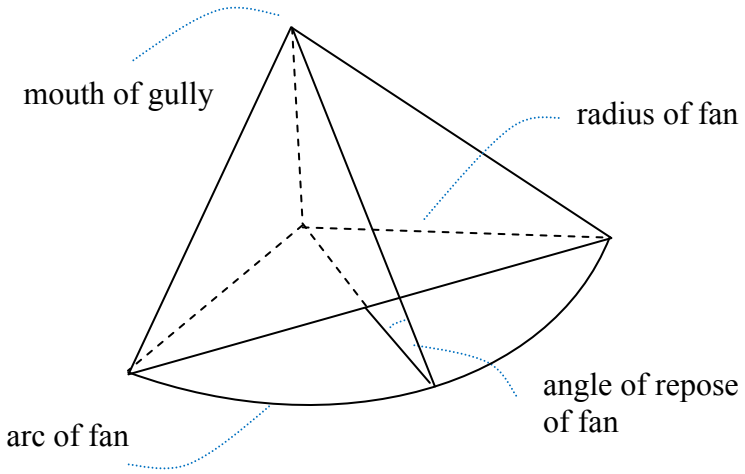

Figure 4. View of the fan in 3 dimensions.

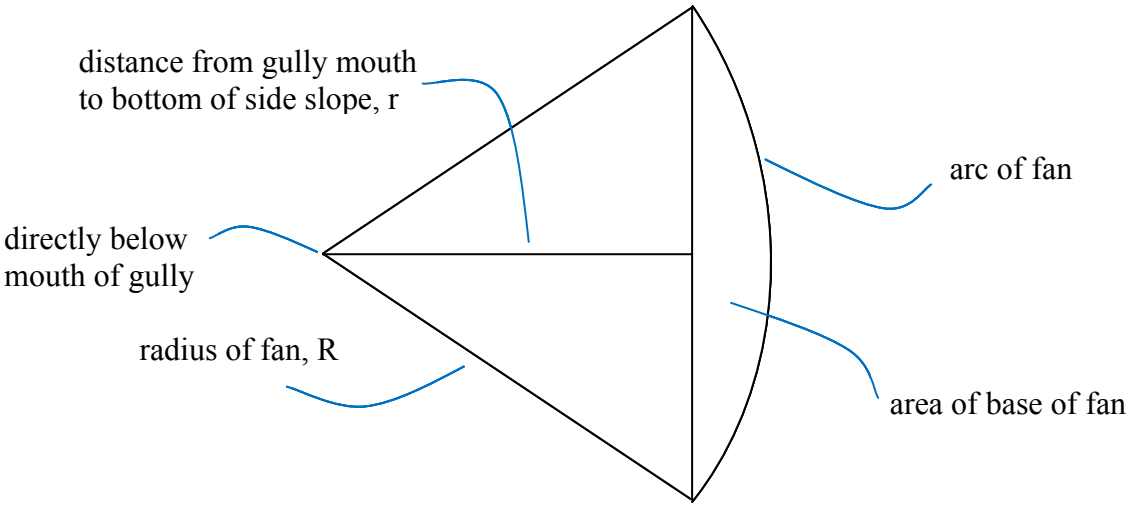

Figure 5. Top view of the fan geometry, looking through the fan to the footprint.

The fan is treated as a pyramidal structure. As such, the volume of the fan corresponds to 1/3 the area of the base multiplied by the height:

$$V_{fan} = \frac{1}{3} Area_{base} \times height \tag{29}$$

For this fan, the area of the base is the area of the circular segment (Figure 5):

$$Area_{base} = R^2 \cos^{-1}\left(\frac{r}{R}\right) - r\sqrt{R^2 - r^2} \tag{30}$$

where

R is the radius of the fan (m), and
r is the horizontal distance from the gully mouth to the bottom, or ground surface, of the side slope (m).

For more information on understanding this area calculation, see Weisstein, 2011a, for example.

The radius of the fan can be expressed in terms of the angle of repose of the fan, see Figure 2 and Figure 4.

$$R = \frac{h}{\tan \alpha_{fan}} \tag{31}$$

where

h is the height of the mouth of the gully (m), and
α_{fan} is the angle of repose of the fan (deg).

Similarly, the distance, r, from the gully mouth to the outer edge of the side slope is

$$r = \frac{h}{\tan \alpha_{SS}} \tag{32}$$

where

α_{SS} is the angle the side slope makes with the ground surface (deg).

Now the volume of fan can be expressed in terms of the area in Eq. (30), with new expressions for R and r, and the height to the mouth of the gully, h.

$$V_{fan} = \frac{h}{3}\left(\frac{h^2}{\tan^2 \alpha_{fan}} \cos^{-1}\left(\frac{\frac{h}{\tan \alpha_{SS}}}{\frac{h}{\tan \alpha_{fan}}}\right) - \frac{h}{\tan \alpha_{SS}} \sqrt{\frac{h^2}{\tan^2 \alpha_{fan}} - \frac{h^2}{\tan^2 \alpha_{SS}}}\right) \tag{33}$$

Simplifying yields

$$V_{fan} = \frac{h^3}{3}\left(\frac{1}{\tan^2 \alpha_{fan}} \cos^{-1}\left(\frac{\tan \alpha_{fan}}{\tan \alpha_{SS}} \right) - \frac{1}{\tan \alpha_{SS}} \sqrt{\frac{1}{\tan^2 \alpha_{fan}} - \frac{1}{\tan^2 \alpha_{SS}}} \right) \quad (34)$$

5.2.4 Expressing *a* in terms of *h*

The components for Eq. (11) are now given by the volume of the gully in the top slope (Eq. (21)), the volume of the gully in the side slope (Eq. (28)), and the volume of the fan (Eq. (33)). Next, Eq. (10) can be expanded to express *a* in terms of *h*, the height of the gully.

$$\frac{a}{b+1} L_{mouth}^{b+1} - B_1 a + z_0 = -\frac{z_{break}}{L_{SS}} L_{mouth} + \frac{z_{break}}{L_{SS}} (L_{SS} + L_{TS}) \quad (35)$$

This equation can be solved for *a* so that

$$a = \frac{\frac{z_{break}}{L_{SS}} L_{mouth} - \frac{z_{break}}{L_{SS}} (L_{SS} + L_{TS}) + z_0}{B_1 - \frac{1}{b+1} L_{mouth}^{b+1}} \quad (36)$$

To express *a* in terms of *h*, an equation for L_{mouth} is used, based on Figure 2.

$$L_{mouth} = L_{SS} + L_{cap} - \frac{h}{\tan \alpha_{SS}} \quad (37)$$

Now there are sufficient equations to solve for *h,* and all other variables can be re-written as a function of *h*. The equation for the elevation of the gully bottom can then be computed at any point along the gully.

6.0 Implementation in GoldSim

The gully calculations presented above are used in the Clive PA GoldSim model to allow the formation of a gully that can be different for each realization, based on four stochastic parameters: the gully slope exponent, *b*, angles of repose of the gully and fan, and the distance from the ridge of the cap to the initial point of the gully. The model checks to see if the gully is deep enough to get into the waste. If it is, then waste material is assumed to cover the surface area of the fan, and the surface area of the exposed waste is calculated. To simplify the calculation, waste concentrations are averaged over the waste layers exposed and then assigned to an exposure area that corresponds to the surface area of the fan plus the area of the waste exposed within the gully.

A random number of gullies sampled from a discrete distribution (min = 1, max = 20) are chosen to occur, to illustrate the effect multiple gullies would have on dose and to evaluate the effects of gullies over a range of more than one gully. Each of these gullies is identical for a given realization, to keep the gully model simple. The fraction of the cap's surface area that is consumed by gullies is calculated as a reality check to determine if the quantity of erosion is physically reasonable for an intact embankment.

6.1 Numerical Solution in GoldSim

GoldSim allows the user to iteratively solve a system of equations, such as what is given above, using Newton's method. This numerical solution is implemented in GoldSim using a previous value element and a looping container for which the user specifies a maximum number of loop counts and/or a convergence criterion.

Newton's method is a successive approximation method that can be used on differentiable functions. In this model, it is the height of the gully mouth that is the function of interest. The formula for Newton's method in terms of gully height is:

$$h_{n+1} = h_n - \frac{f(h_n)}{f'(h_n)} \tag{38}$$

where

- $f(h)$ is the difference between the volume of the gully and the volume of the fan, and
- $f'(h)$ is the derivative of the function $f(h)$.

New values are calculated for h until the difference between h_{n+1} and h_n is sufficiently small. In the Clive PA model, a convergence criterion of 0.01 m^3 is used, such that the difference between the volume of the gully and the volume of the fan is less than 0.01 m^3.

6.2 Representation of Gully and Waste

The biggest concern about gullies is whether or not a gully gets deep enough to expose and remove waste and how much waste is exposed and removed. In the current Clive PA model, waste is buried only under the top slope, so the quantity of concern is the distance from the ridge that the gully gets into the waste. In similar terminology to that used above, this variable can be called $L_{gully.}$, where $L_{gully.}$ is a vector of distances from the ridge of the cap to where the gully enters the waste layer.

Some assumptions need to be made to allow for a simple calculation of $L_{gully.}$. The column of waste and cap, as modeled in the Clive PA model, is a 1-dimensional representation of the cap; however, the gully model is a 2-dimensional representation, to include the slope of the cap in the gully calculations. To calculate L_{gully} and the gully outwash of each waste layer, the 2-D representation must be merged with the 1-D representation. Figure 6 illustrates the potential configurations that were considered in the calculation of gully outwash volume and the calculate

of where the gully first gets into the waste. The top slope has waste layers (outlined in green) with a cap covering the waste layers. The side slope comes off the top slope, with the break in slope being the vertical dotted black line. The fan leans against the side slope on the right side of the illustrations in Figure 6. The gully (drawn in black) intersects the cap and waste layers.

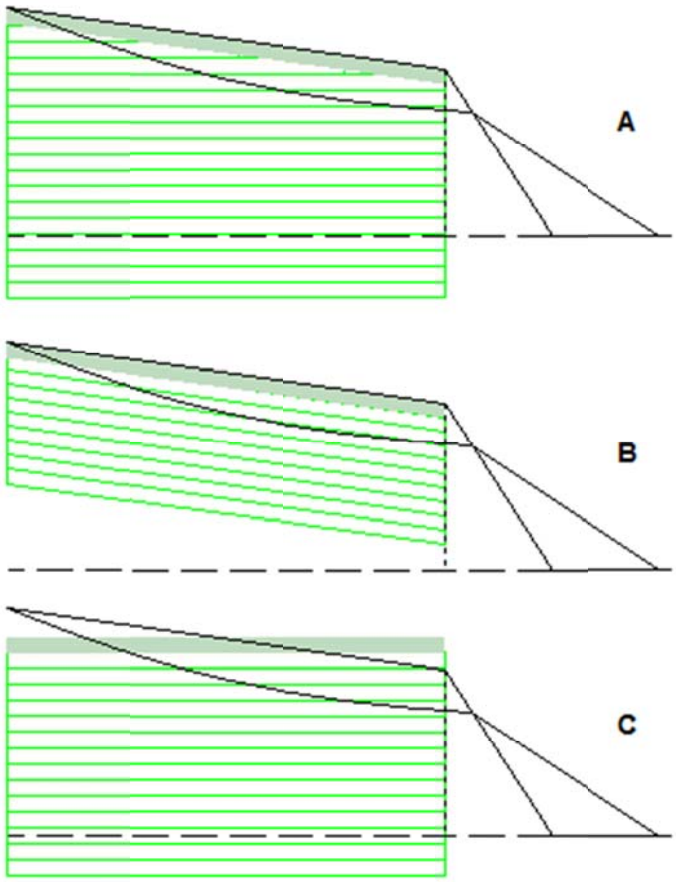

Figure 6. Gully and waste configurations for the gully outwash volume calculation, with the cover represented by the solid green layer and the waste layers outlined in green. A. the embankment as constructed; B. representation of the 1-D column, preserving the slope of the cap throughout the column; C. representation of the 1-D column, preserving the horizontal layering of the waste.

Three different representations were considered to model the intersection of waste with the gully and the gully outwash volume of waste. Figure 6A roughly depicts the embankment as it is intended to be constructed, with the cover (solid green) over horizontal waste layers and a sloping top cap. This representation is difficult to model in GoldSim because the waste layers do not continue across the entire top slope of the cap. Figure 6B represents the waste layers continuing for the length of the cap, at the same slope of the top slope of the cap. The problem with this approach is that the gully can dip into and out of a waste layer, meaning that there are two points in each waste layer that the gully could potentially intersect, rather than one intersection point. With this arrangement, there is considerable computational effort required to ensure that the numerical solution for the volume from each layer converges. Figure 6C shows how the implementation of the gully was chosen for the Clive PA model. The top of the cap and top of

each waste layer is set as the midpoint of each layer in the top slope of the cap. With the horizontal waste layers, the gully intersects each layer only once.

A problem with implementation of the arrangement in Figure 6C is that the top waste layers at the break in slope in this 1-D representation are higher than the actual cap height at the break in the 2-D representation. So the calculation is an approximation of how many waste layers are cut into by the gully and how much waste is washed out by the gully from each waste layer. This approximation is considered tolerable since the overall gully model is a simplification. Furthermore, if there is sufficient fill material between the top of the DU waste and the bottom of the cap, then the effect is negligible. Some caution should be exercised when interpreting output from the gully model if DU waste is disposed within a few meters of the bottom of the cap.

6.3 Calculation of $L_{gully.}$

To calculate the volume of each waste layer removed by the gully and the surface area of the waste layers exposed by the gully, the distance from the ridge of the top slope to where the gully first intersects each waste layer, $L_{gully.}$, must be calculated. These values are calculated by finding the intersection of the gully with the horizontal lines at the heights above ground surface for each waste layer. In other words, solve Eq. (9) for L such that z_{gully} equals the height of each waste layer, z_{waste} :

$$L_{gully} = \left(\frac{b+1}{a} (z_{waste} + B_1 a - B_0) \right)^{\frac{1}{b+1}} \tag{39}$$

where

z_{waste} is a vector of the waste layer heights above ground surface at the mid-point of the top slope of the cap

Note that this calculation in GoldSim requires that $B_1 a - B_0$ is a vector expression of length equal to the number of waste layers.

6.4 Calculation of Surface Area

The surface area of the fan and the surface area of the waste exposed by the gully will be summed and included in exposure area calculations in the dose assessment.

6.4.1 Surface Area of Fan

To approximate the surface area of the fan, a simplifying assumption is used – that the surface area of the fan is the shadow the fan creates on the horizontal plane. This assumption is reasonable since the fan is at such a low angle (5 – 10 degrees, see Section 4.1). Figure 5 shows the shape of this shadow.

The area of a circular sector, $Area_{sector}$, can be found by

$$Area_{sector} = \frac{1}{2} R^2 \theta \tag{40}$$

where

R is the radius of the circle (m), and
θ is the angle cut by the circular segment.

The value of R is the same as in Eq. (31) above. The value of θ is given by

$$\theta = 2\cos^{-1}\left(\frac{r}{R}\right) = 2\cos^{-1}\left(\frac{\frac{h}{\tan\alpha_{SS}}}{\frac{h}{\tan\alpha_{fan}}}\right) = 2\cos^{-1}\left(\frac{\tan\alpha_{fan}}{\tan\alpha_{SS}}\right) \tag{41}$$

where

r is the horizontal distance from the gully mouth to the outer edge of the side slope, as given in Eq. (32) above.

Thus, the surface area of the fan, SA_{fan}, can be expressed as

$$SA_{fan} = \frac{h^2}{\tan^2\alpha_{fan}} \cos^{-1}\left(\frac{\tan\alpha_{fan}}{\tan\alpha_{SS}}\right) \tag{42}$$

For more information on understanding this area calculation, see Weisstein, 2011b, for example.

6.4.2 Surface Area of Waste Exposed by Gully

To calculate the surface area of each waste layer exposed, the cross sectional distance of waste exposed by the gully is integrated over the length of the gully in the top slope. See Figure 7.

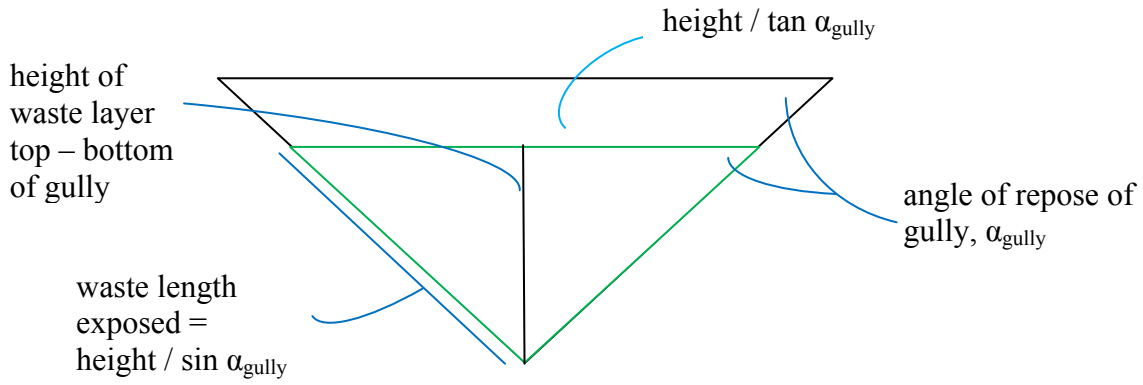

Figure 7. Gully cross section for waste exposure calculations.

The surface area exposed by the gully for each waste layer can be calculated by first calculating the surface area exposed by the gully from the top of each waste layer to the bottom of the gully and then subtracting that calculation from each waste layer. In other words,

$$SAWasteLayer1 = SAWasteLayer1toGullyBottom - SAWasteLayer2toGullyBottom \quad (43)$$

So the surface area exposed from the top of each waste layer to the gully bottom is:

$$SA = \frac{2}{\sin \alpha_{gully}} \int_{L_{waste}}^{L_{TS}} (z_{waste} - z_{gully}) dL \quad (44)$$

where the 2 comes from having two sides of the gully exposed.

Substituting in for z_{gully}

$$SA = \frac{2}{\sin \alpha_{gully}} \int_{L_{waste}}^{L_{TS}} (z_{waste} - (\frac{a}{b+1} L^{b+1} - B_1 a + B_0)) dL \quad (45)$$

Simplifying yields

$$SA = \frac{2}{\sin \alpha_{gully}} \left[(z_{waste} + B_1 a - B_0)(L_{TS} - L_{waste}) - \frac{a}{(b+1)(b+2)} (L_{TS}^{b+2} - L_{waste}^{b+2}) \right] \quad (46)$$

This value of surface area is then evaluated for each waste layer and used as in Eq. (43) to calculate the surface area exposed for each waste layer. The bottom waste layer surface area is simply the value given in Eq. (46).

6.5 Calculation of Volume of Waste Layers Removed

In a similar fashion to the calculation for the surface area of waste exposed by the gully, the volume of each waste layer removed by the gully is calculated by first calculating the volume of waste removed from the top of each waste layer to the bottom of the gully. Then that volume calculation is subtracted from the layer below, similar to Eq. (43):

$$VolWasteLayer1 = VolWasteLayer1toGullyBottom - VolWasteLayer2toGullyBottom \quad (47)$$

The cross-sectional area of the waste exposed by the gully, similar to Eq. (14), is integrated over the length of the gully that incises the waste.

$$Vol = \frac{1}{\tan \alpha_{gully}} \int_{L_{waste}}^{L_{TS}} (z_{waste} - z_{gully})^2 dL \quad (48)$$

Simplifying,

$$Vol = \frac{1}{\tan \alpha_{gully}} \int_{L_{waste}}^{L_{TS}} (z^2{}_{waste} - 2 z_{waste} z_{gully} + z^2{}_{gully}) dL \tag{49}$$

$$Vol = \frac{1}{\tan \alpha_{gully}} \int_{L_{waste}}^{L_{TS}} (z^2{}_{waste} - 2 z_{waste} \left(\frac{a}{b+1} L^{b+1} - B_1 a + B_0 \right) - \frac{a^2}{(b+1)^2} L^{2b+2} + \\ + \frac{2aL^{b+1}}{b+1} (B_0 - B_1 a) + (B_0 - B_1 a)^2) dL \tag{50}$$

$$Vol = \frac{1}{\tan \alpha_{gully}} \int_{L_{waste}}^{L_{TS}} (z^2{}_{waste} + 2 z_{waste} B_1 a - 2 z_{waste} B_0 + (B_0 - B_1 a)^2) + \\ - \frac{2 z_{waste} a}{b+1} L^{b+1} + \frac{2a(B_0 - B_1 a)}{b+1} L^{b+1} + \frac{a^2}{(b+1)^2} L^{2b+2}) dL \tag{51}$$

$$Vol = \frac{1}{\tan \alpha_{gully}} \left[\left(z^2{}_{waste} + 2 z_{waste} B_1 a - 2 z_{waste} B_0 + (B_0 - B_1 a)^2 \right) (L_{TS} - L_{waste}) + \right. \\ - \left(\frac{2 z_{waste} a}{(b+1)(b+2)} + \frac{2a(B_0 - B_1 a)}{(b+1)(b+2)} \right) (L_{TS}^{b+2} - L_{waste}^{b+2}) + \\ \left. + \frac{a^2}{(b+1)^2 (2b+3)} (L_{TS}^{2b+3} - L_{waste}^{2b+3}) \right] \tag{52}$$

This calculation of volume is then evaluated for each waste layer and used as in Eq. (47) to calculate the volume of waste removed by the gully for each waste layer. The bottom waste layer volume is simply that value given in Eq. (52) evaluated for the last waste layer.

6.6 Concentration of Waste Removed by Gully

The concentration of waste removed by the gully is averaged and is assumed to be spread out uniformly over the surface area of the fan. This same averaged concentration of waste is assumed to be present in the surface area exposed by the gully.

To obtain the average waste concentration, the concentration of each radionuclide species is computed as a mass-weighted average. The volume of each layer of waste removed by the gully is multiplied by the bulk density of that waste layer to get the mass of waste removed in each layer. Then the mass in each layer is divided by the total mass of waste removed. The mass of each radionuclide in each waste cell is converted to a mass concentration and then multiplied by the mass fraction of each layer removed by the gully. The concentration of waste removed by the gully is then the sum of each radionuclide over every waste layer. It is this total concentration that is used in the dose calculations.

7.0 References

Clover, Thomas J. Pocket Ref. Littleton, Colorado: Sequoia Publishing, Inc., 1998, referenced in Wikipedia definition for Angle of repose, http://en.wikipedia.org/wiki/Angle_of_repose#cite_ref-3

Energy*Solutions*, 2009. *License Amendment Request: Class A South/11E.(2) Embankment.* Revision 1, June 9, 2009.

GTG (GoldSim Technology Group), 2011. *GoldSim: Monte Carlo Simulation Software for Decision and Risk Analysis*, http://www.goldsim.com

NRC, 2010. Workshop on Engineered Barrier Performance Related to Low-Level Radioactive Waste, Decommissioning, and Uranium Mill Tailings Facilities. Nuclear Regulatory Commission. August 3 – 5.

Weisstein, E. 2011a, May 18. Circular Segment. Wolfram Research. Retrieved 23 May 2011 from http://mathworld.wolfram.com/CircularSegment.html.

Weisstein, E. 2011b, May 18. Circular Sector. Wolfram Research. Retrieved 23 May 2011 from http://mathworld.wolfram.com/CircularSector.html.

Willgoose, G. 2005. User Manual for SIBERIA (Version 8.30). Telluric Research. http://www.telluricresearch.com/siberia_8.30_manual.pdf

Willgoose, G. 2010. *Assessment of the Erosional Stability of Covers at Millennial Timescales: Capabilities, Issues and Needs*. Workshop on Engineered Barrier Performance Related to Low-Level Radioactive Waste, Decommissioning, and Uranium Mill Tailings Facilities. Nuclear Regulatory Commission. August 3 – 5.

Willgoose, G. R., and S. Sharmeen, 2006. A one-dimensional model for simulating armouring and erosion on hillslopes. 1. Model development and event-scale dynamics, *Earth Surface Processes and Landforms*, 31: 970-991. http://onlinelibrary.wiley.com/doi/10.1002/esp.1398/abstract

Neptune and Company Inc.

June 1, 2011 Report for EnergySolutions

Clive DU PA Model, version 1

Appendix 11

Dose Assessment

Dose Assessment for the Clive DU PA

28 May 2011

Prepared by

Neptune and Company, Inc.

This page is intentionally blank, aside from this statement.

CONTENTS

FIGURES

TABLES

1.0 Summary of Input Parameter Values

Following is a brief summary of input values used parameters employed in the "exposure-dose" (ED) component of the Clive Performance Assessment (PA) model that is the subject of this white paper. Please see Appendix I in this document, the companion spreadsheet *Dose Assessment Appendix II*, and the *Clive PA Model Parameters* white paper for further justifications of selected values, and the text for further explanation.

For distributions, the following notation is used:

- N(μ, σ, [*min*, *max*]) represents a normal distribution with mean μ and standard deviation σ, and optional truncation at the specified *min*imum and *max*imum,
- LN(*GM*, *GSD*, [*min*, *max*]) represents a log-normal distribution with geometric mean GM and geometric standard deviation GSD, and optional *min* and *max*,
- U(*min*, *max*) represents a uniform distribution with lower bound *min* and upper bound *max*,
- Beta(μ, σ, *min*, *max*) represents a generalized beta distribution with mean μ, standard deviation σ, minimum *min*, and maximum *max*,
- Gamma(μ, σ) represents a gamma distribution with mean μ and standard deviation σ, and
- TRI(*min*, *m*, *max*) represents a triangular distribution with lower bound *min*, mode *m*, and upper bound *max*.

Table 1. Exposure dose input parameters summary

Parameter	Units	Value	Dependencies	Source	Table	Notes
"Inner Loop" human exposure and dose factors; sampled multiple times within a realization						
Dose conversion factors (DCFs)	Sv/Bq; Sv-m^3 / Bq-s	Distributions for some DCFs are derived based upon Kocher et al, 2005 REFs (see below). See also Dose Assessment Appendix II.xls		EPA, 1999; and others		
Radiation effectiveness factors (REFs)	Unitless	Alpha: LN(1.81e+01, 2.37+00) Photon < 30 keV: LN(2.45, 1.55) Photon 30-250 keV: LN(1.96, 1.48) Electron: LN(2.41, 1.44)		Kocher et al., 2005	14, 15; p. 26	Particle- and energy-specific values. Based upon lognormal fits to percentiles presented in Kocher et al., 2005
Uranium oral reference dose	mg/kg-day	Discrete(0.5, 0.0006; 0.5, 0.003)		EPA, 2011; EPA, 2000		Equal probability assigned to Office of Water and Superfund criteria.
Age	yr	N(25.7, 20.3), truncated at 16 and 60		USFS, 2005	2, p. 8	
Gender		Male: 60.8% Female: 39.2%		USFS, 2005	2, p. 8	

Parameter	Units	Value	Dependencies	Source	Table	Notes
Body weight	kg	Male: LN(exp(4.08+1.64e-2*Age-1.69e-4*Age^2), 1.24) Female: LN(exp(3.94+1.51e-2*Age-1.51e-4*Age^2), 1.28)	Age, Gender	EPA, 2009a	8-4, p. 8-12;, 8-5, p. 8-13	
Ventilation rate: sleeping	m3/min-kg	Male, age 16-20: LN(6.91e-5, 1.24) Male, age 21-60: LN(exp(-9.91+4.93e-3*Age), 1.26) Female, age 16-20: LN(6.71e-5, 1.29) Female, age 21-60: LN(exp(-9.93+3.57e-3*Age), 1.30)	Age, Gender, units in terms of Body Weight	EPA, 2009a, EPA, 2009b	6-13, p. 6-33;, 6-14, p. 6-35	
Ventilation rate: sedentary activity	m3/min-kg	Male, age 16-20: LN(7.58e-5, 1.20) Male, age 21-60: LN(exp(-9.82+5.14e-3*Age), 1.19) Female, age 16-20: LN(7.37e-5, 1.23) Female, age 21-60: LN(exp(-9.86+3.89e-3*Age), 1.24)	Age, Gender, units in terms of Body Weight	EPA, 2009a, EPA, 2009b	6-13, p. 6-33;, 6-14, p. 6-35	
Ventilation rate: light activity	m3/min-kg	Male, age 16-20: LN(1.77e-4, 1.18) Male, age 21-60: LN(exp(-8.82+2.01e-3*Age), 1.17) Female, age 16-20: LN(1.72e-4, 1.18) Female, age 21-60: LN(exp(-8.88+2.55e-3*Age), 1.20)	Age, Gender, units in terms of Body Weight	EPA, 2009a, EPA, 2009b	6-13, p. 6-33;, 6-14, p. 6-35	
Ventilation rate: moderate activity	m3/min-kg	Male, age 16-20: LN(3.80e-4, 1.21) Male, age 21-60: LN(exp(-8.02+1.93e-3*Age), 1.25) Female, age 16-20: LN(3.56e-4, 1.21) Female, age 21-60: LN(exp(-8.10+1.40e-3*Age), 1.25)	Age, Gender, units in terms of Body Weight	EPA, 2009a, EPA, 2009b	6-13, p. 6-34; 6-14, p. 6-36	

Parameter	Units	Value	Dependencies	Source	Table	Notes
Ventilation rate: high activity	m3/min-kg	Male, age 16-20: LN(6.92e-4, 1.25) Male, age 21-60: LN(exp(-7.38+5.56e-4*Age), 1.27) Female, age 16-20: LN(6.76e-4, 1.27) Female, age 21-60: LN(exp(-7.37-4.88e-4*Age), 1.30)	Age, Gender, units in terms of Body Weight	EPA, 2009a, EPA, 2009b	6-13, p. 6-34; 6-14, p. 6-36	
Adult incidental soil ingestion rate	mg/d	Silicon: LN(12.2, 3.29), truncated at 0 and 197 Aluminum: LN(32.7, 3.81), truncated 0 and 814 Titanium: LN(296, 2.76), truncated at 0 and 2900	Selection of tracer element performed outside of the "inner loop"	EPA, 2009a; Davis et al, 2006.	5-11, p. 5-37	Only study with applicable adult data. Truncation maxima based upon maxima reported in Davis et al, 2006, as pathological soil ingestion is not of interest here.
Ingestion rate: "home-produced" beef	g/kg-d	Age 16-39: Gamma(1.45, 0.68) Age 40-60: Gamma(1.84, 0.97)	Age, units in terms of Body Weight	EPA, 2009a	13-33, p. 13-40	
Ingestion rate: "home-produced" game	g/kg-d	Age 16-39: Gamma(1.52, 1.81) Age 40-60: Gamma(1.42, 1.43)	Age, units in terms of Body Weight	EPA, 2009a	13-41, p. 13-48	
Daily exposure time; sedentary+sleeping	hr/day	Males: LN(exp(2.79-1.55e-2*Age+2.09e-4*Age^2), 1.09) Females: LN(exp(2.84-1.71e-2*Age+2.10e-4*Age^2), 1.08) Truncated at 24 hr/day	Age, Gender	EPA, 2009a, EPA, 2009b	6-15, p. 6-37	Sedentary duration alone constructed by subtracting sleeping time.
Daily exposure time; sleeping	hr/day	Males: LN(exp(2.31-1.01e-2*Age+1.05e-4*Age^2), 1.06) Females: LN(exp(2.35-9.94e-3*Age+9.94e-5*Age^2), 1.06) Truncated at Sedentary+Sleeping time	Age, Gender, Sedentary+Sleeping time	EPA, 2009a, EPA, 2009b	6-15, p. 6-37	Sleep duration is excluded for daily-use receptors.

Parameter	Units	Value	Dependencies	Source	Table	Notes
Daily exposure time; light activity	hr/day (un-normalized)	Males: LN(exp(2.38-3.44e-2*Age+4.05e-4*Age^2), 1.49) Females: LN(exp(2.09-1.37e-2*Age+1.69e-4*Age^2), 1.34)	Age, Gender	EPA, 2009a, EPA, 2009b	6-15, p. 6-37	Light, moderate, and high activities are normalized to equal: 24 hr/day – (sedentary + sleeping time).
Daily exposure time; moderate activity	hr/day (un-normalized)	Males: LN(exp(1.86e-1+6.74e-2*Age-8.16e-4*Age^2), 1.88) Females: LN(exp(2.21e-1+6.49e-2*Age-7.85e-4*Age^2), 1.65)	Age, Gender	EPA, 2009a, EPA, 2009b	6-15, p. 6-38	Light, moderate, and high activities are normalized to equal: 24 hr/day – (sedentary + seeping time).
Daily exposure time; high activity	hr/day (un-normalized)	Males: LN(exp(-1.12-2.19e-2*Age+3.14e-4*Age^2), 3.04) Females: LN(exp(-1.97+4.04e-3*Age+6.27e-5*Age^2), 2.84)	Age, Gender	EPA, 2009a, EPA, 2009b	6-15, p. 6-38	Light, moderate, and high activities are normalized to equal: 24 hr/day – (sedentary + sleeping time).
Total number of individuals in vicinity of site	#	TRI(100, 350, 500)		BLM, personal communication, 2010		Assumes area up to approximately 100 sq mi around site. This value, minus the number of ranchers (see text), defines the number of Sport OHVers and Hunters
Number of Ranchers in vicinity of site	#	U(1, 20)		BLM, personal communication, 2010		
Number of Hunters in vicinity of site	#	Binomial(N, 0.25), where N is the number of non-rancher individuals in vicinity of site	Total number of individuals, number of ranchers	USFS, 2005	22, p. 32	"Big game" hunters, all OHV users. Rounded to two significant figures.
Number of Sport OHVers in vicinity of site	#	Number(Recreationalists) - Number(Hunter)	Total number of individuals, number of ranchers and hunters			Number of Recreationists defined as all individuals minus Ranchers.
Ranchers; day trip time in exposure area	hr/d	U(4, 12)				Professional judgment.
Sport OHVers; day trip time in exposure area	hr/d	Beta(6.3, 2.11, 1, 20)		Burr et al, 2008	21, p. 18	Utah data. Minimum, maximum, and standard deviation based upon professional judgment. Rounded to two significant figures.
Hunter/Rancher; fraction of day trip time spent OHVing	fraction	U(0.1, 0.75)				Professional judgment. OHV use related to higher dust concentrations in air.

Parameter	Units	Value	Dependencies	Source	Table	Notes
All receptors; camp trip time spent OHVing	hr/d	U(2.0, 8.0)				Professional judgment. All overnight users assumed to have similar OHV use. OHV use related to higher dust concentrations in air.
Exposure time; overnight trip	hr/d	24				Professional judgment; overnight trip assigned a 24 hr duration.
All receptors; fraction of camp trip exposure time on disposal cell	fraction	U(0.25, 0.75)				Professional judgment. Corresponds to 6 to 18 hr/day. Campers are assumed to set up camp on the disposal cell.
Hunter; fraction of hunting day trip exposure time on disposal cell	fraction	U(0.02, 0.17)				Professional judgment. Corresponds to 0.5 to 4 hr/day.
Rancher and Sport OHVer; fraction of day trip exposure time on disposal cell	fraction	Disposal cell area / Exposure area				Assumes that Ranchers and Sport OHVers visiting the area for a day trip cover the exposure area randomly over the course of a year.
Rancher; exposure frequency	d/yr	Beta(135, 34.9, 0, 180)		BLM, personal communication, 2010; BLM, 2010		All leases are 6 mo., from November 1 to April 30, but can be reduced depending upon grazing conditions. It is assumed that Ranchers only work 5 days per week (i.e. 130 days per year). distribution based upon professional judgment.
Sport OHVer; exposure frequency	d/yr	LN(11.3, 3.45, 1, 200)		USFS, 2005	19, p. 27	Western region, "all groups". Minimum and and maximum based upon professional judgment.

Parameter	Units	Value	Dependencies	Source	Table	Notes
Hunter; exposure frequency	d/yr	LN(4.66, 3.45, 1, 100)		USFWS, 2006	pg. 10	Utah data. Recreationists who are not Hunters are defined as Sport OHVers: # Sport OHVers = # Recreationists in total - # Hunters.. Mean calculated based upon number of hunters and days of hunting. Minimum, maximum, and standard deviation based upon professional judgment.
Ranchers; fraction of exposure frequency related to overnight trips	fraction	U(0.5, 0.67)		BLM, personal communication , 2010		Corresponds to 15 – 20 day/month overnight. Remaining days in ranching EF assumed to be day trips.
Hunters; fraction of exposure frequency related to overnight trips	fraction	U(0, 1.0)				Professional judgment.
Sport OHVers; fraction of exposure frequency related to overnight trips	fraction	U(0, 1.0)				Professional judgment.
Off-Site Receptor Distributions ("Inner Loop")						
Exposure frequency rest area caretaker	d/yr	TRI(327,350,365)				Professional judgment. Minimum represents 28 days vacation, 10 holidays, mode is EPA default (EPA, 1989), high is maximum.
Exposure time rest area caretaker	hrs/day	24				Professional judgment (residential receptor).
Exposure frequency I-80 and west-side access road traveller	d/yr	U(250, 365)				Professional judgment (minimum reflects average number of work days per year).
Exposure time travelers on I-80 and train	min/d	U(2.3, 7.2)				Professional judgment. Minimum represents 80 mph/3 miles 1-way; maximum 50 mph/3 miles 2-way. 3 miles represents 'densest' part of off-site dispersion plume.

Parameter	Units	Value	Dependencies	Source	Table	Notes
Exposure time cars on west-side access road (Utah Test and Training Range access)	min/d	U(2.4,4.0)				Professional judgment. Minimum represents 50 mph/1 mile 2-way upper 30 mph/1 mile 2-way. 1 mile represents size of ES property.
Knolls area Sport OHVer; exposure frequency	d/yr	LN(11.3, 3.45, 1, 200)		USFS, 2005	19, p. 27	Western region, "all groups". Minimum and and maximum based upon professional judgment.
Knolls area Sport OHVers; exposure time	hr/d	Beta(6.3, 2.11, 1, 20)		Burr et al, 2008	21, p.18	Utah data. Minimum , maximum, and standard deviation based upon professional judgment. Rounded to two significant figures.
"Outer Loop" human exposure factors; sampled once each model realization						
Receptor area (exposure area)	acres	U(16000,64000)		BLM, personal communication , 2010; BLM, 2010		Professional judgment. High-end reflects area between I-80 and UTTR, bounded by salt flats and Cedar Mt foothills. Low-end reflects Aragonite and E. Grassy range leases. This defines the exposure area for ranching and recreational receptors.
Meat preparation loss	fraction	N(0.27,0.07, 0.01, 1)		EPA, 1997b	13-5	Converted from fractions. Fraction of meat (which is based upon beef, uncooked weight) lost in preparation. Minimum and maximum based upon professional judgment.
Meat post-cooking loss	fraction	N(0.24, 0.09, 0.01, 1)		EPA, 1997b	13-5	Converted from fractions. Fraction of meat (which is based upon beef, uncooked weight) lost in preparation. Minimum and maximum based upon professional judgment.
OHV dust loading	multiplier for ambient dust concentration	LN(98.1, 1.65)		EPA, 2008	2	Activity based; i.e. OHVs generate increased dust.
Exposure frequency; food	d/yr	365		EPA, 1997b		Food intake rates are annual averages.

Parameter	Units	Value	Dependencies	Source	Table	Notes
Soil ingestion tracer element		Discrete(0.333)				Professional judgment; equal probability assigned to distributions based upon aluminum, silicon, and titanium.
Cattle and game radionuclide uptake exposure factors ("Outer Loop")						
Cattle range area, per operation	acres					See 'outer loop' parameter definition; for receptor exposure area.
Pronghorn range area	acres	U(995, 9192)		Huffman, 2004		Foraging distances for summer and winter were equally weighted and assigned as diameters of a circular home range, from 0.1-0.8 km in the spring and summer to 3.2-9.7 km in the fall and winter.
Cattle beef transfer factor	Bq/kg per Bq/d	(element-specific; see Table 3)		IAEA, 2010; and others		Also applied to pronghorn.
Cattle water ingestion rate	kg/day	U(33, 53)		MSUE, 2011		Range of average daily water intake for "finishing cattle" of weights 600 – 1200 lb is 8.6 to 14 gallons.
Cattle forage ingestion rate	kg/day	U(8.85, 14.75)		EPA 2005	B-3-10, p. B-138	Recommended value is 11.8 kg/day; range of +/- 25% is professional judgment. Value is dry weight.
Cattle soil ingestion rate	kg/day	U(0.05, 0.95)		EPA 2005	B-3-10, p. B-139	Recommended value is 0.5 kg/day; range of +/- 100% is professional judgment.
Cattle time fraction in exposure area	fraction	Discrete(1.0)				Professional judgment. Time grazing around the site is presumed to be sufficient to reach the equilibrium represented by transfer factors.
Pronghorn water ingestion rate	kg/day	U(0.1, 1)		UDWR, 2009	p. 4	Professional judgment. Pronghorn may drink no water at all when fresh browse is available and up to 0.79 gal/day (3.0 L) during dry periods. Maximum set at 1 L/day.

Parameter	Units	Value	Dependencies	Source	Table	Notes
Pronghorn body weight	kg	U(38, 41)		Huffman, 2004		
Pronghorn forage ingestion rate	kg/day	0.577 x Body Weight Factor$^{0.727}$ x 0.001		EPA, 1993b	Equation 3-9, p. 3-6	Allometric scaling based upon body weight for mammalian herbivore. Units converted to kg/d.
Pronghorn soil ingestion rate	kg/day	U(0.005, 0.095)				Professional judgment. Set equal to 10% of soil ingestion distribution for cattle based upon body mass.
Plant ingestion screening calculations exposure factors ("Outer Loop")						
Dry-wet plant weight conversion factor	fraction	U (0.05, 0.30)		EPA, 2009a	9-33, p. 9-59	Professional judgment. Based upon approximate range of moisture contents for edible parts of fruits and vegetables.

2.0 Purpose and Context

A radioactive waste disposal facility located in Clive, Utah (the "Clive facility") and operated by Energy*Solutions* LLC is proposed to receive and store depleted uranium (DU) and associated waste (called "DU waste" here). To assess whether the proposed Clive facility location and containment technologies are suitable for protection of human health, specific performance objectives for land disposal of radioactive waste set forth in Utah Administrative Code (UAC) Rule R313-25-8 (Utah, 2010) must be met. In order to support the required radiological PA, a detailed computer model has been developed to evaluate the potential future radiation doses to human receptors that may result from the disposal of DU waste, and conversely to determine how much DU waste can be safely disposed at the Clive facility.

The site conditions, chemical and radiological characteristics of the wastes, contaminant transport pathways, and potential human receptors and exposure routes at the Clive facility that are used to structure the quantitative PA model are described in the conceptual site model (CSM) documented in the *Conceptual Site Model for Disposal of Depleted Uranium at the Clive Facility* white paper (Clive DU PA CSM.pdf). Note that the referenced white papers as well as an appendix to this document are available via links in the PA GoldSim model. The PA model has been developed as a probabilistic model taking into account site-specific conditions and uncertainties inherent to model variables (termed "parameters" here). The GoldSim systems analysis software (GTG, 2010) was used to construct the probabilistic PA model. This software supports probabilistic analysis of the release and transport of radionuclides from disposal systems. The PA model is intended to reflect the current state of knowledge with respect to the proposed DU disposal, and to support environmental decision making in light of inherent uncertainties.

The dynamic aspects of the PA model may be grouped into two domains. The 'contaminant transport' (CT) component of the PA model encompasses the release of contaminants from disposed wastes and subsequent migration through the environment. The output of the CT component (documented in other white papers) is a time series of contaminant concentrations in different environmental media. These concentrations serve as inputs to the 'exposure-dose' (ED) component of the PA model that is the subject of this white paper. Because the ED component of the PA model is organized within a single "container" in GoldSim, the terms ED model and ED container are used interchangeably.

Assumptions and mathematical equations describing contaminant intake, including external exposure to ionizing radiation, for each exposure scenario are provided here. Equations for estimating radionuclide dose, and non-carcinogenic toxicity associated with uranium, are also provided. The implementation of methods for evaluating uncertainty in the ED calculations are also described. The bases of the deterministic values and/or statistical distributions for each of the ED parameters are discussed in the text below, the attached Appendix I, the spreadsheet *Dose Assessment Appendix II*, and the *Clive PA Model Parameters* documents (Clive PA Model Parameters.pdf and Clive PA Model Parameters.xls).

3.0 Exposure-Dose Model Implementation

3.1 Summary of Exposure-Dose Model Scope

The ED container addresses potential radiation exposure, dose and non-carcinogenic toxicity to human receptors who may come in contact with contaminants released from the disposal facility into the environment subsequent to facility closure. Radiation dose limits for protection of the general population are defined in UAC Rule R313-25-8 (Utah, 2010), and in 10 CFR 61.41 (CFR, 2007). These dose limits implicitly assume a level of health risk (discussed further below). The regulations specify that design, operation, and closure of the land disposal facility must also ensure protection of individuals inadvertently intruding into the disposal site and occupying the site or contacting the waste at any time after loss of active institutional control (e.g., fences, guards, etc.) of the site. Because the definition of inadvertent intruders encompasses exposure of individuals who engage in normal activities without knowing that they are receiving radiation exposure, there is no practical distinction between a member of the public (MOP) and inadvertent intruders with regard to exposure/dose assessment in the ED model.

The UAC Rule R313-25-8 (Utah, 2010) requires a PA for DU to have a minimum compliance period of 10,000 years, with additional simulations for a “qualitative analysis” (i.e., one in which only contaminant migration, and not doses, are modeled) for the period where peak hypothetical dose occurs. The estimation of doses in such long time horizons would be speculative at best, but if total radioactivity is used for a proxy (accounting for radiological decay and ingrowth from the disposed DU), then a peak value would occur once the progeny of U-238 have reached secular equilibrium in about 2.5 million years. With respect to radiation dose and non-carcinogenic uranium toxicity, the ED container quantifies dose only within the regulatory time frame of 10,000 yr. This approach is consistent with the requirements of UAC R313-25-8 (Utah, 2010). No specific time frame is defined in 10 CFR 61 (CFR, 2007) for the exposure/dose assessment.

Key land use characteristics for the Clive facility that pertain to the development of receptor scenarios and dose modeling are summarized in the CSM and in the *Features, Events, and Processes (FEPs) Analysis for Disposal of Depleted Uranium at the Clive Facility* white paper. Current human use of the area surrounding the Clive facility is very limited. Note that a residential scenario is not evaluated here, as there is no evidence that humans have permanently resided at the immediate Clive facility environs in recent history (see CSM). The closest current dwelling is approximately 12 km to the northeast of the site (a caretaker at the Aragonite/Grassy Mountain rest stop on east-bound Interstate-80).

Rancher and recreationist scenarios for the area surrounding the Clive facility are conditioned only on a continuation of present-day land use, whereas the conditions related to other scenarios would be much more speculative. It is not possible to project changes in human biology, society, technology, or behavior over a 10,000 year time frame; thus, current land use characteristics are projected throughout this period of performance, as recommended in NRC (2000). Uncertainty associated with this assumption is not quantified at this time. However, general justifications for this assumption in addition to NRC guidance can be made. The Clive facility environs are currently not amenable to permanent habitation due to the lack of potable groundwater and other factors. Dramatic changes in climate, such as large increases in average annual temperature or decreases in precipitation, would make the site even less hospitable. Changes in the opposite direction; i.e., large decreases in average annual temperature or increases in precipitation, have historically only been associated with ice ages and thus again would result in the site becoming less hospitable than it is today (see CSM). Therefore, the assumption that future land use and receptors will be similar to today's is likely conservative (i.e., protective).

It is possible that the Clive facility disposal cap could become more amenable to plant cover and perhaps increased human use than the surrounding areas post-closure due to the presence of the rip rap cover (e.g., in terms of accumulation of aeolian or wind-borne soil and dust and lower evaporation rates from soil below the rip rap). Nearby areas hosting vegetation (e.g., the alluvial fan of the Cedar Mountains east of the Clive facility, rocky outcrops west of the site) thus potentially offer analogous sites that will be considered for characterizing potential future plant communities on the disposal cap.

3.2 Exposure Scenarios

Based upon current and reasonably anticipated future land uses as summarized above, and as described in the FEP analysis (see *FEP Analysis for Disposal of Depleted Uranium at the Clive Facility* white paper), two future use exposure scenarios were identified for inclusion in the ED model: ranching and recreation. After institutional controls are no longer maintained, exposures to contamination in the ranching and recreation scenarios could occur both on the Clive facility site as well as nearby off-site locations.

Modeling of ranching and recreation scenarios is discussed here. Exposure scenarios are defined according to various human activities, which may result in a complete exposure pathway existing between the contaminant source and receptors. Exposure pathways describe the media, activities and exposure routes by which contamination becomes available to human receptors in the exposure scenarios. Every complete exposure pathway contains the following elements (EPA, 1989):

- Known or potential sources and/or releases of contamination;
- Contaminant transport pathways;
- Potential exposure media;
- A point of potential receptor contact with the impacted medium; and,
- An exposure route (such as ingestion or inhalation).

The primary exposure routes for the ranching and recreation scenarios include ingestion, inhalation, and external irradiation. A summary of potentially complete exposure pathways for each scenario is provided in Table 2. Figure 10 in the CSM depicts the transport mechanisms by which contaminants in the disposed waste may reach the exposure media discussed in this section.

Table 2. Exposure pathways summary

Exposure Pathway	Ranching	Recreation
Inhalation (wind derived dust)	×	×
Inhalation (mechanically-generated dust)	×	×
Inhalation (gas phase radionuclides)	×	×
Ingestion of surface soils (inadvertent)	×	×
Ingestion of game meat		×
Ingestion of beef	×	
Ingestion of wild plant material	×*	×*
Ingestion of seasonal surface water	×*	×*
External irradiation – soil	×	×
External irradiation – immersion in air	×	×

*Not included in the ranching or recreation scenarios; see text.

Note that a single individual could potentially engage in both ranching and recreation in the same area, but these scenarios are modeled separately both because they are expected to be distinct. Groundwater ingestion is not directly evaluated in the ED model, although groundwater concentrations are compared to State of Utah Ground Water Protection Levels (GWPLs). As described in the CSM, the aquifers underlying the area are more saline than seawater, and would not be potable without extensive desalinization. This situation is unlikely to change under any foreseeable conditions that would allow human habitation in the vicinity of the facility.

It is possible that humans may be exposed by ingestion of native plants. Several plants identified in Clive area vegetation plots were historically used as traditional food or medicine. These include shadscale saltbrush (*Atriplex confertifolia*), black greasewood (*Sarcobatus vermiculatus*), and rockcress (*Arabis* sp.), among others. However, present-day use of these plants by potential receptors in the area is unknown. In the absence of such information for plant uses and quantities thereof, a screening-level calculation will be performed to determine what quantity of plant

material from the disposal cap would need to be consumed to exceed the radiation dose performance objective.

A second possible exposure pathway not directly assessed in the ranching and recreation scenarios is human ingestion of intermittent (seasonal) surface water from puddles that may form in the air dispersion area. This surface water is likely to be salty, due to the saline nature of soils adjacent to the Clive facility, and direct human exposure is considered to be unlikely. Although present-day use of surface water by potential receptors in the area is unknown, a screening-level calculation will be performed to determine what volume of water would need to be consumed to exceed the radiation dose performance objective.

3.2.1 Ranching

The land surrounding the Clive facility is currently utilized for cattle and sheep grazing (BLM, 2010). Livestock apparently utilize the area more during winter periods when snow is present and when puddles exist during wet periods (NRC, 1993). The Bureau of Land Management (BLM) currently issues leases for 6 months of the year (November 1 to April 30; BLM, 2010, personal communication: Salt Lake Field Office). The personnel who spend time with the herds in the field are called "Ranchers" here (although this may include a variety of job classifications). Activities are expected to include herding, maintenance of fencing and other infrastructure, and assistance in calving and weaning. Ranchers may be exposed to contamination via the routes outlined in Table 1. It is assumed that any future ranching-related structures that might be constructed will be rough-built, with sufficient air flow that indoor radon accumulation is not an issue.

Ranchers typically use off-highway vehicles (OHVs; including four-wheel drive trucks) for transport. Beef consumption (from cattle exposed to contamination released from the site), is evaluated for the Ranchers, assuming that they may consume some of their own product. Beef, rather than lamb or mutton, is used as a food in the ED ranching scenario because regulatory bodies such as EPA (2005) and others have published information related to modeling of tissue concentrations for cattle.

3.2.2 Recreation

The recreational exposure scenario could potentially encompass a variety of activities. Information is limited regarding current use, as the BLM, the manager of much of the surrounding land, does not specifically track recreational usage in the area. However, based upon discussions with the BLM and reasonable judgment regarding anticipated land use, recreation may involve OHV use, hunting, target shooting of inanimate objects, rock-hounding, wild-horse viewing, and limited camping.

The desirability of recreational activities on or around the disposal units, similar to suitability for ranching, is partially dependent upon assumptions regarding ecological succession on the disposal unit over time. With the possible exceptions of OHV use and as a vantage for hunting (e.g., for pronghorn), recreational use of the disposal unit in an as-closed state of bare rip rap surfaces is likely to be minimal. As soil develops on the cap and plant succession proceeds, the disposal unit may become more attractive for different types of recreational activities. However, for the purpose of exposure assessment, it is assumed that sport OHV riders ("Sport OHVers; i.e., OHV users who use their vehicles for recreation alone) and hunters using OHVs ("Hunters"),

both of whom may also camp at the site, would represent the most highly-exposed receptors (due to dust exposure, game meat ingestion, etc.), and other types of recreationists would have lower exposures.

3.2.3 Other Potential Receptors

The ranching and recreation scenarios are characterized by potential exposure related to activities both on the disposal site and in the adjoining area. Specific off-site points of potential exposure also exist for other receptors based upon present-day conditions and infrastructure. These locations and receptors include:

- Travelers on Interstate-80, which passes 4 km to the north of the site;
- Travelers on the main east-west rail line, which passes 2 km to the north of the site;
- Workers at the Utah Test and Training Range (a military facility) to the south of the Clive facility, who may occasionally drive on a gravel road immediately to the west of the Clive facility fenceline;
- The resident caretaker at the east-bound Interstate-80 rest facility (the Grassy Mountain Rest Area at Aragonite) approximately 12 km northeast of the site, and,
- Sport OHV enthusiasts at the Knolls OHV area (BLM land that is specifically managed for OHV recreation) 12 km to the west of the site.

Exposure to individuals at these off-site locations is expected to be minimal due to either the large distance from the site (Interstate-80 rest area and Knolls OHV area) or because the exposure time for any individual will be very brief (travelers on road, rail, and highway). Unlike ranching and recreational receptors who may be exposed by a variety of pathways on or adjacent to the site, these off-site receptors would likely only be exposed to wind-dispersed contamination, for which inhalation exposures are likely to predominate. These receptors will be evaluated using screening calculations to determine whether exposures at these off-site locations may be important.

3.3 Assessment Endpoints

The biological effect of greatest interest to regulatory agencies for environmental exposure to radionuclides is cancer. Ionizing radiation is a clear cause of cancer and other health effects at high doses. However, the risk of cancer to an individual exposed to radiation at environmental levels is highly uncertain and depends upon a large number of assumptions, the most influential being: 1) The major source of data for radiological risk assessment; i.e., the high doses experienced by the Hiroshima/Nagasaki atomic bomb victims in World War II, is relevant for the doses in the range of regulatory dose limits; and, 2) risks can be extrapolated from large doses to small doses in a linear fashion, with no threshold of effect (i.e., the hypothesis that no dose is without some risk of cancer) (Brenner et al., 2003). Both of these assumptions are controversial (Scott, 2008), but they provide substantive bases for NRC and DOE radiation regulation and guidance at this time. Uncertainty associated with these assumptions is not evaluated in the PA model at this time.

3.3.1 Individual Dose

There are two performance goals that may be applicable in the PA. The first is the individual dose limit. Title 10 CFR 61.41 (CFR, 2007) specifies assessment endpoints for a radiological PA that are related to annual radiation dose. The specific metrics described in §61.41 are organ-specific doses, and restrict the annual dose to an equivalent of 0.25 mSv (25 mrem) to the whole body, 0.75 mSv (75 mrem) to the thyroid, and 0.25 mSv (25 mrem) to any other organ. As described below, the ED model will employ a total effective dose equivalent (TEDE) for comparison with the 0.25 mSv/yr threshold. This dose level will be considered as a deterministic performance goal, with no uncertainty.

As discussed in Section 3.3.7.1.2 of NUREG-1573 (NRC, 2000), the radiation dosimetry underlying the §61.41 dose metrics was based upon a methodology published by the International Commission on Radiation Protection (ICRP) in 1959. Subsequent to Title 10 CFR 61.41, more recent dose assessment methodology has been published by the ICRP (ICRP, 1979; 1991; 1995) that employs the TEDE approach. The TEDE uses weighting factors related to the radiosensitivity of each target organ to arrive at an effective dose equivalent across all organs. The text of Section 3.3.7.1.2 of NUREG-1573 (NRC, 2000) states:

> "As a matter of policy, the Commission considers 0.25 mSv/year (25 mrem/year) TEDE as the appropriate dose limit to compare with the range of potential doses represented by the older limits... Applicants do not need to consider organ doses individually because the low value of TEDE should ensure that no organ dose will exceed 0.50 mSv/year (50 mrem/year)."

The regulations state that this dose limit is applicable to *any* member of the public, yet NRC PA guidance (NRC, 2000) suggests a practical approach of applying the dose limit to an *average* member of a "critical group" (i.e., a group of public receptors who might be reasonably expected to live near or experience exposure to the facility site). The ED model has been developed to support estimates of both average individual dose and various percentiles of the distributions of individual dose for Ranchers, Sport OHVers, and Hunters.

Thus, in terms of PA performance objectives, the modeling question relates to estimating the probability that the total radiation dose attributable to future releases from the site to any or an average member of a critical group (defined here as a Rancher, Sport OHVer, or Hunter) will exceed 25 mrem TEDE in any particular year, during the performance period of the site. As institutional controls in place while the site is operating are designed to prevent public access, there will be no public exposure during this time period. The period of time of interest, therefore, in the ED portion of the PA model is from the time of loss of institutional control to 10,000 years post-closure, although physical transport processes are evaluated beginning at model year zero.

The US Environmental Protection Agency (EPA) has estimated that 15 mrem/year is equivalent to a 3-in-10,000 excess risk of cancer (EPA, 1997a), and has defined that level as:

> "...consistent with levels generally considered protective in other governmental actions, particularly regulations and guidance developed by EPA in other radiation control programs."

A 1- in-1-million excess risk level is typically viewed as a *de minimus* level; i.e. one that is below a level of concern (CFR, 1994). If the estimated EPA risk equivalence for 15 mrem/year is extrapolated to 1- in-1-million, this results in a 0.05 mrem/year *de minimus* dose. This is important both when evaluating the dose to *any* receptor and when collective dose is assessed (discussed below).

3.3.2 As Low As Reasonably Achievable (ALARA)

A second decision rule pertains to the ALARA concept. Ionizing radiation protection limits have been utilized since the 1920s (Hendee and Edwards, 1987). These limits have changed over time as more information regarding the negative biological effects of radiation has become available (especially after World War II). Concurrently, therapeutic and diagnostic (i.e., beneficial) uses of radiation have increased dramatically. Thus, a tradeoff is immediately apparent; radiation can be harmful or helpful, depending upon the context.

An additional consideration is the biological endpoint of concern. Radiation in high doses kills cells, which can be harmful or beneficial to the receptor of the doses (e.g., in the latter case, targeted radiation is used to kill cancer cells). The effects of low doses of radiation are more uncertain. There is ample evidence that ionizing radiation can damage DNA and enhance cell proliferation in doses below those that kill cells, and thus can potentially cause cancer. However, it is uncertain at what level of low doses this becomes a concern.

For many years, there has been a presumption in radiation protection, based upon statistical analysis of animal and human data, that ionizing radiation has a linear dose-response curve at low doses and that there is no threshold of effect; i.e. any dose of radiation can result in an increased probability of cancer (this is termed the linear no-threshold, or LNT, hypothesis). This is not supported by all experimental and clinical observation (Scott, 2008). Additionally, the fact that radiation is associated with a large number of natural sources, ranging from sunlight to radon, and the fact that multiple highly-efficient molecular and cellular defense and repair mechanisms exist, must be considered. Regardless, this LNT hypothesis is the basis for most regulatory standards today, and indeed for the ALARA concept.

ALARA (or the older but similar concept "as low as practicable"; ALAP) essentially assumes no carcinogenic threshold of radiation carcinogenesis. If this assumption is taken at face value, ALARA seems to be a reasonable objective. If not, then a threshold of effect would be a more tractable and achievable objective. Regardless, ALARA could perhaps be applied even in the case of a threshold or 'target' concentration; the threshold would simply be a limit on the amount of risk reduction that should be achieved by a particular management alternative. Proper evaluation of uncertainty associated with the LNT hypothesis would be a large task in itself, but the influence of a LNT assumption can still be evaluated using sensitivity analysis. However, this is beyond the scope of the current PA.

A different sort of threshold exists with regard to natural background levels of radiation. The doses that the public receives from all environmental sources (e.g., local geology, extraterrestrial, etc.) can be quite variable. For example, population *X* who live at high altitude in a location with geologically high levels of uranium may have a much higher level of annual exposure than population *Y* who live at sea level with low levels of uranium in soil (e.g., see http://www.epa.gov/radon/zonemap.html). If population sizes were equivalent, one could then

consider that a larger incremental dose might be acceptable for population *Y* compared to population *X*.

Uranium and many other metals are also associated with non-radiological toxicity; e.g. kidney or liver damage. In such cases, toxicology has developed concepts such as the reference dose and benchmark dose, to account for the clear thresholds of effect that are associated with non-carcinogenic toxicity (Filipsson, 2003). Similar to the discussion above, in these cases the threshold can be viewed as a target, below which risks are not of substantial concern.

The modern ALARA concept, as germane to radiation protection on both individual and population levels, was described by the ICRP in 1977 (ICRP, 1977):

> "Most decisions about human activities are based on an implicit form of balancing of costs and benefits leading to the conclusion that the conduct of a chosen practice is 'worthwhile.' Less generally, it is also recognized that the conduct of the chosen practice should be adjusted to maximize the benefit to the individual or to society. In radiation protection, it is becoming possible to formalize these broad decision-making procedures. . ."

The ICRP (1977) basically recommended a system of radiation protection that included the following principles:

- No practice shall be adopted unless its introduction produces a positive net benefit;
- All exposures shall be kept as low as reasonably achievable, economic and social factors being taken into account; and,
- The dose equivalent to individuals shall not exceed the limits recommended for the appropriate circumstances by the Commission.

These three components are identified by the ICRP by the abbreviated terms:

- The justification of the practice;
- The optimization of radiation protection; and,
- The limits of individual dose equivalent.

For present purposes, as regulatory agencies have adopted and applied clear dose limits for individuals, evaluation of ALARA here will be restricted to population doses and risks, termed collective dose. This is appropriate in the context of design and siting of radioactive waste facilities; as it is likely, if any substantial future risks occur, that health concerns will be at a population level. Further, we assume that facility workers will be protected under existing health and safety regulations and guidance, and will not be evaluated here.

3.3.3 Collective Dose

In order to estimate collective dose, a population needs to be assessed. If cumulative doses are to be estimated over some period of time, then the doses are added over that time period. The 'answer', at the end of the performance period (10,000 years post-closure, in this case) might then

be the individual annual doses added up over a period of 10,000 years (minus the period of time when institutional controls are in place).

For a hypothetical example, say a total population of 50 people is potentially exposed to the site for every year during the performance period (note that all radioactive waste repositories that have been recently evaluated in the US are in fairly remote areas, so a large urban population would be inappropriate). Say institutional controls are in place for 100 years. Then, the cumulative population dose will be the sum of 50 individual doses in mrem/year, multiplied by 9,900 years. Say that every person in the population is exposed just below the individual dose limit (say, 24 mrem/year TEDE). Thus, the cumulative population dose will be 50×24×9900=11,880,000 mrem, or 11,880 person-rem. This number has no meaning by itself, as there is no standard or basis for declaring this is 'unacceptable' or not, or whether it is "reasonable" or "achievable" (according to ALARA). It is only useful in the context of comparing how one site or disposal option might perform compared to another. This is best determined in the context of a decision or economic analysis, which is discussed in a future companion white paper *Decision Analysis Methodology for Assessing ALARA Collective Radiation Doses and Risks*.

In the context of the current assessment, and in lieu of guidance that defines what an 'acceptable' population dose might be; a means must be applied so that all populations (e.g., the entire United States) are not assessed, as this would be burdensome and meaningless. For instance, it is known that a large population will indeed be exposed to the site if current conditions continue; i.e., the population of drivers on Interstate-80. However, as previously mentioned, each of these drivers would be exposed for very short periods of time. In order to gauge the importance of quantifying dose for this population, and indeed any population that might be exposed for brief periods and/or to very low concentrations, the *de minimus* risk approach will be applied. As explained previously, according to the EPA a 0.05 mrem/year dose corresponds to approximately a 1-in-1-million excess cancer risk. Receptors other than Ranchers, Sport OHVers, or Hunters will be evaluated using this individual dose threshold to determine whether their doses should be considered when computing collective dose. Cumulative population dose will not include contributions from these receptors unless individual doses are above 0.05 mrem/year.

3.4 Modeling Doses

3.4.1 Individual Doses

Studies of the health of existing populations (i.e., epidemiological studies) have struggled with how to infer individual risk from population statistics. For example, a study of cigarette smokers and lung cancer may show a clear statistical relationship between the exposure and disease, with a high degree of confidence; yet, for instance, it does not tell *me* what *my* additional risk of cancer will be if I smoke one cigarette. It is indeed impossible to directly estimate health risk for individuals for the majority of exogenous exposures (there are exceptions in the case of some genetic abnormalities; if the abnormality is known to exist in an individual, then the risk of disease in that individual associated with that abnormality is known with almost perfect confidence). Risk for individuals must generally be inferred from populations. In addition to various designs of epidemiological studies, insurance companies, for example, use life tables stratified on gender, age, disease history, etc. to estimate premiums.

In the present case, the issue is estimation of individual radiation doses. As mentioned above, risk is implicit in radiation dose, with many inherent assumptions. Additionally, the PA is projecting into the future, to individuals who do not exist yet. As information as to how humans may or may not change biologically in the space of a 10,000-year performance period does not exist, it is only reasonable to assume that humans will remain essentially the same.

One approach to estimating individual risk, based upon how the EPA has historically conducted exposure assessment (EPA, 1989), is to define a 'simulated' individual based upon their exposure characteristics. The simulated individual is therefore the product of a number of physiological and behavioral parameters. Historically, this has been done deterministically; i.e., single values are used for the exposure and physiological parameters, and a single simulated individual results. With more recent applications of probabilistic methods, this process has been expanded to address variance in the exposure parameter values.

For the Clive facility, following are some major sources of variance related to radiation dose that are directly germane to the ED model at any particular point during the assessment time horizon:

1. The number of receptors, if any, in the vicinity of the disposal site at any point in time;
2. The physiological characteristics of the receptors;
3. The nature and intensity of exposure by various potential exposure routes (ingestion, inhalation, external radiation) based upon behavioral characteristics of the receptors;
4. The concentrations of radionuclides in potential exposure media; and,
5. The annual radiation dose associated with the exposure.

Within some of these five categories there may be multiple exposure parameters employed in the modeling and hence numerous sources of variance. In particular, radionuclide concentrations in exposure media include all the variance from the contaminant transport modeling conducted in the PA that are propagated to the ED assessment.

As discussed above, the PA guidance (NRC, 2000) suggests that the annual dose to an "average member of a critical group" should be estimated. Specifically:

> The average member of the critical group is that individual who is assumed to represent the most likely exposure situation, based on cautious but reasonable exposure assumptions and parameter values. It is generally not practicable, when analyzing future potential doses, to calculate individual doses for each member of a critical group and then re-calculate the average dose to these same members. In general, it is more meaningful to designate a single hypothetical individual, representative of that critical group, who has habits and characteristics equal to the mean value of the various parameter ranges that define the critical group. In this fashion, the dose to the "average member" of the critical group approximates the average dose obtained if each member of the critical group were separately modeled and the results averaged.

Thus, the guidance appears to request definition of:

- A critical group;

- An average member of the critical group; and,
- The annual dose to this member.

The critical groups, in the case of the present PA, are defined as Ranchers, Sport OHVers, and Hunters. An "average member" of these groups is a theoretical or statistical construct, as such a person does not and never will exist. Thus, we can interpret the guidance as referring to the statistical average dose (i.e., arithmetic mean) of a population of individuals' doses. In order to estimate the average simulated individual's dose at a particular time step, doses to a population of simulated individuals need to be estimated (note that hardware and software capabilities have increased dramatically since the NRC's guidance, so it is indeed now possible to calculate doses at an individual level).

In the context of human health risk assessment, variance in parameter values is traditionally split into the categories of variability and uncertainty (EPA, 2001). The term *variability* refers to natural, irreducible variance in the range of values a parameter may take (say, body weights in a population), and *uncertainty* refers to incomplete, imprecise and/or inaccurate knowledge associated with parameter values (Bogen et al., 2009). These particular definitions are not universally accepted however, and in practice may have more or less utility as a basis for the methodology used to assess overall variance in model output.

Returning to the issue of doses to a population of simulated individuals, and to the five major sources of variance for these dose estimates, the first 3 sources of variance apply to population variability. In particular, in any year the physiological and behavioral characteristics of the exposed individuals govern the degree of variance related to sources #2 and #3. The variance related to parameters contributing to exposure concentrations and to radiation dose coefficients do not vary over time and do not vary for different hypothetical individuals. For example, models of carcinogenesis for low-dose radiation are highly uncertain, but this uncertainty does not appreciably differ among individuals nor does it vary from one model year to another. Similarly, we assume essentially static environmental conditions over the 10,000-year performance period for any given model realization; a soil-water distribution coefficient that applies at model year 2,000 also applies at model year 3,000.

There are multiple methods that may be employed to model two different types of variance, but a typical method is termed 2-dimensional (2D) or nested-loop Monte Carlo simulation (Bogen et al., 2009). In the ED model, the exposure parameters are grouped into long-term model uncertainty and population variability categories. The physiological and behavioral parameters related to sources #2 and #3, as well as the number of individuals exposed in any year (source #1), are evaluated annually in the “inner loop” of the 2D Monte Carlo simulation. The remainder of the model parameters, including all aspects of the Contaminant Transport modeling and the radiation dose conversion factors (DCFs) are defined in the “outer loop” of the 2D Monte Carlo simulation. This categorization is further discussed below.

3.4.2 Collective Dose

As described above, an issue of ALARA interest is the collective dose over the performance period. To reiterate, this estimate is of little value in itself as there are no performance objectives for this endpoint; rather, it should ideally be viewed in the context of decision analysis.

Estimating population dose is simple. It is the sum of individual annual doses over the period of time from loss of institutional control to the 10,000 year mark. Contributions from off-site receptors who are anticipated to have very low annual dose rates will only be included in the collective dose sum if individual doses are above a 0.05 mrem/yr threshold (equivalent to approximately a 1-in-1-million excess cancer risk).

3.4.3 Dose Conversion Factors

For both individual doses and population doses, exposures or intakes are converted to TEDEs via so-called DCFs, or dose equivalents per unit intake. DCFs are published by EPA and ICRP. Section 3.3.7.3 of NUREG-1573 specifies DCFs published by EPA in Federal Guidance Reports (FGR) 11 (EPA, 1988) and 12 (EPA, 1993a). EPA subsequently made use of age-specific DCFs published in ICRP Publication 72 (ICRP, 1995) to estimate radionuclide cancer risk coefficients in FGR 13 (EPA, 1999). The DCFs published in EPA (1999) are used in the dose assessment and are available online (http://ordose.ornl.gov/downloads.html). The radionuclide-specific DCFs used in the dose assessment are also provided in the spreadsheet *Dose Assessment Appendix II*.

DCFs are derived using models and data that represent the physics and biology of the interaction of the human body with radiation or radioactive material. Briefly, internal DCFs (typically in units of Sv/Bq) are used to convert from an exposure or intake to an internal dose delivered to target organs. DCFs are radionuclide, receptor-age, and exposure-route dependent (external, inhalation, or ingestion). In addition, separate inhalation dose coefficients are published for different lung absorption rate classes. For external exposure the dose coefficient depends upon whether the receptor is immersed in a plume of radioactive contaminants (such as air) or is standing on the surface of contaminated ground (surface water sources are not evaluated here).

DCFs, like most of the parameters in the PA model, have associated uncertainty. The National Council on Radiation Protection and Measurements (NCRP, 1996), provides examples of the use of distributions for DCFs in probabilistic modeling. The work that led to FGR 13 included a quantitative uncertainty analysis, but unfortunately the results for dose coefficients are not presented. It is also unclear in this work as to the relative contribution to total uncertainty associated with dose for specific radionuclides (although the authors of the report indicate that this is variable).

In order to be useful for probabilistic modeling, the uncertainties associated with DCFs must be represented as statistical distributions. A search of the published literature indicates that uncertainty distributions for DCFs *per se* have only been developed in a few instances; largely focused on a few radionuclides (e.g., I-131, tritium) that have been to focus of worker protection assessments, legal cases, and related dose reconstruction scenarios (e.g., Hamby, 1999; Harvey et al., 2006). For the purpose of the PA, uncertainty distributions for a large number of DCFs would ideally be available. No such 'global' source was identified in the literature.

However, there has been published work that has focused on components of DCFs that are generalizable to different classes of radionuclides. The most relevant work that was identified is the work of Kocher et al. (2005), in the context of "probability of causation" in cases of worker exposure to radiation. This work has been incorporated into the National Institute for Occupational Safety and Health's "Interactive RadioEpidemiological Program" (IREP; http://www.cdc.gov/niosh/ocas/ocasirep.html), which is employed to determine the probability

that a cancer was caused by workers' exposure to radiation during nuclear weapons production. Similar work has been applied in the context of probabilistic dose reconstruction (Linkov et al., 2001.)

Kocher et al. (2005) estimate:

> …so-called radiation effectiveness factors (REFs) [*note*: not to be confused with 'radon emanation factors'] that are intended to represent the biological effectiveness of different types of ionizing radiation for the purpose of estimating cancer risks and probability of causation of radiogenic cancers in identified individuals. An REF is a dimensionless factor used to modify an estimate of average absorbed dose from a given radiation type in an organ or tissue of concern in an identified individual to obtain a biologically significant dose on which the risk of induction of cancer in that organ or tissue is assumed to depend.

Kocher et al. (2005) specify that they are ultimately interested in *risks*, not *doses*; but, the estimates of uncertainty associated with REFs are relevant to the current application. They state that their REFs are essentially analogous to radiation weighting factors (w_R). The w_R is is an additive function of a dimensionless "quality factor" Q, that is dependent upon radiation type; and a dimensionless N, which is dependent upon the tissues irradiated, the time and volume relevant to irradiation, and biological characteristics of the receptor. Consistent and thorough documentation of these terms appear to be lacking in published reports. Regardless, in most cases, these terms have been superseded by another term; Relative Biological Effectiveness (RBE). The radiation dose unit employed in this PA, the sievert (Sv), can vary considerably based upon the RBE.

Kocher et al. (2005) state that their

> …new term "radiation effectiveness factor" (REF) is used in this work to distinguish a quantity that represents biological effectiveness for purposes of estimating cancer risks and probability of causation in identified individuals from similar quantities, including relative biological effectiveness (RBE), which strictly applies only to results of specific radiobiological studies under controlled conditions.

For the purpose of establishing initial, proof-of-principle uncertainty distributions for DCFs for incorporation into the PA, these philosophical and semantic issues will take a subservient position. We will therefore assume that for the carcinogenic effects or radiation, that the REF is equivalent to the RBE, which is in turn equivalent to w_R. This is not strictly the case, but the intent here is to estimate uncertainty in biologically-relevant radiation dose, not exact numerical quantities. REFs account for the fact that some types of radioactive decay result in more biological damage than others. The "reference" type of radiation is typically Co-60 high-dose/dose-rate gamma decay, as this is the type of radiation germane to the atomic-bomb survivor data and similar sources of epidemiological data on cancer resulting from radiation exposure. The REF (or w_R) for such radiation is set at 1.0. However, larger particles such as alpha particles and neutrons can cause more biological damage, thus the REFs for these types of ionizing radiation are larger, and function as multipliers to the DCFs.

In this PA model, radiation-type specific REFs per Kocher et al. (2005) will be used as modifying distributions to the DCF point estimates presented in FGR 13 (note that DCFs are not presented in the written report of FGR 13, but are available via an online database: http://ordose.ornl.gov/downloads.html). Kocher et al. (2005) developed probability distributions for REFs, based upon a combination of exhaustive literature review, statistical analysis, modeling, and subjective judgment. Tables 14 and 15 in that reference provide summaries.

These REF distributions can be essentially viewed as modifiers to published DCFs, in lieu of the published deterministic w_R's used in radiation protection (ICRP, 1991). For example, the published deterministic w_R for alpha particles is 20. The Kocher et al. (2005) REF for alpha particles can be represented by a lognormal distribution with a median of 18, and a 95% confidence interval from 3.4 to 100. Thus, for an alpha-emitting radionuclide, the published DCF would be divided by 20, then multiplied by the distribution provided. As the REFs are radiation-type specific, they are generally applicable to the predominant radiation characteristics of the particular radionuclide of concern.

In the present model, there are no species that decay by neutron emission. The REFs employed represent alpha, beta (electron), and photon (gamma, X-ray) decay. For each radionuclide, the dominant radiation type and its energy are defined based upon information from ICRP (using the program RadSum32, available from http://ordose.ornl.gov/downloads.html). For some radionuclides, the energy of electron or photon emissions is essentially equivalent to the reference radiation (high-energy gamma), resulting in an REF of 1.0 with no uncertainty. For others, an REF distribution is defined based upon the information in Kocher et al. (2005) and this REF is used as a multiplier to the DCF. Please note that radon is evaluated differently from other radionuclides (see Section 4.4); thus the REF distribution development process outlined below does not apply.

Following is a summary of the specific process by which REF distributions are generated and applied in the PA model, along with assumptions (please see Kocher et al. (2005) for assumptions made in that work). Radionuclide-specific deterministic DCFs, and the inputs necessary to calculate stochastic DCFs, are provided in the spreadsheet *Dose Assessment Appendix II*.

1. The 27 radionuclide Species in the PA model were expanded to 63 radionuclides to account for short-lived progeny (Species radionuclides have a half-life of approximately 2 years or longer). The decay chains for identifying progeny were taken from the Nuclear Wallet Cards (Tuli, 2005).

2. DCFs were taken from the the EPA FGR 13 database (available from http://ordose.ornl.gov/downloads.html). DCFs are available for particulate and vapor-phase inhalation, ingestion, and external exposure (including "submersion", "ground plane", and "soil volume" values). In all cases, DCFs for adults are selected (as the receptors of interest are adults), and "effective dose" DCFs (a weighted composite of all organs) are employed. Inhalation DCFs related to the default inhalation absorption class from Table 2.1 of FGR 13 were used. If no default class was specified, the "medium" (Class M) inhalation DCF was usually selected because it is commonly between the DCF values for slow and fast absorption classes, and is therefore considered to be the least

biased point estimate. For external exposure to contaminated soils, the "soil volume" external DCFs are used in this PA consistent with the physical models of contaminant transport over time.

3. A dominant form of radiological decay was assigned for internal DCFs and external DCFs for each of the 63 radionuclides using information from the RadSum32 code. For internal DCFs, the dominant decay mode was identified as the highest contributor to total emitted energy of any radiation type (gamma + x-ray; electron (the maximum of beta, internal conversion electrons, or auger electrons); and, alpha). In all cases, this protocol resulted in alpha emissions being selected as the dominant decay mode when alpha decay occurs. For external DCFs, the dominant decay mode was identified as the energy of gamma + x-ray. If there are no photon emissions for a radionuclide, dominant decay for external irradiation was identified as the highest energy among beta, internal conversion electrons, and auger electrons. Because alpha particles cannot penetrate the stratum corneum to the biologically active lower strata of the skin, alpha particles are not evaluated for the purpose of assigning REF distributions to external DCFs.

4. For radionuclides where the dominant decay mode is electron or photon, the average particle energy of that decay mode (in million electron volts, or MeV) is identified from the RadSum32 code.

5. REF distributions are defined for four categories of decay mode and energy, based upon percentiles in Tables 14 and 15 in Kocher et al. (2005). For radionuclides where the dominant decay mode is photon or electron emission with a mean energy higher than the particular threshold, an REF of 1.0 is assigned, as the REF for these emissions are essentially equivalent to the reference radiation (Co-60 gamma). The REF distribution categories include:

    - alpha (any energy)
    - electron (<0.015 MeV)
    - photon (>0.03 and <=0.25 MeV)
    - photon (<=0.03 MeV)

    With regard to the alpha REF, please note that Kocher et al. (2005) assumed that 100 represented the 97.5th percentile of the distribution. This is likely conservative, as the highest value ever estimated from experimental studies is 100, and this only applies to particular forms of inhaled plutonium (Kocher et al., 2005).

6. The DCFs for each of the 63 radionuclides are divided by the ICRP weighting factor (w_R) in order to apply the REF distributions. For alpha emitters, the w_R value is 20, and for electrons and photons it is 1.0. Stochastic DCFs are then calculated as the product of the DCF and the appropriate REF.

7. DCFs for the 27 radionuclide Species defined in the PA model are assembled using the decay chains and branching fractions from the Nuclear Wallet Cards (Tuli, 2005). These are equivalent to the "plus daughters" (+D) DCFs for primary radionuclides provided in

radiological dose software such as the RESRAD computer code (http://web.ead.anl.gov/resrad/home2/).

8. The stochastic +D DCFs may then be employed in the PA model for radiation dose calculations. Alternatively, a model user may select the option of using the deterministic FGR 13 DCFs in a simulation. This is permitted even when the PA model is run in stochastic mode for all other model parameters.

Note that this method only addresses one component of uncertainty associated with DCFs, and thus must be viewed as a pilot effort. There are likely substantial sources of uncertainty that cannot be readily quantified, or which can only be quantified for a few radionuclides.

3.4.4 Additional Sources of Uncertainty

In addition to variance in the definition of model parameter values, there are other important sources of uncertainty and/or bias to potentially consider. For example, if radiation dose-response model uncertainty (particularly at low doses) were to be considered, it is possible that the uncertainties associated with radiation risk would swamp those associated with the remainder of the PA model, as it is by no means clear that ionizing radiation has *no* threshold of carcinogenic effect.

There is uncertainty associated with the mathematical models defining contaminant transport in the environment over time. These models are designed to represent the system as best they can (although sometimes with known protective biases) but they like all models are simply approximations of reality. Other aspects of the PA model have similar issues associated with model uncertainty.

Most importantly, the overall uncertainty associated with what the natural world and human society will be like in 1,000 or 10,000 years from today is likely much greater than the uncertainty associated with the model form, yet this 'future world' uncertainty is not quantifiable or readily bounded. Such sources of uncertainty must be discussed qualitatively rather than being quantitatively modeled.

3.4.5 Non-Cancer Toxicity Endpoints

DU waste (and potentially other compounds) associated with the Clive facility can be associated with toxicological risks that are independent of radioactive properties. EPA has evaluated available dose response information for many chemicals and has published this information in the form of toxicity values and accompanying information. Potential health effects related to intake of chemicals is assessed by means of slope factors for suspected carcinogens, and reference doses (RfDs) for noncarcinogenic effects of chemicals. Unlike carcinogenic agents, EPA typically views toxicants with non-cancer effects as having thresholds; i.e., levels below which effects would be unlikely. RfDs essentially amount to such thresholds, usually with several layers of 'safety' factors added.

As a proof-of-principle exercise, the potential non-radiation related toxicity of DU at the Clive facility will be evaluated in the PA. The modeling process is very similar to that conducted for radionuclides, other than kidney toxicity (as opposed to radiation dose) of DU will be evaluated, and the toxicity of DU will not change over time (as radioactive decay is not important in this

context).Oral toxicity criteria for uranium are published by EPA in relation to the Superfund program (EPA, 2011) and by EPA's Office of Water in relation to drinking water standards (EPA, 2000). There is a five-fold difference between these criteria, and both will be employed in the assessment of uranium toxicity to determine the sensitivity of uranium health effect results to differences in these recommended toxicity criteria for uranium.

4.0 Equations and Parameters of the Exposure-Dose Container

4.1 Organization

The implementation of the exposure and dose calculations, and associated results, are organized within different subcontainers in the ED container. A description of the main subcontainers and their contents are described below:

- *Environmental Concentrations*: Concentrations of species in various environmental media developed in the Contaminant Transport (CT) component of the PA model are tracked here. These elements are the link between the CT and ED components of the PA model, and take the form of GoldSim vectors defined by the array Species. Environmental concentrations are subsequently defined as a two-dimensional matrices with the addition of arrays for different receptor groups in order to track doses for multiple individuals to tally a population dose.
- *Behavioral Parameters:* Input parameter values related to human activities and behaviors for the Rancher, Sport OHVer, and Hunter exposure scenarios. With few exceptions, these parameters are defined within an 'inner-loop' container that has a separate internal timestep so that they can be sampled on an annual basis regardless of the timestep length of the CT model.
- *DCFs:* Dose conversion factors for radionuclides are grouped in a subcontainer outside the inner-loop container..
- *Dose Calculations:* A series of subcontainers are defined within the inner-loop container for calculation of TEDE related to inhalation, ingestion, and external radiation exposures for the Rancher, Sport OHVer, and Hunter exposure scenarios. A container for off-site receptor doses is also provided. Screening-level dose calculations for ingestion of edible plant materials gathered on the waste disposal cell, and ingestion of standing surface water, are grouped in a subcontainer outside the inner-loop container.
- *Uranium Hazard:* A subcontainer within the inner-loop container holding calculations for systemic toxicity (hazard) related to the nonradiological effects of uranium.

In terms of parameter definitions, GoldSim uses a variety of methods, including deterministic values, scalars, time series data, and “stochastics”, which are user-defined statistical distributions. Parameter distributions employed in the PA model reflect a mixture of site- and receptor-specific data, information modeled in 'upstream' portions of the PA model, literature information, and subjective judgment; as appropriate.

4.2 Environmental Concentrations

The principal link between the CT component and the ED component of the PA model are concentrations of contaminants in different environmental media. Major environmental media evaluated in the ED container include:

- **Soil**. There are several soil concentration terms that are used in the ED container. The contaminant transport portion of the PA model employs a homogenized waste source term and simulates transport over time to produce estimates of soil concentrations for the embankment *top slope* and the embankment *side slopes*. The principal soil term in the ED container is the area-weighted average concentration in the top layer of both the *top slope* and *side slope* of the disposal cap. This is the *disposal cap* soil concentration. Contaminant concentrations in these soils, plus possible contribution from lower soil layers and even the disposed waste itself, are used to calculate soil exposure concentrations for the *embankment*. Embankment soil concentrations are defined as the area-averaged soil concentrations of the disposal cap and of one or more gullies and fans that may develop in the future. Finally, particle resuspension and deposition models are used to calculate area-averaged soil concentrations *off-site air dispersion area* based upon the embankment soil concentrations.

  Area-averaged soil concentrations for the embankment and the off-site air dispersion area are employed because there is no basis for specifying greater or lesser individual exposure intensity as a function of location within these regions. Individuals are presumed to be exposed at random in these areas, and an area-averaged exposure concentration reflects this presumed behavior.

  The human exposure area surrounding the Clive site is where the Ranchers, Sport OHVers, and Hunters identified as likely receptor populations conduct their activities. The maximum size of this area is the approximate area between I-80 and the Utah Test and Training Range (UTTR) in an east-west orientation, and the Cedar Mountain foothills and salt/mud flats in a north-south orientation. The minimum size of this area is the approximate minimum size of the four current grazing leases in the vicinity of the Clive facility. Because the maximum area is roughly equivalent to the largest of the four current grazing leases, the human exposure area and the size of the area over which cattle may graze are equivalent.

- **Air**. Air concentrations of gaseous and particulate contaminants in the atmosphere are calculated using the AERMOD atmospheric dispersion model for breathing-zone air above the embankment and above the off-site dispersion area. Off-site air concentrations are also calculated at the specific exposure locations described previously. These calculations are documented in the Atmospheric Modeling white paper. To evaluate the impacts of dust generated during off-highway vehicle (OHV) use, an adjustment factor for particulate air concentrations is used based upon dust generation data collected by EPA Region 9 for OHV users wearing personal air monitors in a recreational area in California (EPA, 2008).

- **Game**. Contaminant concentrations in the meat of game animals that incorporate the embankment and nearby areas as part of their home range. Based upon communications

with BLM, pronghorn are modeled as the most likely game species of interest to future Hunters. Contaminant concentrations in game tissue are modeled as a function of ingestion of browse plants, standing surface water, and soil inadvertently ingested while browsing.

- **Beef**. Contaminant concentrations in beef from cattle that incorporate the embankment and nearby areas areas as part of their range. Similar to game tissue concentrations, beef concentrations are related to plants, surface water, and soil. The number of cattle grazing in impacted areas is assumed to be sufficient to provide ranchers with beef commensurate with the specified intake rates.
- **Plants**. Wet weight contaminant concentrations in plant tissues. These concentrations are used as an interim step in the calculation of tissue concentrations in cattle and game and are calculated based upon an equilibrium with soil defined by element-specific plant-soil concentration ratios. They are also used for screening-level calculations to determine if potential direct human exposures by plant ingestion may be of concern.
- **Surface Water**. Contaminant concentrations in standing surface water in the air dispersion area. Water concentrations are calculated assuming equilibrium with soil, as defined by element-specific soil-water partition coefficients. These water concentrations are used as an interim step in the calculation of tissue concentrations in cattle and game. They are also used for screening-level calculations to determine if potential direct human exposures by surface water ingestion may be of concern.

Groundwater is not an exposure medium *per se*, because the aquifer below the Clive facility is too saline to be used as a drinking water source, and so is classified by the State of Utah as Class IV (nonpotable) in the ground water quality discharge permit for the Clive facility. However, the permit also states that concentrations of contaminants in groundwater will regardless be compared to published GWPLs.

4.3 Exposure Parameters

The basis of the deterministic values and/or statistical distributions for each of the ED equation parameters is discussed in the *Clive PA Model Parameters* white paper , the attached Appendix I, and the spreadsheet *Dose Assessment Appendix II*. A major source of exposure parameter values is the 2009 update to the EPA *Exposure Factors Handbook* (EPA, 2009a). Although this reference exists as an external review draft, it is much more current and extensive than the 1997 version, and much more distributional information is included. For physiological variables in particular, the primary studies that EPA employed as the basis of recommendations in EPA (2009a) were also reviewed.

Three non-residential human receptor scenarios (Rancher, Sport OHV recreationist, and Hunter recreationist) are defined, each with its own set of exposure parameter values but with similar computational exposure models. Exposure parameters that pertain to inter-individual population variability have been assigned to the "inner loop" of the 2D Monte Carlo simulation. These parameters pertain to physiological characteristics, the fraction of time an individual spends on or near the site, and the number of receptors present at the site. These categorizations of inner or outer loop are noted in Section 1.

Exposure parameters related to inter-individually varying population characteristics, and to the number of receptors within the exposure area, are defined within an “inner-loop” sub-container in the ED model. This sub-container has an annual time step so that the stochastic parameters relating to the number of individuals appearing in the exposure area, and the inter-individual characteristics of these individuals, are sampled annually. This sub-container is the "inner loop" of the 2-dimensional Monte Carlo simulation.

The remainder of the exposure parameters, which include the exposure concentrations in environmental media, the DCFs, and a few other parameters, are defined by uncertainty distributions that apply to each individual in the population over the entire 10,000-yr performance period. These parameters, and all components of the contaminant transport model that produce estimates of exposure concentrations over time, are in the "outer loop" of the 2-dimensional Monte Carlo simulation. The uncertainty distributions for stochastic parameters in the outer loop outside this sub-container are sampled only once at the beginning of each model realization.

In the 2-dimensional model, it is assumed that uncertainties are independent for each member of the ranching and recreational scenario populations. The fraction of time that each individual spends on the disposal cell or in the adjacent off-site area is variable. Because the processes that lead to concentration terms in these two areas are different, they have different uncertainty characteristics. This results in independence in the uncertainties of the individual annual dose results.

The inhalation rate distributions activities are specified according to exertion level as heavy, moderate, light, sedentary, and sleeping. For each exertion level, EPA (2009a) provides information for breathing (ventilation) rate and associated fraction of daily time spent at that level. In the absence of scenario-specific information, the fraction of daily time spent at each exertion level for the general population described in EPA (2009a) has been applied to ranching and recreation receptors. Stochastic distributions for the inhalation rates, and also for meat ingestion rates, are tied to the age and (for inhalation rate) gender of an individual receptor, and are specified as a linear function of their body weight as described in EPA (2009a; 2009b). An adult between the ages of 16 and 60 is defined for the ranching and recreation receptor groups.

The behavioral exposure parameters defined in the inner-loop sub-container relate primarily to the fraction of daily and yearly time spent by receptors in the exposure area generally, and within the exposure area the fractional time spent on the embankment versus other locations. Based upon discussion with BLM, Ranchers are assumed to work within a ranching lease during the day and may also camp overnight. Both Sport OHVers riders and Hunters may visit the area for either a day trip or an overnight trip.

4.4 DCFs

The TEDE is not an effect *per se*, but rather a measure of radiation dose absorbed by a tissue. The DCFs used in the ED model account for the biological effectiveness of the radiation (e.g., alpha particles, photons) in causing cellular damage in different tissues, as well as the sensitivity of different tissues to the effects of ionizing radiation. For external dose, this “effective dose” is calculated. For internal dose, the committed effective dose is calculated, which accounts for

continued dose over time from radionuclides retained in the body. Distribution development for uncertainties inherent in DCFs was described previously.

Section 3.3.7 of NUREG-1573 (NRC, 2000) discusses modeling of radiation dose, including internal and external dosimetry. NRC (2000) notes that the performance objectives set forth in Section 61.41 of Title 10 CFR 61.41 (CFR, 2007) are based upon ICRP 2 dose assessment methods, which pre-date the development of TEDE methodology. NRC recommends the use of current ICRP dosimetry employing TEDE methods in lieu of calculation of individual organ doses. The internal and external DCFs used in the ED model were obtained from the electronic database accompanying FGR 13 (EPA, 1999), available online at http://ordose.ornl.gov/downloads.html and also provided in the spreadsheet *Dose Assessment Appendix II*. The DCFs for all species, as well as the individual short-lived progeny of these parent nuclides, were developed using appropriate decay chains and branching fractions as described in the CSM and documented in the electronic attachment.

The DCF for radon-222 and progeny was derived from recommendations provided in an ICRP draft report for consultation (ICRP, 2009). A range of 3 - 6 mSv-m^3/mJ-hr is given for the radon-222 DCF, calculated using ICRP's Human Respiratory Tract Model. The main sources of uncertainty related to this range are the activity size distribution of aerosols for radon progeny, and the breathing rates (ICRP 2009; Appendix B, paragraph B 6).

In paragraph B 11 of Appendix B to ICRP (2009), the inhalation rate for a "standard worker" associated with the upper-end DCF estimate of 6 mSv-m^3/mJ-hr is given as 1.2 m^3/hr. ICRP states,

> "For typical aerosol conditions in home and mines the effective dose is about 3.7 mSv-m^3/mJ-hr. . . However, assuming the same aerosol conditions as for a home but with a breathing rate for a standard worker (1.2 m^3/hr) the effective dose increases from 3.7 to 6 mSv-m^3/mJ-hr."

This indicates that approximately 75% of the range of 3 - 6 mSv-m^3/mJ-hr given for the Rn-222 DCF may be related to inhalation rate. Based upon this observation, a breathing rate normalized radon-222 DCF was calculated for use in the ED model. The units for alpha energy (mJ) were converted to an equivalent activity (Bq) for radon-222 according to units definitions in the glossary of ICRP (2009).

A radon-222 DCF of 2.8×10^{-8} Sv/Bq was calculated as:

$$\text{Radon-222 DCF} = (0.006 \text{ Sv-m3/mJ-hr} \times 5.56 \times 10\text{-}6 \text{ mJ/Bq}) / 1.2 \text{ m3/hr}$$

Not that the REFs discussed earlier are not applicable to radon, as the DCF was estimated in a different fashion than the other species.

4.5 PDCFs

A PDCF is an equation that combines Exposure Parameter values and DCFs, as described in Section 3.3.7.2 of NRC (2000). PDCFs are combined with estimates of radionuclide concentrations in exposure media to calculate a TEDE. PDCF equations for each exposure route are described in subsections below.

4.5.1 Inhalation PDCF Equations

PDCF for inhalation of particulates and gases

$$PDCF\_Inh\ (\text{Sv}\cdot\text{m}^3/\text{Bq}\cdot\text{yr}) = DCF\_Inh \times InhalationRate \times EF \times ET \quad (1)$$

where

DCF_Inh is the inhalation DCF (Sv/Bq)
InhalationRate is the activity-weighted inhalation rate (m^3/hr)
EF is the yearly exposure frequency (d/yr), and
ET is the total daily exposure time (hr/d).

and

$$InhalationRate\ (\text{m}^3/\text{hr}) = \sum_i (Inhal\_act_i \times ET\_frac_i) \quad (2)$$

where

$Inhal\_act_i$ is the inhalation rate for activity level i (m^3/hr), and
ET_frac_i is the fraction of daily exposure time for activity level i (-)

Activity levels (i) for which population-average breathing rates and daily exposure times are defined include sleeping, sedentary activity, light activity, medium activity, and heavy activity. Breathing rates are body weight adjusted. Population distributions of both breathing rates and daily exposure times at different activity levels are defined as functions of age and gender, as described in EPA (2009a).

4.5.2 External PDCF Equations

PDCF for external radiation from soil

$$PDCF\_Ext\_Soil\ (\text{Sv}\cdot\text{g}/\text{Bq}\cdot\text{yr}) = DCF\_Ext \times EF \times ET \times \rho_b \times CF_1 \quad (3)$$

where

DCF_Ext is the external DCF for a 3-dimensional soil source ($Sv\cdot m^3$/Bq·s)
EF is the yearly exposure frequency (d/yr)
ET is the total daily exposure time (hr/d)
ρ_b is the bulk soil density (g/m^3), and
CF_1 is a unit conversion factor (3600 s/hr)

PDCF for external radiation from immersion in air

$$PDCF\_Imm\ (\text{Sv}\cdot\text{m}^3/\text{Bq}\cdot\text{yr}) = DCF\_Imm \times EF \times ET \times CF_1 \quad (4)$$

where

DCF_Imm is the external DCF for air immersion ($Sv\cdot m^3$/Bq·s)
EF is the yearly exposure frequency (d/yr)
ET is the total daily exposure time (hr/d), and
CF_1 is a unit conversion factor (3600 s/hr)

4.5.3 Ingestion PDCF Equations

PDCF for inadvertent ingestion of soil

$$PDCF\_Ing\_Soil\ (\text{Sv}\cdot\text{g/Bq}\cdot\text{yr}) = DCF\_Ing \times SoilIngRate \times EF \times CF_2 \quad (5)$$

where

DCF_Ing is the ingestion DCF (Sv/Bq)
SoilIngRate is the daily soil ingestion rate (mg/day)
EF is the yearly exposure frequency (d/yr), and
CF_2 is a unit conversion factor (0.001 g/mg).

PDCF for ingestion of game meat or beef

$$PDCF\_Ing\_Meat\ (\text{Sv}\cdot\text{g/Bq}\cdot\text{yr}) = DCF\_Ing \times MeatConsumpRate \times (1 - Prep\_loss) \times (1 - PostCook\_loss) \times EF\_food \quad (6)$$

where

DCF_Ing is the ingestion DCF (Sv/Bq)
MeatConsumpRate is the daily consumption rate of beef or game meat (g/kg body weight/d)
Prep_loss is the fractional preparation and cooking loss of consumed meat related to dripping and volatile losses during cooking (-)
PostCook_loss is the fractional post-cooking loss of consumed meat related to trimming, bones, scraps, etc (-)
EF_food is the intrinsic exposure frequency assumed in the time-averaged ingestion rate data (d/yr), and

PDCF for plant ingestion (screening calculation)

$$PDCF\_Ing\_Plant\ (\text{Sv}\cdot\text{g/Bq}\cdot\text{yr}) = DCF\_Ing \times PlantIngRate \quad (7)$$

where

DCF_Ing is the ingestion DCF (Sv/Bq, and
PlantConsumpRate is the yearly consumption rate of wild plants (g/yr)

PDCF for water ingestion (screening calculation)

$$PDCF\_Ing\_Water\ (\text{Sv}\cdot\text{g/Bq}\cdot\text{yr}) = DCF\_Ing \times WaterIngRate \times WatDens \quad (8)$$

where

DCF_Ing is the ingestion DCF (Sv/Bq,
WaterConsumpRate is the yearly consumption rate of standing water (L/yr), and
WatDens is the density of water (g/L)

4.6 TEDE

The calculation of dose, represented here by TEDE, is the product of a PDCF and the exposure concentration. Separate soil concentrations are developed in the contaminant transport model for the disposal cap and the off-site area impacted by deposition of wind-dispersed particles. Particulate air concentrations, which are related to resuspension of soil, and concentrations of gas-phase radionuclides in air, are also calculated separately for these three exposure areas. Other exposure concentrations used in the dose model include radionuclide concentrations in animal tissue, as well as plant tissue and standing surface water in screening calculations.

All TEDE calculations reference the PA model element describing the time after site closure when institutional controls fail and a receptor can gain access to the site. If this time has not been reached in the model realization, ranching and recreation doses are assigned a zero value.

Note that potential embankment gullies are modeled in a preliminary manner in the PA model to evaluate possible consequences given the current waste disposal configuration. Gully formation can be 'switched' on or off by the model user.

4.6.1 Inhalation TEDE Equations

Gas and particulate inhalation TEDE results (mSv/yr) are vectors dimensioned by Species in the PA model related to the inhalation PDCFs. Concentrations of respirable particles and gas-phase radionuclides in air are calculated by methods described in the Atmospheric Modeling white paper. The inhalation TEDE equation for particulate inhalation is:

$$TEDE\_Inh \text{ (mSv/yr)} = PDCF\_Inh \times C_{air} \quad (9)$$

where

$PDCF\_Inh$ is the inhalation PDCF (Sv·m^3/Bq·yr), and
C_{air} is the spatially-averaged air concentration (Bq/m^3)

Exposure concentrations on the embankment are calculated in an area-weighted manner. This calculation presumes that exposures across the embankment occur in a random manner. Air concentrations above the embankment are calculated as:

$$C_{embnk} \text{ (Bq/m}^3\text{)} = \{([C_{cap} \times A_{cap} + C_{gullies} \times A_{gullies}] / [A_{cap} + A_{gullies}]) \quad (10)$$

where

C_{embnk} is the air concentration above the embankment (Bq/m^3)
C_{cap} is the air concentration above the disposal cap (Bq/m^3)
A_{cap} is the area of the embankment cap (m^2)
$C_{gullies}$ is the air concentration above the gullies and associated fans (Bq/m^3)
$A_{gullies}$ is the surface area of the gullies and associated fans (m^2)

The terms $C_{gullies}$ and $A_{gullies}$ are calculated using a model for possible erosive effects of precipitation subsequent to gully initiation due to OHV activity, grazing animals, or other processes.

With respect to ranching and recreation exposure, there are two concentrations terms to address: a concentration term for the embankment (per Equation 10) and a concentration term for the off-

site air dispersion area. A weighted exposure concentration for particulates in ambient air is calculated for these two concentration terms as follows:

$$C_{air\text{-}dust}\ (\text{Bq/m}^3) = \{\ OHV\_timefrac \times OHV\_dust \times (C_{embnk} \times ET\_frac_{embnk}) + (C_{a\text{-}disp} \times [1 - ET\_frac_{embnk}]\ \} + \{\ [\ 1 - OHV\_timefrac] \times (C_{embnk} \times ET\_frac_{embnk}) + (C_{a\text{-}disp} \times [1 - ET\_frac_{embnk}]\ \} \quad (11)$$

where

$OHV\_timefrac$ is the fraction of exposure time spent OHVing (-)
OHV_dust is the off-highway vehicle dust factor, used to account for the contribution of mechanical dust creation (-)
C_{embnk} is the air concentration above the embankment (Bq/m^3)
ET_frac_{embnk} is the fraction of total daily exposure time spent on the embankment (-)
$C_{a\text{-}disp}$ is the air concentration above the air dispersion area (Bq/m^3)

For particulates, C_{embnk} and $C_{a\text{-}disp}$ are calculated using a particle erosion model, which calculates the amount of dust released from the ground surface, and the AERMOD air dispersion model (see the Atmospheric Modeling white paper). Particle erosion is assessed as a function of both wind and mechanical disturbance from the use of OHVs, but the mechanical dust creation factor is applied as a multiplier to the baseline (wind-derived) dust concentration. The AERMOD air dispersion model is used to estimate particulate deposition in the offsite air dispersion area as well as breathing zone concentrations of respirable particles above contaminated soil.

For radon and other gas-phase radionuclides, C_{embnk} and $C_{a\text{-}disp}$ are calculated using AERMOD (see the Atmospheric Modeling white paper) based upon the embankment surface flux computed in the PA model. The air dispersion area is not a definite region with respect to particle definition, because it's size is defined by the size of the receptor exposure area, which varies as described in Section 4.2. Based upon AERMOD calculations, a protective estimate of respirable particle deposition beyond the embankment is assigned to this area. Radon air concentrations in the off-site air dispersion area are calculated as the average across the entire area.

Because mechanical dust generation by OHVs is not an issue for calculating air concentrations of radon and other gas-phase radionuclides, Equation 11 reduces to:

$$C_{air\text{-}gas}\ (\text{Bq/m}^3) = (C_{embnk} \times ET\_frac_{embnk}) + (C_{a\text{-}disp} \times [1 - ET\_frac_{embnk}]) \quad (12)$$

The current version of the PA model does not fully integrate gully formation into the physical model of the embankment. Therefore, Radon air concentrations in the gully are modeled from estimated radium-226 surface soil concentrations on the gully 'floor'. The contribution of radon from disposed waste below this surface soil layer is presently accounted for. Also, the influence of gully walls on radon air concentrations within the gully has not been modeled. For these reasons, gully radon exposures may be underestimated.

4.6.2 External Radiation TEDE Equations

Soil and air immersion external dose results (mSv/yr) are vectors dimensioned by Species in the PA model related to the external PDCFs.

The air immersion external dose equation is:

$$TEDE\_Imm \text{ (mSv/yr)} = PDCF\_Imm \times C_{air} \quad (13)$$

where

PDCF_Imm is the immersion PDCF (Sv·m^3/Bq·yr), and
C_{air} is the spatially-averaged air concentration (Bq/m^3)

The derivation of C_{air} for air immersion is identical to that described in Equations 10, 11 and 12.
The soil external dose equation is:

$$TEDE\_Ext\_Soil \text{ (mSv/yr)} = PDCF\_Ext\_Soil \times C_{soil} \quad (14)$$

where

PDCF_Ext_Soil is the soil ingestion PDCF (Sv·g/Bq·yr), and
C_{soil} is the spatially-averaged soil concentration (Bq/g)

Similar to Equation 8, soil concentrations on the embankment are calculated as:

$$C_{embnk} \text{ (Bq/g)} = \{([C_{cap} \times A_{cap} + C_{gullies} \times A_{gullies}] / [A_{cap} + A_{gullies}]) \quad (15)$$

where

C_{embnk} is the embankment soil concentration (Bq/g)
C_{cap} is the disposal cap soil concentration (Bq/g)
A_{cap} is the area of the disposal cap (m^2)
$C_{gullies}$ is the soil concentration of the gullies and associated fans (Bq/g)
$A_{gullies}$ is the surface area of the gullies and associated fans (m^2)

And analogous to Equation 12, a weighted exposure concentration for embankment and air dispersion area soil is calculated as follows:

$$C_{soil} \text{ (Bq/g)} = (C_{embnk} \times ET\_frac_{embnk}) + (C_{a\text{-}disp} \times [1 - ET\_frac_{embnk}]) \quad (16)$$

where

ET_frac_{embnk} is the fraction of total daily exposure time spent on the embankment (-)
$C_{a\text{-}disp}$ is the soil concentration for the air dispersion area (Bq/g)

4.6.3 Ingestion TEDE Equations

Inadvertent soil ingestion (i.e., via soil on hands, food, etc.) and meat ingestion dose results (mSv/yr) are vectors dimensioned by Species in the PA model related to the ingestion PDCFs.

The soil inadvertent ingestion dose equation is:

$$TEDE\_Ing\_Soil \text{ (mSv/yr)} = PDCF\_Ing\_Soil \times C_{soil} \quad (17)$$

where

PDCF_Ext_Soil is the soil ingestion PDCF (Sv·g/Bq·yr), and
C_{soil} is the spatially-averaged soil concentration (Bq/g)

and, C_{soil} is calculated according to Equation 16.

The meat ingestion dose equation is:

$$TEDE\_Ing\_Meat \text{ (mSv/yr)} = PDCF\_Ing\_Meat \times C_{meat} \quad (18)$$

where

$PDCF\_Ext\_Soil$ is the soil ingestion PDCF (Sv·g/Bq·yr), and
C_{meat} is the concentration in beef or game meat (Bq/g)

The calculation of C_{meat} is based upon grazing models for beef cattle and pronghorn and uses as inputs the soil concentrations C_{embnk} and $C_{a\text{-}disp}$. Both beef cattle and pronghorn may be exposed to soil contamination by direct soil ingestion while grazing, by ingestion of browse plants growing in contaminated soil, and by ingestion of standing water on contaminated soil. Radionuclide concentrations in beef and game tissue are calculated based upon three animal exposure pathways: direct ingestion of soil while browsing, ingestion of plants growing in contaminated soils, and drinking standing surface water. Cattle and pronghorn are assumed to graze randomly across the entire range area. Hence, exposure to radionuclides in the embankment and air dispersion areas is based upon the relative size of these areas.

For soil, exposure concentrations for cattle are calculated as:

$$C_{soil\text{-}cattle} \text{ (Bq/g)} = ([C_{embnk} \times A_{embnk}] + [C_{a\text{-}disp} \times A_{a\text{-}disp}]) / A_{range\text{-}cattle} \quad (19)$$

where

C_{embnk} is the embankment soil concentration (Bq/g)
A_{embnk} is the area of the embankment (m^2)
$C_{a\text{-}disp}$ is the soil concentration for the air dispersion area (Bq/g)
$A_{a\text{-}disp}$ is the surface area of the air dispersion area (m^2), and
$A_{range\text{-}cattle}$ is the size of the cattle range area (m2)

Soil radionuclide exposure concentrations for pronghorn are calculated in an identical manner, substituting the size of the pronghorn grazing area.

Equation 19 is also used to calculate exposure concentrations in browse plants for cattle and pronghorn. However, plant concentrations on the disposal cap are based upon uptake of contamination across the entire root depth profile of the plants. Different types of plants (differentiated by root depth distributions, biomass, and leaf litter production) are employed in the Contaminant Transport model to evaluate transport of radionuclides on the disposal cap. Plant concentrations on the disposal cap are calculated in the contaminant transport portion of the PA model as the weighted average (based upon leaf litter production) of all plants. Soil concentrations in the air dispersion area, and in the gullies and fans, are only calculated for a single surface soil layer. 100% of plant roots are assumed to be situated in this layer.

For standing surface water, exposure concentrations for cattle and pronghorn are calculated for puddles in the air dispersion area. Puddle water concentrations are based upon bulk soil concentrations using element-specific soil water partition coefficients.

Using the exposure concentrations described above, radionuclide concentrations in beef are calculated as:

$$C_{beef}(\text{Bq/g}) = TF\_beef \times (C_{plant\text{-}cattle} \times cattle\_forage) + (C_{soil\text{-}cattle} \times cattle\_soil) + (C_{water\text{-}cattle} \times cattle\_water) \quad (20)$$

where

TF_beef is the amount of an element taken up into muscle tissue as a function of the daily intake rate of that element by the animal. (Bq/g per Bq/d)

$C_{plant\text{-}cattle}$ is the area-weighted plant concentration on the cap, gullies and fans, and air-dispersion area (Bq/g dry wt)

cattle_forage is the dry-weight forage intake rate for browsing cattle (g/day dry wt)

$C_{soil\text{-}cattle}$ is the weighted soil concentration on the embankment and air-dispersion areas (Bq/g)

cattle_soil is the soil ingestion rate for browsing cattle (g/day)

$C_{water\text{-}cattle}$ is the water concentration for the puddles in the air-dispersion areas (Bq/g)

cattle_water is the water ingestion rate for browsing cattle (g/day)

Concentrations in pronghorn tissue (C_{game}) are calculated in a manner analogous to Equation 20, substituting weighted exposure concentrations and intake rates for pronghorn.

Transfer factors (TFs) determine the amount of an element taken up into muscle tissue as a function of the daily intake rate of that element by the animal. The units are expressed as Bq/kg per Bq/d (d/kg). Element-specific beef transfer factors were preferentially obtained from a recent publication of the International Atomic Energy Agency (IAEA, 2010). A report by Pacific Northwest National Laboratory (Staven et al., 2003) was used as a secondary reference. For many elements, these values are reported as a geometric mean and geometric standard deviation. For a subset of elements with only a single reference, an arithmetic mean is provided with no measure of variance. In these cases (actinium, americium, neptunium, protactinium, radium, and technetium), an estimate of variance was produced by taking the average geometric standard deviation for the all other elements excepting plutonium, which was considered an outlier. A summary of the beef TFs with accompanying notes is provided in Table 3.

Distributional form for the values of geometric mean and geometric standard deviation reported in IAEA (2010) was not discussed in this reference. Also, For sample sizes of less than 3, IAEA (2010) values were originally reported as the arithmetic mean and standard deviation. In order to provide a common set of inputs, values obtained from IAEA (2010) and Staven et al. (2003) were processed to conform to an assumed lognormal distribution. Values originally reported as arithmetic mean and standard deviation were transformed to geometric equivalents.

Beef TF data were reported in IAEA (2010) as a geometric mean, geometric standard deviation, minimum, and maximum. The geometric standard deviations are greater than 2 in nearly every case, suggested high right-skewness in the data, and the minimum and maximum were consistent with samples from a lognormal distribution. In order to establish a distribution for the mean, a parametric bootstrap approach was taken [Efron 1998], simulating bootstrap samples from the lognormal distribution using the maximum likelihood estimates of the lognormal parameters. A lognormal distribution was then fit to the resulting bootstrap simulations of the mean, since some right-skewness was still present in the sampling distribution.

Table 3. Beef transfer factors (Bq/kg per Bq/d)

Element	Sample size	Geometric Mean	Geometric Std. Dev.	Notes
Actinium	1	0.0004	generic*	Mean based upon Staven et al. (2003; table 2-6, p. 2.7); no value in IAEA (2010). Geometric standard deviation based upon 6 surrogate elements.
Americium	1	0.0005	generic*	Geometric standard deviation based upon 6 surrogate elements. (IAEA, 2010; table 30, p. 93)
Cesium	58	0.032	1.15	Based upon values provided in IAEA (2010; table 30, p. 93)).
Iodine	5	0.0107	1.85	Based upon values provided in IAEA (2010; table 30, p. 93).
Neptunium	1	0.001	generic*	Mean based upon Staven et al. (2003; table 2.6, p. 2.7); no value in IAEA 2010. Geometric standard deviation based upon surrogate elements.
Protactinium	1	0.0005	generic*	Americium (IAEA 2010 value) used as a surrogate based upon Staven et al. (2003; table 2.6, p. 2.7).
Lead	5	0.000952	1.59	Based upon values provided in IAEA (2010; table 30, p. 93).
Plutonium	5	0.0000128	7.42	Based upon values provided in IAEA (2010; table 30, p. 93).
Radium	1	0.0017	generic*	Geometric standard deviation based upon surrogate elements. (IAEA 2010; table 30, p. 93)
Radon	--	arbitrarily small value	1	Radon gas is inert and has effectively no potential to establish an equilibrium in animal tissue.
Strontium	35	0.00223	1.26	Based upon values provided in IAEA (2010; table 30, p. 93).
Technetium	1	0.0001	generic*	Mean based upon Staven et al. (2003; table 2.6, p. 2.7); no value in IAEA 2010. Geometric standard deviation based upon surrogate elements.
Thorium	6	0.000355	1.68	Based upon values provided in IAEA (2010; table 30, p. 93).
Uranium	3	0.000421	1.32	Based upon values provided in IAEA (2010; table 30, p. 93).

* A generic GSD for these elements is 1.475

5.0 References

BLM (United States Bureau of Land Management) 2010. *Rangeland Administration System*. United States Bureau of Land Management, www.blm.gov/ras.

Bogen K.T., Cullen A.C., Frey H.C., Price P. 2009. Probabilistic exposure analysis for chemical risk characterization. *Toxicological Sciences* 109(1): 4-17.

Brenner D.J., Doll R., Goodhead D.T., et al. 2003. Cancer risks attributable to low doses of ionizing radiation: Assessing what we really know. *Proc. Natl Acad Sci* 100(24): 13761-6.

Burr S.W., Smith J.W., Reiter D., et al. 2008. *Recreational Off-Highway Vehicle Use on Public Lands in Utah*. Utah State University, Institute for Outdoor Recreation and Tourism, Logan UT.

CFR (Code of Federal Regulations). 1994. *National Oil and Hazardous Substances Pollution Contingency Plan,* Code of Federal Regulations 40 CFR 300, US Government Printing Office, Washington, DC.

CFR. 2007. *Licensing Requirements for Land Disposal of Radioactive Waste*, Code of Federal Regulations Title 10, Part 61 (10 CFR 61), US Government Printing Office, Washington, DC.

Davis S., Mirick D.K. 2006. Soil ingestion in children and adults in the same family. *Journal of Exposure Science and Environmental Epidemiology*, 16: 63-75.

Efron B.,Tibshirani R.J. 1998. *Introduction to the Bootstrap*, CRC Press, Boca Raton, FL.

EPA (United States Environmental Protection Agency). 1988. *Limiting Values of Radionuclide Intake and Air Concentration and Dose Conversion Factors for Inhalation, Submersion, and Ingestion*, EPA 520/1-88-020, Federal Guidance Report (FGR) 11, US Environmental Protection Agency, Washington, DC.

EPA. 1989. *Risk Assessment Guidance for Superfund, Volume I: Human Health Evaluation Manual (Part A)*, Interim Final, Office of Emergency and Remedial Response, US Environmental Protection Agency, Washington, DC.

EPA. 1993a. *External Exposure to Radionuclides in Air, Water, and Soil*, EPA 402-R-93-81, Federal Guidance Report (FGR) 12, US Environmental Protection Agency, Washington, DC.

EPA. 1993b. *Wildlife Exposure Factors Handbook*. Vol. I. EPA/600/R-93/187, Office of Research and Development, US Environmental Protection Agency, Washington, DC.

EPA. 1997a, *Establishment of Cleanup Levels for CERCLA Sites with Radioactive Contamination*, Memorandum from Stephen D. Luftig, Director, Office of Emergency and Remedial Response, and Larry Weinstock, Acting Director, Office of Radiation and Indoor Air, to addressees, OSWER No. 9200.4 18, US Environmental Protection Agency, Washington, DC.

EPA. 1997b. *Exposure Factors Handbook*. Office of Research and Development. US Environmental Protection Agency, Washington, DC.

EPA. 1999. *Cancer Risk Coefficients for Environmental Exposure to Radionuclides: Updates and Supplements*, EPA 402-R-99-001, FGR 13, US Environmental Protection Agency, Washington, DC.

EPA. 2000. *National Primary Drinking Water Regulations; Radionuclides; Final Rule*, Federal Register: December 7, 2000 (Volume 65, Number 236)

EPA. 2001, *Risk Assessment Guidance for Superfund (RAGS), Volume III: Process for Conducting Probabilistic Risk Assessment (Part A)*, EPA 540-R-02-002, OSWER 9285.7-45, Office of Emergency and Remedial Response, US Environmental Protection Agency, Washington, DC.

EPA. 2005, *Human Health Risk Assessment Protocol for Hazardous Waste Combustion Facilities, Final*, EPA/530-R-05-006, Office of Solid Waste and Emergency Response, US Environmental Protection Agency, Washington, DC.

EPA. 2008, *Clear Creek Management Area Asbestos Exposure and Human Health Risk Assessment*, US Environmental Protection Agency, Region 9, San Francisco, CA.

EPA. 2009a. *Exposure Factors Handbook*: 2009 Update. External Review Draft, July 2009. Office of Research and Development, National Center for Environmental Assessment, US Environmental Protection Agency, Washington, DC.

EPA. 2009b. *Metabolically Derived Human Ventilation Rates*. May 2009. Office of Research and Development, National Center for Environmental Assessment, US Environmental Protection Agency, Washington, DC.

EPA, 2011a. *Integrated Risk Information System* (IRIS), Office of Research and Development and National Center for Environmental Assessment, Electronic Database. Available online at: http://www.epa.gov/iris/.

Filipsson A.F., Sand S., Nilsson J., et al. 2003. The benchmark dose method- review of available models, and recommendations for application in health risk assessment. *Crit Rev Toxicol* 33:505-542.

GTG (GoldSim Technology Group), 2010. *GoldSim: Monte Carlo Simulation Software for Decision and Risk Analysis*, http://www.goldsim.com

Hamby D.M. 1999. Uncertainty of the tritium dose conversion factor. *Health Phys* 77(3): 291-7.

Harvey R.P., Hamby D.M., Palmer T.S., 2006. Uncertainty of the thyroid dose conversion factor for inhalation intakes of I-131 and its parametric uncertainty. *Radiat Prot Dosimetry* 118(3):296-306.

Hendee W.R., Edwards F.M. 1986. ALARA and an integrated approach to radiation protection. S*eminars in Nuclear Medicine* 16:142-150.

Huffman B. 2004. *Antilocapra americana. Pronghorn*. Ungulate Fact Sheet. http://www.ultimateungulate.com/Artiodactyla/Antilocapra_americana.html.

IAEA (International Atomic Energy Agency). 2010. *Handbook of Values for the Prediction of Radionuclide Transfer in Terrestrial and Freshwater Environments*, International Atomic Energy Agency Technical Report Series No. 472, Vienna.

ICRP, 1977. *Radiation Protection.* International Commission of Radiological Protection Publication No. 26. Permagon, NY.

ICRP. 1979. *Limits for Intakes of Radionuclides by Workers*, International Commission on Radiological Protection Publication No. 30, *Ann. ICRP* 2(3-4).

ICRP. 1983. *Cost-Benefit Analysis in the Optimization of Radiation Protection.* International Commission of Radiological Protection Publication No. 37. Permagon, NY.

ICRP. 1989. *Age-Dependent Doses from Intakes of Radionuclides: Part 1*, International Commission on Radiological Protection Publication No. 56, *Ann. ICRP* 20(2).

ICRP. 1991. *Recommendations of the International Commission on Radiological Protection* I; International Commission on Radiological Protection Publication No. 60. *Ann. ICRP* 21 (1–3)

ICRP. 1995. *Age-Dependent Doses to Members of the Public from Intake of Radionuclides, Part 5: Compilation of Ingestion and Inhalation Dose Coefficients*, International Commission on Radiological Protection Publication No. 72, *Ann. ICRP* 26(1). P 072 errata in SG 03 JAICRP 32 (1-2).

ICRP. 2009. *ICRP Statement on Radon and Lung Cancer Risk from Radon and Progeny*, Draft Report for Consultation, http://www.icrp.org/docs/ICRP_Statement_on_Radon_AND_Lung_cancer_risk_from_radon_and_progeny%28for_consultation%29.pdf.

Kocher D.C., Apostoaei A.I., Hoffman F.O. 2005. Radiation effectiveness factors for use in calculating probability of causation of radiogenic cancers. *Health Phys* 89(1): 3-32.

Linkov I., Burmistrov D. 2001. Reconstruction of doses from radionuclide inhalation for nuclear power plant worker using air concentration measurements and associated uncertainties. *Health Phys* 81(1): 70-75.

MSUE (Michigan State University Extension). 2011. *Agricultural Water Use Reporting.* Michigan State University Extension. Available at web1.msue.msu.edu/waterqual/WQWEB/Beef.doc.

NCRP (National Council on Radiation Protection and Measurements). 1996. *A Guide for Uncertainty Analysis in Dose and Risk Assessments Related to Environmental Contamination*. National Council on Radiation Protection and Measurements Commentary No. 14, Bethesda, MD.

NRC (United States Nuclear Regulatory Commission). 1993. *Final Environmental Impact Statement to Construct and Operate a Facility to Receive, Store, and Dispose of 11e.(2) Byproduct Material Near Clive, Utah,* NUREG 1476, US Nuclear Regulatory Commission, Washington, DC.

NRC. 2000. *A Performance Assessment Methodology for Low-Level Radioactive Waste Disposal Facilities*, NUREG 1573, US Nuclear Regulatory Commission, Washington, DC.

Scott B.R. 2008. It's time for a new low-dose-radiation risk assessment paradigm- one that acknowledges hormesis. *Dose-Response* 6:333-351.

Staven L.H., Napier B.A., Rhoads K., Strenge DL. 2003. *A Compendium of Transfer Factors for Agricultural and Animal Products,* Pacific Northwest National Laboratory, Richland WA.

Tuli J. K., 2005. *Nuclear Wallet Cards, 7th Edition*, Brookhaven National Laboratory, Upton, NY.

UDWR (Utah Division of Wildlife Resources) 2009. *Utah Pronghorn Statewide Management Plan.*, Utah Department of Natural Resources, Salt Lake City UT.

USFS (United States Forest Service), 2005. *Off-Highway Vehicle Recreation in the United States, Regions, and States: A National Report from the National Survey on Recreation and the Environment.* June, 2005. US Forest Service, University of Georgia; Athens GA.

USFWS (United States Fish and Wildlife Service) 2006. *National Survey of Fishing, Hunting, and Wildlife-Associated Recreation: Utah*. US Fish and Wildlife Service, US Department of Commerce, and US Census Bureau; Washington, DC.

Utah 2010. *Standards for Protection Against Radiation*. Utah Administrative Code Rule R313 15. In effect on March 1, 2010. (http://www.rules.utah.gov/publicat/code/r313/r313-015.htm, accessed 17 Mar 2010).

Appendix I: Discussion of Derivations of Selected Parameter Distributions

Distribution development utilized data where available, and exercised professional judgment where it was not available. For the parameter distributions discussed below, unless specified otherwise, the approach followed the *Fitting Probability Distributions* white paper.

- *Age*: Based upon the observed age quantile breakdown reported in USFS (2005) for recreational receptors, ignoring the age groups outside of the defined adult age range 16-60. For simplicity, and because age data specific to ranchers in the vicinity of Clive were unavailable, the same age distribution was also used for rancher receptors. The age range corresponds to bins used to aggregate ventilation rate data by EPA (2009b).
- *Gender*: Based upon the observed percentage in USFS (2005).
- *Body Weight*: EPA (2009a) reports body weights as quantiles, broken down by various age and gender categories. Mean body weight changes gradually with age, and is significantly different between genders. A lognormal distribution was fit for each gender separately, with the log of the geometric mean was fit as a constant, a linear function of age, and a quadratic function of age, using the quantile likelihood fitting described in the *Fitting Probability Distributions* white paper. The quadratic model produced the best fit, capturing the mean decrease in the population for the oldest age group:

$$\mu = \beta_0 + \beta_1 Age + \beta_2 Age^2 \tag{21}$$

where e^{μ} is the geometric mean.

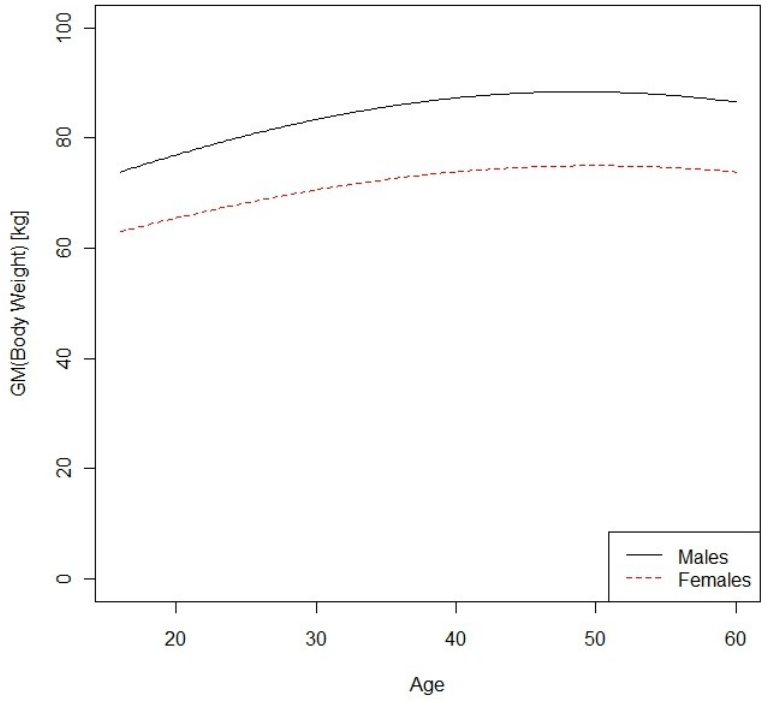

Figure 1. Geometric mean of body weight as a function of age.

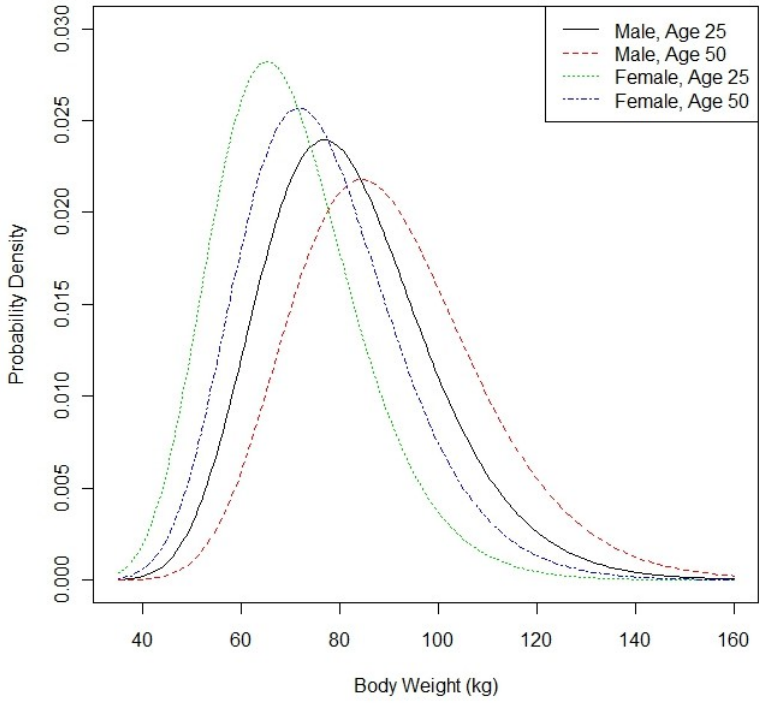

Figure 2. Examples of distributions for body weight.

- *Ventilation Rate*: EPA (2009a) reports inhalation rates as quantiles, broken down by various activity, age, and gender categories. The data are reported as both weight-adjusted and non-weight-adjusted inhalation rates. In order to incorporate correlation in inhalation rates between activity categories, the weight-adjusted data are utilized. That is, a weight-adjusted inhalation rate will be simulated for each activity level, and then the single simulated body weight for the individual is multiplied by the weight-adjusted inhalation rates to obtain the inhalation rates:

$$V_{E,i} = V_{E,i}^{(BW)} \cdot BW \tag{22}$$

where $V_{E,i}$ is inhalation rate for activity level *i* in m^3/min, $V_{E,BW}$ is body-weight adjusted inhalation rate for activity level *i* in m^3/kg-min, and BW is body weight in kg. This approach to constructing inhalation rate is similar to the approach taken in EPA (2009b). Inhalation rate is significantly different between genders, and mean ventilation rate changes gradually with age. A lognormal distribution was fit for each gender separately. The log of the geometric mean was fit as a constant, a linear function of age, and a quadratic function of age; using the quantile likelihood fitting described in the companion white paper *Probability Distribution Development for the Clive PA*. None of these models adequately characterized the data, as the 16-20 age group is significantly

different from the 21-30 age group. As such, the 16-20 age group was fit separately from the remaining data, and a linear fit was adequate for the remaining age ranges.

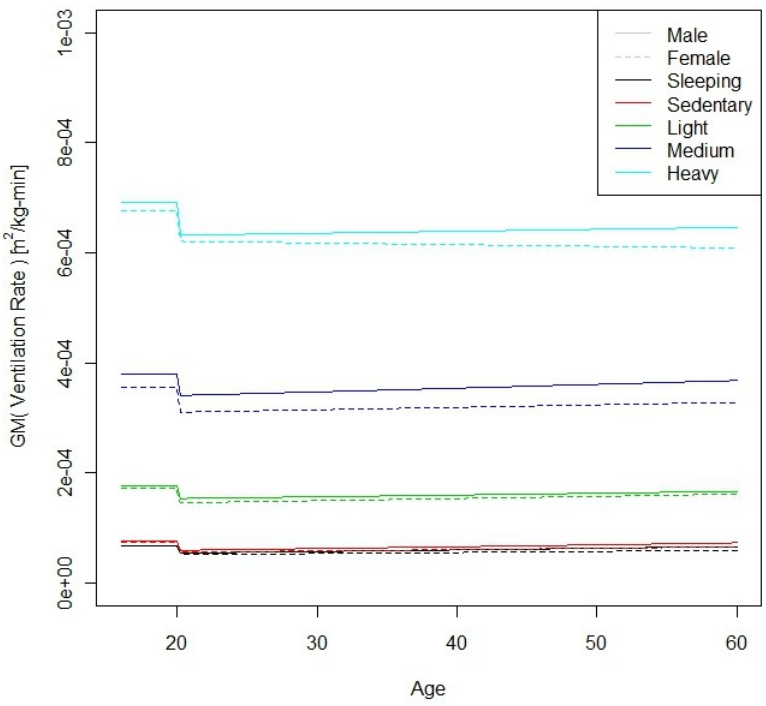

Figure 3. Geometric means for ventilation rate, as a function of age and gender.

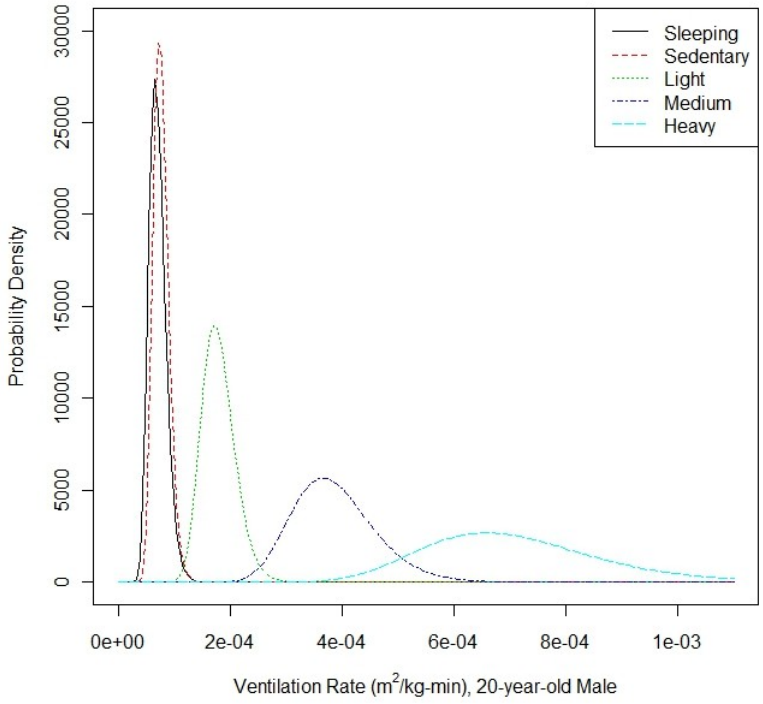

Figure 4. Examples of ventilation rate distributions for different activities (20-year-old male).

- *Soil Ingestion Rate*: EPA (2009a) reports soil ingestion for adults only as a mean, median, and standard deviation. The distribution derived here is based upon the only careful study of adult ingestion that has been conducted to date (Davis and Mirick 2006), identified as a key study in EPA (2009a). Three tracer elements (aluminum, silicon, and titanium) used in Davis and Mirick (2006) provide different bases for quantifying soil ingestion rate. The data distribution is significantly different for the three tracer elements. Thus, rather than combine data across the three tracers, a separate distribution of soil ingestion is established for each tracer. Because there was no significant difference between genders, males and females were combined. Given the significant skew in the data (means much larger than the medians), a lognormal model was fit to the combined data based using maximum likelihood estimates.

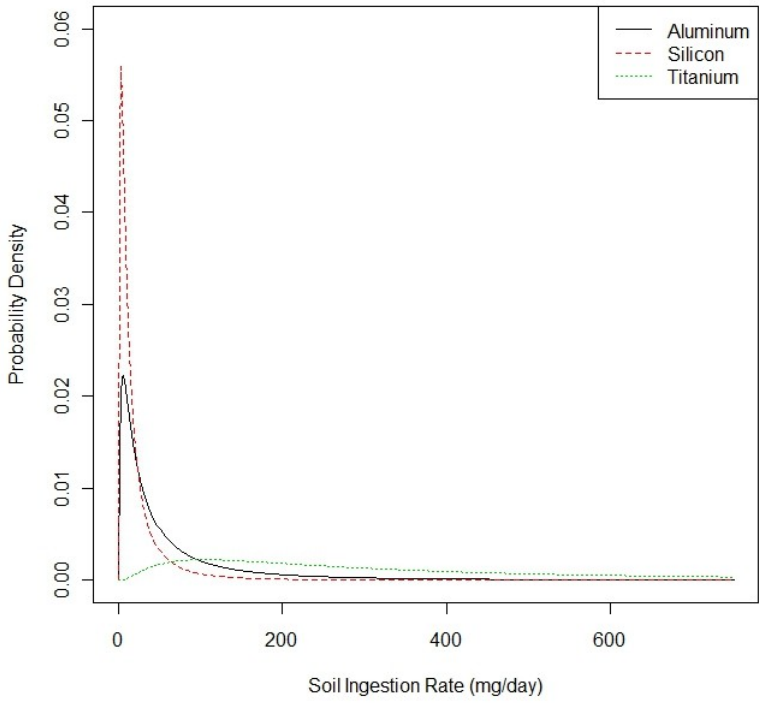

Figure 5. Distributions for soil ingestion, representing different tracers.

- *Ingestion Rates, Home-produced Meat (beef)*: EPA (2009a) reports quantiles of the body-weight-adjusted average intake per day of home-produced meat, broken down by age and type of meat. The age groups given do not correspond perfectly to the range of ages considered in this PA model. Thus, the 20-39 age group was used to represent the 16-39 age group, and the 40-69 age group was used to represent the 40-60 age group. The distributions were significantly different for the two age groups, so they were fit separately. The lognormal distribution provided a good fit to the center of the data, but had poor tail behavior in each case. Thus, a gamma distribution was chosen instead, which provided a better overall fit.

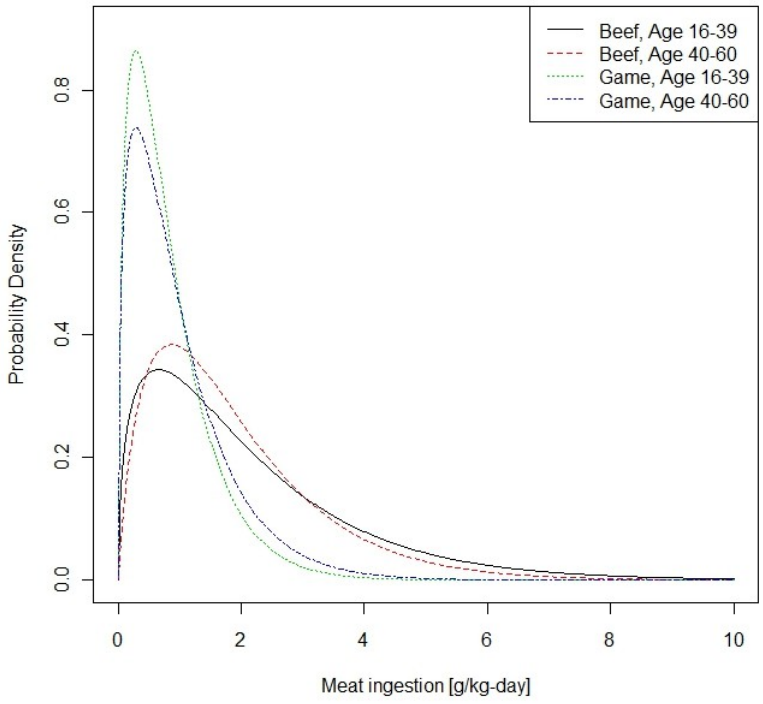

Figure 6. Distributions for home-produced meat ingestion rates.

- *Activity-Based Exposure Time*: EPA (2009a) document reports average time per day spent at different levels of activity as quantiles for adults, broken down by age and gender. The quantiles are reported independently for each activity level, and thus no information regarding the correlation between the times is available. Correlation must exist, as an individual's daily averages must exist on the simplex that sums to 24 hours. Dirichlet distributions are the only standard statistical model that provides a distribution on a simplex. However, Dirichlet distributions could not achieve the long tails observed in the distributions for the more active levels. In order to achieve the tail behavior, the following approach was used. A lognormal model was fitted for combined sleeping and sedentary time (constrained to be no more than 24 hours). Sleeping time alone was also fitted as a lognormal model and constrained to be smaller than combined sleeping and sedentary time. Remaining average time per day was then partitioned into light, medium, and heavy activities. A lognormal distribution was fit to each, but for simulation purposes, the three values are simulated and then normalized to sum to time per day remaining. The resulting distribution induces moderate negative correlation amongst the time spent in each activity level; the greatest negative correlation existing between light and medium activity durations. The tail behavior of medium and heavy activity durations is reduced from that observed in the data (i.e., the upper percentiles are slightly lower than observed).

However, without the detailed correlation structure of the data, a simple model is unlikely to both meet the constraints of the simplex and match the tail behavior.

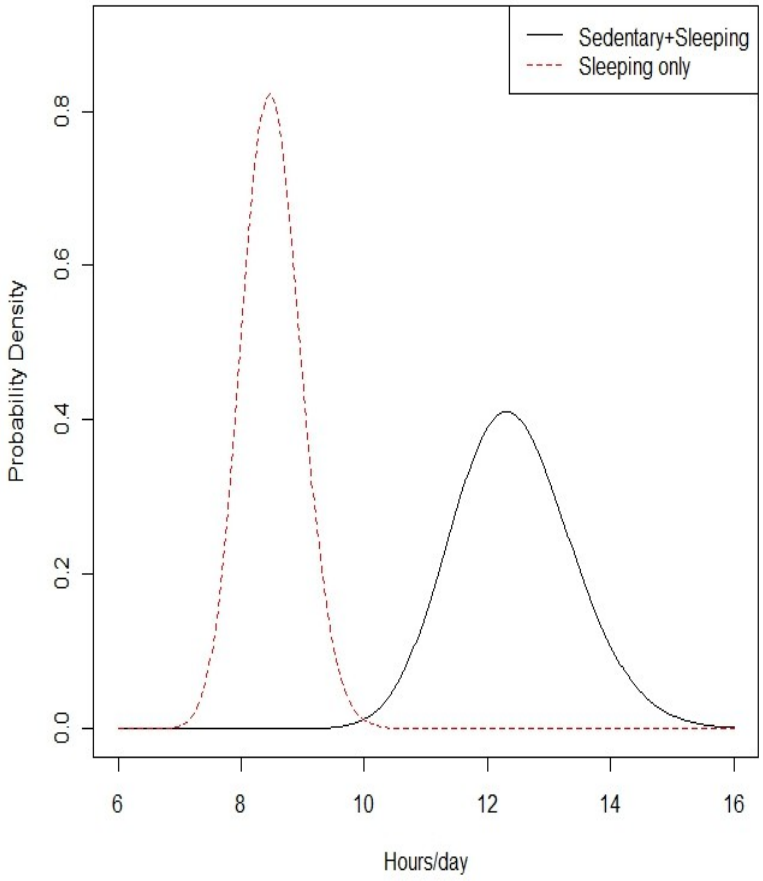

Figure 7. Example distributions for sedentary plus sleeping time/day and sleeping time/day (30-year-old female).

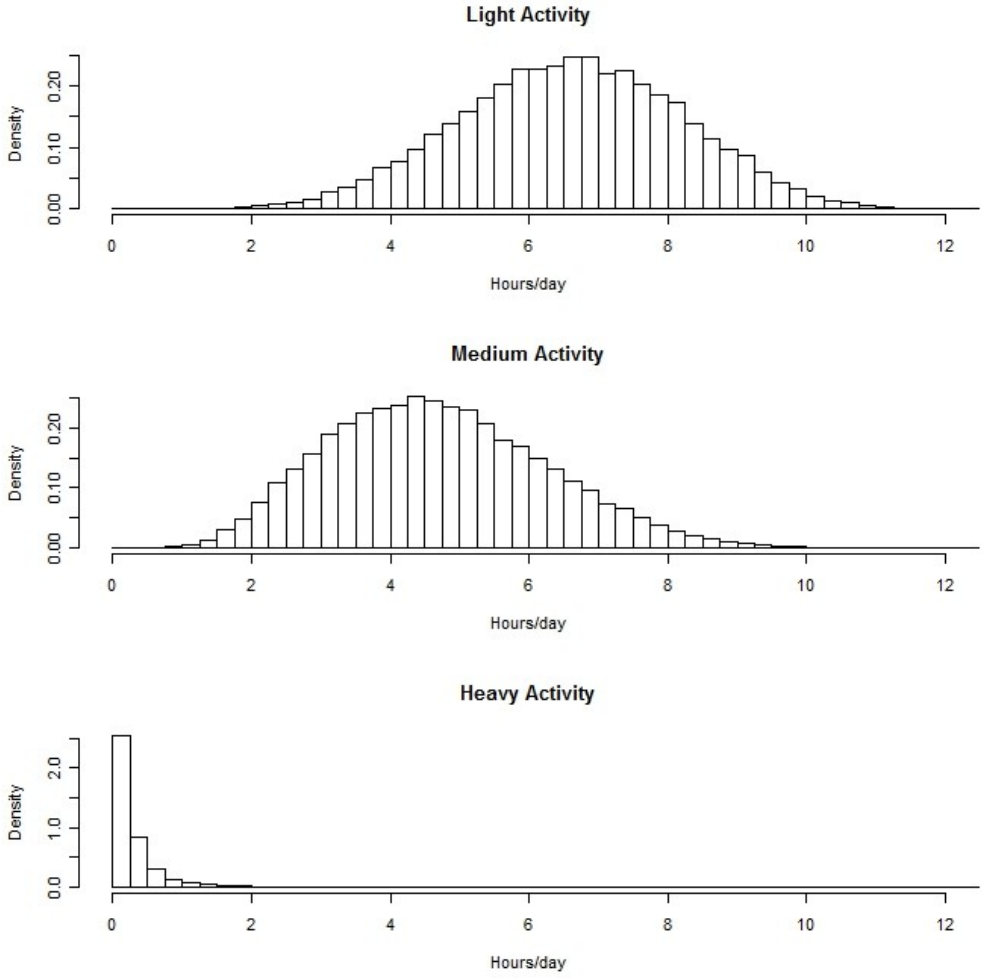

Figure 8. Distributions for light, medium, and heavy activity time/day (30-year-old female).

- *Numbers of Individuals in Vicinity of Site* – Personal communication with BLM staff (Salt Lake Field Office) provided 100 and 500 as bounds and 350 as a best guess. These might be interpreted as 5th and 95th percentiles, along with a mean or median. However, due to the informal nature of the conversation and a programming need to have a fixed upper bound on this distribution, these will be treated as bounds, making a triangular distribution a reasonable representation of the information.

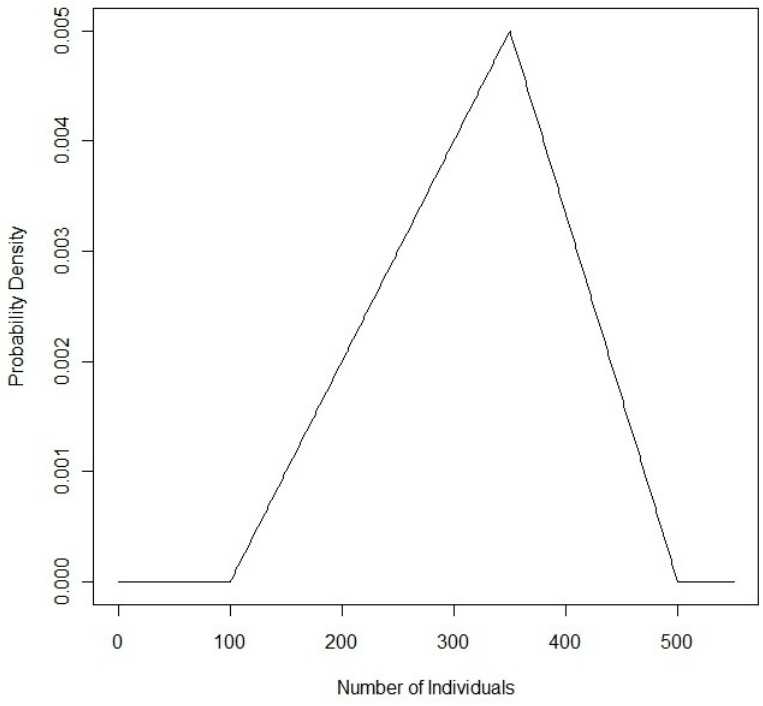

Figure 9. Distribution for the total number of individuals at the site during a given year.

- *Receptor Type* – The individuals in the vicinity of the site are partitioned into Ranchers, Hunters, and Sport OHVers. The distribution for the number of Ranchers was based upon professional judgment and the size of leases, and is independent of the total number of individuals within vicinity of the site. The remaining individuals are then partitioned into Hunters and Sport OHVers by utilizing a binomial distribution with the proportion of hunters equal to 0.25, the value reported from the large survey in USFS (2005).

- *Sport OHVer Day-Trip Time in Area* – The only reported value from the Sport OHVer survey was a mean of 6.3 hr/day. The standard deviation is not reported, so professional judgment was used to choose a standard deviation.

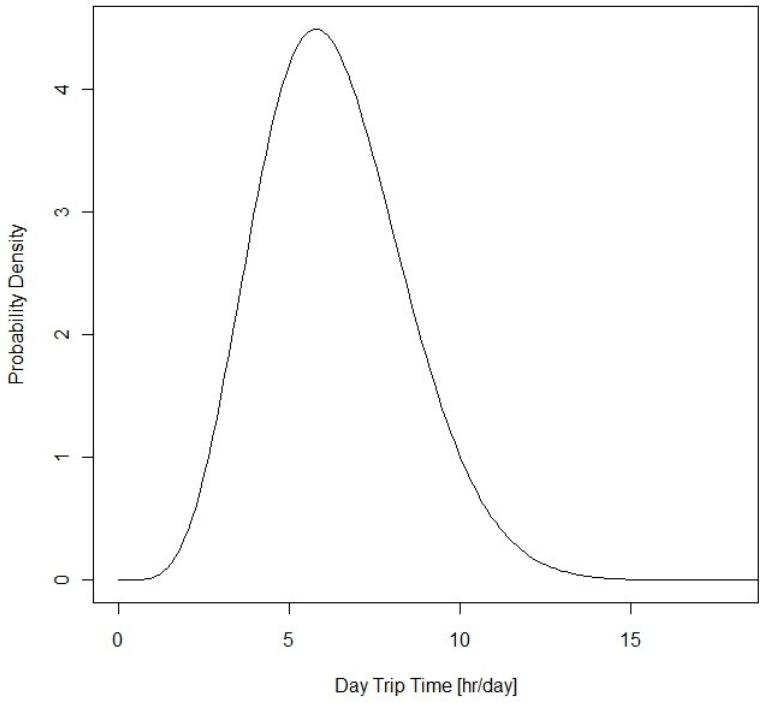

Figure 10. Distribution for the average day-trip time.

- *OHV Dust Loading* – Summary data from EPA (2008) are available both for ambient conditions (CCMA) and near ATV riders. Means are given, and standard errors for the mean can be approximated from the upper confidence limit (UCL) values, by assuming a *t*-UCL. The standard errors are high relative to the mean, so each of these distributions was treated as lognormal. These two distributions were then simulated and a ratio taken, to obtain a distribution on the ratio. The resulting distribution is also approximately lognormal. Figure 11 shows the simulated values, along with the fitted distribution.

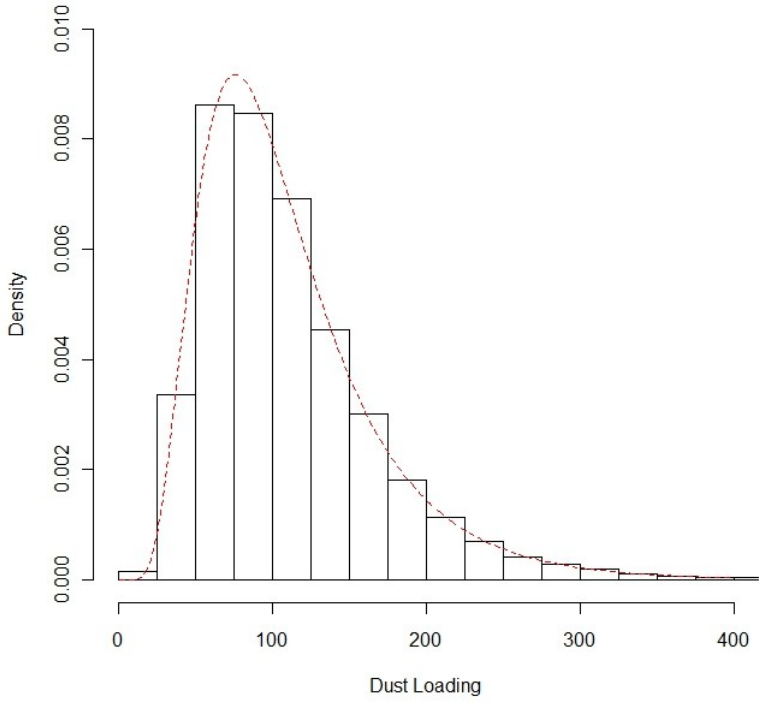

Figure 11. Distribution for dust loading (overlaid on a histogram of simulated values).

- *Rancher Exposure Frequency* – Grazing leases are granted for 180 days each year, giving a natural upper bound for the distribution. There is little other information available to develop a distribution, so professional judgment was used, and a distribution was chosen that has most Ranchers spending a high proportion of the allotted 180 days on site, but allows for Ranchers that spend weekends off-site, do not utilize their full lease, etc.

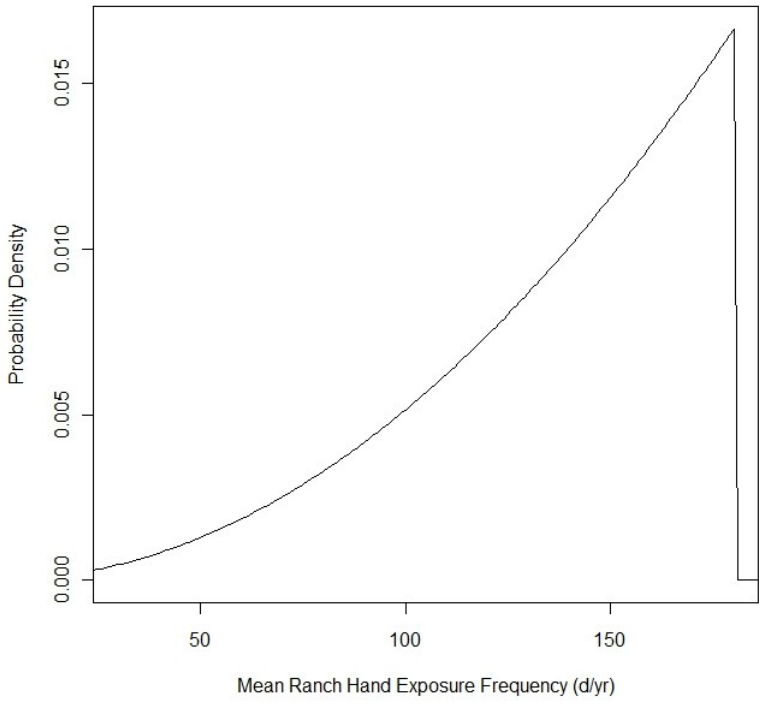

Figure 12. Distribution for Rancher exposure frequency.

- *Sport OHVer Exposure Frequency* – The USFS (2005) document reports a confidence interval for the mean exposure frequency, which can be used to calculate the standard deviation of the exposure frequency. Because the standard deviation is larger than the mean, a lognormal model was used to match the observed mean and standard deviation from the survey data.

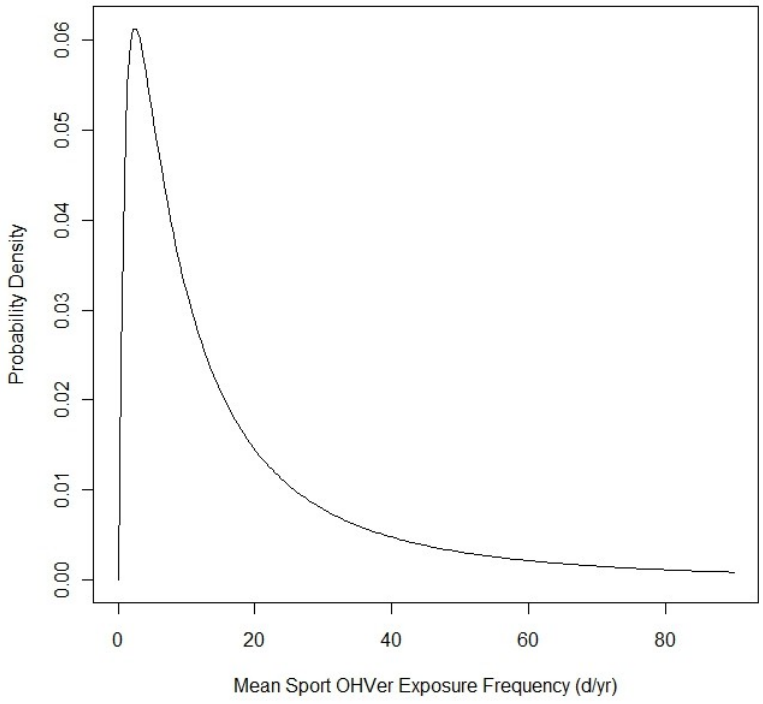

Figure 13. Distribution for Sport OHVer exposure frequency.

- *Hunter Exposure Frequency* – The USFWS (2006) provides a mean estimate of 10 d/yr, but does not provide any other summary information. It may be reasonable to assume that this distribution has a similar shape as the exposure frequency for Sport OHVers; i.e., a right-skewed distribution that has most of the population spending a relatively small amount of time, with a few individuals who dedicate a great deal of time to the activity. Thus, a lognormal distribution was chosen with a mean of 10 d/yr, and a geometric standard deviation that matches the Sport OHVer geometric standard deviation.

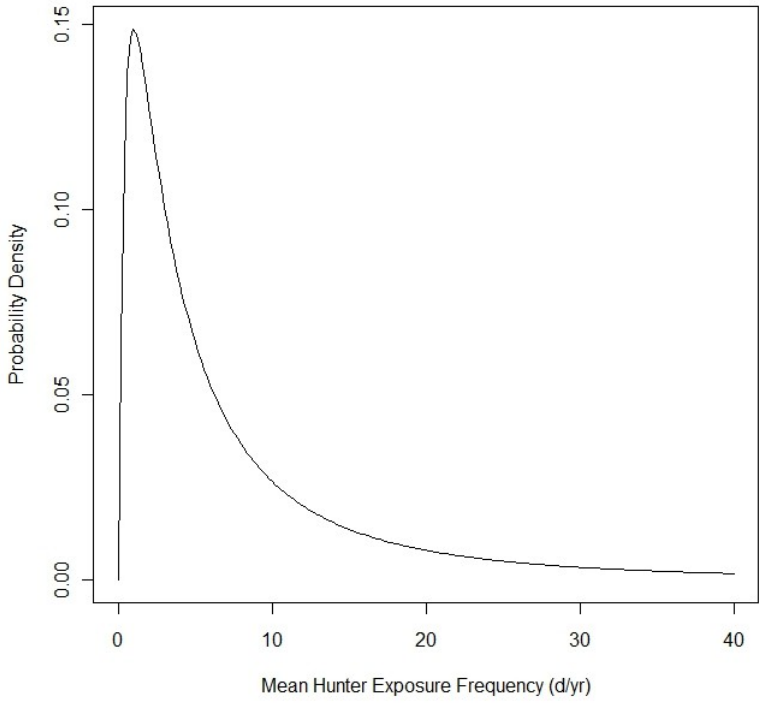

Figure 14. Distribution for Hunter exposure frequency.

- *Rest Area Caretaker Exposure Frequency* – The distribution for this parameter was based on professional judgment. The maximum was conservatively set to the maximum possible exposure of 365 days per year. The mode is set to the EPA default exposure value of 350 days per year, and the minimum allows for 28 days of vacation plus 10 holidays for which the caretaker would be off-site.

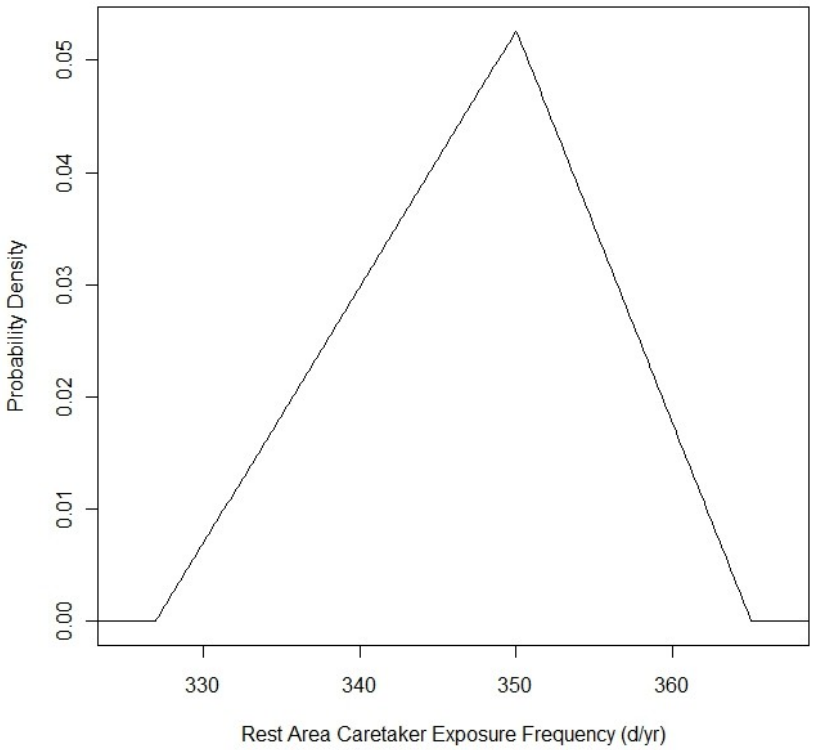

Figure 15. Distribution for rest area caretaker exposure frequency.

- *Meat Loss* – EPA (1997b) provides information on the amount of meat lost in preparation and in post-cooking. An average and a standard deviation are reported for the *mean* loss. As the distribution of interest represents uncertainty about he mean, the average and standard deviation were used for a normal distribution.

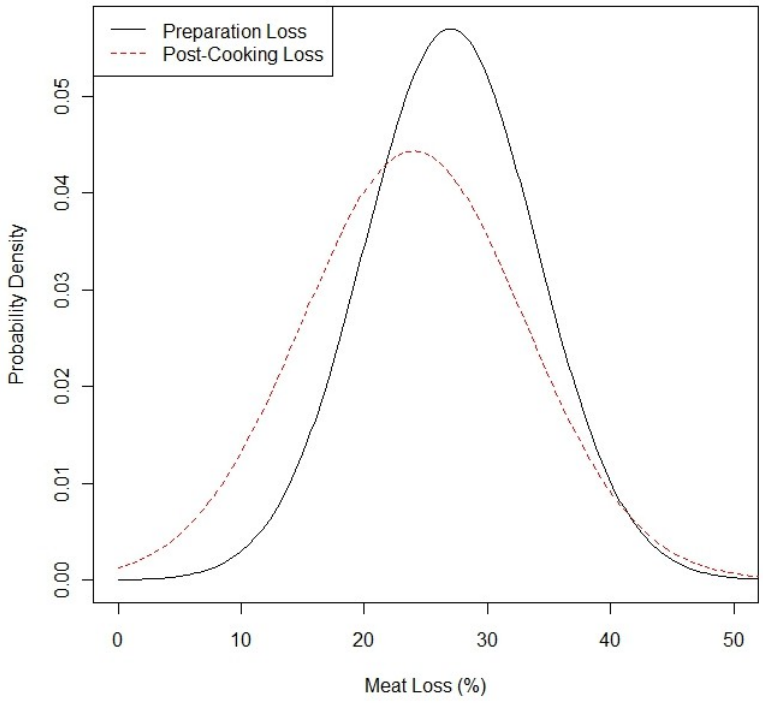

Figure 16. Distributions for meat loss (preparation and post-cooking).

- *Cattle Range Acreage* – There are only four data points available (the four leases in the Clive area), but because the distribution of the mean acreage is desired, the mean and standard error of the mean are used to define a normal distribution.

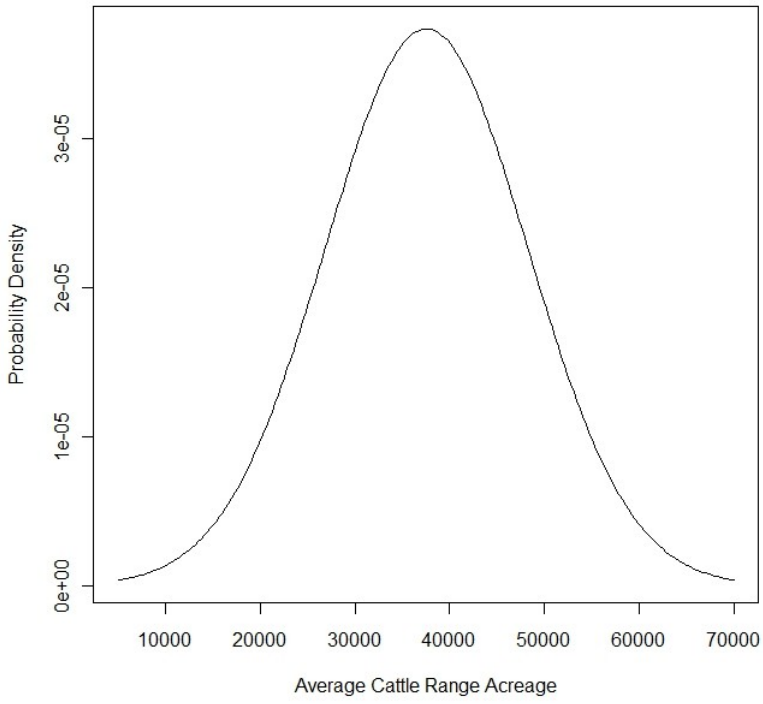

Figure 17. Distribution for the average cattle range acreage.

- *Miscellaneous Uniform Distributions* – For many of the parameters, little information is available that is specific to the Clive facility site. A default distribution in such a case was a uniform distribution over a range of theoretical values, or from the minimum and maximum values found in literature. The uniform distribution is generally a poor representation of uncertainty but has the advantage of spreading its mass across a range of possible values. These uniform distributions are used as defaults until a sensitivity analysis can be performed to demonstrate whether further data collection is needed to construct a better representation of uncertainty.
- *REF Distributions* - Kocher (2005) utilized lognormal distributions to represent the uncertainty in REF parameters. Thus, lognormal distributions were fit to the reported 2.5th, 50th, and 97.5th percentiles of these distributions.

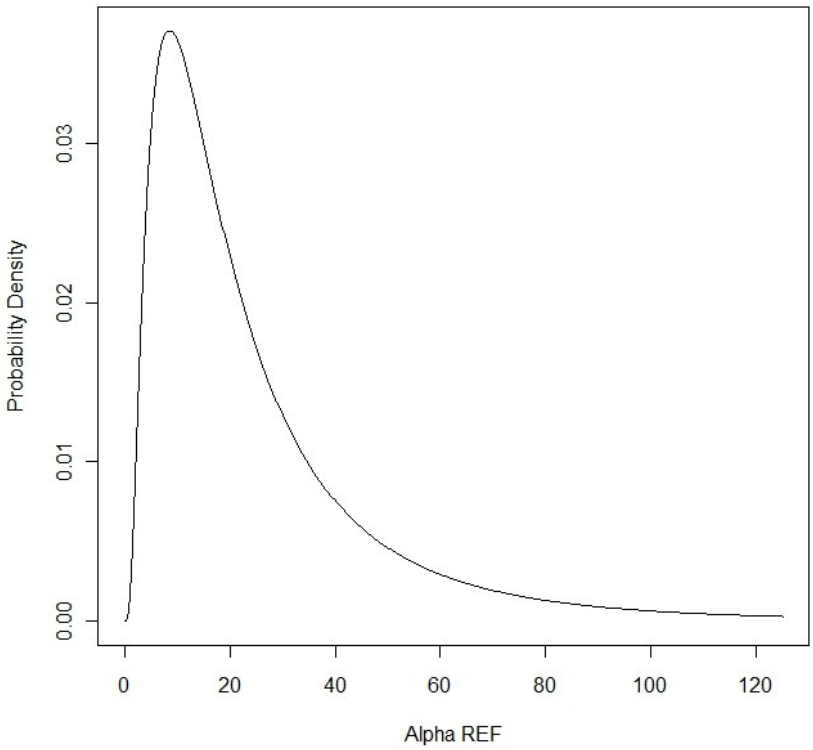

Figure 18. Distribution for alpha particle REF.

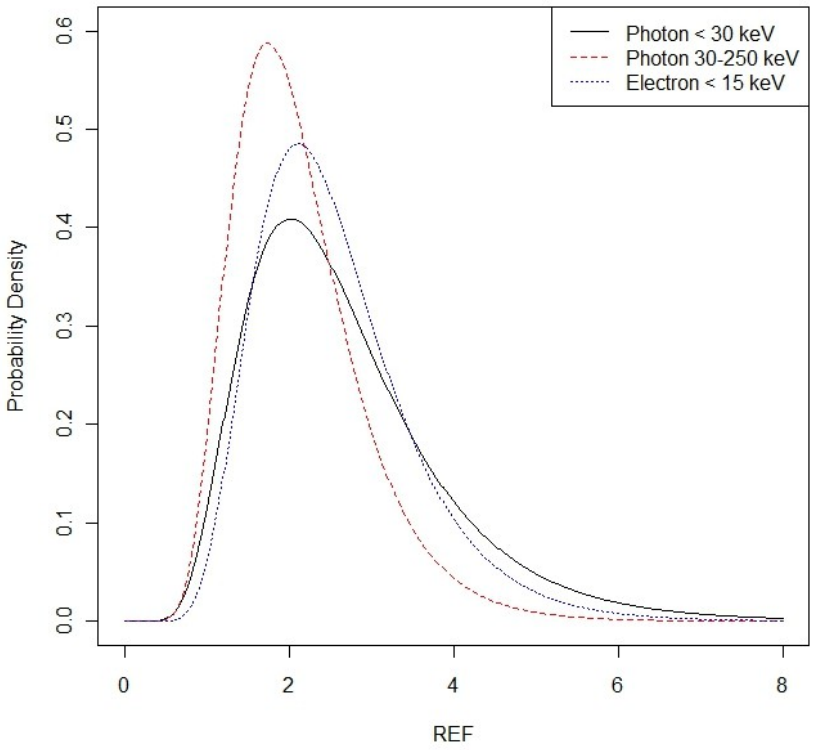

Figure 19. Distribution for electron and photon REFs.

- *Uranium oral reference dose* – EPA has two published values for this value: EPA (2011) and EPA (2000). These two sources are considered equally viable, so each is selected with 50% probability.

This worksheet documents the deterministic DCFs, and the development of inputs to calculate

These DCFs include the contribution of short-lived radioactive daughters (+D) for Species

RADIONUCLIDES (Species)	Inh (particle)	Inh (gas)	Ingestion	External (Immersion)	External (3D)
	Sv/Bq	Sv/Bq	Sv/Bq	(Sv/s)/(Bq/m3)	(Sv/s)/(Bq/m3)
Sr90+D	3.70E-08		3.04E-08	8.91E-16	2.18E-19
Tc99	4.03E-09		6.42E-10	2.87E-17	5.81E-22
I129	3.59E-08	9.59E-08	1.06E-07	2.83E-16	5.14E-20
Cs137+D	4.67E-09		1.36E-08	2.70E-14	1.81E-17
Pb210+D	4.46E-06		9.42E-07	3.03E-16	4.01E-20
Rn222+D	0	2.80E-08	0	1.78E-17	1.17E-20
Ra226	3.46E-06		2.80E-07	2.84E-16	1.56E-19
Ra228+D	2.65E-06		6.97E-07	4.49E-14	3.03E-17
Ac227+D	9.05E-05		4.36E-07	1.74E-14	1.00E-17
Th228+D	4.29E-05		1.43E-07	7.65E-14	5.18E-17
Th229+D	8.49E-05		6.38E-07	1.39E-14	7.88E-18
Th230	1.40E-05		2.14E-07	1.49E-17	5.73E-21
Th232	2.48E-05		2.31E-07	7.27E-18	2.44E-21
Pa231	9.35E-05		4.79E-07	1.57E-15	9.44E-19
U232	7.82E-06		3.36E-07	1.18E-17	4.25E-21
U233	3.55E-06		5.13E-08	1.42E-17	6.77E-21
U234	3.48E-06		4.95E-08	6.13E-18	1.84E-21
U235+D	3.09E-06		4.70E-08	6.94E-15	3.70E-18
U236	3.21E-06		4.69E-08	3.87E-18	9.53E-22
U238+D	2.87E-06		4.79E-08	1.51E-15	6.42E-19
Np237+D	2.27E-05		1.08E-07	9.46E-15	5.41E-18
Pu238	4.62E-05		2.28E-07	3.51E-18	6.25E-22
Pu239	5.01E-05		2.51E-07	3.49E-18	1.41E-21
Pu240	5.02E-05		2.51E-07	3.43E-18	6.03E-22
Pu241	9.01E-07		4.75E-09	6.35E-20	2.84E-23
Pu242	4.76E-05		2.38E-07	2.91E-18	5.32E-22
Am241	4.17E-05		2.04E-07	6.77E-16	1.99E-19

These DCFs for each radionuclide, including short-lived daughters of Species, are used in the GoldSim m

RADIONUCLIDES (DoseSpecies)	inhal absorp type	Inh_particle	Inh_gas	Ingestion	Immersion
Sr90	M	3.56E-08		2.77E-08	9.83E-17
Y90	M	1.39E-09		2.69E-09	7.93E-16
Tc99	M	4.03E-09		6.42E-10	2.87E-17
I129	F	3.59E-08	9.59E-08	1.06E-07	2.83E-16

Cs137	F	4.67E-09		1.36E-08	9.28E-17
Ba137m	M				2.69E-14
Pb210	M	1.10E-06		6.96E-07	4.51E-17
Bi210	M	9.30E-08		1.31E-09	2.58E-16
Po210	M	3.27E-06		1.21E-06	3.89E-19
Rn222	M		2.80E-08		1.78E-17
Po218	M				4.21E-19
Pb214	M	1.36E-08		1.39E-10	1.10E-14
Bi214	M	1.46E-08		1.12E-10	7.25E-14
Po214	M				3.81E-18
Ra226	M	3.46E-06		2.80E-07	2.84E-16
Ra228	M	2.64E-06		6.97E-07	
Ac228	M	1.19E-08		4.01E-10	4.49E-14
Ac227	M	7.28E-05		3.23E-07	5.13E-18
Th227	S	1.04E-05		9.02E-09	4.44E-15
Fr223	M	1.04E-08		2.36E-09	2.21E-15
Ra223	M	7.44E-06		1.04E-07	5.48E-15
Rn219	M				2.46E-15
Po215	M				7.80E-18
Pb211	M	1.11E-08		1.78E-10	2.59E-15
Bi211	M				2.04E-15
Tl207	M				4.53E-16
Th228	S	3.97E-05		7.20E-08	8.13E-17
Ra224	M	2.97E-06		6.45E-08	4.30E-16
Rn220	M				1.72E-17
Po216	M				7.75E-19
Pb212	M	1.72E-07		5.98E-09	6.26E-15
Bi212	M	3.08E-08		2.59E-10	8.96E-15
Po212	M				
Tl208	M				1.69E-13
Th229	S	7.12E-05		5.00E-07	3.37E-15
Ra225	M	6.26E-06		9.95E-08	2.41E-16
Ac225	M	7.39E-06		3.85E-08	6.38E-16
Fr221	M				1.33E-15
At217	M				1.37E-17
Bi213	M	2.98E-08		1.98E-10	6.17E-15
Po213	M				
Tl209	M				9.66E-14
Pb209	M	5.64E-11		5.67E-11	1.00E-16
Th230	S	1.40E-05		2.14E-07	1.49E-17
Th232	S	2.48E-05		2.31E-07	7.27E-18
Pa231	M	9.35E-05		4.79E-07	1.57E-15
U232	M	7.82E-06		3.36E-07	1.18E-17
U233	M	3.55E-06		5.13E-08	1.42E-17

U234	M	3.48E-06	4.95E-08	6.13E-18
U235	M	3.09E-06	4.67E-08	6.48E-15
Th231	S	3.34E-10	3.36E-10	4.59E-16
U236	M	3.21E-06	4.69E-08	3.87E-18
U238	M	2.86E-06	4.45E-08	2.51E-18
Th234	S	7.69E-09	3.40E-09	2.95E-16
Pa234m	M			1.21E-15
Np237	M	2.27E-05	1.07E-07	8.90E-16
Pa233	M	3.33E-09	8.78E-10	8.57E-15
Pu238	M	4.62E-05	2.28E-07	3.51E-18
Pu239	M	5.01E-05	2.51E-07	3.49E-18
Pu240	M	5.02E-05	2.51E-07	3.43E-18
Pu241	M	9.01E-07	4.75E-09	6.35E-20
Pu242	M	4.76E-05	2.38E-07	2.91E-18
Am241	M	4.17E-05	2.04E-07	6.77E-16

stochastic DCFs, for the GoldSim Performance Assessment model for the Clive, UT disposal site.

Development of distributions for internal and external REFs for use in the G

Nuclide	Branching Fraction	Dominant Decay Mode (internal)	Mean Energy; internal (MeV)
Sr90	*1*	electron	0.196
Y90	*1*	electron	0.935
Sr90+D			
Tc99		electron	0.101
I129		electron	0.0489
Cs137	*1*	electron	0.187
Ba137m	*1*	photon	0.662
Cs137+D			
Pb210	*1*	electron	0.0335
Bi210	*1*	electron	0.389
Po210	*1*	alpha	
Pb210+D			
Rn222	*1*	not used	
Po218	*1*	not used	
Pb214	*1*	not used	
Bi214	*1*	not used	
Po214	*1*	not used	
Rn222+D		alpha	
Ra226		alpha	
Ra228	*1*	electron	0.00987
Ac228	*1*	photon	0.771
Ra228+D			
Ac227	*1*	alpha	
Th227	*0.9862*	alpha	
Fr223	*0.0138*	electron	0.343
Ra223	*1*	alpha	
Rn219	*1*	alpha	
Po215	*1*	alpha	
Pb211	*1*	electron	0.453
Bi211	*1*	alpha	
Tl207	*1*	electron	0.493
Ac227+D			
Th228	*1*	alpha	
Ra224	*1*	alpha	

nodel.

External
3.46E-21
2.15E-19
5.81E-22
5.14E-20

4.47E-21		***Rn220***	*1*	alpha	
1.81E-17		***Po216***	*1*	alpha	
1.06E-20		***Pb212***	*1*	photon	0.241
2.92E-20		***Bi212***	*1*	alpha	
2.64E-22		***Po212***	*0.6406*	alpha	
1.17E-20		***Tl208***	*0.3594*	photon	1.46
2.85E-22	***Th228+D***				
6.65E-18		***Th229***	*1*	alpha	
4.99E-17		***Ra225***	*1*	electron	0.094
2.59E-21		***Ac225***	*1*	alpha	
1.56E-19		***Fr221***	*1*	alpha	
		At217	*1*	alpha	
3.03E-17		***Bi213***	*1*	alpha	
2.40E-21		***Po213***	*0.9791*	alpha	
2.57E-18		***Tl209***	*0.0209*	photon	0.773
9.71E-19		***Pb209***	*1*	electron	0.198
2.96E-18	***Th229+D***				
1.53E-18	***Th230***			alpha	
5.06E-21	***Th232***			alpha	
1.56E-18	***Pa231***			alpha	
1.27E-18	***U232***			alpha	
1.23E-19	***U233***			alpha	
3.85E-20	***U234***			alpha	
2.53E-19		***U235***	*1*	alpha	
1.15E-20		***Th231***	*1*	electron	0.0771
5.26E-22	***U235+D***				
3.46E-18	***U236***			alpha	
5.96E-18		***U238***	*1*	alpha	
		Th234	*1*	electron	0.043
1.17E-16		***Pa234m***	*1*	electron	0.819
1.55E-18	***U238+D***				
4.63E-20		***Np237***	*1*	alpha	
3.09E-19		***Pa233***	*1*	photon	0.302
7.56E-19	***Np237+D***				
8.86E-21	***Pu238***			alpha	
3.83E-18	***Pu239***			alpha	
	Pu240			alpha	
6.56E-17	***Pu241***			electron	0.00524
4.04E-21	***Pu242***			alpha	
5.73E-21	***Am241***			alpha	
2.44E-21					
9.44E-19	Branching fractions based on Tuli (2005). Half lives from Chart of the Nucl				
4.25E-21	Default inhalation absorption type from Table 2.1 of FGR 13. I assumed M				
6.77E-21	Dominant decay mode [gamma + x-ray; MAX(beta, IC electrons, auger elec				

1.84E-21
3.53E-18
1.72E-19
9.53E-22
4.27E-22
1.14E-19
5.28E-19
3.73E-19
5.04E-18
6.25E-22
1.41E-21
6.03E-22
2.84E-23
5.32E-22
1.99E-19

RADON-222: Radon inhalation DCF (cell W27) is calculated based on the

FGR13 DCFs	key
Inh F S	Inhalation DCF; Fast lung absorption (particle); Solid tur
Inh M S	Inhalation DCF; Medium lung absorption (particle); Soli
Inh S S	Inhalation DCF; Slow lung absorption (particle); Solid tu
Inh V S	Inhalation DCF; Vapor phase nuclide; Solid tumor
Ing S	Ingestion DCF; Solid tumor (for polonium, this applies to
Ing Ins S	Ingestion DCF; Solid tumor (specific to the insoluble (in
Ext S S	External DCF; Submersion; Solid tumor
Ext GP S	External DCF; 2-D Ground Plane; Solid tumor (infinite a
Ext SV S	External DCF; 3-D Soil Volume; Solid tumor (infinite ar

REF distributions (Kocher et al, 2005 Tables 14 and 15; fitted means by M Fitzgeral

	geo mean	geoSD	LN(
alpha	18.13	3.368	;
beta (<0.015 MeV)	2.415	1.438	)
photon (>0.03 and <=0.25 MeV)	1.935	1.426	
photon (<=0.03)	2.451	1.535	

oldSim model is documented here for each DoseSpecies…

REF distribution (internal DCF)	Dominant Decay Mode (external)	Mean Energy; external (MeV)	REF distribution (external DCF)	half-life (yr)	default inhal absorp type
none	electron	0.196	none	28.78	M
none	photon	0.0155	LN(2.451; 1.535)	0.0073011	none
none	electron	0.101	none	2.13E+05	M
none	photon	0.028	LN(2.451; 1.535)	1.57E+07	F
none	electron	0.187	none	30.07	F
none	photon	0.662	none	4.85E-06	none
none	photon	0.0124	LN(2.451; 1.535)	22.3	M
none	electron	0.389	none	0.0137252	none
LN(18.13; 3.368)	photon	0.802	none	0.3788632	M
	photon	0.510	none	0.010468	none
	photon	0.837	none	5.89E-06	none
	photon	0.333	none	5.10E-05	M
	photon	1.12	none	3.78E-05	none
	photon	0.797	none	5.21E-12	none
LN(18.13; 3.368)					
LN(18.13; 3.368)	photon	0.186	LN(1.935; 1.426)	1599	M
LN(2.415; 1.438)	photon	0.00667	LN(2.451; 1.535)	5.76	M
none	photon	0.771	none	7.02E-04	none
LN(18.13; 3.368)	photon	0.0159	LN(2.451; 1.535)	21.772	none
LN(18.13; 3.368)	photon	0.202	LN(1.935; 1.426)	0.051254	S
none	photon	0.0911	LN(1.935; 1.426)	4.18E-05	none
LN(18.13; 3.368)	photon	0.25	LN(1.935; 1.426)	0.0313082	M
LN(18.13; 3.368)	photon	0.323	none	1.25E-07	none
LN(18.13; 3.368)	photon	0.439	none	5.64E-11	none
none	photon	0.595	none	6.86E-05	M
LN(18.13; 3.368)	photon	0.351	none	4.07E-06	none
none	photon	0.885	none	9.07E-06	none
LN(18.13; 3.368)	photon	0.115	LN(1.935; 1.426)	1.912	S
LN(18.13; 3.368)	photon	0.242	LN(1.935; 1.426)	0.0100208	M

LN(18.13; 3.368)	photon	0.550	none	1.76E-06	none
LN(18.13; 3.368)	photon	0.806	none	4.59E-09	none
LN(1.935; 1.426)	photon	0.241	LN(1.935; 1.426)	0.0012138	M
LN(18.13; 3.368)	photon	0.858	none	1.15E-04	none
LN(18.13; 3.368)	none			9.47E-15	none
none	photon	1.46	none	5.80E-06	none
LN(18.13; 3.368)	photon	0.047	LN(1.935; 1.426)	7.34E+03	S
none	photon	0.040	LN(1.935; 1.426)	0.0407951	M
LN(18.13; 3.368)	photon	0.128	LN(1.935; 1.426)	0.0273793	none
LN(18.13; 3.368)	photon	0.218	LN(1.935; 1.426)	9.32E-06	none
LN(18.13; 3.368)	photon	0.472	none	1.01E-09	none
LN(18.13; 3.368)	photon	0.450	none	8.67E-05	none
LN(18.13; 3.368)	none			1.16E-13	none
none	photon	0.773	none	4.11E-06	none
none	electron	0.198	none	3.71E-04	M
LN(18.13; 3.368)	photon	0.0146	LN(2.451; 1.535)	7.54E+04	S
LN(18.13; 3.368)	photon	0.0146	LN(2.451; 1.535)	1.40E+10	S
LN(18.13; 3.368)	photon	0.164	LN(1.935; 1.426)	3.28E+04	none
LN(18.13; 3.368)	photon	0.0154	LN(2.451; 1.535)	69.8	M
LN(18.13; 3.368)	photon	0.0159	LN(2.451; 1.535)	1.59E+05	M
LN(18.13; 3.368)	photon	0.0154	LN(2.451; 1.535)	246000	M
LN(18.13; 3.368)	photon	0.177	LN(1.935; 1.426)	7.04E+08	M
none	photon	0.0170	LN(2.451; 1.535)	0.0029113	S
LN(18.13; 3.368)	photon	0.0153	LN(2.451; 1.535)	2.34E+07	M
LN(18.13; 3.368)	photon	0.0153	LN(2.451; 1.535)	4.47E+09	M
none	photon	0.0813	LN(1.935; 1.426)	0.065984	S
none	photon	0.928	none	2.22E-06	none
LN(18.13; 3.368)	photon	0.0233	LN(2.451; 1.535)	2.14E+06	M
none	photon	0.302	none	7.38E-02	none
LN(18.13; 3.368)	photon	0.0556	LN(1.935; 1.426)	87.7	M
LN(18.13; 3.368)	photon	0.0163	LN(2.451; 1.535)	2.41E+04	M
LN(18.13; 3.368)	photon	0.0161	LN(2.451; 1.535)	6.56E+03	M
LN(2.415; 1.438)	photon	0.0289	LN(2.451; 1.535)	14.4	M
LN(18.13; 3.368)	photon	0.0161	LN(2.451; 1.535)	3.75E+05	M
LN(18.13; 3.368)	photon	0.0164	LN(2.451; 1.535)	432.7	M

ides, 16th edition, Knoll's Atomic Power Laboratory (2002).

class if there was no information in Table 2.1. Selected inhalation DCFs shown by heavy cell border.

ctrons); alpha] based on highest contribution to total energy emitted (MeV/nt) of these 3 groups from RadSum3

methodology described in the comment field attached to that cell.

ıor
d tumor
ımor

ɔ a soluble (organic) form)
organic) form of polonium)

ırea source)
ea and depth source)

d 8/4/2010)

FGR 13 DCFs copied from workbook "DCF conversions QAed Rev 1.xlsx", worksheet 'FGR 13 D
(see key to FGR 13 DCF headers below)

Sv/Bq	Sv/Bq	Sv/Bq	Sv/Bq	Sv/Bq	Sv/Bq	(Sv/s)/(Bq/m3)	(Sv/s)/(Bq/m2)
Inh F S	***Inh M S***	***Inh S S***	***Inh V S***	***Ing S***	***Ing Ins S***	***Ext S S***	***Ext GP S***
2.39E-08	3.56E-08	1.57E-07		2.77E-08		9.83E-17	1.64E-18
5.36E-10	1.39E-09	1.50E-09		2.69E-09		7.93E-16	1.10E-16
2.44E-08	3.70E-08	1.59E-07		3.04E-08		8.91E-16	1.12E-16
2.86E-10	4.03E-09	1.33E-08		6.42E-10		2.87E-17	6.49E-20
3.59E-08	1.50E-08	9.82E-09	9.59E-08	1.06E-07		2.83E-16	1.96E-17
4.67E-09	9.69E-09	3.92E-08		1.36E-08		9.28E-17	2.99E-18
						2.69E-14	5.78E-16
4.67E-09	9.69E-09	3.92E-08		1.36E-08		2.70E-14	5.81E-16
9.07E-07	1.10E-06	5.61E-06		6.96E-07		4.51E-17	2.13E-18
1.07E-09	9.30E-08	1.33E-07		1.31E-09		2.58E-16	3.51E-17
6.09E-07	3.27E-06	4.27E-06		1.21E-06	2.45E-07	3.89E-19	8.07E-21
1.52E-06	4.46E-06	1.00E-05		9.42E-07	2.45E-07	3.03E-16	3.72E-17
						1.78E-17	3.82E-19
						4.21E-19	8.64E-21
2.92E-09	1.36E-08	1.47E-08		1.39E-10		1.10E-14	2.40E-16
7.23E-09	1.46E-08	1.54E-08		1.12E-10		7.25E-14	1.44E-15
						3.81E-18	7.91E-20
			2.80E-08			8.35E-14	1.68E-15
3.59E-07	3.46E-06	9.51E-06		2.80E-07		2.84E-16	6.11E-18
9.07E-07	2.64E-06	1.60E-05		6.97E-07			
1.19E-08	1.19E-08	1.46E-08		4.01E-10		4.49E-14	9.38E-16
9.19E-07	2.65E-06	1.60E-05		6.97E-07		4.49E-14	9.38E-16
1.56E-04	7.28E-05	5.53E-05		3.23E-07		5.13E-18	1.41E-19
6.69E-07	8.42E-06	1.04E-05		9.02E-09		4.44E-15	9.81E-17
8.97E-10	1.04E-08	1.21E-08		2.36E-09		2.21E-15	7.76E-17
1.25E-07	7.44E-06	8.68E-06		1.04E-07		5.48E-15	1.21E-16
						2.46E-15	5.28E-17
						7.80E-18	1.68E-19
3.88E-09	1.11E-08	1.20E-08		1.78E-10		2.59E-15	9.49E-17
						2.04E-15	4.40E-17
						4.53E-16	5.56E-17
1.57E-04	9.05E-05	7.42E-05		4.36E-07		1.74E-14	4.66E-16
2.96E-05	3.20E-05	3.97E-05		7.20E-08		8.13E-17	2.13E-18
7.59E-08	2.97E-06	3.36E-06		6.45E-08		4.30E-16	9.15E-18

						1.72E-17	3.69E-19
						7.75E-19	1.61E-20
1.80E-08	1.72E-07	1.90E-07		5.98E-09		6.26E-15	1.35E-16
9.04E-09	3.08E-08	3.32E-08		2.59E-10		8.96E-15	2.25E-16
						1.69E-13	2.97E-15
2.97E-05	4.29E-05	4.33E-05		1.43E-07		7.65E-14	1.44E-15
2.39E-04	1.08E-04	7.12E-05		5.00E-07		3.37E-15	7.90E-17
1.29E-07	6.26E-06	7.73E-06		9.95E-08		2.41E-16	1.07E-17
7.97E-07	7.39E-06	8.49E-06		3.85E-08		6.38E-16	1.47E-17
						1.33E-15	2.84E-17
						1.37E-17	2.92E-19
1.05E-08	2.98E-08	3.20E-08		1.98E-10		6.17E-15	1.68E-16
						9.66E-14	1.92E-15
1.73E-11	5.64E-11	6.10E-11		5.67E-11		1.00E-16	3.19E-18
2.40E-04	8.49E-05	8.75E-05		6.38E-07		1.39E-14	3.44E-16
1.02E-04	4.28E-05	1.40E-05		2.14E-07		1.49E-17	6.37E-19
1.10E-04	4.54E-05	2.48E-05		2.31E-07		7.27E-18	4.55E-19
2.30E-04	9.35E-05	2.89E-05		4.79E-07		1.57E-15	3.78E-17
4.05E-06	7.82E-06	3.70E-05		3.36E-07		1.18E-17	8.08E-19
5.80E-07	3.55E-06	9.59E-06		5.13E-08		1.42E-17	6.00E-19
5.59E-07	3.48E-06	9.40E-06		4.95E-08		6.13E-18	5.86E-19
5.21E-07	3.09E-06	8.47E-06		4.67E-08		6.48E-15	1.40E-16
7.86E-11	3.11E-10	3.34E-10		3.36E-10		4.59E-16	1.56E-17
5.21E-07	3.09E-06	8.47E-06		4.70E-08		6.94E-15	1.56E-16
5.30E-07	3.21E-06	8.74E-06		4.69E-08		3.87E-18	5.03E-19
5.02E-07	2.86E-06	8.04E-06		4.45E-08		2.51E-18	4.24E-19
2.49E-09	6.63E-09	7.69E-09		3.40E-09		2.95E-16	7.50E-18
						1.21E-15	1.08E-16
5.04E-07	2.87E-06	8.05E-06		4.79E-08		1.51E-15	1.16E-16
4.97E-05	2.27E-05	1.19E-05		1.07E-07		8.90E-16	2.52E-17
1.03E-09	3.33E-09	3.86E-09		8.78E-10		8.57E-15	1.86E-16
4.97E-05	2.27E-05	1.19E-05		1.08E-07		9.46E-15	2.11E-16
1.08E-04	4.62E-05	1.61E-05		2.28E-07		3.51E-18	6.26E-19
1.19E-04	5.01E-05	1.60E-05		2.51E-07		3.49E-18	2.84E-19
1.19E-04	5.02E-05	1.61E-05		2.51E-07		3.43E-18	6.01E-19
2.29E-06	9.01E-07	1.75E-07		4.75E-09		6.35E-20	1.72E-21
1.13E-04	4.76E-05	1.50E-05		2.38E-07		2.91E-18	4.98E-19
9.64E-05	4.17E-05	1.60E-05		2.04E-07		6.77E-16	2.33E-17

32 software (ICRP38, K Eckerman, http://ordose.ornl.gov/downloads.html).

)CFs'

(Sv/s)/(Bq /m3)

Ext SV S
3.46E-21
2.15E-19
2.18E-19
5.81E-22
5.14E-20
4.47E-21
1.81E-17
1.81E-17
1.06E-20
2.92E-20
2.64E-22
4.01E-20
1.17E-20
2.85E-22
6.65E-18
4.99E-17
2.59E-21
5.66E-17
1.56E-19
3.03E-17
3.03E-17
2.40E-21
2.57E-18
9.71E-19
2.96E-18
1.53E-18
5.06E-21
1.56E-18
1.27E-18
1.23E-19
1.00E-17
3.85E-20
2.53E-19

1.15E-20
5.26E-22
3.46E-18
5.96E-18
1.17E-16
5.18E-17
1.55E-18
4.63E-20
3.09E-19
7.56E-19
8.86E-21
3.83E-18
6.56E-17
4.04E-21
7.88E-18
5.73E-21
2.44E-21
9.44E-19
4.25E-21
6.77E-21
1.84E-21
3.53E-18
1.72E-19
3.70E-18
9.53E-22
4.27E-22
1.14E-19
5.28E-19
6.42E-19
3.73E-19
5.04E-18
5.41E-18
6.25E-22
1.41E-21
6.03E-22
2.84E-23
5.32E-22
1.99E-19

Neptune and Company Inc.

June 1, 2011 Report for EnergySolutions

Clive DU PA Model, version 1

Appendix 12

Decision Analysis (ALARA)

Decision Analysis Methodology for Assessing ALARA Collective Radiation Doses and Risks

30 May 2011

Prepared by

Neptune and Company, Inc.

This page is intentionally blank, aside from this statement.

CONTENTS

1 Introduction

The safe storage and disposal of depleted uranium (DU) waste is essential for mitigating releases of radioactive materials and reducing exposures to humans and the environment. Currently, a radioactive waste facility located in Clive, Utah (the "Clive facility") operated by the company Energy*Solutions* Inc. is being considered to receive and store DU waste that has been declared surplus from radiological facilities across the nation. The Clive facility has been tasked with disposing of the DU waste in a manner that protects humans from future radiological releases.

To assess whether the proposed Clive facility location and containment technologies are suitable for protection of human health, specific performance objectives for land disposal of radioactive waste set forth in Title 10 of the Code of Federal Regulations (CFR) Part 61 (10 CFR 61) Subpart C, and promulgated by the Nuclear Regulatory Commission (NRC), must be met. In order to support the required radiological performance assessment (PA), a detailed computer model will be developed to evaluate the doses to human receptors that would result from the disposal of DU and its associated radioactive compounds (collectively termed "DU waste"), and conversely to determine how much DU waste can be safely disposed at the Clive facility.

The Neptune and Company, Inc. (Neptune) white papers "Conceptual Site Model [CSM] for Disposal of Depleted Uranium at the Clive Facility" and "Exposure and Dose Documentation" detail background, issues, and methods for estimating radiation doses to future human receptors associated with DU and its decay products. The NRC specifies a clear performance goal (25 mrem/yr) that is germane to individual members of the public (MOP). This goal is the result of a complex balance of risk and feasibility, and is not specifically addressed here as it is (at present and in a practical sense) inflexible and non-negotiable.

However, the CFR (Section 61.42) also defines a second decision rule that pertains to populations as well as individuals. The regulation states "reasonable effort should be made to maintain releases of radioactivity in effluents to the general environment as low as is reasonably achievable" (or ALARA). Ionizing radiation protection limits have been utilized since the 1920s, but the concept of keeping radiation doses as low as practicable or achievable was an outgrowth of worker safety in the nuclear weapons development industry (Hendee and Edwards, 1987). The ALARA concept can be applied to either individuals or populations. In the context of the Clive DU PA, ALARA is applied to collective doses germane to the receptor populations described in the "Exposure and Dose Documentation" white paper.

The ALARA process is also described in DOE regulations and associated guidance documents such as 10 CFR Part 834 and DOE 5400.5 ALARA (10 CFR 834; DOE 1993, 1997), and in other NRC documents (NRC, 1995, 2000). The definitions in each case are very similar; indicating that exposures should be controlled so that releases of radioactive material to the environment are as low as is reasonable taking into account social, technical, economic, practical, and public policy considerations. It is also noted that ALARA is not a dose limit, but rather a process which has the objective of attaining doses as far below the applicable limit of this part as is reasonably achievable.

Unfortunately, the words "reasonably" and "achievable" in ALARA are not precise. The two words imply some degree of consideration of tradeoffs, but no clear definition is published.

Assuming that there are trade-offs, then this implies that an analysis should be performed that explicitly evaluates the trade-offs and how different disposal options, designs, or sites may differentially satisfy the objectives and resource constraints (e.g., a decision or economic analysis). Yet, at present, there is limited specific guidance on how to apply ALARA principles to the PA process.

The probabilistic Clive DU PA model is designed to estimate individual annual doses to hypothetical individuals in future populations that may be exposed to radionuclide releases from the Clive facility. The model is also able to aggregate individual doses into estimates of collective and cumulative population dose, on an annual basis as well as over the 10,000 year period of performance. Additionally, the model is able to evaluate non-radiological toxicity; e.g. associated with uranium. The remainder of this discussion will focus upon the concepts of population dose/risk and ALARA, and how these can be integrated into a Bayesian decision analysis (DA) for application to the Clive facility.

2 ALARA

The modern ALARA concept, as germane to radiation protection for both individual and population (collective) levels, was described by the ICRP in 1977 (ICRP, 1977):

> "Most decisions about human activities are based on an implicit form of balancing of costs and benefits leading to the conclusion that the conduct of a chosen practice is 'worthwhile.' Less generally, it is also recognized that the conduct of the chosen practice should be adjusted to maximize the benefit to the individual or to society. In radiation protection, it is becoming possible to formalize these broad decision-making procedures."

The ICRP (1977) basically recommended a system of radiation protection that included the following principles:

- No practice shall be adopted unless its introduction produces a positive net benefit – *justification of the practice*.
- All exposures shall be kept as low as reasonably achievable, economic and social factors being taken into account – *optimization of radiation protection*.
- The dose equivalent to individuals shall not exceed the limits recommended for the appropriate circumstances by the Commission – *the limits of individual dose assessment*.

In other words, ICRP defined radiation protection in the context of decision analysis, at least in terms of the first two principles, considering health, economic, and social objectives; and invoked the concept of net benefit. The third principle can, instead, be interpreted as a compliance objective, so that the decision analysis can only be performed for decision options that first comply with regulatory performance objectives.

The ALARA process is also described in DOE regulations and associated guidance documents such as 10 CFR Part 834 and DOE 5400.5 ALARA (10 CFR 834; DOE 1993, 1997), and in various NRC documents such as NRC, 1995, 2000. The definitions in each case are very similar;

indicating that exposures should be controlled so that releases of radioactive material to the environment are as low as is reasonable taking into account social, technical, economic, practical, and public policy considerations. 10 CFR 834 further describes the ALARA process as a "logical procedure for evaluating alternative operations, processes, and other measures, for reducing exposures to radiation and emissions of radioactive material into the environment, taking into account societal, environmental, technological, economic, practical and public policy considerations to make a judgment concerning the optimum level of public health protection". Although 10 CFR 834 is not aimed specifically at disposal of radioactive waste, the basic goals are protection of the public from DOE activities, of which radioactive waste disposal is one such activity.

NRC also provides guidance on application of the principle of ALARA. For example, although the context is different, 10 CFR Part 20 provides guidance that suggests – "Reasonably achievable" is judged by considering the state of technology and the economics of improvements in relation to all the benefits from these improvements (NRC Regulatory Guide 8.8, Revision 3, 2008). NRC also notes that "...a comprehensive consideration of risks and benefits will include risks from non-radiological hazards".

The overall implication of the various Agency regulations and guidance documents regarding ALARA is that many factors should be taken into account when considering the potential benefits of different options for disposal of radioactive waste. In order to implement ALARA in a logical system, and so that economic factors are taken into consideration, a decision analysis is implied. Decision analysis is the appropriate mechanism for evaluating and optimizing disposal, closure and long term monitoring and maintenance of a radioactive waste disposal system. Decision options for disposal at Clive might include engineering options and waste placement. More generally, if decision analysis is applied, then a much wider range of options can be factored into the decision model, such as transportation of waste, risk to workers, and effect on the environment. However, for the current Clive DU PA, the focus is on different options for waste disposal within the current proposed configuration of the Class A South embankment.

The decision analysis in this context is essentially a benefit-cost analysis, within which different options for the placement of waste are evaluated. For each option, the PA model predicts doses to the array of receptors, and the consequences of those doses are assessed as part of an overall cost model, which also includes the costs of disposal of waste for each option. The goal is to find the best option, which is the option that provides the greatest overall benefit. The consequences of risk can be measured through a simplification that is available in ALARA guidance, including NRC 1995, which provides the basis for, and history of, assigning a dollar value to person-rem as a measure of radiation dose. Prior to the NRC guidance, a single value of $1,000 per person-rem was recommended, with the accompanying assumption that a discount rate would not be applied. The history of the selection of this value is described in NRC, 1995, and further references to prior documents. In 1995, NRC instead promoted the idea of using $2,000 per person-rem as the relevant value, subject to present worth considerations. This appears to be an overt attempt by the NRC to allow an economic decision analysis to be performed, allowing for a discount factor to be used in the assessment of ALARA. This is made clearer in NRC, 2000, which provides examples and formulas for how to implement ALARA, which include discount factors of 7% for the first 100 years, and 3% thereafter. These are steep discounting rates that result in small costs

comparatively at 100 years into the future. DOE guidance also suggests that a range of $1,000 to $6,000 could be considered (DOE, 1997), but that the $2,000 value is sufficient for most purposes. The allowable range presented by DOE, however, could be used to describe uncertainty over the appropriate value.

In assigning a value to the person-rem cost to society of radiation dose, the Agency's have short-circuited a full decision analysis. This is reasonable for a first pass at a decision analysis associated with the Clive DU PA. Hence, the value of $2,000 will be applied, as described below. Prior to describing the specific application, a more generic discussion of decision analysis is provided.

3 Decision Analysis

A generic process for decision analysis has been described in many references, and includes the following basic steps (cf., Berry, 1995, Clemen, 1996):

1. State a problem
2. Identify objectives (and measures of those objectives – i.e., attributes or criteria)
3. Identify decision alternatives or options
4. Gather relevant information, decompose and model the problem (structure, uncertainty, preferences)
5. Choose the 'best' alternative (the option that maximizes the overall benefit)
6. Conduct uncertainty analysis, sensitivity analysis and value of information analysis to determine if the decision should be made, or if more data/information should be collected to reduce uncertainty and, hence, increase confidence in the decision
7. Go back if more data/information are collected

This framework is iterative and flexible; e.g., sensitivity analysis can also be performed before choosing alternatives. Value-of-information analysis can be performed to help determine where further data collection will be most informative. In the case of ALARA as described in Section 2, the only disposal and design options that can be considered are those that first demonstrate compliance. If no options are identified that comply after the first pass through the decision analysis, then it might be necessary to redefine the options, or the problem. In this sense, the decision analysis process is constrained.

Generally, in a decision analysis, there are many considerations for successful applications ranging from identifying the decision makers and stakeholders, the objectives of interest for all parties involved in the decision making process, their preference structures (which attributes of the decision problem do they prefer), characterization of uncertainty in the model, and measures of the probable consequences of the different decision options. The spatial and temporal constraints on the decision are also important.

There are many technical approaches that have been used to provide some form of numerical decision support for a wide variety of decision problems (cf., Kiker et al, 2005, Linkov et al, 2009), however, only one is commonly recognized as rational and logical: Bayesian statistical decision theory, although other names have been used. The main components of Bayesian decision analysis include probability distributions that are used to capture what is known and

uncertainty about the underlying process, and specification of cost and value functions to capture the costs of each decision option that is being considered.

For an ALARA analysis of a PA, implementation of a Bayesian decision analysis requires development of a PA model for different options (e.g., different disposal options, closure options). This includes specification of probability distributions for each input parameter in the PA model so that both the best estimate and its uncertainty is accounted for, subsequent estimation of population doses from the model, and characterization of the costs of implementing each option. The cost-benefit trade-off is performed by comparing options for the risks to human health (as measured through dose), and the costs of each option considered.

In general, Bayesian decision analysis is a powerful means of facilitating decisions under uncertainty. Decision analysis models, developed properly, are transparent and easy to use, even for complex decisions. Decision analysis is also amenable to sensitivity and value-of-information analyses, which can be used to inform decision makers regarding uncertainty in the decision. That is, if the uncertainty is low enough, then confidence is high enough, and a decision can be made. However, if greater confidence is needed, then further data collection is indicated, and this is informed by the sensitivity analysis and a value of information analysis (i.e., which variables are most uncertain and have the most influence on ranking of alternatives). The idea is the reduce uncertainty cost-effectively. At some point the cost of collecting more data outweighs the benefit from the reduction in uncertainty. Then the best decision option should be selected.

4 Scope of ALARA Decision Analysis for the Clive Depleted Uranium Performance Assessment

Decision analysis in the context of ALARA is simplified for the current version of the Clive DU PA. There is one primary objective, which is to maximize human health in the context of disposal of the DU waste. The attribute of interest is dose to the receptors, which is measured in terms of millirem in a year. Note that groundwater concentrations are also of concern, but a simplification similar to the dose costs per person rem are not available for groundwater, hence, the groundwater pathway is not evaluated for this version of the Clive DU PA Model. Groundwater concentrations could be accommodated in a more complete decision analysis, however, it is also noted that groundwater at Clive is not potable, and is more saline than seawater, and, hence, has no real use. The cost consequences to human health are, consequently, negligible or non-existant.

Three decision options will be evaluated. These all assume the same basic engineered design for the Class A South embankment, but the waste is placed differently in each case. The different placement results in different dose estimates for the three types of receptors evaluated – ranchers, hunters and OHV enthusiasts. The options include 3 m of fill material under the cap prior to the first layer of DU waste, 5 m of fill and 10 m of fill. These are fully described in the *Embankment Modeling* white paper.

Assuming the cost of disposal is the same for each configuration (which might not be the case, but is a simplifying assumptions that is made for this purpose), then the differentiating factor is the cost associated with the radiation risk – i.e., the dose costs. The PA model is constructed to present both doses to hypothetical individuals and to the populations of those individuals, as described in the "Exposure and Dose Assessment" white paper. Consequently, the population

doses can be summed and presented by year. Dose costs can be associated with those population doses, with or without a discounting factor.

The is the extent of ALARA analysis that will be performed for the current Version of the Clive DU PA. Extensions that include the costs of disposal, and the varying costs for different engineered designs or waste disposal configurations can be completed for future versions.

Note also, that the evaluation that will be presented sets the stage for a relatively simple optimization of the disposal configuration for the DU waste included in the model. The engineered design includes 27 layers, each about 0.5 m in thickness, in which DU waste can be disposed. Placing the waste away from the bottom layers decreases groundwater concentrations, and placing the waste lower in the system decreases the doses. There is a middle ground in which both groundwater concentrations and doses comply with performance objectives. A reasonable goal is to place the waste optimally with respect to human health using the dose metric and ALARA principles, and groundwater concentration compliance requirements.

In terms of application of a discounting factor, it should be noted that DU has a characteristic that is different than most forms of radioactive waste; i.e., its decay dynamics result in higher radioactivity (and therefore dose) of the waste over time, as opposed to lower radioactivity associated with many other types of radionuclide decay. This perhaps has implications for whether to include a discounting factor for future benefits, risks, and costs. Population doses will be presented, and a dollar multiplier attached both with and without a discounting factor.

The overall decision scenario can be stated as in terms of the ‘best’ alternatives with regard to long-term disposal of DU. As a first application, the decision analysis focuses on the “best” alternatives for achieving ALARA with respect to future population doses/risks at the Clive facility. The decision analysis is presented in terms of the disposal site itself, and does not address other potentially important life-cycle issues such as interim storage, transportation, etc. However, note that the decision analysis framework could be easily expanded to address these other issues. For this decision analysis 'best' is defined in terms of overall benefit-cost in the context of the cost to reduce risk, the cost consequences of the risk, and the uncertainty associated with choosing the best option. That is, the decision problem is framed as a benefit-cost problem, but constrained by the requirement that each decision option considered must comply with the performance objectives.

Most of the inputs to the PA model are specified with uncertainty. As previously mentioned, uncertainty in the output can be evaluated to assess whether the decision can be made, or if more information might be warranted. Sensitivity analyses can determine which variables contribute most to this uncertainty, and value of information analysis can determine the 'value', in dollars, of uncertainty reduction (Morgan and Henrion, 1990, Claxton, 1999). This approach to model evaluation can be used to guide further data collection if the degree of overall uncertainty makes the decision difficult. The sensitivity analysis methods described in the “Sensitivity Analysis” white paper will be applied to the results of this simplified ALARA analysis.

5 Dose Assessment

For present purposes, as regulatory agencies have adopted and applied clear dose limits for individuals, evaluation of ALARA here will be restricted to collective doses and risks. This is appropriate in the context of design and siting of radioactive waste facilities; as it is likely, if any substantial future risks occur, that health concerns will be at a population level. Further, it is assumed that facility workers will be protected under existing health and safety regulations and guidance, and not evaluated as part of ALARA. In a complete decision analysis, however, many other factors could be considered, including health and safety of workers.

Applying formal decision analysis to the ALARA implies evaluation of the trade-off between risk reduction and the costs associated with the actions that can be taken to reduce risk and the benefits of the risk reduction. Risk in a PA is assessed through radiation dose, which is, perhaps, one of the most uncertain aspects of a PA.

Ionizing radiation protection limits have changed over time as more information regarding the negative biological effects of radiation has become available (especially after World War II). Concurrently, therapeutic and diagnostic (i.e., beneficial) uses of radiation have increased dramatically, and nuclear fission is an important source of power in most of the developed world. Thus, a tradeoff is immediately apparent; radiation can be harmful or helpful, depending upon the context.

An additional consideration are the biological endpoints of concern. Radiation in high doses kills cells (so-called 'deterministic' effects), which can be harmful or beneficial to the receptor of the doses (e.g., in the latter case, radiation is used to kill cancer cells). The effects of low doses of radiation are more uncertain. There is ample evidence that ionizing radiation can damage DNA and enhance cell proliferation in doses below those that kill cells, and thus can potentially cause cancer (so-called 'stochastic' effects).

However, it is uncertain at what low doses carcinogenicity becomes a concern (also, note that different tissues have different susceptibility). For many years, there has been a presumption in radiation protection, based upon statistical analysis of animal and human data, that ionizing radiation has a linear dose-response curve at low doses and that there essentially is no threshold of effect; i.e. any dose of radiation can result in an increased probability of cancer (this is termed the linear no-threshold, or LNT, hypothesis). This is not borne out by all experimental and clinical observation. Additionally, the fact that radiation is associated with a large number of natural sources, ranging from sunlight to radon, and the fact that multiple highly-efficient molecular and cellular defense and repair mechanisms exist, must be considered (Scott 2008). Regardless, this LNT hypothesis is the basis for most regulatory standards today. Consequently, if a PA uses the LNT approach to develop dose estimates, then the ALARA analysis essentially assumes no carcinogenic threshold of radiation carcinogenesis.

A threshold of dose effect model is, arguably, more realistic, and could be used to estimate dose and in the ensuing ALARA analysis. If ALARA is applied in the case of a threshold or “target” concentration, then the threshold would be treated as a limit on the amount of risk reduction that can be achieved by a particular management alternative. Proper evaluation of uncertainty

associated with the LNT hypothesis would be a large task in itself, but the influence of a LNT assumption could still be evaluated within the decision analysis framework.

A different sort of threshold exists with regard to natural background levels of radiation. The doses that the public receives from all environmental sources (e.g., local geology, extraterrestrial, etc.) can be quite variable. For example, people who live at a location in the US with high levels of uranium compounds in the local soil and rocks may have a much higher level of annual exposure (due to radon) than people who live at sea level with little uranium compound content of the soil and rocks (http://www.epa.gov/radon/zonemap.html). From an ALARA perspective, it might be reasonable to consider that the *incremental* population dose is of interest; i.e. the dose that is over and above background. If, instead, background is considered part of the dose assessment, then background conditions would need to be characterized. Background is not usually considered in a PA, in which case an assumption is made that the decision analysis is aimed only at risks from exposure to radioactive contaminants in the disposal facility.

Uranium and many other metals are also associated with non-radiological toxicity; e.g. kidney or liver damage. In such cases, toxicology has developed concepts such as the reference dose and benchmark dose, to account for the clear thresholds of effect that are associated with non-carcinogenic toxicity (Filipsson et al., 2003). Similar to the discussion above, in these cases the threshold can be viewed as a target, below which risks are not of substantial concern, and background risks are not considered in the PA or ALARA analysis.

6 References

Berry, D.A., 1995. *Statistics: A Bayesian Perspective*. Wadsworth Press.

Clemen RT. 1996. *Making Hard Decisions*. Duxbury, Pacific Grove.

Claxton K. 1999. Bayesian approaches to the value of information: Implications for the regulation of new pharmaceuticals. *Health Economics* 8:269-274.

DOE 1993. *Radiation Protection of the Public and the Environment,* DOE Order 5400.5 (January 1993).

DOE 1997. *Applying the ALARA Process for Radiation Protection of the Public and Environmental Compliance with 10 CFR 834 and DOE 5400.5 ALARA Program Requirements*, draft DOE standard (April 1997).

Filipsson AF, Sand S, Nilsson J, et al. 2003. The benchmark dose method - review of available models, and recommendations for application in health risk assessment. *Crit Rev Toxicol* 33:505-542.

Hendee WR, Edwards FM. 1986. ALARA and an integrated approach to radiation protection. S*eminars in Nuclear Medicine* 16:142-150.

ICRP. 1977. *Radiation Protection.* International Commission of Radiological Protection Publication No. 26. Permagon, NY.

ICRP. 1983. *Cost-Benefit Analysis in the Optimization of Radiation Protection.* International Commission of Radiological Protection Publication No. 37. Permagon, NY.

Kiker GA, Bridges TS, Varghese A, Seager PT, Linkov I. 2005. Application of multicriteria decision analysis in environmental decision making. *Integrated Environmental Assessment and Management* 1:95-108.

Linkov I, Loney D, Cormier S, Satterstrom FK, Bridges T. 2009. Weight-of-evidence evaluation in environmental assessment: review of qualitative and quantitative approaches. *Science of the Total Environment* 407:5199-5205.

Morgan MG, Henrion M. 1990. *Uncertainty: A Guide to Dealing with Uncertainty in Quantitative Risk and Policy Analysis*. Cambridge University Press, Cambridge.

NRC. 1995. *Reassessment of NRC's Dollar Per Person-Rem Conversion Factor Policy*. NUREG-1530. December 1995.

NRC. 2000. *ALARA Analyses*. NUREG-1727, Appendix D. September 2000.

NRC. 2008. *Generic FSAR Template Guidance for Ensuring that Occupational Radiation Exposures are as Low as is Reasonably Achievable (ALARA)*, Revision 3. NEI 07-08. November 2008.

Pennington CW. 2009. Comparative population dose risks from nuclear fuel cycle closure and renewal of the commercial nuclear energy alternative in the U.S. *Progress in Nuclear Energy* 51:290-296.

Scott BR. 2008. It's time for a new low-dose radiation risk assessment paradigm. *Dose-Response* 6:333-351.

Neptune and Company Inc.

June 1, 2011 Report for EnergySolutions

Clive DU PA Model, version 1

Appendix 13

Deep Time Assessment

Deep Time Assessment for the Clive DU PA

30 May 2011

Prepared by

Neptune and Company, Inc.

This page is intentionally blank, aside from this statement.

CONTENTS

FIGURES

TABLES

1.0 Deep Time Scenarios Distribution Summary

The following is a brief summary of input values used parameters employed in the deep time[1] scenarios component of the Clive Performance Assessment (PA) model that is the subject of this white paper.

For distributions, the following notation is used:

- LN(*GM*, *GSD*, [*min*, *max*]) represents a log-normal distribution with geometric mean GM and geometric standard deviation GSD, and optional *min* and *max*, and
- Beta(μ, σ, *min*, *max*) represents a generalized beta distribution with mean μ, standard deviation σ, minimum *min*, and maximum *max*.

Table 1. Summary of distributions for the Deep Time Scenarios container.

Model Parameter	Value or Distribution	Units	Reference / Comments
LargeLakeStart	LN(GM=14000, GSD=1.2, min=0, max=50000)	yr	See Section 6.1
LargeLakeEnd	LN(GM=6000, GSD=1.2, min=0, max=50000)	yr	See Section 6.1
LargeLakeSedimentationRate	LN(GM=0.00012, GSD=1.2)	m/yr	See Section 6.3
IntermediateLakeDuration	LN(GM=500, GSD=1.5, min=0, max=2500)	yr	See Section 6.2
IntermediateLake SedimentAmount	LN(GM=2.82, GSD=1.71)	m	See Section 6.3
SiteDispersalArea	LN(GM= VolumeAboveGrade / 0.1 m, GSD=1.5, min= VolumeAboveGrade / 1 m, max=Large[1])	km^2	See Section 6.4
IntermediateLakeDepth	beta(μ=30, σ=18, min = 0, max = 100)	m	See Section 6.5
LargeLakeDepth	beta(μ=150, σ=20, min = 100, max = 200)	m	See Section 6.5

[1]"Large" is an arbitrarily large number defined in the Clive DU PA Model as 1E+30.

2.0 Deep Time Scenarios Overview

There are two major components to the Clive depleted uranium (DU) Performance Assessment (PA) model. The first addresses quantitative dose assessment for 10,000 years and is based on projections of current societal conditions into the future, which also assumes no substantial change in climatic conditions. The second addresses simulations until the time of peak radioactivity. For this PA, peak radioactivity associated with radon production from DU, occurs

1 For the purpose of this white paper, deep time refers to the period between 10 thousand years to 2.1 million years

at about 2.1 My. The time frame of this component requires consideration of climatic changes based on the scientific literature that have occurred on approximately 100 ky cycles for more than 1 My. These cycles include periods of extensive glaciation and inter-glacial periods (Figure 1). The planet is currently in an inter-glacial period. In effect, the 10 ky model is projected under inter-glacial conditions, and the deep time model includes an evaluation of the effect on DU disposal in the Class A South embankment of future 100 ky glacial cycles for the next 2.1 My. The focus of this paper is the deep time model.

The objective of the deep time scenarios submodel in the GoldSim (GTG, 2011) PA model is to assess the potential impact of glacial epoch pluvial lake events on the overall DU waste embankment from 10 ky through 2.1 My post-closure. A pluvial lake is a consequence of periods of extensive glaciation, and results from low evaporation, increased cloud cover, increased albedo, and increased precipitation in landlocked areas.

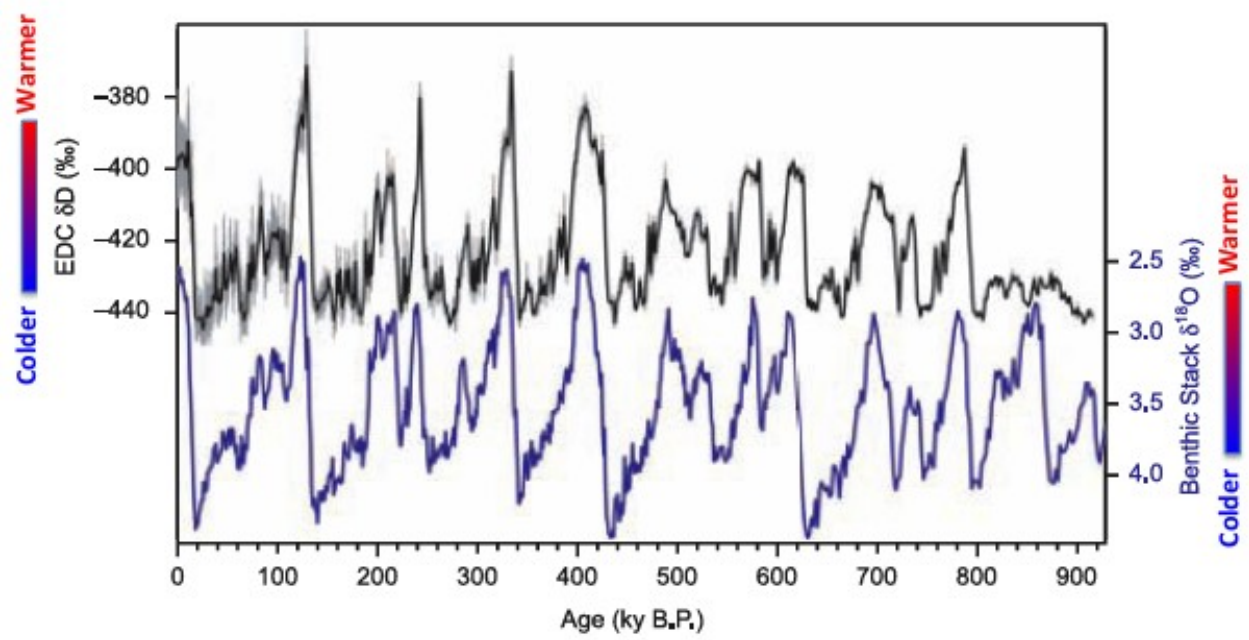

Figure 1. Comparison of delta deuterium (black line) from the European Project for Ice Coring in Antarctica (EPICA) Dome C ice core and benthic (marine) oxygen-18 record (blue line) for the past 900 ky [reproduced from Jouzel et al. (2007)]. Note that the two records are correlated for about the past 800 ky.[2]

The deep time evaluation focuses on potential releases of radioactivity following a series of lake events caused by glacial cycles (Figure 1). The approximate 100 ky glacial cycles can be easily discerned in Figure 1. The current inter-glacial period is shown on the left edge of the figure. The last ice age finished between 12 ky and 20 ky ago. Around the last glacial maxiumum (represented as a trough on the far-left side of Figure 1), Lake Bonneville reached its maximum extent. The ice core data and the benthic marine isotope data show very similar patterns for the

2 Both time series have been used as proxies for representing major shifts (glacial and interglacial shifts, represented by the temperature gradient on the y-axes) in past climate.

past 800 ky. These 100 ky cycles are used as the basis for modeling the return and recurrence of lake events in the Bonneville Basin.

The approach to deep time modeling is briefly described in the *Conceptual Site Model for Disposal of Depleted Uranium at the Clive Facility* (Neptune, 2011a). The model is developed further in this paper, including more detailed conceptual model development, model structuring and model specification based on available data, scientific literature, and expert opinion.

For the deep time evaluation, the PA model provides an assessment of plausible future consequences of present-day disposal of DU waste to the environment. Doses to potential human receptors are not calculated. However, projected concentrations of radioactive species are tracked in both lake water and lake sediments. Although the 100 ky glacial patterns can be used as a basis for modeling lake recurrence, specific temporal information available for assessing the long-term behavior of the DU waste disposal system and the area surrounding the Clive site is highly uncertain. That is, although large lakes are expected to return, the exact timing is uncertain. However, the exact timing is not important. What is important is that the model allows for periodic recurrence of large lakes similar to those that have occurred in the past which could inundate the Clive area in the future. Given this ability, the impact of large lakes on the disposal system can then be evaluated.

Thus the deep time model constructed should be regarded as conceptual and stylized. The intent is to present a picture of what the future might hold for the DU waste disposal embankment, rather than to provide a quantitative, temporally specific, prediction of future conditions, or an assessment of exposure or dose to human receptors who might or might not exist long into the future. The type of glacial climate change envisioned in the deep time model will probably have wide-reaching consequences for the planet, that are far beyond the scope of a PA for disposal of radioactive waste.

The focus of the deep time evaluation is return of large lakes in the Bonneville Basin. Since climatic cycles are considered very likely, in which case the deep time model evaluates the consequences of the return of large lakes. Other less likely geologic events could also occur in the next 2.1 My. Events such as meteor strikes, and volcanic activity such as Yellowstone could also be considered. However, events other than the cyclic return of large lakes are not considered further in this model because their likelihood is small, and their consequences are likely to be much greater and far reaching for human civilization.

The background sections provide a detailed overview of past climatic conditions that have been linked to the formation of pluvial lake events in the Bonneville Basin, which is the large drainage basin in Utah that has been subject to pluvial lake events in the past. For example, the Great Salt Lake is a remnant of Lake Bonneville, the pluvial lake that existed at the last glacial maximum. The background sections are then followed by a presentation of the conceptual site model and the specific functions and parameters implemented in the deep time container in the GoldSim PA model.

3.0 Background on Pluvial Lake Formation in the Bonneville Basin

3.1 Long-term Climate

Large-scale climatic fluctuations over the last 2.6 My (the beginning of the Quaternary Period in geologic time) have been studied extensively in order to understand the mechanisms underlying those changes (Hays et al., 1976, Berger, 1988, Paillard, 2001, Berger and Loutre, 2002). These climatic signals have been observed in marine sediments (Lisiekcki and Raymo, 2005), land records (Oviatt et al., 1999), and ice cores (Jouzel et al., 2007). These large-scale fluctuations in climate have resulted in glacial and interglacial cycles, which have waxed and waned throughout the Quaternary Period. The causes of the onset of the last major Northern Hemisphere glacial cycles 2.6 My ago remain uncertain, but several studies suggest that the closing of the Isthmus of Panama caused a marked reorganization of ocean circulation patterns that resulted in continental glaciation (Haug and Tiedemann, 1998, Driscoll and Haug, 1998). Future glacial events are likely to be caused by a combination of the Earth's orbital parameters as well as increases in freshwater inputs to the world's oceans resulting in a disruption to the ocean's thermohaline circulation (Driscoll and Haug, 1998).

Changes in the periodicity of glacial cycles have been linked to variations in Earth's orbit around the Sun. These variations were described by Milankovitch theory and are based on changes that occur due to the eccentricity (i.e., orbital shape) of Earth's orbit every 100 ky, the obliquity (i.e., axial tilt) of Earth's axis every 41 ky, and the precession of the equinoxes (or solstices) (i.e., wobbling of the Earth on its axis) every 21 ky (Berger, 1988). For the first 2 My of the Pleistocene (the first major Epoch of the Quaternary Period), Northern Hemispheric glacial cycles occurred every 41 ky, while the last million years have indicated glacial cycles occurring every 100 ky, with strong cyclicity in solar radiation every 23 ky (Berger and Loutre, 2002; Paillard, 2006). The shift from shorter to longer cycles is one of the greatest uncertainties associated with utilizing the Milankovitch orbital theory alone to explain the onset of glacial cycles (Paillard, 2006).

The evaluation by Hays et al. (1976), who analyzed changes in the isotopic Oxygen-18 ($\delta^{18}O$) composition of deep-sea sediment cores, suggest that major climatic changes have followed both the variations in obliquity and precession through their impact on planetary insolation (i.e., the measure of solar radiation energy received on a given surface area in a given time). In its most common form, Oxygen in composed of 8 protons and 8 neutrons (giving it an atomic weight of 16). This is know as a "light" oxygen. It is called "light" because a small fraction of oxygen atoms have 2 extra neutrons and a resulting atomic weight of 18 (O^{18}), which is then known as "heavy" oxygen. O^{18} is a rare form and is found in only about 1 in 500 atoms of oxygen. The ratio of these two oxygen isotopes has changed over the ages and these changes are a proxy to changing climate that have been used in both ice cores from glaciers and ice caps and cores of deep sea sediments. Thus, variations in $\delta^{18}O$ reflect changes in oceanic isotopic composition caused by the waxing and waning of Northern Hemispheric ice sheets, and are thus used as a proxy for previous changes in climate (cf. Figure 1).

Slightly different external forcing and internal feedback mechanisms can lead to a wide range of responses in terms of the causes of glacial-interglacial cycles. The collection of longer ice core records, such as the European Project for Ice Coring in Antarctica (EPICA) Dome C core located in Antarctica, has highlighted the clear distinctions between different interglacial-glacial cycles (Jouzel et al., 2007). For example, the last glacial period resulted in the presentation of Lake Bonneville, perhaps the largest glacial lake that has occurred in the Bonneville Basin. However, of the seven most recent 100 ky glacial cycles, it is estimated that only four of them presented very large lakes in the Bonneville Basin. Variation in climatic conditions appears to be sufficient that large differences have occurred in each of the past 100 ky cycles. At the present time, the EPICA Dome C core is the longest (in duration) Antarctic ice core record available, covering the last 800 ky (Jouzel et al., 2007).

Various studies highlight the importance of past atmospheric composition in the dynamics of glaciations across the Northern Hemisphere, in addition to the insolation due to orbital influences (Masson-Delmotte et al., 2010; Clark et al., 2009; Paillard, 2006). Carbon dioxide (CO_2) is a well-known influence on the atmospheric 'greenhouse effect' (i.e. warming due to trapping of solar heat), and is a globally well-mixed gas in the atmosphere due to its long lifetime. Therefore, measurements of this gas that are made in Antarctic ice are globally representative and provide long-term data that are important for understanding past climatic changes. Direct measurement of CO_2 trapped in the EPICA Dome C core indicates that atmospheric CO_2 concentrations decreased during glacial periods due to greater storage in the deep ocean, thereby causing cooler temperatures from a reduction of the atmosphere's greenhouse effect (EPICA, 2004). Warmer temperatures resulting from elevated concentrations of CO_2 that is released from the ocean contribute to further warming and could support hypotheses of rapid wasting at the end of glacial events (Hays et al., 1976). Earlier interglacial events (prior to 420 ky), however, are thought to have been cooler than the most recent interglacial events (since 420 ky) (Masson-Delmotte et al., 2010).

Berger and Loutre (2002) conducted simulations including orbital forcing coupled with insolation and CO_2 variations over the next 100 ky. Their results indicated that the current interglacial period could last another 50 ky with the next glacial maximum occurring about 100 ky from now. The scientific record (cf. Figure 1) supports variability across the 100 ky glacial cycles. Berger and Loutre (2002) effectively indicate that the current 100 ky cycle will not be as glacially intense as some of the previous cycles. They also quote J. Murray Mitchell (Kukla et al, 1972, p. 436) who predicts that "The net impact of human activities on climate of the future decades and centuries is quite likely to be one of warming and therefore favorable to the perpetuation of the present interglacial". Archer and Ganopolski (2005) conducted simulations that predict that a massive carbon release from fossil fuel or methane hydrate deposits could prevent glaciation for the next 500 ky. The potential impact of anthropogenic CO_2 (as opposed to natural sources) is controversial and subject to a large degree of uncertainty, and is not addressed further in this modeling effort. Although human influences might extend the current inter-glacial period, this potential effect is not considered in the deep time model because orbital forcing is expected to dominate further into this glacial cycle.

Berger and Loutre (2002) also report that future increases in atmospheric CO_2 from anthropogenic activity along with small insolation variations could result in a transition between the Quaternary and the next geologic period due to the potential wasting of the Greenland and west Antarctic Ice Sheets. However this would also result in increased freshwater inputs to the oceans and could cause a shift toward a colder climate and the next glacial age (Driscoll and Haug, 1998). Given the uncertainties involved in these speculations, the deep time model focuses on stylized projection of the past 800 ky of 100 ky glacial cycles.

Other gases, such as deuterium, have also been measured in the EPICA Dome C core. Jouzel et al. (2007) assembled a high-resolution deuterium profile from the EPICA Dome C core and used these measurements to extend the climate record back to 800 ky ago (see Figure 1). These data indicate that a 100 ky periodicity primarily dominates the temperature record, however the record also indicates that a strong obliquity (40-41 ky) component exists and increases when going from past to present. Jouzel et al. (2007) also indicate that in general, systematic millennial-scale changes are related to North Atlantic deep water formation (influenced by fresh water inputs and sea ice formation), which is shown for the last glacial cycle and suggested for previous glacial periods.

The following sub-sections present an overall background on past events in the Bonneville Basin that are driven by major shifts in climatic regime that are presumed to occur in the future (10 ky to 2.1 My).

3.2 Deep Lake Cycles

The Bonneville Basin is the largest drainage basin in the Great Basin of the Western US. It is a hydrologically closed basin that covers an area greater than 134,000 km^2, and has previously been occupied by deep pluvial lakes. Pluvial lakes typically form when warm air from arid regions meets chilled air from glaciers, creating cloudy, cool, rainy weather beyond the terminus of the glacier. The increase in rainfall and moisture can fill the drainage basin, forming a lake. This kind of humid climate was evident during the last glacial period in North America, and resulted in more precipitation than evaporation, hence the rise of Lake Bonneville.

Various studies have investigated previous lake cycles in the Bonneville Basin (Table 2; Oviatt et al., 1999; Link et al., 1999). Some of these studies focus on the analysis of sediment cores, which are used to help understand previous lake levels as well as establish the approximate age of previous lake cycles (e.g., Oviatt et al., 1999). Oviatt et al. (1999) analyzed hydrolysate amino acid enantiomers for aspartic acid, which is abundant in ostrocode protein. Ostracodes are small crustaceans that are useful indicators of paleo-environments because of their widespread occurrence and because they are easily preserved. Oviatt et al. (1999) indicate that ostracodes are highly sensitive to water salinity. Therefore, portions of sediment cores that contain ostracodes indicate fresher, and hence probably deeper, lake conditions than the modern Great Salt Lake (Oviatt et al., 1999).

To establish the approximate timing of previous lake cycles, Oviatt et al. (1999) examined sediments from the Burmester sediment core and suggested that a total of four deep-lake cycles occurred during the past 780 ky (Table 2). They found that the four lake cycles correlated with marine $\delta^{18}O$ stages 2 (Bonneville lake cycle: ~24-12 ky), 6 (Little Valley lake cycle: ~186-128 ky), 12 (Pokes Point lake cycle: ~478-423 ky), and 16 (Lava Creek lake cycle: ~659-620 ky).

Oxygen isotope stages are alternating warm and cool periods in the Earth's paleoclimate which are deduced from oxygen isotope data (Figure 2). These correlations suggest that large pluvial lake formation in the Bonneville Basin occurred in the past only during the most extensive Northern Hemisphere glaciations. These extensive glaciations are suggested to have been controlled by the mean position of storm tracks throughout the Pleistocene, which were in turn controlled by the size and shape of the ice sheets (Oviatt, 1997; Asmerom et al., 2010). In addition to these large lake cycles, a smaller cycle known as the Cutler Dam cycle occurred between 80-40 ky (Link et al., 1999).

Table 2. Lake cycles in the Bonneville Basin during the last 700 ky.[3]

Lake Cycle	Approximate Age*	Maximum Elevation	Lake level control
Great Salt Lake (current level)	present	1284 m (4212 ft) in 1873	Inter-glacial climate; human intervention
Bonneville (Gilbert Shoreline)	12.9-11.2 ka	1295 m (4250 ft)	Beginning of inter-glacial climate; possible regressive phase of Lake Bonneville; possible association with the Younger Dryas period
Bonneville (Provo Shoreline)	17.4-15.0 ka	1445 m (4740 ft)	Glacial climate; new threshold at Zenda near Red Rock Pass, Idaho (natural dam collapse)
Bonneville (Bonneville Shoreline)	18.3-17.4 ka	1552 m (5090 ft)	Glacial climate; threshold at Zenda near Red Rock Pass, Idaho
Bonneville Transgression	~30-18.3 ka		Glacial climate
Bonneville (Stansbury Shoreline)	26–24 ka	1372 m (4500 ft)	Glacial climate; transgressive phase of Lake Bonneville
Cutler Dam	~80–40 ka	< 1380 m (< 4525 ft)	Glacial climate
Little Valley	~128–186 ka	1490 m (4887 ft)	Glacial climate
Pokes Point	417–478 ka	1428 m (4684 ft)	Glacial climate
Lava Creek	~620–659 ka	1420 m (4658 ft)	Glacial climate

*Approximate ages derived from Currey, et al. (1984) Link et al. (1999) and Oviatt et al. (1999). Bonneville cycle approximate age presented as calibrated years.
Elevations are not corrected for isostatic variations

3 Note the various levels of the last major lake cycle, Lake Bonneville.

Lake Bonneville is the last major deep lake cycle that took place in the Bonneville Basin and is widely described in the literature (Hart et al., 2004; Oviatt and Nash, 1989; Oviatt et al., 1994; 1999). Lake Bonneville was a pluvial lake that began forming approximately 28-30 thousand years before present (ky BP), forming various shorelines throughout its existence and covering over 51,000 km^2 at its highest level (Matsurba and Howard, 2009). The high-stand (i.e., the highest level reached) of the lake at the Zenda threshold (1,552 m), located north of Red Rock Pass, occurred approximately 18.3-17.4 ky BP. The high-stand of the lake was followed by an abrupt drop in lake level due to the catastrophic failure of a natural dam composed of unconsolidated material at approximately 17.4 ky BP. As a result of this flood, the lake dropped to a level of 1,445 m, called the Provo level. The Provo level is the maximum level that any future deep lake can reach. The lake regressed rapidly during the last deglaciation, then increased again to form the Gilbert shoreline between 11.2-12.9 ky BP which coincided with the Younger Dryas global cooling event (Oviatt et al., 2005). The lake then receded to levels of the current Great Salt Lake at approximately 10 ky BP for the remainder of the Holocene.

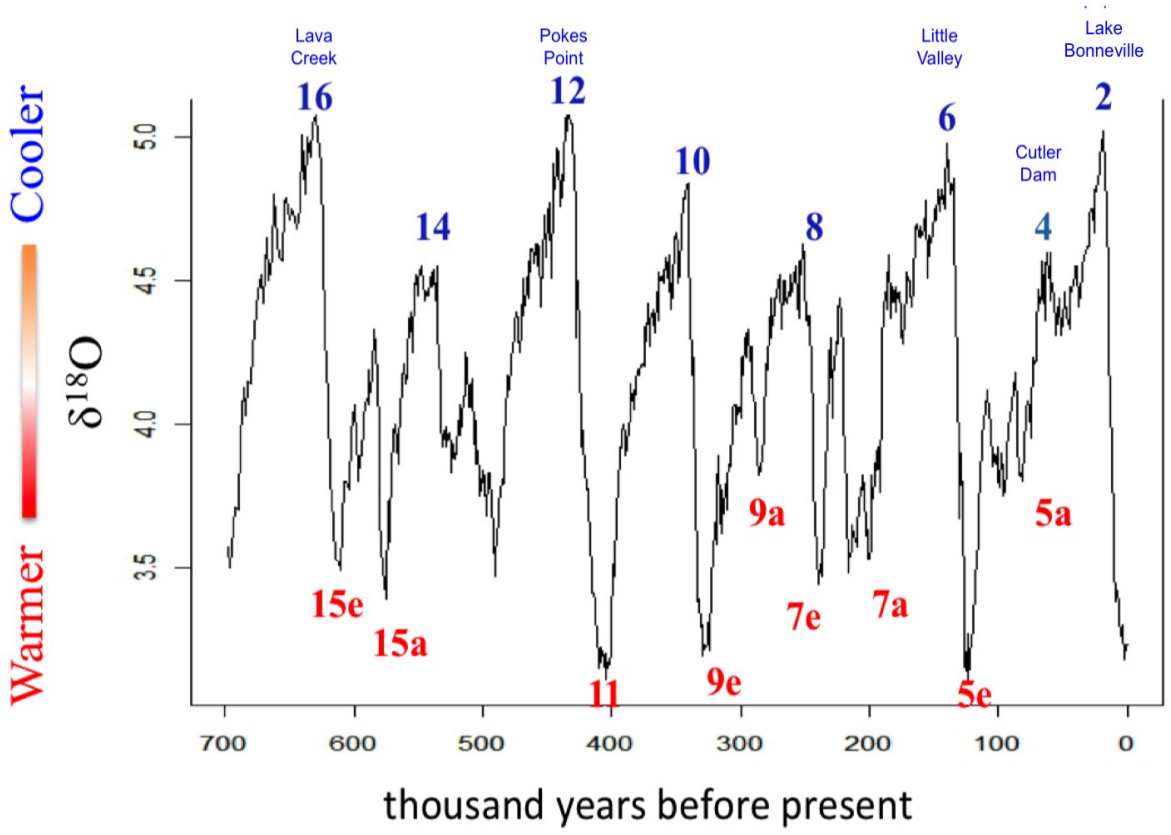

Figure 2. Benthic oxygen isotope record for the last 700,000 years (Lisiecki and Raymo, 2005).[4]

4 Red (warm periods) and blue (cool periods) numbers correspond to marine isotope stages based on Lisiecki and Raymo (2005). Lake stages identified by Oviatt et al. (1999) are also included in blue text.

Glacial cycles can be discerned in Figure 2 by considering each cycle from the beginning of the inter-glacial period and ending each cycle at the peaks that correspond to large lake occurrence. Using this approach, the current glacial cycle started around 12 ky ago, Lake Bonneville occurred at the end of the last complete cycle, and Cutler Dam occurred in the middle of the last 100 ky cycle. The previous 100 ky cycle resulted in Little Valley. Pokes Point occurred five cycles ago, and Lava Creek 7 cycles ago. These large lakes have been identified in sediment cores and in shorelines around the Bonneville Basin. However, it is likely that many more shallower lakes have also occurred in each glacial period, but the shorelines have been destroyed by later lakes. In addition, sedimentation in the Bonneville Basin is caused by several factors including air dispersion in inter-glacial periods, and both terrigenous and biotic sedimentation when lakes are formed in glacial periods. In addition, sedimentation in the Bonneville Basin depends on location within the basin, which determines such things as the presence or absence of river input, wave energy, sediment availability on piedmonts, water chemistry, biological activity, and slope. The mixing of sediment that occurs during lake formation can mask the existence of previous relatively shallow lakes. There is considerable uncertainty in the number of lakes of various sizes that might have existed in the Bonneville Basin. However, the main focus of the modeling is to ensure the presence of lakes that inundate Clive at different times in future glacial cycles, and to approximately match the net sedimentation of the past glacial cycles.

3.3 Shallow Lake Cycles

Smaller lake events have also occurred in the history of the Bonneville Basin. These are documented in Table 3 (C.G. Oviatt, Professor of Geology, Kansas State University, personal communication December 2010, January 2011, and email communication herein referred to as 'C.G. Oviatt, personal communication'). These events are evident when analyzing a pit wall interpretation at the Clive site (Appendix A; C.G. Oviatt, unpublished data) as well as at the ostracode and snail record present in the Knolls sediment core (Appendix B; C.G. Oviatt, unpublished data). The pit wall study conducted by Oviatt occured during early development of the Clive disposal facility. From the Clive pit wall interpretation, it is presumed that at least three shallow lake cycles occurred prior to the Bonneville cycle, although there is some uncertainty associated with that estimate. These shallow cycles could in fact be part of the transgressive phase (i.e., rising lake level) of the Bonneville cycle (C.G. Oviatt, personal communication). By analyzing the Knolls core interpretation, which is more representative of Clive than the Burmester core due to its relative proximity and differences in their regional topography, the Little Valley cycle is present at approximately 16.8 m from the top of the core. Given the pit wall at Clive was 6.1 m deep and does not capture the Little Valley cycle, it can be speculated that other smaller lake cycles occurred in the Clive region in addition to the three shallow lake events noted in Table 3 (labeled as Pre-Bonneville Lacustrine Cycles).

Of interest is that the deep lake cycle of Lake Bonneville did not result in substantial sediment deposition. Each shallower lake cycle, given that they probably occurred for shorter periods of time than Lake Bonneville, deposited sediments at a greater rate. Sediment can also accumulate during inter-glacial periods from air deposition, which is reworked when a lake returns. The Knolls core suggests that 16.8 m of sediment was deposited in the last glacial cycle. This also matches the Burmester core sediment record.

For modeling purposes, a distinction is made between shallow, intermediate and large lakes. Large lakes are assumed to be similar to Lake Bonneville, occurring no more than once per 100 ky glacial cycle. Intermediate lakes are assumed to be smaller lakes that reach and exceed the altitude of Clive, but are not large enough that carbonate sedimentation can occur. Shallow lakes are assumed to exist at all other times. The current Great Salt Lake is an example. Under current climate conditions, it is assumed that intermediate lakes will not occur. Under future climate conditions, some glacial cycles will produce a large lake in the Bonneville Basin, and intermediate lakes will occur during the transgressive and regressive phases of a large lake, or during glacial cycles that do not exhibit a large lake.

Table 3. Lake cycles and sediment thickness from Clive pit wall interpretation (C. G. Oviatt, personal communication)

Lake Cycle	Thickness of Sediment Layer (meters)	Depth Below Ground Surface (meters)
Gilbert Lake transgressive/regressive phase	1.05	1.05
Lake Bonneville Regressive Phase (reworked marl)	0.43	1.48
Lake Bonneville Open Water (white marl)	1.29	2.77
Lake Bonneville Transgressive (littoral facies)	0.76	3.53
Pre-Bonneville Lacustrine Cycle 3 (possible shallow lake)	0.71	4.24
Pre-Bonneville Lacustrine Cycle 2 (possible shallow lake)	0.62	4.86
Pre-Bonneville Lacustrine Cycle 1 (possible shallow lake)	1.14	6.00

3.4 Sedimentation

The types of sediment resulting from the formation and long-term presence of lakes in the Bonneville Basin can be divided into two components: 1) biogenic (i.e., sediment from biological processes), and 2) terrigenous (i.e., sediment that is mechanically and chemically eroded and transported). During the large pluvial lake events, biogenic sediment in the form of calcium carbonate was precipitated as tufas, marls, shells (of mollusks), and ostracodes (Hart et al., 2004). Terrigenous sedimentation however, accounts for the majority of sediment deposited throughout the sediment core record (C.G. Oviatt, personal communication). The geomorphological evidence in the form of various lake shorelines carved into the landscape in the Bonneville Basin is an example of the terrigenous erosional capacity of a deep lake system over long time periods. Given the difficulty in separating biogenic versus terrigenous causes of sedimentation, estimates reported below are assumed to be representative of cumulative sedimentation from all causes during a lake event. During inter-glacial periods air deposition also adds to the sedimentation, although there are no sediment core records of airborne sedimentation perhaps because the formation of each lake results in mixing of the upper range of existing sediments.

Brimhall and Merritt (1981) reviewed previous studies that analyzed sediment cores of Utah Lake, a freshwater remnant of Lake Bonneville that formed at approximately 10 ky BP. They

suggest that up to 8.5 m of sediment has accumulated since the genesis of Utah Lake, implying an average sedimentation rate of 850 mm/ky over 10 ky. Within the Bonneville Basin as a whole the major lake cycles resulted in substantial accumulations of sediment based on the depth of the cores analyzed (e.g., a 110-meter core that corresponds to the past 780 ky, or four large lake cycles [Oviatt et al., 1999]), which averages about 140 mm/ky. Einsele and Hinderer (1997) indicate that sediment accumulation in the Bonneville Basin occurred at a rate of 120 mm/ky during the past 800 ky. The Knolls core suggests that there has been 16.8 m sedimentation in the last glacial cycle, or nearly 170 mm/ky.

Interpretations of the Clive pit wall (Table 3; C.G. Oviatt, unpublished data) indicate that the sedimentation rate at the Clive site for the Lake Bonneville cycle is on the order of 2.75 m over a 17-19 ky time period (140-160 mm/kyr). By contrast, shallow lacustrine cycles that occurred prior to Lake Bonneville (but after the Little Valley cycle) indicate that the amount of sediment deposited during each cycle is approximately 1/3 that of the Bonneville sediment deposited. The timing of these shallow lake cycles is uncertain, however it can be approximated when comparing the Clive pit wall interpretation to the Knolls Core (C.G. Oviatt, personal communication). The Little Valley lake cycle is exhibited in the Knolls Core at a depth of approximately 17 m, which is roughly 14 m deeper than the beginning of the transgressive phase of the Bonneville lake cycle event noted on the Clive pit wall interpretation. Given the Little Valley event occurred 150 ky BP, a sedimentation rate can be approximated for the depth between this event and the transgressive phase of the Bonneville cycle of 110 mm/ky.

These data support greater sedimentation rates in shallow lakes (sedimentation in Utah Lake is much greater, and sedimentation in the Clive Pit Wall indicates lower rates for a deep lake cycle), but also suggest that the sedimentation rate in each glacial cycle is similar.

4.0 Conceptual Overview of Modeling Future Lake Cycles

As stated in the overall Conceptual Site Model (Neptune, 2011a), there is a lack of peer-reviewed literature that allows accurate and precise prediction of the direct effects of future climate change on major lake formation in the Bonneville Basin. However, assuming no major changes from recent climate cycles, the probability of another major lake cycle occurring in the Bonneville basin within the next few million years is high. Variations in the Earth's orbital parameters in combination with increases in inputs of freshwater into the world's oceans are likely to lead to another major ice age and could alter long-term climatic patterns in the Bonneville Basin, resulting in deep lake formation. It is possible that the Clive facility will be subjected to deep lake formation in the future, unless anthropogenic effects on atmospheric CO_2 concentrations cause major changes in climatic patterns (Berger and Loutre, 2002).

The basic intent of the deep-time model is to allow lakes to recur in the Bonneville Basin that are sufficiently large that the above-ground portions of the DU waste embankment will be obliterated, and so that the sedimentation rates for each glacial cycle are similar. The exact timing of the recurring lakes is not important, the current 100 ky cycle excepted. The deep-time model allows a deep lake to return in each 100 ky cycle, which, given the scientific record, might be conservative. It also allows intermediate lakes to recur at a frequency that allows the 100 ky sedimentation rate to be satisfied. The current 100 ky cycle is not modeled explicitly. It is possible that the current inter-glacial period will last for another 50 ky, which is unusually large.

The return of a large lake causes the above-ground features of the site to be obliterated, and the contents of the waste embankment to be dispersed through wave action. The DU waste is assumed to be mixed with lake sediments. Each new lake event causes more sedimentation, which will either bury or continually mix the waste with more sediment over time. This basic conceptual model is described in more detail below.

Future Scenarios

Various Features, Events, and Processes (FEPs) may be associated with the effect of a lake return scenario on the DU waste embankment, including wave action, sedimentation, and site inundation. Details of the FEPs process are provided in the *Features, Events and Processes for the Clive DU Performance Assessment* report (Neptune, 2011b). Starting with current conditions, representative lake occurrence scenarios for the long-term future are described below and depicted in Figure 3. Note that there are two components of the models used to represent these scenarios. The first is modeling lake formation and dynamics, based upon the scientific record. The second is modeling the fate of the DU waste embankment.

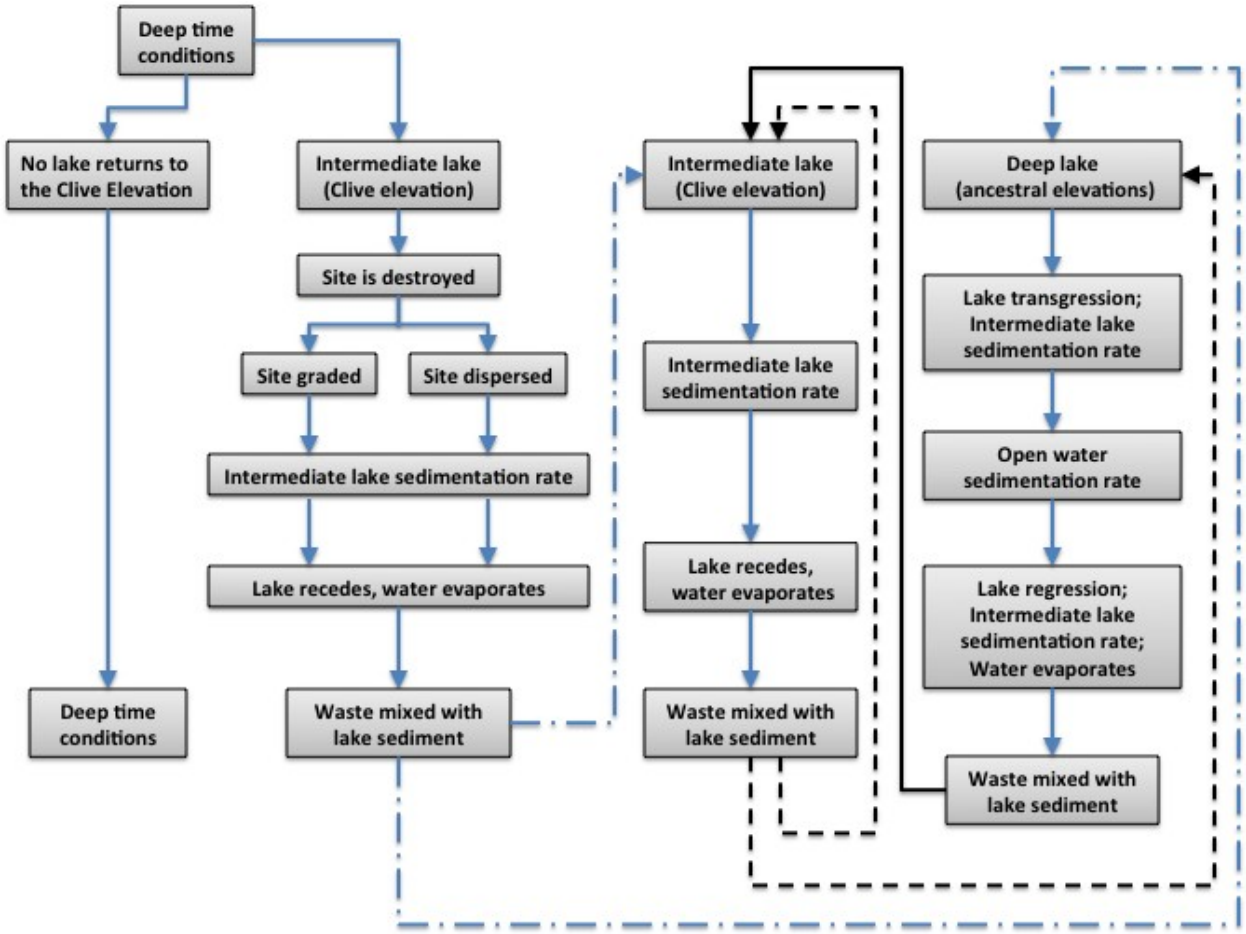

Figure 3. Scenarios for the long-term fate of the Clive facility[5]

5 The scenario that indicates that no lake returns to the Clive elevation implies that a shallow lake is present and never reaches the Clive site.

The Great Salt Lake represents the current condition of a lake in the Bonneville Basin. Lakes such as this are likely to exist in all future climatic cycles, but lakes that do not reach the elevation of the DU waste embankment at Clive will not affect the waste embankment. For the Clive DU waste PA model, it is assumed that destruction of the waste embankment will result from the effects of wave action from an intermediate or large lake. In effect, it is assumed that a lake is large enough that obliteration of a relatively soft pile will occur. This assumption separates shallow and intermediate lakes. In this obliteration scenario, all of the embankment material above grade is assumed to be dispersed through a combination of physical dispersal through wave action and dissolution into the water column above the waste dispersal area.

Waste material that dissolves into the lake eventually returns to the lake bed through precipitation or evaporation as the lake regresses.

While the lake is present, some waste in the water column will bind with carbonate ions and precipitate out into ooilitic sediments, while the remaining waste will fall out with the sediment as the lake eventually recedes. The waste material enters the lake system, creating lake water concentrations. However, all of the waste re-enters the lake sediment once the lake disappears. Sediment concentrations decrease over time because the amount of waste does not change other than through decay and ingrowth, whereas more sediment is added over time.

The model assumes the waste is fully mixed with the accumulated sediment, whereas some waste might be buried by future lake sediments. The model also allows large dispersal areas, and assumes a water column for accepting waste through dissolution that is contained above the dispersal area. These assumptions are conservative, leading to greater concentrations of waste than is probably reasonable. The conservatism is included in this model because of the lack of data that exists to quantify the processes. For example, the extent of mixing of previous sediment with new sediment is not understood, hence an assumption that the sediments completely mix is expedient, but is conservative, since it retains some of the waste near the surface rather than burying it under the latest cycle of sedimentation. Limiting dissolution to a column above the waste dispersal area is conservative because lake water will probably mix more extensively, but the dispersal area is difficult to estimate. An approach that considers the size of the spits from from the Grayback Hills to the north of the Clive facility that were formed during the lake event might provide a better analog. It should be noted that a Gilbert-sized lake would just barely reach Clive and the wave energy would very likely not erode the waste embankment (C. G. Oviatt, personal communication). The size of lake in the PA model that is needed to obliterate the waste embankment can be as small as 1 m, which might not have sufficient wave power to obliterate the site. Dissolution into such a shallow lake might over-estimate lake water concentrations, if such a shallow lake cannot obliterate the waste embankment. There are various reasons why the deep time model might over-estimate lake water and sediment concentrations, but the data needed to better specify the model are not readily available. Depending on the model performance, data collection in support of model refinement might prove to be desirable.

One other factor that is important for this model is that the lake formation model is applied to each 100 ky cycle similarly. That is, the current 100 ky cycle is not treated differently, despite evidence that the current inter-glacial period might last for another 50 ky (Berger and Loutre, 2002). In the model, therefore, an intermediate lake can return sooner than might be expected in the current 100 ky cycle. From the perspective of obliteration of the embankment, the timing is

largely irrelevant. The mass of waste does not change much over time. However, the deep-time model also assumes that the form of DU available for deep-time transport is U_3O_8, which is far less soluble than UO_3 (see *Radioactive Waste Inventory for the Clive PA* (Neptune, 2011c)). The DU waste consists primarily of U_3O_8, from the gaseous diffusion plants. However, the form of the DU waste from the Savannah River Site is UO_3. Fate and transport modeling performed in the GoldSim PA model indicates that the UO_3 will have completely or almost completely migrated to groundwater within 50 ky. Consequently, the deep time model focuses on U_3O_8 as the form of DU available for deep-time migration.

The remainder of this section describes the specifics of the models that have been developed for this PA, including lake formation and sedimentation.

4.1.1 Intermediate and Large Lake Formation

This scenario assumes that changes in climate will continue to cycle in a similar fashion to the climate cycles that have occurred since the onset of the Pleistocene epoch. These changes follow those observed in the marine oxygen isotope record (Figure 2). The record captures major climate regime shifts on a global scale and are used in this scenario in conjunction with expert opinion (C.G. Oviatt, personal communication) and site-specific sediment core and pit wall information to determine the approximate periodicity of lake events. However, uncertainties exist due to the limitations related to the quality of the sediment core data. The following subsections provide more detail with respect to the assumptions for both intermediate and large lake formation.

4.1.1.1 Intermediate Lake Formation

The Great Salt Lake represents the current condition of a lake in the Bonneville Basin. Lakes such as this are likely to exist for periods of time during all future climatic cycles, but lakes that do not reach the elevation of the DU waste embankment at Clive will not affect the waste embankment, so they need are not modeled explicitly. However, it is assumed that during the 100 ky climatic cycles, larger lakes will occur, including lakes that reach the elevation of the DU waste embankment at Clive. Although a definitive distinction is not made, lakes that reach the elevation of Clive but do not develop into a large lake are considered intermediate lakes. These intermediate lakes are also assumed to be large enough that their wave action will destroy the waste embankment. Intermediate lakes might occur during the transgression and regression phases of a large lake, or might occur during a glacial cycle that does not produce a large lake, perhaps in conjunction with glacial cycles that are shorter and less severe than the 100 ky year glacial cycles previously discussed (for example, potentially the current 100 ky cycle).

In general, variation in lake elevation is assumed to occur at all lake elevations. The variation is due to local temporal changes in temperature, evaporation and precipitation. For example, the Great Salt Lake has seen elevation changes of several tens of feet in the past 30-40 years. In addition, the Great Salt Lake has seen greater elevation changes in the past 10 ky, but in no cases since the Younger Dryas has the Great Salt Lake reached the elevation of Clive.

Sedimentation is assumed to occur during these intermediate lake events at greater annual rates than is assumed to occur for the open-water phase of large lakes. This is based on the pre-Bonneville lacustrine cycles that are documented in Table 3 (Clive pit wall interpretation – see Appendix A). The lake is assumed to recede after some period of time, at which point a shallow

lake relative to the Clive facility will occupy Bonneville Basin until the next intermediate or large lake cycle. The details relating to the mathematical approach employed to model this scenario and model parameters are provided in Section 6.0.

4.1.1.2 Large Lake Formation

In this scenario, a large lake forms throughout the Bonneville Basin in response to major glaciation in North America and the Northern Hemisphere, following the ongoing 100 ky glacial cycle. Increases in precipitation and decreases in evaporation over the long-term, and subsequent increases in discharge to the Bonneville Basin via rivers that drain high mountains along the eastern side of the basin in general have resulted in lakes that are more than 30 m deep and cover an area similar to that of the most recent pluvial lake episode (e.g., Lake Bonneville, Provo Shoreline). This same extent of lake formation is assumed to occur in the future. Under such a scenario, the depth of a lake at the location of the Clive facility could be many tens of meters, resulting in sedimentation over the long period of time of the lake's existence. A key difference between this scenario and the intermediate lake scenario is that both the transgressive and regressive phases of lake formation are considered. Transgressive and regressive phases of lake formation can lead to brief periods of rising and falling water levels in both phases. These phases of transgression and regression are also assumed to have higher sedimentation rates than the open-water phase. Upon the complete regression of a large lake, it is assumed that only intermediate lakes will form until the large lake associated with next 100 ky climate cycle occurs. It is assumed that destruction of the waste embankment occurs in response to the formation of a large lake, if the first large lake occurs prior to formation of an intermediate lake.

5.0 A Heuristic Model for Relating Large Lakes to Climate Cycles from Ice Core Temperature

In this section, a model is presented for estimating lake elevation that uses surface temperature deviations from the EPICA Dome C ice core data (Jouzel et al., 2007). The model is not intended to be highly accurate, but rather is aimed at capturing the major lake-cycle features as shown in the studies conducted by Oviatt et al. (1999), Link et al. (1999), and the sediment core and pit wall interpretations (C.G. Oviatt, personal communication). This model is not used as a predictive model but rather to form a basis for the character and dynamics of lake events, which will be implemented in the deep time model developed in Section 6.0.

The deep-sea benthic $\delta^{18}O$ record is in excellent agreement with the EPICA Dome C deuterium measurements for the last approximate 810 ky (Jouzel et al., 2007). Temperature anomaly data for the past 810 ky were obtained from the World Data Center for Paleoclimatology, National Oceanic and Atmospheric Administration/National Climate Data Center. These data are made available based on calculations described in Jouzel et al. (2007), and are plotted in Figure 4. From the 810 ky of data, the temperature deviations range from $T_{min} = -10^{o}C$ to $T_{max} = +5^{o}C$. This range is utilized to bound extreme events.

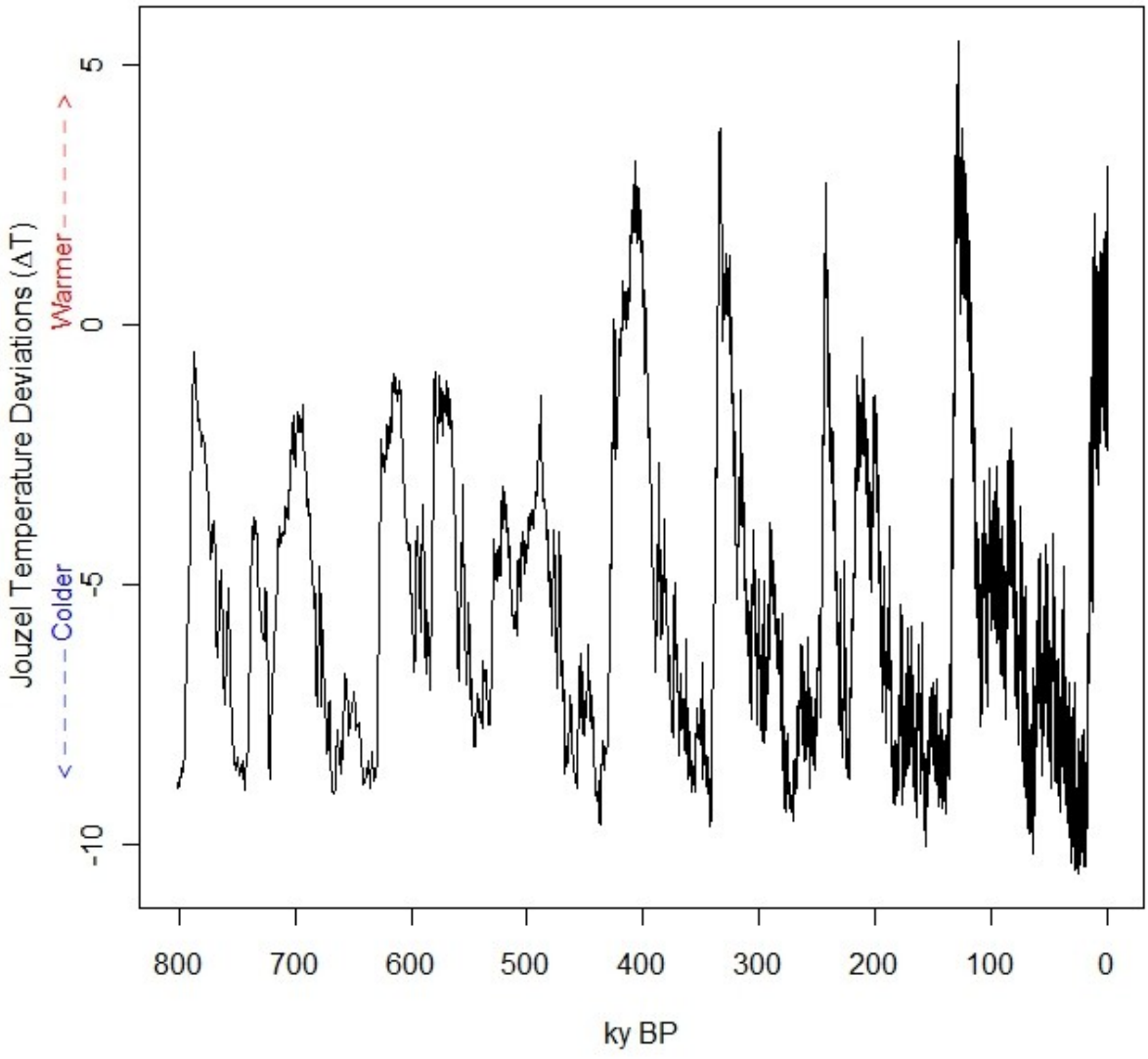

Figure 4. Temperature deviations for the last 810 ky, Jouzel (2007).

5.1 Conceptual Model

Water balance in the Bonneville Basin is affected by many complex processes, so modeling water balance simply as a function of temperature alone is not expected to produce any precise results, but might succeed in representing a coarse feature. The conceptual model is based on a water balance reservoir model of precipitation versus evaporation. If precipitation outpaces evaporation, the lake elevation increases. If evaporation outpaces precipitation, then the lake elevation decreases. Precipitation and evaporation are affected directly by temperature, but long

term patterns of precipitation are affected more greatly by the presence or absence of continental glaciation in North America. Thus, glaciation is modeled first using a simple reservoir model depending on temperature.

5.2 Glaciation

The water balance model begins by constructing a "continental glacier" – an artificial construct that represents a glacier large enough to affect precipitation levels in the Bonneville Basin. The extent of glaciation in proximity to the Bonneville Basin is assumed to be zero initially, which is a reasonable approximation for the start time of 785 ky BP, a start time chosen because it corresponds to a warmer climate phase (data from Jouzel, et al., 2007 – see Figure 4). For each time step of 500 years, an increase in glacial magnitude is dependent on temperature deviation (ΔT) as scaled in Jouzel (see Figure 4):

$$Glacial_{addition}(\Delta T)=\begin{cases} 0 & if\ \Delta T \geq \Delta T_{GMax} \\ \frac{1}{N_{GA}}\left(e^{R_{GA}\cdot(\Delta T_{GMax}-\Delta T)}-1\right) & if\ \Delta T < \Delta T_{GMax} \end{cases} \quad (1)$$

where

- N_{GA} is a normalizing constant:

$$N_{GA}=e^{R_{GA}\cdot(\Delta T_{GMax}-\Delta T_{min})} \quad (2)$$

- R_{GA} is a rate parameter (yr^{-1}), and
- T_{GMax} is a threshold temperature (degrees Celsius).

Since the glacier is an artificial construct for modeling purposes, the units and scale of the glacial "magnitude" are arbitrary. The parameters of the precipitation model described below must be calibrated appropriately to the scale of the glaciation model.

For each time step, the decrease in glacial magnitude is also modeled as a function of temperature:

$$Glacial_{subtraction}(\Delta T)=\begin{cases} 0 & if\ \Delta T \leq \Delta T_{GMin} \\ \frac{S_{GS}}{N_{GS}}\left(e^{R_{GS}\cdot(\Delta T-\Delta T_{GMin})}-1\right) & if\ \Delta T > \Delta T_{GMin} \end{cases} \quad (3)$$

where

- N_{GS} is a normalizing constant:

$$N_{GS}=e^{R_{GS}\cdot(\Delta T_{max}-\Delta T_{GMax})} \quad (4)$$

- R_{GS} is a rate parameter (yr^{-1}), and
- T_{GMin} is a threshold temperature (degrees Celsius).

The change in glacial magnitude for a time step is thus:

$$Glacier_t = max\left\{0, Glacier_{t-1} + Glacial_{addition}\left(\Delta T_t\right) - Glacial_{subtraction}\left(\Delta T_t\right)\right\} \quad (5)$$

where the *t* subscript is a time step index. The time step used for the model is 500 years.

The parameters of the model were calibrated heuristically to compute parameters that produced a glacial cycle that appeared reasonable for this coarse model. The set of parameters computed was:

$$\Delta T_{GMax} = -6;\ R_{GA} = 0.25;\ \Delta T_{GMin} = -6;\ R_{GS} = 0.2;\ S_{GS} = 5 \tag{6}$$

The change in the glacial magnitude for a particular time step as a function of temperature is shown in Figure 5. These values lead to slow growth during the very cold phases (Jouzel temperature deviations of less than -6 ˚C) of the glacial cycle, and rapid recession during warm phases (Jouzel temperature deviations of greater than -6 ˚C).

5.3 Precipitation

A coarse model for precipitation in the Bonneville Basin was developed dependent on global temperature (as precipitation generally increases with global temperature), lake surface area (which affects recharged evaporation), and an additional effect that depends of the magnitude of the continental glacier. The precipitation in meters of annual rainfall is modeled as:

$$P_t\left(\Delta T_t, L_{t-1}, G_{t-1}\right) = B_P + R_{PT} \cdot \Delta T + R_{PLSA} \cdot SA\left(L_{t-1}\right) + S_{PG} \cdot e^{R_{PG} \cdot G_{t-1}} \tag{7}$$

where B_P is a baseline precipitation, R_{PT} is a coefficient of linear effect of global temperature, R_{PLSA} is a coefficient of linear effect of the surface area of the lake, and $SA(L)$ is the surface area in km^2 associated with lake elevation L. The effect of temperature and lake surface area are modeled as linear, while the glacial effect is exponential with respect to glacier size. The set of parameters calibrated to the glacial magnitude model are:

$$B_P = 0.30;\ R_{PT} = 0.005;\ R_{PLSA} = 2\text{e-}6;\ S_{PG} = 0.06;\ R_{PG} = 0.03 \tag{8}$$

The precipitation is then converted to a volume by multiplying by the area of Bonneville Basin (approximately 47,500 km^2).

5.4 Evaporation

Evaporation rate in the region is modeled as a function of temperature:

$$E_t\left(\Delta T_t\right) = B_E + \frac{S_E}{N_E} \cdot e^{R_E \cdot \left(\Delta T - \Delta T_{min}\right)} \tag{9}$$

where N_E is a normalizing constant:

$$N_E = e^{R_E \cdot \left(\Delta T_{max} - \Delta T_{min}\right)} \tag{10}$$

The evaporation is then converted to a volume by multiplying by the area of the basin.

The calibrated parameters are:

$$B_E = 0.32;\ S_E = 0.3;\ R_E = 0.05;\ \Delta T_{min} = -10;\ \Delta T_{max} = 5 \tag{11}$$

If the precipitation volume exceeds the evaporation volume, then the difference is added to the lake volume, and the lake elevation is calculated from the total lake volume.

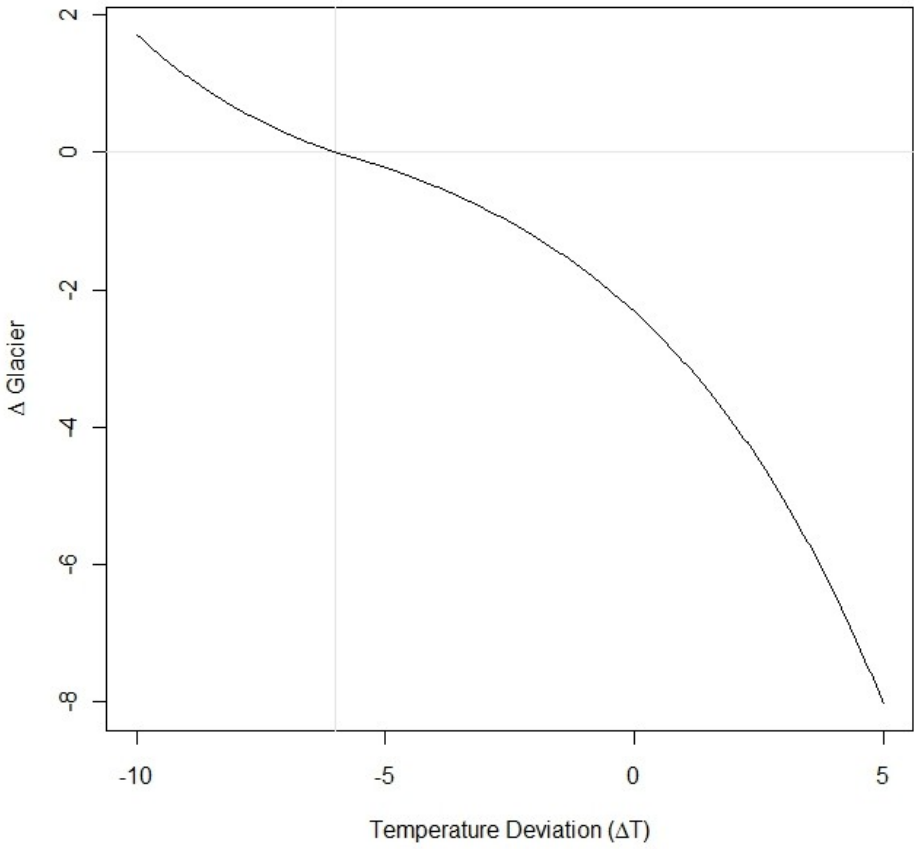

Figure 5. Glacial change as a function of temperature for the coarse conceptual model.

If the evaporation volume is greater than the precipitation volume, then the total evaporation is adjusted downward to adjust for the actual surface area exposed (rather than the full surface area of the basin as used in the initial calculation). The difference between the adjusted evaporation and the precipitation is then subtracted from the lake volume, and the lake surface elevation is calculated from the total lake volume.

$$\Delta\, Volume_t = \begin{cases} \left[P_t(\Delta T_t) - E_t(\Delta T_t)\right] \cdot SA_{basin} & if\ E_t(\Delta T_t) < P_t(\Delta T_t) \\ \left[P_t(\Delta T_t) - E_t(\Delta T_t)\right] \cdot \dfrac{SA(L_{t-1})}{SA_{basin}} & if\ E_t(\Delta T_t) \geq P_t(\Delta T_t) \end{cases} \quad (12)$$

5.5 Simulations

For simplicity, the lake volume and glacial magnitude are assumed to be zero at the first time step (785 ky BP), as that time step corresponds to a warm climate phase. The values for the parameters given above are calibrated graphically to produce reasonable precipitation versus evaporation values. Several lake elevation histories were simulated by simulating the parameter values of the model probabilistically. The distributions for the parameters were lognormal with medians equal to the parameter values listed in Equations (6), (8), and (11). The simulations provide a variety of behaviors depending on the combination of parameters simulated.

A few common features are apparent in the simulated results. The largest lakes tend to occur at the times of Lake Bonneville, Little Valley, and Lava Creek, and the smallest 100 ky cycle lake occurs in δO^{18} cycle 14 (~533 ky BP), which matches the scientific record. When the simulated glaciation effects are small (R_{GA} and R_{GS}) , precipitation change in the model is due primarily to temperature change. In this case, large lakes form with few intermediate lakes, as the lake elevation history in the top graph in Figure 6 shows. When glaciation effects are larger, then large lakes tend to last longer, and intermediate lakes form, as the lake elevation history in the lower graph of Figure 6 shows.

The simulation models were then calibrated further by combining the simulated lake histories with sedimentation rates seen in sediment cores. Based on the results of this coarse model calibration, some assumptions are carried forward to the deep time model.

1. The 100 ky cycle in global temperature is a strong indicator of the return of a large lake. While not all simulations showed a lake returning to the Clive elevation in every 100 ky cycle (particularly δO^{18} cycle 14), the results were consistent enough to treat as systematic behavior for a heuristic model.
2. Intermediate lakes should be a part of the deep time simulation, because sedimentation rates did not calibrate well with simulations that produce only large lakes.
3. Intermediate lakes are more likely to occur in the later stages of the 100 ky cycle than in the early stages, primarily in conjunction with the slowly decreasing temperatures across the cycle (as opposed to the relatively rapid warming period that occurs at the end of a 100 ky cycle).

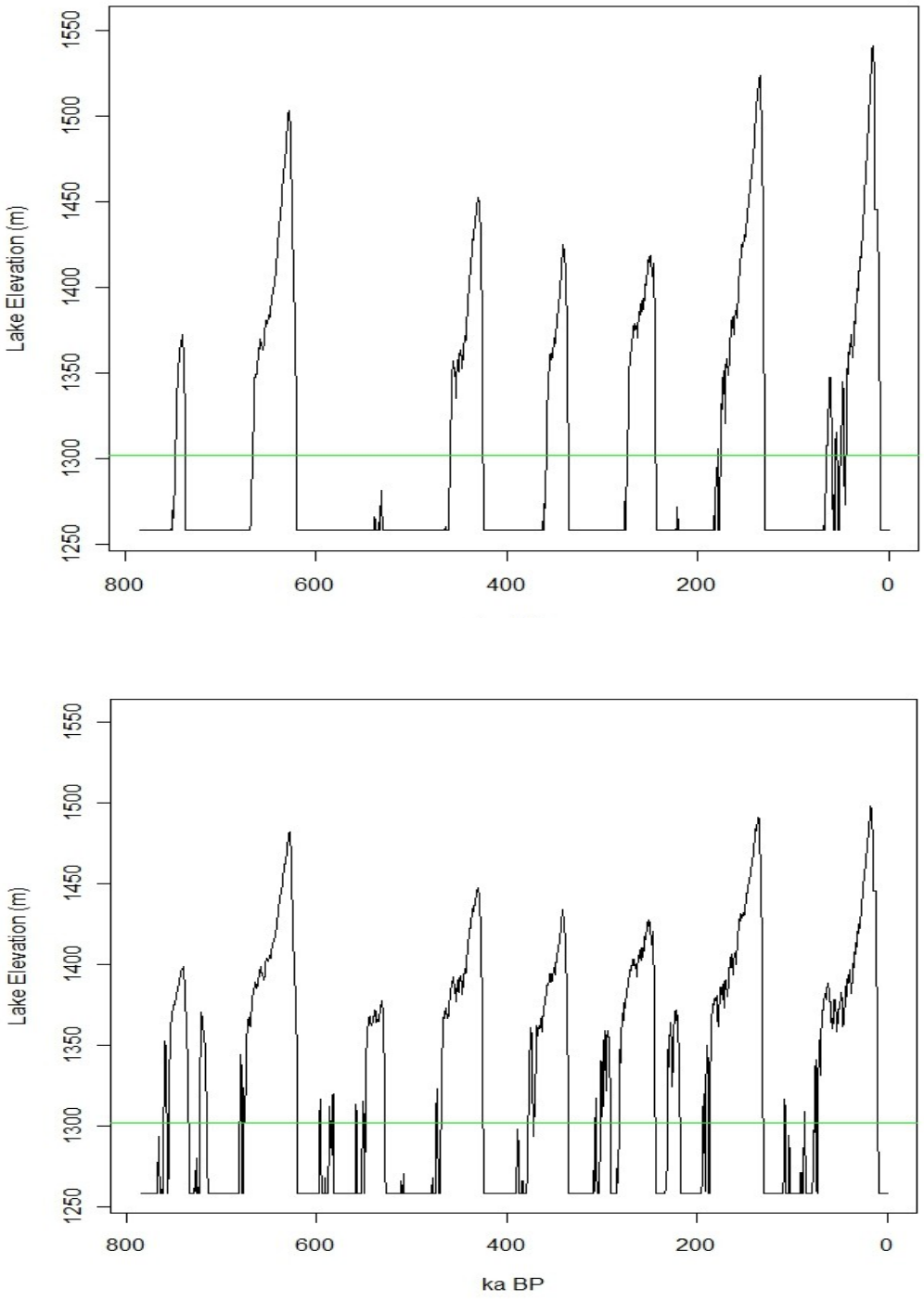

Figure 6. Two example simulated lake elevations as a function of time with Clive facility elevation represented by green line.

6.0 Modeling Approach for the PA Model

Depleted uranium, since it is primarily ^{238}U, has the property of becoming more radioactive with time, due to the ingrowth of decay products that were separated out during processing. The extremely long half-life of ^{238}U regulates this ingrowth, and the DU waste gets more radioactive over a period of about 2.1 My, and remains at that constant activity for billions more years. It is therefore of interest to understand, at least at a qualitative level, what the distant future (beyond 10,000 y) holds for the Clive facility. This deep time modeling includes what might be expected over those 2.1 My, in a stylized depiction of the effects of lakes returning to the Bonneville Basin.

With the return of the first lake that inundates the site, contaminant transport modeling within embankment ceases, and those above-ground portions of the facility are assumed to be obliterated and dispersed to varying degrees. While the lake is present, the dispersal of the site is coincident with dissolution of wastes into the water column, and their burial under fresh lacustrine sediments. Modeling the details of such processes is beyond the scope of this PA, but gross estimates of radionuclide concentrations in sediments and in the lake water are made. The long term concentrations of long-lived isotopes and their decay products are of primary concern. A detailed, precise model of temporal lake cycles is therefore not necessary—rather, a model that captures the major features of lake recurrence is indicated. The basic features of the heuristic lake formation model presented in Section 5.0 are abstracted into the Clive DU PA Model to construct a probabilistic model for the deep time model. The various components of this model are presented here.

6.1 Large Lakes

The 100 ky climate cycle is treated as a sufficiently robust effect to create a hypothetical lake that will reach the elevation of Clive each cycle. The exact time of occurrence is not a crucial parameter, due to the slowly-changing concentrations during deep time. Thus, the lake is set to be present at each 100 ky mark, with time beginning at 10 ky (the end of the quantitative performance period addressed for the quantitative dose assessment component of the PA).

There is little information on the amount of time that the Clive location has been under water. Lake Bonneville has been estimated to have been present at the elevation of Clive for a duration of approximately 16,000 years (Oviatt et al., 1999). Durations of older large lakes are unknown. Thus, a conservative choice was made to allow large lakes to endure an average of about 20,000 years (conservative in the sense that more waste will migrate into the water column). The occurrence time for each large lake is set by choosing a start time some number of years prior to the 100 ky mark. The start time is represented by a lognormal distribution with geometric mean of 14 ky prior to the 100 ky mark, and a geometric standard deviation of 1.2. The end time is represented by a lognormal distribution with geometric mean of 6 ky after the 100 ky mark, and a geometric standard deviation of 1.2. These distributions are depicted in Figure 7.

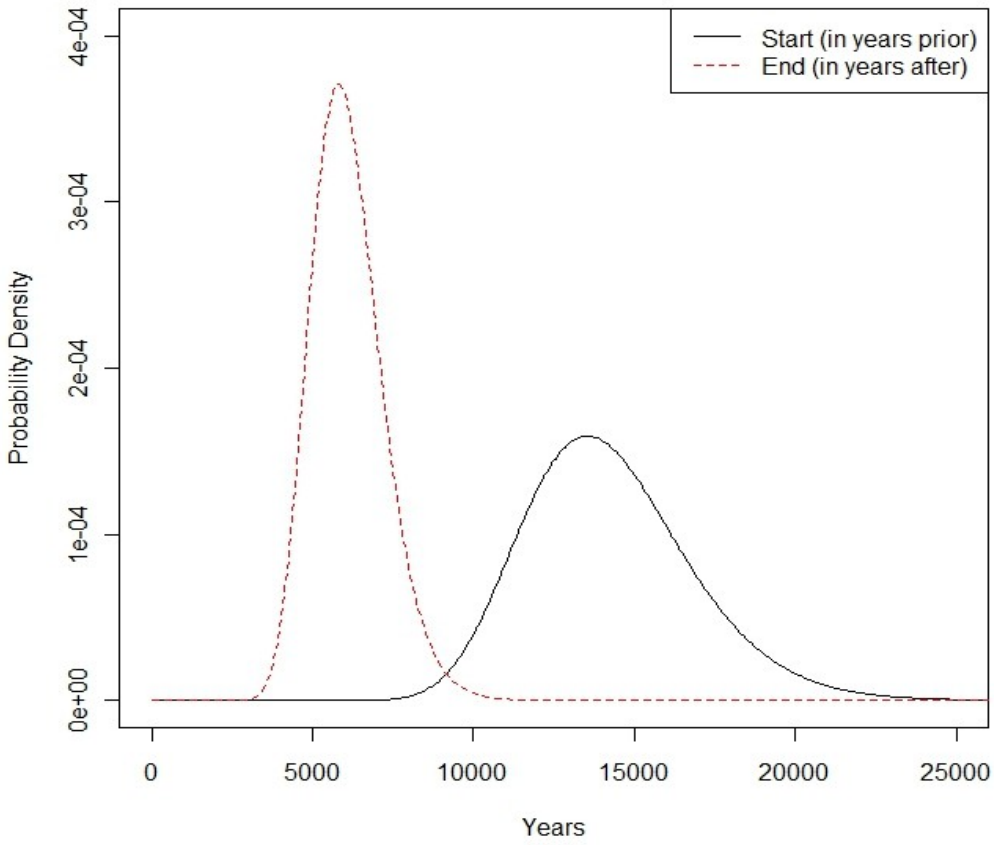

Figure 7. Probability density functions for the start and end times for a large lake, in years prior to the 100 ky mark and years after the 100 ky mark, respectively.

6.2 Intermediate Lakes

Intermediate lakes are modeled as potentially occurring anytime between large lake events. In order to reflect the slow decrease in temperature over the 100 ky cycle, the occurrence time for intermediate lakes is modeled as a Poisson process with a rate that increases linearly over the cycle time, from a rate of 0 to 7.5 lakes per 100 ky. This process produces an average of about 3 intermediate lakes per 100 ky. There is little recorded basis for this number, but it matches reasonably with the heuristic model of Section 5.0, and was chosen so that long-term sedimentation rates matched the average from previous lake cycles, as estimated from the sedimentation of individual lakes developed in Section 6.3.

There is virtually no information for the duration of intermediate lakes, due to the high mixing rate of shallow lake sediments, which makes dating of times within a single stratigraphic layer of a shallow lake sediment core extremely difficult. Thus, a distribution was chosen to roughly

calibrate with the heuristic model: lognormal with geometric mean of 500 y and geometric standard deviation of 1.5.

6.3 Sedimentation Rates

Deposition of material in the area of the Clive facility is a continuous process that occurs during shallow, intermediate and large lake periods. During shallow lake periods, as observed in present-day conditions, air deposition is the primary mechanism. However, air deposition is not evident in sediment cores, presumably because of mixing with lake-derived sediments. Intermediate lake sediments include both terrigenous and oolitic content, with the ratio probably depending on the size and duration of the lake. Any airborne deposition is mixed with the sediments from the first returning lake. However, since air deposition layers are not evident in the sediment cores, the model effectively includes combines material from air deposition with material from lake sediments. The mixing probably occurs with an intermediate lake, which is likely to be the first lake after the inter-glacial period. This also suggests that there is a mixing depth associated with each lake recurrence. However, the mixing process itself makes it very difficult to associate mixing depth with the different layers in the sediment cores.

Large lakes, instead, have similar deposition rates to intermediate lakes in the transgressive and regressive phases, but a different, slower, rate when the lake is large enough that the dominant sedimentation is carbonate in nature. Records from the sediments cores are able to distinguish between layers associated with intermediate lakes that might include mixing of material from air deposition, terrigenous lake deposition, and oolitic lake deposition, and those associated with a stable large lake that are dominated instead by carbonate deposition.

Based on the available data from the sediment cores, sedimentation rates are expected to be higher when lake water is shallow than when a deep lake covers the Clive site.

For large lakes, a sedimentation rate is modeled as a lognormal distribution with geometric mean of 120 mm/ky and geometric standard deviation of 1.2, a distribution that covers the range of observed values for deep lakes in Section 3.4. This distribution is represented in Figure 8. The sedimentation rate is applied for the simulated duration of the large lake. In addition, sedimentation is added at the beginning of the lake cycle as well as the end that represents the shallow phase of the transgressive and regressive lakes. This additional sediment mimics the behavior of an intermediate lake.

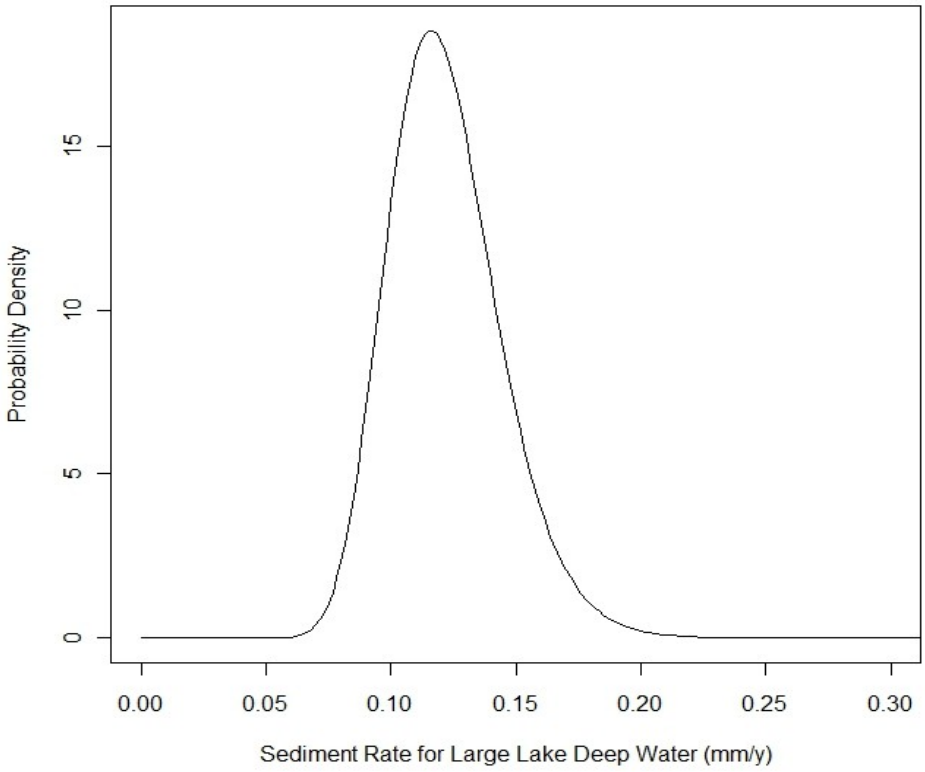

Figure 8. Probability density function for sedimentation rate for the deep-water phase of a large lake.

For intermediate lakes (and shallow phases of large lakes), there is high likelihood of multiple short-term transgressions and regressions with respect to the elevation of Clive. For example, the Clive pit wall (Appendix A) shows three distinct lakes after the deep-water phase of Lake Bonneville and three distinct lakes prior to the deep-water phase of Lake Bonneville. Without further study of a sediment core at the site, including dating, it is impossible to determine if these distinct lakes were separated by a few years or a few hundred years; i.e., whether they are distinct lake events or simply part of the transgression and regression of Lake Bonneville. However, based on current behavior of the lake, some year-to-year variation in the lake elevation occurs, in addition to the longer-term trends in lake elevation.

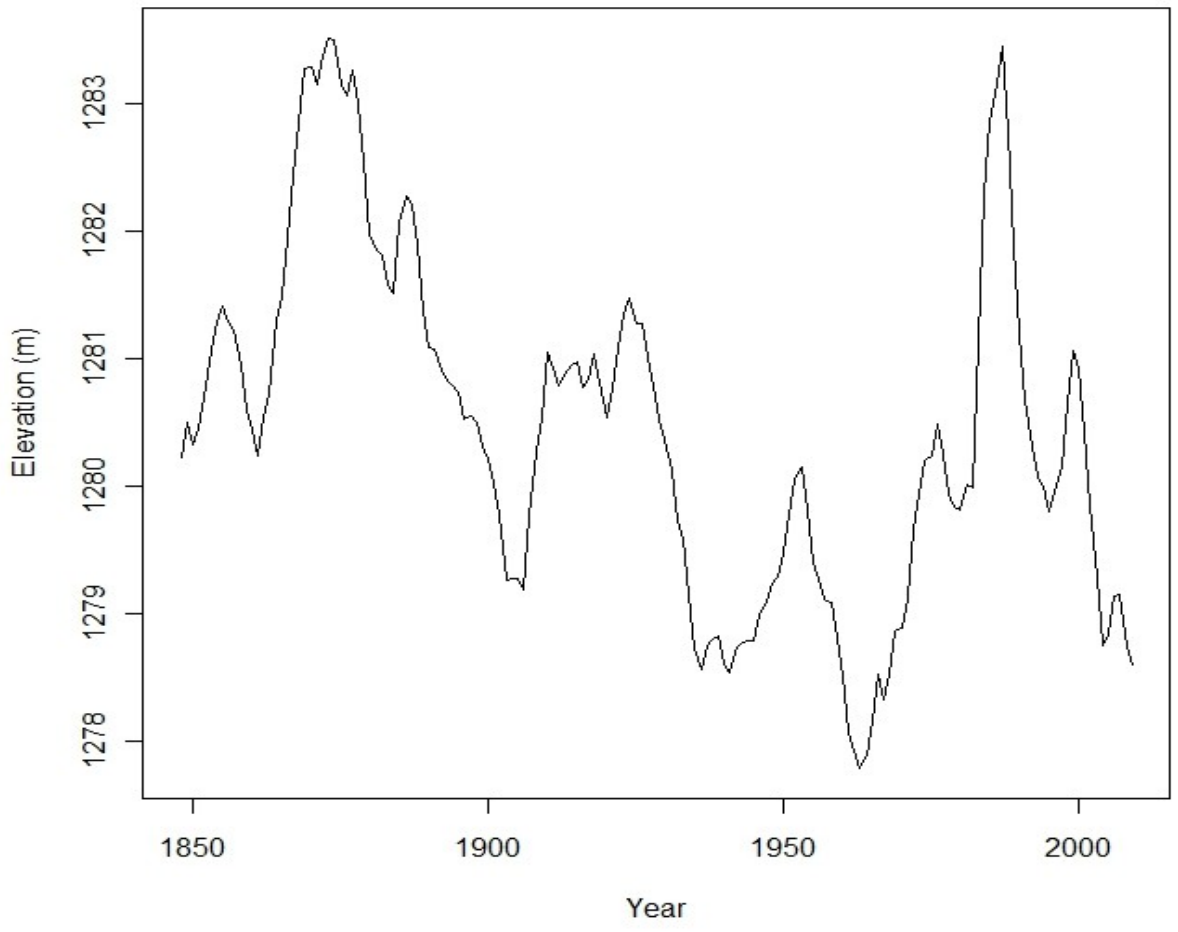

Figure 9. Historical elevations of the Great Salt Lake.

Another heuristic model was constructed to evaluate the effect of the short-term variation. The lake elevation for the years 1848 through 2009 is available from the Saltair Boat Harbor monitoring site (USGS, 2001), as shown in Figure 9. The year-to-year variation can be modeled as a second-order autoregressive process AR(2) (Brockwell and Davis, 1991), a model that accounts for year to year temporal correlations in the variation. An AR(2) process was simulated and added to a transgressive or regressive curve based on the simplified model of Section 5.0. Examples of these simulations are given in Figure 10. As can be seen in the figure, the short-term variation can result in lakes covering the Clive elevation for a short time, receding for a short time, then rising again, often multiple times in a single transgression. A similar simulation was performed for simulated intermediate duration lakes as well. The transgressive and regressive phases of a large lake behaved similarly to the intermediate lakes in that they averaged about 4 total occurrences of "mini-lakes;" i.e., occurrences of a rise above the elevation of Clive followed by a drop below for at least one year.

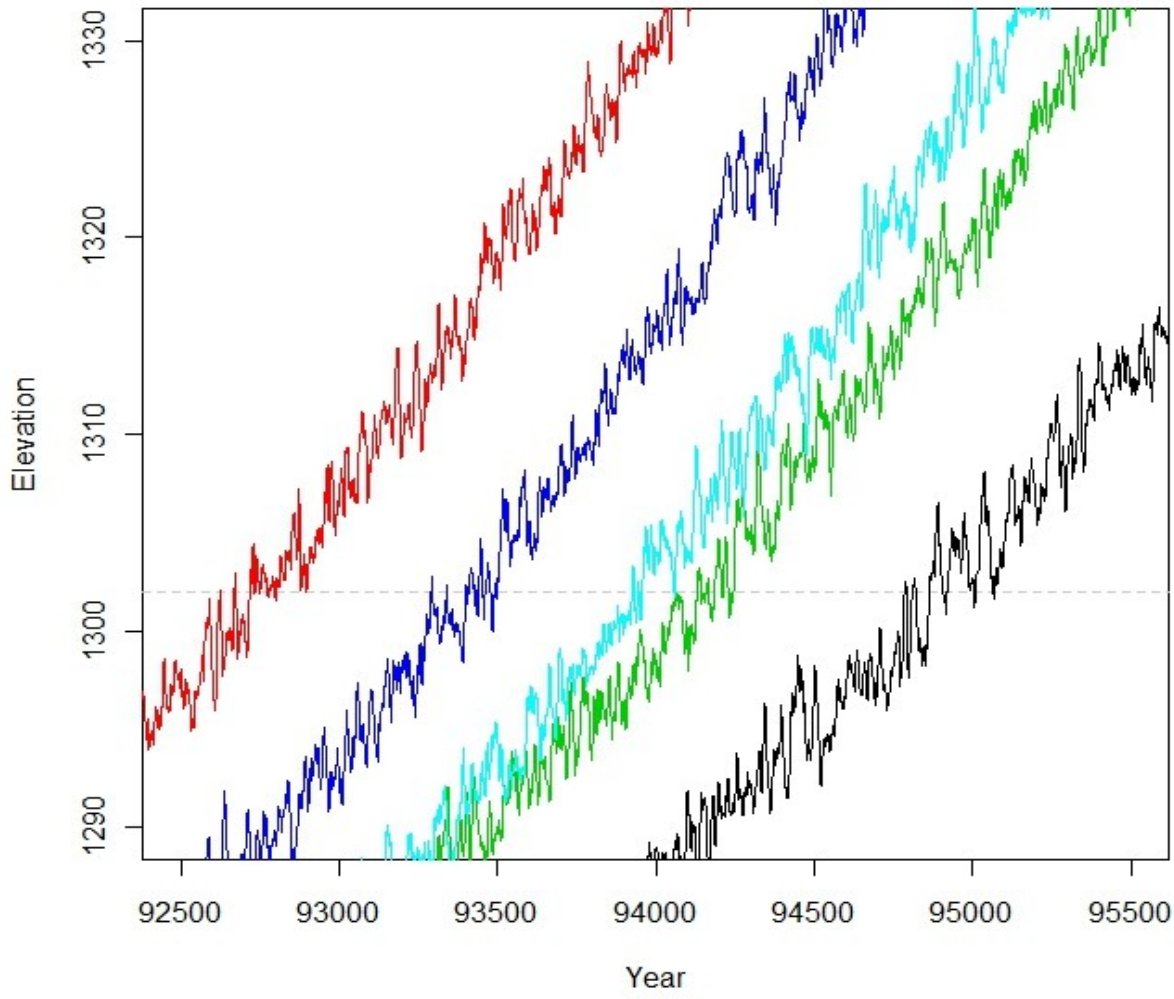

Figure 10. Simulated transgressions of a large lake including short-term variation.

The distribution for sedimentation rates for intermediate lakes was thus based on simulating this multiple mini-lake behavior. First, the number of mini-lakes associated with an intermediate lake was simulated as 1 plus a Poisson random variable with rate 3 (the "plus 1" being necessary to ensure at least one event in order to match the definition of a lake event). The sedimentation for each mini-lake was simulated according to a distribution based on the information for mini-lakes in the Clive pit wall, using the six distinct "mini-lakes" in Table 3 (all layers except the one that corresponds to the deep-water phase of Lake Bonneville), which resulted in a lognormal distribution with geometric mean 0.75 m and geometric standard deviation 1.4. The total sedimentation for all mini-lakes associated with a simulated intermediate lake cycle were then added together to produce a total sedimentation for the intermediate lake. A distribution was

then based on all simulated intermediate lake sedimentations, a lognormal distribution with geometric mean 2.82 m and geometric standard deviation 1.71, as presented in Figure 11.

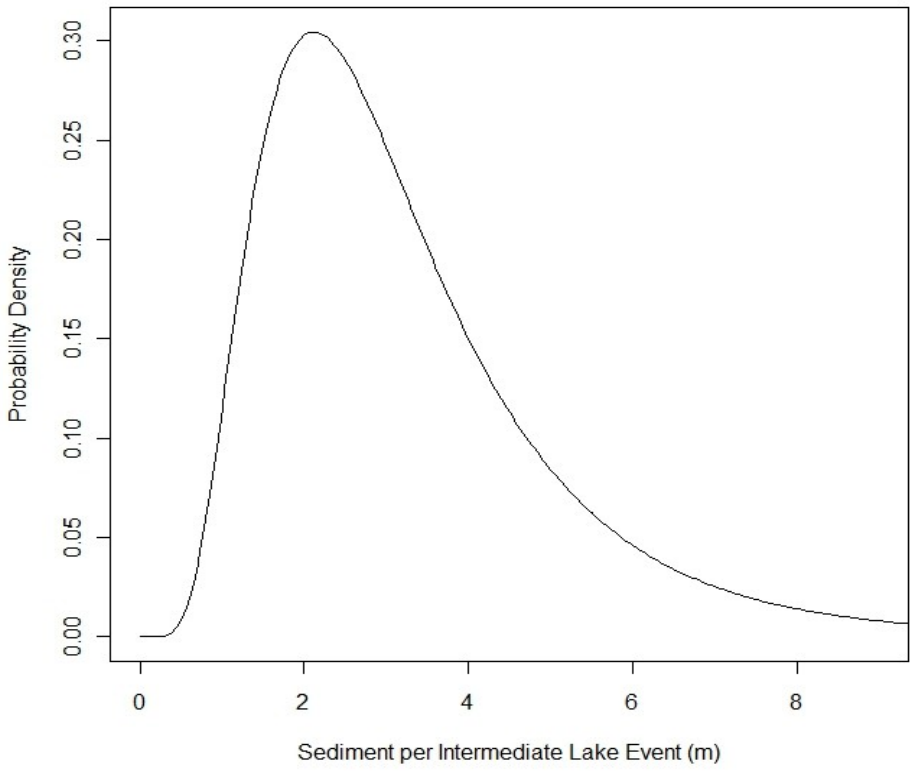

Figure 11. Probability density function for the total sediment thickness associated with an intermediate lake (or the transgressive of regressive phase of a large lake).

The net effect is that the sedimentation rates are on the order of 15-20 m per glacial cycle (100 ky). For the duration of the model (2.1 My), this implies sedimentation of more than 300 m. The Basin and Range system accommodates this rate of sedimentation because it is an extensional system. That is, sedimentation continues as the basins expand and subside, maintaining similar elevation in each cycle.

6.4 Destruction of the Waste Embankment

A scenario involving destruction of the Energy*Solutions* waste embankment was modeled. That is, intermediate lakes are assumed to be sufficiently large that wave energy from such a lake will destroy the above-ground portions of the DU waste cell. In effect, conceptually this differentiates a shallow lake from an intermediate lake. The precise elevation needed for this to happen is not considered for the model, but the intermediate lakes that occur in the model are intended to match this definition.

The first lake in the time period assessed is likely to be an intermediate lake but can be a large lake. The destruction is handled equivalently in either case, as the conceptual model treats the transgressive phase of a large lake as behaving similarly to an intermediate lake.

The mass of material that is within the embankment above the grade of the surrounding land is assumed to be dispersed by wave action. This volume of above grade material in the embankment, including DU waste, fill material and cap material, is assumed to be mixed with the sediment associated with the intermediate lake, and subsequently spread across the dispersal area. It is assumed that the volume of material below grade is simply covered by sediment (i.e., sediment that is mixed with the above-grade waste). However, the DU waste included in the below grade layers is also included in the dispersed waste. That is, the total volume dispersed is the volume above grade, but the total mass of waste dispersed is the entirety of the DU waste that is still contained in the disposal system. Including the below grade DU waste is clearly conservative, but is a simplification that has been taken in this model. Some DU waste could be emplaced below grade, and, if not, then a diffusion gradient will cause mixing with below grade sedimentary layers. That is, some DU waste will move down, but, instead, all of the DU waste still in the disposal system when a lake arrives is made available to lake-related transport processes.

A probability distribution for the area across which the embankment material is spread was developed based on an assumption that a destroyed site would be flattened by wave action. The probability distribution for the area was developed so that the area represents:

- at a minimum, an area that would be covered if the volume of the above-grade material were spread out to a height of 1 m, and
- for a geometric mean, an area that would be covered if the volume of the above-grade material were spread out to a height of 10 cm.

The exact distribution for area depends on the precise volume of the above-grade embankment at the time of destruction, but a lognormal distribution with geometric standard deviation 1.5, and geometric mean defined as above. A typical probability density function is shown in Figure 12.

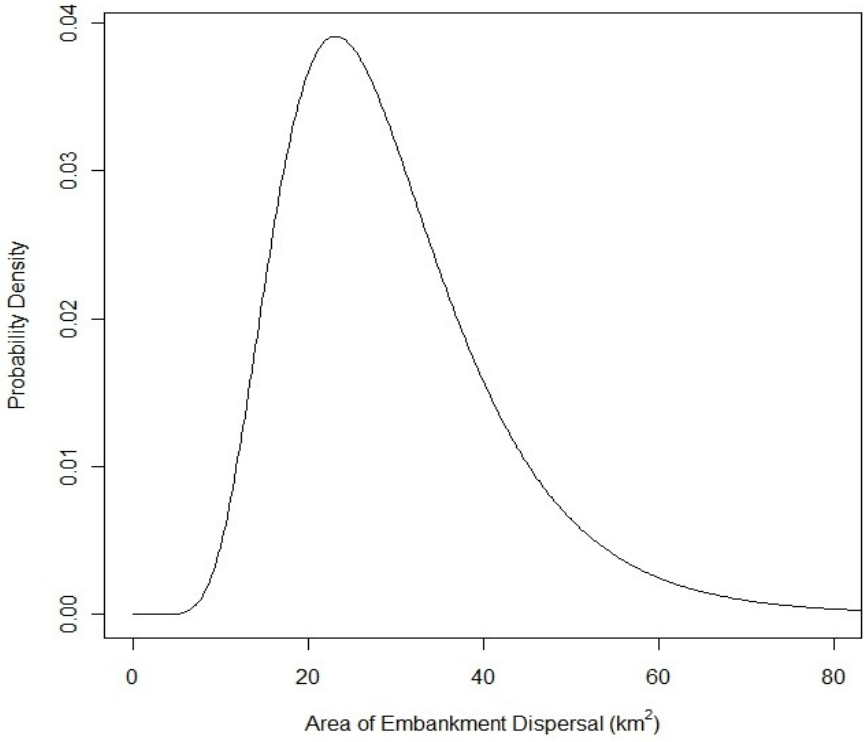

Figure 12. Probability density function for the area over which the waste embankment is dispersed upon destruction.

6.5 Reported Results

As a qualitative assessment, the deep time model does not attempt to calculate dose to human receptors, but rather to simply characterize the fate of the bulk of the waste. After the destruction of the waste embankment, the bulk of the waste will be mixed with sediments and dissolved in lake water.

Upon destruction of the waste embankment, the PA model switches modes from detailed modeling of waste transport through air dispersion, biotic uptake, groundwater flow, and other processes to a much simpler model. These processes are expected to have minor effects on transport once the waste is mixed into a sedimentary layer. The only processes that are modeled after destruction are lake recurrence, radioactive decay and ingrowth, mixing of waste with sediment, and dissolution of waste in lake water.

6.5.1 Concentration in Sediment

Concentration in sediment is initially calculated under the assumption that all of the waste that was above grade in the waste embankment is mixed evenly with the sediment that forms with the

lake that destroys the site. Concentration in sediment is then calculated as the total radioactivity in the dispersed site divided by the volume of material into which the waste is dispersed:

$$C_{sediment} = \frac{R_{above\ grade}}{V_{material\ above\ grade} + V_{sediment}} . \quad (13)$$

The volume of sediment is the depth of sediment associated with the lake times the area over which the waste is dispersed.

This calculation assumes that there is no loss of waste from the initial dispersal region. While this calculation is counter to the modeling of dissolution into the water column of the lake, a simplifying assumption is that all waste that dissolves into the lake precipitates back into the sediment upon recession of the lake.

The concentrations in sediment are modeled as remaining constant, except for decay and ingrowth, until a new lake occurs. When a new lake occurs, the sedimentation associated with that lake is likely to mix with some portion of the top layer of existing sediment and leave the lower layers of the sediment buried beneath. However, for simplicity, a conservative approach is to mix all sediment that contains waste, effectively keeping some portion of the waste near-surface. The concentration is again the total radioactivity divided by the volume containing waste; however, the volume that contains waste now has the additional volume of sediment associated with the current lake.

6.5.2 Radioactivity in Lake Water

When lake water is present, radionuclides will partition between the water phase and the solid phase depending on element-specific solubility and sorption properties. Radionuclides remaining in the pore water will then diffuse into the lake. The waste is likely to mix over a wide area of the lake, and many forms of the waste are likely to bind with carbonate ions in the water, ultimately precipitating into carbonate sediments. As a conservative assumption, upon recession of the lake, all waste is assumed to precipitate back into the *local* sediments – meaning that all radionuclides in the sediments modeled in Section 6.5.1 are returned to the sediments when the lake regresses.

When a lake returns, the sediments are assumed to be fully saturated, and thus radionuclides are partitioned from the sediment to the pore water within the sediment using the same partitioning coefficients (K_d) used for other sedimentary soils in the model. An important difference between the assumptions for this model and the model for transport from the embankment in the 10 ky model is that the lake water is assigned a different solubility for uranium for the deep time assessment. While solubilities for all other radionuclides remain the same, the solubility for uranium is reduced to that of U_3O_8 which is significantly lower than other forms of uranium originally present in the waste. This change in solubility for uranium is adopted because it is expected that by the time the first lake returns, all soluble uranium forms (UO_2 and UO_3) will have been leached from the embankment into the shallow aquifer.

As radionuclides associated with the sediments dissolve into the pore water, they diffuse into the lake water using a constant flux model based on Fick's first law, with the following assumptions:

- There is an interface boundary layer of 0.1 m above the sediment, above which the water has a radionuclide concentration of 0. In fact, there will be some buildup of concentration

as a radionuclide migrates into the water, but it will diffuse into the lake. It is conservative to assume a zero concentration, which results in the highest possible flux.

- The concentration in sediment remains constant over the deep time period. The sediment concentration should in fact diminish over time if enough mass is migrated into the water, but for simplicity, the sediment concentrations are kept constant across time steps.

The activity that is migrated to water is then:

$$R = \Delta T \cdot D_m \cdot \frac{C_V}{0.1\,\text{m}} \cdot A\,, \tag{14}$$

where

- R is radioactivity (Bq or pCi),
- ΔT is the time step (in s),
- D_m is the diffusion coefficient (m^2/s),
- C_V is the concentration in sediment (Bq/m^3 or pCi/m^3), and
- A is the area of the sediment that contains that concentration of waste (the dispersed area, in m^2).

Concentration in lake water is then calculated based on the conservative assumption that the radioactive material does not dilute in a large basin of the lake but rather remains in the water column immediately above the dispersed area. That is, the concentration is calculated as:

$$C = \frac{R}{D \cdot A} \tag{15}$$

where

- C is concentration (Bq/L),
- R is the radioactivity (Bq),
- A is the area of the sediment that contains waste (the dispersed area, in m^2), and
- D is the depth of the lake (m).

There is an insufficient record of lake elevations to construct a data-based distribution for lake depth. Thus, the distributions for lake depth are chosen based on the conceptual model. Depths for intermediate lakes have a Beta distribution with mean 30 m, standard deviation 18 m, minimum of 0 m, and maximum of 100 m. Depths for large lakes have a Beta distribution with mean 150 m, standard deviation 20 m, minimum of 100 m, and maximum of 200 m.

For intermediate lakes, the time step is the duration of the intermediate lake. For large lakes, the lake may exist for several time steps in the GoldSim model, in which case the time step is the portion of the time step for which the lake is present. When large lakes cross multiple time steps, the concentration in sediment is allowed to change between time steps (only due to decay and ingrowth), and the activity in the lake water is accumulated over those time steps.

7.0 References

Archer, D. and A. Ganopolski, 2005. A movable trigger: fossil fuel CO_2 and the onset of the next glaciation. *Geochemistry, Geophysics, Geosystems*, 6(5), doi:10.1029/2004GC000891.

Asmerom, Y., Polyak, V. J., and S. J. Burns, 2010. Variable winter moisture in the southwestern United States linked to rapid glacial climate shifts. *Nature Geoscience*, 3, 114-117.

Berger, A., 1988. Milankovitch theory and climate. *Reviews of Geophysics*, 26(4): 624-657.

Berger, A. and M. F. Loutre, 2002. An exceptionally long interglacial ahead? *Science*, 297: 1287-1288.

Brimhall W. H. and L. B. Merritt, 1981. The geology of Utah Lake – implications for resource management. *Great Basin Naturalist Memoirs*, 5: 24-42.

Brockwell, P.J. and R.A. Davis, 1991. *Time Series: Theory and Methods*. Springer-Verlag, New York, NY.

Clark, P. U., Dyke, A. S., Shakun, J. D., Carlson, A. E., Clark, J., Wohlfarth, B., Mitrovica, J. X., Hostetler, S. W., and A. M. McCabe, 2009. The Last Glacial Maximum. *Science*, 325: 710-714.

Currey, D.R., G. Atwood, and D.R. Mabey, *Map 73 Major Levels of Great Salt Lake and Lake Bonneville*, Utah Geological and Mineral Survey, Salt Lake City, UT, May 1984

Driscoll, N. W. and G. H. Haug, 1998. A short circuit in thermohaline circulation: a cause for Northern Hemisphere glaciation. *Science*, 282: 436-438.

Einselle, G. and M. Hinderer, 1997. Terrestrial sediment yield and the lifetimes of reservoirs, lakes, and larger basins. *Geologische Rundschau*, 86: 288-310.

EPICA community members, 2004. Eight glacial cycles from an Antarctic ice core. *Nature*, 429: 623-628.

GTG (GoldSim Technology Group), 2011. *GoldSim: Monte Carlo Simulation Software for Decision and Risk Analysis*, http://www.goldsim.com

Hart, W. S., Quade, J., Madsen, D. B., Kaufmann, D. S., and C. G. Oviatt, 2004. The $^{87}Sr/^{86}Sr$ Ratios of Lacustrine Carbonates and Lake-level History of the Bonneville Paleolake System. *GSA Bulletin*, 116: 1107-1119.

Haug, G. H. and R. Tiedemann, 1998. Effect of the Formation of the Isthmus of Panama on Atlantic Ocean Thermohaline Circulation. *Nature*, 393: 673-676.

Hays, J. D., Imbire, J., and N. J. Shackleton, 1976. Variations in the Earth's Orbit: Pacemaker of the Ice Ages. *Science*, 194: 1121-1132.

Jouzel, J., Masson-Delmotte, V., Cattani, O., Dreyfus, G., *et al.*, 2007. Orbital and millennial Antarctic climate variability over the past 800,000 years. *Science*, 317: 793-796.

Kukla, G. J., R. K. Matthews, J. M. Mitchell Jr., *Quat. Res.* **2**, 261 (1972)

Lisiecki, L. E. and M. E. Raymo, 2005. A Pliocene-Pleistocene stack of 57 globally distributed benthic $\delta^{18}O$ records. *Paleoceanography*, 20, PA1003, doi:10.1029/2004PA001071.

Link, P. K., Kaufmann, D. S., and Thackray, G. D., 1999. Field guide to Pleistocene lakes Thatcher and Bonneville and the Bonneville flood, southeastern Idaho, *In*: Hughes S. S. and G. D Thackray (eds.), *Guidebook to the Geology of Eastern Idaho*, Idaho Museum of Natural History, p. 251-266.

Masson-Delmotte, V., Stenni, B., Pol, K., Braconnot, P., *et al.*, 2010. EPICA Dome C record of glacial and interglacial intensities. *Quaternary Science Reviews*, 29: 113-128.

Matsurba, Y. and A. D. Howard, 2009. A spatially explicit model of runoff, evaporation, and lake extent: application to modern and late Pleistocene lakes in the Great Basin region, western United States. *Water Resources Research*, 45, W06425, doi:10.1029/2007WR005953.

Oviatt, C. G. and W. P. Nash, 1989. Late Pleistocene basaltic ash and volcanic eruptions in the Bonneville basin, Utah. *Geological Society of America Bulletin*, 101: 292-303.

Oviatt, C. G., McCoy, W. D., and Nash, W. P., 1994. Sequence stratigraphy of lacustrine deposits: a Quaternary example from the Bonneville basin, Utah. *Geological Society of America Bulletin,* 106: 133-144.

Oviatt, C. G., 1997. Lake Bonneville fluctuations and global climate change. *Geology*, 25(2): 155-158.

Oviatt, C. G., Thompson, R. S., Kauffman, D. S., Bright, J., and R. M. Forester, 1999. Reinterpretation of the Burmester core, Bonneville Basin, Utah. *Quaternary Research*, 52: 180-184.

Oviatt, C. G., D. M. Miller, J. P. McGeehin, C. Zachary, and S. Mahan, 2005. The Younger Dryas phase of Great Salt Lake, Utah, USA, *Palaeogeography, Palaeoclimatology, Palaeoecology*, 219: 263-284.

Paillard, D., 2001. Glacial cycles: toward a new paradigm. *Reviews of Geophysics*, 39(3): 325-346.

Paillard, D., 2006. What drives the Ice Age cycle? *Science*, 313: 455-456.

United States Geological Survey (USGS), 2001. National Water Information System data (Water Data for the Nation), accessed December, 2010 URL: http://waterdata.usgs.gov/

Appendix A

A.1 Clive Pit Wall Interpretation (C. G. Oviatt, unpublished data)

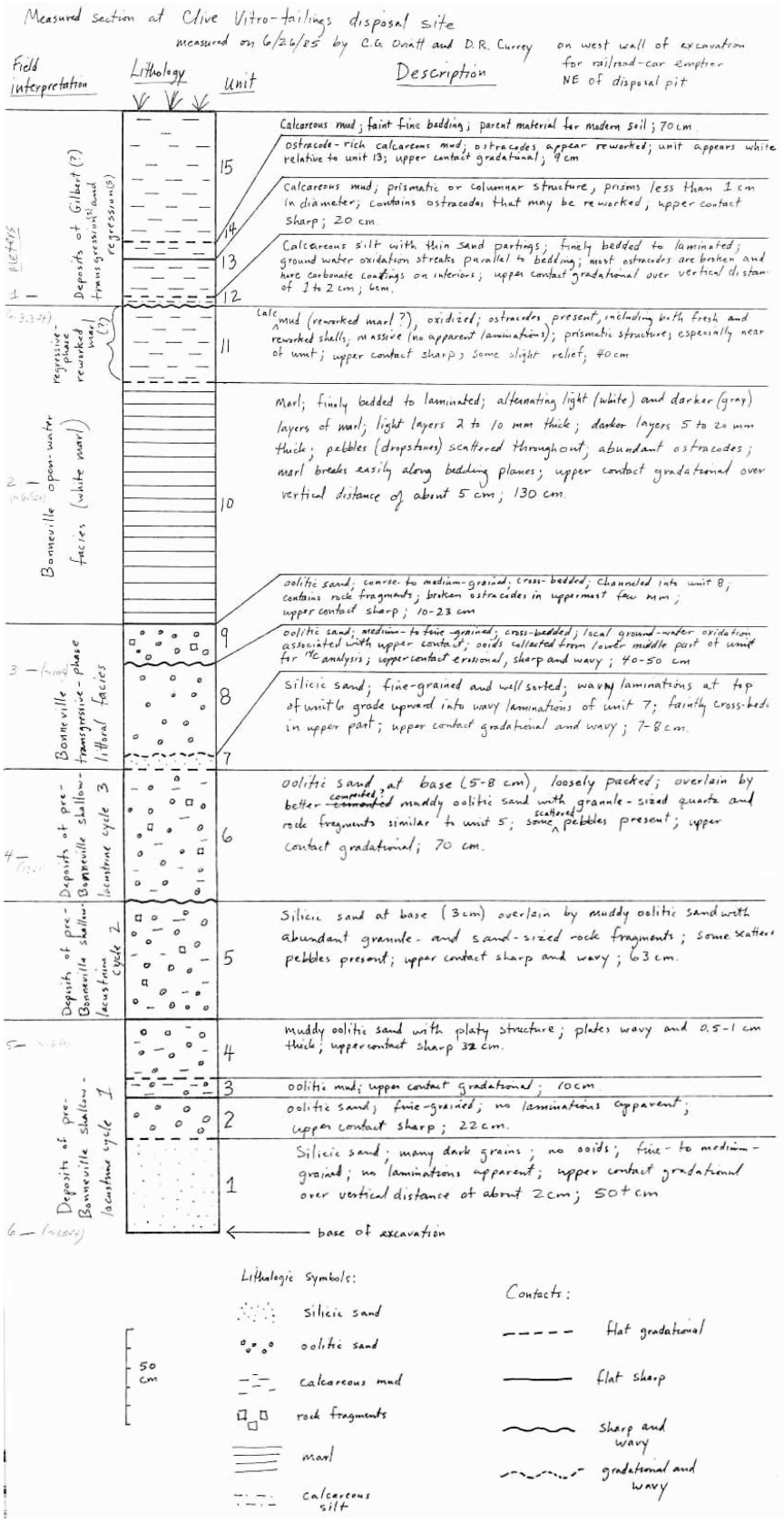
Measured section at Clive Vitro-tailings disposal site
measured on 6/26/85 by C.G. Oviatt and D.R. Currey
on west wall of excavation for railroad-car emptier NE of disposal pit
Field interpretation
Lithology
Unit
Description
Deposits of Gilbert (?) transgressive(?) and regressive(?)
Bonneville open-water facies (white marl)
regressive-phase reworked marl (?)
Bonneville transgressive-phase littoral facies
Deposits of pre-Bonneville shallow-lacustrine cycle 3
Deposits of pre-Bonneville shallow-lacustrine cycle 2
Deposits of pre-Bonneville shallow-lacustrine cycle 1
15 Calcareous mud; faint fine bedding; parent material for modern soil; 70 cm.
Ostracode-rich calcareous mud; ostracodes appear reworked; unit appears white relative to unit 13; upper contact gradational; 9 cm
14 Calcareous mud; prismatic or columnar structure, prisms less than 1 cm in diameter; contains ostracodes that may be reworked; upper contact sharp; 20 cm
13 Calcareous silt with thin sand partings; finely bedded to laminated; ground water oxidation streaks parallel to bedding; most ostracodes are broken and have carbonate coatings on interiors; upper contact gradational over vertical distance of 1 to 2 cm; 64 cm.
12
11 Calc mud (reworked marl?), oxidized; ostracodes present, including both fresh and reworked shells; massive (no apparent laminations); prismatic structure, especially near of unit; upper contact sharp; some slight relief; 40 cm
10 Marl; finely bedded to laminated; alternating light (white) and darker (gray) layers of marl; light layers 2 to 10 mm thick; darker layers 5 to 20 mm thick; pebbles (dropstones) scattered throughout; abundant ostracodes; marl breaks easily along bedding planes; upper contact gradational over vertical distance of about 5 cm; 130 cm.
9 oolitic sand; medium- to fine-grained; cross-bedded; local ground-water oxidation associated with upper contact; ooids collected from lower middle part of unit for 14C analysis; upper contact erosional, sharp and wavy; 40-50 cm
8 Silicic sand; fine-grained and well sorted; wavy laminations at top of unit 8 grade upward into wavy laminations of unit 7; faintly cross-bedded in upper part; upper contact gradational and wavy; 7-8 cm.
7
6 oolitic sand at base (5-8 cm), loosely packed; overlain by better cemented muddy oolitic sand with granule-sized quartz and rock fragments similar to unit 5; some scattered pebbles present; upper contact gradational; 70 cm.
5 Silicic sand at base (3 cm) overlain by muddy oolitic sand with abundant granule- and sand-sized rock fragments; some scattered pebbles present; upper contact sharp and wavy; 63 cm.
4 muddy oolitic sand with platy structure; plates wavy and 0.5-1 cm thick; upper contact sharp 32 cm.
3 oolitic mud; upper contact gradational; 10 cm.
2 oolitic sand; fine-grained; no laminations apparent; upper contact sharp; 22 cm.
1 Silicic sand; many dark grains; no ooids; fine- to medium-grained; no laminations apparent; upper contact gradational over vertical distance of about 2 cm; 50+ cm
base of excavation
50 cm
Lithologic symbols:
Silicic sand
oolitic sand
calcareous mud
rock fragments
marl
calcareous silt
Contacts:
flat gradational
flat sharp
sharp and wavy
gradational and wavy

Appendix B

B.1 Knolls Core Interpretation (C. G. Oviatt, unpublished data)

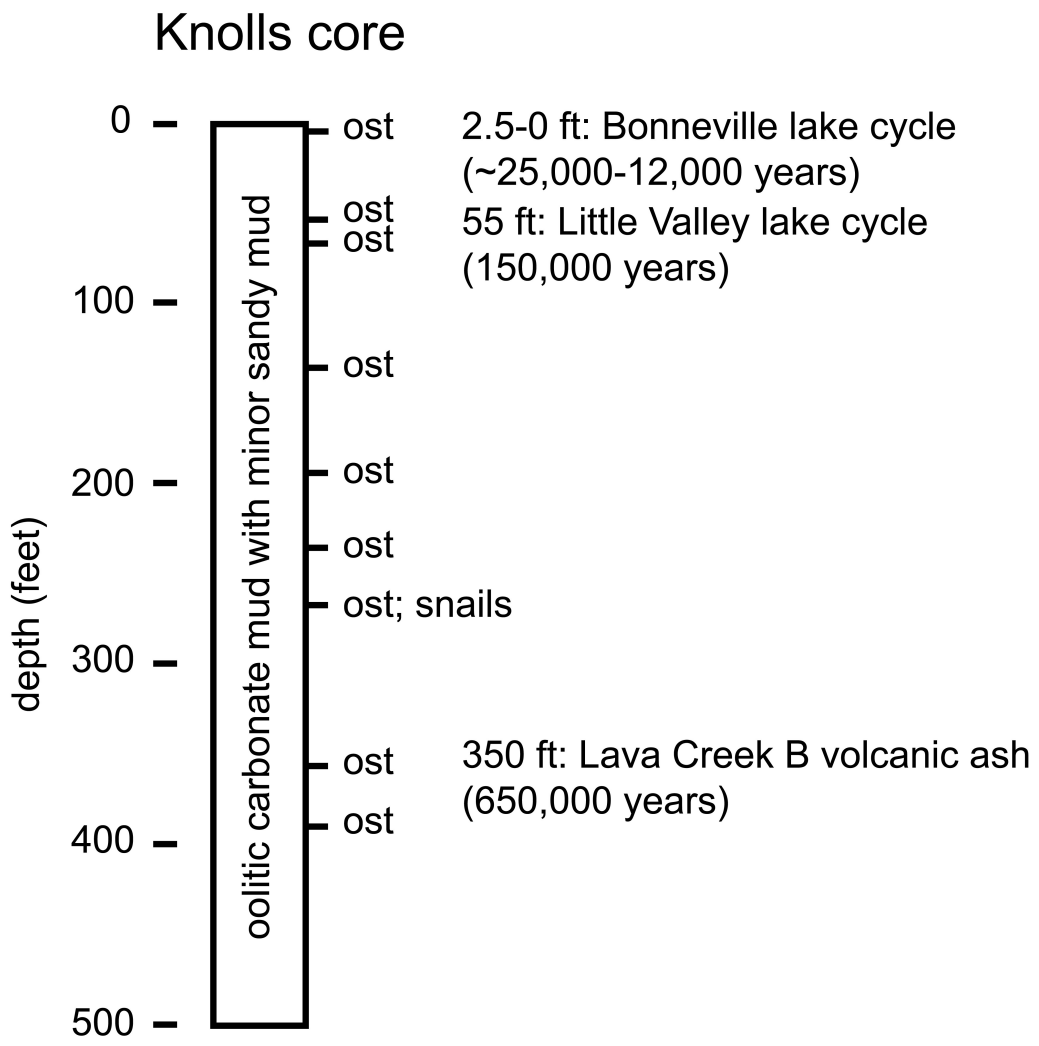

ost = ostracodes (fresh water of a lake or marsh)
snails indicate shallow fresh water

Neptune and Company Inc.

June 1, 2011 Report for EnergySolutions

Clive DU PA Model, version 1

Appendix 14

Development of Probability Distributions

Fitting Probability Distributions

1 June 2011

Prepared by

Neptune and Company, Inc.

This page is intentionally blank, aside from this statement.

CONTENTS

FIGURES

TABLES

1.0 Introduction

In the Clive DU PA model, most of the input parameters are treated as probabilistic. The term *parameter* is used to refer to any numerical quantity in the PA model. his document provides an overview of the approach to construction of probability distributions for parameters.

Note that the term parameter is used here because it is in common use in the PA and modeling community. However, since probability distributions are applied to these parameters, from a statistics perspective they should be termed variables, or even random variables.

2.0 Types of Parameters

Parameters of the PA model are mathematical constructs that represent a variety of different concepts. Assignment of a probabilistic distribution must consider the use of the parameter within the PA model.

The probabilistic behavior associated with the input may also represent a variety of different concepts. The variation may represent aleatory variability, epistemic uncertainty, or some combination of those two. The appropriate probabilistic representation for the parameter can differ greatly depending on the appropriate representation.

- Epistemic uncertainty represents lack of knowledge about the true value of the parameter. Hypothetically, data could be collected to reduce the uncertainty, which would then result in a distribution with less variation.
- Aleatory variability represents inherent randomness in the "outcome" of the parameter. The outcome may represent changes through time or space or the characteristics of individual members of a population. Given assumptions about the population or modeling assumptions underlying the parameter, further information gathering does not reduce aleatory variability. Changing the modeling or population assumptions can lead to a change in the variability (e.g. changing the spatial extent a soil porosity distribution is applied to).

Many parameters in the Clive DU PA contain at least some element of both epistemic uncertainty and aleatory variability, though the probabilistic construction is typically based on assuming one or the other. Although there are exceptions, for the most part, distributions developed assuming aleatory uncertainty are contained in the individual dose model (see the Dose Assessment white paper). Most other input distributions are developed based on epistemic uncertainty, although as noted, most parameters contain some element of both. It is often difficult to completely separate epistemic and aleatory uncertainty. Another, and perhaps better, way of framing the distinction is with respect to the spatial and/or temporal scale of each parameter. Most parameters in the Clive DU PA model represent long time frames or large areas, and the distribution of the average of the trait of interest is needed for the model. These cases are aligned more with the concept of epistemic uncertainty. However, the dose parameters are specific to individuals, representing points space, and time frames that are specific to the available data. These cases are aligned more with the concept of aleatory variability. In effect, in this model, epistemic uncertainty, upscaling and distribution of the average are related, and aleatory variability, and distribution of the data are related without the need for upscaling.

These are important distinctions in the development of complex PA models, not just for model building purposes, but also for model interpretation and comparison with performance objectives. The PA model is constructed so that raw output doses are provided for each hypothetical individual included in the model, in each year of the model. Typically, risk assessment is based on the average risk. In that context, the average dose to the individuals in each year is the relevant statistic for each receptor group (ranchers, hunters, OHV enthusiasts). Since 5,000 simulations are performed, there are 5,000 estimates of the average dose in each year of the model. If the input distributions are specified as epistemic at the appropriate spatio-temporal scale, then, by analogy with typical approaches to risk assessment, the 95th percentile of the average dose in each year is the relevant statistic of interest. This has the added advantage of properly representing uncertainty in the average dose, and hence the uncertainty can be reduced through further data collection.

Typically, doses generated from a PA are compared to performance objectives by using the "peak of the means", however, this does not adequately address the issue of dose in a year (unless the peak of the mean dose is in the same year for every simulation). There are also 5,000 estimates of the peak of the mean, however, it is not clear how to match a statistic from that distribution to the performance objectives. This model will allow exploration of this issue, to evaluate possible approaches to comparison of output doses to performance objectives.

There are other sources of uncertainty that should also be considered in a PA model. These do not fall easily into either the epistemic or aleatory categories.

- Conceptual uncertainty is typically not associated with a parameter, except in conjunction with the model as a whole.
- Numerical uncertainty is similar to model uncertainty, except that it typically relates only to the mathematical aspect of the model, and whether or not a single number can adequately represent the process.

These latter sources of uncertainty are largely ignored when constructing probabilistic distributions for parameters. These uncertainties are typically explored, to limited extent, with sensitivity analyses. However, where expert judgment is utilized in construction of a probability distribution, the presence of conceptual or numerical uncertainty may cause the expert to increase the variation associated with a parameter in order to (perhaps) produce a broader range of model outputs.

More generally, the development of distributions for model input parameters in a PA model needs to accommodate a wide range of options that address spatio-temporal scales, correlation structures, available data, secondary data, literature review information, expert opinion and abstraction from more complex sub-models. Statistical methods that can be considered in each case are described in the following sections. This is a critical component of model development. If not performed properly then the PA model runs the risk of the "garbage in – garbage out" syndrome, uncertainty and sensitivity analysis are compromised, and the results of the model are potentially meaningless. If performed properly, then everything falls into place regarding model results, comparison with performance objectives, and useful uncertainty and sensitivity analysis.

3.0 Fitting Distributions to Data

3.1 Distributions Representing Epistemic Uncertainty

When data are available, whose distribution depends on a parameter of interest, then a Bayesian approach can be used to combine any available prior information with information from the data. The posterior distribution on the parameter represents the uncertainty about the value of the parameter. Prior information could be obtained through expert elicitation, but for nearly every parameter in the Clive DU PA model for which data are available, a non-informative prior is used.

Most parameters in the Clive DU PA model correspond to physical quantities that represent an average of some type. Some parameters represent averages over time, as they represent typical behavior that will be used throughout the 10,000 year performance period, such as annual precipitation. Other parameters represent averages over space. For example, properties of vegetation represent an average vegetation effect across a model area, while soil properties represent an average across a volume of material represented by a model cell. When data are available that represent small amounts of time relative to the 10,000 years, or small areas/volumes relative to the model cells, then it is the *mean* of the data distribution that needs to be modeled. Under most regularity conditions (such as finite variance and the true parameter not on the border of the parameter space), the asymptotic distribution of a posterior distribution of a parameter is normally distributed (Gelman 2004). When a non-informative prior is used, the posterior distribution is generally well-approximated by the sample distribution of the statistic used to estimate the parameter. Thus, the posterior distribution for a mean μ is generally well-approximated by a normal distribution, according to the Central Limit Theorem, if the sample size n is sufficiently large:

$$\mu \,|\, \boldsymbol{X} \sim N\left(\bar{X}, \frac{s}{\sqrt{n}}\right) \tag{1}$$

where $\bar{X}$ is the sample mean, and s is the sample standard deviation. This approximation can be generalized to most other types of parameters, with the posterior distribution well-approximated by:

$$N\left(\hat{\theta}, s.e.(\theta)\right) \tag{2}$$

where $\hat{\theta}$ is an estimate of the parameter of interest θ, and $s.e.(\theta)$ is the standard error associated with the estimate. Stricter regularity conditions may be required for the general approximation to hold, and larger sample sizes may be needed for the posterior distribution to converge to normality.

For parameters whose sampling distributions are difficult to calculate, due to the type of parameter or the small sample size, a bootstrap approach can be utilized to simulate a sampling distribution (Efron and Tibshirani 1994). The bootstrap method simulates a sampling distribution for a parameter by simulating new sets of data of the same size and structure as the existing data.

The data simulation may be either parametric, assuming an underlying distribution for the data, or non-parametric, simulating from the empirical distribution of the data. The simulated bootstrap samples of the parameter are then fit to a distribution following the guidelines of fitting presented in Section 3.2, since the bootstrap data represent hypothetical data that can be precessed similarly to the processing of data that represent aleatory uncertainty.

3.2 Distributions Representing Aleatory Variability

For cases where the goal is to find a distribution that reflects the variability in the data, a goodness-of-fit approach is used. When the complete data set is available, the Akaike Information Criterion (AIC) is used to choose a distribution (Akaike 1974). The special case of data that are reported only as quantiles is address in Section 4.0.

AIC provides a measure of fit based on the likelihood function that attempts to discourage over-fitting by penalizing models with larger numbers of fitted parameter values. AIC could be used directly to choose a distribution by selecting the distribution that minimizes AIC. However, in order to allow for scientific judgment to choose between models that are close in fit, Akaike weights can be used for model selection (Burnham 2002). Akaike weights can be interpreted as conditional probabilities for each model when all models are treated as equally likely a priori. The Akaike approach is the following:

- Choose a set of distributions to be considered: M_1, M_2, …, M_k.
- Fit each distribution via maximum likelihood, and calculate the AIC for each model: A_1, A_2, …, A_k.
- Calculate the Akaike weights for each model:

$$W_i = \frac{e^{-0.5\cdot(A_i - A_{min})}}{\sum_{j=1}^{k} e^{-0.5\cdot(A_j - A_{min})}} \tag{3}$$

where A_{min} is the smallest AIC amongst the models being considered. Distributions with low weights are removed from consideration, and scientific considerations are used to choose between distributions with similarly high weights.

The following descriptions and figures (Figures 1 through 4) provide a list of distributions that are commonly considered for parameters in the Clive PA model: Normal, Lognormal, Gamma, Beta. Note that the uniform distribution is special case of the Beta distribution. Many other distributions are considered for special cases, but these four are adequate for most purposes. Log-uniform distributions are used for Kd and solubility as described in the Geochemistry white paper, and triangular distributions are used for a few parameters in the dose model, which represent aleatory variability, when there was insufficient data and expert elicitation has not yet been performed.

- *Normal* – N(*m*, *s*), where *m* is the mean, and *s* is the standard deviation. This distribution is unimodal and symmetric and has support on the entire real line. This distribution occurs naturally in many settings and is generally preferred for parameters representing averages or sums. Since the normal distribution has infinite support, the distribution must be left-truncated at 0 (or some other natural boundary) for certain types of parameters.

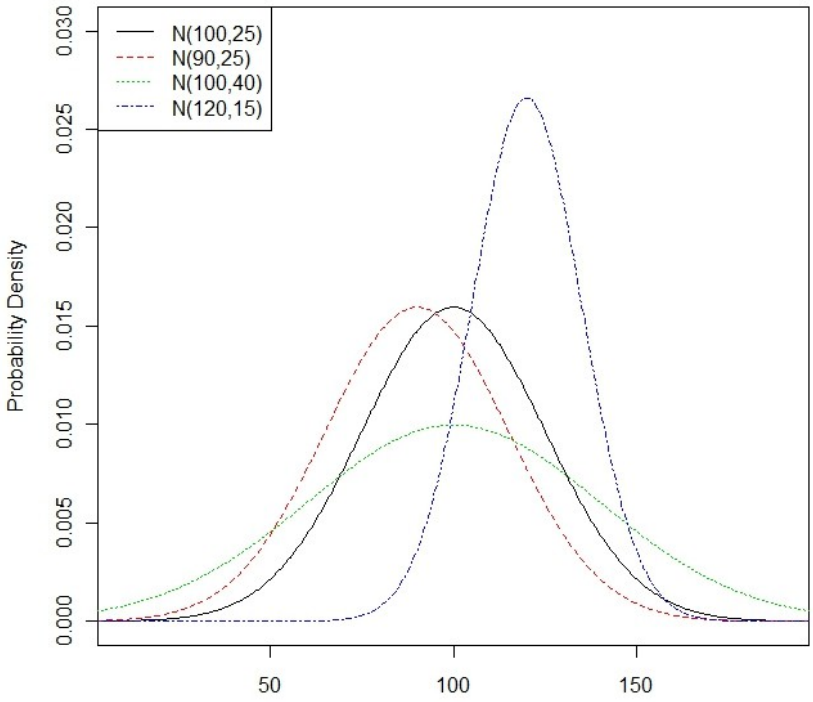

Figure 1. Examples of normal probability density functions

- *Lognormal* – LN(m, s, θ), where m is the geometric mean, and s is the geometric standard deviation, and θ is a location parameter specifying the minimum. This distribution is unimodal and right-skewed and has support on all real values greater than θ. When the geometric standard deviation is near 1, the lognormal distribution closely approximates the normal distribution. Physical quantities can often be modeled well with a lognormal distribution, and typically θ=0, forcing those quantities to be positive.

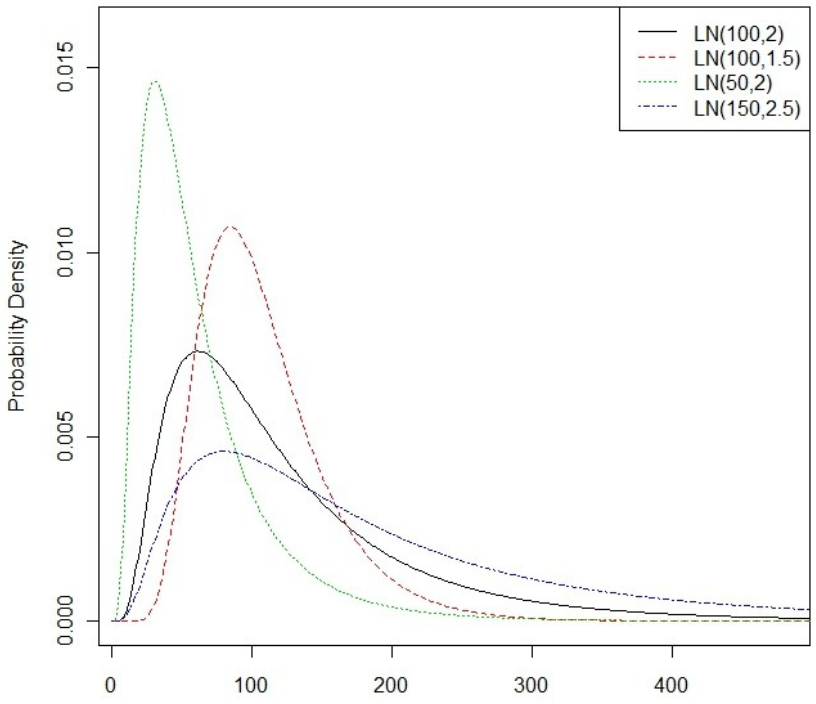

Figure 2. Examples of lognormal probability density functions

- *Gamma* – Gamma(m, s, θ), m is the mean, s is the standard deviation, and θ is a location parameter specifying the minimum. This distribution is unimodal and right-skewed and has support on all real values greater than θ. Fitted gamma distribution and lognormal distributions often appear quite similar, and the lognormal is typically preferred for physical quantities. However, the gamma distribution can fit certain types of tail behavior that the lognormal distribution cannot.

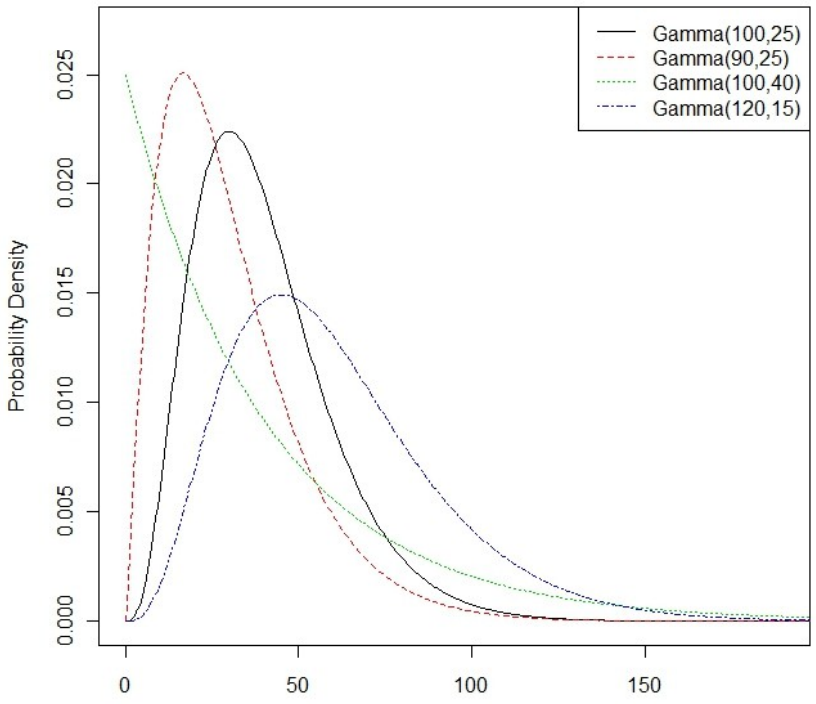

Figure 3. Examples of gamma probability density functions

- *Beta* - Beta(*m*, *s*, *l*, *u*), where *m* is the mean, *s* is the standard deviation, *l* is the lower bound, and *u* is the upper bound. The beta distribution can take on a variety of shapes. It is typically unimodal, but can be bimodal, with modes at the lower and upper bounds. The beta distribution is sufficiently flexible that it might provide a reasonable fit where other distributions cannot, and it is the only standard distribution that has finite support. For many parameters, finite support does not make good sense, so the beta distribution is typically only chosen when it is the only distribution that provides a reasonable fit, or when there is a natural lower and upper bound.

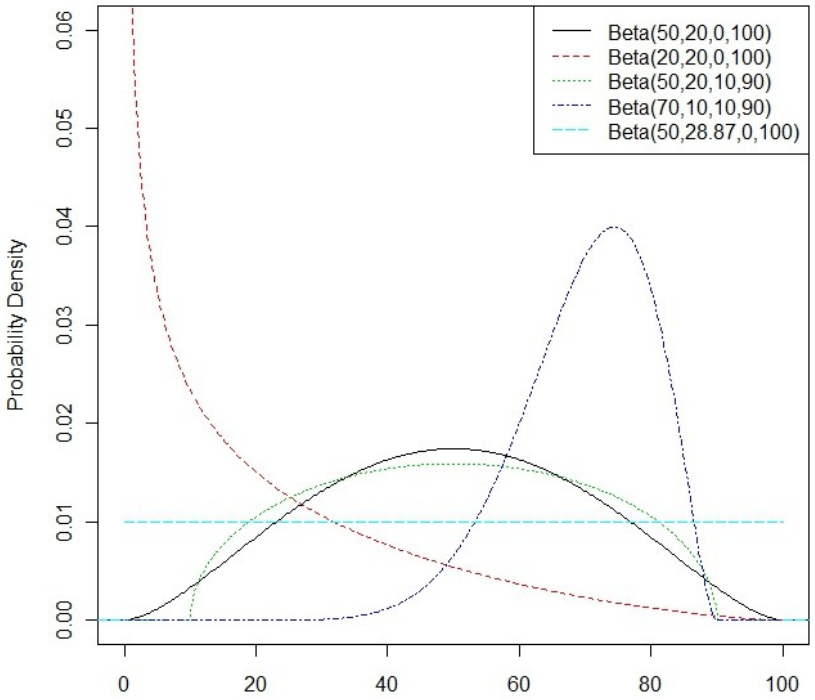

Figure 4. Examples of beta probability density functions

4.0 Fitting Distributions to Reported or Elicited Quantiles

In many cases, data are available only in the form of reported quantiles of the distribution. A formal method for fitting a distribution and choosing amongst possible distributions is needed. While the focus here is on empirical quantiles, the same approach may also apply to quantiles achieved via expert elicitation, though some assumptions about the expert's knowledge base must be considered. This section begins with a definition of quantiles, and follows up with a likelihood estimation method for estimating distributions based on quantile input, and ends with an example.

4.1 Quantiles

Let X be a random variable whose distribution is of interest. Suppose that a random sample of n observations from this distribution has been collected, $\boldsymbol{X}=\{X_i\}_{i=1}^{n}$, but that the reported summaries of this sample are restricted to a set of k empirical quantiles, $\{\hat{q}_j\}_{j=1}^{k}$, corresponding to a set of proportions $\{p_j\}_{j=1}^{k}$ (considered to be given in increasing order for convenience; i.e., $p_j < p_{j+1}$).

The empirical cumulative distribution function (CDF) is defined as:

$$\hat{F}_X(x)=\frac{\#\ of\ sample\ values\ less\ than\ \ x}{n}=\frac{\sum_{i=1}^{n} I\{X_i<x\}}{n}, \tag{4}$$

where I is the indicator function. An empirical quantile corresponds to the inverse of the empirical distribution function:

$$\hat{q}_i=\hat{F}_X^{-1}(p_i)\ . \tag{5}$$

Since $\hat{F}_X$ is a step function, the inverse is not uniquely defined. However, there are many common methods for defining a unique quantile (Hyndman and Fan, 1996). In practice, the exact method of defining the quantile is rarely cited. Thus, there is some potential error associated with a reported quantile. The relative size of the error is dependent on the underlying distribution and the quantile of interest. When sample sizes are large and/or the underlying distributions are smooth (as is the case with named families of distributions that one is likely to fit), the error associated with non-uniqueness should be small, though sensitivity analysis to this error should be performed in assessing fits based on reported quantiles. For the purposes of this document, $\hat{q}_i$ will be considered to be uniquely defined.

4.2 Likelihood Functions

If the original data set were available, then a reasonable choice for fitting the parameters of a distribution is maximum likelihood. Suppose that the random variable of interest, X, is assumed

to come from a parametric family of distributions (e.g. Gaussian, gamma, etc.), that are uniquely defined by a set of parameters $\boldsymbol{\theta}$. The likelihood function for a sample $\boldsymbol{X}$ is defined as:

$$L(\theta|\boldsymbol{X}) = \prod_{i=1}^{n} f_X(x_i|\theta) \ , \tag{6}$$

where f_X is the probability density (or mass) function corresponding to the parametric family of distributions. The maximum likelihood estimator (MLE) of the parameters is then defined by:

$$\hat{\theta} = arg\ max_{\theta} L(\theta|\boldsymbol{X}) \ , \tag{7}$$

or equivalently when maximizing the log-likelihood:

$$\hat{\theta} = arg\ max_{\theta} \ln L(\theta|\boldsymbol{X}) = arg\ max_{\theta} l(\theta|\boldsymbol{X}) \ . \tag{8}$$

When the sample has been summarized by quantiles, the likelihood function for the data takes a different form. The reported data are effectively $\boldsymbol{Y} = \{Y_j\}_{j=1}^{k+1}$, where Y_j is the number of observations between q_{j-1} and q_j.

$$Y_j = \sum_{i=1}^{n} I\{q_{j-1} < X_i \le q_j\} \ , \tag{9}$$

where $q_0 = -\infty$ and $q_{k+1} = \infty$ for notational convenience.

The reported data thus follow a multinomial distribution:

$$\boldsymbol{Y} \sim Multinomial_{k+1}(n, \boldsymbol{\pi}(\theta)) \ , \tag{10}$$

where

$$\pi_j(\theta) = F_X(q_j|\theta) - F_X(q_{j-1}|\theta) \ , \tag{11}$$

and F_X represents the CDF for X.

The likelihood function associated with the reported data is then:

$$L(\theta|\boldsymbol{Y}) = n! \prod_{j=1}^{k+1} \frac{[\pi_j(\theta)]^{Y_j}}{Y_j!} \propto \prod_{j=1}^{k+1} [\pi_j(\theta)]^{Y_j} \ , \tag{12}$$

Where proportionality is with respect to the parameters of interest, $\boldsymbol{\theta}$. Maximizing the log-likelihood is thus equivalent to maximizing:

$$l^*(\boldsymbol{\theta}|\boldsymbol{Y}) = \sum_{j=1}^{k+1} Y_j \ln\left[\pi_j(\boldsymbol{\theta})\right] = \sum_{j=1}^{k+1} n\hat{\pi}_j \ln\left[\pi_j(\boldsymbol{\theta})\right] \propto \sum_{j=1}^{k+1} \hat{\pi}_j \ln\left[\pi_j(\boldsymbol{\theta})\right] \quad , \tag{13}$$

where

$$\hat{\pi}_j = \frac{Y_j}{n} \quad . \tag{14}$$

Note that maximizing Equation (13) does not depend on knowing the sample size n, which may not be available for some data reports, and is only an abstract concept if the quantiles represent elicited values.

For most parametric families, $\pi_j(\boldsymbol{\theta})$ does not have a functional form that lends itself to analytical maximization of Equation (13). However, the CDF for most parametric families is sufficiently smooth that maximization routines work robustly.

Note also that the use of maximum likelihood estimation is similar to intent to using Bayesian statistical methods with some types of non-informative prior distributions. This approach, therefore, is similar in intent for quantile data as the methods described in Section 3.1. Use of least squares minimization instead is not recommended, because the underlying assumptions will probably not be met (e.g., normality, independence, identically distributed data).

4.3 Example: Gaussian Distribution

Suppose that data are reported as in Table 1:

Table 1. Example data, reported only as quantiles

$p_1 = 0.05 = 5\%$	$p_2 = 0.25 = 25\%$	$p_3 = 0.5 = 50\%$	$p_2 = 0.75 = 75\%$	$p_5 = 0.95 = 95\%$
$q_1 = 31$	$q_2 = 58$	$q_3 = 76$	$q_4 = 89$	$q_5 = 120$

Five quantiles are reported, and thus the data are separated into 6 bins. In fitting a Gaussian distribution to these quantiles, $\boldsymbol{\pi}$ can be expressed in terms of the standard Gaussian CDF, Φ, as in Table 2.

Table 2. Calculation of quantities for the log-likelihood

$\hat{\pi}_1 = 0.05 - 0 = 0.05$	$\pi_1 = \Phi\left(\frac{31-\mu}{\sigma}\right)$
$\hat{\pi}_2 = 0.25 - 0.05 = 0.2$	$\pi_2 = \Phi\left(\frac{58-\mu}{\sigma}\right) - \Phi\left(\frac{31-\mu}{\sigma}\right)$
$\hat{\pi}_3 = 0.50 - 0.25 = 0.25$	$\pi_3 = \Phi\left(\frac{76-\mu}{\sigma}\right) - \Phi\left(\frac{58-\mu}{\sigma}\right)$
$\hat{\pi}_4 = 0.75 - 0.50 = 0.25$	$\pi_4 = \Phi\left(\frac{89-\mu}{\sigma}\right) - \Phi\left(\frac{76-\mu}{\sigma}\right)$

$\hat{\pi}_5 = 0.95 - 0.75 = 0.2$	$\pi_5 = \Phi\left(\frac{120-\mu}{\sigma}\right) - \Phi\left(\frac{89-\mu}{\sigma}\right)$
$\hat{\pi}_6 = 1 - 0.95 = 0.05$	$\pi_6 = 1 - \Phi\left(\frac{120-\mu}{\sigma}\right)$

Maximum likelihood estimators can thus be calculated: $\hat{\mu} = 74.6$ and $\hat{\sigma} = 25.8$, resulting in a value of -1.65 for the (right portion of) Equation (13). The CDF and probability density function (pdf) for the fitted distribution are plotted in Figure 5.

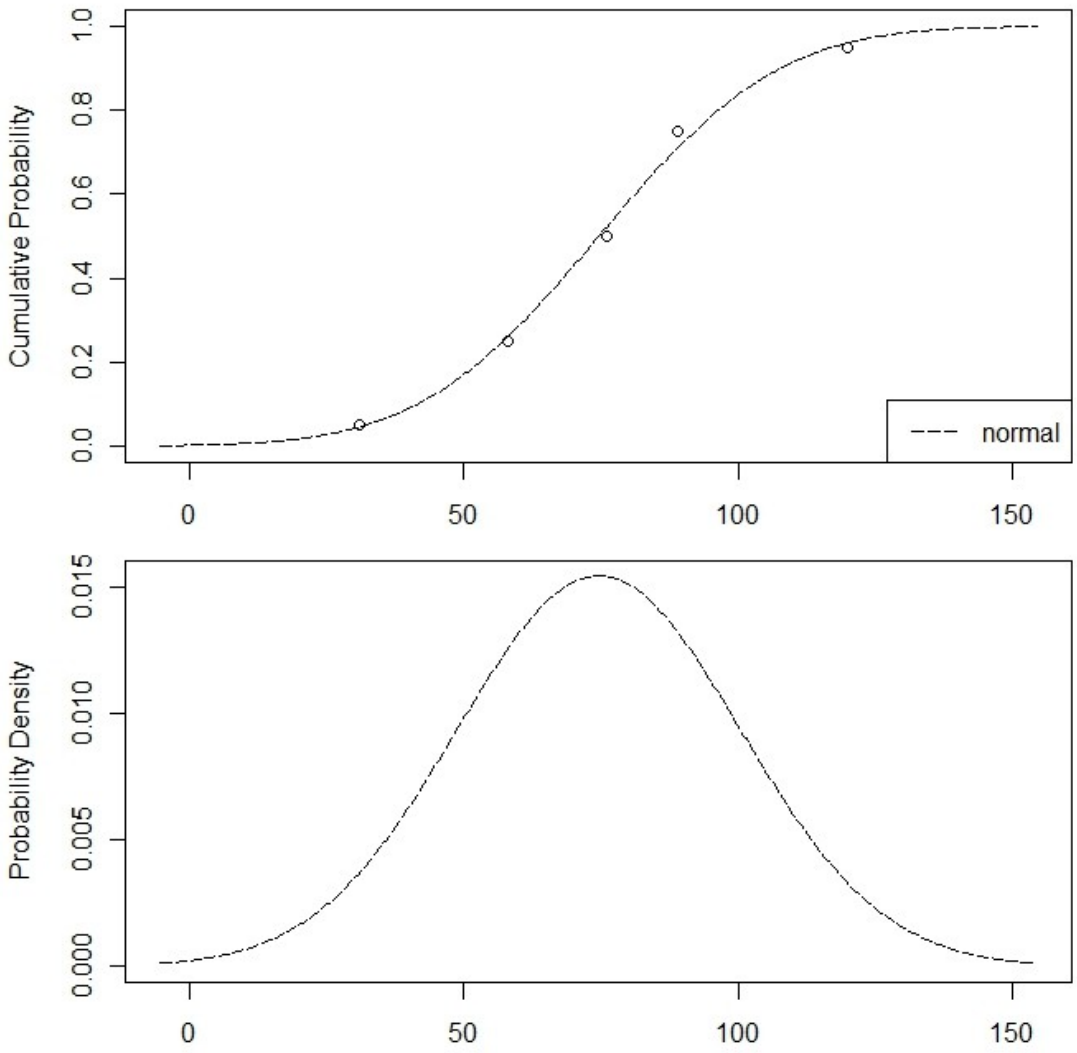

Figure 5. Fitted distribution to the quantiles of the example data

5.0 Parameter Relationships and Conditioning

Many parameters in the Clive DU PA model are related to one another. One parameter may be physically constrained by the value of another parameter, or they may simply tend to vary together. Information about the joint behavior is often unavailable, but where it is, the preferred approach is to construct joint distributions for the parameters.

When joint data are available, a simple approach is to simply calculate the sample correlation of the parameters in the data and apply the same correlation to the parameters in the model to induce a joint distribution. A simple correlation structure may not fully capture the relationship between two parameters but often provides a reasonable first approximation. Where a correlation structure is used in the Clive DU PA model, the correlation algorithms implemented in GoldSim for Gaussian copula are used (Iman and Conover 1982, Embrechts et al. 2001).

Where data and expertise are available, it is generally preferable to construct joint distributions for the parameters by constructing a marginal distribution for one parameter and *conditional* distributions for the remaining parameters. By fitting a distinct conditional distribution of the second parameter for each possible value of the first parameter, a more realistic relationship might be constructed than can be achieved through simple correlation.

For example, for the population of American males the distribution of body weight changes as a function of age, even after reaching adulthood. Beyond age 20, the median body weight tends to increase as a function of age, until middle-age, after which median body weight decreases. The variation in body weight across the population also changes with the mean. Thus, a reasonable approach might be to model body weight as:

$$BW_{males} \sim LN\left(e^{a+b\cdot Age+c\cdot Age^2}, e^{\sigma}\right) \quad . \tag{15}$$

where a, b, c, and σ are estimated from data. This general approach was utilized for the Clive PA model (including for this body weight example), by using the fitting techniques outlined in Section 4.0 to quantile data available for age and body weight.

6.0 Summary

For the Clive DU PA considerable effort has been expended to provide statistical rigor and defense for the PA model. There are few, if any, previous examples of PA for low-level waste that have achieved this level of statistical support. Regulations and guidance that could be used are sadly lacking in sufficient definition of how PA models should be constructed and the role that statistics should play to ensure proper construction. The Clive DU PA model provides an opportunity for others who perform PA for low level radioactive waste to follow this path, and improve the statistical defense for PA more generally.

7.0 References

Akaike, H. (1974). "A New Look at the Statistical Model Identification," *IEEE Transactions on Automatic Control* **19** (6): 716-723.

Burnham, K.P., Anderson, D.R. (2002). "Understanding AIC and BIC in Model Selection." *Sociological Methods and Research. Sociological Methods and Research,* **33** (2): 261-304.

Efron, B. and Tibshirani, R.J. (1994). *Introduction to the Bootstrap*. CRC Press LLC, Boca Raton, FL.

Embrechts, P., Lindskog, F., and McNeil, A. (2001). *Modelling Dependence with Copulas and Applications to Risk Management*, Department of Mathematics, Swiss Federal Institute of Technology, Zurich.

Gelman, A., Carlin, J.B., Stern, H.S., and Rubin, D.B. (2004). *Bayesian Data Analysis, 2nd Edition*. Chapman and Hall/CRC, Boca Raton, FL.

Hyndman, R.J., and Fan, Y. (1996). "Sample Quantiles in Statistical Packages," *American Statistician*, 50: 361-365.

Iman, R.L., and Conover, W.J. (1982). "A Distribution-Free Approach to Inducing Rank Correlation Among Input Variables," *Communications in Statistics: Simulation and Computation,*11 (3): 311-334.

Neptune and Company Inc.

June 1, 2011 Report for EnergySolutions
Clive DU PA Model, version 1

Appendix 15

Sensitivity Analysis Methods

Machine Learning for Sensitivity Analysis of Probabilistic Environmental Models

29 May 2011

Prepared by

Neptune and Company, Inc.

This page is intentionally blank, aside from this statement.

CONTENTS

FIGURES

TABLES

1.0 Introduction

Complex models are useful for investigating dynamics of systems where multiple variables are interacting in a nonlinear manner. Increasingly these investigations are being conducted using probabilistic simulation approaches such that the uncertainty in the understanding of the system can be propagated through to the predicted response. Quantitatively assessing the importance of inputs becomes important when uncertainty in the response is deemed to be unacceptable for the decision at hand. Sensitivity analysis (SA) can be used to help identify those inputs for which uncertainty reduction through further information collection will have the most impact on reducing uncertainty in the model response. However, sensitivity analysis of high dimensional probabilistic models can be computationally challenging. These challenges can be met through machine learning methods applied to probabilistic simulation results.

Quantitative assessment of the importance of inputs is necessary when the level of uncertainty in the system response exceeds the acceptable threshold specified in the decision making framework. One of the goals of sensitivity analysis is to identify which variables have distributions that exert the greatest influence on the response.

2.0 Sensitivity Analysis Approaches

Sensitivity analysis deals with estimating influence measures for input variables for a given model. In general, this estimate can span the *qualitative* to *quantitative* spectrum, as well as the *local* to *global* spectrum. A *qualitative* SA attempts to provide a relative ranking of the importance of input factors without incurring the computational cost of *quantitatively* estimating the percentage of the output variation accounted for by each input factor. A *local* SA involves varying one input factor while holding all other input factors constant and assessing the impact on the model output. This is *local* in the sense that only a minimal portion of the full volume of the input factor space is explored (*i.e.*, the point at which the input factors are held constant). Although local sensitivity analysis is useful in some applications, the region of possible realizations for the model of interest is left largely unexplored. Global sensitivity analysis attempts to explore the possible realizations of the model more completely. The space of possible realizations for the model can be explored through the use of search curves or evaluation of multi-dimensional integrals using Monte Carlo methods. However, global sensitivity becomes more difficult as the dimensionality of the model increases.

An example of *quantitative local* SA approach is differential analysis based on the partial derivatives of the model with respect to each input factor. Given a model of the form $y = f(X)$, the *local* relative sensitivity measure, S_i, of each input factor, x_i, on model output y can be calculated as:

$$S_i = \left\{ E_x \left[\frac{\partial f(X)}{\partial x_i} \right]^2 \mathrm{var}_x[x_i] \right\}^{1/2} \quad \textbf{(1)}$$

Quantitative global SA attempts to explore the full volume defined by the input factors and then averages over the variation of all input factors to provide an estimate of sensitivity:

$$S_i = \frac{\mathrm{var}_{x_i}[E(y \mid x_i)]}{\mathrm{var}(y)} \tag{2}$$

The analysis is successful if $\sum_{i=1}^{p} S_{x_i} \cong 1$, where p is the number of model parameters.

2.1 Regression Based Methods

Quantitative SA approaches include squared standardized regression coefficients (SSRC) and squared standardized rank regression coefficients (SSRRC).

Given a linear regression model of the form

$$y = \beta_0 + \sum_{i=1}^{p} \beta_i x_i \tag{3}$$

the variance of the model output can be estimated as

$$\mathrm{var}(y) = \sum_{i=1}^{p} \beta_i^2 \,\mathrm{var}(x_i) \tag{4}$$

assuming the input factors are independent. If the model output and input factors are standardized to a mean of 0 and a variance of 1 then the square of the regression coefficients (β_i^2) provides an estimate of S_i. Alternatively, regressing the input factors on the *ranks* of the model output can help to fit nonlinearities in the model.

The coefficient of determination, R^2, provides a measure of how far along the continuum towards being both *quantitative* and *global* these SA methods achieve for a given application. The closer the R^2 is to one the closer the results are to being both *global* and *quantitative*. 1-R^2 represents the percentage of output variation not accounted for by the SA method. As this percentage increases, confidence in the influence estimates is reduced although the resulting relative ranking may still be of value. However, at some unknown percentage, the validity of the relative rankings also come into question as the potential increases that account for this output variation would change the relative rankings. Standardized regression and rank correlation methods assume a monotonic linear relationship between the input factors and the model output. A low R^2 may be reflective of a model structure that does not meet this assumption.

The essence of these approaches is an analysis of variance (ANOVA) decomposition, decomposing the response variance into partial variances of increasing dimensionality. The total number of terms involved in this type of decomposition is $2^p - 1$. The dimensionality of an ANOVA decomposition analysis becomes prohibitive at even moderate values of p. "the larger the number of factors, the higher the likelihood of non-negligible higher-order terms".

2.2 Fourier Amplitude Sensitivity Test (FAST)

Several approaches have been proposed to handle nonlinear, nonmonotonic models. Two of these approaches include the Fourier Amplitude Sensitivity Test (FAST) (Saltelli *et al*. 1999) and Sobol's design of experiment (SDOE) approach (Sobol 1993). These methods provide an estimate of the proportion of the variation in the model output due to an input factor through

an ANOVA-like decomposition of the output variation. The two methods use a different computational strategy for decomposing the partial variances of increasing dimensionality (main-effects, two-way interactions, three-way interactions, etc.). In the context of SA, this ANOVA decomposition can be described in terms of total sensitivity indices for each input factor, S_{Ti}. An S_{Ti} for input factor i is calculated as the sum across all main and interaction sensitivities that involve the i^{th} input factor:

$$S_{T_i} = S_i + \sum_{j \neq i}^{n} S_{ij} + \sum_{j,k \neq i}^{n} S_{ijk} + \cdots \quad (5)$$

where S_i is the first-order or (main effect) sensitivity index and S_{ij} is the second-order (interaction effect) sensitivity index and so on. The total number of sensitivity indices is $2^n - 1$, where n is the number of input factors. Because SDOE requires multi-dimensional integration to estimate the sensitivity indices, this method can be prohibitive computationally for moderately complex models (complexity is defined by the number of input factors, n).

FAST is a computationally elegant alternative to SDOE for side stepping this "curse of dimensionality". FAST involves simulating input factors using a *random phase-shift* sampling scheme:

$$x(s)_i = \frac{1}{2} + \frac{1}{\pi}\arcsin(\sin(\omega_i s + \zeta_i)) \quad (6)$$

where s varies from $(-\pi, \pi)$, the ω_i's are a linearly independent set of frequencies (a unique frequency for each input factor), and ζ_i is a random phase shift chosen uniformly in $[0,2\pi)$. The model output based on this sampling scheme for the input factors shows different periodicities at each of the ω_i. The amplitude of the oscillation at the ω_i's and their harmonics provides a measure of the model output sensitivity to the corresponding input x_i. Fast Fourier Transform of the resulting model output provides the pieces from which the S_T's can be computed.

This is accomplished by a Fourier series expansion of $y = f(x(s)_i)$

$$y = \sum_{-\infty}^{+\infty} \{A_j \cos js + B_j \sin js\} \quad (7)$$

where A_j and B_j are the Fourier coefficients and can be estimated via a fast Fourier transform algorithm.

The spectrum of the Fourier transform is

$$\Lambda_j = A_j^2 + B_j^2 \quad (8)$$

Summing all Λ_j provides an estimate of the total variance in y

$$\hat{D} = \sum_{j \in Z} \Lambda_j \quad (9)$$

Summing all Λ_j excluding the frequency embedded in x_i and its associated higher harmonics, Z^0, provides an estimate of the variance due to the uncertainty in x_i

$$\hat{D}_i = \sum_{j \in Z^0} \Lambda_j \quad (10)$$

The sensitivity of y to x_i is then given by

$$\hat{S}_i = \hat{D}_i / \hat{D} \tag{11}$$

Unfortunately, global sensitivity methods such as the FAST require construction of model simulations in which a signal is embedded in each input parameter and then the strength of the signal in the model realizations is a measure of parameter sensitivity. This requires construction of a separate model with distributions for input parameters constructed specifically for sensitivity analysis, rather than for uncertainty analysis. The space of possible realizations for the model can be explored through the use of search curves or evaluation of multi-dimensional integrals using Monte Carlo methods. However, these approaches to global sensitivity analysis become more computationally intensive as the dimensionality of the model (i.e., the number of model parameters) increases and can be prohitbitive for models that include hundreds or thousands of stochastic parameters.

Results from a typical probabilistic model run design for uncertainty analysis can be difficult to use in FAST. A probabilistic model run could be designed for both uncertainty analysis and FAST if the cumulative distribution functions (cdf) for all input factors are available analytically. Analytic cdf's are available for distributions such as the uniform and Weibull but not for the normal. Thus FAST may not be feasible when model run times are long and when uncertainty and sensitivity analysis are both part of the decision process.

2.3 Machine Learning Approaches

Because of the computational cost, sensitivity analysis of high-dimensional probabilistic models requires efficient algorithms for practical application. Machine learning provides tools that allow for the partitioning of the variance in the model response to the input parameters by exploration of the realizations from a model run for uncertainty analysis. Two common machine learning approaches that could be brought to bear for sensitivity analysis are bagging (Breiman 2001) and boosting (Friedman 2001) of regression trees. The advantages of machine learning approaches include the ability to fit non-monotonic and non-linear effects, the ability to fit parameter interaction effects, and the ability to visualize these effects and their interaction across the range of the response and input parameters. Bagging, boosting and other machine learning approaches typically produce similar results for noisy data. In the case of realizations from a probabilistic process model, each realization is a deterministic evaluation of the model and all the stochastic predictor variables are available. As such there is no unexplainable variation in the process model response (as is the case with observed data) and the choice of machine learning algorithm should have negligible impact of the results of the sensitivity analysis.

2.3.1 Multivariate Adaptive Regression Splines (MARS)

Multivariate Adaptive Regression Splines (MARS) is a recursive partitioning approach (similar to Classification and Regression Trees) that helps deal with the ANOVA decomposition "curse of dimensionality", making estimation of sensitivity indices computationally achievable for large n (Friedman, 1991). MARS accomplishes this by optimally partitioning or, splitting the model output and input factors into subsets, from which splines are fit. The recursive nature of the algorithm results in increasingly local splits of the model results in which all significant interaction effects in subregions are found. MARS is

able to find and fit only the significant nonlinear and thresholds relationships between the model input and output. An input factor's influence is calculated as the sum of the partial residuals removing all main and interaction effects that variable enters.

$$S_{x_i} = \sum \left[f - a_o + \sum_{i \neq 1} f(x_i) + \sum_{i,j \neq 1} f(x_i, x_j) + \sum_{i,j,k \neq 1} f(x_i, x_j, x_k) + \cdots \right]^2 \qquad (12)$$

2.3.2 Gradient Boosting Machines (GBM)

Boosting of decision trees provides a technique that adds to the flexiblity offered by recusive partioning methods such as MARS. The Gradient Boosting Machines (GBM) approach utilizes boosting of binary recursive partitioning algorithms that deconstruct a response into the relative influence from a given set of explanatory variables (stochastic model input parameters). That is, the collection of results (the process model response) is broken up into parts, and each part is examined separately. This process is repeated with smaller and smaller parts, each analyzed for the relationship between the model inputs (explanatory variables) and the results. This sensitivity analysis methodology identifies which stochastic model input parameters are most influential in determining the results, such as media concentrations or future potential doses. It also identifies the ranges over which the influence is strongest.

Variance decomposition of the GBM fit is then used to estimate SIs. Under this decomposition approach, the goal is to identify the most influential explanatory variables that are identified within a model. The necessary degree of model complexity is assessed using validation metrics, based on comparison of model predictions, with randomly selected subsets of the data. This approach uses the "deviance" of the model as a measure of goodness of fit. The concept of deviance is fundamental to classical statistical hypothesis tests (e.g., the common *t*-test can be derived using a deviance-based framework) and guides the model selection process applied here.

The GBM fitting approach is based on finding the values of each explanatory variable that result in the greatest difference in mean for the corresponding subsets of the response. For example, if there were only a single explanatory variable, the GBM would identify the value of the explanatory variable that corresponds to a split of the response into two parts. This will ensure that no other split would result in corresponding groups of the response variable with a greater difference in means. When multiple explanatory variables are present, these multiple splits are referred to as "trees." Each tree results in an estimate (e.g., prediction) of the response. As multiple potential trees are evaluated, they are compared to the observed data using a loss function. The selection of the loss function is an influential aspect of the GBM process, and depends on the distribution of the response variable. For data that are sufficiently skewed (e.g., non-normal), the absolute error loss function typically produces more reliable results.

There is a trade-off that exists when considering which loss function to use. The squared-error loss function results in better fitting models, but can do so at the expense of introducing spurious variables into the model selection process when the response distribution is sufficiently skewed. The absolute error loss function produces model predictions with more variability, but is less likely to result in the selection of spurious variables in the model. For this application, the focus has been on using a deviance-based method to obtain models that

identify the most important explanatory variables with respect to the observed variability in the response. Therefore, the squared-error function was used in these applications.

With standard linear regression techniques, it is assumed that the relationship between the response and the explanatory variable is a constant (e.g., the parameter estimates in the linear model). With the GBM approach, this relationship is not constrained by assumptions of linearity, and the partial dependence plots show the data-based estimate of the relationship between the response and the explanatory variable. This is useful for understanding the influence of changes in a single explanatory variable, when integrating across all other explanatory variables.

2.4 Example

2.4.1 "Sobol g-function"

The Sobol *g*-function (Saltelli *et. al.* 1999) provides an analytic non-monotonic test function for evaluating the performance of various sensitivity analysis approaches. This function is defined as:

$$f = \prod_{i=1}^{p} g_i(x_i) \tag{13}$$

where p is the total number of input factors and $g_i(x_i)$ is given by

$$g_i(x_i) = \frac{|4x_i - 2| + a_i}{1 + a_i}, \tag{14}$$

with

$$x_i = \frac{1}{2} + \frac{1}{\pi}\arcsin(\sin(\omega_i s + \phi_i)), \tag{15}$$

and s varing along (-π,π), $\varphi_i \sim U[0,2\pi)$, and ω_i are specified frequencies.

The Sobol *g* function was simulated for $p = 8$ and frequencies $\{\omega_i\} = \{23, 55, 77, 97, 107, 113, 121, 125\}$ for a specific set of a_i's. Table 1 provides a comparison of sensitivity indices calculated analytically (S) and using of GBM, MARS, FAST, differential analysis (DERIV), squared standardized regression coefficients (SSRC), and squared standardized rank regression coefficients (SSRRC).

Note that the GBM, MARS and FAST methods return sensitivity indices that are close to the actual sensitivities for the Sobol function (S). The Sobol function is highly non-liniear, hence the standardized regression approaches do not work very well. As described, FAST is computationally challenging. The difference between MARS and GBM is close, but preference is given overall to the GBM approach.

A goodness-of-fit statistic is also presented in the bottom row of Table 1. This is calculated as the standard chi-square good ness –of-fit statistic – the sum of the square of the observed (SA method) minus the expected (S value) all divided by the expected value, in which case a small value implies a better fit. These goodness-of-fit statistics show that the GBM method outperforms the other methods, although the difference is small for GBM and FAST.

	a	*S*	*GBM*	*MARS*	*FAST*	*DERIV*	*SSRC*	*SSRRC*
x_1	99	0.0001	0.0003	0.0000	0.0043	0.0037	0.6880	0.7805
x_2	0	0.4227	0.4146	0.4397	0.4287	0.3151	0.0137	0.0036
x_3	9	0.0058	0.0011	0.0084	0.0190	0.0401	0.0003	0.0000
x_4	0	0.4227	0.4200	0.4239	0.4269	0.3169	0.0163	0.0098
x_5	99	0.0001	0.0001	0.0000	0.0006	0.0037	0.0350	0.1152
x_6	4.5	0.0182	0.0335	0.0239	0.0141	0.0787	0.0012	0.0554
x_7	1	0.1304	0.1303	0.1041	0.1063	0.2382	0.0574	0.0344
x_8	99	0.0001	0.0000	0.0000	0.0002	0.0037	0.1881	0.0012
Goodness-of-Fit statistic			3.3	14.8	3.6	470	7,250	535

Table 1. ***Sensitivity Indices by Sensitivity Analysis Method for Sobol g-function application with p = 8.***

GBM is run on the realizations themselves, whereas FAST requires set up interms of an embedded signal. This makes FAST cumbersome to deal with comparatively. Also, GBM outperforms MARS, which is not as flexible and runs slower. GBM tends to provide the best fit, is flexible and is applied directly to the realizations. Consequently, it is the preferred method, and the one that is used for the sensitivity analyses for the Clive DU PA.

2.4.2 Visualization

Once a GBM has been is constructed, each of the explanatory variables that exist in the model can be assigned an SI. The SI is obtained through variance decomposition and can be interpreted as the percentage of variability explained in the model by a given explanatory variable. The sum of the SI's across the entire set of explanatory variables in the machine will approximately equal the R^2 of the linear regression of the process model predictions versus the machine learning predictions. The R^2 values for this version of the model indicate the high degree of predictive power of the machine learning in fitting the process model predictions.

For a GBM model, the partial dependence is determined through the integration across the joint density to obtain a marginal distribution. The integration is performed using a "weighted tree traversal" measure that is analogous to more common integration procedures performed with Riemann or Lebesgue measures. The vertical axis of the partial dependence plot shows the change in the response variable as a function of the changes in the explanatory variable.

In order to assess the relationship between an individual explanatory variable and the response of interest, partial dependence plots are used (**Figure 1**). The first panel depicts a density estimate of the simulated response from the process model as well as the machine goodness-

of-fit and summary statistics for the response. The percentiles of the response distribution in this panel are shaded to provide a context for the partial dependence plots presented in the remaining panels. The colors indicate the percentile range of the response as follows:

1. The 0th - 25th percentile region is shaded orange-brown
2. The 25th - 50th percentile region is shaded dark yellow-green
3. The 50th - 75th percentile region is shaded light green
4. The 75th - 100th percentile region is shaded light blue

The y-axis scale of the partial dependence plots is in units of the response distribution (the x axis of the first panel). Given that each parameter has a different range and strength of influence on the response, the y axes of the partial dependence panels depict only the range of the response over which a particular parameter is influential. If the original scale of the response were maintained on each partial dependence panel, then the influence of the least influential parameter would not be visible in many cases. To counteract this scale issue, the background of the partial dependence panels is shaded to depict the percentile of the response over which the parameter is influential. For example, if the background of the partial dependence plot under the partial dependence line is light blue, then that indicates the parameter's influence on the upper end of the response distribution (i.e., the 75th to 100th percentile of the response).

The partial dependence panels in each figure show the distributions of the explanatory variables (black line), and the partial dependence curve (blue line) shows changes in the response as a function of each explanatory variable.

The plots show that the distributions for the three input parameters are uniform, and that the effects show sensitivity across the entire range of the inputs. The effects are first negative, and then positive, which is to be expected given Equation 15. Also note that the linear regression methods would not be able to track the non-linearity, and instead fits a straight, horizontal line for these parameters, which shows them to be non-sensitive. This is a prime example of why methods such as GBM are advantageous.

Note:

An implementation of Friedman's gradient boosting machine approach is available in the R statistical software in the gbm package. The gbm package functions were tailored to generate global sensitivity indices and partial dependence visualization of the impact of model input parameters on the model response based on a set of realizations from the probabilisticly run model.

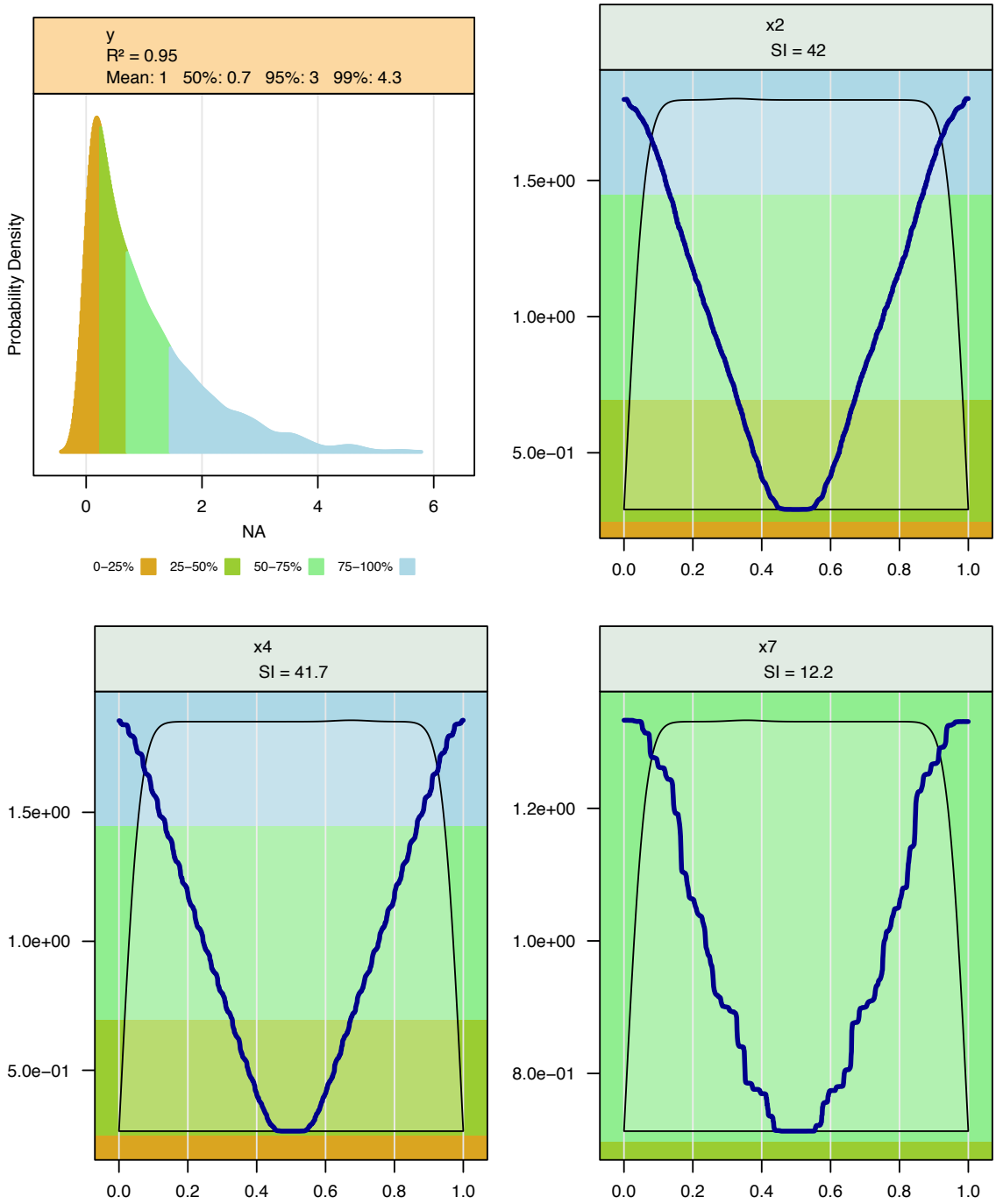

Figure 1. Sensitivity and Partial Dependence Plots for the GBM fit to the Sobol Function.

3.0 References

Friedman, J.H. (1991), "Multivariate Adaptive Regression Splines," *The Annals of Statistics*, 19, 1-141.

Friedman, J.H. (2001). "Greedy Function Approximation: A Gradient Boosting Machine," Annals of Statistics 29(5):1189-1232.

Saltelli A., Tarantola S., and Chan K.P.-S. (1999), "A Quantitative Model-Independent Method for Global Sensitivity Analysis of Model Output," *Technometrics*, 41, 39-55.

Sobol, I.M. (1993), "Sensitivity Analysis for Nonlinear Mathematical Models," *Mathematical Modeling & Computational Experiment*, 1, 407-414.

Neptune and Company Inc.

June 1, 2011 Report for EnergySolutions
Clive DU PA Model, version 1

Appendix 16

GoldSim Parameters

Model Parameters for the Clive DU PA Model

version 1.0

28 May 2011

Prepared by

Neptune and Company, Inc.

This page is intentionally blank, aside from this statement.

CONTENTS

FIGURES

TABLES

1.0 Introduction

This document, along with the complementary Excel workbook, Clive PA Model Parameters.xls, is a collection of all the input parameters used in the Clive DU PA GoldSim model. The workbook contains those parameters that are most conveniently stored in arrays (such as collections of values by contaminant Species or by chemical Elements), and this document contains individual parameter values and distributions, organized by Containers in the model. Expressions and other operators that do not have model inputs are not represented in these documents. Some input distributions refer to other expression for part of their specification. Rather than writing in those expressions, these are generally noted here as simply "$f(x)$".

2.0 Distribution Specification

Distributions in this document are specified according to the notation shown in Table 1.

Table 1. Statistical distribution types used in the parameter specifications.

distribution type	value or distribution
discrete	value
uniform	U(minimum, maximum)
log uniform	LU(minimum, maximum)
triangular	Tri(minimum, expected, maximum)
normal	N(mean μ, standard deviation σ)
truncated normal	N(mean μ, standard deviation σ, minimum, maximum)
log-normal	LN(geometric mean GM, geometric standard deviation GSD)
truncated log-normal	LN(GM, GSD, minimum, maximum)
beta (generalized)	beta(mean μ, standard deviation σ, minimum, maximum)
Weibull	W(minimum, Weibull slope, mean - minimum)

3.0 \SimulationSettings

The SimulationSettings container has two primary subcontainers, Chronology and Switches. A standard set of simulation settings is suggested in order to control intercomparisons between various runs. The standard set includes Simulation Settings and the values of the various Switches.

Table 2. Generic constants used in simulations

GoldSim element	value	units	reference / comment
Small	1×10^{-30}	—	arbitrarily small number for use in modeling constructs
Large	1×10^{30}	—	arbitrarily large number for use in modeling constructs
U_mask	vector by species of 1's for U species, 0's for non-U species		Modeling construct: All uranium isotopes have a value of 1, and all other radionuclides have a value of 0.

3.1 Simulation Settings (the GoldSim dialog)

The GoldSim Simulation Settings dialog (accessed through the F2 key, or from the menu as Run | Simulation Settings...) controls a number of settings controlling the probabilistic and deterministic modeling runs (Table 3) as well as the specification of time steps (Table 4). Time steps are specific so that values of time-varying outputs are recorded at various times during the simulation. These values, the saving of which is identified by checking the "FV" column, are then available for post-processing analysis. Users of GoldSim are able to modify these time steps, but GoldSim Player users may not. Do not modify the 2500-yr time step length in the later time steps, as these are assumed to exist for the deep time assessment.

If the user desires to run a shorter simulation than the full 2.1 My, this should be done using the model's Control Panel dashboard—not by entering in a shorter duration in the Simulation Settings dialog. See the *Clive PA Model User Guide* for more details on the use of model controls and dashboards.

Table 3. Monte Carlo simulation settings

setting	value	comments
Time		
Time Display Units	yr	This is a fixed model setting.
Duration	21000000 yr	2.1 million years is required for U-238 to reach secular equilibrium with its decay products.
Start-time / End-time	—	These are ignored.
Probabilistic Simulation		
# Realizations	variable	Set by user.
# Histories to save	variable	Set to # Realizations for viewing all realizations; set to zero for sensitivity analysis.
Use Latin Hypercube Sampling	checked	Use of LHC sampling is advisable in order to evenly sample distributions.
Repeat Sampling Sequences	checked	Check to ensure reproducibility.
Random Seed	variable	This is a user-selected value.
Deterministic Simulation		
Solve Simulation deterministically using:	Element Deterministic Values	

Table 4. Times step settings for the full 2.1-million year run

time range (y)	# steps	time step length (y)	plot every	FV
0 - 100	20	5	1	
100 - 400	15	20	1	
400 - 1000	12	50	1	X
1000 - 2000	10	100	1	
2000 - 3000	10	100	1	
3000 - 4000	10	100	1	
4000 - 5000	10	100	1	
5000 - 6000	5	200	1	
6000 - 7000	4	250	1	
7000 - 8000	2	500	1	
8000 - 9000	2	500	1	
9000 - 10000	2	500	1	X
10000 - 50000	40	1000	1	
50000 - 100000	50	1000	1	X
100000 - 200000	40	2500	10	
200000 - 300000	40	2500	10	
300000 - 400000	40	2500	10	
400000 - 500000	40	2500	10	
500000 - 600000	40	2500	10	
600000 - 700000	40	2500	10	
700000 - 800000	40	2500	10	
800000 - 900000	40	2500	10	
900000 - 1000000	40	2500	10	X
1000000 - 1100000	40	2500	10	
1100000 - 1200000	40	2500	10	
1200000 - 1300000	40	2500	10	
1300000 - 1400000	40	2500	10	
1400000 - 1500000	40	2500	10	
1500000 - 1600000	40	2500	10	
1600000 - 1700000	40	2500	10	
1700000 - 1800000	40	2500	10	
1800000 - 1900000	40	2500	10	
1900000 - 2000000	40	2500	10	
2000000 - 2100000	40	2500	10	X

3.2 \SimulationSettings\Chronology

The model chronology is documented in this container, referenced throughout the model (Table 5).

Table 5. Global events and their probability of occurrence

GoldSim element	value or distribution	units	reference / comment
ModelTimeZero time at which calculations start	2012		Assumed date for first disposal of DU in the Class A South embankment.
IC_Period time since time zero of loss of institutional control	discrete, 100	yr	Assumed duration of active institutional control, per regulatory language.
CapNaturalization_Time time since time zero to when the cap is fully naturalized	N(μ=40, σ=10, min=10, max=Large)	yr	see Unsaturated Zone Modeling white paper
Dose_Simulation_Duration time since time zero that dose	user-selected	yr	User can set this value, up to 10,000 yr, per UAC R313-28-8

3.3 \SimulationSettings\Switches

Switches that control the model are not model inputs documented here, as they are user-selectable via the Control Panel and other dashboards.

4.0 \Materials

Most of the Species-specific properties are defined in the Excel workbook, Clive DU PA Model Parameters.xls, since they are tabulated lists and therefore better suited to a spreadsheet format from which values can be electronically transferred to the model. A number of parameters, however, as well as the overall decay chain scheme, are presented in the decay chain diagrams, shown in Figures 1 and 2. Radionuclides in black are modeled for contaminant transport and dose contributions, those in green are modeled for dose contributions only, and those in gray are not modeled. Figure 3 shows details of those actinide decay chains where some radionuclides are omitted from the model calculations. These are radionuclides with exceedingly small branching fractions and/or no dose conversion factors, so they could not possibly affect model results or decisions based on those results.

One value defined for each contaminant species in the Species element cannot be referenced to an array: the molecular (or in this case, atomic) mass, also called the molecular or atomic weight. GoldSim assumes the same atomic mass for all isotopes for a given chemical element. For example, all isotopes of uranium are assigned the atomic mass of the first isotope encountered — ^{232}U in this case. Therefore, the atomic masses shown in Table 6 are defined for each element, not for each radionuclide. These values are entered manually into the Species element in the \Materials container of the model. In all cases, the most abundant isotope is used, based on inventory mass as developed in \Inventory\Total_DU_Inventory for disposed radionuclides, and the corresponding decay products for radionuclides that ingrow. For example, the disposed mass of thorium is reported as zero, but since most of the thorium would be ingrowing from the large

mass of ^{238}U, the corresponding thorium isotope of greatest mass would be ^{230}Th. This ignores the half-life of the decay products, but any error in averaged or presumed atomic masses is expected to be quite minor, since ^{230}Th and ^{232}Th have very similar atomic masses anyway.

Table 6. Atomic mass of Species

Species ID	atomic mass (g/mol)	Species ID	atomic mass (g/mol)
Sr90	90	Ac227	227
Tc99	99	Th228, Th229, Th230, Th232	230
I129	129	Pa231	231
Cs137	137	U232, U233, U234, U235, U236, U238	238
Pb210	210	Np237	237
Rn222	222	Pu238, Pu239, Pu240, Pu241, Pu242	239
Ra226, Ra228	226	Am241	241

Other chemical elements used in the model have their atomic masses listed in Table 7.

Table 7. Atomic masses of other elements

GoldSim element	value or distribution	units	reference / comment
Fluorine_AtomicMass	19.0	g/mol	Chart of the Nuclides, 16th Edition
Oxygen_AtomicMass	16.0	g/mol	*ibid.*

4.1 \Materials\DecayChains

Decay chains are illustrated in this container and reproduced below in Figures 1 through 3.

Decay chains implemented in contaminant transport and dose calculations

Note that the radionuclides and stable nuclides in black are maintained in the Species list. Any modification to the decay chain diagram needs to have an associated modification to the Species list, and vice versa.

The radionuclides noted in green italic are considered in the dose assessment only, through dose coversion factors. Environmental transport of these progeny is assumed to follow their respective parents, with which they are in secular equilibrium.

Radionuclides, stable nuclides, and decay arrows in gray are not represented in the model, but are shown here for completeness. Details in the Actinide_detail Container are also not modeled.

These decay chains are based on the branching fractions in the Nuclear Wallet Cards (Tuli, 2005). Unless noted at a branch, the branching fraction is always 1. Alpha decay is indicated by a red arrow. In a few cases, complex decay paths have been simplified, and are shown in the detail Container. These cases are invariably inconsequential, as the branching fractions in question are extremely small.
Revised 12 April 2011 - JT

Non-actinide decay to dose-producing progeny:

Non-actinide decay to stable progeny that are not modeled:

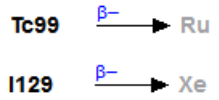

Neptunium Series, simplified

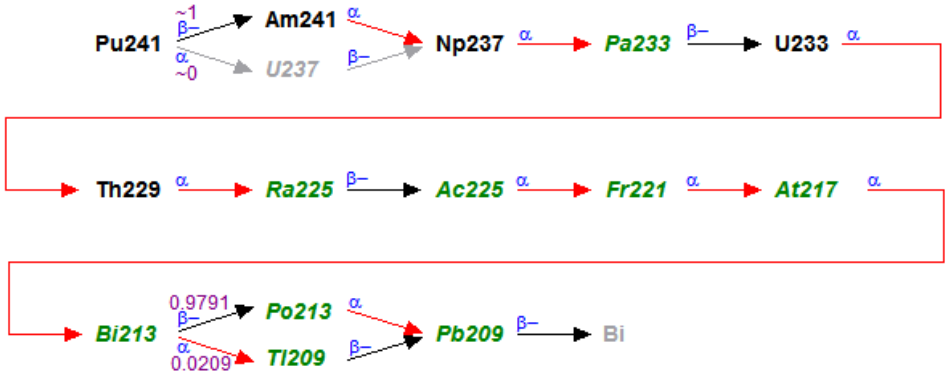

Figure 1. Decay chains modeled in the Clive DU PA Model, part 1 of 2.

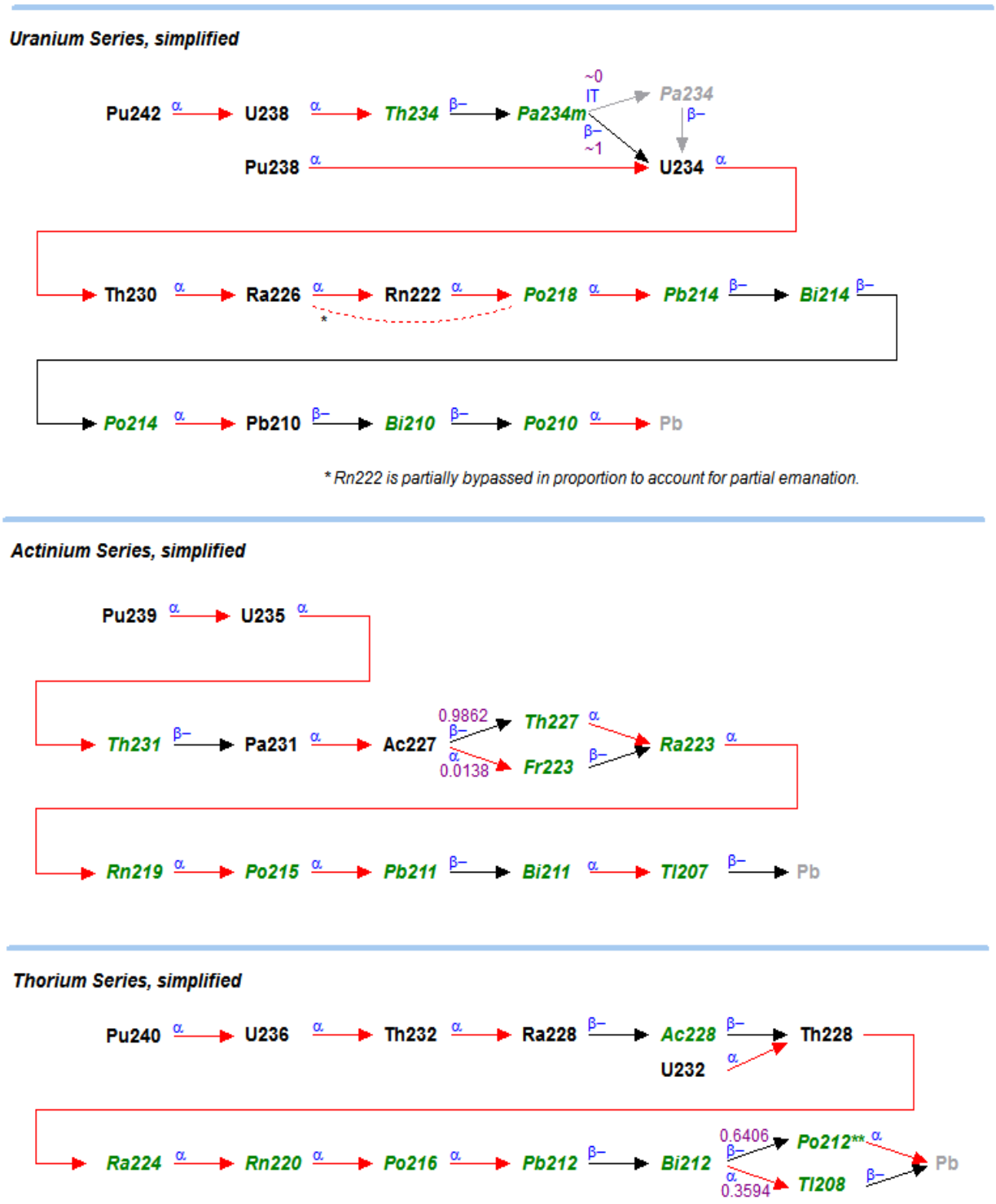

Figure 2. Decay chains modeled in the Clive DU PA Model, part 2 of 2.

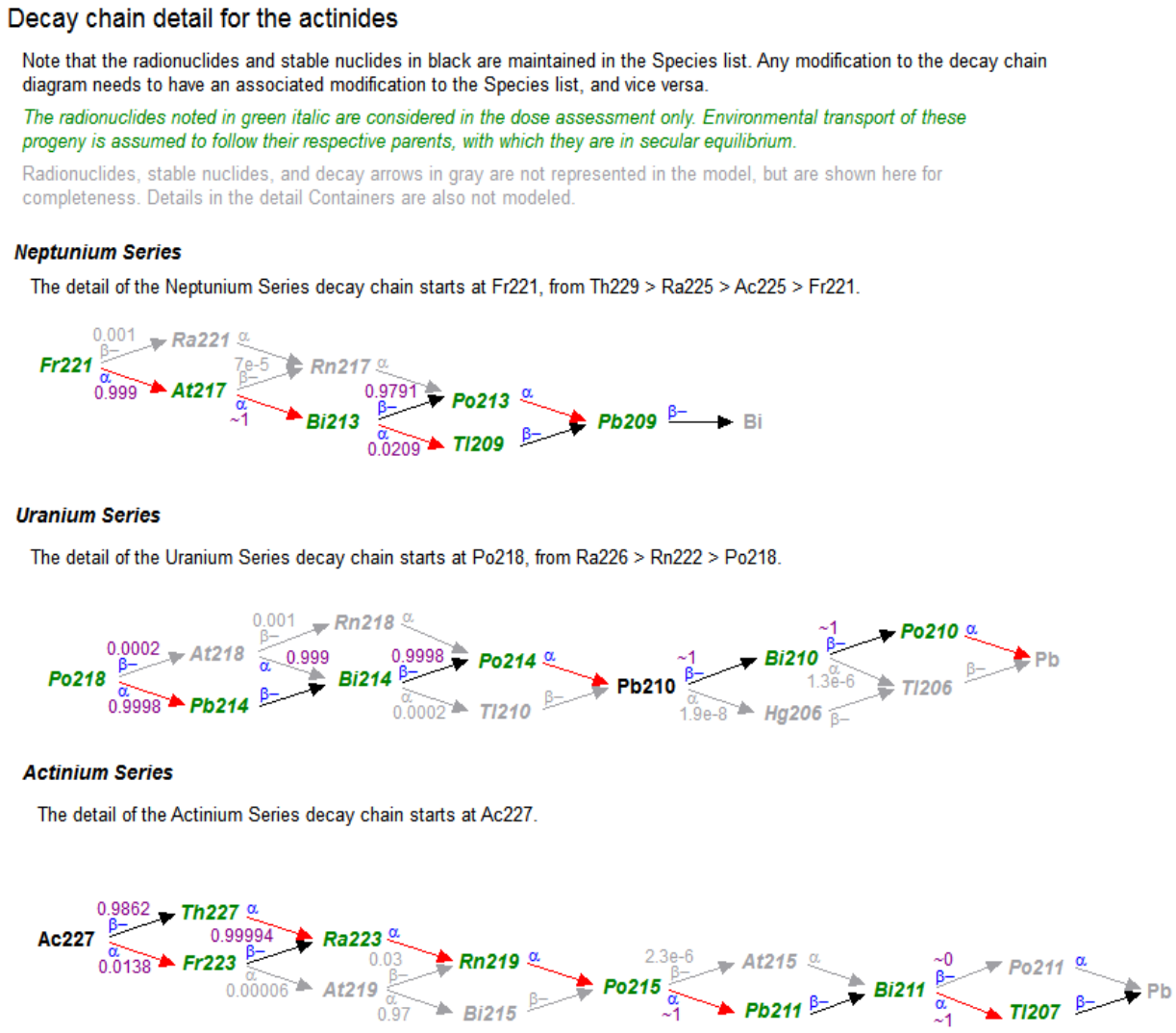

Figure 3. Details of the actinide decay chains modeled in the Clive DU PA Model, showing which species are omitted, in gray.

4.2 \Materials\Loess_Properties

Since loess (windblown sediment) is derived from the surrounding Unit 4 surface soils, the material properties for Loess are redirected to those of Unit 4 (see Table 8).

4.3 \Materials\Unit4_Properties

Unit 4 is a silty clay, the uppermost unit deposited in the region by ancestral lakes. Windblown loess that deposits in the upper cover layers is derived from Unit 4, and shares its material properties. This is also used for a source material for certain parts of the engineered system (clay liner and upper and lower radon barriers), and has materials properties listed in Table 8. Unit 4 is

also used for the basic material properties of the clay liner and the upper and lower radon barrier clay layers. Unit 4 is assigned K_d values for silt.

Table 8. Unit 4 material properties

GoldSim element	value or distribution	units	reference / comment
ParticleDensity_Unit4 particle density of Unit 4 material	2.65	g/cm^3	see Unsaturated Zone Modeling white paper
Porosity_Unit4 porosity of Unit 4 material	N(μ=0.428, σ=6.08e-3, min=Small, max=1-Small)	—	*ibid.*, truncated just above 0 and just below 1
BulkDensity_Unit4 dry bulk density of Unit 4 material	N(μ =$f(x)$, σ=0.1, min=Small, max=Large)	g/cm^3	*ibid.*, truncated just above 0
D_Unit4 Brooks-Corey fractal dimension parameter for Unit 4 material	N(μ=2.81, σ=9.93e-5, min=0, max=3)	—	*ibid.*, truncated at 0 and 3
Hb_Unit4 bubbling pressure head of Unit 4 material	N(μ=104., σ=1.72, min=Small, max=Large) correlated to D_Unit4 as -0.66	cm	*ibid.*, truncated just above 0
MCres_Unit4 residual moisture content for Unit 4 material	N(μ=0.108, σ=8.95e-4, min=Small, max=Large)	—	*ibid.*, truncated just above 0
Ksat_Unit4 saturated hydraulic conductivity for Unit 4 material	N(μ=5.16e-5, σ=5.97e-7 , min=Small, max=Large) correlated to D_Unit4 -0.37	cm/s	*ibid.*, truncated just above 0

4.4 \Materials\Unit3_Properties

Material properties for the unsaturated zone below the liner of the disposal embankment, comprised of stratigraphic Unit 3, a silty sand, are provided in Table 9. Unit 3 is assigned K_d values for sand.

Table 9. Unit 3 material properties

GoldSim element	value or distribution	units	reference / comment
ParticleDensity_Unit3 particle density of Unit 3 material	2.65	g/cm^3	see Unsaturated Zone Modeling white paper

GoldSim element	value or distribution	units	reference / comment
Porosity_Unit3 porosity of Unit 3 material	N(μ=0.393, σ=6.11e-3, min=Small, max=1-Small)	—	*ibid.*, truncated just above 0 and just below 1
BulkDensity_Unit3 dry bulk density of Unit 3 material	N(μ =$f(x)$, σ=0.1, min=Small, max=Large)	g/cm^3	*ibid.*, truncated just above 0
D_Unit3 Brooks-Corey fractal dimension parameter for Unit 3 material	N(μ=2.73, σ=5.21e-3, min=0, max=3)	—	*ibid.*, truncated at 0 and 3
Hb_Unit3 bubbling pressure head of Unit 3 material	N(μ=8.85, σ=0.929, min=Small, max=Large); [*correlated to D_Unit3 -0.85*]	cm	*ibid.*, truncated just above 0
MCres_Unit3 residual moisture content for Unit 3 material	N(μ=6.78e-3, σ=2.05e-3, min=Small, max=Large)	—	*ibid.*
Ksat_Unit3 saturated hydraulic condictivity for Unit 3 material	N(μ=5.14e-5, σ=5.95e-6, min=Small, max=Large); [*correlated to D_Unit3 -0.98*]	cm/s	*ibid.*, truncated just above 0

4.5 \Materials\Unit2_Properties

Material properties for the saturated zone, comprised of stratigraphic Unit 2, a silty clay, are provided in Table 10. Unit 2 is assigned K_d values for clay.

Table 10. Unit 2 material properties

GoldSim element	value or distribution	units	reference / comment
BulkDensity_Unit2 dry bulk density for Unit 2 material	N(μ=1.57, σ=0.05, min=Small, max=Large)	g/cm^3	see Saturated Zone Modeling white paper truncated just above 0
Porosity_Unit2 porosity for Unit 2 material	N(μ=0.29, σ=0.05, min=Small, max=1-Small)	—	*ibid.*, truncated just above 0 and just below 1
Ksat_Unit2 saturated hydraulic conductivity for Unit 2	N(μ=9.6e-4, σ=9.67e-5, min=Small, max=Large)	cm/s	*ibid.*, truncated just above 0

4.6 \Materials\RipRap_Properties

Rip Rap is used to construct the uppermost layer: Armor. It quickly becomes infilled with Loess. The Rip Rap itself is assumed to be an inert material.

Table 11. Rip rap material properties

GoldSim element	value or distribution	units	reference / comment
ParticleDensity_RipRap	2.65	g/cm^3	see Unsaturated Zone Modeling white paper
BulkDensity_RipRap	N(μ=*f*(*x*), σ=0.1, min=Small, max=Large)	g/cm^3	*ibid.*, truncated just above 0
Porosity_RipRap	N(μ=0.18, σ=0.01, min=Small, max=1-Small)	—	*ibid.*, truncated just above 0 and just below 1

4.7 Materials\FineCobbleMix_Properties

Fine Cobble Mix is used to construct the upper filter layer. It also becomes quickly infilled with Loess. The Fine Cobble Mix itself is assumed to be an inert material.

Table 12. Fine cobble mix material properties

GoldSim element	value or distribution	units	reference / comment
ParticleDensity_ FineCobbleMix	2.65	g/cm^3	see Unsaturated Zone Modeling white paper
BulkDensity_ FineCobbleMix	N(μ=*f*(*x*), σ=0.1, min=Small, max=Large)	g/cm^3	*ibid.*, truncated just above 0
Porosity_ FineCobbleMix	N(μ=0.19, 0.01, min=Small, max=1-Small)	—	*ibid.*, truncated just above 0 and just below 1

4.8 Materials\SiltSandGravel_Properties

Silt Sand Gravel is used to construct the Sacrificial Soil layer.

Table 13. Silt sand gravel material properties

GoldSim element	value or distribution	units	reference / comment
ParticleDensity_ SiltSandGravel	2.65	g/cm^3	see Unsaturated Zone Modeling white paper
BulkDensity_ SiltSandGravel	N(μ=*f*(*x*), σ=0.1, min=Small, max=Large)	g/cm^3	*ibid.*, truncated just above 0
Porosity_ SiltSandGravel	N(μ=0.31, 0.01, min=Small, max=1-Small)	—	*ibid.*, truncated just above 0 and just below 1

4.9 Materials\FineGravelMix_Properties

Fine Gravel Mix is used to construct the lower filter layer. It becomes infilled with Silt Sand Gravel from the Sacrificial Soil layer over time. The Fine Gravel Mix itself is assumed to be an inert material.

Table 14. Fine gravel mix material properties

GoldSim element	value or distribution	units	reference / comment
ParticleDensity_ FineGravelMix	2.65	g/cm^3	see Unsaturated Zone Modeling white paper
BulkDensity_ FineGravelMix	N(μ=*f*(*x*), σ=0.01, min=Small, max=Large)	g/cm^3	*ibid.*, truncated just above 0
Porosity_ FineGravelMix	N(μ=0.28, 0.01, min=Small, max=1-Small)	—	*ibid.*, truncated just above 0 and just below 1

4.10 Materials\UpperRnBarrierClay_Properties

The Radon Barrier layers are divided into upper and lower layers. Both are constructed of local Unit 4 clay, compacted to different hydraulic conductivities. UpperRnClay represents the upper of the two layers, and has significantly lower K_{sat} (see Table 15). Other material properties for this material are redirected to those of Unit 4 (see Table 8).

Table 15. Upper radon barrier clay material properties

GoldSim element	value or distribution	units	reference / comment
Ksat_RnClayUpper	LN(GM=5e-8, GSD=1.2)	cm/s	see Unsaturated Zone Modeling white paper

4.11 Materials\LowerRnBarrierClay_Properties

The Lower Radon Barrier is constructed of compacted local Unit 4 clay, but has its own K_{sat} (see Table 16). LowerRnClay represents the lower of the two layers. Other material properties for this material are redirected to those of Unit 4 (see Table 8).

Table 16. Lower radon barrier clay material properties

GoldSim element	value or distribution	units	reference / comment
Ksat_RnClayLower	LN(GM=1e-6, GSD=1.2)	cm/s	see Unsaturated Zone Modeling white paper

4.12 Materials\LinerClay_Properties

The Liner is constructed of compacted local Unit 4 clay, but has its own K_{sat} (see Table 17). Other material properties for this material are redirected to those of Unit 4 (see Table 8).

Table 17. Liner clay material properties

GoldSim element	value or distribution	units	reference / comment
Ksat_LinerClay	LN(GM=1e-6, GSD=1.2)	cm/s	see Unsaturated Zone Modeling white paper

4.13 \Materials\UO3_Waste_Properties

UO_3 waste is typical of the Savannah River Site DU waste stream. Note, however, that given that the DU-containing waste layer is overwhelmingly inert fill by volume, the material properties for this layer as modeled are set to those of Unit 3 (see Table 9).

4.14 \Materials\Waste_U3O8_Properties

U_3O_8 waste is typical of the gaseous diffusion plant DU waste streams. Like the UO_3 waste, the material properties for this layer as modeled are set to those of Unit 3 (see Table 9).

4.15 \Materials\Generic_Waste_Properties

The current Clive DU PA Model has no generic waste inventory, but this material is defined as a placeholder. Any layers to be filled with generic LLW borrow material properties from Unit 3 (see Table 9).

4.16 \Materials\Water_Properties

Water is the reference fluid in GoldSim.

Table 18. Properties of water, the reference fluid.

GoldSim element	value or distribution	units	reference / comment
RefDiffusivity_Water reference diffusivity in Water	1×10^{-9}	m^2/s	as given in the GoldSim manual
Dm molecular diffusivity in Water	U(3e-6, 2e-5)	cm^2/s	see the Geochemical Modeling white paper

4.17 \Materials\Kd

Since the K_d distribution for each element and each material can be defined independently, with a different distributional form, the Model Parameters workbook does not lend itself to listing these as a vector. Instead, each chemical element is listed in the following tables, one table for each material. Materials are limited to sand, silt, and clay, which spans the gross material properties found at the site. Since the depleted uranium is assumed to be dispersed in a large volume of fill material of as yet unspecified characteristics, the material properties of the disposed waste

generally assumes the properties of this fill material. For now, then, the uranium oxide wastes are not assigned their own chemical properties.

4.17.1 \Materials\Kd\Kd_Sand_Values

Table 19. Soil/water partition coefficients (K_ds) for sand

chemical element	value or distribution	units	reference / comment
Ac	LU(min=16.8, max=535)	mL/g	see Geochemical Modeling white paper
Am	LU(min=43.2, max=811)	mL/g	*ibid.*
Cs	LU(min=2.70, max=22.2)	mL/g	*ibid.*
I_dist	N(0.428, 0.605), with values less than 0 set to 0.	mL/g	*ibid.*; Values sampled below 0 are set to 0, within the Expression I.
Np	LU(min=0.392, max=51)	mL/g	*ibid.*
Pa	LU(min=8.32, max=331)	mL/g	*ibid.*
Pb	LU(min=2.70, max=22.2)	mL/g	*ibid.*
Pu	LU(min=66.9, max=2390)	mL/g	*ibid.*
Ra	LU(min=0.387, max=64.6)	mL/g	*ibid.*
Rn	0	mL/g	*ibid.*
Sr	LU(min=2.7, max=22.2)	mL/g	*ibid.*
Tc_dist	N(0.102, 0.145), with values less than 0 set to 0.	mL/g	*ibid.*; Values sampled below 0 are set to 0, within the Expression Tc.
Th	LU(min=19.2, max=41.6)	mL/g	*ibid.*
U	LU(min=0.344, max=6.77)	mL/g	*ibid.*

4.17.2 \Materials\Kd\Kd_Silt_Values

Table 20. Soil/water partition coefficients (K_ds) for silt

chemical element	value or distribution	units	reference / comment
Ac	LU(min=15.7, max=1910)	mL/g	see Geochemical Modeling white paper
Am	LU(min=88.0, max=1140)	mL/g	*ibid.*
Cs	LU(min=4.23, max=118)	mL/g	*ibid.*

chemical element	value or distribution	units	reference / comment
I	Equal to Kd for I in Sand	mL/g	*ibid.*
Np	LU(min=0.805, max=62.1)	mL/g	*ibid.*
Pa	LU(min=184, max=978)	mL/g	*ibid.*
Pb	LU(min=4.23, max=118)	mL/g	*ibid.*
Pu	LU(min=80.5, max=6210)	mL/g	*ibid.*
Ra	LU(min=0.797, max=75.3)	mL/g	*ibid.*
Rn	0	mL/g	*ibid.*
Sr	LU(min=4.23, max=118)	mL/g	*ibid.*
Tc	Equal to Kd for Tc in Sand	mL/g	*ibid.*
Th	LU(min=34.4, max=697)	mL/g	*ibid.*
U	LU(min=0.880, max=11.4)	mL/g	*ibid.*

4.17.3 \Materials\Kd\Kd_Clay_Values

Table 21. Soil/water partition coefficients (K_ds) for clay

chemical element	value or distribution	units	reference / comment
Ac	LU(min=83.6, max=2990)	mL/g	see Geochemical Modeling white paper
Am	LU(min=88.0, max=1140)	mL/g	*ibid.*
Cs	LU(min=6.69, max=239)	mL/g	*ibid.*
I	Equal to Kd for I in Sand	mL/g	*ibid.*
Np	LU(min=4.32, max=81.1)	mL/g	*ibid.*
Pa	LU(min=180, max=1560)	mL/g	*ibid.*
Pb	LU(min=6.69, max=239)	mL/g	*ibid.*
Pu	LU(min=914, max=5470)	mL/g	*ibid.*
Ra	LU(min=1.42, max=1410)	mL/g	*ibid.*
Rn	0	mL/g	*ibid.*
Sr	LU(min=6.69, max=239)	mL/g	*ibid.*
Tc	Equal to Kd for Tc in Sand	mL/g	*ibid.*
Th	LU(min=84.7, max=2360)	mL/g	*ibid.*
U	LU(min=9.05, max=66.3)	mL/g	*ibid.*

4.18 \Materials\WaterSolubility

Since the aqueous solubility distribution for each element and each material could be defined independently, with a different distributional form, the Model Parameters workbook does not lend itself to listing these as a vector. Instead, each chemical element is listed in the following table.

4.18.1 \Materials\WaterSolubility\Solubilities_Saltwater

Table 22. Aqueous solubilities in saltwater, by chemical element

chemical element	value or distribution	units	reference / comment
Ac	LU(min=6.81e-9, max=1.47e-5)	mol/L	see Geochemical Modeling white paper
Am	LU(min=6.81e-10, max=1.47e-6)	mol/L	*ibid.*
Cs	LU(min=6.81e-3, max=1.47e1)	mol/L	*ibid.*
I	LU(min=5.99e-5, max=1.67e0)	mol/L	*ibid.*
Np	LU(min=6.81e-6, max=1.47e-2)	mol/L	*ibid.*
Pa	LU(min=6.81e-9, max=1.47e-5)	mol/L	*ibid.*
Pb	LU(min=6.81e-9, max=1.47e-5)	mol/L	*ibid.*
Pu	LU(min=5.27e-11, max=1.90e-5)	mol/L	*ibid.*
Ra	LU(min=5.99e-10, max=1.67e-5)	mol/L	*ibid.*
Rn	LU(min=7.74e-4, max=1.29e-1)	mol/L	*ibid.*
Sr	LU(min=6.81e-7, max=1.47e-3)	mol/L	*ibid.*
Tc	LU(min=7.74e-5, max=1.29e-2)	mol/L	*ibid.*
Th	LU(min=7.74e-9, max=1.29e-6)	mol/L	*ibid.*
UO3	LU(min=3.58e-6, max=2.79e-3)	mol/L	*ibid.*
U3O8	LU(min=1e-16, max=6.5e-10)	mol/L	*ibid.*

4.19 \Materials\AirDiffusivities

Currently, the only gaseous radionuclide in the model is ^{222}Rn, which diffuses in the air phase.

Table 23. Parameters relevant to diffusion in air..

GoldSim element	value or distribution	units	reference / comment
RefDiffusivity_Air	1	cm^2/s	arbitrary value in GoldSim, as it falls out in math
Da_Rn	0.11	cm^2/s	Rogers and Nielson (1991)

4.20 \Materials\Kh

Radon also partitions into water according to its Henry's Law constant.

Table 24. Henry's Law constants and related parameters.

GoldSim element	value or distribution	units	reference / comment
SoilTemp average soil temperature	N(μ=12, σ=1)	°C	Estimated from the Clive Test Cell temperature data "Temp and Dose Data 9-19-01 to 1-15-09.xls" provided by Energy*Solutions.*
Khcp_Rn parameter used in devising Henry's Law constant	9.3e-3	mol/L·atm	Sander (1999), table 7, page 13

5.0 \Processes

Physical process parameters global in scope (general to the entire model) are defined in this container.

5.1 \Processes\AirTransport

Contaminant transport in air includes both pore air in porous media, and the dispersion into and within the atmosphere. Chi/Q values for gas and particles that are specific to the Class A South embankment are listed in Table 43 (for the \Disposal\AtmosphericDispersion\AirConc_Remote container).

Table 25. Radon diffusive transport parameters.

GoldSim element	value or distribution	units	reference / comment
EPRatio_Radon radon escape/production ratio	beta(0.290, 0.156, min=0, max=1)	—	see Unsaturated Zone Modeling white paper
ThicknessAtm mixing thickness of the atmosphere, for purposes of diffusion from soil layers	N(μ=2.0, σ=0.5, min=Small, max=Large)	m	*ibid.*
WindSpeed average wind speed, for purposes of diffusion from soil layers	N(μ=3.14, σ=0.5, min=Small, max=Large)	m/s	*ibid.*

GoldSim element	value or distribution	units	reference / comment
AtmDiffusionLength diffusion length for the atmosphere, for purposes of diffusion from soil layers	N(μ=0.1, σ=0.02, min=Small, max=Large)	m	*ibid.*

Table 26. Atmospheric transport parameters.

GoldSim element	value or distribution		units	reference / comment
Dust_mask logical mask to identify PM-10 particles	Rn = 0, all others = 1 (see workbook)		—	masks Species with 0/1 to be those found in dust particles
Gas_mask logical mask to identify gases	Rn = 1, all others = 0 (see workbook)		—	masks Species with 0/1 to be those found in gaseous phase
ResuspensionFlux mass flux of soil particles into atmosphere	LU(Small, 0.3)		kg/m^2-yr	see Atmospheric Modeling white paper
Particle_Fraction the fraction of PM-10 particles in the 0 to 2.5 μm size bin	U(0,1)		—	based on physical limits
Frac_OffSite_ Deposition fraction of all particles that migrate off site that are deposited in the off-site air dispersion area. a lookup table based on Particle_Fraction	0	0.11	—	see Atmospheric Modeling white paper
	0.05	0.11	—	
	0.1	0.11	—	
	0.2	0.099	—	
	0.4	0.086	—	
	0.6	0.072	—	
	0.8	0.057	—	
	1.0	0.041	—	
OnSiteRedepos_ Ratio_bySize a lookup table based on Particle_Fraction	0	4.224e-7	g/m^2-yr per g/yr	*ibid.*
	0.05	4.114e-7		
	0.1	4.002e-7		
	0.2	3.776e-7		
	0.4	3.311e-7		
	0.6	2.827e-7		
	0.8	2.321e-7		
	1.0	1.794e-7		

5.2 \Processes\AnimalTransport

Burrowing animals have the potential to exhume waste or contaminated cap materials. All burrowers are collected into one of two types: ants and small mammals.

5.2.1 \Processes\AnimalTransport\AntData

Table 27. Model parameters for ants.

GoldSim element	value or distribution	units	reference / comment
NestVolume volume of each nest	N(μ=0.161, σ=0.024, min=0, max=Large)	m^3	see Biological Modeling white paper
ColonyLifespan lifespan of each colony	N(μ=20.2, σ=3.6, min=Small, max=Large)	yr	*ibid.*
ColonyDensity area density of colonies on the ground	see below for each field study plot	1/ha	*ibid.*
_Plot1	Gamma(33,1, min=0, max=Large)	1/ha	*ibid.*
_Plot2	Gamma(2, 1, min=0, max=Large)	1/ha	*ibid.*
_Plot3	Gamma(7, 1, min=0, max=Large)	1/ha	*ibid.*
_Plot4	Gamma(17, 1, min=0, max=Large)	1/ha	*ibid.*
_Plot5	Gamma(6, 1, min=0, max=Large)	1/ha	*ibid.*
MaxDepth maximum depth for any colony	212	cm	*ibid.*
b fitting parameter for nest shape	N(μ=10, σ=0.71, min=1, max=Large)	—	*ibid.*

5.2.2 \Processes\AnimalTransport\MammalData

Table 28. Model parameters for small mammals.

GoldSim element	value or distribution	units	reference / comment
MoundDensity area density of mounds on the ground	see below for each plot	1/ha	see Biological Modeling white paper
_Plot1	Gamma(235, 1, min=0, max=Large)	1/ha	*ibid.*
_Plot2	Gamma(239, 1, min=0, max=Large)	1/ha	*ibid.*

GoldSim element	value or distribution	units	reference / comment
_Plot3	Gamma(1.33, 1, min=0, max=Large)	1/ha	*ibid.*
_Plot4	Gamma(1.33, 1, min=0, max=Large)	1/ha	*ibid.*
_Plot5	Gamma (1.33, 1, min=0, max=Large)	1/ha	*ibid.*
ExcavationRate volumetric rate of a single burrow excavation	N(μ=0.0006, σ=0.00015, min=Small, max=Large)	m^3/yr	*ibid.*
MaxDepth maximum depth for any burrow	200	cm	*ibid.*
b fitting parameter for burrow shape	N(μ=4.5, σ=0.84, min=1, max=Large)	—	*ibid.*

5.3 \Processes\PlantTransport

Plants have the potential to translocate contaminants in waste or contaminated cap materials. All plants are collected into one of five types: greasewood, grasses, forbs, trees, and shrubs. Each of these plant types is characterized in each of the five plot locations that were studied, corresponding to five vegetation associations:

- Plot 1: Mixed Grassland
- Plot 2: Juniper - Sagebrush
- Plot 3: Black Greasewood
- Plot 4: Halogeton - Disturbed
- Plot 5: Shadscale - Gray Molly

Each of these vegetation associations is picked at random for a given realization.

Table 29. Parameters general to all plants.

GoldSim element	value or distribution	units	reference / comment
BiomassProductionRate	U(300, 1500)	kg/ha-yr	see *Biological Modeling* white paper
VegetationAssociationPicker	discrete(1, 2, 3, 4, 5)	—	*ibid.*

5.3.1 \Processes\PlantTransport\PlantCR

Table 30. Plant/soil concentration ratio parameters.

GoldSim element	value or distribution	units	reference / comment
CR_GM	tabulated in Clive PA Model Parameters.xls workbook	—	see *Biological Modeling* white paper
CR_GSD	tabulated in Clive PA Model Parameters.xls workbook	—	*ibid.*
CR_GM_radon	Small	—	*ibid.*
CR_GSD_radon	1	—	*ibid.*

5.3.2 \Processes\PlantTransport\BiomassCalcs

Table 31. Biomass calculation parameters.

GoldSim element	value or distribution	units	reference / comment
percent cover tables, such as PctCover_Plot4_Forb	tabulated in Clive PA Model Parameters.xls workbook	%	These are 25 tables, one for each Plot and for each plant type. Source: plant.cover.percent.simulations.xlsx in Clive PA Model Parameters.xls workbook
PctCoverRandomSelector	probability of 0.001 assigned to discrete values from 1 to 1000	%	An index generator used to pick correlated sets of percent cover

5.3.3 \Processes\PlantTransport\GreasewoodData

Table 32. Greasewood parameters.

GoldSim element	value or distribution	units	reference / comment
RootShoot_Ratio	U(0.30, 1.24)	—	see Biological Modeling white paper
MaxDepth	570	cm	*ibid.*
b	N(μ=14.6, σ=0.0807, min=1, max=Large)	—	*ibid.*

5.3.4 \Processes\PlantTransport\GrassData

Table 33. Grass parameters.

GoldSim element	value or distribution	units	reference / comment
RootShoot_Ratio	T(1, 1.2, 2)	—	see Biological Modeling white paper
MaxDepth	150	cm	*ibid.*
b	N(μ=2.19 σ=0.036, min=1, max=Large)	—	*ibid.*

5.3.5 \Processes\PlantTransport\ForbData

Table 34. Forb parameters.

GoldSim element	value or distribution	units	reference / comment
RootShoot_Ratio	U(0.40, 1.80)	—	see Biological Modeling white paper
MaxDepth	51	cm	*ibid.*
b	N(μ=23.9 σ=0.313, min=1, max=Large)	—	*ibid.*

5.3.6 \Processes\PlantTransport\TreeData

Table 35. Tree parameters.

GoldSim element	value or distribution	units	reference / comment
RootShoot_Ratio	U(0.55, 0.76)	—	see Biological Modeling white paper
MaxDepth	450	cm	*ibid.*
b	N(μ=14.6 σ=0.0807, min=1, max=Large)	—	*ibid.*

5.3.7 \Processes\PlantTransport\ShrubData

Table 36. Other shrub parameters.

GoldSim element	value or distribution	units	reference / comment
RootShoot_Ratio	U(0.4, 1.8)	—	see Biological Modeling white paper
MaxDepth	110	cm	*ibid.*
b	N(μ=23.9 σ=0.313, min=1, max=Large)	—	*ibid.*

5.4 \Processes\WaterTransport

Flow within moving water (advection) and diffusion within water are typically significant contaminant transport mechanisms. Global parameters for water transport are located here. Other parameters specific to a modeled column are located within that column's modeling container (e.g. Section 7.2.3 Table 46).

Table 37. Water transport parameters.

GoldSim element	value or distribution	units	reference / comment
AnnualPrecipitation_Avg	N(μ=8.61, σ=0.822,min=0, max=Large)	in/yr	see Unsaturated Zone Modeling white paper
Evapotranspiration_Cover	N(μ=5.14, σ=0.762, min=0, max=Large)	in/yr	*ibid.*
MoistureContent_Armor	N(μ=0.125, σ=0.0175, min=Small, max= Porosity_Unit4)	—	*ibid.*
MoistureContent_UpperFilter	use value for Armor	—	*ibid.*
MoistureContent_SacSoil	N(μ=0.243, σ=0.0175, min=Small, max=Porosity_ SiltSandGravel)	—	*ibid.*
MoistureContent_LowerFilter	use value for SacSoil	—	*ibid.*
WaterContent_Exponent exponent to water content in water phase tortuosity calc	U(4/3, 7/3)	—	*ibid*
Porosity_Exponent exponent to porosity in water phase tortuosity calculation	U(0.5, 2)	—	*ibid.*

5.5 \Processes\ErosionTransport

Erosion through the formation of gullies can be a significant mechanism for exposing waste to the environment. Global parameters for erosion are located here. Other parameters specific to an embankment are located within that embankment's modeling container (e.g. Section 7.2.5 Table 60).

Table 38. Water transport parameters.

GoldSim element	value or distribution	units	reference / comment
AngleOfRepose_Gully angle of repose for gully walls	N(μ=38, σ=5, min=Small, max=90-Small)	degrees	see Erosion Modeling white paper
Gully_b_parameter shape parameter for gully thalweg	N(μ=-0.4, σ=0.15, min=-0.75, max=-0.05)	—	*ibid.*

6.0 \Inventory

The DU waste is characterized by analysis of the SRS DU. To date, insufficient information exists to thoroughly characterize the DU wastes expected to arrive from the gaseous diffusion plants (GDPs).

6.1 \Inventory\SRS_DU_Inventory

The SRS DU, which consists of several thousand 208-L (55-gal) drums of powdered DUO_3, has been subjected to laboratory analysis, so activity concentrations are based on that information.

Table 39. SRS DU inventory parameters.

GoldSim element	value or distribution	units	reference / comment
ActivityConc_DUWaste_Mean	See parameters workbook, sheet "Inventory"	pCi/g	see Waste Inventory white paper
ActivityConc_DUWaste_StdDev	See parameters workbook, sheet "Inventory"	pCi/g	see Waste Inventory white paper
SRS_DU_Drums_Disposed	21000	—	(not considered in this PA)
SRS_DU_Drums_ProposedUT	5408	—	see Waste Inventory white paper
SRS_DU_Drums_ProposedEW	5408 × 2	—	(not considered in this PA)
Drum_Mass	20	kg	see Waste Inventory white paper
ShippedMass_Proposed_UT	3577	Mg	see Waste Inventory white paper

6.2 \Inventory\GDP_DU_Inventory

Since insufficient information exists to exactly characterize the DU wastes expected to arrive from the GDPs, the activity concentrations and other waste material characteristics are borrowed from the SRS DUO_3 waste, as a proxy.

Table 40. GDP DU inventory parameters.

GoldSim element	value or distribution	units	reference / comment
Num_DUF6_Cylinders_PGDP	36191	—	see Waste Inventory white paper
Num_DUF6_Cylinders_PORTS	16109	—	*ibid.*
Num_DUF6_Cylinders_K25	4822	—	*ibid.*
Mass_DUF6_PGDP	436400	Mg	*ibid.*
Mass_DUF6_PORTS	195800	Mg	*ibid.*
Mass_DUF6_K25	54300	Mg	*ibid.*
CylinderDiameter	4	ft	*ibid.*
CylinderLength	12	ft	*ibid.*
FractionGDP_Contaminated	Beta(0.0392, 0.0025, 0, 1)	—	*ibid.*
CleanDU_Mask	see workbook	—	simply a mask for uranium

6.3 \Inventory\Other_DU_Inventory

This is a placeholder container. No other DU inventory is assumed in the model.

6.4 \Inventory\ClassA_LLW_Inventory

This is a placeholder container. No other LLW inventory is assumed in the model.

7.0 \Disposal

The Disposal container hosts all the actual contaminant calculations, including atmospheric transport, transport mechanisms within each column of each embankment (water, air, biological, etc.) and the saturated zone. While global transport parameters are defined in the \Processes container (Section 5.0), parameters and calculations specific to local mechanisms are defined here.

7.1 \Disposal\AtmosphericDispersion

The values for the ratio of airborne contaminant concentration to source release rate into the atmosphere are known as X/Q (Chi/Q) values. These are implemented as lookup tables on Particle_Fraction.

7.1.1 \Disposal\AtmosphericDispersion\AirConc_Onsite

OnSite air concentrations are used for exposures to receptors that traverse the embankment itself.

Table 41. Atmosphere dispersion parameters for on-site exposures.

GoldSim element	value or distribution		units	reference / comment
ChiQ_Embankment _538m	0	222	(μg/m^3)/(g/s)	see Atmospheric Modeling white paper
	0.05	223		
	0.1	224		
	0.2	225		
	0.4	228		
	0.6	231		
	0.8	234		
	1.0	238		
ChiQ_Gas_Onsite (Embankment)	234		same	*ibid.*

7.1.2 \Disposal\AtmosphericDispersion\MediaConc_Offsite

OffSite air concentrations are used for exposures to receptors that traverse the area surrounding the embankment. These receptors also have access to the embankment itself. Functionally, the air concentrations are set to those same values used for OnSite air.

Table 42. Atmosphere dispersion parameters for off-site exposures (in the "air dispersion" area.)

GoldSim element	value or distribution	units	reference / comment
ChiQ_Dust_Offsite	set equal to ChiQ_Dust _Onsite	(μg/m^3)/(g/s)	see Atmospheric Modeling white paper
ChiQ_Gas_Offsite	0.38	same	*ibid.*

7.1.3 \Disposal\AtmosphericDispersion\AirConc_Remote

Various receptors are at specific geographic locations farther away from the site, including Interstate-80, the rail road, the Grassy Rest Area, the Knolls OHV Recreation Area, and the UTTR access road.

Table 43. Atmosphere dispersion parameters for remote off-site exposures.

GoldSim element	value or distribution		units	reference / comment
ChiQ_RestArea_1K	0	0.0069	(μg/m^3)/(g/s)	see Atmospheric Modeling white paper
	0.05	0.0069		
	0.1	0.0069		
	0.2	0.0070		

GoldSim element	value or distribution		units	reference / comment
	0.4	0.0071		
	0.6	0.0072		
	0.8	0.0073		
	1.0	0.0074		
ChiQ Gas RestArea	0.0088		same	*ibid.*
ChiQ_Knolls	0	0.043	same	*ibid.*
	0.05	0.044		
	0.1	0.044		
	0.2	0.046		
	0.4	0.049		
	0.6	0.052		
	0.8	0.055		
	1.0	0.058		
ChiQ Gas Knolls	0.053		same	*ibid.*
ChiQ_I80_1K	0	0.26	same	*ibid.*
	0.05	0.26		
	0.1	0.26		
	0.2	0.27		
	0.4	0.27		
	0.6	0.28		
	0.8	0.28		
	1.0	0.28		
ChiQ Gas I80	0.28		same	*ibid.*
ChiQ_Railroad_1K	0	0.43	same	*ibid.*
	0.05	0.43		
	0.1	0.43		
	0.2	0.43		
	0.4	0.43		
	0.6	0.44		
	0.8	0.44		
	1.0	0.44		
ChiQ Gas Railroad	0.44		same	*ibid.*
ChiQ_UTTRaccess_1K	0	222	same	*ibid.*
	0.05	223		
	0.1	224		
	0.2	225		
	0.4	228		

GoldSim element	value or distribution	units	reference / comment
	0.6 231		
	0.8 234		
	1.0 238		
ChiQ Gas UTTRaccess	234	same	*ibid.*

7.2 \Disposal\ClassASouthCell

This PA model considers only the Class A South cell, part of the Federal Cell embankment.

7.2.1 \Disposal\ClassASouthCell\ClassASouth_Cell_Dimensions

Exact dimensions of the embankment are somewhat irregular, so the shape of the cell has been somewhat idealized to facilitate calculations. Elevations for the top of the waste are read from drawing 07021 V1, which has the note "1. All elevations shown are for top of waste..." Elevation of bottom of waste is from drawing 07021 V3.

Table 44. Interior (waste) dimensions of the Federal Cell, Class A South section.

GoldSim element	value or distribution	units	reference / comment
AverageOriginalGrade Average original grade elevation	4272	ft amsl	see Embankment Modeling.pdf
WasteTopElev_Ridge Elevation of top of the waste at the ridgeline	4317.25	ft amsl	*ibid.*
AverageWasteTopElev_Break Elevation of top of the waste at the break in slope	4299.20	ft amsl	*ibid.*
WasteBottomElev Elevation of the bottom of the waste	4264.17	ft amsl	*ibid.*
LengthOverall Length overall	1429.6	ft	*ibid.*
WidthOverall Width overall	1775	ft	*ibid.*
LengthToBreak Length from edge to the break in slope	153.2	ft	*ibid.*
WidthToBreak Width from edge to the break in slope	152.1	ft	*ibid.*

GoldSim element	value or distribution	units	reference / comment
RidgeLength Length along the ridge	542.1	ft	*ibid.*

7.2.2 \Disposal\ClassASouth\NaturalSystemGeometry

Table 45. Natural system geometry parameters for the Class A South cell.

GoldSim element	value or distribution	units	reference / comment
UZ_Thickness thickness of the unsaturated zone below the CAS cell	N(μ=12.9, σ=0.25, min=Small, max=Large)	ft	see Unsaturated Zone Modeling white paper

7.2.3 \Disposal\ClassASouthCell\TopSlope

No input elements are defined at this level.

7.2.3.1 \Disposal\ClassASouthCell\TopSlope\Column_Transport

No input elements are defined at this level.

7.2.3.1.1 \Disposal\ClassASouthCell\TopSlope\Column_Transport \WaterTransport

No input elements are defined at this level.

7.2.3.1.1.1 \Disposal\ClassASouthCell\TopSlope\Column_Transport \WaterTransport\WaterTransport_CapCells

Water balance and flow calculations for the top slope column are performed here.

Table 46. Infiltration parameters for cap cells.

GoldSim element	value or distribution	units	reference / comment
SurfaceRunoff	LN(GM=0.0252, GSD=3.33, min=0, max=0.1)	in/yr	see Unsaturated Zone Modeling white paper
LatDiversion_UpperFilter_Early	N(μ=0.0427, σ=0.0111, min=Small, max=Large)	in/yr	*ibid.*
LatDiversion_LowerFilter_Early	N(μ=3.39, σ=0.214, min=Small, max=Large)	in/yr	*ibid.*
VerticalFlow_RnBarrier_Early	N(μ=0.104, σ=0.00417, min=Small, max=Large)	in/yr	*ibid.*
LatDiversion_UpperFilter_Late	0.0	in/yr	*ibid.*
LatDiversion_LowerFilter_Late	N(μ=0.345, σ=0.0815, min=Small, max=Large)	in/yr	*ibid.*
VerticalFlow_RnBarrier_Late	N(μ=0.0482, σ=0.00351, min=Small, max=Large)	in/yr	*ibid.*

7.2.3.2 \Disposal\ClassASouthCell\TopSlope\Column_MoistureProfile

7.2.3.2.1 \Disposal\ClassASouthCell\TopSlope\Column_MoistureProfile \WaterContentCalcs_RnBarrier

Table 47. Parameters for moisture profile calculations for the radon barrier.

GoldSim element	value	units	reference / comment
NumNodes	5		this is the number of modeled radon barrier layers +1
UpperRn_NodeNumber	2		middle node in part of column
LowerRn_NodeNumber	4		middle node in part of column

7.2.3.2.2 \Disposal\ClassASouthCell\TopSlope\Column_MoistureProfile \WaterContentCalcs_Waste

Table 48. Parameters for moisture profile calculations for the waste.

GoldSim element	value	units	reference / comment
NumNodes	28	—	this is the number of modeled waste layers +1

7.2.3.2.3 \Disposal\ClassASouthCell\TopSlope\Column_MoistureProfile \WaterContentCalcs_Liner

Table 49. Parameters for moisture profile calculations for the clay liner.

GoldSim element	value	units	reference / comment
NumNodes	5		this is the number of modeled liner layers +1
MiddepthNodeNumber	3		middle node in column

7.2.3.2.4 \Disposal\ClassASouthCell\TopSlope\Column_MoistureProfile \WaterContentCalcs_Unsat

Table 50. Parameters for moisture profile calculations for the unsaturated zone below the clay liner.

GoldSim element	value or distribution	units	reference / comment
NumNodes	24		see Unsaturated Zone Modeling white paper
ZoneThickness specified from the bottom up	-0.0204 -0.0204 -0.0204 -0.0204 -0.0204 -0.0510 -0.0510 -0.0510 -0.2550 -0.2550 -0.2550 -0.2550 -0.2550 -0.2550 -0.2550 -0.2550 -0.2550 -0.2550 -0.2550 -0.2550 -0.2550 -0.2550 0	m	*ibid.*
MiddepthNodeNumber	16		middle node in column

7.2.3.3 \Disposal\ClassASouthCell\TopSlope\Cap_Layers

7.2.3.3.1 \Disposal\ClassASouthCell\TopSlope\CapLayers\CapCell_Dimensions

Table 51. Cap layering dimensions for the top slope.

GoldSim element	value or distribution	units	reference / comment
TArmor Type B rip rap thickness	18	in	see Embankment Modeling white paper
TUpperFilter Type A filter zone thickness	6	in	*ibid.*
TSacrificialSoil Sacrificial soil thickness	12	in	*ibid.*
TLowerFilter Type B filter zone thickness	6	in	*ibid.*
TUpperRadon upper radon barrier clay thickness	12	in	*ibid.*
TLowerRadon lower radon barrier clay thickness	12	in	*ibid.*
NArmorCells	3	—	modeling construct
NUpperFilterCells	1	—	modeling construct
NSacrificialSoilCells	2	—	modeling construct
NLowerFilterCells	1	—	modeling construct
NUpperRadonCells	2	—	modeling construct
NLowerRadonCells	2	—	modeling construct
TopCell_Thickness	U(1 cm, TArmor – NArmorCells × 1 cm)	cm	modeling construct This allows the thickness of the topmost cell to vary between 1 cm and the maximum so that the other cells in this layer are at least 1 cm.

7.2.3.4 \Disposal\ClassASouthCell\TopSlope\Liner

Table 52. Number of liner cells.

GoldSim element	value or distribution	units	reference / comment
NumLinerCells	4	—	modeling construct

7.2.3.5 \Disposal\ClassASouthCell\TopSlope\UnsatLayer

Table 53. Number of unsaturated zone cells.

GoldSim element	value or distribution	units	reference / comment
NumUnsatCells	10	—	modeling construct

7.2.3.6 \Disposal\ClassASouthCell\TopSlope\WasteLayers

No input elements are defined at this level.

7.2.3.6.1 \Disposal\ClassASouthCell\TopSlope\WasteLayers\ WasteCell_Dimensions

Table 54. Top slope waste cell dimensions.

GoldSim element	value or distribution	units	reference / comment
NumWasteCells_TS	27	—	modeling construct

7.2.4 \Disposal\ClassASouthCell\SideSlope

No input elements are defined at this level.

7.2.4.1 \Disposal\ClassASouthCell\SideSlope\Column_Transport

No input elements are defined at this level.

7.2.4.1.1 \Disposal\ClassASouthCell\SideSlope\Column_Transport \WaterTransport

No input elements are defined at this level.

7.2.4.2 \Disposal\ClassASouthCell\SideSlope\Column_MoistureProfile

7.2.4.2.1 \Disposal\ClassASouthCell\SideSlope\Column_MoistureProfile \WaterContentCalcs_RnBarrier

Table 55. Parameters for moisture profile calculations for the radon barrier.

GoldSim element	value	units	reference / comment
NumNodes	5		this is the number of modeled radon barrier layers +1
UpperRn_NodeNumber	2		middle node in part of column
LowerRn_NodeNumber	4		middle node in part of column

7.2.4.2.2 \Disposal\ClassASouthCell\SideSlope\Column_MoistureProfile \WaterContentCalcs_Waste

Table 56. Parameters for moisture profile calculations for the waste.

GoldSim element	value	units	reference / comment
NumNodes	13	—	this is the number of modeled waste layers +1

7.2.4.2.3 \Disposal\ClassASouthCell\SideSlope\Column_MoistureProfile \WaterContentCalcs_Liner

Table 57. Parameters for moisture profile calculations for the clay liner.

GoldSim element	value	units	reference / comment
NumNodes	5		this is the number of modeled liner layers +1
MiddepthNodeNumber	3		middle node in column

7.2.4.2.4 \Disposal\ClassASouthCell\SideSlope\Column_MoistureProfile \WaterContentCalcs_Unsat

Parameters for moisture profile calculations for the unsaturated zone below the clay liner in teh side slope are identical to those for the top slope, as listed in Table 50.

7.2.4.3 \Disposal\ClassASouthCell\SideSlope\Cap_Layers

7.2.4.3.1 \Disposal\ClassASouthCell\SideSlope\CapLayers\CapCell_Dimensions

Table 58. Cap layering dimensions for the side slope.

GoldSim element	value or distribution	units	reference / comment
TArmor Type A rip rap thickness	18	in	see Embankment Modeling white paper
TUpperFilter Type A filter zone thickness	6	in	*ibid.*
TSacrificialSoil Sacrificial soil thickness	12	in	*ibid.*
TLowerFilter Type B filter zone thickness	18	in	*ibid.* (Note how this is different from the TopSlope value.)
TUpperRadon upper radon barrier clay thickness	12	in	*ibid.*

GoldSim element	value or distribution	units	reference / comment
TLowerRadon lower radon barrier clay thickness	12	in	*ibid.*
NArmorCells	3	—	modeling construct
NUpperFilterCells	1	—	modeling construct
NSacrificialSoilCells	2	—	modeling construct
NLowerFilterCells	1	—	modeling construct
NUpperRadonCells	2	—	modeling construct
NLowerRadonCells	2	—	modeling construct
TopCell_Thickness	U(1 cm, TArmor – NArmorCells × 1 cm)	cm	modeling construct This allows the thickness of the topmost cell to vary between 1 cm and the maximum so that the other cells in this layer are at least 1 cm.

7.2.4.4 \Disposal\ClassASouthCell\SideSlope\Liner

Parameters in this section are identical to those defined for the Top Slope in Section 7.2.3.4.

7.2.4.5 \Disposal\ClassASouthCell\SideSlope\UnsatLayer

Parameters in this section are identical to those defined for the Top Slope in Section 7.2.3.5.

7.2.4.6 \Disposal\ClassASouthCell\SideSlope\WasteLayers

No input elements are defined at this level.

7.2.4.6.1 \Disposal\ClassASouthCell\SideSlope\WasteLayers\ WasteCell_Dimensions

Table 59. Side slope waste cell dimensions.

GoldSim element	value or distribution	units	reference / comment
NumWasteCells	12	—	modeling construct

7.2.5 \Disposal\ClassASouthCell\GullyAndFan

The calculation of the volume, depth, and potential to expose waste by gullies is examined here. This work is preliminary, designed to evaluate whether more sophisticated landform evolution modeling is warranted.

Table 60. Basic gully and fan definition parameters.

GoldSim element	value or distribution	units	reference / comment
NumberOfGullies	discrete(1, ..., 20) equal probability (0.05)	—	See Erosion Modeling white paper.
AngleOfRepose_Fan	U(5, 10)	deg	*ibid.*

7.2.5.1 \Disposal\ClassASouthCell\GullyAndFan\GullyVolumeCalcs

The numerical (iterative) solution for gully and fan formation is done here.

Table 61. Gully and fan numerical solution parameters.

GoldSim element	value or distribution	units	reference / comment
ConvergenceCriterion	0.01	m^3	modeling construct

7.2.5.1.1 \Disposal\ClassASouthCell\GullyAndFan\GullyVolumeCalcs\ Dimensions

More numerical solution work for gully and fan formation is done here.

Table 62. More gully and fan numerical solution parameters.

GoldSim element	value or distribution	units	reference / comment
L_init	U(Small, 5)	m	see Erosion Modeling white paper

7.3 \Disposal\SatZone

The saturated zone underlies and accepts recharge from all the embankments at the Clive Facility. All contaminated recharge flows down-gradient to a monitoring well.

7.3.1 \Disposal\SatZone\SatZone_Parameters

Table 63. Saturated zone parameters.

GoldSim element	value or distribution	units	reference / comment
SZ_Thickness	N(μ=16.2, σ=0.25, min=0.1, max=Large)	ft	see Saturated Zone Modeling white paper
MonitoringWellDistance	90	ft	*ibid.*
WaterTableGradient	N(μ=6.94e-4, σ=1.27e-4, min=0, max=Large)	—	*ibid.*

7.3.2 \Disposal\SatZone\SZ_ClassASouthFootprint

Table 64. Total number of cells in the saturated footprint zone.

GoldSim element	value or distribution	units	reference / comment
NumCells_Footprint	25		modeling construct

7.3.2.1 \Disposal\SatZone\SZ_ClassASouthFootprint\Waste_to_Footprint

Table 65. Total number of cells in both footprint ends.

GoldSim element	value or distribution	units	reference / comment
NumCells_Footprint_Ends	4		modeling construct

7.3.3 \Disposal\SatZone\SZ_ToWell

Table 66. Total number of cells from footprint to well.

GoldSim element	value or distribution	units	reference / comment
NumCells_ToWell	20		modeling construct

7.4 \Disposal\EngineeredSystemGeometry

Table 67. Engineered system geometry parameters.

GoldSim element	value	units	reference / comment
ClayLiner_Thickness	2	ft	see Embankment Modeling white paper

8.0 \Exposure_Dose

The Data element Dose_Timestep_Length is controlled by the user, and so has no set value.

8.1 \Exposure_Dose\Media_Concs

Concentrations of contaminants in environmental media to which receptors may be exposed are collected and calculated in this container.

Table 68. Mechanically generated dust

GoldSim element	value or distribution	units	reference / comment
OHV_DustAdjustment OHV dust loading	LN(GM=98.1, GSD=1.65, min=Small, max=Large)	—	See Dose Assessment white paper

8.1.1 \Exposure_Dose\Media_Concs\Exposure_Areas

Table 69. Exposure areas used in the calculation of exposure media concentrations

GoldSim element	value or distribution	units	reference / comment
Receptor_Area Receptor area (exposure area)	U(16,000, 64,000)	acres	See Dose Assessment white paper
AntelopeRange_Area Pronghorn range area	U(995, 9192)	acres	*ibid.*

8.1.2 \Exposure_Dose\Media_Concs\Animal_Concentrations

Table 70. Animal tissue concentrations for the recreational and ranching scenarios

GoldSim element	value or distribution	units	reference / comment
TF_Beef_GM Beef transfer factor, geometric mean	Tabulated in workbook	day/kg	"Clive PA Model Parameters.xls", Elements worksheet; see also Dose Assessment white paper
TF_Beef_GSD Beef transfer factor, geometric standard deviation	Tabulated in workbook	—	*ibid.*
WaterIngRate_Cattle Cattle water ingestion rate	U(33, 53)	kg/day	See Dose Assessment white paper
ForageIngRate_Cattle Cattle forage ingestion rate	U(8.85, 14.75)	kg/day	*ibid.*
SoilIngRate_Cattle Cattle soil ingestion rate	U(0.05, 0.95)	kg/day	*ibid.*
GrazingTimeFrac_Cattle Cattle time fraction in exposure area	1	—	*ibid.*
WaterIngRate_Antelope Pronghorn water ingestion rate	U(0.1, 1)	kg/day	*ibid.*

GoldSim element	value or distribution	units	reference / comment
BodyWtFactor_Antelope Pronghorn body weight, as a unitless factor for allometric scaling	U (38,000, 41,000)	—	*ibid.* Body mass in Dose Assessment white paper reported in units of kg.
ForageIngRate_Antelope Pronghorn forage ingestion rate	0.577 × BodyWtFactor _Antelope$^{0.727}$ × 0.001	kg/day	*ibid.*
SoilIngRate_Antelope Pronghorn soil ingestion rate	U(0.005, 0.095)	kg/day	*ibid.*

8.1.2.1 \Exposure_Dose\Media_Concs\Animal_Concentrations\Beef_TFs

The beef transfer factors are tabulated in the Parameters Workbook, but some values in those table point to fixed values in the GoldSim model. These are tabulated here:

Table 71. Parameters related to beef transfer factors

GoldSim element	value or distribution	units	reference / comment
BeefTF_GM_radon Beef transfer factor for radon, geometric mean	Small	day/kg	See Dose Assessment white paper
BeefTF_GSD_radon Beef transfer factor for radon, geometric standard deviation	1	—	*ibid.*
BeefTF_GSD_generic Generic beef transfer factor, geometric standard deviation	1.475	—	*ibid.*

8.2 \Exposure_Dose\DCFs

Table 72. Dose conversion factors

GoldSim element	value or distribution	units	reference / comment
BranchingFractions Radionuclide branching fractions	Tabulated in workbook	—	"Dose Assessment Appendix II.xls", see also Dose Assessment white paper
DCF_Inh_Dust_determ Dose conversion factor, inhalation dust	Tabulated in workbook	Sv/Bq	*ibid.*

GoldSim element	value or distribution	units	reference / comment
DCF_Inh_Gas_determ Dose conversion factor, inhalation gas	Tabulated in workbook	Sv/Bq	*ibid.*
DCF_Ing_determ Dose conversion factor, ingestion	Tabulated in workbook	Sv/Bq	*ibid.*
DCF_Ext_Imm_determ Dose conversion factor, immersion	Tabulated in workbook	(Sv-m^3)/ (Bq-s)	*ibid.*
DCF_Ext_Soil_determ Dose conversion factor, external	Tabulated in workbook	(Sv-m^3)/ (Bq-s)	*ibid.*
Rn222_EffectiveDose Effective dose for Radon-222	6	(mSv-m^3)/ (mJ-hr)	See Dose Assessment white paper
Rn_progeny_equil energy per Bq of radon at equilibrium	5.56E-06	mJ/Bq	*ibid.*
Rn_Inh_rate Breathing rate for a standard worker	1.2	m^3/hr	*ibid.*

8.2.1 \Exposure_Dose\DCFs\Stochastic_REFs

Table 73. Stochastic radiation effectiveness factors

GoldSim element	value or distribution	units	reference / comment
Alpha_GM Alpha radiation effectiveness factor, geometric mean	18.1	—	"Dose Assessment Appendix II.xls", see also Dose Assessment white paper
Alpha_GSD Alpha radiation effectiveness factor, geometric standard deviation	2.37	—	*ibid.*
Alpha_REF Alpha radiation effectiveness factor, distribution	LN(GM=Alpha_GM, GSD=Alpha_GSD)	—	*ibid.*
Beta_GM Electron radiation effectiveness factor, geometric mean	2.41	—	*ibid.*

GoldSim element	value or distribution	units	reference / comment
Beta_GSD Electron radiation effectiveness factor, geometric standard deviation	1.44	—	*ibid.*
Beta_REF Electron radiation effectiveness factor, distribution	LN(GM=Beta_GM, GSD= Beta_GSD)	—	*ibid.*
Photon1_GM Photon radiation effectiveness factor (30-250 keV), geometric mean	1.96	—	*ibid*. (>0.03 and <=0.25 MeV)
Photon1_GSD Photon radiation effectiveness factor (30-250 keV), geometric standard deviation	1.48	—	*ibid.*
Photon1_REF Photon radiation effectiveness factor (30-250 keV), distribution	LN(GM=Photon1_GM, GSD= Photon1_GSD)	—	*ibid.*
Photon2_GM Photon radiation effectiveness factor (< 30 keV), geometric mean	2.45	—	*ibid.*
Photon2_GSD Photon radiation effectiveness factor (< 30 keV), geometric standard deviation	1.55	—	*ibid.* (<=0.03 MeV)
Photon2_REF Photon radiation effectiveness factor (< 30 keV), distribution	LN(GM=Photon2_GM, GSD=Photon2_GSD)	—	*ibid.*
Deterministic_REF Deterministic radiation effectiveness factor	1	—	See Dose Assessment white paper
WeightingFactor_Alpha Weighting factor for alpha radiation	20	—	*ibid.*
WeightingFactor_Beta Weighting factor for beta radiation	1	—	*ibid.*
WeightingFactor_Gamma Weighting factor for gamma radiation	1	—	*ibid.*

8.3 \Exposure_Dose\OuterLoop_Exposure_Parameters

Table 74. Exposure parameters, sampled once per realization

GoldSim element	value or distribution		units	reference / comment
SoilIngestionTracerElement Adult incidental soil ingestion rate tracer elements	*Probability*	*Value*	—	See Dose Assessment white paper
	0.3333	0		Tracer element: silicon
	0.3334	1		Tracer element: aluminum
	0.3333	2		Tracer element: titanium
EF_food Exposure frequency, food	365		day/yr	See Dose Assessment white paper
Meat_PrepLoss Meat preparation loss	N(μ=0.27, σ=0.07, min = 0.01, max = 1)		—	*ibid.*
Meat_PostCookLoss Meat post-cooking loss	N(μ=0.24, σ=0.09, min = 0.01, max = 1)		—	*ibid.*

8.4 \Exposure_Dose\Dose_Calculations

This looping container performs calculations on a finer time step than the outer model, and has parameters that are sampled on the inner time steps.

8.4.1 \Exposure_Dose\Dose_Calculations\Physiology_Rancher

Table 75. Attributes of inter-individual uncertainty in physiological characteristics for rancher receptors (ranch hands)

GoldSim element	value or distribution	units	reference / comment
Age	N(μ=25.7, σ=20.3, min = 16, max = 60)	yr	See Dose Assessment white paper
Gender	Male 60.8%, Female 39.2%	—	*ibid.*
BodyWeight Body mass	LN(GM=$f(x)$, GSD=$f(x)$)	kg	Inputs denoted as *f(x)* are calculated based on other outputs from the model and are documented in the Dose Assessment white paper

GoldSim element	value or distribution	units	reference / comment
SoilIngestionRate Adult incidental soil ingestion rate	LN(GM=$f(x)$, GSD=$f(x)$, Min=0, Max=$f(x)$)	mg/day	*ibid.*
BeefIngestionRate_BWA Ingestion rate: "home-produced" beef	Gamma(μ=$f(x)$, σ=$f(x)$)	g/kg-day	*ibid.*
VentilationRateSleep_BWA Ventilation rate: sleeping	LN(GM=$f(x)$,GSD=$f(x)$)	m^3/min-kg	*ibid.*
ActivityDurationSleep_dist Daily exposure time: sleeping	LN(GM=$f(x)$, GSD=$f(x)$, Min=1, Max=24)	hr/day	*ibid.*
VentilationRateSedentary_BWA Ventilation rate: sedentary activity	LN(GM=$f(x)$,GSD=$f(x)$)	m^3/min-kg	*ibid.*
ActivityDurationSedSleep Daily exposure time: sedentary+sleeping	LN(GM=$f(x)$,GSD=$f(x)$)	hr/day	*ibid.*
VentilationRateLight_BWA Ventilation rate: light activity	LN(GM=$f(x)$,GSD=$f(x)$)	m^3/min-kg	*ibid.*
VentilationRateMedium_BWA Ventilation rate: moderate activity	LN(GM=$f(x)$,GSD=$f(x)$)	m^3/min-kg	*ibid.*
VentilationRateHeavy_BWA Ventilation rate: high activity	LN(GM=$f(x)$,GSD=$f(x)$)	m^3/min-kg	*ibid.*
ActivityDurationLight_UN Daily exposure time: light activity	LN(GM=$f(x)$,GSD=$f(x)$)	hr/day	*ibid.*
ActivityDurationMedium_UN Daily exposure time: moderate activity	LN(GM=$f(x)$,GSD=$f(x)$)	hr/day	*ibid.*
ActivityDurationHeavy_UN Daily exposure time: high activity	LN(GM=$f(x)$,GSD=$f(x)$)	hr/day	*ibid.*

8.4.2 \Exposure_Dose\Dose_Calculations\Physiology_SportOHV

Table 76. Attributes of inter-individual uncertainty in physiological characteristics for Sport OHV receptors

GoldSim element	value or distribution	units	reference / comment
Age	N(μ=25.7, σ=20.3, min = 16, max = 60)	yr	See Dose Assessment white paper
Gender	Male 60.8%, Female 39.2%	—	*ibid.*
BodyWeight Body mass	LN(GM=*f*(*x*), GSD=*f*(*x*))	kg	Inputs denoted as *f(x)* are calculated based on other outputs from the model and are documented in the Dose Assessment white paper
SoilIngestionRate Adult incidental soil ingestion rate	LN(GM=*f*(*x*), GSD=*f*(*x*), Min=0, Max=*f*(*x*))	mg/day	*ibid.*
VentilationRateSleep_BWA Ventilation rate: sleeping	LN(GM=*f*(*x*),GSD=*f*(*x*))	m^3/min-kg	*ibid.*
ActivityDurationSleep_dist Daily exposure time: sleeping	LN(GM=*f*(*x*), GSD=*f*(*x*), Min=1, Max=24)	hr/day	*ibid.*
VentilationRateSedentary_BWA Ventilation rate: sedentary activity	LN(GM=*f*(*x*),GSD=*f*(*x*))	m^3/min-kg	*ibid.*
ActivityDurationSedSleep Daily exposure time: sedentary+sleeping	LN(GM=*f*(*x*),GSD=*f*(*x*) 1.09 or 1.08)	hr/day	*ibid.*
VentilationRateLight_BWA Ventilation rate: light activity	LN(GM=*f*(*x*),GSD=*f*(*x*))	m^3/min-kg	*ibid.*
VentilationRateMedium_BWA Ventilation rate: moderate activity	LN(GM=*f*(*x*),GSD=*f*(*x*))	m^3/min-kg	*ibid.*
VentilationRateHeavy_BWA Ventilation rate: high activity	LN(GM=*f*(*x*),GSD=*f*(*x*))	m^3/min-kg	*ibid.*
ActivityDurationLight_UN Daily exposure time: light activity	LN(GM=*f*(*x*),GSD=*f*(*x*))	hr/day	*ibid.*

GoldSim element	value or distribution	units	reference / comment
ActivityDurationMedium_UN Daily exposure time: moderate activity	LN(GM=*f*(*x*),GSD=*f*(*x*))	hr/day	*ibid.*
ActivityDurationHeavy_UN Daily exposure time: high activity	LN(GM=*f*(*x*),GSD=*f*(*x*))	hr/day	*ibid.*

8.4.3 \Exposure_Dose\Dose_Calculations\Physiology_Hunter

Table 77. Attributes of inter-individual uncertainty in physiological characteristics for Hunter receptors

GoldSim element	value or distribution	units	reference / comment
Age Age	N(μ=25.7, σ=20.3, min = 16, max = 60)	yr	See Dose Assessment white paper
Gender Gender	Male 60.8%, Female 39.2%	—	*ibid.*
BodyWeight Body weight	LN(GM=*f*(*x*), GSD=*f*(*x*))	kg	Inputs denoted as *f(x)* are calculated based on other outputs from the model and are documented in the Dose Assessment white paper, Section 1.0.
SoilIngestionRate Adult incidental soil ingestion rate	LN(GM=*f*(*x*), GSD=*f*(*x*), Min=0, Max=*f*(*x*))	mg/day	*ibid.* function of age
GameIngestionRate_BWA Ingestion rate: "home-produced" game	Gamma(μ=*f*(*x*), σ=*f*(*x*))	g/kg-day	*ibid.*
VentilationRateSleep_BWA Ventilation rate: sleeping	LN(GM=*f*(*x*),GSD=*f*(*x*))	m^3/min-kg	*ibid.*
ActivityDurationSleep_dist Daily exposure time: sleeping	LN(GM=*f*(*x*), GSD=*f*(*x*), Min=1, Max=24)	hr/day	*ibid.*
VentilationRateSedentary_BWA Ventilation rate: sedentary activity	LN(GM=*f*(*x*),GSD=*f*(*x*))	m^3/min-kg	*ibid.*

GoldSim element	value or distribution	units	reference / comment
ActivityDurationSedSleep Daily exposure time: sedentary+sleeping	LN(GM=*f*(*x*),GSD=*f*(*x*))	hr/day	*ibid.*
VentilationRateLight_BWA Ventilation rate: light activity	LN(GM=*f*(*x*),GSD=*f*(*x*))	m^3/min-kg	*ibid.*
VentilationRateMedium_BWA Ventilation rate: moderate activity	LN(GM=*f*(*x*),GSD=*f*(*x*))	m^3/min-kg	*ibid.*
VentilationRateHeavy_BWA Ventilation rate: high activity	LN(GM=*f*(*x*),GSD=*f*(*x*))	m^3/min-kg	*ibid.*
ActivityDurationLight_UN Daily exposure time: light activity	LN(GM=*f*(*x*),GSD=*f*(*x*))	hr/day	*ibid.*
ActivityDurationMedium_UN Daily exposure time: moderate activity	LN(GM=*f*(*x*),GSD=*f*(*x*))	hr/day	*ibid.*
ActivityDurationHeavy_UN Daily exposure time: high activity	LN(GM=*f*(*x*),GSD=*f*(*x*))	hr/day	*ibid.*

8.4.4 \Exposure_Dose\Dose_Calculations\ExposureTime_Rancher

Table 78. Attributes of inter-individual uncertainty in physiological characteristics for Rancher receptors – Exposure Time

GoldSim element	value or distribution	units	reference / comment
ET_Ranch_DayTrip Ranchers; day trip time in exposure area	U(min=4, max=12)	hr/day	See Dose Assessment white paper
ET_Overnight Exposure frequency, overnight trips	24	hr/day	*ibid.*
ET_Camp_OnsiteFrac All receptors; fraction of camp trip exposure time on disposal cell	U(min=0.25, max=0.75)	—	*ibid.*
OHV_timeFrac_Camper All receptors; camp trip time spent OHVing	U(min=2, max=8)	hr/day	*ibid.*
OHV_timeFrac_HuntRanch_DayTrip Hunter/Rancher; fraction of day trip time spent OHVing	U(min=0.1, max=0.75)	hr/day	*ibid.*

GoldSim element	value or distribution	units	reference / comment
EF_Ranch_dist Rancher; exposure frequency	beta(μ=135, σ=34.9, min = 0, max = 180)	day/yr	*ibid.*
Frac_Ranch_Overnight_dist Ranchers; fraction of exposure frequency related to overnight trips	U(min=0.5, max=0.67)	—	*ibid.*

8.4.5 \Exposure_Dose\Dose_Calculations\ExposureTime_SportOHV

Table 79. Attributes of inter-individual uncertainty in physiological characteristics for Sport OHV receptors – Exposure Time

GoldSim element	value or distribution	units	reference / comment
ET_Rec_DayTrip Sport OHVers; day trip time in exposure area	beta(μ=6.3, σ=2.11, min = 1, max = 20)	hr/day	See Dose Assessment white paper
ET_Overnight Exposure frequency, overnight trips	24	hr/day	*ibid.*
ET_Camp_OnsiteFrac All receptors; fraction of camp trip exposure time on disposal cell	U(min=0.25, max=0.75)	—	*ibid.*
OHV_timeFrac_Camper All receptors; camp trip time spent OHVing	U(min=2, max=8)	hr/day	*ibid.*
EF_Recreational_dist Sport OHVer; exposure frequency	LN(GM=11.3, GSD=3.45, Min=1, Max=200)	d/yr	*ibid.*
Frac_recOHV_Overnight_dist Sport OHVers; fraction of exposure frequency related to overnight trips	U(min=0, max=1)	—	*ibid.*

8.4.6 \Exposure_Dose\Dose_Calculations\ExposureTime_Hunter

Table 80. Attributes of inter-individual uncertainty in physiological characteristics for Hunter receptors – Exposure Time

GoldSim element	value or distribution	units	reference / comment
ET_Rec_DayTrip Sport OHVers; day trip time in exposure area	beta(μ=6.3, σ=2.11, min = 1, max = 20)	hr/day	See Dose Assessment white paper
ET_Overnight Exposure frequency, overnight trips	24	hr/day	*ibid.*
ET_Hunt_DayTrip_OnsiteFrac Hunter; fraction of hunting day trip exposure time on disposal cell	U(min=0.02, max=0.17)	—	*ibid.*
ET_Camp_OnsiteFrac All receptors; fraction of camp trip exposure time on disposal cell	U(min=0.25, max=0.75)	—	*ibid.*
OHV_timeFrac_Camper All receptors; camp trip time spent OHVing	U(min=2, max=8)	hr/day	*ibid.*
OHV_timeFrac_HuntRanch_DayTrip Hunter/Rancher; fraction of day trip time spent OHVing	U(min=0.1, max=0.75)	—	*ibid.*
EF_Hunting_dist Hunter; exposure frequency	LN(GM=4.66, GSD=3.45, min=1, max=100)	day/yr	*ibid.*
Frac_Hunt_Overnight_dist Hunters; fraction of exposure frequency related to overnight trips	U(min=0, max=1)	—	*ibid.*
EF_Recreational_dist Sport OHVer; exposure frequency	LN(GM=11.3, GSD=3.45, min=1, max=200)	day/yr	*ibid.*

8.4.7 \Exposure_Dose\Dose_Calculations\Population_Size_Variables

Table 81. Attributes of population variability.

GoldSim element	value or distribution	units	reference / comment
Number_Individuals_Total Total number of individuals in vicinity of site, per year	Tri(100, 350, 500)	—	See Dose Assessment white paper
Ranch_Hands_dist Number of ranchers in vicinity of site, per year	U(1, 20)	—	*ibid.*
Ranchers_Picker This element is used to identify the number of ranch receptors present.	Binomial(Batch Size = 1, Probability = $f(x)$/20)	—	For probability, the denominator corresponds to the size of the receptor array and *f(x)* to the value of Ranch_Hands_dist.
Number_Hunter Number of hunters in vicinity of site, per year	Binomial(Batch Size = round(Number_Individuals_Total – Number_Ranch_Hands), Probability = 0.25)	—	See Dose Assessment white paper
Hunters_Picker This element is used to identify the number of hunter receptors present.	Binomial(Batch Size = 1, Probability = Number_Hunter/175)	—	Analogous to Ranchers_Picker.
Number_Recreationalists Number of recreationalists in vicinity of site	$f(x)$ = Number_Individuals_Total - Ranch_Hands_Dist	—	See Dose Assessment white paper
Number_SportOHV Number of OHVers in vicinity of site	$f(x)$ = Number_Recreationalists - Number_Hunter	—	See Dose Assessment white paper
SportOHVers_Picker This element is used to identify the number of SportOHV receptors present.	Binomial(Batch Size = 1, Probability = Number_SportOHV/424)	—	Analogous to Ranchers_Picker.

8.4.8 \Exposure_Dose\Dose_Calculations\UraniumHazard

Table 82. Uranium hazard for Rancher and Recreationists.

GoldSim element	value or distribution		units	reference / comment
Uranium_RfD Reference dose for uranium	Probability	Value		See Dose Assessment white paper
	0.5	0.0006	mg/kg-day	
	0.5	0.0030	mg/kg-day	

8.4.9 \Exposure_Dose\Dose_Calculations\OffSite_Receptors

Table 83. Inhalation dose for off-site receptors.

GoldSim element	value or distribution	units	reference / comment
ET_RestArea Exposure time rest area caretaker	24	hr/day	See Dose Assessment white paper
EF_RestArea Exposure frequency rest area caretaker	Tri(327, 350, 365)	day/yr	*ibid.*
ET_Knolls Exposure time for day trip, Knolls OHVer	Beta(μ=6.3, σ=2.11, min=1, max=20)	hr/day	*ibid.*
EF_Knolls Exposure frequency, Knolls OHVer	LN(μ=11.3, σ=3.45, min=1, max=200)	day/yr	*ibid.*
ET_Traveller Exposure time travelers on I-80 and train	U(2.3, 7.2)	min/day	*ibid.*
EF_Traveller Exposure frequency I-80 and west-side access road traveller	U(250, 365)	day/yr	*ibid.*
ET_UTTR_Road Exposure time cars on west-side access road (Utah Test and Training Range access)	U(2.4, 4.0)	min/day	*ibid.*

8.4.10 \Exposure_Dose\Screening_Calculations

Table 84. Parameters used in screening dose calculations.

GoldSim element	value or distribution	units	reference / comment
NativePlant_Ing_Rate	1	kg/yr	See Dose Assessment white paper
FreshWeightConversion	U(0.05, 0.3)	—	*ibid.*
OffsiteWater_Ing_Rate	1	L/yr	*ibid.*

9.0 \GWPLs

The model estimates concentrations in a hypothetical monitoring well down gradient of the waste embankment. Certain radionuclides are of interest, and their concentrations are displayed for comparison to Ground Water Protection Limits (GWPLs) as specified in State of Utah (2010) Table 1A.

Table 85. Groundwater protection limits.

GoldSim element	value or distribution	units	reference / comment
MaxTime_WellConcs	500	yr	State of Utah (2010)
GWPL_Sr90	42	pCi/L	*ibid.*
GWPL_Tc99	3790	pCi/L	*ibid.*
GWPL_I129	21	pCi/L	*ibid.*
GWPL_Th230	83	pCi/L	*ibid.*
GWPL_Th232	92	pCi/L	*ibid.*
GWPL_Np237	7	pCi/L	*ibid.*
GWPL_U233	26	pCi/L	*ibid.*
GWPL_U234	26	pCi/L	*ibid.*
GWPL_U235	27	pCi/L	*ibid.*
GWPL_U236	27	pCi/L	*ibid.*
GWPL_U238	26	pCi/L	*ibid.*

10.0 DeepTimeScenarios

Deep time scenarios are developed to provide information for a qualitative analysis of effects from the Clive Facility on future conditions after 10,000 years.

Table 86. Deep time scenario parameters.

GoldSim element	value or distribution	units	reference / comment
Unit_U238	vector by species with 0's for all except U238, with 1 g	g	Used to explore U238 decay and ingrowth of daughters
LargeLakeStart	LN(GM=14000, GSD=1.2, min=0, max=50000)	yr	see Deep Time Assessment white paper
LargeLakeEnd	LN(GM=6000, GSD=1.2, min=0, max=50000)	yr	*ibid.*
LargeLakeSedimentationRate	LN(GM=0.00012, GSD=1.2)	m/yr	*ibid.*
IntermediateLakeDuration	LN(GM=500, GSD=1.5, min=0, max=2500)	yr	*ibid.*
IntermediateLakePoissonRate	$f(x)$	1/yr	*ibid.*
IntermediateLake SedimentAmount	LN(GM=2.82, GSD=1.71)	m	*ibid.*
SiteDispersalArea	LN(GM= VolumeAboveGrade / 0.1 m, GSD=1.5, min= VolumeAboveGrade / 1 m, max=Large)	km^2	*ibid.*
IntermediateLakeDepth	beta(μ=30, σ=18, min = 0, max = 100)	m	*ibid.* resampled at each intermediate lake event
LargeLakeDepth	beta(μ=150, σ=20, min = 100, max = 200)	m	*ibid.* resampled at each large lake recurrence

QA Notes for *Clive PA Model Parameters.xls*

Values in green or italics are entered; others are linked to other places in the spreadsheet or are calculated
Values in blue are to be used for populating GoldSim array elements

when	who	what
2 Nov 09	JT	This workbook of spreadsheets documents the development of information to be used in the EnergySolutions Depleted Uranium (ES DU) GoldSim model.
2 Nov 09	JT	Species worksheet added from early work on the model, v0.000e. This includes all long-lived progeny from uranium-232, -233, 234 -235, -236, and -238.
2 Nov 09	JT	Added IAEA's recipe for DU, in the Abundance worksheet.
3 Nov 09	JT	Re-exported Species worksheet from the model (v0.000f) with Species list reduced to just the Uranium and Actinium series (assuming that DU is only U234, U235, and U238). Added ChemElements worksheet. Updated half-lives from Chart of the Nuclides, 16th Edition.
7 Dec 09	JT	Added information about abundance of isotopes in DU from Kozak et al. (1992) to Abundance worksheet. Now we need to work up distributions for these values.
21 Jan 10	JT	Major update, starting with a new Species list based on the SRS Waste Profile, and exported from the GoldSim model. All references and associated lists were also updated. Rebuilt the Abundance worksheet for new Species list, but it still needs updating with new information from the SRS DU Waste Profile. Renamed ChemElements to simply Elements.
22 Jan 10	JT	Added DCF rollup calculations, plant/soil CRs and animal transfer factors adapted from the NTS Area 5 Parameters workbook. The larger Area 5 lists were pared down to match the ES DU Species list.
4 Feb 10	JT	Replaced references to a separate workbook on the worksheet "DCFs" to references to the local worksheet "DCF calcs". Added new reference for DU abundance from ORNL-TM-2000-10
21 May 10	JL	QA'd half lives on Species Properties worksheet with source (16th Ed. of Chart of the Nuclides)
1 Jun 10	JL	Created checkprint for half-lives from Species Properties worksheet.
6 Jun 10	DAG	Added Atomic Weights for each of radionuclide species based on number of protons and nuetrons
8 Jun 10	DAG	Added Henry's Constant for Iodine gas (I2) on species properties sheet
15 Jun 10	DAG	Added some deterministic values for solubilities in the Species Properties tab.
16 Jun 10	DAG	Added solubility for Radon at 12C. Estimated from solubility at 3 temperatures, reference in Gratson's spreadsheet with all solubility references. Looks very high to me, O2 is 9.1 mg/L (2.8e-4 mol/l) at 20C
30 Jul 10	DAG	Added notes on U solubility and changed to 100 mg/L = 4.2e-4
30 Sep 10	JT	Moved plant/soil concentration ratios and animal transfer factors to the "Elements" worksheet. Moved Henry's Law constants to the Parameters Document.
5th Nov 2010	DAG	I don't understand JT's comment on the Elements tab that that we need a better source for the atomic weight. The species property tab is more precise and these values are in the GS model for ES.
13 Jan 11	DAG	revised solubilities to include ranges and central value in both salt and fresh water. Most values for fresh water are unchanged with the exception of uranium. True distributions have not yet been developed.
13 Jan 11	DAG	Also added Kd ranges for both salt and fresh water. These are a decent starting point for most, some need a bit of calculation still based on input from Chuck Vandergraaf. True distributions have not yet been developed.
4 Feb 11	JT	Moved the listings of solubility for "U as UO3" and "U as U3O8" to a separate line on the Elements sheet. For purposes of copy and paste into GoldSim, we cannot change the list of Elements.
10 Feb 11	JT	Added Inventory worksheet and populated with concentration values.
10 Feb 11	mjp	Added values to inventory sheet.
10 Feb 11	JT	Replaced the NAs with zeros and removed the commas in Matt's Inventory sheet entries. Put ordering of Species back in proper order, and rearranged values to match.
12 Feb 11	JT	Removed Kd and solubility listings from the workbook. These will be documented in the Model Parameters document, since each chemical element can have its own distribution.
23 Feb 11	DAG	Verified that the UO3 inventory (in pCi/g) found in the Waste Inventory White Paper matches the numbers in this document. I also confirmed that version .806 of the GS model contains the same values. These are then scaled up for the GDP U3O8 inventory using the mass of DU3O8 accounting for stoichiometry differences: IncludeInv_GDP_DU_Proposed * GDP_DU_TotalMass * ActivityConc_DUWaste / Species.Specific_Activity.
24 Feb 11	JT	Added logical masks to the Species Properties worksheet
1 Mar 11	DAG	Put a note about the DU U3O8 concentrations. These are calculated in the model using the SRS activity concentrations. This is also documented in the Waste Inventory white paper. The abundance worksheet has very little information. This is better found in the Waste Inventory white paper. Solubilities and Kd values are documented in the Geochemical Modeling white paper.
8 Mar 11	JT	Removed atomic mass references from the workbook. These are defined in the Parameters Document, since they are not entered into the GoldSim model as an array. Also updated the Species worksheet from the model, as these values changed.
17 Mar 11	JT	Replaced Plant/Soil CRs and Beef TFs on the worksheet Elements
1 Apr 11	JT	Added DoseSpecies worksheet, with a reordering of dose species by Z number. This will eventually replace the "DCFs" worksheet.
12 Apr 11	RP	Updated DoseSpecies branching fractions to reflect approximation to 1.0 for isotopes with branches of >99%. Deleted 'DCFs' sheet.

when	who	what
9 May 11	JT	Added U_Mask column to Species Properties. Corrected value for half-life of U-234 (was "2.46e4 yr" is corrected to "2.46e5 yr". It was correct in the GoldSim model, fortunately.
10 May 11	JT	Added notes to find source documentation for plant/soil CRs and animal transfer factors on the sheet Elements. Added the VegPctCover worksheet and populated it.
11 May 11	JT	Changed reference to "GreenDU_Mask" to "CleanDU_Mask" in Species Properties sheet.
23 May 11	JT	Modified the standard deviation for SRS DUO3 inventory concentration for isotopes of Am, Cs, I, Np, Pu, Ra, and Sr, following a check print of values in the Waste Inventory white paper.
28 May 11	JT	Removed Abundance page, since this work is done in the Waste Inventory white paper. Performed page formatting for printing the workbook.

Species ID	Isotope	Atomic Weight	Half-life	Radioactive	Daughter1	Stoichiometry1	Daughter2	Stoichiometry2	Description
Sr90	Y	90	HalfLives[Sr90]	Y					Strontium 90
Tc99	Y	99	HalfLives[Tc99]	Y					Technetium 99
I129	Y	129	HalfLives[I129]	Y					Iodine 129
Cs137	Y	137	HalfLives[Cs137]	Y					Cesium 137
Pb210	Y	210	HalfLives[Pb210]	Y					Lead 210
Rn222	Y	222	HalfLives[Rn222]	Y	Pb210	1			Radon 222
Ra226	Y	226	HalfLives[Ra226]	Y	Pb210	1 - EPRatio_Radon	Rn222	EPRatio_Radon	Radium 226
Ra228	Y	226	HalfLives[Ra228]	Y	Th228	1			Radium 228
Ac227	Y	227	HalfLives[Ac227]	Y					Actinium 227
Th228	Y	230	HalfLives[Th228]	Y					Thorium 228
Th229	Y	230	HalfLives[Th229]	Y					Thorium 229
Th230	Y	230	HalfLives[Th230]	Y	Ra226	1			Thorium 230
Th232	Y	230	HalfLives[Th232]	Y	Ra228	1			Thorium 232
Pa231	Y	231	HalfLives[Pa231]	Y	Ac227	1			Protactinium 231
U232	Y	238	HalfLives[U232]	Y	Th228	1			Uranium 232
U233	Y	238	HalfLives[U233]	Y	Th229	1			Uranium 233
U234	Y	238	HalfLives[U234]	Y	Th230	1			Uranium 234
U235	Y	238	HalfLives[U235]	Y	Pa231	1			Uranium 235
U236	Y	238	HalfLives[U236]	Y	Th232	1			Uranium 236
U238	Y	238	HalfLives[U238]	Y	U234	1			Uranium 238
Np237	Y	237	HalfLives[Np237]	Y	U233	1			Neptunium 237
Pu238	Y	239	HalfLives[Pu238]	Y	U234	1			Plutonium 238
Pu239	Y	239	HalfLives[Pu239]	Y	U235	1			Plutonium 239
Pu240	Y	239	HalfLives[Pu240]	Y	U236	1			Plutonium 240
Pu241	Y	239	HalfLives[Pu241]	Y	Am241	0.999975	Np237	2.50E-05	Plutonium 241
Pu242	Y	239	HalfLives[Pu242]	Y	U238	1			Plutonium 242
Am241	Y	241	HalfLives[Am241]	Y	Np237	1			Americium 241

Parameter Values by DoseSpecies

DoseSpecies is an array defined in the Clive DU PA Model. Columns on this page correspond to that array.

GoldSim element in the container \Exposure_Dose\DCFs

	DCF_Inh_Dust_determ	DCF_Inh_Gas_determ	DCF_Ing_determ	DCF_Ext_Imm_determ	DCF_Ext_Soil_determ	BranchingFraction
Species	**Inhalation Dust**	**Inhalation Gas**	**Ingestion**	**Immersion**	**External**	**Branching Fraction**
	Sv/Bq	**Sv/Bq**	**Sv/Bq**	**(Sv-m^3)/(Bq-s)**	**(Sv-m^3)/(Bq-s)**	
Sr90	3.56E-08	0	2.77E-08	9.83E-17	3.46E-21	1
Y	1.39E-09	0	2.69E-09	7.93E-16	2.15E-19	1
Tc99	4.03E-09	0	6.42E-10	2.87E-17	5.81E-22	1
I129	3.59E-08	9.59E-08	1.06E-07	2.83E-16	5.14E-20	1
Cs137	4.67E-09	0	1.36E-08	9.28E-17	4.47E-21	1
Ba137m	0	0	0	2.69E-14	1.81E-17	1
Tl207	0	0	0	4.53E-16	1.23E-19	1
Tl208	0	0	0	1.69E-13	1.17E-16	0.3594
Tl209	0	0	0	9.66E-14	6.56E-17	0.0209
Pb209	5.64E-11	0	5.67E-11	1.00E-16	4.04E-21	1
Pb210	1.10E-06	0	6.96E-07	4.51E-17	1.06E-20	1
Pb211	1.11E-08	0	1.78E-10	2.59E-15	1.56E-18	1
Pb212	1.72E-07	0	5.98E-09	6.26E-15	3.46E-18	1
Pb214	1.36E-08	0	1.39E-10	1.10E-14	6.65E-18	1
Bi210	9.30E-08	0	1.31E-09	2.58E-16	2.92E-20	1
Bi211	0	0	0	2.04E-15	1.27E-18	1
Bi212	3.08E-08	0	2.59E-10	8.96E-15	5.96E-18	1
Bi213	2.98E-08	0	1.98E-10	6.17E-15	3.83E-18	1
Bi214	1.46E-08	0	1.12E-10	7.25E-14	4.99E-17	1
Po210	3.27E-06	0	1.21E-06	3.89E-19	2.64E-22	1
Po212	0	0	0	0	0	0.6406
Po213	0	0	0	0	0	0.9791
Po214	0	0	0	3.81E-18	2.59E-21	1
Po215	0	0	0	7.80E-18	5.06E-21	1
Po216	0	0	0	7.75E-19	5.26E-22	1
Po218	0	0	0	4.21E-19	2.85E-22	1
At217	0	0	0	1.37E-17	8.86E-21	1
Rn219	0	0	0	2.46E-15	1.53E-18	1
Rn220	0	0	0	1.72E-17	1.15E-20	1
Rn222	0	Rn222_DCF	0	1.78E-17	1.17E-20	1
Fr221	0	0	0	1.33E-15	7.56E-19	1
Fr223	1.04E-08	0	2.36E-09	2.21E-15	9.71E-19	0.0138
Ra223	7.44E-06	0	1.04E-07	5.48E-15	2.96E-18	1
Ra224	2.97E-06	0	6.45E-08	4.30E-16	2.53E-19	1
Ra225	6.26E-06	0	9.95E-08	2.41E-16	4.63E-20	1

Species	Inhalation Dust	Inhalation Gas	Ingestion	Immersion	External	Branching Fraction
	Sv/Bq	Sv/Bq	Sv/Bq	(Sv-m^3)/(Bq-s)	(Sv-m^3)/(Bq-s)	
Ra226	3.46E-06	0	2.80E-07	2.84E-16	1.56E-19	1
Ra228	2.64E-06	0	6.97E-07	0	0	1
Ac225	7.39E-06	0	3.85E-08	6.38E-16	3.09E-19	1
Ac227	7.28E-05	0	3.23E-07	5.13E-18	2.40E-21	1
Ac228	1.19E-08	0	4.01E-10	4.49E-14	3.03E-17	1
Th227	1.04E-05	0	9.02E-09	4.44E-15	2.57E-18	0.9862
Th228	3.97E-05	0	7.20E-08	8.13E-17	3.85E-20	1
Th229	7.12E-05	0	5.00E-07	3.37E-15	1.55E-18	1
Th230	1.40E-05	0	2.14E-07	1.49E-17	5.73E-21	1
Th231	3.34E-10	0	3.36E-10	4.59E-16	1.72E-19	1
Th232	2.48E-05	0	2.31E-07	7.27E-18	2.44E-21	1
Th234	7.69E-09	0	3.40E-09	2.95E-16	1.14E-19	1
Pa231	9.35E-05	0	4.79E-07	1.57E-15	9.44E-19	1
Pa233	3.33E-09	0	8.78E-10	8.57E-15	5.04E-18	1
Pa234m	0	0	0	1.21E-15	5.28E-19	1
U232	7.82E-06	0	3.36E-07	1.18E-17	4.25E-21	1
U233	3.55E-06	0	5.13E-08	1.42E-17	6.77E-21	1
U234	3.48E-06	0	4.95E-08	6.13E-18	1.84E-21	1
U235	3.09E-06	0	4.67E-08	6.48E-15	3.53E-18	1
U236	3.21E-06	0	4.69E-08	3.87E-18	9.53E-22	1
U238	2.86E-06	0	4.45E-08	2.51E-18	4.27E-22	1
Np237	2.27E-05	0	1.07E-07	8.90E-16	3.73E-19	1
Pu238	4.62E-05	0	2.28E-07	3.51E-18	6.25E-22	1
Pu239	5.01E-05	0	2.51E-07	3.49E-18	1.41E-21	1
Pu240	5.02E-05	0	2.51E-07	3.43E-18	6.03E-22	1
Pu241	9.01E-07	0	4.75E-09	6.35E-20	2.84E-23	1
Pu242	4.76E-05	0	2.38E-07	2.91E-18	5.32E-22	1
Am241	4.17E-05	0	2.04E-07	6.77E-16	1.99E-19	1

Properties of Modeled Species

NOTES:
Half-lives are from Chart of the Nuclides, 16th Ed. - JT

Species ID	half-life (units as reported)	Gas_ Mask	Dust_ Mask	CleanDU _Mask	U _Mask
Sr90	*28.78 yr*	*0*	*1*	*0*	*0*
Tc99	*2.13e5 yr*	*0*	*1*	*0*	*0*
I129	*1.57e7 yr*	*0*	*1*	*0*	*0*
Cs137	*30.07 yr*	*0*	*1*	*0*	*0*
Pb210	*22.3 yr*	*0*	*1*	*1*	*0*
Rn222	*3.8235 d*	*1*	*0*	*1*	*0*
Ra226	*1599 yr*	*0*	*1*	*1*	*0*
Ra228	*5.76 yr*	*0*	*1*	*1*	*0*
Ac227	*21.772 yr*	*0*	*1*	*1*	*0*
Th228	*1.912 yr*	*0*	*1*	*1*	*0*
Th229	*7.3e3 yr*	*0*	*1*	*1*	*0*
Th230	*7.54e4 yr*	*0*	*1*	*1*	*0*
Th232	*1.40e10 yr*	*0*	*1*	*1*	*0*
Pa231	*3.28e4 yr*	*0*	*1*	*1*	*0*
U232	*69.8 yr*	*0*	*1*	*1*	*1*
U233	*1.592e5 yr*	*0*	*1*	*1*	*1*
U234	*2.46e5 yr*	*0*	*1*	*1*	*1*
U235	*7.04e8 yr*	*0*	*1*	*1*	*1*
U236	*2.342e7 yr*	*0*	*1*	*1*	*1*
U238	*4.47e9 yr*	*0*	*1*	*1*	*1*
Np237	*2.14e6 yr*	*0*	*1*	*0*	*0*
Pu238	*87.7 yr*	*0*	*1*	*0*	*0*
Pu239	*2.410e4 yr*	*0*	*1*	*0*	*0*
Pu240	*6.56e3 yr*	*0*	*1*	*0*	*0*
Pu241	*14.4 yr*	*0*	*1*	*0*	*0*
Pu242	*3.75e5 yr*	*0*	*1*	*0*	*0*
Am241	*432.7 yr*	*0*	*1*	*0*	*0*

Properties of Modeled Chemical Elements

NOTES:
The list of elements is derived from the Species List.

GoldSim element:	\Processes \PlantTransport \PlantCR \PlantCR_GM	\Processes \PlantTransport \PlantCR \PlantCR_GSD	\Exposure_Dose \Media_Concs \Animal_Concentrations \Beef_TFs\BeefTF_GM	\Exposure_Dose \Media_Concs \Animal_Concentrations \Beef_TFs\BeefTF_GSD

chemical element name	plant/soil concentration ratio (Ci/kg dry Plant) per (Ci/kg dry Soil)		animal product transfer factors (d/kg)	
	GM	GSD	GM	GSD
Ac	*3.70E-03*	*1.49*	*4.00E-04*	*BeefTF_GSD_generic*
Am	*3.73E-03*	*1.50*	*5.00E-04*	*BeefTF_GSD_generic*
Cs	*6.70E-01*	*1.13*	*3.20E-02*	*1.15*
I	*6.70E-02*	*3.92*	*1.07E-02*	*1.85*
Np	*9.51E-02*	*1.36*	*1.00E-03*	*BeefTF_GSD_generic*
Pa	*3.72E-03*	*1.49*	*5.00E-04*	*BeefTF_GSD_generic*
Pb	*2.84E-01*	*1.54*	*9.52E-04*	*1.59*
Pu	*9.57E-04*	*1.35*	*1.28E-05*	*7.42*
Ra	*4.38E-01*	*1.81*	*1.70E-03*	*BeefTF_GSD_generic*
Rn	*CR_GM_radon*	*CR_GSD_radon*	*BeefTF_GM_radon*	*BeefTF_GSD_radon*
Sr	*1.77E+00*	*1.07*	*2.23E-03*	*1.26*
Tc	*1.31E+02*	*1.39*	*1.00E-04*	*BeefTF_GSD_generic*
Th	*3.89E-01*	*1.47*	*3.55E-04*	*1.68*
U	*1.70E-01*	*1.50*	*4.21E-04*	*1.32*

Inventory by Species

NOTES:
• SRS DU Inventory is entered as a concentration, and later converted to gram inventory using the entire mass of the waste stream.
• DU3O8 is assumed to have the same concentration of each species, for now. The mass of each species is scaled from the total DUF6 in the GDP inventory, each individual species is based on the SRS DU concentrations. This table has values of zero for the GDP DU3O8 since the GoldSim model

	SRS DUO_3 concentration		GDP DU_3O_8 concentration	
Species ID	**mean**	**standard deviation**	**mean**	**standard deviation**
	pCi/g	**pCi/g**	**pCi/g**	**pCi/g**
Sr90	*4.70E+1*	*1.28E+1*	*0*	*0*
Tc99	*2.38E+4*	*1.10E+4*	*0*	*0*
I129	*1.86E+1*	*1.59E+0*	*0*	*0*
Cs137	*1.21E+1*	*7.10E-1*	*0*	*0*
Pb210	*0*	*0*	*0*	*0*
Rn222	*0*	*0*	*0*	*0*
Ra226	*3.17E+2*	*1.91E+1*	*0*	*0*
Ra228	*0*	*0*	*0*	*0*
Ac227	*0*	*0*	*0*	*0*
Th228	*0*	*0*	*0*	*0*
Th229	*0*	*0*	*0*	*0*
Th230	*0*	*0*	*0*	*0*
Th232	*0*	*0*	*0*	*0*
Pa231	*0*	*0*	*0*	*0*
U232	*0*	*0*	*0*	*0*
U233	*5.29E+3*	*4.78E+2*	*0*	*0*
U234	*3.31E+4*	*2.17E+3*	*0*	*0*
U235	*2.97E+3*	*7.50E+2*	*0*	*0*
U236	*4.91E+3*	*1.17E+3*	*0*	*0*
U238	*2.72E+5*	*6.64E+3*	*0*	*0*
Np237	*5.68E+0*	*1.17E+0*	*0*	*0*
Pu238	*2.10E-1*	*4.00E-2*	*0*	*0*
Pu239	*1.28E+0*	*2.00E-1*	*0*	*0*
Pu240	*3.40E-1*	*5.00E-2*	*0*	*0*
Pu241	*4.04E+0*	*7.40E-1*	*0*	*0*
Pu242	*0*	*0*	*0*	*0*
Am241	*1.42E+1*	*9.10E-1*	*0*	*0*

Percent Cover by Plant Type and by Plot
Source: plant.cover.percent.simulations.xlsx

Plant Type:	Greasewood					Grass					Forb					Tree					Shrub				
Plot:	1	2	3	4	5	1	2	3	4	5	1	2	3	4	5	1	2	3	4	5	1	2	3	4	5
sample #																									
1	0	0	8.044	0.51	0	25.986	11.262	0	0	0.008	1.307	1.393	0.959	3.779	0.688	0	4.4	0	0	0	1.819	21.963	0.566	3.672	6.905
2	0	0	5.442	0	0	27.292	10.304	0	0.001	0.004	1.982	0.784	0.503	3.418	0.35	0	5.7	0	0	0	2.75	15.299	0.383	3.991	6.408
3	0	0	8.491	0.34	0	29.882	9.516	0	0	0.004	0.826	1.42	0.915	4.246	1.279	0	4.65	0	0	0	2.163	18.375	0.283	4.414	5.505
4	0	0	5.223	0.68	0	24.449	10.63	0	0.001	0.004	1.844	1.905	0.792	4.824	0.028	0	3.65	0	0	0	1.826	19.793	0.325	3.37	7.937
5	0	0	8.28	0.51	0	26.834	11.967	0	0	0.001	2.077	1.429	0.497	6.128	0.621	0	8.2	0	0	0	2.309	24.469	0.191	2.616	7.328
6	0	0	5.5	0	0	28.755	11.309	0	0.005	0	0.8	1.658	1.02	4.966	0.362	0	3.35	0	0	0	2.131	23.284	0.414	3.863	5.275
7	0	0	7.86	0.51	0	27.67	11.253	0	0.001	0.001	2.119	2.325	1.208	2.919	0.007	0	2.2	0	0	0	1.546	21.141	0.537	4.77	7.045
8	0	0	5.262	0.85	0	31.148	11.882	0	0	0.004	1.723	1.846	1.174	3.766	0.335	0	4.65	0	0	0	1.937	20.16	0.443	3.084	5.322
9	0	0	4.306	0.51	0	33.992	12.829	0	0.004	0	1.091	2.493	0.607	4.261	0.875	0	0	0	0	0	2.145	20.094	0.252	3.822	5.582
10	0	0	3.735	0	0	28.236	11.972	0	0.001	0.003	1.073	1.081	0.936	3.527	0.089	0	3.7	0	0	0	2.25	19.963	0.635	3.993	6.661
11	0	0	9.202	1.02	0	24.79	11.181	0	0.001	0.001	2.294	1.772	0.836	2.677	0.941	0	3.05	0	0	0	1.436	22.436	0.433	3.522	6.348
12	0	0	6.49	0.17	0	31.212	11.142	0	0.002	0.003	0.776	2.132	0.808	3.287	0.619	0	1.45	0	0	0	1.759	18.52	0.474	4.371	7.059
13	0	0	4.026	0.68	0	30.24	12.766	0	0.003	0.003	1.197	1.947	0.823	4.762	0.713	0	2	0	0	0	2.228	22.6	0.548	3.215	7.228
14	0	0	4.54	0.17	0	32.059	11.369	0	0	0.004	1.632	2.173	1.026	3.58	0.027	0	1	0	0	0	2.145	18.675	0.548	3.951	6.718
15	0	0	5.504	0	0	29.648	11.553	0	0.002	0.002	1.708	1.845	0.971	3.19	0.029	0	2.85	0	0	0	1.882	21.379	0.45	4.392	8.323
16	0	0	6.99	0.34	0	31.826	11.174	0	0.002	0	1.795	1.278	0.813	5.696	0.548	0	3.3	0	0	0	1.923	19.227	0.384	4.032	5.672
17	0	0	4.973	0.17	0	28.419	11.681	0	0.005	0.001	1.034	1.235	0.852	3.45	0.419	0	4.95	0	0	0	1.735	18.495	0.647	4.202	5.752
18	0	0	5.945	0.17	0	33.293	11.679	0	0.002	0.001	0.393	2.167	0.672	5.145	0.472	0	1.15	0	0	0	2.012	18.692	0.408	3.772	7.967
19	0	0	6.041	0.68	0	29.39	10.855	0	0.002	0	0.957	1.183	1.151	4.338	0.709	0	2.6	0	0	0	2.063	19.214	0.427	3.574	6.471
20	0	0	6.61	0.34	0	30.117	10.149	0	0.002	0.002	2.191	2.134	1.218	2.704	0.609	0	1.15	0	0	0	2.553	17.276	0.733	3.701	6.469
21	0	0	4.261	0	0	28.125	12.098	0	0	0.006	1.871	2.636	0.893	5.706	0.987	0	2.65	0	0	0	1.273	18.838	0.388	2.063	5.936
22	0	0	6.231	0	0	31.926	11.719	0	0	0	1.966	1.172	0.766	4.394	0.752	0	4.15	0	0	0	2.568	19.573	0.788	3.223	6.97
23	0	0	6.171	0	0	30.894	13.267	0	0.007	0.001	0.864	2.303	0.868	2.954	0.477	0	2	0	0	0	2.108	24.175	0.444	5.06	6.496
24	0	0	7.251	0.85	0	30.244	10.711	0	0.003	0.002	0.832	1.212	1.078	2.827	0.09	0	2.9	0	0	0	2.798	16.873	0.364	3.5	7.445
25	0	0	7.13	0.51	0	28.032	10.455	0	0.004	0	1.428	1.424	0.598	3.305	0.513	0	2	0	0	0	3.002	20.767	0.519	4.42	8.2
26	0	0	5.535	0.17	0	30.457	12.183	0	0	0	1.218	1.833	0.798	4.102	0.251	0	1.4	0	0	0	3.608	20.195	0.353	4.076	5.758
27	0	0	6.37	0.51	0	29.453	12.596	0	0.004	0.001	1.452	2.011	0.901	3.01	0.221	0	2.05	0	0	0	2.525	18.505	0.38	4.362	9.086
28	0	0	6.943	0.51	0	30.771	12.51	0	0.001	0.003	1.747	1.585	0.855	5.17	0.047	0	7.3	0	0	0	2.908	19.918	0.422	3.163	7.554
29	0	0	5.441	0.34	0	30.703	11.418	0	0	0.001	1.062	1.821	0.915	3.217	1.1	0	2.9	0	0	0	1.762	20.455	0.7	4.23	4.913
30	0	0	3.32	0.17	0	31.002	11.761	0	0	0	0.633	1.418	0.865	4.117	1.06	0	5.7	0	0	0	1.732	20.244	0.275	3.361	8.097
31	0	0	4.8	0.85	0	31.442	12.851	0	0.002	0.001	1.176	2.198	1.056	3.891	1.399	0	4.35	0	0	0	2.787	20.543	0.428	3.021	6.894
32	0	0	6.281	0	0	28.435	11.977	0	0.006	0	1.685	2.108	1.189	3.362	0.472	0	1.5	0	0	0	3.968	21.741	0.855	3.793	8.659
33	0	0	6.521	0.85	0	28.301	10.94	0	0.002	0.002	1.334	1.802	1.353	3.958	0.712	0	5.35	0	0	0	1.438	22.466	0.436	3.711	6.964
34	0	0	5.511	0.34	0	29.553	12.441	0	0.002	0	0.714	1.356	1.224	4.494	0.77	0	5.9	0	0	0	1.929	21.124	0.511	5.22	6.587
35	0	0	6.785	0.51	0	26.242	11.321	0	0.001	0.004	2.121	1.86	0.722	2.96	0.596	0	1.7	0	0	0	2.418	19.785	0.632	5.05	5.547
36	0	0	4.211	0.34	0	27.448	13.313	0	0.002	0.003	0.816	1.122	0.679	2.968	0.721	0	5.65	0	0	0	3.613	20.545	0.778	3.64	6.132
37	0	0	7.113	0.34	0	28.063	11.746	0	0.002	0.002	1.772	1.961	0.769	3.182	0.786	0	4.35	0	0	0	2.688	18.297	0.271	4.031	7.743
38	0	0	2.971	0.17	0	30.736	13.932	0	0.002	0.003	2.301	2.007	0.839	3.813	0.505	0	5.2	0	0	0	1.601	21.623	0.4	3.551	6.775
39	0	0	6.14	0.17	0	29.219	11.177	0	0	0.004	1.155	3.022	0.902	3.962	0.09	0	0	0	0	0	2.111	20.619	0.316	3.161	7.4
40	0	0	8.61	0.51	0	27.941	11.988	0	0.005	0.001	1.632	2.023	1.067	3.279	0.668	0	2.4	0	0	0	1.606	22.897	0.633	4.201	7.762
41	0	0	7.282	0.85	0	28.839	11.344	0	0.002	0.002	1.418	1.792	0.792	4.384	0.492	0	2.2	0	0	0	1.999	15.318	0.722	4.44	6.975
42	0	0	5.633	0	0	27.606	12.944	0	0.003	0.005	3.269	1.737	0.433	3.234	0.345	0	4.2	0	0	0	1.329	22.325	0.503	3.901	5.763
43	0	0	8.291	0	0	30.816	12.884	0	0.005	0	1.322	1.642	0.931	5.979	1.171	0	2.45	0	0	0	1.322	20.504	0.325	3.742	7.009
44	0	0	4.821	0	0	26.218	11.731	0	0.004	0.004	2.225	2.35	1.388	5.42	0.368	0	3.9	0	0	0	1.877	22.075	0.548	4.08	5.976
45	0	0	4.238	0	0	30.493	12.441	0	0.003	0.004	1.137	1.716	1.251	3.869	0.327	0	5.65	0	0	0	2.769	19.711	0.484	4.992	5.924
46	0	0	6.431	0.68	0	29.562	11.247	0	0.002	0	1.83	2.414	0.842	3.656	0.587	0	0.95	0	0	0	1.5	22.012	0.304	3.742	6.458
47	0	0	6.49	0.34	0	28.221	13.195	0	0.004	0.002	1.736	1.917	0.643	3.69	0.472	0	1.85	0	0	0	2.483	26.018	0.568	3.82	8.795
48	0	0	5.911	0.17	0	28.592	11.444	0	0.002	0.009	1.131	1.351	1.346	3.592	0.024	0	2.15	0	0	0	1.808	19.915	0.705	4.153	6.099
49	0	0	7.132	0	0	29.855	13.482	0	0.003	0	1.694	2.442	0.662	3.239	0.401	0	0.5	0	0	0	2.589	25.864	0.4	4.251	6.85
50	0	0	6.872	0.68	0	27.736	12.289	0	0.003	0	2.192	1.307	0.914	3.611	1.092	0	5.05	0	0	0	2.235	22.477	0.252	3.173	5.289
51	0	0	4.97	0.17	0	29.633	11.972	0	0	0.002	2.015	2.573	0.789	4.066	1.107	0	1.7	0	0	0	1.338	20.289	0.568	3.731	6.685
52	0	0	7.961	0	0	26.347	10.988	0	0.003	0.003	0.864	1.914	0.809	2.795	1.507	0	1.75	0	0	0	2.391	20.264	0.639	4.26	7.53
53	0	0	6.893	0	0	26.679	11.112	0	0.002	0.003	2.424	1.467	0.857	3.937	1.537	0	5.05	0	0	0	2.066	18.616	0.661	4.041	7.312
54	0	0	7.172	0.51	0	28.965	11.335	0	0	0.002	2.331	1.84	0.7	3.586	0.285	0	1.5	0	0	0	1.551	22.908	0.369	4.263	7.367
55	0	0	6.86	0	0	29.18	12.087	0	0.004	0.009	1.927	2.629	0.979	4.254	0.523	0	2.5	0	0	0	2.239	23.477	0.318	3.372	6.364
56	0	0	8.78	0.51	0	28.525	12.71	0	0.003	0.002	1.656	2.75	0.848	2.822	0.161	0	0	0	0	0	2.571	23.881	0.401	4.88	6.65
57	0	0	3.977	0.68	0	27.28	12.121	0	0.004	0.002	1.44	2.384	0.834	4.792	0.024	0	1.5	0	0	0	1.507	22.764	0.489	3.111	7.389
58	0	0	6.861	0.85	0	26.831	11.024	0	0.002	0.001	1.492	1.477	0.874	2.82	0.581	0	3.35	0	0	0	2.1	20.665	0.356	3.952	7.433
59	0	0	9.882	0.51	0	29.746	11.494	0	0.001	0.001	1.287	1.651	0.905	4.137	0.664	0	5.25	0	0	0	1.617	18.6	0.835	4.533	8.045
60	0	0	7.32	1.02	0	30.634	11.405	0	0	0.004	1.705	2.02	0.787	3.269	0.197	0	1.85	0	0	0	2.293	21.971	0.428	3.752	7.425
61	0	0	6.483	0.51	0	23.263	11.592	0	0.006	0.002	2.299	1.249	1.077	4.648	0.572	0	4.15	0	0	0	2.39	20.84	0.405	3.733	6.69
62	0	0	4.071	0.68	0	27.436	14.369	0	0.004	0.005	1.93	2.572	0.701	3.678	0.607	0	0.4	0	0	0	1.525	22.312	0.687	3.621	5.147
63	0	0	6.461	0.34	0	29.353	10.923	0	0.007	0.001	1.469	2.476	0.845	3.454	1	0	1.7	0	0	0	1.84	19.18	0.23	3.94	5.623
64	0	0	5.203	0.17	0	31.611	12.47	0	0.002	0.003	0.961	1.24	0.576	4.344	0.76	0	1.9	0	0	0	2.767	16.162	0.364	3.51	7.342
65	0	0	7.693	0.51	0	28.814	11.381	0	0.003	0.003	1.059	1.882	1.147	4.124	0.468	0	1.75	0	0	0	1.985	21.863	0.556	3.532	7.983
66	0	0	8.691	0	0	31.131	14.034	0	0	0.001	1.557	1.435	0.575	3.831	0.493	0	5.7	0	0	0	1.587	19.937	0.326	5.981	6.08
67	0	0	8.392	0	0	25.742	12.267	0	0.002	0.003	2.136	2.003	0.871	3.377	0.37	0	1.35	0	0	0	1.649	21.262	0.641	4.472	5.476
68	0	0	6.93	1.19	0	29.597	12.122	0	0.004	0	1.174	2.087	0.963	3.886	1.111	0	2.45	0	0	0	3.116	19.403	0.358	2.801	7.537
69	0	0	6.241	0.17	0	27.221	11.985	0	0	0.001	1.961	1.556	0.775	5.906	0.971	0	3.15	0	0	0	2.937	19.929	0.167	3.647	5.805
70	0	0	3.76	0.51	0	27.577	12.12	0	0.003	0.003	1.911	1.853	0.824	2.93	0.582	0	4.4	0	0	0	2.041	23.299	0.519	4.16	7.135
71	0	0	4.921	0	0	25.52	12.001	0	0.002	0.001	1.821	2.001	1.103	3.677	0.29	0	0.9	0	0	0	4.011	24.428	0.481	3.941	5.832
72	0	0	7.311	0.68	0	32.402	12.721	0	0.001	0.002	1.268	1.37	0.606	5.438	0.91	0	7	0	0	0	0.931	20.068	0.379	2.24	5.224
73	0	0	7.442	0.51	0	27.856	11.33	0	0	0	2.137	1.583	1.329	5.575	1.547	0	3.45	0	0	0	1.556	21.147	0.43	3.352	5.208
74	0	0	7.25	0.51	0	30.901	12.381	0	0.001	0.002	1.352	1.041	0.899	4.174	0.396	0	2.5	0	0	0	1.973	17.805	0.565	4.882	7.905
75	0	0	4.958	0	0	30.681	12.808	0	0.002	0.001	0.9	1.874	0.737	5.233	0.599	0	2.5	0	0	0	2.747	23.756	0.594	3.674	4.988
76	0	0	4.942	0.34	0	27.783	10.168	0	0.001	0	2.136	2.261	1.419	4.135	1.197	0	2.2	0	0	0	2.541	20.568	0.816	2.971	7.48
77	0	0	7.922	1.02	0	33.837	11.399	0	0	0.001	0.441	1.858	0.709	4.088	0.78	0	0.4	0	0	0	2.153	20.966	0.329	3.951	6.528
78	0	0	6.91	0	0	26.677	12.222	0	0.003	0.002	1.458	2.42	0.684	5.128	0.047	0	1	0	0	0	1.603	22.336	0.49	4.403	8.224
79	0	0	6.441	0.34	0	25.431	11.689	0	0.001	0.003	2.853	1.82	0.86	4.418	1.425	0	2	0	0	0	0.901	16.368	0.667	3.774	3.999
80	0	0	6.84	0.68	0	27.943	11.475	0	0.002	0.002	1.977	1.703	0.878	3.182	0.284	0	7.2	0	0	0	1.626	18.986	0.427	3.722	7.459
81	0	0	3.115	0.17	0	31.777	11.554	0	0.003	0.005	0.992	1.532	0.75	5.117	0.326	0	4.1	0	0	0	2.292	23.358	0.538	3.513	7.141
82	0	0	6.52	0	0	28.767	11.037	0	0.001	0	2.225	1.388	0.555	4.988	1.111	0	2.7	0	0	0	1.963	16.234	0.415	5.012	5.313
83	0	0	6.81	0	0	32.696	11.614	0	0.006	0	2.404	1.31	0.863	3.911	0.479	0	3.15	0	0	0	2.116	20.099	0.516	3.941	8.078
84	0	0	6.441	0.51	0	28.101	11.93	0	0.006	0.005	1.307	1.994	1.013	2.537	0.294	0	0.5	0	0	0	1.518	18.267	0.467	4.97	7.31
85	0	0	5.055	0.34	0	28.81	12.828	0	0.001	0.004	1.675	1.353	0.934	3.752	0.378	0	2.65	0	0	0	2.589	20.267	0.561	2.912	6.932
86	0	0	7.193	0	0	28.742	10.729	0	0.002	0.001	1.222	1.712	0.55	4.887	0.722	0	2.75	0	0	0	2.216	20.116	0.407	3.063	6.637
87	0	0	7.663	0.68	0	26.098	12.002	0	0	0.004	1.117	2.423	0.785	4.146	0.936	0	1	0	0	0	2.809	22.874	0.572	3.695	7.97
88	0	0	4.612	0	0	30.408	11.654	0	0.002	0	2.403	2.367	0.924	3.346	0.311	0	0.9	0	0	0	1.994	18.408	0.417	3.81	7.48
89	0	0	7.821	0.17	0	33.035	11.359	0	0.001	0.003	1.353	1.159	0.78	2.758	0.914	0	2.45	0	0	0	2.508	17.958	0.396	5.092	6.893
90	0	0	6.163	0	0	34.221	12.202	0	0.004	0.001	0.714	1.882	0.795	4.782	0.851	0	6.65	0	0	0	1.045	22.233	0.253	3.872	5.647
91	0	0	4.442	0.51	0	27.109	11.227	0	0	0.003	2.452	2.123	1.105	4.747	0.197	0	1.45	0	0	0	2.105	20.911	0.87	3.102	6.425
92	0	0	7.72	0	0	24.752	12.941	0	0.004	0	2.201	2.29	1.115	3.943	0.685	0	2.2	0	0	0	2.286	22.312	0.387	4.346	5.767
93	0	0	4.884	0	0	23.631	10.952	0	0.007	0.001	2.506	2.25	1.029	2.907	0.008	0	1	0	0	0	1.685	17.682	0.473	5.68	7.139
94	0	0	4.721	0.17	0	28.166	11.06	0	0.003	0	1.405	1.319	0.895	4.139	1.06	0	2.9	0	0	0	2.314	16.995	0.282	3.911	6.433
95	0	0	5.273	0.51	0	27.969	11.891	0	0	0	1.436	1.876	0.505	4.886	0.968	0	4.1	0	0	0	1.976	20.926	0.389	2.958	6.395
96	0	0	6.49	0	0	31.531	12.814	0	0.003	0.001	0.78	1.34	0.93	4.129	0.03	0	5.1	0	0	0	2.712	18.385	0.318	4.413	7.453
97	0	0	6.052	1.02	0	27.647	11.434	0	0	0	1.792	1.411	0.785	4.857	0.96	0	6.4	0	0	0	1.775	17.436	0.365	3.237	5.258
98	0	0	6.044	0.34	0	29.952	12.662	0	0	0.002	1.542	2.119	0.74	4.655	0.659	0	1	0	0	0	2.464	23.18	0.341	4.182	8.209
99	0	0	6.312	0.51	0	28.654	11.897	0	0.001	0.002	0.854	1.558	0.674	4.937	0.77	0	0.95	0	0	0	3.083	21.55	0.763	3.706	7.12
100	0	0	4.514	0.17	0	31.822	11.354	0	0.003	0.003	0.828	2.504	0.878	3.088	0.455	0	1.75	0	0	0	2.742	22.341	0.608	4.75	6.356

Plant Type:	Greasewood					Grass					Forb					Tree					Shrub				
Plot:	1	2	3	4	5	1	2	3	4	5	1	2	3	4	5	1	2	3	4	5	1	2	3	4	5
sample #																									
101	0	0	5.733	0.68	0	31.029	11.747	0	0.001	0.001	0.956	2.122	1.28	3.07	0.452	0	0.4	0	0	0	2.138	20.561	0.7	5.312	8.099
102	0	0	5.883	0.68	0	30.686	12.294	0	0	0.005	1.439	2.142	0.71	2.824	0.389	0	4.6	0	0	0	1.628	18.594	0.467	3.641	6.696
103	0	0	4.961	0	0	28.662	10.886	0	0.003	0.002	1.652	1.512	1.266	4.123	0.937	0	2.25	0	0	0	1.727	18.43	0.558	2.691	7.746
104	0	0	5.97	0.17	0	27.457	11.004	0	0.002	0.004	1.338	1.931	0.946	4.382	0.089	0	1.85	0	0	0	2.076	17.492	0.38	5.012	8.762
105	0	0	6.401	0.51	0	27.933	12.876	0	0.004	0.001	0.914	2.214	0.761	5.271	0.349	0	2.6	0	0	0	2.8	21.384	0.553	2.873	6.151
106	0	0	4.334	0	0	31.936	11.293	0	0	0.001	0.877	1.983	0.932	3.332	0.52	0	0.5	0	0	0	2.503	17.077	0.384	4.7	6.226
107	0	0	6.363	0.17	0	26.745	12.264	0	0.003	0.003	2.298	1.582	0.507	4.358	0.777	0	4	0	0	0	1.934	16.889	0.456	3.901	5.403
108	0	0	3.725	0.17	0	26.958	13.03	0	0	0.003	1.977	1.941	0.905	3.237	0.046	0	3.45	0	0	0	2.808	21.356	0.216	3.701	7.539
109	0	0	8.571	0.51	0	27.111	13.143	0	0.004	0.003	1.967	1.889	1.268	4.146	0.179	0	4	0	0	0	2.683	19.227	0.554	3.425	7.119
110	0	0	8.244	0	0	32.621	10.968	0	0.002	0.004	1.025	1.966	0.79	3.547	0.392	0	3	0	0	0	1.581	21.027	0.55	3.475	5.939
111	0	0	6.283	0.85	0	28.44	12.054	0	0	0.004	1.089	1.428	0.92	3.27	0.122	0	1.4	0	0	0	2.943	22.839	0.605	3.641	8.096
112	0	0	3.953	0.17	0	28.781	12.893	0	0	0.001	1.15	1.6	0.979	4.627	0.54	0	2	0	0	0	2.429	20.118	0.564	4.522	6.433
113	0	0	5.881	0.17	0	29.629	11.51	0	0.001	0.002	1.312	2.594	0.997	4.215	0.777	0	0	0	0	0	1.742	20.485	0.459	4.134	6.648
114	0	0	5.4	1.19	0	25.357	12.18	0	0.001	0.001	2.518	2.337	0.92	2.891	0.957	0	3.25	0	0	0	2.552	23.077	0.453	3.62	5.844
115	0	0	5.871	0	0	30.743	12	0	0.001	0.001	0.791	2.454	0.85	3.868	0.782	0	3.6	0	0	0	3.693	22.681	0.315	4.152	7.495
116	0	0	5.281	0.34	0	27.937	12.269	0	0.002	0	2.118	1.97	0.716	4.293	0.874	0	3.75	0	0	0	1.381	19.581	0.438	3.901	6.455
117	0	0	6.44	0.51	0	29.133	10.834	0	0.002	0.001	1.247	1.552	1.001	5.975	0.58	0	5.3	0	0	0	2.112	18.242	0.438	2.485	7.203
118	0	0	4.065	0.68	0	26.264	12.576	0	0	0.003	1.894	1.261	1.088	3.524	0.359	0	2.25	0	0	0	1.846	19.921	0.473	3.272	7.236
119	0	0	5.991	0	0	29.406	12.682	0	0	0	1.357	1.467	0.892	3.825	0.987	0	2.95	0	0	0	2.671	18.171	0.281	3.444	6.655
120	0	0	5.482	0.85	0	26.777	13.139	0	0	0.008	1.813	1.984	1.206	3.095	1.199	0	3.95	0	0	0	2.27	21.344	0.556	5.164	6.715
121	0	0	7.231	0.17	0	25.34	11.853	0	0.004	0.008	1.401	1.752	0.86	3.802	0.293	0	2	0	0	0	3.064	22.611	0.452	3.84	6.498
122	0	0	4.832	0.51	0	26.862	10.707	0	0	0.002	1.496	1.518	0.779	3.793	0.49	0	2.15	0	0	0	1.119	17.067	0.584	4.002	6.058
123	0	0	4.426	0.34	0	25.066	12.014	0	0	0.008	1.923	1.842	1.266	5.429	0.486	0	1.65	0	0	0	2.459	21.733	0.672	3.86	7.698
124	0	0	5.322	0.68	0	29.649	12.437	0	0	0.002	1.204	1.823	0.946	2.727	0.307	0	3.25	0	0	0	1.944	22.464	0.453	4.71	6.647
125	0	0	6.093	0.17	0	26.012	11.303	0	0.003	0.003	1.278	1.445	0.806	5.114	0.338	0	7.35	0	0	0	2.738	21.464	0.475	2.824	6.262
126	0	0	4.165	0.34	0	24.792	12.001	0	0.003	0.002	2.542	1.632	0.557	3.788	0.297	0	2.95	0	0	0	2.242	21.387	0.285	4.22	7.488
127	0	0	4.651	0.51	0	25.769	11.211	0	0.002	0.004	2.698	2.176	0.927	4.554	0.205	0	1.2	0	0	0	3.309	21.029	0.251	4	7.415
128	0	0	6.261	0	0	32.642	9.858	0	0.005	0.001	0.757	1.287	1.769	2.85	1.303	0	2.25	0	0	0	2.471	18.308	0.919	5.75	6.714
129	0	0	6.631	1.02	0	28.62	11.898	0	0	0	1.788	2.146	0.447	2.968	0.44	0	2	0	0	0	2.169	25.017	0.232	2.95	5.415
130	0	0	5.363	0.34	0	32.974	11.478	0	0	0	0.76	1.463	1.459	3.491	0.621	0	4	0	0	0	3.061	20.754	0.69	3.322	6.066
131	0	0	7.651	0	0	31.878	11.32	0	0.003	0.003	1.637	1.951	0.848	2.876	0.639	0	2	0	0	0	2.458	22.253	0.374	4.59	6.986
132	0	0	6.446	0.68	0	27.04	10.21	0	0.003	0.001	1.758	1.846	0.564	3.979	0.603	0	0.7	0	0	0	2.374	22.007	0.201	3.441	6.057
133	0	0	7.561	0.51	0	32.459	13.905	0	0	0.001	1.164	1.357	1.015	4.067	0.617	0	1.5	0	0	0	2.209	21.689	0.511	3.113	5.77
134	0	0	6.317	0.51	0	26.166	11.33	0	0	0.003	2.448	1.505	0.472	2.794	0.649	0	4.15	0	0	0	2.097	17.991	0.692	4.411	6.214
135	0	0	4.935	0.17	0	29.748	12.17	0	0.001	0	0.908	1.699	0.839	5.071	0.548	0	5.1	0	0	0	1.728	21.395	0.678	4.083	7.435
136	0	0	7.565	0.85	0	30.413	12.168	0	0.001	0.002	1.496	2.661	1.33	4.836	0.601	0	0.5	0	0	0	2.218	22.488	0.672	4.055	6.539
137	0	0	5.743	1.19	0	27.74	10.78	0	0.007	0.003	1.42	1.558	1.018	2.854	0.617	0	2.5	0	0	0	3.097	23.229	0.407	4.3	6.9
138	0	0	7.942	0	0	27.149	12.011	0	0.003	0.003	1.226	2.1	1.389	3.93	0.871	0	1.15	0	0	0	1.629	21.973	0.639	4.61	6.52
139	0	0	4.924	0	0	29.654	11.044	0	0.004	0.003	1.12	1.345	0.816	4.039	0.376	0	5.4	0	0	0	1.47	18.112	0.462	4.39	7.295
140	0	0	5.904	0.17	0	26.207	12.118	0	0.004	0.001	3.042	1.287	0.874	3.984	0.98	0	1.25	0	0	0	2.368	17.193	0.304	3.141	6.965
141	0	0	8.333	0.34	0	31.521	11.906	0	0.005	0.003	2.061	1.949	0.883	6.309	0.269	0	2.35	0	0	0	2.584	20.775	0.257	2.385	7.652
142	0	0	5.88	0.85	0	24.909	12.525	0	0	0.004	1.986	1.985	1.269	3.872	1.088	0	1.35	0	0	0	2.381	23.46	0.618	3.036	6.696
143	0	0	5.21	0	0	31.105	11.543	0	0.005	0.004	1.561	1.41	0.892	3.316	0.796	0	2.2	0	0	0	1.086	18.242	0.279	5.642	5.245
144	0	0	4.711	0.34	0	31.808	9.765	0	0.003	0	0.91	1.535	0.997	2.875	0.881	0	2.1	0	0	0	1.805	18.003	0.433	4.25	6.262
145	0	0	7.112	0.51	0	27.04	11.888	0	0.002	0.001	2.925	1.956	0.831	4.565	0.714	0	1.95	0	0	0	1.624	22	0.293	2.911	6.417
146	0	0	4.306	0.34	0	26.702	12.15	0	0.001	0.005	1.428	1.374	0.923	3.186	0.281	0	3.15	0	0	0	3.488	20.187	0.735	5.7	6.867
147	0	0	4.433	0.17	0	29.937	12.349	0	0.005	0.002	1.964	1.876	1.388	5.472	0.246	0	2.9	0	0	0	2.289	21.349	0.409	2.584	6.407
148	0	0	6.211	0	0	28.564	11.367	0	0.002	0	0.945	1.67	0.79	3.586	0.551	0	2.55	0	0	0	2.847	22.055	0.247	4.75	8.441
149	0	0	4.172	0.34	0	26.089	11.816	0	0.002	0	1.114	2.094	0.845	4.362	0.666	0	2.2	0	0	0	1.827	19.005	0.332	3.002	6.202
150	0	0	4.582	0.85	0	23.33	11.466	0	0.003	0.004	3.155	1.61	0.917	3.164	0.88	0	4.95	0	0	0	2.18	21.353	0.526	4.38	5.974
151	0	0	6.731	0.17	0	29.775	11.199	0	0.002	0	1.065	1.166	1.199	5.059	0.34	0	4.3	0	0	0	0.821	15.552	0.331	3.953	8.048
152	0	0	6.232	0	0	25.3	12.468	0	0.003	0.01	2.628	2.025	0.786	6.076	0.246	0	3.4	0	0	0	1.967	21.061	0.522	2.415	6.524
153	0	0	6.801	0.17	0	25.464	11.32	0	0	0	2.377	2.162	0.853	2.464	0.371	0	1.2	0	0	0	1.882	19.341	0.39	4.51	7.594
154	0	0	5.236	0.85	0	28.418	12.41	0	0	0	1.13	1.993	0.776	3.74	0.714	0	3.15	0	0	0	1.921	17.672	0.376	3.15	6.494
155	0	0	5.101	0.17	0	30.407	12.011	0	0.003	0.001	1.179	1.316	1.06	4.536	0.1	0	8.1	0	0	0	1.191	18.744	0.572	3.953	5.665
156	0	0	7.33	0.68	0	31.584	12.698	0	0.002	0.002	1.437	1.518	0.882	3.138	0.109	0	3.1	0	0	0	2.921	17.428	0.383	4.65	8.184
157	0	0	6.471	0	0	25.763	11.675	0	0.007	0.003	2.115	1.696	0.88	4.019	0.227	0	1.4	0	0	0	1.568	22.545	0.224	5.012	8.56
158	0	0	5.732	0.17	0	32.469	12.496	0	0.002	0.002	1.962	1.941	0.708	3.896	0.697	0	4.1	0	0	0	2.089	21.271	0.599	3.504	6.219
159	0	0	5.136	0.17	0	31.143	11.418	0	0	0.001	1.545	1.772	1.354	3.708	0.92	0	1.75	0	0	0	1.457	18.853	0.648	3.882	5.625
160	0	0	6.05	0	0	29.505	12.044	0	0	0.003	2.201	1.474	1.462	3.12	0.897	0	3	0	0	0	2.02	22.572	0.75	4.59	7.164
161	0	0	5.522	0.34	0	23.637	12.17	0	0.001	0.002	1.825	2.032	0.817	3.513	0.937	0	4.75	0	0	0	2.437	18.561	0.329	4.972	7.162
162	0	0	7.921	0.34	0	28.907	14.103	0	0.002	0.002	2.514	2.818	1.12	3.766	0.778	0	1.5	0	0	0	1.816	24.618	0.379	4.182	6.876
163	0	0	2.836	0.68	0	31.135	10.227	0	0	0.003	1.035	1.329	0.868	6.319	0.568	0	4.15	0	0	0	2.435	22.952	0.41	2.907	7.432
164	0	0	6.071	0	0	25.429	11.382	0	0.002	0	1.77	1.413	0.83	2.935	0.561	0	4.1	0	0	0	1.794	20.216	0.441	3.493	6.316
165	0	0	5.38	0.17	0	26.206	12.597	0	0.002	0	1.972	2.195	1.138	5.574	1.082	0	2.4	0	0	0	2.19	20.458	0.401	3.611	7.183
166	0	0	7.032	0.68	0	27.013	14.198	0	0.006	0	2.489	2.459	0.885	5.35	0.348	0	2	0	0	0	1.607	26.422	0.329	3.79	8.428
167	0	0	6.851	1.36	0	27.031	10.822	0	0	0.003	0.898	1.558	0.797	3.015	1.24	0	1.15	0	0	0	2.179	15.272	0.449	4.39	6.39
168	0	0	6.614	0.51	0	26.404	12.299	0	0.002	0.001	3.308	1.284	0.83	3.654	1.277	0	2.5	0	0	0	0.904	16.018	0.69	3.613	4.829
169	0	0	5.064	0	0	33.865	12.136	0	0.004	0.002	0.865	1.101	1.324	4.273	0.363	0	5.6	0	0	0	2.078	16.856	0.623	5.761	5.306
170	0	0	8.781	0.51	0	30.653	12.496	0	0	0.006	0.809	1.562	0.637	3.398	0.615	0	1.2	0	0	0	2.78	19.142	0.55	3.454	7.303
171	0	0	6.891	0.68	0	30.408	11.345	0	0.001	0.006	0.592	1.715	0.711	4.32	0.724	0	3.1	0	0	0	2.785	18.629	0.315	3.461	6.427
172	0	0	7.331	0.34	0	27.628	10.613	0	0	0.005	2.063	1.703	0.847	3.551	0.332	0	3.95	0	0	0	1.337	19.113	0.243	4.73	6.689
173	0	0	6.313	0.51	0	27.768	11.858	0	0	0.001	1.582	1.723	1.18	2.941	1.634	0	3.45	0	0	0	2.377	19.776	0.439	4.94	5.543
174	0	0	6.2	0	0	26.067	12.768	0	0.004	0.005	1.313	2.922	0.983	3.76	1.247	0	0.75	0	0	0	2.298	23.991	0.291	3.901	5.189
175	0	0	4.202	0	0	27.445	11.312	0	0.002	0.002	2.225	1.344	1.17	5.707	0.108	0	4.5	0	0	0	2.53	19.646	0.517	3.502	8.814
176	0	0	7.95	0	0	33.294	11.741	0	0.002	0.005	1.885	1.37	1.251	3.659	0.819	0	5.35	0	0	0	2.09	21.963	0.35	3.371	7.611
177	0	0	6.132	0.51	0	32.747	11.197	0	0.001	0.001	1.226	1.645	0.862	3.611	0.888	0	3.05	0	0	0	1.593	16.796	0.417	3.72	6.355
178	0	0	6.302	0.34	0	27.521	12.293	0	0	0.001	0.826	1.912	1.288	3.422	1.052	0	3.7	0	0	0	2.739	20.926	0.372	3.78	6.236
179	0	0	6.971	0.17	0	33.133	12.242	0	0	0.001	0.719	2.556	0.946	2.945	1.213	0	0.5	0	0	0	1.7	21.547	0.265	4.131	5.807
180	0	0	6.486	0.85	0	27.384	11.345	0	0.005	0.001	1.275	2.014	0.697	4.178	0.412	0	0.4	0	0	0	2.055	17.366	0.613	3.461	8.06
181	0	0	3.652	0.17	0	26.959	11.973	0	0.002	0.006	1.453	1.509	1.316	3.045	0.897	0	3.4	0	0	0	2.815	21.678	0.619	4.432	5.24
182	0	0	5.233	0.17	0	30.545	11.528	0	0.003	0.003	1.201	2.114	0.998	3.832	0.59	0	1.7	0	0	0	2.824	21.324	0.677	5.691	6.208
183	0	0	6.181	0.68	0	27.991	11.733	0	0	0.001	1.951	1.724	1.498	3.26	0.401	0	3.65	0	0	0	1.599	21.131	0.49	4.332	6.721
184	0	0	7.183	0.17	0	32.48	11.98	0	0.001	0.005	0.842	1.721	1.014	3.329	0.693	0	1.95	0	0	0	3.11	19.479	0.698	4.771	4.704
185	0	0	6.651	0.17	0	28.733	11.845	0	0.001	0	1.047	1.85	0.735	4.505	0.295	0	5.3	0	0	0	2.971	23.901	0.465	4.571	8.183
186	0	0	5.634	0	0	32.42	11.853	0	0.005	0.005	1.214	2.436	0.908	4.905	1.057	0	0.5	0	0	0	1.734	20.44	0.23	3.642	5.189
187	0	0	6.821	0.34	0	30.436	10.886	0	0.004	0.003	1.11	2.52	1.007	2.867	0.025	0	2.4	0	0	0	2.651	15.663	0.665	3.961	5.486
188	0	0	5.633	0.51	0	27.779	12.529	0	0.006	0.003	2.216	1.201	1.128	3.477	1.007	0	4.4	0	0	0	1.393	21.017	0.569	4.146	7.781
189	0	0	6.114	0	0	25.836	11.578	0	0	0	1.54	1.456	1.035	2.803	0.557	0	3.95	0	0	0	3.179	22.177	0.534	4.304	6.026
190	0	0	6.325	0.51	0	26.41	13.692	0	0	0	1.44	1.222	0.517	4.059	0.512	0	7.15	0	0	0	3.099	17.745	0.344	3.782	7.311
191	0	0	6.231	1.02	0	31.873	13.171	0	0.004	0.001	1.48	1.596	0.491	3.78	0.351	0	0	0	0	0	2.791	17.057	0.615	3.7	6.709
192	0	0	7.372	0.17	0	29.759	14.015	0	0.004	0	1.057	1.844	1.03	6.082	0.425	0	3.65	0	0	0	2.243	22.031	0.317	3.348	8.792
193	0	0	8.412	0	0	25.898	11.971	0	0	0.006	2.158	1.779	0.819	4.047	0.023	0	5.05	0	0	0	1.88	19.433	0.488	4.182	7.854
194	0	0	5.441	0.51	0	26.079	11.914	0	0.002	0.004	2.032	1.828	1.073	3.22	0.349	0	2.95	0	0	0	2.211	18.487	0.282	5.21	6.543
195	0	0	5.505	0	0	30.573	11.093	0	0.001	0.001	1.129	1.824	1.267	3.813	1.003	0	3.9	0	0	0	1.416	18.011	0.423	5.511	6.108
196	0	0	7.372	0.85	0	27.679	12.603	0	0.002	0.002	1.805	1.81	0.84	2.888	0.599	0	6.1	0	0	0	2.732	19.568	0.537	4.35	7.692
197	0	0	7.812	1.36	0	29.632	12.162	0	0.003	0.001	2.022	1.541	0.905	3.427	0.581	0	5.45	0	0	0	0.566	19.124	0.361	3.991	6.718
198	0	0	6.476	0.85	0	25.666	11.959	0	0.003	0.001	1.256	1.828	0.796	4	0.539	0	0.7	0	0	0	2.258	16.555	0.351	3.635	6.894
199	0	0	7.39	0.68	0	31.09	12.196	0	0.002	0.002	0.78	1.91	0.948	3.454	0.764	0	3.15	0	0	0	3.802	22.559	0.448	3.29	5.708
200	0	0	5.813	0.34	0	31.357	11.731	0	0.002	0.002	1.389	2.168	1.141	3.553	0.802	0	0.5	0	0	0	2.282	20.376	0.422	3.791	6.152
201	0	0	7.19	0.68	0	35.991	12.288	0	0.002	0.002	1.319	1.11	1.064	3.613	0.523	0	4.35	0	0	0	1.98	22.329	0.523	3.72	7.702
202	0	0	4.13	0	0	27.136	11.779	0	0	0.001	0.852	1.966	0.916	4.908	0.449	0	0.5	0	0	0	2.838	19.573	0.712	3.123	6.664
203	0	0	7.092	0.51	0	28.577	10.677	0	0.001	0.005	1.557	1.257	0.867	4.749	0.42	0	6	0	0	0	2.242	14.881	0.304	3.755	5.824

Plant Type:	Greasewood					Grass					Forb					Tree					Shrub				
Plot:	1	2	3	4	5	1	2	3	4	5	1	2	3	4	5	1	2	3	4	5	1	2	3	4	5
sample #																									
204	0	0	5.93	0.68	0	28.361	11.793	0	0.002	0.009	1.964	2.364	1.2	2.212	0.937	0	0.9	0	0	0	2.13	23.602	0.534	3.67	5.491
205	0	0	7.92	0	0	27.322	11.563	0	0	0	1.957	2.041	0.918	2.799	0.901	0	3.4	0	0	0	2.9	23.595	0.381	3.801	6.342
206	0	0	6.181	0	0	29.757	13.906	0	0	0.001	1.54	1.767	0.93	5.365	0.341	0	2	0	0	0	1.348	19.463	0.483	3.129	8.336
207	0	0	6.491	0.85	0	28.355	12.215	0	0.001	0.003	1.165	1.231	0.802	3.735	0.519	0	5.45	0	0	0	1.551	20.527	0.413	3.363	6.534
208	0	0	4.951	0.17	0	26.732	10.754	0	0.001	0.002	1.439	1.793	1.139	3.565	0.4	0	1.95	0	0	0	2.174	22.317	0.591	3.335	8.153
209	0	0	5.762	0	0	30.935	11.054	0	0.001	0.002	1.95	1.153	1.011	4.029	0.749	0	3.65	0	0	0	1.916	17.901	0.314	4.181	6.752
210	0	0	7.334	0.85	0	26.404	13.129	0	0.001	0.001	1.582	1.905	0.883	2.857	0.14	0	2.7	0	0	0	2.808	22.382	0.533	4.35	6.206
211	0	0	6.071	0.17	0	28.702	12.123	0	0	0.003	1.225	2.222	0.994	5.878	1	0	0.7	0	0	0	2.577	24.941	0.442	3.224	6.045
212	0	0	6.173	0.51	0	26.711	12.752	0	0.001	0.002	1.584	2.369	0.758	4.712	0.37	0	1.15	0	0	0	1.848	23.219	0.517	3.583	6.444
213	0	0	4.292	0.34	0	29.738	11.883	0	0.004	0.002	1.55	1.981	0.702	2.792	0.689	0	1.5	0	0	0	2.847	23.747	0.73	4.202	6.993
214	0	0	3.602	0	0	30.255	12.164	0	0.004	0	1.673	2.454	0.993	4.489	0.369	0	1.25	0	0	0	2.297	24.467	0.499	2.935	8.79
215	0	0	6.091	0.85	0	28.486	10.841	0	0.005	0.002	1.773	1.696	1.059	3.995	0.339	0	5.3	0	0	0	2.173	21.659	0.489	3.345	4.478
216	0	0	7.054	0.68	0	25.552	11.957	0	0.001	0.001	1.543	1.685	1.124	3.277	0.541	0	7	0	0	0	1.912	22.092	0.925	3.65	7.276
217	0	0	4.68	0	0	29.388	12.608	0	0.004	0.002	1.829	2.455	0.796	2.971	0.139	0	2.1	0	0	0	1.711	22.159	0.378	4.251	7.355
218	0	0	7.771	0.51	0	25.851	11.666	0	0.002	0.004	1.39	2.778	1.016	4.029	0.087	0	0.4	0	0	0	3.461	23.809	0.475	3.961	7.593
219	0	0	5.052	0.51	0	27.677	14.147	0	0.003	0.004	1.169	1.875	1.076	3.404	0.577	0	1.25	0	0	0	3.298	18.005	0.487	5.36	5.329
220	0	0	5.802	0	0	28.966	13.298	0	0.001	0	1.243	2.048	0.782	4.887	0.673	0	4.4	0	0	0	1.289	15.46	0.325	4.121	6.391
221	0	0	6.453	0.34	0	27.066	12.026	0	0.002	0.009	1.801	2.587	1.098	2.865	0.325	0	1.25	0	0	0	2.152	21.287	0.638	4.19	6.049
222	0	0	5.224	0.51	0	30.931	10.945	0	0.002	0.001	1.646	2.087	0.932	3.093	0.619	0	4.05	0	0	0	2.971	19.861	0.485	3.61	5.884
223	0	0	6.23	0	0	28.339	12.63	0	0.001	0	2.078	2.769	0.857	4.682	0.782	0	0.95	0	0	0	3.066	20.029	0.35	3.623	7.106
224	0	0	6.084	0.34	0	25.652	11.217	0	0	0.007	1.55	2.085	0.723	3.121	0.496	0	6.15	0	0	0	1.549	19.845	0.529	4.691	5.659
225	0	0	5.921	1.02	0	27.576	12.014	0	0.006	0.003	1.56	2.263	1.533	2.424	1.482	0	2.65	0	0	0	1.58	23.803	0.411	3.68	6.014
226	0	0	5.371	0	0	29.269	11.94	0	0.002	0.004	1.773	1.483	1.294	5.146	1.301	0	4.25	0	0	0	2.563	22.286	0.526	4.032	5.995
227	0	0	7.851	0.51	0	32.591	10.784	0	0.002	0.004	1.102	1.463	0.846	3.403	0.797	0	1.65	0	0	0	2.006	17.722	0.179	4.391	5.827
228	0	0	5.083	0.34	0	31.967	12.164	0	0	0	1.436	1.559	1.094	5.062	1.028	0	4.5	0	0	0	1.722	19.106	0.436	3.692	5.925
229	0	0	7.194	0.51	0	26.35	12.045	0	0.002	0.001	2.285	1.754	1.398	3.759	0.992	0	1.75	0	0	0	2.083	23.224	0.469	3.862	5.511
230	0	0	7.18	0.17	0	26.721	10.965	0	0.003	0.002	1.848	2.433	0.763	3.518	0.905	0	0.8	0	0	0	1.401	22.887	0.493	3.793	6.4
231	0	0	4.844	1.02	0	29.428	11.496	0	0.001	0.003	1.05	1.969	1.151	2.553	0.048	0	5.05	0	0	0	2.7	20.854	0.399	4.691	6.991
232	0	0	8.205	0.17	0	31.979	10.257	0	0.008	0.003	0.862	1.364	0.736	4.819	0.638	0	4.15	0	0	0	1.577	21.893	0.548	4.383	8.635
233	0	0	8.191	0	0	34.093	11.05	0	0.006	0.001	1.09	1.846	0.946	4.377	0.741	0	4.45	0	0	0	2.437	25.451	0.464	5.02	7.408
234	0	0	8.54	0.85	0	27.474	12.173	0	0	0	1.306	1.81	0.795	4.709	0.027	0	2.2	0	0	0	3.202	24.234	0.292	3.41	7.445
235	0	0	4.631	0	0	24.637	11.813	0	0	0.003	2.745	2.113	1.013	3.662	0.518	0	0.6	0	0	0	1.424	19.852	0.261	4.2	6.661
236	0	0	3.563	0.68	0	31.783	13.274	0	0.003	0.007	1.776	1.955	1.013	2.129	0.935	0	1.5	0	0	0	2.199	25.958	0.916	5.11	6.488
237	0	0	6.55	0	0	31.995	13.12	0	0.002	0.004	0.651	1.737	0.898	3.66	0.674	0	3.25	0	0	0	1.532	18.744	0.787	4.301	6.652
238	0	0	7.033	0.17	0	27.546	12.183	0	0.003	0.001	1.099	1.911	1.453	3.366	0.393	0	4.95	0	0	0	1.878	18.011	0.49	3.453	8.032
239	0	0	5.721	0.34	0	31.184	11.905	0	0.001	0.001	1.451	1.919	1.206	3.926	0.861	0	0.5	0	0	0	2.683	18.809	0.421	2.71	8.278
240	0	0	6.3	0.34	0	29.659	11.884	0	0.004	0.002	1.298	1.785	0.808	3.92	0.267	0	3.85	0	0	0	2.561	18.921	0.228	4.02	6.543
241	0	0	5.52	0.17	0	27.329	11.288	0	0	0.005	0.939	1.538	1.08	3.016	0.254	0	5.35	0	0	0	2.798	17.079	0.569	4.162	5.678
242	0	0	8.48	0.17	0	28.966	13.754	0	0.001	0	1.514	2.072	0.816	5.785	0.272	0	1.2	0	0	0	2.937	24.294	0.57	2.643	6.799
243	0	0	7.993	0.34	0	26.127	10.247	0	0	0.001	2.033	1.294	0.806	3.679	1.325	0	4.6	0	0	0	1.762	18.988	0.232	5.145	6.073
244	0	0	6.573	0	0	32.151	12.307	0	0	0.004	1.023	2.032	1.031	3.636	0.409	0	0.95	0	0	0	2.529	21.615	0.364	5.122	5.959
245	0	0	5.532	1.02	0	28.066	11.753	0	0	0.004	1.512	2.214	0.821	4.759	1.243	0	4.85	0	0	0	3.438	21.835	0.381	3.573	5.212
246	0	0	5.411	0.34	0	28.897	13.633	0	0	0	2.145	1.935	0.931	3.292	0.753	0	0.5	0	0	0	2.887	22.528	0.485	3.842	7.387
247	0	0	4.914	0.51	0	32.669	12.725	0	0.005	0	0.911	1.924	0.953	4.5	0.279	0	1.45	0	0	0	1.326	19.989	0.921	4.283	8.238
248	0	0	5.863	0	0	26.622	11.553	0	0.006	0	1.649	0.759	0.691	2.959	0.437	0	1.5	0	0	0	1.829	17.215	0.258	5.54	5.904
249	0	0	4.982	0.17	0	31.134	11.447	0	0	0.001	1.239	2.299	0.766	5.134	0.674	0	1.25	0	0	0	2.15	16.173	0.461	2.725	7.655
250	0	0	7.643	0.17	0	33.942	12.912	0	0.002	0.002	1.248	1.375	0.699	3.137	1.31	0	3.25	0	0	0	2.793	17.736	0.495	3.231	5.719
251	0	0	5.184	0	0.15	25.267	8.129	0	0.002	0.003	1.456	1.051	1.478	4.689	1.001	0	5.37	0	0	0	2.423	19.736	0.163	3.722	12.821
252	0	0	5.225	0.51	0.15	28.733	9.45	0	0.003	0.034	2.46	0.794	1.12	5.293	1.794	0	8.5	0	0	0	1.165	16.675	0.326	2.63	12.362
253	0	0	3.619	0.17	0	26.223	8.51	0	0	0.074	2.136	1.346	1.223	6.648	0.496	0	4.62	0	0	0	1.511	17.559	0.352	2.484	17.302
254	0	0	3.81	0	0	27.289	9.076	0	0	0.086	1.426	1.286	1.2	4.853	0.269	0	4.52	0	0	0	2.977	16.159	0.242	4.64	14.37
255	0	0	3.667	0.51	0	27.586	9.702	0	0	0.107	1.772	1.995	0.846	4.415	0.343	0	3.25	0	0	0	1.459	20.445	0.361	4.152	18.922
256	0	0	4.822	0.17	0.15	29.275	8.33	0	0	0.007	2.733	0.92	1.015	5.575	1.491	0	8.32	0	0	0	1.988	19.627	0.418	2.58	10.783
257	0	0	3.663	0.51	0.3	24.009	8.98	0	0.001	0.019	1.856	1.453	0.936	4.416	0.785	0	6.1	0	0	0	2.318	18.543	0.456	4.18	12.791
258	0	0	3.176	0.34	0	25.356	8.757	0	0.001	0.177	2.159	0.929	0.615	5.208	0.557	0	5.87	0	0	0	2.028	20.394	0.436	4.803	13.609
259	0	0	4.678	0.17	0	28.707	8.704	0	0	0.011	2.693	2.356	1.23	5.509	0.914	0	6.9	0	0	0	1.271	20.492	0.408	2.711	12.745
260	0	0	6.537	0.17	0	23.737	6.937	0	0.001	0.154	2.834	0.726	1.396	3.936	0.364	0	5.35	0	0	0	1.47	17.333	0.506	4.481	15.96
261	0	0	4.776	0.34	0.3	26.644	7.843	0	0.002	0.004	1.879	0.587	1.169	5.302	0.87	0	8.02	0	0	0	2.233	17.294	0.384	2.89	12.531
262	0	0	4.574	0	0	23.086	7.961	0	0	0.037	2.368	1.235	1.07	6.119	1.561	0	2.57	0	0	0	1.553	16.263	0.305	3.13	12.799
263	0	0	4.749	0	0	21.529	8.309	0	0.002	0.015	1.782	1.3	0.668	4.171	1.369	0	5.6	0	0	0	2.152	17.912	0.213	3.611	11.185
264	0	0	4.752	0.17	0	24.679	10.533	0	0	0.164	1.858	1.211	0.842	4.172	1.247	0	3.62	0	0	0	2.442	18.621	0.305	2.771	13.255
265	0	0	3.988	0.51	0.15	24.949	8.449	0	0	0.002	2.233	1.406	0.985	4.622	1.821	0	4.92	0	0	0	2.909	18.494	0.515	2.624	10.053
266	0	0	3.231	0.17	0	25.483	8.964	0	0.001	0.16	2.013	1.684	1.258	5.347	0.855	0	9.2	0	0	0	2.288	16.581	0.366	3.532	16.305
267	0	0	5.081	0	0.15	29.952	7.885	0	0.001	0.076	2.334	0.941	0.864	3.852	0.538	0	3.5	0	0	0	2.2	19.284	0.307	3.972	14.573
268	0	0	2.653	0.68	0	24.426	7.849	0	0	0.15	2.684	1.22	0.925	3.744	0.477	0	6.05	0	0	0	1.336	17.697	0.317	3.392	13.166
269	0	0	4.18	0.17	0	26.858	7.947	0	0.001	0.049	2.46	1.096	1.113	7.602	0.808	0	5.35	0	0	0	2.435	13.19	0.534	3.201	13.573
270	0	0	3.466	0	0	29.349	7.199	0	0.003	0.005	2.286	1.182	0.876	6.347	2.089	0	6.55	0	0	0	1.857	16.623	0.471	2.99	9.684
271	0	0	3.647	0.34	0	26.591	7.629	0	0.002	0.107	1.534	0.851	1.101	6.716	0.844	0	10.15	0	0	0	1.661	15.229	0.412	3.803	12.793
272	0	0	6.356	0.34	0.45	26.949	8.237	0	0	0.024	1.022	0.478	1.27	4.467	0.742	0	5	0	0	0	2.65	15.856	0.329	3.533	13.445
273	0	0	3.906	0.85	0	25.846	7.388	0	0	0.113	1.643	1.425	1.306	4.698	0.246	0	3.42	0	0	0	2.629	22.202	0.463	2.4	16.039
274	0	0	3.844	0	0.15	24.231	9.4	0	0.002	0.077	1.633	1.227	0.905	4.744	0.476	0	7.55	0	0	0	2.077	15.256	0.442	2.952	14.097
275	0	0	2.438	0	0.15	24.676	7.054	0	0	0.009	2.461	0.333	0.801	5.371	0.583	0	7	0	0	0	2.411	13.639	0.308	4.405	14.365
276	0	0	5.003	0.17	0.15	26.718	8.639	0	0.001	0.108	1.325	0.913	1.477	4.204	0.864	0	5.07	0	0	0	2.176	15.36	0.368	3.411	14.196
277	0	0	5.617	0.17	0	26.075	7.517	0	0.002	0.09	3.424	1.023	0.996	5.075	1.232	0	4.45	0	0	0	1.036	19.336	0.622	3.92	11.855
278	0	0	3.875	0	0	28.077	7.728	0	0.001	0.004	1.607	0.905	0.618	5.14	1.909	0	8.77	0	0	0	1.543	17.309	0.332	3.061	11.128
279	0	0	4.456	0	0	22.422	8.32	0	0.005	0.028	2.843	1.533	0.756	3.861	1.054	0	6.7	0	0	0	1.279	15.975	0.567	3.741	12.35
280	0	0	3.334	0.17	0	24.4	8.987	0	0	0.056	2.114	0.67	1.055	4.07	0.426	0	2.07	0	0	0	2.378	18.808	0.485	3.27	13.86
281	0	0	2.83	0	0	30.078	9.062	0	0	0.054	1.852	0.908	0.899	4.785	1.444	0	8.97	0	0	0	1.052	13.793	0.512	5.001	12.509
282	0	0	4.396	0	0.75	28.421	9.659	0	0	0.039	1.584	1.328	1.03	5.629	0.601	0	9.1	0	0	0	1.446	15.436	0.215	3.311	12.58
283	0	0	4.235	0.34	0	22.73	7.602	0	0	0.13	2.762	1.064	1.466	4.166	1.534	0	5.9	0	0	0	1.748	15.857	0.587	4.93	14.383
284	0	0	3.612	0.34	0	25.498	8.429	0	0.003	0.083	2.715	1.368	1.071	4.055	1.465	0	4.52	0	0	0	1.56	21.696	0.359	3.643	13.6
285	0	0	4.645	0	0	28.088	8.249	0	0	0.015	2.066	1.475	0.984	5.223	0.202	0	6.8	0	0	0	2.781	17.288	0.349	2.724	13.228
286	0	0	4.757	0	0.3	24.58	8.921	0	0	0.046	2.433	1.274	0.953	4.91	0.989	0	10.11	0	0	0	2.342	15.241	0.449	3.431	11.682
287	0	0	4.004	0	0.3	26.071	9.121	0	0.002	0.058	2.733	1.261	1.111	4.996	0.82	0	8.05	0	0	0	1.337	18.725	0.394	3.163	12.484
288	0	0	3.058	0	0.15	29.072	7.846	0	0.001	0.01	2.035	0.765	1.119	5.848	0.328	0	10.2	0	0	0	2.21	16.503	0.424	3.251	12.79
289	0	0	3.433	0	0	24.247	7.048	0	0.001	0.025	1.617	1.282	0.878	5.513	1.549	0	6.3	0	0	0	2.553	13.643	0.149	3.166	11.528
290	0	0	5.253	0	0.3	23.141	8.894	0	0	0.093	1.844	2.083	1.183	4.565	2.231	0	6.2	0	0	0	2.39	16.845	0.345	2.552	14.411
291	0	0	4.007	0.17	0.3	26.52	9.027	0	0.001	0.011	2.213	0.766	0.972	4.525	0.842	0	4.58	0	0	0	1.074	19.354	0.379	3.934	11.583
292	0	0	5.048	0	0	24.393	8.453	0	0.001	0.006	1.546	1.681	0.94	6.798	0.538	0	2.44	0	0	0	1.473	19.329	0.347	1.641	14.337
293	0	0	3.894	0.34	0.15	23.762	8.418	0	0	0.094	1.959	1.13	1.214	5.655	0.71	0	4.75	0	0	0	2.441	16.984	0.397	3.67	13.86
294	0	0	3.526	0.17	0	26.714	8.103	0	0	0.001	2.979	1.015	1.181	3.93	1.878	0	5.32	0	0	0	0.657	19.248	0.448	3.29	9.541
295	0	0	5.374	0.17	0.15	21.417	8.3	0	0.003	0.005	1.929	1.028	0.634	4.887	1.734	0	3.94	0	0	0	1.805	16.363	0.507	3.951	11.584
296	0	0	6.206	0.34	0.45	23.655	6.792	0	0	0.045	2.317	0.603	0.772	4.943	1.268	0	5.9	0	0	0	2.773	18.106	0.342	2.845	13.858
297	0	0	6.61	0	0.45	23.294	8.042	0	0.001	0.027	1.86	1.516	1.236	4.031	0.803	0	3.95	0	0	0	1.893	15.785	0.36	4.66	13.256
298	0	0	4.712	0.51	0.45	28	8.051	0	0	0.02	2.728	0.614	0.859	5.261	0.71	0	4.22	0	0	0	1.559	18.959	0.509	4.033	11.972
299	0	0	3.146	0	0.3	25.722	9.222	0	0.001	0.051	1.457	1.269	1.489	4.6	2.027	0	5.47	0	0	0	3.05	16.746	0.463	3.34	10.893
300	0	0	4.682	0.34	0	23.569	9.298	0	0	0.148	2.389	0.814	1.027	4.667	0.265	0	11.6	0	0	0	2.93	17.915	0.355	2.651	17.006
301	0	0	3.706	0.17	0.3	27.617	8.273	0	0	0.101	2.23	1.578	0.95	4.222	0.875	0	3.9	0	0	0	2.044	16.949	0.458	5.15	14.085
302	0	0	4.458	0	0.45	23.109	8.887	0	0.001	0.007	2.524	1.517	1.114	6.553	0.484	0	1.59	0	0	0	1.321	24.806	0.27	2.223	13.051
303	0	0	4.488	0.17	0	22.811	8.951	0	0	0.151	1.767	0.986	0.725	4.323	1.214	0	4.18	0	0	0	2.245	18.299	0.361	3.571	12.029
304	0	0	3.894	0.17	0	26.436	7.833	0	0	0.115	2.185	1.355	0.948	4.269	1.674	0	5.8	0	0	0	2.278	14.796	0.41	2.454	11.125
305	0	0	3.384	0	0	25.003	10.148	0	0.002	0.003	1.389	1.6	0.98	5.178	0.481	0	8.01	0	0	0	2.341	19.314	0.289	3.113	14.155
306	0	0	4.36	0.68	0.3	25.311	8.467	0	0.004	0.021	2.314	1.143	1.103	6.03	1.811	0	2.96	0	0	0	2.952	23.055	0.34	2.834	10.943

Plant Type:	Greasewood					Grass					Forb					Tree					Shrub				
Plot:	1	2	3	4	5	1	2	3	4	5	1	2	3	4	5	1	2	3	4	5	1	2	3	4	5
sample #																									
307	0	0	4.046	0	0	21.613	9.132	0	0	0.01	1.502	1.146	0.84	4.065	1.556	0	6.9	0	0	0	1.927	17.854	0.389	2.932	11.499
308	0	0	6.005	0	0	25.672	8.797	0	0	0.015	1.888	1.433	0.876	4.144	1.834	0	9.12	0	0	0	2.3	18.861	0.142	5.27	10.801
309	0	0	4.088	0	0.45	25.684	9.34	0	0.001	0.016	2.385	1.026	0.511	4.624	1.397	0	5.92	0	0	0	1.086	17.593	0.427	3.55	9.901
310	0	0	5.966	0.34	0.3	25.381	9.308	0	0	0.011	1.577	1.728	0.948	4.076	0.82	0	6.03	0	0	0	2.538	20.436	0.493	3.504	10.143
311	0	0	5.239	0.68	0.45	23.152	8.25	0	0.003	0.016	3.342	0.703	0.614	5.505	1.669	0	7.15	0	0	0	1.145	14.847	0.38	3.086	11.881
312	0	0	5.242	0	0	25.925	7.798	0	0	0.026	2.695	0.986	0.832	6.569	1.381	0	5.82	0	0	0	1.099	20.876	0.386	1.923	11.146
313	0	0	4.451	0	0.15	28.344	10.837	0	0.004	0.07	1.4	1.491	1.397	3.846	1.383	0	5.01	0	0	0	2.173	18.625	0.312	3.502	12.39
314	0	0	5.064	0	0	23.532	9.148	0	0	0.02	2.196	2.044	0.754	5.005	1.848	0	5.2	0	0	0	1.499	19.512	0.426	4.872	10.745
315	0	0	6.086	0.34	0	26.706	8.681	0	0	0.005	1.458	2.053	1.088	3.211	1.9	0	1.3	0	0	0	2.439	17.466	0.346	2.91	10.324
316	0	0	3.113	0.34	0.45	27.464	9.616	0	0	0.013	1.66	0.948	0.678	4.499	0.8	0	8.5	0	0	0	1.72	16.163	0.267	2.862	11.33
317	0	0	5.263	0	0.3	27.471	10.121	0	0.002	0.027	1.921	2.668	0.488	4.613	1.089	0	7.12	0	0	0	1.868	15.962	0.252	4	12.65
318	0	0	4.118	0.17	0.15	28.476	9.228	0	0	0.003	2.032	1.577	1.04	3.452	1.498	0	5.6	0	0	0	2.482	11.751	0.486	3.02	12.894
319	0	0	3.297	0	0.15	24.365	8.338	0	0.002	0.118	2.173	1.384	0.849	5.373	0.155	0	5.05	0	0	0	2.443	21.905	0.474	2.534	16.109
320	0	0	5.306	0.34	0	25.597	8.496	0	0	0.032	2.442	1.385	1.091	5.578	0.746	0	1.98	0	0	0	1.758	21.308	0.164	3.421	12.008
321	0	0	4.5	0	0.3	28.976	8.85	0	0	0.055	2.759	1.281	1.116	6.006	0.266	0	7.32	0	0	0	2.347	18.258	0.391	4.612	12.95
322	0	0	4.458	0.34	0	25.544	9.069	0	0.002	0.092	1.962	0.881	1.081	4.255	0.32	0	5.94	0	0	0	2.219	18.229	0.356	3.523	14.208
323	0	0	4.127	0.17	0	31.649	9.791	0	0	0.108	1.573	1.269	0.421	4.96	0.549	0	5.9	0	0	0	1.685	17.147	0.407	1.792	14.34
324	0	0	4.532	0	0	21.241	7.453	0	0.003	0.203	2.058	1.481	1.004	6.216	0.437	0	7.7	0	0	0	1.824	13.737	0.373	2.7	16.315
325	0	0	4.59	0	0	27.106	9.242	0	0	0.006	2.824	0.816	1.077	5.629	1.472	0	7.55	0	0	0	2.113	16.648	0.368	3.151	10.172
326	0	0	4.653	0.34	0	24.887	7.509	0	0.003	0.074	1.827	1.102	0.678	4.828	0.979	0	5.32	0	0	0	2.315	15.043	0.374	3.543	11.247
327	0	0	3.994	0	0.3	23.941	8.493	0	0	0.035	2.064	1.04	1.51	4.795	0.968	0	1.76	0	0	0	2.238	21.359	0.217	2.403	11.898
328	0	0	6.414	0	0	28.95	9.298	0	0.002	0.124	3.298	0.852	0.909	3.78	1.071	0	6.7	0	0	0	0.721	14.785	0.677	3.451	12.827
329	0	0	3.593	0.51	0.45	23.792	8.606	0	0.001	0.032	2.725	1.148	1.319	6.577	0.349	0	3.12	0	0	0	1.88	22.605	0.345	2.953	12.88
330	0	0	4.729	0	0.3	24.061	8.241	0	0	0.093	2.567	0.779	0.698	4.362	0.925	0	2.12	0	0	0	1.369	21.065	0.51	3.272	13.383
331	0	0	4.15	0	0.45	22.923	8.028	0	0.001	0.004	1.625	0.847	0.708	4.976	1.029	0	4.5	0	0	0	1.674	15.983	0.534	3.203	11.627
332	0	0	2.693	0	0	28.165	8.089	0	0.002	0.165	2.199	0.533	0.658	5.194	1.09	0	6.1	0	0	0	2.421	16.234	0.374	3.811	12.92
333	0	0	5.282	0.34	0.15	25.067	9.175	0	0	0.037	2.459	1.696	0.739	2.734	0.419	0	6.12	0	0	0	1.959	23.092	0.484	5	12.599
334	0	0	3.782	0	0.15	27.526	7.666	0	0.004	0.024	2.459	1.547	0.669	5.347	0.879	0	2.67	0	0	0	2.427	19.757	0.501	3.366	11.662
335	0	0	4.069	0	0.15	28.909	8.22	0	0.001	0.004	2.009	0.689	0.683	6.931	2.041	0	4.72	0	0	0	1.368	17.273	0.416	2.8	10.799
336	0	0	4.858	0	0.3	26.491	10.461	0	0	0.001	2.781	1.175	0.679	3.342	1.689	0	2.95	0	0	0	1.748	19.045	0.537	3.26	10.167
337	0	0	4.833	0	0.3	29.049	7.692	0	0.004	0.012	2.777	1.424	1.049	3.749	1.112	0	12.8	0	0	0	2.046	15.771	0.253	4.42	11.656
338	0	0	4.077	0	0	24.195	8.211	0	0.003	0.087	1.883	1.079	0.78	5.409	1.419	0	6.77	0	0	0	2.295	17.565	0.155	2.781	13.038
339	0	0	4.895	0	0.15	23.761	7.667	0	0.003	0.01	2.115	1.295	0.936	4.586	0.608	0	2.59	0	0	0	2.019	18.097	0.548	3.781	14.701
340	0	0	4.928	0.17	0.3	24.243	7.321	0	0	0.031	1.64	0.937	0.591	4.631	1.217	0	1.27	0	0	0	1.245	16.897	0.356	4.775	13.476
341	0	0	4.844	0.17	0.15	26.953	8.743	0	0	0.125	1.976	1.688	1.244	4.791	0.8	0	5.69	0	0	0	2.554	21.878	0.498	3.85	13.526
342	0	0	6.063	0.34	0	21.995	8.944	0	0.002	0.053	1.77	1.18	1.447	4.922	0.542	0	8.62	0	0	0	2.623	17.574	0.369	3.95	11.947
343	0	0	4.013	0.34	0	29.593	10.663	0	0.002	0.026	1.587	1.479	0.719	5.207	1.285	0	6.74	0	0	0	2.252	20.465	0.499	3.655	11.339
344	0	0	5.033	0	0.15	25.034	9.294	0	0	0.092	1.816	1.019	0.821	4.49	0.615	0	6.92	0	0	0	2.316	19.895	0.272	4.093	16.289
345	0	0	2.987	0.17	0	25.337	6.56	0	0	0.104	1.405	1.168	0.904	4.881	2.142	0	8.5	0	0	0	1.457	17.762	0.602	3.104	11.199
346	0	0	3.806	0.85	0	24.794	7.294	0	0.002	0.016	2.59	0.945	1.349	3.987	0.729	0	7.1	0	0	0	1.285	12.312	0.377	3.244	14.028
347	0	0	4.602	0.17	0.6	26.024	7.825	0	0	0	2.456	0.826	0.963	3.909	1.291	0	1.4	0	0	0	2.131	19.83	0.299	3.663	11.226
348	0	0	4.848	0	0	22.728	8.629	0	0.003	0.114	2.18	1.152	0.51	4.559	0.507	0	6.87	0	0	0	2.95	15.579	0.507	3.19	13.76
349	0	0	5.461	0.17	0	24.964	7.729	0	0	0.054	2.121	0.643	0.764	4.112	1.551	0	7	0	0	0	1.619	16.084	0.263	5.521	13.211
350	0	0	3.907	0.51	0	27.305	8.507	0	0	0.086	2.772	1.418	0.965	6.717	1.297	0	12.52	0	0	0	1.827	19.244	0.377	2.854	12.298
351	0	0	3.878	0.17	0.3	24.671	9.143	0	0.003	0.071	2.573	1.039	1.012	3.82	0.759	0	4.22	0	0	0	2.229	18.889	0.373	3.892	16.199
352	0	0	5.066	0.17	0.3	27.406	9.638	0	0	0.067	1.408	1.023	0.994	4.266	0.137	0	9.05	0	0	0	2.341	18.134	0.372	3.703	14.879
353	0	0	3.622	0	0	22.383	9.515	0	0.002	0.039	1.578	1.101	0.754	5.786	1.036	0	2.68	0	0	0	1.952	22.813	0.365	2.813	12.878
354	0	0	3.442	0	0	26.301	8.177	0	0	0.055	1.948	1.533	0.832	4.506	1.117	0	8	0	0	0	2.689	17.35	0.486	3.603	13.981
355	0	0	2.962	0	0.15	28.594	9.592	0	0	0.055	2.609	1.831	1.16	3.45	0.719	0	3.22	0	0	0	1.728	22.257	0.301	3.462	13.91
356	0	0	5.948	0.17	0	24.615	9.092	0	0	0.256	1.885	1.372	0.801	4.255	1.357	0	4.6	0	0	0	1.952	20.255	0.337	3.93	11.862
357	0	0	4.593	0.51	0	22.354	7.36	0	0	0.19	2.477	1.392	1.083	4.522	0.576	0	3.5	0	0	0	2.982	16.67	0.539	4.404	14.401
358	0	0	3.149	0.34	0.15	24.902	8.994	0	0	0.006	1.737	1.148	0.837	3.142	1.051	0	2.12	0	0	0	1.79	20.177	0.325	2.771	11.001
359	0	0	4.03	0.34	0.3	26.751	8.49	0	0.001	0.023	2.293	1.653	1.108	4.289	1.586	0	4.4	0	0	0	1.699	18.442	0.292	2.371	12.111
360	0	0	5.31	0.34	0.15	24.56	8.401	0	0.002	0.047	1.24	0.889	0.656	3.754	0.565	0	4.9	0	0	0	2.857	23.584	0.259	3.69	14.221
361	0	0	4.596	0.68	0.6	25.423	8.494	0	0	0.005	2.027	0.546	0.91	5.129	1.224	0	2.74	0	0	0	1.642	18.252	0.674	3.58	10.689
362	0	0	6.008	0	0	28.499	9.011	0	0	0.06	2.155	1.497	0.778	4.531	0.629	0	5.76	0	0	0	0.906	21.169	0.359	3.485	14.873
363	0	0	3.187	0.17	0.15	28.12	8.634	0	0.002	0.042	2.351	1.257	0.674	4.285	0.637	0	5.49	0	0	0	1.981	19.266	0.492	4.172	14.272
364	0	0	3.688	0.34	0.3	26.271	9.039	0	0.003	0.116	2.983	1.039	1.263	3.72	1.499	0	4.7	0	0	0	1.334	21.848	0.432	3.621	11.659
365	0	0	5.001	0	0.3	21.979	8.969	0	0	0.06	1.575	1.477	1.19	5.429	1.063	0	7	0	0	0	2.047	21.143	0.374	2.825	12.763
366	0	0	2.692	0.68	0.15	24.076	8.191	0	0.002	0.019	2.471	1.706	0.663	5.335	0.313	0	6.5	0	0	0	3.23	16.434	0.362	3.511	11.912
367	0	0	3.563	0.17	0.15	23.067	9.055	0	0.003	0.003	2.77	1.364	1.094	4.415	2.238	0	6.17	0	0	0	2.149	19.887	0.426	3.22	8.773
368	0	0	3.521	0	0.15	25.606	8.858	0	0	0.027	2.541	1.423	0.96	5.627	0.469	0	4.15	0	0	0	2.431	18.467	0.305	4.177	12.577
369	0	0	4.205	0	0	25.194	10.628	0	0	0.053	2.59	1.83	1.352	4.774	0.359	0	3.2	0	0	0	1.338	20.891	0.435	3.17	14.015
370	0	0	4.115	0	0	26.686	8.761	0	0.002	0.021	3.637	1.021	0.908	6.084	1.17	0	8.85	0	0	0	1.88	16.346	0.471	3.27	11.826
371	0	0	4.684	0.34	0	22.949	8.447	0	0	0.082	2.336	1.568	0.802	4.202	0.915	0	5.7	0	0	0	1.392	15.587	0.32	3.06	13.826
372	0	0	5.553	0.68	0	26.472	10.194	0	0	0.009	3.356	1.029	0.582	5.501	1.27	0	7.34	0	0	0	1.606	20.603	0.432	2.73	12.213
373	0	0	5.134	0	0.3	24.587	8.473	0	0.002	0.048	1.666	0.5	0.904	4.712	0.985	0	7.45	0	0	0	1.91	20.323	0.509	4.321	13.304
374	0	0	5.544	0.51	0.15	26.303	9.466	0	0.001	0.115	2.074	1.954	0.807	5.092	1.74	0	6.7	0	0	0	1.799	21.015	0.332	3.252	12.907
375	0	0	4.499	0	0	24.25	8.11	0	0	0.031	1.958	1.665	1.061	6.018	1.034	0	5.7	0	0	0	2.419	14.814	0.294	3.382	13.766
376	0	0	5.505	0.34	0	24.059	9.709	0	0.002	0.025	1.839	1.049	0.998	6.057	1.874	0	4.46	0	0	0	1.879	22.602	0.507	2.653	10.232
377	0	0	6.514	0.51	0	31.265	8.175	0	0	0.088	1.759	1.072	0.961	4.809	1.117	0	9.25	0	0	0	1.851	14.995	0.522	2.241	12.417
378	0	0	4.757	0.17	0	26.804	7.288	0	0	0.048	2.323	1.416	1.403	6.79	0.779	0	4.5	0	0	0	1.421	14.045	0.251	3.193	13.341
379	0	0	3.794	0	0	28.014	8.394	0	0	0.022	2.232	0.831	0.653	4.272	1.709	0	2.84	0	0	0	2.276	19.254	0.38	2.992	12.425
380	0	0	5.932	0.34	0.15	27.269	7.421	0	0.002	0.011	2.596	0.542	0.444	6.272	2.349	0	8.5	0	0	0	1.511	16.366	0.457	3.39	11.908
381	0	0	4.879	0	0	25.305	9.297	0	0	0.047	1.949	1.106	1.238	5.864	0.368	0	6.84	0	0	0	3.156	17.649	0.397	3.274	14.759
382	0	0	2.994	0.17	0.45	26.164	7.354	0	0	0.075	2.195	0.437	0.952	6.567	0.786	0	11.57	0	0	0	2.19	15.956	0.297	3.01	14.329
383	0	0	5.364	0	0	21.406	8.665	0	0.002	0.063	2.049	1.381	1.162	4.737	0.348	0	5	0	0	0	2.137	16.078	0.178	4.651	13.071
384	0	0	2.728	0.51	0	24.284	10.762	0	0	0.028	2.596	2.21	0.536	4.216	2.115	0	3.12	0	0	0	1.879	21.4	0.482	3.574	10.872
385	0	0	6.438	0	0.45	28.07	9.021	0	0	0.015	2.89	1.103	0.903	4.371	1.314	0	6.95	0	0	0	1.128	16.648	0.376	4.422	10.857
386	0	0	3.027	0.17	0.15	24.115	7.537	0	0	0.06	2.799	1.991	0.851	5.151	0.996	0	4.95	0	0	0	1.644	21.384	0.65	3.591	13.513
387	0	0	3.54	0.68	0.3	27.519	8.106	0	0	0.152	2.393	1.137	0.896	4.589	1.408	0	7.89	0	0	0	1.214	13.259	0.449	4.113	13.614
388	0	0	3.446	0	0	23.738	8.303	0	0.002	0.093	2.753	0.389	0.768	6.012	1.028	0	6.65	0	0	0	0.791	18.305	0.347	3.742	13.306
389	0	0	2.744	0	0.3	26.507	8.159	0	0.001	0.124	2.69	0.918	1.133	3.601	0.73	0	4.65	0	0	0	2.167	20.699	0.239	3.912	14.885
390	0	0	4.861	0.34	0	30.969	8.226	0	0	0.088	1.555	0.92	0.921	4.8	0.117	0	6.02	0	0	0	2.248	22.973	0.161	3.09	17.091
391	0	0	4.366	0	0.3	21.997	8.636	0	0.002	0.014	2.402	0.822	0.694	3.487	1.544	0	7.78	0	0	0	1.985	19.857	0.477	4.042	10.673
392	0	0	2.94	0.17	0	24.138	7.803	0	0.002	0.114	2.794	1.621	0.837	5.416	0.004	0	0.8	0	0	0	1.709	18.635	0.501	2.9	15.547
393	0	0	3.978	0.34	0	26.161	8.379	0	0.003	0.119	2.662	0.907	0.695	4.733	0.502	0	6.4	0	0	0	2.218	18.475	0.258	3.54	15.893
394	0	0	4.454	0	0.3	21.478	8.331	0	0	0.027	2.198	1.144	1.212	5.16	1.219	0	4.32	0	0	0	1.762	17.773	0.431	3.54	13.114
395	0	0	4.153	0.17	0	24.669	9.048	0	0	0.134	1.007	1.372	1.143	4.841	0.23	0	8.22	0	0	0	2.941	20.838	0.364	3.143	16.015
396	0	0	4.823	0.34	0.15	24.167	8.18	0	0	0.031	2.526	0.665	1.233	5.45	0.475	0	8.9	0	0	0	1.967	17.793	0.219	2.751	13.25
397	0	0	3.84	0	0.15	27.619	9.622	0	0	0.064	2.629	1.166	0.942	4.41	1.191	0	5.16	0	0	0	1.467	17.825	0.302	3.38	13.304
398	0	0	5.393	0	0.3	26.507	8.362	0	0	0.022	2.644	1.223	0.54	4.924	1.097	0	4.04	0	0	0	1.658	19.72	0.238	3.952	10.731
399	0	0	4.137	0.17	0	27.92	8.936	0	0	0.022	1.599	1.563	1.515	6.468	0.003	0	6.9	0	0	0	2.507	19.495	0.315	2.204	14.969
400	0	0	5.29	0.34	0	27.132	9.342	0	0	0.022	2.13	1.065	1.102	5.515	1.553	0	6.17	0	0	0	1.687	19.876	0.53	2.401	12.61
401	0	0	5.237	0.17	0.15	28.29	7.055	0	0	0.008	2.135	0.814	0.684	6.283	0.93	0	7.2	0	0	0	1.379	13.517	0.368	2.345	13.04
402	0	0	5.141	0.34	0	25.151	9.101	0	0	0.018	1.248	1.05	0.947	5.432	1.938	0	5.99	0	0	0	2.351	19.495	0.362	2.815	11.576
403	0	0	2.231	0	0.45	25.231	8.751	0	0.002	0.012	1.599	1.442	0.801	4.148	0.961	0	10.95	0	0	0	1.58	14.483	0.325	5.212	12.196
404	0	0	4.112	0.34	0	24.745	8.333	0	0	0.002	1.602	1.438	0.585	5.318	1.204	0	4.66	0	0	0	2.957	19.267	0.295	3.87	12.565
405	0	0	3.636	0.34	0.3	24.718	9.711	0	0	0.021	1.153	1.644	0.943	4.602	0.733	0	3.57	0	0	0	2.424	19.949	0.367	3.73	11.022
406	0	0	5.075	0.51	0.15	23.91	7.791	0	0.001	0.036	1.643	0.615	1.105	4.466	0.447	0	5.57	0	0	0	1.597	18.655	0.302	3.81	13.119
407	0	0	4.71	0.17	0.3	25.294	8.811	0	0	0.004	1.212	1.178	0.877	3.637	1.168	0	6.74	0	0	0	1.443	18.687	0.581	3.867	10.64
408	0	0	5.424	0	0	24.921	8.476	0	0	0.04	1.833	0.944	0.382	4.781	1.22	0	1.19	0	0	0	1.299	19.556	0.254	3.632	11.877
409	0	0	4.363	0	0.15	28.13	8.242	0	0.002	0.128	1.371	1.106	0.875	4.873	1.024	0	6.32	0	0	0	2.371	21.203	0.375	5.425	14.291

Plant Type:	Greasewood					Grass					Forb					Tree					Shrub				
Plot:	1	2	3	4	5	1	2	3	4	5	1	2	3	4	5	1	2	3	4	5	1	2	3	4	5
sample #																									
410	0	0	4.039	0	0	27.84	7.545	0	0	0.022	2.21	1.144	0.822	4.926	1.396	0	4.75	0	0	0	1.856	17.416	0.662	2.95	10.554
411	0	0	4.636	0.85	0.3	24.177	8.666	0	0.002	0.011	2.567	1.098	0.956	4.9	1.297	0	2.44	0	0	0	1.796	19.119	0.751	3.654	10.654
412	0	0	3	0.17	0.3	23.615	8.335	0	0	0.036	2.473	1.019	0.806	5.679	0.817	0	11.87	0	0	0	1.767	19.783	0.342	2.571	14.784
413	0	0	3.304	0.68	0	26.651	9.285	0	0	0.043	2.276	1.051	1.22	3.383	1.437	0	3.46	0	0	0	1.22	20.306	0.279	3.311	10.588
414	0	0	4.212	0.17	0	25.172	7.987	0	0.003	0.189	1.825	1.682	0.693	3.262	0.293	0	4.1	0	0	0	1.943	15.904	0.413	3.882	16.543
415	0	0	4.805	0.34	0	24.877	9.148	0	0.002	0.129	2.358	1.513	0.752	4.732	1.513	0	3.19	0	0	0	1.477	18.777	0.451	2.77	11.928
416	0	0	3.792	0	0	26.526	7.411	0	0	0.031	2.856	1.274	0.965	4.426	1.404	0	6.02	0	0	0	1.767	17.327	0.295	2.861	12.108
417	0	0	6.403	0	0.45	29.135	8.43	0	0.004	0.003	2.378	1.042	1.109	4.648	0.76	0	7.39	0	0	0	1.491	16.684	0.536	4.141	12.632
418	0	0	6.306	0.17	0.3	27.2	7.181	0	0	0.086	2.278	1.02	1.085	4.73	0.52	0	5.25	0	0	0	1.044	17.314	0.204	4.45	14.611
419	0	0	4.412	0.51	0	26.494	9.198	0	0.001	0.008	2.263	0.99	1.483	4.431	1.67	0	7.22	0	0	0	1.869	18.935	0.349	2.854	11.436
420	0	0	4.643	0.17	0	26.405	9.03	0	0.001	0.19	2.154	1.439	1.471	5.466	0.328	0	4.85	0	0	0	1.79	18.431	0.147	3.474	16.527
421	0	0	2.652	0.51	0	28.255	7.395	0	0.001	0.05	1.969	1.523	0.704	5.4	1.588	0	12.05	0	0	0	2.953	16.818	0.599	4.611	12.001
422	0	0	4.547	0	0	25.469	8.496	0	0	0.057	2.06	1.265	0.782	4.24	1.7	0	6.7	0	0	0	2.048	17.397	0.341	2.82	11.429
423	0	0	4.899	0	0	28.399	7.961	0	0	0.018	1.82	1.148	0.858	3.954	1.448	0	10.7	0	0	0	1.524	17.013	0.254	2.931	11.828
424	0	0	6.426	0.17	0.15	22.982	8.271	0	0	0.01	1.949	1.596	0.632	3.698	0.44	0	4.02	0	0	0	1.297	21.315	0.275	3.661	13.514
425	0	0	5.369	0.85	0	24.943	9.536	0	0	0.044	1.849	1.703	0.72	5.27	0.045	0	12.4	0	0	0	1.471	17.428	0.193	2.812	14.869
426	0	0	4.294	0	0	26.301	9.478	0	0.001	0.243	2.02	1.581	1.356	4.599	0.277	0	5.9	0	0	0	2.301	19.602	0.64	3.705	18.067
427	0	0	4.952	0.51	0.15	23.631	7.014	0	0.001	0.068	2.102	0.842	0.954	3.163	0.682	0	5.55	0	0	0	1.631	15.625	0.407	4.12	12.65
428	0	0	3.845	0	0	24.638	8.304	0	0.002	0.009	1.872	0.701	0.821	4.725	0.821	0	5.15	0	0	0	1.795	20.688	0.378	3.521	12.171
429	0	0	4.603	0	0.15	22.595	8.289	0	0	0.076	2.579	1.76	1.168	3.871	1.223	0	1.84	0	0	0	1.606	17.088	0.306	2.79	12.72
430	0	0	4.339	0.17	0	28.767	8.738	0	0.001	0.054	1.429	1.796	1.118	5.152	0.627	0	7.3	0	0	0	1.77	15.399	0.42	4.291	13.802
431	0	0	3.544	0.51	0	25.959	8.656	0	0.001	0.016	1.096	1.324	1.185	4.001	0.774	0	4.32	0	0	0	2.495	17.462	0.546	4.34	12.675
432	0	0	3.405	0	0	25.046	8.253	0	0	0.104	2.664	2.013	0.982	4.891	0.63	0	5.5	0	0	0	2.168	13.725	0.7	2.371	15.26
433	0	0	3.46	0.68	0	27.844	8.715	0	0	0.045	2.596	0.896	0.987	5.003	0.979	0	2.83	0	0	0	1.594	22.985	0.311	3.432	14.833
434	0	0	4.819	0.34	0	26.354	7.617	0	0.004	0.017	1.691	0.507	0.536	3.98	1.484	0	5.89	0	0	0	3.111	17.955	0.373	2.442	12.203
435	0	0	4.984	0.34	0	31.797	9.488	0	0	0.049	2.083	0.732	1.359	5.494	1.575	0	8.89	0	0	0	1.472	18.345	0.239	3.423	10.123
436	0	0	4.223	0	0.75	27.837	10.008	0	0	0.002	2.41	1.358	1.074	5.382	1.579	0	8.4	0	0	0	1.036	18.983	0.373	6.06	9.748
437	0	0	4.006	0.51	0.3	27.387	7.551	0	0	0.002	1.389	1.568	1.025	6.194	0.368	0	7.9	0	0	0	1.633	17.116	0.302	2.72	14.196
438	0	0	4.621	0.17	0	25.506	8.765	0	0	0.032	1.399	0.952	0.784	3.739	1.03	0	5.64	0	0	0	2.046	19.381	0.298	3.29	12.499
439	0	0	5.7	0	0	26.441	8.466	0	0	0.016	2.059	1.225	0.952	5.338	1.538	0	3.12	0	0	0	1.382	23.979	0.23	3.391	10.989
440	0	0	6.124	0.34	0	24.78	7.008	0	0.001	0.04	2.429	0.91	0.881	4.533	1.742	0	7.35	0	0	0	2.358	14.908	0.371	4.24	13.455
441	0	0	5.815	0	0.15	26.012	9.205	0	0	0.134	2.285	1.438	0.843	6.752	0.359	0	7.34	0	0	0	2.036	16.156	0.215	2.742	14.158
442	0	0	7.235	0	0	24.167	8.487	0	0.003	0.014	2.72	1.447	0.594	3.469	1.336	0	4.2	0	0	0	1.866	20.897	0.198	4.452	11.507
443	0	0	3.614	0	0.3	25.737	9.678	0	0	0.164	2.642	1.404	1.192	4.465	0.618	0	4.84	0	0	0	1.248	21.324	0.457	4.081	13.421
444	0	0	6.121	0.51	0.3	27.909	8.642	0	0.001	0.03	2.698	1.365	1.277	4.302	2.071	0	6.52	0	0	0	1.876	18.735	0.433	4.186	10.361
445	0	0	5.282	0.34	0.3	25.141	8.996	0	0.004	0.013	2.6	1.379	0.995	4.657	1.34	0	3.79	0	0	0	1.741	18.611	0.382	3.312	12.591
446	0	0	4.124	0	0	26.233	7.914	0	0.001	0.103	2.518	1.181	0.967	3.661	0.302	0	9.55	0	0	0	2.351	20.024	0.347	3.96	14.108
447	0	0	4.998	0.34	0	29.063	9.196	0	0	0.029	2.166	1.541	0.883	4.255	1.12	0	7.7	0	0	0	1.436	17.84	0.298	3.89	12.817
448	0	0	3.744	0	0	26.772	8.216	0	0.002	0.017	2.448	1.217	1.114	4.304	0.994	0	6.35	0	0	0	1.727	16.436	0.458	3.862	13.485
449	0	0	3.33	0.17	0.6	24.186	7.614	0	0.003	0.014	2.435	0.924	1.358	4.739	1.825	0	6.7	0	0	0	1.944	16.251	0.421	3.151	11.136
450	0	0	5.46	0.17	0.3	23.79	7.7	0	0.002	0.081	2.267	0.867	0.577	5.702	0.727	0	2.86	0	0	0	2.212	23.088	0.339	3.113	12.619
451	0	0	4.404	0.17	0	26.11	7.827	0	0.003	0.079	2.158	0.872	1.248	4.649	1.632	0	5.6	0	0	0	1.32	14.983	0.194	3.34	12.078
452	0	0	3.051	0.17	0	27.653	8.127	0	0	0.029	3.025	1.134	1.408	3.763	0.153	0	13.6	0	0	0	1.061	19.964	0.342	3.791	14.365
453	0	0	6.936	0	0	25.364	8.769	0	0	0.113	2.487	1.366	0.659	5.02	0.628	0	2.52	0	0	0	2.535	17.405	0.361	2.554	13.826
454	0	0	5.625	0	0	27.042	9.324	0	0.001	0.035	1.436	1.502	1.096	5.156	1.584	0	7.07	0	0	0	1.154	16.731	0.51	3.312	11.297
455	0	0	5.756	0	0	26.713	8.272	0	0	0.15	1.893	0.369	0.781	3.747	0.632	0	12.82	0	0	0	1.844	15.973	0.319	4.185	15.625
456	0	0	5.233	0	0.6	29.162	8.446	0	0.002	0.002	1.832	1.279	1.641	2.771	1.556	0	2.82	0	0	0	1.376	19.322	0.364	4.78	11.134
457	0	0	2.66	0.17	0	25.368	9.086	0	0	0.064	2.815	1.57	0.902	3.942	0.891	0	3.06	0	0	0	1.667	21.824	0.405	3.94	12.985
458	0	0	4.447	0.85	0.3	29.234	9.262	0	0	0.023	2.537	0.839	1.172	4.374	1.262	0	2.64	0	0	0	1.618	23.457	0.263	4.34	11.615
459	0	0	4.486	0	0.6	27.427	7.641	0	0.001	0.005	1.911	1.189	0.766	5.278	1.111	0	9	0	0	0	2.064	14.236	0.306	2.942	11.012
460	0	0	5.162	0	0.45	23.39	8.093	0	0.005	0.002	2.513	0.754	0.84	3.454	0.694	0	5.45	0	0	0	2.815	20.308	0.375	3.271	14.167
461	0	0	5.151	0.51	0.3	28.564	8.809	0	0.002	0.166	2.478	1.5	0.984	4.09	0.003	0	10.7	0	0	0	1.098	23.154	0.456	2.733	16.561
462	0	0	3.567	0	0	26.547	8.55	0	0.003	0.18	1.185	1.329	1.227	4.134	0.725	0	7.75	0	0	0	2.374	13.927	0.353	3.681	16.005
463	0	0	4.821	0.34	0.45	23.806	8.199	0	0.001	0.021	1.461	1.501	0.68	3.9	1.711	0	6.6	0	0	0	2.091	17.429	0.15	3.673	11.573
464	0	0	3.848	0	0.15	25.216	9.526	0	0.003	0.083	2.037	1.073	0.949	5.382	0.361	0	9.02	0	0	0	0.968	18.934	0.517	4.502	12.665
465	0	0	4.184	0	0.3	25.858	7.862	0	0.001	0.022	2.251	1.035	1.18	4.662	0.877	0	9	0	0	0	2.515	14.689	0.495	4.455	12.783
466	0	0	6.801	0	0	24.242	8.291	0	0.001	0.147	2.596	1.693	0.363	6.055	0.535	0	3.94	0	0	0	2.071	21.315	0.522	2.864	17.277
467	0	0	5.788	0	0	28.648	9.088	0	0	0.033	2.158	0.951	0.768	5.924	1.127	0	6.25	0	0	0	1.267	16.934	0.327	3.011	13.569
468	0	0	5.082	0.34	0.6	23.007	9.194	0	0	0.004	2.357	1.196	1.026	4.349	2.22	0	5.9	0	0	0	1.643	16.007	0.463	4.083	10.604
469	0	0	4.507	0.34	0.15	25.347	9.287	0	0	0.113	2.937	1.411	0.782	6.776	0.768	0	5.47	0	0	0	2.216	20.677	0.395	2.394	16.406
470	0	0	4.874	0.68	0.45	23.952	7.835	0	0	0.125	1.526	1.139	0.878	5.202	0.651	0	7.7	0	0	0	1.791	17.529	0.462	2.826	15.427
471	0	0	3.871	0.17	0.3	24.325	6.449	0	0.001	0.041	2.728	0.948	0.731	4.087	0.859	0	7	0	0	0	1.548	16.639	0.346	4.141	12.522
472	0	0	4.816	0.17	0	22.232	9.399	0	0.002	0.017	2.015	0.911	0.677	3.674	1.467	0	11.05	0	0	0	2.195	14.073	0.536	5.54	11.648
473	0	0	4.888	0	0	28.482	8.948	0	0.001	0.024	1.32	1.274	0.841	3.217	0.906	0	4.22	0	0	0	2.179	20.434	0.22	3.96	13.086
474	0	0	3.514	0.34	0	26.919	8.635	0	0	0.107	2.123	0.668	1.088	4.092	0.47	0	9.45	0	0	0	1.983	15.298	0.147	4.052	13.945
475	0	0	5.992	0	0	28.922	9.488	0	0.004	0.142	1.039	0.912	0.958	5.631	1.477	0	5.55	0	0	0	2.033	19.007	0.121	4.001	12.661
476	0	0	3.074	0.17	1.2	29.723	8.662	0	0	0	2.409	1.239	1.306	4.52	1.208	0	2.76	0	0	0	2.112	19.439	0.22	3.951	10.802
477	0	0	3.274	0.17	0	24.787	8.016	0	0	0.077	2.18	0.859	1.274	4.844	1.132	0	5.25	0	0	0	1.838	19.758	0.42	3.966	14.689
478	0	0	3.712	0.17	0	28.212	8.6	0	0	0.016	1.619	1.374	1.082	6.089	1.196	0	3.92	0	0	0	4.03	19.268	0.356	3.515	11.655
479	0	0	4.495	0	0	27.319	10.407	0	0	0.03	1.238	1.466	0.975	3.226	0.692	0	4.47	0	0	0	2.092	20.216	0.546	4.352	13.913
480	0	0	5.243	1.02	0.3	27.278	8.482	0	0	0.004	2.68	0.661	1.088	5.144	1.876	0	1.85	0	0	0	1.503	19.036	0.174	3.141	10.133
481	0	0	3.923	0.17	0	29.374	9.689	0	0.001	0.109	2.383	2.328	0.962	4.42	0.376	0	4.1	0	0	0	1.294	16.886	0.194	4.663	15.023
482	0	0	3.432	0	0.3	25.093	8.873	0	0.002	0.099	1.97	0.759	1.011	2.791	1.183	0	6.37	0	0	0	1.846	20.183	0.346	4.47	13.879
483	0	0	4.004	0	0.15	23.976	7.676	0	0.001	0.003	2.756	0.814	0.965	3.415	1.249	0	8.42	0	0	0	1.863	16.354	0.529	3.591	11.727
484	0	0	3.655	0	0	21.85	7.643	0	0	0.129	2.264	1.472	0.929	3.839	0.927	0	12.4	0	0	0	2.224	16.288	0.423	3.762	15.587
485	0	0	4.158	0	0.15	23.617	7.659	0	0.001	0.026	2.138	1.358	1.162	5.028	0.729	0	7.8	0	0	0	2.327	14.917	0.355	4.053	13.61
486	0	0	5.136	0.34	0	29.687	9.452	0	0	0.068	1.988	1.239	0.566	4.944	0.595	0	7.47	0	0	0	2.011	20.785	0.513	3.852	15.644
487	0	0	5.341	0.51	0	28.639	9.562	0	0	0.056	1.987	0.95	0.516	4.388	0.409	0	8.6	0	0	0	2.467	16.065	0.308	2.623	13.63
488	0	0	3.824	0.34	0.3	26.927	8.703	0	0	0.021	1.678	1.622	1.022	4.01	0.758	0	5.86	0	0	0	1.361	20.055	0.511	3.991	13.74
489	0	0	2.92	0	0.3	25.929	8.36	0	0	0.038	1.732	0.407	0.648	3.982	0.938	0	4.62	0	0	0	2.095	19.263	0.547	4.22	12.872
490	0	0	4.191	0	0	23.42	9.635	0	0.002	0.106	1.58	1.265	1.438	4.35	1.061	0	5.06	0	0	0	1.907	20.498	0.347	3.23	14.981
491	0	0	5.204	0.85	0	30.129	8.887	0	0	0.105	1.221	1.406	1.12	5.713	1.345	0	5.74	0	0	0	2.099	19.646	0.479	2.782	11.082
492	0	0	3.144	1.19	0.75	25.284	8.323	0	0.002	0.013	2.423	1.089	0.776	3.084	1.016	0	4.5	0	0	0	2.994	13.617	0.441	4.95	11.665
493	0	0	5.557	0	0.15	27.065	9.48	0	0	0.002	1.827	1.357	1.086	6.166	1.463	0	7.92	0	0	0	1.567	19.803	0.224	2.684	11.232
494	0	0	5.271	0.51	0.45	26.192	10.414	0	0	0.007	1.383	1.08	0.693	5.654	1.202	0	2.97	0	0	0	1.423	22.754	0.292	3.916	12.035
495	0	0	5.405	0	0	26.003	9.367	0	0	0.121	2.61	0.929	0.841	3.336	0.644	0	3.36	0	0	0	1.559	16.932	0.316	3.9	13.999
496	0	0	4.695	0.34	0.6	26.418	8.144	0	0.002	0.014	3.158	0.696	0.992	5.312	0.855	0	12.45	0	0	0	1.491	15.554	0.361	4.344	11.561
497	0	0	5.321	0	0	25.658	8.527	0	0.003	0.089	2.469	0.689	0.892	4.897	1.251	0	7.74	0	0	0	1.644	22.308	0.329	2.44	13.581
498	0	0	3.452	0	0.15	27.816	7.491	0	0	0.025	1.856	1.079	0.577	5.273	0.969	0	10.4	0	0	0	2.165	20.427	0.292	3.796	12.774
499	0	0	4.163	0	0	28.168	9.458	0	0.003	0.004	2.125	0.936	0.954	4.534	0.77	0	7.56	0	0	0	2.072	15.579	0.4	4.033	12.11
500	0	0	3.444	0.51	0.15	24.619	7.732	0	0	0.171	2.405	1.164	0.954	6.083	1.095	0	9.2	0	0	0	1.877	13.187	0.6	3.536	17.186
501	0	0	5.384	0	0	24.635	9.527	0	0	0.032	2.418	1.259	0.506	6.424	1.385	0	9.3	0	0	0	1.672	13.47	0.648	2.293	11.517
502	0	0	4.867	0.17	0	24.73	8.631	0	0	0.169	2.868	1.663	0.901	4.836	0.006	0	3.59	0	0	0	1.832	16.598	0.45	3.403	15.851
503	0	0	4.646	0	0.15	25.93	8.154	0	0	0.066	2.845	1.464	1.338	3.448	0.221	0	8.1	0	0	0	1.981	15.799	0.225	3.693	15.357
504	0	0	5.305	0.34	0	23.289	7.713	0	0	0.059	2.102	0.814	0.797	5.174	0.88	0	8.29	0	0	0	1.956	18.697	0.293	3.684	14.957
505	0	0	3.358	0.51	0	25.217	7.19	0	0	0.091	2.458	1.439	0.863	5.502	0.576	0	7.55	0	0	0	2.879	14.135	0.409	2.544	14.381
506	0	0	4.615	0	0	27.776	8.626	0	0	0.101	2.248	1.373	0.981	3.949	1.322	0	2.04	0	0	0	2.334	21.652	0.665	3.991	13.846
507	0	0	5.661	0	0.45	27.583	8.208	0	0.001	0.037	2.285	1.528	0.989	5.367	1.189	0	4.9	0	0	0	1.358	22.037	0.251	2.7	13.061
508	0	0	5.225	0.85	0.3	24.96	7.619	0	0.003	0.003	1.462	0.804	1.037	4	0.664	0	4.95	0	0	0	2.266	18.596	0.376	2.942	15.566
509	0	0	4.001	0	0	25.915	8.089	0	0	0.023	2.374	1.75	0.739	6.055	1.176	0	7.5	0	0	0	2.108	20.035	0.427	2.542	12.139
510	0	0	6.409	0	0.45	26.911	9.344	0	0.006	0.035	3.059	1.474	0.98	4.164	0.829	0	6.72	0	0	0	1.584	17.301	0.199	3.381	9.801
511	0	0	4.377	0.17	0	27.092	9.243	0	0.003	0.009	2.207	1.089	1.038	5.178	0.685	0	8.49	0	0	0	2.46	20.176	0.299	5.73	14.204
512	0	0	4.407	0.34	0.15	26.636	7.518	0	0.001	0.15	2.192	0.479	0.812	5.463	0.432	0	8.1	0	0	0	1.285	20.031	0.324	3.7	13.891

Plant Type:	Greasewood					Grass					Forb					Tree					Shrub				
Plot:	1	2	3	4	5	1	2	3	4	5	1	2	3	4	5	1	2	3	4	5	1	2	3	4	5
sample #																									
513	0	0	5.815	0	0.3	26.296	7.656	0	0.003	0.117	2.256	0.856	0.871	5.256	0.983	0	12.7	0	0	0	0.832	16.632	0.298	3.735	13.033
514	0	0	3.906	0.17	0	26.473	9.605	0	0	0.08	2.192	1.551	0.874	4.357	0.583	0	1.58	0	0	0	2.195	22.156	0.535	2.894	13.578
515	0	0	5.971	0.17	0.15	23.7	7.382	0	0	0.005	2.345	0.881	0.805	5.523	1.027	0	3.8	0	0	0	2.4	17.507	0.401	2.26	10.674
516	0	0	4.517	0.51	0.15	27.844	8.873	0	0	0.026	2.123	1.28	0.824	5.371	1.434	0	5.3	0	0	0	1.305	18.611	0.254	3.02	12.068
517	0	0	6.367	0	0	28.777	8.632	0	0.004	0.149	2.806	1.165	1.144	5.9	1.567	0	3.92	0	0	0	1.808	19.755	0.325	4.491	13.196
518	0	0	4.963	0	0.3	27.704	6.984	0	0.002	0.002	2.641	1.218	1.251	4.93	1.487	0	5.65	0	0	0	2.41	16.873	0.245	4.492	12.538
519	0	0	4.907	0	0.3	25.924	8.738	0	0.002	0.106	1.851	1.098	0.93	4.969	0.564	0	5	0	0	0	2.681	17.978	0.386	5.28	14.501
520	0	0	5.636	0	0.15	24.91	8.669	0	0.001	0.02	1.458	1.051	1.186	4.594	0.902	0	4.5	0	0	0	1.974	15.111	0.214	3.843	11.687
521	0	0	3.519	0	0.15	25.231	10.495	0	0.001	0.016	1.773	1.919	0.696	5.44	0.403	0	7.02	0	0	0	1.47	17.676	0.402	4.513	14.157
522	0	0	2.954	0.34	0	23.218	7.72	0	0.002	0.018	2.223	1.37	0.706	4.863	0.285	0	5.75	0	0	0	1.33	17.226	0.393	3.844	13.839
523	0	0	3.65	0.34	0.3	28.28	8.492	0	0	0.052	2.076	0.592	0.855	4.574	1.33	0	8.05	0	0	0	1.865	18.265	0.453	3.891	12.081
524	0	0	4.415	0.34	0.3	21.643	8.627	0	0	0.11	1.965	1.189	0.718	4.878	0.735	0	8.25	0	0	0	2.608	17.149	0.505	4.404	13.548
525	0	0	4.013	0	0.15	27.638	8.59	0	0.001	0.106	2.057	0.348	0.677	5.637	0.405	0	7.45	0	0	0	2.009	21.443	0.386	3.581	15.411
526	0	0	5.935	0	0	24.853	9.27	0	0	0.06	2.425	1.532	0.532	3.099	0.716	0	2.74	0	0	0	2.791	19.597	0.292	4.531	13.395
527	0	0	5.526	0	0	26.886	10.146	0	0.001	0.105	2.333	1.736	1.268	3.349	1.305	0	4.84	0	0	0	1.248	25.799	0.382	4.08	14.657
528	0	0	4	0.34	0	26.922	9.622	0	0.001	0.186	2.114	1.081	0.936	4.785	0.077	0	7.3	0	0	0	1.097	14.894	0.307	4.791	14.725
529	0	0	4.39	0	0.6	29.53	7.938	0	0.001	0.082	2.396	1.202	1.156	3.929	0.391	0	8.1	0	0	0	0.78	17.935	0.401	4.35	12.156
530	0	0	3.063	0.17	0	24.743	7.819	0	0	0.059	2.611	1.838	1.312	3.622	1.003	0	7.4	0	0	0	1.849	19.129	0.307	3.77	13.971
531	0	0	4.368	0.34	0	27.982	8.523	0	0	0.112	2.586	1.033	0.807	4.553	0.769	0	5.24	0	0	0	2.375	15.07	0.352	3.742	12.519
532	0	0	6.196	0.34	0	25.147	8.794	0	0.002	0.039	2.44	0.51	0.803	3.666	0.784	0	7.21	0	0	0	1.708	18.198	0.561	2.661	12.211
533	0	0	3.057	0	0.3	27.336	8.355	0	0	0.132	2.499	1.217	0.815	3.136	1.4	0	8.75	0	0	0	1.533	15.07	0.384	4.013	12.733
534	0	0	3.845	0	0.15	22.386	9.089	0	0.001	0.031	2.01	0.826	0.912	6.25	0.489	0	5.87	0	0	0	2.703	21.014	0.201	4.443	13.997
535	0	0	4.052	0.51	0	26.478	8.245	0	0.001	0.178	2.278	1.244	0.621	4.506	1.237	0	3.5	0	0	0	1.677	16.587	0.259	3.584	14.4
536	0	0	5.686	0	0	28.827	8.448	0	0	0.061	2.449	1.173	0.634	4.04	0.408	0	9.46	0	0	0	1.482	14.444	0.326	3.722	15.01
537	0	0	4.83	0.68	0	24.706	8.815	0	0	0.054	2.41	0.791	0.687	4.938	0.38	0	4.12	0	0	0	2.332	22.463	0.209	3.183	13.727
538	0	0	3.56	0.17	0.15	26.977	8.804	0	0	0.024	2.612	1.33	0.807	4.193	1.053	0	1.95	0	0	0	1.869	20.387	0.194	4.183	11.625
539	0	0	4.336	0	0	27.097	7.577	0	0	0.065	2.072	1.264	0.655	5.694	1.333	0	8.3	0	0	0	1.834	18.935	0.487	2.591	13.911
540	0	0	4.031	0.17	0	23.785	8.545	0	0.001	0.04	2.105	0.865	1.378	5.802	1.05	0	2.4	0	0	0	2.642	18.054	0.344	3.406	12.036
541	0	0	4.035	0	0	28.282	9.582	0	0	0.052	2.391	1.783	0.785	5.039	0.549	0	4.9	0	0	0	2.479	18.916	0.345	4.053	14.096
542	0	0	3.586	0.17	0	24.397	10.296	0	0.002	0.012	2.078	1.796	0.482	6.928	0.707	0	4.64	0	0	0	1.512	19.764	0.272	2.385	13.446
543	0	0	5.169	0	0	24.004	7.447	0	0	0.008	3.157	1.041	0.774	5.44	1.757	0	5.7	0	0	0	1.518	17.528	0.269	3.048	9.944
544	0	0	3.786	0	0.3	27.645	9.185	0	0.004	0.064	2.442	1.26	0.838	6.494	1.507	0	10.81	0	0	0	2.126	19.435	0.633	4.045	13.886
545	0	0	4.227	0	0.15	27.02	9.517	0	0.001	0.006	2.305	1.46	0.877	3.7	2.277	0	8.56	0	0	0	1.816	18.477	0.411	3.725	9.887
546	0	0	3.72	0	0	26.521	8.587	0	0.002	0.073	2.366	0.938	1.06	5.981	0.845	0	3.97	0	0	0	2.009	18.156	0.562	2.87	14.145
547	0	0	5.807	0	0.15	25.065	8.36	0	0.003	0.078	1.065	1.449	0.783	7.082	0.354	0	6.55	0	0	0	2.98	19.136	0.506	2.884	14.922
548	0	0	3.797	0.34	0	24.259	7.891	0	0	0.031	2.83	1.156	0.936	4.821	0.693	0	9.77	0	0	0	2.236	17.533	0.355	3.58	14.989
549	0	0	5.147	0.17	0	26.671	9.2	0	0	0.059	2.08	1.386	1.213	4.572	1.429	0	2.19	0	0	0	2.329	17.788	0.278	4.86	12.881
550	0	0	5.413	0	0.45	27.871	7.416	0	0.002	0.032	2.722	1.099	0.894	5.243	1.636	0	10.85	0	0	0	1.577	19.666	0.26	3.232	10.912
551	0	0	4.28	0.51	0.45	29.341	8.133	0	0	0.065	3.19	0.743	0.861	3.647	1.236	0	6	0	0	0	1.824	15.133	0.175	4.362	12.957
552	0	0	5.828	0.17	0	23.279	7.878	0	0	0.161	2.238	0.956	0.818	3.989	2.049	0	13.15	0	0	0	2.391	13.132	0.448	3.402	13.356
553	0	0	4.334	0.17	0	24.141	8.212	0	0.002	0.035	1.862	1.413	1.085	4.732	0.984	0	7.6	0	0	0	1.849	17.264	0.317	3.302	12.846
554	0	0	5.059	0	0.15	25.781	9.954	0	0.001	0.064	1.274	1.48	0.475	4.213	0.939	0	4.11	0	0	0	2.164	16.962	0.41	2.551	12.751
555	0	0	3.69	0	0	31.61	8.859	0	0	0.053	1.341	1.316	0.751	4.476	0.36	0	6.62	0	0	0	1.856	17.206	0.351	3.502	14.679
556	0	0	5.796	0	0.15	26.008	7.244	0	0.002	0.055	2.123	1.494	0.557	4.604	0.591	0	7.15	0	0	0	1.919	14.853	0.343	2.593	12.07
557	0	0	4.3	0.17	0	24.185	8.979	0	0.004	0.05	1.683	1.13	0.952	6.296	1.058	0	5.39	0	0	0	1.922	18.01	0.447	3.73	12.266
558	0	0	5.62	0	0	24.209	7.491	0	0.001	0.05	2.415	1.558	0.537	5.891	0.532	0	3.2	0	0	0	2.1	14.484	0.145	4.196	12.556
559	0	0	2.995	0	0.15	24.554	7.33	0	0	0.012	1.808	0.735	1.053	4.48	0.4	0	7.12	0	0	0	2.987	17.403	0.546	5.001	14.14
560	0	0	4.344	0	0.3	26.727	7.961	0	0	0.024	1.597	0.649	1.274	4.695	1.056	0	11.95	0	0	0	2.029	17.164	0.239	2.452	11.892
561	0	0	4.989	0	0.15	28.536	7.382	0	0.003	0.091	1.998	1.289	0.688	5.289	1.041	0	4.9	0	0	0	2.289	18.41	0.409	4.14	14.233
562	0	0	4.105	0.17	0.45	26.829	9.041	0	0	0.014	2.784	1.493	0.571	4.126	0.997	0	7.7	0	0	0	2.18	15.725	0.461	3.374	11.529
563	0	0	2.989	1.02	0.15	26.06	8.283	0	0.002	0.11	2.722	1.101	0.669	4.747	1	0	6.12	0	0	0	1.796	21.02	0.457	3.23	11.701
564	0	0	3.868	0	0	24.727	8.2	0	0	0.117	2.724	1.65	0.826	4.175	0.59	0	5.5	0	0	0	1.987	20.763	0.251	4.023	13.525
565	0	0	6.321	0	0.15	29.301	7.909	0	0	0.016	2.218	1.261	1.107	5.098	0.673	0	11.25	0	0	0	1.277	16.483	0.435	3.372	12.314
566	0	0	4.173	0	0.15	26.683	9.147	0	0	0.051	2.431	1.384	1.108	4.494	1.353	0	2	0	0	0	2.609	21.037	0.377	3.127	13.62
567	0	0	3.702	0	0	27.161	9.56	0	0.003	0.079	3.758	1.383	0.779	5.589	0.529	0	2.3	0	0	0	1.341	20.085	0.432	4.39	13.145
568	0	0	3.747	0	0.15	21.764	8.245	0	0	0.186	3.181	1.016	1.628	4.177	0.107	0	4.84	0	0	0	1.159	19.605	0.206	4.034	14.758
569	0	0	3.045	0.17	0	23.528	6.932	0	0	0.049	2.146	1.047	0.551	4.8	1.049	0	5.7	0	0	0	1.562	17.622	0.329	3.1	12.855
570	0	0	3.373	0	0.9	27.627	8.593	0	0.001	0.036	1.711	1.414	0.744	4.005	0.941	0	9.3	0	0	0	2.141	20.26	0.577	4.043	11.321
571	0	0	5.635	0.34	0	31.425	7.521	0	0.001	0.078	1.022	1.286	1.082	5.243	1.054	0	5.16	0	0	0	2.194	20.984	0.271	4.59	10.928
572	0	0	5.847	0.51	0	27.001	9.885	0	0.001	0.096	1.797	1.561	0.602	3.821	0.475	0	10.37	0	0	0	2.271	17.278	0.343	3.651	14.955
573	0	0	4.689	0	0.45	27.128	9.619	0	0.005	0.148	2.745	1.657	0.889	4.626	0.113	0	8.6	0	0	0	1.576	17.23	0.228	3.79	16.939
574	0	0	6.209	0	0	25.499	9.773	0	0	0.037	2.442	2.01	0.884	3.342	0.226	0	5.32	0	0	0	2.656	18.182	0.251	2.712	16.215
575	0	0	4.743	0	0.15	26.451	8.421	0	0	0.067	1.778	0.688	0.647	5.745	0.025	0	5	0	0	0	2.117	14.951	0.327	3.133	14.054
576	0	0	3.772	0	0.15	25.628	8.861	0	0.002	0.035	1.9	1.352	1.159	3.432	1.47	0	1.9	0	0	0	2.677	22.139	0.536	4.602	13.181
577	0	0	4.105	0	0	25.079	7.968	0	0	0.016	1.58	1.238	1.235	5.266	1.574	0	6.82	0	0	0	2.624	16.658	0.266	3.261	10.999
578	0	0	4.833	0	0	26.934	8.006	0	0.001	0.078	2.105	0.823	0.843	4.376	0.295	0	4.25	0	0	0	2.747	20.501	0.179	2.121	14.979
579	0	0	4.543	0.17	0.45	26.617	9.533	0	0	0.018	2.169	1.634	1.091	3.816	0.773	0	7.46	0	0	0	1.274	22.328	0.449	3.68	13.316
580	0	0	5.698	0.34	0	24.086	9.015	0	0.001	0.022	2.418	1.485	1.217	4.48	0.656	0	3.92	0	0	0	1.584	17.625	0.307	3.202	13.819
581	0	0	4.619	0.17	0	30.403	8.6	0	0	0.014	2.468	0.907	0.797	4.405	1.554	0	4.1	0	0	0	1.532	18.681	0.45	4.823	10.441
582	0	0	4.396	0	0.15	29.043	7.611	0	0	0.119	2.549	0.947	0.639	4.709	1.064	0	6.52	0	0	0	2.517	14.836	0.637	2.851	13.89
583	0	0	4.915	0	0	24.757	8.408	0	0	0.096	1.73	1.881	1.161	3.675	1.521	0	4.4	0	0	0	2.221	19.436	0.222	4.461	12.277
584	0	0	4.863	0.17	0.15	28.645	8.492	0	0.004	0.02	2.625	1.432	1.025	5.635	1.828	0	7.5	0	0	0	1.865	19.671	0.548	4.691	13.173
585	0	0	5.147	0	0.15	25.064	6.989	0	0.002	0.071	3.121	0.961	0.998	4.28	0.485	0	2.16	0	0	0	2.567	16.961	0.414	4	15.42
586	0	0	4.538	0.17	0	26.987	8.948	0	0	0.037	1.791	0.844	1.031	5.588	0.263	0	11.68	0	0	0	2.1	19.659	0.366	2.673	16.179
587	0	0	4.965	0.17	0.15	26.323	8	0	0	0.009	2.34	1.287	0.662	3.749	0.949	0	5.76	0	0	0	2.959	16.961	0.404	2.771	11.854
588	0	0	3.321	0	0	22.95	8.137	0	0.001	0.061	2.574	1.297	1.122	4.444	1.087	0	7.02	0	0	0	1.235	15.163	0.356	3.55	13.035
589	0	0	4.106	0	0.15	25.545	9.423	0	0	0.064	2.006	1.82	0.698	5.031	1.247	0	0.96	0	0	0	1.653	18.238	0.421	3.37	12.374
590	0	0	5.086	0	0	29.02	8.113	0	0	0.137	1.175	0.639	1.078	5.218	0.589	0	6.5	0	0	0	1.966	15.37	0.545	3.255	16.385
591	0	0	3.199	0.51	0	22.96	7.314	0	0	0.089	2.096	1.331	1.142	6.212	1.421	0	6.95	0	0	0	2.524	17.534	0.34	2.564	14
592	0	0	4.694	0	0	24.068	12.794	0	0.005	0.025	1.915	0.791	0.83	4.826	1.305	0	1.52	0	0	0	1.82	16.41	0.305	4.122	12.372
593	0	0	3.292	0.17	0.15	26.701	8.836	0	0	0.151	2.285	0.848	0.742	4.815	0.457	0	6	0	0	0	1.876	20.094	0.176	2.775	15.745
594	0	0	4.369	0.17	0.15	27.812	8.02	0	0	0.018	1.991	0.926	1.075	6.814	0.742	0	9.8	0	0	0	1.858	14.295	0.53	3.745	12.137
595	0	0	5.366	0	0	27.637	8.947	0	0.003	0.024	1.537	0.843	0.743	5.409	1.196	0	5.52	0	0	0	1.504	18.523	0.317	3.644	13.423
596	0	0	5.074	0.17	0.3	25.138	6.55	0	0.004	0.015	2.017	0.767	0.921	4.691	0.643	0	4.45	0	0	0	2.136	17.957	0.39	3.121	13.556
597	0	0	1.546	0	0	27.025	9.091	0	0.001	0.174	1.984	0.842	0.923	4.732	0.86	0	9.8	0	0	0	2.109	20.532	0.39	2.612	13.956
598	0	0	4.516	0	0.3	26.107	8.29	0	0	0.038	2.245	0.946	0.846	7.321	1.002	0	3.74	0	0	0	2.48	20.725	0.257	1.98	12.009
599	0	0	5.273	0	0.15	24.399	8.42	0	0.003	0.03	1.364	0.786	0.609	5.048	0.516	0	4.97	0	0	0	1.871	17.715	0.467	2.953	13.225
600	0	0	3.918	0	0.3	24.944	8.088	0	0.001	0.027	2.797	1.727	1.192	3.348	1.232	0	2.3	0	0	0	1.375	19.537	0.464	3.865	11.839
601	0	0	4.608	0.34	0.15	25.589	8.863	0	0.002	0.018	3.338	1.246	1.019	6.095	0.617	0	7.83	0	0	0	2.045	19.684	0.324	3.182	12.64
602	0	0	2.745	0	0	24.623	8.732	0	0	0.071	2.794	1.614	0.71	5.042	0.019	0	4.52	0	0	0	1.185	21.806	0.605	3.703	15.543
603	0	0	3.044	0.34	0	25.91	8.436	0	0	0.096	1.843	1.155	0.937	4.725	2.002	0	9.44	0	0	0	2.023	19.746	0.578	2.832	12.782
604	0	0	3.933	0.51	0	26.28	8.529	0	0.001	0.021	2.453	1.75	1.345	3.854	1.896	0	3.2	0	0	0	1.186	19.769	0.493	2.85	8.917
605	0	0	5.642	0.17	0	30.165	9.335	0	0.001	0.222	2.415	1.732	1.284	5.604	0.356	0	5.12	0	0	0	1.919	19.947	0.319	5.28	15.138
606	0	0	4.399	0.17	0.45	26.716	7.361	0	0.003	0.035	1.987	0.614	1.044	5.749	0.844	0	6.5	0	0	0	2.128	16.274	0.396	3.095	13.356
607	0	0	3.568	0	0.15	22.663	8.716	0	0	0.003	1.86	0.933	1.79	5.543	1.314	0	5.2	0	0	0	1.704	17.726	0.237	3.735	14.401
608	0	0	3.483	0.17	0	29.313	8.215	0	0.001	0.019	1.523	0.796	1.323	3.701	1.506	0	6.45	0	0	0	1.977	14.367	0.308	3.84	10.749
609	0	0	4.239	0	0.15	25.516	9.303	0	0	0.008	1.082	0.705	1.198	3.806	0.56	0	4.94	0	0	0	2.114	18.484	0.176	3.172	12.71
610	0	0	4.966	0	0	30.922	7.638	0	0.002	0.075	2.218	1.171	0.553	5.286	1.141	0	8.35	0	0	0	1.719	17.231	0.494	3.411	13.285
611	0	0	3.485	0	0.15	24.62	7.884	0	0	0.017	2.54	1.4	0.868	5.457	0.775	0	2.7	0	0	0	1.239	18.009	0.369	2.824	13.364
612	0	0	5.287	0	0	26.463	7.248	0	0	0.046	2.555	1.536	1.024	5.181	1.282	0	9.5	0	0	0	1.261	15.89	0.33	3.432	11.959
613	0	0	6.264	0	0.15	25.442	8.995	0	0	0.044	2.495	1.171	0.815	5.792	0.771	0	7.87	0	0	0	2.1	20.175	0.255	2.534	14.083
614	0	0	3.332	0.17	0.75	24.503	9.411	0	0	0.062	2.815	1.035	0.785	4	0.795	0	3.48	0	0	0	1.786	19.776	0.286	4.32	13.48
615	0	0	6.632	0	0.45	23.158	9.023	0	0.001	0.02	2.387	1.128	0.956	5.759	1.142	0	5.6	0	0	0	1.712	19.627	0.907	2.871	11.194

Plant Type:	Greasewood					Grass					Forb					Tree					Shrub				
Plot:	1	2	3	4	5	1	2	3	4	5	1	2	3	4	5	1	2	3	4	5	1	2	3	4	5
sample #																									
616	0	0	4.907	0	0.3	29.755	10.071	0	0.002	0.026	2.143	1.509	1.298	5.658	0.861	0	2.67	0	0	0	1.337	16.187	0.308	2.914	12.694
617	0	0	4.601	0	0.3	24.096	7.572	0	0	0.002	2.716	0.668	0.836	4.691	1.842	0	9.7	0	0	0	1.866	16.105	0.26	4.172	10.523
618	0	0	7.334	0.17	0.3	29.117	8.826	0	0	0.046	2.117	0.734	0.791	4.866	1.15	0	4.8	0	0	0	2.033	14.598	0.273	2.601	9.899
619	0	0	5.108	0	0	24.044	8.202	0	0.001	0.043	1.677	1.406	0.927	5.018	1.873	0	6.3	0	0	0	1.706	16.594	0.408	4.305	11.762
620	0	0	5.393	0	0	26.868	9.171	0	0	0.134	2.041	1.313	0.931	5.598	0.664	0	2.87	0	0	0	2.072	17.907	0.44	3.964	14.097
621	0	0	5.843	0	0	25.308	10.345	0	0	0.004	1.959	1.767	1.261	4.056	0.862	0	3.02	0	0	0	1.852	24.425	0.248	4.574	11.38
622	0	0	5.086	0.51	0.15	29.961	8.816	0	0.001	0.006	2.123	1.912	0.897	3.691	0.969	0	4.4	0	0	0	2.269	20.683	0.539	3.51	12.499
623	0	0	4.388	0.51	0	21.692	8.684	0	0	0.032	2.174	1.424	0.961	3.136	1.444	0	6.32	0	0	0	1.562	17.001	0.553	3.571	10.075
624	0	0	4.296	0	0	26.397	8.709	0	0.002	0.087	2.583	1.385	0.672	4.379	1.81	0	3.94	0	0	0	1.985	24.875	0.339	3.604	11.67
625	0	0	3.251	0.17	0.15	26.274	9.161	0	0	0.009	1.433	1.891	1.226	4.728	0.792	0	4	0	0	0	3.023	18.285	0.392	3.521	11.109
626	0	0	4.861	0.34	0.15	29.214	8.444	0	0.001	0.017	1.413	1.141	1.148	4.726	0.259	0	5.84	0	0	0	2.512	18.828	0.279	3.854	12.418
627	0	0	4.116	0.17	0	25.568	8.426	0	0	0.199	1.267	0.717	0.876	5.988	0.769	0	8.95	0	0	0	1.703	18.063	0.344	3.551	16.233
628	0	0	3.875	0.85	0	27.326	10.524	0	0	0.054	3.154	1.789	1.061	4.236	0.743	0	7.52	0	0	0	1.597	17.192	0.377	3.24	12.761
629	0	0	6.32	0.17	0.45	25.755	8.326	0	0.001	0.007	2.244	1.235	0.843	4.791	1.196	0	8.45	0	0	0	2.628	9.824	0.246	3.97	10.58
630	0	0	6.225	0.17	0.15	23.551	8.649	0	0	0.066	2.803	1.66	1.499	4.508	0.425	0	6.02	0	0	0	1.943	19.869	0.307	2.58	13.455
631	0	0	6.107	0	0	31.924	8.729	0	0.003	0.018	1.939	0.698	1.083	5.217	1.355	0	5.3	0	0	0	0.739	19.706	0.48	3.231	13.973
632	0	0	5.288	0.34	0	29.594	7.485	0	0.001	0.04	1.956	1.038	1.209	4.575	0.634	0	6.35	0	0	0	2.32	15.438	0.316	3.673	14.545
633	0	0	5.539	0	0.3	25.715	8.95	0	0	0.099	2.356	2.007	0.691	7.243	0.839	0	11.1	0	0	0	1.81	16.504	0.39	2.754	13.294
634	0	0	4.713	0.34	0.15	26.294	9.307	0	0	0.084	1.885	0.923	0.395	5.971	0.808	0	3.34	0	0	0	1.756	16.348	0.406	3.203	16.441
635	0	0	5.506	0.17	0.6	23.707	7.699	0	0	0.186	1.465	0.832	0.877	4.815	0.426	0	11.1	0	0	0	2.11	13.724	0.34	3.102	15.545
636	0	0	3.227	0	0.3	26.475	10.242	0	0.001	0.055	1.602	0.787	1.246	3.123	0.691	0	7.55	0	0	0	1.871	14.843	0.319	4.081	13.565
637	0	0	4.115	0.51	0	24.26	7.418	0	0	0.048	2.096	0.946	1.26	4.455	1.143	0	4.02	0	0	0	2.149	18.66	0.186	2.26	12.462
638	0	0	3.417	0.34	0.3	27.315	8.435	0	0.001	0.118	2.015	1.113	0.844	3.269	0.618	0	8.4	0	0	0	2.102	20.124	0.269	3.71	14.428
639	0	0	4.787	0	0	28.176	10.983	0	0.002	0.094	2.066	1.871	1.008	4.603	0.485	0	1.5	0	0	0	1.986	20.888	0.253	3.744	13.583
640	0	0	4.507	0	0	24.262	8.444	0	0.002	0.006	2.827	1.06	1.034	4.765	1.475	0	6.8	0	0	0	1.53	19.776	0.456	3.542	12.37
641	0	0	5.291	0	0	26.254	8.252	0	0.001	0.043	1.819	0.813	0.953	6.854	0.704	0	4.06	0	0	0	2.267	16.516	0.291	2.896	13.553
642	0	0	4.184	0.68	0.45	27.46	10.029	0	0	0.005	1.328	1.237	1.279	4.687	1.057	0	6.29	0	0	0	2.02	17.763	0.397	2.861	11.656
643	0	0	3.775	0.17	0	26.62	7.572	0	0.003	0.014	1.781	1.061	0.969	3.81	1.626	0	7.1	0	0	0	2.343	16.744	0.494	3.53	11.621
644	0	0	2.827	0	0	25.34	7.679	0	0.002	0.013	3.309	1.023	0.648	4.508	0.89	0	6.65	0	0	0	1.708	14.036	0.301	4.381	11.587
645	0	0	3.862	0.17	0.15	26.939	8.377	0	0	0.015	1.926	1.409	1.102	5.894	0.974	0	5.86	0	0	0	2.136	19.675	0.446	3.73	11.831
646	0	0	5.692	0	0	25.468	8.245	0	0.001	0.037	2.139	1.244	0.604	3.035	0.637	0	6.5	0	0	0	1.327	19.644	0.28	2.99	14.571
647	0	0	3.944	0.17	0.3	28.511	8.782	0	0.001	0.011	1.264	1.072	0.9	4.828	1.437	0	7.34	0	0	0	2.324	16.627	0.371	3.111	12.977
648	0	0	3.215	0.17	0.3	27.61	8.587	0	0.001	0.104	2.006	0.776	1.159	4.275	1.105	0	7.5	0	0	0	2.054	17.381	0.471	2.334	14.406
649	0	0	3.923	0.17	0.6	23.296	9.422	0	0	0.053	1.433	1.366	1.044	4.542	0.41	0	0.78	0	0	0	2.09	20.755	0.37	4.343	13.99
650	0	0	5.395	0.34	0	24.55	8.903	0	0.003	0.071	2.305	0.753	1.638	4.132	0.989	0	7.51	0	0	0	1.492	18.24	0.544	3.65	11.19
651	0	0	5.219	0	0.15	21.263	8.613	0	0.001	0.007	2.006	0.963	0.712	5.486	2.105	0	8.4	0	0	0	2.258	15.821	0.347	4.593	9.342
652	0	0	4.761	0.17	0.15	27.545	7.567	0	0	0.087	2.537	0.697	0.988	4.952	0.985	0	7.1	0	0	0	2.188	16.553	0.438	2.301	14.07
653	0	0	6.504	0	0	22.923	8.749	0	0	0.154	1.642	1.178	1.144	5.943	0.28	0	7.62	0	0	0	1.551	17.814	0.384	3.761	14.439
654	0	0	7.356	0.17	0	24.513	9.909	0	0	0.057	3.182	1.043	0.521	4.571	1.227	0	5.77	0	0	0	1.608	18.455	0.388	3.901	13.171
655	0	0	4.965	0.17	0	24.104	8.302	0	0	0.056	1.838	0.744	0.977	4.395	0.82	0	4.97	0	0	0	1.988	19.663	0.603	3.27	14.009
656	0	0	8.088	0.17	0	24.464	9.18	0	0.001	0.047	2.677	0.666	1.356	4.018	1.019	0	4.42	0	0	0	1.422	19.622	0.212	3.48	12.988
657	0	0	4.401	0.17	0.15	24.673	8.7	0	0	0.179	2.681	1.581	0.89	4.998	0.146	0	4.7	0	0	0	1.76	18.539	0.725	3.34	17.532
658	0	0	4.025	0	0.3	21.587	9.532	0	0	0.089	2.222	1.367	1.032	5.999	0.446	0	6.77	0	0	0	2.659	16.047	0.503	3.323	14.106
659	0	0	4.005	0.51	0.45	25.69	7.853	0	0	0.026	3.237	1.193	0.803	5.491	0.241	0	6.3	0	0	0	0.606	16.521	0.27	3.493	13.724
660	0	0	6.564	0	0	25.617	8.278	0	0	0.084	1.645	0.962	1.143	4.804	1.121	0	5.69	0	0	0	1.825	15.986	0.422	3.152	12.868
661	0	0	6.622	0	0.6	29.43	7.197	0	0	0.005	1.151	1.315	0.955	4.467	1.361	0	5.9	0	0	0	1.434	17.575	0.167	3.39	12.894
662	0	0	3.095	0.34	0	25.158	8.111	0	0.002	0.098	2.219	1.295	1.135	3.889	0.894	0	14.1	0	0	0	2.202	16.754	0.334	5.022	15.326
663	0	0	5.166	0.51	0.15	25.295	8.336	0	0.001	0.113	2.15	1.001	1.015	4.366	0.347	0	8.67	0	0	0	1.185	18.056	0.401	3.781	14.668
664	0	0	4.493	0.51	0	29.944	7.382	0	0	0.085	1.854	0.922	1.105	4.476	0.658	0	6	0	0	0	1.708	15.065	0.353	4.55	13.217
665	0	0	3.963	0	0	27.073	8.518	0	0	0.056	2.308	1.395	0.967	5.6	1.276	0	5.9	0	0	0	1.723	16.289	0.256	2.912	12.511
666	0	0	5.714	0.34	0	23.188	6.766	0	0.001	0.133	2.195	0.678	1.501	3.318	0.336	0	8.5	0	0	0	1.452	13.805	0.297	5.24	14.583
667	0	0	3.76	0	0	27.674	8.358	0	0.003	0.107	2.458	1.615	0.882	3.702	0.543	0	11.85	0	0	0	1.055	18.169	0.301	3.663	14.28
668	0	0	5.468	0	0.3	27.94	9.204	0	0.003	0.021	2.408	1.123	0.811	4.395	0.808	0	4.75	0	0	0	1.842	25.435	0.16	4.754	13.484
669	0	0	5.216	0.17	0	22.968	9.077	0	0.003	0.036	1.998	1.922	0.948	6.265	0.978	0	8.8	0	0	0	2.259	17.7	0.392	3.503	12.439
670	0	0	5.177	0.17	0	25.087	8.456	0	0.002	0.058	1.533	1.452	0.887	3.622	0.785	0	7.4	0	0	0	2.784	17.063	0.538	3.902	14.252
671	0	0	4.416	0	0	23.811	6.945	0	0.001	0.01	1.486	0.934	0.622	4.34	1.071	0	8.2	0	0	0	2.672	13.671	0.383	3.054	11.491
672	0	0	3.935	0.68	0.3	27.351	8.789	0	0	0.062	2.19	1.338	0.974	3.057	0.989	0	7.4	0	0	0	1.729	16.283	0.395	3.15	12.336
673	0	0	7.072	0.51	0.3	27.249	9.033	0	0	0.061	2.51	1.373	0.563	6.137	0.8	0	9.57	0	0	0	1.034	18.378	0.22	2.482	13.691
674	0	0	4.798	0	0	22.992	8.407	0	0.001	0.187	2.35	1.629	0.617	4.661	0.563	0	8.2	0	0	0	2.223	18.845	0.313	3.443	15.477
675	0	0	3.66	0	0	23.731	8.575	0	0.001	0.034	2.327	1.23	1.09	4.279	0.914	0	2.52	0	0	0	1.111	16.949	0.307	5.03	12.855
676	0	0	3.906	0	0.45	31.112	9.049	0	0	0.025	2.522	1.3	1.207	3.562	1.021	0	10.85	0	0	0	1.754	17.645	0.334	4.042	11.595
677	0	0	4.931	0.34	0	22.794	10.448	0	0.002	0.11	2.269	1.206	0.864	5.251	1.067	0	7.8	0	0	0	1.408	18.353	0.502	3.771	13.106
678	0	0	4.717	0.85	0.15	30.249	8.206	0	0.002	0.065	1.982	1.547	1.015	4.836	0.89	0	4.3	0	0	0	1.307	18.551	0.481	3.225	13.17
679	0	0	3.815	0.17	0.3	30.895	8.521	0	0	0.07	1.675	1.465	1.263	4.612	0.653	0	5.02	0	0	0	1.453	20.629	0.215	2.882	13.465
680	0	0	6.5	0.17	0.75	25.85	7.732	0	0	0.023	2.376	1.197	0.672	4.443	0.738	0	5.27	0	0	0	2.687	19.895	0.435	2.332	12.294
681	0	0	3.045	0.17	0.6	26.682	7.752	0	0.003	0.014	1.888	1.489	0.597	4.871	0.971	0	6.1	0	0	0	2.349	17.153	0.608	4.591	11.788
682	0	0	4.096	0	0	26.406	8.465	0	0	0.044	3.376	0.751	1.524	3.848	0.961	0	10.22	0	0	0	1.637	13.428	0.175	3.382	13.255
683	0	0	5.324	0.34	0	26.601	8.151	0	0	0.103	2.007	0.762	0.646	5.471	1.607	0	6.97	0	0	0	1.542	19.485	0.196	2.754	11.48
684	0	0	6.573	0.34	0.6	23.568	8.019	0	0.001	0.001	2.479	1.054	1.013	4.181	0.645	0	4.79	0	0	0	0.569	20.44	0.459	4.14	12.201
685	0	0	5.718	0	0.45	28.198	8.072	0	0	0.071	1.626	0.675	0.969	4.511	0.732	0	8.45	0	0	0	1.68	13.965	0.4	2.024	12.811
686	0	0	4.247	0.51	0.15	24.26	10.002	0	0.001	0.008	2.264	1.315	1.066	4.944	1.204	0	4.92	0	0	0	1.979	21.219	0.322	3.333	10.568
687	0	0	3.704	0	0.15	27.028	8.379	0	0	0.071	2.897	0.998	1.049	3.92	1.338	0	6.71	0	0	0	1.048	19.773	0.182	2.831	12.543
688	0	0	3.275	0.17	0.45	26.371	9.025	0	0.001	0.002	1.759	1.562	0.769	6.287	0.408	0	1.26	0	0	0	2.267	19.97	0.404	3.671	14.391
689	0	0	3.26	0.51	0.15	25.022	8.432	0	0	0.012	2.578	0.794	0.71	5.065	0.979	0	6.4	0	0	0	2.059	17.952	0.341	3.872	13.743
690	0	0	5.161	0	0	23.936	7.82	0	0.003	0.092	2.507	1.083	0.911	4.082	2.027	0	9.05	0	0	0	2.658	19.424	0.26	3.511	13.89
691	0	0	3.795	0.34	0.75	23.742	7.922	0	0.001	0.004	2.894	1.182	0.919	4.798	0.754	0	8	0	0	0	0.877	20.157	0.26	3.342	13.023
692	0	0	4.294	0.34	0	31.723	8.886	0	0	0.185	2.854	1.802	1.162	3.741	0.748	0	6.92	0	0	0	1.674	20.337	0.352	2.34	13.775
693	0	0	3.068	0.34	0	23.858	9.078	0	0.002	0.062	2.291	1.963	1.293	5.383	0.617	0	2.72	0	0	0	2.77	16.378	0.513	2.662	14.256
694	0	0	5.106	0.34	0	23.897	8.833	0	0	0.148	2.22	1.835	0.979	4.534	0.315	0	5.1	0	0	0	2.461	19.748	0.237	3.11	14.751
695	0	0	5.872	0	0.3	25.012	8.929	0	0.001	0.131	1.72	0.718	1.192	4.264	0.688	0	8.04	0	0	0	2.074	16.799	0.253	3.034	13.024
696	0	0	4.678	0	0	27.419	8.527	0	0.001	0.089	2.147	1.509	1.023	6.023	0.419	0	4	0	0	0	1.977	15.633	0.458	3.663	14.895
697	0	0	4.646	0	0.3	27.224	9.161	0	0.003	0.037	2.146	0.597	1.126	4.442	0.105	0	7.65	0	0	0	2.268	17.473	0.446	4.23	14.634
698	0	0	4.604	0	0.15	25.347	8.285	0	0	0.078	1.874	1.394	1.277	5.683	0.543	0	4.9	0	0	0	2.031	17.942	0.209	2.682	14.367
699	0	0	5.49	0.17	0.3	27.185	8.748	0	0	0.007	1.272	1.622	0.644	4.266	0.37	0	13	0	0	0	1.949	19.307	0.426	2.851	13.892
700	0	0	5.247	0	0.3	24.158	8.723	0	0.001	0.063	2.461	0.726	1.144	5.697	0.716	0	12.21	0	0	0	1.929	19.106	0.305	4.399	16.017
701	0	0	3.657	0	0	24.631	8.419	0	0.001	0.005	2.639	0.882	1.293	5.316	0.966	0	6.87	0	0	0	1.164	17.115	0.302	2.581	11.324
702	0	0	4.36	0.34	0	23.586	10.498	0	0	0.042	2.797	1.044	0.759	5.763	0.639	0	6.06	0	0	0	1.631	16.848	0.395	2.635	14.131
703	0	0	3.751	0	0.15	30.923	8.412	0	0.001	0.09	2.234	1.1	0.927	4.481	0.524	0	7.7	0	0	0	2.413	17.942	0.336	3.21	14.717
704	0	0	5.927	0.51	0.45	25.91	9.197	0	0	0.005	2.104	1.395	0.653	4.336	1.227	0	4.14	0	0	0	1.579	19.006	0.309	3.81	10.701
705	0	0	4.308	0	0.3	25.597	8.633	0	0	0.014	1.57	1.914	1.08	4.743	0.482	0	8.5	0	0	0	1.508	17.356	0.507	2.711	11.391
706	0	0	4.471	0	0.45	24.938	7.129	0	0.001	0.074	1.899	0.8	0.506	6.251	0.035	0	5.1	0	0	0	1.457	13.958	0.404	2.385	14.998
707	0	0	5.063	0.34	0	25.793	8.916	0	0	0.138	2.147	1.68	1.126	4.466	0.758	0	6.4	0	0	0	1.941	22.523	0.524	3.651	16.168
708	0	0	4.247	0.34	0.15	23.909	7.632	0	0	0.095	1.757	1.001	0.432	4.864	0.839	0	11.15	0	0	0	2.185	18.116	0.384	3.141	16.178
709	0	0	4.034	0.68	0.15	24.699	8.652	0	0.002	0.015	2.051	1.875	1.291	4.621	0.456	0	10.65	0	0	0	2.119	16.813	0.175	4.171	16.029
710	0	0	3.5	0	0	22.17	8.817	0	0.004	0.01	2.24	1.214	1.198	3.902	0.65	0	7.45	0	0	0	1.802	16.754	0.339	4.29	13.894
711	0	0	3.295	0.17	0.15	24.681	7.703	0	0	0.072	1.434	1.14	1.213	6.666	0.748	0	5.14	0	0	0	1.667	19.395	0.274	2.945	13.612
712	0	0	3.873	0	0	24.722	7.004	0	0.002	0.081	3.077	1.232	1.138	4.242	0.244	0	8.9	0	0	0	1.904	19.817	0.514	4.222	15.628
713	0	0	3.26	0.51	0.15	28.933	7.79	0	0.001	0.006	1.882	1.303	0.842	4.32	1.581	0	6.5	0	0	0	1.89	21.604	0.443	3.2	11.338
714	0	0	6.951	0	0.45	23.967	9.467	0	0.001	0.116	2.413	1.57	0.783	4.666	1.713	0	1.26	0	0	0	3.45	24.467	0.27	4.614	11.905
715	0	0	5.485	0.17	0.45	28.643	8.411	0	0.001	0.017	2.551	0.861	0.889	6.077	0.139	0	5.77	0	0	0	1.33	16.293	0.164	3.624	12.848
716	0	0	3.766	0	0	29.408	9.309	0	0.004	0.023	2.187	0.681	1.6	3.607	0.511	0	6.97	0	0	0	1.868	14.717	0.318	4.96	12.525
717	0	0	4.473	0	0.3	24.616	8.761	0	0	0.044	2.521	0.644	0.609	6.561	1.895	0	2.21	0	0	0	1.526	22.796	0.665	3.612	11.114
718	0	0	4.093	0	0.3	26.911	8.525	0	0	0.019	1.478	1.032	1.119	3.534	1.36	0	11.2	0	0	0	2.671	16.513	0.307	3.12	12.442

Plant Type:	Greasewood					Grass					Forb					Tree					Shrub				
Plot:	1	2	3	4	5	1	2	3	4	5	1	2	3	4	5	1	2	3	4	5	1	2	3	4	5
sample #																									
719	0	0	4.703	0.51	0.3	23.518	8.218	0	0.001	0.03	1.83	1.348	0.852	4.215	0.497	0	10.3	0	0	0	1.505	15.25	0.588	3.222	13.481
720	0	0	4.04	0	0	25.114	8.832	0	0	0.056	1.594	1.559	1.197	4.828	1.157	0	4.48	0	0	0	2.514	20.603	0.213	2.826	12.066
721	0	0	4.347	0	0.3	26.454	7.25	0	0.003	0.026	2.392	0.522	1.27	4.761	1.252	0	7.4	0	0	0	2.58	14.844	0.222	3.66	13.229
722	0	0	4.602	0.17	0	28.255	8.528	0	0	0.068	2.667	1.418	0.818	3.946	0.546	0	6.7	0	0	0	1.27	16.416	0.446	3.793	16.329
723	0	0	5.907	0	0.45	30.559	7.946	0	0.003	0.046	3.167	1.108	0.919	4.056	1.429	0	8.42	0	0	0	1.159	18.707	0.503	2.85	11.41
724	0	0	3.266	0	0.45	26.484	9.52	0	0.002	0.021	2.297	0.977	0.488	4.199	1.273	0	6.89	0	0	0	2.494	16.736	0.308	3.233	11.591
725	0	0	5.672	0	0.6	22.825	9.043	0	0.003	0.013	2.562	1.152	1.072	5.602	0.733	0	5.8	0	0	0	1.355	14.746	0.539	3.96	10.086
726	0	0	3.586	0.34	0.3	26.188	7.972	0	0.001	0.019	1.559	0.885	1.073	5.259	0.741	0	7.9	0	0	0	2.123	18.742	0.399	4.65	14.798
727	0	0	4.825	0.17	0.3	27.813	8.041	0	0	0.089	2.019	1.532	1.375	5.67	1.064	0	3.67	0	0	0	1.949	20.284	0.401	3.644	13.855
728	0	0	3.791	0.17	0.75	26.518	9.054	0	0.001	0.036	3.345	1.308	1.261	4.088	1.051	0	8.84	0	0	0	1.01	20.827	0.452	3.754	11.627
729	0	0	4.075	0.51	0	22.956	8.513	0	0.002	0.207	1.947	1.542	1.123	3.986	1.552	0	3.92	0	0	0	2.033	15.633	0.353	2.982	14.955
730	0	0	4.323	0.34	0	22.967	10.241	0	0	0.099	2.165	1.457	0.743	4.402	1.203	0	5.97	0	0	0	2.441	19.985	0.547	2.951	13.618
731	0	0	4.13	0	0	26.883	8.786	0	0	0.11	1.326	0.735	0.873	6.521	1.009	0	5.35	0	0	0	2.448	11.682	0.543	2.445	14.398
732	0	0	2.287	0	0.15	25.349	9.444	0	0	0.087	1.316	1.53	0.847	4.817	0.702	0	4.12	0	0	0	2.908	20.839	0.501	2.454	14.318
733	0	0	3.336	1.02	0	23.086	9.969	0	0	0	2.125	1.082	1.072	4.663	1.428	0	8.97	0	0	0	1.585	16.558	0.267	3.372	9.616
734	0	0	3.214	0.17	0	25.218	8.51	0	0.001	0.065	1.151	1.525	0.949	3.835	0.909	0	10.9	0	0	0	2.074	16.583	0.468	2.901	14.206
735	0	0	6.669	0	0	23.925	7.429	0	0	0.073	2.429	0.871	1.045	5.06	1.257	0	7.1	0	0	0	1.59	15.58	0.263	3.293	11.521
736	0	0	4.789	0	0	23.551	9.544	0	0.001	0.052	2.625	1.451	0.634	5.2	0.402	0	6.42	0	0	0	2.162	18.34	0.311	3.281	13.3
737	0	0	6.845	0.17	0.15	27.228	9.091	0	0	0.031	3.268	0.99	0.973	4.614	1.564	0	5.2	0	0	0	1.837	20.837	0.364	3.333	11.822
738	0	0	3.687	0	0.15	31.072	8.812	0	0.001	0.101	2.282	0.721	1.212	5.288	0.657	0	8.15	0	0	0	0.89	18.21	0.369	2.333	14.673
739	0	0	5.393	0.68	0	21.719	7.75	0	0	0.016	2.39	1.186	0.677	5.831	1.478	0	6.3	0	0	0	2.006	14.102	0.551	2.661	10.839
740	0	0	4.862	0	0	27.425	7.487	0	0	0.065	2.009	1.502	0.982	5.303	1.795	0	7.15	0	0	0	2.5	16.455	0.411	2.673	12.562
741	0	0	3.575	0.17	0	29.184	8.202	0	0	0.017	2.767	1.272	1.107	4.919	0.63	0	6.55	0	0	0	0.99	16.647	0.418	3.681	12.6
742	0	0	5.759	0.17	0.15	27.194	9.526	0	0.001	0.113	1.3	1.52	0.811	4.787	2.059	0	2.66	0	0	0	2.071	24.597	0.368	2.862	11.474
743	0	0	4.267	0.34	0	27.323	8.433	0	0.001	0.103	1.505	0.811	0.605	3.94	1.406	0	6.17	0	0	0	3.144	17.799	0.239	3.84	12.68
744	0	0	6.118	0.34	0	26.825	9.306	0	0	0.008	1.128	1.14	1.165	5.111	0.669	0	8.35	0	0	0	1.73	15.211	0.208	2.795	14.301
745	0	0	4.021	0	0.15	25.742	8.395	0	0.001	0.116	1.509	1.276	1.042	3.985	1.012	0	4.27	0	0	0	2.051	16.598	0.307	3.75	12.175
746	0	0	6.13	0	0.6	25.744	8.06	0	0.003	0.028	3.069	1.041	1.194	4.114	1.949	0	8.1	0	0	0	1.375	15.215	0.473	2.92	11.576
747	0	0	4.046	0	0.3	27.358	8.801	0	0.001	0.076	3.523	0.709	0.881	5.189	0.475	0	9.7	0	0	0	1.233	17.826	0.626	3.727	13.829
748	0	0	7.206	0.51	0	26.809	8.904	0	0	0.004	2.744	0.614	1.127	4.708	1.018	0	7.85	0	0	0	1.779	20.595	0.118	3.61	11.385
749	0	0	3.769	0.17	0	28.096	7.91	0	0.005	0.083	1.931	0.748	0.882	4.311	1.138	0	7.22	0	0	0	1.897	17.688	0.327	4.033	12.976
750	0	0	6.339	0	0.15	23.189	10.156	0	0	0.121	1.708	1.202	0.634	4.033	0.963	0	2.74	0	0	0	2.443	20.766	0.258	3.89	13.839
751	0	0	2.419	0	0.75	23.948	4.727	0	0	0.06	2.973	0.443	0.908	6.732	0.945	0	12.12	0	0	0	1.598	14.103	0.151	3.302	18.077
752	0	0	3.581	0	0.15	21.445	5.8	0	0	0.109	2.717	0.406	1.263	5.931	1.559	0	7.88	0	0	0	1.865	19.865	0.187	2.921	18.614
753	0	0	3.208	0	0	22.86	3.9	0	0	0.151	2.839	0.299	0.841	5.804	1.492	0	10.94	0	0	0	1.726	11.103	0.357	1.74	18.977
754	0	0	2.859	0	0.45	22.903	7.585	0	0	0.126	2.901	0.408	1.058	6.06	2.32	0	11.48	0	0	0	2.171	18.448	0.403	3.354	18.692
755	0	0	3.515	0	0.45	23.955	5.814	0	0	0.058	3.238	1.104	1.373	6.764	2.262	0	12.36	0	0	0	2.346	15.334	0.112	3.992	15.619
756	0	0	3.322	0	0.15	20.736	4.722	0	0	0.132	2.402	0.26	1.082	6.308	2.618	0	6.8	0	0	0	1.013	16.954	0.185	4.952	17.064
757	0	0	4.838	0	0	21.765	6.169	0	0	0.102	2.577	0.694	1.221	7.843	1.486	0	11.86	0	0	0	1.57	17.173	0.152	3.733	17.463
758	0	0	2.296	0	0.3	27.405	6.699	0	0	0.111	3.499	0.319	1.588	5.418	1.416	0	2.74	0	0	0	1.044	21.959	0.121	3.022	18.193
759	0	0	3.478	0	0.6	21.455	4.369	0	0	0.185	2.709	0.429	0.963	5.615	1.447	0	7.46	0	0	0	2.235	13.786	0.189	2.897	20.994
760	0	0	3.007	0	0.6	21.503	4.947	0	0	0.124	2.792	0.255	0.702	5.106	1.268	0	6.2	0	0	0	2.049	16.604	0.162	2.832	20.584
761	0	0	3.958	0	0.45	21.949	4.683	0	0	0.023	3.042	0.429	1.196	7.087	0.738	0	6.4	0	0	0	1.228	14.63	0.255	3.551	19.69
762	0	0	4.312	0	0.75	23.404	5.807	0	0	0.03	2.838	0.411	0.995	6.081	0.783	0	8.42	0	0	0	1.924	17.693	0.218	2.775	18.459
763	0	0	2.89	0	0.6	22.55	5.524	0	0	0.147	2.923	0.734	1.292	5.292	0.989	0	8.94	0	0	0	1.801	13.191	0.249	4.201	19.164
764	0	0	2.855	0	0.15	23.548	5.468	0	0	0.075	2.832	0.412	0.629	4.645	2.041	0	9.54	0	0	0	2.012	20.604	0.186	2.475	15.469
765	0	0	5.126	0	0.15	22.943	4.437	0	0	0.229	3.281	0.612	0.699	5.466	1.474	0	10.4	0	0	0	1.645	12.571	0.12	3.352	17.825
766	0	0	3.884	0	0.3	22.494	5.338	0	0	0.08	2.119	0.818	1.18	5.046	1.174	0	13.92	0	0	0	1.954	12.611	0.385	3.382	17.997
767	0	0	3.637	0	0.3	20.884	6.117	0	0	0.013	2.348	0.675	1.446	5.303	1.78	0	8.96	0	0	0	1.633	16.285	0.188	3.08	18.964
768	0	0	4.092	0	0.6	24.02	5.273	0	0	0.101	3.399	0.59	1.202	5.106	1.06	0	11.68	0	0	0	1.507	15.546	0.258	1.79	18.423
769	0	0	4.141	0	0.45	25.623	5.169	0	0	0.162	3.377	0.471	0.83	4.985	0.881	0	9.62	0	0	0	1.384	13.403	0.263	1.961	21.627
770	0	0	3.499	0	0.15	24.101	5.95	0	0	0.077	3.472	0.63	0.801	5.366	2.772	0	7.14	0	0	0	1.819	18.26	0.236	2.232	15.135
771	0	0	3.212	0	0.15	22.345	4.935	0	0	0.077	2.912	0.447	0.37	3.899	0.853	0	4.02	0	0	0	1.194	14.656	0.33	2.56	19.619
772	0	0	4.071	0	0.6	18.46	5.514	0	0	0.135	2.102	0.881	0.911	4.197	1.174	0	8.18	0	0	0	1.738	12.977	0.221	2.745	21.148
773	0	0	2.159	0	0	21.608	6.883	0	0	0.02	2.403	0.505	0.685	5.128	1.875	0	10.12	0	0	0	2.371	16.013	0.395	3.496	16.644
774	0	0	3.329	0	0.15	24.511	5.319	0	0	0.131	2.573	0.334	0.873	4.655	2.337	0	7.72	0	0	0	1.396	16.962	0.226	2.531	17.712
775	0	0	4.283	0	0.15	21.683	4.62	0	0	0.072	2.764	0.602	0.91	4.073	1.101	0	9.4	0	0	0	1.769	13.563	0.144	3.91	20.406
776	0	0	2.71	0	0.6	22.979	5.862	0	0	0.028	2.773	0.26	0.965	6.556	2.125	0	5.22	0	0	0	2.09	19.445	0.169	4.063	17.72
777	0	0	3.869	0	0	21.758	6.436	0	0	0.041	2.956	1.29	1.19	6.918	0.33	0	20.7	0	0	0	1.857	14.261	0.136	3.072	22.055
778	0	0	1.671	0	0.3	24.84	3.42	0	0	0.129	2.643	0.16	0.866	6.21	0.895	0	3.3	0	0	0	1.604	13.872	0.254	2.933	18.912
779	0	0	2.228	0	0.15	21.091	5.24	0	0	0.197	2.151	0.687	0.822	7.122	0.628	0	11.44	0	0	0	2.848	17.376	0.268	2.312	22.338
780	0	0	4.614	0	0.45	21.756	4.627	0	0	0.208	2.815	0.868	0.754	5.088	1.081	0	13.32	0	0	0	1.614	13.904	0.171	2.56	19.688
781	0	0	3.506	0	0.3	22.276	5.36	0	0	0.149	1.89	0.686	1.307	5.666	0.314	0	13.4	0	0	0	2.086	12.24	0.188	2.311	21.302
782	0	0	3.082	0	0.45	25.997	5.212	0	0	0.184	3.304	0.36	0.834	5.038	1.653	0	6.54	0	0	0	1.523	19.737	0.181	3.6	18.912
783	0	0	2.47	0	0.45	23.941	5.918	0	0	0.055	2.793	0.29	0.512	4.161	0.553	0	6.18	0	0	0	1.253	17.679	0.283	3.681	20.219
784	0	0	2.144	0	0.3	24.085	5.297	0	0	0.207	2.791	0.311	0.743	5.452	2.139	0	5.9	0	0	0	1.539	15.495	0.357	2.89	18.159
785	0	0	4.359	0	0.6	24.191	5.458	0	0	0.312	3.296	0.728	0.78	5.811	0.327	0	7.6	0	0	0	2.713	13.856	0.206	2.455	22.898
786	0	0	2.52	0	0.45	22.956	6.029	0	0	0.088	2.768	0.484	0.937	5.286	0.777	0	7.94	0	0	0	1.991	15.777	0.294	3.33	20.944
787	0	0	3.335	0	0.3	24.765	4.974	0	0	0.062	3.016	0.618	0.652	6.613	0.705	0	13.62	0	0	0	1.041	14.332	0.351	3.533	19.849
788	0	0	4.31	0	0.6	20.984	5.862	0	0	0.199	3.04	0.707	1.12	5.132	1.154	0	12.52	0	0	0	2.01	13.543	0.208	3.323	19.381
789	0	0	3.442	0	0.3	22.217	4.571	0	0	0.1	2.796	0.609	1.02	5.403	1.572	0	8.44	0	0	0	2.055	15.464	0.271	3.021	19.314
790	0	0	2.83	0	0.15	21.989	7.318	0	0	0.111	2.653	0.706	1.489	5.195	0.78	0	9.14	0	0	0	2.552	17.708	0.159	2.692	19.659
791	0	0	2.046	0	0.45	24.081	7.204	0	0	0.144	3.045	0.782	0.798	5.603	1.604	0	3.12	0	0	0	2.215	21.272	0.333	1.72	18.611
792	0	0	2.337	0	0.9	23.674	5.657	0	0	0.122	2.933	0.477	1.006	6.016	1.426	0	13.8	0	0	0	1.932	9.051	0.31	2.614	20.663
793	0	0	3.027	0	0.45	26.666	4.158	0	0	0.163	3.014	0.462	0.951	6.268	0.811	0	12.9	0	0	0	1.303	13.694	0.319	2.422	20.279
794	0	0	3.965	0	0.45	21.662	5.37	0	0	0.209	1.991	0.946	0.594	6.251	0.951	0	7.46	0	0	0	2.638	15.924	0.263	3.614	19.738
795	0	0	2.793	0	0.45	23.091	6.026	0	0	0.016	3.246	0.265	1.028	4.283	1.182	0	12.1	0	0	0	1.094	16.278	0.184	2.902	19.268
796	0	0	2.76	0	0.45	26.504	5.027	0	0	0.035	3.499	0.704	0.841	6.398	0.849	0	12.32	0	0	0	1.947	12.391	0.268	4.691	17.847
797	0	0	4.519	0	0.6	22.312	3.58	0	0	0.136	2.547	0.22	1.193	6.381	1.525	0	10.5	0	0	0	2.039	14.414	0.294	2.973	17.069
798	0	0	2.705	0	0.15	20.201	6.668	0	0	0.026	2.395	0.718	0.642	6.172	1.189	0	5.12	0	0	0	1.518	15.226	0.184	2.882	19.84
799	0	0	1.82	0	0.6	22.085	5.267	0	0	0.12	2.337	0.847	1.294	3.645	0.835	0	7.76	0	0	0	2.381	15.141	0.225	4.56	22.578
800	0	0	2.746	0	0	22.583	6.484	0	0	0.045	2.56	0.892	0.9	6.286	2.611	0	7.18	0	0	0	2.149	23.275	0.19	1.842	18.152
801	0	0	2.626	0	0.45	24.855	5.287	0	0	0.096	3.224	0.383	1.391	5.81	0.451	0	11.64	0	0	0	1.42	21.151	0.35	2.263	19.768
802	0	0	2.877	0	0.15	24.047	5.812	0	0	0.103	2.708	0.527	0.876	4.37	1.935	0	9.22	0	0	0	2.757	20.99	0.337	2.33	18.359
803	0	0	4.354	0	0.15	24.151	4.559	0	0	0.066	3.191	0.492	1.041	5.485	0.841	0	13.3	0	0	0	2.396	12.305	0.191	3.112	17.517
804	0	0	2.336	0	0	23.953	5.487	0	0	0.067	4.055	0.89	1.254	6.651	1.044	0	7.1	0	0	0	1.039	15.192	0.221	1.58	19.741
805	0	0	2.268	0	0.15	25.803	5.454	0	0	0.057	3.241	0.662	1.026	5.472	2.842	0	10.3	0	0	0	1.303	16.434	0.302	3.254	16.556
806	0	0	3.409	0	0.45	21.244	4.973	0	0	0.045	3.595	0.519	1.154	3.676	0.937	0	10	0	0	0	1.737	11.146	0.236	1.931	17.672
807	0	0	3.543	0	0.45	21.639	4.445	0	0	0.03	2.717	0.248	1.243	5.019	1.699	0	11.24	0	0	0	1.141	15.092	0.264	3.542	16.34
808	0	0	2.718	0	0.45	22.286	5.104	0	0	0.065	3.084	0.348	1.142	5.832	1.923	0	9.04	0	0	0	2.029	13.825	0.296	2.691	17.711
809	0	0	2.99	0	0.45	23.552	5.569	0	0	0.016	2.547	0.321	0.661	5.594	1.178	0	9.84	0	0	0	1.75	16.853	0.383	2.624	18.657
810	0	0	2.008	0	0.15	24.355	5.405	0	0	0.027	2.79	0.508	0.859	4.279	2.103	0	9.54	0	0	0	2.068	17.54	0.375	2.9	14.705
811	0	0	2.656	0	0.6	21.413	7.267	0	0	0.065	2.629	1.129	0.381	5.758	1.3	0	4.24	0	0	0	1.683	20.622	0.337	2.54	17.895
812	0	0	2.242	0	0.15	24.749	6.524	0	0	0.101	3.202	0.642	1.579	5.466	1.686	0	9.32	0	0	0	1.346	20.031	0.141	2.665	19.937
813	0	0	2.582	0	0.3	23.325	5.94	0	0	0.03	2.572	0.62	1.344	5.193	0.654	0	7.44	0	0	0	1.426	13.212	0.239	3.481	20.273
814	0	0	3.004	0	0.15	27.69	5.364	0	0	0.057	3.044	0.233	0.98	4.63	1.205	0	8.74	0	0	0	1.049	20.104	0.22	5.37	18.757
815	0	0	3.812	0	0	23.219	5.367	0	0	0.215	3.252	0.247	1.327	6.369	0.912	0	7.4	0	0	0	2.146	16.332	0.194	2.536	24.366
816	0	0	3.242	0	0	23.22	5.331	0	0	0.053	2.772	0.712	1.4	4.854	2.019	0	10.86	0	0	0	1.784	18.715	0.152	3.592	19.098
817	0	0	2.806	0	0.45	22.733	5.688	0	0	0.175	3.242	0.518	1.249	3.151	0.887	0	12.14	0	0	0	1.45	14.912	0.375	5.444	21.542
818	0	0	2.178	0	1.05	19.977	5.43	0	0	0.208	2.632	0.729	1.076	4.636	0.505	0	12.14	0	0	0	1.783	15.147	0.183	1.813	22.049
819	0	0	3.288	0	0.3	22.659	6.521	0	0	0.254	2.684	1.017	0.906	4.45	0.746	0	6.74	0	0	0	1.629	16.86	0.325	3.234	23.108
820	0	0	3.132	0	0.3	24.505	5.589	0	0	0.251	2.911	0.851	1.209	7.216	0.364	0	10.8	0	0	0	2.07	16.688	0.173	3.403	21.708
821	0	0	2.64	0	0	22.973	6.648	0	0	0.053	3.526	0.589	0.788	7.664	1.351	0	5.46	0	0	0	1.736	18.912	0.366	1.913	18.445

Plant Type:	Greasewood					Grass					Forb					Tree					Shrub				
Plot:	1	2	3	4	5	1	2	3	4	5	1	2	3	4	5	1	2	3	4	5	1	2	3	4	5
sample #																									
822	0	0	2.372	0	0.15	26.07	5.467	0	0	0.043	2.565	0.805	0.975	5.586	1.16	0	6.44	0	0	0	1.7	18.214	0.252	2.066	18.924
823	0	0	2.729	0	0.15	25.048	5.939	0	0	0.154	3.164	0.489	1.146	5.795	1.573	0	11.64	0	0	0	1.607	14.275	0.249	2.16	18.507
824	0	0	2.778	0	0.45	24.18	4.825	0	0	0.082	2.711	0.34	0.774	5.634	1.171	0	11.6	0	0	0	1.364	12.854	0.177	2.152	18.67
825	0	0	3.27	0	0.15	19.924	4.03	0	0	0.107	2.447	0.483	1.112	5.442	0.883	0	6.22	0	0	0	1.999	15.086	0.225	3.221	22.293
826	0	0	5.386	0	0.15	22.797	5.851	0	0	0.08	2.435	0.739	1.136	5.548	1.939	0	6.84	0	0	0	2.566	19.727	0.244	3.86	17.696
827	0	0	2.958	0	0.15	21.759	4.323	0	0	0.083	2.704	0.286	1.311	5.189	1.124	0	10.1	0	0	0	1.522	13.752	0.132	3.752	19.857
828	0	0	3.395	0	0.15	21.128	5.518	0	0	0.032	2.597	0.628	1.279	6.31	1.88	0	6.46	0	0	0	1.94	16.493	0.22	2.321	17.013
829	0	0	2.618	0	0	22.654	6.391	0	0	0.074	2.918	0.593	1.175	6.618	1.34	0	11.78	0	0	0	1.939	13.253	0.126	3.014	19.787
830	0	0	3.623	0	0.3	20.228	5.207	0	0	0.082	2.361	0.49	0.802	6.091	1.229	0	9.98	0	0	0	1.534	15.895	0.179	2.856	18.869
831	0	0	1.708	0	0.3	22.209	6.367	0	0	0.168	2.599	0.731	1.484	6.484	1.388	0	8.64	0	0	0	1.834	18.697	0.188	2.014	19.705
832	0	0	2.347	0	0.15	23.255	5.827	0	0	0.046	3.17	0.37	0.942	6.307	1.549	0	16.32	0	0	0	1.816	15.726	0.187	3.77	17.046
833	0	0	3.799	0	0	25.143	5.858	0	0	0.17	2.639	0.766	0.874	5.826	1.136	0	6.26	0	0	0	1.477	20.435	0.366	3.691	19.062
834	0	0	2.957	0	0.45	21.184	4.937	0	0	0.126	2.233	0.551	1.124	4.045	1.106	0	5.12	0	0	0	1.842	15.924	0.275	3.54	19.624
835	0	0	3.186	0	0	19.342	7.341	0	0	0.147	2.7	0.65	0.465	4.45	1.063	0	7.18	0	0	0	1.944	17.713	0.346	3.836	20.841
836	0	0	2.816	0	0.15	22.632	6.899	0	0	0.216	2.611	0.67	0.965	4.204	1.423	0	3	0	0	0	1.955	17.148	0.353	2.641	20.485
837	0	0	3.13	0	0	21.955	5.167	0	0	0.039	2.492	0.66	0.98	5.499	0.674	0	12.84	0	0	0	2.268	12.974	0.21	2.84	21.152
838	0	0	2.817	0	0.3	22.246	5.479	0	0	0.036	3.062	0.554	0.679	5.788	0.409	0	11.74	0	0	0	1.92	14.236	0.189	2.76	20.977
839	0	0	2.812	0	0.45	21.851	5.443	0	0	0.116	2.341	0.599	1.056	5.099	0.831	0	6.02	0	0	0	2.053	14.273	0.396	3.073	19.998
840	0	0	3.148	0	0.15	21.557	4.98	0	0	0.092	2.396	0.715	0.654	5.08	2.33	0	9.74	0	0	0	1.631	11.71	0.273	2.1	17.765
841	0	0	3.123	0	0.3	21.779	5.448	0	0	0.187	2.572	0.694	1.079	5.015	0.628	0	11.44	0	0	0	2.074	12.536	0.351	1.84	23.201
842	0	0	3.997	0	0.3	24.992	4.751	0	0	0.118	3.353	0.43	1.677	6.381	0.714	0	11.14	0	0	0	1.158	18.773	0.122	1.982	19.279
843	0	0	2.219	0	0.45	21.511	5.909	0	0	0.108	2.971	0.689	1.296	5.248	1.108	0	7.94	0	0	0	2.488	20.767	0.17	3.312	18.298
844	0	0	5.124	0	0	23.376	5.685	0	0	0.174	2.965	0.253	0.721	5.671	1.884	0	5.18	0	0	0	1.76	18.32	0.211	3.293	18.487
845	0	0	2.265	0	0.6	20.526	5.775	0	0	0.152	2.274	0.677	0.977	3.814	1.951	0	5.3	0	0	0	3.321	20.179	0.272	2.391	19.097
846	0	0	2.113	0	0.45	23.804	5.791	0	0	0.034	3.461	0.411	1.488	6.349	1.272	0	9	0	0	0	2.515	16.156	0.217	3.77	16.079
847	0	0	2.401	0	1.05	23.113	6.487	0	0	0.089	2.544	1.036	0.727	5.356	0.777	0	7.4	0	0	0	1.703	17.953	0.294	1.35	20.306
848	0	0	2.057	0	0.75	21.698	5.487	0	0	0.065	2.475	0.244	1.17	4.992	1.863	0	11.78	0	0	0	2.242	16.522	0.215	3.494	17.128
849	0	0	3.222	0	0.15	28.46	5.524	0	0	0.183	3.153	0.889	0.854	5.611	0.458	0	10.74	0	0	0	1.301	18.321	0.277	3.511	23.068
850	0	0	2.52	0	0.6	21.937	4.765	0	0	0.051	3.02	0.345	0.945	4.89	0.887	0	9.76	0	0	0	1.593	16.194	0.256	3.642	17.133
851	0	0	1.625	0	0.15	24.515	3.56	0	0	0.087	3.059	0.129	0.426	6.186	1.89	0	12.1	0	0	0	2.659	10.843	0.519	2.69	16.785
852	0	0	2.436	0	0.15	24.958	3.348	0	0	0.217	3.396	0.344	1.178	5.612	0.105	0	8.2	0	0	0	1.207	11.028	0.256	3.07	26.233
853	0	0	2.607	0	0.6	19.77	4.986	0	0	0.051	2.04	0.219	0.591	4.808	1.069	0	10.14	0	0	0	2.536	17.051	0.229	2.86	20.221
854	0	0	2.598	0	0.6	20.687	5.512	0	0	0.125	2.063	0.455	1.36	5.027	0.202	0	8.48	0	0	0	1.581	16.975	0.346	3.461	23.332
855	0	0	3.58	0	0.45	23.513	4.066	0	0	0.248	2.916	0.478	0.851	4.223	1.164	0	13.4	0	0	0	1.826	11.762	0.194	2.041	20.457
856	0	0	4.071	0	0.15	24.29	6.247	0	0	0.09	2.712	0.635	0.912	4.972	1.059	0	4.6	0	0	0	1.365	18.665	0.217	3.192	18.816
857	0	0	3.371	0	0.6	22.661	4.901	0	0	0.049	3.107	0.411	1.421	6.087	1.741	0	12.4	0	0	0	1.777	15.733	0.18	2.63	16.009
858	0	0	3.195	0	0.45	22.128	5.421	0	0	0.123	2.656	0.378	0.952	5.247	1.572	0	11.18	0	0	0	2.455	19.458	0.241	3.132	20.569
859	0	0	2.624	0	0.45	21.098	5.667	0	0	0.02	2.999	0.964	1.012	5.725	2.021	0	10.56	0	0	0	1.582	14.327	0.328	3.216	16.629
860	0	0	2.774	0	0.45	23.566	5.001	0	0	0.137	2.606	0.51	0.724	6.391	0.948	0	6.32	0	0	0	1.589	15.265	0.224	2.691	19.626
861	0	0	2.801	0	0.15	25.148	6.616	0	0	0.228	4.004	0.976	0.851	6.313	0.985	0	10.12	0	0	0	1.631	16.095	0.208	1.76	23.032
862	0	0	2.255	0	0	21.717	6.019	0	0	0.186	2.533	0.785	0.693	7.131	1.15	0	13.42	0	0	0	2.187	13.8	0.285	2.851	20.146
863	0	0	3.783	0	0.3	23.077	5.347	0	0	0.035	2.53	0.382	0.965	5.463	1.178	0	7.56	0	0	0	2.149	15.305	0.253	3.371	16.937
864	0	0	2.444	0	0.3	21.663	6.214	0	0	0.019	2.526	1.259	0.898	5.282	1.415	0	17.2	0	0	0	2.501	15.342	0.377	3.52	19.27
865	0	0	3.688	0	0.45	18.374	4.77	0	0	0.111	2.324	0.185	0.639	8.852	1.493	0	11	0	0	0	1.585	12.622	0.427	2.691	16.783
866	0	0	2.501	0	0.3	23.509	5.944	0	0	0.269	2.6	0.436	0.418	6.321	1.409	0	8.76	0	0	0	2.033	15.677	0.197	2.381	20.565
867	0	0	2.154	0	0.45	25.146	5.234	0	0	0.225	2.888	0.733	0.96	5.552	1.09	0	20.2	0	0	0	0.987	13.944	0.324	1.87	21.974
868	0	0	3.851	0	0.15	22.582	6.326	0	0	0.086	2.753	0.479	0.848	4.048	2.03	0	4.9	0	0	0	1.367	20.63	0.253	3.061	18.337
869	0	0	2.342	0	0	21.28	6.916	0	0	0.182	2.872	0.803	1.148	5.396	0.53	0	7.32	0	0	0	1.911	22.142	0.176	2.87	25.484
870	0	0	2.226	0	0	22.837	5.579	0	0	0.096	3.391	0.532	0.792	4.078	1.296	0	4.84	0	0	0	0.875	15.178	0.291	3.641	20.173
871	0	0	2.055	0	0.6	22.992	4.386	0	0	0.227	2.515	0.627	0.882	5.787	0.515	0	5.7	0	0	0	1.552	16.48	0.149	1.543	24.862
872	0	0	2.808	0	0.75	25.119	6.772	0	0	0.127	3.203	0.916	1.646	5.141	1.53	0	10.54	0	0	0	1.684	17.622	0.186	4.511	19.255
873	0	0	5.224	0	0.45	23.085	7.375	0	0	0.005	2.594	0.349	1.003	6.863	2.585	0	11.46	0	0	0	1.471	20.695	0.163	2.246	14.965
874	0	0	2.911	0	0.75	27.156	5.756	0	0	0.224	3.518	0.394	0.77	5.688	1.065	0	9.6	0	0	0	1.365	18.32	0.212	3.24	21.554
875	0	0	1.96	0	0	24.606	4.133	0	0	0.099	3.041	0.278	1.123	6.225	1.295	0	10.7	0	0	0	2.393	16.023	0.367	2.662	16.738
876	0	0	1.721	0	0	22.725	4.96	0	0	0.043	2.423	0.35	1.031	4.658	0.711	0	12.12	0	0	0	2.019	14.053	0.381	3.462	19.83
877	0	0	2.387	0	0.3	22.822	5.377	0	0	0.174	2.655	0.605	0.555	4.087	0.553	0	15.4	0	0	0	2.468	13.714	0.27	4.3	21.641
878	0	0	1.527	0	0	23.585	5.87	0	0	0.042	2.773	0.844	0.849	4.423	1.651	0	11.5	0	0	0	1.687	12.615	0.235	2.502	16.354
879	0	0	2.104	0	0	23.293	6.238	0	0	0.265	2.447	0.784	0.916	5.002	1.671	0	10	0	0	0	2.641	9.893	0.375	3.411	21.076
880	0	0	3.289	0	0.45	21.457	5.022	0	0	0.037	3.042	0.374	1.019	5.313	1.346	0	5.42	0	0	0	1.393	16.853	0.385	3.475	16.663
881	0	0	2.706	0	0	20.23	6.252	0	0	0.073	2.245	0.622	0.6	5.223	0.882	0	4.56	0	0	0	1.643	22.527	0.331	3.281	19.24
882	0	0	4.253	0	0	28.091	6.233	0	0	0.174	3.197	0.582	1.134	5.815	1.044	0	8.24	0	0	0	0.967	13.982	0.127	2.574	22.338
883	0	0	4.174	0	0.3	24.808	4.687	0	0	0.099	2.61	0.279	0.544	5.597	1.736	0	4.92	0	0	0	1.981	18.494	0.186	3.8	18.107
884	0	0	2.728	0	0.6	23.997	5.73	0	0	0.026	2.88	1.037	1.115	5.575	1.818	0	13.74	0	0	0	1.844	14.455	0.199	2.79	17.776
885	0	0	3.171	0	0	25.133	4.526	0	0	0.167	2.34	0.552	0.776	5.293	1.229	0	5.8	0	0	0	2.025	14.574	0.234	5.021	19.942
886	0	0	4.588	0	0.9	22.988	5.806	0	0	0.172	3.18	0.327	1.057	4.33	0.595	0	11.94	0	0	0	1.456	20.99	0.137	2.33	21.857
887	0	0	2.156	0	0.15	24.502	6.713	0	0	0.121	2.587	0.83	1.054	6.441	0.578	0	7.36	0	0	0	1.181	17.472	0.569	2.71	20.505
888	0	0	2.179	0	0.45	23.986	7.822	0	0	0.132	2.645	0.863	1.253	5.353	0.994	0	13.92	0	0	0	1.763	20.78	0.392	3.893	21.608
889	0	0	2.557	0	0.15	25.717	6.151	0	0	0.123	2.905	0.799	0.338	7.111	1.148	0	12.22	0	0	0	1.892	18.057	0.244	3.554	19.462
890	0	0	2.627	0	0.45	23.886	6.071	0	0	0.198	2.803	0.438	1.093	5.388	0.941	0	9.32	0	0	0	2.311	18.665	0.171	4	21.328
891	0	0	2.065	0	0	25.017	4.82	0	0	0.253	2.861	0.689	0.778	5.231	0.841	0	8.2	0	0	0	1.355	15.844	0.376	4.141	21.618
892	0	0	2.439	0	0	22.059	4.856	0	0	0.11	2.653	0.488	0.667	6.492	1.292	0	12.42	0	0	0	2.406	16.023	0.223	2.42	20.21
893	0	0	4.713	0	0.6	23.089	5.559	0	0	0.115	2.401	0.18	0.616	7.591	0.525	0	5.62	0	0	0	1.404	19.044	0.308	2.113	20.402
894	0	0	2.648	0	0.15	21.499	4.968	0	0	0.161	2.09	0.262	0.67	7.731	1.163	0	10.82	0	0	0	2.011	17.256	0.307	2.742	22.56
895	0	0	2.848	0	0.75	24.453	5.615	0	0	0.032	2.875	0.45	1.575	4.515	1.699	0	9	0	0	0	1.092	16.746	0.238	3.335	14.576
896	0	0	3.072	0	0	21.081	5.004	0	0	0.14	2.254	0.507	1.252	6.326	1.095	0	11.7	0	0	0	1.479	11.928	0.176	2.484	20.221
897	0	0	2.75	0	0.3	25.768	5.964	0	0	0.035	2.92	0.705	0.904	5.789	2.061	0	9.08	0	0	0	1.768	20.523	0.252	3.987	16.817
898	0	0	3.964	0	0.45	21.253	5.999	0	0	0.184	3.006	1.229	1.011	5.1	0.576	0	12.02	0	0	0	1.934	17.262	0.217	4.03	22.635
899	0	0	2.318	0	0.6	24.726	4.803	0	0	0.176	3.194	0.418	1.078	5.605	1.082	0	8.12	0	0	0	2.379	13.814	0.384	2.591	18.855
900	0	0	3.693	0	0.15	18.539	4.676	0	0	0.043	3.034	0.29	0.766	5.506	1.097	0	6.06	0	0	0	1.675	16.925	0.213	3.992	19.025
901	0	0	1.766	0	0.75	23.313	5.731	0	0	0.103	2.898	0.63	0.752	4.971	1.371	0	7	0	0	0	1.71	10.567	0.212	3.272	17.675
902	0	0	3.345	0	0.15	21.745	5.756	0	0	0.109	1.981	0.429	0.802	6.296	0.954	0	1.94	0	0	0	2.41	20.463	0.309	2.783	20.865
903	0	0	2.117	0	0.3	22.396	6.013	0	0	0.145	2.664	0.506	0.92	3.555	1.208	0	12.1	0	0	0	1.603	10.781	0.221	2.19	22.408
904	0	0	4.095	0	0.15	22.852	6.104	0	0	0.205	2.976	0.291	0.661	3.576	0.6	0	8.9	0	0	0	1.757	13.948	0.382	3.693	23.918
905	0	0	1.839	0	0.15	24.395	7.187	0	0	0.111	2.531	0.529	1.615	6.068	1.661	0	4.44	0	0	0	1.958	20.807	0.264	3.263	19.948
906	0	0	3	0	0	21.058	5.534	0	0	0.114	2.97	0.416	1.352	5.002	0.595	0	11.22	0	0	0	2.431	16.321	0.199	3.02	21.962
907	0	0	1.899	0	0.3	24.906	6.003	0	0	0.167	3.269	0.713	0.908	5.231	1.847	0	8.88	0	0	0	2.038	16.653	0.324	3.22	18.671
908	0	0	3.605	0	0	23.948	5.955	0	0	0.043	2.767	0.626	0.835	7.773	1.883	0	4.56	0	0	0	2.934	17.322	0.179	2.897	16.78
909	0	0	2.889	0	0.3	22.06	5.505	0	0	0.049	2.691	1.16	1.015	4.564	2.698	0	6.94	0	0	0	1.906	16.941	0.328	2.561	16.993
910	0	0	2.778	0	1.05	22.104	5.469	0	0	0.09	3.727	0.268	1.255	5.435	0.466	0	8.08	0	0	0	1.211	18.95	0.133	3.322	22.194
911	0	0	2.917	0	0.15	24.64	5.678	0	0	0.048	2.838	0.34	1.082	4.108	0.402	0	6.16	0	0	0	2.377	17.005	0.23	3.131	21.345
912	0	0	2.908	0	0.15	27.546	5.051	0	0	0.125	3.045	0.283	1.373	3.795	1.678	0	10.8	0	0	0	1.312	13.321	0.316	3.152	19.398
913	0	0	2.982	0	0.15	24.81	6.646	0	0	0.151	2.772	0.792	0.955	5.347	1.269	0	13.86	0	0	0	2.267	18.411	0.319	3.282	20.09
914	0	0	2.645	0	0.15	23.394	5.51	0	0	0.082	2.717	0.408	0.591	4.934	0.884	0	7.68	0	0	0	1.877	18.036	0.221	3.023	21.016
915	0	0	2.854	0	0.15	23.667	6.188	0	0	0.096	2.762	0.784	0.954	5.813	2.495	0	12.24	0	0	0	1.975	14.193	0.24	3.172	18.147
916	0	0	3.499	0	0.6	25.403	4.749	0	0	0.111	3.108	0.645	1.014	7.953	0.905	0	3.36	0	0	0	1.378	18.475	0.254	2.564	20.76
917	0	0	2.801	0	0.3	22.224	6.947	0	0	0.087	2.194	0.955	1.579	5.423	1.603	0	8.7	0	0	0	2.665	15.502	0.204	3.054	20.853
918	0	0	2.2	0	0.15	22.054	4.919	0	0	0.123	3.101	0.661	0.588	5.903	1.219	0	8.34	0	0	0	1.677	15.682	0.236	3.235	20.966
919	0	0	1.817	0	0	21.481	4.713	0	0	0.108	2.496	0.659	1.341	4.601	1.277	0	15.44	0	0	0	1.602	15.592	0.203	3.33	17.665
920	0	0	3.36	0	1.65	21.832	5.175	0	0	0.114	2.629	1.025	1.093	4.873	1.298	0	14.76	0	0	0	1.767	14.964	0.158	2.964	17.907
921	0	0	2.154	0	0	20.29	5.737	0	0	0.193	2.981	0.638	0.956	6.368	1.286	0	7.6	0	0	0	1.654	14.583	0.318	3.861	21.906
922	0	0	3.353	0	0.15	20.563	5.514	0	0	0.132	2.386	0.712	0.926	6.106	0.119	0	2.84	0	0	0	1.423	18.249	0.28	2.014	20.724
923	0	0	2.413	0	0.9	23.559	5.932	0	0	0.025	2.87	0.474	0.908	6.448	1.166	0	10.92	0	0	0	1.845	16.235	0.473	2.062	17.073
924	0	0	1.97	0	0	25.043	6.236	0	0	0.084	2.942	0.718	1.483	7.394	2.349	0	3.24	0	0	0	1.669	16.696	0.323	3.02	15.961

Plant Type:	Greasewood					Grass					Forb					Tree					Shrub				
Plot:	1	2	3	4	5	1	2	3	4	5	1	2	3	4	5	1	2	3	4	5	1	2	3	4	5
sample #																									
925	0	0	2.997	0	0	22.634	5.867	0	0	0.073	2.776	0.997	0.662	8.493	2.449	0	15.02	0	0	0	1.722	15.541	0.341	5.295	14.964
926	0	0	2.938	0	0.6	19.764	4.678	0	0	0.05	2.542	0.343	0.804	3.78	0.457	0	11.74	0	0	0	1.376	15.924	0.337	5.162	20.412
927	0	0	1.838	0	0	25.746	6.243	0	0	0.096	2.993	0.643	0.816	5.427	0.921	0	8.98	0	0	0	1.302	20.875	0.239	2.791	18.664
928	0	0	3.173	0	0	20.767	6.001	0	0	0.148	2.506	0.939	1.119	4.869	0.791	0	14.7	0	0	0	1.881	12.124	0.262	1.942	20.013
929	0	0	4.206	0	0	23.436	5.249	0	0	0.042	3.192	0.19	1.28	5.918	1.478	0	7.7	0	0	0	1.376	20.333	0.181	3.474	17.54
930	0	0	3.348	0	0.75	20.812	4.761	0	0	0.145	2.109	0.88	0.589	4.979	0.843	0	8.12	0	0	0	2.005	13.706	0.195	2.616	19.47
931	0	0	4.633	0	0.6	23.819	5.275	0	0	0.112	2.599	0.854	1.27	5.907	0.609	0	6.1	0	0	0	2.761	19.271	0.12	2.052	20.863
932	0	0	3.362	0	0.3	22.893	6.363	0	0	0.155	3.552	0.466	0.866	5.937	1.203	0	8.12	0	0	0	1.405	17.687	0.273	2.77	20.37
933	0	0	2.167	0	0.9	19.7	5.183	0	0	0.164	2.282	0.655	1.283	5.394	0.598	0	8.34	0	0	0	2.53	15.296	0.297	2.07	18.713
934	0	0	1.789	0	0.15	25.26	4.293	0	0	0.111	3.007	0.396	0.881	6.093	0.829	0	10.9	0	0	0	1.211	10.68	0.256	3.275	19.944
935	0	0	5.736	0	0.6	20.936	5.516	0	0	0.198	2.483	0.611	0.768	6.579	1.207	0	7.04	0	0	0	2.233	14.482	0.23	2.702	20.604
936	0	0	3.207	0	0.15	21.85	5.081	0	0	0.094	2.449	0.867	0.857	4.945	1.92	0	9.92	0	0	0	1.398	10.864	0.231	1.98	17.51
937	0	0	3.137	0	0.6	23.812	4.994	0	0	0.15	2.777	0.448	0.618	4.23	1.603	0	14.98	0	0	0	2.067	15.074	0.291	1.82	19.169
938	0	0	3.251	0	0.75	24.221	7.153	0	0	0.068	2.578	0.478	0.588	7.969	1.383	0	8.96	0	0	0	2.357	21.077	0.297	2.86	20.187
939	0	0	3.075	0	0	26.282	6.136	0	0	0.104	2.664	0.723	0.968	5.988	1.961	0	10.5	0	0	0	1.37	17.726	0.196	3.331	17.719
940	0	0	2.53	0	0.15	21.625	4.307	0	0	0.137	2.904	0.557	0.601	7.222	0.69	0	15.1	0	0	0	2.045	11.084	0.388	2.753	22.216
941	0	0	2.799	0	0.6	23.795	5.808	0	0	0.091	2.461	0.92	0.933	4.145	0.568	0	9.4	0	0	0	2.275	12.34	0.203	3.381	19.582
942	0	0	3.003	0	0	20.72	6.428	0	0	0.158	2.937	0.535	0.647	4.945	1.663	0	8.72	0	0	0	1.818	19.864	0.286	2.721	18.884
943	0	0	3.129	0	0.45	21.874	4.797	0	0	0.146	2.68	0.301	0.859	5.594	1.071	0	8.42	0	0	0	1.639	11.765	0.303	2.676	18.911
944	0	0	2.57	0	0.6	24.01	5.27	0	0	0.061	2.576	0.742	0.765	4.515	0.962	0	8.34	0	0	0	1.684	13.315	0.249	1.82	20.07
945	0	0	3.613	0	0	23.021	5.977	0	0	0.103	2.919	0.477	0.689	5.656	0.621	0	12.02	0	0	0	1.679	17.045	0.172	2.961	21.865
946	0	0	2.747	0	0.15	22.182	5.772	0	0	0.053	2.72	0.778	0.947	6.476	2.13	0	9.44	0	0	0	1.947	14.303	0.219	3.881	17.829
947	0	0	3.457	0	0	20.599	5.439	0	0	0.181	2.306	0.631	0.793	3.93	1.127	0	7.32	0	0	0	1.754	15.132	0.313	3.311	22.978
948	0	0	3.393	0	1.05	20.738	5.073	0	0	0.082	2.755	0.968	0.71	7.214	1.396	0	6.8	0	0	0	2.756	12.832	0.25	3.633	18.696
949	0	0	3.071	0	0.6	24.257	4.543	0	0	0.137	3.371	0.393	1.053	5.148	1.454	0	12.1	0	0	0	1.646	11.191	0.285	3.685	18.703
950	0	0	3.041	0	0.45	24.155	4.167	0	0	0.081	2.792	0.284	0.785	7.207	0.437	0	10.92	0	0	0	1.87	13.402	0.326	1.922	23.121
951	0	0	2.846	0	0	22.629	4.757	0	0	0.119	2.357	0.934	0.971	5.364	2.412	0	15	0	0	0	1.521	15.59	0.314	2.814	18.372
952	0	0	2.496	0	0.15	25.037	5.832	0	0	0.097	2.962	0.442	0.89	4.565	1.402	0	7.54	0	0	0	1.597	20.458	0.396	4.142	17.86
953	0	0	2.981	0	0	22.988	5.811	0	0	0.132	2.862	0.428	0.739	4.741	1.319	0	9.04	0	0	0	2.273	18.714	0.329	3.904	20.696
954	0	0	3.69	0	0.45	22.585	6.793	0	0	0.033	2.912	0.405	0.494	6.284	2.536	0	5.44	0	0	0	1.79	23.048	0.296	3.044	15.559
955	0	0	2.547	0	0.3	25.581	5.442	0	0	0.112	3.094	0.35	1.376	4.646	0.723	0	9.26	0	0	0	1.163	19.908	0.21	2.403	20.951
956	0	0	4.22	0	0.45	22.011	5.162	0	0	0.209	2.969	0.625	1.378	6.438	1.052	0	9.12	0	0	0	1.481	17.804	0.2	1.525	23.26
957	0	0	2.543	0	0	22.207	6.157	0	0	0.181	2.274	0.707	1.029	6.038	0.91	0	11.68	0	0	0	2.59	17.437	0.273	2.132	22.744
958	0	0	3.447	0	0.45	20.258	4.237	0	0	0.119	2.155	0.29	1.282	5.008	1.104	0	5.82	0	0	0	2.213	14.294	0.253	1.9	19.359
959	0	0	1.857	0	0.15	21.807	6.216	0	0	0.006	2.173	0.516	0.882	6.525	3.023	0	6.64	0	0	0	1.847	20.763	0.397	2.351	15.914
960	0	0	3.074	0	0.45	22.268	5.15	0	0	0.086	2.688	0.299	1.009	5.533	0.72	0	12.22	0	0	0	2.091	14.188	0.297	2.621	18.625
961	0	0	2.776	0	0	21.319	5.721	0	0	0.111	2.538	0.74	0.919	6.281	2.317	0	8.36	0	0	0	2.231	13.065	0.327	3.003	18.831
962	0	0	3.211	0	0.15	23.121	4.573	0	0	0.074	2.189	0.214	0.818	5.006	1.607	0	6.64	0	0	0	1.398	17.693	0.24	3.54	18.471
963	0	0	2.249	0	0.15	23.349	4.206	0	0	0.121	2.823	0.336	1.527	5.262	1.266	0	7.6	0	0	0	1.87	9.065	0.175	2.371	19.355
964	0	0	3.797	0	0.45	22.295	3.8	0	0	0.22	2.283	0.12	1.005	5.98	0.615	0	6.8	0	0	0	1.41	13.001	0.158	2.894	21.488
965	0	0	3.06	0	0.45	20.481	4.66	0	0	0.142	2.562	0.395	0.829	6.074	1.087	0	11.2	0	0	0	1.581	11.464	0.203	3.268	19.852
966	0	0	2.733	0	0	22.131	5.341	0	0	0.061	2.603	0.412	0.971	7.194	2.18	0	3.94	0	0	0	2.932	20.584	0.302	3.63	18.694
967	0	0	3.378	0	0.15	24.37	4.942	0	0	0.052	3.147	0.773	0.798	5.712	3.073	0	13.3	0	0	0	0.981	13.025	0.184	2.052	15.214
968	0	0	2.976	0	0	25.517	3.333	0	0	0.194	3.345	0.581	0.671	5.515	1.182	0	14.52	0	0	0	1.406	13.623	0.258	3.662	19.66
969	0	0	4.462	0	0.75	21.284	5.125	0	0	0.171	2.851	0.401	1.282	5.083	1.091	0	13.32	0	0	0	2.686	11.493	0.159	1.831	20.683
970	0	0	2.81	0	0	19.973	5.457	0	0	0.058	2.719	0.406	1.151	6.836	2.9	0	6.26	0	0	0	2.093	19.906	0.199	3.283	17.212
971	0	0	2.617	0	0	24.212	4.09	0	0	0.04	3.848	0.474	0.93	5.532	1.368	0	6.32	0	0	0	0.832	12.861	0.27	2.832	18.488
972	0	0	2.493	0	0	21.767	6.013	0	0	0.106	2.673	0.76	1.052	4.983	1.073	0	13.94	0	0	0	0.801	17.624	0.086	3.475	19.695
973	0	0	4.011	0	0.6	25.581	4.656	0	0	0.193	2.603	0.455	0.778	5.468	0.876	0	11.94	0	0	0	2.156	13.795	0.247	2.662	20.578
974	0	0	2.573	0	0	19.667	6.67	0	0	0.134	1.82	0.623	1.497	4.693	0.993	0	3.56	0	0	0	2.201	22.153	0.243	3.374	20.023
975	0	0	3.646	0	0.3	23.568	4.623	0	0	0.304	3.002	0.358	1.623	4.743	0.697	0	8.02	0	0	0	2.051	14.064	0.137	3.281	23.493
976	0	0	3.924	0	0.15	24.657	4.258	0	0	0.027	3.29	0.286	0.76	6.739	2.228	0	9.52	0	0	0	1.406	16.224	0.165	3.284	17.08
977	0	0	2.021	0	0.3	21.597	5.566	0	0	0.048	2.258	0.525	1.002	5.338	0.896	0	6.98	0	0	0	2.528	19.163	0.25	2.17	18.568
978	0	0	3.251	0	0.45	22.487	5.324	0	0	0.031	2.752	0.719	1.015	7.285	0.498	0	8.22	0	0	0	1.822	14.743	0.153	1.731	19.6
979	0	0	2.255	0	1.2	24.06	6.227	0	0	0.05	3.646	0.854	0.897	4.441	0.504	0	8.42	0	0	0	2.545	15.492	0.275	2.812	21.259
980	0	0	3.058	0	0	20.705	5.463	0	0	0.063	3.149	0.682	1.312	6.592	1.482	0	5.92	0	0	0	1.665	13.116	0.14	1.693	17.463
981	0	0	3.429	0	0.45	21.318	5.136	0	0	0.153	3.015	0.547	1.084	6.032	0.613	0	10.6	0	0	0	2.112	14.905	0.211	4.372	20.603
982	0	0	3.096	0	0.3	23.789	7.516	0	0	0.111	2.479	0.72	0.857	6.322	2.524	0	6.8	0	0	0	2.033	18.395	0.282	3.112	15.613
983	0	0	2.451	0	0.45	22.757	4.055	0	0	0.115	2.431	0.288	0.471	5.657	1.199	0	9.02	0	0	0	2.126	14.477	0.227	4.46	18.696
984	0	0	1.69	0	0	22.674	6.826	0	0	0.142	3.055	0.552	0.924	4.916	1.43	0	9.8	0	0	0	0.971	11.896	0.344	2.54	21.477
985	0	0	3.492	0	0.45	20.896	5.585	0	0	0.167	2.87	0.539	1.291	5.657	0.662	0	10.38	0	0	0	1.921	14.604	0.14	3.04	22.164
986	0	0	2.841	0	0	23.099	4.914	0	0	0.129	2.903	0.861	1.044	4.771	0.381	0	16.42	0	0	0	1.41	18.264	0.241	3.292	20.432
987	0	0	2.968	0	0.6	24.913	4.966	0	0	0.059	2.492	0.285	1.378	4.93	1.436	0	8.94	0	0	0	1.938	18.166	0.395	2.5	18.709
988	0	0	3.246	0	0.45	22.306	5.596	0	0	0.065	3.104	0.407	1.22	3.975	1.6	0	12.02	0	0	0	1.344	14.636	0.328	1.813	16.3
989	0	0	3.857	0	1.5	24.012	5.213	0	0	0.032	2.912	0.643	0.744	5.117	1.681	0	13.02	0	0	0	1.292	16.922	0.287	1.782	18.22
990	0	0	2.466	0	0.6	21.873	4.01	0	0	0.023	2.788	0.303	0.979	6.911	1.661	0	11.04	0	0	0	2.167	10.897	0.26	3.141	15.972
991	0	0	2.788	0	0.75	24.932	5.398	0	0	0.093	2.981	0.937	1.203	4.548	0.796	0	8.32	0	0	0	1.689	14.825	0.22	3.901	20.973
992	0	0	4.596	0	0.15	23.218	5.358	0	0	0.084	2.661	0.722	1.012	4.351	0.917	0	8.8	0	0	0	1.607	14.23	0.317	2.73	18.548
993	0	0	2.671	0	0.15	22.065	4.932	0	0	0.087	2.634	0.596	0.991	5.684	1.475	0	16.5	0	0	0	2.036	11.789	0.277	1.25	20.195
994	0	0	3.097	0	0.3	27.919	6.314	0	0	0.238	3.28	0.583	1.43	5.954	0.912	0	3.38	0	0	0	1.442	23.573	0.16	3.795	20.807
995	0	0	3.221	0	0.45	24.893	6.555	0	0	0.118	3.408	0.358	1.345	6.75	0.452	0	8.44	0	0	0	1.222	23.475	0.319	2.703	22.972
996	0	0	3.901	0	0.45	19.451	5.733	0	0	0.06	1.651	0.63	1.078	4.928	1.013	0	9.3	0	0	0	2.574	16.65	0.232	2.782	18.485
997	0	0	2.56	0	0.6	23.903	4.816	0	0	0.07	2.905	0.819	1.114	4.658	0.659	0	11.6	0	0	0	1.581	14.483	0.229	3.4	21.525
998	0	0	2.122	0	0.6	21.487	5.666	0	0	0.093	2.412	0.135	0.952	3.633	1.299	0	2.22	0	0	0	2.633	19.815	0.297	2.33	17.112
999	0	0	3.557	0	0.6	24.459	5.15	0	0	0.071	2.907	0.263	1.151	5.966	1.142	0	10.16	0	0	0	1.324	15.814	0.181	1.611	18.107
1000	0	0	2.347	0	0.3	22.38	6.054	0	0	0.047	3.037	0.128	0.451	5.777	0.89	0	1.06	0	0	0	1.202	22.036	0.364	2.52	19.407

Neptune and Company Inc.

June 1, 2011 Report for EnergySolutions

Clive DU PA Model, version 1

Appendix 17

Quality Assurance Project Plan

Quality Assurance Project Plan
Performance Assessment Model
Clive, Utah

Prepared by

Neptune and Company

1505 15th St Suite B
Los Alamos, NM 87544

Document No: 06245-001

APPROVALS

_____ _____

Paul Black Date
Neptune and Company Project Manager

_____ _____

James Markwiese Date
Neptune and Company
Corporate Quality Assurance Officer

Contents

Figures

Tables

Distribution List

K. Catlett
D. Gratson
W. Houghteling
R. Lee
J. Markwiese
G. McDermott
R. Perona
T. Stockton
M. Sully
J. Tauxe
Neptune and Company
1505 15th Street, Suite B
Los Alamos, NM 87544

P. Black
M. Balshi
M. Fitzgerald
M. Pocernich
Neptune and Company
8550 W. 14th Ave., Suite 100
Lakewood, CO 80215

M. Gross
MG Enterprises
415 Riveria Drive
San Rafael, CA 94901-1530

1.0 Introduction

This document describes the quality assurance project plan (QAPP) for modeling services provided for the development of a performance assessment model for the disposal of depleted uranium by Energy*Solutions* at the Clive, Utah facility. Throughout this document, the term Quality Assurance (QA) refers to a program for the systematic monitoring and evaluation of the various aspects of performance assessment model development to ensure that the models and analyses are of the type and quality of that needed and expected by the client.

2.0 Project Management and Organization

Neptune and Company (N&C) has developed this QAPP for conducting work for Energy*Solutions* under purchase order 008404. This QAPP is based on the Environmental Protection Agency (EPA) QA/G-5M Guidance for Quality Assurance Project Plans for Modeling, and our company's nineteen year history working in the environmental quality arena. A tiered approach is used that includes specific procedures developed by N&C that have been developed for modeling projects. This project-specific QAPP will work as an umbrella plan that ensures quality across all tasks.

The N&C quality program includes:

- Experienced and trained personnel who understand the QA requirements of each task.
- An experienced Project Manager.
- A corporate Quality Assurance Officer
- Task planning, tracking, and operation via internal SOPs.
- Emphasis on continuous improvement via internal reviews and customer feedback.

It is the policy of N&C to implement a quality program designed to generate products or services that meet or exceed the expectations established by our clients. This quality policy addresses all products delivered to our Energy*Solutions* client under the contract. We will ensure quality through the use of a quality program that includes program and project management, systematic planning, work and product assessment and control along with continuous improvement to ensure that data and work products of acceptable quality to support the intended use are produced.

To achieve this goal, N&C will assign appropriately qualified and trained staff and ensure that all products are carefully planned. Tasks will be conducted according to the QAPP or applicable SOP and any and all problems affecting quality will be brought to the immediate attention of the project or task manager for resolution. All products will be reviewed by another technical expert. Adequate budget and time will be planned to execute the quality system.

As indicated on Figure 1, the N&C organizational structure ensures direct reporting between the N&C Project QA Officer and the Project Manager. This structure requires that all N&C technical staff report to the N&C Project Manager who is responsible for the work.

The N&C Quality Assurance Officer has the authority and responsibility to ensure that the project-specific QAPP is implemented by N&C staff. Roles and Responsibilities for this project are detailed in Table 1. The QA aspects of the project are handled by those project members responsible for any particular part of the project. The lead modeler is responsible for QA for the GoldSim models. For probabilistic models, the lead statistician is responsible for QA of statistical routines and products that feed into the model. The responsibility for other QA tasks may be assigned to other project members at the direction of the lead modeler or lead statistician. The *model custodian* is responsible for configuration control of the model. The role of *model custodian* may be assumed by any project team member, but only one person at a time may be the custodian.

3.0 Personnel Qualifications and Training

N&C technical staff is composed of highly qualified chemists, engineers, statisticians, IT professionals, QA specialists, and biologists with advanced degrees in their fields and direct training experience. Many of the N&C staff have participated in GoldSim training courses and GoldSim User Conferences. Qualifications for the staff are shown in Table 1. Each N&C employee or contractor involved with this project will be required to read this QAPP and associated standard operating procedures (SOPs).

Figure 1: N&C Organizational Chart

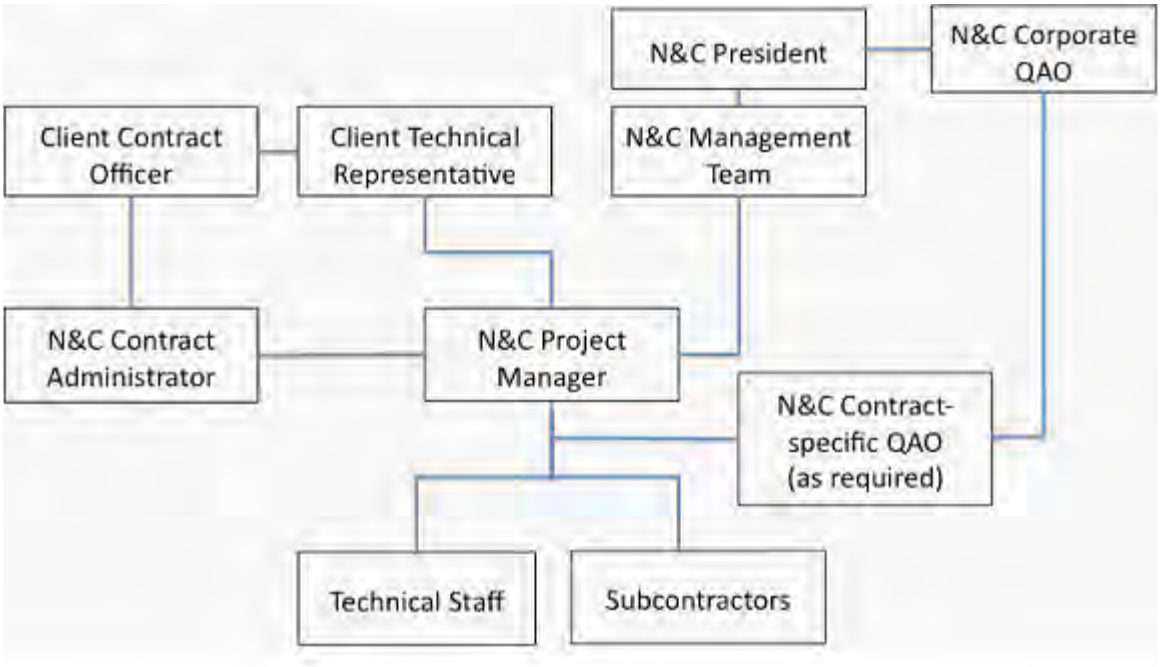

Table 1: Roles, Responsibilities, and Training

Roles	Personnel	Training
Project Manager	Paul Black	Ph.D. Statistics
QA Officer	Jim Markwiese	Ph.D. Biology
Technical Lead	John Tauxe	Ph.D. Civil Engineer, Professional Engineer (New Mexico), GoldSim Training
Modeler Biologist	Mike Balshi	Ph.D. Ecological Modeling System model training
Modeler	Katie Catlett	Ph.D. Soil Science GoldSim Training
Statistician	Mark Fitzgerald	Ph.D. Statistics
Chemist	Dave Gratson	M.S. Environmental Science and Engineering Certified Environmental Analytical Chemist GoldSim Training
Modeler	Mike Gross	Ph.D. Mechanical Engineering GoldSim Training
Project planner	Warren Houghteling	IT Specialist
Risk and analyst	Robert Lee	M.S. Environmental Health
Ecologist	Greg McDermott	M.S. Entomology
Exposure and Dose Assessment Modeler	Ralph Perona	M.S. Environmental Health DABT
Statistician Modeler	Matt Pocernich	M.S. Environmental Engineering M.S. Applied Mathematics (Statistics)
Statistician	Tom Stockton	Ph.D. Environmental Modeling GoldSim Training
Hydrologist	Michael Sully	Ph.D. Soil Science GoldSim Training

4.0 Project Description

The safe storage and disposal of depleted uranium (DU) waste is essential for mitigating releases of radioactive materials and reducing exposures to humans and the environment. Currently, a radioactive waste facility located in Clive, Utah operated by Energy*Solutions* is proposed to receive and store DU waste that has been declared surplus from radiological facilities across the nation. The Clive facility has been tasked with disposing of the DU waste in an economically feasible manner that protects humans from future radiological releases.

To assess whether the proposed Clive facility location and containment technologies are suitable for protection of human health, specific performance objectives must be met for land disposal of

radioactive waste set forth in Title 10 Code of Federal Regulations Part 61 (10 CFR 61) Subpart C, and promulgated by the Nuclear Regulatory Commission (NRC). In order to support the required radiological performance assessment (PA), a detailed computer model will be developed to evaluate the doses to human receptors that would result from the disposal of DU and its associated radioactive contaminants (collectively termed "DU waste"), and conversely to determine how much DU waste can be safely disposed at the Clive facility.

5.0 Critical Tasks and Schedule

Critical tasks for meeting project objectives are described in Table 2 below including the associated product and scheduled deliverable dates.

Table 2: Critical tasks for meeting project objectives, task products, and scheduled completion dates.

Task	*Product*	*Scheduled Completion Date*
Task 1. Develop a Performance Assessment Model		
SubTask 1a. Attend Kick-off Meetings	Meeting Attendance	September 2009
SubTask 1b. Model structuring based on Features, Events and Processes	Conceptual Site Model Report Preliminary GoldSim Model	February 2010
SubTask 1c. Develop a Model Representative of a Single Disposal Embankment Cell	Fully-functional probabilistic GoldSim model for a single cell	December 2010
SubTask 1d. Compare results of the initial model to the existing modeling effort	Model comparison report	August 2010
SubTask 1e. Perform Uncertainty and Sensitivity Analyses on the initial model	Uncertainty and Sensitivity Analysis report	September 2010
SubTask 1f. Demonstrate Preliminary Model and Solicit Feedback	Presentation and Training	October 2010
Task 2. Develop a Complete Model Encompassing All Candidate Disposal Cells	Complete GoldSim ES DU Model v1.0 including QA documentation, User Guide, electronic references, and supporting information	February 2011

Task	*Product*	*Scheduled Completion Date*
	Delivered on CD or DVD media	
Task 3. Training		
SubTask 3a. Train Various Audiences in Use of the Model	Training sessions	TBD
SubTask 3b. Provide Technical Information, Training, and Interactions with the Utah Division of Radiation Control and/or other Stakeholders	Technical presentations, training sessions, question and answer sessions, and other interactions as required	TBD
SubTask 3c. Assist in Technical Interactions with the Nuclear Regulatory Commission.	Provide responses to comments and requests for additional information as needed	TBD
Task 4. SQAP	SQAP revisions	Version 1 December 2009
Task 6. Project Management	Administration, reporting, planning, participation in presentations and publications	

6.0 Quality Objectives and Model Performance Criteria

Systematic planning to identify required GoldSim model components will be accomplished through the development of a conceptual site model (CSM) for the disposal of depleted uranium at the Clive facility. This CSM describes the physical, chemical, and biological characteristics of the Clive facility.

The CSM encompasses everything from the inventory of disposed wastes, the migration of radionuclides contained in the waste through the engineered and natural systems, and the exposure and radiation doses to hypothetical future humans. These site characteristics are used to define variables for the quantitative PA model that is used to provide insights and understanding of the future potential human radiation doses from the disposal of DU waste. The content of the CSM provides the basis for selection of the significant regional and site-specific features, events

and processes that need to be represented mathematically in the PA model. A report describing the CCM will be developed as part of Task 1.

As described in Section 4.0 the objective of the PA is to provide a tool for determining if specific performance objectives will be met for land disposal of radioactive waste set forth in Title 10 Code of Federal Regulations Part 61 (10 CFR 61) Subpart C, and promulgated by the Nuclear Regulatory Commission (NRC). The quality objective for the model is to provide results that are consistent with the site characteristics, the waste characteristics, and the CSM. If data are available, the demonstration of consistency will be supported by available site monitoring data and other field investigations. The model predictions of transport of radionuclides and the inadvertent intrusion into the disposal facility, and the sensitivity and uncertainty of the calculated results should be comprehensive representations of the existing knowledge of the site and the disposal facility design and operations.

7.0 Documentation and Records

Subversion version-control software will be used to maintain records of ownership and traceability of all project-specific files and database contents. Original data are stored in version-controlled repositories. Additions, deletions and file modifications within the repository are tracked by the version control software, which documents the file user and the date and time of modification. The version control software also offers a "compare between revisions" feature for text files that denotes line-by-line changes between previous and current versions of a file. User-entered comments are also maintained by the version control software as files are added, deleted, or modified. Version control of records is described in more detail in the Energy*Solutions* Subversion SOP in Appendix A.

Internal documentation of the GoldSim model, version change notes, change log, model versioning, and model error reporting and resolution are described in the Energy*Solutions* GoldSim Model Development SOP in Appendix B and the Energy*Solutions* Issue Tracker SOP in Appendix C.

8.0 Data Acceptance Criteria

The choice of data sources depends on data availability and data application in the model. The following hierarchy outlines different types of information and their application. The information becomes increasingly site-specific and parameter uncertainty is generally reduced moving down the list.

- Physical limitations on parameter ranges, used for bounding values when no other supporting information is available. *Example: Porosity must be between 0 and 1 by definition.*
- Generic information from global databases or review literature, used for bounding values and initial estimates in the absence of site-specific information. *Example: A common value for porosity of sand is 0.3.*

- Local information from regional or national sources, used to refine the above distributions, but with little or no site-specific information. *Example: Sandy deposits in the region have been reported to have porosities in the range of 0.30 to 0.37, based on drilling reports.*

- Information elicited from experts regarding site-specific phenomena that cannot be measured. *Example: The likelihood of farming occurring on the site sometime within the next 1000 years is estimated at 50% to 90%.*

- Site-specific information gathered for other purposes. *Example: Water well drillers report the thickness of the regional aquifer to be 10 to 12 meters.*

- Site-specific modeling and studies performed for site-specific purposes. *Example: The infiltration of water through the planned engineered cap is estimated by process modeling to be between 14 and 22 cm/yr.*

- Site-specific data gathered for specific purposes in the models. *Example: The density of* Pogonomyrmex *ant nests adjacent to the site is counted, and found to be 243 nests per hectare.*

The determination of data adequacy is informed by a sensitivity analysis of the model, which identifies those parameters most significant to a given model result. Such parameters are candidates for improved quality. As the model development cycle proceeds, sensitive parameters are identified, and their sources are evaluated to determine the cost/benefit of reducing their uncertainty.

9.0 Data Management and Software Configuration

The acquired data, developed statistical distributions and results generated by the GoldSim model and the uncertainty and sensitivity analyses will be archived in a version-control repository as described in Section 7.0 above. Configuration management for the GoldSim model is described in the Energy*Solutions* GoldSim SOP in Appendix B.

10.0 Model Assessment and Response Actions

During model development assessments will be conducted using a graded approach with the level of testing proportional to the importance of the model feature. Assessments will consist of:

- reviews of model theory

- reviews of model algorithms

- reviews of model parameters and data

- sensitivity analysis

- uncertainty analysis

- tests of individual model modules using alternate methods of calculation such as analytic solutions or spreadsheet calculations
- reasonableness checks

Response actions including error reporting and resolution processes are described in the Energy*Solutions* GoldSim SOP and the Energy*Solutions* Issue Tracker SOP.

11.0 Model Requirements Assessment

The purpose of these assessments is to confirm that the modeling process was able to produce a model that meets project objectives. Model results will be reviewed to ensure that results are consistent with the site characteristics, the waste characteristics, and the CSM as described in Section 6.0. Model results will be assessed to determine that the requirements of Energy*Solutions* for the use of the model have been met. Any limitations on the use of the model results will be reported to the project manager and discussed with Energy*Solutions*.

Appendix A - Energy*Solutions* Subversion Standard Operating Procedure

Neptune and Company (N&C) Internal Procedure
Confidential

General Procedure: Standard Operating Procedure (SOP) Contract Specific: Internal N&C product	**Document No.** 06245-002	Version: 01
Document Status: Final		
Title: Energy*Solutions* Subversion SOP		**Author:** Warren Houghteling **Revised by: N/A**
Final Approval Signatures		**Date**
Corporate Quality Assurance Officer: Print Name: James Markwiese Signature:		12/21/1010
Neptune and Company Project Manager Print Name: Paul Black Signature:		12/21/2010
Effective Date: 12/21/2010		Page 1 of 11

Date Stamp: 2/22/2011

Energy*Solutions* Subversion SOP

Introduction

Subversion is an open source version control system. Version control is the management of changes to documents, programs, and other information stored as electronic files. Neptune uses subversion to manage work products and other project information that can be stored as electronically. Subversion has two major features that support increased productivity and better Quality Assurance:

1) Subversion allows the easy sharing of file in a way that allows all project participants to have access to the latest version of the file. No longer is it necessary to send emails back and forth with updates to work products, a process which can often lead to confusion as to which document version contains all the latest changes
2) Subversion keeps a copy of every "committed" version of the file in its database, making it easy to go back to earlier versions of a file. No file version is ever deleted in subversion. The progression of changes in any file can be tracked via the comment feature, which allows the user to add a comment describing what had changed each time they commit an edited version of a file to the database.

Repositories

As the Subversion online manual (http://svnbook.red-bean.com/) states, Subversion is a centralized system for sharing information. At its core is a repository, which is a central store of data. The SVN repositories live on a central server, SVN.neptuneinc.org. New repositories can be created on the server at any time. To the user, a repository appears as a collection of files and directories (although they are not actually stored that way on the SVN server).

Users access the contents of a repository by "checking out" a local copy of the repository. This process copies files from the repository to the user's computer, creating a local "working copy" of the repository. The user can then make changes to their local copy and "commit" these changes back to the repository, so they become part of the centralized data store. To get the latest changes committed by others, the user should periodically "update" their repository, a process which pulls down any new changes from the server that are not yet part of the user's working copy.

Repositories have typically been created on a per-project basis, but some have instead been created to house all the data associated with a particular client (for example, the EPA repository). The latter approach produces very large repositories,

which can make downloading the whole repository very time consuming, especially for users outside the Los Alamos office where the server resides. However, this can be worked around by the user checking out only the sub-folders they need from a given repository. This will be discussed in more detail later in this document.

Accessing Repositories

To access Neptune's subversion repositories, you will need two things:

1) a subversion user account on the server
2) a client program running on your computer which can interact with the subversion server to allow you to check out, update, and commit files

Obtaining a Subversion Account

This should be done automatically as part of your new-employee setup; however, if for some reason you find yourself without an account, any member of the IT team can set you up with one. You will receive a username and a password, which need to be submitted for most SVN transactions. Fortunately, all SVN clients provide the opportunity to cache your identity so that you do not have to repeatedly enter your credentials.

Subversion Clients

Windows GUI

On Windows machines, the main client we use is Tortoise SVN, which is available from Tigris.org. Its home page is http://tortoisesvn.tigris.org/. Downloading and installing Tortoise SVN is a straightforward process, but IT staff will always be glad to offer assistance if needed. Tortoise works as a plugin to Windows Explorer (NOT Internet Explorer the web browser, but the file explorer); once you have Tortoise installed, you will see special icons next to files that are part of working copies, and you will have access to SVN commands via right-clicking on any file or folder in Windows Explorer.

Other clients are available – the other client that software developers use is a plugin to the Eclipse development environment called Subclipse (also from Tigris).

Mac GUI

There are two main Mac clients currently in use at Neptune, SCplugin (http://scplugin.tigris.org/) , which mimics some of the Tortoise functionality but unfortunately does not have all features enabled on the latest OS version (Snow Leopard), and svnX (http://www.lachoseinteractive.net/en/community/subversion/svnx/), which has a richer feature set but a very different UI concept. Both clients are useful and can even coexist on the same machine. As is the case on Windows, plugins are also available for various development environments (e.g. Netbeans, Eclipse).

Command Line

On Linux and other Unix-based systems (including the Mac), there is a command-line client program called SVN. The command line client is the most flexible and powerful way to interact with subversion, and may be needed in special situations to address issues that the GUI clients cannot handle. In these cases, IT personnel can lead you through the necessary steps.

Getting Started with Subversion

Your first experience with subversion will likely involve someone on your project team telling you to check out a repository (or sub-section of a repository) so you can examine and/or modify files. You will need the URL of the repository (or sub-directory) to be able to check it out. All Neptune SVN URLs will begin with http://SVN.neptuneinc.org/repos followed by the repository name. So if I wanted to check out the entire Neptune repository (not recommended, as it is very large), I would use the URL http://SVN.neptuneinc.org/repos/neptune.

Trunk, Branches, and Tags

Most repositories have three top-level directories called trunk, branches, and tags. The trunk represents the main line of work in the repository – the branches and tags folders have specialized uses, which will be discussed later (they are mainly relevant to programmers). When someone asks you to check out the "project1" repository, and that repository has a trunk, the URL you will want to use is http://SVN.neptuneinc.org/repos/project1/trunk. However, the name of the directory you will create to check the files out into should be called project1, so you will know what repository you are working with.

Checking Out

Once you have been given the URL of the repository you want to check out, you will enter that URL into your subversion client as part of a "checkout" operation. Depending on you client, you may need to create the containing directory first, or the client may do it for you if you indicate a directory that does not yet exist. Either way, the files you have requested will be copied from the SVN server to the location you have specified. Subversion does NOT CARE where on your machine you chose to store your files. Subversion keeps hidden "metadata" folders inside each folder of your working copy. One of the things these metadata folders keep track of is what URL on the server the current directory corresponds to. This means that you can move the location of the working copy on your computer, and this will *not affect subversion at all* – it still knows where to go on the server to get updates for those files, or commit changes to those files

If the repository is large, and especially if you are not in the Los Alamos office where the SVN server resides, this initial checkout could take a long time. Your client will show you a running progress display, usually listing each file that is pulled down from the server. If the listing seems to get "stuck" on a particular file, that probably means that the next file in the list is very large, as the files are not listed until their download is complete. Occasionally, you will some kind of "timeout" error message during a long checkout. In this case, it almost always works to simply update your working copy to get the rest of the files (see the next section for updating).

Updating

As time passes, other team members may make changes to files in the repository you have checked out. The only way for you to see these changes to update your working copy of the repository. Your SVN client will allow you to select any directory or file in a working copy and request that it be updated. Usually, you will want to pick the top-level directory, so you can get all the updates at once. As with checking out, your client will give you a listing of files, but in this case it will only be files that have versions newer than the one you already have in your working copy. If nothing has changed, you will see a message confirming that your working copy is already at the latest version, for example "at revision 258."

Conflicts

If you have changed a file in your working copy, and someone else has changed the same file in their working copy and committed (uploaded) their change back to the server, you may get a conflict notification. If the file is plain text, and the changes in the repository are in a different part of the file than the changes you made, you will see a notification that those changes have been merged into your version of the file

(there will be a G after the file name in the list of changes). However, if your text changes conflict with the changes from the repository, or if the file is a binary file, you will get a conflict. We will talk about resolving conflicts later in this document.

Committing

When you have made changes to one or more files and want to publish those changes back to the repository, you need to commit them. Your SVN client will allow you to select a file or directory and issue the commit command. The client will show you a list of the changed files it found, and offer you the option of unselecting any files that might have changes you are not ready to commit. It will also provide you a space to enter a comment describing the changes made to the file(s) in question. It is critical that a meaningful comment always be filled in. This requirement will be discussed in more detail later in the document.

Adding New Files or Folders

If you create a new file or folder inside a directory that is part of your working copy, it has no effect on the repository until you first add the file to the working copy and then commit that addition. Most GUI clients allow you to combine these operations by including new files in the list of changes when you begin the process of committing a directory. New files will usually appear with a question mark next to them. If you check the box next to a new file, you are telling the client program to first add the file to the containing directory and then include that addition in the final commit operation. Some GUIs will have a check box that allows you to toggle whether or not new files are shown in the commit list.

Why Commits Can Fail

The main reason that a commit will fail is if one of the files to be committed is not the latest version from the repository. Subversion will not allow you to potentially overwrite someone else's changes. For example, you cannot commit a file that is based on an earlier version than the latest version from the repository. When a commit fails for this reason, the only thing to do is to update. If the file is a text file, you may find that the changes in the repository are simply merged into your file. However, the most likely scenario is that you will get a conflict, which you will then have to resolve (see Resolving Conflicts later in this document).

Practically speaking, this means that just before you begin editing a file, you need to do an update to make sure you have the latest version. Also, if the file is binary (e.g. a MS Word document), you will want to let other members of your team know that you are editing the document, so that they won't start editing in parallel. Of course, for large documents, there are strategies that allow for editing files in parallel when

you know that your changes will not conflict with your colleagues' (for example when two people are editing different sections of the document). These strategies will be discussed later under the Workflow section.

Reverting Changes

Sometimes you may be working on a file and wish to discard all your changes and return to the base revision from the repository. This might happen if you were to realize that you had been modifying the wrong file, or for a variety of other reasons. The revert command will discard all local changes and restore your working copy with a "pristine" version of the last version of the file or files you checked out.

Sometimes reverting is the best way to resolve a conflict. You can always save your version of the changed file to a different location and then revert the conflicted file. This will give you the latest file from the repository, and allow you to examine that file and see how it differs from yours, so you can incorporate your changes into the new version.

Subversion Workflow

Repository Creation

A repository can be created at any time by a member of the IT staff. Repository names must conform to the following requirements (not that not all existing repositories conform):

- all lower case
- no spaces – use underscores instead
- alphanumeric characters only – no special characters

Repositories are created on an as-needed basis. Once again, communication is key – team members should decide if their project needs a new repository or if it best fits inside an existing repository.

The structure of the files within the repository is also a team decision. Several templates have been used on different types of projects. Specific template examples may be made available in the future to use as starting points for new projects.

Working with Existing Repositories

You always have the option to check out an entire repository, or just a subsection of a repository. The only difference between the two is the URL that is passed to the checkout command. To check out an entire repository, your URL will look like this:

http://SVN.neptuneinc.org/repos/repository_name/trunk

or, in the case of a repository with no trunk,

http://SVN.neptuneinc.org/repos/repository_name

If you only want to check out a sub-section of the repository, you simply include the path to the sub-section in your URL. Here is an example of how to check out just the QA folder (containing the new company QA plan documents) from the Neptune repository:

http://SVN.neptuneinc.org/repos/neptune/trunk/QA

This way you only get a folder with three documents rater than an entire repository with many Gigabytes of data.

Repository Browsing

Many of the GUI clients include a feature that allows you to "browse" the repository on the server. By entering the base URL of the repository (for example, http://SVN.neptuneinc.org/repos/neptune) in the browser window, you can view the structure of the repository as it is on the server without having to download anything. This is a great way to figure out what you might need to check out for a given purpose. For example, the browser will show you that under the trunk of the Neptune repository there is a Business Development folder, which in turn contains a proposals folder. If you are just interested in seeing the proposal work done for DOD, you can just check out the DOD folder from inside the proposals folder. Most repository browser GUIs allow you to select a sub-folder from within a repository and ask to check it out. At worst, you can use the browser view to see how to build the URL you will need to check out the sub-folder you are interested in.

One thing that a repository browser GUI will NOT do is allow you to see all the different repositories on the server. To see a list of all repositories, visit to the password-protected web page at http://repositories.neptuneinc.org/index.php. You can get the username and password from one of the IT staff.

Making Changes

There are three kinds of changes you can make to a repository:

1) Modify existing files in a repository
2) Add new files to a repository
3) Reorganize the structure of a repository

Modifying Existing Files

As noted earlier, always do an update before you begin modifying files, to make sure that you are working on the latest versions. Also, especially in the case of binary files, notify other team members that you will be modifying the file(s).

Using Locks to Enforce Serial Editing of Binary Documents

The best way to avoid conflicts when editing files is to use subversion's locking feature. Both svnX on the Mac and Tortoise on Windows give you access to this feature. Locking a file is simple. First be sure you have the latest version of the file by running an update. Then use the GUI (or command line) to invoke the lock command. (you will get an error message if a more recent version of the file exists in the repository). Once a file is locked, no one else can commit changes to that file – they will receive an error when trying to commit, telling them the file is locked and the name of the user who has the lock.

Therefore, when editing a binary file, one should ALWAYS lock the file first. If someone else already has the file locked, you will get an error with the lock owner's username, and you know that you need to wait for that team member to finish his or her edits before you can work on the file. If you successfully gain the lock, you can be sure that no one will commit a new version that will then cause a conflict when you try to commit yours. When you commit your version of the file, the lock is automatically released.

In case someone locks a file and then forgets about it and goes on vacation, locks can be broken (you may need help from an IT staff member to do this). Locks are not a strict enforcement mechanism – rather they are a way to enhance team communication.

Editing Binary Documents in Parallel

In cases of large binary documents with many sections, team members may work on a file in parallel, with the understanding that the different team members are working on different sections of the file. When one team member is ready to commit their changes, they may do so, and the other member(s) then need to update their versions. Before doing so, they should save their versions with changes to a location outside of their working copy, or save their changes to a new filename, perhaps with their initials appended (for example, save Report1.docx as Report1_WH.docx. This way, before the other members update, they can revert their changes in the repository to avoid a conflict when they updated to get their colleague's changes (the revert operation can also happen after the conflict – this will discard all local changes and leave the working copy with the latest version from the repository). The next team member to finish their edits can then copy just their section into the new version of the document and commit those changes. As discussed in the previous section, locks can be used to enforce the order in which

changes are made to the document. Needless to say, this process requires good communication among team members to make sure that no ones changes are unintentionally overwritten.

In all cases it is REQUIRED that a comment be entered which summarizes the changes to the file as part of the commit process. This is essential to leveraging the full power of Subversion to provide support for Quality Assurance by providing a clear trail of comments explaining how documents evolve over time. If the project is using Bugzilla to track tasks, the comment should include references to Bugzilla task numbers where appropriate (for more details see the Bugzilla SOP).

Adding New Files

Generally, there are two kinds of new files we add to a repository. The first are new Neptune-created files, which may become work products or simply supporting project information. In these cases, it is REQUIRED to enter a comment describing the purpose of the file and perhaps its initial content.

The second type of files we add to repositories are files received from outside sources – reports, data, communications from clients, meeting minutes, etc. In these cases it is CRUCIAL that the comment contain as much detail as possible about the provenance of the file. Being able to track down exactly where we got the file and from whom is crucial to the QA process. So the comment "adding new Eco data" is fairly useless, whereas "adding new mammal field data received from Brett Tiller via email on 7/21/2008" gives us solid backward traceability to the source of the data.

Reorganizing the Structure of a Repository

This operation is the one most likely to lead to confusion and errors if it is done incorrectly. As mentioned earlier in the document, each directory in a working copy keeps hidden metadata about how it corresponds to the data in the repository on the server. This means that moving directories around on your computer has NO EFFECT on the structure of the repository on the server. You must move a special "SVN move" command to let the working copy know that you want to modify the directories in the working copy by adding or removing files from the (a move operation will delete files from one directory and add them to another). The actual effect on the repository will not take place until you commit your changes which include the moved files.

Similarly, deleting files from your working copy will have NO EFFECT on those files in the repository. You must use a special "SVN delete" command to let the directory containing those files that they are scheduled for deletion. The actual deletion of the files will not take place until you commit your changes that include the SVN deletes.

It is important to realize that deleting a file does NOT delete the file from the repository. It simply deletes the file from the latest version of the repository. It is always possible to go back to earlier versions of the repository to "resurrect" deleted files.

Finally, because deleting files from your hard disk does not affect the repository, this can be a good last-ditch solution for solving SVN problems. Occasionally, the metadata in some part of a working copy may become corrupted, leading to error messages when you try to update the repository or delete files. You can always delete the directory to which the error message refers and then run an update on the containing directory to get a fresh copy of the data pulled down from the repository. Of course, if you have changed files in the problem directory or any of its sub-directories, you should first copy the changed files to a location outside your working copy before deleting the problem directory. Then once you have done the update to get a clean copy of the directory, you can copy your changed files back into their appropriate locations in the working copy, and they will once again show up as changed files that you can commit.

Appendix B - Energy*Solutions* GoldSim Model Development Standard Operating Procedure

Neptune and Company (N&C) Internal Procedure
Confidential

General Procedure: Standard Operating Procedure (SOP) Contract Specific: Internal N&C product	**Document No.** 06245-003	Version: 01
Document Status: Final		
Title: Energy*Solutions* GoldSim Model Development SOP		**Author:** John Tauxe **Revised by: N/A**
Final Approval Signatures		**Date**
Corporate Quality Assurance Officer: Print Name: James Markwiese Signature:		
Neptune and Company Project Manager: Print Name: Paul Black Signature:		
Effective Date: 12/21/2010		

Date Stamp: 2/22/2011

Energy*Solutions* GoldSim Model Development SOP

22 February 2011

Prepared by

Neptune and Company, Inc.

1. Title: GoldSim Model Development SOP			
2. File Name: GoldSim Model Development SOP.docx			
3. Describe Use: This document describes the standard operating procedure for the development of GoldSim Models. Some language is specific to model development for Performance Assessment-type models.			
	Printed Name	Signature	Date
4. Originator	John Tauxe		15 Dec 2009
5. Reviewer	Warren Houghteling		21 Dec 2009
6. Remarks: Revised to generalize to all PA-type GoldSim model development. - 16 Jun 09 JT Minor revisions and clarifications. - 15 Dec 09 JT Review and additional modifications for Energy*Solutions* work. - 29 Dec 09 JT Revised to SOP content – 2 Feb 2011 MS			

CONTENTS

FIGURES

1.0 Introduction

This standard operating procedure (SOP) describes the development of GoldSim-based computer models. These models are used to perform contaminant transport and dose assessment calculations as the computational basis for radiological Performance Assessments (PA). They are developed using the GoldSim™ systems analysis software, developed by the GoldSim Technology Group (GTG), as a principal platform, commonly in conjunction with various supporting computer programs and data sources. Throughout this document, the term Quality Assurance (QA) refers to a program for the systematic monitoring and evaluation of the various aspects of a GoldSim model development to ensure that standards of quality are being met.

2.0 Modeling Lifecycle

GoldSim model development follows a structured process or lifecycle that requires a graded approach to quality assurance at each phase. The lifecycle for GoldSim model development is described below and correlates with the work process shown in Figure 1.

2.1 Conceptual Model Development

Model development begins with the development of a Conceptual Site Model (CSM). The conceptual site model identifies important features and processes of the system being modeled that are consistent with the existing data. While the process of developing the CSM does not fall under the scope of this SOP, it is mentioned here because it forms the basis for the GoldSim model design.

The CSM is documented in a Conceptual Site Model document, which explains and provides justification for the mathematical approaches for modeling geological, hydrogeological, contaminant fate and transport, and other component process of the overall model. Existing data and literature and expert opinion are used to support the modeling approach described by the CSM.

2.2 Model Requirements Evaluation

The CSM provides a description of the attributes and capabilities of the software required to meet the project objectives. An evaluation is conducted to verify that the GoldSim modeling platform is capable of providing these required attributes and capabilities.

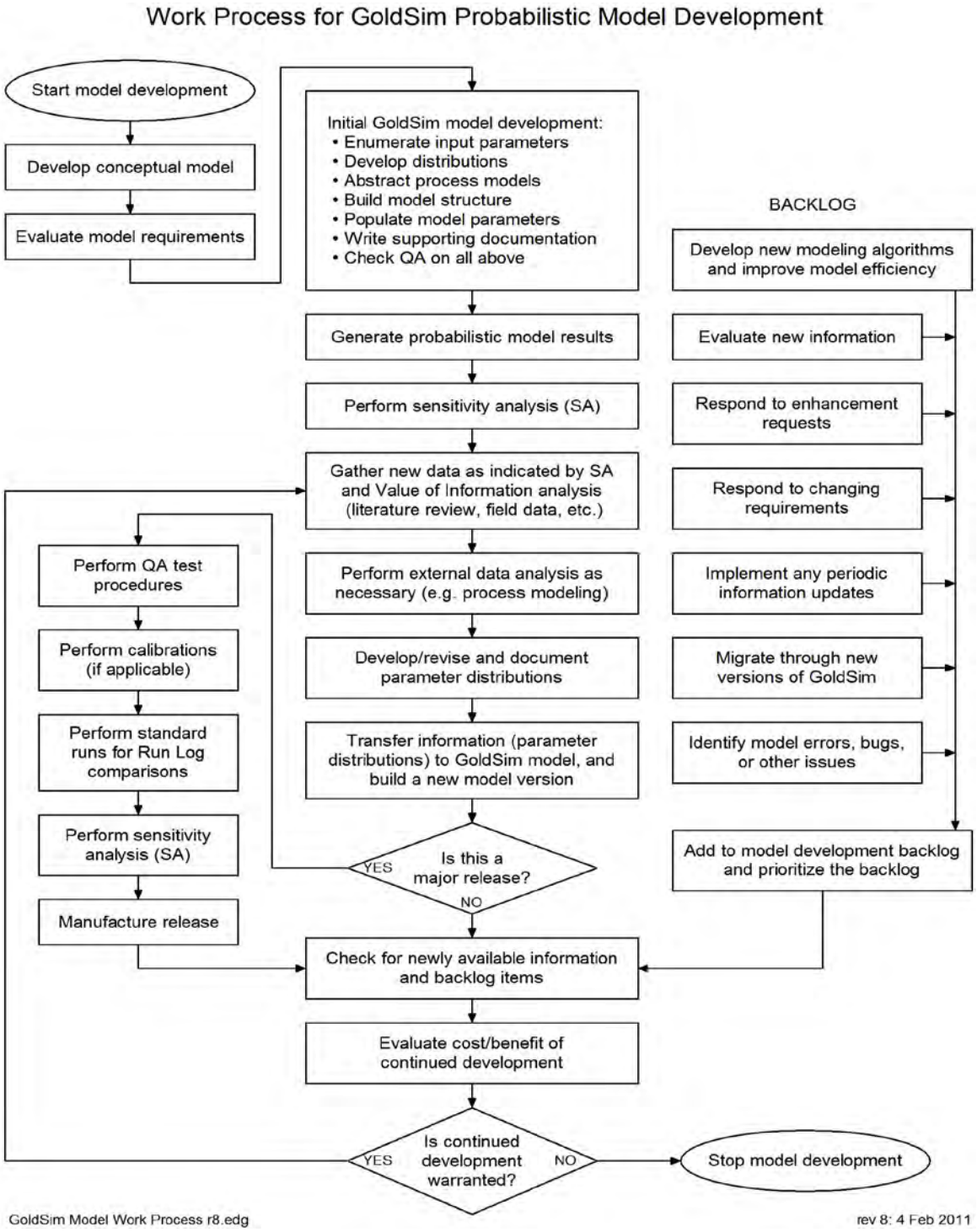

Figure 1: Model development work process flow diagram.

2.3 Verification of Software Installation

The GoldSim software is installed and registered as described in the GoldSim User's Guide (GTG 2010a). Following the installation and registration the user runs the example model "FirstModel.gsm" located in the "General Examples" directory and verifies that the output obtained matches the chart shown on page 26 of the User's Guide (GTG 2010a).

The GoldSim User's Guide (GTG 2010a) and the GoldSim Contaminant Transport Module User's Guide (GTG 2020b) provide complete descriptions of the features and capabilities of GoldSim and the Contaminant Transport Module.

2.4 GoldSim Model Development

To begin model development individual modelers work in parallel to model specific sub-processes described in the CSM. For example, existing mathematical models are translated into specific algorithms to be used in the modeling process. GoldSim offers a level of model structure that can closely resemble a conceptual model, so the structural implementation of the GoldSim model will follow the conceptual model developed by the project team. As the different components of the model are developed in GoldSim, they are integrated to form a coherent model of the overall process being studied. GoldSim's object-oriented structure facilitates this process, often allowing independently developed sub-modules to be copied and pasted into the main model. GoldSim's "self-documenting"features allow the graphical user interface (GUI) design to incorporate documentation of modeling concepts and parameter derivation, so that it is relatively easy to crosswalk between individual GoldSim pages and sections of the CSM document.

2.5 Model Data Inputs

2.5.1 Input Data Selection

The development of appropriate definitions of input parameters is guided by model sensitivity analyses, which identify those parameters most important in determining the model results. In some cases, the definition of an input value matters little to the results and in these cases less effort is expended in developing distributions. Sensitive parameters, however, warrant a closer investigation, and their input distributions are devised with great care where possible. All parameters in the model are based on some sort of information source, be it a "literature value", the result of a site-specific data collection campaign, or the result of expert professional judgment.

2.5.2 Input Data Placeholders

On occasion, a modeling element must be added to the model in order to proceed with construction, but no value has yet been developed. In this case, an *ad hoc* placeholder value is chosen so that model development may continue, and the parameter is noted as a placeholder.

Before the model can be relied upon for any purpose, however, all such placeholder values must be replaced with suitably-derived and documented values.

2.5.3 Data Acceptance Criteria

The sources of input data for the model are various, and the quality of the source is a compromise between model sensitivity (identifying the need for high-quality data), availability, appropriateness, and the ability (budget and/or practicality) to generate data of sufficient quality. Input parameters that have a strong influence on the model results as determined by sensitivity analyses are given higher priority than those with little influence.

The choice of data sources depends on the availability and application of the data in the model. The following hierarchy outlines different types of information and their application. The information becomes increasingly site-specific and parameter uncertainty is generally reduced moving down the list.

- Physical limitations on parameter ranges, used for bounding values when no other supporting information is available. *Example: Porosity must be between 0 and 1 by definition.*

- Generic information from global databases or review literature, used for bounding values and initial estimates in the absence of site-specific information. *Example: A common value for porosity of sand is 0.3.*

- Local information from regional or national sources, used to refine the above distributions, but with little or no site-specific information. *Example: Sandy deposits in the region have been reported to have porosities in the range of 0.30 to 0.37, based on drilling reports.*

- Information elicited from experts regarding site-specific phenomena that cannot be measured. *Example: The likelihood of farming occurring on the site some time within the next 1000 years is estimated at 50% to 90%.*

- Site-specific information gathered for other purposes. *Example: Water well drillers report the thickness of the regional aquifer to be 10 to 12 meters.*

- Site-specific modeling and studies performed for site-specific purposes. *Example: The infiltration of water through the planned engineered cap is estimated by process modeling to be between 14 and 22 cm/yr.*

- Site-specific data gathered for specific purposes in the models. *Example: The density of* Pogonomyrmex *ant nests adjacent to the site is counted, and found to be 243 nests per hectare.*

The determination of data adequacy is informed by a sensitivity analysis of the model, which identifies those parameters most significant to a given model result. Such parameters are candidates for additional measurements or more deliberate estimation. As the model development cycle proceeds, sensitive parameters are identified and their sources are evaluated to determine the cost/benefit of reducing their uncertainty.

2.5.4 Records of Parameter Values

One limitation of the GoldSim platform is that there is no straightforward way to examine all the values of inputs (data and stochastic elements) in one place. The user must search the model and open (or "mouse-over") each input element individually in order to see its value. In order to overcome this inconvenience, all the parameter inputs are stored external to the model, in the Parameter List documents.

2.5.5 The Parameter List

The Parameter List is a complete list of the input parameters for the model, and may consist of a text document, a workbook of spreadsheets, a database, or a combination of these, depending on the changing capabilities of the GoldSim modeling platform. Each parameter is listed in only one place, so that there is no ambiguity about the proper value of a parameter. Accompanying the listing of the parameter value in the Parameter List is a reference to its origin, which may be in a white paper or literature reference. Any change to a parameter is made to the Parameter List first, and then the change is made to the model. The value in the Parameter List is cross-checked to its source via a check print (see below), and the value in the model is then changed, noted in the Version Change Note for the modified element, and in the Change Log.

2.5.6 Check Prints

Whenever information (e.g. a parameter distribution) is transferred from one record to another (e.g. from a site document to the Parameter List) a QA Check Print process is invoked. This process is intended to positively and unambiguously document the source of information for each model input parameter or distribution. Since GoldSim is not capable of printing out a list of all the parameters that exist in the model, a separate document—the Parameter List—is maintained in exact concordance with the model at all times.

The flow of information is from primary sources (field data, literature, expert elicitations, etc.) to white papers that develop the input distributions (this step may not apply to all cases), to the Parameter List to the GoldSim model. QA check prints are maintained in all but the final step—transferring input values to the model. The check print process consists of obtaining paper copies of the data source and its destination, such as a paper from the literature and the Parameter List, for example. A comment field in the Parameter List (either a column in a table, a comment attached to a spreadsheet cell, or other location unambiguously associated with the data) identifies the value's origin. A paper copy of that page or pages of the Parameter List is stapled to a paper copy of the data source (which may be simply the page from the identified source), and the QA reviewer annotates each page. Typically, a yellow highlighter is used to indicate each

positively-checked value, and a red pen identifies any value that does not match. After checking each value against its source, the check print is documented with the date and the signature of the checker. Errors discovered in the process are noted, the errors are corrected in the destination document, and the values are rechecked with a subsequent check print, which is stapled to the original. This process is repeated until the check prints can document that information transfers are error-free. Check prints are stored as hard copy at N&C.

The final step of information transfer—from the Parameter Document to the GoldSim model—does not lend itself to check printing. However, traceability of parameter information can be maintained using GoldSim's internal QA tools, such as Note Panes and Version Change Notes discussed in Sections 3.0 and 4.0.

2.6 Model Assessment

Assessment of the proper operation of the Model is done on two levels. The overall model, as represented in the results, is subjected to benchmarking with process model results if a process model is available, and is compared to previous versions of the Model to assure that incremental changes are in line with those expected from modifications to the Model. On a submodel scale, particular parts of the Model may be assessed independently.

2.6.1 Validation/Verification

Many computer models that attempt to predict the outcomes of processes and events can be validated (verified) with measurable results. Due to the nature of performance assessments, which attempt to estimate concentrations and fluxes of materials in environmental media and the possible doses resulting from those materials far into the future, the results are not amenable to this validation. It is not possible to “test” the model to see if it has done a good job of predicting the dose to a hypothetical individual 10,000 years from now. The methods listed below, however, are used to demonstrate that reasonable efforts have been taken to ensure that the models are valid.

2.6.2 Benchmarking

Benchmarking consists of reproducing the deterministic results of the process model calculations using an established process model and GoldSim. This “benchmarking” is a fundamental high-level corroboration of the model implementation and calculations. Agreement between the two models serves to build confidence in the validity of the GoldSim model.

2.6.3 Reasonableness Checking

A model can incorporate several tools for checking the reasonableness of certain inputs and results. Examples follow:

- Intermediate results are provided where they are useful for checking calculations.

- Mass balance checks demonstrate that the mass of materials (soil, water, air) and radionuclides is preserved. This is a fundamental requirement of physical environmental models.

- To check the reasonableness of the results of a particular algorithm, the modeler may set up equation(s) both as an element in GoldSim and also using another tool, for example a Microsoft Excel Spreadsheet. This allows the modeler to compare results using two different calculation methods to provide a higher level of confidence that the algorithm has been implemented correctly in the GoldSim environment.

2.7 Model Review

Model development is subject to review by a modeler different from the one who did the original model building. As parts of the model are revised, with changes in parameters, expressions, or other functional elements, or model structure, these changes are reviewed for accuracy and completeness. Any accompanying text on the model pages is also reviewed for clarity and accuracy. The modeler making the changes identifies which parts of the model are subject to review, and another N&C GoldSim modeler examines these in detail, providing review comments to the originating modeler. The entire model is subjected to review before release to the client (see Section 4.7).

3.0 Model Documentation

3.1 Documentation Components

The Model is documented both internally and externally. Internal documentation includes the Change Log, Version Change Notes, modeling element Note Panes, and GoldSim's versioning capability. External documentation includes white papers, check prints, and a Parameter List. White papers document the development of specific algorithms and other inputs to the GoldSim model and are intended to explain and justify the approach taken.

A typical page in the model consists of model elements and explanatory text. Each page represents a modeling concept, and the model is logically divided into parts that will fit onto pages. Text at the top of each page explains the function of the page, and text juxtaposed with the model elements explains the function of the element, and provides information about its source. Each element also has a description field that is used for a short descriptive identifier.

The influence of one model element on another can be easily traced through the model using the “Show All Links” function attached to the triangle-shaped arrows on each side of the element graphic. The left triangle, pointing into the element, shows the other elements referenced by the current one, and the right triangle, pointing out of the element, shows the other elements that are dependent on it. By following these links, the complete interdependency of elements can be

traced through the model. In addition to descriptive text on the page, illustrations made with native drawing tools can be added to better communicate modeling concepts.

3.2 Model Element Note Panes

Associated with each GoldSim modeling element is the optional Note Pane feature. If an element has a note, it is identified by an underlined element name. Note panes have a dual purpose in the model. They are used for general information, describing the purpose of a container or element. They also serve the QA process, as a convenient place to make notes about the source of information or the status of QA review. While most of the note pane is free-format, the QA-related notes are to include a date (which can be cross-indexed to a version number using the Change Log, described below), the name of the person making the note, and a description about the nature of the QA check. For example, a QA note for an entire container might read:

1 Apr 05	JT	QA for this container completed
13 Apr 05	JT	QA updated with cross-check of water tortuosity exponent parameter values

and one for an individual element:

13 Aug 04	JT	Verified source of these data: Each value was checked against the 15th edition of the Chart of the Nuclides (General Electric Co. and Knolls Atomic Power Laboratory, 1996), wall chart version.
28 Sep 04	JT	Updated and verified source of these data: Each value was checked against the 16th edition of the Chart of the Nuclides (General Electric Co. and Knolls Atomic Power Laboratory, 1996), booklet version.

If an element is actually changed in the process of a QA review (or for any other reason), such change is noted in the Version Change Note associated with that element.

4.0 Model Configuration Management

Managing the model configuration through its various versions is critical to the production of a usable modeling product that meets client requirements. The following sections discuss various topics relevant to model modification and control.

4.1 Model Custody

During model development, the baseline model is tracked by the lead modeler. In the event that another modeler needs to have custody of the model for development purposes, the custody will be passed to that modeler and returned when the work is finished. The current custodian is always known, and is recorded on the topmost page of the model (except in released versions).

Modelers make use of the internal GoldSim versioning and Change Log in order to document changes made to the model.

A GoldSim model differs from many other software development projects in that it exists in a single binary file (with the ".gsm" extension). There are no separate files for subroutines as in a more low-level programming language like C, FORTRAN, or even Java. Therefore, the model cannot be edited by more than a single person at a time. At any given time, there is a single "main" model file. The custody of the main model must be explicitly passed from the lead modeler to another, and the custody is always known by the lead modeler, who is also the default custodian. The lead modeler may assign custody to another for a particular modeling task, but will resume custody when that task is completed. Upon return of custody, the returned model is inspected and one of two paths is chosen: 1) The returned model is maintained as the baseline model, or 2) the baseline model is modified appropriately to incorporate changes made in the returned model, and the modified baseline model is retained as the new baseline model. The baseline model resides on the custodian's computer, and is backed up by several methods; including off-site media (see Section 4.5).

4.1.1 Experimental Module Development

On occasion, model development requires some experimentation that may not be desirable in the main model. In such cases, a copy of the main model is made and given a unique file name in order to keep it distinct from the main model. This "branch copy" is used for module development and prototyping of modeling methods. Once the prototype of a specific module is complete, tested, and accepted, the new model parts are re-integrated into the main model, either by copying model containers and elements from the branch copy into the main model (the preferred method), or by re-entering elements directly into the main model in cases where GoldSim will not allow copying between model files. Either way, the additions and/or changes to the main model are cross checked for accuracy (by a modeler other than the one implementing the change), and the modifications are noted in the Change Log (see Section 4.2.211). At all times, however, there is only one main model file.

4.1.2 Criteria for Making Changes

Changes to the model occur at different levels. Minor changes to internal documentation language, including clarifications of text and correction of typographical errors, are made as they are identified, and without formal documentation. Changes involving any type of data input or calculation that could potentially affect the modeling results are documented in the Change Log.

A change to an input parameter (e.g. a distribution) may be precipitated by the following:

- QA review, in which model parameters are found to not match their values as documented outside the model. In such a case, the value in the model would be determined to be in error.

- A decision by a subject matter expert (SME), generally in consultation with other project team members, that a value should be changed for some technical reason, such as the availability of new data on which a distribution is based. This would be considered an update, and the change would cascade through the proper sequence, from an update to the data set, through development of an updated distribution, updating of the documentation in a white paper (if applicable) and in the Parameter List and finally an update to the model itself, with an accompanying entry in the Change Log and in the parameter element's Version Change Note (see Section 4.2.1. Each step in the change sequence is reviewed by an individual other than the person implementing the change.

- Major changes to the model, such as changing the species list, adding a contaminant transport process, a waste configuration, or an exposure scenario, are discussed and planned by Team SMEs.

4.2 Documentation of Changes

The documentation of changes made to the model is done at a level appropriate to the changes. If individual parameters are modified or added, this is documented with a note provided in the model element's Version Change Note, referencing the nature of the change, who made it, and date of the change. The name of the changed element is noted in the Change Log, along with the model version number, date of the change, the name of the person executing the change, and the name of the reviewer of the change process. Such changes may also be noted in the element's Note Pane or that of its container.

4.2.1 Version Change Notes

Version Change Notes (Figure 2) are automatically attached by GoldSim to any model element that has been modified, and are used to store information about changes in any particular element. GoldSim keeps a versioning database within the Model, consisting of a list of all changes to the model between version-stamps, and the text supplied in the Version Change Notes. At any time, GoldSim can generate a report of changes made between versions. Once a model version number has been incremented, all Version Change Notes are "reset" and a new set begins for that version. Any information that is to be maintained through versions for viewing by users or reviewers, such as QA reviews, is kept in the Note Panes associated with model elements or containers. Any time an element is edited, a log entry is generated internally by GoldSim documenting the event. Note that this happens even if nothing is actually changed in the element when the "OK" button is chosen in the dialog. Use of the "Cancel" button does not signal a change.

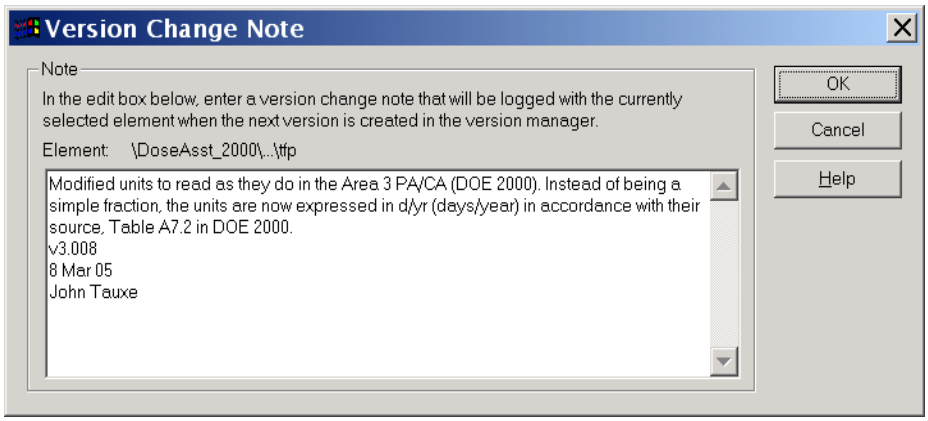

Figure 2: GoldSim provides for annotation regarding any change in an element's definition through the Version Change Note.

4.2.2 The Change Log

Neptune and Company GoldSim Models have a Change Log, which is stored in the note pane of the ChangeLog element as shown in Figure 3. This log is maintained by the modelers, and documents when a change was made, who made it, the model version number, and descriptive details. Modifications that could potentially change modeling results are noted to the level of the element changed, with more detail included in the element's Version Change Note or Note Pane. Modifications to explanatory text and changes to diagrams and other supporting material are noted in broad terms, such as "Modified figures depicting waste cell geometries." Typographical corrections are generally not noted.

All of these documentation techniques are used in model development. If a change was made to the model, or if part of the model was reviewed, this will be noted in the Change Log. A note regarding the QA review (and details, if necessary) will be made in the element's note pane or in its container's note pane. The container's note pane is appropriate if there are many similar elements in the container. If a change is made to an element, either from a QA review or for another reason, GoldSim will automatically provide the element with a Version Change Note, which is used for recording the change.

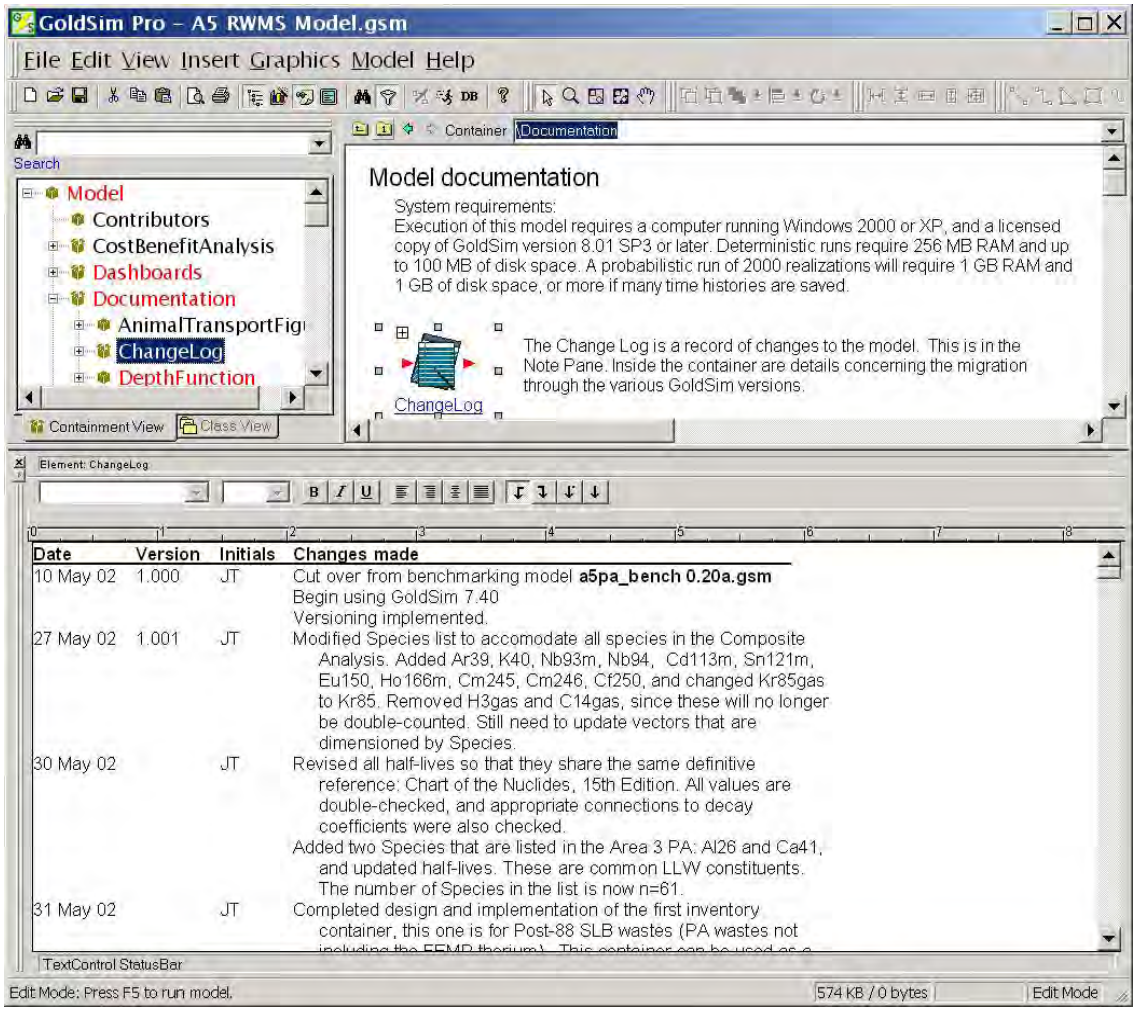

Figure 3: The model's Change Log can be maintained using a note pane or a formatted text box.

4.3 GoldSim Versioning

Introduced specifically as a model QA feature, GoldSim has model-level and element-level versioning built in to the Version Manager.

4.3.1 Model Version Numbers

At the model level, illustrated in Figure ***4***, version numbers are incremented at the modeler's discretion. The model version number is incremented as described below. GoldSim keeps track of changes made to the model in any given version, and can generate a report of changes made.

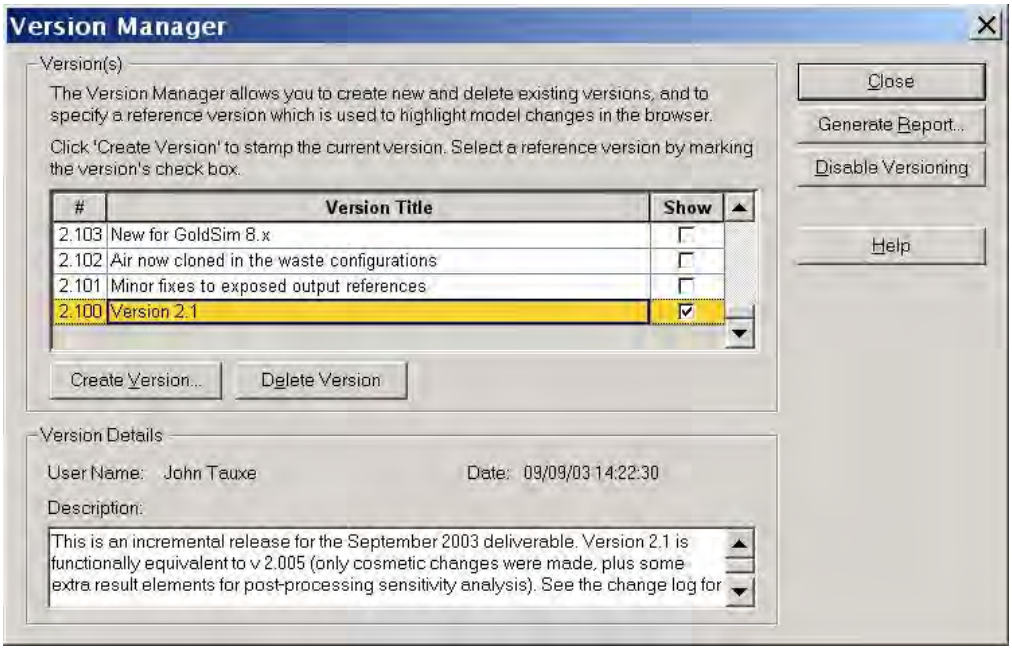

Figure 4: GoldSim's Version Manager.

Neptune GoldSim models use versioning at two levels: Release versions and development versions. Major revisions to the model, resulting in planned CD releases, generally proceed in increments of X.Y, with a change in X signifying a more significant model evolution than a change in Y. The assignment of these values is subjective, and may be decided upon in coordination with the client.

Model development uses GoldSim's minor version definition, which increments the Y in the three digits following the decimal point. For example, development following the release of version 2.1 starts with version 2.101. After making some changes to the model, a modeler decides to preserve the incremental version. At this point, the version number is incremented to 2.102 and the work proceeds, with 2.101 being archived.

Day-to-day and hour-to-hour development versions are noted with letters appended to the version number, such as 2.010a, 2.010b, etc. This is done so that during the process of editing the model, any change can be easily undone. When a specific modeling task is accomplished, the model is saved with the next letter in the sequence. As the changes are tested and accepted, the letter suffixes are dropped, and these intermediate versions are generally not archived. If a problem is found during testing of daily builds, or if the model file becomes corrupted, then the modeler can easily revert to a previously saved version of the model file and rebuild the part that caused the problem. This is preferable to attempting to "undo" the work, which takes time, can be prone to error, and clutters the internal versioning record.

4.3.1.1 Incrementing the version number

The following insert illustrates the documentation of incrementing development versions, as recorded in the Change Log:

1) Make a final entry in the Change Log under version 1.034 that you are incrementing the version number (see Figure 3):

   29 Jun 02 1.034 JJ Versioning counter updated to 1.034, and model saved.

2) Immediately change the internal versioning to 1.034 using “Model | Versioning...” (see Figure 4)

3) Save the model as "name v1.034.gsm", (any name plus the version number) overwriting all previous versions of that name.

4) Change the file attributes to “read only” so that the model file will not be inadvertently overwritten.

5) Change the front page and the Change Log entries to 1.035.

   29 Jun 02 1.035 JJ Begin work on v1.035.

6) Save the model as "name v1.035a.gsm" (or similar)

7) Begin work on version 1.035, starting at intermediate development version 1.035a.

8) After developing using intermediates 1.035a, 1.035b, 1.035c, etc., determine when to save the model as 1.035, and return to step 1) using the new version number.

4.3.1.2 Creating a versioning report

A report can be generated from GoldSim (using the “Generate Report...” button shown in Figure 4), listing all changes to the model for a particular version. The report is a text file with global changes as well as changes to individual elements, including the text from the Version Change Notes.

4.4 Model Testing

Any time a change is made to the model calculations that could change the results; the effects of the change are assessed. Model testing is relatively easy using GoldSim, since the results of any element in the model can be examined through a time series or final value. This enables straightforward parallel calculations to be done in order to verify correct and consistent operation. The modeling environment also allows the simple creation of temporary elements to perform calculations parallel to any others in the model.

Model testing is most readily done on discrete parts of the model, where results of a small number of straightforward calculations can be examined. Confirmation of discrete parts of the model are done by constructing a test model in GoldSim that is focused in its analysis. Ideally, this test model is excised directly from the main model, so that all relationships and definitions

are preserved. For example, to verify that GoldSim is performing diffusion calculations as expected, a simple GoldSim model can be constructed to examine the diffusion of materials between various media in two cells, and the results can be compared to an analytical solution to the diffusion equation. Calculations verified in the test model give confidence in the correct operation in the model.

4.5 Model Backup

Preservation of electronic model files is paramount in any software development project. Several redundant methods are employed for backup of the GoldSim model files and all other files and documentation. Foremost are project files maintained on an N&C server, which are backed up daily on a separate hard drive. Incremental versions of the model are likewise backed up locally and in addition to this, the lead modeler keeps a copy on his/her computer, and backs that copy up to a N&C server. Off-site backups are also maintained.

4.6 Error Reporting and Resolution

As errors are discovered, they must be identified, reported, and resolved. This section discusses the handling of errors in the development of a model. Formal tracking of errors, bugs, and other issues will be done using an issue-tracking system maintained by the QA manager and lead modeler.

4.6.1 Reporting Error Candidates

Errors such as typographical errors in supporting text are not considered in this process. Errors considered for this process include errors in parameter data entry or GoldSim programming. If an error is suspected, it is to be reported to the lead modeler along with any supporting information. It is the responsibility of the lead modeler to evaluate the error candidate and see that the issue is resolved.

Data entry errors may be discovered in input elements (Data or Stochastic GoldSim model elements). These are also brought to the attention of the lead modeler. These or any other modeling issues are to be entered into the issue-tracking system.

4.6.2 Assessing Error Candidates

Once an error candidate has been brought to the attention of the lead modeler via the issue-tracking system an assessment must be made to determine if the candidate is in fact an error. This is usually a simple process, involving examining a mathematical expression or a piece of entered data. Real errors are subject to resolution. False errors are commonly dismissed, noting the resolution in the issue-tracking system. If, however, the problem was due to some other cause, such as an ambiguity in documentation, the causes of the identification of a false error may require attention.

4.6.3 Resolving Errors

Errors, once discovered and confirmed, are usually easily remedied. Like other changes to the model, fixing an error is documented at least in Version Change Notes and the Change Log. Resolution is also noted in the issue-tracking system.

4.6.4 Error Resolution Verification

Checking the error resolution may be as simple as cross-checking an input value with the value in the Parameters List to ensure it is correct. Alternatively, a modification to an expression may involve an independent check of the calculation, using a spreadsheet, calculator, or a separate GoldSim model.

4.6.5 Error Impact Assessment

Each resolved error is assessed regarding its potential effect on the results. If the effect is anything more than negligible, its discovery and resolution are reported to the project participants via email. Similarly, if the error could have had an effect on the results of previous versions of the model, this is also reported.

4.7 Model Distribution

GoldSim models, like other computer model software, are open to modification. This is a benefit for modelers and researchers, since the logic is transparent and the model is easily maintained. This is a potential detriment to model integrity for the same reason. There are ways to tell if a model has been tampered with, however, as discussed above. Versioning, and the tracking of all changes between versions is important. Nevertheless, developers and clients alike need to know the configuration status of the model they are using, and the read-only media-released versions always provide unambiguous starting points.

Release versions of the model(s) are delivered to the client on read-only media (such as a CD-ROM), which inherently precludes modification of the models and supporting files. Using this method of delivery ensures that there is no ambiguity about the model and supporting documentation that constitutes the deliverable.

The standard GoldSim software allows for complete construction and editing of models. The companion GoldSim Player, however, is currently available at no cost and can run GoldSim models that have been specifically “exported” as Player versions. The Player version of the model is not editable. For distribution to the general public, a GoldSim Player version of a Model can be provided as part of the deliverable. The Player model cannot be modified in its significant parts, though the user can still operate switches and controls to evaluate various effects.

5.0 References

GTG (GoldSim Technology Group), 2010a, *GoldSim User's Guide: Volumes 1 and 2*, GoldSim Technology Group LLC, Issaquah, WA.

GTG (GoldSim Technology Group), 2010b, *GoldSim Contaminant Transport Module User's Guide*, GoldSim Technology Group LLC, Issaquah, WA.

Appendix C - Energy*Solutions* Issue Tracker Standard Operating Procedure

Neptune and Company (N&C) Internal Procedure
Confidential

General Procedure: Standard Operating Procedure (SOP) Contract Specific: Internal N&C product	**Document No.** 06245-004	Version: 01
Document Status: Final		
Title: Energy*Solutions* Issue Tracker SOP		**Author:** Warren Houghteling **Revised by: N/A**
Final Approval Signatures		**Date**
Corporate Quality Assurance Officer: Print Name: James Markwiese Signature:		
Neptune and Company Project Manager: Print Name: Paul Black Signature:		
Effective Date: 12/21/2010		

Date Stamp: 2/22/2011

Energy Solutions Issue Tracker for the Clive Performance Assessment Model
Standard Operating Procedure

Introduction

For the Energy Solutions Clive Facility Performance Assessment, Neptune and Company has set up an issue tracking system for the performance assessment model and associated documentation. An issue tracking system contributes to product quality in two major ways:

1. It assures that issues, once discovered, are not overlooked or "lost in the shuffle" by providing a centralized location for all issue reports.
2. It provides documentation of how the issue was identified, the steps taken to correct it, and the steps taken to verify that issue was in the end resolved in a satisfactory manner.

Without a formal issue tracking system, this kind of information is often contained in emails or other more transient forms of communications (e.g., instant messaging), making it difficult to reconstruct the process that was followed in identifying and resolving an issue. An issue tracking system provides a high level of transparency to the issue discovery and resolution process, lending a much higher level of confidence to the quality of the product being tracked.

The "ES Issue Tracker" is based on the open-source Bugzilla software defect tracking system (http://www.bugzilla .org). As stated on the Bugzilla web site,

> Bugzilla is a "Defect Tracking System" or "Bug-Tracking System." Defect Tracking Systems allow individual or groups of developers to keep track of outstanding bugs in their product effectively. Most commercial defect-tracking software vendors charge enormous licensing fees. Despite being "free", Bugzilla has many features its expensive counterparts lack. Consequently, Bugzilla has quickly become a favorite of thousands of organizations across the globe.

Bugzilla is a web-based application, which makes is easy to access by anyone with a web browser. The Neptune "ES Issue Tracker" uses version 3.4.6 of the Bugzilla software and is hosted at http://zeus.neptuneinc.org/es-issuetracker/.

Bugzilla can be configured for use with one of a number of different database management systems (DBMS) for its database back end. The ES Issue Tracker uses the PostgreSQL open-source database management system (http://www.postgresql.org). The current installation uses PostgreSQL version 8.3.9. The issues database is backed up nightly by an automated script that runs on the database server machine.

Creating a User Account

To use the issue tracker, one must first create a user account. The site's main page features a large "Open a New Account" button as well as having "New Account" links that appear on

both the top and bottom toolbars found on each page of the site. Once a user has created an account and logged in, these links are replaced by "Log out" links.

Clicking on the button or on one of the links brings up a screen where the user is prompted to enter a valid email address. All Bugzilla usernames are email addresses – this makes it easy for Bugzilla to keep users informed of the status of the issues it tracks via email. Once the user has entered an email address, they will receive an email confirming that their account has been created. The email will provide a temporary password and instructions for logging on to the site and setting up a permanent password and other aspects of their user profile.

Bugzilla is designed to allow anyone who can access the site to create a user account. However, the software can be configured with security permissions that strictly control which users can access the different aspects of the site's functionality. In other words, despite its open architecture, Bugzilla is also able to tightly control "who sees what" in terms of the information stored in the Bugzilla database.

Filing an Issue

When a problem is discovered with the performance assessment model or documentation, anyone on the team may file an issue report. The home page features a large "File an Issue" button, plus "new" links in the top and bottom toolbars. Upon clicking one of these, the user will be directed to one of two pages. If they have not yet logged in, they will be prompted to do so, and upon successful login they will be redirected to the Issue entry form, or they will go straight to the entry form if already logged in.

At the top of the entry page are the following instructions: "Before reporting an issue, please read the issue writing guidelines, please look at the list of most frequently reported issues, and please search for the issue." For the ES Issue Tracker, Neptune has customized the issue reporting guidelines that come with Bugzilla to make them specific to performance assessment model development. All users of the system MUST read this document, as it specifies requirements for filling out an effective issue report, including required fields (these are also covered in the following section). The other two links are designed to help the user avoid entering duplicate information into the system, given that more than one person may come across the same issue at more or less the same time.

Required Form Parameters

Product / Component

Bugzilla supports tracking issues with multiple different products in a single installation. Each product has at least one "component," a distinct functional unit against which issues are tracked. The ES Issue Tracker is dedicated to a single product, the "Clive PA Model," so it is only necessary to choose a component.

Version

The user must select a version of the product against which to report the issue. If there is a newer version of the model available, the user must try to reproduce the issue with the latest version, in case it has already been addressed. The procedure for assigning versions to GoldSim models is described in section 4.3 of the Neptune document "GoldSim Model Development SOP."

Summary

The summary field describes the issue in approximately 60 or fewer characters. A good summary **should quickly and uniquely identify an issue report**. It should explain the problem, not a suggested solution.

Description

This section provides the details of the problem report, including:

- **Overview**: More detailed restatement of summary.
  - e.g. "Crash occurs on realization 138 when 1,000 realizations are selected."
- **Steps to Reproduce**: Minimized, easy-to-follow steps that will trigger the issue. Include any special setup steps.
  - e.g. "Run v1.103 in probabilistic mode, with 1,000 realizations and the seed set to 1."
- **Actual Results**: What the application did after performing the above steps.
    - e.g. "GoldSim crashes, without even an error dialog."
- **Expected Results**: What the application should have done were the issue not present.
  - e.g. "Expected simulation to continue."
- **GoldSim Version**: GoldSim version in which issue first encountered.
  - e.g. "GoldSim v10.02"
- **Additional Versions**: Whether the issue exists in other model or GoldSim versions.
  - e.g. "Also occurs using GoldSim 10.11, but cannot test older versions."
- **Additional Information**: Any other useful information.

For crashing issues:

- Any information provided in an error message.

Optional Parameters

These parameters are preset with default values and do not necessarily need to be adjusted by the person filing the new issue.

Severity

This parameter indicates the severity of the issue. Values range from "enhancement" (essentially a new feature request rather than a defect) to "blocker" (an issue so severe that it is preventing development from moving forward). Defaults to "normal" and can be adjusted throughout the lifecycle of the issue.

Hardware

This value is hard-coded to "PC" as this is the only hardware that GoldSim currently supports.

OS

Operating system – currently hard-coded to 'Windows."

Advanced Fields

At the top of the issue entry form is a link titled "Show Advanced Fields." By clicking on this link the user can adjust some fields that have already received default values based on the values of the standard fields.

Priority

This field represents the priority that will be assigned to the issue. Priorities are used to determine the order in which issues will be addressed. Priority may correlate with severity, but do not necessarily need to do so. The default priority is P5, the lowest. Priorities will be managed (usually by the technical lead in conjunction with the project manager) during the issue triage process described during succeeding sections of this document.

Initial State

This defaults to "NEW," but could be set to "ASSIGNED" if the issue is being reported by the technical lead and they are ready to assign the issue to a team member. The meanings of the different issue states will be discussed in the following section.

Assign To

Each component is given a default assignee when it is created. For the ES Issue Tracker, all issues are initially assigned to the technical lead to be reviewed and assigned to the appropriate team member. However, if the technical lead is reporting the issue, he might choose to assign it directly to a team member.

CC

The CC list for an issue defines a list of users who will be cc'd on all emails generated by the issue. Anyone who wants to be kept abreast of developments on the issue can be added to the list. When a component is created, it can be assigned a default CC list. For the ES Issue Tracker, the default CC list for each component includes the project manager and the technical lead.

URL

This Bugzilla field is not used in the ES Issue Tracker implementation and can be ignored.

Depends on

This field can be used to indicate that the resolution of an issue depends on the resolution of one or more existing issues. Input to the field should be a comma-separated list of existing issue numbers. Bugzilla can use this information to create dependency trees that

illustrate the relationship(s) between issues. Bugzilla will also prevent issues that are marked as depending on other issues from being changed to status RESOLVED until the all its blocking issues are first marked as resolved.

Blocks

This field can be used to indicate that resolution of this issue blocks the resolution of one or more existing issues. In other words, the other issues cannot be effectively resolved unless this issue has been resolved first. Input to the field should be a comma-separated list of existing issue numbers. Bugzilla can use this information to create dependency trees that illustrate the relationship(s) between issues. As noted above, Bugzilla also requires that issues blocking a given issue be resolved before the blocked issue may be marked as resolved.

Committing the Issue Report

When all required fields (and possibly some or all of the optional fields) have had values entered, the user clicks on the "Commit" button to add the issue report to the database. If any required fields have not been set, the user will receive an error message and be asked to hit the "back" button in their browser and fill in the missing information.

Once the issue is created, Bugzilla will send email to the issue assignee (unless the assignee is the same user as the issue reporter) and anyone on the CC list for the issue, notifying them of the creation of the issue and providing brief summary information and a URL link to the full issue report. The reporter of the issue will not receive an email. Bugzilla's default behavior is to assume that a user who creates or updates an issue report knows that they have done so and does not need an email notification. However, once the issue begins to progress through its life cycle (described in the following section), the reporter will receive email notifications whenever anyone else adds information to or changes the status of the issue report.

Issue Life Cycle

Once it has been created, an issue report has a life cycle in which it moves from one status state to the next until it reaches the "CLOSED" status, which indicates that the issue has been resolved and the resolution verified. The management of this life cycle is the core of how Bugzilla contributes to product quality by ensuring a rigorous QA process is followed for issue resolution.

Issue Status

During its life cycle, an issue goes through a series of states described by the Status field. There are two basic sets of states – "Open" states indicating that the issue is still active and unsolved, and "Resolved" states indicating varying degrees of resolution of the issue. Some Bugzilla tools, including the simple search page, use the term "open" to refer to all open status states.

"Open" States

NEW

The NEW status indicates only that an issue has been entered into the system. Is has not necessarily been interacted with in any way by anyone other than the original issue reporter. NEW issues should be transitioned as quickly as possible to the ASSIGNED status.

ASSIGNED

The ASSIGNED status indicates that the issue has been initially triaged by the technical lead and assigned to a team member for further investigation. The "assigned to" field does not necessarily have to change during this step – the technical lead could keep the issue assigned to himself. The most important thing about this state is that it indicates that the first level of triage has been carried out – that at least the technical lead has looked at the issue and made some decisions accordingly.

ACCEPTED

This status indicates that the issue assignee has seen and read the issue report and has been able to reproduce the issue. By setting the issue status to ACCEPTED, the assignee accepts responsibility for beginning the process of resolving the issue.

REOPENED

Once an issue is marked RESOLVED (see the following section), it must be independently verified that a correct resolution to the problem has in fact been implemented. If this QA step reveals that the issue was not correctly or completely resolve, the status should be changed to REOPENED.

"Resolved" States

RESOLVED

This status is self-explanatory – it indicates that the issue is claimed to be resolved. When status is changed to RESOLVED, the person doing so MUST explain how the issue was resolved and refer to a **specific version** of the GoldSim model and/or documentation in which the fix has been implemented. This is necessary so that the claimed resolution can be independently tested rather than taken at face value.

While an issue is most frequently marked as RESOLVED because code and/or documentation have been changed to correct the reported issue, it can also be marked RESOLVED for a number of other reasons. Therefore Bugzilla has a "Resolution" field that allows the user to indicate how the issue was resolved. The possible values for the Resolution field (which only appears in the interface when Status is set to RESOLVED) are:

- FIXED – the default value; indicates that code and/or documentation has been changed to address the issue
- DUPLICATE – indicates that the issue report is actually a duplicate of another issue report. Sometimes this does not become apparent until after initial investigation of

the issue report. As part of assigning this status to a report, the user must indicate the issue number of which the current issue is a duplicate.

- WONTFIX – indicates that while the issue described is valid, it will not be corrected in the current release. For example, the issue might be of severity "enhancement," and while the team might agree that this is a worthwhile enhancement, implementing it does not fall within current project scope or budget.
- WORKSFORME – indicates that all attempts to reproduce the issue have been futile. If the issue re-surfaces in later testing, the issue report can be re-opened.
- INVALID – after investigating the issue, the assignee concludes that the issue does not in fact represent a defect or problem that needs to be solved.

VERIFIED

This status indicates that someone other than the team member who marked the issue as RESOLVED – FIXED had independently verified that the issue is indeed resolved.

CLOSED

Indicates that the issue's life cycle is at an end. Once an issue is marked as VERIFIED, it can be transitioned to CLOSED. However, some resolutions, such as INVALID and WONTFIX, do not need to be verified -- they can be moved directly to CLOSED.

Issue Workflow

The workflow for a given issue is summarized in the following diagram, taken from the Bugzilla User's Guide and modified for the ES Issue Tracker:

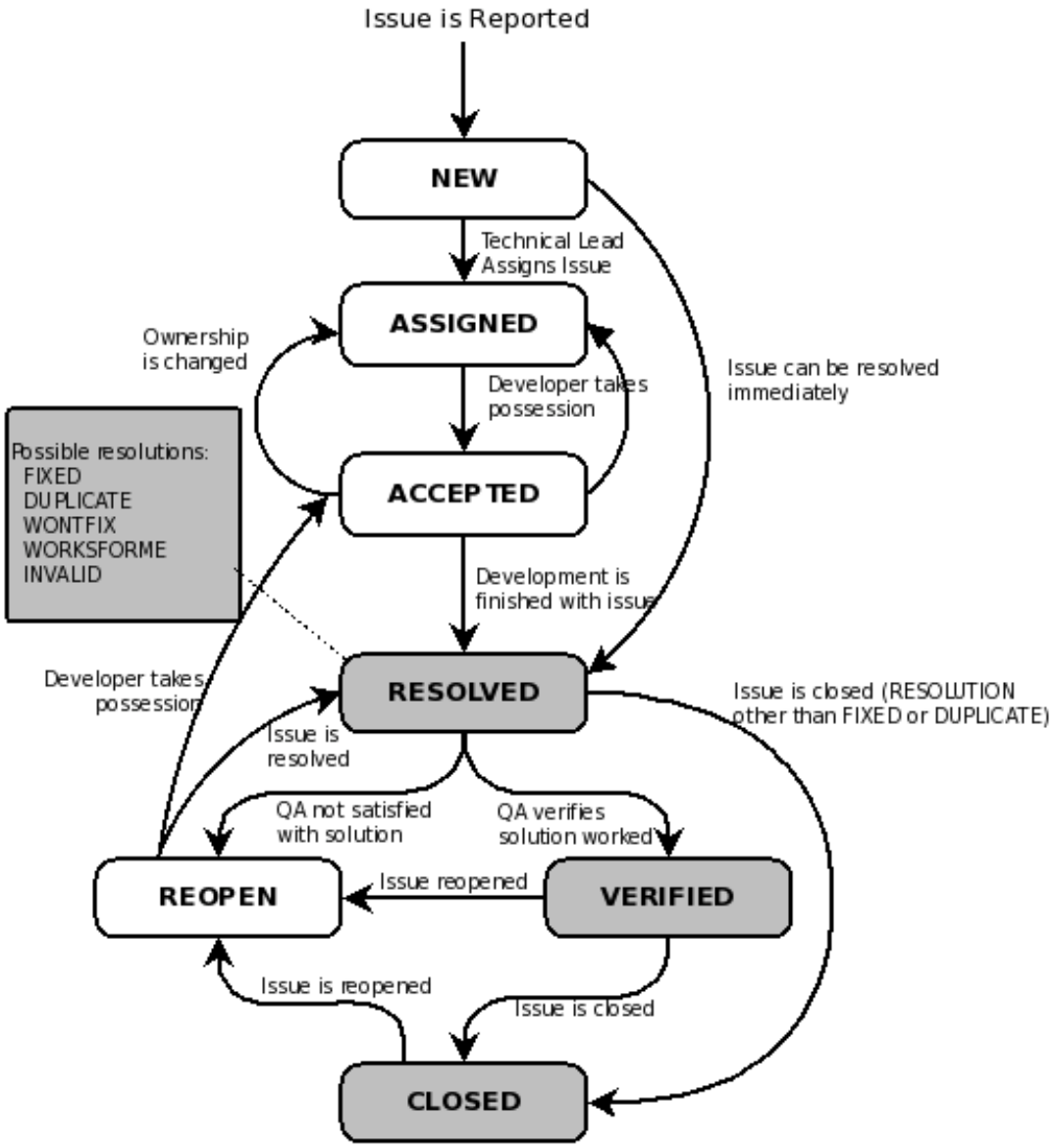
Issue is Reported
NEW
Technical Lead
Assigns Issue
ASSIGNED
Ownership
is changed
Developer takes
possession
Issue can be resolved
immediately
Possible resolutions:
FIXED
DUPLICATE
WONTFIX
WORKSFORME
INVALID
ACCEPTED
Development is
finished with issue
Developer takes
possession
RESOLVED
Issue is closed (RESOLUTION
other than FIXED or DUPLICATE)
Issue is
resolved
QA not satisfied
with solution
QA verifies
solution worked
REOPEN
Issue reopened
VERIFIED
Issue is reopened
Issue is closed
CLOSED

The above workflow can be summarized as follows:

1. Issue report is created with status = NEW and assigned to the technical lead.
2. Technical lead triages the issue and assigns it to a team member – status changes to ASSIGNED.
3. The team member to whom the issue has been assigned reviews the issue and possession of it by changing status to ACCEPTED. At the very least, this indicates that the team member is aware that a new issue has been assigned to them.
4. The assignee works to investigate and resolve the issue. At this point two basic scenarios are possible:
    a. The team member takes action that they feel resolves the issue, and they change the status to RESOLVED with a resolution of FIXED. The team member **must** add a comment to explain exactly what was done to resolve the issue. If the issue was with a documentation component of the model (i.e. the white papers, parameters document, etc.) the Subversion revision number that contains the corrected document(s) **must** be included in the resolution comment. If the issue was with the GoldSim model, the version of the model in which the fix was implemented **must** be included in the comment. Attempting to commit a change of status to RESOLVED without including a comment will transfer to an error page which directs the user to click the browser's "back" button and add a comment.
    b. The team member determines that the issue should be marked as resolved using one of the other resolutions (DUPLICATE, WONTFIX, WORKSFORME or INVALID – for the meanings of these, please see the previous section.). Again, the team member **must** enter a comment explaining the rationale behind this decision. At this point, we skip ahead to step 7 below.
5. As part of changing the status of an issue to status RESOLVED, the team member **must** re-assign the issue to another team member to independently verify that the issue has been successfully resolved. If the team member has any doubts as to whom they should assign the report at this point, they should assign it back to the technical lead, who will determine who should verify the issue's resolution.
6. The new assignee attempts to independently verify that the issue is resolved.
    a. If they agree, they changed the issue status to VERIFIED, and we progress to step 7 below.
    b. Otherwise, they change the status to REOPENED and assign the issue back to the team member who marked it as resolved, taking us back to step 3 in the process

    In either case, the validator **must** provide a comment explaining in as much detail as necessary why the issue either passed or failed verification.
7. This issue has its status changed to CLOSED and its lifecycle is ostensibly ended. However, future testing might lead to the conclusion that the issue was not in fact fully resolved, in which case the issue will have its status changed to REOPENED and it will be assigned to the technical lead for triage, taking us back to step 2.

Interacting with Issue Reports

Once an issue report has been created and saved in the database, it can be accessed in several ways:

- Via the link to the issue report included in the automated emails that Bugzilla sends when the issue report is created or modified
- By entering the report's issue number in the text field to the left of the "Find" button in the top and bottom toolbar of each page of the ES Issue Tracker
- By searching for the issue

Searching for Issues

The ES Issue Tracker provides a large "Search" button on its home page and "search" links in the top and bottom toolbars of each page of the site. All of these lead the user to the search page. The search page has two tabs, entitled "Find a Specific Issue" (the default) and "Advanced Search."

Simple Search

The first tab (from this point on referred to as the "simple search interface") has a form with three fields, Status, Product, and Words.
"Status" is a drop-down list with the terms Open, Closed, and All. "Open" reports are all those whose status field contains "Open Status" as described in the previous section. For the purposes of the search interface, "Closed" reports are all those reports whose status field contains "Resolves Status" as described in the previous section. Choosing "All" means that the query will not filter on status.
"Product" is another drop down list containing the values "All" and "Clive PA Model." Since the ES Issue Tracker is limited to single product, this field can essentially be ignored.
"Words" is a text field where the user can issue words that it wants to include in the query. Bugzilla will search all "content" fields – the report summary, the description, and any comments that have been added to the report (see below) for any of the words entered in this field.

Advanced Search

The advanced search page provides the ability to create highly detailed searches by specifying desired values for any of the different fields as well as specifying date ranges for criteria such as when various aspects of the issue report changed (e.g. status, priority, severity, etc.)
Team members who are new to this interface may find it daunting.
Because documenting all features of the advanced search would unnecessarily lengthen this SOP, team members are advised to consult the team's IT specialist for personal training and assistance in using the interface if needed.

Saved Searches

Saved searches are an extremely powerful and useful Bugzilla feature. Once a search has been defined using either the simple or advanced interface, the search can be given a name and saved. The saved search will then show up as a link in the top and bottom toolbars. Bugzilla provides one built-in saved search, called "My Issues," that searches for all "open" issue reports where the user is either the issue reporter or the current assignee. It is easy to create other useful saved searches, such as all open issues dealing a given component, or all issues assigned to a particular team member. Because Bugzilla stores these searches as

URLs, with the search criteria included in the URL's query string, saved searches can easily be shared among team members by simply sending an email or IM with the search URL, which can then be used to execute and save the search in the target user's profile.

The Issue Tracker as the Sole Means of Communication for Issue Tracking and Resolution

As mentioned in the introduction, a major goal of the issue tracking system is to provide documentation of how an issue was identified, the steps taken to correct it, and the steps taken to verify that the issue was in the end resolved in a satisfactory manner. Therefore, once an issue has been identified, the Issue Tracker should be the sole means of written communication about the issue. The team accomplishes this by adding comments to the issue report, and reassigning the issue among team members as necessary.

Adding Comments to the Issue Report

As the issue report transitions between states and is otherwise modified, team members should add comments to the issue report that explain the state transitions and modifications. For example, if the priority or severity fields are changed, a comment should be added to explain why the priority is considered to be different (raised or lowered) than it was previously. Most crucially, as mentioned earlier, when an issue is marked RESOLOVED, a comment MUST be added to explain exactly what was done to resolve the issue. This constraint is enforced by the software – attempting to commit a change of status to RESOLVED without including a comment will transfer to an error page which directs the user to click the browser's "back" button and add a comment. If the issue was with a documentation component of the model (i.e. the white papers, parameters document, etc.) the Subversion revision number that contains the corrected document(s) **must** be included in the resolution comment. If the issue was with the GoldSim model, the version of the model in which the fix was implemented **must** be included in the comment.

Comments are also extremely useful for tracking progress in resolving non-trivial issues. If debugging the issue involves significant testing and/or research, recording intermediate results and progress in comments is an excellent way to preserve and share important technical information. This also has the added benefit of keeping the technical lead and project manager (plus potentially other interested parties) informed of progress on the issue, as Bugzilla generates automated email notifications every time a change to the issue report is committed to the database.

Adding Attachments to the Issue Report

Bugzilla also allows users to upload attachments to issue reports. This feature is especially useful for attaching screen shots, spreadsheets, and other non-text information to the report. Other candidates for attachments might be intermediate versions of documents that are in the process of being amended and correspondence from interested parties who might not have access to the Issue Tracker. Also, incremental versions of the GoldSim model (versions whose version number ends in a letter – see section 4.3 of the "GoldSim Model Development SOP" for details) may be attached to an issue report as a way to share

these versions during the process of issue resolution. Because of their size, GoldSim Models should always be marked as "Big Files" by checking the "BigFile" check box on the attachment upload interface. This means that they will be stored directly on the server's hard disk and can be deleted by the site administrator when appropriate (for example, when a newer intermediate version is available, or the issue has been closed).

Reassigning an Issue

Sometimes a developer may need to reassign an issue to get help from another team member. The other team member may go on to resolve the issue, or may simply provide information or other help that allows the original assignee to complete the resolution. In this latter case, the team member to whom the issue was re-assigned should assign the issue back to the original team member once they have provided the requested assistance (which should of course be recorded in one or more comments in the issue report).

Appendix D - Energy*Solutions* Checkprint Standard Operating Procedure

Neptune and Company (N&C) Internal Procedure
Confidential

General Procedure: Standard Operating Procedure (SOP) Contract Specific: Internal N&C product	**Document No.** 06245-005	Version: 02
Document Status: Final		
Title: Energy*Solutions* Checkprint SOP		**Author:** Michael Sully **Revised by:** Michael Sully
Final Approval Signatures		**Date**
Corporate Quality Assurance Officer: Print Name: James Markwiese Signature:		
Neptune and Company Project Manager: Print Name: Paul Black Signature:		
Effective Date: 12/21/2010		

Date Stamp: 2/22/2011

Energy*Solutions* Check Print Process for Verification of Data Entry

---

Purpose

This procedure describes the method for providing a check for the completeness and accuracy of data entry processes.

Scope

This procedure applies to manual or electronic data entry including data documentation packages developed for model input, databases or spreadsheets supporting models, and data/results tables included in reports.

In this procedure

This procedure addresses the following major topics:

General information about this procedure

Attachments

This procedure has the following attachments:

Number	Attachment Title	No. of pages
1	Check print 1 example	1
2	Check print 1 example data source document	1
3	Check print 2 example	1

History of revision

This table lists the revision history and effective dates of this procedure

Revision	Date	Description of Changes
0	8 Sep 2004	New document
1	21 Dec 2010	Revised signature page

Who requires training to this procedure?

Personnel verifying data entry processes.

Training method

The training method for this procedure is on-the-job training by a previously trained individual and is documented by signature on training form and archived with project records

Prerequisites

None.

Check print process

Overview

This procedure applies to work processes requiring the manual entry or electronic transfer of data. Examples of entities that receive data include data documentation packages for model input parameters, external spreadsheets and databases used to provide input parameters for modeling, and tables of data/results in documents. Using this procedure data entry or transfer is verified by comparing values in the receiving entity with values in the source documents/files to insure accuracy and completeness of the data entry or transfer. An individual other than the one compiling the data in the receiving entity should perform this check. For manual data entry 100 percent of the entries are checked. For electronic data transfer, 10 percent of the entries are checked. Inputs are checked using the check print process described below. This process can be used to verify most data entry tasks. Large files may require a modified procedure.

Check print process

To check print manually entered or electronically transferred data perform the following steps:

Step	Action
1	Obtain a paper copy of the receiving entity and a copy of the data source document. For example, see attachments 1 and 2.
2	Compare the parameter value in the source document including units with the value in the receiving entity to determine if it was entered accurately and completely.
3	If the value is correct, mark with a highlighter
4	If the value is incorrect, circle in red ink and note the correct value.
5	Verify that the cited reference for the value is correct and complete with page number, table number, or other reference as required.
6	If the reference is accurate and complete, mark with a highlighter.
7	If the reference is inaccurate or incomplete, note corrections in red ink.
8	Label the checked receiving entity as “Check Print 1”, sign, date and return to the author for corrections.
9	When the corrections to the receiving entity are completed follow the same process as described in Steps 1 through 7, however, only the corrected values/references identified in check print 1 need to be checked. See attachment 3.
10	Label this check print as “Check Print 2”. Date and sign.
11	Repeat this process until all data/references entered are accurate and complete. The check print number is incremented for each iteration. Keep all iterations for archiving.

Records resulting from this procedure

Records

The following records are created as a result of this procedure. Paper or electronic copies are maintained at Neptune and Company as described in the QAPP.

- All check prints
- Data source documents (or relevant sections thereof)

Attachment 1

An example GoldSim Parameter List - Check Print 1

\DoseAssessment\PlantCRFood

Plant/soil concentration ratios are taken from Kennedy and Strenge (1992) [Table 6.16 p. 6-25]. All values in the table are defined as geometric means. The following table presents geometric mean values for four different plant parts and for each chemical element. These values are also used in plant-induced contaminant transport calculations (see the container \TransportProcesses\PlantTransport\PlantCRTransport).

element	Leafy Veg (Ci/kg dry Plant) per (Ci/kg dry Soil)	Root (Ci/kg dry Plant) per (Ci/kg dry Soil)	Fruit (Ci/kg dry Plant) per (Ci/kg dry Soil)	Grain (Ci/kg dry Plant) per (Ci/kg dry Soil)
C	7.00E-01	7.00E-01	7.00E-01	7.00E-01
Cl	7.11E+01 7.00E+01	7.00E+01	7.00E+01	7.00E+01
Ar	0.00E+00	0.00E+00	0.00E+00	0.00E+00

Reference

Kennedy, W.E.Jr., and D.L. Strenge, 1992. *Residual Radioactive Contamination From Decommissioning*, NUREG\CR-5512, Vol. 1 Pacific Northwest Laboratory, Richland, Washington.

Check Print 1 8 Sep 2004

_____

Mary Jones

An error was found for the entry for Cl for Leafy veg. The incorrect value was marked in red and the correct value was noted directly below it. The reference was determined to be incomplete since the data source was a single table in a 376 page document. The specific location of the table used as the data source was noted in red ink. The copy is labeled as Check Print 1 and is signed and dated by the reviewer.

Attachment 2

Source Document Referenced in the Parameter List
Kennedy and Strenge (1992)

Table 6.16 Soil-to-plant concentration factors

Element/atomic number	Soil-to-plant concentration factors (pCi/kg dry weight per pCi/kg soil)			
	Leafy vegetables	Root vegetables	Fruit	Grain
H 1	(-)*	(-)*	(-)*	(-)*
Be 4	1.0E-2	1.5E-3	1.5E-3	1.5E-3
C 6	7.0E-1	7.0E-1	7.0E-1	7.0E-1
N 7	3.0E+1	3.0E+1	3.0E+1	3.0E+1
F 9	6.0E-2	6.0E-3	6.0E-3	6.0E-3
Na 11	7.5E-2	5.5E-2	5.5E-2	5.5E-2
Mg 12	1.0E+0	5.5E-1	5.5E-1	5.5E-1
Si 14	3.5E-1	7.0E-2	7.0E-2	7.0E-2
P 15	3.5E+0	3.5E+0	3.5E+0	3.5E+0
S 16	1.5E+0	1.5E+0	1.5E+0	1.5E+0
Cl 17	7.0E+1	7.0E+1	7.0E+1	7.0E+1
Ar 18	(-)**	(-)**	(-)**	(-)**

* Concentration factors for ^{3}H are not needed because a special model is used to determine ^{3}H uptake in plants.

** Noble gas radionuclides are not assumed to be taken up by plants.

Attachment 3

An example GoldSim Parameter List - Check Print 2

\DoseAssessment\PlantCRFood

Plant/soil concentration ratios are taken from Kennedy and Strenge (1992) [Table 6.16, p. 6-25]. All values in the table are defined as geometric means. The following table presents geometric mean values for four different plant parts and for each chemical element. These values are also used in plant-induced contaminant transport calculations (see the container \TransportProcesses\PlantTransport\PlantCRTransport).

element	Leafy Veg (Ci/kg dry Plant) per (Ci/kg dry Soil)	Root (Ci/kg dry Plant) per (Ci/kg dry Soil)	Fruit (Ci/kg dry Plant) per (Ci/kg dry Soil)	Grain (Ci/kg dry Plant) per (Ci/kg dry Soil)
C	7.00E-01	7.00E-01	7.00E-01	7.00E-01
Cl	7.00E+01	7.00E+01	7.00E+01	7.00E+01
Ar	0.00E+00	0.00E+00	0.00E+00	0.00E+00

Reference

Kennedy, W.E.Jr., and D.L. Strenge, 1992. *Residual Radioactive Contamination From Decommissioning*, NUREG\CR-5512, Vol. 1 Pacific Northwest Laboratory, Richland, Washington.

Check Print 2 8 Sep 2004

_____

Mary Jones

The correction of the entry for Cl for Leafy veg and the additional data source information are verified and marked. The check print number is incremented and the copy is signed and dated by the reviewer. This is the final check print since the document is now accurate and complete.

Neptune and Company Inc.

June 1, 2011 Report for EnergySolutions
Clive DU PA Model, version 1

ATTACHMENT

User Guide for Clive PA Model
version 1.0

User Guide for the Clive PA Model

version 1.0

May 2011

Prepared by

Neptune and Company, Inc.

This page is intentionally blank, aside from this statement.

CONTENTS

FIGURES

1.0 Introduction

This User Guide accompanies the Clive DU PA Model v1.0 computer model (the model).

This radiological performance assessment (PA) computer model, written using the GoldSim systems modeling platform, has been developed to assess the effects of specific proposed disposals of depleted uranium (DU) at the Clive low-level radioactive waste (LLW) disposal facility, operated by Energy*Solutions*, LLC (Energy*Solutions*). The model presents calculations useful in comparison to performance objectives specified by the State of Utah, in UAC 313-25-8.(2)(a), and for comparison to groundwater protection limits (GWPLs) identified in the site's groundwater discharge permit.

The intent of this model is to inform decisions regarding this proposed disposal, considering its possible effects on local groundwater and estimated risk, in terms of radiological dose and uranium toxicity, to human receptors. A complete description of the Model and its purpose is provided in the *Conceptual Site Model* (CSM) white paper, provided as part of the reference set as `Clive DU PA CSM.pdf`.

1.1 Objectives

Effects within the first 10,000 years are measured as concentrations of radionuclides from these wastes in groundwater, and estimates of possible radiological doses and uranium toxicity hazards to hypothetical receptors.

Effects beyond 10,000 years until peak activity is reached (at secular equilibrium—about 2.1 million years) are measured as concentrations of radionuclides from these wastes in water of a future lake, and concentrations of radionuclides from these wastes in sediments deposited by future lakes.

1.2 Model Development

The model was developed by Neptune and Company, Inc. (Neptune) for Energy*Solutions*, with the first version (v1.0) delivered in May 2011. It was developed using the GoldSim probabilistic system modeling platform, developed by GoldSim Technology Group (GTG) of Issaquah, Washington. While the full version of the GoldSim modeling software is required to build and modify the model, full functionality of the model is also available through use of the GoldSim Player, freely downloadable from the GTG web site at http://www.goldsim.com

2.0 Getting Started

It is the intent of the model developers that anyone with access to a personal computer can run the Clive DU PA model, and examine its inner workings. This section covers what is needed to get up and running with the model.

2.1 System Requirements

The GoldSim software is designed to run under the Microsoft Windows operating system, and can run under wither 32- or 64-bit versions of Windows XP, Windows Vista, or Windows 7. A current and more definitive description of the operating constraints under various versions of Windows is available at the GTG website. Running the model in a simple deterministic mode requires modest resources in terms of disk space and random access memory (RAM), but more ambitious runs of perhaps thousands of realizations would be better handled by a computer with a 64-bit version of Windows and at least 4 GB of RAM.

Electronic references supplied with the model are in Adobe Portable Document Format (PDF) and as Microsoft Excel workbooks. In order to view these resources, the user will need to have Acrobat or Acrobat Reader installed, as well as Excel or the Excel Viewer. Acrobat Reader is available at http://get.adobe.com/reader/, and the Microsoft Excel Viewer at http://www.microsoft.com/downloads.

2.2 Installation of GoldSim and the GoldSim Player

The installation of GoldSim or the GoldSim Player is straightforward, much like any other contemporary computer software. The installation files for both the licensed version and the free Player are available for download at the GTG web site. Evaluation and academic versions are also available. An install file for the GoldSim Player is also provided on the distribution disc for the convenience of the user, though it is advised to check the GTG web site for more recent service packs or versions.

2.2.1 Installation on a personal computer running Microsoft Windows

After obtaining the installation file, simply run it like any other software installation, and GoldSim will be ready to run. Licensed versions will require license activation with GTG, and the user will be prompted to go through this process upon running GoldSim for the first time.

2.2.2 Installation on an Apple Macintosh computer

GoldSim runs well on Macintosh computers that have been outfitted with virtual machines (VMs) running Windows. One such platform that has been successfully implemented at Neptune is VMWare, but others may also work. See http://www.apple.com/macosx/compatibility/ for compatibility with your Macintosh system. Once VMWare is installed, the Microsoft Windows operating system is to be installed within it, and GoldSim installed within that.

2.2.3 Installation on computers running Linux

Although Neptune has not tested the running of GoldSim on Windows VMs under other Linux or Unix platforms, given our experience with VMWare and Macintosh, we expect that this could work.

2.3 Installation of the Clive DU PA Model

The Clive DU PA Model is provided on the distribution DVD. The disc includes all files needed to run the model, including the model file in full GoldSim form (`*.gsm`) and as a Player version (`*.gsp`). After installing GoldSim or the GoldSim Player, the installation of the model is straightforward.

In order to run the full model or the player version, create a directory on your computer hard drive where the model will reside. The location of the model on your hard drive(s) can be easily changed at any time, since there is no complex installation procedure for the model. Copy the `Clive DU PA Model v1.0.gsm` and/or the `Clive DU PA Model v1.0.gsp` file from the DVD (in the `\model` directory) to the chosen directory on your hard drive, and run the model or the player version in GoldSim.

The model comes with a collection electronic references—mostly PDF documents and URLs to document sources. To facilitate locating supporting information, the Clive DU PA Model contains links to these references in appropriate locations in the model. In order for the model to find these reference materials from links embedded in the model, the user must also copy the entire `\model\references` directory from the disc to the directory where the model resides. That is, the model always looks for a directory called `\references` relative to its installed location.

For example, if you copied the model into a directory named

```
D:\CliveDU\
```

then the model will expect to find references here

```
D:\CliveDU\references\
```

The reference set includes PDFs of white papers written by Neptune that describe details of the CSM, processes included in the model, statistical techniques used, and model calculations and inputs. While many papers are provided in PDF format, many other are subject to copyright and cannot be provided. These are available, however, from their respective publishers, and links to sources for these papers are provided. In total, nearly 1 GB of information is provided on the DVD, all of it relevant to the Clive DU PA.

A complete list of Neptune white papers is provided at the end of this User Guide, in Table 1.

3.0 Running the Model

Run the model as you would other Windows software, either by double-clicking on the `.gsm` or `.gsp` model file name, or by launching GoldSim or the Player from a shortcut, and loading the file by navigating to the directory that contains the models. If you are running the Player version, the Welcome screen will appear, depicted in Figure 1.

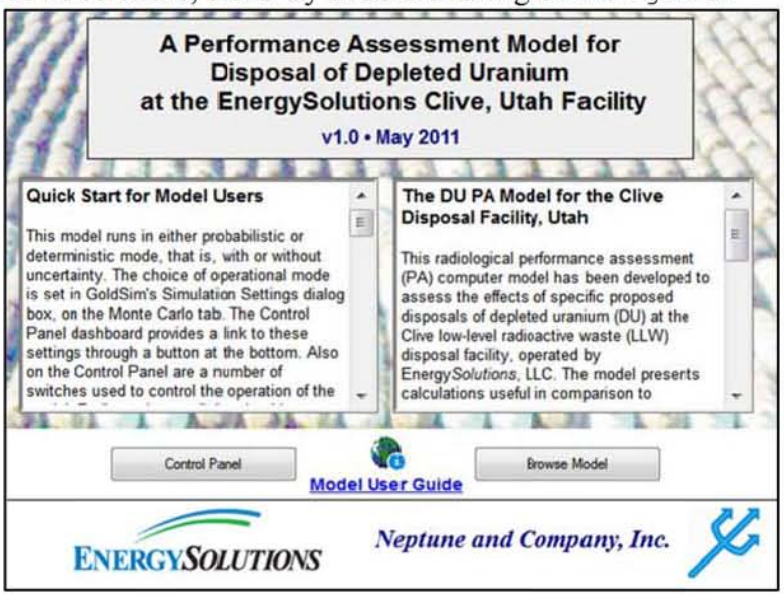

If you are running the full version of GoldSim, the model will open to its top level page, as shown in Figure 2. This is also available to the Player user by clicking the Browse Model button.

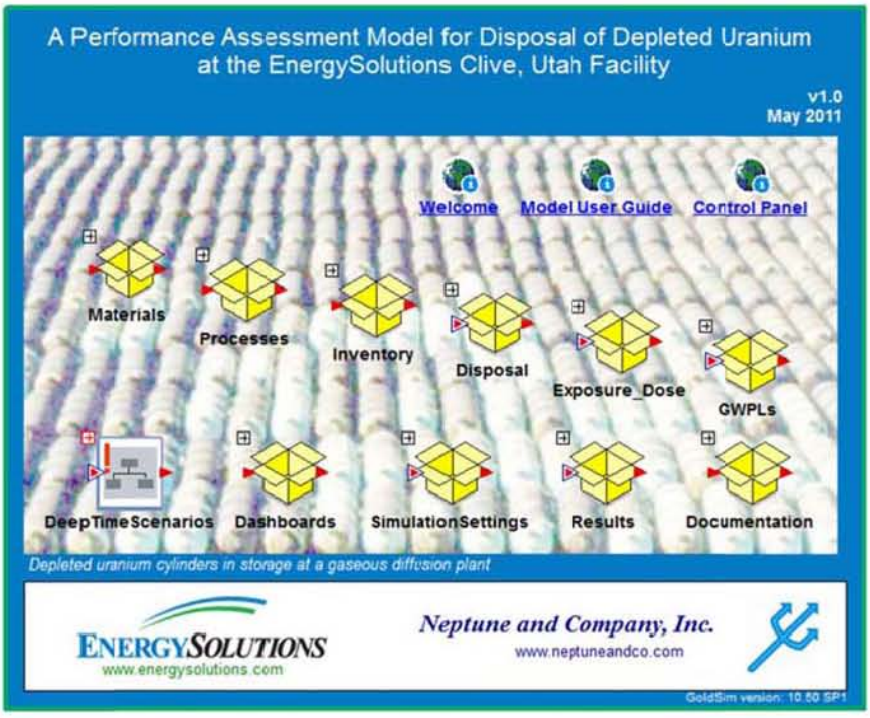

Either way, the user can switch between the two views by selecting the "Browse Model" button from the Welcome screen, or the "Welcome" icon from the top level page.

3.1 Control Panel Setup

From either a button on the Welcome screen or the icon on the top level page, the user can access the model's main Control Panel, shown in Figure 3. The Control Panel is an example of what GoldSim calls a dashboard, which is dialog box-like interface for model users. Dashboards provide information about the model, and buttons that take the user to other dashboards, model controls, or to the model itself, and a number of controls such as check boxes and edit boxes. Each of these controls sports fly-out explanatory text that appears when the user floats the mouse over the control.

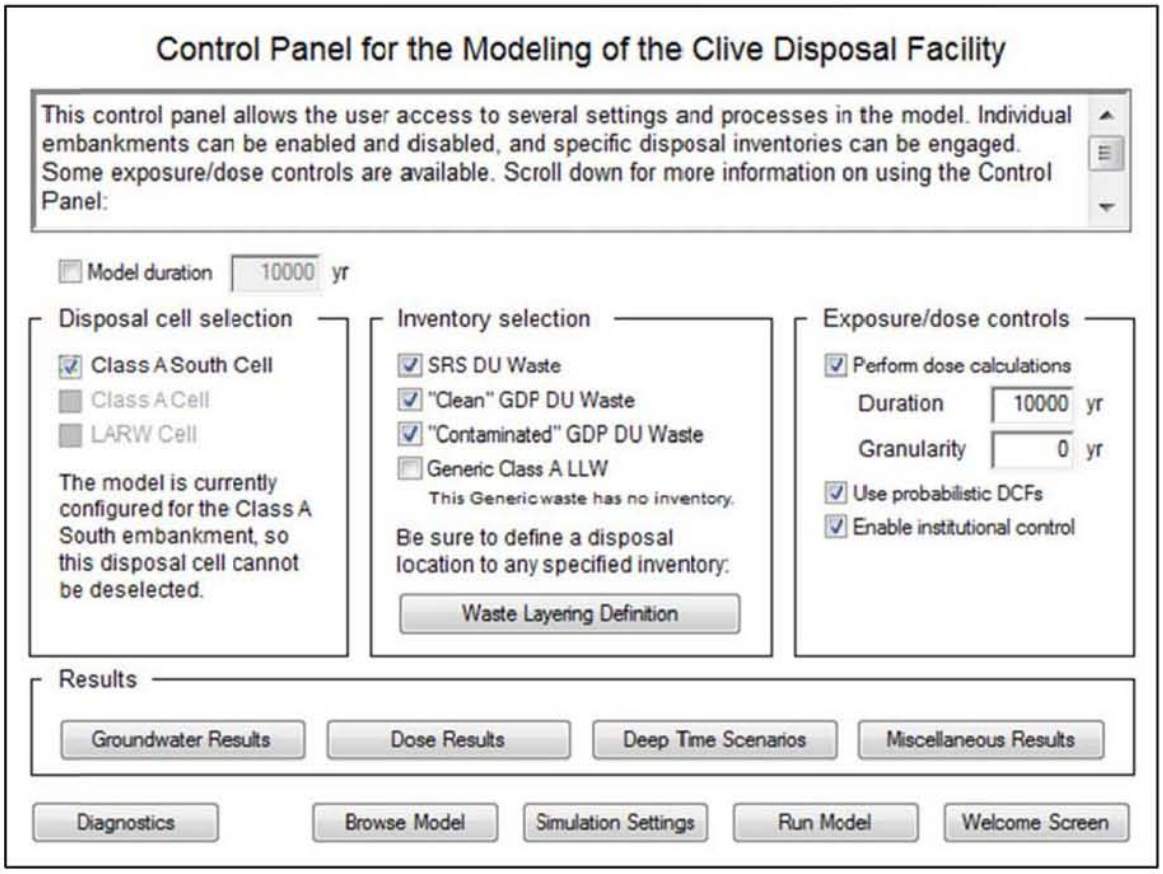

Discussion of each of the Control Panel settings follows. A scrolling paragraph of explanatory text is provided at the top of the Control Panel.

3.1.1 Model Duration

Upon checking the Model duration checkbox, the user may enter the number of years to be simulated. If the box is not checked, then the full 2.1 million years (My) is simulated. If the user puts in a shorter duration, the model stops calculations at that time, and makes no new calculations out to the end of the 2.1 My. Using this option saves in computation time. This is the preferred method for running simulation durations shorter than the full 2.1 My.

3.1.2 Disposal Cell Selection

The current version of the Clive DU PA Model considers only the Class A South disposal cell, or embankment. The checkbox selecting this disposal cell is permanently checked. Subsequent versions of the Clive PA Model are expected to include other disposal cells, hinted at by the grayed text listing them below the Class A South Cell. See the *Embankment Modeling* white paper for more details.

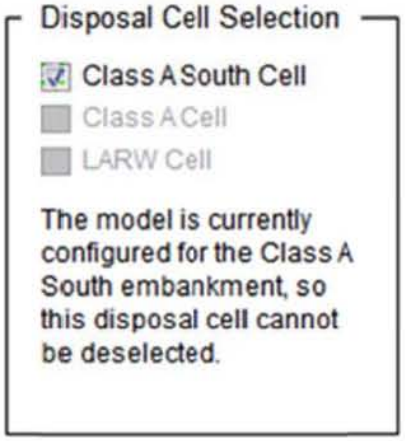

3.1.3 Inventory Selection

Similarly, the current model is configured to examine the effects of only that DU proposed for disposal. There are three principal sources of this material: the DUO_3 waste in drums from the Savannah River Site (SRS DU) and the two types of DU_3O_8 waste in process cylinders from the gaseous diffusion plants (GDP DU) at Portsmouth, Ohio and Paducah, Kentucky. These GDP DU wastes are subdivided into "clean" DU, which contains only uranium and its decay products, and "contaminated" DU, which has been contaminated with fission and activation products present in uranium from reactor returns that was introduced to the process. All of the SRS DU is contaminated with such reactor returns. The user can select different combinations of these waste streams, and both are assumed to be disposed in the Class A South Cell. Subsequent versions of the Clive PA Model are expected to include other Class A LLW as well, as suggested by their listing in gray below the two DU waste types. For more information about the various waste types in the model, see the *Waste Inventory* white paper.

In addition to selecting the various types of waste to be included in a given realization, the user can select where, in a vertical stack, these wastes are to be emplaced. The Waste Layering Definition dashboard, shown in Figure 4, offers a layer-by-layer choice of waste types.

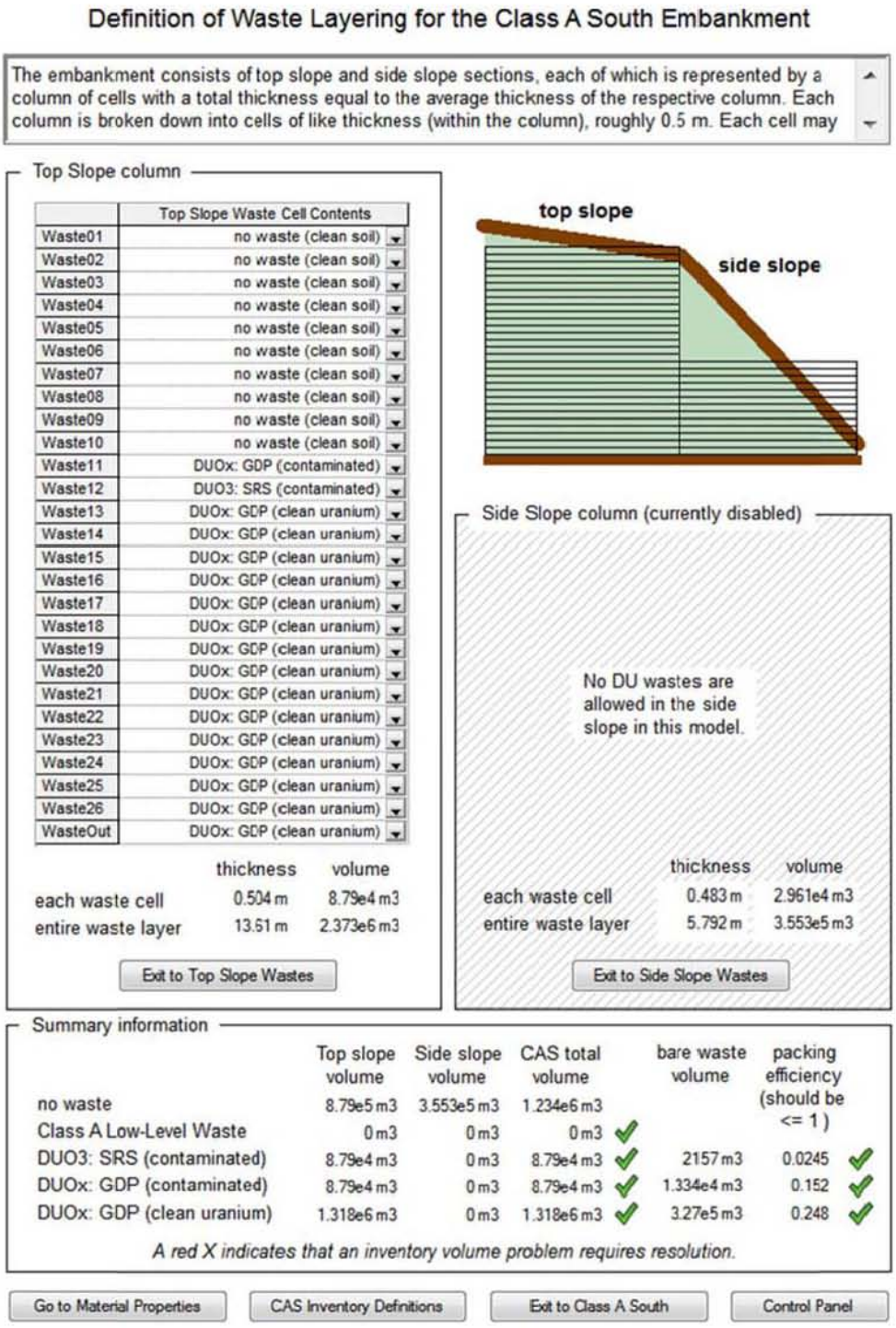

In the example of waste layering shown, Clean GDP DU wastes are on the bottom several layers, overlain by a layer of SRS DU wastes, all of which are contaminated, and that by a layer of Contaminated GDP DU waste. These can be rearranged in any combination that accommodates the volumes of wastes. The information necessary to assure such accommodation is posted at the bottom of the Waste Layering Dashboard. As each waste layer is assigned a material, the volume of that layer is allocated to that waste. If the total volume of the allocated layers is insufficient to contain the volume of the waste type, a red **X** is displayed in the volume calculation table. Assigning more layers to the waste in question will spread it evenly among the layers. Volume should be added by adding layers until the waste volume is exceeded by the total layer volume assigned to that waste type, or a packing efficiency is achieved that is within range of what can be expected in disposal operations. The packing efficiency is the ratio of the volume of the waste type to the assigned layer volume, so therefore must be < 1 in order to accommodate even a perfectly packed waste form, having no voids to contend with.

Waste placement is limited to the layers available in the dashboard. Each of the 27 layers can contain only one waste type at a time. Each is about 50 cm (20 in) thick, and covers the entire Top Slope area of the embankment. For the purposes of this PA, the side slope column is not considered for waste disposal.

3.1.4 Exposure/Dose Controls

A few options are available to the user for controlling the calculation of human exposures and resulting doses and uranium hazards:

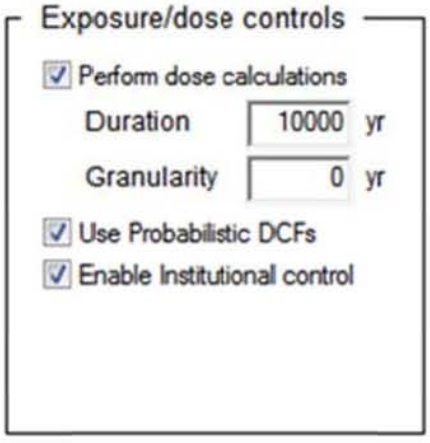

Perform dose calculations enables the dose calculations. This would ordinarily be checked, but if the user is interested only in groundwater concentrations or deep time scenarios, for example, computational effort can be saved by not calculating doses.

Duration: If Perform dose calculations is checked, then the user can select the duration of the dose simulation, up to 10,000 yr, in accordance with UAC 313-25-8.(2)(a).

Granularity: If Perform dose calculations is checked, then the user can also select the "granularity" of the calculations for individual receptors. The individual receptor calculations run at a finer time step than the rest of the model, and this setting defines that time step. This could be as low as 1 yr, which brings in a new set of receptors (ranchers and recreationalists, including hunters and off-highway vehicle enthusiasts) each year for the duration of the dose calculations. Doing so will be more computationally intensive, but the dose to each receptor is calculated and compiled with doses to all receptors, so that individual physiological differences are accounted for. The user might also consider setting this to 10 yr (a new set of receptors is determined every 10 years) to save computational time. A choice of granularity of 0 yr tells the model to use no

granularity at all, defining a new set of receptors only at each of the larger modeling time steps, defined in Simulation Settings. The model runs fastest with the granularity = 0 yr setting.

Use probabilistic DCFs: The user can select between using the fixed (deterministic) and uncertain (probabilistic) values for dose conversion factors (DCFs) with this checkbox. By choosing the probabilistic DCFs, the uncertainty inherent in DCFs is accounted for in the calculations. If the model is run in probabilistic mode. DCFs come from EPA's Federal Guidance Report (FGR) 13. Details on the effects of this and other Exposure/Dose controls are provided in the *Dose Assessment* white paper.

Enable institutional control: The institutional control period is a time when receptors are kept off the site. If this is unchecked, receptors may gain access to the site at any time. Institutional control is otherwise assumed to be effective for 100 yr.

3.1.5 Simulation Settings

GoldSim provides model users and developers with a number of tools for modifying the simulation. These are available through the Simulation Settings dialog, a part of GoldSim. Users of the full version of GoldSim can access these controls with the F2 key, or by Run | Simulation Settings on the GoldSim menu. Users of the Player version of the Clive DU PA Model can access simulation settings from a button on the model's Control Panel dashboard.

The simulation settings of greatest utility to the user for this probabilistic model are on the Monte Carlo tab. Here, the user can selected between probabilistic and deterministic modes of operation. Deterministic modeling, while not offering a sense of the uncertainty in any given results, is a quick way to experiment with model behavior given different scenarios. The user can also choose whether to use the deterministic values set in each Stochastic element definition (these are generally means values), or force the use of mean values, or any given percentile of values from the input distributions. Median values would be selected by specifying the quantile 0.5. Many cases can be considered in

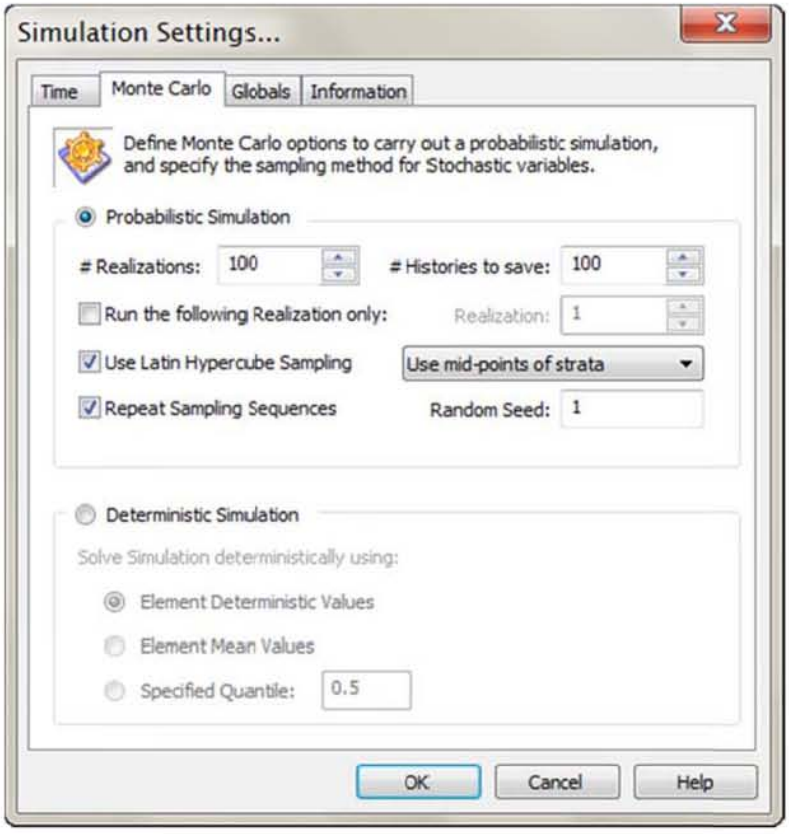

manipulating the settings on the Control Panel. Some of the more common cases to be considered are discussed in the following section.

For users interested in the uncertainty surrounding a particular scenario or result, the model can be run in probabilistic mode. On the Monte Carlo tab, the number of realizations to run can be selected. 100 is a reasonable starting point, offering a rough span of the uncertainty in a short amount of time. A global sensitivity analysis should use something more like 5000 realizations. The # Histories to save should generally be set to be the same number. Latin Hypercube Sampling should be enabled.

More information on these settings and others in the dialog is available in the GoldSim User Manual that is installed with the software.

3.2 Displaying Results

Model results are available in a variety of forms. Time histories show the value of one or more outputs as they change in time. Maximum values show the peak value an output has reached over the duration of the simulation. Final values show outputs values at the end of the simulation. If the model is run probabilistically, each of these results will also include the statistical summary of the value, indicating the uncertainty surrounding its estimation. Most outputs of interest are available through the dashboards linked from the control panel. For example, outputs related to human exposures (dose and hazard) are shown on the Dose Results dashboard (Figure 6), with final values displayed and full time histories available via buttons. As the model runs through

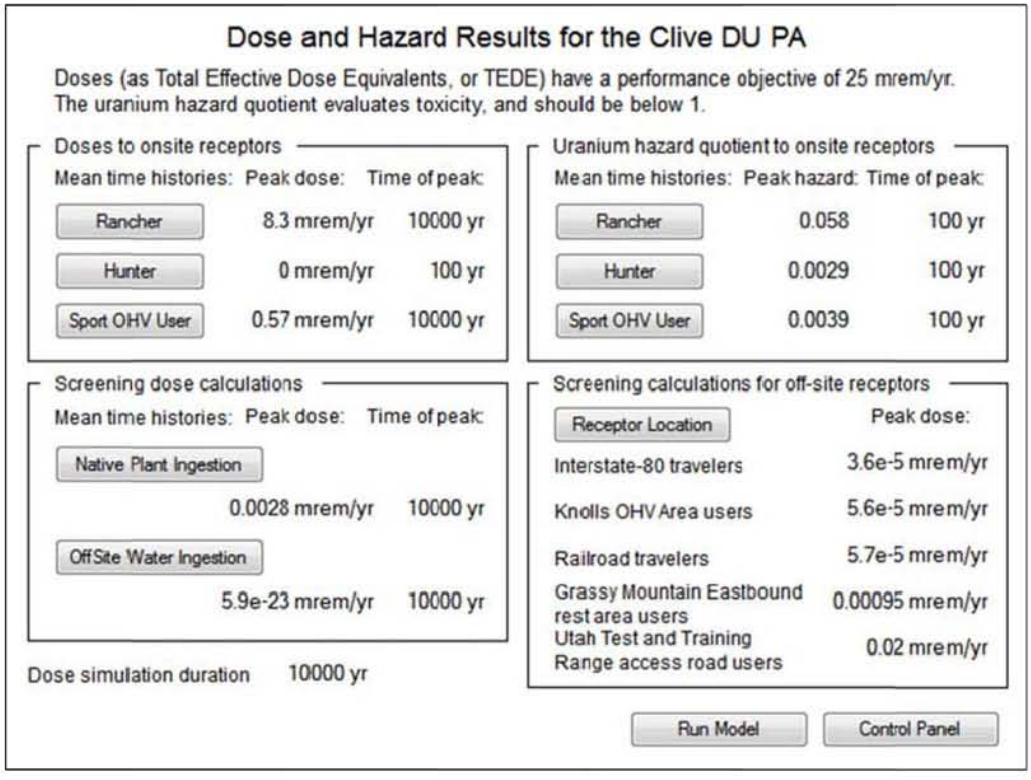

various realizations, the displayed values are updated. In a probabilistic run, therefore, the values displayed on the dashboard are from only the final realization, and do not represent the entire suite of realizations.

3.2.1 Time History graphs

A time history of a deterministic estimate of dose to a ranch hand receptor is shown in Figure 7. Time is shown along the abscissa (the horizontal axis), and dose is shown on the vertical. Both axes may be linear or logarithmic scales. Since this is a deterministic simulation, only a single realization is shown. This graph shows the dose time history over the full 10,000 yr, and represents the annual dose that a ranch hand would receive if he were to show up in any given year. In very early time, the effect of 100 years of institutional control can be seen, where receptors are kept off the site and no doses are achievable. After the loss of institutional control, the dose steadily increases to its maximum value at 10,000 yr, which can be seen by positioning the computer mouse over the graph: 8.3 mrem in a year, in this example. This value is also seen on the dashboard as the peak dose to this receptor.

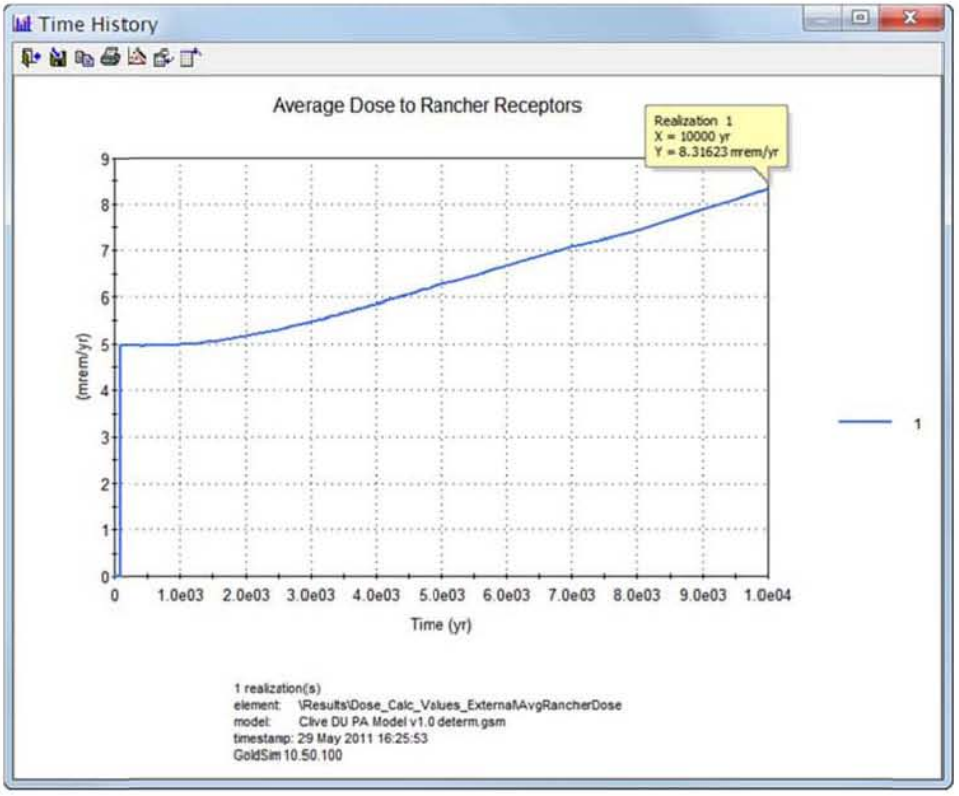

At the bottom of the graph window is displayed information about the simulation, including

- the number or realizations run,
- the name of the GoldSim model element whose output is displayed (in this case, AvgRancherDose),
- the exact name of the model file that was run (Clive DU PA Model v1.0 determ.gsm),
- the date and time of the model run, and
- the version of GoldSim used to run the model.

This information aids in recording and reproducing information from model simulations. The user is strongly advised to save different simulations using descriptive file names.

To continue with our example of dose to the ranch receptor, several additional results not available directly from dashboards are available in the **Results** container. For example, the contributions to dose from individual radionuclides is shown in Figure 8. Clearly, U238 is the leading contributor, followed by Rn222.

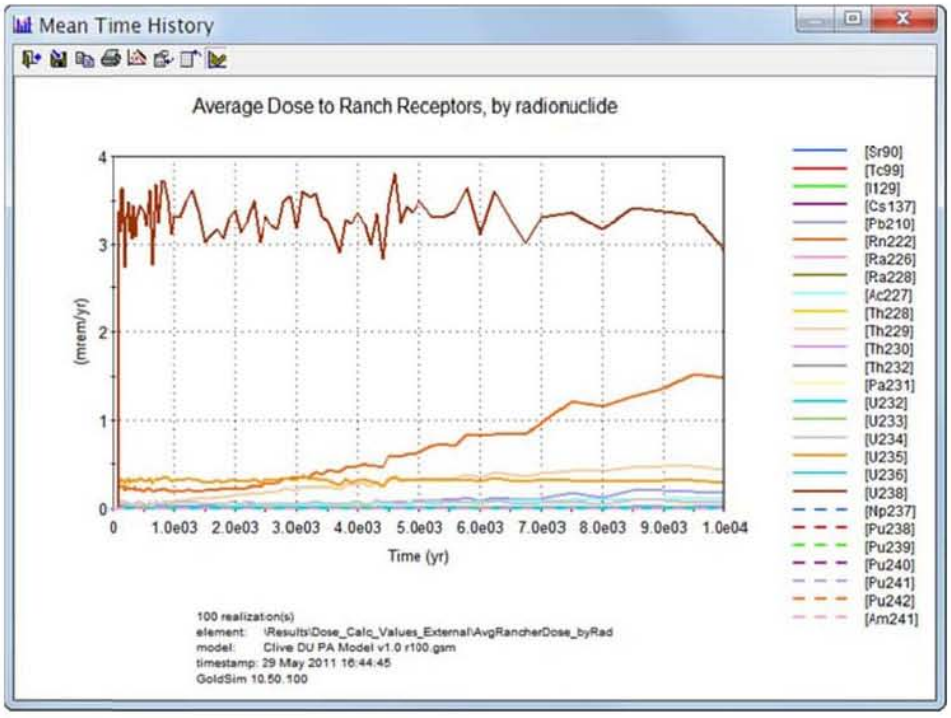

de

A probabilistic simulation of the same output (rancher dose) is shown in Figure 9, having run 100 realizations. Here, the vertical axis (dose) has been displayed as using a logarithmic scale, in order to aid in viewing the results. The peak mean dose is seen to be just over 6 mrem in a year at 9500 yr. The legend identifies various percentiles of the dose at each time step.

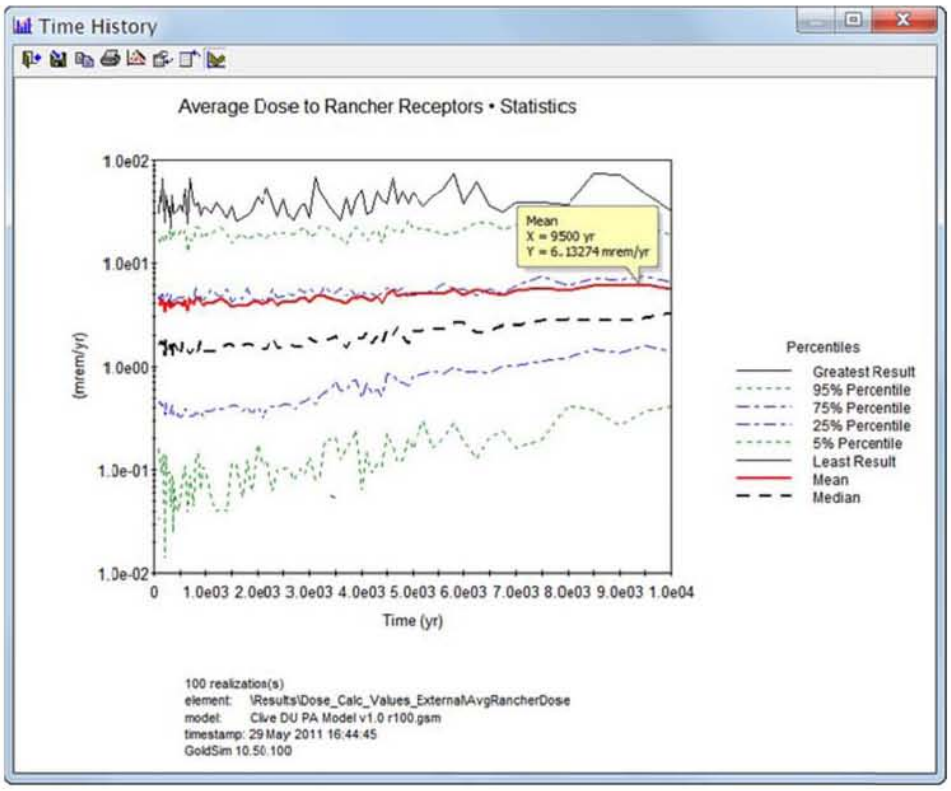

See the GoldSim User Manual for information about manipulating time history plots.

3.2.2 Outputs of values directly on the results dashboards

Many dashboards display values for results directly. These output values are useful for showing deterministic simulation results, but not for probabilistic ones. After a probabilistic simulation, the values displayed are the final values for the last realization, not mean values or any other representation of probabilistic results.

3.2.3 Intermediate Model Results

One feature in GoldSim that aids in transparency is that any model output can be examined to see how it behaves in the simulation. Most element definition dialogs have options for saving results either as final values or as full time histories. In order to examine results from any particular GoldSim element, simply check the Save Final Values or Save Time History checkboxes in the element. More information on saving specific results is available in the GoldSim Manuals or Help.

The Player version does not allow the user to select specific time histories or final values to record.

3.3 Executing Common Scenarios

Depending on the user's particular interest, various simulation scenarios may be run, as discussed in this section.

3.3.1 Selecting Waste Types and Layering

The selection of waste types to be included in a simulation is discussed in Section 3.1.3, and is done using the Control Panel dashboard (Figure 3). As shown in Figure 4, the user can also specify where specific waste types are to be layered. In general, arranging wastes deeper in the embankment will reduce their influence on doses, but may increase their groundwater concentrations, and *vice versa*.

3.3.2 Optimizing Simulations for Specific Endpoints of Interest

If a large number of probabilistic realizations needs to be run, it is often desirable to disable unnecessary calculations to improve computer run time. The scenarios presented below represent the most common methods of streamlining calculations.

3.3.2.1 Comparisons to Groundwater Protection Limits

If one is interested solely in groundwater concentrations, for example to compare to GWPLs, there is no need to run the dose calculations, or even to run the model past 500 yr, the duration of GWPL applicability. Therefore, the Control Panel could be set up as shown in Figure 10: The model duration is set to 500 yr, and dose calculations are turned off.

3.3.2.2 Human Exposure Scenarios

If the user is interested only in evaluating human exposures, the dose calculations should be enabled, and the duration could be limited to only 10,000 yr, so as to save time in not calculating to 2.1 My. The granularity of the dose calculations, described in Section 3.1.4, should be set to the desired value.

3.3.2.3 Deep Time Results

For examining deep time results, the Model duration checkbox should be left unchecked, so that the full 2.1-My simulation is run. The dose calculations should be disabled, as was done for the groundwater calculations.

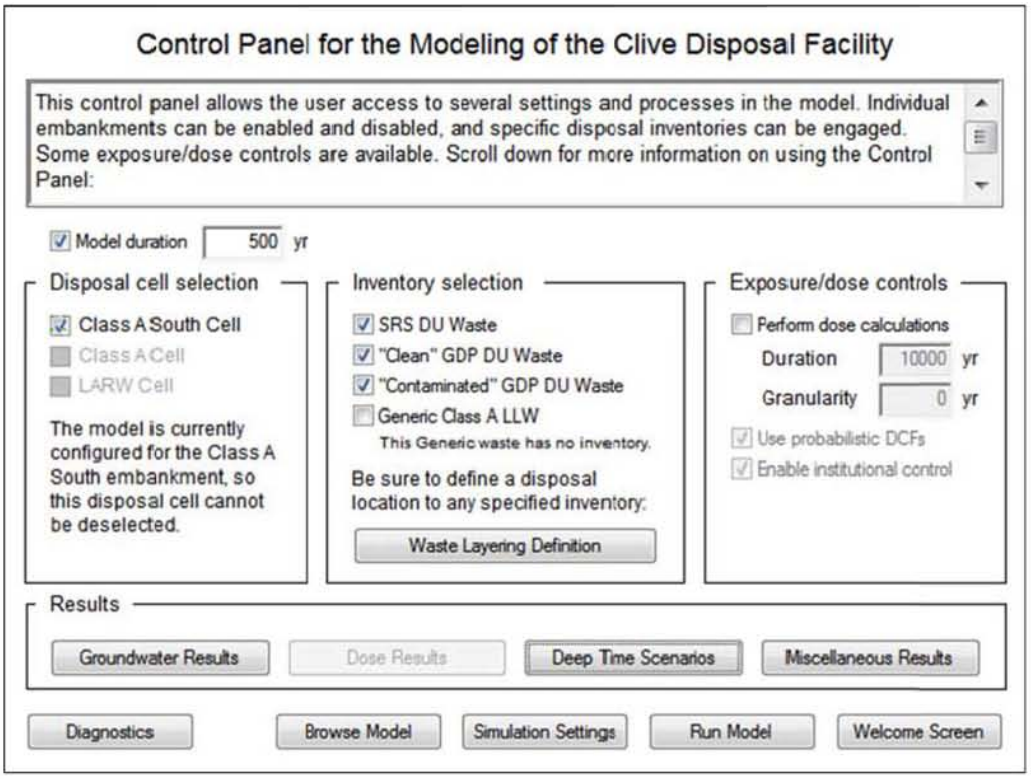

is alone

3.3.2.4 Comprehensive Simulations

Unless the user is running on a particularly slow computer, or desired to run a large number of realizations, it may be fine to leave all the calculations enabled. This allows exploration of all results within a single model. In this case, the Control Panel should be set up as shown in Figure 3, with consideration given to dose calculation granularity, as described in Section 3.1.4.

3.4 Diagnostics

The diagnostics dashboard (Figure 11) provides access to model controls that enable or disable a number of physical, chemical, and biological processes in the model. The principal use of these is to verify that certain modeled processes are working in response to the controls, and it is of little value in running simulations for information. The result elements accessed by button controls on this dashboard show various outputs that indicate whether a process is working or not.

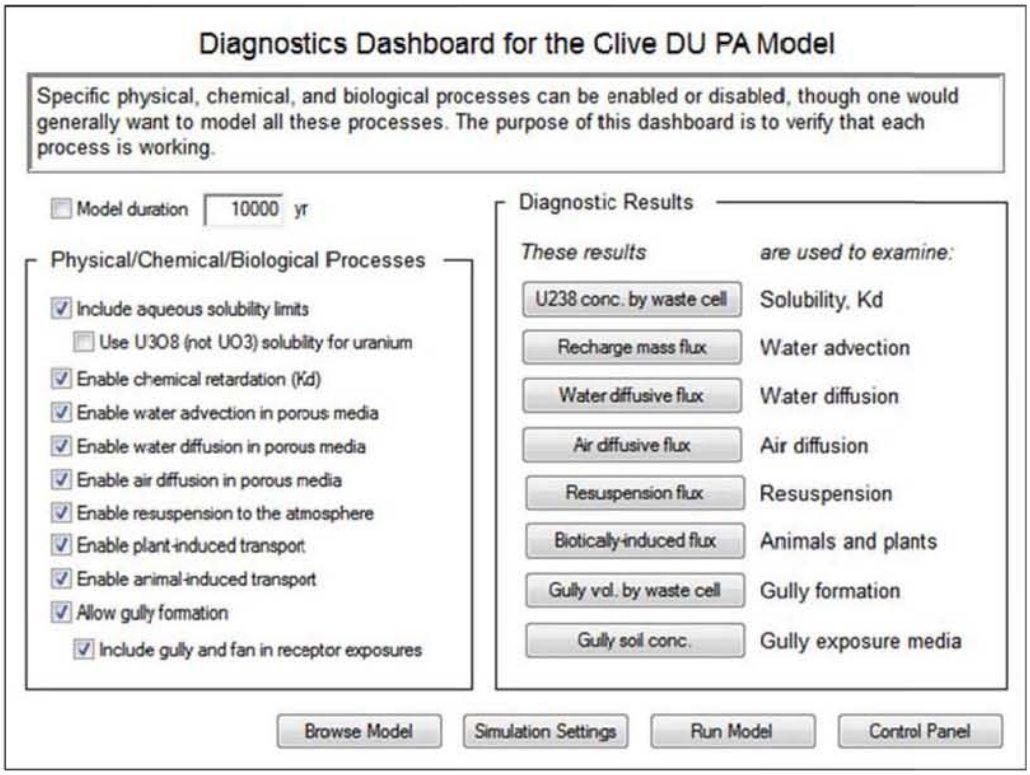

4.0 Error Messages, Alerts, and Warnings

The Clive DU PA Model has a few interrupts and warnings that alert the user to certain situations that may require attention. The GoldSim software produces its own set of warnings and errors as well.

4.1 Messages from the Model

4.1.1 Waste Requires Layering

If a waste inventory is selected, then it must be assigned to the waste layering. If no layer has been specified to host a selected waste type, the model issues a message to the user about how to fix the problem. An example of such a message is shown here.

4.1.2 Waste Packing Efficiency Warning

The Waste Layering dashboard (Figure 4) displays information at the bottom regarding the packing of the waste into the selected volume. A table of values is calculated by the model, as discussed in Section 3.1.3. A detail of this table is shown below:

Summary information

	Top slope volume	Side slope volume	CAS total volume		bare waste volume	packing efficiency (should be <= 1)	
no waste	1.934e6 m3	3.553e5 m3	2.289e6 m3				
Class A Low-Level Waste	0 m3	0 m3	0 m3	✓			
DUO3: SRS (contaminated)	8.79e4 m3	0 m3	8.79e4 m3	✓	2157 m3	0.0245	✓
DUOx: GDP (contaminated)	8.79e4 m3	0 m3	8.79e4 m3	✓	1.334e4 m3	0.152	✓
DUOx: GDP (clean uranium)	2.637e5 m3	0 m3	2.637e5 m3	✓	3.27e5 m3	1.24	✗

A red X indicates that an inventory volume problem requires resolution.

The red **X** indicates that one of the selected inventories has an estimated volume that exceeds the volume allocated to it using the Waste Layering controls—that is, the packing efficiency is greater than 1. The user must add more layers for the indicated inventory type ("DUOx: GDP (clean uranium)" in this example) until the packing efficiency drops below 1, or within the range of estimated packing efficiency that could be achieved in disposal operations.

4.1.3 Run Log Warnings and Error Messages

After every simulation, GoldSim generates a run log to document it. This information, which is stored within the model in results mode, includes metadata (software version, model name, run time, etc.) as well as a record of warnings and errors that GoldSim encountered during the run. These warnings are intended to indicate problems in the model, but most are benign. For example, most of them identify differences in fluid fluxes that are intentionally programmed. For reasons that are explained in the model itself, some material balances are deliberately crafted this way, and doing so does not indicate a mathematical mass balance error.

Specifically, references to the "Footprint" cells, or cells called Cap03, Cap04, etc. are expected to display warnings, and will be found in the Run Log file. These are not errors, and apparent mass balance errors are accounted for in the model design.

4.2 GoldSim Error Messages

The GoldSim software may generate its own error messages, independent of any messages generated by the model. These messages may refer to something occurring in the model, or something in GoldSim itself. Should such a message appear, consult the GoldSim help. If the problem cannot be resolved, try to reproduce it and contact GoldSim support. Methods of contact

are found by selecting Help | Contact Technical Support or Help | Report a Problem from the GoldSim menu.

5.0 Supporting References

A number of references, or "white papers" have been developed as background information supporting the development of the performance assessment model. These are listed below, and are to be found in the `\model\references` directory on the DVD. If this `\references` subdirectory is installed in the same directory as the GoldSim model, these reference papers and others referenced from within the model itself will be found through hyperlinks.

Table 1. White papers supporting the Clive DU PA Model

white paper title	file name
Model Parameters for the Clive DU PA	Clive PA Model Parameters.pdf and Clive PA Model Parameters.xls
Features, Events, and Processes for the Clive DU PA	Clive DU PA FEP Analysis.pdf
Conceptual Site Model for the Clive DU PA	Clive DU PA CSM.pdf
Atmospheric Transport Modeling for the Clive DU PA	Atmospheric Modeling.pdf
Biologically-Induced Transport for the Clive DU PA	Biological Modeling.pdf
Decision Analysis for the Clive DU PA	Decision Analysis.pdf
Deep Time Assessment for the Clive DU PA	Deep Time Assessment.pdf
Dose Assessment for the Clive DU PA	Dose Assessment.pdf
Embankment Modeling for the Clive DU PA	Embankment Modeling.pdf
Erosion Modeling for the Clive DU PA	Erosion Modeling.pdf
Geochemical Modeling for the Clive DU PA	Geochemical Modeling.pdf
Probability Distribution Development for the Clive DU PA	Probability Distributions.pdf
Saturated Zone Modeling for the Clive DU PA	Saturated Zone Modeling.pdf
Sensitivity Analysis for the Clive DU PA	Sensitivity Analysis.pdf
Unsaturated Zone Modeling for the Clive DU PA	Unsaturated Zone Modeling.pdf
Radioactive Waste Inventory for the Clive DU PA	Waste Inventory.pdf